



UNIVERSITAT DE
BARCELONA

Allosteric interactions between catecholamine receptors and other G protein-coupled receptors: Pharmacological and functional characterization

Verònica Casadó Anguera

ADVERTIMENT. La consulta d'aquesta tesi queda condicionada a l'acceptació de les següents condicions d'ús: La difusió d'aquesta tesi per mitjà del servei TDX (www.tdx.cat) i a través del Dipòsit Digital de la UB (diposit.ub.edu) ha estat autoritzada pels titulars dels drets de propietat intel·lectual únicament per a usos privats emmarcats en activitats d'investigació i docència. No s'autoritza la seva reproducció amb finalitats de lucre ni la seva difusió i posada a disposició des d'un lloc aliè al servei TDX ni al Dipòsit Digital de la UB. No s'autoritza la presentació del seu contingut en una finestra o marc aliè a TDX o al Dipòsit Digital de la UB (framing). Aquesta reserva de drets afecta tant al resum de presentació de la tesi com als seus continguts. En la utilització o cita de parts de la tesi és obligat indicar el nom de la persona autora.

ADVERTENCIA. La consulta de esta tesis queda condicionada a la aceptación de las siguientes condiciones de uso: La difusión de esta tesis por medio del servicio TDR (www.tdx.cat) y a través del Repositorio Digital de la UB (diposit.ub.edu) ha sido autorizada por los titulares de los derechos de propiedad intelectual únicamente para usos privados enmarcados en actividades de investigación y docencia. No se autoriza su reproducción con finalidades de lucro ni su difusión y puesta a disposición desde un sitio ajeno al servicio TDR o al Repositorio Digital de la UB. No se autoriza la presentación de su contenido en una ventana o marco ajeno a TDR o al Repositorio Digital de la UB (framing). Esta reserva de derechos afecta tanto al resumen de presentación de la tesis como a sus contenidos. En la utilización o cita de partes de la tesis es obligado indicar el nombre de la persona autora.

WARNING. On having consulted this thesis you're accepting the following use conditions: Spreading this thesis by the TDX (www.tdx.cat) service and by the UB Digital Repository (diposit.ub.edu) has been authorized by the titular of the intellectual property rights only for private uses placed in investigation and teaching activities. Reproduction with lucrative aims is not authorized nor its spreading and availability from a site foreign to the TDX service or to the UB Digital Repository. Introducing its content in a window or frame foreign to the TDX service or to the UB Digital Repository is not authorized (framing). Those rights affect to the presentation summary of the thesis as well as to its contents. In the using or citation of parts of the thesis it's obliged to indicate the name of the author.

**ALLOSTERIC INTERACTIONS BETWEEN
CATECHOLAMINE RECEPTORS AND
OTHER G PROTEIN-COUPLED
RECEPTORS: PHARMACOLOGICAL AND
FUNCTIONAL CHARACTERIZATION**



**VERÒNICA CASADÓ ANGUERA
2018**



UNIVERSITAT DE
BARCELONA

FACULTAT DE BIOLOGIA

DEPARTAMENT DE BIOQUÍMICA I BIOMEDICINA MOLECULAR

**ALLOSTERIC INTERACTIONS BETWEEN
CATECHOLAMINE RECEPTORS AND OTHER G
PROTEIN-COUPLED RECEPTORS:
PHARMACOLOGICAL AND FUNCTIONAL
CHARACTERIZATION**

Verònica Casadó Anguera

2018



UNIVERSITAT DE
BARCELONA

FACULTAT DE BIOLOGIA

DEPARTAMENT DE BIOQUÍMICA I BIOMEDICINA MOLECULAR

ALLOSTERIC INTERACTIONS BETWEEN CATECHOLAMINE RECEPTORS AND OTHER G PROTEIN-COUPLED RECEPTORS: PHARMACOLOGICAL AND FUNCTIONAL CHARACTERIZATION

Memòria presentada per la graduada en Bioquímica

VERÒNICA CASADÓ ANGUERA

per optar al grau de Doctor per la Universitat de Barcelona

Aquesta Tesi s'ha adscrit al Departament de Bioquímica i Biomedicina Molecular de la
Universitat de Barcelona, dins el programa de doctorat de Biomedicina.

El treball experimental i la redacció de la present memòria han estat realitzats per Verònica
Casadó Anguera sota la direcció del Dr. Enric Isidre Canela i del Dr. Antoni Cortés

Dr. Enric I. Canela Campos

Dr. Antoni Cortés Tejedor

Verònica Casadó Anguera

Barcelona, Abril 2018

INDEX

LIST OF ABBREVIATIONS	i
I. INTRODUCTION	1
1. G PROTEIN COUPLED RECEPTORS	1
1.1. STRUCTURE	1
1.2. CLASSIFICATION	2
1.3. SIGNALING PATHWAYS	3
1.4. INTERACTING PROTEINS	5
1.4.1. <i>G proteins</i>	5
1.4.2. β -arrestin	8
1.4.3. Cytoskeletal-anchoring polypeptides	10
1.4.4. Adenosine deaminase	10
1.4.5. Oligomerization with other receptors	10
2. GPCR OLIGOMERIZATION	11
2.1. TYPES OF GPCR OLIGOMERIZATION	12
2.1.1. Heteromerization	12
2.1.2. Homodimerization	13
2.1.3. Higher order oligomerization	13
2.2. GPCR LIGANDS	14
2.2.1. Orthosteric	14
2.2.2. Allosteric	15
2.2.3. Bitopic	17
2.3.4. Photoswitchable	18
2.3.5. Multivalent	19
2.3.6. Heteromer-selective	19
2.3.7. Bivalent	20
2.4. METHODS TO STUDY GPCR OLIGOMERIZATION	21
2.4.1. Early and classical methods	21
2.4.2. Biophysical methods	22
2.4.3. Immunochemical methods	27
2.4.4. Physiological methods	28
2.4.5. X-ray crystallography of GPCRs	28
2.4.6. Computational methods	29
2.4.7. Ligand binding in oligomeric receptors	30

2.4.8. Signaling fingerprint	31
3. ANALYZING RADIOLIGAND BINDING DATA: MONOMERIC vs DIMERIC MODELS	32
4. CATECHOLAMINES	37
4.1. STRUCTURE, BIOSYNTHESIS AND RELEASE	37
4.2. DOPAMINE SYSTEM	39
4.2.1. Dopamine system in the brain	39
4.2.2. Structure of dopamine receptors	40
4.2.3. Dopamine receptor expression in the brain	43
4.2.4. Neuronal functions of dopamine receptors	46
4.3. NOREPINEPHRINE SYSTEM.....	50
4.3.1. Adrenergic system in the brain	50
4.3.2. Structure of adrenergic receptors	51
4.3.3. Adrenergic receptor expression in the brain	53
4.3.4. Neuronal functions of adrenergic receptors	55
5. ADENOSINE SYSTEM.....	58
5.1. Adenosine system in the brain.....	59
5.2. Structure of adenosine receptors	60
5.3. Adenosine receptor expression in the brain.....	62
5.4. Neuronal functions of adenosine receptors	63
5.4.1 Caffeine interactions with adenosine receptors.....	64
6. CATECHOLAMINE AND ADENOSINE SYSTEM INTERACTIONS.....	66
6.1 Dopamine and adenosine system interaction	66
6.1.1 Direct and indirect pathway.....	66
6.1.2. Adenosine-dopamine receptor heteromers: control of motor function	67
6.1.3 Dopamine-adenosine system in Parkinson's disease	68
6.2. Dopamine and adrenaline system interaction	69
6.2.1. Catecholamine systems and ADHD.....	70
II. AIM AND OBJECTIVES.....	75
III. RESULTS.....	79
Chapter 1. Reinterpreting anomalous competitive binding experiments assuming radioligand-competitor allosteric interactions within G protein-coupled receptor homodimers	79
Chapter 2.1. Allosteric interactions between agonists and antagonists within the adenosine A2A receptor-dopamine D2 receptor heterotetramer	105

Chapter 2.2. Evidence for the heterotetrameric structure of the adenosine A2A-dopamine D2 receptor complex.....	119
Chapter 2.3. Functional pre-coupled complexes of receptor heteromers and adenylyl cyclase	127
Chapter 3. Design of a true bivalent ligand with picomolar binding affinity for a G protein-coupled receptor homodimer	155
Chapter 4. α_{2A} - and α_{2C} -Adrenoceptors as Targets for Dopamine and Dopamine Receptor Ligands	211
Chapter 5. Revisiting the functional role of dopamine D4 receptor gene polymorphisms: Heteromerization-dependent gain of function of the D4.7 receptor variant	231
Chapter 6. Functional differences between dopamine D4.4 and D4.7 receptor variants within the dopamine D4-adrenergic α_{2A} receptor heteromer in the brain	247
IV. GENERAL DISCUSSION	283
V. CONCLUSIONS	297
VI. BIBLIOGRAPHY	305
VII. ANNEXES	365

LIST OF ABBREVIATIONS

5-HT: 5-hydroxytryptamine or serotonin

α_1 R: α_1 -adrenoceptor

α_2 R: α_2 -adrenoceptor

β R: beta-adrenoceptor

AC: adenylyl cyclase

ADA: adenosine deaminase

ADHD: attention-deficit hyperactivity disorder

ADR: adrenergic receptor

AR: adenosine receptor subtypes: A_1 (**A₁R**), A_{2A} (**A_{2A}R**), A_{2B} (**A_{2B}R**), A_3 (**A₃R**)

BiFC: bimolecular fluorescence complementation

BiLC: bimolecular luminescence complementation

BRET: bioluminescent resonance energy transfer

cAMP: cyclic adenosine monophosphate

CNS: central nervous system

CODA-RET: complemented donor-acceptor resonance energy transfer

Co-IP: co-immunoprecipitation

DA: dopamine

DAG: diacyl glycerol

DR: dopamine receptor subtypes: D_1 (**D₁R**), D_2 (**D₂R**), D_3 (**D₃R**), D_4 (**D₄R**), D_5 (**D₅R**)

E: epinephrine

ECL: extracellular loop

ERK: extracellular signal-regulated kinase

FRAP: fluorescence recovery after photobleaching

FRET: fluorescent resonance energy transfer

GABA: gamma-aminobutyric acid

GDP: guanosine diphosphate

GFP: green fluorescent protein

GIRK: G protein-coupled inwardly-rectifying potassium channels

GP: globus pallidus, external (**GPe**) and internal (**GPI**)

GPCR: G protein-coupled receptor

GRK: G protein-coupled receptor kinase

GTP: guanosine triphosphate

HEK: human embryonic kidney

ICL: intracellular loop
IP3: inositol triphosphate
LC: locus coeruleus
MAO: monoamine oxidase enzyme
MAPK: mitogen-activated protein kinase
MSN: medium spiny neuron
NAC: nucleus accumbens
NAM: negative allosteric modulator
NE: norepinephrine
PAM: positive allosteric modulator
PCL: photochromic ligand
PD: Parkinson's disease
PFC: prefrontal cortex
PI3K: phosphatidylinositol 3-kinase
PKA and PKC: protein kinase A and C
PLA: proximity ligation assay
PLC: phospholipase C
PNMT: phenylethanolamine N-methyl transferase
RGS: regulators of G protein signaling
RLS: restless leg syndrome
RLuc: Renilla luciferase
SN: substantia nigra, pars compacta (**SNc**) and pars reticulata (**SNr**)
SRET: sequential resonance energy transfer
STN: subthalamic nucleus
SUD: substance use disorders
TAT: HIV transactivator of transcription
TM and 7TM: transmembrane and seven transmembrane domain
TR: tandem repeats
TR-FRET: time-resolved FRET
VMAT: vesicular monoamine transporter
VNTR: variable number of tandem repeats
VTA: ventral tegmental area
YFP: yellow fluorescent protein

I- INTRODUCTION

I. INTRODUCTION

1. G PROTEIN COUPLED RECEPTORS

G protein-coupled receptors (GPCRs), also known as seven transmembrane domain (7TM) receptors, comprise the largest superfamily of plasma membrane proteins in the body. In the human genome, more than 2% of the genome codes for more than 1000 GPCRs (Jacoby et al., 2006; Kochman, 2014) being 90% of them expressed in the central nervous system (CNS) (Vassilatis et al., 2003).

GPCRs have an enormous biomedical importance because they are involved in 80% or more of the signal transduction processes that occur across cell membranes. For this reason, they are a main focus of research efforts in academia, government and pharma to develop new therapeutic drugs. Nowadays, it is estimated that about 700 approved drugs target GPCRs, implying that approximately 35% of approved drugs target GPCRs (Sriram and Insel, 2018). In addition, to date, over 600 inactivating and almost 100 activating mutations in GPCR have been identified responsible for more than 30 different human diseases (Schöneberg et al., 2004).

This superfamily of receptors exerts their effects primarily through their association with heterotrimeric G- proteins in response to a wide range of extracellular ligands, including single photons, neurotransmitters, hormones and peptides (Wells, 2014).

Agonist binding to a GPCR and the subsequent G protein activation is rapidly followed by several coordinated events common to most GPCRs. These include recruitment of GPCR kinases (GRKs), which phosphorylate the receptor at multiple intracellular residues, followed by the recruitment of β -arrestins, which trigger receptor endocytosis. However, in addition to canonical G protein-mediated signaling, GPCRs can also bind to other cytosolic adaptors, including β -arrestins, which elicit G-protein independent signaling through activation of mitogen-activated-protein kinase (MAPK) and Akt. Most known endogenous and synthetic ligands can signal through both signaling mechanisms. However, there are some examples of biased ligands that preferentially signal through β -arrestins over G-proteins or vice versa. This mechanism can be due a ligand-dependent phosphorylation pattern that make the receptor more suitable for signaling through β -arrestins or the differential ligand-induced conformational change of the receptor that make it more specific for certain G proteins.

GPCRs represent a potentially fruitful area for further study in order to find more druggable GPCRs and drugs to target them. Moreover, efforts to design new types of GPCR-targeted drugs with signaling bias (via G proteins or β -arrestins), allosteric modulators, new types of therapeutic agents (antibodies/nanobodies, aptamers, anti-sense oligonucleotides, and gene therapies), or ligands delivered in novel ways, makes us to predict that GPCRs will continue to play a prominent role as therapeutic targets (Sriram and Insel, 2018).

1.1. STRUCTURE

The hydrophobic 7TMs of the GPCRs define their common structural feature. The α -helices have approximately 25 to 35 residues of length and are connected by intra- and extracellular loops (ICL and ECL). Helices are placed in a lipidic environment, while loop regions are surrounded by an aqueous medium (Martinelli and Ortore, 2013). Another common feature are the two cysteine residues which are conserved in most GPCRs, one is in the ECL1 and another one in the ECL2, which form a disulfide bond that is supposed to have an important role in the packaging

and stabilization of a restricted number of conformations of the 7TMs (see Fig. 1) (Probst et al., 1992; Baldwin, 1994).

All GPCRs have also in common the existence of an amino-terminal extracellular domain for stimulus recognition, and a carboxyl-terminal intracellular domain for signal propagation to transducers such as G proteins (Schmitz et al., 2014). Over the past decade, more than 130 structures of 24 different class A GPCRs and 5 GPCRs from other classes have been determined in complex with ligands of diverse pharmacology, peptides, antibodies and G proteins (Venkatakrisnan et al., 2013; Cohen et al., 2014; Shonberg et al., 2015; Zhang et al., 2015).

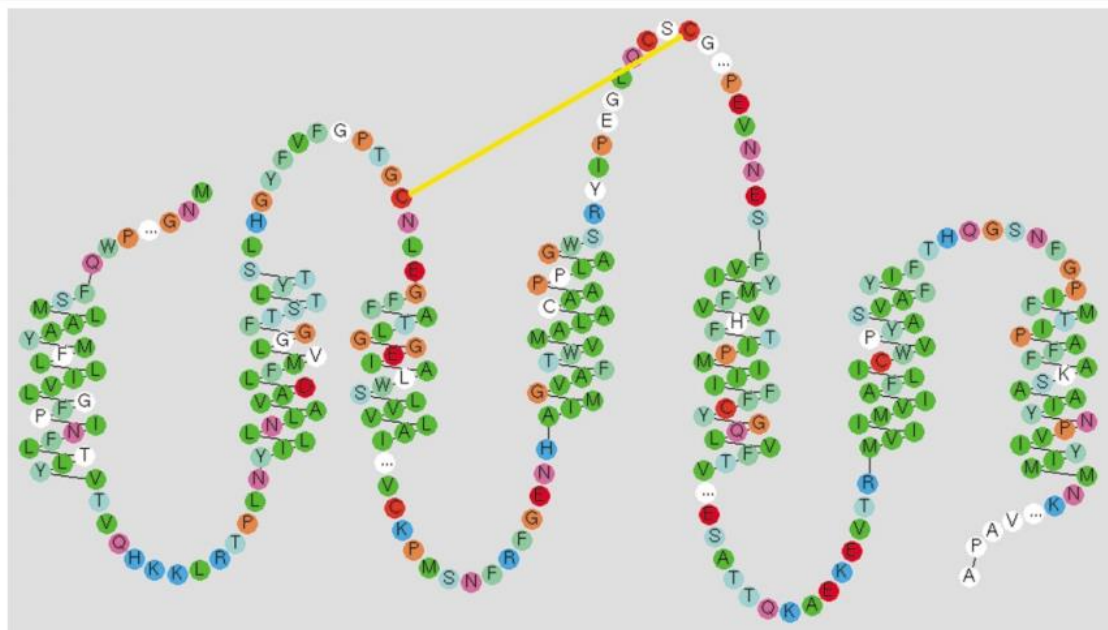


Figure 1. Snake-like diagram of the human Rhodopsin receptor. This plot was generated with the RbDe software. Extracted from Horn et al. (2003).

The correct integration and orientation of the protein occurs in the endoplasmic reticulum and the α -helices are stabilized inside the phospholipid bilayer due to the GPCR hydrophobicity, facing the polar amino acids to the center of the α -helices, minimizing the contact with the hydrophobic bilayer. Finally, the functional tertiary structure is formed by the specific interactions between α -helices generating the ring-shape compact structure of the GPCRs (Bulenger et al., 2005).

1.2. CLASSIFICATION

Horn et al. (2003) developed a system for classifying GPCR for the GPCRDB database, which is currently the only regularly updated GPCR information system available on the World Wide Web. This system divides GPCRs into six classes: three major and three minor families. The three major families are family A, that include those related to the rhodopsin and the β 2-adrenergic receptor, family B, composed of those associated with the glucagon receptor, and family C, that comprise those related to the metabotropic neurotransmitter receptors. The three minor families include class D (pheromone receptors), class E (cAMP receptors) and class F (Frizzled/smoothened family).

- *Family A* comprises the largest and most studied class of GPCRs. The also called rhodopsin-like receptor family, binds a variety of ligands, including biogenic amines (catecholamines, histamine

and serotonin), adenosine, cannabinoids and peptides. The only residue that is conserved among all family A members is the Arg in the Asp-Arg-Tyr motif in the cytosolic site of the third transmembrane domain, important for G-protein activation. Despite that the overall homology among type A receptors is low, they exhibit identical structural organization (Probst et al., 1992). The N-terminal domain is involved in ligand binding and possibly receptor activation; the extracellular loops are important elements for peptide binding and have a key role in receptor selectivity towards ligands, and the transmembrane core is formed by seven alpha-helices that provide a hydrophobic environment for nonpeptide and small-peptide ligand binding. The intracellular site has the elements responsible to the direct or indirect interaction with intracellular effectors such as G proteins. Moreover, the C-terminal can have posttranslational modifications, important for the modulation of receptor activation state, G protein coupling, internalization and desensitization. Furthermore, many of family A receptors, have a palmitoylated cysteine on the C-terminal that anchors the receptor to the plasma membrane (Papac et al., 1992; Kennedy and Limbird, 1993).

There are about 60 “orphan” GPCRs that have in common the sequence pattern with family A but that does not have defined ligands or functions (Gloriam et al., 2005).

- *Family B receptors*, also known as the secretin-like receptor family, are regulated by several hormones and neuropeptides and comprise about 15 different receptors. They have in common with the family A receptors the disulfide bridge between ECL1 and ECL2 but do not have the Asp-Arg-Tyr motif. They have an extracellular N-terminal domain with conserved cysteine residues and disulfide bridges (Ulrich et al., 1998) important for the ligand recognition (Jacoby et al., 2006).

- *Family C receptors* have also the conserved cysteines forming the disulfide bridge between ECL1 and ECL2 but, in contrast, have a large N-terminal extracellular domain that contains the ligand binding site (Conn and Pinn, 1997). They also have a short ICL3 domain highly conserved. This family, among others, includes the metabotropic glutamate, the calcium receptors and the gamma-aminobutyric acid (GABA) receptors.

1.3. SIGNALING PATHWAYS

GPCRs owe their name to their ability to interact with heterotrimeric G-proteins ($G_{\alpha\beta\gamma}$), from which most of the receptor signaling is directed. The heterotrimeric G-proteins, that have a crucial role in defining the specificity and temporal characteristics of the cellular response, are constituted of α (39-46 kDa), β (37 kDa) and γ (8 kDa) subunits. Upon ligand activation, there is a conformational change that is transmitted to the G-protein α -subunit (G_{α}), which exchanges guanosine diphosphate (GDP) nucleotide (inactive conformation) for guanosine triphosphate (GTP) (active conformation). This provokes that the G_{α} subunit bound to GTP dissociates from the receptor and from the $\beta\gamma$ dimer ($G_{\beta\gamma}$) (Marinissen and Gutkind, 2001). The two resulting subunits, G_{α} bound to GTP and $G_{\beta\gamma}$ are capable of interact and modulate the activity downstream cellular signaling pathways such as adenylyl cyclase (AC) activation or inhibition, phospholipases activation or potassium and calcium ion channel activity regulation (Hamm, 1998). Apart from these typical second-messenger pathways, $G_{\beta\gamma}$ subunits can control the activity of intracellular signal-transducing molecules, including small GTP-binding proteins of the Ras and Rho family members of the mitogen-activated protein kinase (MAPK) family of serine-threonine kinases.

These include extracellular signal-regulated kinase (ERK), p38, ERK5 and c-jun N-terminal kinase (JNK) through a complex network of signaling procedures.

The signal terminates when the GTP is hydrolyzed by the GTPase activity of the G_{α} subunit, to GDP and phosphate and the $G_{\beta\gamma}$ complex binds to the G_{α} forming the inactive G-protein (Hamm, 1998).

The agonist binding to GPCRs often results in a rapid attenuation of receptor responsiveness. This receptor desensitization process is the consequence of a combination of different mechanisms that include the receptor uncoupling from the heterotrimeric G-protein complex in response to receptor phosphorylation (Hausdorff et al., 1989; Lohse et al., 1990; Ferguson, 2001), the internalization of cell surface receptors to various intracellular compartments (Hermans et al., 1997; Trejo et al., 1998), and the down-regulation of the total number of receptors in the cell. This down-regulation is achieved through mechanisms to reduce receptor mRNA and protein synthesis and through lysosomal degradation of pre-existing receptors (Jockers et al., 1999; Pak et al., 1999). These processes can occur within seconds (phosphorylation), minutes (endocytosis) or hours (down-regulation of surface receptors) and the amount of receptor desensitization varies from the complete termination of receptor signaling to the attenuation of agonist potency and maximal responsiveness (Sakmar, 1998).

Some years ago was proved that GPCR can produce signals independently of G-protein (Daaka et al., 1998; Lefkowitz, 1998). It was suggested that agonist-induced receptor phosphorylation through GRK and the subsequent arrestin and surface receptor recruiting are not only important mechanisms for decreasing the signaling capacity of the receptor but also play a key role in switching the receptor from G-protein-coupled-dependent signaling pathways to G-protein-independent signaling cascades (see Fig. 2) (Ferguson, 2001; Krupnick and Benovic, 1998; Luttrell and Lefkowitz, 2002; Woehler and Ponimaskin, 2009).

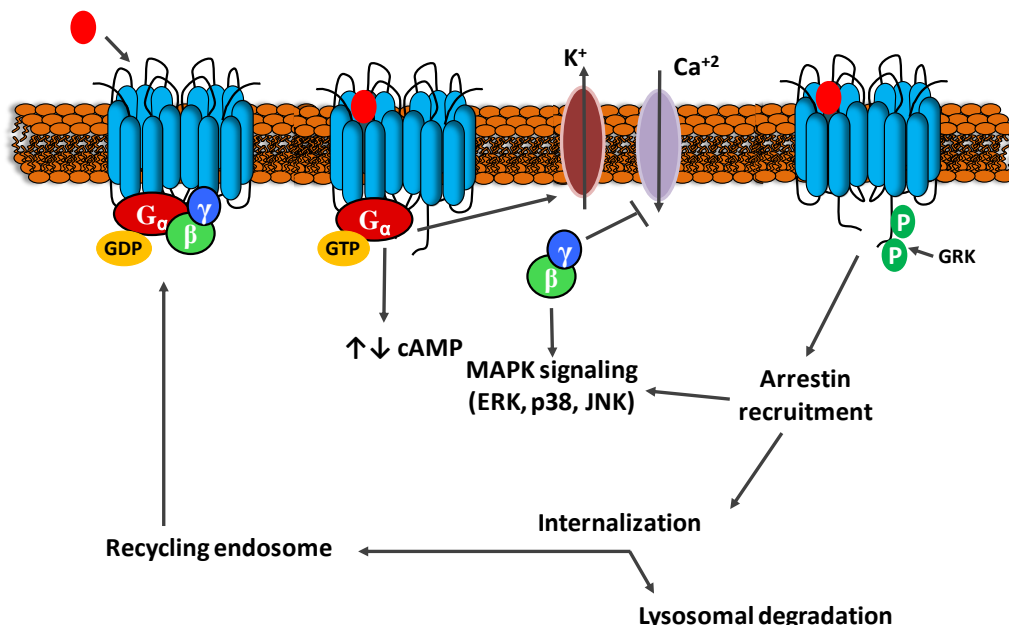


Figure 2. Signaling of GPCRs

There are some studies with rhodopsin receptor, M3-muscarinic receptor, thyrotropin-releasing hormone receptor and β_2 adrenergic receptor that seems to indicate that, at least for the rhodopsin family, there is a common activation-dependent reorientation of the cytoplasmic end

of helix VI. Additional work is required to extend these observations to the other families of GPCRs (Farrens et al., 1996; Sheikh et al., 1996; Jensen et al., 2001; Huang et al., 2005; Ward et al., 2006).

1.4. INTERACTING PROTEINS

Many GPCRs contain sequence motifs that are known to direct protein-protein interactions and, therefore, have the theoretical capacity to interact with a wide range of other proteins. Such interactions might determine receptor properties, like cellular compartmentalization or signaling, and can promote complexes that integrate their functions through protein scaffolding (Milligan and White, 2001).

On the intracellular site of GPCR, both the C-terminus tail and the third intracellular loop can be of a considerable size. Thus, these regions are more likely to interact with signaling and other intracellular proteins like cytoskeletal proteins or trafficking-related proteins. The length of these interactions varies from transitory such as signaling purposes to more stable interactions. Either way, these complexes are considered dynamic (Canals et al., 2003). In contrast, GPCR extracellular loops are relatively short causing extracellular interactions to take place in the N-terminus tail. However, some extracellular proteins can also interact with extracellular loops, such as the enzyme adenosine deaminase in the case of adenosine receptors (ARs). A third group of interactions are extended along GPCR 7TM with other GPCRs or with other membrane receptors.

1.4.1. G proteins

In contrast with the number and diversity of the GPCR superfamily, there are a relatively small number of different G-proteins to initiate the intracellular signaling cascades. In humans, there are 21 G_{α} subunits encoded by 16 genes, 6 G_{β} subunits (5 plus a splice variant) encoded by 5 genes, and 12 G_{γ} subunits (Downes and Gautam, 1999). G proteins have a crucial role in defining the specificity and temporal characteristics of the cellular response and their switching function depends on the ability of the G_{α} to cycle between an inactive GDP-bound conformation that is primed for interaction with an activated receptor, and an active GTP-bound conformation that can modulate the activity of downstream effector proteins (Fig. 3) (Oldham and Hamm 2008).

G protein heterotrimers are typically divided into four main classes based on the primary sequence similarity of the G_{α} subunit: $G_{\alpha s}$, $G_{\alpha i/o}$, $G_{\alpha q/11}$ and $G_{\alpha 12/13}$ (Simon et al., 1991). $G_{\alpha s}$ family stimulates AC and has two members: $G_{\alpha s}$ which is expressed in most cell types and $G_{\alpha olf}$ which is mainly expressed in the olfactory sensory neurons.

$G_{\alpha i/o}$ family inhibits AC and is the biggest and most varied family, including $G_{\alpha i1}$, $G_{\alpha i2}$, $G_{\alpha i3}$, $G_{\alpha o}$, $G_{\alpha t}$, $G_{\alpha g}$ and $G_{\alpha z}$. While $G_{\alpha i}$ subunits have been found in most cell types, $G_{\alpha o}$ is highly expressed in neurons and has two splice variants: $G_{\alpha o1}$ and $G_{\alpha o2}$ (or $G_{\alpha oA}$ and $G_{\alpha oB}$). $G_{\alpha t}$ has also two isoforms: $G_{\alpha t1}$ is expressed in the rod cells in the eye and $G_{\alpha t2}$ in the cone cells of the eye. In addition, $G_{\alpha g}$ is found in taste receptor cells and $G_{\alpha z}$ in neuronal tissues and in platelets.

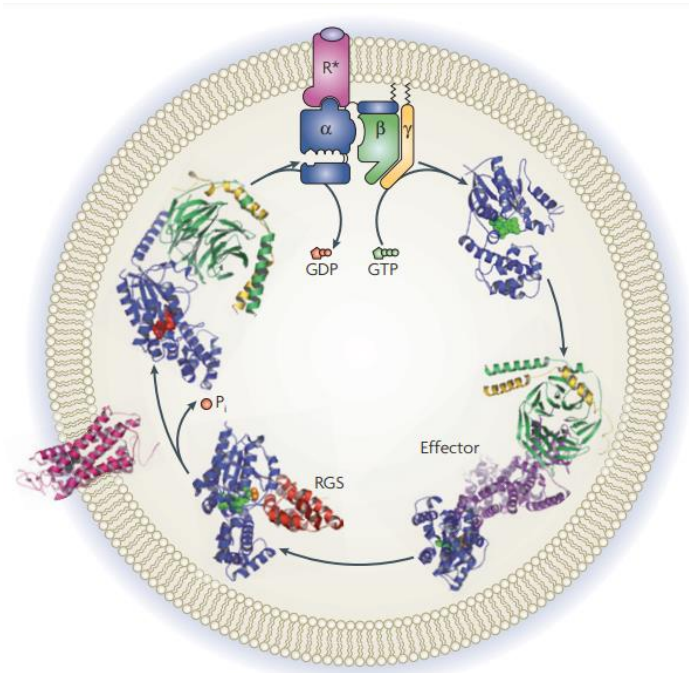


Figure 3. The G protein cycle. In the resting state, G proteins are heterotrimers of GDP-bound α - (blue), β - (green) and γ - (yellow) subunits. On binding of an extracellular stimulus (light purple), receptors (pink) undergo a conformational change that permits G protein binding and catalyses GDP release from G_{α} . Once GDP is released, a stable, high-affinity complex is formed between the activated receptor (R^*) and G protein. Binding of GTP (green) to G_{α} destabilizes this complex, allowing both subunits, G_{α} and $G_{\beta\gamma}$, to interact with downstream effector proteins (purple). The signal is terminated on hydrolysis of GTP to GDP by G_{α} , which may be catalysed by regulator of G protein signalling proteins (dark red). Extracted from Oldham and Hamm 2008

In humans, $G_{\alpha q}$ activates phospholipase $C\beta$ (PLC β) and promotes cleavage of phosphatidylinositol biphosphate into inositol triphosphate (IP3) and diacyl glycerol (DAG). IP3 mobilizes calcium of endoplasmatic reticulum via IP3 receptors (calcium channel) while DAG can activate protein kinase C (PKC). $G_{\alpha q}$ family consists of $G_{\alpha q}$, $G_{\alpha 11}$, $G_{\alpha 14}$ and $G_{\alpha 15/16}$. $G_{\alpha q}$ and $G_{\alpha 11}$ are expressed ubiquitously; in contrast, $G_{\alpha 14}$ and $G_{\alpha 15/16}$ have a more restricted expression.

The $G_{\alpha 12}$ family regulates Rho proteins and has two subfamilies: $G_{\alpha 12}$ and $G_{\alpha 13}$ which are expressed in most types of cells.

$G_{\beta 1}$, $G_{\beta 2}$, $G_{\beta 3}$ and $G_{\beta 4}$ share 80-90% of similarities, while $G_{\beta 5}$ is more dissimilar, only shares 50% of the sequence with the other G_{β} subunits. $G_{\beta 5}$ is mostly found in the brain but, in contrast, the other G_{β} subunits are widely distributed. G_{γ} subunits are more diverse and share sequence similarities ranging from 20 to 80% (Syrovatkina et al., 2016).

At the brain level, especially $G_{\alpha o}$ but also $G_{\alpha i1}$, $G_{\alpha i2}$ and $G_{\alpha i3}$ are expressed. $G_{\alpha s}$ and $G_{\alpha q}$ are also widely expressed. Concerning the $G_{\alpha s}$ family, there are evidences for a different distribution of $G_{\alpha olf}$ and $G_{\alpha s}$ mRNAs in rat forebrain. $G_{\alpha olf}$ mRNA is highly expressed in striatal areas, including caudate putamen, nucleus accumbens, and olfactory tubercle. These areas show almost no expression of $G_{\alpha s}$, except for some sparse neurons. On the contrary, $G_{\alpha s}$ mRNA is highly expressed in many brain areas including all cortical areas, septum, most of the hypothalamic and thalamic nuclei, hippocampus, and amygdala, in which $G_{\alpha olf}$ mRNA expression is very low. In few brain regions, substantial expression of both $G_{\alpha olf}$ and $G_{\alpha s}$ mRNAs is observed: piriform cortex, medial habenula, and dentate gyrus (Hervé, 2011). However, to our knowledge, no clear region-specific pattern of mRNA expression for $G_{\alpha i/o}$ protein subtypes has been reported.

Many crystal structures of these proteins have been resolved in various conformations, and provide the framework for understanding the biomechanics of G protein signaling (Oldham et al., 2006). Concretely, the structures of the G_{α} subunit reveal a conserved protein fold that is composed of a GTPase domain and a helical domain. The GTPase domain is conserved in all members of the G protein superfamily and its function is to hydrolyze GTP and provide the binding surfaces for the $G_{\beta\gamma}$ dimer, GPCRs and effector proteins. The helical domain is unique to G_{α} proteins and is composed of a six α -helix bundle that forms a lid over the nucleotide-binding pocket, burying bound nucleotides in the core of the protein. All G_{α} subunits, except $G_{\alpha t}$, are post-translationally modified with the fatty acid palmitate at the N terminus. Members of the $G_{\alpha i}$ family are also myristoylated at the N terminus. These modifications regulate membrane localization and protein-protein interactions (Chen and Manning, 2001; Smotryś and Linder, 2004).

The G_{β} subunit has a seven-bladed β -propeller structure that is composed of seven WD40 sequence repeats. The N terminus of G_{β} adopts an α -helical conformation that forms a coiled-coil with the N terminus of G_{γ} , and the C terminus of G_{γ} binds to blades five and six (Wall et al., 1995; Sondek et al., 1996). The G protein β - and γ -subunits form a functional unit that can only be dissociated under denaturing conditions (Schmidt et al., 1992). Although most G_{β} subunits can interact with most G_{γ} subunits, not all of the 60 possible dimer combinations occur (Clapham and Neer, 1997). Additionally, several $G_{\beta\gamma}$ dimers can interact with the same G_{α} isoform (Milligan and Kostenis, 2006), which suggests that differential expression or subcellular localization are determinant in the regulation of downstream signaling (Graf et al., 1992).

Due to the fact that relatively few types of G proteins are able to transduce signals from a large number of GPCRs, so each member of the G protein family is able to interact with many different receptors. Moreover, each receptor can activate multiple G proteins, generating different signaling cascades, some of which with opposite effects. Thus, the receptor–G-protein interface must encode vital information that determines which G proteins can interact with a specific receptor. However, despite identifying many of the contact sites that contain this interface, the patterns that define the coupling between the receptor and the specific G protein are still unclear. This is because the poor sequence homology of the intracellular loops that comprise the G protein binding site. Moreover, it has also been seen that the global conformation of the receptor or changes in its dynamics may be just as important as specific side-chain interactions in determining receptor–G-protein selectivity (Gilchrist et al., 1996; Pérez et al., 1996), so different agonists can imprint on the receptor a particular but subtle conformation that affect that G protein is activated (Kenakin, 2003; Perez and Karnik, 2005).

Preassembled receptor–G protein complexes

The generally accepted model, deduced largely from *in vitro* studies, proposes that receptor-mediated G protein activation involves an initial recruitment of $G_{\alpha\beta\gamma}$ to the activated receptor followed by a rapid dissociation of G_{α} and $G_{\beta\gamma}$ into free active subunits (Gilman, 1987; Bourne, 1997; Cabrera-Vera et al., 2003). However, this classical collision-based model has been challenged by several studies (Rebois et al., 1997; Klein et al., 2000; Bunemann et al., 2003; Frank et al., 2005; Galés et al., 2005) suggesting that stable receptor–G protein complexes, heterotrimeric G protein complexes or both may persist during the activation process.

Galés et al. (2005) found several consistent evidences that indicate that there is a preassembled complex between the receptor and the G protein before activation. First, they observed a basal BRET signal between several receptors and either $G_{\alpha 1}$, $G_{\beta 1}$ or $G_{\gamma 2}$ in the absence of agonist stimulation. Second, BRET₅₀ values did not reveal any change in the apparent affinity of receptors for G protein subunits after agonist stimulation. Moreover, both increases and decreases in BRET signals between receptor and $G_{\alpha 1}$ were observed after agonist stimulation, depending on the positions of the probes at $G_{\alpha 1}$ subunit, indicating that the change in BRET reflected not $G_{\alpha 1}$ recruitment but rather a structural change in a preformed complex. They also found that preassembly did not result from altered stoichiometry between heterologously expressed partners, as specific BRET signals were observed for all expression ratios.

Despite there is some controversy (Bondar and Lazar, 2006), these results are according to a large body of evidence indicating that receptor-promoted activation of G proteins does not result only from random collision but involves organized modules that include precoupled receptor–G protein complexes (Neubig, 1994; Rebois and Hebert, 2003; Ferré, 2015). Moreover, their work also suggest that $G_{\beta\gamma}$ do not fully dissociate from G_{α} upon activation and it is still compatible with the existence of overlapping binding sites of G_{α} for AC and $G_{\beta\gamma}$ that suggested that $G_{\beta\gamma}$ must leave G. It is possible because $G_{\beta\gamma}$ is displaced away from its original site of association with G_{α} , but it is not dissociated from the protein complex.

1.4.2. β -arrestin

After ligand binding and G protein activation, GPCRs are desensitized to attenuate continued signaling. First, GRKs family members selectively phosphorylate agonist-activated receptors in their cytoplasmic loops and C-terminus, thereby promoting the binding of cytosolic cofactor proteins called β -arrestins, which uncouple the receptor from heterotrimeric G-proteins (Lohse et al., 1990; Kendall and Luttrell, 2009; Luttrell and Gesty-Palmer, 2010; Kang et al., 2013). β -arrestins were first discovered for their role in mediating receptor desensitization (Lohse et al., 1990), a process by which repeated stimulation decreases the signalling response over seconds to minutes, through steric hindrance of GPCR interaction with G proteins. In addition, β -arrestins scaffold second messenger degrading enzymes that degrade cyclic adenosine monophosphate (cAMP) and DAG.

β -Arrestins also mediate receptor internalization with components of the clathrin-coated vesicle pathway (Goodman et al., 1996; Oakley et al., 1999; Laporte et al., 2000). β -arrestins have specific binding domains for clathrin, AP2 and other endocytic proteins required for efficient receptor internalization. Furthermore, the interaction between β -arrestins and E3 ubiquitin ligase Mdm2 promotes ubiquitination of β -arrestins, facilitating the robust binding of β -arrestins with both the GPCR and the endocytic machinery (clathrin and AP2). Following the internalization, receptors can be recycled or lysosomal degraded. Internalized receptors that are not degraded can also be dephosphorylated in endosomes and recycled to the plasma membrane (Fig. 4) (Hanyaloglu and Zastrow, 2008).

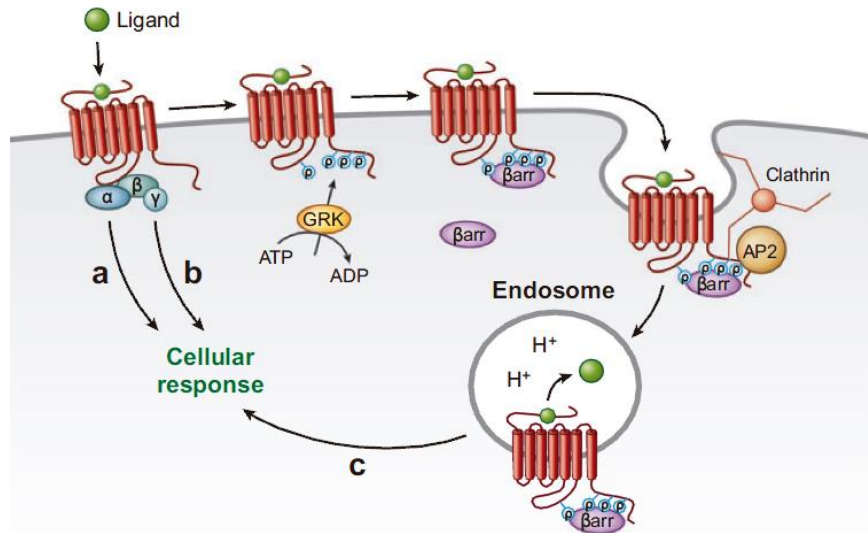


Figure 4. Rapid desensitization and endocytosis of GPCRs mediated by GRKs, arrestins, and clathrin-coated pits.

Ligand-activated receptors activate heterotrimeric G proteins, which signal to downstream effects via α and/or $\beta\gamma$ subcomplexes (arrows a and b). Receptor phosphorylation promotes recruitment of arrestins from the cytoplasm, preventing subsequent activation of G proteins by receptors and promoting receptor endocytosis via clathrin-coated pits. There is emerging evidence that some GPCR-mediated- signaling events may occur from the endosome membrane (arrow c). Extracted from Hanyaloglu and Zastrow (2008).

It is now established that, surprisingly, in addition to acting as negative regulators of G protein signaling, β -arrestins also couple to numerous signaling mediators (Smith et al., 2018). In fact, β -arrestins have the ability to interact with MAPKs (which control many cellular functions including cell cycle, regulation of transcription and apoptosis) the serine/threonine kinase AKT, the tyrosine kinase SRC, nuclear factor- κ B (NF- κ B) and phosphatidylinositol 3-kinase (PI3K), by acting as adaptors and scaffolds. These pathways are separated from classical G protein signaling but can involve similar signaling cascades that are often temporally distinct. More recently, it has also been appreciated that some receptors that tightly interact with β -arrestins maintain catalytic GEF activity on endosomes, continuing to promote G protein signaling after internalization (Ferrandon et al., 2009; Calebiro et al., 2009; Irannejad et al., 2013). Thus, β -arrestins regulate nearly all aspects of receptor activity, including desensitization, downregulation, trafficking and signaling (Fig. 5) (Shenoy and Lefkowitz, 2011; Smith et al., 2018).

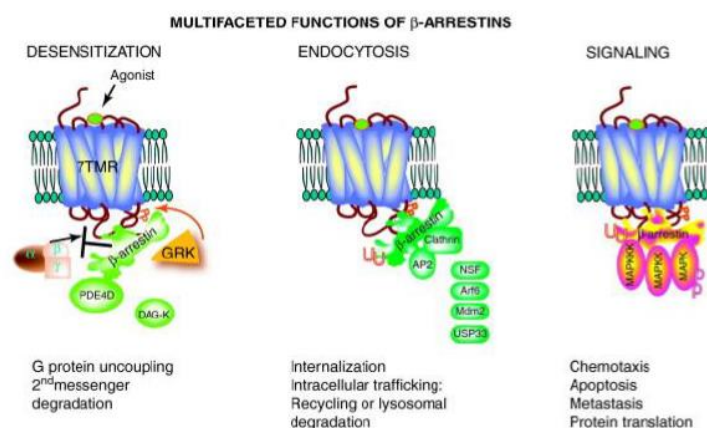


Figure 5. Multifaceted functions of β -arrestins. Extracted from Shenoy and Lefkowitz, 2011.

Other internalization processes

Not all GPCRs necessarily internalize in a β -arrestin-/clathrin-dependent manner but may also be internalized through alternative endocytic pathways. Some GPCRs have been found in cholesterol rich plasma membrane structures termed caveolae (Chun et al., 1994; Huang et al., 1997; Burgueño et al., 2003; Parton and Simons, 2007). These domains are also known as signaling domains, but appear to contain proteins involved in the formation of vesicles such as dynamin (Cho et al., 2006). Finally, some receptors seem to use a third alternative endocytic pathway. No coat or adaptor proteins have been identified for the generation of these vesicles (Claing et al., 2000).

1.4.3. Cytoskeletal-anchoring polypeptides

One classical example of GPCR interacting proteins is cytoskeletal-anchoring polypeptides. This is the case of α -actinin and adenosine A_{2A} receptors ($A_{2A}R$) (Fig. 6) (Burgueño et al., 2003), α -filamin and dopamine D_2 receptors (D_2R) (Lin et al., 2001) or the Shank family of proteins and several other GPCR including type I metabotropic glutamate receptor (mGluR1) (Sheng and Kim, 2000).

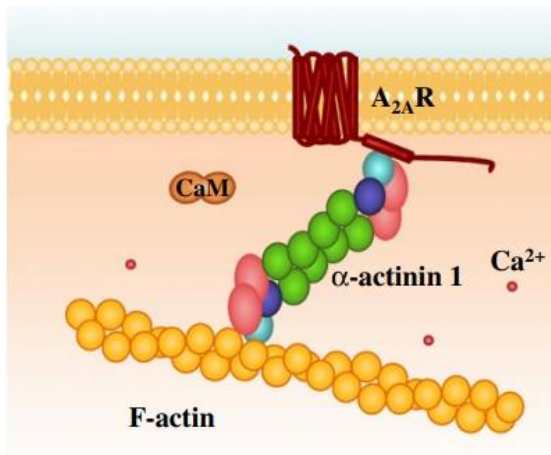


Figure 6. Schematic illustration of α -actinin1- $A_{2A}R$ interaction that anchors the receptor to the actin cytoskeleton. Extracted from Piirainen et al. (2017).

1.4.4. Adenosine deaminase

Adenosine deaminase (ADA) plays a central role in purine catabolism (Camici et al., 2010; Grunebaum et al., 2013) and catalyzes the deamination of both adenosine and 2'-deoxyadenosine by converting them to inosine and 2'-deoxyinosine, and ammonia (Conway and Cooke, 1939; Brady, 1942). ADA can be present intracellularly in all cells, but also on the cell surface of neurons (Ruiz et al., 2000; Hawryluk et al., 2012) working as an ecto-enzyme. Cell surface ADA can form heteromeric complexes with adenosine A_1 (A_1R), $A_{2A}R$ and A_{2B} (A_{2BR}) receptors through their extracellular loops which are relatively short. Several ADA amino acids have been identified as crucial for its interaction with ARs (Gracia et al., 2013a). In this scenario, ADA acts as an allosteric regulator, enhancing agonist and antagonist binding and increasing receptor signaling (Ciruela et al., 1996; Saura et al., 1996, 1998; Sarrió et al., 2000; Herrera et al., 2001; Sun et al., 2005; Gracia et al., 2008, 2011, 2013b; Cortés et al., 2015).

1.4.5. Oligomerization with other receptors

Protein-protein interactions can also take place at the plasma membrane level. Since the nineties, a great number of studies have shown GPCR oligomerization that is further detailed along the next chapter.

2. GPCR OLIGOMERIZATION

The long perceived notion that GPCRs only function in monomeric form (Whorton et al., 2007, 2008; Chabre et al., 2009; Kuszak et al., 2009) has recently been changed by the description of a number of GPCRs of classes A, B and C found as homodimers, heterodimers and higher order oligomers that are often essential for modulation of GPCR function (Casadó et al., 2007; Ciruela, 2008; Ferré et al., 2009a, 2010a,b, 2014; Milligan, 2009; Rivero-Muller et al., 2010; Albizu et al., 2010; Gonzalez-Maeso, 2011; Ciruela et al., 2012; Lane and Canals, 2012; Miller et al., 2012; Steel et al., 2014). In many cases, oligomeric structures of GPCRs are essential for receptor activation, maturation, regulation and signal transduction once they are brought to the cell surface (Milligan et al., 2006; López-Giménez et al., 2007; Milligan, 2008, 2013; Ciruela et al., 2011; Rivero-Muller et al., 2013; Mondal et al., 2014; Ulloa-Aguirre et al., 2014). So, targeting GPCRs dimers or higher order oligomers with oligomeric-specific ligands may result in more selective and potent compounds with fewer side effects.

Several reports in the literature suggested that GPCR dimers were not constitutive but ligand promoted (Rodriguez-Frade, et al., 1999; Horvat et al., 2001). These studies challenge the most accepted concept that early GPCR dimerization in the biosynthetic pathway is a general feature that is necessary for the plasma membrane targeting of all members of this receptor family (Bulenger et al., 2005). Concretely, accumulating evidence pointed out that the homodimerization of many GPCRs is constitutive (i.e. does not require receptor activation) (McVey et al., 2001; Ayoub et al., 2002; Issafras et al., 2002; Jensen et al., 2002; Terrillon et al., 2003) and that both 'obligatory heterodimerization' and homodimerization of GPCRs occurs most probably in the endoplasmic reticulum (ER) (Ayoub et al., 2002; Jensen et al., 2002; Terrillon et al., 2003), an organelle that has a central role in the quality control of protein synthesis. Thus, dimerization might be a common requirement for GPCRs to pass quality-control checkpoints along the biosynthetic pathway, with homodimerization being the general rule and heterodimerization being a special case of this general rule (Fig. 7) (Bulenger et al., 2005).

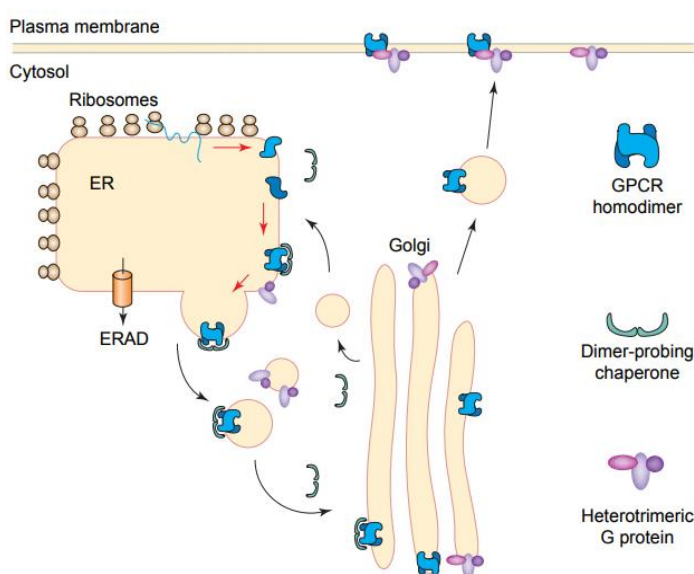


Figure 7. A model proposing that GPCR dimerization is a necessary step to pass quality-control checkpoints along the biosynthetic pathway. Nascent GPCR folding in the endoplasmic reticulum (ER) dimerize and interact with dimer-probing cytosolic chaperone proteins. Unfolded and monomeric GPCRs are degraded rapidly by the ER-associated degradation (ERAD) pathway. After maturation through the Golgi apparatus, GPCR homodimers are exported to the plasma membrane where they interact with a single heterotrimeric G protein. It is noteworthy that previous studies have suggested that $G\alpha\beta\gamma$ subunits also form a heterotrimer at an endomembrane location before reaching the plasma membrane. Extracted from Bulenger et al. (2005).

It is important to notice that, when ligands were apparently found to regulate dimer formation, a basal level of constitutive dimerization was observed (Kroeger et al., 2003). Moreover, the fact that ligands were found to modulate or even induce GPCR dimerization in some studies but not in others probably reflects differences in result interpretation rather than true differences between receptor behaviors. In addition, there are studies where it has been seen that conformational changes resulting from ligand binding (Villardaga et al., 2003) might stabilize the dimers, which become partially resistant to the solubilization conditions, hence leading to the erroneous conclusion that ligand binding could induce dimerization.

To sum up, it is more widely accepted that oligomerization can be implicated in GPCR ontogenesis, which means in the protein folding control and membrane targeting of the newly synthesized receptors as well as in their endocytic pattern (Breit et al., 2004; Terrillon and Bouvier, 2004; Bulenger et al., 2005; Law et al., 2005) which can be as dimers or oligomers (Yesilaltay and Jenness, 2000). Moreover, it has also consequences in pharmacology, signaling and desensitization (for further information read Prinster et al., 2005)

2.1. TYPES OF GPCR OLIGOMERIZATION

2.1.1. Heteromerization

GPCR heteromers are macromolecular complexes composed of at least two receptor units (protomers), with biochemical properties that are demonstrably different from those of its individual components (Ferré et al., 2009b, 2014; Gomes et al., 2016). The γ -aminobutyric acid (GABA_B) receptor is the first known GPCR that requires heteromerization for function. In fact, it is an obligatory heterodimer composed by two subunits, GBR1 and GBR2, which bear functions complimentary to each other in signal transmission. While the extracellular domain of GRB1 is responsible for ligand recognition, the transmembrane domain of GRB2 is required for G-protein activation. In addition, GRB2 facilitates the cell surface expression of GRB1 through coiled-coil interactions in the cytoplasmic region (Fan et al., 2017). More recent work demonstrated that the adrenergic receptor β_2 ($\beta_{2A}R$), a class A GPCR, despite of being functional without making heteromers (Whorton et al., 2007), was able to heterodimerize with different consequences depending on the GPCR involved; this type of heteromerization is called receptor heteromer (Ferré et al., 2009b). For example, it was able to associate with the adrenergic β_{1A} receptor ($\beta_{1A}R$) and the β_{3A} receptor ($\beta_{3A}R$) causing a reduction in the rate of agonist-induced internalization and a reduction in the ability of the receptor to stimulate extracellular signal-regulated kinase phosphorylation (Lavoie et al., 2002; Breit et al., 2004). Moreover, the same receptor was also able to heterodimerize with α_{2A} adrenergic receptors ($\alpha_{2A}R$), resulting in cross-internalization of the receptors following agonist stimulation of one of the subtypes (Xu et al., 2003) and with AT1 angiotensin receptors, resulting in a cross-inhibition of receptor signaling by their antagonists (cross-antagonism) (Barki-Harrington et al., 2003).

A number of specific interactions between purinergic receptors, key actors in the CNS, cardiovascular and immune system, and in other tissues, have been detected. For example, dopamine D₁ receptor (D₁R) heterodimerizes with A₁R (Gines et al., 2000) and none of them with D₂R (Gines et al., 2000; Kamiya et al., 2003; Frederick et al., 2015). In contrast, D₂Rs specifically heteromerize with A_{2A}R (Hillion et al., 2002; Ciruela et al., 2004), which do not heteromerize with D₁Rs (Hillion et al., 2002). In the case of the A₁R-D₁R heteromer, coactivation of both receptors led to the canonical negative interaction at the level of AC signaling. D₁R also

heteromerizes with dopamine D₃ receptor (D₃R). Within this heteromer, there is a positive crosstalk of D₁R and D₃R agonists at the level of mitogen-activated protein kinase (MAPK) signaling. In the context of the A_{2A}R-D₂R heteromer, A_{2A}R agonists are able to decrease the affinity and efficacy of D₂R for its agonists (Ferré et al., 1991; Hillion et al., 2002; Canals et al., 2003) and D₂R agonists, through the activation of G_{i/o} proteins, are able to counteract A_{2A}R agonist-mediated G_{s/oif}-dependent activation of AC (Trincavelli et al., 2012; Fernández-Dueñas et al., 2013). Moreover, A₁R specifically heteromerizes with A_{2A}R which is able, when activated, to allosterically shut down A₁R signaling (Ciruela et al., 2006; Casadó et al., 2010; Navarro et al., 2016, 2018). Both A₁R and A₂R also interact with non-dopamine receptors (DR) such as with some mGluR subtypes acquiring a synergistic signaling between adenosine and glutamate receptor agonists (Ciruela et al., 2001; Ferré et al., 2002).

2.1.2. Homodimerization

Moreover, there is also a growing list of receptors that have been found to form homomers, such as adenosine A₁ (Gracia et al., 2013b; Navarro et al., 2016), A_{2A} (Łukasiewicz et al., 2007; Gracia et al., 2011; Navarro et al., 2016) and A₃ (May et al., 2011), dopamine D₁ (Guitart et al., 2014), D₂ (Guo et al., 2003; Pou et al., 2012) and D₃ (Pou et al., 2012; Guitart et al., 2014), serotonin 5-HT_{1A} (Łukasiewicz et al., 2007), 5-HT_{2A} (Herrick-Davis et al., 2013), 5-HT_{2C} (Herrick-Davis et al., 2004, 2012; Mancía et al., 2008) and 5-HT₇ (Teitler et al., 2010), adrenergic α_{1B} (Herrick-Davis et al., 2013), β₁ (Mercier et al., 2002; Gherbi et al., 2015) and β₂ (Angers et al., 2000; Mercier et al., 2002; Herrick-Davis et al., 2013; Parmar et al., 2017), cannabinoid CB₁ (Bagher et al., 2017), angiotensin AT₁ (Szalai et al., 2012), metabotropic glutamate mGlu₂ (Levitz et al., 2016), muscarinic M₁ (Goin and Nathanson, 2006; Herrick-Davis et al., 2013), M₂ (Park and Wells, 2003; Goin and Nathanson, 2006; Herrick-Davis et al., 2013) and M₃ (Goin and Nathanson, 2006; McMillin et al., 2011), δ (Cvejic and Devi, 1997; McVey et al., 2001; Johnston et al., 2011), κ (Jordan and Devi, 1999) and μ (He et al., 2002) opioid, neurotensin 1 (White et al., 2007), melatonin MT₂ (Ayoub et al., 2004), niacin (Mandrika et al., 2010), and chemokine CXCR4 (Babcock et al., 2003). There are evidences suggesting that homodimers are the predominant species with potential dynamic formation of higher-order oligomers, and that the pentameric structure consisting of one GPCR homodimer and one heterotrimeric G protein is the minimal functional unit (Banères and Parello, 2003; Han et al., 2009; Pellissier et al., 2011, Ferré et al., 2014).

2.1.3. Higher order oligomerization

To add more complexity, during the last few years, it has been suggested that functional GPCRs are complexes of heteromers mostly constituted by different homodimers (Guitart et al., 2014). In the case of the dopamine D₁R and D₃R heteromers, it was found a minimal tetrameric stoichiometry comprised of homodimers of both receptors that were able to couple to G_{qs} and G_{qi} proteins respectively (Guitart et al., 2014). Moreover, the heterotetramer of A₁R and A_{2A}R has also been suggested (Cristóvão-Ferreira et al., 2013; Navarro et al., 2016, 2018). Recently, the heterotetramer formed by homodimers of A_{2A}R and D₂R was confirmed in transfected mammalian cells and striatal tissue. This tetrameric model explains why the occupancy of the A_{2A}R homodimer with either an agonist or an antagonist produces a conformational change that conduces the same allosteric modulation to the D₂R, a decrease of the affinity and efficacy of any D₂R ligand; whereas the simultaneous occupancy of the A_{2A}R homodimer by an agonist and

an antagonist not allow this conformational change. In the brain, there is a tone of adenosine under physiological conditions that can explain why caffeine and $A_{2A}R$ antagonists produce locomotor activation and not locomotor depression (results derived from this Thesis).

2.2. GPCR LIGANDS

2.2.1. Orthosteric

Orthosteric ligands are ligands that bind to the binding site for the endogenous ligand on a receptor, the orthosteric site. The mechanism of action for many drugs is often based on mimicking (as in the case of agonists) or blocking (as in the case of antagonists and inverse agonists) the action of an endogenous signaling molecule by competing for the orthosteric site on a specific receptor

Early models of GPCR signaling considered that receptors had two states: "off" and "on" depending on their ability to trigger downstream responses. Orthosteric ligands were classified as agonists if they elicited a maximal response, partial agonists if they generated a submaximal response at saturating ligand concentration, antagonists if they lacked efficacy but competitively inhibited agonist responses, and inverse agonists if they preferentially stabilized the "off" state, leading to a suppression of basal receptor activity (Black and Leff, 1983; Samama et al., 1993). First with the β_2 -adrenergic receptor and then with δ -opioid receptor, the constitutive activity of these receptors was probed: they had an intrinsic activity without the presence of an agonist that diminished when adding an inverse agonist (Cerione et al., 1984).

This early conceptualization began to evolve in the mid-1990s, driven by the recognition that many GPCRs were able to couple to several effectors' pathways simultaneously (Offermanns et al., 1994; Laugwitz et al., 1996) or differentially depending on the tissue (Jin et al., 2001; Mahon et al., 2002). Furthermore, structurally distinct ligands could activate the same GPCR in different ways contradicting the classical idea that agonist had the capacity to activate equally all signaling pathways. All of the above indicate that most, if not all, GPCRs possess more than one "active" receptor state and that the structure of the ligand can "bias" downstream signaling (Kenakin, 1995; Christopoulos and Kenakin, 2002). Now, we have evolved from the "off" and "on" model to a non binary model where receptors, when bound to the ligand, can have a finite number of discrete active and inactive states within the sterically permissible conformational (Kenakin and Miller, 2010) that links them to a particular downstream effector and efficacy. In this scenario, "functional selectivity or ligand-biased signaling" may arise from differences in the ligand efficiency to stabilize different active states (Luttrell et al., 2015).

In this context, Galés et al. (2005) linked conformational changes to signaling efficacy. In that study, the use of BRET probes at different positions in the receptor-G protein complex, revealed distinct conformations stabilized by ligands with different efficacies. The general profile of the changes distinguishes the full and partial agonists from the antagonists. In particular, agonists promoted BRET changes at several positions that were silent with antagonists. Concretely, the probes that sensed the opening of the protein $G_{\alpha i}$ nucleotide binding pocket ($G_{\alpha i 1}$ -91RLuc and GFP10- $G_{\gamma 2}$) promoted by agonist stimulation did not respond to antagonist treatment. Moreover, partial agonists lead to a fraction of the BRET signal promoted by the full agonist in $G_{\alpha i 1}$ -91RLuc and GFP10- $G_{\gamma 2}$. A similar correspondence between ligand efficacy and amplitude of BRET changes was observed when monitoring relative movements between the receptor and either G_{β} , G_{γ} or position 91 in $G_{\alpha i 1}$ (Fig. 8).

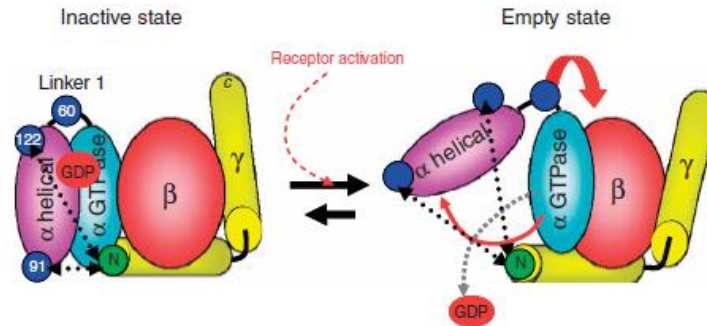


Figure 8. Schematic representation of structural rearrangement within the $G_{\alpha i1}\beta_1\gamma_2$ heterotrimer detected by BRET after receptor activation. RLuc probes appear in blue and GFP probe in green. Scheme depicts opening of the $G_{\alpha i1}$ GTPase and helical domain through linker 1 which increases distances between RLuc91 or RLuc122 and $G_{\gamma 2}$ -GFP and shortens that of RLuc60- $G_{\gamma 2}$ -GFP. These structural rearrangements create an exit route for the GDP. Extracted from Galés et al. (2005).

Nowadays, a variety of GPCR agonists have been described, which differ in their ability to promote receptor coupling to different G protein families or even subunits, recruit signal transducers such as arrestins, activate a variety of downstream molecular pathways and induce certain phosphorylation signatures or gene expression patterns (Fig. 9). As an example, α_2 -adrenergic receptor subtypes are able to couple to multiple G proteins even from $G_{\alpha s}$ and $G_{\alpha i}$ (Eason et al., 1992, 1995) and activate multiple signaling pathways. So, depending on the cell population, they may couple to different G protein subtype activating different signaling pathways. Moreover, signaling through these parallel pathways may differ depending on the ligand used to stimulate the receptor, resulting in a biased response (Roth et al., 2015).

Biased ligands could provide an opportunity to modulate GPCR function in a finer way and to separate therapeutic from side effects improving safety profiles (Kenakin, 2011; Kenakin and Christopoulos, 2013; Rankovic et al., 2016).

2.2.2. Allosteric

Allostery is a widespread biological phenomenon that describes the ability of interactions occurring at a site of a macromolecule to modulate interactions at a spatially distinct binding site on the same macromolecule (Gentry et al., 2015).

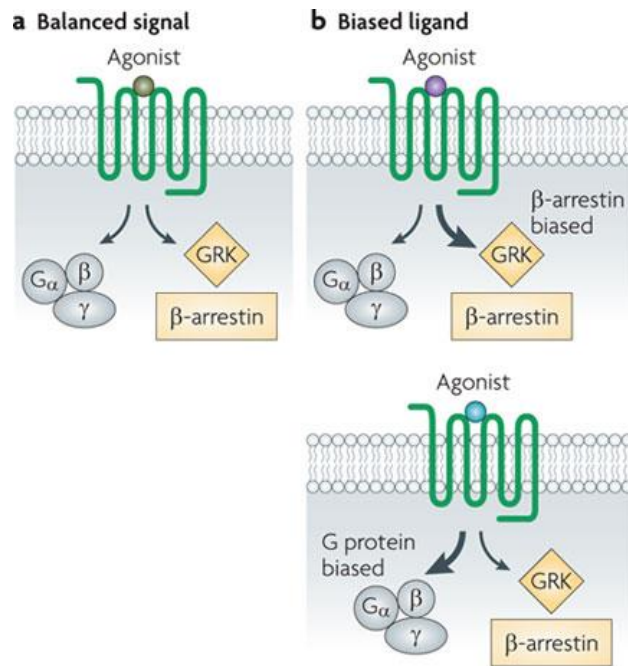


Figure 9. Biased agonism or functional selectivity. In a balanced signal, a specific agonist had the capacity to activate equally all signaling pathways. In a biased agonism, agonist A produces a biased stimulus for β -arrestin signaling pathway whereas agonist B stabilizes another receptor conformation that selectively induces bias for G protein signaling pathway. Adapted from Rajagopal et al. (2010).

It is increasingly recognized that one important mechanism for the regulation of the biological functions of the most, if not all, GPCR is through allosteric modulation (Christopoulos and Kenakin, 2002; Gao and Jacobson, 2006, 2013; May et al., 2007; Conn et al., 2009; De Amici et al., 2010; Smith and Milligan, 2010; Canals et al., 2011; Göblyös and Ijzerman, 2011; Changeux, 2012; Kenakin, 2012; Melancon et al., 2012; Dror et al., 2013; Lane et al., 2013; Wang and Lewis, 2013; Wootten et al., 2013; Christopoulos, 2014; Christopoulos et al., 2014; Nickols and Conn, 2014; Wu et al., 2014; Ferré et al., 2014; Feng et al., 2015; Harpsoe et al., 2015; van der Westhuizen et al., 2015; Changeux and Christopoulos, 2016; Dawaliby et al., 2016; Shivnaraine et al., 2016; Rossi et al., 2017). In fact, GPCR signal transduction is intrinsically allosteric as it involves the binding of an extracellular stimulus and subsequent propagation of the signal through the protein to a topographically distinct intracellular site recognized by G proteins, β -arrestins, and others (Gentry et al., 2015). In classical allosterism, the allosteric ligand, by binding to a non-orthosteric site, can modify either affinity or efficacy of the orthosteric agonists (Fig. 10) (Conn et al., 2009; Ferré et al., 2016).

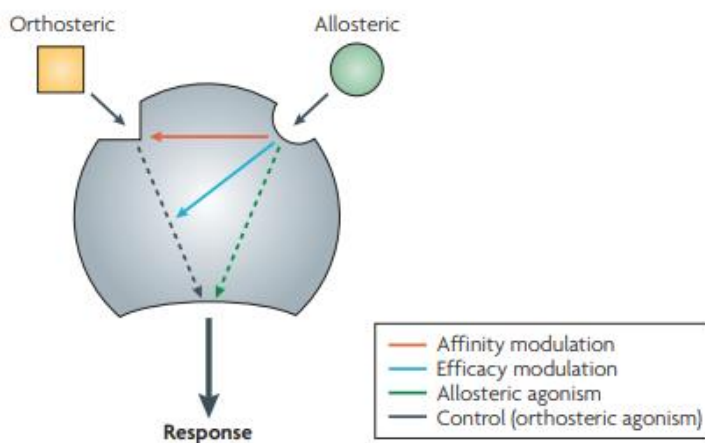


Figure 10. Modes of action of allosteric modulators. Allosteric ligands bind to a topographically distinct site on a receptor to modulate orthosteric ligand affinity (red) and/or efficacy (blue). Some allosteric ligands can directly perturb signaling in their own right (green). Extracted from Conn et al. (2009).

Allosteric modulators of GPCRs can either potentiate (positive allosteric modulators, PAMs) or inhibit (negative allosteric modulators, NAMs) the receptor response by inducing conformational changes in the GPCR protein that are transmitted from the allosteric binding site to the orthosteric site and/or directly to the effectors protein coupling sites (Gao and Jacobson, 2006; Conn et al., 2009; Kenakin and Miller, 2010). There are also neutral allosteric ligands (NALs), also termed silent allosteric modulators (SAMs), which bind to the allosteric site but have no effects on the responses to the orthosteric ligand but, by simple competition, inhibit the actions of other allosteric modulators that bind to that same site (Conn et al., 2009). Experimental evidence has also identified PAMs with intrinsic activity (PAM-ago) (Christopoulos et al., 2014).

The classification of an allosteric ligand as a modulator is conditional on the nature of the reference ligand that is being used to probe receptor function (Kenakin, 2005); the use of terms as positive, negative and neutral must be placed within the context of the interacting ligand against which the allosteric ligand is been tested and the experimental conditions (Christopoulos et al., 2014).

Most of allosteric modulators are exogenous drugs, but there are a variety of endogenous substances that can act as allosteric modulators of GPCRs, including the G protein, but also a variety of ions (e.g. Na^+ , Zn^{2+} , Mg^{2+}), lipids (e.g. cholesterol, anandamide), amino acids (e.g. L-Phe, homoCys), peptides (e.g. glutathione), and accessory proteins or other GPCRs that display different degrees of receptor-specific modulatory effects (van der Westhuizen et al., 2015; Manna et al., 2016; Guixà-González et al., 2017).

The previously solved GPCR structures reveal various allosteric binding sites, especially within the 7TM helical bundle, but also in the extracellular region of the receptor or on the external lipidic interface of the transmembrane domain (Zhang et al., 2015; Changeux and Christopoulos, 2016). As an example, the $\text{A}_{2\text{A}}\text{R}$ structure suggests that sodium ion may act as an allosteric modulator to alter the dynamics and activation profiles of GPCRs (Gutierrez-de-Teran et al., 2013).

Allosteric ligands are emerging as promising alternatives for therapeutic intervention because they may obviate several of the inherent challenges of orthosteric target-centered approaches. Moreover, a property of allosteric modulators is the saturability which means that a negative allosteric modulator that modifies the affinity of an orthosteric agonist will displace the functional dose-response curve to higher concentrations but only up to a certain extent. In contrast, a competitive orthosteric antagonist would displace the curve ad infinitum. This is useful and has medical implications by reducing overdose effects, compared with orthosteric ligands. (Kenakin and Miller, 2010; Smith and Milligan, 2010).

2.2.3. Bitopic

A third type of new GPCR ligands (besides orthosteric and allosteric) are bitopic ligands, which are bifunctional ligands comprised of two pharmacophores that simultaneously interact with an orthosteric and an allosteric site (Mohr et al., 2013; Christopoulos et al., 2014; Shonberg et al., 2015; Fronik et al., 2017).

Bitopic ligands have emerged as a new approach to develop selective GPCR ligands with improved binding affinity (via orthosteric sites) and high selectivity (via allosteric sites) owing to

a greater number of ligand-GPCRs contacts (Lane et al., 2013; Mohr et al., 2013), stabilizing receptors (Feng et al., 2015). Moreover, well designed dualistic bitopic ligands, can combine the high receptor subtype selectivity of the allosteric sites with the capacity to fine-tune the natural signaling pattern of the receptor engendering signaling bias (Langmead and Christopoulos, 2014; Grundmann et al., 2016).

In addition, bitopic ligands give the opportunity for the development of more selective drugs with reduced adverse side effects because allosteric binding sites are usually less structurally conserved than their corresponding orthosteric sites due to the fact that they did not sustain direct evolutionary pressure to preserve key functional residues (Capra et al., 2009; Gao and Jacobson, 2013, Wang and Lewis, 2013; Nussinov and Tsai, 2015).

As an example of a bitopic ligand, the compound SB269652, originally discovered as an antagonist of D₂R and D₃R, was proposed by Silvano et al. (2010) as a bitopic ligand. Lane et al. (2014) also provided evidence to confirm that SB269652 acted as a bitopic ligand at D₂R dimer (Fig. 11).

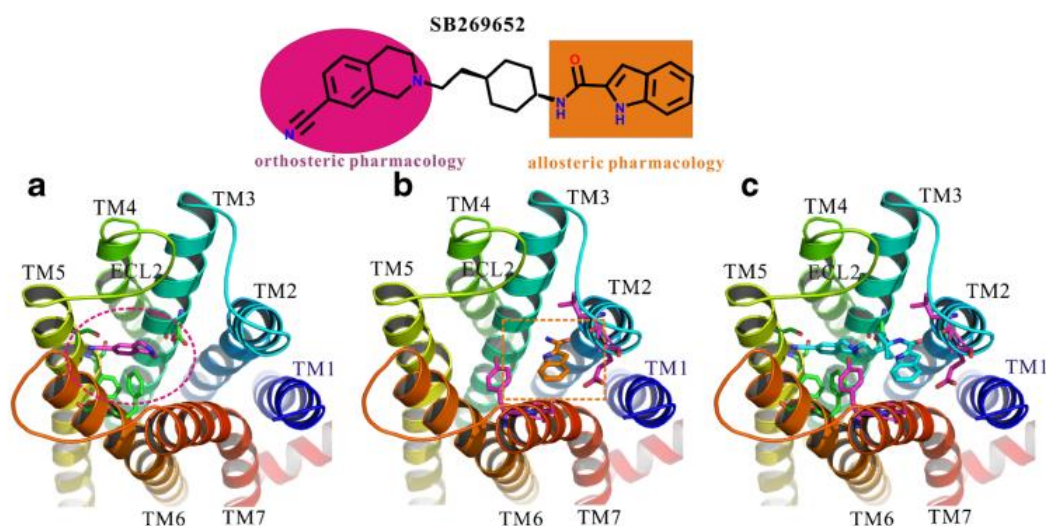


Figure 11. Docking results of bitopic ligand SB269652 at D₂R. a) the binding mode of the orthosteric fragment at the orthosteric site. b) the binding mode of the allosteric fragment at the allosteric binding site. c) the binding mode of the whole structure of SB269652. Extracted from Feng et al. (2015).

2.3.4. Photoswitchable

It is known that, when studying neural circuits and synapses, standard diffusion and partitioning of the ligand mean poor spatial and temporal control of ligand activity. Light-based techniques have been developed to overcome these challenges. Photoswitchable ligands contain a synthetic photoswitch which is a small molecule that absorbs light to reversibly change its shape. The most commonly used photoswitch in biological applications is azobenzene due to its synthetic tractability, tunable photochemical properties, and biological compatibility (Figure 12a). The lowest energy isomer, the straight trans-azobenzene, isomerizes to the bent cis-azobenzene configuration upon irradiation with near-UV light. Subsequent irradiation with longer wavelength visible light, or thermal relaxation, leads the metastable cis-azobenzene to revert to the trans-azobenzene isomer (Kienzler and Isacoff, 2017).

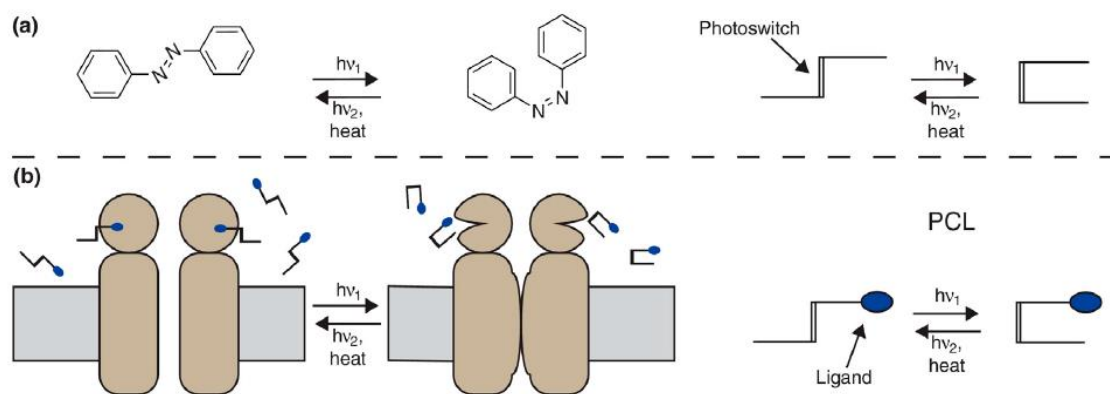


Figure 12. Strategies for incorporating synthetic photoswitches into neuroscience tools. a) The trans and cis isomers of azobenzene can be interconverted with different wavelengths of light. Cartoons show how the core azobenzene structure can be elaborated into photoswitchable tools. b) Photochromic ligands (PCLs) switch between active and inactive compounds that freely diffuse and link to endogenous channels and receptors. Extracted from Kienzler and Isacoff (2017).

To make a light-sensitive probe, the photoswitch is chemically attached to a biologically active ligand. Freely diffusible photoswitch-ligand constructs, called photochromic ligands (PCLs) (Figure 12b), interact with the native target protein such that one photoisomer is active and the other is not. PCLs have the capability to operate as blockers (e.g. of a pore or active site), agonists, antagonists, or allosteric modulators. In addition, this system is an improvement upon conventional pharmacology because PCLs can be rapidly photoswitched to provide exceptional spatial and temporal control. Several PLCs of GPCRs have been reported for metabotropic glutamate receptors (Font et al., 2017; Levitz et al., 2017) or $A_{2A}R$ (Bahamonde et al., 2014).

2.3.5. Multivalent

The privileged structure based approach has been widely used to design libraries that possess both a high probability of producing compounds against a variety of targets and good “drug-like” properties (Guo and Hobbs, 2003). The term “privileged structure” was introduced by Evans and co-workers at Merck in 1988 and was defined as “a single molecular framework able to provide ligands for diverse receptors”.

Privileged structures are an ideal source of scaffolds for the design and synthesis of combinatorial libraries for multiple receptors (Guo and Hobbs, 2003; Messer, 2004; Costantino and Barlocco, 2006). Vendrell et al. (2007), used ergot alkaloid structure to create several multivalent compounds that behaved as A_1R antagonists, $A_{2A}R$ inverse agonists or antagonists, D_1R agonists and D_2R agonists or antagonists that would be useful for the treatment of Parkinson disease. In this pathology, the combined therapy using DA agonists and adenosine antagonists is currently being evaluated (Kanda et al., 2000; Jenner, 2005; Kase et al., 2003).

The application of a multitarget ligand approach is particularly useful for disorders in which the alteration of a single receptor is therapeutically insufficient and a balanced modulation of a small number of targets has been shown to have more efficacy and fewer side effects than single-target treatments (Morphy et al., 2004; Vendrell et al., 2007).

2.3.6. Heteromer-selective

Based on experiments in transfected cells and on their potencies for blocking striatal glutamate release and inducing psychomotor activation in rats, Orrú et al. (2011) demonstrated that the $A_{2A}R$ antagonist SCH-442416 bound with higher affinity $A_{2A}R$ s when forming heteromers with

A₁Rs. In contrast, the A_{2A}R antagonist KW-6002 showed the best relative affinity for A_{2A}Rs when forming heteromers with D₂Rs. Another heteromer-specific ligand described is the opioid agonist 6'-guanidinonaltrindole, which selectively activates delta opioid receptors only when forming heteromers with kappa opioid receptors (Waldhoer et al., 2005). A specific case of heteromer-selective ligands are hetero-bivalent ligands (see 2.3.7) (Hübner et al., 2016). At present, the number of clearly described heteromer-specific ligands remains small, but it is likely that many heteromer-selective ligands will be discovered in the near future. It therefore seems reasonable to assume that customized drugs targeting a specific receptor heteromer in the CNS might improve safety and efficacy for their therapeutic targets (Cortés et al., 2016).

2.3.7. Bivalent

Bivalent ligands are composed of two covalently tethered chemical groups (pharmacophores) that can tolerate the addition of a linker onto their structure (Arnatt and Zhang, 2014) and that are potentially capable of binding into the two protomers of a receptor dimer target simultaneously (Shonberg et al., 2011). Potentially, these two pharmacophores can be agonist or antagonist orthosteric ligands.

Berque-Bestel et al. (2008) reported that due to constitutive nature of GPCR dimers (see above), bivalent ligands are expected in most cases to bind and stabilize preexisting dimers rather than to promote ligand-induced-dimerization.

Generally, bivalent ligands can either be classified as homobivalent or heterobivalent, that is, they either have two of the same pharmacophores or two different ones. These two pharmacophores are attached to each other with a linker that should not interfere with receptor binding and that must be of the appropriate length and composition to allow the two pharmacophores to interact with both receptors at the same time (Arnatt and Zhang, 2014). The average distance between GPCR dimers is thought to be between 27-32 Å (Portoghese, 2001). Several different linker types have been reported and range from aliphatic chains to polyethers (Shonberg et al., 2011). Bivalent ligands have been developed for a variety of GPCR targets, including adenosine, dopamine, opioid, melanocortin, oxytocin, chemokine and cannabinoid receptors (Soriano et al., 2009; Kuhhorn et al., 2011; Shen et al., 2013; Arnatt and Zhang, 2014; Nimczick and Decker, 2015; Arnatt et al., 2016; Busnelli et al., 2016; Lensing et al., 2016; Bonifazi et al., 2017).

The binding of the first pharmacophore would increase the local concentration of the second tethered pharmacophore and, therefore, increase its binding to the dimer partner, resulting in either substantially steeper binding curves than for monovalent ligands or higher affinity; examples of such behavior are observed in the bivalent ligand literature (Glass et al., 2016).

If the bivalent ligand is too short, only one or the other pharmacophore would be bound at any one time. In this scenario, higher affinity or cooperative binding behavior may be due to the effect of 'statistical binding': the binding of one pharmacophore of a bivalent ligand to its receptor increases the local concentration of the other pharmacophore, potentially driving the binding equilibrium of the second receptor towards greater receptor binding (Fig. 13). However, differentiating between dual activation of the receptors and simultaneously binding is near impossible (Glass et al., 2016).

Both dual-acting and bivalent ligands would have the potential to result in simultaneous activation of both receptors, but dual-acting ligands would lack the theoretical ability of bivalent ligands to only target those receptors within the specific dimer pair and cannot be considered heteromer-specific ligands (see 2.3.6). Thus, because of their selective recognition properties, bivalent ligands can be used for tissue specific targeting cells expressing an individual GPCR dimer (Hübner et al., 2016).

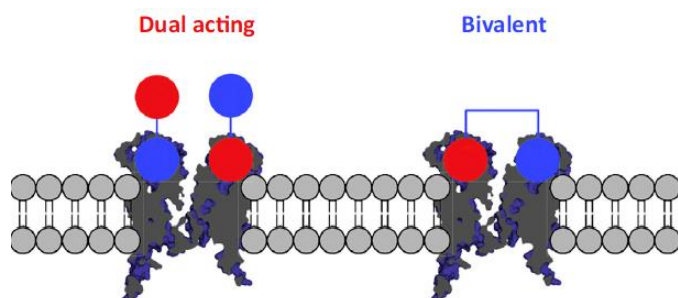


Figure 13. Schematic diagram illustrating the difference between dual-acting and bivalent ligands. Both comprise two pharmacophores linked together by a spacer; however, only the bivalent ligand is able to bind simultaneously to both receptors. Image extracted from Glass et al. (2016).

2.4. METHODS TO STUDY GPCR OLIGOMERIZATION

In order to define the physiological relevance of GPCR dimers, the International Union of Basic and Clinical Pharmacology (IUPHAR) released three criteria of which at least two have to be fulfilled. First, the physical interaction of GPCRs has to be verified in native tissues or primary cells. Second, evidence of dimer-specific properties, like specific signaling or binding properties or the existence of dimer-selective ligands, must be given. The third criterion recommends the *in vivo* validation of GPCR dimerization by knock-out animals or RNAi technology (Pin et al., 2007; Gomes et al., 2016).

There are many experimental techniques used to study the GPCR oligomerization. From those based on traditional biochemistry such as co-immunoprecipitation (Co-IP) and western blot, to biophysical methods including fluorescence and bioluminescence resonance energy transfer (FRET and BRET), bimolecular luminescence complementation (BiFC), a combination of them, time resolution fluorescence resonance energy transfer (TR-FRET) and complemented donor-acceptor resonance energy transfer (CODA-RET). There are also immunochemical techniques such as proximity ligation assays (PLA), co-localization and immunoelectromicroscopy and the detection of allosteric effects by binding assays or by analyzing signaling pathways.

2.4.1. Early and classical methods

Co-IP and Western blotting. Early and classical but one of the most used techniques that probed GPCR dimerization (Hillion et al, 2002). Several publications reported that GPCRs sometimes migrated on SDS-PAGE (sodium dodecyl sulfate-polyacrylamide gel electrophoresis) in a way that seemed to indicate about twice the expected molecular mass. To investigate if it was actually a direct physicochemical interaction between two GPCRs it was established the Co-IP. With this technique, the potentially formed dimers are immunoprecipitated by using a specific antibody against one epitope, followed by immunoblotting using a specific antibody against the other protomer. Co-IP studies have revealed, for example, that the A_{2A}R, D₂R and glutamate mGlu₅R were able to form higher order oligomers (Díaz-Cabiale et al., 2002). However, this technique has a significant restriction to be used in native tissues due to the lack of specific and high-affinity antibodies to detect GPCRs. Moreover, it is necessary to lysate and

solubilize the tissue for releasing the protein of interest from the insoluble membrane environment and this step by itself can create nonspecific protein-protein interactions and disrupt native associations. However, to avoid the disruption of existing receptor-receptor interactions, cross-linking agents have been applied prior to the solubilization process to stabilize the preformed dimers during the subsequent steps (Shenton et al, 2005).

2.4.2. Biophysical methods

Resonance energy transfer (RET) based techniques have facilitated the visualization of GPCR dimers in intact living cells. The most widely used approaches involve either fluorescence resonance energy transfer (FRET) or bioluminescence resonance energy transfer (BRET), which are based on the nonradiative transfer of energy from a donor to an acceptor molecule. In FRET assays, energy transfer-competent pairs of fluorescent proteins have been attached to the C-terminus of the GPCR (i. e. GFP2, green fluorescent protein2, as donor and YFP, yellow fluorescent protein, as acceptor). In BRET, the donor molecule is an enzyme (commonly luciferase from *Renilla reniformis* (Rluc) which becomes bioluminescent upon reaction of its substrate and the acceptor is a fluorescent protein (YFP, GFP2, or mOrange).

BRET has the advantage over FRET that does not require an external illumination to initiate the energy transfer, which leads to higher background noise resulting from excitation of the acceptor or photobleaching. Nevertheless, FRET and BRET signals cannot distinguish between cell surface receptors and receptors retained inside the cells.

There exists a variant of BRET assay, named BRET2. In this case, the donor uses Deep Blue C as the substrate emitting light at 400 nm and the acceptor is GFP2 that emits at 510 nm. The advantage of BRET2 is that there is a bigger separation between the donor and acceptor peaks but the disadvantage is that it has 100 to 300 times lower intensity of emitted light as compared with the luminescence emitted by RLuc. In addition, Deep Blue C experiences a faster signal decay and lower quantum yield than that emitted by coelenterazine H (Fig. 14).

In this Thesis, almost all of the BRET experiments performed are BRET1 and the two pairs used are RLuc8 and mVenus. RLuc8 is a variant of RLuc with enhanced enzymatic activity since it is ~4 times brighter than RLuc and more stable in different environments (Loening et al., 2006). mVenus is a variant of the YFP, a genetic mutant of the GFP and it has the advantage of improved maturation and brightness as well as reduced environmental dependence (Nagai et al., 2002; Rekas et al., 2002).

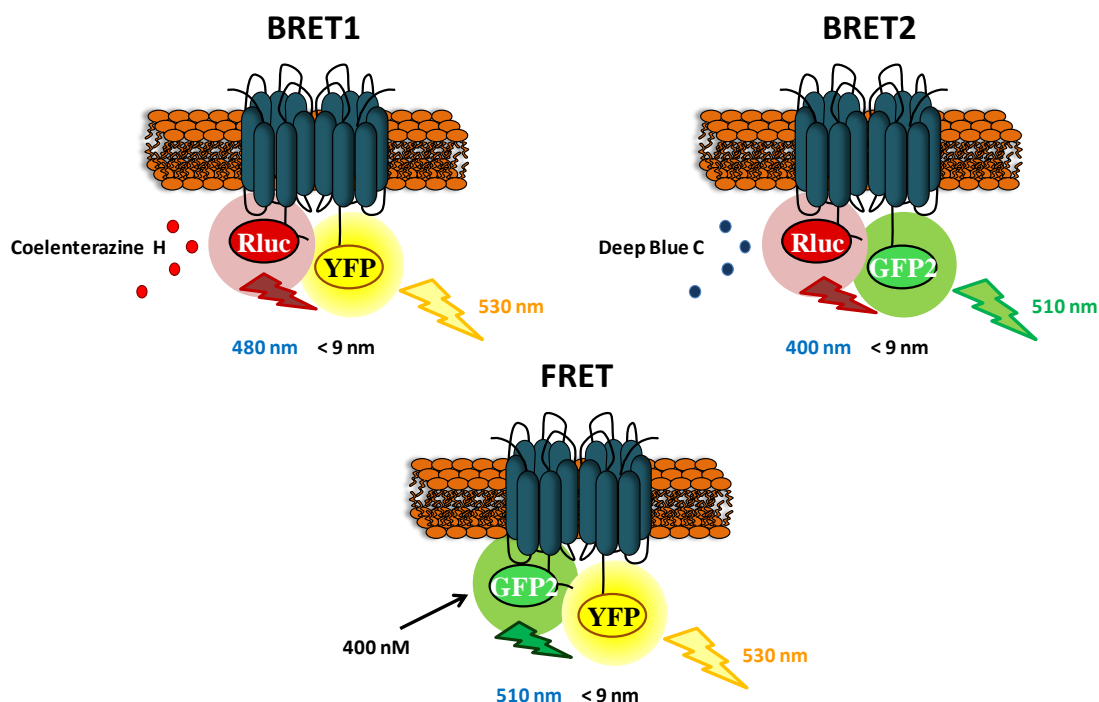


Figure 14. Schematic representation of BRET1, BRET2 and FRET techniques.

Bimolecular fluorescence complementation (BiFC) and bimolecular luminescence complementation (BiLC) assays are based on the reconstitution of a fluorescent or luminescent protein by interaction of two GPCRs fused to its inactive and complementary half. For BiFC the protein could be mVenus, Cerulean or mCherry and for BiLC *Renilla reniformis* and *Gaussia princeps* (Vidi and Watts, 2009). Dimerization of the GPCRs brings the fragments in close proximity, leading to the reconstitution of the protein and the fluorescence/luminescence can be detected (Kerppola, 2008; Vidi et al., 2011). When combined with approaches such as FRET and BRET, BiFC and BiLC allowed the detection of multiple protein interactions. As an example, BiFC-BiLC assays were used to demonstrate the ability of D₁R and D₃R to form heterotetramers (Guitart et al., 2014). In this experiment, complemented RLuc and YFP from D₁R-D₃R heteromers were used as donor and acceptor molecules in BRET assays demonstrating the formation of the heterotetramer. To demonstrate that the reconstitution is not driven by the hemiproteins, it is necessary to transfect the cells with one receptor fused to the hemiprotein and another receptor that it is known that does not interact, fused to the complementary hemiprotein. In this Thesis, this method has also been applied to the study of the A_{2A}R-D₂R heterotetramer and the negative controls were A₁R-D₂R and A_{2A}R-D₁R pairs, in agreement with the suggested ability of A_{2A}R to heteromerize with D₂R and not with D₁R and with the ability of D₂R to heteromerize with A_{2A}R and not with A₁R (Hillion et al., 2002; Ferré et al., 2014) (Fig. 15).

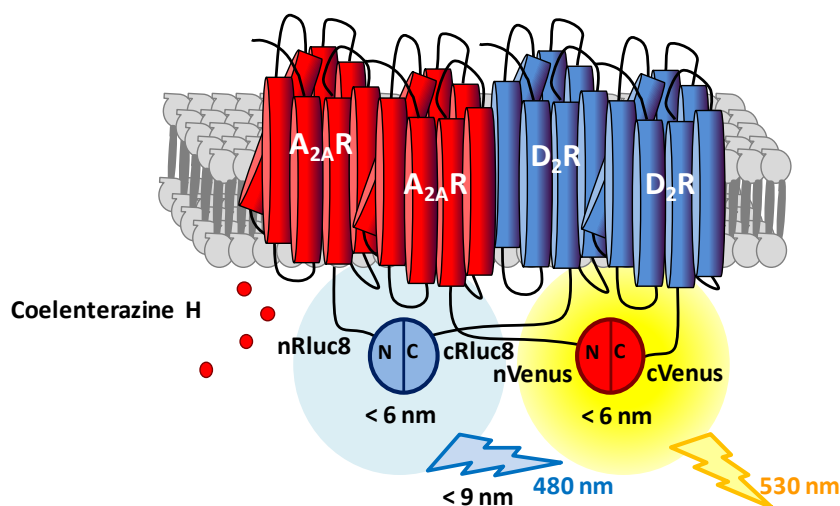


Figure 15. Schematic representation of the tetrameric structure of A_{2A}R–D₂R heteromer detected by BRET using BiFC/BiLC BRET was measured in human embryonic kidney (HEK) cells expressing A_{2A}R–nRluc, D₂R–cRluc, A_{2A}R–nVenus and D₂R–cVenus. Coelenterazine H is the substrate of Rluc. Extracted from Results of this Thesis.

BiFC combined with the application of TM peptides with the aminoacid sequences of receptors have been used in several studies to determine the interfaces of different receptor oligomers. To perform these experiments, TMs peptides of the receptors are fused to the HIV transactivator of transcription (TAT) peptide, allowing their effective insertion and orientation in the plasma membrane due to their capacity to penetrate it (He et al., 2011; Guitart et al., 2014; Navarro et al., 2015). Only the transmembrane peptide that is able to bind to the receptor and disturb the quaternary structure of the oligomer will cause a significant fluorescence decrease indicating that is involved in the interface of the oligomer.

Recently, our group successfully used this method to demonstrate the involvement of specific TM domains in the heteromerization of D₁R and D₃R (Guitart et al., 2014), corticotropin-releasing factor CRF1 (CRF1R) and orexin OX1 receptors (OX1R) (Navarro et al., 2015), serotonin 5-HT_{2A} (5-HT_{2A}R) and cannabinoid CB1 receptors (CB1R) (Viñals et al., 2015) and A_{2A}R and A₁R (Navarro et al., 2018). Specifically, in these studies we showed that TM5 and TM6 of D₁R are implicated in the D₁R–D₃R heteromerization; TM5 and TM6 of CB₁Rs in the 5-HT_{2A}R–CB₁R heteromer interface; TM5 and TM1 of OX1R in the CRF1R–OX1R heteromer.

In addition, BRET experiments can be conducted under conditions that more closely reflect the biochemical environment occurring in living organisms than FRET assays. So, BRET is not only widely used to investigate receptor interactions but also has played a major role in the characterization of GPCR activation and signaling (Kaczor et al., 2014). Recently, several studies have applied BRET for the study of dynamic cellular processes, such as the modulation of the interaction of two proteins following pharmacological treatment or the development of biosensors for various signaling pathways. These biosensors are important tools to understand GPCR signal transduction by providing optical tools to study real time interactions between receptors, the recruitment of binding partners to receptors, and variations in concentrations of second messengers generated downstream of receptors such as cAMP and calcium. Most importantly, BRET studies are conducted in living cells and enable the study of a wide variety of signaling systems to be probed under biologically relevant conditions, with minimal perturbation and in a quantitative manner.

In this Thesis, several BRET biosensors have been used to investigate the biology, pharmacology, and signaling of GPCRs in a dynamic fashion:

- *Complemented donor-acceptor resonance energy transfer (CODA-RET) technology.* Urizar et al. (2011) developed this technique that merges properties of BiLC and BRET to study conformational changes in response to activation of a defined GPCR dimer (Fig. 16). The BRET assay requires a donor molecule (nRLuc8 and cRLuc8 hemiproteins) fused to the C terminus of the receptors of interest, and an acceptor molecule (mVenus) fused to the G_{α} subunit at the same position. This technique requires not only the expression of the G_{α} biosensor but also the untagged $G_{\beta\gamma}$ proteins. When the luminescent protein is reconstituted, indicating the presence of the dimer, and the receptor activated, conformational changes occur at the level of the GPCR-G protein interaction that are seen as an increase of the BRET values depending on the concentration of the ligand. In this scenario, the luminescence signal will only result from complementation of the receptors; thus, any homomeric species will be silent at the level of the BRET readout.

An alternative to CODA-RET are the called G protein engagement and the G-protein BRET. Interestingly, the first it is named “engagement” and not “recruitment” because it suggests a precoupled state between receptor and G protein (Galés et al., 2005). In G protein engagement, the RLuc8 reconstitution is not necessary. RLuc8 is fused to the receptor and mVenus to the G_{α} subunit. In contrast, the G-protein BRET measures the interaction between two G protein subunits after receptor activation. It requires the use of tagged-fused G-protein subunits and untagged receptors (Fig. 16). The first group that used BRET in living cells to monitor the activation of G proteins after the receptor activation was Bouvier’s laboratory (Galés et al., 2006).

In this Thesis, in collaboration with Dr. Ferre’s laboratory, we use both CODA-RET and G-protein BRET to study DA and NE receptor interaction and signaling.

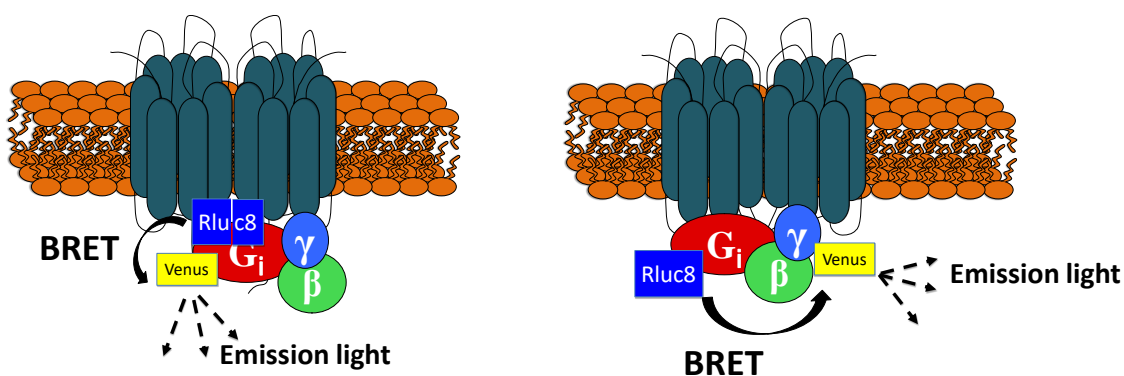


Figure 16. CODA-RET and G-protein BRET schemes. (Left) CODA-RET: nRLuc8 and cRLuc8 hemiproteins are fused to the C terminus of the receptors and mVenus is fused to the G_{α} subunit. When the luminescent protein is reconstituted, and the receptor activated, GPCR-G protein closely interact and this is seen as an increase of the BRET values. (Right) G-protein BRET: RLuc8 is fused to the G_{α} subunit and mVenus is fused to the G_{γ} subunit. BRET decrease between G_{α} and G_{γ} is recorded after activation of the receptor by a ligand.

- *β -arrestin.* In this assay, β -arrestin is fused to mVenus and receptor is fused to RLuc8 or vice versa and drug-induced BRET is measured. GRK is usually cotransfected since it facilitates β -arrestin recruitment (Evron et al., 2012).

- *cAMP dynamics*. In order to measure changes in cAMP concentration in living cells, the AC inhibition assay uses the CAMYEL biosensor construct. It was developed by Jiang et al. (2007), and consists on a catalytically inactive Epac1 sandwiched between the RLuc and YFP (or mVenus). When Epac1 binds to cAMP, a conformational change occurs that alters the relative orientation between the donor and acceptor molecules. This conformational change following the binding to cAMP, results in a decrease in BRET values. Therefore, a decrease in BRET is related to an increase of cAMP, typical of Gs coupled receptors or treatment with forskolin. In contrast, an increase in BRET is interpreted as a decrease in cAMP such as the one mediated by Gi coupled receptors.

Sequential resonance energy transfer (SRET) allows the identification of heterotrimeric in living cells. In SRET, the oxidation of an RLuc substrate by an RLuc-fusion protein leads to acceptor excitation by BRET and subsequent FRET with the third fusion protein. Applying BRET1 or BRET2 gives rise to SRET1 or SRET2. SRET will only occur between these fusion proteins if the two coupling pairs, RLuc/GFP2 and GFP2/YFP or RLuc/YFP and YFP/DsRed, are at a distance less than 10 nm (Fig. 17) (Carriba et al., 2008).

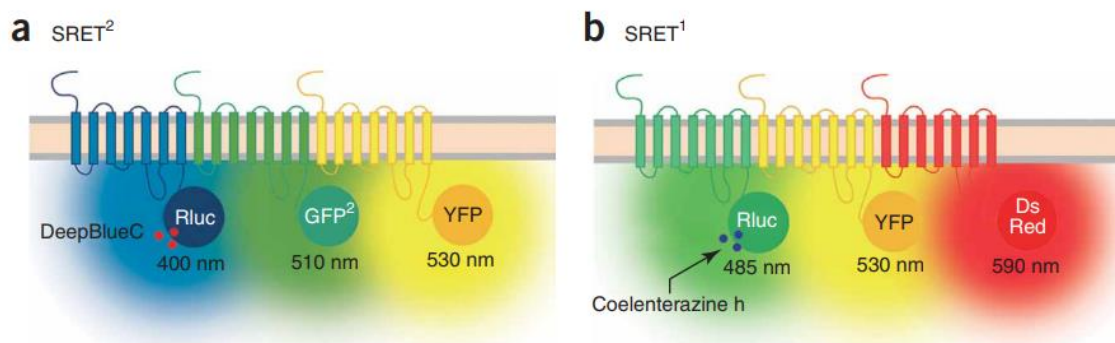


Figure 17. Scheme of SRET2 and SRET1. Extracted from Carriba et al. (2008).

Lately, more variants of FRET have been developed, like time-resolved FRET, photobleaching FRET and *FRET spectrometry* (Pfleger and Eidne, 2005).

Time-resolved FRET (TR-FRET), the inability to define the cellular location of the signal was overcome by fluorescence markers that are not able to penetrate the cell membrane. TR-FRET is based on the energy transfer between a lanthanide (terbium, dysprosium, samarium, or europium) that exhibits a long-lasting fluorescent light emission, and a compatible fluorophore (Alexa Fluor 647, DY-647, or d2). In this technique, receptor can be labeled non-covalently for instance with donor and acceptor- labeled antibodies or covalently using tag proteins. Alternatively, fluorescence-labeled ligands can be used with the advantage of a smaller size compared to antibodies and fluorescent proteins. Using ligands covalently linked to TR-FRET-compatible fluorophores, Albizu et al. (2010), observed GPCR dimerization in native tissue for the first time (Fig. 18). With this approach, using compatible specific fluorescent ligands (NAPSLumio4Tb and SCH442416dy647), Dr. Ciruela's group observed endogenous receptor oligomers between D₂R and A_{2A}R in native tissue (Fig. 18) (Fernández-Dueñas et al., 2015). Similarly, with TR-FRET compatible ligands, Hounsou et al. (2015) detected D₁R-D₃R heterodimers.



Figure 18. Detection of endogenous receptor oligomers of D_2R and $A_{2A}R$ s in native tissue by TR-FRET compatible specific fluorescent ligands (NAPSLumio4Tb and SCH442416^{dy647}). Adapted from Fernández-Dueñas et al. (2015).

FRAP (fluorescence recovery after photobleaching) is used to study the diffusion within membranes of fluorescently labeled proteins and real time interactions. In this technique, non-bleached fluorescent receptors diffuse into a defined region of interest, whose molecules have been photobleached by the application of an intense pulse of laser light. The diffusion coefficient and the mobile fraction depends on the mobility properties of the molecules studied (Kraft and Kenworthy, 2012; Guo et al., 2017).

FRET spectrometry. Experimental approach used to determine the stoichiometry and quaternary structure of proteins. It is based on FRET and uses optical microspectroscopy technology in order to probe the structure of dynamic protein complexes in living cells (Raicu and Singh, 2013). It depends on measuring and analyzing the distributions of apparent FRET efficiency (E_{app}), across FRET-image pixels of individual cells expressing proteins of interest (Raicu and Singh, 2013). From the obtained data can be deduced the most probable quaternary structure of protein complexes and their size and shape (Guo et al., 2017).

2.4.3. Immunochemical methods

Proximity ligation assays (PLAs). This technique allows the direct detection of molecular interactions between two endogenous or transfected proteins without the need of fusion proteins and with the advantage, compared to immunoprecipitation, which do not require membrane solubilization. Labeling heterodimers by PLA requires both receptors to be sufficiently close to allow the two antibody-DNA probes to form double stranded segments (<17 nm), a signal that is further amplified in the presence of fluorescent oligonucleotides (Söderberg et al., 2008) (Fig. 19). Heteromers are observed as red dots when observed in a confocal microscope equipped with an apochromatic 63X oil-immersion objective, and a 561nm laser line (Taura et al., 2015). This technique has been recently used to demonstrate GPCR heteromerization in mammalian tissues (Farré et al., 2015; Viñals et al., 2015; Fernández-Dueñas et al., 2015; Moreno et al., 2017, 2018) but also to demonstrate A_1R homodimerization (Gracia et al., 2013b).

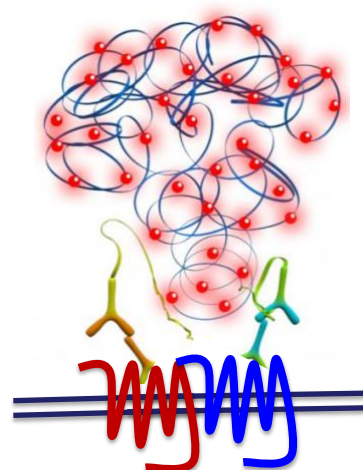


Figure 19. Schematic representation of PLA technique.

Co-localization. Using properly labeled antibodies against the receptors of interest and using confocal microscopy, it is possible to localize the receptors in native tissues. It is also possible to hypothesize that they are interacting if the emission of both receptors superposes. As an example, this technique has been used as a tool to demonstrate D₁R-Galanin receptor 1 and D₅R-Galanin receptor 1 heteromers in transfected living cells (Moreno et al., 2011).

2.4.4. Physiological methods

Single fluorescent-molecule video imaging appears to be a highly suitable method for determining both whether GPCRs form dimers or oligomers and how long these forms last. By using these techniques, all fluorescent GPCR molecules at the cell surface could be tracked. The first step is the labeling of the protein of interest with a ligand conjugated with a fluorescent dye. Using TIRF illumination, the process by which ligands bind to the receptor molecules was observed at the single-molecule level. Based on the single-molecule images, a 2D–3D Scatchard plot was constructed and used to determine the number of receptor molecules bound by the fluorescent ligand, the dynamic equilibrium of the monomer and dimers, the 2D equilibrium constant and the dissociation and association rate constants (Guo et al., 2017).

Spatial intensity distribution analysis can measure protein oligomeric size (in subunit counts) and density distributions from the intensity information recorded in individual conventional laser scanning fluorescence microscopy images. SpIDA was previously used to quantify the density of spatially mixed monomeric and dimeric populations of receptors localized on the plasma membrane of intact cells. The method is based on fitting fluorescence intensity histograms obtained from regions of interest (selected within single images) to obtain density maps of fluorescent molecules and molecular aggregates along with their quantal brightness, which indicates their oligomeric state. Because distributions are measured from single images, this analysis can be applied to both live and chemically fixed cells and tissues (Godin et al., 2015).

2.4.5. X-ray crystallography of GPCRs

The determination of GPCR structure at high resolution using X-ray crystallography began with the structure of rhodopsin (Palczewski et al., 2000), whose first crystal structure was solved from diffraction data extending to 2.8-Å resolution. Now, an increasing number of X-ray crystallographic GPCR structures have appeared (Fig. 20) (Wu et al., 2010; Choe et al., 2011; Wu et al., 2012; Shonberg et al., 2015; Zhang et al., 2015). The relevance of crystal structures to GPCR oligomerization is the suggestion that the proteins will crystallize utilizing the same intermolecular contacts and faces as can be found when diffusing through the cell membrane and indeed several distinct potential dimer interfaces are starting to emerge from crystallographic studies. However, some of these interfaces might be artificial and potentially may not represent a functional biological assembly but still suggest possible scenarios related to the manner in which GPCRs interact with each other (Guo et al., 2017).

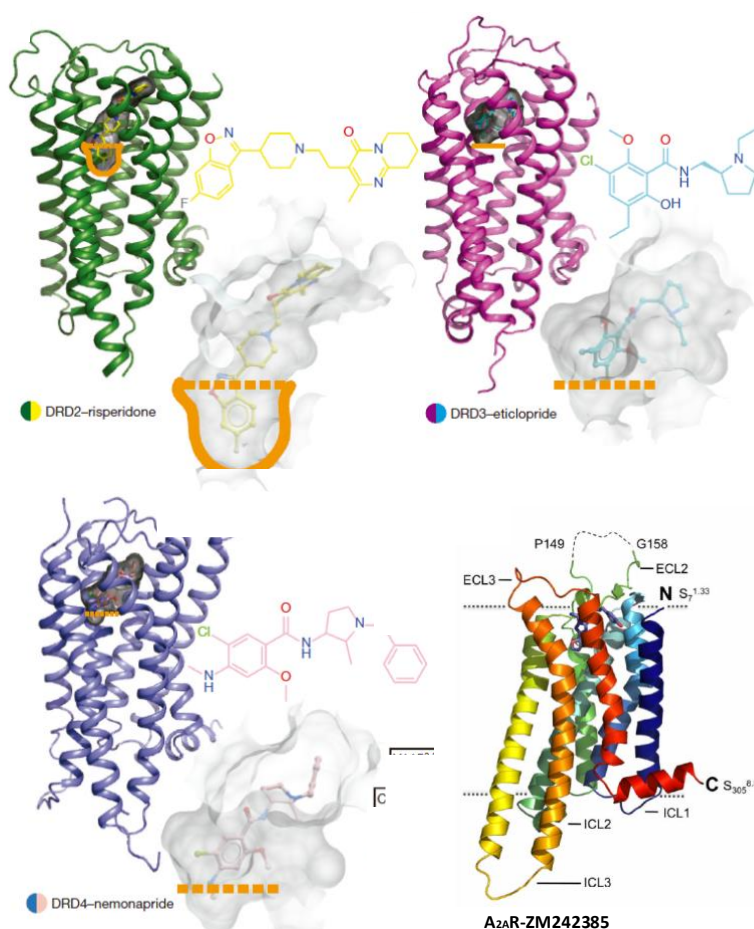


Figure 20. D₂R, D₃R, D₄R and A_{2A}R structures. Overview of D₂R-risperidone, D₃R-eticlopride, D₄R-nemonapride and A_{2A}R-ZM 242385 complex structures deduced from crystal structures in their inactive states. Dopamine receptor structures extracted from Wang et al. (2018) and Adenosine receptor structure from Doré et al. (2011).

2.4.6. Computational methods

Because of the limited high-resolution structural information on GPCRs, computational techniques such as protein–protein docking, molecular dynamics (MD) simulation and coarse-grained MD (CGMD) simulation are useful to predict their structure from the amino acid sequence (Pieper et al., 2013). Despite not having structure data of a particular protein, the computational model can be built using homologous proteins of known structure and similar sequence as a template. This is feasible because structure is more conserved than sequence. Moreover, a significant set of membrane proteins maintains a strong conservation of the TM structure even at low sequence identity because membrane proteins contain only two types of folds in their TM domains: α -helix bundles and β -barrels (Gonzalez et al., 2014).

In the context of GPCR oligomerization, the recent release of the high-resolution crystal structures of μ OR (Manglik et al., 2012) and β_1 -AR (Huang et al., 2013) in the form of homo-oligomers have facilitated the task of modeling GPCR dimers and higher order oligomers (Gonzalez et al., 2014).

In conclusion, computational models have been useful to study ligand binding, receptor specificity, receptor activation, G protein coupling, allosteric communication between protomers, among others but it is clear that the inclusion of experimental results are essential to improve the reliability of the models, and their predictive character (Gonzalez et al., 2014).

2.4.7. Ligand binding in oligomeric receptors

Saturation, competition and kinetic assays are the three types of ligand binding assays more commonly used to characterize GPCRs. In saturation experiments, tissue sections, cultured cells, or homogenates are incubated with an increasing concentration of a radioligand, which is usually a radiolabeled synthetic drug. The subsequent analysis using nonlinear regression programs measures the affinity of the labeled ligand for the receptor (equilibrium dissociation constant K_D), and the receptor density (B_{max}). In kinetic experiments, samples are incubated with a constant radioligand concentration and it is measured the rate of association (k_+) or dissociation (k_-) from a receptor, measuring its binding along the time. However, in pharmacological studies, competition binding assays are the most widely used to determine the affinity and selectivity of an unlabeled ligand to compete for the binding of a fixed concentration of a radiolabeled ligand to a receptor (Fig. 21). Quantitative autoradiography and positron emission tomography (PET) image analysis are other sensitive techniques used to detect low levels of radiolabeled ligands and to determine the anatomical distribution of receptors in tissue slices or in whole organs (Maguire et al., 2012).

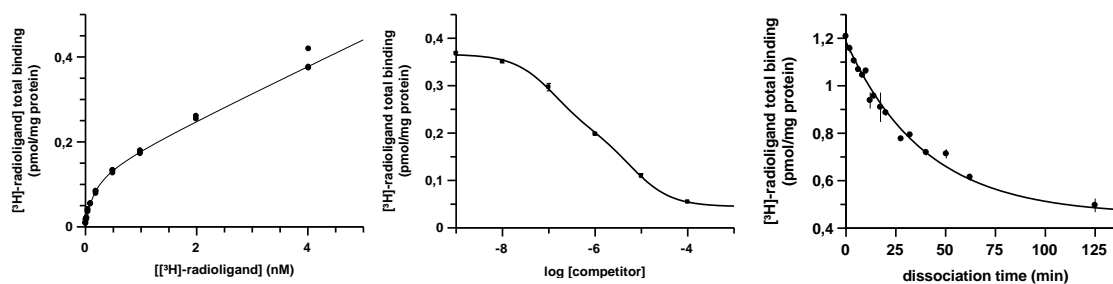


Figure 21. From left to right: saturation, competition and kinetic binding assays.

Recent literature has confirmed altered pharmacological properties of GPCR oligomers resulting from allosteric communication between protomers. Concretely, three major allosteric modulations emerge within GPCR oligomers (homo- and heteromers). First, the binding of a ligand to an allosteric site can modify the efficacy (which determines the power of a ligand to induce a functional response) and/or affinity of any ligand binding to the orthosteric site in any protomer of the oligomer. Second, conformational changes induced by the binding of an orthosteric ligand can be transmitted from the binding site of one protomer to the other, resulting in an increased or decreased propensity of the second molecule to bind, which results in a modification of the affinity and/or efficacy of the partner receptor. This phenomenon is known as positive or negative cooperativity when talking about the same agonist that bind to a homodimer, positive or negative crosstalk when talking about agonists that bind to a heteromer or crossantagonism when talking about how an antagonist can alter the binding/signaling properties of the partner receptor within the heteromer. Third, there exists a ligand-independent allosteric modulation that occurs when one receptor of the oligomer acts as a modulator of the pharmacological properties of the other molecularly different receptor; in this case, the modulator is not a ligand, but a protein (Kenakin and Miller, 2010; Ferré et al., 2014, 2016).

In conclusion, GPCR dimerization can result in altered binding properties that are not compatible with the model that one single independent GPCR binds one ligand. Upward concave nonlinear Scatchard plots in saturation experiments and biphasic curves in agonist-antagonist

competitive-inhibition experiments are examples of radioligand binding experiments with complex binding only explainable by the existence of oligomers.

Dissociation kinetic experiments of a tracer ligand in the absence or presence of a second ligand is a key and sensitive method to detect interactions between two topographically distinct binding sites. This is because ligands that compete for the same site on a monomeric receptor do not influence one another's dissociation kinetics. In contrast, allosteric modulations between two simultaneously bound and interacting sites (within a receptor monomer or across a receptor dimer or oligomer) alter ligand dissociation parameters (May et al., 2007). This analysis has been used to demonstrate homomerization of several GPCRs (Urizar et al., 2005; Albizu et al., 2006, 2010; Springael et al., 2006; May et al., 2011).

2.4.8. Signaling fingerprint

Once proved the possibility of oligomer formation among specific GPCRs, more techniques such as the analysis of the signaling, are needed in order to prove its existence in native tissues or at least to be able to detect some of specific characteristics that could be used as oligomerization fingerprints *in vivo*. Some of the most frequently studied signaling pathways are those that modulate ERK and AKT phosphorylation and cAMP and Ca²⁺ intracellular levels.

Conformational changes caused by GPCR dimerization can modify signaling properties of a receptor such as leading to signaling empowerment or attenuation (crosstalk if both ligands are agonists and crossantagonism if we test the ability of an antagonist to decrease the effect of the agonist of the partner receptor) or even can lead to the generation of novel pharmacological effects through a switch in signaling due to induction of coupling to another G-protein subtype. As an example, within the A_{2A}R-D₂R heteromer, the binding of an A_{2A}R agonist is able to reduce the binding efficacy of D₂R ligands by the mechanism of negative crosstalk (Ferré et al., 2001), similarly as in the A_{2A}R-A₁R heteromer, where the binding of A_{2A}R agonists to the receptor, leads to a reduction of the efficacy of A₁R (Ciruela et al., 2006). As an example of a signaling enhancement, D₃R agonists increase the affinity of D₁R for their agonists within the D₁R-D₃R heteromer (Marcellino et al., 2008). This causes a positive crosstalk at the level of MAPK signaling (Guitart et al., 2014). Moreover, as an example of a signaling switch, D₁R normally signals through G_s but, when heteromerizes with histamine H₃ receptor, signals through G_i (Ferrada et al., 2009). In addition, the formation of the CB₁R-5-HT_{2A}R heteromer may lead to a switch in G protein coupling for 5-HT_{2A}R from G_q to G_i (Viñals et al, 2015). Moreover, A_{2A}R normally signals through G_s and CB₁R through G_i but, surprisingly, the A_{2A}R- CB₁R heteromer signals through G_q (Moreno et al., 2018).

The ligand-induced allosteric interactions (crosstalk and crossantagonism) within the oligomer can be reverted by using selective peptides with the sequence of specific TMs of the studied receptors. These peptides can destabilize the homodimer or heteromer interface and are an innovative approach to confirm not only that the allosteric modulations observed are due to the homo- or hetero-dimerization but also which transmembrane domains of the receptors are involved in the oligomerization (Guitart et al., 2014, Viñals et al., 2015; Moreno et al., 2017, 2018).

3. ANALYZING RADIOLIGAND BINDING DATA: MONOMERIC vs DIMERIC MODELS

Colquhoun (1973) and Thron (1973) pioneered some studies that led to the subsequent development of models for neurotransmitter and/or hormone receptors that wanted to explain the behavior of GPCRs. Most of the developed models consider that there are at least 2 or 3 conformational forms that can be in equilibrium or not. One of the conformational forms is capable of signaling, and it is considered the “active” molecule, another one is considered to be the inactive state of the receptor and the last one is weakly active. These models can imply or not the coupling and decoupling of G proteins to GPCRs that act as allosteric modulators of the ligand binding. Most of these models generate an overparameterization except the “two-independent-site model” that is the approach most simple and most often used to deal with radioligand binding data. This model can explain both monophasic and biphasic binding curves and is based on two assumptions: one is that receptors are monomeric and another is that there are two populations of receptors, one is coupled to a G-protein and displays high-affinity (K_{DH}), whereas another is uncoupled from any G-protein and displays low-affinity (K_{DL}) binding for agonists. High affinity receptors can be converted to low affinity receptors by adding GTP, which uncouple the G protein from the receptor (De Lean et al., 1980). These two different forms of the receptor have to be independent and cannot be in equilibrium (see Fig. 22).

When there is only one population of receptors or when the ligand recognizes with the same affinity both populations (R_H and R_L), such as the case of an antagonist, a simplification of the “two-independent-site model” is used: the classical one-site receptor model. In this scenario, monophasic competition curves are observed.

$$A_{bound} = \frac{R IC_{50}}{IC_{50} + B}$$

When there are two populations, a biphasic curve is observed in competition assays, and the equation used is:

$$A_{bound} = \frac{R_H IC_{50H}}{IC_{50H} + B} + \frac{R_L IC_{50L}}{IC_{50L} + B}$$

where R , R_H and R_L are the specific binding in the absence of competing ligand. IC_{50} , IC_{50H} and IC_{50L} of the compound B are apparent constants and are related with the respective equilibrium dissociation constants K_D , K_{DH} and K_{DL} according to Cheng and Prusoff (1973) equation:

$$IC_{50H} = K_{DH} \left(1 + \frac{A}{K_{DA}}\right) \quad IC_{50L} = K_{DL} \left(1 + \frac{A}{K_{DA}}\right)$$

However, this approach is meaningful only if the two states of the receptor with high- and low-affinity for ligands are totally independent, i.e. they are not in equilibrium and they cannot be converted into each other. This is possible in artificial systems such as that described by Whorton et al. (2007) but there is evidence that it is not likely to happen in cells. Moreover, in order to explain complex radioligand binding curves, the monomer-G protein model assumes a preexisting proportion of both populations of receptors and, consequently, a limited pool of G proteins. This assumption is difficult to reconcile with the fact that the expression levels of G proteins in native cell systems clearly exceeds those of GPCRs (Neubig, 1994).

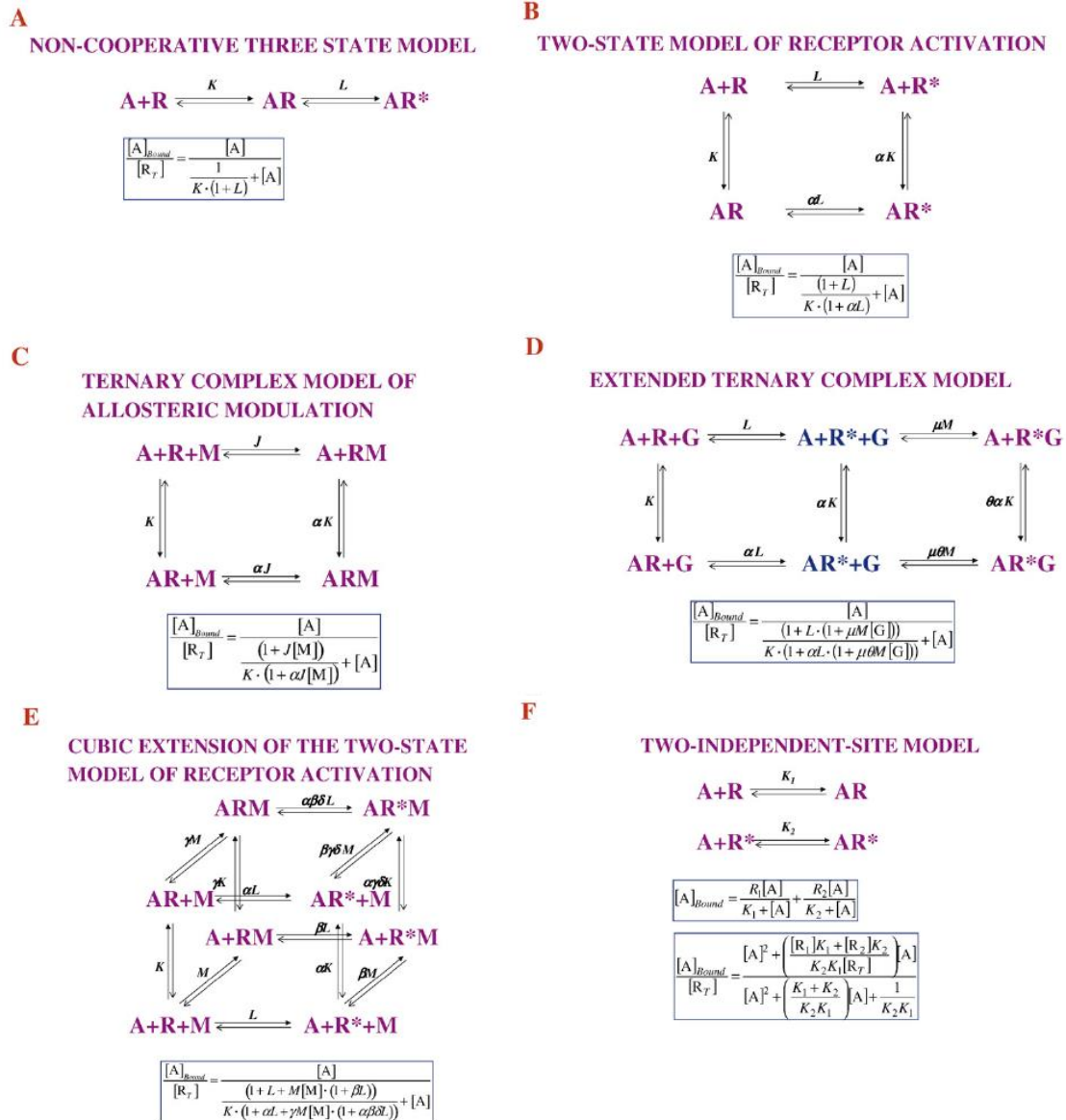


Figure 22. Different models of receptor operation assuming that receptors are monomeric. For each model, the binding isotherm equation is provided. R denotes receptor, R* denotes activated receptor (able to couple to the signaling machinery), A denotes the agonist/antagonist, G denotes a G protein, and M denotes the allosteric modulator which can be a G protein. Each equation can be further studied in: A) del Castillo and Katz (1957); B) Leff, (1995); C) De Lean et al. (1980) and Tuček and Proška, (1995); D) Samama et al. (1993); E) Weiss et al. (1996a, 1996b, 1996c) and Hall (2000); F) Casadó et al. (1990). Extracted from Casadó et al. (2007).

In contrast, the dimer-cooperativity models, considers oligomerization (Wreggett and Wells, 1995; Chidiac et al., 1997), or at least GPCR dimers (Durrux, 2005; Franco et al., 2005; Casadó et al., 2007; Rovira et al., 2008, 2009). In this scenario, communication through the two protomers allows negative cooperativity, meaning that the binding of a ligand to the first protomer decreases the affinity of the ligand for the second protomer.

Cooperativity (positive or negative) is a particular type of allosteric modulation in receptor oligomers, where the protomers of a homodimer are the conduit of the allosteric modulation and the same ligand, when bound to the first protomer, is the allosteric modulator to the binding to the second protomer. This mechanism does not assume a limited pool of G proteins, which are always present and act as additional allosteric modulators that increase the affinity of the

agonist and provide the conformation of the dimer that allows the negative cooperativity of a ligand through the protomers (Cui and Karplus, 2008; Ferré et al., 2014).

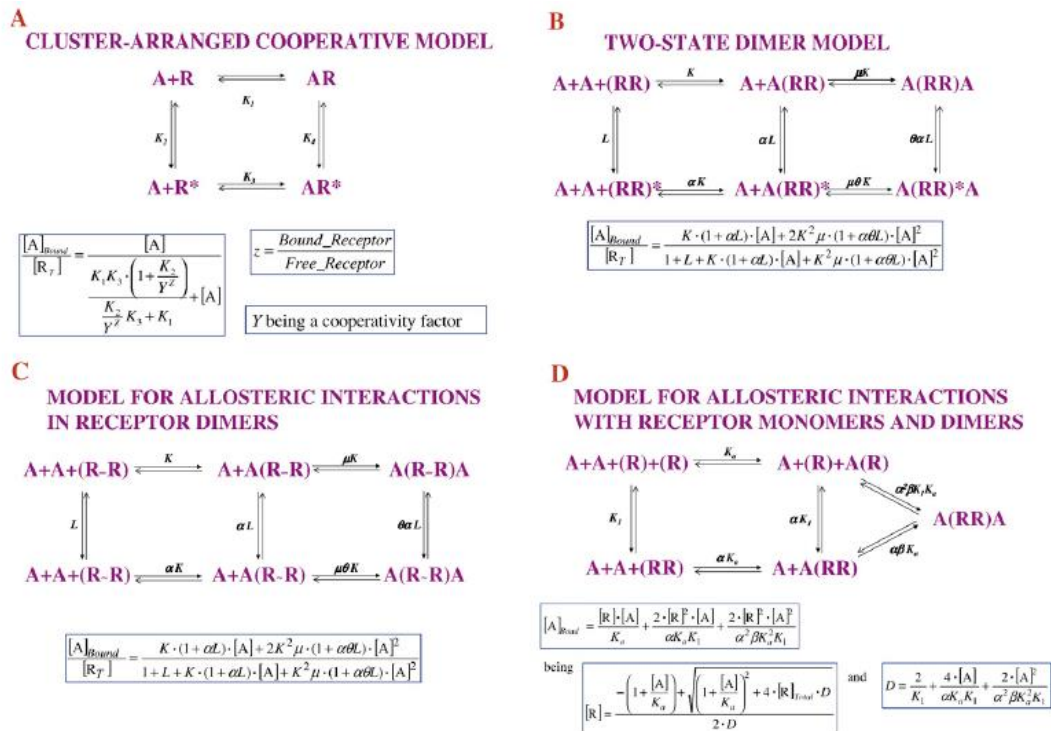


Figure 23. Different models of receptor cooperativity (panels A–D) assuming receptor monomers or receptors dimers. For each model, the binding isotherm equation is provided. Schemes taken (with modifications) from the work of A) Franco et al. (1996); B) Franco et al. (2005, 2006); C) and D) Durroux (2005). Extracted from Casadó et al. (2007).

When handling with complex radioligand-binding curves, the use of the traditional two-independent-site model generates values for the equilibrium dissociation constants and for the number of receptors that vary significantly depending on the concentration of the radioligand employed. This indicates a lack of robustness of the two-independent-site model that can be overcome by using a dimer receptor model (Casadó et al., 2009a; Ferré et al, 2014). In other cases, when working with receptor dimers and using monomeric models, dissociation constants determined in saturation and competition experiments are not the same (Strange, 2005; Maggio et al., 2013). In addition, concave-downward Scatchard plots, i.e. positive cooperativity (Albizu et al., 2006), only can be explained by dimeric models. Moreover, discrepancies in dissociation rate constants obtained with different radioligand concentrations (Casadó et al., 1991; Franco et al., 1996) and mismatches in constant values obtained when dissociation is performed by dilution vs. by an excess of unlabeled ligand (De Meyts et al., 1973; Urizar et al., 2005; Kara et al., 2010; Gracia et al., 2013b) cannot be explained by monomeric receptor models either. In contrast, with the two-state dimer model, the equilibrium dissociation constants are obtained irrespective of the concentration of the radioligand (Casadó et al., 2009b).

The dimer receptor model (Casadó et al., 2009a) is essential because it is the first that, by assuming the formation of receptor homodimers, can explain several experimental results previously considered erroneous due to their impossibility to be fitted. Furthermore, is easy-to-use, in contrast with other dimer receptor models (Durroux, 2005; Rovira et al., 2008, 2009)

Durroux (2005) presented two complex mathematical models: one considers that receptors oscillate between 2 dimeric states: The R~R in which the protomers are independent from one another and the R-R in which the protomers are able to establish a crosstalk. The other model considers that receptors oscillate between a monomeric state and a dimeric state in which protomers are able to crosstalk. It is not known if this switch is possible and if so, which is the proportion. Moreover, this model generates an overparameterization that makes them unlikely to be used.

Despite the evidence of GPCR homodimerization, the fact that biphasic competition curves can be also fitted with the two-independent-site model has caused that, for simplicity, most research groups still use classic equations instead of using dimer receptor models.

In our model, the equation describing a saturation experiment with the radioligand A is:

$$A_{\text{bound}} = \frac{(K_{DA2} A + 2 A^2) R_T}{(K_{DA1} K_{DA2} + K_{DA2} A + A^2)} \quad (\text{Eq. 1})$$

where A represents the free radioligand concentration, R_T is the total amount of receptor dimers, and K_{DA1} and K_{DA2} are the macroscopic equilibrium dissociation constants describing the binding of the first and the second ligand molecule to the receptor homodimer (Fig. 24).

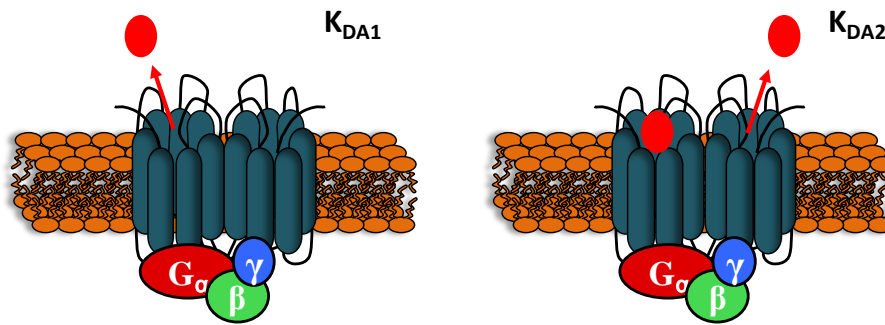


Figure 24. Schematic representation of the parameters obtained from a saturation radioligand binding assay fitting the data according to the dimer receptor model.

In addition, to calculate the macroscopic equilibrium dissociation constants involved in the binding of the agonist, the following equation for a competition binding experiment deduced by Casadó et al. (2007) is considered:

$$A_{\text{bound}} = \frac{\left(K_{DA2} A + 2 A^2 + \frac{K_{DA2} A B}{K_{DAB}} \right) R_T}{K_{DA1} K_{DA2} + K_{DA2} A + A^2 + \frac{K_{DA2} A B}{K_{DAB}} + \frac{K_{DA1} K_{DA2} B}{K_{DB1}} + \frac{K_{DA1} K_{DA2} B^2}{K_{DB1} K_{DB2}}} \quad (\text{Eq. 2})$$

where A represents the radioligand, R_T is the total amount of receptor dimers ($B_{\text{max}} = 2R_T$) and K_{DA1} and K_{DA2} are the macroscopic dissociation constants describing the binding of the first and the second radioligand molecule (A) to the receptor dimer; B represents the assayed competing compound concentration and K_{DB1} and K_{DB2} are, respectively, the equilibrium dissociation constants of the first and second binding of B ; K_{DAB} can be described as a hybrid equilibrium radioligand/competitor dissociation constant, which is the dissociation constant of B binding to a receptor dimer semi-occupied by A (Fig. 25).

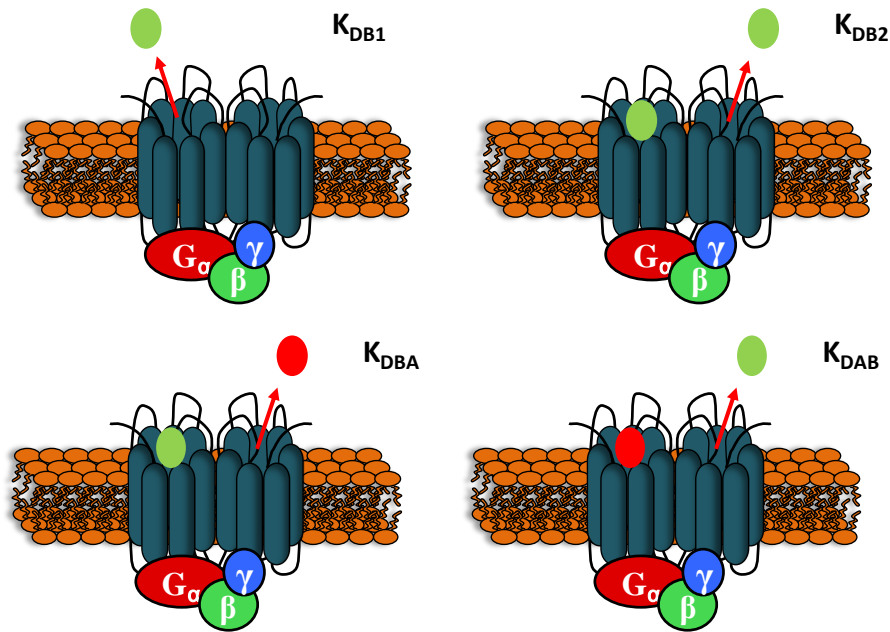


Figure 25. Schematic representation of the parameters obtained from a competition radioligand binding assay fitting the data according to the dimer receptor model.

Depending on the characteristics of the ligands (the radioligand A and the competitor B) the following simplifications of the equation (2) can be developed:

For A non-cooperative, the equation is simplified due to the fact that $K_{DA2} = 4K_{DA1}$:

$$A_{\text{bound}} = \frac{\left(4 K_{DA1} A + 2 A^2 + \frac{4 K_{DA1} A B}{K_{DAB}}\right) R_T}{4 K_{DA1}^2 + 4 K_{DA1} A + A^2 + \frac{4 K_{DA1} A B}{K_{DAB}} + \frac{4 K_{DA1}^2 B}{K_{DB1}} + \frac{4 K_{DA1}^2 B^2}{K_{DB1} K_{DB2}}} \quad (\text{Eq. 3})$$

For A and B non-cooperative, the equation is simplified due to the fact that $K_{DA2} = 4K_{DA1}$ and $K_{DB2} = 4K_{DB1}$:

$$A_{\text{bound}} = \frac{\left(4 K_{DA1} A + 2 A^2 + \frac{4 K_{DA1} A B}{K_{DAB}}\right) R_T}{4 K_{DA1}^2 + 4 K_{DA1} A + A^2 + \frac{4 K_{DA1} A B}{K_{DAB}} + \frac{4 K_{DA1}^2 B}{K_{DB1}} + \frac{K_{DA1}^2 B^2}{K_{DB1}^2}} \quad (\text{Eq. 4})$$

There is another important parameter, the dimer cooperativity index, important for pharmacological purposes. This dimer is calculated as follows:

$$D_{CA} = \log\left(4 \frac{K_{DA1}}{K_{DA2}}\right) \quad (\text{Eq. 5})$$

where 0 means noncooperative value, positive values indicate positive cooperativity, whereas negative values imply negative cooperativity.

The radioligand-competitor allosteric index can be calculated according to the equation:

$$D_{AB} = \log\left(2 \frac{K_{DB1}}{K_{DAB}}\right) \quad (\text{Eq. 6})$$

4. CATECHOLAMINES

Conventional neurotransmitters are endogenous chemical messengers that transmit signals across a chemical synapse, such as from a neuron to another target neuron, muscle, cell organ or other tissue. They are stored in synaptic vesicles, get released into the synaptic cleft when Ca^{2+} enters the axon terminal in response to an action potential, and act by binding to receptors on the membrane of the postsynaptic cell (Deutch, 2013).

The biogenic amines dopamine (3-hydroxytyramine, DA), norepinephrine (NE) and epinephrine (E), constitute a class of conventional neurotransmitters and hormones that occupy key positions in the regulation of physiological processes and in the development of neurological, psychiatric, endocrine and cardiovascular diseases (Eisenhofer et al. 2004). DA has been shown to have a key role in regulating affect, attention, behavior and cognition, motivation and reward, sleep and voluntary movement (Jauhar et al., 2017). NE is involved in alertness, mood, arousal, learning and memory, blood flow, and metabolism (Costa et al., 2012). E is the body's activator and is released in response to anxiety, exercise or fear and is a potent enhancer of learning and memory processing (Gold, 2015).

4.1. STRUCTURE, BIOSYNTHESIS AND RELEASE

These catecholamines are biosynthesized in both neuronal and non-neuronal cells, including the CNS, sympathetic nerves, adrenal medulla, gastrointestinal tract, pancreas, kidneys... They are now believed to be largely metabolized in the cells in which they are biosynthesized. In the CNS, DA and NE are widely distributed, whereas E is found in the mammalian brain in relatively low concentrations.

DA is incapable of crossing the blood-brain barrier so it must be synthesized inside the brain to perform its functions. Midbrain dopaminergic neurons are located in three major nuclei, including the substantia nigra pars compacta (SNc), that accounts for approximately of 70% DA in the brain, the ventral tegmental area (VTA) and the retrorubral field (Nair-Roberts et al., 2008).

NE is synthesized and released by the CNS in a part of the brain called the locus coeruleus (LC), that is the largest noradrenergic site in the brain of mammals and is the main source of NE to the neocortex (Chandler, 2016). It is a small pontine nucleus containing the entire population of noradrenergic neurons projecting to every major part of the brain and also to the spinal cord, that modulates sensory processing, motor behavior, attention, arousal and cognitive processes, and is implicated in a wide array of disease states (Berridge and Waterhouse, 2003; Sara and Bouret, 2012; Chandler, 2016; Llorca-Torralba et al., 2016).

NE is also synthesized by a division of autonomic nervous system called the sympathetic nervous system and is the main neurotransmitter used by this system. These sympathetic ganglia are connected to numerous organs, including the eyes, salivary glands, heart, lungs, liver, intestine, kidneys, urinary bladder, reproductive organs, muscles, skin, adrenal glands... and the effect of NE on each target organ is to modify its state in a way that makes it more conducive to activate body movement (Hamill et al., 2012).

Finally, E is normally produced by both the adrenal medulla (outside the CNS) and certain neurons (Kvetnansky et al., 2009).

Catecholamines are derived from the amino acid tyrosine, which is obtained mostly from dietary sources and some in the liver from the essential amino acid phenylalanine by the enzyme phenylalanine hydroxylase. The biosynthesis of DA and NE takes place within dopaminergic or noradrenergic neurons near the terminus of the axon and junction with the effector cell and begins with the active transport of the amino acid L-tyrosine (Tyr) into these neurons.

In the first step within the cytoplasm, tyrosine is converted to DOPA by tyrosine hydroxylase followed by conversion of DOPA to DA by DOPA decarboxylase (Fig. 26). This enzyme is not considered to be rate-limiting in physiological catecholamines synthesis, but it becomes rate-limiting in several pathological states, such as Parkinson's disease (PD) or the bipolar syndrome (Bertoldi, 2014).

In neurons that use DA as neurotransmitter, no further biosynthetic enzymatic modification occurs and DA is transported from the cytoplasm into synaptic vesicles by vesicular monoamine transporter (VMAT). Two closely related VMATs with distinct pharmacological properties and tissue distribution have been characterized: VMAT1 and VMAT2. DA, NE and E have 3-fold higher affinity for VMAT2 in comparison to VMAT1 (Erickson et al., 1996; Wimalasena, 2011).

DA is stored in these vesicles until it is ejected into the synaptic cleft by voltage-dependent calcium channels that trigger the fusion of the DA filled vesicles with the presynaptic membrane. These transporters permit vesicular uptake, storage, and regulated release of different catecholamines and other biogenic amines. Vesicular uptake prevents rapid degradation of monoamines in the cytoplasm, reduces cytoplasmic production of toxic metabolites of DA and other monoamines and sequesters neural toxins such as MPTP (1-methyl-4-phenyl-1,2,3,6-tetrahydro pyridine) (Guillot and Miller, 2009). The internal environment of these storage vesicles is more acidic (2.0–2.4 pH units lower) than the pH in the cytoplasm (Guillot and Miller, 2009). This low pH is essential to store high concentrations of protonated DA hydroxyl groups, protecting DA from auto-oxidation. DA sequestration also protects DA from enzymatic metabolism and keeps cytoplasmic DA levels down.

In the adrenal medullary chromaffin cells and in noradrenergic neurons, a proportion of the DA that is formed in the cytoplasm of the nerve terminal is actively transported into the storage vesicle by the VMAT and converted into NE by dopamine β-hydroxylase (Fig. 26). NE is in turn

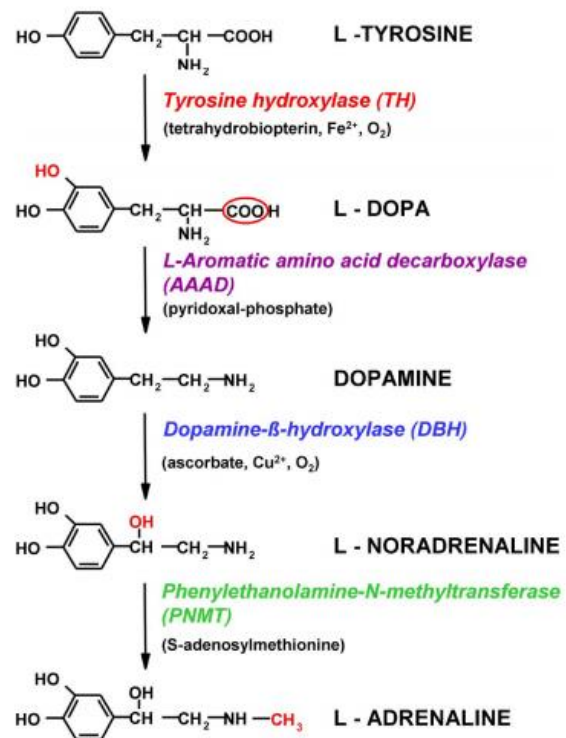


Figure 26. Pathway for catecholamine biosynthesis and its enzymatic steps. The steps of conversion L-tyrosine to L-NE are typical for sympathetic and some brain neurons, and the conversion of L-NE to L-E is typical for the adrenal medullary cells and some peripheral and brain neurons. Extracted from Kvetnansky et al. (2009).

stored in these vesicles until is ejected into the synaptic cleft. NE synthesis also requires a proton pump that drives down intravesicular pH and the synthesized neurotransmitter is stored in the vesicles, which concentrate it and protect it from metabolism until NE is released following nerve stimulation.

Cells and neurons using epinephrine as a neurotransmitter contain one additional enzyme, phenylethanolamine N-methyl transferase (PNMT), which catalyzes the S-adenosyl methionine (SAM)-dependent conversion of NE to E and S-adenosyl-L-homocysteine. Expression of PNMT in humans occurs largely in the adrenal gland where E functions as a hormone but with detectable levels in several other organs including the brain (Stratton et al., 2017).

4.2. DOPAMINE SYSTEM

Once in the synapse, DA binds to and activates DRs. These can be postsynaptic or presynaptic. Upon binding, the activation of the receptor triggers a complex chain of intracellular events that ultimately will lead to the activation or inhibition of the postsynaptic neuron. Finally, the dopaminergic signaling is terminated through the reuptake of DA from the synaptic cleft to the presynaptic terminal by the DA transporter. Once back in the cytosol, DA can either be broken down by the monoamine oxidase enzyme (MAO) or repackaged into vesicles by VMAT2 making it available for future release (Amara and Kuhar, 1993; Eiden et al., 2004)

Since the discovery of the physiological functions DA almost 60 years ago (Carlsson et al., 1957), this catecholaminergic neurotransmitter has attracted enormous attention. Although dopaminergic neurons are rare ($<1/10^5$ brain neurons), they regulate several key aspects of basic brain function including locomotor activity, motivation, memory and endocrine regulation. DA also plays an important role in the brain reward system that controls and stimulates the learning of many behaviors (Girault and Greengard, 2004). In the periphery, this catecholamine also plays multiple roles as a modulator of cardiovascular function, catecholamine release, hormone secretion, vascular tone, renal function, and gastrointestinal motility (reviewed in Missale et al., 1998 and Iversen and Iversen, 2007).

4.2.1. Dopamine system in the brain

Brain areas that synthesize DA have projections that give rise to four axonal pathways, named nigrostriatal, mesolimbic, mesocortical and tuberoinfundibular systems (Fig. 27) (reviewed in Iversen and Iversen, 2007).

The *nigrostriatal pathway* is formed by projections that arise from DA-synthesizing neurons of the midbrain nucleus, the SNc, which innervates the dorsal striatum (caudate and putamen) and is involved in motor control. Degeneration of nigrostriatal neurons causes Parkinson's disease.

The *mesolimbic pathway* originates from the midbrain VTA and innervates the olfactory tubercle, the ventral striatum (nucleus accumbens, NAc) and parts of the limbic system (amygdala and hippocampus). This pathway is implicated in the control of memory, motivation and emotional response, behavior and learning. It is also involved in the psychomotor effects generated by drugs of abuse including cocaine and methamphetamine (Koob, 1992; Wise, 2009).

The *mesocortical pathway* arises from the VTA and innervates different regions of the frontal cortex and it is involved in the control of cognitive functions. Finally, the *tuberoinfundibular pathway* arises from cells of the periventricular and arcuate nuclei of the hypothalamus and goes to the pituitary gland and is involved in hormone regulation, maternal behavior, pregnancy and sensory processes.

The dopaminergic system has been the focus of much research over the past decades mainly because several high impact pathological conditions such as PD, attention-deficit hyperactivity disorder (ADHD), schizophrenia, Tourette's syndrome, Huntington's disease, restless leg syndrome (RLS) and substance use disorders (SUD) among others, have been linked to a deregulation of dopaminergic transmission.

As an example, PD originates from a loss of striatal dopaminergic innervations in the brain (Ehringer and Hornykiewicz, 1960) and ADHD from a deregulation of adrenergic and dopaminergic systems (Mink, 2006; Swanson et al., 2007; Gizer et al., 2009). A role for abnormal dopaminergic signaling has also been suggested for other brain disorders, such as bipolar disorder, major depression, dyskinesias, and various somatic disorders, including hypertension and kidney dysfunction (Missale et al., 1998; Aperia, 2000; Carlsson, 2001; Iversen and Iversen, 2007). Hundreds of pharmacologically active compounds that interfere with DA receptor functions at the level of ligand binding have been developed, and many of these compounds have been used for clinical applications in the treatment of these and other disorders.

4.2.2. Structure of dopamine receptors

The physiological actions of DA are mediated by five distinct but closely related GPCRs that are divided into two major groups: the D₁-like, which comprises D₁ and D₅ receptors, and D₂-like, including D₂, D₃ and D₄ (D₄R) receptors. D₁-like receptors produce an increase of cAMP levels via G_{αs/olf} which stimulates AC and also produce activation of protein kinase A (PKA); moreover, their localization is mostly postsynaptic on DA-receptive cells, such as GABA-ergic medium spiny neurons (MSNs) in the striatum (Civelli et al., 1993). In contrast, D₂-like receptors inhibit AC via G_{αi/o} coupling and decrease cAMP, they also negatively modulate the activity of PKA and its effectors (Rangel-Barajas et al., 2015). In addition, D₂-like receptors activate K⁺ channels and reduce Ca²⁺ entry through voltage-gated channels (Nicola et al., 2000). D₂-like receptors are expressed postsynaptically on DA target cells and presynaptically on dopaminergic neurons (Sokoloff et al., 2006; Rondou et al., 2010).

The individual members of the subfamilies of the D₁- and D₂-like receptors share a high level of homology of their transmembrane domains and have distinct pharmacological properties. D₁R and D₅R are 80% homologous in their transmembrane domains, whereas D₃R and D₄R are 75% and 53% homologous, respectively, with the D₂R. Despite that the N-terminal domain has a similar number of amino acids in all DRs, the C-terminal of D₁-like receptors is seven-fold longer than the C-terminal of D₂-like receptors (Missale et al., 1998). They also differ on the IC3 domain

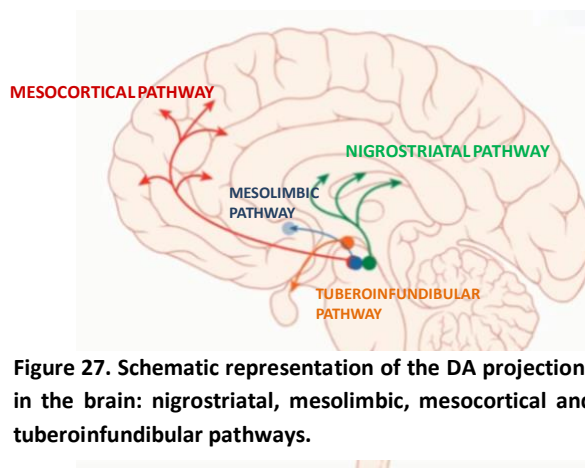


Figure 27. Schematic representation of the DA projections in the brain: nigrostriatal, mesolimbic, mesocortical and tuberoinfundibular pathways.

that is much longer for the D₂-like family than for the D₁-like. This is a common feature for G_i and G_s coupled receptors (Fig. 28) (reviewed in Civelli et al., 1993; Gingrich and Caron, 1993).

Sánchez-Soto et al. (2016) performed radioligand competition experiments in HEK-293 cells stably transfected with D_{2S}R, D_{2L}R, D₃R. These experiments revealed a high affinity (low K_i values) of DA for all the D₂-like receptors, with a rank order of D₃R > D₄R ≥ D_{2S}R = D_{2L}R. Moreover, NE showed high and similar affinity (around 50 nM) for the four D₂-like receptor subtypes. In the same study, by determining the cAMP inhibition, they saw that both DA and NE showed significantly low EC₅₀ values with D₃R and D₄R variants compared with D_{2L}R. Finally, by using G-protein BRET assays, they found that DA and NE had higher potencies for the D₄Rs than for the D₂R variants when coupled to G_{αi1} and G_{αi2} proteins but similar potencies when coupled to G_{αo1} or G_{αo2}. DA and NE showed higher potency for D₃R than for the other D₂-like receptors with all G_{αi/o} protein subunits with the exception of G_{αi2}, which seemed to be completely insensitive to DA or NE-induced D₃R activation.

D₁- and D₂-like receptors are also different at the level of genetic structure, primarily in the presence of introns in their coding sequences. The D₁R and D₅R genes do not contain introns in their coding regions; in contrast, the genes that encode D₂-like receptors have several introns. Therefore, the genetic organization of the D₂-like receptors provides the basis for the generation of receptor splice variants. For example, the alternative splicing of an 87-base-pair exon between introns 4 and 5 of the D₂R leads to the generation of two major D₂R variants that have been named D_{2S} (D₂-short) and D_{2L} (D₂-long) (Giros et al., 1989; Monsma et al., 1989). These two alternatively spliced isoforms differ in the presence of an additional 29 amino acids in the third intracellular loop. D_{2S} has been shown to be mostly expressed presynaptically and to be mostly involved in autoreceptor functions, whereas D_{2L} seems to be predominantly a postsynaptic isoform (Usiello et al., 2000; De Mei et al., 2009). Splice variants of the D₃R have also been described, and some of the encoding proteins have been shown to be essentially nonfunctional (Giros et al., 1991).

The D₄R gene contains quite a large number of polymorphisms in its coding sequence (La Hoste et al., 1996). The most extended polymorphism is found in exon 3, in a region that codifies for third cytoplasmic loop. It consists of a variable number of tandem repeats (TR), in which 48-base-pair sequence exists as a 2- to 11-fold repeat (Wang et al., 2004). The three most common variants in humans contain 2, 4 and 7 TR and code for a D₄R receptor with 2, 4 and 7 repeats of a proline rich sequence of 16 amino acids (D_{4.2}, D_{4.4} and D_{4.7} receptors). These repeats cause this protein to have a very high disorder index which increments with the number of repetitions (Fig. 29) (Woods, 2010). The DRD4 gene with four TRs constitutes the most frequent variant, with a global allelic frequency of 64%, followed by the variants with seven TRs (21%) and two TRs (8%) (Chang et al., 1996). It is interesting to notice that the seven-repeat allele is, at least, five to ten times younger than the common four-repeat allele but, nevertheless, have increased in frequency in human populations by positive selection (Ding et al., 2002).

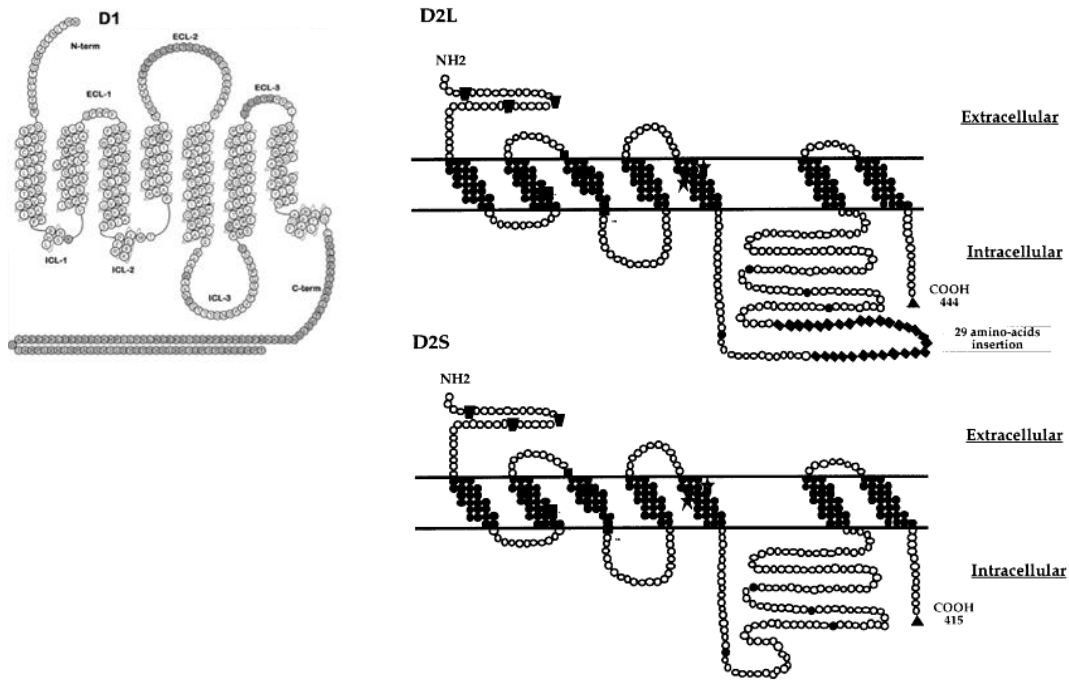


Figure 28. Scheme of D₁Rs and D₂Rs. Adapted from Vallone et al. (2000).

DRD4 polymorphic variants have been suggested to be associated with numerous behavioral individual differences and neuropsychiatric disorders. The most reported association is the link between the variant with seven repeats and ADHD (Faraone et al., 2005; Li et al., 2006; Gizer et al., 2009) and SUDs (McGeary, 2009; Belcher et al., 2014). Yet, very little is known about the role of the D₄R in the brain and even less about the functional differences between the products of the different polymorphic variants, which should explain their noticeable influence at the behavioral level.

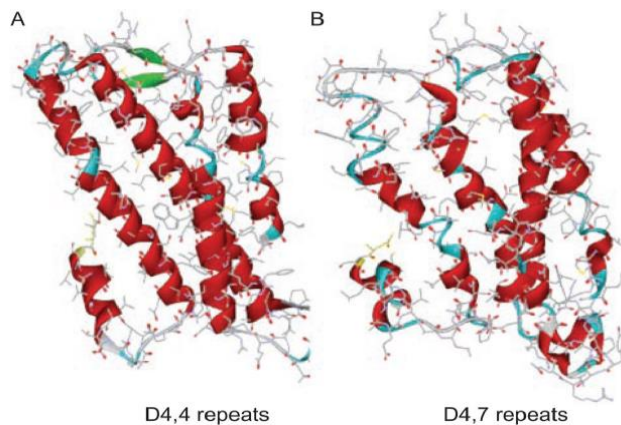


Figure 29. Model of the D_{4.4}R and D_{4.7}R. The third intracellular loop of D_{4.4}R has more α -helices than the D_{4.7}R. Extracted from Woods (2010).

In an effort to understand the functional and pharmacological role of the D₄R, it was generated a knock-in mouse with a humanized mouse DRD4 gene containing seven TRs of the human DRD4 in the homologous region of the mouse gene, which codes for the 3IL (D_{4.7}R mouse) (Gonzalez et al., 2012a). Curiously, the rodent gene does not have polymorphisms in the region coding for the 3IL of the D₄R, and wild-type control littermates (WT mouse) express a D₄R with a short 3IL comparable to the human D_{4.2} receptor (Gonzalez et al., 2012a). An *in vitro* study using D_{4.7}R mice showed a blunted MAPK signaling in striatal slices from these mice compared to WT D₄R,

as well as low ability of D_{4.7}R to interact with D₂R in transfected cells (Gonzalez et al., 2012a). Other groups also suggested that the D_{4.7}R variant could be less efficient at inhibiting AC but contradictory results have been reported (Asghari et al., 1995; Jovanovic et al., 1999). In Table 1 there is a summary of several studies performed in order to find dissimilarities between D₄R variants.

D₄Rs are able to form homodimers in HEK-293T transfected cells (Borroto-Escuela et al., 2011; Van Craenenbroeck et al., 2011). D_{4.4}Rs but not D_{4.7}Rs is also able to form heteromers with D_{2S}R in HEK-293T transfected cells and in striatal mice and rat slices (Gonzalez et al., 2012a). However, both variants are able to heteromerize with D_{2L}R in HEK-293T transfected cells but with less potency in the case of D_{4.7}R -D_{2L}R (Borroto-Escuela 2011). In addition, it has been reported that D₄Rs are also able to form heteromers with the adrenergic receptors α_{1B} and β_1 in rat pineal gland and in CHO transfected cells (Gonzalez et al., 2012b).

4.2.3. Dopamine receptor expression in the brain

DRs have broad expression patterns in the brain and in the periphery. In the brain, D₁Rs are the most widespread DA receptor and they are expressed at higher levels than any other DA receptor (Dearry et al., 1990; Fremeau et al., 1991; Weiner et al., 1991). D₁R has been found at a high density in the nigrostriatal, mesolimbic, and mesocortical areas, such as the caudate-putamen (dorsal striatum), nucleus accumbens, substantia nigra (SN), olfactory bulb, amygdala and frontal cortex, as well as at lower levels in the hippocampus, cerebellum and in thalamic and hypothalamic areas (Beaulieu and Gainetdinov, 2011).

D₅Rs are poorly expressed compared to D₁Rs. They are located at low levels in multiple brain regions, including pyramidal neurons of the prefrontal cortex (PFC), the premotor cortex, the cingulate cortex, the entorhinal cortex, the SN, the hypothalamus, the hippocampus, and the dentate gyrus. A very low level of expression has also been observed in the MSNs of the caudate nucleus and nucleus accumbens (Choi et al., 1995; Khan et al., 2000; Berlanga et al., 2005). A recent study in macaque frontal eye field, an area within the PFC involved in the control of visual spatial attention, indicated that D₅Rs are more prevalent on pyramidal neurons than on inhibitory interneurons and that are disproportionately expressed on putative long-range projecting pyramidal neurons, compared to interneurons, particularly in layers II–III (Mueller et al., 2018).

Post-synaptic D₂Rs are present in dopaminergic projection areas such as the striatum (50%), limbic areas (nucleus accumbens, olfactory tubercle), hypothalamus and pituitary gland. D₂R are also located pre-synaptically in the SNc, VTA and striatum, where they modulate the release of DA (De Mei et al., 2009). They are also expressed at significant levels in the cortical areas, septum, amygdala, and hippocampus (Missale et al., 1998; Gerfen, 2000a; Vallone et al., 2000; Seeman et al., 2006).

Table 1. Comparative characteristics of D₄R variants.

	D _{4.2}	D _{4.4}	D _{4.7}	References
DA release induced by METH	-	-	Significantly lower DA increase in D _{4.7} mice as compared to WT	Bonaventura et al., 2017
Psychomotor activation induced by METH	-	-	Significantly lower locomotor activation in D _{4.7} mice as compared to WT	Bonaventura et al., 2017
Glu Release in the NAC shell induced by METH	-	-	Significantly lower corticostriatal GLU release in D _{4.7} mice as compared to WT	Bonaventura et al., 2017
Optogenetic stimulation induced GLU release in the striatum	-	-	Significantly lower increase in extracellular GLU levels in D _{4.7} mice striatum as compared with WT	Bonaventura et al., 2017
Inhibition of forskolin stimulated cAMP levels by DA (EC ₅₀ nM)	Not significant differences found			Sánchez-Soto et al., 2016
	1.8 ± 0.2	1.4 ± 0.2	1.6 ± 0.3	
Inhibition of forskolin stimulated cAMP levels by NE (EC ₅₀ nM)	Not significant differences found			Sánchez-Soto et al., 2016
	54 ± 8	53 ± 8	53 ± 13	
Differences in the inhibition of β-arrestin-2 recruitment	Not significant differences found			Sánchez-Soto et al., 2016
Differences in the activation by DA and NE involving different Gai/o subtypes	Not significant differences found			Sánchez-Soto et al., 2016
Interaction with β-arrestin-1 and 2	+	+	+	Skieterska et al., 2016
Activation of the synchronous network activity in the PFC by PD168077	ND	Normal effects on excitatory and inhibitory network bursts	Over-suppression of Glu excitatory network bursts and under suppression of GABAergic inhibitory network bursts	Zong et al., 2016
Non-lysine ubiquitination promoted by KLHL12	+	+	Hardly observed	Skieterska et al., 2016
Formation of functional heteromers with D ₂₅ R	+	+	-	González et al., 2012
Allosteric interactions within D ₄ R- D ₂₅ R by MAPK	+	+	-	González et al., 2012
Formation of functional heteromers with D ₂₁ R	+	+	+ but lower BRET _{max} and higher BRET ₅₀ values	Borroto-Escuela et al., 2011
Allosteric interactions within D ₄ R- D ₂₁ R by MAPK	+	+	-	Borroto-Escuela et al., 2011
Functional activation by DA (EC ₅₀ in nM)	1.02 ± 0.06	4.89 ± 0.28*	1.07 ± 0.04	Wedemeyer et al., 2007
Functional activation by NE (EC ₅₀ in nM)	40.80 ± 0.97	43.50 ± 1.76	58.80 ± 2.31*	Wedemeyer et al., 2007
Potency of [³⁵ S]GTPγS binding (EC ₅₀ nM) following stimulation by DA or NE (100 mM NaCl)	Not significant differences found			Czermak et al., 2006
	92 ± 34 (DA) 756 ± 151 (NE)	129 ± 76 (DA) 1220 ± 209 (NE)	102 ± 58 (DA) 1190 ± 259 (NE)	
Inhibition of forskolin stimulated cAMP levels by DA (EC ₅₀ nM)	18.8 ± 2.7*	13.8 ± 2.7*	36.9 ± 4.6	Asghari et al., 1995

ND: not determined. *: statically significant (for more information, see references).

The D₃R and D₄R subtypes are much less abundant than the D₂R subtype and have different and more restricted tissue localization. The D₃R has a more limited pattern of distribution, the highest level of expression being observed in the limbic areas, such as in the shell of the nucleus accumbens, the olfactory tubercle, and the islands of Calleja (Sokoloff et al., 1992, 2006; Missale et al., 1998). At significantly lower levels, the D₃R is also detectable in the striatum, SNc, VTA, hippocampus, septal area, and in various cortical areas (Cortés et al., 2016). Notably, D₃Rs possess a high affinity for DA (420-fold higher than that of D₂R) and, unlike D₂Rs, small changes in their number or function may lead to dramatic effects on synaptic transmission, suggesting that D₃R could be critical modulators of normal dopaminergic function and, despite their localization, also of cognition (Maramai et al., 2016).

Low levels of D₄R have been found in the basal ganglia. In contrast, this receptor appears predominantly localized in the PFC, in GABAergic interneurons and in glutamatergic pyramidal neurons, including their striatal projections (Tarazi et al., 1998; Svingos et al., 2000; Lauzon and Laviolette, 2010), amygdala, hippocampus, hypothalamus, globus pallidus, substantia nigra pars reticulata (SNr), and thalamus (Missale et al., 1998; Rondou et al., 2010). In Rivera et al. (2008), authors performed an image analysis of the D₄R in the rat cerebral cortex. They saw a bilaminar organization of the D₄R in the rodent cortical layers that were in agreement with other studies (Ariano et al., 1997a; Defagot et al., 1997; Mauger et al., 1998; Wedzony et al., 2000) with the receptor being mainly concentrated in layers II/III, and IV. An interesting finding was that the laminar organization of the D₄Rs is complementary to the ones of other DAergic receptors. Thus, D₁Rs (Savasta et al., 1986; Al-Tikriti et al., 1992; Vincent et al., 1993), D₂Rs (Al-Tikriti et al., 1992; Vincent et al., 1993) and D₅Rs (Ariano et al., 1997b; Khan et al., 2000) are reported to be mainly localized in the deeper layers of the rat cerebral cortex. The differential localization of DRs in cortical layers could reflect the particular function that each one have in processing DAergic inputs (Gonzalez-Islas and Hablitz, 2003; Young and Yang, 2005; Wu and Hablitz, 2005). D₄Rs were mainly localized in cell bodies and dendrites of glutamatergic pyramidal neurons as well as in GABAergic interneurons. It has been reported that the D₄R could be an inhibitory modulator of cortical glutamate activity in the PFC (Rubinstein et al., 2001). Rivera et al. (2008) also concluded that the relationship between D₄R structures and DA and NE nerve terminal plexuses indicates, in view of the relative mismatches observed, that the D₄R may be activated by both DA and NE signals, results in agreement with the recently published Sánchez-Soto et al. (2016).

Khan et al. (1998), studied the distribution of D₄Rs in human brain tissues. They saw immunopositive neurons to D₄R antibodies in motor, visual and prefrontal cortices. In all three areas D₄R labeled neurons were located in all cortical layers, but particularly in layers IV–V. Labeling was predominantly associated with neural cell bodies and initial dendritic segments. Pyramidal and nonpyramidal D₄R positive neurons were visualized. Moreover, in the striatal compartments of human brain caudate and putamen, a diffuse neuropil immunostaining and numerous small size immunostained neurons could be detected with D₄R antibodies. This study is in agreement with Almeida and Mengod (2010), who studied the mRNA distribution of D₄R in monkey PFC. They detected D₄R mRNA in glutamatergic and GABAergic neurons in all cortical layers but layer I (predominantly in layer V) (Fig. 30).

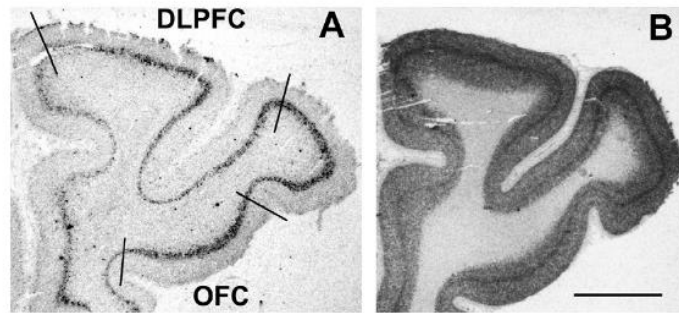


Figure 30. Autoradiographic localization of D2R (A) and D4R (B) mRNA in monkey prefrontal cortex. Both mRNA transcripts were visualized by in situ hybridization with oligonucleotides labeled with ^{33}P . Extracted from Almeida and Mengod (2010).

Interestingly, D_4R and D_2R seem to be colocalizing in the pyramidal glutamatergic neurons of the PFC and in their striatal terminals (Gaspar et al., 1995; Tarazi et al., 1998; Svingos et al., 2000; Lauzon and Laviolette, 2010; González et al., 2012b, Bonaventura et al., 2017).

4.2.4. Neuronal functions of dopamine receptors

The striatum is the main input structure of the basal ganglia (Kase, 2001), which is located in the telencephalon. The basal ganglia consist of several interconnected nuclei: the striatum, external globus pallidus (GPe), internal globus pallidus (GPi), SN, and the subthalamic nucleus (STN). Although in humans and non-human primates it has been classically subdivided into NAc, caudate and putamen, it can be functionally subdivided in three different compartments according to the cortical inputs: ventral, rostral-dorsal and caudal-dorsal striata (Fig. 31).

The ventral striatum, mostly the NAc with its two compartments, core and shell, and the olfactory tubercle, is innervated by the dopaminergic cells of the VTA. Moreover, the ventral striatum receives glutamatergic inputs from the ventromedial PFC, orbitofrontal cortex and anterior cingulate cortex (Haber and Behrens, 2014) (Fig. 31). In fact, the orbitofrontal cortex and the anterior cingulate cortex respectively receive partial and predominant dopaminergic innervation from the SNc (Haber and Behrens, 2014). Furthermore, the ventral striatum receives afferent glutamatergic projections from the insular cortex, amygdala and hippocampus (Haber and Behrens, 2014). The ventral striatum participates in motivation, reward and reinforcement learning and plays an important role in addiction (Koob, 1992; Hyman et al., 2006; Iversen and Iversen, 2007; Everitt and Robbins, 2016).

The rostral-dorsal striatum receives glutamatergic input from frontal and parietal association areas, such as the dorsolateral PFC, premotor cortex and parietal cortex and the caudal-dorsal striatum from the primary motor and somatosensory cortices (Fig. 31). Both rostral-dorsal and caudal-dorsal striata receive their dopaminergic input from the SNc (Haber, 2014; Haber and Behrens, 2014). The dorsal striatum is implicated in execution of learning and complex motor behavior (Koob, 1992; Hyman et al., 2006; Iversen and Iversen, 2007; Everitt and Robbins, 2016).

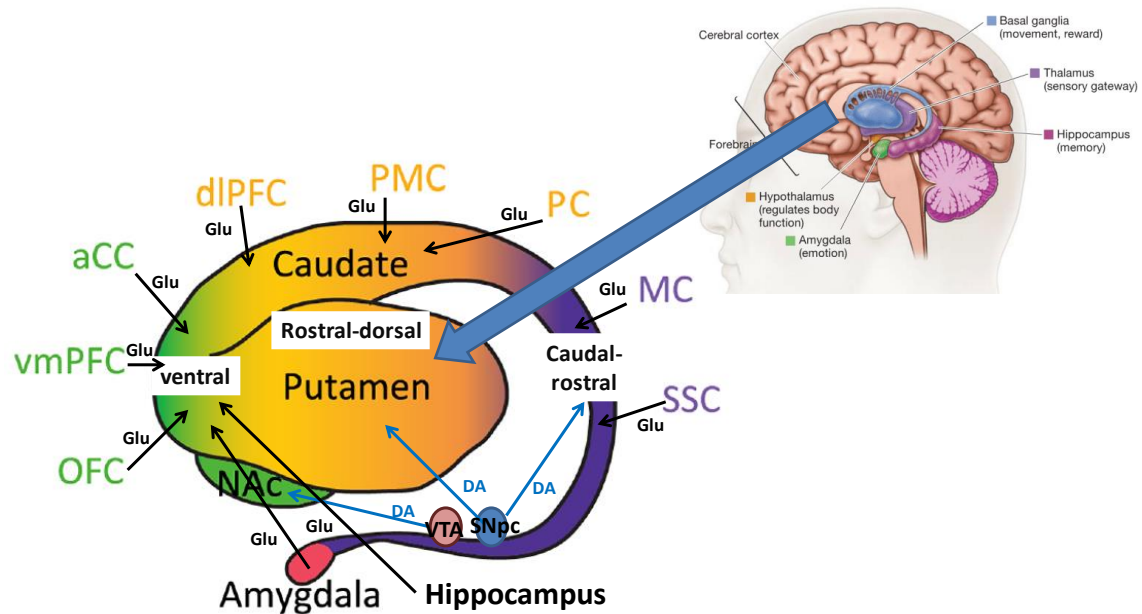


Figure 31. Inputs and outputs of the striatum. Lateral view of the striatum and amygdala (of human and non-human primates). vmPFC: ventromedial prefrontal cortex; OFC: orbitofrontal cortex; aCC: anterior cingulate cortex; dIPFC: dorsolateral prefrontal cortex; PMC: premotor cortex; PC: parietal cortex; MC: primary motor cortex; SSC: somatosensory cortex.

Striatum has high levels of DA and this catecholamine controls and regulates movement. Multiple lines of evidence indicate that locomotor activity is primarily controlled by D_1R , D_2R , D_3R and D_4R (Missale et al., 1998; Sibley, 1999; Bonaventura et al., 2017). An anatomical scheme for understanding the control of movement by the striatum was defined in the late 1980s (Penney and Young, 1986; Albin et al., 1989; DeLong, 1990). This scheme recognized that the majority of dorsal-striatal neurons are MSNs, of which there are two distinct classes, termed direct and indirect pathways (Alexander and Crutcher, 1990; DeLong, 1990; Gerfen et al., 1990; Graybiel and Kimura, 1995; Le Moine and Bloch, 1995). These populations exhibit distinct neurochemical expression patterns and anatomical projection targets (Fig. 32).

Direct pathway MSNs express D_1R s and project to the internal globus pallidus and SNr, whereas indirect pathway MSNs express D_2R s and project indirectly to the SNr by way of the GPe and STN. Based on this anatomy, DA produced by neurons from substantia nigra pars compacta induces motor activation via both activation of D_1R s in striatopallidal neurons of direct pathway and inhibition of striatonigral neurons of indirect pathway when acting on D_2R s. It has been demonstrated in many studies that activation of direct pathway striatal neurons promotes movement whereas activation of the indirect pathway inhibits movement (Sano et al., 2003; Durieux et al., 2009; Kravitz et al., 2010) so, due to the differential expression of D_1R s and D_2R s in the direct and indirect pathway, respectively, DA affects the neurons of each pathway differently allowing controlled movement (Gerfen et al., 1990). Thus, it is clear that the activation of both the postsynaptic D_1R and D_2R is necessary for the full manifestation of locomotor activity (White et al., 1988).

The activation of D_1R that are exclusively expressed on the postsynaptic neurons has a moderate stimulatory effect on locomotor activity. D_1R is coupled to $G_{\alpha s}$, which activates AC and increases intracellular cAMP (Kebabian and Calne, 1979; Stoof and Kebabian, 1981; Gerfen, 2000b). This

increase in cAMP results in multiple intracellular effects that increase the excitability of direct pathway neurons.

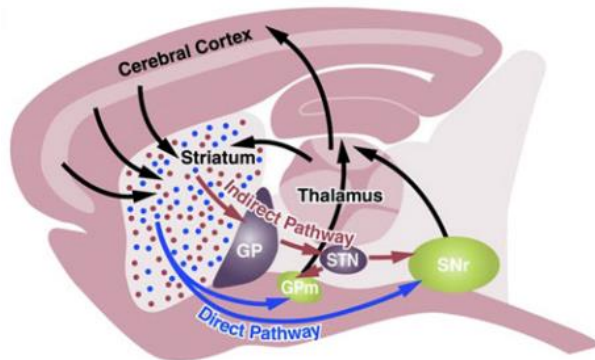


Figure 32. Direct- and indirect-pathway basal ganglia circuits. Sagittal view of a mouse brain, depicting cortex-basal ganglia-thalamus-cortex circuits. Extracted from Kreitzer and Malenka, (2008).

In contrast, the role of D_2 Rs is much more complex than of D_1 Rs because they result from both presynaptic and postsynaptic expression of these subtypes of receptors (Missale et al., 1998; Sibley, 1999). Presynaptically localized autoreceptors generally provide an important negative feedback mechanism that adjusts neuronal firing rate, synthesis, and release of the neurotransmitter in response to changes in extracellular neurotransmitter levels (Wolf and Roth, 1990; Missale et al., 1998; Sibley, 1999). Activation of postsynaptic D_2 Rs, coupled to $G_{\alpha i}$, inhibits AC and decreases intracellular cAMP which in turn decreases the excitability of indirect pathway neurons. In addition, regulation of cAMP/PKA signaling by DRs may directly or indirectly regulate the induction of striatal synaptic plasticity (Kreitzer and Malenka, 2008; Surmeier et al., 2009).

It should be noted that the splice variants of the D_2 Rs, D_{2L} Rs and D_{2S} Rs, seem to have different neuronal distributions, D_{2S} Rs being predominantly presynaptic and D_{2L} Rs being postsynaptic. D_3 Rs seem to exert a moderate inhibitory action on locomotion either by acting as autoreceptors or through the involvement of postsynaptic receptor populations (Sibley, 1999; Joseph et al., 2002). The roles of D_4 Rs and D_5 Rs in locomotor activity is unclear.

When striatal DA levels decrease in Parkinson's disease, activity in the direct pathway decreases and activity in the indirect pathway increases (Albin et al., 1989; Graybiel et al., 2000; Obeso et al., 2008; Smith and Villalba, 2008). On the other hand, excess of dopaminergic stimulation would lead to hyperkinesias. In Huntington's disease, hyperkinetic choreic movements are due to a gradual disappearance of the contribution of the indirect inhibitory pathway followed by the degeneration of the direct pathway and the nigrostriatal neurons (Glass et al., 2000). Therapies aimed at rebalancing the activity in these pathways are the basis for most therapeutic interventions (Filion et al., 1991; Kanda et al., 1998; Dostrovsky et al., 2000; Levy et al., 2001; Baron et al., 2002; Matsubara et al., 2002; Jenner, 2003).

Many other vital functions depend on the activation of brain DRs. D_1 Rs, D_2 Rs, and, to a lesser degree, D_3 Rs, are critically involved in reward and reinforcement mechanisms. Multiple studies have shown that pharmacological and genetic approaches that alter DA receptor function result in a significant modulation of the responses to natural rewards and addictive drugs. Thus, DRs remain an important topic of interest in drug addiction research (Missale et al., 1998; Hyman et al., 2006; Sokoloff et al., 2006; Di Chiara and Bassareo, 2007; De Mei et al., 2009; Koob and Volkow, 2010).

Both D₁Rs and D₂Rs seem to be critical for learning and memory mechanisms, such as working memory, that are mediated primarily by the PFC (Goldman-Rakic et al., 2004). At the same time, D₃Rs, D₄Rs and, potentially, D₅Rs, seem to have a minor modulatory influence on some specific aspects of cognitive functions (Missale et al., 1998; Sibley, 1999; Sokoloff et al., 2006; Rondou et al., 2010). In addition, the fact that essentially all clinically effective antipsychotics have the ability to block D₂Rs indicates that these receptors are likely to play a critical role in the psychotic reactions observed in schizophrenia and bipolar disorder (Snyder et al., 1970; Roth et al., 2004). Other functions are mediated, in part, by various dopamine receptor subtypes in the brain, such as affect, attention, impulse control, decision making, motor learning, sleep, reproductive behaviors, and the regulation of food intake (Missale et al., 1998; Di Chiara and Bassareo, 2007; Iversen and Iversen, 2007; Koob and Volkow, 2010; Rondou et al., 2010; Yoon and Baik, 2015).

In general, the specific physiological roles played by D₃R, D₄R, and D₅R in the brain are not well known. However, a recent study published by Bonaventura et al. (2017), led to the demonstration of a significant role of D₄R in the modulation of corticostriatal glutamatergic transmission. In the same article, Bonaventura et al. (2017) revealed that the D_{4.7}R subtype could have important implications for the understanding of neuropsychiatric disorders such as ADHD and SUD.

Moreover, it has been established a main role of the D₄R-D₂5R heteromer in the brain: the inhibitory dopaminergic control of corticostriatal neurotransmission (Maura et al., 1988, Gonzalez et al., 2012a; Bonaventura et al., 2017), both at the dendritic level (PFC) and at the terminal level (NAc shell). Concretely, they are involved in the decrease of glutamate release in the striatum. This can explain the previously documented increases of striatal extracellular Glu levels in DRD4 knock-out mice (Thomas et al., 2009).

It was demonstrated, with D₄Rs expressed in cultured cells, a specific decreased ability of the D_{4.7}R to molecularly interact (oligomerize) with the D₂R than the more common D_{4.4}R receptor (Gonzalez et al., 2012a). If we add this to the fact that DA is significantly more potent at activating any D₄R variant (D_{4.2}R, D_{4.4}R and D_{4.7}R) than D₂Rs (D_{2.5}R or D_{2L}R) according to Sánchez-Soto et al. (2016), and that DA is also more potent at activating D₄Rs (including the D_{4.7}R variant) than D₂R-D₄R heteromers (results from this Thesis), the inability of D_{4.7}R to heteromerize should lead to a gain of function. These experiments performed in transfected cells, are in according with those published by Bonaventura et al. (2017). In this study, the analysis of cortical ERK1/2 phosphorylation and the measurement of striatal glutamate release with the optogenetic-microdialysis technique allowed the demonstration that D₄Rs mediate a significant inhibitory role of DA that was higher in the case of D_{4.7}R knock-in mice. These results are also in agreement with Zhong et al. (2016) who, with an *in vitro* electrophysiological study in cortical slices from DRD4 knock-out mice, reported an increased ability of a putative selective D₄R agonist to suppress glutamatergic excitatory network bursts upon viral infection with human D_{4.7}R, as compared with D_{4.4}R cDNA or as compared with the suppression observed in slices from WT mice.

In the cerebral cortex, a predominant localization of the D₄R has been extensively described in the prefrontal and entorhinal cortices, in both pyramidal and non-pyramidal neurons (Ariano et al., 1997a; Defagot et al., 1997; Primus et al., 1997; Tarazi et al., 1997; Wedzony et al., 2000). This evidence supports the notion of a crucial role of the D₄Rs in dopaminergic (DAergic)

mechanisms that regulate cortical function, through pyramidal neurons or via modulation of GABA interneurons that innervate pyramidal neurons (Mrzljak et al., 1996; Goldman-Rakic, 1998).

Other functions mediated by DRs that are localized outside the CNS include olfaction, vision, and hormonal regulation, such as the pituitary D₂R-mediated regulation of prolactin secretion; kidney D₁R-mediated renin secretion; adrenal gland D₂R-mediated regulation of aldosterone secretion; the regulation of sympathetic tone; D₁R, D₂R, and D₄R-mediated regulation of renal function; blood pressure regulation; vasodilatation; and gastrointestinal motility (Missale et al., 1998; Aperia, 2000; Carlsson, 2001; Witkovsky, 2004; Li et al., 2006; Iversen and Iversen, 2007; Villar et al., 2009).

4.3. NOREPINEPHRINE SYSTEM

NE is synthesized and released by the CNS and also by the sympathetic nervous system. In the brain, NE is mainly produced in the locus coeruleus (LC). In the sympathetic nervous system, NE is used as a neurotransmitter by sympathetic ganglia located near the spinal cord or in the abdomen, and it is also released directly into the blood stream by the adrenal glands as sympathetic effector organs.

The main function of NE is to mobilize the brain and body for the so-called fight-or-flight response, i.e., the ability to react to acute stress. NE release is lowest during sleep, rises during wakefulness, and reaches much higher levels during situations of stress or danger. In the brain, NE increases arousal and alertness, promotes vigilance, enhances formation and retrieval of memory, and focuses attention; it also increases restlessness and anxiety. NE also increases heart rate and blood pressure, triggers the release of glucose from energy stores, increases blood flow to skeletal muscle, reduces blood flow to the gastrointestinal system, and inhibits voiding of the bladder and gastrointestinal motility.

4.3.1. Adrenergic system in the brain

The LC was the first modulatory system to be delineated anatomically and specified neurochemically (Dahlström and Fuxe, 1964). LC is comprised of only 1,500 neurons in the rat (around 15000 in humans/hemisphere) and is situated deep in the pons. It receives afferents from the midbrain and brainstem conveying information about visceral and sympathetic nervous system function as well as pain and threat. It also receives inputs from the forebrain such as the hypothalamus, the amygdala and the PFC that provide complex emotional homeostatic and cognitive information. The LC also receives projections from various neuromodulatory brain regions, including the VTA (dopamine) and dorsal raphe (serotonin). Together, these afferents connections allow for modulation of the LC neural processing by basic sensory and visceral experiences, as well as regulation by top-down influences from forebrain structures conveying highly processed cognitive/emotional information (Berridge and Waterhouse, 2003; Aston-Jones and Cohen, 2005; Sara and Bouret, 2012).

Despite the small number of neurons in the LC, it projects broadly to most forebrain regions as well as some midbrain and brainstem nuclei and the cerebellum and spinal cord (Berridge and Waterhouse, 2003; Aston-Jones and Cohen, 2005; Valentino and Van Bockstaele, 2008; Sara and Bouret, 2012). Related to learning and memory, the LC sends also strong efferent projections to the amygdala and PFC (Fig. 33) (Fallon et al., 1978; Arnsten and Goldman-Rakic, 1984).

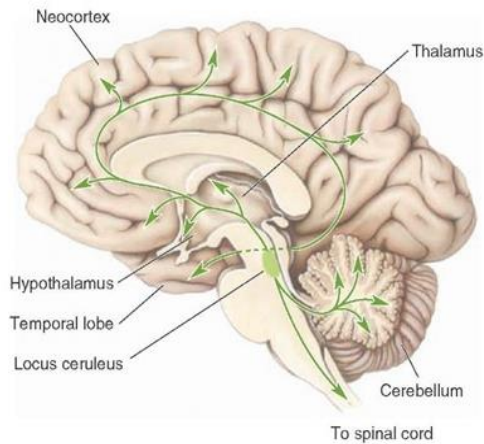


Figure 33. Noradrenergic pathways that arise from the nucleus locus coeruleus and other regions of the brainstem reticular formation. Both of these monoaminergic systems project to all parts of the CNS, but in particular, to the forebrain. Source: <http://what-when-how.com/neuroscience/behavioral-and-psychiatric-disorders-integrative-systems-part-2>

4.3.2. Structure of adrenergic receptors

Both NE and E transmit their biological signals via three subfamilies of adrenoceptors: α_1 -adrenoceptors (ADRA1, subdivided into ADRA1A, ADRA1B, and ADRA1D), α_2 -adrenoceptors (ADRA2, subdivided into ADRA2A, ADRA2B, and ADRA2C), and β -adrenoceptors (ADRB, subdivided into ADRB1, ADRB2, and ADRB3) (Bylund et al., 1994). These receptors are mostly localized in the plasma membrane of noradrenergic neurons and neuronal and non-neuronal target cells.

All adrenoceptor subtypes belong to the GPCR family so, upon binding of the endogenous activators (E and NE), adrenoceptors undergo a conformational change that leads to the activation of a heterotrimeric G protein. The three groups of adrenoceptors couple to and activate certain G protein subtypes leading to different intracellular changes. α_1 -adrenoceptors (α_1R) are coupled to $G_{q/11}$, which activates PLC and increases intracellular IP₃ and Ca²⁺ concentrations. α_2 -adrenoceptors (α_2R) mostly mediate their intracellular effects via $G_{i/o}$, which inhibits AC producing a decrease in cAMP. In addition, $G_{\beta\gamma}$ subunits released from activated $G_{i/o}$ proteins are important regulators of neuronal function by inhibiting neuronal Ca²⁺ channels and activating G protein-coupled inwardly-rectifying potassium channels (GIRK) and ERK1/2 phosphorylation (Cussac et al., 2001). Finally, β -adrenoceptors couple to $G_{s/olf}$ which leads to activation of adenylyl cyclase and increase of cAMP in the cell. Adrenoceptors, like other GPCRs, recruit arrestins which prevents further G protein activation as well as generates a protein scaffold for further signaling processes including MAPK, AKT and PI3K (Fig. 34).

Within the 7 transmembrane domains, the adrenergic receptors contain considerable amino acids sequence identity. The highest identity (~70%) is usually found among members of the same subfamily. Within members of the adrenergic receptor family, the identity within the transmembrane segments falls to about 45%. The regions of greatest diversity even among related receptor subtypes are the extracellular amino terminus, the third cytoplasmic loop, as well as the carboxyl terminal (Roth et al., 1991). Interestingly, adrenoceptors are highly dynamic proteins that may adopt multiple distinct conformations depending on the type of ligand bound, the associated signaling proteins, and the membrane environment (Deupi and Kobilka, 2010).

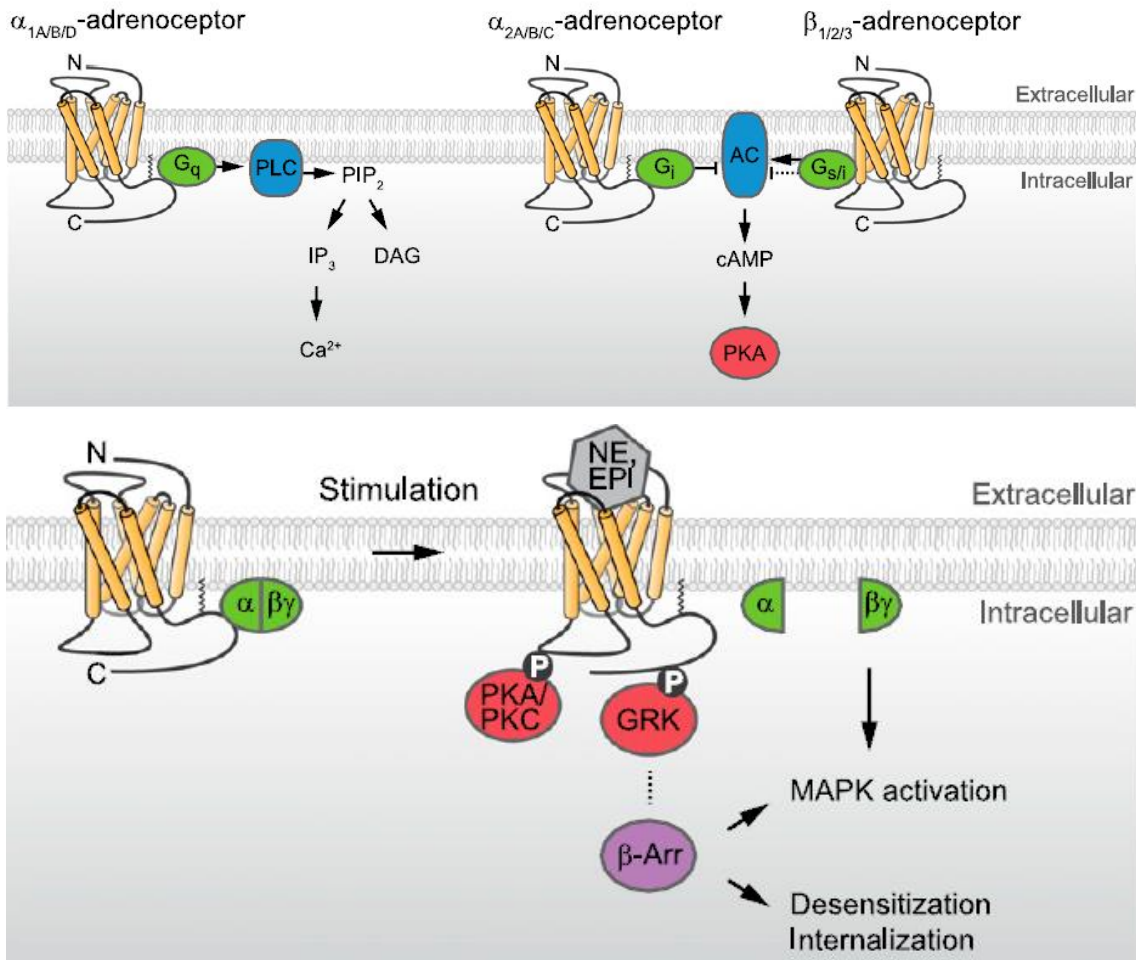


Figure 34. Signal transduction of adrenoceptors. Ga-dependent signaling pathways activated by the three families of adrenoceptor subtypes. Extracted from Ahles and Engelhardt (2014).

The primary structures of the nine adrenergic receptor subtypes display similar characteristic features: a single polypeptide chain from 400 to over 500 residues long comprising amino and carboxy-terminal regions variable both in length and sequence, and three intracellular, three extracellular and seven well conserved hydrophobic transmembrane domains. The α_2 R subtype C-terminal regions are shorter than those of the β and much shorter than those of the α_1 R subtypes. This goes in line with the observation that $G_s/G_{i/o}$ -coupled receptors generally have short intracellular loop 3 and C-terminal segment than receptors involved in other effector systems such as phospholipase C which have longer sequences in these regions (Fig. 35).

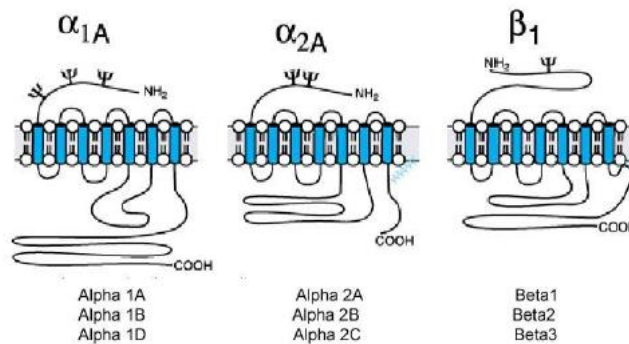


Figure 35. Schematic representation of adrenergic receptors.

One important distinguishing feature among α_2 R subtypes is their pattern of subcellular distribution and agonist-induced trafficking (Saunders and Limbird, 1999). The α_{2A} R subtype is efficiently targeted to the cell surface membrane and only a small proportion of receptor internalizes in response to agonist activation (von Zastrow et al., 1993), α_{2B} Rs are rapidly and reversibly internalized after agonist binding, whereas α_{2C} Rs reside in an intracellular compartment in many cell types and are not effectively targeted to the plasma membrane (Daunt et al., 1997; Hurt et al., 2000).

Within the adrenergic receptor family, the β_2 R was the first member for which homo-oligomerization was described, using co-immunoprecipitation of epitope-tagged receptors (Hebert et al., 1996). BRET technology was then used to test the existence of receptor oligomers *in vitro* in transfected cells (Hebert et al., 1996; Angers et al., 2000). Homo-oligomerization has been demonstrated for the β_2 R (Hebert et al., 1996; Angers et al., 2000), β_1 R (Mercier et al., 2002), α_{1A} R and α_{1B} R (Stanasila et al., 2003; Uberti et al., 2003), α_{1D} R (Uberti et al., 2003), α_{2A} R and α_{2C} R (Small et al., 2006), and for the α_{2B} R (Zhou et al., 2006). Within the ADR family, the following main heteromers have been found: β_1 R/ β_2 R (Lavoie et al., 2002), β_2 R/ β_3 R (Breit et al., 2004), α_{1B} R/ α_{1A} R and α_{1B} R/ α_{1D} R (Stanasila et al., 2003; Uberti et al., 2003), α_{1D} R/ β_2 R (Uberti et al., 2003), α_{1B} R/ β_2 R (Stanasila et al., 2003), α_{2A} R/ α_{2C} R (Small et al., 2006), α_{2A} R/ β_1 R (Xu et al., 2003) and α_{2C} R/ β_1 R (Prinster et al., 2006). All these interactions have specific consequences, as an example, within the α_{2A} R/ α_{2C} R heterodimer, the GRK-dependent phosphorylation and β -arrestin recruitment at the α_{2A} R, is inhibited (Small et al., 2006). Moreover, in the α_{2A} R/ β_1 R heterodimers, stimulation of the α_{2A} R triggered the internalization of the β_1 R (Xu et al., 2003) which, in addition, displayed altered pharmacology. Heteromers of ADR with other GPCRs have also been reported. As described before, α_{1B} R and β_1 R heteromerize with D_4 R. Likewise, α_{2A} R forms heteromers with μ opioid receptor (Glass and Pickel, 2002), β_2 R with κ (Jordan et al., 2001) and δ (Ramsay et al., 2002) opioid receptor.

4.3.3. Adrenergic receptor expression in the brain

The majority of cells in the human body express one or several of the nine adrenoceptor subtypes at their surface (Brunton et al., 2011). One particular receptor often dominates in certain cells in effector organs of the sympathetic nervous system or in the CNS. Likewise, the equipment of different cell types with G proteins and downstream signaling molecules is different. This heterogeneity allows for diverse responses of tissues and organs to catecholamines released from the sympathetic nervous system or within the CNS.

In the brain, α_1 R is found throughout the mesocorticolimbic system with high levels in the rat striatum, the VTA and the substantia nigra (Rommelfanger et al., 2009). α_1 R was also found in cortex, hippocampus, hypothalamus, midbrain, cerebellum and spinal cord (Papay et al., 2006).

When looking α_2 R, the lack of selective ligands for α_2 -subtypes prevents their proper study by autoradiography or binding. Nevertheless, the use of [3 H]rauwolscine, which preferably binds to the α_{2C} subtype, has helped to study the distribution of this receptor subtype in some detail, especially in rodent tissues where this radioligand offers better discrimination of α_{2C} R versus α_{2A} R compared to the situation in humans (MacDonald et al., 1992). Holmberg et al. (2003) compared the binding of [3 H]RX821002 (non-selective α_2 R ligand) and [3 H]rauwolscine (α_{2C} R preferred ligand) to account for the expression of α_{2C} R versus α_{2A} R in mice brain. They found high [3 H]RX821002 binding density (α_{2A} R and α_{2C} R expression) in cortex and within the basal

ganglia, especially in the nucleus accumbens but also in caudate-putamen nucleus, islands of Calleja, olfactory tubercle and ventral pallidum. Moderate levels of [³H]rauwolscine binding were observed in the caudate-putamen nucleus and the olfactory tubercle. Sparse binding was seen over the nucleus accumbens, the islands of Calleja, the ventral pallidum and the cortex. So, the main subtype in the brain is clearly $\alpha_{2A}R$. $\alpha_{2c}Rs$ are thus present in brain regions involved in the processing of sensory information and in the control of motor and emotion-related activities such as the accumbens and caudate putamen nuclei, the olfactory tubercle, the lateral septum, the hippocampus, the amygdala, and the frontal and somatosensory cortices (Fig. 36 and 37).

Another technique used to map the distribution of α_2 -adrenoceptor subtypes is *in situ* hybridization. With this technique, it has been described that the $\alpha_{2A}R$ is the predominant α_2R whereas $\alpha_{2c}R$ has a more restricted expression pattern and is highly enriched in the striatum (Fagerholm et al., 2008; Lehto et al., 2015), although with a lower density than $\alpha_{2A}R$ (Ordway et al., 1993; Uhlen et al., 1997), confirming the results obtained by autoradiographic experiments.

Finally, in total brain membrane fractions, the abundance of $\alpha_{2B}R$ was too low for detection by radioligand binding (Bucheler et al., 2002). However, mRNA of the α_{2B} subtype was detectable in thalamic nuclei of the rat brain, suggesting that this subtype is mostly restricted to the thalamus (Nicholas et al., 1993, 1996; Scheinin et al., 1994; MacDonald and Scheinin, 1995).

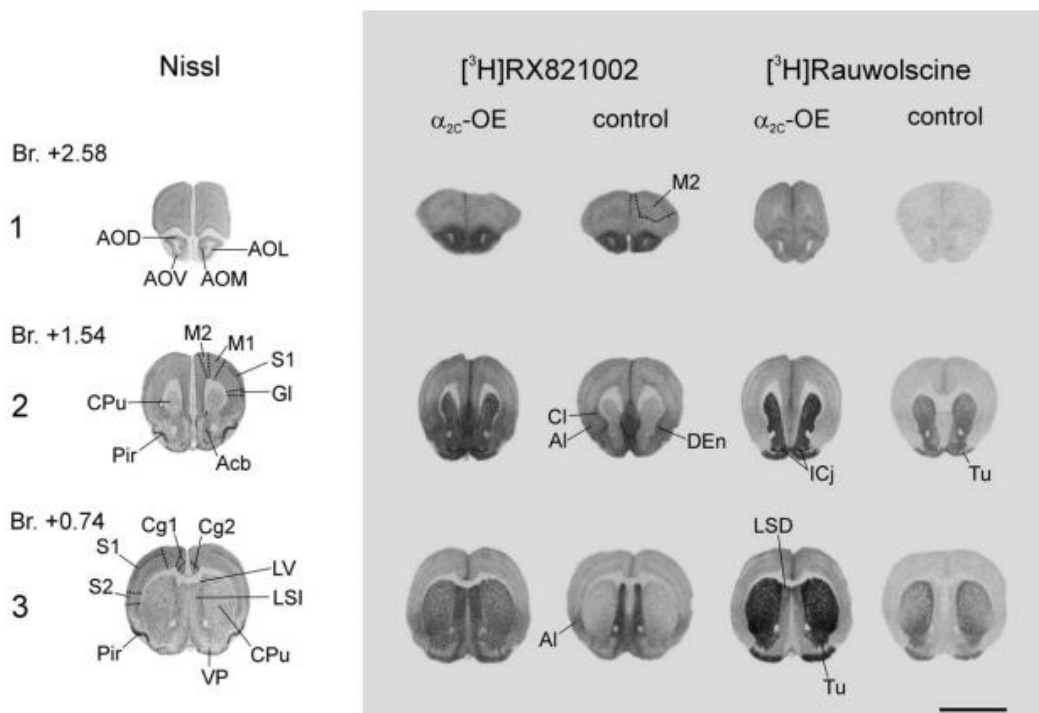


Figure 36. [³H]RX821002 and [³H]rauwolscine binding in forebrain structures at different levels. Increased binding of both radioligands is evident over the accumbens and caudate putamen nuclei, the islands of Calleja (ICj), the olfactory tubercle (Tu), and the cortical regions of mice overexpressing (OE) the α_2R compared with control mice. Extracted from Holmberg et al. (2003).

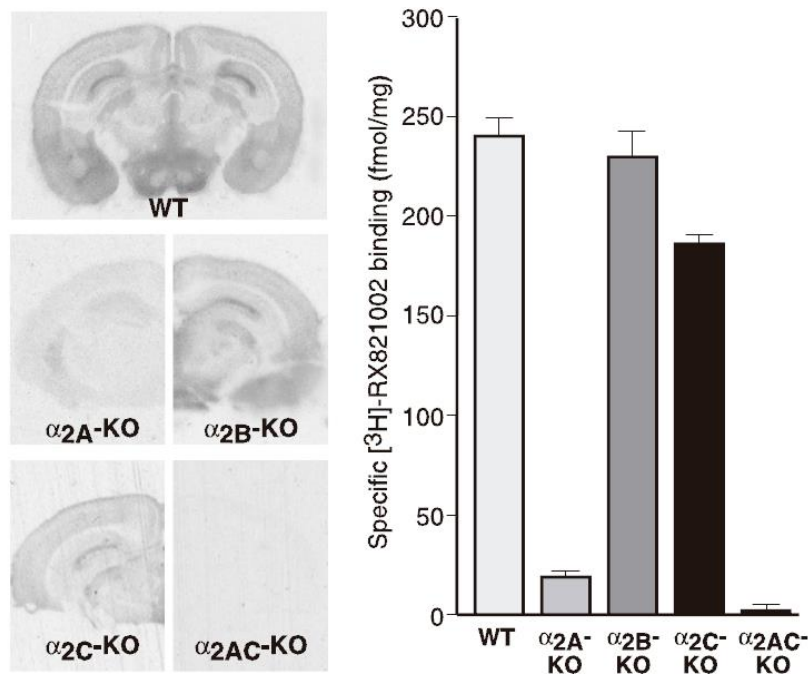


Figure 37. Expression of α_2R subtypes in the brain of α_2R -KO mice. (left) Autoradiograms of [3H]RX821002 specific binding in the brain of wild-type (WT) and α_2R -KO mice. In wild-type mouse brain, highest levels of α_2R s were expressed in brain cortex and hippocampus. (right) Quantification of the autoradiograms of mouse brain slices. Extracted from Bucheler et al. (2002).

β -adrenergic receptor subtypes have differential expression patterns. β_1 -adrenoceptors are found at their highest levels in the heart and brain (Friele et al., 1987), especially in the cortex, and more concretely in the intermediate layers of the PFC, where thalamic inputs are concentrated (Rainbow et al. 1984; Goldman-Rakic et al., 1990; Nicholas et al., 1993), but also in the thalamus, pineal gland and sympathetic ganglia (Nicholas et al., 1996). β_2 adrenoceptors are more widely expressed. They are present in the olfactory bulb, cerebral cortex, hippocampus, thalamus, hypothalamus, pineal gland and spinal cord (Nicholas et al., 1996). Moreover, they are found on dendritic spines of the PFC pyramidal neurons and on GABAergic interneurons (Aoki et al., 1998). Finally, β_3 adrenoceptors are found mainly in adipose tissue (Emorine et al., 1989; Summers et al., 1995). All β -adrenoceptors are found on glia (Hansson and Ronnback, 1991; Fillenz and Lowry, 1998; Fillenz et al., 1999).

4.3.4. Neuronal functions of adrenergic receptors

Neurons in the LC play a critical role in many functions including physiological responses to stress and panic, learning and memory. A large body of literature implicates NE also in cellular excitability, synaptic plasticity and long-term potentiation (Harley, 1987, 2007). An equally large number of studies have demonstrated the role of NE in gating and tuning sensory signals in the thalamus and the cortex (Berridge and Waterhouse, 2003). Pharmacological studies have provided evidence that NE, interacting with other neuromodulators and hormones, modulates memory formation, mainly through actions in the amygdala and the hippocampus (Cahill and McGaugh, 1996).

Other pharmacological approaches have revealed a noradrenergic influence in frontal cortical regions that are engaged in attention and working memory functions (Arnsten and Li, 2005; Robbins and Roberts, 2007). In addition, electrophysiological studies in behaving primates and

rodents have shown a clear relationship between activity in the locus coeruleus neurons and cognitive behaviors (Aston-Jones and Cohen, 2005; Bouret and Sara, 2005; Yu and Dayan, 2005).

Because of the lack of sufficiently subtype-selective ligands, the physiological properties of each adrenoceptor subtype have not been fully elucidated until recently. However, new approaches using mice carrying deletions in the genes encoding individual adrenoceptor subtypes have greatly advanced the knowledge regarding the specific functions of these receptors (MacDonald et al., 1997; Rohrer, 1998; Rohrer and Kobilka, 1998; Bücheler et al., 2002; Brette et al., 2004; Philipp and Hein, 2004).

Whereas NE exerts a wide spectrum of effects in the CNS, the contribution of the α_1 R to these neuronal functions is largely unknown. Some studies suggest that the noradrenergic pathway is important for the modulation of behaviors such as reaction to novelty and exploration and propose that this behavior is mediated, at least partly, through α_{1B} R (Spreng et al., 2001). Other studies indicate the critical role of α_{1B} R and NE transmission in the vulnerability of addiction (Drouin et al., 2002). Moreover, according with Arnsten et al. (2000), high levels of NE released during stress, bind to α_1 R and impair PFC function altering working memory. In contrast, α_1 R-antagonists protect PFC cognitive function from stress-induced impairment.

In mammalian species, both α_{2A} R and α_{2C} R seem to be localized mostly postsynaptically, preferentially in GABAergic striatal efferent neurons (Holmberg et al., 1999; Hara et al., 2010). However, α_2 R can also be expressed presynaptically as autoreceptors, where they work as presynaptic feedback inhibitors of neurotransmitter release (Langer, 1997; Starke, 2001). The α_{2A} subtype is found to be the main inhibitory presynaptic feedback receptor in the sparse striatal noradrenergic terminals (Fig. 38) (Altman et al., 1999; Hein et al., 1999; Trendelenburg et al., 2003; Ihalainen and Tanila, 2004). Additionally to the α_{2A} R subtype, α_{2C} R participates in presynaptic regulation in the CNS (Trendelenburg et al., 2003). In addition to their function as inhibitory autoreceptors, α_2 Rs can also regulate a number of other neurotransmitters in the central and peripheral nervous system and thus operate as “heteroreceptors” (presynaptic receptors activated by transmitters from neighboring neurons). Also, α_{2A} R and α_{2C} R presynaptically inhibit DA release in basal ganglia (DA terminals from SN) (Bucheler et al., 2002), being α_{2A} R the principal subtype involved (Trendelenburg et al., 1994). This inhibition can be mediated by NE and, probably, by DA binding to α_2 R (Zhang et al., 1999). Both adrenoceptors also control serotonin secretion in mouse hippocampus and brain cortex (Scheibner et al., 2001). The inhibition of neurotransmitter release has also been linked with the neuroprotective effects of α_2 -agonists, which are mostly mediated via the α_{2A} -subtype (Ma et al., 2003, 2005; Paris et al., 2006). Other functions of α_2 R in the brain are analgesia, sedation/hypnosis, processing of sensory information and centrally-mediated cardiovascular control (MacMillan et al., 1996; Altman et al., 1999; Philipp et al., 2002). In the PFC α_{2A} Rs are instrumental for spatial working memory (Arnsten et al., 1988; Wang et al., 2007) as well as emotional behavior (Zang et al., 2009). The activation of α_{2A} Rs improves regulation of attention, behavioral inhibition and task planning in humans, whereas NE depletion has been shown to increase distractibility during neuropsychological testing.

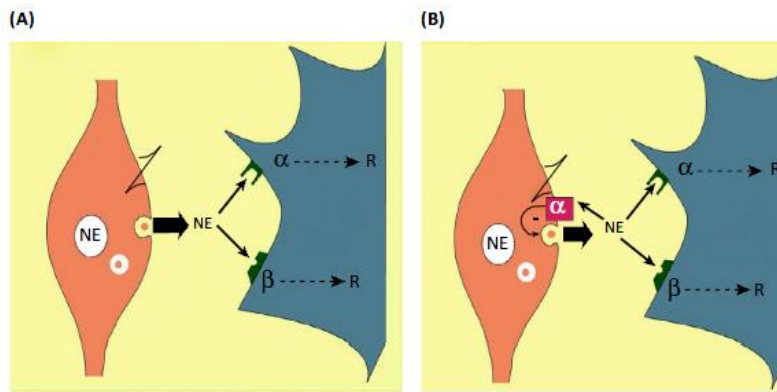


Figure 38. The basic elements of neurochemical transmission. In anterograde neurotransmission (A), NE is released from nerve terminals and crosses the synaptic cleft to activate α or β ADR postsynaptically, generating a cellular response. In retrograde neurotransmission (B), released NE acts on presynaptic inhibitory α ADR located on the membrane of the nerve terminal to inhibit further transmitter release through a negative feedback mechanism mediated by the transmitter of the neuron (i.e., NE). Presynaptic inhibitory autoreceptors correspond to the α_2 R subtype. Extracted from Langer (2015).

In contrast to α_2 Rs, which are important for the control of neurotransmitter release, the β_1 Rs are mostly known for their role in the regulation of cardiovascular, uterine, and peripheral metabolic functions. In the CNS, an important aspect of β_1 R is their expression in medium spiny neurons (Nahorski et al., 1979; Waeber et al., 1991), where the loss of β_1 R in the striatum was reported in the late stages of Huntington's disease (Waeber et al., 1991). In the pineal gland, NE released from sympathetic nerves controls the circadian rhythm of melatonin synthesis via β -adrenoceptors (Simonneaux and Ribelayga, 2003) and/or D_4 R heteromers (González et al., 2012a). Several studies using knock-out mice of each β -adrenoceptor indicate that these receptors play a central role in regulating numerous functions of the CNS, including the regulation of sympathetic tone, learning and memory, mood and food intake. NE acting at β_1 R has been found to be essential for the retrieval of contextual and spatial memory but is not essential for the retrieval of emotional memories (Winder et al., 1999; Murchison et al., 2004). Presynaptic β -adrenoceptors may also play an important role in the regulation of neurotransmitter release (Trendelenburg et al., 2000). In humans, many drugs are currently being used that may interact with β -adrenoceptors. β -blockers are used to treat chronic migraine, glaucoma, or essential tremor (Hoffman and Lefkowitz, 1996). However, the exact mechanism of action of these drugs in these conditions has not been clearly identified.

5. ADENOSINE SYSTEM

Adenosine is an endogenous nucleoside formed by a purinic base adenine bound to a ribose by a β -N-glycosilic bond. Adenosine and its derivatives are an essential constituent for all living cells. Adenosine plays a structural role as a building block of nucleic acids, in cellular metabolism (energy storage: ATP), as intracellular regulator (cofactors: NAD^+ , NADP^+ , FAD; second messenger in cellular neuromodulator: cAMP) (Arch and Newsholme, 1978; Pull and McIlwain, 1972) and as neuromodulator in the control of synaptic transmission acting on ARs (Cobbin et al., 1974).

Its physiological concentration rapidly increases in conditions of injury or stress such as ischemia, hypoxia, trauma and inflammation (Hasko et al., 2008; Wei et al., 2013). Extracellular adenosine levels are also increased in cancer tissues as the result of genetic alterations that occur during tumor progression and have a crucial role in the alteration of immune cell activity (Gessi et al., 2011; Antonioli et al., 2013, 2014). Likewise, adenosine is an important neuromodulator involved in many physiological and pathological processes in the mammalian CNS (Sebastiao and Ribeiro, 2000; Fredholm et al., 2005; Abbracchio et al., 2009; Paul et al., 2011; Acton and Miles, 2015). Consequently, adenosine signaling has a relevant role in pathological states as epilepsy, pain, ischemic organ injury, inflammation and cancer (Borea et al., 2016).

Adenosine is produced both intracellularly and extracellularly and it is transported via concentrative and equilibrative nucleoside transporter proteins across the plasma membrane (Gray et al., 2004; Molina-Arcas et al., 2009; Huang et al., 2017). Inside the cell, adenosine is formed from ATP, cAMP or SAH, while outside the cell it arises from equilibrating nucleotide transporter-mediated release or metabolism by ecto-nucleotidases from ATP or cAMP (Sawynok and Liu, 2003) (see Fig. 39). Several enzymes are responsible of intracellular or extracellular adenosine degradation, such as adenosylhomocysteine hydrolase (SAHase), adenosine kinase (AK), and adenosine deaminase (ADA).

Apart from these enzymes, the levels of intra- and extracellular adenosine are under the control of equilibrative nucleoside transporters (ENT) in the plasma membrane, which can either release or capture adenosine according to its concentration across the membrane. As the synaptic concentration of adenosine is usually higher than the intracellular one, its transport across ENT is usually in the inward direction (Sebastiao and Ribeiro, 2015). ENTs are the most abundant nucleoside transporters in the brain, and they are expressed both in neurons and glia (Parkinson et al., 2011). During seizures, there is a high energy demand, and therefore an intense catabolism of ATP; in these circumstances neurons provide the source of adenosine into the synapse whereas astrocytes, with ENT and AK, act as removers of extracellular nucleoside (Sebastiao and Ribeiro, 2015).

5.2. Structure of adenosine receptors

Extracellular adenosine exerts numerous physiological functions throughout the entire human body by interacting with specific ARs expressed on the surface of the target cells. There are four known adenosine receptor subtypes, A₁R, A_{2A}R, A_{2B}R and A₃R (Fig. 40), each of which has a unique pharmacological profile, tissue distribution and effector coupling. These AR subtypes can either inhibit (A₁R and A₃R) or activate (A_{2A}R and A_{2B}R) AC. A_{2B}R also signals via G_q proteins (Fig. 40) (Vecchio et al., 2016).

All of the ARs have glycosylation sites and all except A_{2A}R a palmitoylation site near the carboxyl terminus, that would allow another insertion in the membrane generating a fourth intracellular loop that has been suggested to participate in the coupling of the receptor to the G-protein (Bouvier et al., 1995). Moreover, ARs contain several features common to all G-protein coupled receptors: cysteine residues on the extracellular loop that may be involved on disulfide bond formation and confer a conformational stability to receptors after insertion to the plasma membrane (Dohlman et al., 1990). All the cloned ARs present a “DRY” motif that has been suggested to mediate G-protein activation. Each of the ARs possesses consensus sites for N-linked glycosylation on their second extracellular loops that is involved in membrane targeting (Fig. 41) (Klotz and Lohse, 1986). Intracellular domain phosphorylation sequence consensus is present and phosphorylation is implicated in receptors desensitization (Palmer et al., 1994; Saura et al., 1998).

A₁R, A_{2A}R and A₃R have a molecular weight of 36.7, 36.4 and 36.6 kDa respectively, whereas, due to its long C-terminal tail, A_{2A}R has a molecular weight of 45 kDa (Palmer and Stiles, 1995). Human ARs exhibit high sequence homology and are usually clustered into A₁R and A₃R (49% similarity) and A_{2A}R and A_{2B}R (59%) (Moro et al., 2006; Jacobson and Gao, 2006). Although the affinity of adenosine for these receptors may vary, depending on the type of test used to evaluate it (Fredholm, 2014), adenosine presents higher affinity for A₁R (100 nM), A_{2A}R (310 nM) and A₃R (290 nM) than for A_{2B}R (15 μM) (Yan et al., 2003). Among these four ARs, A₁R and A_{2A}R are mostly responsible for the effects of adenosine in the brain (Fredholm et al., 2005) because present more affinity for adenosine and are expressed in higher levels than A₃R.

A_{2A}R complexes have been crystallized, facilitating the discovery of more effective and selective A_{2A}R ligands and the knowledge of the molecular determinants of subtype specificity and ligand efficacy (Bertheleme et al., 2014; Carpenter et al., 2016). The first crystal structure of the A_{2A}R was solved in complex with ZM241385 and demonstrated that the ligand binding pocket was located in a different position and orientation, relative to other structures available at that time, and that ligand selectivity could be achieved through targeting hydrophobic residues extending from the aromatic core of ZM241385 (Jaakola et al., 2008). There is a quite large number of A_{2A}R crystals in complex with agonists and antagonists

Very recently, Glukhova et al. (2017) have determined the crystal structure of the A₁R in complex with a covalent antagonist, DU172. Compared to the A_{2A}R, the A₁R structure contains a more open binding site cavity that can accommodate orthosteric and allosteric ligands.

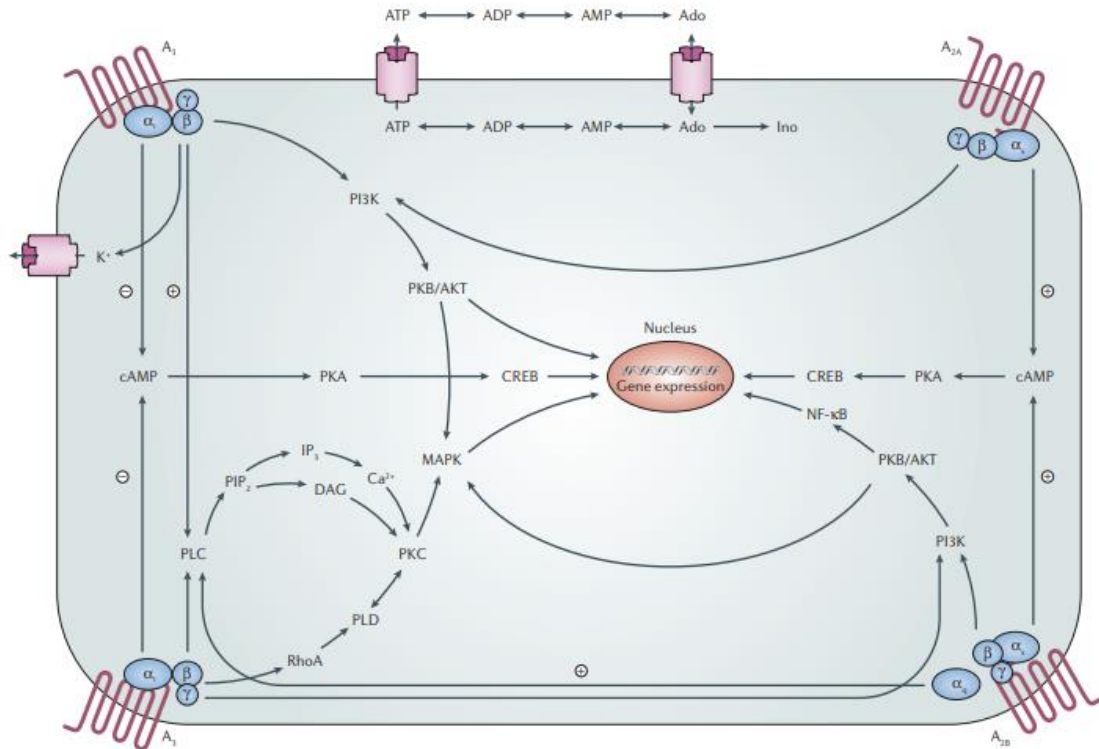


Figure 40. Adenosine receptor signalling pathways. Activation of the A₁R and A₃R inhibits AC activity through activation of pertussis toxin-sensitive G_i proteins and results in increased activity PLC via G_{βγ} subunits. Activation of the A_{2A}R and A_{2B}R increases AC activity through activation of G_s proteins. Activation of the A_{2A}R to induce formation of IP₃ can occur under certain circumstances, possibly via the pertussis toxin-insensitive G_{α15} and G_{α16} proteins. A_{2B}R-induced activation of PLC is through G_q proteins. All four subtypes of ARs can couple to MAPK, giving them a role in cell growth, survival, death and differentiation. CREB: cAMP response element binding protein; PIP₂: phosphatidylinositol-4,5-bisphosphate; PLD: phospholipase D; NF-κB: nuclear factor-κB. Extracted from Jacobson and Gao (2006).

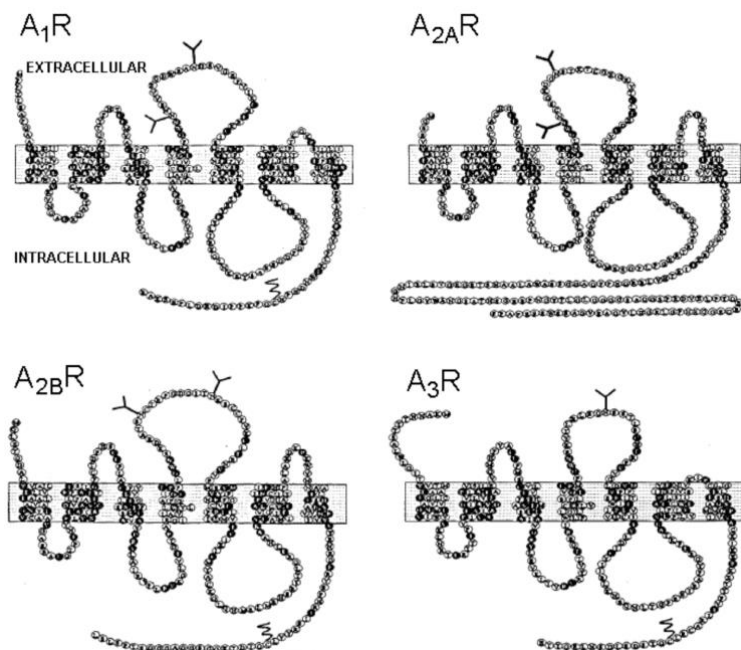


Figure 41. Adenosine receptor scheme. Very long C-terminal tail of the A_{2A}R lacking palmitoylation site. Glycosylation sites in the second extracellular loop of all ARs. Taken from Dr. F. Ciruela's PhD thesis.

5.3. Adenosine receptor expression in the brain

A₁Rs are very ubiquitous and are expressed in the highest density in kidney, heart atria, adipose tissue and brain areas as the hippocampus, cerebral cortex, thalamus, basal ganglia, cerebellar cortex and dorsal horn of spinal cord in human and experimental animals (Fukumitsu et al., 2005; Vallon and Osswald, 2009; Gharibi et al., 2012; Li et al., 2016; Stockwell et al., 2017). In conclusion, A₁Rs are the most abundant and widespread distributed in the brain; concretely they are the second most abundant cerebral metabotropic receptor. A₁Rs can be at pre- and post-synaptic sites, as well as in astrocytes, to influence synaptic function; they are mostly located in excitatory glutamatergic synapses, but they are also present in GABAergic, cholinergic, dopaminergic, serotonergic and noradrenergic synapses (Sebastiao and Ribeiro, 2015; Cunha, 2016).

A_{2A}Rs are more abundant in the basal ganglia, almost exclusively in the striatopallidal GABAergic neurons of the indirect pathway cells that co-express dopamine D₂R and is not present (or at best only to a limited extend) in medium spiny neurons of the direct pathway (Fredholm et al., 2005). By means of more sensible techniques, like immunohistochemistry or radioligand binding assays, lower levels of A_{2A}R were also detected in other brain regions, such as the cortex, amygdala, hippocampus, hypothalamus, thalamus and cerebellum (Rebola et al., 2005b; Hasko and Pacher, 2008; Chen et al., 2013; Stockwell et al., 2017). A_{2A}Rs are found predominantly at post-synaptic neurons in striatum, in the indirect motor pathway (Hettinger et al., 2001), but they are also detected as important presynaptic neuromodulators, controlling glutamate release in the direct motor pathway (Schiffmann et al., 2007) or GABA release (Cunha and Ribeiro, 2000). A_{2A}R could also be found presynaptically in the hippocampus (Rebola et al., 2005b).

Upon agonist stimulation, the A_{2A}R response “quickly” desensitizes within a time frame of less than an hour. Desensitization involves A_{2A}R phosphorylation mostly by GRK in the proximal portion of the C-terminus (Thr298) of A_{2A}R (Palmer et al., 1994). A longer agonist exposure induces receptor internalization, a necessary step for either resensitization or down-regulation of A_{2A}R through clathrin-coated vesicles (Palmer et al., 1994; Mundell and Kelly, 2011).

A_{2B}Rs are highly expressed in peripheral tissues but they have a very low expression levels throughout the brain and a very low affinity by the endogen ligand adenosine; for this reason, A_{2B}Rs are only activated when adenosine is released at high levels as one of the consequences of tissue damage (Trincavelli et al., 2014).

The A₃R is less widely distributed than other AR subtypes with low expression brain (Rivkees et al., 2000; Borea et al., 2015). Using autoradiographic and immunohistochemical experiments, Haeusler et al. (2015) showed the existence of low levels of A₃R in human post-mortem brain tissues (thalamus, putamen, cerebellum, hippocampus, caudate nucleus and cortex). These receptors are present in both presynaptic and postsynaptic terminals, but its role in synaptic transmission remains to be elucidated (Dixon et al., 1996; Gundlfinger et al., 2007; Huang and Thathiah, 2015). Recent studies have shown that A₃R is critical in regulating pain induced by chronic constriction injury or chemotherapy and in the progression of diabetic neuropathy and it can be targeted to provide effective pain relief from chronic pain (Janes et al., 2016; Yan et al., 2016).

5.4. Neuronal functions of adenosine receptors

In the brain, adenosine acts as an important upstream neuromodulator of a broad spectrum of neurotransmitters, receptors and signaling pathways that converge to contribute to the expression of an array of important brain functions (Fig. 42) (Gomes et al., 2011). Adenosine is the main molecule involved in the coordination of brain activity (Sebastiao and Ribeiro, 2009) and it has a key endogenous neuroprotective role in this tissue, predominantly mediated by adenosine A_1 Rs. This nucleoside maintains brain homeostasis and regulates complex behavior via activation of inhibitory and excitatory ARs in a brain region-specific manner (Cortés et al., 2016).

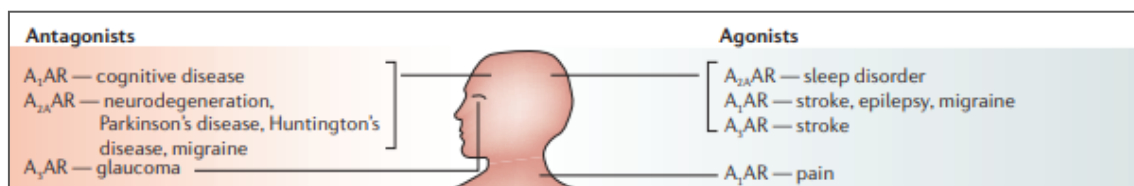


Figure 42. Novel disease targets for selective adenosine receptor ligands. Most promising prospects exist for treatment of arrhythmias, ischemia of the heart and brain, pain, neurodegenerative diseases, sleep disorders, inflammation, diabetes, renal failure, cancer and glaucoma, and in cardiovascular imaging. Adapted from Jacobson and Gao (2006).

Adenosine modulates the function of two principal neurotransmitter systems: one that is involved in motor activation and reward (dopaminergic systems) and another that is involved in arousal processes (cholinergic, noradrenergic, histaminergic, and orexinergic systems) (Ferré, 2010). It was reported that A_1 R and A_{2A} Rs contribute to the sleep homeostasis (Elmenhorst et al., 2007; Huang et al., 2011). Serchov et al. (2015) showed that upregulating A_1 R in forebrain neurons evokes both resilience against depressive-like behavior and antidepressant effects in a chronic depression model.

A_{2A} Rs seem to operate as metamodulators, regulating other receptors and neuromodulators fine-tuning neuronal activity, with implications for the control of synaptic plasticity and, therefore, of learning and memory (Sebastiao and Ribeiro, 2015). Simoes et al. (2016) have identified the presence of A_{2A} R in glutamatergic terminals in the amygdala, where they selectively control synaptic plasticity processes that are considered the neurophysiological basis of conditional fear memory. At the synaptic level, activation of stimulatory A_{2A} R by adenosine also contributes to synaptotoxicity and is a rational explanation for the neuroprotective effects of caffeine and other A_{2A} R antagonists (Cunha, 2005, 2008). Therefore, A_{2A} R agonists provide protection by controlling massive infiltration and neuroinflammation in the hours and days after brain ischemia (Pedata et al., 2016). A_{2A} Rs also play an important role in the control of neuropathic pain because of modulation of glial cytokines (Gao and Jacobson, 2007), in the regulation of inflammatory and immune responses, and in neurodegenerative disorders (Sitkovsky et al., 2004; Lappas et al., 2005; Naganuma et al., 2006; Popoli et al., 2008; Bura et al., 2008; Palmer and Trevethick, 2008; Morello et al., 2009; Huang et al., 2011; Impellizzeri et al., 2011; Chan et al., 2013; Ouyang et al., 2013; Rissanen et al., 2013; Ahmad et al., 2013; Kanda and Uchida, 2014; Chiu et al., 2015; Arosio et al., 2016; Hatfield and Sitkovsky, 2016; Stockwell et al., 2017). A_{2A} Rs also control glial function and brain metabolic adaptation and are important in controlling the demise of neurodegeneration (Cunha et al., 2008; Santiago et al., 2014).

Moreover, it has been indicated that A_{2A} Rs can be attractive targets to manage psychiatric disorders (Cunha et al., 2008; Krugel, 2016) and drug addiction (Filip et al., 2012).

5.4.1 Caffeine interactions with adenosine receptors

The psychostimulant caffeine (1,3,7-trimethylxanthine) (Fig. 43) is a non-selective adenosine receptor antagonist and one of the most important naturally occurring methylated xanthine alkaloids and is the most widely used psychoactive drug in the world (Fredholm et al., 1999; Fisone et al., 2004). Once consumed, it is rapidly distributed throughout the body and readily crosses the blood–brain barrier (Dager and Friedman, 2000); once in the brain, it produces a variety of behavioral effects including an increase in performance, subjective alertness and attention (an important prerequisite for many cognitive processes, such as memory and reasoning), and it also reduces fatigue and enhances motor activity (Fisone et al., 2004).

New research indicates that coffee consumption may be useful to restore memory dysfunction associated with aging and neurodegenerative diseases (González de Mejia and Ramirez-Mares, 2014). In fact, healthy people can tolerate low and moderate (<400 mg/day for a 70-kg person) ingestions of caffeine, but heavy caffeine consumption has been associated with serious adverse health effects, including tachycardia, hypertension, anxiety, restlessness, and tremors (Seifert et al., 2011).

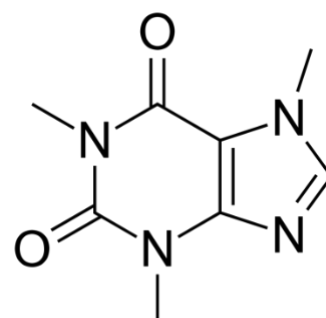


Figure 43. Structure of caffeine.

Caffeine acts as antagonist when bind to ARs with a low micromolar range of affinities. Concretely, caffeine has similar *in vitro* affinities for A_1 R, A_{2A} R and A_{2B} R and much lower for A_3 R. It is known that caffeine exerts its psychostimulant effects by counteracting the tonic effects of endogenous adenosine on ARs. Karcz-Kubicha et al. (2003) suggested that the tolerance to the motor-activating effects of caffeine may be due to the tolerance to the effects of A_1 R blockade and that the residual motor-activating effects of caffeine in tolerant individuals might be mostly because of A_{2A} R blockade. Both striatal A_1 Rs and A_{2A} Rs are involved in the motor-activating and probably reinforcing effects of caffeine, although they play a different role under conditions of acute or chronic caffeine administration (Ferré, 2008).

Caffeine also affects the brain by a localized combination of neuronal and vascular responses. Increased neuronal activity is thought to be exerted mainly through action on A_1 Rs (Dunwiddie and Masino, 2001), whereas vasoconstriction is mediated mainly through action on A_{2A} Rs and also, in a lesser degree, by A_{2B} Rs (Pelligrino et al., 2010; Cortés et al., 2016). Both caffeine-mediated blockade of ARs and vasoconstriction have direct repercussions on brain connectivity at resting states and during cognitive activation. Whereas the effects of acute caffeine consumption seem mostly to be due to the antagonism of A_1 Rs, the effects resulting from the chronic consumption of caffeine seem to be mainly due to the antagonism of A_{2A} Rs (Chen et al., 2007; Ferré, 2008; Pelligrino et al., 2010).

Caffeine also has molecular effects on cognitive functions, enhancing cognition through the blockade of A_1 R in hippocampal CA1 and CA2 neurons. In animals, caffeine has been found to counteract certain kinds of memory impairments, such as those associated with sleep deprivation or attention deficit disorder. It has been indicated that caffeine administration enhances consolidation of long-term memories in humans (Borota et al., 2014). In this context,

it has been reported that the regular human consumption of caffeine has neuroprotective effects in aging and in neurodegenerative diseases such as Alzheimer's and Parkinson's diseases (Ribeiro and Sebastião, 2010; Kolahehdouzan and Hamadeh, 2017).

A₁Rs localized in the basal forebrain and A_{2A}Rs localized in the hypothalamus are believed to be mostly responsible for the arousing properties of caffeine. These properties depend on the blockade of multiple inhibitory mechanisms that adenosine, as an endogenous sleep-promoting substance, exerts on the multiply interconnected ascending arousal systems (Ferré, 2008, 2010). These mechanisms include a direct A₁R-mediated modulation of the corticopetal basal forebrain system and an indirect A_{2A}R mediated modulation of the hypothalamic, histaminergic, and orexinergic systems (Ferré, 2010). The blockage of these receptors by caffeine leads to an increase in adenosine within the noradrenergic, cholinergic, dopaminergic, and serotonergic systems, which are regulated by adenosine (Lopez-Garcia et al, 2014). The stimulation of these neurotransmitter systems increases alertness, attention, arousal, and motor activation (Ferré, 2010; Lopez-Garcia et al., 2014). Despite that the relative contribution of A₁R and A_{2A}R to sleep induction remains controversial (Porkka-Heiskanen et al., 2013; Huang et al., 2014) it has been suggested by Huang et al. (2014) that A_{2A}R plays a predominant role in sleep induction, whereas A₁R regulates the sleep–wake cycle in a site-dependent manner.

The presence of A₁R-A₁R homodimers demonstrated in cell cultures and *in vivo* (Gracia et al., 2013b) allows modulations within the homomer in which caffeine binding to one protomer increases the agonist affinity for the other protomer, a pharmacological characteristic that correlates with the low caffeine concentration-induced activation of agonist-promoted A₁R signaling. This pharmacological property can explain the biphasic effects obtained at low and high concentrations of caffeine on locomotor activity: at low caffeine concentrations, caffeine increase, instead of decrease, the agonist-induced signaling, eliciting locomotor depression, and at high concentrations, caffeine inhibits agonist-induced signaling, inducing locomotor activation (Gracia et al., 2013b). If an interligand allosteric interaction is detected on a GPCR target, the usage of antagonist for blocking the effect of agonist drugs has to be taken with caution. These results open new perspectives on the actions of antagonists that must be taken into account in drug handling.

6. CATECHOLAMINE AND ADENOSINE SYSTEM INTERACTIONS

6.1 Dopamine and adenosine system interaction

6.1.1 Direct and indirect pathway

Dorsal striatum (caudate nucleus and putamen) is implicated in learning or complex motor behavior. MSNs are the most numerous in the dorsal striatum, with at least 75% of neurons belonging to this type in primates (Graveland and DiFiglia, 1985; Tepper et al., 2010), and up to 95% in rodents and cats (Kemp and Powell, 1971; Graveland and DiFiglia, 1985). The second class of neurons present in the dorsal striatum are interneurons (GABAergic or cholinergic), that are typically spiny, and unlike the medium spiny neurons, do not send projections outside the striatum (Phelps et al., 1985; Cowan et al., 1990; Kawaguchi, 1993; Kawaguchi et al., 1995; Wu et al., 2000; Tepper et al., 2010). Finally, the striatum also contains a small number of dopaminergic neurons. Although the amount of these neurons is almost vestigial in normal rodent striatum, it is more prevalent in primates (Dubach et al., 1987; Ikemoto et al., 1996).

Mesencephalic DA and cortical glutamate inputs converge in the GABA medium spiny projection neurons. MSNs can be divided into two types according to expression of different peptides and neurotransmitter receptors. Direct pathway MSN express dynorphin and substance P and D₁R coupling stimulatory G_s. They are also called striatonigral MSN. They project directly to the internal globus pallidus (GPI) and SNr. Stimulation of the direct pathway results in motor activation. Indirect pathway MSN express enkephalin and D₂R coupling inhibitory G_i. They are also called striatopallidal MSN and project indirectly to the SNr by way of the GPe and STN. Stimulation of indirect pathway MSN results in motor inhibition.

Direct and indirect pathways converge in GPI/SNr, the main output of basal ganglia motor circuitry. GPI/SNr neurons are inhibitory and project to the thalamus. The thalamus projects back to cortex, constituting the well-known parallel cortical-striatal-thalamic-cortical circuits. But, apart from this well-known, largely segregated, parallel processing, a non-appreciated substantial convergence of cortical inputs takes place in the striatum, in the striatonigral and striatopallidal neurons. This convergence includes: inputs from the two types of cortical pyramidal neurons: the intratelencephalic and pyramidal tract neurons (simplified in Fig. 44) (Shepherd, 2003), coming from the same cortical area or from different and separated cortical areas. These convergent corticostriatal glutamate inputs provide the convergent input necessary for establishing the DA-mediated stamping-in of stimulus-reward and reward response associations that follows the receipt of the reward (Ferré et al., 2017).

According to both inputs from direct and indirect pathway the final outcome is transmitted back to cortex. Direct pathway is considered to promote voluntary movements and indirect pathway to suppress unwanted movements. An adequate equilibrium between both pathways produces normal movements (Mink, 2003; Nambu, 2008; Cohen and Frank, 2009).

DA produced by neurons from substantia nigra pars compacta, is the key regulator for the correct functioning of basal ganglia. It induces motor activation via activation of D₁Rs in striatopallidal neurons of direct pathway and inhibition of D₂Rs in striatonigral neurons of indirect pathway, which means potentiating the stimulatory direct pathway and depressing the inhibitory indirect pathway. Thus, DA stimulates movement acting upon both pathways.

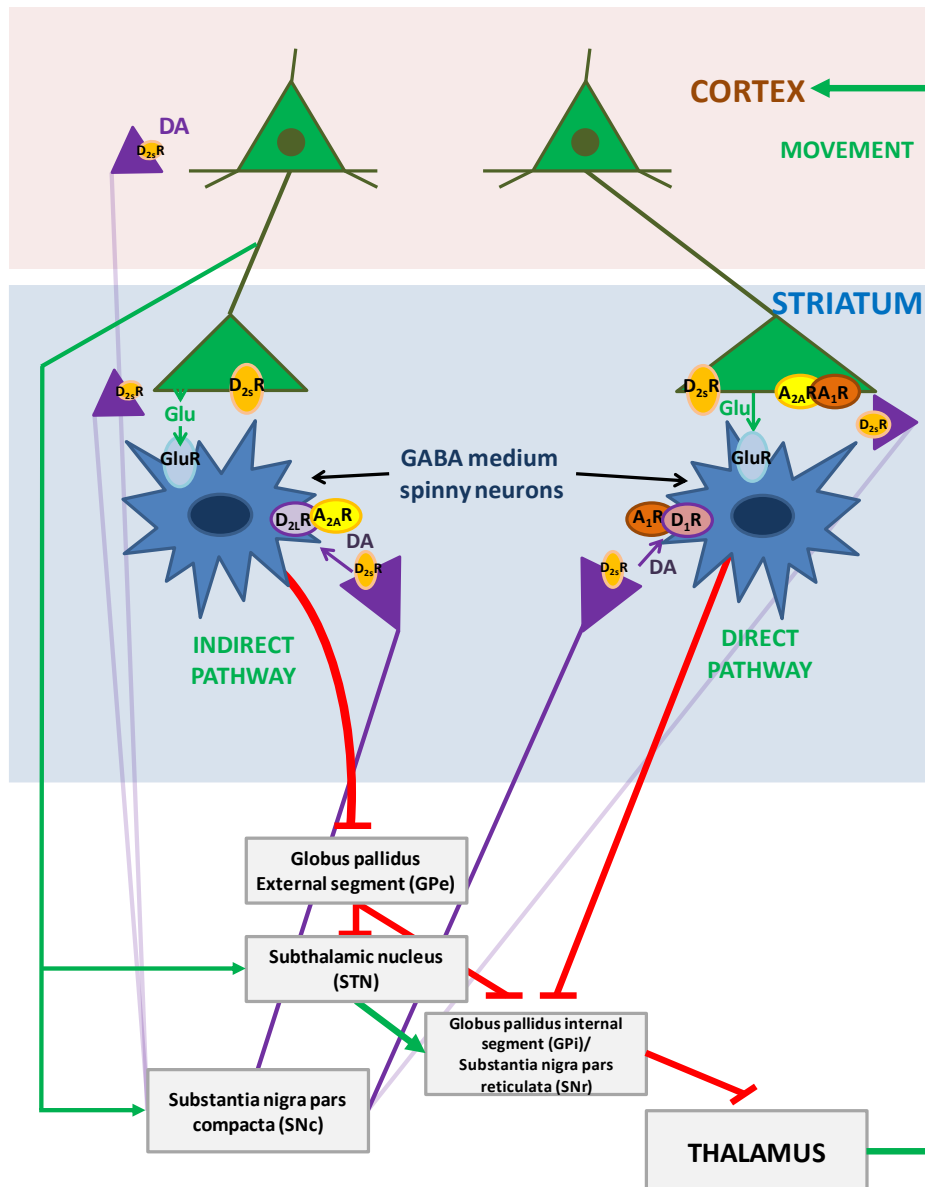


Figure 44. Schematic representation of the direct and indirect pathway of basal ganglia motor circuitry.

However, the differential affinities of DA for D₁R and D₂R (higher affinity for D₂R than for D₁R), provide a fine-tuning device by which bursts and pauses of DA neurons can differentially influence their activity. D₂R are more sensitive to DA pauses and D₁R are more sensitive to DA bursts. DA bursts activate and stimulate D₁Rs and cause the direct pathway to promote high value reward associate movements, the “GO” response. And DA pauses remove activation of inhibitory D₂Rs and cause the indirect pathway to suppress low-value reward-associate or high-value punishment associate movements, the “NO GO” response (Ferré et al., 2017).

6.1.2. Adenosine-dopamine receptor heteromers: control of motor function

In the striatum, both D₂R and A_{2A}R are expressed in striatopallidal neurons (indirect pathway) forming functional heteromers. It was largely known that A_{2A}R agonists selectively counteract and antagonists selectively potentiate the psychomotor-activating effects of D₂R agonists (Popoli et al., 1998; Rimondini et al., 1998; Strömberg et al., 2000; Ferré et al., 2001) (see also 5.4.1. section). The allosteric mechanisms within the A_{2A}R-D₂R heteromer plus the

heterotetrameric structure of the complex provided the rationale for the use of A_{2A}R antagonists in PD (results from this Thesis: Bonaventura et al., 2015). The most salient interaction between the complex are the ability of adenosine or exogenous A_{2A}R ligands to decrease the affinity and efficacy of DA or exogenous D₂R ligands (allosteric A_{2A}R-D₂R interaction) and the ability of D₂R agonist-mediated and G_{i/o} protein-dependent counteraction of A_{2A}R agonist-mediated and G_{s/olf}-dependent activation of AC (canonical G_s-G_i interaction). One more recently discovered interaction is a negative allosteric modulation between an orthosteric A_{2A}R agonist and an orthosteric A_{2A}R antagonist binding simultaneously to the A_{2A}R homodimer within the A_{2A}R-D₂R heterotetramer. This interaction provides the frame for the apparent psychostimulant effects of the non-selective A₁R and A_{2A}R antagonist caffeine (this work will be further explained in the Results section of this Thesis).

Thus, the A_{2A}R-D₂R heteromer acts as an integrative device that allows complex interactions between adenosine and DA controlling the function of the indirect pathway of the “NoGo” pathway. Preferential A_{2A}R versus D₂R activation leads to an increased activity of the “NoGo” pathway with a signal of not responding to reward-associated stimuli. Preferential D₂R versus A_{2A}R activation leads to a decreased activity of the “NoGo” pathway (Ferré et al., 2017).

Moreover, adenosine also modulates the “Go” pathway (direct pathway) through A₁R-D₁R postsynaptic complex that has been demonstrated in transfected cells, striatal neurons in culture (Ferré et al., 1998; Ginés et al., 2000) and in striatal tissue. A₁R activation leads to a selective significant counteraction of D₁R-mediated activation of striatal neurons both at the allosteric and AC interaction level (Ferré et al., 1996). At the behavioral level A₁R agonists selectively depress psychomotor activation induced by D₁R agonists.

Finally, the A₁R-A_{2A}R heteromer also plays a role in the fine-tune control of the glutamate release at the striatal glutamate terminal. Adenosine has more affinity for A₁R, thus, at low concentrations, adenosine will activate A₁R, which activates G_{i/o} proteins and inhibits glutamate release. Higher concentrations also activate A_{2A}R, which allosterically shuts down A₁R signaling, promotes G_s signaling, activation of cAMP and glutamate release (Ciruela et al., 2006; Cristóvão-Ferreira et al., 2013). Some studies have linked this heteromer with the direct pathway (Quiroz et al., 2009).

6.1.3 Dopamine-adenosine system in Parkinson’s disease

Dysfunctions of the central DA system are involved in a variety of disorders, including PD. The main motor symptoms of PD are bradykinesia, rigidity, tremors, akinesia and postural instability and are attributed to dysfunctions of the brain circuits involved in the execution and coordination of body movements, the “motor circuit”. In PD, neurodegeneration of dopaminergic neurons tends to occur initially and predominantly in the lateral part of the SNC, which projects mainly to the caudal dorsal striatum. In consequence, there is a predominant deficit of the more automatic versus intentional action skills and most sequential psychomotor responses need to be performed with full attention.

The reduced concentration of DA in the striatum induces hyperactivation of the globus pallidus internus via inhibition of the direct pathway and excitation of the indirect pathway and consequently, a hypoactivation of the thalamus. The net effect of the DA depletion and the decrease of the cortical output via pyramidal neurons correlate with hypokinetic movements that are typical for PD. Excess of dopaminergic stimulation would lead to hyperkinesia.

Patients with PD are usually treated with DA-related drugs including levodopa, monoamine oxidase B inhibitors and dopamine agonists, which in turn increase the risk of motor and non-motor complications (Stocchi et al., 2010; Chondrogiorgi et al., 2014; Moore et al., 2014). Non-dopaminergic agents are thus needed for improving PD therapy and limiting side effects. The antagonistic relationship between A_{2A}Rs and D₂Rs in the striatum has provided a rationale for evaluating A_{2A}R antagonists in PD that could reduce the risk of the onset of PD and subsequent dyskinesia caused by long-term dopaminergic drug therapy (Hernan et al., 2002; Kachroo et al., 2012; Wills et al., 2013; Preti et al., 2015). Moreover, A_{2A}R antagonists not only provide symptomatic relief but also decelerate the neurodegeneration of dopaminergic cells in patients with Parkinson's disease (Xu et al., 2005).

As an example, epidemiological evidence shows an inverse relationship between caffeine consumption and risk of developing PD (Ross, et al., 2000; Ascherio et al., 2001). In the same context, the A_{2A}R antagonist KW-6002 (istradefylline), was approved in Japan in 2013 (under the brand name NouriasTM) as adjunctive therapy to levodopa/carbidopa for the treatment of idiopathic PD reducing dyskinesia in patients who experience motor response complications (Jenner et al., 2009; Kondo et al., 2015) resulting from long-term treatment with classical antiparkinson drugs such as levodopa (Uchida et al., 2015; Ko et al., 2016). Istradefylline also exerts antidepressant-like effects via modulation A_{2A}R activity (Dungo and Deeks, 2013; Pinna, 2014; Yamada et al., 2014).

Besides KW-6002, other A_{2A}R antagonists are or have been in clinical trials such as SCH- 420814 (Merck-Schering), SYN-115 (Roche), vipadenant (Juno Therapeutics) or ST-1535 (Weiss et al., 2003; Peng et al., 2004; Cutler et al., 2012; Factor et al., 2013; Wang et al., 2013; Jenner, 2014; Pinna, 2014; Hauser et al., 2015; Sakata et al., 2017), but none of them has yet got the approval by the U.S. FDA mainly because of the difficulties in translating very promising preclinical assays into medications due to the tight requirements for being approval. It is well known that quite a number of current drugs would not pass today the tight requirements asked by the regulatory bodies.

6.2. Dopamine and adrenaline system interaction

The PFC is the most recently evolved region of the brain, subserving our highest order cognitive abilities. The cellular networks of the PFC are able to maintain representations of goals and rules and use remembered information to guide attention, behavior, and emotion (Goldman-Rakic, 1995). Current evidence supports the role of the PFC in the regulation of top-down attention, i.e. attention based on relevance (Buschman and Miller, 2007). Extensive projections to the sensory association cortices allow the PFC to suppress processing of irrelevant distractions and enhance processing of meaningful stimuli that may not be inherently captivating (e.g. homework) (Barbas et al., 2005; Yamaguchi and Knight, 1990). Depending on task demands, the PFC facilitates sustained attention on a single task (Wilkins et al., 1987) or manages rapid shifts in attention to accomplish multiple sequential tasks (Robbins and Roberts, 2007).

The right inferior PFC is especially important for reducing impulsive behavior and inhibiting inappropriate actions (Aron et al., 2004), while the orbital and ventromedial PFC is essential for the regulation of emotion, such as the inhibition of aggressive impulses (Best et al., 2002; Izquierdo et al., 2005; Price et al., 1996). These PFC regions act in concert to carry out the executive functions of planning and organizing appropriate actions, thoughts, and emotions. The

PFC regulates attention, behavior, and emotion through networks of pyramidal neurons that interconnect on dendritic spines. A unique feature of PFC networks is that neurons are able to excite each other in the absence of external environmental stimulation, thus representing information such as goals for behavior, even in the presence of distracting stimuli (Miller et al., 1993; Goldman-Rakic, 1995).

Lesions to the PFC produce symptoms such as forgetfulness, distractibility, impulsivity and/or perseveration, and disorganization. Patients with PFC lesions are easily distracted (Godefroy and Rousseaux, 1996; Woods and Knight, 1986), are impaired at gating sensory stimuli (Knight et al., 1989; Yamaguchi and Knight, 1990), have poor concentration and organization, and are more vulnerable to disruption from proactive interference (Thompson-Schill et al., 2002). There is also an old but consistent literature demonstrating that PFC lesions cause locomotor hyperactivity in monkeys (French, 1959; Gross, 1963; Kennard, 1941). Moreover, the PFC network activity is fragile, and extremely sensitive to the neurochemical environment. Thus, small changes in the arousal systems can markedly alter the connectivity of PFC networks (Arnsten et al., 2010). In particular, these PFC connections require that catecholamine concentrations be maintained at optimal levels (Arnsten, 2007)

Concretely, NE transmission in PFC through modulation of dopamine in NAc, is a necessary condition for motivational salience attribution to both reward- and aversion-related stimuli. In addition, NAc is involved in processing the information underlying the motivational control of goal-directed behavior, processing both rewarding and aversive stimuli (Wise, 2004). NE in PFC might activate mesoaccumbens DA release through excitatory prefrontal cortical projection to VTA DA cells (Sesack and Pickel, 1992; Shi et al., 2000) and/or through corticoaccumbal glutamatergic projections (Darracq et al., 1998). Moreover, a role for PFC projections to the LC in exerting an excitatory influence can be envisaged because this nucleus has been shown to activate VTA DA neurons (Grenhoff et al., 1993; Liprando et al., 2004), which could lead to increased DA release in NAc.

6.2.1. Catecholamine systems and ADHD

In summary, the PFC controls many of the executive functions that are altered in the pathology of ADHD. Moreover, it is important to note that, in the “Information Age,” when we are bombarded with stimuli and valued based on our abilities to organize and use large amounts of information efficiently. The more frequent diagnosis and treatment of ADHD may be related to this increased need for PFC abilities to succeed in modern society (Arnsten and Li, 2005).

Several imaging studies have shown that the dorsolateral PFC has a smaller volume and reduced blood flow or metabolism in patients with ADHD compared with controls (Castellanos et al., 2002, 2008; Mostofsky et al., 2002; Rubia et al., 1999; Seidman et al., 2005). Decreased PFC activity is particularly evident in the performance of tasks that require sustained attention or inhibition of inappropriate movement (Rubia et al., 2005). In patients with ADHD, the white matter tracts that link the PFC to other brain regions also appear less well organized (Casey et al., 2007; Makris et al., 2008), and functional connectivity is reduced (Castellanos et al., 2008). In addition, the volumes of other brain regions, such as the caudate and cerebellum, which have reciprocal connections with the PFC, have been reported to be smaller in children with ADHD than in control subjects in some studies (Castellanos et al., 2002). There is also evidence of delayed maturation of the PFC in children with ADHD (Shaw et al., 2007) that may vary in degree,

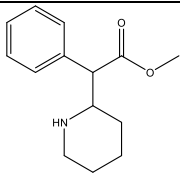
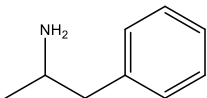
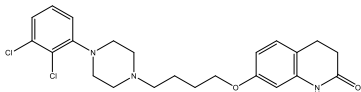
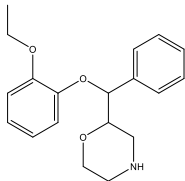
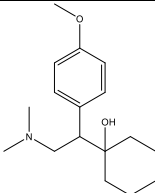
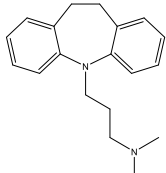
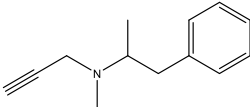
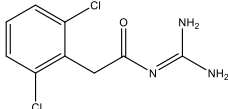
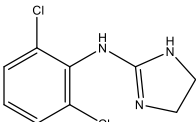
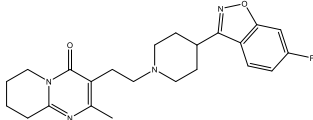
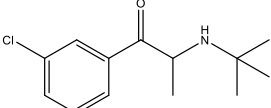
which may explain why ADHD continues into adulthood for some individuals, yet may resolve in others.

There is also suggestive evidence of reduced catecholamine, especially DA and NE, inputs to the PFC in adults with ADHD based on fluorodopa positron-emission tomography (PET) imaging (Ernst et al., 1998). These data are especially compelling, given that most medications used to treat ADHD enhance DA and NE transmission (Table 2). Genetic studies have also indicated linkage of vulnerability for developing ADHD and a variety of genes related to DA (the DA transporter, the DA degrading enzyme COMT, D₁R and D₄R) and NE (the synthetic enzyme dopamine beta hydroxylase and α_{2A} R) (Cook et al., 1995; Gill et al., 1997; Roman et al., 2003; Park et al., 2005; Arnsten and Li, 2005; Belcher et al., 2014).

Low to moderate levels of NE have important beneficial effects on PFC function, whereas high concentrations of NE released during stress contribute to impaired PFC function. Moderate levels of NE, when the subject is alert and interested, improve PFC function via α_2 R (Li and Mei, 1994), whereas high levels of NE released under stressful conditions engage lower affinity α_1 - and β -receptors and impair PFC function (Arnsten et al., 2000; Birnbaum et al., 2004; Ramos et al., 2005). α_{2A} R have been associated with ADHD and action impulsivity (Ma et al., 2003, 2005; Arnsten and Li, 2005; Cummins et al. 2014). Concretely, α_{2A} R agonists improve PFC function in mice (Franowicz et al., 2002), rats (Tanila et al., 1996), monkeys (Arnsten et al., 1988; Rama et al., 1996), and humans (Jakala et al., 1999a, 1999b) thus improving working memory and behavioral inhibition and protecting against distractibility. Moreover, the blocking of α_{2A} R with local yohimbine infusions in monkey PFC can recreate many of the symptoms of ADHD, including impulsivity and locomotor hyperactivity (Li and Mei, 1994; Ma et al., 2003, 2005). In contrast, α_1 R agonists impair working memory, while α_1 R antagonists protect PFC cognitive function from stress-induced impairment.

Among the α_2 Rs, the α_{2A} R subtype is the most prevalent in the PFC and is found both presynaptically on noradrenergic terminals and postsynaptically on the dendritic spines of PFC pyramidal cells that receive network inputs (Aoki et al., 1998; Wang et al., 2007). The effectiveness of PFC network connections relies on noradrenergic stimulation of α_{2A} Rs on the spines of PFC pyramidal cells (Wang et al., 2007). These α_{2A} R are localized on the dendritic spines near ion channels that control the impact of synaptic inputs on the spine (Wang et al., 2007). When these ion channels are open, nearby synaptic inputs are diverted and the incoming information escapes, weakening the synaptic connection (Fig. 45). Alternatively, stimulation of α_{2A} R, activates $G_{\alpha_{i/o}}$ proteins, decreasing cAMP levels via inhibition of adenylate cyclase and causing the closure of the ion channel, strengthening the synaptic connection.

Table 2. ReCompilation of prescribed medications for ADHD.

Compound	Commercial name	Action mechanism
Metilphenidate 	Ritalin [®] , Metadate CD [®] , Methylin ER [®] , Ritalin SR [®] , Contempla XR-ODT [®] , Focalin [®] , Focalin XR [®]	block reuptake of NE and DA into presynaptic neurons
Dextroamphetamine and amphetamine mixtures 	Adderall [®] , Mydayis, Dexedrine [®] , Vyvanse [®] , Dyanavel XR [®] , Evekeo [®]	block NE and DA reuptake in presynaptic neurons and increases release of these monoamines in extraneuronal spaces
Atomoxetine 	Strattera [®]	inhibit neuronal NE reuptake
Reboxetine 	Irenor [®]	inhibit neuronal NE reuptake
Venlafaxine 	Effexor [®]	inhibit neuronal serotonin and NE reuptake
Imipramine 	Tofranil [®]	inhibits the reuptake of NE or serotonin at presynaptic neurons
Selegiline 	Plurimen [®]	MAO B inhibitor, causes an increase of DA
Guanfacine 	Intuniv [®]	central alpha2 agonist
Clonidine 	Kapvay [®]	central alpha2 agonist
Risperidona 	Risperidal [®]	5-HT2n and D2 receptor agonist
Bupropion 	Wellbutrin [®]	NE and DA agonist

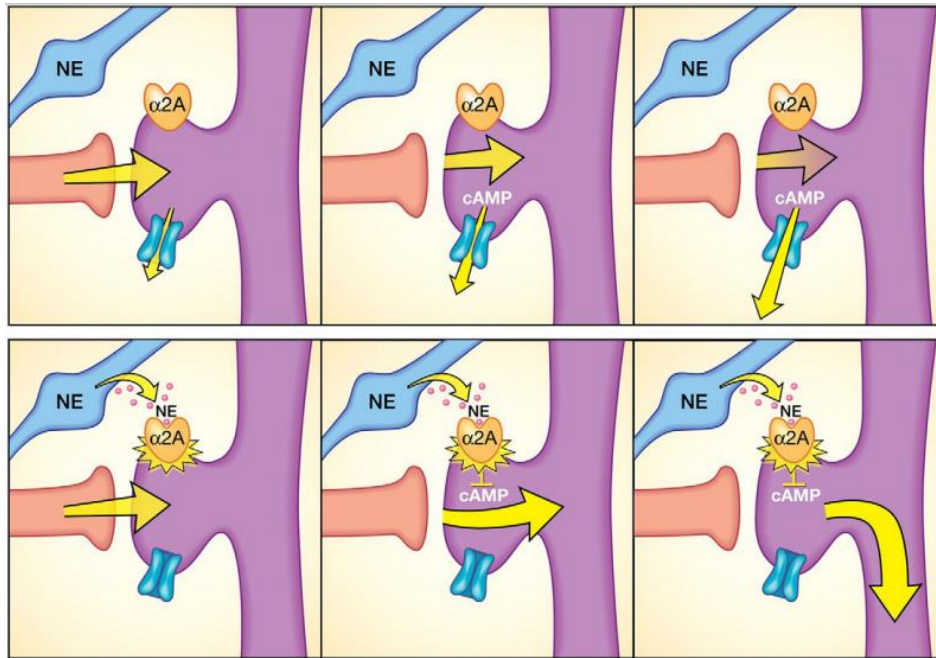


Figure 45. Stimulation of postsynaptic, α_{2A} R on PFC neurons by NE or guanfacine strengthens the functional connections between PFC neurons. Many α_{2A} R are found on the dendritic spines where PFC neurons form network connections. Top row: When there is no α_{2A} R stimulation, cAMP levels are high, potassium channels open, weakening nearby synaptic inputs. As a result, PFC network firing decreases, and there is weakened capability to regulate attention, behavior, or emotion. Bottom row: When α_{2A} R are stimulated by NE or by guanfacine, they close nearby potassium channels, increasing the efficacy of network inputs, and facilitating PFC function. Source: Wang et al. (2007).

Furthermore, according to Arnsten et al. (2000) and Arnsten and Li (2005), guanfacine and clonidine, two drugs approved by the FDA for the treatment of ADHD, produce their memory-enhancing effects by acting as agonists on a postsynaptic α_{2A} R without different sedative and hypotensive effects. A third possibility involves the report by Miller et al. (2014) of aberrant glutamate signaling in the PFC. These authors reported that the spontaneously hypertensive rat (SHR) model of ADHD involves a hyperfunctional glutamate system. The glutamatergic nerve terminals have α_{2A} R acting as heteroreceptors reducing glutamate release presynaptically in the PFC (Miller et al., 2014).

The most prominent dopaminergic actions in the PFC arise from actions at D_1 R, which are found in both superficial and deep layers of the primate PFC (Lidow et al., 1991). In the PFC, DA stimulation of D_1 R plays a role complementary to that of NE, decreasing PFC neuronal activity in response to irrelevant stimuli (Vijayraghavan et al., 2007). Activated D_1 Rs open ion channels on a set of dendritic spines that receive inputs irrelevant to focused working memory and attention. Opening channels on these spines weakens irrelevant network connections, reducing noisy input to the neuron and enhancing the efficiency of PFC function. However, diminishing these connections excessively may be harmful in situations that require broad attention or creative solutions; concretely, ADHD appears to be associated with depressed DA activity in the brain (Volkow et al., 2007). In addition, DA D_1 R overstimulation (e.g., under a stressful condition) may lead to disconnection of all network inputs and the cell may stop firing.

DA also binds at D_2 R in the PFC which are concentrated in layer V neurons where they also increase response-related firing (Wang et al., 2004). DA also acts at D_4 R in the PFC, where regulate cortical function, through pyramidal neurons or via modulation of GABA interneurons

that innervate pyramidal neurons (Mrzljak et al., 1996; Goldman-Rakic, 1998) or interneurons (Mrzljak et al., 1996; Wang et al., 2002).

Moreover, both D₂R and D₄R are involved in the modulation of corticostriatal glutamatergic transmission in the striatum (Maura et al., 1988, Gonzalez et al., 2012a; Bonaventura et al., 2017), both at the dendritic level (PFC) and at the terminal level (NAc shell) that is higher in the case of D_{4,7}R knock-in mice. A blunted corticostriatal transmission should affect the activity of both the “Go” and “NoGo” GABAergic striatal efferent pathways, decreasing their respective ability to increase the reactivity to reward-related stimuli and to suppress the reactivity to non-rewarded- or aversive-related stimuli (Bromberg-Martin et al., 2010). The outcome should be an increased “interest” for irrelevant stimuli and a reduced inhibition of irrelevant responses, which could be important in explaining the attention deficit and impulsivity of ADHD.

II- AIM AND OBJECTIVES

II. AIM AND OBJECTIVES

The catecholamines dopamine (DA) and norepinephrine (NE) constitute a class of conventional neurotransmitters and hormones that occupy key positions in the regulation of physiological processes and in the development of neurological, psychiatric, endocrine and cardiovascular diseases. DA has been shown to have a key role in regulating affect, attention, behavior and cognition, motivation and reward, sleep and voluntary movement. NE is involved in alertness, mood, arousal, learning and memory, motor control, blood flow, and metabolism. DA system has been a main focus of interest during the last decades mainly due to its role in pathologies such as Parkinson's disease, attention deficit hyperactivity disorder (ADHD), schizophrenia, Tourette syndrome, Huntington disease, Restless Leg syndrome and substance abuse disorder (SUD), among others, all related to a deregulation in the dopaminergic transmission. NE system has also been related with several diseases within the CNS such as psychiatric disorders including major depression and ADHD, among others. DA activates two families of receptors: D₁-like (D₁R and D₅R) and D₂-like receptors (D₂R, D₃R, and D₄R) and NE binds and activates three subfamilies of adrenoceptors: α_1 R, α_2 R and β R. These receptors are involved in the complex regulation system of the prefrontal cortex (PFC) and in the motor control. Both NE and DA receptors belong to the GPCR family, also known as seven transmembrane domain receptors. GPCRs comprise the largest superfamily of plasma membrane proteins in the body and are involved in 80% or more of the signal transduction processes that occur across cell membranes, acquiring an enormous biomedical importance. It is estimated that about 35% of approved drugs target GPCRs.

During the last two decades, a large number of GPCRs have been described to form homodimers, heterodimers and higher order oligomers that are often essential for the fine modulation of GPCR function. For these reasons, **we hypothesized** that *allosteric interactions between catecholamine receptors and other GPCR could be involved in neurologic and motor dysfunctions, and their study will help to rationally design new more effective drugs targeting these receptor heteromers with less secondary effects*. To test our hypothesis, we formulated the following **aim** of this Thesis: *to study and characterize the molecular interactions at pharmacological and functional level of heterodimers between catecholamine receptors and between catecholamine and adenosine receptors involved in several neurological pathologies related to imbalances in attention, impulsivity and motor control*.

To accomplish this main aim, we designed several specific objectives:

Most of the developed models that wanted to explain the behavior of drug-GPCR interactions, consider GPCRs as monomers. However, since oligomers have biochemical properties that are demonstrably different from those of their individual components, when working with receptor dimers but using monomeric models, some parameters obtained may be erroneous. This can be solved by using a dimer receptor model that considers oligomerization. Nevertheless, there are still several aspects to further investigate, such as the obtaining of different curve patterns in competitive radioligand binding experiments depending on the radioligand and its concentration. For this reason, we formulated the following objective:

- **Objective 1. To characterize the consequences of radioligand-competitor allosteric interactions within G protein-coupled receptor homodimers on the curve pattern and parameter values obtained in competitive experiments using the dimer receptor model.**

The biochemical, pharmacological and biological characterization of receptor oligomers is essential for understanding the normal function of the body as well as their alterations and roles in pathologies and has important implications in the field of GPCR pharmacology. It is well known that DA D₂Rs have an important role in the regulation of motor activity in the indirect pathway of the basal ganglia. In this pathway D₂Rs heteromerize with adenosine A_{2A}R, which negatively regulate their function through a complex system of allosteric modulations. For this reason, we formulated the following objective:

- Objective 2. To further biochemically, pharmacologically and biologically characterize the repercussions derived from the quaternary structure of the dopamine D₂ receptor and adenosine A_{2A} receptor heteromer, with an emphasis on both the ligand-protein and protein-protein allosteric interactions.

Customized drugs targeting a specific receptor oligomer in the CNS might improve safety and efficacy for their therapeutic targets. In this context, bivalent ligands are the best example of oligomers-selective ligands that can interact simultaneously with a (homo/hetero) GPCR dimer with high affinity and subtype selectivity. The main problem with bivalent ligands is that, if the orientation or the spacer length is not the appropriate may lead to dual-acting ligands. Thus, it is crucial to know the dimer interface and the quaternary structure of the receptor and also to choose the best pharmacophores for properly design these compounds. Due to knowledge acquired with the Objective 2 about the structure and function of homodimers, heterodimers and higher-order oligomers of D₂R, we formulated the following objective as a first step to design a true bivalent ligand between D₂-like receptors or with other catecholamine or adenosine receptors for the treatment of motor dysfunctions:

- Objective 3. To rationally design and evaluate bivalent ligands for dopamine D₂ receptor homodimers, using a combination of computational, chemical and biochemical tools.

In the brain, catecholamine innervations generally coincide with the distribution of its receptors but it is not always the case. There is compelling evidence indicating that DA and NE promiscuously interact with each other's receptors in some situations. As an example, striatum receives low striatal NE innervations and, in contrast, has high density of α_2 -adrenoceptors. It has been previously postulated that dopamine could provide the endogenous neurotransmitter for striatal α_2 Rs, although with discrepancies in the efficacy of this interaction, leaving the question unanswered. For this reason, we formulated the following objective:

- Objective 4. To characterize by radioligand binding assays the affinity of DA and synthetic DA receptor ligands for α_2 Rs and to determine the effectiveness of this binding in activating several signaling pathways.

The two most common polymorphisms of the human *DRD4* gene encode a D₄R with four or seven repeats of a proline-rich sequence of 16 amino acids (D_{4.4}R or D_{4.7}R). Although D_{4.7}R has been associated with ADHD, the differential functional properties between both variants remained enigmatic until recent electrophysiological and optogenetic-microdialysis

experiments that indicated a gain of function of D_{4.7}R. Since no clear differences in the biochemical properties of individual D_{4.4}R and D_{4.7}R have been reported, it has been suggested that those differences may emerge upon heteromerization with dopamine D₂R. Both D₂-like receptors co-localize in the corticostriatal pyramidal neurons of the layer V both pre- and post-synaptically, controlling glutamate release in the striatum and, consequently, the activation of the indirect pathway of the movement. Thus, we formulated the following objective:

- Objective 5. To functionally characterize heteromers between dopamine D₂R and dopamine D_{4.4}R, as well as with D_{4.7}R, prevalent in ADHD patients in order to find differences between variants that may explain the pathophysiology of this disorder.

Similar to D₄R, α_{2A} R has been associated with ADHD and action impulsivity and is present both in the PFC and basal ganglia. In view of the common epidemiological and pharmacological involvement of D₄R and α_{2A} R in impulse control and the apparent promiscuity of DA and NE in their ability to activate both receptors, we formulated the last objective of this Thesis:

- Objective 6. To characterize biochemically and pharmacologically new heteromers between human α_{2A} R and D_{4.4}R, as well as with the D_{4.7}R variant, prevalent in ADHD patients, in cell cultures and in striatum and PFC slices of control and human D_{4.7} knock-in mice to know if dopamine modulates adrenergic signaling and vice versa.

III- RESULTS



Report provided by the directors of the Doctoral Thesis presented as a compendium of articles.

Enric I Canela Campos and Antoni Cortés Tejedor of the Molecular Neurobiology Group from the Department of Biochemistry and Molecular Biomedicine, Faculty of Biology, University of Barcelona (Diagonal, 643, Edifici Prevosti, planta -2; 08028-Barcelona), directors of the Doctoral Thesis "Allosteric interactions between catecholamine receptors and other G protein-coupled receptors: pharmacological and functional characterization" presented by Verònica Casadó Anguera in the compendium of articles format expose that:

The manuscript **"Reinterpreting anomalous competitive binding experiments assuming radioligand-competitor allosteric interactions within G protein-coupled receptor homodimers"** has been submitted to Drug Discovery Today journal (IF: 6,369). The manuscript **"Allosteric interactions between agonists and antagonists within the adenosine A2A receptor-dopamine D2 receptor heterotetramer"** has been published in Proceedings of the National Academy of Sciences of the United States of America (PNAS) journal (IF: 9,423). The manuscript **"Evidence for the heterotetrameric structure of the adenosine A2A-dopamine D2 receptor complex"** has been published in Biochemical Society Transactions journal (IF: 2,765). The manuscript **"Functional pre-coupled complexes of receptor heteromers and adenylyl cyclase"** has been published in Nature Communications journal (IF: 12.124). The manuscript **"Design of a true bivalent ligand with picomolar binding affinity for a G protein-coupled receptor homodimer"** has been submitted to Journal of Medicinal Chemistry (IF: 6.259). The manuscript **" α_{2A} - and α_{2C} -Adrenoceptors as Targets for Dopamine and Dopamine Receptor Ligands"** has been published in Molecular Neurobiology journal (IF: 6,190). The manuscript **"Revisiting the functional role of dopamine D₄ receptor gene polymorphisms: Heteromerization-dependent gain of function of the D_{4.7} receptor variant"** has been submitted to ACS Chem. Biol (IF: 4,995). The manuscript **"Functional differences between dopamine D_{4.4} and D_{4.7} receptor variants into the dopamine D₄-adrenergic α_{2A} receptor heteromer in the brain"** is ready to be submitted to Neuropsychopharmacology journal (IP: 6.403).

In the article **"Reinterpreting anomalous competitive binding experiments assuming radioligand-competitor allosteric interactions within G protein-coupled receptor homodimers"** the PhD student Verònica Casadó is the first author and performed all the experimental part and the simulations assays and also participated in the design of the experiments and in the writing process of the manuscript.

In the article **"Allosteric interactions between agonists and antagonists within the adenosine A2A receptor-dopamine D2 receptor heterotetramer"** the PhD student Verònica Casadó performed radioligand experiments and proximity ligation assays and participated in the discussions of the manuscript.

In the article **"Evidence for the heterotetrameric structure of the adenosine A2A-dopamine D2 receptor complex"** the PhD student Verònica Casadó is the first author. She wrote most of the



manuscript and performed the novel experiments of radioligand dissociation of [³H]YM-09151-2 in the absence or presence of selective D₂R ligands.

In the article “**Functional pre-coupled complexes of receptor heteromers and adenylyl cyclase**” the PhD student Verònica Casadó performed experiments to determinate the canonical interaction between dopamine D₂ receptors and adenosine A_{2A} receptors at the adenylyl cyclase level in different cell models and participated in the discussion of the manuscript.

In the manuscript “**Design of a true bivalent ligand with picomolar binding affinity for a G protein-coupled receptor homodimer**” the PhD student Verònica Casadó is a first co-author with Dr. Daniel Pulido and Dr. Laura Pérez-Benito. Verònica Casadó participated in the design of the experiments and performed the bimolecular fluorescence complementation assay of D₂R homodimers in the presence of interference peptides. She also performed the pharmacological characterization of the bivalent ligands by binding assays (in the presence or absence of interference peptides) and tested the real-time signaling signature by a label-free method. She also participated in the writing process of the manuscript.

In the article “**α_{2A}- and α_{2C}-Adrenoceptors as Targets for Dopamine and Dopamine Receptor Ligands**” the PhD student Verònica Casadó is a first co-author with Dr. Marta Sánchez-Soto. Both researchers performed all the experiments except the modeling of the binding mode of dopamine at each receptor type that appears in Fig. 9 that was performed by Dr. Bryan Bender and Dr. Jens Meiler at Vanderbilt University, Nashville, USA.

In the manuscript “**Revisiting the functional role of dopamine D₄ receptor gene polymorphisms: Heteromerization-dependent gain of function of the D_{4.7} receptor variant**” the PhD student Verònica Casadó performed CODA-RET assays with Dr. Marta Sánchez Soto during her stay at Dr. Sergi Ferré lab at the NIH, Baltimore, USA, from September-December, 2016 and participated in the discussion and in the writing process of the manuscript.

In the manuscript “**Functional differences between dopamine D_{4.4} and D_{4.7} receptor variants within the dopamine D₄-adrenergic α_{2A} receptor heteromer in the brain**” the PhD student Verònica Casadó is the first author and participated in the design of the experiments and performed the totality of the experimental part. She also participated in the discussions and in writing the manuscript.

Dr. Marta Sánchez-Soto, for the elaboration of her Doctoral Thesis, used the results obtained in the article “**α_{2A}- and α_{2C}-Adrenoceptors as Targets for Dopamine and Dopamine Receptor Ligands**”, in a preliminary version of the manuscript prior to its publication. The results that appear in the manuscript “**Revisiting the functional role of dopamine D₄ receptor gene polymorphisms: Heteromerization-dependent gain of function of the D_{4.7} receptor variant**” pendent to be accepted for publication.

Dr. Laura López, for the elaboration of her Doctoral Thesis, used the results that appear in the manuscript “**Design of a true bivalent ligand with picomolar affinity for a G protein-coupled receptor homodimer**” pendent to be accepted for publication.

Dr. Jordi Bonaventura and Dr. Marc Brugarolas for the elaboration of their Doctoral Thesis used results that appear in the article “**Allosteric interactions between agonists and antagonists**”



UNIVERSITAT DE
BARCELONA

Departament de Bioquímica
i Biomedicina Molecular
Facultat de Biologia

Av. Diagonal, 643
Edifici Prevosti planta -2
08028 Barcelona

Tel. +34 934021523
Fax +34 934021559

within the adenosine A2A receptor-dopamine D2 receptor heterotetramer” when it was in a preliminary phase.

Barcelona, April 23rd, 2018

Dr. Enric I. Canela Campos

Dr. Antoni Cortés Tejedor



**UNIVERSITAT DE
BARCELONA**

**Departament de Bioquímica
i Biomedicina Molecular
Facultat de Biologia**

Av. Diagonal, 643
Edifici Prevosti planta -2
08028 Barcelona

Tel. +34 934021523
Fax +34 934021559

III. RESULTS

The results derived from this Thesis appear in the following articles and manuscripts:

Chapter 1. Reinterpreting anomalous competitive binding experiments assuming radioligand-competitor allosteric interactions within G protein-coupled receptor homodimers

Casadó-Anguera V, Moreno E, Mallol J, Ferré S, Canela EI, Cortés A, Casadó V.

Drug Discovery Today, submitted.

Reinterpreting anomalous competitive binding experiments assuming radioligand-competitor allosteric interactions within G protein-coupled receptor homodimers

Verònica Casadó-Anguera^{1,2}, Estefanía Moreno^{1,2}, Josefa Mallol^{1,2}, Sergi Ferré³, Enric I. Canela^{1,2}, Antoni Cortés^{1,2} and Vicent Casadó^{1,2}

¹ Centro de Investigación Biomédica en Red sobre Enfermedades Neurodegenerativas (CIBERNED), Spain

²Institute of Biomedicine of the University of Barcelona (IBUB), and Department of Biochemistry and Molecular Biomedicine, Faculty of Biology, University of Barcelona, Av. Diagonal 643, 08028 Barcelona, Spain

³National Institute on Drug Abuse, I.R.P., N.I.H., D.H.H.S., Baltimore, MD 21224, USA.

* Corresponding author: Vicent Casadó. Laboratory of Molecular Neurobiology, Department of Biochemistry and Molecular Biomedicine, Faculty of Biology, University of Barcelona, Av. Diagonal 643, 08028 Barcelona, Spain. Tel.: (34) 934039279; fax: (34) 934021559; vcasado@ub.edu

Author's e-mail addresses: vcasadoanguera@gmail.com (V. Casadó-Anguera), fifa877@hotmail.com (E. Moreno), jmallol@ub.edu (J. Mallol), sferre@intra.nida.nih.gov (S. Ferré), ecanela@ub.edu (E.I. Canela), antonicortes@ub.edu (A. Cortés), vcasado@ub.edu (V. Casadó)

Short title: Radioligand-competitor allosteric interactions

Key words: G-protein coupled receptor, pharmacological parameter, allosteric modulation, protein-protein interaction, receptor homodimer, dimer receptor model, molecular cross-talk

ABSTRACT

An increasing number of G protein-coupled receptors (GPCRs) have been reported to be expressed in the plasma membrane as dimers. Since most ligand binding data are currently fitted by classical equations developed only for monomeric receptors, the interpretation of data could be misleading in the presence of GPCR dimers. On the other hand, the equations developed from dimer receptor models assuming the existence of two orthosteric binding sites within the dimeric molecule offer the possibility to directly calculate macroscopic equilibrium dissociation constants for the two sites, an index of cooperativity (D_c) that reflects the molecular communication within the dimer and, importantly, a constant of radioligand-competitor allosteric interaction (K_{AB}). Here, we provide a practical new way to fit competitive binding data that allows to interpret apparently anomalous results, such as competition curves that could be either biphasic, monophasic or bell-shaped depending on the assay conditions. Considering a radioligand-competitor allosteric interaction allows fitting these data both under simulation conditions and in real radioligand binding experiments. Our approach is novel because it is the first that, assuming the formation of receptor homodimers, is able to explain several experimental results previously considered erroneous due to their impossibility to be fitted. We also deduce the radioligand concentration responsible for the conversion of biphasic to monophasic or to bell-shaped curves in competitive radioligand binding assays. In addition, we demonstrate that bell-shaped curves in competitive binding experiments constitute evidence for GPCR homodimerization.

INTRODUCTION

G protein-coupled receptors (GPCRs) comprise the largest protein superfamily in mammalian genomes, covering around 3% of the human proteome (Cvick et al., 2016). They are involved in 80% or more of the signal transduction processes that occur across cell membranes, exerting their intracellular effects in response to a wide array of extracellular ligands, including single photons, neurotransmitters, hormones and peptides (Wells, 2014). Their critical role in the mediation of transmembrane signal transduction makes GPCRs therapeutic targets in a large number of diseases, either due to their direct role in the pathophysiology of specific disease or due to their ability to modulate a set of signaling cascades implicated in a specific disease (Lefkowitz, 2004; Cvick et al., 2016). Therefore, GPCRs are the most important class of membrane proteins in clinical medicine, accounting for about 40% of all current marketed drugs. Moreover, 20% of recently Food and Drug Administration (FDA) approved drugs act through modulating GPCR functions (Garland, 2013; Katrich et al., 2013; Wang and Lewis, 2013), providing treatments for CNS disorders, cardiac dysfunction, cancer, diabetes, obesity, inflammation, and pain (Hauser et al., 2017).

The long perceived notion that GPCRs only function in monomeric form (Chabre and Le Maire, 2005; Ernst et al., 2007; Whorton et al., 2007, 2008; Chabre et al., 2009; Kuszak et al., 2009) has been changed in the last decades by the description of a number of GPCRs of classes A, B and C that are found as homodimers, heterodimers and higher order oligomers (for review, see Bouvier, 2001; Devi, 2001; George et al., 2002; Milligan, 2004, 2007, 2008; Ferré et al., 2009, 2014; Casadó et al., 2009a; Fuxe et al., 2010; Hiller et al., 2013; Ferré, 2015; Gomes et al., 2016 for review). In many cases, oligomeric structures of GPCRs are essential for receptor maturation, ligand pharmacology, signal transduction, and cellular trafficking (Milligan et al., 2006; López-Gimenez et al., 2007; Milligan 2008, 2013; Ciruela et al., 2011; Ulloa-Aguirre et al., 2014).

Radioligand binding is widely used to characterize receptors and determine their anatomical distribution. Saturation, competition and kinetic assays are the three types of experiments more commonly used. In saturation experiments, tissue sections, cultured cells, or homogenates are incubated with an increasing concentration of a radioligand, which is usually a radiolabeled synthetic drug. The subsequent analysis using nonlinear regression programs measures the affinity of the labeled ligand for the receptor (equilibrium dissociation constant K_D), and the receptor density (B_{max}). In kinetic experiments, samples are incubated with a constant radioligand concentration and, measuring its binding along the time, the rate of association (k_+) to or dissociation (k_-) from a receptor is calculated. However, in pharmacological studies, competition binding assays are the most widely used to determine the affinity and selectivity of an unlabeled ligand to compete for the binding of a fixed concentration of radiolabeled ligand to a receptor. Quantitative autoradiography and positron emission tomography (PET) image analysis are other sensitive techniques to detect low levels of radiolabeled ligands and to determine the anatomical distribution of receptors in tissue slices or in whole organs (Maguire et al., 2012).

Monomeric GPCRs have a single binding site and drug–receptor interactions are driven by the law of mass action, where a drug bounds to a particular receptor at a rate that depends on the concentration of both the drug and the receptor (Maggio et al., 2013). Therefore, at equilibrium, in saturation-binding studies, the B_{max} expressed by the sample must be the same

for all radioligands and should be independent of assay conditions. In competitive binding assays, all ligands should fully compete with each other, and dissociation constants determined in saturation and competition studies must be the same (Maggio et al., 2013). In this context of monomeric receptors, complex saturation or competition curves are interpreted considering two independent receptor populations that are not in equilibrium: one bound to G protein and the other not. In this scenario, the receptors coupled to G proteins have higher affinity (K_{DH}) for the agonist. These receptors could then be converted into low affinity (K_{DL}) receptors with the addition of GTP, which uncouple the G protein from the receptor (De Lean et al., 1980).

However, if oligomerization is taking place, it would be expected that this could alter the properties of the receptor, with equilibrium and kinetic binding assays exhibiting cooperativity (Strange, 2005). In fact, there is a growing list of receptors that have been found to form homomers, such as adenosine A_1 (Gracia et al., 2013; Navarro et al., 2016), A_{2A} (Łukasiewicz et al., 2007; Gracia et al., 2011; Bonaventura et al., 2015; Navarro et al., 2016, 2018) and A_3 (May et al., 2011), dopamine D_1 (Herrick-Davis et al., 2013; Guitart et al., 2014), D_2 (Guo et al., 2003; Pou et al., 2012; Bonaventura et al., 2015; Casadó-Anguera et al., 2016; Navarro et al., 2018) and D_3 (Pou et al., 2012; Guitart et al., 2014), serotonin $5HT_{1A}$ (Łukasiewicz et al., 2007), $5HT_{2A}$ (Herrick-Davis et al., 2013), $5HT_{2C}$ (Herrick-Davis et al., 2004, 2012; Mancía et al., 2008) and $5HT_7$ (Teitler et al., 2010), adrenergic α_{1B} (Herrick-Davis et al., 2013), β_1 (Mercier et al., 2002; Gherbi et al., 2015) and β_2 (Angers et al., 2000; Mercier et al., 2002; Herrick-Davis et al., 2013; Parmar et al., 2017), cannabinoid CB_1 (Bagher et al., 2017), angiotensin AT_1 (Szalai et al., 2012), metabotropic glutamate $mGlu_2$ (Levitz et al., 2016), muscarinic M_1 (Goin and Nathanson, 2006; Herrick-Davis et al., 2013), M_2 (Park and Wells, 2003; Goin and Nathanson, 2006; Herrick-Davis et al., 2013) and M_3 (Goin and Nathanson, 2006; McMillin et al., 2011), δ (Cvejic and Devi, 1997; McVey et al., 2001; Johnston et al., 2011), κ (Jordan and Devi, 1999) and μ (He et al., 2002) opioid, neurotensin 1 (White et al., 2007), melatonin MT_2 (Ayoub et al., 2004), niacin (Mandriks et al., 2010), and chemokine $CXCR4$ (Babcock et al., 2003) receptors. Analysis of complex radioligand binding curves, such as upward concave nonlinear Scatchard plots in saturation experiments and as biphasic curves in agonist-antagonist competitive experiments, have contributed to this notion. To deal with receptor homodimers, dimeric models have been developed (Chidiac et al., 1997; Durroux, 2005; Franco et al., 2005; Casadó et al., 2007; Rovira et al., 2008, 2009). These models consider an allosteric communication through the two protomers that allows negative cooperativity, meaning that the binding of a ligand to the first protomer decreases the affinity of the same ligand for the second protomer. In these cases, when handling with complex radioligand-binding curves, the use of the traditional two-independent-site model generates values for the equilibrium dissociation constants and for the number of receptors that vary significantly depending on the concentration of the radioligand employed (Casadó et al., 1991; Franco et al., 1996). This indicates a lack of robustness of the two-independent-site model that can be solved by using a dimer receptor model (Casadó et al., 2009a; Ferré et al., 2014). In other cases, when working with dimeric receptors and using monomeric models, dissociation constants determined in saturation and competition experiments do not match (Strange, 2005; Albizu et al., 2006). Moreover, concave-downward Scatchard plots, i.e. positive cooperativity (Albizu et al., 2006), only can be explained by dimeric models. In addition, mismatches in constant values obtained when dissociation is performed by dilution vs. by an excess of unlabeled ligand (De Meyts et al., 1973; Urizar et al., 2005; Kara et al., 2010; Gracia et al., 2013) cannot be explained by monomeric receptor models either.

Here, we focus on anomalous competitive binding experiments, when curves appear as biphasic, monophasic or bell-shaped depending on the assay conditions. Previously, Wreggett and Wells (1995), working with cardiac muscarinic receptors, reported that non-hydrolysable guanyl nucleotides induced bell-shaped curves in competitive radioligand binding assays which would only be interpretable assuming tetrameric receptors and a modulation between agonist and radioligand. Albizu et al. (2006) also showed some competition curves exhibiting an increase of the radioligand binding to vasopressin receptors for low concentrations of competitors, suggesting a cooperative binding process. Later, we provided experimental evidence showing the effect of radioligand concentration on the conversion of biphasic to monophasic curves (Casadó et al., 2009b). Now, we demonstrate that the existence of a radioligand-competitor allosteric interaction deduced from our dimer receptor model allows the fitting of bell-shaped curves, typically considered as anomalous or erroneous results. We also deduce the radioligand concentration responsible for the conversion of biphasic to monophasic or to bell-shaped curves in competitive radioligand binding assays. These curves are only interpretable assuming the formation of receptor homodimers.

MATERIALS AND METHODS

Membrane preparation and protein determination

Membrane suspensions from sheep brain striatum were processed as described previously (Casadó et al., 1990; Sarrió et al., 2000). Tissue was disrupted with a Polytron homogenizer (PTA 20 TS rotor, setting 3; Kinematica, Basel, Switzerland) for three 5 s-periods in 10 volumes of 50 mM Tris-HCl buffer, pH 7.4 containing a protease inhibitor cocktail (1:1000, Sigma, St. Louis, MO, USA). Cell debris were eliminated and membranes were obtained by centrifugation at 105,000 x g (60 min, 4°C), and the pellet was resuspended and recentrifuged under the same conditions. The resulting pellet was stored at -80°C and washed once more as described above and resuspended in 50 mM Tris-HCl buffer for immediate use. Protein was quantified by the bicinchoninic acid method (Pierce Chemical Co., Rockford, IL, USA) using bovine serum albumin dilutions as standard.

Radioligand binding experiments

Membrane suspensions (0.2 mg protein/ml) were incubated 2 h in 50 mM Tris-HCl buffer, pH 7.4, containing 10 mM MgCl₂ and 0.2 U/ml (1 µg/ml) desalted bovine adenosine deaminase (EC 3.5.4.4; Roche, Basel, Switzerland; only in adenosine A_{2A} receptor binding experiments) with the indicated free concentration of the adenosine A₁ receptor (A₁R) antagonist [³H]DPCPX (PerkinElmer, Wellesley, MA, USA), the adenosine A_{2A} receptor (A_{2A}R) agonist [³H]CGS21680 (PerkinElmer, Wellesley, MA, USA) or the dopamine D₁ receptor (D₁R) antagonist [³H]SCH23390 (PerkinElmer) and increasing concentrations of the A₁R agonist R-PIA, the A_{2A}R antagonist SCH442416, or the D₁R agonist SKF81297 (triplicates of 10-13 different concentrations from 0.1 nM to 50 µM; Tocris, Ellisville, MO, USA), respectively. Incubations were carried out at 25°C, except for A_{2A}R binding assays that were at 12 °C.

Nonspecific binding was determined in the presence of an excess of the corresponding unlabeled antagonist and confirmed that the value was the same as calculated by extrapolation of the competition curves. Free and membrane bound radioligands were separated by rapid filtration of 500 µl aliquots in a cell harvester (Brandel, Gaithersburg, MD, USA) through Whatman GF/C filters embedded in 0.3% polyethylenimine that were subsequently washed for

5 s with 5 ml of ice-cold Tris–HCl buffer. The filters were incubated with 10 ml of Ultima Gold MV scintillation cocktail (PerkinElmer, Boston, MA, USA) overnight at room temperature and radioactivity counts were determined using a Tri-Carb 2800 scintillation counter (PerkinElmer, Boston, MA, USA) with an efficiency of 62% (Sarrió et al., 2000).

Binding data analysis

Radioligand saturation curves were analyzed by nonlinear regression using the commercial Graft curve-fitting software (Erithacus Software, Surrey, UK), by fitting the specific binding data to our dimer receptor model (Casadó et al., 2007, 2009a,b). To calculate the macroscopic equilibrium dissociation constants involved in the binding of the radioligand, the following equation deduced by Casadó et al. (2007) was considered:

$$A_{\text{bound}} = \frac{(K_{\text{DA}2} A + 2 A^2) R_T}{(K_{\text{DA}1} K_{\text{DA}2} + K_{\text{DA}2} A + A^2)} \quad (\text{Eq. 1})$$

where A represents the free radioligand (the A₁R antagonist [³H]DPCPX, the A_{2A}R agonist [³H]CGS21680, or the D₁R antagonist [³H]SCH23390) concentration, R_T is the total amount of receptor dimers and K_{DA1} and K_{DA2} are the macroscopic dissociation constants describing the binding of the first and the second radioligand molecule (A) to the receptor homodimer.

Radioligand competition curves were also analyzed by nonlinear regression fitting experimental data to the following equation deduced from our dimer receptor model (Casadó et al., 2007):

$$A_{\text{bound}} = \frac{\left(K_{\text{DA}2} A + 2 A^2 + \frac{K_{\text{DA}2} A B}{K_{\text{DAB}}} \right) R_T}{K_{\text{DA}1} K_{\text{DA}2} + K_{\text{DA}2} A + A^2 + \frac{K_{\text{DA}2} A B}{K_{\text{DAB}}} + \frac{K_{\text{DA}1} K_{\text{DA}2} B}{K_{\text{DB1}}} + \frac{K_{\text{DA}1} K_{\text{DA}2} B^2}{K_{\text{DB1}} K_{\text{DB2}}}} \quad (\text{Eq. 2})$$

where A represents the radioligand (the A₁R antagonist [³H]DPCPX, the A_{2A}R agonist [³H]CGS21680, or the D₁R antagonist [³H]SCH23390) concentration, R_T is the total amount of receptor dimers and K_{DA1} and K_{DA2} are the macroscopic dissociation constants describing the binding of the first and the second radioligand molecule (A) to the dimeric receptor; B represents the assayed competing compound (the A₁R agonist R-PIA, the A_{2A}R antagonist SCH442416, or the D₁R agonist SKF81297) concentration and K_{DB1} and K_{DB2} are, respectively, the equilibrium dissociation constants of the first and second binding of B; K_{DAB} can be described as a hybrid equilibrium radioligand-competitor dissociation constant, which is the dissociation constant of B binding to a receptor dimer semi-occupied by A.

Since the radioligand A (the antagonist [³H]DPCPX, the agonist [³H]CGS21680, or the antagonist [³H]SCH23390) showed non-cooperative behavior (Casadó et al., 2007, 2009b, and results not shown), Eq. (2) was simplified to Eq. (3) due to the fact that K_{DA2} = 4K_{DA1} (see Casadó et al., 2007):

$$A_{\text{bound}} = \frac{\left(4 K_{DA1} A + 2 A^2 + \frac{4 K_{DA1} A B}{K_{DAB}}\right) R_T}{4 K_{DA1}^2 + 4 K_{DA1} A + A^2 + \frac{4 K_{DA1} A B}{K_{DAB}} + \frac{4 K_{DA1}^2 B}{K_{DB1}} + \frac{4 K_{DA1}^2 B^2}{K_{DB1} K_{DB2}}} \quad (\text{Eq. 3})$$

The dimer cooperativity index for the radioligand A or the competing ligand B was calculated as (see Casadó et al., 2007):

$$D_{CA} = \log \left(4 \frac{K_{DA1}}{K_{DA2}}\right) \quad D_{CB} = \log \left(4 \frac{K_{DB1}}{K_{DB2}}\right) \quad (\text{Eq. 4})$$

where 0 means non-cooperative value, positive values indicate positive cooperativity, whereas negative values imply negative cooperativity.

In the experimental conditions when both the radioligand A and the competitor B show non-cooperativity, it results that $K_{DA2} = 4K_{DA1}$ and $K_{DB2} = 4K_{DB1}$, and Eq. (2) and (3) were simplified to:

$$A_{\text{bound}} = \frac{\left(4 K_{DA1} A + 2 A^2 + \frac{4 K_{DA1} A B}{K_{DAB}}\right) R_T}{4 K_{DA1}^2 + 4 K_{DA1} A + A^2 + \frac{4 K_{DA1} A B}{K_{DAB}} + \frac{4 K_{DA1}^2 B}{K_{DB1}} + \frac{K_{DA1}^2 B^2}{K_{DB1}^2}} \quad (\text{Eq. 5})$$

The radioligand-competitor allosteric index can be calculated according to the equation:

$$D_{AB} = \log \left(2 \frac{K_{DB1}}{K_{DAB}}\right) \quad (\text{Eq. 6})$$

For comparison, data were also fitted to the classical one-site receptor model when monophasic competition curves were observed and to the classical two-independent-site receptor model when biphasic competition curves were obtained, using respectively the equations:

$$A_{\text{bound}} = \frac{R IC_{50}}{IC_{50} + B} \quad (\text{Eq. 7})$$

$$A_{\text{bound}} = \frac{R_H IC_{50H}}{IC_{50H} + B} + \frac{R_L IC_{50L}}{IC_{50L} + B} \quad (\text{Eq. 8})$$

where R , R_H and R_L are the specific binding in the absence of competing ligand. IC_{50} , IC_{50H} and IC_{50L} of the B compound are related with the respective equilibrium dissociation constants K_D , K_{DH} and K_{DL} according with Cheng and Prusoff (1973) equation:

$$K_{DH} = \frac{IC_{50H}}{1 + \frac{A}{K_{DA}}} \quad K_{DL} = \frac{IC_{50L}}{1 + \frac{A}{K_{DA}}} \quad (\text{Eq. 9})$$

Goodness of fit was tested according to reduced χ^2 value given by the nonlinear regression program. The test of significance for two different model population variances was based upon the F distribution (see Casadó et al. 1990, for details). Using this F test, a probability greater than 95% ($p < 0.05$) was considered the criterion to select a more complex model (cooperativity in Eq. (3) or two-sites in Eq. (8)) over the simplest one (non-cooperativity in Eq. (5) or one site in Eq. (7)). In all cases, a probability of less than 70% ($p > 0.30$) resulted when one model was not significantly better than the other. Results are given as parameter values \pm SEM of three independent experiments.

RESULTS

Adenosine A₁ receptors show slightly bell-shaped competitive curves

Working with A₁R, competition experiments are usually performed with an antagonist radioligand, such as [³H]DPCPX, displaced by a non-labeled agonist, such as R-PIA. Sometimes the curves obtained show a slight increase in the radioligand binding at low concentrations of the displacer R-PIA. This small bell-shaped pattern cannot be fitted by classical mathematical models based on monomeric receptors, such as the commonly used two-independent site model of radioligand binding to receptors. Data showed in Figure 1A are an example of a competition experiment of 0.009 nM [³H]DPCPX vs. R-PIA. Parameter values obtained by fitting these data to the classical two-independent-site model (Eq. (8)) appear in Table 1 and the fitting curve is represented in Figure 1A. The affinity values of R-PIA deduced from Cheng and Prusoff equation (Eq. 9) are much higher than those obtained from saturation assays that were in the low nM range (Gracia et al., 2013). As we can see, the points showing enhanced radioligand binding are left out. However, if we use our dimer receptor model (see Methods), and the points showing enhanced radioligand binding have low experimental dispersion, the bell-shaped curve can be accurately fitted by Eq. (3) using $K_{DA1} = 0.038$ nM (Gracia et al., 2013) (see Figure 1B). The parameter values obtained also appear in Table 1 and they are more according to the reported saturation data. Our dimer receptor model is able to explain the enhanced radioligand binding at low displacer concentrations due to the existence of an allosteric interaction between the two orthosteric ligands, radioligand ([³H]DPCPX) and competitive displacer (R-PIA), which is measured by the K_{DAB} parameter (see Methods and Table 1). By including this parameter in the fit, the two affinity values obtained for cooperative R-PIA are closer to the expected values from saturation assays.

However, if the points showing enhanced radioligand binding have high experimental dispersion, the inclusion of a new parameter (K_{AB}) does not significantly improve data fit to the dimer receptor model and the best fit is a slight biphasic curve defined only by the K_{DB1} and the K_{DB2} parameters, in addition to the total amount of dimers (R_T) and the K_{DA1} of the radioligand (Figure 1C). In this case, the points showing enhanced radioligand binding are underestimated. This curve overlaps with that obtained using the two-independent-site model.

Adenosine A_{2A} receptors show moderate bell-shaped competitive curves

Next, we moved to competitive radioligand binding assays with the A_{2A}R due to our expertise with the displacement of the A_{2A}R agonist [³H]CGS21680 by unlabeled competitive antagonists of this receptor. With these ligands, the curves obtained frequently show a more evident bell-shaped pattern despite that the experimental dispersion with this radioligand is high. In this particular experiment, we used 24 nM [³H]CGS21680 as free radioligand and increasing concentrations of SCH442416 as competitor. In the conditions pointed out in Figure 2, we obtained a bell-shaped curve when the concentrations of competitor (from 0.1 nM to 30 nM) clearly increased the binding of [³H]CGS21680, significantly more than in Figure 1. When these data are fitted by the classical one site or two-independent site models (Eq. (7) or (8)), the first points are not correctly fitted, and the points showing enhanced radioligand binding are left out (Figure 2A, dashed line). When fitting binding data to our dimer receptor model, we can consider the competitor SCH442416 as non-cooperative and only use the K_{DB1} parameter (Eq. (5) with $K_{DAB}=2K_{DB1}$). The values obtained, using $K_{DA1}=41$ nM (Gracia et al., 2011), appear in Table 2 and

the regression curve (solid line) roughly overlaps with the dashed line in Figure 2A. In contrast, if we consider that the antagonist shows cooperativity, we must include a second parameter, K_{DB2} (Eq. (3) with $K_{DAB}=2K_{DB1}$). In this case the fit is not better and overlaps with the solid line. Only when we consider the presence of an allosteric modulation between radioligand and competitor (K_{DAB} parameter), we obtain a bell-shaped curve and all points are correctly fitted (Eq. (5)) (see Figure 2B). All parameter values obtained also appear in Table 2. Again, only the high affinity value obtained for SCH442416 by fitting the bell-shaped curve with K_{DAB} is according with the high affinity value reported for this antagonist (Shinkre et al., 2010; Orrú et al., 2011). These results again show that the radioligand-competitor allosteric interaction measured by K_{DAB} is responsible for obtaining bell-shaped curves in competitive binding assays.

Dopamine D₁ receptors clearly show bell-shaped competitive curves

Then, we wanted to test our model with competitive curves working with D₁R because we previously reported the existence of a great radioligand-competitor allosteric interaction between [³H]SCH23390 and the agonist SKF81297 and because of the low experimental dispersion when working with this radioligand. The K_{DAB} value was 2 ± 1 nM, two times lower than the K_{DB1} value (7 ± 1 nM), pointing out a positive effect of [³H]SCH23390 on the SKF81297 affinity ($D_{AB}=+0.7\pm 0.1$, according to Eq. (6)) (see Methods section and Casadó et al., 2009b). This inter-ligand allosteric interaction was higher than between [³H]SCH23390 and SKF38393, where D_{AB} value was $+0.3\pm 0.1$. Here, first of all, we developed saturation curves of [³H]SCH23390 being aware of the light sensitivity of this radioligand. In Figure 3A we show saturation experiments of [³H]SCH23390 non-exposed to light, fitted to Eq. (1). This radioligand did not show cooperativity ($D_{CA}=0$), as expected for an antagonist (Eq. (4)), and the affinity value (K_{DA1}) was 0.27 nM. Surprisingly, when we developed competition curves of [³H]SCH23390 vs. SKF81297 at high (1.4 nM, Figure 3B, red line) or at low (0.15 nM, Figure 3B, blue line) radioligand concentration, we obtained two different curve patterns: biphasic (red line) and bell-shaped (blue line) curves when fitting to Eq. (5) of the dimer receptor model. Considering cooperativity in B binding (Eq. (3)), the fit was not better (see Methods). In Figure 3C we show a magnification of the bell-shaped results, also fitted to monomeric models (dotted line) according to Eq. (7). The parameter values obtained with Eq. (5) appear in Table 3. The affinity values of SKF81297 are highly robust (3 to 9 nM) at the three concentrations of radioligand used, and are in the range of reported values (Casadó et al., 2009b). Conversely, the affinity value obtained by the monomeric one-site model is much higher ($K_D=28$ nM), as observed in the other competition assays when fitting with monomeric models (Tables 1 and 2).

Simulating biphasic, monophasic and bell-shaped competitive binding curves with the dimer receptor model

Previously, we reported that competition experiments between [³H]SCH23390 and SKF81297 showed biphasic curves even in the absence of any cooperativity of the radioligand or the competitor (Casadó et al. 2009b). Assuming a marked positive radioligand-competitor modulation ($D_{AB}\gg 0$), our dimer receptor model predicted the evolution from biphasic to monophasic patterns when decreasing the radioligand concentration in the assay (Casadó et al. 2009b). Now, we simulate a set of competition curves considering the general competitive Eq. (5) and a set of parameters in the range of the [³H]SCH23390/SKF81297 system: , $K_{DA1}=1$ nM ($K_{DA2}=4$ nM, $D_{CA}=0$), $K_{DB1}=10$ nM ($K_{DB2}=40$ nM, $D_{CB}=0$) and $K_{DAB}=2$ nM ($D_{AB}=1$), and $R_T=0.5$ pmol/mg

protein. Importantly, decreasing the radioligand concentration (A) from 10 nM to 0.2 nM, curves evolve not only from biphasic to monophasic but also to bell-shaped patterns (Figure 4A). Next, we investigate the effect of K_{DAB} values at high (A=5 nM, Figure 4B) and low radioligand concentrations (A=1 nM, Figure 4C). As showed in Figure 4B, at high radioligand concentrations, when K_{DAB} values are low (with $D_{AB} \gg 0$, i.e. positive allosteric modulation between ligands), curves are clearly biphasic, and when K_{DAB} values are higher ($D_{AB} \ll 0$, i.e. negative allosteric modulation) curves abruptly decay; when $K_{DAB} \sim 2K_{DB1}$ ($D_{AB} \sim 0$) curves are monophasic. On the other hand, at low radioligand concentration (see Figure 4C), low K_{DAB} values ($D_{AB} \gg 0$) generate bell-shaped curves. Again, high K_{DAB} values ($D_{AB} \ll 0$) generate abruptly decreasing curves and with $K_{DAB} \sim 2K_{DB1}$ ($D_{AB} \sim 0$) curves show a normal monophasic pattern. The main conclusion of our simulation with the dimer receptor model is that there is a difference between the experiments performed at high or at low radioligand concentration when there is positive radioligand-competitor allosteric modulation ($D_{AB} \gg 0$). In this case, curve pattern is biphasic (for high radioligand concentration) or bell-shaped (for low radioligand concentration).

At this point, the question is: what concentration of radioligand causes competition curves to have a biphasic pattern? To answer this question, we analyzed Figure 4B, which shows a set of curves for high radioligand concentrations. These curves clearly show a pinched point, i.e. a common point for all curves. At this competitor concentration (B), all the curves (and all potential K_{DAB}) have the same radioligand binding (A_{bound}). The next question to answer was: what is this concentration of competitor? The mathematical expression of competitive binding used to generate the simulated curves when A and B are non-cooperative (Figure 4B) is Eq. (5) (see Methods). Then, for any two curves n and m of this figure, the radioligand bound is:

$$A_{bound\ n} = \frac{\left(4 K_{DA1} A + 2 A^2 + \frac{4 K_{DA1} A B}{K_{DAB\ n}}\right) R_T}{4 K_{DA1}^2 + 4 K_{DA1} A + A^2 + \frac{4 K_{DA1} A B}{K_{DAB\ n}} + \frac{4 K_{DA1}^2 B}{K_{DB1}} + \frac{K_{DA1}^2 B^2}{K_{DB1}^2}}$$

$$A_{bound\ m} = \frac{\left(4 K_{DA1} A + 2 A^2 + \frac{4 K_{DA1} A B}{K_{DAB\ m}}\right) R_T}{4 K_{DA1}^2 + 4 K_{DA1} A + A^2 + \frac{4 K_{DA1} A B}{K_{DAB\ m}} + \frac{4 K_{DA1}^2 B}{K_{DB1}} + \frac{K_{DA1}^2 B^2}{K_{DB1}^2}}$$

where all parameters are the same except for K_{DABn} and K_{DABm} (in red in the equations). At the B concentration of the competitor corresponding to the singular pinched point, all curves have the same radioligand bound and, then, $A_{bound\ n} = A_{bound\ m}$. Therefore, equaling the two expressions and solving the system, we obtain the quadratic equation:

$$\frac{K_{DA1}^2}{K_{DB1}^2} B^2 + \frac{4K_{DA1}^2}{K_{DB1}} B + 4K_{DA1}^2 - A^2 = 0$$

Only one solution is possible (positive):

$$B = \frac{(A - 2K_{DA1})K_{DB1}}{K_{DA1}}$$

but just if $A > 2K_{DA1}$. In any other case, the concentration of B would be negative at the pinched point. The B concentration for this point with the simulated parameter values is 30 nM with $A_{bound} = R_T$, i.e. with the dimers semi-occupied, exactly as deduced from Figure 4B.

Which graph pattern is obtained when $A=2K_{DA1}$? To answer this question, we simulated this scenario in Figure 4D, obtaining only monophasic curves. Thus, for the parameters employed in the simulations of the Figure 4, the critical concentration of the radioligand is $A=2$ nM.

The last question is: what radioligand concentration (A) is responsible for obtaining bell-shaped curves? The answer to this question can be found determining the slope of the curve corresponding to Eq. (5). The derivative of A_{bound} with respect to competitor concentration (B), when B tends to zero, must be positive to observe a bell-shaped curve, and its value must be negative for obtaining decreasing monophasic curves. When the derivative is zero, we obtain the quadratic expression:

$$\frac{1}{K_{DAB}} A^2 + \frac{2K_{DA1}}{K_{DB1}} A + \frac{4 K_{DA1}^2}{K_{DB1}K_{DAB}} (K_{DAB} - K_{DB1}) = 0$$

Solving the equation, we find the maximum critical A concentration that allows the obtaining of a bell-shaped curve:

$$A = \frac{2K_{DA1}}{K_{DB1}} (K_{DB1} - K_{DAB})$$

It is easily deduced that A must be lower than $2K_{DA1}$, tending to $2K_{DA1}$ value when K_{DAB} is much lower than K_{DA1} (high positive radioligand-competitor allosteric interaction). In addition, K_{DB1} must be higher than K_{DAB} . We can also deduce the competitor B corresponding to the maximum of the bell-shaped curve, being always $B \leq 2K_{DB1} - 2K_{DAB}$ and tending to $2K_{DB1} - 2K_{DAB}$ for low radioligand concentrations (A tending to 0).

In conclusion, if A and B are non-cooperative and there is a positive radioligand-competitor interaction (positive D_{AB}), when using radioligand concentrations higher than $2K_{DA1}$, the curves will be biphasic in competition experiments (Figure 4B); in contrast, when $A=2K_{DA1}$, monophasic curves are always obtained (Figure 4D) and, when $A < 2K_{DA1}$, we can obtain bell-shaped curves if $K_{DAB} < K_{DB1}$ and A specifically lower than $2K_{DA1} (K_{DB1} - K_{DAB}) / K_{DB1}$ (Figure 4C) or, in any other cases, curves will be always monophasic.

Bell-shaped competitive curves with dopamine D₁ receptors can be modulated according with the radioligand concentration used

Finally, we prove the hypothesis deduced above from our dimer receptor model. Effectively, the bell-shaped curve (Figure 3B, blue line) was obtained at a free radioligand concentration of 0.15 nM, lower than $2K_{DA1}=0.54$ nM. Under these conditions the above simulation predicts that the existence of a radioligand-competitor interaction ($K_{DAB}=2.5$ nM) can generate bell-shaped competition curves. The same experiment showed a biphasic pattern (Figure 3B, red line) at a high free radioligand concentration of 1.4 nM, higher than 0.54 nM. However, the same experiment performed at an intermediate free radioligand concentration, near to 0.54 nM, should generate monophasic curves.

Finally, we developed [³H]SCH23390 vs. SKF81297 competition curves at 0.4 nM of free radioligand and, as showed in Figure 3B (black line), curves fitted to Eq. (3) are now monophasic. These results experimentally demonstrate that the pattern of the competitive curves can vary according to the radioligand concentration employed, due to the existence of a positive radioligand-competitor interaction ($D_{AB} > 0$) in a receptor homodimer.

DISCUSSION

When analyzing competitive binding experiments, we sometimes obtain the surprising findings of a biphasic curve using an antagonist ligand or a monophasic curve using an agonist ligand, as competitors. Even more anomalous are those curves showing a bell-shaped pattern, where increasing concentrations of a competitor produce an increase of the radioligand binding before causing the expected displacement. This increase is usually from low to moderate; for example, when working with vasopressin receptors, increases in radioligand binding were frequently observed which did not exceed 20% of the binding in the absence of competitor (Berde et al., 1964; Albizu et al., 2006). Now, we demonstrate that the existence of a radioligand-competitor allosteric interaction, deduced from our dimer receptor model (Casadó et al., 2009b), allows the fitting of bell-shaped curves, typically considered as anomalous or erroneous results. We also deduce the radioligand concentration responsible for the conversion from biphasic to monophasic or to bell-shaped curves in competitive radioligand binding assays. Moreover, we demonstrate that bell-shaped curves are only interpretable assuming the formation of receptor homodimers and, therefore, obtaining bell-shaped curves in competition experiments is a clear evidence for receptor dimerization *in vitro* (working with membrane preparations from transfected cells) and *ex-vivo* (working with membrane preparations from tissues).

According to our results, we can decrease the radioligand concentration under its affinity value ($2K_{DA1}$ or lower) to obtain bell-shaped competition curves. This is a demonstration of the existence of positive radioligand-competitor interaction ($D_{AB}>0$), denoted by a low K_{DAB} value. In this scenario, if $K_{DAB}<K_{DB1}$, we will obtain bell-shaped curves but, if K_{DAB} is between K_{DB1} and $2K_{DB1}$, we will obtain monophasic curves. Working with high affinity radioligands, radioligand concentration much higher than their K_{DA1} values are usually used, which precludes the observation of bell-shaped curves. In addition, if the value of D_{AB} is low, in order to observe the bell-shaped curves, the radioligand concentration should be significantly reduced. Otherwise, the bound ligand would be low and the experimental dispersion could mask the bell-shaped pattern of the competitive curves, as showed in Figure 1. The use of radioligand concentrations under their $2K_{DA1}$ values is more common when working with low affinity radioligands. In these cases, competition experiments similar to those shown in Figure 2 exhibit evident bell-shaped patterns, if D_{AB} is clearly positive (especially higher than +0.5).

It is interesting to note that, although there is clear evidence of the dimerization of GPCRs, currently, radioligand binding data are still fitted to equations deduced for one site or for two-independent site models. This is because experimental data usually fit equally to these simpler models or to the dimer receptor model. The experiments showed here, i.e. bell-shaped curves in competition assays, only can be explained considering homodimeric/oligomeric receptors and fitting data to a dimer receptor model. Chidiac et al. (1997) also suggested that a bell-shaped pattern cannot be obtained from a system of independent sites. Likewise, the conversion of the curve pattern from biphasic to monophasic (Casadó et al., 2009b) and to bell-shaped curves, decreasing the radioligand concentration in the competition assay, only can be interpreted by dimeric or oligomeric models. Our model explains all these cases due to the existence of a radioligand-competitor allosteric interaction, only explainable if receptors form homodimers. Our dimer receptor model can overcome scenarios where different affinity values for a competitive drug are obtained, when different radioligands are used and monomeric models are applied (Maggio et al., 2013). This is because our model takes in account that each

pair of radioligand-competitor has a particular K_{DAB} value according to the magnitude of its allosteric interaction. If this K_{DAB} value is not included in the mathematical fitting model, the affinity values of the competitor obtained with the monomeric one-site and two-independent-site models will not be robust, but inconsistent and erroneous. Furthermore, when bell-shaped curves are obtained in competitive radioligand binding assays, the affinity values of the competitor obtained from equations including K_{DAB} are closer to the actual values. On the contrary, the K_D values obtained from classical monomeric models are usually much higher.

In summary, by assuming the formation of receptor homodimers, our study is the first that can explain several experimental results previously considered erroneous due to their impossibility to be well fitted. Furthermore, our model is easy to use, in contrast to the over-parameterization of other dimer receptor models, and it can successfully predict the pattern of competition curves according to the experimental conditions.

ACKNOWLEDGEMENTS

This research was supported by “Ministerio de Economía y Competitividad” and European Regional Development Funds of the European Union (Grant SAF2014-54840-R and SAF2017-87629-R), “Centro de Investigación Biomédica en Red sobre Enfermedades Neurodegenerativas” (Grant CB06/05/0064), the “Fundació La Marató de TV3” (Grant 20140610), and intramural funds of the National Institute on Drug Abuse.

REFERENCES

- Albizu, L., Balestre, M.N., Breton, C., Pin, J.P., Manning, M., Mouillac, B., Barberis, C., Durroux, T. (2006). Probing the existence of G protein-coupled receptor dimers by positive and negative ligand-dependent cooperative binding. *Mol Pharmacol* 70, 1783-1791.
- Angers, S., Salahpour, A., Joly, E., Hilairret, S., Chelsky, D., Dennis, M., Bouvier, M. (2000). Detection of beta 2-adrenergic receptor dimerization in living cells using bioluminescence resonance energy transfer (BRET). *Proc Natl Acad Sci USA* 97, 3684-3689.
- Ayoub, M.A., Levoye, A., Delagrangé, P., Jockers, R. (2004). Preferential formation of MT1/MT2 melatonin receptor heterodimers with distinct ligand interaction properties compared with MT2 homodimers. *Mol Pharmacol* 66, 312-321.
- Babcock, G.J., Farzan, M., Sodroski, J. (2003). Ligand-independent dimerization of CXCR4, a principal HIV-1 coreceptor. *J Biol Chem* 278, 3378–3385.
- Bagher, A.M., Laprairie, R.B., Toguri, J.T., Kelly, M.E.M., Denovan-Wright, E.M. (2017). Bidirectional allosteric interactions between cannabinoid receptor 1 (CB1) and dopamine receptor 2 long (D2L) heterotetramers. *Eur J Pharmacol* 813, 66-83. doi: 10.1016/j.ejphar.2017.07.034.
- Berde, B., Boissonnas, R.A., Huguenin, R.L., Sturmer, E. (1964). Vasopressin analogues with selective pressor activity. *Experientia* 20, 42–43.
- Bonaventura, J., Navarro, G., Casadó-Anguera, V., Azdad, K., Rea, W., Moreno, E., Brugarolas, M., Mallol, J., Canela, E.I., Lluís, C., Cortés, A., Volkow, N.D., Schiffmann, S.N., Ferré, S., Casadó, V. (2015). Allosteric interactions between agonists and antagonists within the adenosine A2A receptor-dopamine D2 receptor heterotetramer. *Proc Natl Acad Sci USA* 112, E3609-3618. doi: 10.1073/pnas.1507704112.
- Bouvier, M. (2001). Oligomerization of G-protein-coupled transmitter receptors. *Nat Rev Neurosci* 2, 274–286.

- Casadó, V., Cantí, C., Mallol, J., Canela, E.I., Lluís, C., Franco, R. (1990). Solubilization of A1 adenosine receptor from pig brain: characterization and evidence of the role of the cell membrane on the coexistence of high- and low-affinity states. *J Neurosci Res* 26, 461–473.
- Casadó, V., Mallol, J., Canela, E.I., Lluís, C., Franco, R. (1991). The binding of [3H]R-PIA to A1 adenosine receptors produces a conversion of the high- to the low-affinity state. *FEBS Lett* 286, 221-224.
- Casadó, V., Cortés, A., Ciruela, F., Mallol, J., Ferré, S., Lluís, C., Canela, E.I., Franco, R. (2007). Old and new ways to calculate the affinity of agonists and antagonists interacting with G-protein-coupled monomeric and dimeric receptors: the receptor-dimer cooperativity index. *Pharmacol Ther* 116, 343-354.
- Casadó, V., Cortés, A., Mallol, J., Pérez-Capote, K., Ferré, S., Lluís, C., Franco, R., Canela, E.I. (2009a). GPCR homomers and heteromers: a better choice as targets for drug development than GPCR monomers? *Pharmacol Ther* 124, 248-257. doi: 10.1016/j.pharmthera.2009.07.005
- Casadó, V., Ferrada, C., Bonaventura, J., Gracia, E., Mallol, J., Canela, E.I., Lluís, C., Cortés, A., Franco, R. (2009b). Useful pharmacological parameters for G-protein-coupled receptor homodimers obtained from competition experiments. Agonist-antagonist binding modulation. *Biochem Pharmacol* 78, 1456-1463. doi: 10.1016/j.bcp.2009.07.012.
- Casadó-Anguera, V., Bonaventura, J., Moreno, E., Navarro, G., Cortés, A., Ferré, S., Casadó, V. (2016). Evidence for the heterotetrameric structure of the adenosine A2A-dopamine D2 receptor complex. *Biochem Soc Trans* 44, 595-600. doi: 10.1042/BST20150276.
- Chabre, M., le Maire, M. (2005). Monomeric G-protein coupled receptor as a functional unit. *Biochemistry* 44, 9395-9403.
- Chabre, M., Deterre, P., Antony, B. (2009). The aparent cooperativity of some GPCRs does not necessarily imply dimerization. *Trends Pharmacol Sci* 30, 182-187.
- Cheng, Y.C., Prusoff, W.H. (1973). Relationship between the inhibition constant (K_i) and the concentration of inhibitor which causes 50 percent inhibition (I₅₀) of an enzymatic reaction. *Biochem Pharmacol* 22, 3099–3108.
- Chidiac, P., Green, M.A., Pawagi, A.B., Wells, J.W. (1997). Cardiac muscarinic receptors. Cooperativity as the basis for multiple states of affinity. *Biochemistry* 36, 7361-7379.
- Ciruela, F., Gomez-Soler, M., Guidolin, D., Borroto-Escuela, D.O., Agnati, L.F., Fuxe, K., Fernandez-Dueñas, V. (2011). Adenosine receptor containing oligomers: their role in the control of dopamine and glutamate neurotransmission in the brain. *Biochim Biophys Acta* 1808, 1245-1255.
- Cvejic, S., Devi, L.A. (1997). Dimerization of the delta opioid receptor: implication for a role in receptor internalization. *J Biol Chem* 272, 26959-26964.
- Cvick, V., Goddard, W.A., Abrol, R. (2016). Structure-based sequence alignment of the transmembrane domains of all human GPCRs: Phylogenetic, structural and functional implications. *PLoS Comput Biol* 12, e1004805. doi: 10.1371/journal.pcbi.1004805.
- De Lean, A., Stadel, J.M., Lefkowitz, R.J. (1980). A ternary complex model explains the agonist-specific binding properties of the adenylate cyclase-coupled b-adrenergic receptor. *J Biol Chem* 255, 7108-7117.
- De Meyts, P., Roth, J., Neville, D.M., Gavin, J.R., Lesniak, M.A. (1973). Insulin interactions with its receptors, experimental evidence for negative cooperativity. *Biochem Biophys Res Commun* 55, 154e161.

- Devi, L.A. (2001). Heterodimerization of G-protein-coupled receptors: pharmacology, signaling and trafficking. *Trends Pharmacol Sci* 22, 532–537.
- Durroux, T. (2005). Principles: a model for the allosteric interactions between ligand binding sites within a dimeric GPCR. *Trends Pharmacol Sci* 26, 376–384.
- Ernst, O.P., Gramse, V., Kolbe, M., Hofmann, K.P., Heck, M. (2007). Monomeric G protein-coupled receptor rhodopsin in solution activates its G protein transducin at the diffusion limit. *Proc Natl Acad Sci USA* 104, 10859–10864.
- Ferré, S. (2015). The GPCR heterotetramer: challenging classical pharmacology. *Trends Pharmacol Sci* 36, 145–152. doi: 10.1016/j.tips.2015.01.002
- Ferré, S., Baler, R., Bouvier, M., Caron, M.G., Devi, L.A., Durroux, T., Fuxe, K., George, S.R., Javitch, J.A., Lohse, M.J., Mackie, K., Milligan, G., Pflieger, K.D., Pin, J.P., Volkow, N.D., Waldhoer, M., Woods, A.S., Franco, R. (2009). Building a new conceptual framework for receptor heteromers. *Nat Chem Biol* 5, 131–134. doi: 10.1038/nchembio0309-131.
- Ferré, S., Casadó, V., Devi, L.A., Filizola, M., Jockers, R., Lohse, M.J., Milligan, G., Pin, J.P., Guitart, X. (2014). G protein-coupled receptor oligomerization revisited: functional and pharmacological perspectives. *Pharmacol Rev* 66, 413–434. doi: 10.1124/pr.113.008052.
- Franco, R., Casadó, V., Ciruela, F., Mallol, J., Lluís, C., Canela, E.I. (1996). The cluster-arranged cooperative model: a model that accounts for the kinetics of binding to A1 adenosine receptors. *Biochemistry* 35, 3007–3015.
- Franco, R., Casadó, V., Mallol, J., Ferré, S., Fuxe, K., Cortés, A., Ciruela, F., Lluís, C., Canela, E.I. (2005). Dimer-based model for heptaspanning membrane receptors. *Trends Biochem Sci* 30, 360–366.
- Fuxe, K., Marcellino, D., Borroto-Escuela, D.O., Frankowska, M., Ferraro, L., Guidolin, D., Ciruela, F., Agnati, L.F. (2010). The changing world of G protein-coupled receptors: from monomers to dimers and receptor mosaics with allosteric receptor-receptor interactions. *J Recept Signal Transduct Res* 30, 272–283. doi: 10.3109/10799893.2010.506191.
- Garland, S.L. (2013). Are GPCRs still a source of new targets? *J Biomol Screen* 18, 947–66.
- George, S.R., O'Dowd, B.F., Lee, S.R. (2002). G-protein-coupled receptor oligomerization and its potential for drug discovery. *Nat Rev Drug Discovery* 1, 808–820.
- Gherbi, K., May, L.T., Baker, J.G., Bridson, S.J., Hill, S.J. (2015). Negative cooperativity across β 1-adrenoceptor homodimers provides insights into the nature of the secondary low-affinity CGP 12177 β 1-adrenoceptor binding conformation. *FASEB J* 29, 2859–2871. doi: 10.1096/fj.14-265199.
- Goin, J.C., Nathanson, N.M. (2006) Quantitative analysis of muscarinic acetylcholine receptor homo- and heterodimerization in live cells: regulation of receptor down-regulation by heterodimerization. *J Biol Chem* 281, 5416–5425.
- Gomes, I., Ayoub, M.A., Fujita, W., Jaeger, W.C., Pflieger, K.D., Devi, L.A. (2016). G Protein-Coupled Receptor Heteromers. *Annu Rev Pharmacol Toxicol* 56, 403–425. doi: 10.1146/annurev-pharmtox-011613-135952.
- Gracia, E., Pérez-Capote, K., Moreno, E., Barkešová, J., Mallol, J., Lluís, C., Franco, R., Cortés, A., Casadó, V., Canela, E.I. (2011). A2A adenosine receptor ligand binding and signalling is allosterically modulated by adenosine deaminase. *Biochem J* 435, 701–709. doi: 10.1042/BJ20101749.

- Gracia, E., Moreno, E., Cortés, A., Lluís, C., Mallol, J., McCormick, P.J., Canela, E.I., Casadó, V. (2013). Homodimerization of adenosine A₁ receptors in brain cortex explains the biphasic effects of caffeine. *Neuropharmacology* 71, 56-69. doi: 10.1016/j.neuropharm.2013.03.005.
- Guitart, X., Navarro, G., Moreno, E., Yano, H., Cai, N.S., Sánchez-Soto, M., Kumar-Barodia, S., Naidu, Y.T., Mallol, J., Cortés, A., Lluís, C., Canela, E.I., Casadó, V., McCormick, P.J., Ferré, S. (2014). Functional selectivity of allosteric interactions within G protein-coupled receptor oligomers: the dopamine D1-D3 receptor heterotetramer. *Mol Pharmacol* 86, 417-429. doi: 10.1124/mol.114.093096.
- Guo, W., Shi, L., Javitch, J.A. (2003). The fourth transmembrane segment forms the interface of the dopamine D2 receptor homodimer. *J Biol Chem* 278, 4385-4388.
- Hauser, A.S., Attwood, M.M., Rask-Andersen, M., Schiöth, H.B., Gloriam, D.E. (2017). Trends in GPCR drug discovery: new agents, targets and indications. *Nat Rev Drug Discov* 16, 829-842. doi: 10.1038/nrd.2017.178.
- He, L., Fong, J., von Zastrow, M., Whistler, J.L. (2002). Regulation of opioid receptor trafficking and morphine tolerance by receptor oligomerization. *Cell* 108, 271-282.
- Herrick-Davis, K., Grinde, E., Mazurkiewicz, J.E. (2004). Biochemical and biophysical characterization of serotonin 5-HT_{2C} receptor homodimers on the plasma membrane of living cells. *Biochemistry* 43, 13963-13971.
- Herrick-Davis, K., Grinde, E., Lindsley, T., Cowan, A., Mazurkiewicz, J.E. (2012). Oligomer size of the serotonin 5-hydroxytryptamine 2C (5-HT_{2C}) receptor revealed by fluorescence correlation spectroscopy with photon counting histogram analysis: evidence for homodimers without monomers or tetramers. *J Biol Chem* 287, 23604-23614. doi: 10.1074/jbc.M112.350249.
- Herrick-Davis, K., Grinde, E., Cowan, A., Mazurkiewicz, J.E. (2013). Fluorescence correlation spectroscopy analysis of serotonin, adrenergic, muscarinic, and dopamine receptor dimerization: the oligomer number puzzle. *Mol Pharmacol* 84, 630-642. doi: 10.1124/mol.113.087072.
- Hiller, C., Kühhorn, J., Gmeiner, P. (2013). Class A G-protein-coupled receptor (GPCR) dimers and bivalent ligands. *J Med Chem* 56, 6542-6559.
- Johnston, J.M., Aburi, M., Provasi, D., Bortolato, A., Urizar, E., Lambert, N.A., Javitch, J.A., Filizola, M. (2011). Making structural sense of dimerization interfaces of delta opioid receptor homodimers. *Biochemistry* 50, 1682-1690. doi: 10.1021/bi101474v.
- Jordan, B.A., Devi, L.A. (1999). G-protein-coupled receptor heterodimerization modulates receptor function. *Nature* 399, 697-700.
- Kara, E., Lin, H., Strange, P.G. (2010). Co-operativity in agonist binding at the D2 dopamine receptor: evidence from agonist dissociation kinetics. *J Neurochem* 112, 1442-1453. doi: 10.1111/j.1471-4159.2009.06554.x.
- Katritch, V., Cherezov, V., Stevens, R.C. (2013). Structure-function of the G-protein-coupled receptor superfamily. *Annu Rev Pharmacol Toxicol* 53, 531-556.
- Kuszak, A.J., Pitchiaya, S., Anand, J.P., Mosberg, H.I., Walter, N.G., Sunahara, R.K. (2009). Purification and functional reconstitution of monomeric mu-opioid receptors: allosteric modulation of agonist binding by Gi2. *J Biol Chem* 284, 26732-26741.
- Lefkowitz, R.J. (2004). Historical review: a brief history and personal retrospective of seven-transmembrane receptors. *Trends Pharmacol Sci* 25, 413-422.

- Levitz, J., Habrian, C., Bharill, S., Fu, Z., Vafabakhsh, R., Isacoff, E.Y. (2016). Mechanism of Assembly and Cooperativity of Homomeric and Heteromeric Metabotropic Glutamate Receptors. *Neuron* 92, 143-159. doi: 10.1016/j.neuron.2016.08.036.
- Lopez-Gimenez, J.F., Canals, M., Pediani, J.D., Milligan, G. (2007). The alpha 1b-adrenoreceptor exists as a higher-order oligomer: effective oligomerization is required for receptor maturation, surface delivery and function. *Mol Pharmacol* 71, 1015-1029.
- Łukasiewicz, S., Błasiak, E., Faron-Górecka, A., Polit, A., Tworzydło, M., Górecki, A., Wasylewski, Z., Dziedzicka-Wasylewska, M. (2007). Fluorescence studies of homooligomerization of adenosine A2A and serotonin 5-HT1A receptors reveal the specificity of receptor interactions in the plasma membrane. *Pharmacol Rep* 59, 379-392.
- Maggio, R., Rocchi, C., Scarselli, M. (2013). Experimental strategies for studying G protein-coupled receptor homo- and heteromerization with radioligand binding and signal transduction methods. *Methods Enzymol* 521, 295-310. doi: 10.1016/B978-0-12-391862-8.00016-8.
- Maguire, J.J., Kuc, R.E., Davenport, A.P. (2012). Radioligand binding assays and their analysis. *Methods Mol Biol* 897, 31-77. doi: 10.1007/978-1-61779-909-9_3.
- Mancia, F., Assur, Z., Herman, A.G., Siegel, R., Hendrickson, W.A. (2008). Ligand sensitivity in dimeric associations of the serotonin 5HT2c receptor. *EMBO Rep* 9, 363–369.
- Mandrika, I., Petrovska, R., Klovin, J. (2010). Evidence for constitutive dimerization of niacin receptor subtypes. *Biochem Biophys Res Commun* 395, 281-287. doi: 10.1016/j.bbrc.2010.04.011.
- Maurice, P., Kamal, M., Jockers, R. (2011). Asymmetry of GPCR oligomers supports their functional relevance. *Trends Pharmacol Sci* 32, 514-520.
- May, L.T., Bridge, L.J., Stoddart, L.A., Briddon, S.J., Hill, S.J. (2011). Allosteric interactions across native adenosine-A3 receptor homodimers: quantification using single-cell ligand-binding kinetics. *FASEB J* 25, 3465-3476. doi: 10.1096/fj.11-186296.
- McMillin, S.M., Heusel, M., Liu, T., Costanzi, S., Wess, J. (2011). Structural basis of M3 muscarinic receptor dimer/oligomer formation. *J Biol Chem* 286, 28584-28598. doi: 10.1074/jbc.M111.259788.
- McVey, M., Ramsay, D., Kellett, E., Rees, S., Wilson, S., Pope, A.J., Milligan, G. (2001). Monitoring receptor oligomerization using time-resolved fluorescence resonance energy transfer and bioluminescence resonance energy transfer. The human delta-opioid receptor displays constitutive oligomerization at the cell surface, which is not regulated by receptor occupancy. *J Biol Chem* 276, 14092-14099.
- Mercier, J.F., Salahpour, A., Angers, S., Breit, A., Bouvier, M. (2002). Quantitative assessment of beta 1- and beta 2-adrenergic receptor homo- and heterodimerization by bioluminescence resonance energy transfer. *J Biol Chem* 277, 44925-44931.
- Milligan, G. (2004). G protein-coupled receptor dimerization: function and ligand pharmacology. *Mol Pharmacol* 66, 1–7.
- Milligan, G. (2007). G protein-coupled receptor dimerisation: molecular basis and relevance to function. *Biochim Biophys Acta* 1768, 825–835.
- Milligan, G. (2008). A day in the life of a G protein-coupled receptor: the contribution to function of G protein-coupled receptor dimerization. *Br J Pharmacol* 153, 216–229.
- Milligan, G. (2013). The prevalence, maintenance and relevance of G protein-coupled receptor oligomerization. *Mol Pharmacol* 84, 158-169.

- Milligan, G., Canals, M., Padiani, J.D., Ellis, J., Lopez-Gimenez, J.F. (2006). The role of GPCR dimerisation/oligomerisation in receptor signaling. *Ernst Schering Found Symp Proc* (2), 145-161.
- Navarro, G., Cordoní, A., Zelman-Femiak, M., Brugarolas, M., Moreno, E., Aguinaga, D., Perez-Benito, L., Cortés, A., Casadó, V., Mallol, J., Canela, E.I., Lluís, C., Pardo, L., García-Sáez, A.J., McCormick, P.J., Franco, R. (2016). Quaternary structure of a G-protein-coupled receptor heterotetramer in complex with Gi and Gs. *BMC Biol* 14, 26. doi: 10.1186/s12915-016-0247-4.
- Navarro, G., Cordoní, A., Casadó-Anguera, V., Moreno, E., Cai, N.S., Cortés, A., Canela, E.I., Dessauer, C.W., Casadó, V., Pardo, L., Lluís, C., Ferré, S. (2018). Evidence for functional pre-coupled complexes of receptor heteromers and adenylyl cyclase. *Nat Commun* 9, 1242. doi: 10.1038/s41467-018-03522-3.
- Orru, M., Bakešová, J., Brugarolas, M., Quiroz, C., Beaumont, V., Goldberg, S.R., Lluís, C., Cortés, A., Franco, R., Casadó, V., Canela, E.I., Ferré, S. (2011). Striatal pre- and postsynaptic profile of adenosine A_{2A} receptor antagonists. *PLoS One* 6, e16088
- Park, P.S., Wells, J.W. (2003) Monomers and oligomers of the M2 muscarinic cholinergic receptor purified from Sf9 cells. *Biochemistry* 42, 12960–12971.
- Parmar, V.K., Grinde, E., Mazurkiewicz, J.E., Herrick-Davis, K. (2017). Beta₂-adrenergic receptor homodimers: Role of transmembrane domain 1 and helix 8 in dimerization and cell surface expression. *Biochim Biophys Acta* 1859, 1445-1455. doi: 10.1016/j.bbamem.2016.12.007.
- Pou, C., Mannoury la Cour, C., Stoddart, L.A., Millan, M.J., Milligan, G. (2012). Functional homomers and heteromers of dopamine D2L and D3 receptors co-exist at the cell surface. *J Biol Chem* 287, 8864-8878. doi: 10.1074/jbc.M111.326678.
- Rovira, X., Roche, D., Serra, J., Kniazeff, J., Pin, J.P., Giraldo, J. (2008). Modeling the binding and function of metabotropic glutamate receptors. *J Pharmacol Exp Ther* 325, 443-456. doi: 10.1124/jpet.107.133967
- Rovira, X., Vivó, M., Serra, J., Roche, D., Strange, P.G., Giraldo, J. (2009). Modelling the interdependence between the stoichiometry of receptor oligomerization and ligand binding for a coexisting dimer/tetramer receptor system. *Br J Pharmacol* 156, 28-35. doi: 10.1111/j.1476-5381.2008.00031.x.
- Sarrió, S., Casadó, V., Escriche, M., Ciruela, F., Mallol, J., Canela, E.I., Lluís, C., Franco, R. (2000). The heat shock cognate protein hsc73 assembles with A(1) adenosine receptors to form functional modules in the cell membrane. *Mol Cell Biol* 20, 5164–5174.
- Shinkre, B.A., Kumar, T.S., Gao, Z.G., Deflorian, F., Jacobson, K.A., Trenkle, W.C. (2010). Synthesis and evaluation of 1,2,4-triazolo[1,5-c]pyrimidine derivatives as A_{2A} receptor-selective antagonists. *Bioorg Med Chem Lett* 20, 5690-5694. doi: 10.1016/j.bmcl.2010.08.021.
- Strange, P.G. (2005). Oligomers of D2 dopamine receptors. Evidence from ligand binding. *J Mol Neurosci* 26, 155-160. doi: 10.1385/JMN/26:02:155.
- Szalai, B., Barkai, L., Turu, G., Szidonya, L., Várnai, P., Hunyady, L. (2012). Allosteric interactions within the AT₁ angiotensin receptor homodimer: role of the conserved DRY motif. *Biochem Pharmacol* 84, 477-485. doi: 10.1016/j.bcp.2012.04.014.
- Teitler, M., Toohey, N., Knight, J.A., Klein, M.T., Smith, C. (2010). Clozapine and other competitive antagonists reactivate risperidone-inactivated h5-HT₇ receptors: radioligand binding and functional evidence for GPCR homodimer protomer interactions. *Psychopharmacology (Berl)* 212, 687-697. doi: 10.1007/s00213-010-2001-x.

- Ulloa-Aguirre, A., Zariñan, T., Dias, J.A., Conn, P.M. (2014). Mutations in G protein-coupled receptors that impact receptor trafficking and reproductive function. *Mol Cell Endocrinol* 382, 411-423.
- Urizar, E., Montanelli, L., Loy, T., Bonomi, M., Swillens, S., Gales, C., Bouvier, M., Smits, G., Vassart, G., Costagliola, S. (2005). Glycoprotein hormone receptors: link between receptor homodimerization and negative cooperativity. *EMBO J* 24, 1954–1964.
- Wang, C.I., Lewis, R.J. (2013). Emerging opportunities for allosteric modulation of G-protein coupled receptors. *Biochem Pharmacol* 85, 153-162.
- Wells, G.J. (2014). Allosteric modulators of G protein-coupled receptors. *Curr Top Med Chem* 14, 1735-1737.
- White, J.F., Grodnitzky, J., Louis, J.M., Trinh, L.B., Shiloach, J., Gutierrez, J., Northup, J.K., Grisshammer, R. (2007). Dimerization of the class A G protein-coupled neurotensin receptor NTS1 alters G protein interaction. *Proc Natl Acad Sci USA* 104, 12199-12204.
- Whorton, M.R., Bokoch, M.P., Rasmussen, S.G.F., Huang, B., Zare, R.N., Kobilka, B., Sunahara, R.K. (2007). A monomeric G protein-coupled receptor isolated in a high-density lipoprotein particle efficiently activates its G protein. *Proc Natl Acad Sci USA* 104, 7682–7687.
- Whorton, M.R., Jastrzebska, B., Park, P.S., Fotiadis, D., Engel, A., Palczewski, K., Sunahara, R.K. (2008). Efficient coupling of transducin to monomeric rhodopsin in a phospholipid bilayer. *J Biol Chem* 283, 4387-4394.
- Wreggett, K.A., Wells, J.W. (1995). Cooperativity manifest in the binding properties of purified cardiac muscarinic receptors. *J Biol Chem* 270, 22488-22499.

TABLES

Table 1. Parameter values obtained by fitting data from competition experiments of the antagonist [³H]DPCPX binding to adenosine A₁ receptors vs. the agonist R-PIA to different models.

Model	Parameter	0.009 nM [³ H]DPCPX
Two-independent-site model	B _{maxH} (pmol/mg protein)	0.7±0.1
	K _{DH} (nM)	5±2
	B _{maxL} (pmol/mg protein)	0.18±0.09
	K _{DL} (nM)	120±60
Dimer receptor model	R _T (pmol(mg protein))	0.38±0.01
	K _{DB1} (nM)	0.02±0.01
	K _{DB2} (nM)	5.3±0.5
	K _{DAB} (nM)	0.018±0.007
	D _{CB}	-1.8
	D _{AB}	+0.35

Data are mean±SEM values from three experiments. The radioligand affinity was $K_{DA1}=0.038$ nM. B_{maxH} and B_{maxL} are, respectively, the maximum specific binding corresponding to, respectively, high- and low-affinity sites, and K_{DH} and K_{DL} are the equilibrium dissociation constants of the competing ligand B (R-PIA) for, respectively, high- and low-affinity sites. R_T is the total amount of receptor dimers, K_{DB1} and K_{DB2} are, respectively, the equilibrium dissociation constants of the first and second binding of B to the dimer. K_{DAB} is the hybrid equilibrium dissociation constant of B binding to a receptor dimer semioccupied by the A ([³H]DPCPX). D_{CB} is the dimer cooperativity index for the binding of ligand B and D_{AB} is the dimer radioligand-competitor modulation index (see Methods).

Table 2. Parameter values obtained by fitting data from competition experiments of the agonist [³H]CGS21680 binding to adenosine A_{2A} receptors vs. the antagonist SCH442416 to different models.

Model	Parameter	24 nM [³ H]CGS21680
One-site model	B _{max} (pmol/mg protein)	1.7±0.2
	K _D (nM)	180±90
Dimer receptor model (without radioligand /competitor modulation)	R _T (pmol/mg protein)	0.8±0.1
	K _{DB1} (nM)	90±50
	K _{DB2} (nM)	-
	K _{DAB} (nM)	-
	D _{CB}	0
Dimer receptor model	D _{AB}	0
	R _T (pmol/mg protein)	0.56±0.07
	K _{DB1} (nM)	1.2±0.5
	K _{DB2} (nM)	-
	K _{DAB} (nM)	0.03±0.02
	D _{CB}	0
	D _{AB}	+1.9

Data are mean±SEM values from three experiments. The radioligand affinity was K_{DA1}=41 nM. B_{max} is the maximum specific binding and K_D is the equilibrium dissociation constant for the competing ligand B (SCH442416). R_T is the total amount of receptor dimers, K_{DB1} and K_{DB2} are, respectively, the equilibrium dissociation constants of the first and second binding of B to the dimer. K_{DAB} is the hybrid equilibrium dissociation constant of B binding to a receptor dimer semioccupied by A ([³H]CGS21680). D_{CB} is the dimer cooperativity index for the binding of ligand B and D_{AB} is the dimer radioligand-competitor modulation index (see Methods).

Table 3. Parameter values obtained by fitting data from competition experiments of the antagonist [³H]SCH23390 binding to dopamine D₁ receptors vs. the agonist SKF81297 to different models.

Model	Parameter	0.15 nM [³ H]SCH	0.40 nM [³ H]SCH	1.4 nM [³ H]SCH
One-site model	B _{max} (pmol/mg protein)	0.9±0.1	nd	nd
	K _D (nM)	28±5	nd	nd
Dimer receptor model	R _T (pmol/mg protein)	0.41±0.02	0.39±0.01	0.44±0.01
	K _{DB1} (nM)	3±1	7±3	9±1
	K _{DB2} (nM)	-	-	-
	K _{DAB} (nM)	0.9±0.5	5±4	4±1
	D _{CB}	0	0	0
	D _{AB}	+0.7	+0.4	+0.7

Data are mean±SEM values from three experiments. The radioligand affinity was K_{DA1}=0.27 nM. B_{max} is the maximum specific binding and K_D is the equilibrium dissociation constant for the competing ligand B (SKF81297). R_T is the total amount of receptor dimers, K_{DB1} and K_{DB2} are, respectively, the equilibrium dissociation constants of the first and second binding of B to the dimer. K_{DAB} is the hybrid equilibrium dissociation constant of B binding to a receptor dimer semioccupied by the A ([³H]SCH23390). D_{CB} is the dimer cooperativity index for the binding of ligand B and D_{AB} is the dimer radioligand-competitor modulation index (see Methods). nd: not determined.

FIGURE LEGENDS

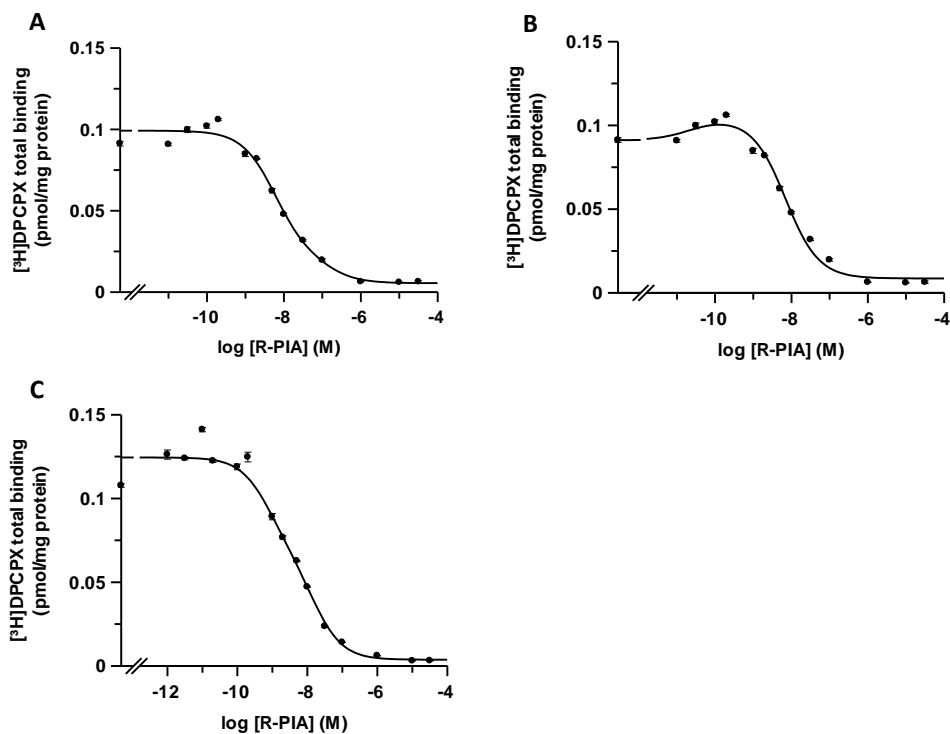


Figure 1. Competition experiments using 0.009 nM of the A_1 R antagonist $[^3\text{H}]\text{DPCPX}$ vs. increasing concentrations of the A_1 R R-PIA using sheep brain striatum membranes (0.2 mg protein/ml) were performed as indicated in Methods. Binding data of the same experiment were fitted to the two-independent-site model (Eq. (8)) (A) or to the dimer receptor model (Eq. (3)) using $K_{DA1}=0.038$ nM) (B). Another experiment was fit with both equations and the curves overlapped (C). Mean \pm SEM values from a representative experiment performed in triplicates are shown.

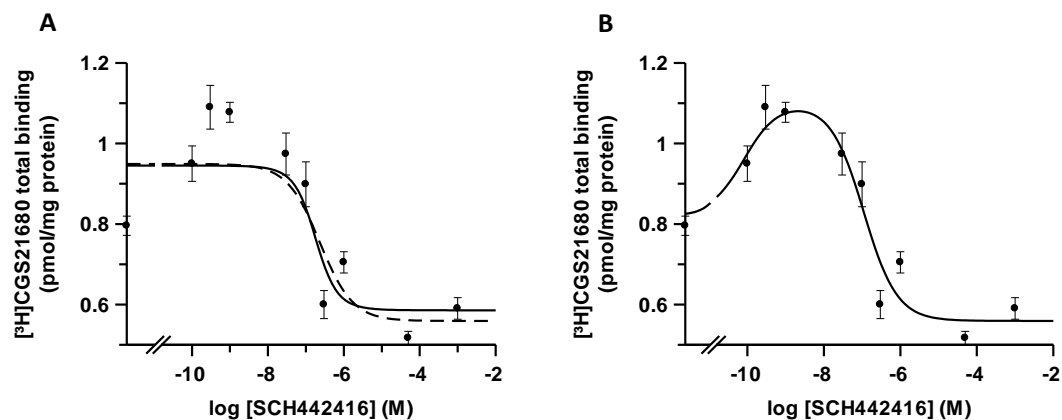


Figure 2. Competition experiments using 24 nM of the A_{2A} R agonist $[^3\text{H}]\text{CGS21680}$ vs. increasing concentrations of the A_{2A} R antagonist SCH442416 using sheep brain striatum membranes (0.2 mg protein/ml) were performed as indicated in Methods. In (A) Binding data were fitted to the one-site model (Eq. (7), dashed line) or to the dimer receptor model with B non-cooperative (Eq. (5)) and non-considering K_{AB} , using $K_{DA1}=41$ nM (solid line). In (B) The same binding data were fitted to the dimer receptor model with B non-cooperative (Eq. (5)) and considering K_{AB} . Mean \pm SEM values from a representative experiment performed in triplicates are shown.

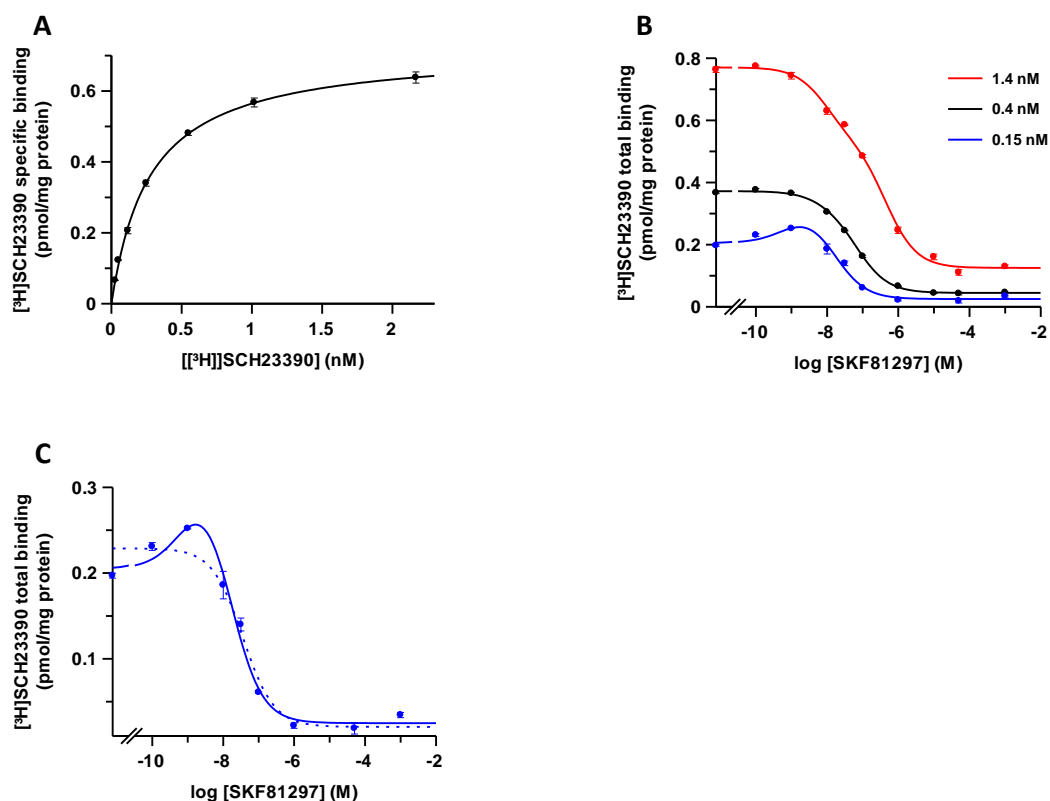


Figure 3. Binding assays of D₁R in sheep brain striatum membranes (0.2 mg protein/ ml) were performed as indicated in Methods. In (A) saturation experiment performed with increasing concentrations of the D₁R antagonist [³H]SCH23390. Binding data were fitted to the Eq. (1), and K_{DA1} was 0.27 nM. In (B) competition experiments using several D₁R antagonist [³H]SCH23390 concentrations (0.15 nM in blue; 0.4 nM in black and 1.4 nM in red) vs. increasing concentrations of the D₁R agonist SKF81297. Binding data were fitted to the dimer receptor model with non-cooperative competitor (Eq. (5)). In (C), magnification of competition assay of 0.15 nM [³H]SCH23390 vs. increasing concentrations of SKF81297 fitted to the dimer receptor model (Eq. (5)) (solid line) or to the one-site model (Eq. (7)) (dotted line). Mean \pm SEM values from a representative experiment performed in triplicates are shown.

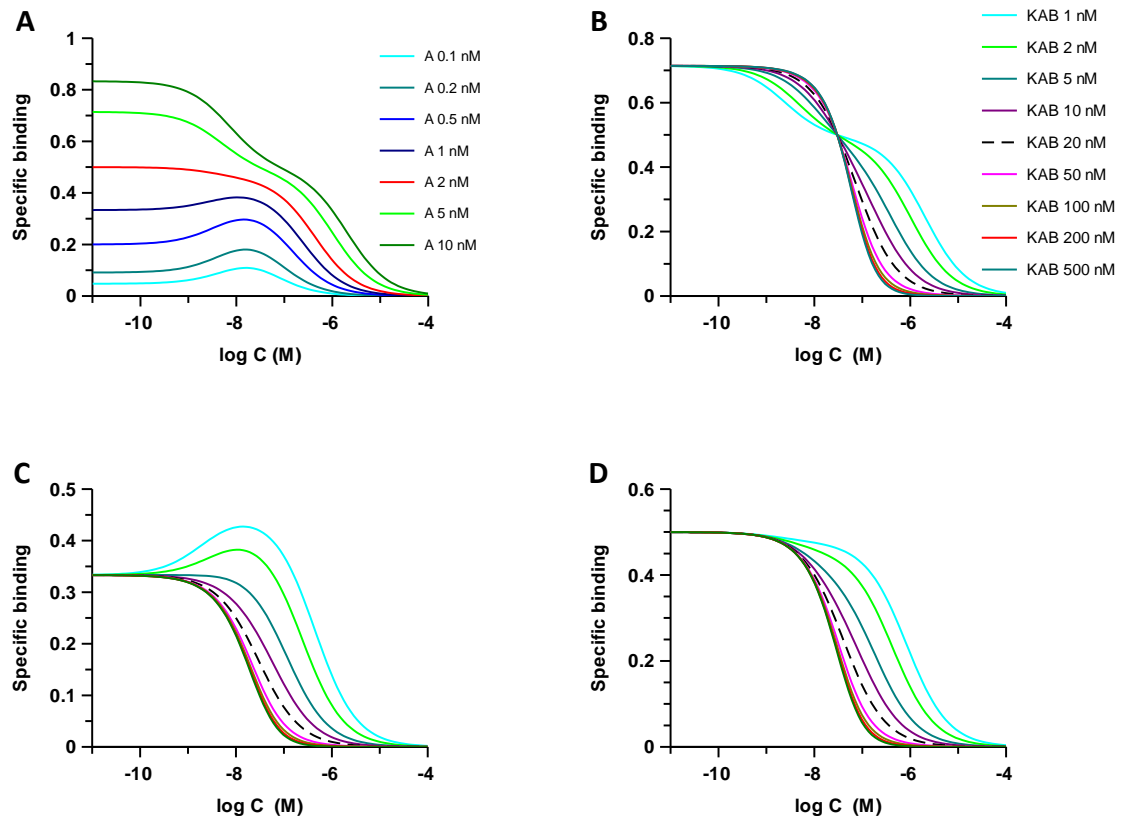


Figure 4. Competition curve simulations considering the Eq. (5). In (A) simulation was performed following the parameter values: $R_T=0.5$ pmol/mg protein, $K_{DA1}=1$ nM ($D_{CA}=0$, $K_{DA2}=4$ nM), $K_{DB1}=10$ nM ($D_{CB}=0$, $K_{DB2}=40$ nM) and $K_{DAB}=2$ nM ($D_{AB}=1$), varying the radioligand concentration (A in Eq. (5); 0.1, 0.2, 0.5, 1.0, 2.0, 5.0 and 10 nM, bottom to top) and with increasing concentrations of the competitor (B in Eq. (5)). In (B), (C) and (D) simulation was performed following the parameter values: $R_T=0.5$ pmol/mg protein, $[A] = 5$ nM (B), 1 nM (C) or 2 nM (D), $K_{DA1}=1$ nM, $K_{DA2}=4$ nM ($D_{CA}=0$), $K_{DB1}=10$ nM, $K_{DB2}=40$ nM ($D_{CB}=0$), varying the K_{DAB} value (1, 2, 5, 10, 20, 50, 100, 200, 500) and with increasing concentrations of the competitor (B in Eq. (5)).

Chapter 2.1. Allosteric interactions between agonists and antagonists within the adenosine A2A receptor-dopamine D2 receptor heterotetramer

Bonaventura J, Navarro G, **Casadó-Anguera V**, Azdad K, Rea W, Moreno E, Brugarolas M, Mallol J, Canela EI, Lluís C, Cortés A, Volkow ND, Schiffmann SN, Ferré S, Casadó V.

Proceedings of the National Academy of Sciences of the United States of America (PNAS), 2015, 112:E3609-18.

Allosteric interactions between agonists and antagonists within the adenosine A_{2A} receptor-dopamine D₂ receptor heterotetramer

Jordi Bonaventura^{a,b}, Gemma Navarro^a, Verònica Casadó-Anguera^a, Karima Azdad^c, William Rea^b, Estefanía Moreno^a, Marc Brugarolas^a, Josefa Mallol^a, Enric I. Canela^a, Carme Lluís^a, Antoni Cortés^a, Nora D. Volkow^d, Serge N. Schiffmann^c, Sergi Ferré^{b,1}, and Vicent Casadó^{a,1}

^aDepartment of Biochemistry and Molecular Biology, Faculty of Biology, University of Barcelona, and Centro de Investigación Biomédica en Red Sobre Enfermedades Neurodegenerativas and Institute of Biomedicine of the University of Barcelona, 08028 Barcelona, Spain; ^bIntegrative Neurobiology Section, National Institute on Drug Abuse, Intramural Research Program, National Institutes of Health, Baltimore, MD 21224; ^cLaboratory of Neurophysiology, Université Libre de Bruxelles-Neuroscience Institute, 1070 Brussels, Belgium; and ^dNational Institute on Alcohol Abuse and Alcoholism, National Institutes of Health, Bethesda, MD 20892

Edited by Susan G. Amara, National Institute of Mental Health, Bethesda, MD, and approved May 27, 2015 (received for review April 21, 2015)

Adenosine A_{2A} receptor (A_{2A}R)-dopamine D₂ receptor (D₂R) heteromers are key modulators of striatal neuronal function. It has been suggested that the psychostimulant effects of caffeine depend on its ability to block an allosteric modulation within the A_{2A}R-D₂R heteromer, by which adenosine decreases the affinity and intrinsic efficacy of dopamine at the D₂R. We describe novel unsuspected allosteric mechanisms within the heteromer by which not only A_{2A}R agonists, but also A_{2A}R antagonists, decrease the affinity and intrinsic efficacy of D₂R agonists and the affinity of D₂R antagonists. Strikingly, these allosteric modulations disappear on agonist and antagonist coadministration. This can be explained by a model that considers A_{2A}R-D₂R heteromers as heterotetramers, constituted by A_{2A}R and D₂R homodimers, as demonstrated by experiments with bioluminescence resonance energy transfer and bimolecular fluorescence and bioluminescence complementation. As predicted by the model, high concentrations of A_{2A}R antagonists behaved as A_{2A}R agonists and decreased D₂R function in the brain.

adenosine A_{2A} receptor | dopamine D₂ receptor | caffeine | GPCR heteromers

Most evidence indicates that G protein-coupled receptors (GPCRs) form homodimers and heteromers. Homodimers seem to be a predominant species, and oligomeric entities can be viewed as multiples of dimers (1). It has been proposed that GPCR heteromers are constituted mainly by heteromers of homodimers (1, 2). Allosteric mechanisms determine a multiplicity of unique pharmacologic properties of GPCR homodimers and heteromers (1, 3). First, binding of a ligand to one of the receptors in the heteromer can modify the affinity of ligands for the other receptor (1, 3, 4). The most widely reproduced allosteric modulation of ligand-binding properties in a GPCR heteromer is the ability of adenosine A_{2A} receptor (A_{2A}R) agonists to decrease the affinity of dopamine D₂ receptor (D₂R) agonists in the A_{2A}R-D₂R heteromer (5). A_{2A}R-D₂R heteromers have been revealed both in transfected cells (6, 7), striatal neurons in culture (6, 8) and in situ, in mammalian striatum (9, 10), where they play an important role in the modulation of GABAergic striatopallidal neuronal function (9, 11).

In addition to ligand-binding properties, unique properties for each GPCR oligomer emerge in relation to the varying intrinsic efficacy of ligands for different signaling pathways (1–3). Intrinsic efficacy refers to the power of the agonist to induce a functional response, independent of its affinity for the receptor. Thus, allosteric modulation of an agonist can potentially involve changes in affinity and/or intrinsic efficacy (1, 3). This principle can be observed in the A_{2A}R-D₂R heteromer, where a decrease in D₂R agonist affinity cannot alone explain the ability

of an A_{2A}R agonist to abolish the decreased excitability of GABAergic striatopallidal neurons induced by high concentration of a D₂R agonist (9), which should overcome the decrease in affinity. Furthermore, a differential effect of allosteric modulations of different agonist-mediated signaling responses (i.e., functional selectivity) can occur within GPCR heteromers (1, 2, 8). Again, the A_{2A}R-D₂R heteromer provides a valuable example. A recent study has shown that different levels of intracellular Ca²⁺ exert different modulations of A_{2A}R-D₂R heteromer signaling (8). This depends on the ability of low and high Ca²⁺ to promote a selective interaction of the heteromer with different Ca²⁺-binding proteins, which differentially modulate allosteric interactions in the heteromer (8).

It has been hypothesized that the allosteric interactions between A_{2A}R and D₂R agonists within the A_{2A}R-D₂R heteromer provide a mechanism responsible not only for the depressant effects of A_{2A}R agonists, but also for the psychostimulant effects of adenosine A_{2A}R antagonists and the nonselective adenosine receptor antagonist caffeine (9, 11, 12), with implications for several neuropsychiatric disorders (13). In fact, the same mechanism has provided the rationale for the use of A_{2A}R antagonists

Significance

G protein-coupled receptors (GPCRs) constitute the largest plasma membrane protein family involved in cell signaling. GPCR homodimers are predominant species, and GPCR heteromers likely are constituted by heteromers of homodimers. The adenosine A_{2A} receptor (A_{2A}R)-dopamine D₂ receptor (D₂R) heteromer is a target for the nonselective adenosine receptor antagonist caffeine. This study uncovers allosteric modulations of A_{2A}R antagonists that mimic those of A_{2A}R agonists, challenging the traditional view of antagonists as inactive ligands. These allosteric modulations disappear when agonist and antagonist are coadministered, however. A model is proposed that considers A_{2A}R-D₂R heteromers as heterotetramers, constituted by A_{2A}R and D₂R homodimers. The model predicted that high concentrations of A_{2A}R antagonists would behave as A_{2A}R agonists and decrease D₂R function in the brain.

Author contributions: J.B., G.N., C.L., N.D.V., S.N.S., S.F., and V.C. designed research; J.B., G.N., V.C.-A., K.A., W.R., E.M., M.B., A.C., and V.C. performed research; J.B., G.N., V.C.-A., K.A., W.R., E.M., M.B., J.M., E.I.C., C.L., A.C., S.N.S., S.F., and V.C. analyzed data; and J.B., G.N., C.L., S.N.S., S.F., and V.C. wrote the paper.

The authors declare no conflict of interest.

This article is a PNAS Direct Submission.

¹To whom correspondence may be addressed. Email: sferré@intra.nida.nih.gov or vcasado@ub.edu.

This article contains supporting information online at www.pnas.org/lookup/suppl/doi:10.1073/pnas.1507704112/-DCSupplemental.

in patients with Parkinson's disease (13, 14). The initial aim of the present study was to study in detail the ability of caffeine to counteract allosteric modulations between $A_{2A}R$ and D_2R agonists (affinity and intrinsic efficacy) within the $A_{2A}R$ - D_2R heteromer. Unexpectedly, when performing control radioligand-binding experiments, not only an $A_{2A}R$ agonist, but also caffeine, significantly decreased D_2R agonist binding. However, when coadministered, the $A_{2A}R$ agonist and caffeine counteracted their ability to modulate D_2R agonist binding. By exploring the molecular mechanisms behind these apparent inconsistencies, the present study provides new insight into the quaternary structure and function of $A_{2A}R$ - D_2R heteromers.

Results

Caffeine Modulates D_2R Agonist Binding: A New Biochemical Property of the $A_{2A}R$ - D_2R Heteromer. As expected, the $A_{2A}R$ agonist CGS 21680 significantly decreased D_2R agonist [3H]quinpirole binding in membrane preparations from both sheep striatum (Fig. 1A, black bars) and Chinese hamster ovary (CHO) cells transiently transfected with $A_{2A}R$ and D_2R (Fig. 1A, red bars). Unexpectedly, caffeine also produced the same effect (Fig. 1B), and the effective concentrations of CGS 21680 and caffeine were in the same range as those able to displace the binding of the selective $A_{2A}R$ antagonist [3H]ZM 241385 in the respective preparations (Fig. S1A and B). In transfected cells, the average B_{max} value for [3H]ZM 241385 binding was 1.6 pmol/mg of protein, and that for [3H]raclopride binding was 0.7 pmol/mg of protein. In sheep striatum, the respective average values were 1.8 and 0.4 pmol/mg

protein. The decrease in [3H]quinpirole binding by CGS 21680 and caffeine was related to a noncompetitive inhibition, with decreasing affinity (i.e., increase in K_{D1} values), as shown in competition experiments of [3H]quinpirole vs. quinpirole (Table 1).

Previous studies have shown that in the $A_{2A}R$ - D_2R heteromer, a strong electrostatic interaction occurs between an arginine-rich epitope localized in the N-terminal part of the third intracellular loop of the D_2R and a phosphorylated residue, serine-374, localized in the distal part of the C terminus of the $A_{2A}R$ (15, 16). Bioluminescence energy transfer experiments demonstrated that transfection with mutant $A_{2A}R$ (A_{2A}^{A374R}) or D_2R lacking these key interacting residues leads to pronounced modification of the quaternary structure of the heteromer (15, 17, 18). In transfected cells, A_{2A}^{A374R} showed a very similar expression (B_{max} for [3H]ZM 241385 binding of 2.0 pmol/mg protein) and the same affinity for caffeine or CGS 21680 compared with the wild-type $A_{2A}R$. Identical competition curves of [3H]ZM 241385 vs. CGS 21680 or caffeine were obtained from cells transfected with D_2R and either A_{2A}^{A374R} or wild-type $A_{2A}R$ (Fig. S1B). The ability of CGS 21680 and caffeine at modulating [3H]quinpirole binding was significantly reduced in the CHO cells transfected with D_2R and the mutant A_{2A}^{A374R} , however (Fig. 1A and B, blue bars). This indicates that the allosteric modulations between an $A_{2A}R$ agonist or antagonist and a D_2R agonist depend on the quaternary structure of the $A_{2A}R$ - D_2R , determined by the electrostatic interaction between intracellular domains of both receptors, and thus constitute a biochemical property of the $A_{2A}R$ - D_2R heteromer.

$A_{2A}R$ Agonists and Antagonists Counteract Their Ability to Modulate D_2R Agonist Binding and Function: Two $A_{2A}R$ Protomers in the $A_{2A}R$ - D_2R Heteromer.

Because both $A_{2A}R$ agonists and antagonists produce a conformational change in the $A_{2A}R$ - D_2R heteromer that leads to the same effect, a reduced affinity of agonists for D_2R (Table 1), this questions the validity of the allosteric interactions between $A_{2A}R$ and D_2R agonists as a main mechanism involved in the opposite and counteracting behavioral effects of $A_{2A}R$ agonists and antagonists. We evaluated the combined effect of $A_{2A}R$ agonists and caffeine or selective $A_{2A}R$ antagonists on D_2R agonist binding. [3H]Quinpirole binding in membrane preparations from sheep striatum was measured in the presence of CGS 21680 (100 nM) and increasing concentrations of caffeine (Fig. 2A) or the selective $A_{2A}R$ antagonists SCH 58261 (Fig. 2C) and KW 6002 (Fig. 2E). Caffeine and the selective $A_{2A}R$ antagonists produced a biphasic effect on the ability of CGS 21680 to decrease [3H]quinpirole binding. Low concentrations counteracted the effect of CGS 21680, whereas high concentrations were associated with a significant decrease in [3H]quinpirole binding. These results show that $A_{2A}R$ agonists and antagonists that bind competitively to the orthosteric site (19–21) produce the same allosteric modulation of D_2R agonist binding when individually administered, and yet they can cancel each other's effect when coadministered. This strongly suggests the presence of the

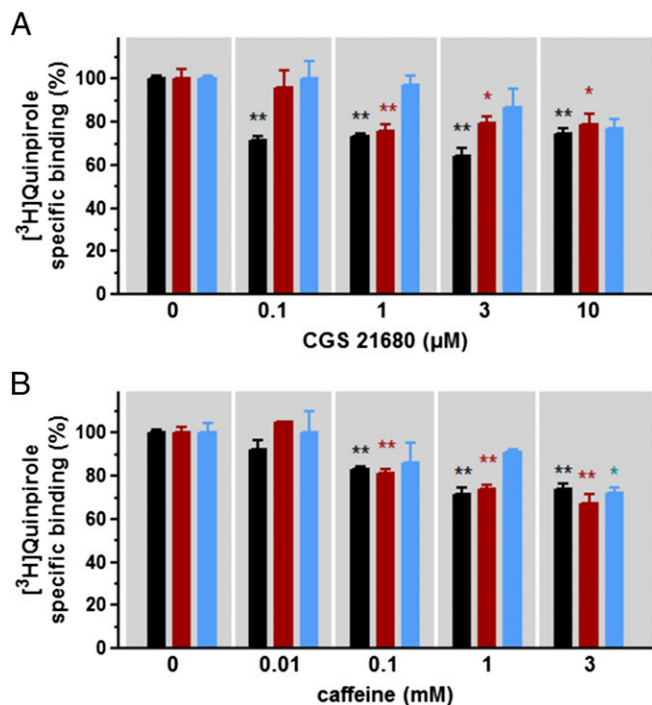


Fig. 1. Effect of an $A_{2A}R$ agonist and caffeine on [3H]quinpirole binding to D_2R . [3H]Quinpirole binding (6 nM) was determined in membrane preparations from sheep striatum (black bars) or CHO cells transfected with D_2R cDNA (2 μ g) and $A_{2A}R$ cDNA (3 μ g) (red bars) or D_2R cDNA (2 μ g) and cDNA (3 μ g) from mutated $A_{2A}R$ (A_{2A}^{A374R} ; blue bars) in the presence or the absence of increasing concentrations of the $A_{2A}R$ agonist CGS21680 (A) or caffeine (B). Values are mean \pm SEM from between three and five different experiments of relative [3H]quinpirole-specific binding (% of nontreated membranes). Statistical significance was calculated by one-way ANOVA followed by Dunnett's post hoc test. * P < 0.05; ** P < 0.01, compared with nontreated membrane preparations.

Table 1. Effect of $A_{2A}R$ ligands on [3H]quinpirole and [3H]raclopride affinity for D_2R

Treatment	[3H]Quinpirole-binding K_{DA1} , nM	[3H]Raclopride-binding K_{DA1} , nM
Control	5 \pm 2	1.8 \pm 0.7
CGS 21680 (3 μ M)	10 \pm 2*	4.2 \pm 0.7*
Caffeine (3 mM)	14 \pm 3*	3.7 \pm 0.7*

K_{DA1} is the equilibrium dissociation constant. Values are mean \pm SEM from three to five different experiments. Statistical significance was calculated using the Student t test. * P < 0.05 compared with controls.

$A_{2A}R$ homodimer with two orthosteric binding sites. A corollary of this assumption would be that simultaneous occupancy of the $A_{2A}R$ homodimer in the $A_{2A}R$ - D_2R heteromer by an agonist and an antagonist should not induce an allosteric modulation of D_2R agonist binding.

The dimeric nature of the $A_{2A}R$ was confirmed with dissociation experiments of [3H]ZM 241385 in sheep striatal preparations. The $A_{2A}R$ agonist CGS 21680, but not caffeine or SCH 58261, significantly modified the dissociation rate of the labeled antagonist (Fig. 3), indicating formation of a hybrid species with both agonist and antagonist simultaneously binding to the dimer. Therefore, only the agonist can exert an allosteric modulation of the labeled antagonist when both are

occupying orthosteric sites in an $A_{2A}R$ oligomer, because the four ligands—caffeine, ZM 241385, SCH 58261, and CGS 21680—all bind and compete for the same orthosteric site (19–21). This implies a different conformation of the $A_{2A}R$ homodimer when occupied simultaneously with an agonist and an antagonist compared with when occupied with two antagonists. This different conformation could then explain the differential ability of the $A_{2A}R$ homodimer, when occupied only by an agonist or an antagonist or simultaneously by an agonist and antagonist, to allosterically modulate D_2R agonist binding and intrinsic efficacy within the $A_{2A}R$ - D_2R heteromer.

The same allosteric modulation exerted by $A_{2A}R$ agonists and antagonists on D_2R agonist affinity was also evident on

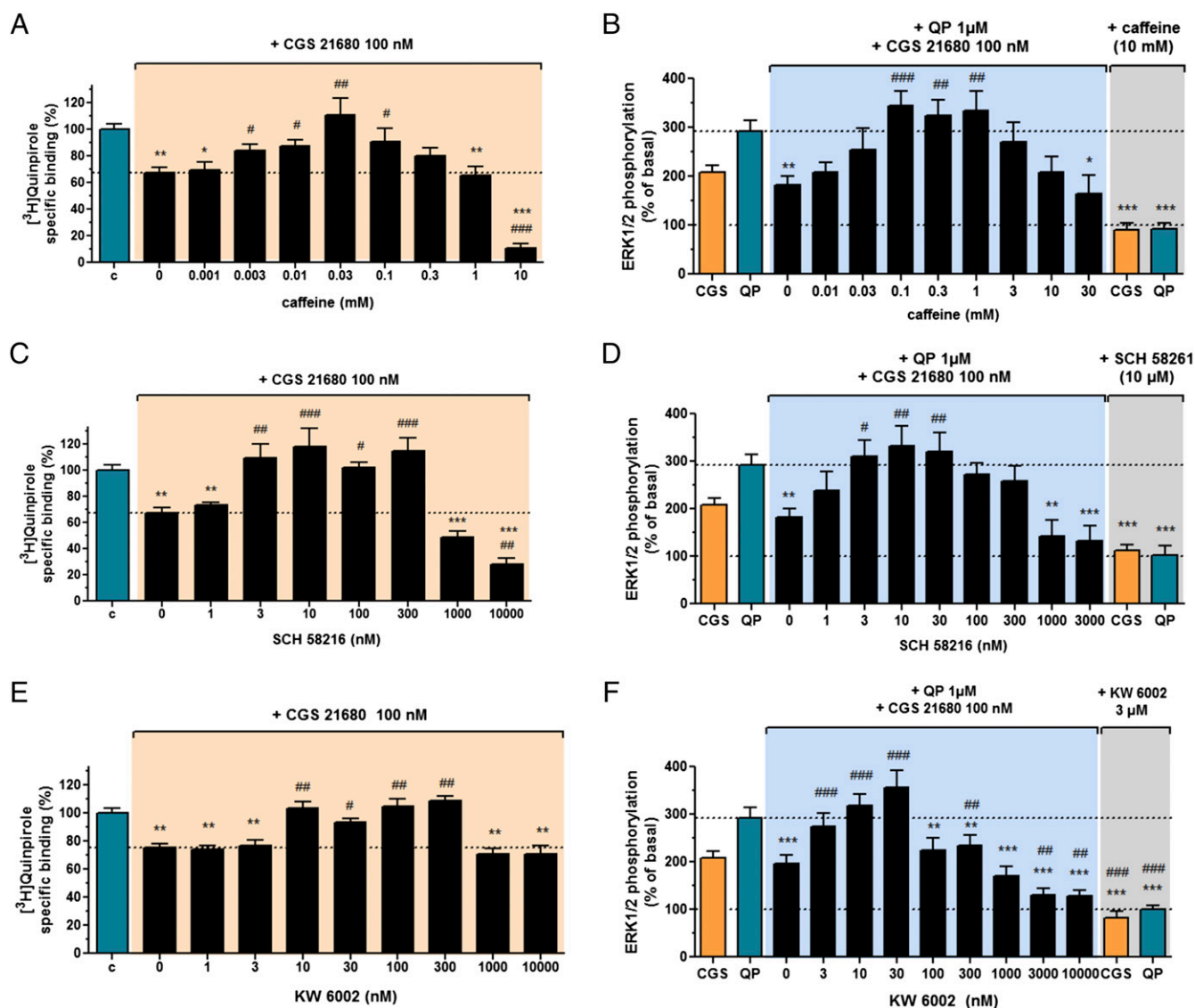


Fig. 2. Biphasic effect of caffeine and selective $A_{2A}R$ antagonists on [3H]quinpirole binding and D_2R -mediated ERK1/2 phosphorylation. (A, C, and E) [3H]Quinpirole binding (6 nM) was determined in membrane preparations from sheep striatum not preincubated (control, blue bars) or preincubated (black bars) for 30 min with the $A_{2A}R$ agonist CGS 21680 (100 nM) and increasing concentrations of caffeine (A) or the selective $A_{2A}R$ antagonists SCH 58216 (C) or KW 6002 (E). Values are mean \pm SEM from four to eight different experiments of relative [3H]quinpirole binding (% of nontreated control membranes, c). Statistical significance was calculated by one-way ANOVA followed by the Newman–Keuls post hoc test. * P < 0.05; ** P < 0.01; *** P < 0.001, compared with c. # P < 0.05; ## P < 0.01; ### P < 0.001 compared with only CGS 21680. (B, D, and F) ERK1/2 phosphorylation was determined in HEK-293 cells transfected with D_2R cDNA (0.8 μ g) and $A_{2A}R$ cDNA (1.2 μ g), stimulated for 5 min with CGS 21680 (CGS; 100 nM) or quinpirole (QP; 1 μ M) alone (orange and blue bars, respectively) or in combination (black bars) after incubation for 10 min with vehicle or with caffeine (B), SCH 58216 (D), or KW 6002 (F). ERK1/2 phosphorylation was quantified; values represent mean \pm SEM from three to six different experiments of the percentage of phosphorylation relative to basal levels in nontreated cells (100%). Statistical significance was calculated by one-way ANOVA followed by Dunnett's post hoc test. * P < 0.05; ** P < 0.01; *** P < 0.001, compared with QP. # P < 0.05; ## P < 0.01; ### P < 0.001, compared with cells treated with QP plus CGS.

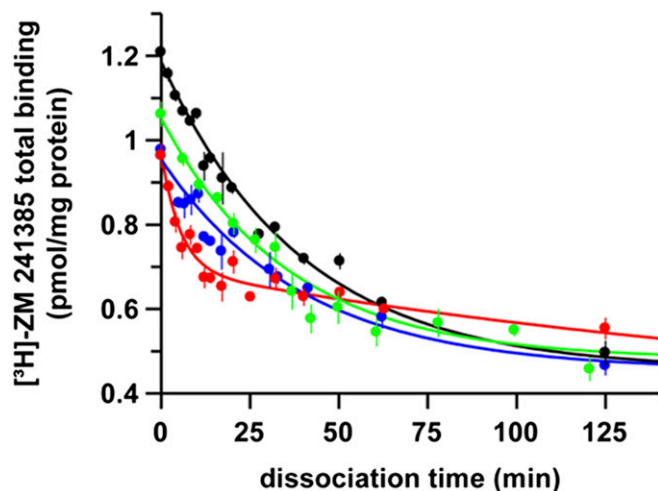


Fig. 3. Dissociation kinetics of [^3H]ZM 241385 in the presence of caffeine or selective $A_{2A}R$ ligands. Dissociation curves of the $A_{2A}R$ antagonist [^3H]ZM 241385 (1.5 nM) in the absence (black curve) or presence of either the $A_{2A}R$ antagonists SCH 58260 (10 nM, blue curve) or caffeine (30 μM , green curve), or the $A_{2A}R$ agonist CGS 21680 (10 nM, red curve). Data points are means \pm SD of triplicates. Fitted K_{off} values of [^3H]ZM 241385 dissociation were $0.025 \pm 0.002 \text{ min}^{-1}$ (i.e., a residence time of 40 min) for control, $0.025 \pm 0.003 \text{ min}^{-1}$ (residence time of 40 min) in the presence of SCH 58260, and $0.028 \pm 0.004 \text{ min}^{-1}$ (residence time of 36 min) in the presence of caffeine. A biphasic curve was obtained in the presence of CGS 21680 (red curve) with a K_{off1} value of $0.19 \pm 0.03 \text{ min}^{-1}$ and a K_{off2} value of $0.004 \pm 0.003 \text{ min}^{-1}$ (residence time of 5 and 250 min, respectively).

D_2R agonist intrinsic efficacy. In HEK-293 cells transfected with $A_{2A}R$ and D_2R , quinpirole (1 μM) and CGS 21680 (100 nM) produced increases in ERK1/2 phosphorylation over basal levels of approximately 300% and 200%, respectively (Fig. 2B). The effect of quinpirole was partially but significantly counteracted by CGS 21680 to the levels of ERK1/2 phosphorylation induced by CGS 21680 alone. Given that the high concentration of quinpirole used (1 μM) should overcome the decrease in affinity induced by CGS 21680 (100 nM) (Table 1), this indicates the ability of the $A_{2A}R$ agonist to decrease not only D_2R agonist affinity, but also its intrinsic efficacy, as previously shown in electrophysiological experiments on striatal neurons (9). Increasing concentrations of caffeine (Fig. 2B), SCH 58261 (Fig. 2D), or KW 6002 (Fig. 2F) produced the same biphasic effect as seen in the radioligand-binding experiments (Fig. 2): low concentrations counteracted the effect of CGS 21680, and this effect disappeared with larger concentrations, when caffeine, SCH 58261, and KW 6002 by themselves completely antagonized the effect of both CGS 21680 and quinpirole. Therefore, simultaneous occupancy of the $A_{2A}R$ homodimer in the $A_{2A}R$ - D_2R heteromer by an agonist and an antagonist blocks the allosteric modulation of both D_2R agonist binding and intrinsic efficacy. Considering that there is a tone of adenosine under physiological conditions, this in fact could be the main mechanism by which caffeine and $A_{2A}R$ antagonists counteract the functional and behavioral effects that depend on D_2R signaling by the $A_{2A}R$ - D_2R heteromer.

$A_{2A}R$ - D_2R Heteromers Assemble Into Tetrameric Complexes. A bimolecular luminescence and fluorescence complementation approach was used to demonstrate the ability of $A_{2A}R$ and D_2R to form heterotetramers. First, in HEK-293 cells, *Renilla* luciferase (Rluc) reconstitution after transfection of $A_{2A}R$ fused to the Rluc N-terminal hemiprotein ($A_{2A}R$ -nRluc) and D_2R fused to the Rluc C-terminal hemiprotein (D_2R -cRluc) was demonstrated by strong bioluminescence after addition of the Rluc substrate

coelenterazine H, indicating $A_{2A}R$ (nRluc)- D_2R (cRluc) heteromerization (Fig. S2). A_1R - D_2R and $A_{2A}R$ - D_1R pairs (fused to corresponding hemiproteins) served as negative controls, in agreement with the suggested ability of $A_{2A}R$ to heteromerize with D_2R and not with D_1R and with the ability of D_2R to heteromerize with $A_{2A}R$ and not with A_1R (6, 22) (Fig. S2).

Second, significant fluorescence could be observed when HEK-293 cells were transfected with $A_{2A}R$ fused to the YFP Venus N-terminal hemiprotein ($A_{2A}R$ -nYFP) and with D_2R fused to the YFP Venus C-terminal hemiprotein (D_2R -cYFP), indicating YFP reconstitution and therefore $A_{2A}R$ (nYFP)- D_2R (cYFP) heteromerization (Fig. 4A). A_1R - D_2R and $A_{2A}R$ - D_1R pairs (fused to corresponding hemiproteins) served as negative controls here as well (Fig. 4A).

Finally, complemented Rluc from $A_{2A}R$ (nRluc)- D_2R (cRluc) heteromers and complemented YFP from $A_{2A}R$ (nYFP)- D_2R (cYFP) heteromers were used as donor and acceptor molecules in bioluminescence resonance energy transfer (BRET) experiments (Fig. 4B). Significant BRET values were obtained with cotransfection of $A_{2A}R$ -nRluc, D_2R -cRluc, $A_{2A}R$ -nYFP, and D_2R -cYFP (Fig. 4B). A_1R - D_2R and $A_{2A}R$ - D_1R pairs (fused to corresponding hemiproteins) again served as negative controls (Fig. 4B). Further controls included independent experiments replacing each receptor fused to its hemiprotein with the same nonfused (soluble) hemiprotein (Table S1).

Bimolecular fluorescence complementation was also used to evaluate the ability of peptides with the amino acid sequence of transmembrane domains (TMs) to destabilize $A_{2A}R$ - D_2R heteromers, as recently described for dopamine D_1R - D_3R heteromers (2). Previous BRET experiments with disrupting peptides had suggested the involvement of TM5 from D_2R in $A_{2A}R$ - D_2R heteromerization (18). We investigated whether synthetic peptides with the sequence of TM5 and TM7 of $A_{2A}R$ or D_2R fused to HIV TAT were able to destabilize receptor heteromerization. Both TM5 peptides, but none of the TM7 peptides, reduced fluorescence complementation in cells expressing $A_{2A}R$ -nYFP and D_2R -cYFP (Fig. 4A), suggesting that, in addition to intracellular domains, TM5 forms part of the heteromerization interface. In contrast, neither TM5 or TM7 from $A_{2A}R$ or D_2R was able to decrease fluorescence complementation in cells expressing $A_{2A}R$ -nYFP and $A_{2A}R$ -cYFP or D_2R -nYFP and D_2R -cYFP (Fig. 4A), supporting the selective involvement of TM5 on the heteromer interface.

Pharmacologic Evidence for $A_{2A}R$ Agonist/Antagonist-Mediated Allosteric Modulation of D_2R Function in Striatal Cells and in the Experimental Animal.

Previous patch-clamp experiments in rat striatal slices showed that CGS 21680 completely antagonizes the decrease of neuronal excitability (i.e., NMDA-induced neuronal firing) induced by D_2R agonists, which was demonstrated to depend on an allosteric modulation of D_2R agonist efficacy and on $A_{2A}R$ - D_2R heteromerization (9). It was also shown that SCH 58261 counteracts the allosteric effect of CGS 21680 on D_2R function (9), but the effect of the $A_{2A}R$ antagonist alone was not analyzed. Under these experimental conditions, the slice bathing solution is free of endogenous neurotransmitters, thereby allowing testing in situ of the $A_{2A}R$ agonist/antagonist-mediated allosteric modulation of D_2R function without the interference of endogenous adenosine. We first reproduced the effect of NMDA (5 μM ; increase in neuronal firing) and the counteraction of this effect by the D_2R agonist agonist R(-)-propylnorapomorphine hydrochloride (NPA; 10 μM) (Fig. 5A). Remarkably, the $A_{2A}R$ antagonist SCH 58261 (1 μM) completely counteracted the effect of the D_2R agonist (Fig. 5A and B), as reported for CGS 21680. These results mirror those obtained with transfected cells and demonstrate that both $A_{2A}R$ agonists and antagonists are able to modulate D_2R function in the striatum.

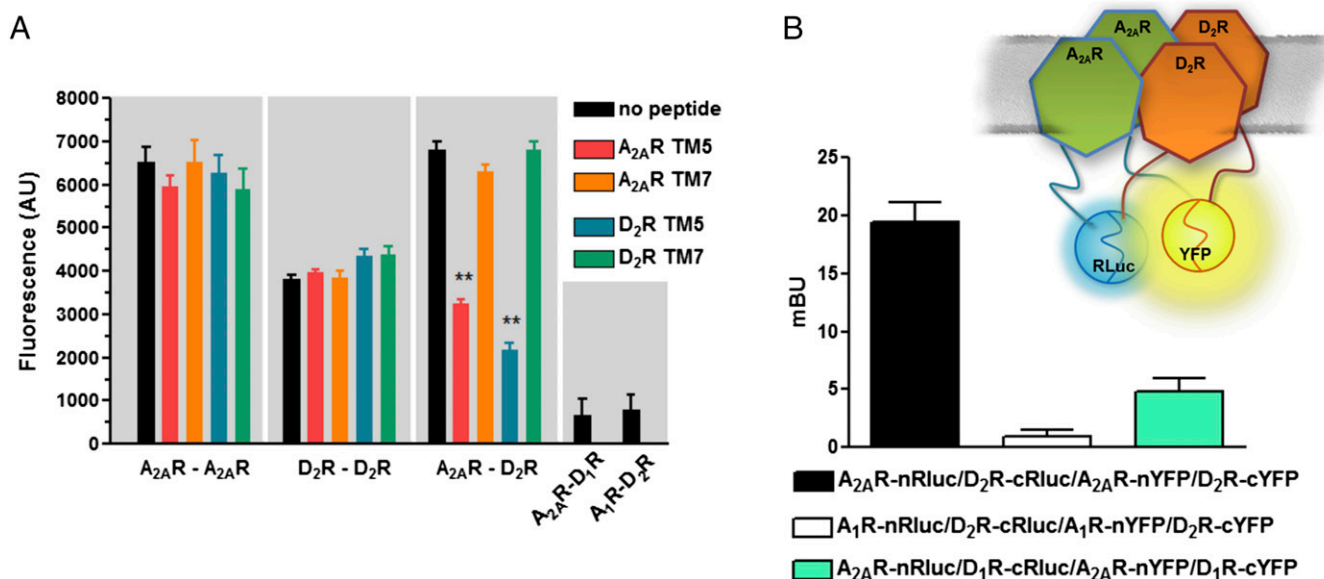


Fig. 4. Tetrameric structure of the A_{2A}R-D₂R heteromer. (A) Fluorescence due to complementation [in arbitrary units (AU)] of YFP Venus was determined in HEK-293 cells coexpressing A_{2A}R-nYFP and A_{2A}R-cYFP, D₂R-nYFP and D₂R-cYFP, or A_{2A}R-nYFP and D₂R-cYFP either not treated or treated with the indicated HIV TAT peptides (4 μM) for 4 h. Values represent means ± SEM from seven or eight different experiments. Statistical significance was calculated by one-way ANOVA followed by Dunnett's post hoc test. ***P* < 0.01, compared with the nontreated cells. (B) BRET was determined in cells expressing A_{2A}R-nRluc, D₂R-cRluc, A_{2A}R-nYFP and D₂R-cYFP, or A_{2A}R-nYFP and D₂R-cYFP and the respective controls replacing A_{2A}R for A₁R or D₂R for D₁R. Values are mean ± SEM of three different experiments. (Upper) Schematic representation of BRET with bimolecular luminescence and fluorescence complementation.

It is well known that locomotor activation by A_{2A}R antagonists or caffeine shows an inverted U-shaped dose-response curve, with a depressant effect at high doses (23–25). This de-

pressant effect could be related to the ability of the antagonists to largely displace endogenous adenosine and occupy both protomers in the A_{2A}R homodimer of the A_{2A}R-D₂R hetero-

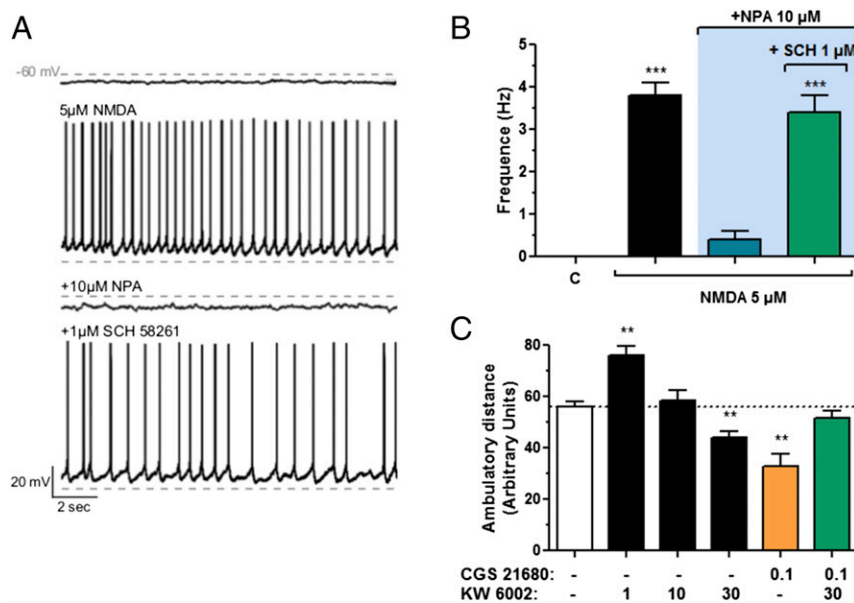


Fig. 5. Allosteric modulation of A_{2A}R antagonists on D₂R-mediated modulation of neuronal function. (A and B) Effect of the A_{2A}R antagonist SCH 58261 on NMDA-mediated depolarized plateau potential on D₂R-responsive neurons in rat ventral striatal slices. (A) Consecutive traces showing typical transitions where the action of NMDA (5 μM) was recorded before and in the presence of D₂R NPA (10 μM) and the A_{2A}R antagonist SCH 58261 (1 μM). On a D₂R-responsive neuron, subsequent application of SCH 58261 totally counteracts the effect of NPA, i.e., inhibition of the depolarized plateau potential and firing frequency. (B) Summary histogram obtained from D₂R-responsive neurons illustrating the antagonistic effect of SCH 58261 on the action potential firing frequency. Data represent mean ± SEM (*n* = 7). Statistical significance was calculated by one-way ANOVA followed by Dunnett's post hoc test. ****P* < 0.001, compared with the untreated slice preparation (c). (C) Locomotor activity in nonhabituated rats during the first 20 min after the administration of vehicle or the A_{2A}R antagonist KW 6002 (1–30 mg/kg, i.p.), or vehicle, was administered 30 min before the administration of CGS 21680. A high dose of KW 6002 produced significant locomotor depression, which was counteracted by a previous administration of the additional depressant dose of CGS 21680. Statistical significance was calculated by one-way ANOVA followed by Dunnett's post hoc test. ***P* < 0.01 compared with controls (animals only treated with vehicle).

mer. In that case, we would predict that coadministration of a depressant dose of an $A_{2A}R$ agonist should not produce more depression, but rather should counteract the depressant effect of the antagonists. We tested locomotor activity in rats during the first 20 min of activity of nonhabituated animals with doses of the $A_{2A}R$ antagonist KW 6002 above 1 mg/kg, reportedly the maximal effective dose (23). KW 6002 also produced a biphasic effect on D_2R binding and MAPK signaling (Fig. 2*F*), and it was selected because of its pronounced locomotor effects compared with SCH 58261 (23). At 10 mg/kg, KW 6002 did not produce any activation, and at 30 mg/kg it had a depressant effect (Fig. 5*C*). As predicted, coadministration of a depressant dose of CGS 21680 (0.1 mg/kg) (24) counteracted the depressant effect of KW 6002 (30 mg/kg) (Fig. 5*C*). The same dose of CGS 21680 did not significantly counteract (although it did not potentiate) the motor depressant effects of high doses of caffeine (56 and 100 mg/kg) (Fig. S3). Thus, these results

agree with previous studies indicating that mechanisms other than adenosine receptor antagonism are involved in the depressant effects of high doses of caffeine (25).

$A_{2A}R$ Agonists and Antagonists Also Modulate D_2R Antagonist Binding in the $A_{2A}R$ - D_2R Heteromer. Because both $A_{2A}R$ agonists and antagonists can allosterically modulate the affinity and intrinsic efficacy of D_2R agonists, we questioned whether $A_{2A}R$ ligands also could modulate the binding of D_2R antagonists in the $A_{2A}R$ - D_2R heteromer. We found that both CGS 21680 and caffeine significantly reduced [3H]raclopride binding in membrane preparations from sheep and human striatum and from CHO cells transfected with $A_{2A}R$ and D_2R (Fig. 6*A* and *B*). The decrease in [3H]raclopride binding by CGS 21680 and caffeine was related to a decrease in the affinity of D_2R antagonist (increase in K_{D1} values), as shown in competition experiments (sheep striatum) of [3H]raclopride vs. raclopride (Table 1). As

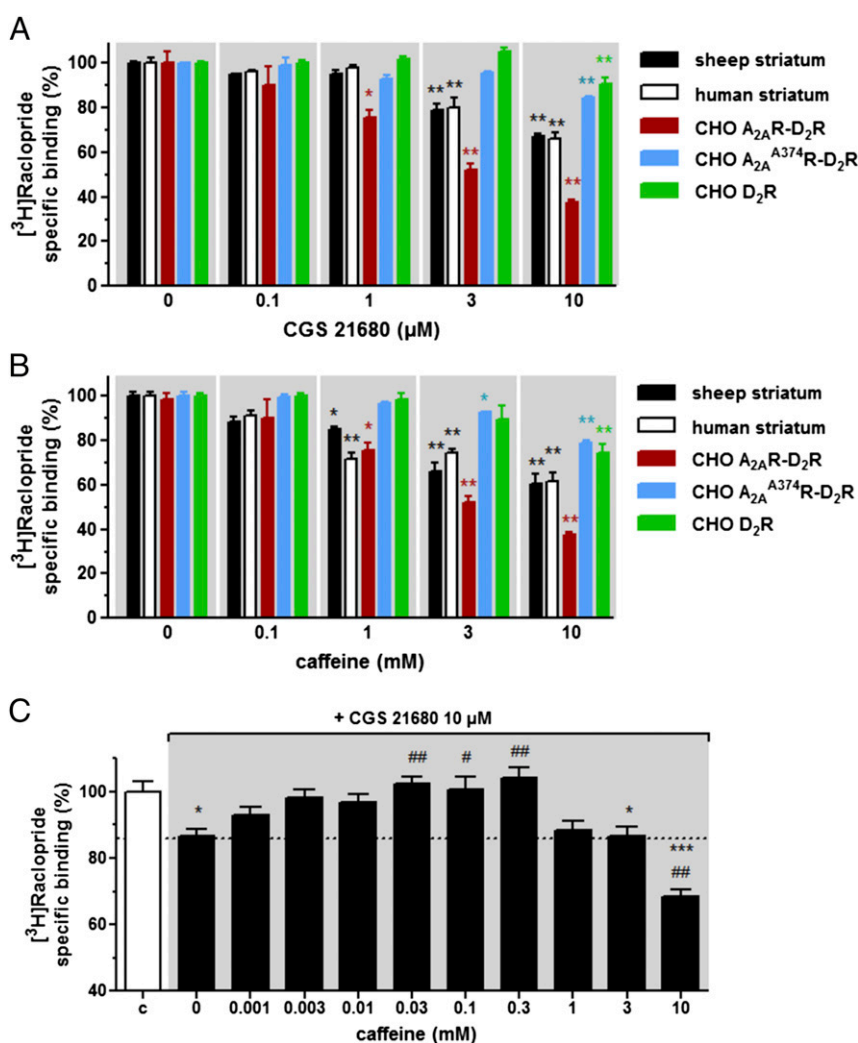


Fig. 6. Effect of an $A_{2A}R$ agonist and caffeine on [3H]raclopride binding. (*A* and *B*) [3H]raclopride (4 nM) binding was determined in membrane preparations from sheep striatum (black bars), human caudate nucleus (white bars), or CHO cells transfected with D_2R cDNA (2 μ g) and $A_{2A}R$ cDNA (3 μ g; red bars), D_2R cDNA (2 μ g) and cDNA (3 μ g) from mutated $A_{2A}R$ (A_{2A}^{A374R} ; blue bars), or CHO cells transfected only with D_2R cDNA (2 μ g; green bars) in the presence or the absence of increasing concentrations of the $A_{2A}R$ agonist CGS21680 (*A*) or caffeine (*B*). (*C*) [3H]raclopride (4 nM) binding determined in membrane preparations from sheep striatum either untreated (white bar, c) or treated with CGS 21680 (10 μ M) in the absence or presence of increasing concentrations of caffeine (black bars). Values are mean \pm SEM from three to five different experiments of the relative [3H]raclopride-specific binding (% of nontreated membranes). Statistical significance was calculated by one-way ANOVA followed by Dunnett's post hoc test or the Newman-Keuls post hoc test. * P < 0.05; ** P < 0.01; *** P < 0.001, compared with the untreated membrane preparations. # P < 0.05; ## P < 0.01, compared with the membranes treated only with CGS 21680.

controls of adenosine receptor selectivity, neither the A_1R agonist CCPA nor the A_1R antagonist DPCPX modulated [3H]raclopride binding at concentrations that do not bind to $A_{2A}R$ (Fig. S4). Again, the potency of both CGS 21680 and caffeine in modulating [3H]raclopride binding was significantly reduced in cells expressing the mutant $A_{2A}^{A374}R$, indicating dependence on $A_{2A}R$ - D_2R heteromerization (Fig. 6A and B). In fact, the same reduction in the potency of CGS 21680 and caffeine observed in cells expressing the mutant $A_{2A}^{A374}R$ was observed in cells transfected only with D_2R (Fig. 6A and B), which were found to constitutively express relatively low levels of $A_{2A}R$ (B_{max} for [3H]ZM 241385 binding of 0.25 pmol/mg protein). Furthermore, the same biphasic effect observed with increasing concentrations of caffeine on the ability of the $A_{2A}R$ agonist CGS 21680

to decrease [3H]quinpirole binding was also observed with [3H]raclopride binding in membrane preparations from sheep striatum (Fig. 6C). Thus, low concentrations of caffeine antagonized the effect of CGS 21680, whereas high concentrations were also associated with a significant decrease in [3H]raclopride binding (Fig. 6C).

We then used disrupting TM peptides to demonstrate that heteromerization is involved in the $A_{2A}R$ ligand-mediated modulation of D_2R binding in striatal tissue. We first checked endogenous $A_{2A}R$ - D_2R heteromer expression in sheep striatal slices by a proximity ligation assay (PLA). This technique permits the detection of molecular interactions between two endogenous proteins and it is similar to immunoprecipitation, but with the additional advantage of not requiring membrane

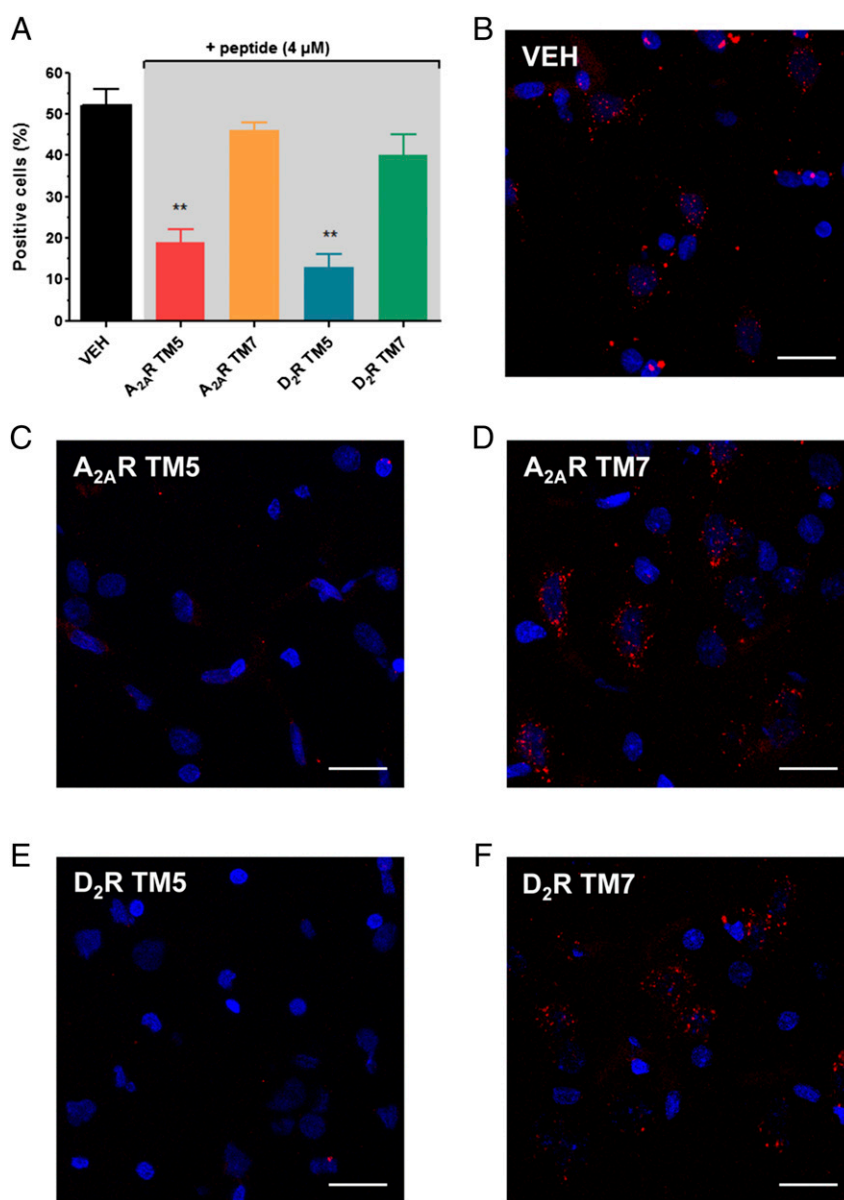


Fig. 7. Detection of $A_{2A}R$ - D_2R heteromers in sheep striatum and effect of HIV TAT-TM peptides. The PLA was performed in coronal slices from sheep striatum treated with vehicle or with HIV TAT-fused TM peptides (4 μ M) corresponding to TM5 or TM7 of $A_{2A}R$ or D_2R . (A) Number of cells containing one or more red spots expressed as the percentage of the total number of cells (blue nucleus). Data (% of positive cells) are the mean \pm SEM of counts from a total of 800–1,000 cells, considering between five and 12 different fields. Statistical significance was calculated by one-way ANOVA followed by Dunnett's post hoc test. ** $P < 0.01$, compared with the slices treated with vehicle (c). (B–F) Representative confocal microscopy images from each experimental condition, in which heteromers appear as red spots. In all cases, cell nuclei were stained with DAPI (blue). (Scale bars: 20 μ m.)

solubilization. Labeling heterodimers by PLA requires that both receptors be sufficiently close to allow the two antibody-DNA probes to form double-stranded segments (<16 nm) (10), a signal that is further amplified in the presence of fluorescent nucleotides (Fig. 7). On the PLA, A_{2A}R-D₂R heteromers were observed as red punctate staining in slices treated with vehicle or with TM7 peptides, but not in slices treated with TM5 peptides from A_{2A}R or D₂R (Fig. 7 C and E). Because TM5 peptides disrupted both fluorescence complementation (Fig. 3A) and the PLA signal (Fig. 7), we expected that this alteration of the quaternary structure should result in the loss of the allosteric interactions within the heteromer. Indeed, TM5 peptides from both A_{2A}R (Fig. 8A) and D₂R (Fig. 8B), but not TM7 peptides, counteracted caffeine-mediated decrease in [³H]raclopride binding in sheep striatal membrane preparations (Fig. 8).

Discussion

Several conclusions can be drawn from this study. First, any orthosteric A_{2A}R ligand, agonist or antagonist, can decrease the affinity and intrinsic efficacy of any D₂R ligand. These features constitute biochemical properties of the A_{2A}R-D₂R heteromer, because they depend on the integrity of the right quaternary structure of the heteromer, as demonstrated in transfected mammalian cells and striatal tissue, by using heteromer-disrupting mutations and peptides, respectively. Second, the results from radioligand dissociation and double complementation of BRET donor and acceptor units provide strong evidence for a tetrameric structure of the A_{2A}R-D₂R heteromer constituted by A_{2A}R and D₂R homodimers. Third, the A_{2A}R-D₂R heterotetramer offers a model that explains the apparent contradiction of orthosteric A_{2A}R agonists and antagonists being able to produce the same modulatory effects on D₂R function and yet counteract each other's effects. The model assumes that occupancy of

the A_{2A}R homodimer with either an agonist or an antagonist produces a conformational change that conduces the same allosteric modulation to the D₂R, whereas simultaneous occupancy of the A_{2A}R homodimer by an agonist and an antagonist would not allow this conformational change (as indicated by dissociation experiments with the radiolabeled A_{2A}R antagonist).

The model has important heuristic value. As the model predicted, in the brain, under specific pharmacologic conditions, orthosteric A_{2A}R antagonists behave as A_{2A}R agonists and decrease D₂R function, effects that can be counteracted by coadministration of both A_{2A}R agonists and antagonists (electrophysiological and locomotor activity experiments). Given the tone of adenosine under physiological conditions, this in fact could be the main mechanism by which caffeine and A_{2A}R antagonists produce locomotor activation, by counteracting the functional effects that depend on D₂R signaling by the A_{2A}R-D₂R heteromer. Nevertheless, motor depression by caffeine or A_{2A}R antagonists implies a significant displacement of endogenous adenosine and occupancy of the A_{2A}R homodimer in the A_{2A}R-D₂R heteromer, which can be attained only by high concentrations of caffeine that cannot be obtained through habitual consumption of coffee. Thus, a 12-oz cup of coffee may contain between 107 and 420 mg of caffeine (26), and oral doses of 250 and 500 mg (human adults) produce peak plasma levels of approximately 0.03 and 0.06 mM (27), which is in the range of concentrations at which caffeine counteracts the allosteric effects of CGS 21680 in the present radioligand-binding experiments (Figs. 2A and 6C). However, therapeutic doses of more potent and selective A_{2A}R antagonists may have differential effects depending on their A_{2A}R affinity and on the levels of endogenous adenosine. Therefore, our model still provides support for the use of A_{2A}R antagonists in treating patients with Parkinson's disease. In addition, the complementing results obtained from functional experiments in mammalian cells in culture, in striatal slices, and in the intact experimental animal provide a basis for understanding the previously claimed significant dependence of D₂R signaling and A_{2A}R-D₂R heteromerization on the pharmacologic effects of caffeine and other A_{2A}R ligands (9, 11–13).

Finally, the present results indicate that a large proportion of D₂R forms heteromers with A_{2A}R in transfected cells and striatal tissue. A similar degree of allosteric modulation of D₂R by A_{2A}R ligands was observed in both artificial and native systems. Particularly notorious was the ability of caffeine to allosterically (noncompetitively) decrease D₂R antagonist binding by approximately 60% and 40% in membrane preparations of transfected cells and striatal tissue, respectively. Furthermore, the experiments with MAPK signaling in transfected cells and the electrophysiological experiments in striatal neurons demonstrate an additional strong allosteric modulation of A_{2A}R ligands on the intrinsic efficacy of D₂R ligands, which can explain, for instance, the complete counteraction by A_{2A}R antagonists on MAPK activation and the decrease in neuronal excitability induced by high concentrations of D₂R agonists, which should surmount the reduction in affinity.

More generally, our study calls for an awareness of homodimers as predominant GPCR species, providing a significant role of allosteric interactions between orthosteric ligands within GPCRs and building blocks for heterotetramers (28), which should have important implications in the field of GPCR pharmacology.

Methods

Animals. Male Sprague–Dawley rats (Charles River Laboratories) weighting 300–350 g were used for all experiments. All animals were handled in accordance with the National Institutes of Health's animal care guidelines. The animal research protocol followed for this study (09-BNRB-73) was approved by the National Institute on Drug Abuse Intramural Research Program's Animal Care and Use Committee.

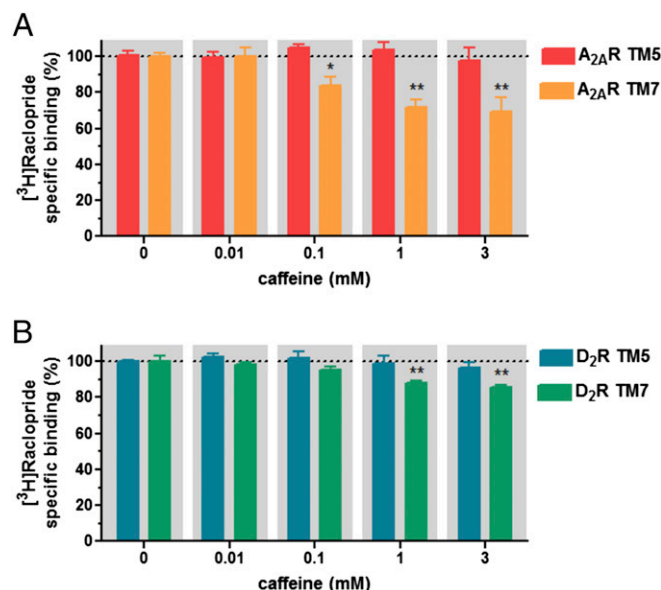


Fig. 8. Effect of HIV TAT-TM peptides on caffeine-induced allosteric modulation of [³H]raclopride binding. Membrane preparations from sheep striatum were pretreated for 2 h with the indicated A_{2A}R (A) or D₂R (B) HIV TAT peptides (4 μM) and [³H]raclopride (4 nM) binding was performed in the absence or the presence of increasing concentrations of caffeine. Values are means ± SEM from three to five different experiments of the relative [³H]raclopride-specific binding (% of the caffeine untreated membranes). Statistical significance was calculated by one-way ANOVA followed by Dunnett's post hoc test. **P* < 0.05; ***P* < 0.01, compared with the caffeine-untreated membranes.

Human Samples. Human brain samples from the nucleus caudate (head area) were obtained by family consent at autopsy in the Basque Institute of Legal Medicine (University of the Basque Country, Bilbao, Spain) from four male subjects without history of neurological or psychiatric disorders and who died suddenly of a car accident. Toxicological screening was negative for all subjects and brain samples were histologically determined as normal. Samples were dissected at the time of autopsy, stored at -70°C until assay and encoded in order to protect the identity of the subject. The time interval between death and autopsy (postmortem delay at 4°C) was 26 ± 4 h.

Fusion Proteins and Expression Vectors. Sequences encoding amino acid residues 1–155 and 156–238 of the YFP Venus protein and amino acid residues 1–229 and 230–311 of the RLuc8 protein were subcloned in the pcDNA3.1 vector to obtain YFP Venus (nYFP, cYFP) and RLuc8 (nRLuc, cRLuc) hemitruncated proteins expressed in the pcDNA3.1 vector. Human cDNA for dopamine D₂R (long isoform) and D₁R, adenosine A_{2A}R and A₁R cloned in pcDNA3.1 were amplified without their stop codons using sense and antisense primers harboring either unique EcoRI or BamHI sites. The fragments were then subcloned to be in-frame with the hemitruncated RLuc or YFP into the EcoRI and BamHI restriction sites of the hemitruncated proteins expressing vector, to render the plasmids that express receptors fused to the hemitruncated proteins (D₂R-cYFP, D₂R-cRLuc, A_{2A}R-nYFP, A_{2A}R-nRLuc, D₁R-cYFP, D₁R-cRLuc, A₁R-nYFP, A₁R-nRLuc). A peptide derived from the HIV transactivator of transcription, HIV TAT (YGRKKRRQRRPQ), was fused to a peptide with the amino acid sequence of human A2AR or D₂R TM domains 5 and 7 (TM5 and TM7; Genesys Synthesis 124), to promote integration of the TM domains in the plasma membrane. Because HIV TAT binds to the phosphatidylinositol-(4, 5)-bisphosphate found on the inner surface of the membrane, HIV TAT peptide was fused to the C terminus of TM5 and TM7 to obtain the right orientation of the inserted peptide (2).

Cell Culture and Transient Transfection. CHO and human embryonic kidney (HEK-293) cells were grown in Minimum Essential Medium (MEM α ; Gibco) and DMEM (Gibco), respectively, supplemented with 2 mM L-glutamine, 100 $\mu\text{g}/\text{mL}$ sodium pyruvate, MEM nonessential amino acid solution (1/100), 100 U/mL penicillin/streptomycin, and 5% (vol/vol) of heat-inactivated FBS (all supplements from Invitrogen). CHO and HEK-293 cells growing in 25-cm² flasks or 150-cm² dishes were transiently transfected by the polyethylenimine (PEI) method. In brief, cells were incubated for 4 h with the indicated amount of cDNA together with ramified PEI (Sigma-Aldrich; 5 mL of 10 mM PEI for each μg of cDNA) and 150 mM NaCl in a serum-starved medium. After 4 h, the medium was changed to a fresh complete culture medium. Cells were used at 48 h after transfection.

ERK1/2 Phosphorylation Assays. The effect of different ligand combinations on ERK1/2 phosphorylation was studied in HEK-293 cells transfected with A_{2A}R and D₂R. The methodology is described in detail elsewhere (2).

BRET and Bimolecular Bioluminescence and Fluorescence Complementation. HEK-293 cells growing in six-well plates were transiently cotransfected with 1 μg of cDNA encoding for the receptors fused to nRLuc8 and cRLuc8 proteins and with 1 μg of cDNA corresponding to the receptors fused to nVenus and cVenus proteins. To quantify receptor-reconstituted YFP Venus expression, cells (20 μg of total protein per well) were distributed in 96-well microplates (black plates with a transparent bottom), and fluorescence was read in a FLUOstar Optima fluorimeter (BMG Labtech). Receptor fluorescence expression was determined as fluorescence of the sample minus the fluorescence of cells expressing the BRET donor alone. For BRET with bimolecular bioluminescence and fluorescence complementation measurements, cells (10 μg of total protein per well) were distributed in 96-well microplates (Corning 3600 white plates), and 5 μM coelenterazine H (Molecular Probes) was added. At 5 min after the addition of coelenterazine H, the readings were collected using a Mithras LB 940 microplate reader (Berthold Technologies), which allows integration of the signals detected in the short-wavelength filter at 485 nm (440–500 nm) and the long-wavelength filter at 530 nm (510–590 nm). To quantify receptor-reconstituted RLuc8 expression, luminescence readings were also performed at 10 min after the addition of 5 mM coelenterazine H. Both the fluorescence and luminescence of each sample were measured before each experiment to confirm similar donor expression ($\sim 150,000$ luminescent units). Net BRET was defined as [(long-wavelength emission)/(short-wavelength emission)] – C_f , where C_f corresponds to [(long-wavelength emission)/(short-wavelength emission)] for the donor construct expressed alone in the same experiment. BRET is expressed as mili BRET units (mBU; net BRET $\times 1,000$).

Radioligand-Binding Experiments. Crude membranes from sheep or human striatum (caudate) or cultured CHO cells were prepared as described else-

where (23). Protein was quantified by the bicinchoninic acid method (Pierce Chemicals). Binding experiments were performed with membrane suspensions at room temperature in 50 mM Tris-HCl buffer, pH 7.4, containing 10 mM MgCl₂ and 0.2 IU/mL adenosine deaminase (EC 3.5.4.4; Roche). For D₂R agonist-binding assays, membrane suspensions (0.2 mg of protein/mL) were incubated with a free concentration (6 nM) of the radiolabeled D₂R agonist [³H]quinpirole (37.2 Ci/mmol; Perkin-Elmer), the indicated concentrations of caffeine (Sigma-Aldrich), the A_{2A}R agonist CGS 21680 (Sigma-Aldrich), and the A_{2A}R antagonist SCH 58261 (Tocris). For D₂R antagonist-binding assays, the medium was supplemented with 120 mM NaCl and 5 mM KCl, and the membrane suspensions (0.2 mg of protein/mL) were incubated with a free concentration (4 nM) of the radiolabeled D₂R antagonist [³H]raclopride (81.9 Ci/mmol; Perkin-Elmer) and the indicated concentrations of caffeine, CGS 21680, or SCH 58261. For experiments with the HIV TAT TM peptides, membranes were preincubated for 2 h with 4 μM of the indicated peptide before the addition of other ligands. For competition experiments, the membrane suspensions were incubated with a constant free concentration of [³H]quinpirole (6 nM) or [³H]raclopride (4 nM) and increasing concentrations of quinpirole (0.01 nM–3 μM) or raclopride (0.01 nM–3 μM), respectively, in the presence or absence of caffeine (3 mM) or CGS 21680 (3 μM). In all cases, free and membrane-bound ligands were separated by rapid filtration, and radioactivity counts were determined as described elsewhere (23).

Two-state dimer model equations were used to determine radioligand-binding parameters, as described in detail elsewhere (29). In dissociation kinetic assays, sheep striatal membranes (0.2 mg of protein/mL) were incubated at 12°C in Tris-HCl buffer (50 mM, pH 7.4) containing 10 mM MgCl₂ and 0.2 IU/mL adenosine deaminase in the absence or presence of CGS 21680 (10 nM), SCH 58261 (10 nM), or caffeine (30 μM). After 30 min, 1.5 nM of the A_{2A}R antagonist [³H]ZM 241385 (50 Ci/mmol; American Radiolabeled Chemicals) was added for an additional 2-h period of radioligand association. Dissociation was initiated by the addition of 10 μM of ZM 241385. At the indicated time intervals, total binding was measured as described above.

Patch-Clamp Recording. Whole-cell patch-clamp recordings were performed on individual neurons from the rat ventral striatum. The method is described in detail elsewhere (9).

Locomotor Activity. Rats received an i.p. injection of 0.1 mg/kg CGS 21680 or vehicle (saline plus 5% DMSO and 5% Tween-80). After 30 min, they received a second i.p. injection of KW 6002 (1, 10, or 30 mg/kg) or vehicle, and locomotor activity was measured by placing the animals individually in motility chambers (50 \times 50 cm; Coulbourn Instruments). Locomotion was measured by counting the number of breaks in the infrared beams of the chambers for the first 20 min after the last i.p. injection.

Proximity Ligation Assay. Sheep striatum placed in ice-cold oxygenated (95% O₂/5% CO₂) Krebs-HCO₃⁻ buffer (124 mM NaCl, 4 mM KCl, 1.25 mM KH₂PO₄, 1.5 mM MgCl₂, 1.5 mM CaCl₂, 10 mM glucose, and 26 mM NaHCO₃; pH 7.4) were dissected and sliced at 4°C using a brain matrix to obtain 0.5-mm coronal slices. Each slice was transferred to a plate and incubated for 4 h at 30°C under constant oxygenation in an Eppendorf Thermomixer (5 Primer Inc.) with Krebs-HCO₃⁻ buffer containing or not containing 4 μM of the indicated HIV TAT TM peptides. Slices were fixed with 4% paraformaldehyde solution for 1 h at room temperature, washed in Tris-buffered saline, and stored at -20°C in a 30% sucrose solution until sectioning. The 20- μm -thick coronal sections were cut on a freezing cryostat (Leica Jung CM-3000), mounted on glass slides, and permeabilized for 10 min at 4°C with 0.1% Triton X-100. A_{2A}R-D₂R complexes were detected using the Duolink II PLA detection kit (OLink Bioscience) following the manufacturer's instructions using a mixture containing equal amounts of rabbit polyclonal anti-D₂R antibody (1:200, AB5084P; Millipore) and monoclonal mouse anti-A_{2A}R antibody (1:200, 05-717; Millipore). The samples were mounted and observed under a Leica SP2 confocal microscope and processed with ImageJ software. Cells containing one or more spots vs. total cells were determined considering 800–1,000 cells from between five and 12 different fields from three different animals per group using the Fiji package (pacific.mpi-cbg.de) as described previously (30).

ACKNOWLEDGMENTS. We acknowledge the technical assistance of Jasmina Jiménez and Edgar Angelats, and thank Dr. Javier Meana and Dr. Joan Sallés (University of the Basque Country) for providing the human samples. This study was supported by the National Institute on Drug Abuse and grants from the Government of Catalonia (2009-SGR-12), Centro de Investigación Biomédica en Red sobre Enfermedades Neurodegenerativas (CB06/05/0064), and the Spanish Ministerio de Ciencia y Tecnología (SAF 2011-23813).

1. Ferré S, et al. (2014) G protein-coupled receptor oligomerization revisited: Functional and pharmacological perspectives. *Pharmacol Rev* 66(2):413–434.
2. Guitart X, et al. (2014) Functional selectivity of allosteric interactions within G protein-coupled receptor oligomers: The dopamine D1-D3 receptor heterotetramer. *Mol Pharmacol* 86(4):417–429.
3. Smith NJ, Milligan G (2010) Allosterism at G protein-coupled receptor homo- and heteromers: Uncharted pharmacological landscapes. *Pharmacol Rev* 62(4):701–725.
4. Ferré S, et al. (2009) Building a new conceptual framework for receptor heteromers. *Nat Chem Biol* 5(3):131–134.
5. Ferré S, von Euler G, Johansson B, Fredholm BB, Fuxe K (1991) Stimulation of high-affinity adenosine A2 receptors decreases the affinity of dopamine D2 receptors in rat striatal membranes. *Proc Natl Acad Sci USA* 88(16):7238–7241.
6. Hillion J, et al. (2002) Coaggregation, cointernalization, and codesensitization of adenosine A2A receptors and dopamine D2 receptors. *J Biol Chem* 277(20):18091–18097.
7. Canals M, et al. (2003) Adenosine A2A-dopamine D2 receptor-receptor heteromerization: Qualitative and quantitative assessment by fluorescence and bioluminescence energy transfer. *J Biol Chem* 278(47):46741–46749.
8. Navarro G, et al. (2014) Intracellular calcium levels determine differential modulation of allosteric interactions within G protein-coupled receptor heteromers. *Chem Biol* 21(11):1546–1556.
9. Azdad K, et al. (2009) Dopamine D2 and adenosine A2A receptors regulate NMDA-mediated excitation in accumbens neurons through A2A-D2 receptor heteromerization. *Neuropsychopharmacology* 34(4):972–986.
10. Trifilieff P, et al. (2011) Detection of antigen interactions ex vivo by proximity ligation assay: Endogenous dopamine D2-adenosine A2A receptor complexes in the striatum. *Biotechniques* 51(2):111–118.
11. Ferré S, O'Connor WT, Fuxe K, Ungerstedt U (1993) The striopallidal neuron: A main locus for adenosine–dopamine interactions in the brain. *J Neurosci* 13(12):5402–5406.
12. Ferré S (2008) An update on the mechanisms of the psychostimulant effects of caffeine. *J Neurochem* 105(4):1067–1079.
13. Ferré S, et al. (2004) Adenosine A2A-dopamine D2 receptor-receptor heteromers: Targets for neuro-psychiatric disorders. *Parkinsonism Relat Disord* 10(5):265–271.
14. Armentero MT, et al. (2011) Past, present and future of A(2A) adenosine receptor antagonists in the therapy of Parkinson's disease. *Pharmacol Ther* 132(3):280–299.
15. Ciruela F, et al. (2004) Combining mass spectrometry and pull-down techniques for the study of receptor heteromerization: Direct epitope-epitope electrostatic interactions between adenosine A2A and dopamine D2 receptors. *Anal Chem* 76(18):5354–5363.
16. Woods AS, Ferré S (2005) Amazing stability of the arginine–phosphate electrostatic interaction. *J Proteome Res* 4(4):1397–1402.
17. Navarro G, et al. (2010) Interactions between intracellular domains as key determinants of the quaternary structure and function of receptor heteromers. *J Biol Chem* 285(35):27346–27359.
18. Borroto-Escuela DO, et al. (2010) Characterization of the A2AR–D2R interface: Focus on the role of the C-terminal tail and the transmembrane helices. *Biochem Biophys Res Commun* 402(4):801–807.
19. Bennett KA, et al. (2013) Pharmacology and structure of isolated conformations of the adenosine A2A receptor define ligand efficacy. *Mol Pharmacol* 83(5):949–958.
20. Doré AS, et al. (2011) Structure of the adenosine A(2A) receptor in complex with ZM241385 and the xanthines XAC and caffeine. *Structure* 19(9):1283–1293.
21. Lebon G, Edwards PC, Leslie AG, Tate CG (2015) Molecular determinants of CGS21680 binding to the human adenosine A2A receptor. *Mol Pharmacol* 87(6):907–915.
22. Ginés S, et al. (2000) Dopamine D1 and adenosine A1 receptors form functionally interacting heteromeric complexes. *Proc Natl Acad Sci USA* 97(15):8606–8611.
23. Orru M, et al. (2011) Striatal pre- and postsynaptic profile of adenosine A(2A) receptor antagonists. *PLoS ONE* 6(1):e16088.
24. Karcz-Kubicha M, et al. (2003) Involvement of adenosine A1 and A2A receptors in the motor effects of caffeine after its acute and chronic administration. *Neuropsychopharmacology* 28(7):1281–1291.
25. Halldner L, et al. (2004) The adenosine A1 receptor contributes to the stimulatory, but not the inhibitory effect of caffeine on locomotion: A study in mice lacking adenosine A1 and/or A2A receptors. *Neuropharmacology* 46(7):1008–1017.
26. Juliano LM, Ferré S, Griffiths RR (2009) The pharmacology of caffeine. *Principles of Addiction Medicine*, eds Ries RK, Fiellin DA, Miller SC, Saitz R (Lippincott Williams & Wilkins, Philadelphia), pp 159–178.
27. Bruce M, Scott N, Lader M, Marks V (1986) The psychopharmacological and electrophysiological effects of single doses of caffeine in healthy human subjects. *Br J Clin Pharmacol* 22(1):81–87.
28. Ferré S (2015) The GPCR heterotetramer: Challenging classical pharmacology. *Trends Pharmacol Sci* 36(3):145–152.
29. Casadó V, et al. (2007) Old and new ways to calculate the affinity of agonists and antagonists interacting with G-protein-coupled monomeric and dimeric receptors: The receptor-dimer cooperativity index. *Pharmacol Ther* 116(3):343–354.
30. Bonaventura J, et al. (2014) L-DOPA treatment in primates disrupts the expression of A(2A) adenosine-CB(1) cannabinoid-D(2) dopamine receptor heteromers in the caudate nucleus. *Neuropharmacology* 79:90–100.

Supporting Information

Bonaventura et al. 10.1073/pnas.1507704112

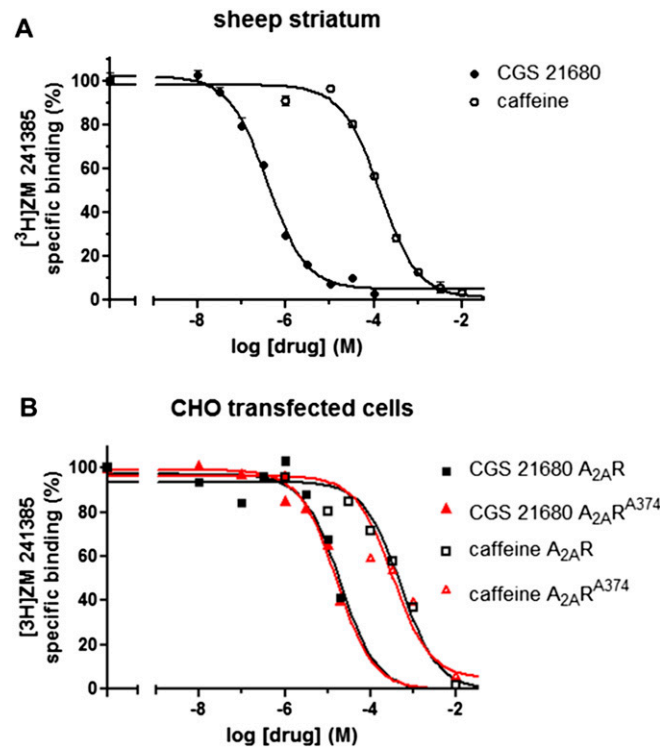


Fig. S1. Competition curves of [³H]ZM 241385 vs. CGS 21680 or caffeine. Membrane preparations from sheep striatum (A) or CHO cells (B) transfected with D₂R cDNA (2 μg) and A_{2A}R cDNA (3 μg) (B, black curves) or with D₂R cDNA (2 μg) and A_{2A}^{A374}R cDNA (or 3 μg) (B, red curves) were incubated with [³H]ZM 241385 (2 nM) and increasing concentrations of CGS 21680 (10 nM–10 μM) or caffeine (1 μM–10 mM). Values are mean ± SEM from a representative experiment performed in triplicate of the relative [³H]ZM 241385-specific binding, where 100% corresponds to 0.96 ± 0.04 pmol/mg protein for sheep striatum and to 0.74 ± 0.03 pmol/mg protein for CHO cells transfected with A_{2A}R or 0.90 ± 0.03 for CHO cells transfected with A_{2A}^{A374}R.

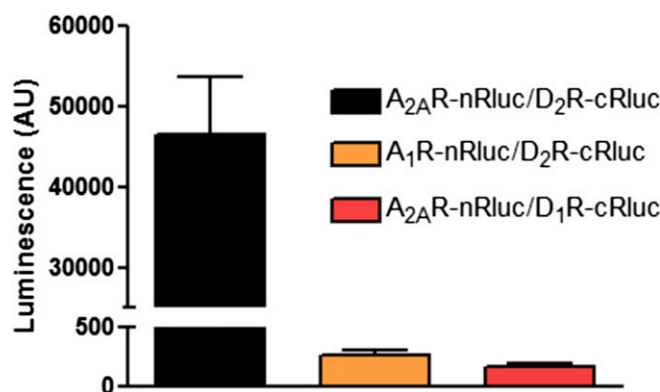


Fig. S2. Bioluminescence complementation within the A_{2A}R-D₂R heteromer. Luminescence due to Rluc in HEK-293 cells cotransfected with A_{2A}R-nRluc and D₂R-cRluc, A₁R-nRluc and D₂R-cRluc, or A_{2A}R-nRluc and D₁R-cRluc. On addition of coelenterazine H, strong luminescence could be observed only in cells co-expressing A_{2A}R-nRluc and D₂R-cRluc.

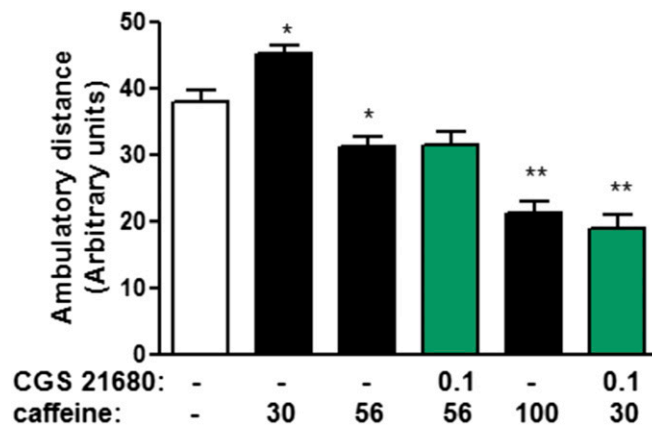


Fig. S3. Locomotor depressant effects of high doses of caffeine. Locomotor activity in nonhabituated rats during the first 20 min after the administration of vehicle or caffeine (30–100 mg/kg, i.p.). The $A_{2A}R$ agonist CGS 21680 (0.1 mg/kg i.p.) or vehicle was administered 30 min before the administration of caffeine. High doses of caffeine produced significant locomotor depression, which was neither counteracted nor potentiated by a previous administration of the additional depressant dose of CGS 21680. Statistical significance was calculated by one-way ANOVA followed by Dunnett's post hoc test. * $P < 0.05$; ** $P < 0.01$, compared with controls (animals treated only with vehicle).

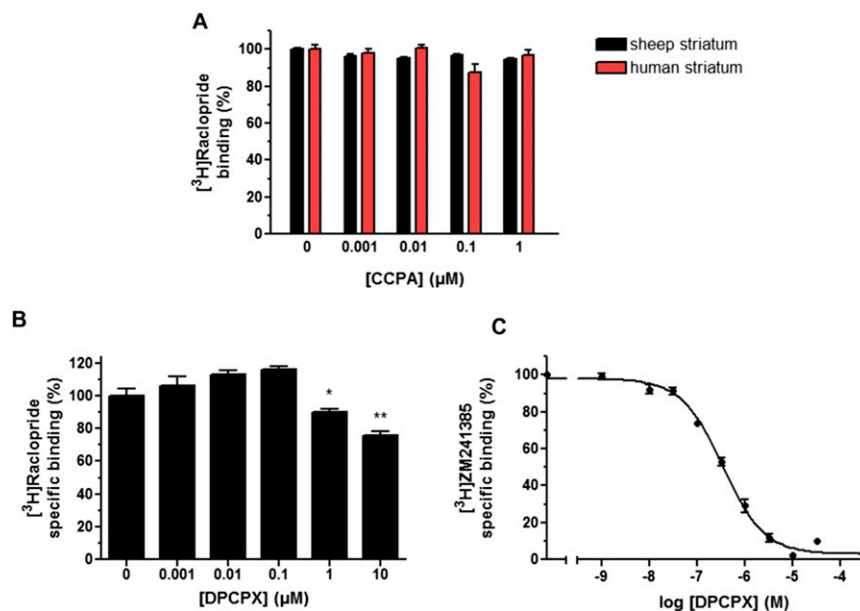


Fig. S4. Effect of A_1R agonist or antagonist on [3H]raclopride binding. (A and B) [3H]raclopride binding (4 nM) was determined in membrane preparations from sheep striatum (black bars) or human caudate nucleus (red bars) in the presence or the absence of increasing concentrations of the A_1R agonist CCPA (A) or the antagonist DPCPX (B), with higher selectivity for A_1R over $A_{2A}R$. Values are means \pm SEM (three to five different experiments) of the relative [3H]raclopride-specific binding (% respect to samples without A_1R ligands). Statistical significance was calculated by one-way ANOVA, followed by Dunnett's post hoc test. * $P < 0.05$; ** $P < 0.01$, compared with the untreated membrane preparations. (C) Competition curve of the $A_{2A}R$ antagonist [3H]ZM 241385 (2 nM) vs. the A_1R -selective antagonist DPCPX. Membrane preparations from sheep striatum were incubated with [3H]ZM 241385 (2 nM) and increasing concentrations of DPCPX (1 nM–300 μ M). Values are mean \pm SEM from a representative experiment performed in triplicate of the relative [3H]ZM 241385-specific binding, where 100% corresponds to 0.96 ± 0.05 pmol/mg protein.

Table S1. BRET with bimolecular bioluminescence and fluorescence complementation

Constructs transfected	mBU
$A_{2A}R$ -nRluc/D ₂ R-cRluc/ $A_{2A}R$ -nYFP/D ₂ R-cYFP	19 ± 2 (8)
nRluc/D ₂ R-cRluc/ $A_{2A}R$ -nYFP/D ₂ R-cYFP	3 ± 2 (7)
$A_{2A}R$ -nRluc/cRluc/ $A_{2A}R$ -nYFP/D ₂ R-cYFP	2 ± 1 (7)
$A_{2A}R$ -nRluc/D ₂ R-cRluc/nYFP/D ₂ R-cYFP	1.4 ± 0.9 (7)
$A_{2A}R$ -nRluc/D ₂ R-cRluc/ $A_{2A}R$ -nYFP/cYFP	2 ± 1 (7)

BRET is represented as mBU (*Materials and Methods*). Values are mean \pm SEM (no. of different experiments in parentheses).

Chapter 2.2. Evidence for the heterotetrameric structure of the adenosine A2A-dopamine D2 receptor complex

Casadó-Anguera V, Bonaventura J, Moreno E, Navarro G, Cortés A, Ferré S, Casadó V.

Biochemical Society Transactions, 2016, 44:595-600.

Evidence for the heterotetrameric structure of the adenosine A_{2A}–dopamine D₂ receptor complex

Verónica Casadó-Anguera*†‡¹, Jordi Bonaventura†§, Estefanía Moreno*†‡, Gemma Navarro*†‡, Antoni Cortés*†‡, Sergi Ferré§ and Vicent Casadó*†¹

*Centro de Investigación Biomédica en Red sobre Enfermedades Neurodegenerativas (CIBERNED), 28031 Madrid, Spain

†Department of Biochemistry and Molecular Biology, Faculty of Biology, University of Barcelona, 08028 Barcelona, Spain

‡Institute of Biomedicine of the University of Barcelona (IBUB), 08028 Barcelona, Spain

§Integrative Neurobiology Section, National Institute on Drug Abuse, Intramural Research Program, National Institutes of Health, Baltimore, MD 21224, U.S.A.

Abstract

Heteromers of G-protein-coupled receptors (GPCRs) have emerged as potential novel targets for drug development. Accumulating evidence indicates that GPCRs can form homodimers and heteromers, with homodimers being the predominant species and oligomeric receptors being formed as multiples of dimers. Recently, heterotetrameric structures have been proposed for dopamine D₁ receptor (D₁R)–dopamine D₃ receptor (D₃R) and adenosine A_{2A} receptor (A_{2A}R)–dopamine D₂ receptor (D₂R) heteromers. The structural model proposed for these complexes is a heteromer constituted by two receptor homodimers. The existence of GPCR homodimers and heteromers provides a structural basis for inter-protomer allosteric mechanisms that might account for a multiplicity of unique pharmacological properties. In this review, we focus on the A_{2A}R–D₂R heterotetramer as an example of an oligomeric structure that is key in the modulation of striatal neuronal function. We also review the interfaces involved in this and other recently reported heteromers of GPCRs. Furthermore, we discuss several published studies showing the *ex vivo* expression of A_{2A}R–D₂R heteromers. The ability of A_{2A}R agonists to decrease the affinity of D₂R agonists has been reported and, on the basis of this interaction, A_{2A}R antagonists have been proposed as potential drugs for the treatment of Parkinson's disease. The heterotetrameric structure of the A_{2A}R–D₂R complex offers a novel model that can provide new clues about how to adjust the drug dosage to the expected levels of endogenous adenosine.

Introduction

The long-perceived notion that G-protein-coupled receptors (GPCRs) only function in monomeric form [1,2] has recently been changed by the description of a number of GPCRs of classes A, B and C found as homodimers, heterodimers and higher order oligomers [3–9]. Receptor oligomers are defined as macromolecular complexes composed of at least two functional receptor units (protomers) with biochemical properties that are demonstrably different from those of their individual components [10]. It has been suggested that GPCR heteromers are mostly constituted by heteromers of homodimers [11]. This is supported by evidence for a minimal tetrameric stoichiometry of D₁R and dopamine D₃ receptor (D₃R) heteromers, comprised of D₁R and D₃R homodimers able to couple to G_s and G_i proteins respectively [11].

By using selective peptides with the sequence of specific transmembrane domains (TM) of the D₁R, this previous study demonstrated ligand-induced allosteric interactions within the D₁R–D₃R heteromer (positive cross-talk and cross-antagonism) that constitute specific biochemical characteristics of the D₁R–D₃R heteromer [11]. The expression of adenosine A₁ receptor (A₁R)–adenosine A_{2A} receptor (A_{2A}R) complex as a receptor heterotetramer in transfected cells has also been suggested [12].

In the context of homo- and heteromers of GPCRs, allosteric mechanisms are responsible for a multiplicity of unique pharmacological properties [6,13]. These mechanisms account for the process by which the interaction of a particular chemical or protein with an allosteric site on a protein or on a macromolecular complex influences the binding or the function of the same or another chemical or protein at a topographically distinct site, i.e. the orthosteric site [13]. Three major allosteric modulations may occur in GPCR oligomers (homo- and heteromers). First, the binding of a ligand to an allosteric site can modify the intrinsic efficacy and/or affinity of any ligand binding to the orthosteric site in any protomer of the oligomer. Second, the binding of a ligand to the orthosteric site of one protomer in the receptor oligomer can modify the affinity and/or intrinsic efficacy of ligands for the orthosteric site of the partner receptor, intrinsic efficacy being the power of an agonist to induce a functional

Key words: adenosine receptors, allosteric modulation, dopamine receptors, G-protein-coupled receptor (GPCR), heteromerization, homodimerization.

Abbreviations: A₁R, adenosine A₁ receptor; A_{2A}R, adenosine A_{2A} receptor; BiFC/BiLC, bimolecular fluorescence or luminescence complementation; BRET, bioluminescence resonance energy transfer; CB₁R, cannabinoid CB₁ receptor; CODA-RET, complemented donor-acceptor resonance energy transfer; CRF₁R, corticotropin-releasing factor CRF₁ receptor; D₁R, dopamine D₁ receptor; D₂R, dopamine D₂ receptor; D₃R, dopamine D₃ receptor; GPCR, G-protein-coupled receptor; 5-HT_{2A}R, serotonin 5-HT_{2A} receptor; MAPK, mitogen-activated protein kinase; OX₁R, orexin OX₁ receptor; PLA, proximity ligation assay; *luc*, *Renilla* luciferase; RT, residence time; TM, transmembrane domain.

¹Correspondence may be addressed to either of these authors (email vcasadoanguera@gmail.com or vcasado@ub.edu).

response, independently of its affinity for the receptor [6,13–15]. Third, a ligand-independent allosteric modulation may occur when one of the receptors in the oligomer acts as a modulator of the pharmacological properties of the other molecularly different receptor; in this case, the modulator is not a ligand, but a protein [6,16].

An example of the second type of major allosteric modulation in a GPCR heteromer, i.e. modulation of ligand-binding properties, is the ability of $A_{2A}R$ agonists to decrease the affinity of dopamine D_2 receptor (D_2R) for its agonists in the $A_{2A}R$ – D_2R heteromer [17–21]. $A_{2A}R$ – D_2R heteromers have been found in transfected cells [22,23], primary cultures of striatal neurons [22] and, *in situ*, in mammalian striatum [21,24–26], where they play an important role in the modulation of GABAergic striato-pallidal neuronal function [24,27]. It has previously been hypothesized that allosteric interactions between $A_{2A}R$ and D_2R agonists within the $A_{2A}R$ – D_2R heteromer provide a mechanism responsible for both the behavioural depressant effects of adenosine analogues and for the psychostimulant effects of selective adenosine $A_{2A}R$ antagonists and the non-selective adenosine receptor antagonist caffeine; this mechanism is of particular relevance in several neuropsychiatric disorders such as Parkinson's disease [15,21,28–31].

The $A_{2A}R$ – D_2R heteromer also provides an interesting example of the third type of major allosteric modulation in receptor heteromers. Screening with diverse *in vitro* and *in vivo* techniques led to the discovery of very different qualitative properties of several selective $A_{2A}R$ antagonists. The most striking finding was a change in the binding properties of the antagonist SCH 442416 for $A_{2A}R$ when forming heteromers with D_2R compared with when not forming heteromers or forming heteromers with A_1R [32]. Application of the dimer receptor model indicated that SCH 442416 binds with a strong negative co-operativity that appears when D_2R interacts with $A_{2A}R$ in the heteromer [3,6,14,15,32]. This suggested for the first time that the $A_{2A}R$ – D_2R comprises at least two $A_{2A}R$ protomers, supporting the existence of the $A_{2A}R$ – D_2R heterotetramer. SCH 442416 acts preferentially on presynaptic striatal $A_{2A}R$ – A_1R heteromers, potently blocking the cortico-striatal glutamatergic neurotransmission at doses that do not produce locomotor activation because it does not bind to postsynaptic $A_{2A}R$ – D_2R heteromers [15,32]. The opposite pharmacological profile was obtained with KW 6002, which produced strong locomotor activation at doses that were ineffective at blocking glutamate release from cortical afferents in the striatum [32]. KW 6002 is thus a promising anti-parkinsonian agent and is already being successfully used for the treatment of Parkinson's disease [33–35].

Homodimeric nature of both $A_{2A}R$ and D_2R

The allosteric modulator effect of orthosteric ligands on the rates of dissociation is commonly used to detect and quantify allosteric interactions [36]. Affinity modulators induce a conformational change that might alter only one or both

association and dissociation rates of binding to the orthosteric site. The most common method of quantification involves assaying the dissociation kinetics, because the dissociation of a prebound GPCR orthosteric ligand complex can only be modified by the concomitant binding of a modulator to a topographically distinct site [36], which can be on the same protomer (allosteric site) or on another protomer in a homodimer (orthosteric or allosteric site). For this purpose, dissociation experiments of radiolabelled orthosteric ligands were performed in the presence of modulators demonstrating, for instance, that IP28 is a negative allosteric modulator that increases the dissociation rate of the radiolabelled neutral antagonist [3H]SCH 23390 bound to D_1R [37].

We have recently determined the presence of A_{2A} and D_2 receptors as homodimers *ex vivo* by radioligand dissociation kinetic assays in sheep striatum membranes. In these experiments we found that the presence of the $A_{2A}R$ agonist CGS 21680 changed the dissociation constant of the radiolabelled $A_{2A}R$ antagonist [3H]ZM 241385 [21]. This constant did not change in the presence of several $A_{2A}R$ antagonists, such as caffeine or SCH 58261 (Table 1). Due to the fact that both agonists and antagonists of $A_{2A}R$ bind and compete for the same orthosteric site according to crystallographic studies [38–41], agonist-induced changes seen in the dissociation constant of the antagonist occur because both are bound simultaneously to different protomers in an $A_{2A}R$ – $A_{2A}R$ homodimer [15,21]. Likewise, dissociation experiments of [3H]YM-09151-2 in the same striatal preparations showed that the D_2R agonist quinpirole, but not the antagonist raclopride, significantly modified the dissociation rate of the radiolabelled antagonist [3H]YM-09151-2 (Table 1), indicating the formation of a hybrid species with both agonist and antagonist simultaneously binding to the D_2R – D_2R homodimer. Table 1 also shows the residence time (RT) in each experimental condition. This parameter may be of greater importance than the affinity when determining the drug's effect and efficacy in patients; this is because the body, unlike an *in vitro* scenario, is an open system where the concentration of free drugs fluctuates over time [42] and the longer the drug occupies the receptor, the more profoundly the drug may exert its effect [43]. Nevertheless, there are some cases, such as when talking about antipsychotic D_2R antagonists, where the toxicity associated with strong extrapyramidal motor effects is more important than the therapeutic advantages of long receptor occupancy. In this particular situation, a fast dissociating compound displaying low RT is desired [44]. As shown in Table 1, agonists, but not antagonists, significantly modified the RT of $A_{2A}R$ or D_2R radiolabelled antagonists.

Allosteric modulation by $A_{2A}R$ ligands of ligand binding to D_2R

Using radioligand binding and mitogen-activated protein kinase (MAPK) signalling assays, we showed that any orthosteric $A_{2A}R$ ligand (either agonists or antagonists) can

Table 1 | Effect of modulators/ligands on dissociation kinetic parameters of A_{2A}R and D₂R radiolabelled antagonists

Dissociation kinetic assays were performed at 12 °C on sheep striatum membranes with the corresponding radioligand (1.5 nM [³H]ZM 241385 or 0.4 nM [³H]YM-09151-2) in the absence or presence of either ligand receptor (10 nM SCH 58260, 30 μM caffeine, 10 nM CGS 21680, 10 nM raclopride or 100 nM quinpirole). Dissociation was initiated by the addition of an excess of the corresponding unlabelled radioligand. *K*_{off} values are means ± S.E.M. from three experiments. [³H]ZM 241385 dissociation data are adapted from [21]: Bonaventura, J., Navarro, G., Casadó-Anguera, V., Azdad, K., Rea, W., Moreno, E., Brugarolas, M., Mallol, J., Canela, E.I., Lluís, C. et al. (2015) Allosteric interactions between agonists and antagonists within the mechanism adenosine A_{2A}-dopamine D₂ receptor heterotetramer. *Proc. Natl. Acad. Sci. U.S.A.* **11**, E3609–E3618 and [³H]YM-09151-2 results are unpublished data.

Receptor	Radioligand	Modulator	<i>K</i> _{off1} (min ⁻¹)	<i>K</i> _{off2} (min ⁻¹)	RT ₁ (min)	RT ₂ (min)
A _{2A}	[³ H]ZM 241385	–	0.025 ± 0.002	–	40	–
		SCH 58261	0.025 ± 0.003	–	40	–
		Caffeine	0.028 ± 0.004	–	36	–
		CGS 21680	0.19 ± 0.03	0.004 ± 0.004	5	250
D ₂	[³ H]YM-09151-2	–	0.031 ± 0.008	0.0029 ± 0.0004	32	354
		Raclopride	0.035 ± 0.008	0.0027 ± 0.0004	29	370
		Quinpirole	0.014 ± 0.003	0.0002 ± 0.0001	71	5000

produce a negative cross-talk on D₂R, decreasing its affinity for both agonists and antagonists and the intrinsic efficacy of agonists [21]. However, when administering A_{2A}R agonists and antagonists together they can counteract each other's negative cross-talk on D₂R, an effect only explainable by the presence of an A_{2A}R homodimer with two orthosteric-binding sites, in accordance with the above discussed dissociation experiments. These conclusions were deduced by measuring the [³H]quinpirole binding in membrane preparations from sheep striatum in the presence of the A_{2A}R agonist CGS 21680 and increasing concentrations of several A_{2A}R antagonists. The antagonists induced a biphasic effect on the ability of CGS 21680 to decrease [³H]quinpirole binding to D₂R. Moderate concentrations of the antagonists counteracted the effect of CGS 21680, whereas high concentrations were associated with a significant decrease in [³H]quinpirole binding, like that caused by the agonist CGS 21680 [21]. The conclusions derived from binding experiments correlate with MAPK signalling assays. In HEK293 cells transfected with A_{2A}R and D₂R, both quinpirole acting through D₂R and CGS 21680 binding to A_{2A}R produced an increase in ERK1/2 phosphorylation. The effect of quinpirole was partially counteracted by CGS 21680 to the phosphorylation levels induced by CGS 21680 alone, indicating the ability of CGS 21680 to decrease not only the affinity of quinpirole for D₂R, but also its intrinsic efficacy. Moderate concentrations of different A_{2A}R antagonists counteracted the effects of CGS 21680. However, this effect disappeared with larger concentrations, where the antagonists by themselves antagonized the effect of both CGS 21680 and quinpirole [21], in the latter case by a phenomenon of cross-antagonism also reported for other receptor heteromers [11].

Since under physiological conditions there is a tone of adenosine, this could in fact be the main mechanism by which caffeine and other A_{2A}R antagonists can promote D₂R-induced locomotor activity. It is the double occupancy of the homodimer by an agonist and an antagonist that disrupts

the negative allosteric modulation. These results imply a different conformation of the receptor homodimers when occupied simultaneously by an agonist and an antagonist compared with when occupied by two antagonists [15,21]. This different conformation could explain the differential ability of the A_{2A}R homodimer to allosterically modulate D₂R agonist binding and intrinsic efficacy within the A_{2A}R–D₂R heteromer [21].

Confirmation of A_{2A}R–D₂R heterotetramer expression *in vitro*

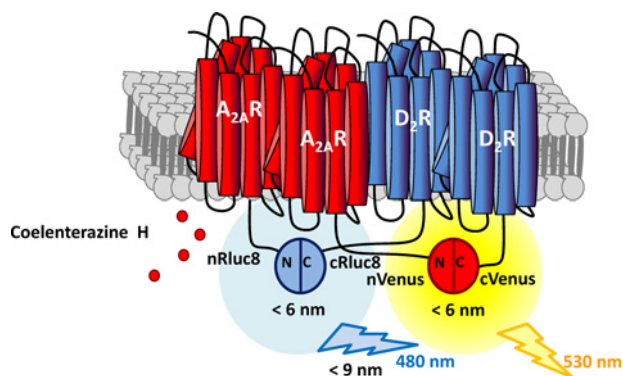
We have recently demonstrated the heterotetrameric structure of the D₁R–D₃R heteromer [11] by combining bimolecular fluorescence/luminescence complementation (BiFC/BiLC) with bioluminescence resonance energy transfer (BRET) [45,46], and complemented donor-acceptor resonance energy transfer (CODA-RET) assays [47]. These studies demonstrated, for the first time, that GPCR heteromers can be arranged as heterotetramers. To assess whether the A_{2A}R–D₂R complex could also be assembled as a heterotetramer constituted by two receptor homodimers, we also used BiFC and BiLC assays in HEK293 cells (see Figure 1) [21]. For this purpose, A_{2A}R was fused to the N-terminal portion of the hemitruncated protein *Renilla* luciferase (Rluc) (A_{2A}R–nRluc) and D₂R to the C-terminal (D₂R–cRluc), which only upon co-expression and complementation can act as a BRET donor. The BRET acceptor protein was obtained upon complementation of the A_{2A}R fused to the N-terminal portion of the YFP Venus (A_{2A}R–nYFP) and the D₂R fused to the C-terminal (D₂R–cYFP). When all four receptor constructs were transfected into the cell, we obtained a positive and saturable BRET signal [21].

Clues to the interfaces involved in the A_{2A}R–D₂R heterotetramer

It has been suggested that, in addition to intracellular domains [24,48], interactions between specific TMs are also involved

Figure 1 | Schematic representation of the tetrameric structure of A_{2A}R–D₂R heteromer detected by BRET using BiFC/BiLC

BRET was measured in HEK cells expressing A_{2A}R–nRluc, D₂R–cRluc, A_{2A}R–nVenus and D₂R–cVenus. Coelenterazine H is the substrate of Rluc.



in GPCR oligomerization [11,49–51]. BiFC assays can be used to evaluate the ability of peptides with the amino acid sequence of TMs to destabilize receptor heteromers. This technique is useful for determining which TMs are involved in the heterotetrameric interfaces. Recently, we successfully used this method to demonstrate the involvement of specific TM domains in the heteromerization of A_{2A}R and D₂R [21], D₁R and D₃R [11], corticotropin-releasing factor CRF₁ (CRF₁R) and orexin OX₁ receptors (OX₁R) [51] and serotonin 5-HT_{2A} (5-HT_{2A}R) and cannabinoid CB₁ receptors (CB₁R) [52]. In these studies, TMs of the receptors were fused to the HIV transactivator of transcription (TAT) peptide, allowing their effective insertion and orientation in the plasma membrane due to its capacity to penetrate it [11,21,51,53]. Specifically, we showed that TM5 and TM6 of D₁R are implicated in the heteromerization of D₁R and D₃R [11]. Likewise, TM5 and TM6 of CB₁R were found to be involved in the 5-HT_{2A}R–CB₁R heteromer interface [52]. However, TM5 and TM1 of OX₁R were involved in the CRF₁R–OX₁R heteromer interface [51]. In all cases, the

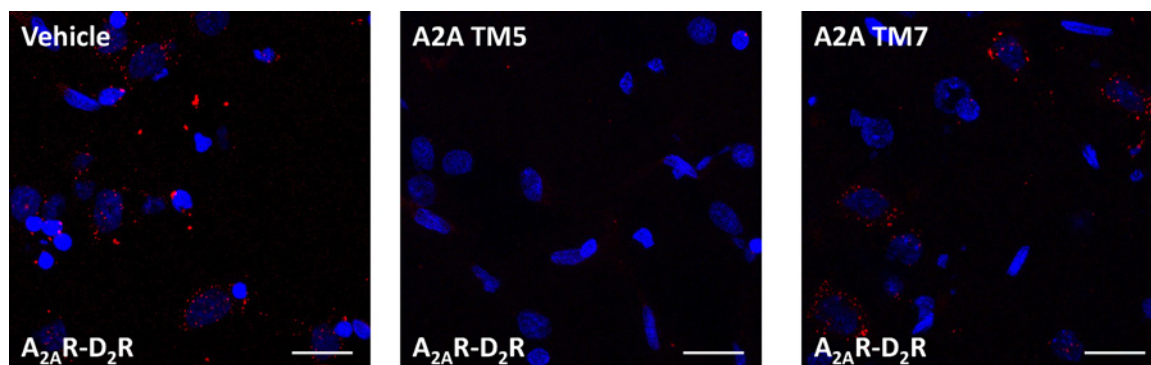
TM7 peptide of the corresponding receptors did not affect the BiFC of the heteromers. In the particular case of the A_{2A}R–D₂R heteromer, disrupting peptides with the sequence of TM5 of both A_{2A}R and D₂R, but none of the TM7 peptides, reduced BiFC in cells expressing A_{2A}R–nYFP and D₂R–cYFP, suggesting that TM5 but not TM7 of both receptors is present at the heteromer interface [21]. Neither TM5 nor TM7 were able to decrease BiFC in cells expressing reconstituted YFP fused to A_{2A}R–A_{2A}R or to D₂R–D₂R [21]. These data support the selective involvement of TM5 at the heteromer interface and show that TM5 and TM7 are not involved at the homodimer interface.

Confirmation of A_{2A}R–D₂R heterotetramer expression *ex vivo*

The proximity ligation assay (PLA) allows the detection of molecular interactions between two endogenous proteins *ex vivo*, and is similar to immunoprecipitation, but with the additional advantage of not requiring membrane solubilization. PLA requires that both receptors be sufficiently close to allow the two antibody–DNA probes to form double-stranded segments (<16 nm) [25], a signal that is further amplified in the presence of fluorescent nucleotides. By PLA, the heteromerization of 5-HT_{2A}R and CB₁R was detected in HEK cells and, *in situ*, in mouse brain slices untreated or treated with the TM7 peptide of CB₁R, but not in samples treated with the TM5 or TM6 peptides of this receptor [52]. We also used this technique to test the endogenous A_{2A}R–D₂R heteromer expression in sheep striatal slices [21]. A_{2A}R–D₂R heteromers were seen as red dots in slices treated with vehicle or with TM7 peptides but not in slices treated with TM5 peptides from both A_{2A}R and D₂R (Figure 2). From these experiments we concluded that these heteromers exist in sheep striatum and that the interfaces of the heteromer detected in transfected cells are the same that occur *ex vivo* in the striatum. Moreover, TM5 peptides from both A_{2A}R and D₂R but not TM7 peptides also counteracted the

Figure 2 | Detection of A_{2A}R–D₂R heteromers in sheep striatum slices and effect of 4 μM TM5 and TM7 A_{2A}R peptides

Representative confocal microscopy images from each experimental condition are shown. Heteromers appear as red dots and cell nuclei stained with DAPI in blue. See [21] for details. Scale bars: 20 μm.



caffeine-mediated decrease in [3 H]raclopride binding to D₂R in sheep striatal membrane preparations [21].

By PLA experiments, Trifilieff et al. [25] confirmed the existence of A_{2A}R–D₂R complexes in striatal brain slices of wild-type mice *ex vivo*, showing a positive PLA signal that was significantly reduced in both D₂R and A_{2A}R KO mice slices. Furthermore, using the same technique we detected the presence of A_{2A}R–D₂R oligomers in monkey striatum [54] and in rat striatum via radioligand-binding experiments [55]. Significantly, these studies indicated that A_{2A}R–D₂R heteromer formation might be disrupted in L-DOPA-induced dyskinetic animals [54,55]. Recently, Fernández-Dueñas et al. [26] identified by PLA native A_{2A}R–D₂R heteromers in the striatum of healthy rats which also decreased in the striatum of parkinsonian rats.

Conclusions

The above-mentioned evidence demonstrates that A_{2A}R–D₂R heteromer is constituted by A_{2A}R and D₂R homodimers assembled in a heterotetramer. From the reported data, we can hypothesize that any orthosteric A_{2A}R ligand (agonist or antagonist) can decrease (negative cross-talk) the affinity and intrinsic efficacy of any D₂R ligand (agonist or antagonist). Furthermore, when administering both A_{2A}R agonists and antagonists they counteract each other's effects, a fact only explainable by the heterotetrameric model.

Since under physiological conditions there is a tone of adenosine, this could explain why A_{2A}R antagonists can produce locomotor activation (a simultaneous occupation of the A_{2A}R dimer by an antagonist and the endogenous adenosine). When adding larger concentrations of potent and selective A_{2A}R antagonists, they might generate the same effects as agonists, causing problems in the treatment of Parkinson's patients. However, the A_{2A}R–D₂R heterotetramer model still provides support for the therapeutic use of A_{2A}R antagonists in Parkinson's disease, providing new clues as to how to adjust the dosage according to the expected levels of endogenous adenosine.

Funding

This study was supported by the Government of Catalonia [grant number 2014-SGR-1236]; the Centro de Investigación Biomédica en Red sobre Enfermedades Neurodegenerativas [grant number CB06/05/0064]; the Spanish Ministerio de Economía y Competitividad [grant number SAF2014-54840-R]; and by intramural funds of the National Institute on Drug Abuse.

References

- Whorton, M.R., Bokoch, M.P., Rasmussen, S.G., Huang, B., Zare, R.N., Kobilka, B. and Sunahara, R.K. (2007) A monomeric G protein-coupled receptor isolated in a high-density lipoprotein particle efficiently activates its G protein. *Proc. Natl. Acad. Sci. U.S.A.* **104**, 7682–7687 [CrossRef PubMed](#)
- Chabre, M., Deterre, P. and Antony, B. (2009) The apparent cooperativity of some GPCRs does not necessarily imply dimerization. *Trends Pharmacol. Sci.* **30**, 182–187 [CrossRef PubMed](#)
- Casadó, V., Cortés, A., Mallol, J., Perez-Capote, K., Ferré, S., Lluís, C., Franco, R. and Canela, E.I. (2009) GPCR homomers and heteromers: a better choice as targets for drug development than GPCR monomers? *Pharmacol. Ther.* **124**, 248–257 [CrossRef PubMed](#)
- Milligan, G. (2009) G protein-coupled receptor hetero-dimerization: contribution to pharmacology and function. *Br. J. Pharmacol.* **158**, 5–14 [CrossRef PubMed](#)
- Ferré, S., Navarro, G., Casadó, V., Cortés, A., Mallol, J., Canela, E.I., Lluís, C. and Franco, R. (2010) G-protein coupled receptor heteromers as new targets for drug development. *Prog. Mol. Biol. Transl. Sci.* **91**, 41–52 [CrossRef PubMed](#)
- Ferré, S., Casadó, V., Devi, L.A., Filizola, M., Jockers, R., Lohse, M.J., Milligan, G., Pin, J.P. and Guitart, X. (2014) G protein-coupled receptor oligomerization revisited: functional and pharmacological perspectives. *Pharmacol. Rev.* **66**, 413–434 [CrossRef PubMed](#)
- Ciruela, F., Fernandez-Dueñas, V., Llorente, J., Borroto-Escuela, D., Cuffi, M.L., Carbonell, L., Sanchez, S., Agnati, L.F., Fuxe, K. and Tasca, C.I. (2012) G protein-coupled receptor oligomerization and brain integration: focus on adenosinergic transmission. *Brain Res.* **1476**, 86–95 [CrossRef PubMed](#)
- Miller, L.J., Dong, M. and Harikumar, K.G. (2012) Ligand binding and activation of the secretin receptor, a prototypic family B G protein-coupled receptor. *Br. J. Pharmacol.* **166**, 18–26 [CrossRef PubMed](#)
- Steel, E., Murray, V.L. and Liu, A.P. (2014) Multiplex detection by homo- and heterodimerization of g protein-coupled receptors by proximity biotinylation. *PLoS One* **9**, e93646 [CrossRef PubMed](#)
- Ferré, S., Baler, R., Bouvier, M., Caron, M.G., Devi, L.A., Durroux, T., Fuxe, K., George, S.R., Javitch, J.A., Lohse, M.J. et al. (2009) Building a new conceptual framework for receptor heteromers. *Nat. Chem. Biol.* **5**, 131–134 [CrossRef PubMed](#)
- Guitart, X., Navarro, G., Moreno, E., Yano, H., Cai, N.S., Sánchez-Soto, M., Kumar-Barodia, S., Naidu, Y.T., Mallol, J., Cortés, A. et al. (2014) Functional selectivity of allosteric interactions within GPCR oligomers: the dopamine D1–D3 receptor heterotetramer. *Mol. Pharmacol.* **86**, 417–429 [CrossRef PubMed](#)
- Cristóvão-Ferreira, S., Navarro, G., Brugarolas, M., Pérez-Capote, K., Vaz, S.H., Fattorini, G., Conti, F., Lluís, C., Ribeiro, J.A., McCormick, P.J. et al. (2013) A1R–A2AR heteromers coupled to Gs and Gi/o proteins modulate GABA transport into astrocytes. *Purinergic Signal.* **9**, 433–449 [CrossRef PubMed](#)
- Smith, N.J. and Milligan, G. (2010) Allosteric at G protein-coupled receptor homo- and heteromers: uncharted pharmacological landscapes. *Pharmacol. Rev.* **62**, 701–725 [CrossRef PubMed](#)
- Casadó, V., Ferrada, C., Bonaventura, J., Gracia, E., Mallol, J., Canela, E.I., Lluís, C., Cortés, A. and Franco, R. (2009) Useful pharmacological parameters for G-protein-coupled receptor homodimers obtained from competition experiments. Agonist-antagonist binding modulation. *Biochem. Pharmacol.* **78**, 1456–1463 [CrossRef PubMed](#)
- Ferré, S., Bonaventura, J., Tomasi, D., Navarro, G., Moreno, E., Cortés, A., Lluís, C., Casadó, V. and Volkow, N.D. (2015) Allosteric mechanisms within the adenosine A2A-dopamine D2 receptor heterotetramer. *Neuropharmacology* **4**, [CrossRef](#)
- Kenakin, T. and Miller, L.J. (2010) Seven transmembrane receptors as shapeshifting proteins: the impact of allosteric modulation and functional selectivity on new drug discovery. *Pharmacol. Rev.* **62**, 265–304 [CrossRef PubMed](#)
- Ferré, S., von Euler, G., Johansson, B., Fredholm, B.B. and Fuxe, K. (1991) Stimulation of high-affinity adenosine A2 receptors decreases the affinity of dopamine D2 receptors in rat striatal membranes. *Proc. Natl. Acad. Sci. U.S.A.* **88**, 7238–7241 [CrossRef PubMed](#)
- Dasgupta, S., Ferré, S., Kull, B., Hedlund, P.B., Finnman, U.B., Ahlberg, S., Arenas, E., Fredholm, B.B. and Fuxe, K. (1996) Adenosine A2A receptors modulate the binding characteristics of dopamine D2 receptors in stably cotransfected fibroblast cells. *Eur. J. Pharmacol.* **316**, 325–331 [CrossRef PubMed](#)
- Diaz-Cabiale, Z., Vivo, M., Del Arco, A., O'Connor, W.T., Harte, M.K., Muller, C.E., Martinez, E., Popoli, P., Fuxe, K. and Ferré, S. (2001) Metabotropic glutamate mGlu5 receptor-mediated modulation of the ventral striatopallidal GABA pathway in rats: interaction with adenosine A2A and dopamine D2 receptors. *Neurosci. Lett.* **324**, 154–158 [CrossRef](#)
- Kudlacek, O., Just, H., Korkhov, V.M., Vartian, N., Klinger, M., Pankevych, H., Yang, Q., Nanoff, C., Freissmuth, M. and Boehm, S. (2003) The human D2 dopamine receptor synergizes with the A2A adenosine receptor to stimulate adenylyl cyclase in PC12 cells. *Neuropsychopharmacology* **28**, 1317–1327 [CrossRef PubMed](#)

- 21 Bonaventura, J., Navarro, G., Casadó-Anguera, V., Azdad, K., Rea, W., Moreno, E., Brugarolas, M., Mallol, J., Canela, E.I., Lluís, C. et al. (2015) Allosteric interactions between agonists and antagonists within the mechanism adenosine A2A-dopamine D2 receptor heterotetramer. *Proc. Natl. Acad. Sci. U.S.A.* **11**, E3609–E3618 [CrossRef](#)
- 22 Hillion, J., Canals, M., Torvinen, M., Casadó, V., Scott, R., Terasmaa, A., Hansson, A., Watson, S., Olah, M.E., Mallol, J. et al. (2002) Coaggregation, cointernalization, and codesensitization of adenosine A2A receptors and dopamine D2 receptors. *J. Biol. Chem.* **277**, 18091–18097 [CrossRef](#) [PubMed](#)
- 23 Canals, M., Marcellino, D., Fanelli, F., Ciruela, F., de Benedetti, P., Goldberg, S.R., Neve, K., Fuxe, K., Agnati, L.F., Woods, A.S. et al. (2003) Adenosine A2A-dopamine D2 receptor-receptor heteromerization: qualitative and quantitative assessment by fluorescence and bioluminescence energy transfer. *J. Biol. Chem.* **278**, 46741–46749 [CrossRef](#) [PubMed](#)
- 24 Azdad, K., Gall, D., Woods, A.S., Ledent, C., Ferré, S. and Schiffmann, S.N. (2009) Dopamine D2 and adenosine A2A receptors regulate NMDA-mediated excitation in accumbens neurons through A2A-D2 receptor heteromerization. *Neuropsychopharmacology* **34**, 972–986 [CrossRef](#) [PubMed](#)
- 25 Trifilieff, P., Rives, M.L., Urizar, E., Piskrowski, R.A., Vishwasrao, H.D., Castrillon, J., Schmauss, C., Slätman, M., Gullberg, M and Javitch, J.A. (2011) Detection of antigen interactions *ex vivo* by proximity ligation assay: endogenous dopamine D2-adenosine A2A receptor complexes in the striatum. *Biotechniques* **51**, 111–118 [PubMed](#)
- 26 Fernández-Dueñas, V., Taura, J.J., Cottet, M., Gómez-Soler, M., López-Cano, M., Ledent, C., Watanabe, M., Trinquet, E., Pin, J.P., Luján, R. et al. (2015) Untangling dopamine-adenosine receptor-receptor assembly in experimental parkinsonism in rats. *Dis. Model Mech.* **8**, 57–63 [CrossRef](#) [PubMed](#)
- 27 Ferré, S., Agnati, L.F., Ciruela, F., Lluís, C., Woods, A.S., Fuxe, K. and Franco, R. (2007) Neurotransmitter receptor heteromers and their integrative role in “local modules”: the striatal spine module. *Brain Res. Rev.* **55**, 55–67 [CrossRef](#) [PubMed](#)
- 28 Ferré, S. (2008) An update on the mechanisms of the psychostimulant effects of caffeine. *J. Neurochem.* **105**, 1067–1079 [CrossRef](#) [PubMed](#)
- 29 Ferré, S., Ciruela, F., Canals, M., Marcellino, D., Burgueño, J., Casadó, V., Hillion, J., Torvinen, M., Fanelli, F., de Benedetti, P. et al. (2004) Adenosine A2A-dopamine D2 receptor-receptor heteromers. Targets for neuro-psychiatric disorders. *Parkinsonism Relat. Disord.* **10**, 265–271 [CrossRef](#) [PubMed](#)
- 30 Müller, C.E. and Ferré, S. (2007) Blocking striatal adenosine A2A receptors: a new strategy for basal ganglia disorders. *Recent Pat. CNS Drug Discov.* **2**, 1–21 [PubMed](#)
- 31 Armentero, M.T., Pinna, A., Ferré, S., Lanciego, J.L., Muller, C.E. and Franco, R. (2011) Past, present and future of A(2A) adenosine receptor antagonists in the therapy of Parkinson's disease. *Pharmacol. Ther.* **132**, 280–299 [CrossRef](#) [PubMed](#)
- 32 Orrú, M., Bakesová, J., Brugarolas, M., Quiroz, C., Beaumont, V., Goldberg, S.R., Lluís, C., Cortés, A., Franco, R., Casadó, V. et al. (2011) Striatal pre- and postsynaptic profile of adenosine A(2A) receptor antagonists. *PLoS One* **6**, e16088 [CrossRef](#) [PubMed](#)
- 33 Jenner, P. (2014) An overview of adenosine A2A receptor antagonists in Parkinson's disease. *Int. Rev. Neurobiol.* **119**, 71–86 [CrossRef](#) [PubMed](#)
- 34 Uchida, S., Soshiroda, K., Okita, E., Kawai-Uchida, M., Mori, A., Jenner, P. and Kanda, T. (2015) The adenosine A2A receptor antagonist, istradefylline enhances anti-parkinsonian activity induced by combined treatment with low doses of L-DOPA and dopamine agonists in MPTP-treated common marmosets. *Eur. J. Pharmacol.* **766**, 25–30 [CrossRef](#) [PubMed](#)
- 35 Pinna, A. (2014) Adenosine A2A receptor antagonists in Parkinson's disease: progress in clinical trials from the newly approved istradefylline to drugs in early development and those already discontinued. *CNS Drugs* **28**, 455–474 [CrossRef](#) [PubMed](#)
- 36 May, L.T., Leach, K., Sexton, P.M. and Christopoulos, A. (2007) Allosteric modulation of G protein-coupled receptors. *Annu. Rev. Pharmacol. Toxicol.* **47**, 1–51 [CrossRef](#) [PubMed](#)
- 37 Soriano, A., Vendrell, M., González, S., Mallol, J., Albericio, F., Royo, M., Lluís, C., Canela, E.I., Franco, R., Cortés, A. and Casadó, V. (2010) A hybrid indoloquinolizidine peptide as allosteric modulator of dopamine D₁ receptors. *J. Pharmacol. Exp. Ther.* **332**, 876–885 [CrossRef](#) [PubMed](#)
- 38 Bennett, K.A., Tehan, B., Lebon, G., Tate, C.G., Weir, M., Marshall, F.H. and Langmead, C.J. (2013) Pharmacology and structure of isolated conformations of the adenosine A_{2A} receptor define ligand efficacy. *Mol. Pharmacol.* **83**, 949–958 [CrossRef](#) [PubMed](#)
- 39 Doré, A.S., Robertson, N., Errey, J.C., Ng, I., Hollenstein, K., Tehan, B., Hurrell, E., Bennett, K., Congreve, M., Magnani, F. et al. (2011) Structure of the adenosine A(2A) receptor in complex with ZM241385 and the xanthines XAC and caffeine. *Structure* **19**, 1283–1293 [CrossRef](#) [PubMed](#)
- 40 Lebon, G., Warne, T., Edwards, P.C., Bennett, K., Langmead, C.J., Leslie, A.G. and Tate, C.G. (2011) Agonist-bound adenosine A2A receptor structures reveal common features of GPCR activation. *Nature* **474**, 521–525 [CrossRef](#) [PubMed](#)
- 41 Lebon, G., Edwards, P.C., Leslie, A.G. and Tate, C.G. (2015) Molecular determinants of CGS21680 binding to the human adenosine A2A receptor. *Mol. Pharmacol.* **87**, 907–915 [CrossRef](#) [PubMed](#)
- 42 Tummino, P.J. and Copeland, R.A. (2008) Residence time of receptor–ligand complexes and its effect on biological function. *Biochemistry* **47**, 5481–5492 [CrossRef](#) [PubMed](#)
- 43 Zhang, R. and Monsma, F. (2009) The importance of drug-target residence time. *Curr. Opin. Drug Discov. Dev.* **12**, 488–496
- 44 Guo, D., Hillger, J.M., Ilzerman, A.P. and Heitman, L.H. (2014) Drug-target residence time – a case for G protein-coupled receptors. *Med. Res. Rev.* **34**, 856–892 [CrossRef](#) [PubMed](#)
- 45 Kerppola, T.K. (2006) Design and implementation of bimolecular fluorescence complementation (BiFC) assays for the visualization of protein interactions in living cells. *Nat. Protoc.* **1**, 1278–1286 [CrossRef](#) [PubMed](#)
- 46 Vidi, P.A. and Watts, V.J. (2009) Fluorescent and bioluminescent protein-fragment complementation assays in the study of G protein-coupled receptor oligomerization and signaling. *Mol. Pharmacol.* **75**, 733–739 [CrossRef](#) [PubMed](#)
- 47 Urizar, E., Yano, H., Kolster, R., Galés, C., Lambert, N. and Javitch, J.A. (2011) CODA-RET reveals functional selectivity as a result of GPCR heteromerization. *Nat. Chem. Biol.* **7**, 624–630 [CrossRef](#) [PubMed](#)
- 48 Banères, J.L. and Parello, J. (2003) Structure-based analysis of GPCR function: evidence for a novel pentameric assembly between the dimeric leukotriene B4 receptor BLT1 and the G-protein. *J. Mol. Biol.* **329**, 815–829 [CrossRef](#) [PubMed](#)
- 49 Hebert, T.E., Moffett, S., Morello, J.P., Loisel, T.P., Bichet, D.G., Barret, C. and Bouvier, M. (1996) A peptide derived from a beta2-adrenergic receptor transmembrane domain inhibits both receptor dimerization and activation. *J. Biol. Chem.* **271**, 16384–16392 [CrossRef](#) [PubMed](#)
- 50 Borroto-Escuela, D.O., Romero-Fernandez, W., Tarakanov, A.O., Gómez-Soler, M., Corrales, F., Marcellino, D., Narvaez, M., Frankowska, M., Flajolet, M., Heintz, N. et al. (2010) Characterization of the A2AR-D2R interface: focus on the role of the C-terminal tail and the transmembrane helices. *Biochem. Biophys. Res. Commun.* **402**, 801–807 [CrossRef](#) [PubMed](#)
- 51 Navarro, G., Quiroz, C., Moreno-Delgado, D., Sierakowiak, A., MacDowell, K., Moreno, E., Aguinaga, D., Rea, W., Cai, N.S., Howell, L.A. et al. (2015) Orexin-corticotropin-releasing factor receptor heteromers in the ventral tegmental area as targets for cocaine. *J. Neurosci.* **35**, 6639–6653 [CrossRef](#) [PubMed](#)
- 52 Viñals, X., Moreno, E., Lanfumey, L., Cordomi, A., Pastor, A., de La Torre, R., Gasperini, P., Navarro, G., Howell, L.A., Pardo, L. et al. (2015) Cognitive impairment induced by delta9-tetrahydrocannabinol occurs through heteromers between cannabinoid CB1 and serotonin 5-HT2A receptors. *PLoS Biol.* **13**, e1002194 [CrossRef](#) [PubMed](#)
- 53 He, S.Q., Zhang, Z.N., Guan, J.S., Liu, H.R., Zhao, B., Wang, H.B., Li, Q., Yang, H., Luo, J., Li, Z.Y. et al. (2011) Facilitation of m-opioid receptor activity by preventing d-opioid receptor-mediated codegradation. *Neuron* **69**, 120–131 [CrossRef](#) [PubMed](#)
- 54 Bonaventura, J., Rico, A.J., Moreno, E., Sierra, S., Sanchez, M., Luquin, N., Farre, D., Muller, C.E., Martinez-Pinilla, E., Cortés, A. et al. (2014) L-DOPA-treatment in primates disrupt the expression of A2A adenosine-CB1 cannabinoid-D2 dopamine receptor heteromers in the caudate nucleus. *Neuropharmacology* **79**, 90–100 [CrossRef](#) [PubMed](#)
- 55 Pinna, A., Bonaventura, J., Farré, D., Sánchez, M., Simola, N., Mallol, J., Lluís, C., Costa, G., Baqi, Y., Müller, C.E. et al. (2014) L-DOPA disrupts adenosine A(2A)-cannabinoid CB(1)-dopamine D(2) receptor heteromer cross-talk in the striatum of hemiparkinsonian rats: biochemical and behavioral studies. *Exp. Neurol.* **253**, 180–191 [CrossRef](#) [PubMed](#)

Received 04 February 2016
doi:10.1042/BST20150276

Chapter 2.3. Functional pre-coupled complexes of receptor heteromers and adenylyl cyclase

Navarro G, Cordoní A, **Casadó-Anguera V**, Moreno E, Cai NS, Cortés A, Canela EI, Dessauer CW, Casadó V, Pardo L, Lluís C, Ferré S.

Nature Communications, 2018, 9:1242.

ARTICLE

DOI: 10.1038/s41467-018-03522-3

OPEN

Evidence for functional pre-coupled complexes of receptor heteromers and adenylyl cyclase

Gemma Navarro^{1,2}, Arnau Corderó³, Verónica Casadó-Anguera², Estefanía Moreno², Ning-Sheng Cai⁴, Antoni Cortés², Enric I. Canela², Carmen W. Dessauer⁵, Vicent Casadó², Leonardo Pardo³, Carme Lluís² & Sergi Ferré⁴

G protein-coupled receptors (GPCRs), G proteins and adenylyl cyclase (AC) comprise one of the most studied transmembrane cell signaling pathways. However, it is unknown whether the ligand-dependent interactions between these signaling molecules are based on random collisions or the rearrangement of pre-coupled elements in a macromolecular complex. Furthermore, it remains controversial whether a GPCR homodimer coupled to a single heterotrimeric G protein constitutes a common functional unit. Using a peptide-based approach, we here report evidence for the existence of functional pre-coupled complexes of heteromers of adenosine A_{2A} receptor and dopamine D₂ receptor homodimers coupled to their cognate G_s and G_i proteins and to subtype 5 AC. We also demonstrate that this macromolecular complex provides the necessary frame for the canonical G_s-G_i interactions at the AC level, sustaining the ability of a G_i-coupled GPCR to counteract AC activation mediated by a G_s-coupled GPCR.

¹Department of Biochemistry and Physiology of the Faculty of Pharmacy of the University of Barcelona, 08028 Barcelona, Spain. ²Department of Biochemistry and Molecular Biomedicine of the Faculty of Biology and Institute of Biomedicine of the University of Barcelona and Center for Biomedical Research in Neurodegenerative Diseases Network, 08028 Barcelona, Spain. ³Laboratory of Computational Medicine, School of Medicine, Autonomous University of Barcelona, 08193 Bellaterra, Spain. ⁴Integrative Neurobiology Section, National Institute on Drug Abuse, National Institutes of Health, Baltimore, MD 21224, USA. ⁵Department of Integrative Biology and Pharmacology, McGovern Medical School, University of Texas Health Science Center, Houston, TX 77030, USA. These authors contributed equally: Gemma Navarro, Arnau Corderó. Correspondence and requests for materials should be addressed to S.Fé. (email: sferre@intra.nida.nih.gov)

Interactions between G protein-coupled receptors (GPCRs), $G\alpha$ and $G\beta\gamma$ protein subunits and adenylyl cyclase (AC) have been classically analyzed in the frame of ‘collision-coupling’ mechanisms, which implies they are freely mobile molecules in the plasma membrane able to couple by random collision. Binding of an agonist to its GPCR induces the binding and subsequent activation of the heterotrimeric G protein, which leads to the dissociation of $G\alpha$ and $G\beta\gamma$ subunits and binding of free $G\alpha$ subunit to AC, leading to its regulation¹. However, accumulating experimental evidence suggests that GPCR activation commonly occurs without dissociation of the receptor from its G protein, without G-protein subunit dissociation and even with pre-coupling of the heterotrimeric G protein to AC (reviewed in ref.²). Moreover, growing evidence suggests that the pentameric complex formed by one GPCR homodimer (two identical protomers) and one heterotrimeric G protein constitutes a common GPCR functional unit^{3–6}. Therefore, classical GPCR physiology needs to be revisited in the frame of pre-coupling mechanisms and GPCR oligomerization.

The topology of mammalian transmembrane AC consists of a variable cytoplasmic N terminus (NT) and two large cytoplasmic domains, C1 and C2, separated by two membrane-spanning domains, M1 and M2, each comprising six putative transmembrane domains (TMs)⁷. C1 and C2 interact to form the enzyme catalytic core at their interface and their arrangement allows, at least in theory, the simultaneous binding of their external sides to $G\alpha$ and $G\beta\gamma$ ⁸, providing the structural framework for the canonical antagonistic interaction between Gs-coupled and Gi-coupled receptors at the AC level of specific AC isoforms, including AC1, AC5, and AC6^{2,7}. $G\alpha$ subunit binds to C2 and increases the affinity of C1 and C2, promoting catalysis, while $G\beta\gamma$, by binding to C1, works in the opposite direction and counteracts AC activation⁷.

It is becoming accepted that GPCRs can form heteromers^{6,9}, defined as macromolecular complexes composed of at least two different protomers with biochemical properties that are demonstrably different from those of its individual components⁶. Considering homodimers as main functional GPCR units, heteromers could be viewed as constituted by different interacting homodimers⁶. Of special functional significance could be those heteromers constituted by one homodimer coupled to a Gs/olf (Gs for short) protein and another different homodimer coupled to a Gi/o (Gi for short) protein. Our hypothesis is that such a ‘GPCR heterotetramer’ would be part of a pre-coupled macromolecular complex that also includes AC, a necessary frame for the canonical antagonistic interaction at the AC level. Recent studies have provided experimental evidence for the existence of GPCR heterotetramers that fulfill this scheme, like the adenosine A_{2A} -dopamine D_2 receptor ($A_{2A}R$ - D_2R) heterotetramer¹⁰. In the present study, using interfering peptides with amino acid sequences of TMs of adenosine $A_{2A}R$ and D_2R and putative TMs of AC5, we provide evidence for the existence of functional pre-coupled complexes of $A_{2A}R$ and D_2R homodimers, their cognate Gs and Gi proteins and AC5, and demonstrate that this macromolecular complex provides the sufficient but necessary condition for the canonical Gs–Gi interactions at the AC level.

Results

Symmetrical TM interfaces in the $A_{2A}R$ - D_2R heterotetramer.

To identify the arrangement of $A_{2A}R$ and D_2R protomers in the heterotetramer (TMs involved in the homo and heterodimerization interfaces), we used synthetic peptides with the amino acid sequence of TMs 1–7 of $A_{2A}R$ and D_2R (TMs and TM peptides are abbreviated TM 1, TM 2, ... and TM1, TM2, ... respectively) fused to the HIV transactivator of transcription (TAT) peptide,

which determines the orientation of the peptide when inserted in the plasma membrane (see ref.¹¹ and Methods section). Peptides were first tested in bimolecular fluorescence complementation (BiFC) experiments, in HEK-293T cells expressing receptors fused to two complementary halves of YFP (Venus variant; cYFP and nYFP). Functionality of all fused receptors was shown with cAMP accumulation experiments (Supplementary Fig. 1). Fluorescence was detected when cells were transfected with $A_{2A}R$ -nYFP and $A_{2A}R$ -cYFP cDNA (broken lines in Fig. 1a) or with D_2R -nYFP and D_2R -cYFP cDNA (broken lines in Fig. 1b), indicating the formation of both $A_{2A}R$ - $A_{2A}R$ and D_2R - D_2R homodimers. Notably, when BiFC assay was performed in the presence of TM peptides (Fig. 1a, b), fluorescence complementation of $A_{2A}R$ -nYFP and $A_{2A}R$ -cYFP was only significantly reduced in the presence of TM6 of $A_{2A}R$ (Fig. 1a; see Methods and Supplementary Fig. 2 for justification of the optimal concentration and time of incubation of the TM peptides). Similarly, only TM6 of D_2R reduced fluorescence complementation of D_2R -nYFP and D_2R -cYFP (Fig. 1b). These results indicate that TM 6 forms part of a symmetric interface for both $A_{2A}R$ and D_2R homodimers when expressed alone. The same results were obtained in cells expressing $A_{2A}R$ -nYFP and $A_{2A}R$ -cYFP co-transfected with non-fused D_2R cDNA (Fig. 1a) or in cells expressing D_2R -nYFP and D_2R -cYFP co-transfected with non-fused $A_{2A}R$ cDNA (Fig. 1b). These results therefore indicate that TM 6 also forms part of a symmetric interface for both $A_{2A}R$ and D_2R homodimers in the heterotetramer. Fluorescence was also detected in cells expressing $A_{2A}R$ -nYFP and D_2R -cYFP (broken lines in Fig. 1c), indicating the formation of $A_{2A}R$ - D_2R heteromers. This fluorescence was only significantly reduced in the presence of TM4 and TM5 of both $A_{2A}R$ and D_2R (Fig. 1c), suggesting a TMs 4/5 interface for $A_{2A}R$ and D_2R heterodimer in the heterotetramer. Additional evidence of heteromer formation via TMs 4/5 was obtained from proximity ligation assay (PLA). This technique permits the direct detection of molecular interactions between two proteins without the need of fusion proteins. $A_{2A}R$ - D_2R heteromers were observed as red punctate staining in HEK-293T cells expressing both $A_{2A}R$ and D_2R (Supplementary Fig. 3a–c). Pretreatment of cells with TM4 and TM5 of $A_{2A}R$ and D_2R but not with TM6 or TM7 (negative control), significantly decreased PLA staining (Supplementary Fig. 3d), decreasing the number of stained cells and red spots per stained cell (Fig. 2a), supporting TMs 4/5 as the interface of the $A_{2A}R$ - D_2R heteromer.

In HEK-293T cells expressing both receptors, the $A_{2A}R$ agonist CGS21680 (100 nM; minimal concentration with maximal effect) significantly increased basal cAMP and the D_2R agonist quinpirole (1 μ M; minimal concentration with maximal effect) decreased forskolin-induced cAMP (Fig. 2b). Pertussis toxin, by catalyzing ADP-ribosylation of the alpha-subunit of Gi, impeded D_2R -mediated Gi activation and thus the ability of quinpirole to inhibit forskolin-induced cAMP accumulation (Fig. 2b). Cholera toxin, by selectively catalyzing ADP-ribosylation of the alpha-subunit of Gs and leading to persistent AC stimulation, impeded an additional effect of CGS21680 but left unaltered the Gi-mediated quinpirole-induced inhibition of forskolin-induced cAMP accumulation (Fig. 2b). These results support the coupling of $A_{2A}R$ and D_2R to their respective cognate Gs and Gi proteins in the $A_{2A}R$ - D_2R heterotetramer. We could then demonstrate that neither $A_{2A}R$ or D_2R activation leads to rearrangements of the TM interfaces in the $A_{2A}R$ - D_2R heterotetramer, since, in the presence of CGS21680 (100 nM) or quinpirole (1 μ M), fluorescence in cells expressing $A_{2A}R$ -nYFP and D_2R -cYFP was still selectively reduced by TM4 and TM5 of $A_{2A}R$ and D_2R (Fig. 1c). Similarly, $A_{2A}R$ activation by CGS21680 (Fig. 1a) or D_2R activation by quinpirole (Fig. 1b) did not modify the corresponding specific homomer TM 6 interface determined in ligand-free experiments.

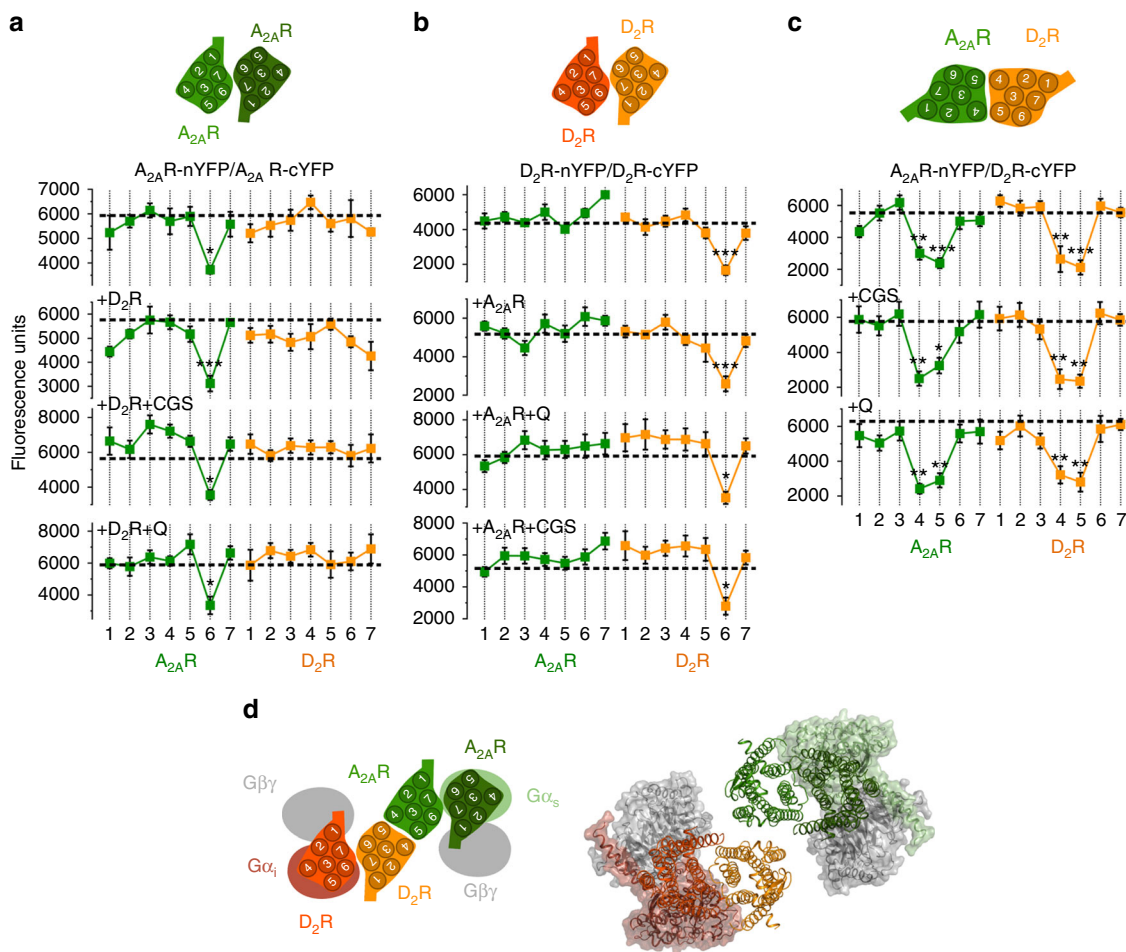


Fig. 1 Quaternary structure of $A_{2A}R$ - D_2R heterotetramer coupled to Gs and Gi proteins. **a-c** BiFC experiments in HEK-293T cells transfected with $A_{2A}R$ -nYFP (0.5 μ g) and $A_{2A}R$ -cYFP (0.5 μ g) cDNA in the absence or presence of D_2R cDNA (0.5 μ g) (**a**), with D_2R -nYFP (0.75 μ g) and D_2R -cYFP (0.75 μ g) cDNA in the absence or the presence of $A_{2A}R$ cDNA (0.4 μ g) (**b**) or with $A_{2A}R$ -nYFP (0.6 μ g) and D_2R -cYFP (0.6 μ g) cDNA (**c**); cells were treated for 4 h with medium (broken lines) or 4 μ M of indicated TM peptides (numbered 1-7) of $A_{2A}R$ (green squares) or D_2R (orange squares) before addition of medium, CGS21680 (CGS; 100 nM) or quinpirole (Q; 1 μ M); fluorescence was detected at 530 nm and values (in means \pm SEM) are expressed as fluorescence arbitrary units ($n = 8$, with triplicates); *, **, and *** represent significantly lower values as compared to control values ($p < 0.05$, $p < 0.01$ and $p < 0.001$, respectively; one-way ANOVA followed by Dunnett's multiple comparison tests). **d** Computational model of the $A_{2A}R$ - D_2R heterotetramer built using the experimental interfaces predicted in panels (**a-c**) (TMs 4/5 for heterodimerization and TM 6 for homodimerization) with Gs and Gi binding to the external protomers; schematic slice-representation (left) and the constructed molecular model (right; with the same color code as the schematic slice-representation), viewed from the extracellular side

We then constructed a molecular model of the $A_{2A}R$ - D_2R heterotetramer (Fig. 1d), considering: (i) the crystal structures of GPCRs and G proteins, as well as homology models (see Methods section); (ii) the structural details of TM interfaces of GPCR oligomers, observed in crystal structures¹² as well as predicted by molecular dynamics simulations (see Methods section); (iii) the results from BiFC experiments with interfering TM peptides; (iv) the general assumption of a common minimal functional unit of GPCRs constituted by a homodimer coupled to its cognate G protein (see Introduction section); (v) the suggested tetrameric structure of the $A_{2A}R$ - D_2R heteromer constituted by two interacting homodimers, from previous results obtained with bioluminescence resonance energy transfer (BRET) experiments with complementation of both the donor and the acceptor biosensors¹⁰; and (vi) the previously enunciated assumption about the necessity of a simultaneous activation of Gs and Gi coupled to the interacting catalytic domains of the same molecule of AC for a canonical antagonistic interaction⁸. This resulted in one minimal computational solution that accommodates the TMs 4/5 interface for $A_{2A}R$ - D_2R heterodimerization and the TM 6

interface for both $A_{2A}R$ - $A_{2A}R$ and D_2R - D_2R homodimerization (see Methods and Supplementary Fig. 4). The existence of these interfaces implies two internal interacting $A_{2A}R$ and D_2R protomers and two external $A_{2A}R$ and D_2R protomers in which the α -subunits of Gi and Gs bind to the corresponding external protomers of the D_2R or $A_{2A}R$ homodimers. This would be the only feasible configuration to avoid any steric clash between the two G proteins simultaneously bound to the complex. Finally, the model also predicts a large distance between both $\beta\gamma$ -subunits (Fig. 1d).

Asymmetrical TM interfaces of the heterotetramer with AC5.

Although several studies have provided direct evidence for pre-coupling between G protein subunits and AC^{7,13-15}, specifically with the AC NT^{7,14}, to our knowledge, the existence of pre-coupling between TMs of a GPCR and TMs of AC had not been previously addressed. We first analyzed the ability of AC5 to establish direct intermolecular interactions with $A_{2A}R$ or D_2R or with $A_{2A}R$ - D_2R heteromers via saturation BRET experiments in

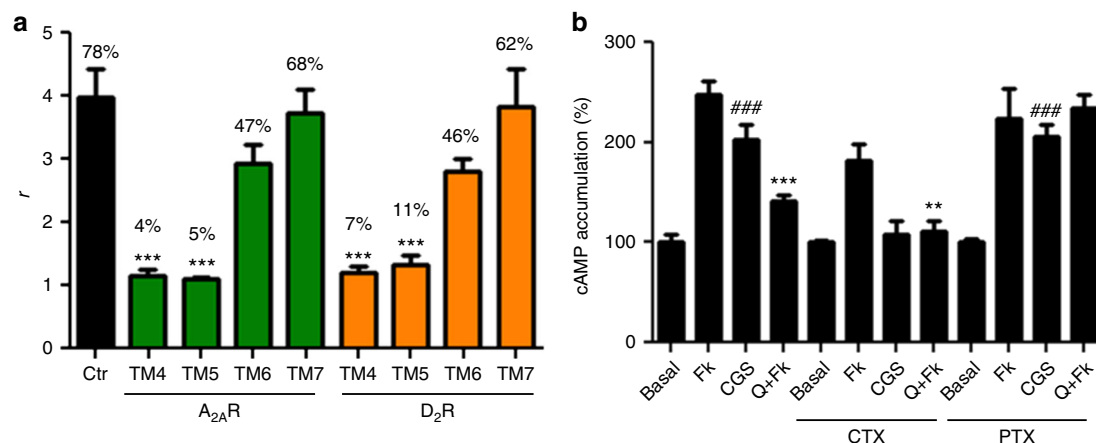


Fig. 2 Functional A_{2A}R–D₂R heterotetramers in transfected cells. **a** Quantification from PLA experiments (see Supplementary Fig. 1) performed in HEK-293T cells transfected with 0.4 μ g of A_{2A}R and 0.5 μ g of D₂R cDNA treated for 4 h with medium (control) or 4 μ M of indicated TM peptides of A_{2A}R or D₂R; values are expressed as the ratio between the number of red spots representing heteromers in confocal microscopy images and the number of cells showing spots (r) (30–50 cells from three independent preparations); % values represent the percentage of cells showing one or more red spots; *** p < 0.001, as compared to control (one-way ANOVA followed by Dunnett’s multiple comparison tests). **b** cAMP production in HEK-293T cells transfected as in (a); cells were incubated overnight with vehicle or pertussis toxin (PTX; 10 ng/ml), or for 2 h with cholera toxin (CTX; 100 ng/ml), and exposed to CGS21680 (CGS; 100 nM) or quinpirole (Q; 1 μ M) in the absence or in the presence of forskolin (Fk; 0.5 μ M), respectively; values are expressed as percentage over cAMP accumulation in non-treated cells (basal) (n = 5–7, with triplicates); ### p < 0.001, as compared to basal values; ** and *** p < 0.01 and p < 0.001 as compared to Fk, respectively; one-way ANOVA followed by Tukey’s multiple comparison tests. Results are always represented as means \pm SEM

the absence of ligands (results are always shown as means \pm SEM). Clear-cut saturation BRET curves were obtained with HEK-293T cells transfected with a constant amount of A_{2A}R fused to *Renilla* Luciferase (A_{2A}R-RLuc) cDNA and increasing quantities of AC5 fused to YFP (AC5-YFP) cDNA (Fig. 3a; BRET_{max} = 54 \pm 6 mBU and BRET₅₀ = 42 \pm 13) or with cells transfected with a constant amount of D₂R-RLuc cDNA and increasing amounts of AC5-YFP cDNA (Fig. 3b; BRET_{max} = 38 \pm 5 mBU and BRET₅₀ = 28 \pm 14), indicating that AC5 interacts with A_{2A}R or D₂R in the absence of ligands. Also, saturation BRET curves were obtained when HEK-293T cells transfected with A_{2A}R-RLuc and increasing amounts of AC5-YFP cDNAs were co-transfected with D₂R cDNA (Fig. 3c; BRET_{max} = 39 \pm 3 mBU and BRET₅₀ = 24 \pm 8) or when cells transfected with D₂R-RLuc and increasing amount of AC5-YFP cDNAs were co-transfected with A_{2A}R cDNA (Fig. 3d; BRET_{max} = 30 \pm 2 mBU and BRET₅₀ = 20 \pm 7). All saturation BRET curves were best-fitted to a monophasic model. We also verified that over-expression of AC5 did not alter A_{2A}R–D₂R heteromerization with BRET experiments in HEK-293T cells transfected with A_{2A}R-RLuc (0.4 μ g) and D₂R-YFP (0.6 μ g) and increasing amounts of AC5 cDNA. No BRET differences were observed between the results obtained with 0, 0.3, 1.0 and 3.0 μ g of AC5 cDNA (56 \pm 7, 53 \pm 6, 53 \pm 3, and 52 \pm 4 mBU, respectively). Altogether, these results suggest that AC5 oligomerize with A_{2A}R–D₂R heteromers in the absence of ligands.

Next, we performed BiFC assays in HEK-293T cells expressing AC5-nYFP, A_{2A}R-cYFP, and D₂R (Fig. 3e) as well as AC5-nYFP, D₂R-cYFP and A_{2A}R (Fig. 3f). Normal functionality of AC5-YFP has been previously reported¹⁶. Significant fluorescence was detected in all cases, providing additional support to direct interactions between AC5 and A_{2A}R–D₂R heteromers (broken lines in Fig. 3e, f). To determine the possible involvement of receptor TMs in the A_{2A}R–D₂R heterotetramer–AC5 interface, we performed BiFC experiments with all different A_{2A}R (Fig. 3e) or D₂R (Fig. 3f) TM peptides. In the absence of ligands, pretreatment of cells with TM1, TM5, or TM6 of A_{2A}R significantly decreased complementation between AC5 and A_{2A}R (Fig. 3e, top panel). Similarly, pretreatment with TM1,

TM4, TM5, or TM6 of D₂R significantly decreased complementation between AC5 and D₂R (Fig. 3f, top panel). This suggests a discrete interaction between TM1 of both receptors with AC5. Since TMs 4–5 of the inner receptor protomers and TMs 6 of inner and outer receptor protomers participate in homo- and heterodimerization (see above), respectively, their apparent involvement in the interactions with AC5 must be indirect, implying that the optimal interaction of the A_{2A}R–D₂R heterotetramer and AC5 requires the optimal quaternary structure of the heterotetramer. When BiFC experiments were performed in the presence of CGS21680 (100 nM, Fig. 3e, bottom panel) or quinpirole (1 μ M, Fig. 3f, bottom panel), the pattern of interfering synthetic peptides changed: In addition to TM5 and TM6 of A_{2A}R and D₂R, TM7 of A_{2A}R and TM2 of D₂R decreased fluorescence complementation in the presence of CGS21680 and quinpirole, respectively, while TM1 of A_{2A}R and D₂R were no longer effective (Fig. 3e, f).

We then investigated the involvement of TMs of AC5 in the oligomerization with A_{2A}R–D₂R heteromers. Since the structure of M1 and M2 domains of any AC isoform is unknown, we used five commonly used algorithms to predict their most probable TMs (Supplementary Table 1). All algorithms predicted the same six TMs for the M2 domain (TM 7 to TM 12), but there was discrepancy on the predicted TMs of the M1 domain. Taking into account the orientation of the predicted TM helices, only Uniprot and TOPCONS solutions were compatible with the well-established intracellular N-terminal and C-terminal domains of AC5⁷. First, TM peptides mimicking right-oriented TMs derived from Uniprot predictions (abbreviated TM1 to TM12) were tested for their ability to destabilize complementation in HEK-293T cells expressing AC5-nYFP, A_{2A}R-cYFP, and D₂R (Fig. 4a), as well as AC5-nYFP, D₂R-cYFP and A_{2A}R (Fig. 4b). In the absence of agonists, pretreatment of cells with TM1 or TM12 significantly decreased complementation between AC5 and A_{2A}R, while TM5 showed a small but not significant decrease (Fig. 4a, top panel). Similarly, pretreatment with TM6 or TM12 significantly decreased complementation between AC5 and D₂R while TM5 again showed a small but not significant decrease (Fig. 4b, top panel). Remarkably, when BiFC

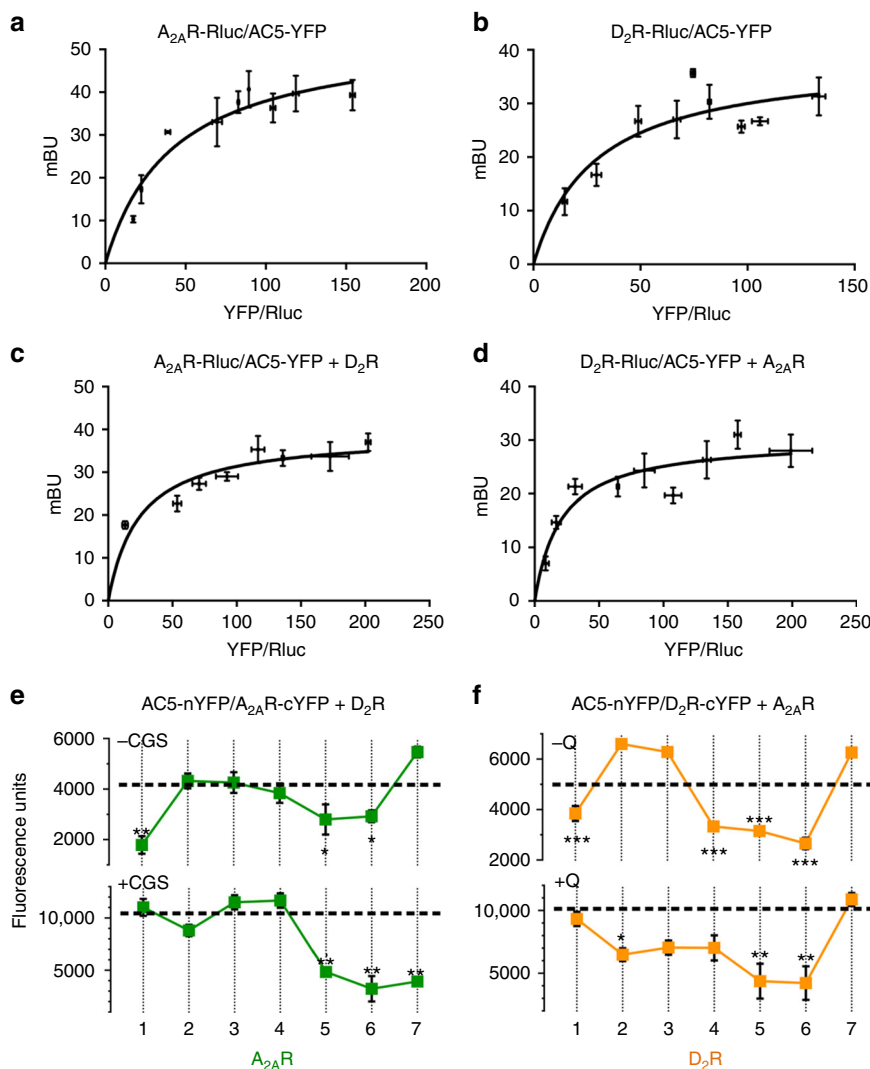


Fig. 3 Involvement of receptor TMs in $A_{2A}R$ - D_2R heterotetramer-AC5 oligomerization. **a-d** BRET saturation experiments in HEK-293T cells transfected with 0.5 μ g of $A_{2A}R$ -Rluc cDNA and increasing amounts of AC5-YFP cDNA (0.3–2.5 μ g) not co-transfected (**a**) or co-transfected (**c**) with D_2R cDNA (0.5 μ g), or with 0.75 μ g of D_2R -Rluc cDNA and increasing amounts of AC5-YFP cDNA (0.3–2.5 μ g) not co-transfected (**b**) or co-transfected (**d**) with $A_{2A}R$ cDNA (0.4 μ g); the relative amount of BRET is given as a function of 1000 \times the ratio between the fluorescence of the acceptor (YFP) and the luciferase activity of the donor (Rluc) and expressed as milli BRET units (mBU) (6–8 experiments, with duplicates, grouped as a function of the amount of BRET acceptor). **e, f** BiFC experiments in HEK-293T cells transfected with AC5-nYFP (0.75 μ g), $A_{2A}R$ -cYFP (0.5 μ g) and D_2R (0.75 μ g) cDNA (**e**) or AC5-nYFP (0.75 μ g), D_2R -cYFP (0.75 μ g) and $A_{2A}R$ (0.4 μ g) cDNA (**f**); cells were treated for 4 h with medium (dotted lines) or 4 μ M of indicated TM peptides (numbered 1–7) of $A_{2A}R$ (**e**) or D_2R (**f**) before addition of medium, CGS21680 (CGS; 100 nM; **e**) or quinpirole (Q; 1 μ M; **f**); fluorescence was detected at 530 nm and values are expressed as arbitrary fluorescent units ($n = 8$, with triplicates); *, ** and *** represent significantly lower values as compared to control values ($p < 0.05$, $p < 0.01$ and $p < 0.001$, respectively; one-way ANOVA followed by Dunnett's multiple comparison tests). Results are always represented as means \pm SEM

experiments were performed in the presence of CGS21680 (100 nM, Fig. 4a, bottom panel) or quinpirole (1 μ M, Fig. 4b, bottom panel), the pattern of interfering synthetic peptides dramatically changed. When receptors were activated, TM1, TM2, TM3, TM5 and TM6 significantly decreased fluorescence complementation between AC5-nYFP and $A_{2A}R$ -cYFP and between AC5-nYFP and D_2R -cYFP. The results imply a major rearrangement of the membrane-spanning domains of the activated pre-coupled complex with an increase in the number of TMs of AC5 directly or indirectly involved in the oligomerization with the $A_{2A}R$ - D_2R heterotetramer.

Opposite-oriented TM peptides, abbreviated as TM2n, TM3n, TM4n, TM5n and TM6n, were tested to examine the specificity of their destabilizing effect (see Supplementary Table 2), which should insert in the membrane in the opposite direction and act

as scrambled control peptides. The peptides were tested in HEK-293T cells expressing AC5-nYFP, $A_{2A}R$ -cYFP, and D_2R (Fig. 4c) as well as AC5-nYFP, D_2R -cYFP, and $A_{2A}R$ (Fig. 4d) in the absence or in the presence of agonists. The same as TM4, TM4n did not have a significant effect, and TM2n, TM3n and TM6n did behave as negative controls to their opposite-oriented peptides, since they did not decrease AC5-nYFP- $A_{2A}R$ -cYFP or AC5-nYFP- D_2R -cYFP complementation in the absence (Fig. 4c, d, top panels) or in the presence (Fig. 4c, d, bottom panels) of agonists. Intriguingly, both TM5 and the opposite-oriented TM5n were able to decrease AC5-nYFP- $A_{2A}R$ -cYFP and AC5-nYFP- D_2R -cYFP complementation (Fig. 4c, d). Importantly, TM5 and TM5n had the lowest hydrophobicity as compared to all the other putative TM sequences (Supplementary Table 1), decreasing the probability of being embedded in the membrane bilayer¹⁷. This

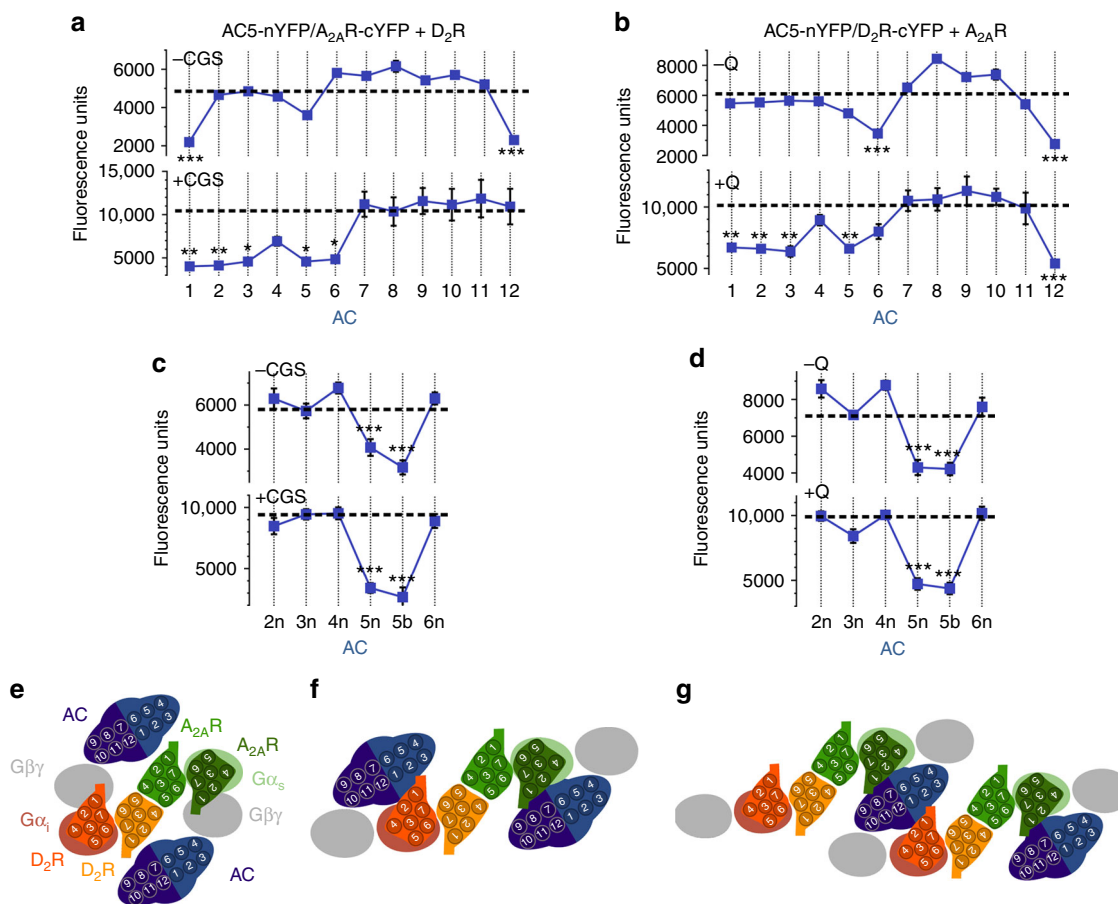


Fig. 4 Involvement of AC5 TMs in A_{2A}R-D₂R heterotetramer-AC5 oligomerization. **a-d** BiFC experiments in HEK-293T cells transfected with AC5-nYFP (0.75 μg), A_{2A}R-cYFP (0.5 μg) and D₂R (0.75 μg) cDNA (**a, c**) or AC5-nYFP (0.75 μg), D₂R-cYFP (0.75 μg) and A_{2A}R (0.4 μg) cDNA (**b, d**); cells were treated for 4 h with medium (dotted lines) or 4 μM of indicated TM peptides predicted from Uniprot algorithm (numbered 1–12) (**a, b**) or control peptides (numbered 2n–6n and 5b; see text) (**c, d**), before addition of medium, CGS21680 (CGS; 100 nM) or quinpirole (Q; 1 μM); fluorescence was detected at 530 nm and values (in means ± SEM) are expressed as arbitrary fluorescent units ($n = 8$, with triplicates); *, ** and *** represent significantly lower values as compared to control values ($p < 0.05$, $p < 0.01$, and $p < 0.001$, respectively; one-way ANOVA followed by Dunnett's multiple comparison tests). **e-g** Schematic slice-representations of A_{2A}R-D₂R heterotetramer-AC5 models: heterotetramer coupled with two AC5 molecules in the absence (**e**) and in the presence (**f**) of agonists; extension of the agonist-bound complex with a second A_{2A}R-D₂R heterotetramer, with simultaneous binding of both Gαs and Gαi to the central C1 and C2 domains of AC5 (**g**). Schematic slice-representation viewed from the extracellular side of the A_{2A}R-D₂R heterotetramer in complex with Gs, Gi, and AC5 in the absence and presence of agonists are shown in Supplementary Fig. 6

could indicate that the AC5 325–345 amino acid sequence forms part of the second intracellular loop (IL2), which could establish direct or indirect intermolecular interactions with the A_{2A}R-D₂R heteromer. Then, the 348–368 aa sequence predicted by the TOPCONS algorithm (TM 5b in Supplementary Table 1), which has the right orientation, becomes a very plausible TM that could interact with the A_{2A}R-D₂R heterotetramer. In fact, TM5b peptide significantly decreased AC5-nYFP-A_{2A}R-cYFP or AC5-nYFP-D₂R-cYFP complementation in the absence or in the presence of agonists (Fig. 4c,d). In agreement with this interpretation, a scrambled TM5-TM5n peptide (AC5-TM5s in Supplementary Table 2) did not decrease AC5-nYFP-A_{2A}R-cYFP or AC5-nYFP-D₂R-cYFP complementation in the absence of ligands (93 ± 7 , and $95 \pm 6\%$, respectively, in means ± SEM and expressed as percentage of change of fluorescent values without peptide; $n = 9$, with triplicates). As additional controls, we also tested AC5 TM1 to TM12 peptides on A_{2A}R-nYFP-D₂R-cYFP complementation and all the D₂R TM and A_{2A}R TM peptides on AC5-nYFP-A_{2A}R-cYFP and AC5-nYFP-D₂R-cYFP complementation, respectively, in the absence of ligands; no changes in BiFC were observed under any condition

(Supplementary Fig. 5). Considering TM 1, TM 2, TM 3, TM 4, TM 5b, and TM 6 as the six putative TMs of the M1 domain of AC5, altogether these results indicate that TM 1 and TM 6, as well as IL2 and TM 5b, are involved in pre-coupling of A_{2A}R-D₂R heterotetramer and AC5 in the absence of agonists. Upon A_{2A}R or D₂R activation there is a rearrangement with an apparent participation of almost all TMs of the M1 domain.

Two A_{2A}R-D₂R heterotetramers and two AC5 molecules. It seems reasonable to hypothesize that the membrane-spanning domains of AC5 are formed by two interacting antiparallel six-helix-bundle domains (M1–M2) with an elliptical ring shape⁷. In the absence of ligands, since it is not feasible that TM 1 from both A_{2A}R and D₂R interact simultaneously with the same TM 5 or TM 12 or the same IL2 of a single AC5 molecule, this suggests the presence of two AC5 molecules simultaneously binding to the A_{2A}R-D₂R heterotetramer in complex with Gi and Gs, possibly with TM1 of D₂R and TM 1 of A_{2A}R interacting specifically with TM 1 and TM 6 of AC5, respectively (Fig. 4e). The ability of peptides that mimic TM 5, TM 12, and IL2 of AC to destabilize

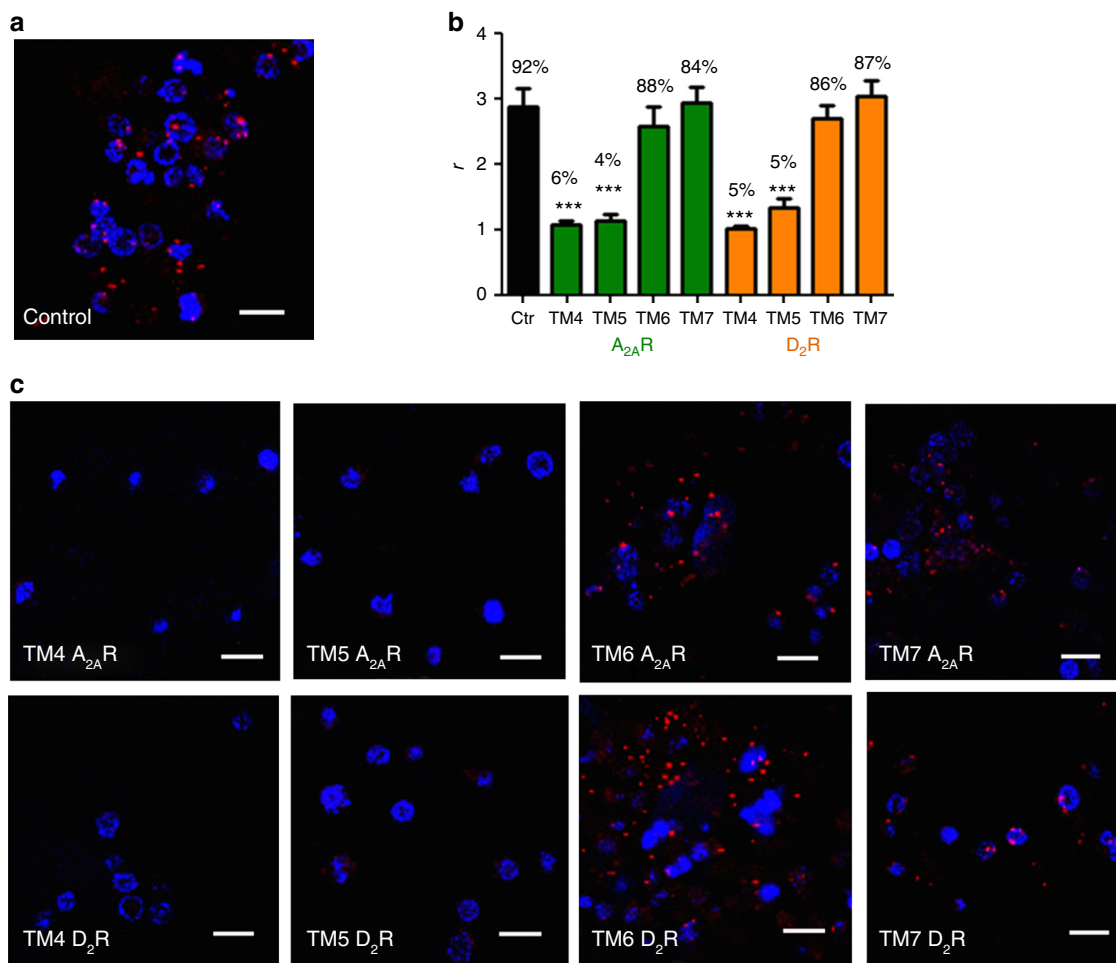


Fig. 5 A_{2A}R–D₂R heterotetramer expression in striatal neurons in culture. Proximity ligation assay (PLA) in rat striatal primary cultures. **a**, **c** Confocal microscopy images (superimposed sections) are shown in which A_{2A}R–D₂R heteromers appear as red spots. Primary cultures were treated for 4 h with medium (**a**) or 4 μM of indicated TM peptides (numbered 1–7) of A_{2A}R or D₂R (**c**); cell nuclei were stained with DAPI (blue); scale bars: 20 μm. **b** Quantification from PLA experiments: values (in means ± SEM) are expressed as the ratio between the number of red spots and the number of cells showing spots (*r*) (20–30 neurons from three independent preparations); % values represent the percentage of cells showing one or more red spots; ****p* < 0.001, as compared to control (one-way ANOVA followed by Dunnett’s multiple comparison tests)

oligomerization between AC5 and the A_{2A}R–D₂R heterotetramer might depend on an indirect modification of their discrete asymmetrical interfaces.

It is well established that the G_α binding site for G_{βγ} overlaps with the G_α binding sites for the effector, the cytoplasmic domains C1 and C2 of AC. During G protein activation, G_{βγ} relative movement promotes G_α binding to AC^{18,19}. These swapping interactions can take place within the frame of the A_{2A}R–D₂R heterotetramer with two AC5 molecules binding simultaneously to G_s and G_i in the complex (Fig. 4e, f). The rearrangement of TM interfaces between the A_{2A}R–D₂R heterotetramer and AC5 upon receptor activation occurs simultaneously with the rearrangement of the G_{βγ} subunit, by its established stable coupling with the NT of AC5¹⁶, which facilitates the interaction between the G_α subunit and its corresponding catalytic AC5 domain. This rearrangement in the frame of the heteromer gives a computational molecular model of activated complex schematized in Fig. 4f. Details about the model are shown in Supplementary Fig. 6. However, within the frame of the constraints imposed by a pre-coupled A_{2A}R–D₂R heterotetramer–G_s–G_i–AC5 complex, a single A_{2A}R–D₂R heterotetramer cannot accomplish the model proposed by Dessauer et al.⁸, in which one G_s and one G_i bind simultaneously to one single AC5 (see below). Therefore, we propose that AC5 should oligomerize

with an additional A_{2A}R–D₂R heterotetramer (Fig. 4g). The results with interfering peptides, together with the proposed simultaneous binding of G_s and G_i to AC5, suggest a minimal functional complex composed of two A_{2A}R–D₂R heterotetramers and two AC5 molecules (Fig. 4g).

The canonical G_s–G_i antagonistic interaction. To corroborate the proposed model we studied the functional characteristics of the A_{2A}R–D₂R heterotetramer–AC5 complex in rat striatal neuronal primary cultures, which express endogenous A_{2A}R–D₂R heteromer complexes²⁰. Furthermore, AC5 is the predominant AC subtype in striatal neurons²¹. First, we analyzed by PLA the expression of A_{2A}R–D₂R heteromers, as well as the ability of the synthetic peptides mimicking the TMs of A_{2A}R and D₂R to modify the quaternary structure of the endogenous A_{2A}R–D₂R heterotetramer. A_{2A}R–D₂R heteromers were observed as red punctate staining in neuronal cells (Fig. 5a, b). As expected, pretreatment of cells with TM4 and TM5 of A_{2A}R and D₂R, but not with TM6 or with TM7, produced a significant decrease in the number of red spots per cell (Fig. 5b, c). These results mirrored those obtained in HEK-293T cells (see Fig. 2a and Supplementary Fig. 3), confirming the same TMs 4/5 interface of

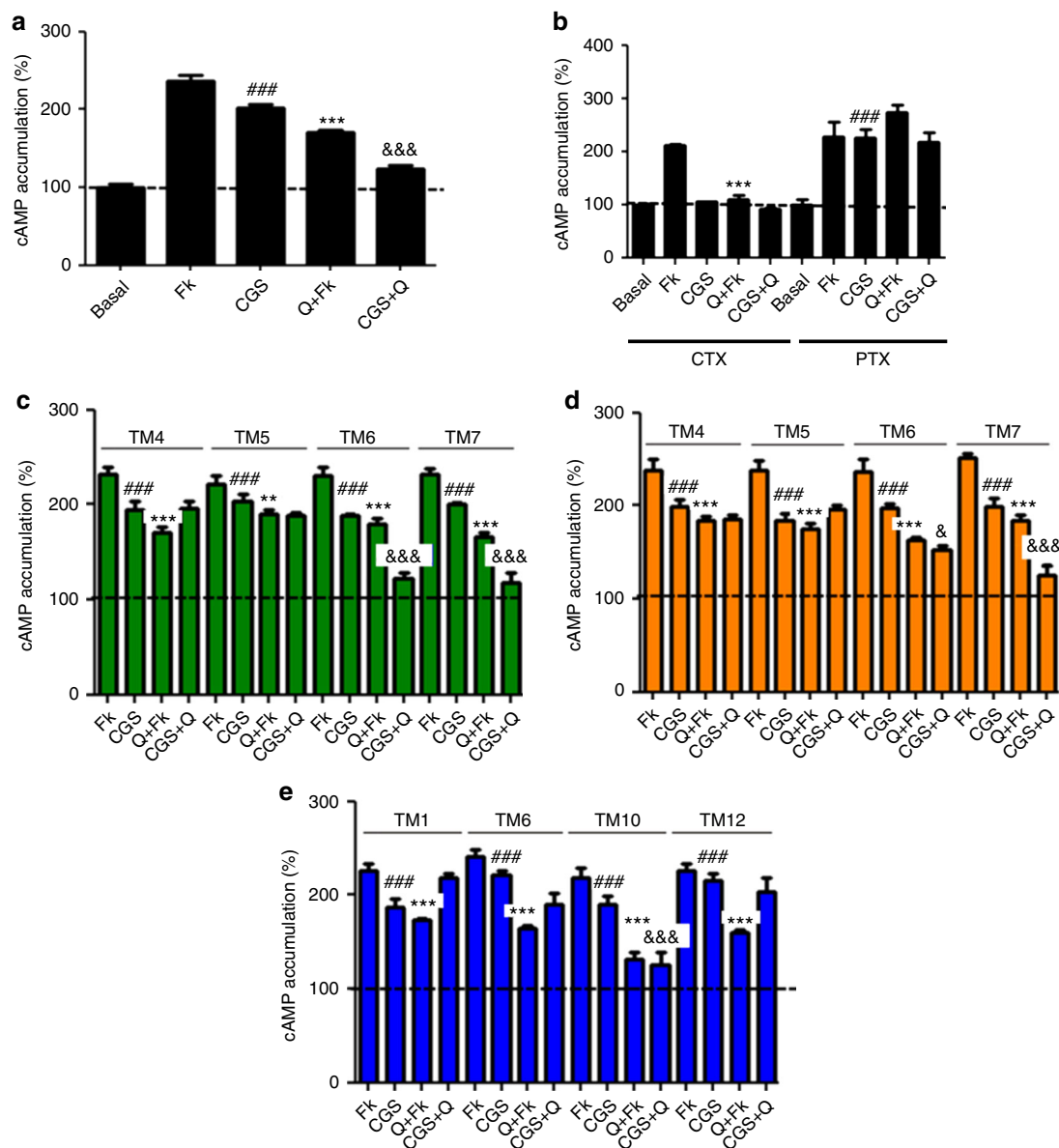


Fig. 6 Canonical Gs-Gi antagonistic interaction in striatal neurons in culture. **a, b** cAMP production determined in rat striatal primary cultures incubated overnight with vehicle (**a**) or with pertussis toxin (PTX; 10 ng/ml), or for 2 h with cholera toxin (CTX; 100 ng/ml) (**b**), and exposed to CGS21680 (CGS; 100 nM), quinpirole (Q; 1 μ M) or both in the absence or in the presence of forskolin (Fk; 0.5 μ M), respectively. **c-e** cAMP production determined in rat striatal primary cultures incubated 4 h with 4 μ M of indicated TM peptides of A_{2A}R (**c**), D₂R (**d**), or AC5 (**e**) and exposed to agonists as in **a, b**. Values (in means \pm SEM) are expressed as percentage of cAMP accumulation in non-treated cells (basal) ($n = 5-7$, with triplicates); ### $p < 0.001$, as compared to basal values; ** and *** $p < 0.01$ and $p < 0.001$ as compared to Fk, respectively; &&& $p < 0.05$ and $p < 0.001$ as compared to CGS, respectively; one-way ANOVA followed by Tukey's multiple comparison tests

A_{2A}R–D₂R heteromers in striatal cells and that TM6 does not destabilize heterodimerization. PLA experiments were also performed with a recently characterized AC5 antibody²². A_{2A}R–AC5 and D₂R–AC5 complexes could be revealed as red punctate staining in neuronal cells (Supplementary Fig. 7). Next, we measured cAMP production to analyze the functional characteristics of the A_{2A}R–D₂R heteromer and the effect of the interfering peptides. As expected, CGS21680 (100 nM) increased the synthesis of cAMP (Fig. 6a) and quinpirole (1 μ M) decreased forskolin-induced cAMP accumulation (Fig. 6a). Pertussis toxin, selectively counteracted the ability of quinpirole to inhibit forskolin-induced cAMP (Fig. 6b), while cholera toxin impeded the activating effect of CGS21680 while leaving unaltered quinpirole-induced inhibition of forskolin-induced AC5

activation (Fig. 6b). Simultaneous exposure to both agonists demonstrated the ability of quinpirole to inhibit the effect of CGS21680, revealing the canonical Gs–Gi interaction at AC5 (Fig. 6a).

Accumulation of cAMP was also determined in striatal cultures upon exposure to ligands and interfering TM peptides. Pretreatment with TM7 (as negative control) or with TM6 of A_{2A}R or D₂R did not modify receptor signaling or the canonical interaction (Fig. 6c, d). In contrast, although pretreatment with TM4 and TM5 of A_{2A}R (Fig. 6c) or D₂R (Fig. 6d) did not modify receptor signaling, it blocked the canonical interaction (Fig. 6c, d). These results indicate that TMs that destabilize receptor heteromerization do not disrupt the individual functional interactions between the receptors and AC5, most probably

because of stable pre-coupling between the G proteins and AC5, as recently demonstrated for the specific $G_{\alpha_{ol}\beta_2\gamma_7}$ -AC5 complex in the rodent striatum²². Nevertheless, the peptides that destabilize receptor heteromerization alter the correct coupling of AC5 to the complex that allows the simultaneous binding of Gas and Gai subunit to AC, impeding the canonical interaction. In conclusion, $A_{2A}R$ - D_2R heteromerization is a necessary condition for the canonical antagonistic interaction between Gs-coupled $A_{2A}R$ and Gi-coupled D_2R at AC in striatal neurons in culture. In agreement with this conclusion, cAMP accumulation induced by CGS21680 was not counteracted by an agonist of dopamine D_4R , which does not heteromerize with $A_{2A}R$ ²³ (Supplementary Fig. 8). Finally, pretreatment of striatal cultures with interfering peptides TM1, TM6 or TM12 of AC5 did not change receptor signaling but also blocked the canonical interaction, while TM10 was ineffective (Fig. 6e). These results confirm the involvement of the AC5 subtype in striatal cultures and indicate that these AC5 TM peptides are not able to destabilize the interactions between AC5 and the receptors but induce an alteration of the quaternary structure of the complex that impedes the simultaneous binding of Gas and Gai subunit to AC5, the canonical interaction. Thus, the correct intermolecular interaction between AC5 and the $A_{2A}R$ - D_2R heterotetramer is also a necessary condition for the presence of the canonical Gs-Gi interaction at AC5.

The ability of quinpirole to reduce cAMP accumulation induced by CGS21680 implies that Gi acts on a Gs-activated AC5. Thus, simultaneous binding of Gsa to the C2 domain and Gia to the C1 domain of a single AC5 must occur⁸. This, in fact, agrees with the suggested complex of two $A_{2A}R$ - D_2R heterotetramers that simultaneously bind to the same AC5 molecule (see Fig. 4g). In this model AC5 acts as a link between two heterotetramers, which makes compatible the antagonistic canonical interaction between Gsa and Gia activated proteins at the same AC5 molecule. Moreover, the membrane-spanning M1 and M2 domains of AC5 can accommodate between the two $A_{2A}R$ - D_2R heterotetramers (Supplementary Fig. 6), providing the frame for the series of experimentally determined TM contacts between $A_{2A}R$, D_2R , and AC5 (see above). However, with the model that includes two $A_{2A}R$ - D_2R heterotetramers and two AC5 molecules (Fig. 4g), only one AC5 simultaneously interacts with Gsa and Gia. This would imply that quinpirole could only produce a partial inhibition of CGS21680-induced cAMP accumulation, while the results showed in Fig. 5a–e demonstrate that quinpirole produces an almost complete blockade. We therefore propose that the minimal functional quaternary structure (see Fig. 4g) forms a linearly arranged high-order oligomeric structures (Supplementary Fig. 6e).

Discussion

Striatal $A_{2A}R$ and D_2R are known to form functionally and pharmacologically significant heteromers that modulate basal ganglia function¹⁰. Here, we demonstrate the existence of intermolecular interactions between $A_{2A}R$, D_2R , and AC5 with the emergence of functional $A_{2A}R$ - D_2R heterotetramer-AC5 complexes. These complexes sustain the canonical Gs-Gi interaction at the AC level, the ability of a Gi-coupled GPCR to counteract AC activation mediated by a Gs-coupled GPCR.

We first identified the symmetrical TM 6 homodimer and TMs 4/5 heterodimer interfaces in the $A_{2A}R$ - D_2R heterotetramer from results of BiFC experiments obtained with specific TM peptides mimicking TM receptor domains. While BiFC complex formation under in vitro conditions has been considered to be essentially irreversible²⁴, several studies indicate that under in vivo conditions BiFC complex formation can be reversible^{25–27}. The

present results provide additional support to that reversibility, which lies on the specificity of the peptide approach, demonstrated by the qualitative identical results from BiFC, PLA, and cAMP accumulation experiments. From these results, we could develop a computational model, where only the two internal protomers participate in the heteromeric interface and the two external protomers participate in the homomeric interface of the $A_{2A}R$ - D_2R heterotetramer. A pattern of similar symmetrical interfaces of GPCR homomers and heteromers involving specific TMs has emerged from several studies also using TM interfering peptides, cross-linking techniques or crystallographic analysis (see ref.⁶, for review). The consistent results we obtained with interfering peptides in experiments with biosensor-fused receptors in transfected cells and with native receptors in striatal neurons in culture, provide strong support for the involvement of TM 6 in the homomeric interfaces and TM 4 and TM 5 in the heteromeric interface of the $A_{2A}R$ - D_2R heterotetramer in its natural environment. The differences in the apparent interfaces of $A_{2A}R$ and D_2R homomers here reported as compared to previous studies (TM 6 versus TMs 4 or/and 5)^{28,29}, could be due to the different experimental approaches and, most likely, due to the presence of heteromeric partner receptors that influence the TM interfaces. The fact that rearrangement of TM 6 constitutes main ligand-induced conformational changes that determine G protein activation and modulation of ligand affinity³⁰, provides a frame for the understanding of allosteric communications through the protomers in GPCR oligomers^{4–6}. Thus, in our constructed models, TM 6 in the inactive closed conformation of the unliganded protomer interacts with TM 6 in the active open conformation of the G protein-bound protomer (Supplementary Fig. 4).

An important conclusion from this study is that the non-activated or agonist-activated $A_{2A}R$ - D_2R heterotetramer is able to establish different molecular interactions with AC5. By using specific interfering peptides, we demonstrate that these interactions involve TMs from the receptors and the AC5. The specificity of the peptide approach was unambiguously demonstrated with their orientation-dependent selectivity on their ability to destabilize the asymmetrical interfaces between AC5 and the receptors. The differential effect of interfering TM peptides in the absence and presence of agonists implies a major rearrangement of the membrane-spanning domains of the activated pre-coupled complex with an increase in the number of TMs of AC5 directly or indirectly involved in the oligomerization with the $A_{2A}R$ - D_2R heterotetramer during agonist exposure. This rearrangement could be driven by the agonist-induced relative movement of the $G\beta\gamma$ subunit away from the helical-domain of the $G\alpha$ subunit, simultaneously pulling the NT domain of AC5¹⁶ and facilitating the interaction of its catalytic domains with the corresponding $G\alpha$ subunit^{18,19}. This key role of the G protein in determining changes in the quaternary structure of the $A_{2A}R$ - D_2R heterotetramer-AC5 complex upon receptor activation would agree with the recently described stable pre-coupling of striatal Golf and AC5²² and the here described less stable interactions between TMs of AC5 and $A_{2A}R$ and D_2R .

Probably the most significant conclusion of the study is that the $A_{2A}R$ - D_2R heterotetramer-AC5 complex sustains the canonical antagonistic Gs-Gi interaction at the AC level. This was also demonstrated with specific interfering TM peptides, by the very selective ability of the TM peptides that mimic the heteromeric interface in the $A_{2A}R$ - D_2R heterotetramer to block the canonical antagonistic interaction in striatal neurons in culture. The significant control of $A_{2A}R$ signaling by D_2R implied that most $A_{2A}R$ that signal through AC5 are forming heteromers with D_2R in this neuronal preparation. Previous studies indicate that the same situation occurs in vivo in the striatum, where the pharmacological or genetic blockade of D_2R disinhibits adenosine-mediated

activation of AC in the striato-pallidal neuron³¹. In fact, A_{2A}R blockade counteracts most biochemical and behavioral effects induced by interruption of D₂R signaling³¹. In complete agreement are also the results obtained by Lee et al. with AC5 knockout mice²¹, which show that AC5 is the principal AC integrating signals from A_{2A}R and D₂R in the striatum and that the signaling cascade involving AC5 is essential for the behavioral effects of D₂R antagonists, and therefore antipsychotic drugs. The efficient D₂R-mediated antagonism of A_{2A}R-mediated AC activation, however, cannot be explained by a minimal functional structure of an A_{2A}R–D₂R heterotetramer–AC5 complex that can sustain a canonical Gs–Gi interaction at AC, which is composed of two A_{2A}R–D₂R heterotetramers and two AC5 molecules. Such a complex would not allow the D₂R agonist to exert the almost complete inhibition of A_{2A}R agonist-mediated cAMP revealed in the experiments on striatal neurons in culture. In fact, this quaternary structure suggests the possible formation of zig-zagged arranged high-order oligomeric structures (Supplementary Fig. 6), as proposed for other GPCRs, including D₂R and rhodopsin homomers^{20,32}. To our knowledge, these are the first data suggesting higher-order linear arrangements of GPCR heteromers and effectors.

The present study represents a proof of concept of the significant functional role of GPCR heteromers within a signalosome, since it demonstrates that GPCR heteromers provide the frame for biochemical interactions previously thought to be independent of intermolecular receptor–receptor interactions, on classical receptor cross-talk at the second-messenger level³³. Therefore, we postulate that pre-coupling should not only apply to other Gs–Gi–AC-coupled heteromers, but also to heteromers coupled to other G proteins and effectors, such as the well-established Gi–Gq-coupled metabotropic glutamate receptor mGlu₂ receptor-serotonin 5-HT_{2A} receptor heteromer³⁴, which could be pre-coupled to potassium channels³⁵. At a more general level, the present results represent a very significant support to the still controversial concepts of GPCR pre-coupling and oligomerization.

Methods

Vectors and fusion proteins. Sequences encoding amino acid residues 1–155 and 156–238 of YFP Venus protein were subcloned into the pcDNA3.1 vector to obtain the YFP Venus hemi-truncated proteins (pcDNA3.1-cVenus or pcDNA3.1-nVenus vectors). The cDNA constructs encoding human A_{2A}R or D₂R in pcDNA3 vectors were subcloned in pRLuc-N1 (PerkinElmer, Wellesley, MA) to generate A_{2A}R–RLuc or D₂R–RLuc fusion proteins on the C-terminal end or were subcloned to be in-frame with restriction sites of pcDNA3.1-cVenus or pcDNA3.1-nVenus vectors to give the plasmids that express proteins fused to hemi-YFP Venus on the C-terminal end (A_{2A}R–cYFP, D₂R–cYFP, A_{2A}R–nYFP or A_{2A}R–nYFP). Human AC5 cDNA was amplified without its stop codon using sense and antisense primers harboring unique KpnI and EcoRV. The amplified fragment was subcloned to be in-frame with restriction sites of pEYFP-N1 (enhanced yellow variant of GFP; Clontech, Heidelberg, Germany) or pcDNA3.1-nVenus vectors to give the plasmids that express AC5 fused to YFP or hemi-YFP Venus on the C-terminal end (AC5–YFP or AC5–nYFP).

Cell cultures and transfection. Primary cultures of striatal neurons were obtained from fetal Sprague Dawley rats of 19 days. All experiments were carried out in accordance with EU directives (2010/63/EU and 86/609/CEE) and were approved by the Ethical Committee of the University of Barcelona. Striatal cells were isolated as described elsewhere²⁰ and plated at a confluence of 40,000 cells/0.32 cm². Cells were grown in Neurobasal medium supplemented with 2 mM L-glutamine, 100 U/ml penicillin/streptomycin, and 2% (v/v) B27 supplement (GIBCO) in a 96-well plate for 12 days. HEK-293T cells were grown in Dulbecco's modified Eagle's medium (DMEM) supplemented with 2 mM L-glutamine, 100 U/ml penicillin/streptomycin, and 5% (v/v) heat inactivated fetal bovine serum (Invitrogen). HEK-293T cells (ATCC, Manassas, VA) were transfected with the plasmids encoding receptors by the PEI (PolyEthylenimine) method as previously described²⁰.

TAT-TM peptides. Peptides with the sequence of transmembrane domains (TM) of A_{2A}R and D₂R and putative TM peptides of AC5 fused to the HIV transactivator of transcription (TAT) peptide (YGRKKRRQRRR) were used as oligomer-destabilizing molecules. The cell-penetrating TAT peptide allows intracellular delivery of fused peptides³⁶. The TAT-fused TM peptide can then be inserted effectively into the

plasma membrane because of the penetration capacity of the TAT peptide and the hydrophobic property of the TM moiety¹¹. To obtain the right orientation of the inserted peptide, the HIV-TAT peptide was fused to the C-terminus or to the N-terminus as indicated. The amino acid sequences of the fusion peptides are shown in Supplementary Table 2. Several algorithms were used to identify putative TMs in the primary amino acid sequence of AC5 (Supplementary Table 1).

Bimolecular fluorescence complementation. HEK-293T cells were transiently co-transfected with the cDNA encoding a protein fused to nYFP and a protein fused to cYFP. After 48 h, cells were treated or not with the indicated TM peptides (4 μM) for 4 h at 37 °C. The time of incubation and concentration of TM peptides were chosen from results of concentration-dependent and time-dependent response experiments of the possible BiFC destabilization by all seven TM peptides of the A_{2A}R in HEK-293T cells transfected with A_{2A}R–nYFP and A_{2A}R–cYFP (Supplementary Fig. 3). The same parameters were applied with D₂R and AC5 TM peptides and in PLA and cAMP experiments. To quantify protein reconstituted YFP Venus expression, cells (20 μg protein; 50,000 cells/well) were distributed in 96-well microplates (black plates with a transparent bottom, Corning, King's Lynn, UK), and emission fluorescence at 530 nm was monitored in a FLUOstar Optima Fluorimeter (BMG Labtechnologies, Offenburg, Germany) equipped with a high-energy xenon flash lamp, using a 10-nm bandwidth excitation filter at 400 nm reading. Protein fluorescence expression was determined as the fluorescence of the sample minus the fluorescence of cells not expressing the fusion proteins (basal). Cells expressing protein-cVenus and nVenus or protein-nVenus and cVenus showed similar fluorescence levels than non-transfected cells.

Bioluminescence resonance energy transfer assay. HEK-293T cells were transiently cotransfected with a constant amount of expression vectors encoding for proteins fused to RLuc and with increasing amounts of the expression vectors corresponding to proteins fused to YFP. To quantify protein-YFP expression, cells (20 μg protein, around 50,000 cells/well) were distributed in 96-well microplates (black plates with a transparent bottom), and fluorescence was read in a Fluor Star Optima Fluorimeter (BMG Labtechnologies, Offenburg, Germany) equipped with a high-energy xenon flash lamp, using a 10-nm bandwidth excitation filter at 400 nm reading. Fluorescence expression was determined as fluorescence of the sample minus the fluorescence of cells only expressing the BRET donor. For BRET measurements, the equivalent of 20 μg of cell suspension was distributed into 96-well microplates (Corning 3600, white plates; Sigma) and 5 μM coelenterazine H (Molecular Probes, Eugene, OR) was added. The readings were taken 1 min later using a Mithras LB 940. The integration of the signals detected in the short-wavelength filter at 485 nm and the long-wavelength filter at 530 nm was recorded. To quantify protein-RLuc expression luminescence, readings were performed 10 min after adding 5 μM of coelenterazine H. Fluorescence and luminescence of each sample were measured before every experiment to confirm similar donor expressions (approximately 100,000 bioluminescence units) while monitoring the increase in acceptor expression (1000 to 30,000 fluorescence units). The net BRET is defined as [(long-wavelength emission)/(short-wavelength emission)] – Cf, where Cf corresponds to [(long-wavelength emission)/(short-wavelength emission)] for the donor construct expressed alone in the same experiment. BRET is expressed as millibRET units (mBU; net BRET x 1000). Data were fitted to a nonlinear regression equation, assuming a single-phase saturation curve with GraphPad Prism software (San Diego, California, US). BRET_{max} and BRET₅₀ values were obtained from the analysis of the BRET saturation curves. BRET₅₀ is a magnitude related to the affinity of the protein-protein interaction, with low values representing high affinity (as in the present results; Fig. 2a–d).

Proximity ligation assay. HEK293T cells or neuronal primary cultures were grown on glass coverslips and fixed in 4% paraformaldehyde for 15 min, washed with phosphate-buffered saline (PBS) containing 20 mM glycine, permeabilized with the same buffer containing 0.05% Triton X-100, and successively washed with TBS. Heteromers and AC5-receptor complexes were detected using the Duolink II in situ PLA detection Kit (OLink; Bioscience, Uppsala, Sweden) following supplier's instructions. A mixture of the primary antibodies [mouse or rabbit anti-A_{2A}R antibodies (1:100; 05-717 and AB1559P, Millipore, Darmstadt, Germany), rabbit anti-D₂R antibody (1:100; AB5084P, Millipore) and the recently characterized mouse anti-AC5 antibody²² (1:50)] was used to detect A_{2A}R–D₂R heteromers together with PLA probes detecting mouse or rabbit antibodies. The specificity of the same A_{2A}R and D₂R antibodies for PLA assays has been previously demonstrated³⁷. Then, samples were processed for ligation and amplification with a Detection Reagent Red and were mounted using a DAPI-containing mounting medium. Samples were analyzed in a Leica SP2 confocal microscope (Leica Microsystems, Mannheim, Germany) equipped with an apochromatic 63X oil-immersion objective (1.4 numerical aperture), and 405-nm and 561-nm laser lines. For each field of view a stack of two channels (one per staining) and 4 to 6 Z-stacks with a step size of 1 μm were acquired. Images were opened and processed with Image J software (National Institutes of Health, Bethesda, MD). Quantification of the total number of red dots versus total cells (blue nuclei) was counted on the maximum projections of each image stack. After getting the projection, each channel was processed individually.

Determination of cAMP. Homogeneous time-resolved fluorescence energy transfer (HTRF) assays were performed using the Lance Ultra cAMP kit (PerkinElmer), based on competitive displacement of a europium chelate-labeled cAMP tracer bound to a specific antibody conjugated to acceptor beads. We first established the optimal cell density for an appropriate fluorescent signal. This was done by measuring the TR-FRET signal as a function of forskolin concentration using different cell densities. The forskolin dose-response curves were related to the cAMP standard curve, to establish which cell density provides a response that covers most of the dynamic range of the cAMP standard curve. Cells (1000–2000 HEK-293T or 4000 to 5000 primary cultures per well) growing in medium containing 50 μ M zardaverine were pre-treated with toxins or the corresponding vehicle in white ProxiPlate 384-well microplates (PerkinElmer) at 25 °C for the indicated time and stimulated with agonists for 15 min before adding 0.5 μ M forskolin or vehicle and incubating for an additional 15 min period. Fluorescence at 665 nm was analyzed on a PHERAstar Flagship microplate reader equipped with an HTRF optical module (BMGLab technologies, Offenburg, Germany).

Computational models. Inactive models of the human A_{2A}R and D₂R were constructed based on the crystal structures of inactive A_{2A}R (PDB id 5IU4)³⁸ and D₂R (PDB id 3PBL)³⁹, respectively. The “active” conformations of A_{2A}R bound to Gs and D₂R bound to Gi were modeled by incorporating the active features of the crystal structure of β_2 -adrenoceptor in complex with Gs (PDB code 3SN6)³⁰. The globular α -helical domain of the α -subunit was modeled in the “closed” conformation, using the crystal structure of either Gsa (PDB id 1AZT)⁴⁰ or Gia (PDB id 3UMR)⁴¹. The absence of crystal structures of the M1 and M2 domains of AC or close protein templates impede their inclusion on the models. Nevertheless, the results with interfering peptides provide significant information about the putative location of the TM segments, which have been considered to form an antiparallel six-helix bundle with an elliptical ring shape as most of the membrane proteins. The structure of the intracellular C1 and C2 domains of AC in complex with Gsa and Gia was modeled as in the crystal structure of C1 and C2 in complex with Gsa (PDB id 1CUL)⁴². All homology models were built using Modeller 9.16⁴³. The structure of A_{2A}R and D₂R heterodimer, using the TMs 4/5 interface, was modeled as in the oligomeric structure of the β_1 -adrenoceptor (PDB code 4GPO)⁴⁴, whereas the structures for A_{2A}R (inactive and Gs-bound “active” A_{2A}R) and D₂R (inactive and Gi-bound “active” D₂R) homodimers were modeled using molecular dynamics simulations (see Supplementary Fig. 2) due to the absence of crystal structures of oligomers using exclusively the TM6 interface¹¹.

Statistical information. One-way ANOVA followed by Dunnett’s or Tukey’s multiple comparison tests were used for statistical comparisons between different groups of results. Number of experiments and replications as well as the statistical results are shown in the corresponding figure legends.

Data availability. All data that support the findings of this study are available from the corresponding author upon reasonable request.

Received: 12 September 2017 Accepted: 21 February 2018

Published online: 28 March 2018

References

- Gilman, A. G. G proteins: transducers of receptor-generated signals. *Annu. Rev. Biochem.* **56**, 615–649 (1987).
- Ferré, S. The GPCR heterotetramer: challenging classical pharmacology. *Trends Pharmacol. Sci.* **36**, 145–152 (2015).
- Bañeres, J. L. & Parelló, J. Structure-based analysis of GPCR function: evidence for a novel pentameric assembly between the dimeric leukotriene B4 receptor BLT1 and the G-protein. *J. Mol. Biol.* **329**, 815–829 (2003).
- Han, Y., Moreira, I. S., Urizar, E., Weinstein, H. & Javitch, J. A. Allosteric communication between protomers of dopamine class A GPCR dimers modulates activation. *Nat. Chem. Biol.* **5**, 688–695 (2009).
- Pellissier, L. P. et al. G protein activation by serotonin type 4 receptor dimers: evidence that turning on two protomers is more efficient. *J. Biol. Chem.* **286**, 9985–9997 (2011).
- Ferré, S. et al. G protein-coupled receptor oligomerization revisited: functional and pharmacological perspectives. *Pharmacol. Rev.* **66**, 413–434 (2014).
- Sadana, R. & Dessauer, C. W. Physiological roles for G protein-regulated adenylyl cyclase isoforms: insights from knockout and overexpression studies. *Neurosignals* **17**, 5–22 (2009).
- Dessauer, C. W., Tesmer, J. J., Sprang, S. R. & Gilman, A. G. Identification of a G α binding site on type V adenylyl cyclase. *J. Biol. Chem.* **273**, 25831–25839 (1998).
- Gomes, I. et al. G protein-coupled receptor heteromers. *Annu. Rev. Pharmacol. Toxicol.* **56**, 403–425 (2016).
- Bonaventura, J. et al. Allosteric interactions between agonists and antagonists within the adenosine A_{2A} receptor-dopamine D₂ receptor heterotetramer. *Proc. Natl Acad. Sci. USA* **112**, E3609–E3618 (2015).
- He, S. Q. et al. Facilitation of mu-opioid receptor activity by preventing delta-opioid receptor-mediated codegradation. *Neuron* **69**, 120–131 (2011).
- Cordomi, A., Navarro, G., Aymerich, M. S. & Franco, R. Structures for G-protein-coupled receptor tetramers in complex with G proteins. *Trends Biochem. Sci.* **40**, 548–551 (2015).
- Rebois, R. V. et al. Heterotrimeric G proteins form stable complexes with adenylyl cyclase and Kir3.1 channels in living cells. *J. Cell Sci.* **119**, 2807–2818 (2006).
- Gao, X., Sadana, R., Dessauer, C. W. & Patel, T. B. Conditional stimulation of type V and VI adenylyl cyclases by G protein betagamma subunits. *J. Biol. Chem.* **282**, 294–302 (2007).
- Rebois, R. V. et al. D₂-like dopamine and β -adrenergic receptors form a signaling complex that integrates Gs- and Gi-mediated regulation of adenylyl cyclase. *Cell. Signal.* **24**, 2051–2060 (2012).
- Sadana, R., Dascal, N. & Dessauer, C. W. N terminus of type 5 adenylyl cyclase scaffolds Gs heterotrimer. *Mol. Pharmacol.* **76**, 1256–1264 (2009).
- Kyte, J. & Doolittle, R. F. A simple method for displaying the hydrophobic character of a protein. *J. Mol. Biol.* **157**, 105–132 (1982).
- Cabrera-Vera, T. M. et al. Insights into G protein structure, function, and regulation. *Endocr. Rev.* **24**, 765–781 (2003).
- Galés, C. et al. Probing the activation-promoted structural rearrangements in preassembled receptor-G protein complexes. *Nat. Struct. Mol. Biol.* **13**, 778–786 (2006).
- Navarro, G. et al. Intracellular calcium levels determine differential modulation of allosteric interactions within G protein-coupled receptor heteromers. *Chem. Biol.* **21**, 1546–1556 (2014).
- Lee, K. W. et al. Impaired D₂ dopamine receptor function in mice lacking type 5 adenylyl cyclase. *J. Neurosci.* **22**, 7931–7940 (2002).
- Xie, K. et al. Stable G protein-effector complexes in striatal neurons: mechanism of assembly and role in neurotransmitter signaling. *eLife* **4**, e10451 (2015).
- Carriba, P. et al. Detection of heteromerization of more than two proteins by sequential BRET-FRET. *Nat. Methods* **5**, 727–733 (2008).
- Rose, R. H., Bridson, S. J. & Holliday, N. D. Bimolecular fluorescence complementation: lighting up seven transmembrane domain receptor signalling networks. *Br. J. Pharmacol.* **159**, 738–750 (2010).
- Schmidt, C. et al. Mechanisms of proinflammatory cytokine-induced biphasic NF- κ B activation. *Mol. Cell.* **12**, 1287–1300 (2003).
- Guo, Y., Rebecchi, M. & Scarlata, S. Phospholipase C β 2 binds to and inhibits phospholipase C δ 1. *J. Biol. Chem.* **280**, 1438–1447 (2005).
- Anderie, I. & Schmid, A. In vivo visualization of actin dynamics and actin interactions by BiFC. *Cell Biol. Int.* **31**, 1131–1135 (2007).
- Guo, W., Shi, L., Filizola, M., Weinstein, H. & Javitch, J. A. Crosstalk in G protein-coupled receptors: changes at the transmembrane homodimer interface determine activation. *Proc. Natl Acad. Sci. USA* **102**, 17495–17500 (2005).
- Navarro, G. et al. Quaternary structure of a G-protein-coupled receptor heterotetramer in complex with Gi and Gs. *BMC Biol.* **14**, 26 (2016).
- Rasmussen, S. G. et al. Crystal structure of the β_2 adrenergic receptor-Gs protein complex. *Nature* **477**, 549–555 (2011).
- Taura, J. et al. Behavioral control by striatal adenosine A(2A) -dopamine D(2) receptor heteromers. *Genes Brain Behav.* <https://doi.org/10.1111/gbb.12432> (2018).
- Jastrzebska, B. et al. Disruption of rhodopsin dimerization with synthetic peptides targeting an interaction interface. *J. Biol. Chem.* **290**, 25728–25744 (2015).
- Agnati, L. F., Tarakanov, A. O., Ferré, S., Fuxe, K. & Guidolin, D. Receptor-receptor interactions, receptor mosaics, and basic principles of molecular network organization: possible implications for drug development. *J. Mol. Neurosci.* **26**, 193–208 (2005).
- Fribourg, M. et al. Decoding the signaling of a GPCR heteromeric complex reveals a unifying mechanism of action of antipsychotic drugs. *Cell* **147**, 1011–1023 (2011).
- Baki, L. et al. Cross-signaling in metabotropic glutamate 2 and serotonin 2A receptor heteromers in mammalian cells. *Pflug. Arch.* **468**, 775–793 (2016).
- Schwarze, S. R., Ho, A., Vocero-Akbani, A. & Dowdy, S. F. In vivo protein transduction: delivery of a biologically active protein into the mouse. *Science* **285**, 1569–1572 (1999).
- Trifilieff, P. et al. Detection of antigen interactions ex vivo by proximity ligation assay: endogenous dopamine D₂-adenosine A_{2A} receptor complexes in the striatum. *Biotechniques* **51**, 111–118 (2011).
- Segala, E. et al. Controlling the dissociation of ligands from the adenosine A_{2A} receptor through modulation of salt bridge strength. *J. Med. Chem.* **59**, 6470–6479 (2016).

39. Chien, E. Y. et al. Structure of the human dopamine D3 receptor in complex with a D2/D3 selective antagonist. *Science* **330**, 1091–1095 (2010).
40. Sunahara, R. K., Tesmer, J. J. G., Gilman, A. G. & Sprang, S. R. Crystal structure of the adenylyl cyclase activator G(s alpha). *Science* **278**, 1943–1947 (1997).
41. Johnston, C. A. et al. Structural determinants underlying the temperature-sensitive nature of a Galpha mutant in asymmetric cell division of *Caenorhabditis elegans*. *J. Biol. Chem.* **283**, 21550–21558 (2008).
42. Tesmer, J. J., Sunahara, R. K., Gilman, A. G. & Sprang, S. R. Crystal structure of the catalytic domains of adenylyl cyclase in a complex with Gsalpha-GTPgammaS. *Science* **278**, 1907–1916 (1997).
43. Martí-Renom, M. A. et al. Comparative protein structure modeling of genes and genomes. *Annu. Rev. Biophys. Biomol. Struct.* **29**, 291–325 (2000).
44. Huang, J., Chen, S., Zhang, J. J. & Huang, X. Y. Crystal structure of oligomeric β 1-adrenergic G protein-coupled receptors in ligand-free basal state. *Nat. Struct. Mol. Biol.* **20**, 419–425 (2013).

Acknowledgements

This study was supported by the Intramural funds of the National Institute Drug Abuse, grants from the Spanish “Ministerio de Economía y Competitividad” and European Regional Development Funds of the European Union (SAF2014-54840-R, SAF2015-74627-JIN, SAF2016-77830-R and SAF2017-84117-R), and “Fundació La Marató de TV3” (20140610) and Government of Catalonia Grant (2014-SGR-1236).

Author contributions

G.N., Ar.C., V.C.-A., E.M. and N.-S.C. performed experiments. G.N., Ar.C., V.C.-A., E.M., N.-S.C., An.C. E.I.C, C.W.D, V.C., L.P., C.L. and S.F. performed data analysis and interpretation. G.N., Ar.C., C.W.D, V.C., L.P., C.L. and S.F. wrote and prepared the manuscript.

Additional information

Supplementary Information accompanies this paper at <https://doi.org/10.1038/s41467-018-03522-3>.

Competing interests: The authors declare no competing interests.

Reprints and permission information is available online at <http://npg.nature.com/reprintsandpermissions/>

Publisher's note: Springer Nature remains neutral with regard to jurisdictional claims in published maps and institutional affiliations.



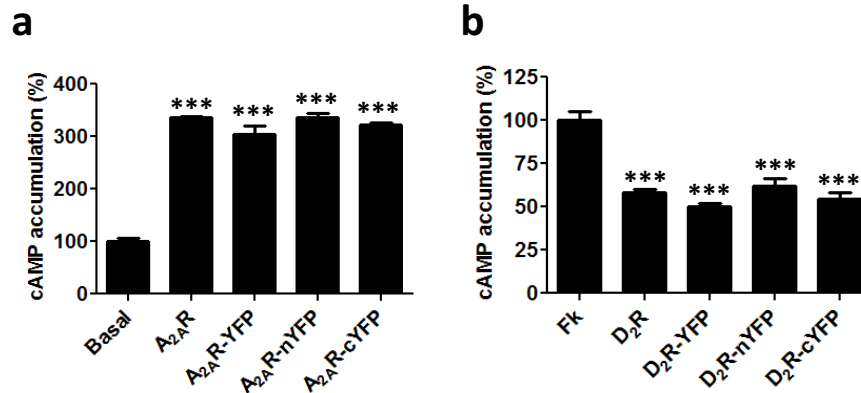
Open Access This article is licensed under a Creative Commons Attribution 4.0 International License, which permits use, sharing, adaptation, distribution and reproduction in any medium or format, as long as you give appropriate credit to the original author(s) and the source, provide a link to the Creative Commons license, and indicate if changes were made. The images or other third party material in this article are included in the article's Creative Commons license, unless indicated otherwise in a credit line to the material. If material is not included in the article's Creative Commons license and your intended use is not permitted by statutory regulation or exceeds the permitted use, you will need to obtain permission directly from the copyright holder. To view a copy of this license, visit <http://creativecommons.org/licenses/by/4.0/>.

© The Author(s) 2018

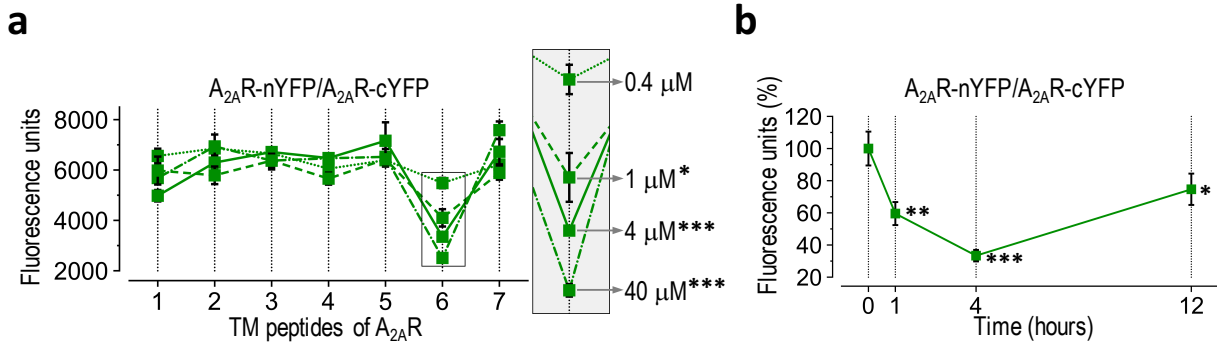
Supplementary Information

Evidence for functional pre-coupled complexes of receptor heteromers and adenylyl cyclase

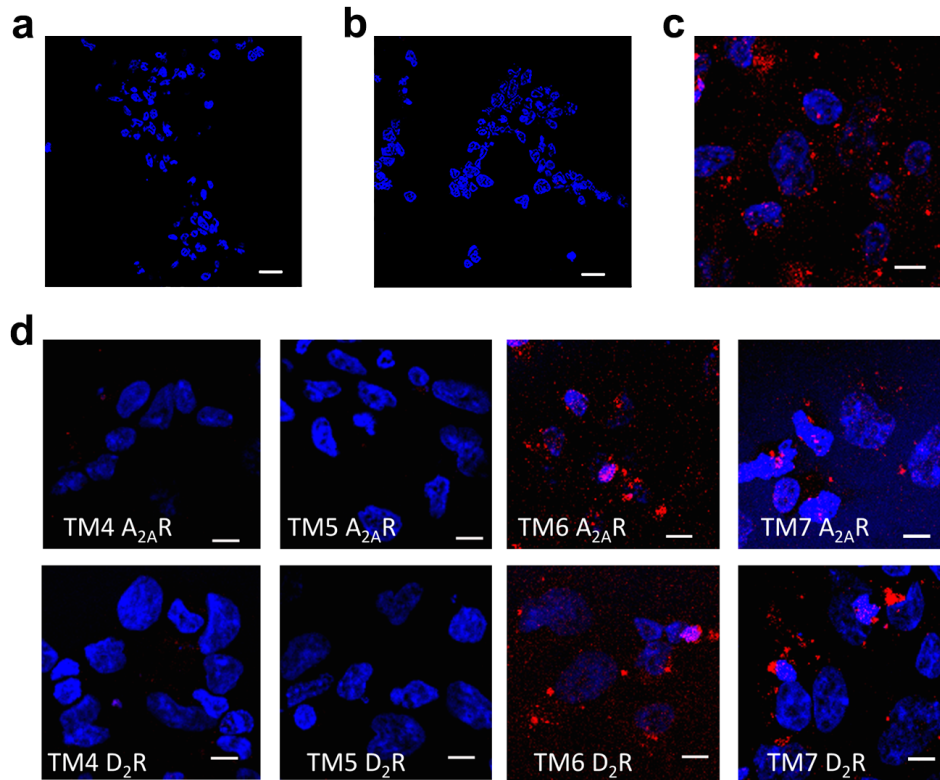
Navarro *et al.*



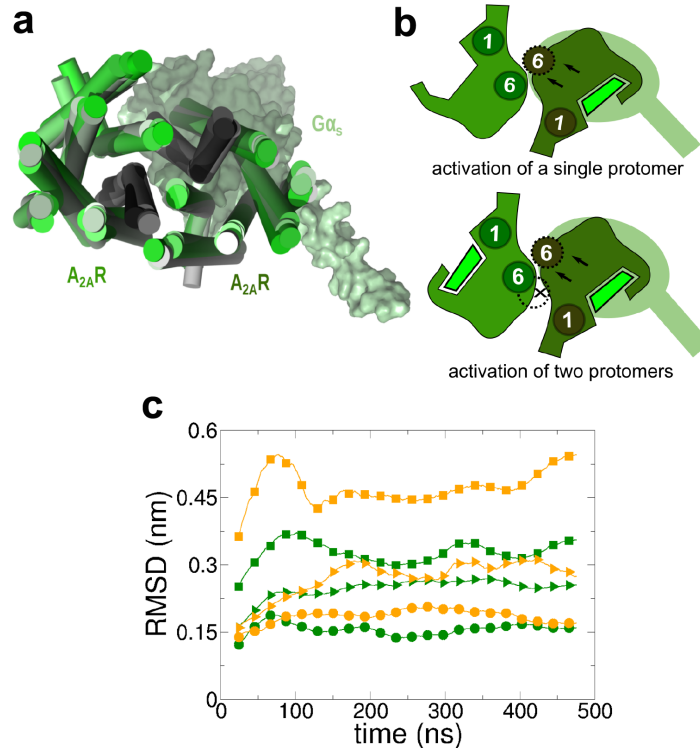
Supplementary Fig. 1 Functionality of fusion proteins. **a.** cAMP production in HEK-293T cells transfected with A_{2A}R, A_{2A}R-YFP, A_{2A}R-nYFP or A_{2A}R-cYFP cDNA (0.5 μg), stimulated with CGS 21680 (100 nM). **b.** cAMP production in HEK-293T cells transfected with D₂R, D₂R-YFP, D₂R-nYFP or D₂R-cYFP cDNA (0.75 μg), stimulated with forskolin (Fk; 0.5 μM) in the presence of quinpirole (1 μM). Values (in means ± SEM) are expressed as percentage of cAMP accumulation in non-treated cells (**a**) or as percentage of Fk-treated cells (n = 8, with triplicates) (**b**). ***: p < 0.001 as compared as compared to basal values or to Fk; no significant differences were observed with the effects of the different fusion proteins versus the respective non-fused receptor (one-way ANOVA followed by Tukey's multiple comparison tests).



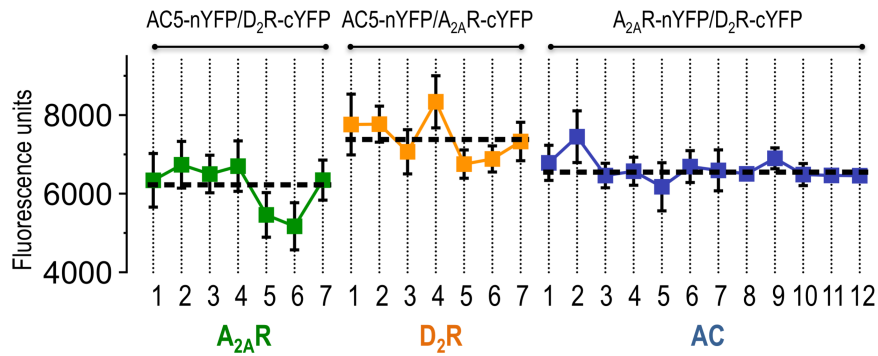
Supplementary Fig. 2 Concentration- and time-dependent destabilizing effect of A_{2A}R TM peptides. BiFC experiments in HEK-293T cells transfected with A_{2A}R-nYFP and A_{2A}R-cYFP cDNA (0.5 μg) and treated: **(a)** 4 h with different concentrations (0.4, 1, 4 and 40 μM) of TM peptides of A_{2A}R (numbered 1-7) or **(b)** with medium with A_{2A}R TM6 peptide (4 μM) during different incubation times (0, 1, 4 and 12 h). In **a**, magnification of values corresponding to A_{2A}R TM6 peptide is shown. Fluorescence (in means ± S.E.M.) was detected at 530 nm and values are expressed as fluorescence arbitrary units (n = 9, with triplicates); *, ** and *** represent significantly lower values as compared to cells treated with the 0.4 μM concentration **(a)** or with the 0-hour incubation time **(b)** (p < 0.05, p < 0.01 and p < 0.001, respectively; one-way ANOVA followed by Dunnett's multiple comparison tests).



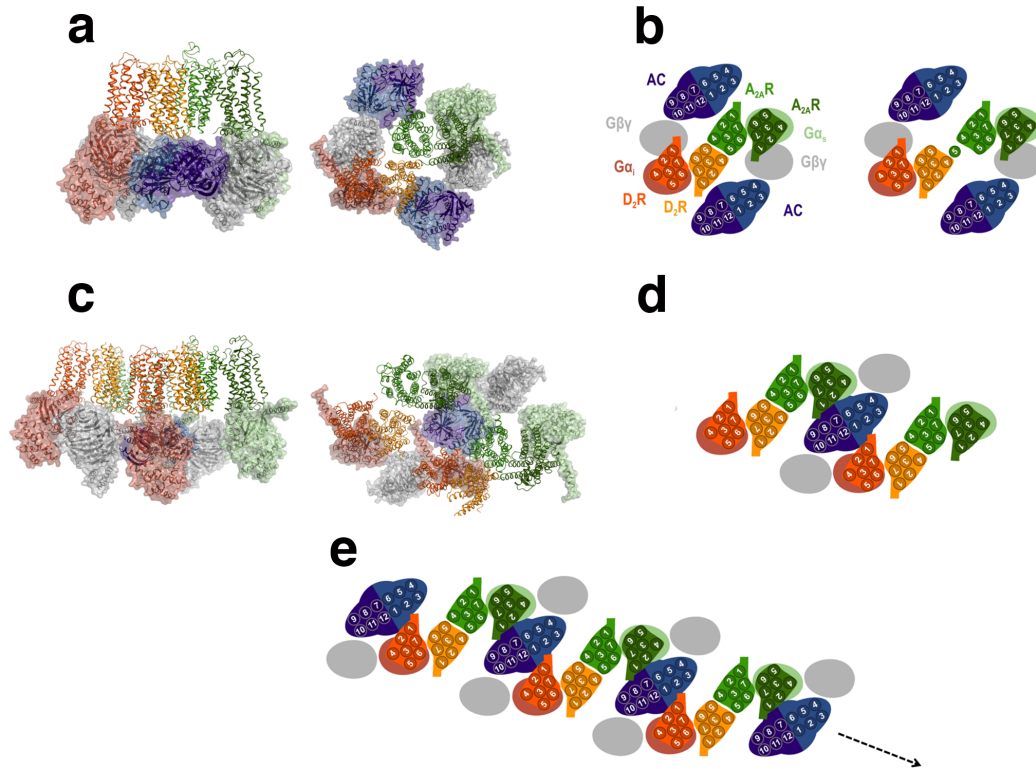
Supplementary Fig. 3 Destabilizing effect of TM peptides on A_{2A}R-D₂R heteromerization in transfected cells. Proximity Ligation assay (PLA) in HEK-293T cells transfected with 0.4 μg of A_{2A}R cDNA (a), 0.5 μg of D₂R cDNA (b) or both (c and d), treated for 4 h with medium (a-c) or with 4 μM of indicated TM peptides of A_{2A}R or D₂R (d); confocal microscopy images (superimposed sections) shows A_{2A}R-D₂R heteromers as red spots; cell nuclei were stained with DAPI (blue); scale bars: 20 μm.



Supplementary Fig. 4 Construction of computational models of the A_{2A}R homodimer in complex with G_s and the D₂R homodimer in complex with G_i. **a** and **b**. Agonist binding opens an intracellular cavity, required for the binding of the C-terminal $\alpha 5$ helix of the G-protein, mainly through the outward movement of TM 6. Thus, the structures for A_{2A}R and D₂R homodimers were modeled with TM 6 in the inactive closed conformation for the unliganded protomer and with TM 6 in the active open conformation for the G protein-bound protomer. TM 6 of the unliganded protomer interacts with TM 6 of the G protein-bound protomer (see cartoon models). It is important to note that, in these models, simultaneous outward movements of TM 6 in the homodimer is not feasible due to a steric clash between active open conformation of both TM 6. Likewise, simultaneous binding of two G proteins to the homodimer would not be possible due to a steric clash between both bulky G proteins. The structures of the A_{2A}R (inactive and G_s-bound “active”) and D₂R (inactive and G_i-bound “active”) homodimers were constructed using molecular dynamics (MD) simulations due to the absence of crystal structures of oligomers using exclusively the TM 6 interface. In **(a)**, representation of 6 evenly spaced snapshots extracted from 500 ns explicit membrane MD trajectories of the A_{2A}R homodimer in complex with G α_s ; A_{2A}R homodimers are shown as cylinders in white-to-green color gradient in relation to simulation time; G α_s is shown as a surface, and lipid and solvent molecules are not shown for clarity; similar results were obtained for the D₂R homodimer (data not shown). These results indicate that the possible rotation of “active” protomers relative to inactive protomers through the TM 6 interface is highly limited, since the accessible area of TM 6 is small. In **(c)**, time-evolution of the root-mean-square deviations (rmsd) on protein α -carbons in the MD simulations of the A_{2A}R homodimer in complex with G α_s (green) and the D₂R homodimer in complex with G α_i (orange) computed for the whole system (squares), for the homodimers (triangles), and for the residues forming TM 6 (circles). Simulations were performed with the GROMACS 5.0.6 simulation package¹, using the AMBER99SB force field and Berger parameters for POPC lipids. This procedure has been previously validated². The systems consisted on rectangular boxes containing a lipid bilayer (~380 molecules of POPC), explicit solvent (~44,000 water molecules) and a 0.15 M concentration of Na⁺ and Cl⁻.

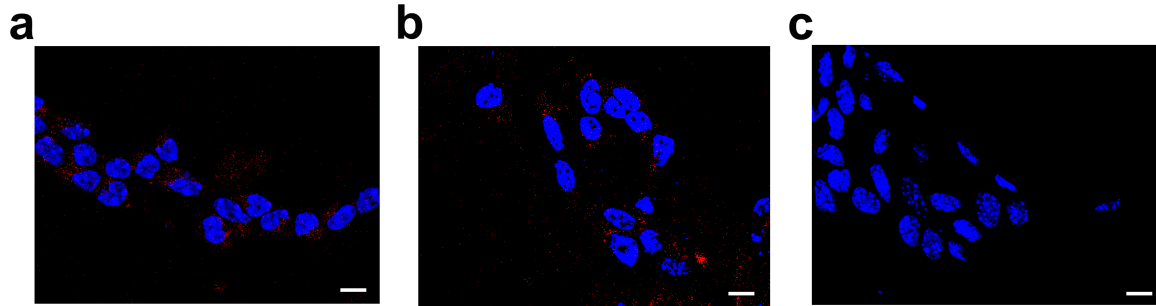


Supplementary Fig. 5 Negative controls for the disrupting effect of TMs peptides. BiFC experiments in HEK-293T cells transfected with AC5-nYFP (0.75 μ g) and D₂R-cYFP (0.75 μ g) and cDNA (AC5-nYFP/D₂R-cYFP), AC5-nYFP (0.75 μ g) and A_{2A}R-cYFP (0.5 μ g) cDNA (AC5-nYFP/A_{2A}R-cYFP) or A_{2A}R-nYFP (0.6 μ g) and D₂R-cYFP (0.6 μ g) cDNA (A_{2A}R-nYFP/D₂R-cYFP). Cells were treated for 4 h with medium (control, broken lines), TM peptides of A_{2A}R (4 μ M; numbered 1-7, green squares), TM peptides of D₂R (4 μ M; numbered 1-7, orange squares) or TM peptides of AC5 (4 μ M; numbered 1-12, blue squares). Fluorescence was detected at 530 nm and values (in means \pm S.E.M) are expressed as fluorescence arbitrary units (n = 8, with triplicates); no significant differences were observed between any of the peptide-treated groups versus the respective control (one-way ANOVA followed by Dunnett's multiple comparison tests).

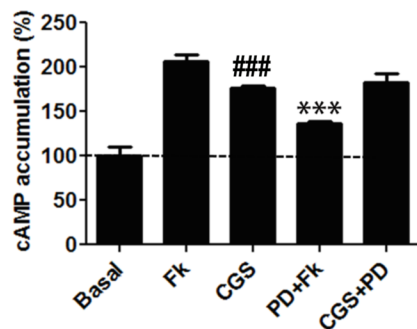


Supplementary Fig. 6 Construction of a computational model of the A_{2A}R-D₂R heterotetramer in complex with G_s, G_i and AC5 in the absence and presence of agonists. **a.** Computational molecular model of the A_{2A}R-D₂R heterotetramer in complex with G_s, G_i, and the C1 and C2 domains of AC5 in the absence of agonists viewed from the membrane (left image) and from the extracellular side (right image). The A_{2A}R-D₂R heterotetramer was built by superimposing the modeled A_{2A}R homodimer in complex with G_s and the D₂R homodimer in complex with G_i (Supplementary Fig. 2) into the oligomeric structure of the β₁-adrenoceptor (PDB code 4GPO) that contains the proposed TMs 4/5 interface between protomers³. The relative orientation of pre-coupled G proteins (G_s and G_i) relative to their bound receptors was modeled based on the crystal structure of β₂-adrenoceptor in complex with G_s (PDB code 3SN6)⁴. The topology of AC consists of a variable cytoplasmic N-terminus and two large cytoplasmic C1 and C2 domains, separated by two membrane-spanning M1 and M2 domains, each comprised by six TM helices. The TMs of the M1 and M2 domains of AC are not included in the model due to the absence of crystal structures of these domains or close protein templates suitable for accurate homology modeling. Nevertheless, the results with interfering peptides indicate a direct interaction between TM domains of AC5 and the A_{2A}R-D₂R heterotetramer. Moreover, despite there is not structural information regarding the relative localization of the C1 and C2 domains of AC5 relative to the G proteins in the inactive state, the existence of intermolecular interactions of G_sα and G_sβ subunits with the cytoplasmic N-terminus of AC5 have been reported^{5,6}. Thus, the C1 and C2 domains (PDB id 1CUL)⁷ were positioned between the A_{2A}R-D₂R heterotetramer and the G protein to facilitate these transmembrane and intracellular interactions. **b.** Scheme of the molecular model shown in A (viewed from the extracellular side); the scheme at the right side shows the effect of TM5 of A_{2A}R interfering with A_{2A}R-D₂R heteromerization and with TM-dependent oligomerization of AC5 with A_{2A}R and D₂R; NT-dependent pre-coupling of AC5 with G_sβ subunits keeps each homodimer separately functional. **c.** Computational molecular model of the A_{2A}R-D₂R heterotetramer in complex with G_s, G_i, and the C1 and

C2 domains of AC5 in the presence of agonists viewed from the membrane (left image) and from the extracellular side (right image). **d.** Scheme of the molecular model shown in C (viewed from the extracellular side). The crystal structure of the C1 and C2 domains of AC5 in complex with G α (PDB id 1CUL)⁷ was used to model the simultaneous binding of G α and G $\beta\gamma$ to a single AC5. The structure of the A_{2A}R-D₂R heterotetramer is as in panels A and B. G $\beta\gamma$ subunits were arbitrarily positioned to facilitate the interaction with the cytoplasmic N-terminus of AC5⁵. The same color code applies to schematical and tridimensional models. **e.** The experimental data suggests the possible formation of zig-zagged arranged high-order oligomeric structures, constituted by alternative links of A_{2A}R-D₂R heterotetramers and AC5 molecules. The black arrow indicates the direction of possible further expansion.



Supplementary Fig. 7 Receptor-AC5 complexes in striatal neurons in culture. Proximity Ligation assay (PLA) in striatal neurons in culture using antibodies against A_{2A}R and AC5 (**a**), D₂R and AC5 (**b**) or only AC5, as negative control (**c**); confocal microscopy images (superimposed sections) shows A_{2A}R-AC5 or D₂R-AC5 complexes as red spots; cell nuclei were stained with DAPI (blue); scale bars: 5 μ m.



Supplementary Fig. 8 Lack of canonical Gs-Gi antagonistic interaction between $A_{2A}R$ and D_4R in striatal neurons in culture. cAMP production determined in rat striatal primary cultures exposed to CGS21680 (CGS; 100 nM), the D_4R agonist PD168,077 (PD; 100 nM) or both in the absence or in the presence of forskolin (Fk; 0.5 μ M), respectively. Values (in means \pm SEM) are expressed as percentage of cAMP accumulation in non-treated cells (basal) (n = 4-6, with triplicates); ###: p < 0.001, as compared to basal values; ***: p < 0.001 as compared to Fk; no significant differences were detected between cells treated with CGS plus PD treated compared to CGS alone (one-way ANOVA followed by Tukey's multiple comparison tests).

Supplementary Table 1 Prediction of the topology of the TMs of AC5 with current algorithms

	Uniprot	TOPCONS	TMHMM	TMMOD	Phobius	Hydropathy
TM 1	196-216 ↑		194-216 ↑	196-216 ↑	197-216 ↑	1.676
TM 2	242-262 ↓	241 – 261 ↑	237-259 ↓	241-261 ↓	237-262 ↓	2.567
TM 3	268-288 ↑	268 – 288 ↓	269-287 ↑	268-288 ↑	268-288 ↑	2.614
TM 4	299-319 ↓	299 – 319 ↑	299-318 ↓	299-319 ↓	300-319 ↓	2.495
TM 5	325-345 ↑	326 – 346 ↓	328-345 ↑	328-345 ↑	325-343 ↑	1.148
TM 5b		348 – 368 ↑			350-367 ↓	2.194
TM 6	374-394 ↓	379 – 399 ↓			379-400 ↑	1.524
TM 7	770- 90 ↑	763 – 783 ↑	761-783 ↓	761-783 ↓	762-783 ↓	2.276
TM 8	792-812 ↓	789 – 809 ↓	787-809 ↑	790-810 ↑	788-813 ↑	2.119
TM 9	836-856 ↑	833 – 853 ↑	834-856 ↓	835-855 ↓	834-855 ↓	2.186
TM 10	910-930 ↓	909 – 929 ↓	909-931 ↑	910-930 ↑	909-927 ↑	1.910
TM 11	935-955 ↑	933 – 953 ↑	933-955 ↓	935-955 ↓	934-955 ↓	2.050
TM 12	984-1004 ↓	985 – 1005 ↓	984-1003 ↑	984-1004 ↑	984-1003 ↑	2.124

All algorithms predict the same 6 TMs for the M2 domain, but there is discrepancy on the predicted TMs of the M1 domain. According to TOPCONS (<http://topcons.cbr.su.se>), the first transmembrane helix corresponds to the same sequence predicted by the other algorithms for TM 2. Thus, another transmembrane helix (TM 1) is predicted more proximal to the AC5 N-terminus according to Uniprot (<http://www.uniprot.org>), TMHMM (<http://www.cbs.dtu.dk/services/TMHMM>), TMMOD (<http://liao.cis.udel.edu/website/servers/TMMOD/scripts/frame.php?p=submit>) and Phobius (<http://phobius.sbc.su.se>) algorithms. All algorithms predict the same TM 2 to TM 5, which correspond to the first four TMs according to TOPCONS. Two more TMs (TM 5b and TM 6) are then predicted according to TOPCONS and Phobius before the M2 domain and the TM 6 is also predicted by Uniprot. On the other hand, TM 5b and TM 6 are missing from TMHMM and TMMOD predictions, which leave M1 with only 5 TMs, while Phobius predicts a total of 7 TMs for the M1 domain. Outward and inward orientations are represented by upward and downward arrows, respectively. The last column indicates the average of Kyte-Doolittle hydropathy values of the putative TMs.

Supplementary Table 2 Amino acid sequence of TAT-TM peptides

A2AR-TM1	V ⁸ YITVELAIAVLAILGNVLCWAVW ³² YGRKKRRQRRR
A2AR-TM2	YGRKKRRQRRRY ⁴³ FVVSLLAAADIAVGVLAIPFAITI ⁶⁶
A2AR-TM3	L ⁷⁸ FIACFVLVLTQSSIFSLIAI ¹⁰⁰ YGRKKRRQRRR
A2AR-TM4	YGRKKRRQRRRA ¹²¹ KGIIAICWVLSFAIGLTPMLGW ¹⁴³
A2AR-TM5	M ¹⁷⁴ NYMVYFNFFACVLVPLLLMLGVYL ¹⁹⁸ YGRKKRRQRRR
A2AR-TM6	YGRKKRRQRRRL ²³⁵ AIIVGLFALCWLPPLHIINCFTFF ²⁵⁸
A2AR-TM7	L ²⁶⁷ WLMYLAIVLSHTNSVNPFIYAY ²⁹⁰ YGRKKRRQRRR
D2R-TM1	A ³⁸ TLTLLIAIVVFGNVLCMAVS ⁶⁰ YGRKKRRQRRR
D2R-TM2	YGRKKRRQRRRY ⁷¹ LIVSLAVADLLVATLVMPWVVY ⁹³
D2R-TM3	I ¹⁰⁹ FVTLDVMMCTASILNLCAISI ¹³⁰ YGRKKRRQRRR
D2R-TM4	YGRKKRRQRRRV ¹⁵² TVMISIVWVLSFTISCPLLF ¹⁷²
D2R-TM5	F ¹⁸⁹ VVYSSIVSFYVPFIVTLLVYIKIY ²¹³ YGRKKRRQRRR
D2R-TM6	YGRKKRRQRRRM ³⁷⁴ LAIVLGVFIICWLPFFITHIL ³⁹⁵
D2R-TM7	A ⁴¹⁰ FTWLGYN SAVNPIIYTTFNI ⁴³¹ YGRKKRRQRRR
AC5-TM1	YGRKKRRQRRRG ¹⁹⁶ AGPGAVLSLGACCLALLQIF ²¹⁶
AC5-TM2	L ²⁴² TMLMAVLVCLVCLVMLAFHAA ²⁶² YGRKKRRQRRR
AC5-TM2n	YGRKKRRQRRRL ²⁴² TMLMAVLVCLVCLVMLAFHAA ²⁶²
AC5-TM3	YGRKKRRQRRRL ²⁶⁸ PYLAVLAAAVGVILIMAVLC ²⁸⁸
AC5-TM3n	L268PYLAVLAAAVGVILIMAVLC ²⁸⁸ YGRKKRRQRRR
AC5-TM4	G ²⁹⁹ LACYALIAVVLAVQVVGLL ³¹⁹ YGRKKRRQRRR
AC5-TM4n	YGRKKRRQRRRG ²⁹⁹ LACYALIAVVLAVQVVGLL ³¹⁹
AC5-TM5	YGRKKRRQRRRA ³²⁵ SEGIWWTVFFIYTIYTLTPV ³⁴⁵
AC5-TM5n	A ³²⁵ SEGIWWTVFFIYTIYTLTPV ³⁴⁵ YGRKKRRQRRR
AC5-TM5s	YGRKKRRQRRRLFATVITEVGSIPFYWWIYT
AC5-TM5b	YGRKKRRQRRRA ³⁴⁹ AVLSGVLLSALHLAIAL ³⁶⁶
AC5-TM6	F ³⁷⁴ LLKQLVSNVLFISCTNIVGV ³⁹⁴ YGRKKRRQRRR
AC5-TM6n	YGRKKRRQRRRF ³⁷⁴ LLKQLVSNVLFISCTNIVGV ³⁹⁴
AC5-TM7	YGRKKRRQRRRL ⁷⁷⁰ VFLFICFVQITIVPHSIFML ⁷⁹⁰
AC5-TM8	F ⁷⁹² YLTCSLLLTLVVFVSVIYSC ⁸¹² YGRKKRRQRRR
AC5-TM9	YGRKKRRQRRRL ⁸³⁶ VGVFITLVFLAAFVNMFTC ⁴⁵⁶
AC5-TM10	F ⁹¹⁰ TYSVLLSLLACSVFLQISCI ⁹³⁰ YGRKKRRQRRR
AC5-TM11	YGRKKRRQRRRL ⁹³⁵ MLAIELIYVLIVEVPGVTLF ⁹⁵⁵
AC5-TM12	V ⁹⁸⁴ ALKVVTPHISVFLALYLH ¹⁰⁰⁴ YGRKKRRQRRR

References

1. Pronk, S. et al. GROMACS 4.5: a high-throughput and highly parallel open source molecular simulation toolkit. *Bioinformatics* **29**, 845-854 (2013).
2. Cordoní, A., Caltabiano, G. & Pardo, L. Membrane Protein Simulations Using AMBER Force Field and Berger Lipid Parameters. *J. Chem. Theory Comput.* **8**, 948-958 (2012).
3. Martí-Renom, M. A. et al. Comparative protein structure modeling of genes and genomes. *Annu. Rev. Biophys. Biomol. Struct.* **29**, 291-325 (2000).
4. Rasmussen, S. G. et al. Crystal structure of the β_2 adrenergic receptor-Gs protein complex. *Nature* **477**, 549-555 (2011).
5. Sadana, R., Dascal, N. & Dessauer, C. W. N terminus of type 5 adenylyl cyclase scaffolds Gs heterotrimer. *Mol. Pharmacol.* **76**, 1256-1264 (2009).
6. Xie, K. et al. Stable G protein-effector complexes in striatal neurons: mechanism of assembly and role in neurotransmitter signaling. *Elife* **4**, e10451 (2015).
7. Tesmer, J. J., Sunahara R. K., Gilman, A. G. & Sprang, S. R. Crystal structure of the catalytic domains of adenylyl cyclase in a complex with G α -GTP γ S. *Science* **278**, 1907-1916 (1997).

Chapter 3. Design of a true bivalent ligand with picomolar binding affinity for a G protein-coupled receptor homodimer

Pulido D*, **Casadó-Anguera V***, Pérez-Benito L*, Moreno E, Cordero A, López L, Cortés A, Ferré S, Pardo L*, Casadó V*, Royo M*.

Journal of Medicinal Chemistry, submitted

Design of a true bivalent ligand with picomolar binding affinity for a G protein-coupled receptor homodimer

Daniel Pulido,^{†,‡,#} Verònica Casadó-Anguera,^{§,||,⊥,#} Laura Pérez-Benito,^{∇,#} Estefanía Moreno,^{§,||,⊥} Arnau Cordoní,[∇] Laura López,[∇] Antoni Cortés,^{§,||,⊥} Sergi Ferré,[¶] Leonardo Pardo,^{} ∇ Vicent Casadó^{*,§,||,⊥} and Miriam Royo^{*,†,‡}*

[†] Biomedical Research Networking Center in Bioengineering, Biomaterials and Nanomedicine (CIBER-BBN), Barcelona Science Park, 08028 Barcelona, Spain

[‡] Combinatorial Chemistry Unit, Barcelona Science Park, 08028 Barcelona, Spain

[§] Department of Biochemistry and Molecular Biomedicine, Faculty of Biology, University of Barcelona, 08028 Barcelona, Spain

^{||} Biomedical Research Networking Center in Neurodegenerative Diseases (CIBERNED), 08028 Barcelona, Spain

[⊥] Institute of Biomedicine of the University of Barcelona (IBUB), 08028 Barcelona, Spain

[∇] Laboratory of Computational Medicine, Biostatistics Unit, Faculty of Medicine, Universitat Autònoma de Barcelona, 08193 Bellaterra, Spain

[¶] Integrative Neurobiology Section, National Institute on Drug Abuse, Intramural Research Program, National Institutes of Health, Baltimore, MD 21224

ABSTRACT

Bivalent ligands have emerged as chemical tools to study G protein-coupled receptor dimers. Using a combination of computational, chemical, and biochemical tools, here we describe the design of bivalent ligand **13** with high affinity ($K_{DBI}=21$ pM) for the dopamine D₂ receptor (D₂R) homodimer. Bivalent ligand **13** enhances the binding affinity relative to monovalent compound **15** by 37-fold, indicating simultaneous binding at both protomers. Using synthetic peptides with amino acid sequences of transmembrane (TM) domains of D₂R, we provide evidence that TM6 forms the interface of the homodimer. Notably, the disturber peptide TAT-TM6 decreased the binding of bivalent ligand **13** by 52-fold and had no effect on monovalent compound **15**, confirming the D₂R homodimer through TM6 *ex-vivo*. In conclusion, using a versatile multivalent chemical platform, we have developed a precise strategy to generate a true bivalent ligand that simultaneously targets both orthosteric sites of the D₂R homodimer.

INTRODUCTION

It is now well accepted that many G protein-coupled receptors (GPCRs) form, in addition to functional monomers,¹ dimers and higher-order oligomeric complexes constituted by a number of equal (homo) or different (hetero) monomers.² Oligomerization plays an important role in terms of receptor function and structure, introducing changes in signaling pathways which are due to the allosteric mechanisms of these complexes. Thus, these oligomers present functional properties different from those of the constituent monomers (protomers), making oligomerization a biological resource to generate pharmacological diversity.³ Considering the involvement of GPCRs in the regulation of many physiological processes, these novel functional units have recently received special attention as new targets for drug development.⁴ Besides the set of existing biochemical and biophysical tools,⁵ to gain insight into the mechanisms by which oligomers signal, specific chemical tools can also contribute to evaluate their pharmacology and to assess their potentiality as drug targets.

One of these tools are bivalent ligands, defined as single chemical entities composed of two pharmacophore units covalently linked by an appropriate linker/spacer. These ligands are designed to interact simultaneously with a (homo/hetero) GPCR dimer to enhance affinity and subtype selectivity.⁶ Homobivalent ligands contain two copies of the same pharmacophore,⁷ whereas heterobivalent ligands link two different pharmacophores.⁸ A requirement for bivalent ligands is the simultaneous binding of the two pharmacophores at the orthosteric sites of the (homo/hetero) dimer. Thus, the linker/spacer length is a key factor in these ligands and depends on the dimer interface, the structure of the pharmacophores, and the geometry of the attachment points.⁹ If the spacer length is not suitable to cover the distance between the orthosteric sites of both GPCR dimer protomers these ligands act in a non-simultaneous interaction mode, with a dual-acting profile.¹⁰ Other types of ligands composed by two pharmacophores connected by a linker, but designed to interact simultaneously with orthosteric and allosteric sites, are referred as bitopic ligands.¹¹

Considering the above-mentioned diversity of interaction modes of these types of compounds, the generation of a bivalent ligand requires not only a precise design, but also an accurate validation of its type of interaction. Using a combination of computational, chemical and biochemical tools, here we describe the design of a true bivalent ligand with high affinity for the dopamine D₂ receptor (D₂R) homodimer. We have selected the D₂R as a test case for two reasons: a) because it forms homo/heterodimers¹² and higher-order oligomers¹³ implicated in several neuropsychiatric disorders, such as Parkinson disease or schizophrenia;¹⁴ and b) due to the existing controversy regarding the interaction mode of some of the described D₂R homodimer bivalent ligands.¹⁵

RESULTS AND DISCUSSION

Design. The design of bivalent ligands requires the selection of: *i.* a scaffold that contains at least two chemical functionalities that can be properly derivatized; *ii.* a ligand that binds the orthosteric binding site with high affinity (pharmacophore unit); *iii.* an appropriate length spacer to cover the distance between both protomers; and, finally, *iv.* if necessary, a linker between this pharmacophore and the bivalent system, adequate in terms of both the topological position of the attachment point and the chemistry used for the conjugation (Figure 1).⁹

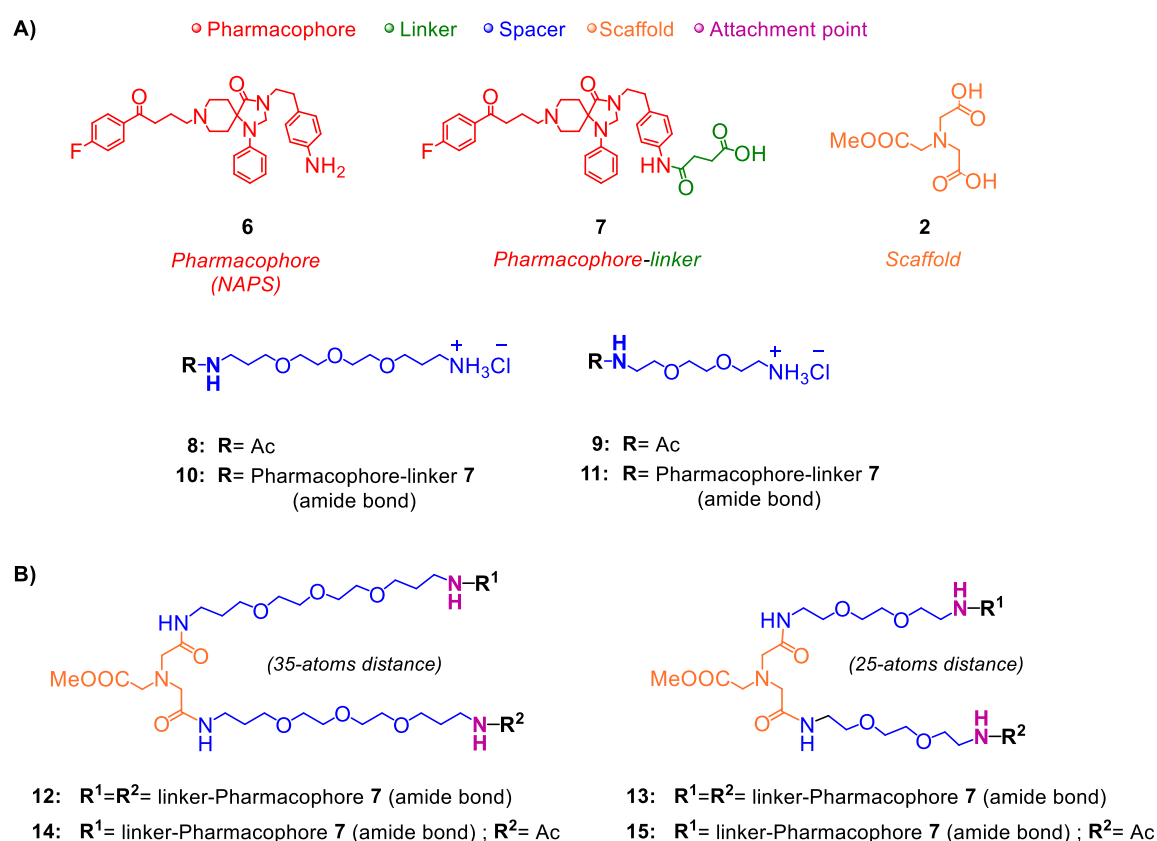


Figure 1. A) Components for the design of bivalent ligands. B) Bivalent ligands (**12-13**) and their corresponding monovalent counterparts (**14-15**).

Herein, the selected scaffold (*i*) is the nitrilotriacetic acid (NTA), which contains three symmetric carboxylic acids and permits the controlled desymmetrization of each of these

functional groups.¹⁶ This multivalent platform allows not only the attachment of two pharmacophore units, but also the introduction of a reporter molecule for imaging studies or another pharmacophore unit to study higher-order oligomers, such as trimers.¹⁷

As a proof of concept, a neutral antagonist has been selected as pharmacophore with the aim to design bivalent ligands whose potential simultaneous interaction with the D₂R homodimer would result only in increased affinity values, avoiding cooperative mechanisms that could difficult the evaluation of the interaction mode. The selected pharmacophore unit (*ii*) is a derivative of the D₂R antagonist spiperone, namely the *N*-(*p*-aminophenethyl)spiperone **6** (NAPS),¹⁸ which was functionalized with an extra succinic acid linker (*iv*) to facilitate its incorporation to the bivalent system (Figure 1). The resulting pharmacophore-linker derivative **7** was docked into a D₃-based homology model of D₂R to determine the orientation of the linker and the attachment point at the extracellular domain (Figure S1). Results showed that the pharmacophore unit (red) remains highly stable at the binding site during the simulation, whereas the linker moiety (green) is very flexible and achieves diverse conformations between extracellular loops (ECL) 2 and 3, always at the extracellular aqueous environment, which makes the selected attachment point (purple) adequate to link the spacer moieties.

The selected spacers (*iii*) were different length oligoethylene glycol (OEG) moieties with the aim to increase water solubility of the final bivalent ligands. A key factor in the design of bivalent ligands is the spacer length, which depends on the dimer interface. Crystal structures of GPCRs display several dimerization interfaces¹⁹ that can be grouped into three clusters, depending on the transmembrane helices (TMs) involved: TMs 1 and 2 (TM1/2 interface), TMs 4 and 5 (TM4/5 interface), and TMs 5 and 6 (TM5/6 interface). Using a MOE-based tool we calculated, for each different interface, a protein surface for the D₂R homodimer in complex with derivative **7** (Table S1). The shortest path across the surface between the attachment points of **7** was used to fit and optimize the different length spacers. The TM5/6 dimerization interface led to the ligand with the shortest spacer (25-atoms), because this interface has the shortest distance between orthosteric sites (33 Å), and also the attachment point directs toward TMs 5 and 6 (Figure S1, Table S1). The TM4/5 interface gave the largest spacer (43-atoms, 43 Å), whereas the TM1/2 interface is in between (31 atoms, 36 Å) (Table S1). Based on these data, we designed two bivalent ligands: **13** (25-atoms spacer), representing the shortest possible bivalent interaction (via TM5/6), and a longer alternative, **12** (35-atoms), which could also interact at other dimer interaction interfaces, excluding TM4/5, which is on the opposite side to the direction of the linker elongation, and therefore implausible to reach it.

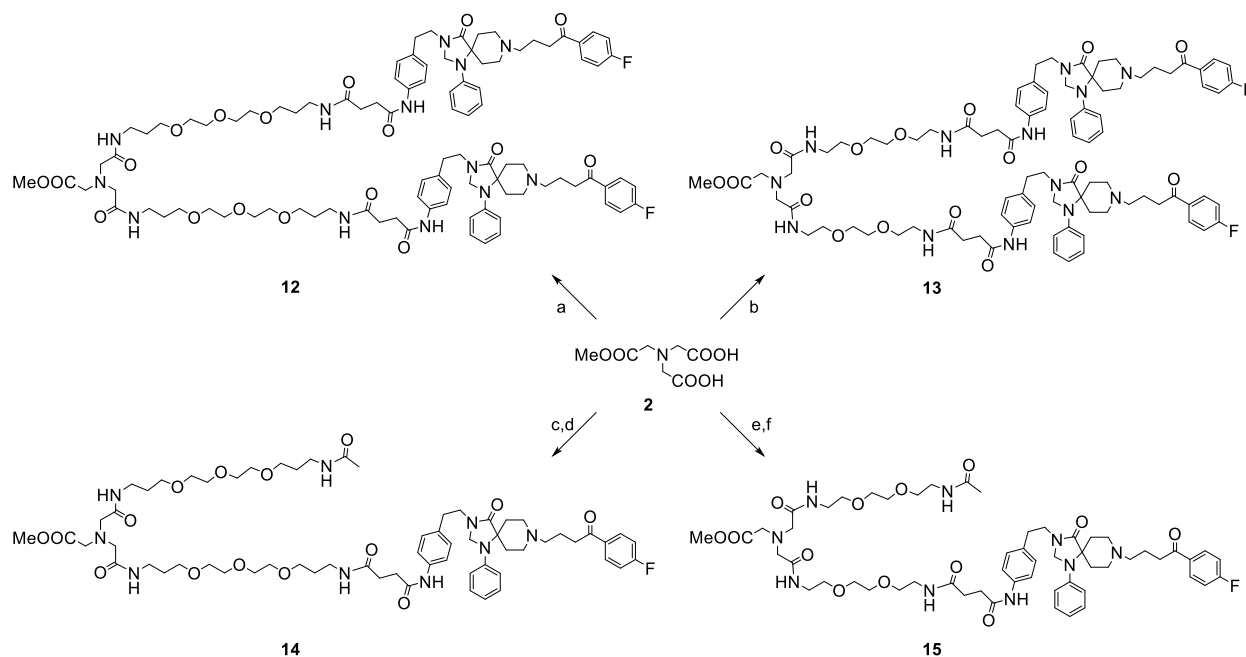
Chemical synthesis. The NTA-based core **2** was prepared starting from glycine methyl ester hydrochloride, which was dialkylated with benzyl bromoacetate, and then hydrogenated to remove the benzyl protecting groups, affording desired compound in 83% yield (Scheme S1).²⁰

The pharmacophore-linker derivative **7** was prepared following the described procedures with minor modifications.^{18a} Briefly, the *N*-alkylation of spiperone with 4-(*N*-*tert*-

butyloxycarbonyl)aminophenethyl bromide afforded **5** in 65% yield. Removal of Boc group using HCl (2 M in dioxane) provided NAPS (**6**, 66% yield) which was subsequently acylated with succinic anhydride to afford compound **7** (90% yield).

OEG-based precursors **8**, **10** and **9**, **11** were prepared from commercially available OEGs in good yields (88% for **8**, 87% for **9**, and 57% for **10**, 56% for **11**) (Scheme S3). The final bivalent ligands **12** and **13** were synthesized by acylation of two carboxylic acids of the NTA scaffold (**2**) with compounds **10** or **11**, respectively (Scheme 1). Finally, the synthesis of monovalent ligands **14** and **15** required differentiation between the free carboxylic acids of **2**. This desymmetrization was accomplished by means of the favored formation of a six-membered ring cyclic anhydride between the pair of carboxylic acids, which reacted selectively with only one equivalent of **8** or **9** to form the amide. Then, the resulting free carboxylic acid could be acylated in a further step using the corresponding compounds **10** or **11** respectively (Scheme 1).

Scheme 1. ^a Synthesis of the bivalent ligands **12** and **13** and the monovalent ligands **14** and **15**.



^a Reagents and conditions: (a) **10**, EDC·HCl, HOBt·H₂O, DIEA, DMF, rt, 16 h (49%); (b) **11**, EDC·HCl, HOBt·H₂O, DIEA, DMF, rt, 16 h (64%); (c) EDC·HCl, dry DMF, rt, 2 h, then **8**, DIEA, dry DMF, rt, 90 min (79%); (d) **10**, EDC·HCl, HOBt·H₂O, DIEA, DMF, rt, 16 h (25%); (e) EDC·HCl, dry DMF, rt, 2 h, then **9**, DIEA, dry DMF, rt, 90 min (80%); (f) **11**, EDC·HCl, HOBt·H₂O, DIEA, DMF, RT, 16 h (24%).

Biological assays. *In vitro* binding affinities of the bivalent ligands (**12** and **13**) and the corresponding monovalent counterparts (**14** and **15**) were obtained from [³H]YM-09151-2 radioligand competition-binding assays using membranes from sheep brain striatum that naturally express D₂R. Data were analyzed according to a ‘two-state dimer model’ (Table 1).²¹ The model assumes GPCR dimers as a main functional unit and provides a more robust analysis of parameters obtained from saturation and competition experiments with orthosteric ligands, as compared with the commonly used ‘two-independent-site

model'.^{21,22} In competition experiments the model analyzes the interactions of the radioligand with a competing ligand and it provides the affinity of the competing ligand for the first protomer in the unoccupied dimer (K_{DB1}) and the affinity of the competing ligand for the second protomer when the first protomer is already occupied by the competing ligand (K_{DB2}). All studied compounds show monophasic non-cooperative curves, as expected for an antagonist with a non-cooperative binding to D₂R dimer. In these conditions, K_{DB1} is enough to characterize the binding of these compounds.

Table 1. Affinity constants (K_{DB1}) of the D₂R ligands **7**, **12-15** with or without TM6 peptides.

Compound	K_{DB1} (nM)	+ TM6 D ₂ R	+ TM6 A _{2A} R
7	0.70±0.06		
12	0.07±0.03*###		
13	0.021±0.003**###	1.1±0.3^^	0.05±0.01
14	1.5±0.6*		
15	0.77±0.04	0.8±0.2	0.8±0.2

Values are mean±SEM from 3-10 determinations. Statistical significance was calculated by one-way ANOVA followed by Bonferroni's post hoc test. *p<0.05, **p<0.01 compared with **7**. ###p<0.001 compared with the corresponding monovalent ligand. ^^p<0.01 compared with the respective control without TM peptides

Compound **7** has high affinity for D₂R (K_{DB1} =0.70 nM). Monovalent compound **15** (25-atoms, K_{DB1} =0.77 nM) has similar affinity for D₂R than compound **7**, whereas monovalent compound **14** (35-atoms, K_{DB1} =1.5 nM) shows a slightly less favorable binding affinity. These results are remarkable since attachment of the spacer should decrease binding affinity unless it has an enthalpic contribution to binding. This suggests that the OEG spacer favorably interacts with residues at the groove connecting both protomers. Notably, bivalent ligands **12** (35-atoms, K_{DB1} =0.07 nM) and **13** (25-atoms, K_{DB1} =0.021 nM) significantly enhance the binding affinity relative to monovalent counterparts **14** and **15** (21-fold and 37-fold, respectively). Clearly, addition of the second pharmacophore unit increases binding affinity due to its higher local concentration in a close radius above the second protomer. Thus, compounds **12** and **13** seem to act as bivalent ligands, that is, both pharmacophores simultaneously target both orthosteric sites of the homodimer.

To further test that the antagonistic nature of these compounds on D₂R signaling remains unaltered, we resolved the real-time signaling signature by using a label-free method (DMR).²³ This approach detects changes in local optical density due to cellular mass movements induced upon receptor activation (see Experimental Section). The magnitude of the signaling by sumanirole, a highly selective D₂R full agonist, significantly decreased in the presence of both bivalent ligands **12** and **13** as much as when adding spiperone (Figure S2). Because the affinity of compound **13** is 3.5-fold higher than **12**, additional biochemical experiments were carried out with **13** and its

corresponding monovalent counterpart **15**. Compound **13** at 100 nM was significantly more efficient ($57\pm 2\%$) antagonizing sumanirole signal (100%) than 200 nM of the corresponding monovalent ligand **15** ($74\pm 3\%$), given that **13** has higher affinity than **15** (Figure 2).

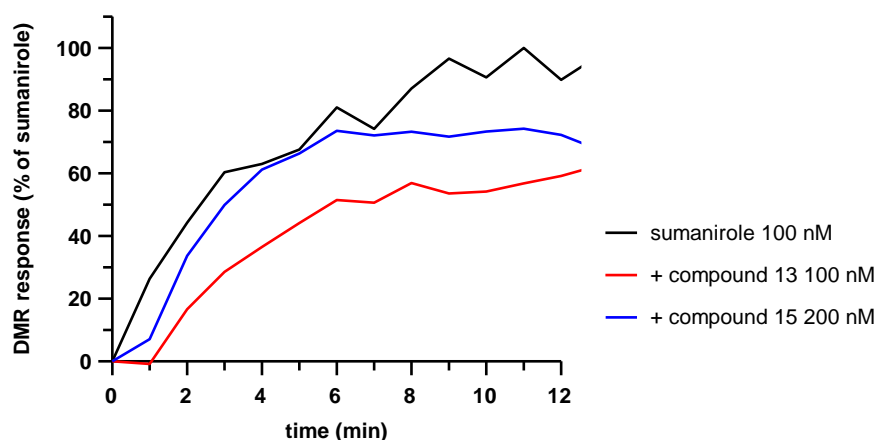


Figure 2. Antagonistic effect of compounds **13** and **15** on global cellular response induced by sumanirole determined by DMR assay in CHO cells stably co-expressing D₂R and A_{2A}R. This panel is a representative experiment of $n = 3$ different experiments. Each curve is the mean of a representative optical trace experiment carried out in triplicates. Data is presented as percentage of the effect of sumanirole 100 nM at 11 minutes after the addition of the agonist (maximal effect).

Because of the higher affinity of **13**, we predicted the TM5/6 interface for homodimerization of D₂R. To validate this hypothesis with a bimolecular fluorescence complementation (BiFC) assay, we used synthetic peptides with the amino acid sequence of TMs 5 and 6 and TM7 (negative control) of D₂R fused to the cell-penetrating HIV transactivator of transcription (TAT) peptide to alter inter-protomer interactions.^{13,24} In this assay, two complementary halves of YFP (Venus variant; cYFP and nYFP) are separately fused to the D₂ receptor and the fluorescence is obtained after reconstitution of the functional YFP when the D₂ receptors homodimerize. Only the transmembrane peptide TAT-TM6 bound to the receptor and disturbed the quaternary structure of the homodimer, causing a significant fluorescence decrease (Figure 3), indicating that only TM6 forms the interface of the D₂R homodimer, according to the recently reported results.²⁴

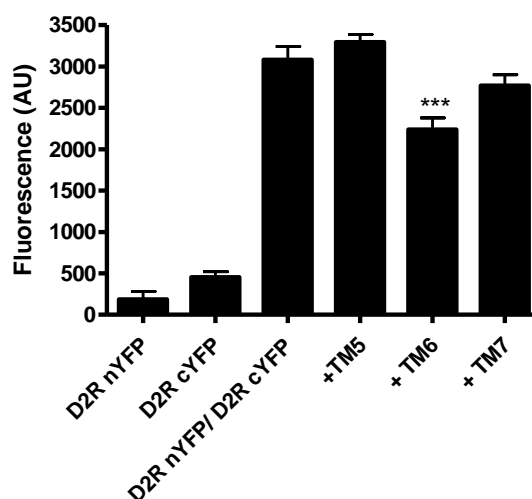


Figure 3. Effect of TM peptides on disturbance of the D₂R homodimer. Values are mean±SEM from 6-9 determinations. Statistical significance was calculated by one-way ANOVA followed by Bonferroni's post hoc test. ***p<0.001 compared to non TM treated complementation.

Because we have identified the TM6 peptide as a disturber of the inter-protomer interaction, we tested the binding affinity of compounds **13** and **15** in the presence of TM6 peptides of D₂R and adenosine A₂R (negative control) in native tissue (Figure 4). Neither TM6 peptide of D₂R nor A₂R influenced the binding of monovalent compound **15**. In contrast, TM6 peptide of D₂R, but not TM6 peptide of A₂R, decreased the binding of the bivalent ligand **13** (K_{DB1} (**13**)=0.021nM vs. K_{DB1} (**13**+TM6)=1.1nM). Remarkably, in the presence of the TM6 peptide of D₂R, bivalent compound **13** performed as the monovalent compound **15** (K_{DB1} (**13**+TM6)=1.1nM vs. K_{DB1} (**15**)=0.77nM).

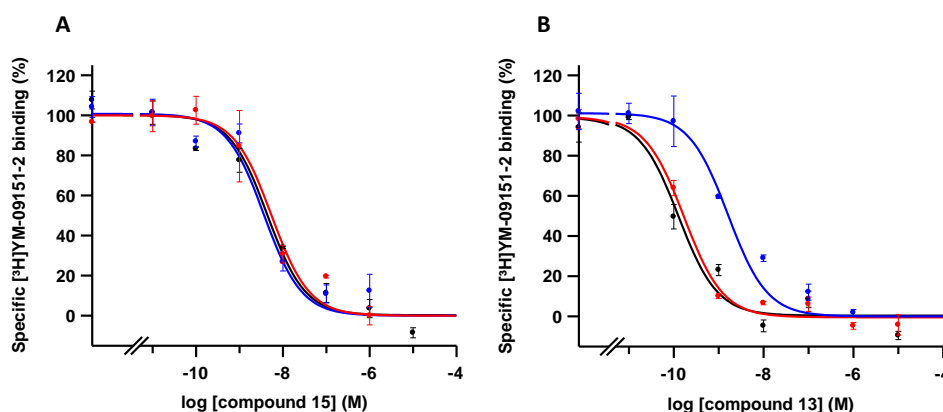


Figure 4. Effect of TM peptides on competition experiments of [³H]YM-09151-2 vs. D₂R ligands. Competition curves with increasing concentrations of monovalent **15** (in A) or bivalent **13** (in B) D₂R ligands in the absence (black) or in the presence of TM6 of A₂AR (red) or TM6 of D₂R (blue), using membranes from sheep brain striatum. Data are mean±SEM from a representative experiment (n=3) performed in triplicate.

This suggests that the TM6 peptide alters the homodimer in such a way that compound **13** binds the orthosteric binding site of the first protomer without reaching the second one. These results show the importance of the simultaneous binding of the two

pharmacophore units at both orthosteric sites of the homodimer for obtaining an improvement in affinity, and confirm the inter-protomer interaction of D₂R homodimer through TM6. These results also ratify the bivalent interaction mode of compound **13**, validating it as a true bivalent ligand.

Molecular modelling of bivalent ligand 13 into D₂R homodimer model. Accordingly, we constructed a computational model of the D₂R homodimer, using exclusively TM6 as the molecular interface, and performed microsecond timescale molecular dynamics (MD) simulations to evaluate the stability of compound **13** in the model (Figure 5). This TM6 interface predicts similar distances between orthosteric binding sites than the TM5/6 interface, thus, leading to the same number of atoms for the spacer. The MD simulations showed that compound **13** comfortably fulfills and maintains simultaneous binding of the two pharmacophoric units at both orthosteric sites throughout the simulation, thus, providing further confidence in the bivalent interaction and the picomolar binding affinity.

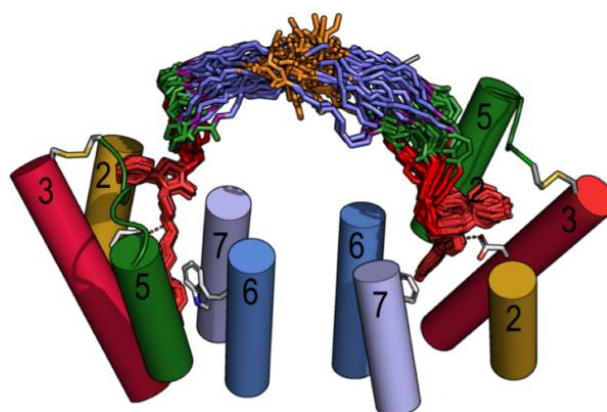


Figure 5. Evolution of bivalent ligand **13** (20 structures collected every 50 ns) in the D₂R homodimer, constructed via the TM6 interface, as devised from MD simulations. The color code is as in Figure 1. A detailed analysis of the simulation (Figure S3) confirms that the designed bivalent ligand **13** remains stable at the orthosteric binding cavities through the unbiased 1 μ s MD simulation.

CONCLUSIONS

We have developed a precise strategy to create bivalent ligands of GPCR (homo/hetero) dimers based on a versatile multivalent chemical platform. The use of computational tools that consider the TM interfaces, distances between orthosteric binding sites and mode of interaction of the pharmacophore units, allows a reduction in the number of synthesized bivalent ligands, yet a high success in the affinity results. Bivalent ligand **13** showed picomolar binding affinity, and the use of different TAT-TM6 disturber peptides allowed the confirmation, in native tissue, of its simultaneous interaction with both orthosteric sites of the D₂R homodimer, constituted through TM6. Furthermore, our results confirm the recently described interface interaction of D₂R homodimer through TM6.

This strategy can be applied to other GPCR oligomers, thus allowing the generation and validation of novel ligands with a clear bivalent interaction mode. These ligands can be used as pharmacological tools in combination with disturber TM peptides to validate inter-protomer GPCR interactions, both *in vitro* and in native tissue, and this information could be potentially used for the design of new therapeutic compounds targeting GPCR oligomers.

EXPERIMENTAL SECTION

General Methods. Reagents and solvents were purchased from commercial sources and were used without further purification. TLC was performed on Merck 60F254 silica plates were visualized by UV light (254 nm), or by potassium permanganate stains. Flash chromatography on silica was carried out on a Teledyne Isco Combiflash Rf instrument using Rediseq Rf silica columns. ¹H-NMR (400 MHz) and ¹³C-NMR (101 MHz) spectroscopy was performed on a Varian Mercury 400 MHz instrument at the NMR unit of the Scientific and Technological Centers of the University of Barcelona (CCiTUB). Chemical shifts (δ) are expressed in ppm relative to tetramethylsilane (TMS). Coupling constants (J) are expressed in Hertz (Hz). The following abbreviations are used to indicate multiplicity: s: singlet; d: doublet, t: triplet, m: multiplet, and br: broad signal. Analytical RP-HPLC and mass spectra were performed on a Waters Alliance 2795 with an automated injector and a photodiode array detector Waters 2996 coupled to an electrospray ion source (ESI-MS) Micromass ZQ mass detector, using a XSelectTM C₁₈ reversed-phase analytical column (4.6 mm×50 mm, 3.5 μ m), and the MassLynx 4.1 software. The instrument was operated in the positive ESI (+) ion mode. Analyses were carried out with several elution systems. System A: a linear gradient 5–100% CH₃CN (0.07% HCOOH) in H₂O (0.1% HCOOH) over 4.5 min at a flow rate of 2 mL/min; and System B: a linear gradient 5–100% CH₃CN (0.07% HCOOH) in H₂O (0.1% HCOOH) over 3.5 min at a flow rate of 1.6 mL/min. High-Resolution Mass Spectroscopy (HRMS) was carried out using an LC/MSD-TOF spectrometer from Agilent Technologies, at the molecular characterization mass spectrometry unit of the Scientific and Technological Centers of the University of Barcelona (CCiTUB). Semi-preparative RP-HPLC purification was performed on a Waters system with a 2545 binary gradient module, a 2767 manager collector and a 2489 UV detector, coupled to an electrospray ion source

(ESI-MS) Micromass ZQ mass detector, and the MassLynx 4.1 software. Gradients and columns used are detailed in each case.

Synthesis. *N,N*-bis(benzyloxycarbonylmethyl)-glycine methyl ester (**1**). To a suspension of glycine methyl ester hydrochloride (1.00 g, 7.96 mmol, 1.0 eq) and K₂CO₃ (4.85 g, 35.1 mmol, 4.4 eq) in acetonitrile (30 mL) was added a solution of benzyl bromoacetate (2.8 mL, 17.7 mmol, 2.2 eq) in acetonitrile (8 mL). The resulting mixture was stirred at room temperature overnight (20 h). After this time the solvents were evaporated to dryness. The crude was suspended in CH₂Cl₂ (50 mL) and washed with saturated NaHCO₃ (2×50 mL) and brine (1×50 mL). The organic phase was dried over MgSO₄ and evaporated. The resulting crude was purified by flash chromatography on silica using hexane and ethyl acetate as solvents (5 to 30% ethyl acetate in hexane), affording compound **1** (2.57 g, 6.67 mmol, 84%). ¹H NMR (400 MHz, CDCl₃, 298 K) δ 7.38 – 7.28 (m, 10H), 5.13 (s, 4H), 3.72 (s, 4H), 3.68 (s, 2H), 3.67 (s, 3H); ¹³C NMR (101 MHz, CDCl₃, 298 K) δ 171.3, 170.7, 135.6, 128.7, 128.4, 128.4, 66.6, 55.3, 55.1, 51.8; HPLC: System A, t_R: 3.48 min, >99% (214 nm); MS: calculated exact mass for C₂₁H₂₄NO₆: 386.2 [M+H]⁺, found by HPLC-MS (ESI): 385.9.

N,N-bis(carboxymethyl)-glycine methyl ester (**2**). Compound **1** (1.80 g, 4.67 mmol, 1.0 eq) was dissolved in MeOH (25 mL) and 10% Pd/C (0.18 g, 10% w/w) was added to this solution. The resulting suspension was stirred at room temperature for 3 h under H₂ atmosphere. The catalyst was removed by filtration through Celite and the solvent was evaporated to dryness to afford compound **2** (950 mg, 4.63 mmol, 99%). ¹H NMR (400 MHz, D₂O, 298 K) δ 4.29 (s, 2H), 4.09 (s, 4H), 3.83 (s, 3H); ¹³C NMR (101 MHz, D₂O, 298 K) δ 169.7, 168.0, 56.0, 54.6, 53.3; MS: calculated exact mass for C₇H₁₂NO₆: 206.1 [M+H]⁺, found by HPLC-MS (ESI): 205.8.

4-(*N*-*tert*-butoxycarbonyl)aminophenethyl bromide (**3**). To a suspension of 4-aminophenethyl alcohol (2.15 g, 15.7 mmol, 1.0 eq) in AcOEt (30 mL) was added a solution of di-*tert*-butyl dicarbonate (3.79 g, 17.4 mmol, 1.1 eq) in AcOEt (10 mL). The resulting mixture was stirred at room temperature for 16 h under Ar atmosphere. After this time, the crude was washed with H₂O (3×50mL), dried over MgSO₄ and evaporated. The crude obtained (white solid) was used for the next reaction without further purification. To a 0 °C cooled solution of the previous crude in CH₂Cl₂ (50 mL) were added triphenyl phosphine (6.17 g, 23.5 mmol, 1.5 eq) and *N*-bromosuccinimide (4.19 g, 23.5 mmol, 1.5 eq). The resulting mixture was stirred at 0 °C for 2 h. Then, the solvent was removed by evaporation. The resulting crude was purified by flash chromatography on silica using hexane and methyl *tert*-butyl ether as solvents (5 to 30% methyl *tert*-butyl ether in hexane), affording compound **3** (2.92 g, 9.72 mmol, 62%). ¹H NMR (400 MHz, CDCl₃, 298 K) δ 7.35 – 7.27 (m, 2H), 7.16 – 7.09 (m, 2H), 6.46 (br s, NH), 3.52 (t, *J* = 7.6 Hz, 2H), 3.10 (t, *J* = 7.6 Hz, 2H), 1.51 (s, 9H); ¹³C NMR (101 MHz, CDCl₃, 298 K) δ 152.9, 137.3, 133.7, 129.3, 118.9, 80.7, 38.9, 33.2, 28.5; HPLC: System A, t_R: 3.72 min, >99% (214 nm), >99% (240 nm); MS: calculated exact mass for C₁₃H₁₉BrNO₂: 300.1 [M+H]⁺, found by HPLC-MS (ESI): 300.0.

8-[4-(4-fluorophenyl)-4-oxobutyl]-1-phenyl-1,3,8-triazaspiro[4.5]decan-4-one (4). A stirred suspension of 1-phenyl-1,3,8-triazaspiro[4.5]decan-4-one (1.00 g, 4.32 mmol, 1.1 eq), 4-chloro-4'-fluorobutyrophenone (0.65 mL, 3.95 mmol, 1.0 eq), potassium iodide (0.718 g, 4.32 mmol, 1.1 eq) and triethylamine (0.66 mL, 4.73 mmol, 1.2 eq) in anhydrous acetonitrile (8 mL) was refluxed under argon for 20 h. After this time the solvent was removed by evaporation. The resulting crude was dissolved in CH₂Cl₂ (50 mL) and washed with saturated NaHCO₃ (3×50 mL). The organic phase was dried over MgSO₄ and evaporated. The residue was dissolved in CH₂Cl₂ (30 mL) and the solution was added dropwise to cold hexane (150 mL). The white precipitate is filtered and dried by vacuum to obtain the desired compound **4** (0.99 g, 2.50 mmol, 63%). ¹H NMR (400 MHz, DMSO-d₆, 298 K) δ 8.59 (s, 1H), 8.10 – 8.00 (m, 2H), 7.40 – 7.29 (m, 2H), 7.21 – 7.11 (m, 2H), 6.81 – 6.69 (m, 3H), 4.55 (s, 2H), 3.02 (t, *J* = 6.8 Hz, 2H), 2.78 – 2.59 (m, 4H), 2.48 – 2.34 (m, 4H), 1.88 – 1.75 (m, 2H), 1.52 (d, *J* = 13.6 Hz, 2H); ¹³C NMR (101 MHz, DMSO-d₆, 298 K) δ 198.6, 176.2, 164.8 (d, *J* = 251.0 Hz), 143.3, 133.8, 133.8, 130.8 (d, *J* = 9.3 Hz), 128.9, 117.6, 115.6 (d, *J* = 21.9 Hz), 114.2, 58.6, 58.3, 57.1, 49.2, 35.9, 28.4, 21.6; HPLC: System A, *t*_R: 1.83 min, 95% (214 nm), 96% (240 nm); MS: calculated exact mass for C₂₃H₂₇FN₃O₂: 393.2 [M+H]⁺, found by HPLC-MS (ESI): 396.1.

*8-[4-(4-fluorophenyl)-4-oxobutyl]-1-phenyl-3-[4-(*N*-tert-butoxycarbonyl)aminophenethyl]-1,3,8-triazaspiro[4.5]decan-4-one (5)*. A mixture of **4** (940 mg, 2.38 mmol, 1.0 eq), potassium hydroxide (67.8 mg, 1.21 mmol, 0.5 eq), potassium carbonate (1.32 g, 9.55 mmol, 4.0 eq) and tetrabutylammonium bisulfate (243 mg, 0.72 mmol, 0.3 eq) suspended in anhydrous toluene (50 mL) was stirred at 90 °C for 30 min under Ar atmosphere. Then, a solution of 4-(*N*-tert-butoxycarbonyl)aminophenethyl bromide (**3**) (1.43 g, 4.76 mmol, 2.0 eq) in anhydrous toluene (6 mL) was added over 5 min. The resulting mixture was stirred at 90 °C for 2 days under Ar atmosphere. After this time, the mixture was allowed to cool to room temperature, washed with brine (3×50 mL), dried with MgSO₄ and evaporated. The resulting crude was purified by flash chromatography on silica using CH₂Cl₂ and MeOH as solvents (0 to 6% MeOH in CH₂Cl₂), affording compound **5** (950 mg, 1.54 mmol, 65%). ¹H NMR (400 MHz, CDCl₃, 298 K) δ 7.98 – 7.90 (m, 2H), 7.25 – 7.12 (m, 4H), 7.10 – 7.01 (m, 4H), 6.81 – 6.72 (m, 3H), 6.42 (s, 1H), 4.45 (s, 2H), 3.57 (t, *J* = 7.2 Hz, 2H), 2.96 (t, *J* = 7.1 Hz, 2H), 2.93 – 2.78 (m, 6H), 2.65 – 2.46 (m, 4H), 1.98 – 1.89 (m, 2H), 1.52 – 1.43 (m, 2H), 1.43 (s, 9H); ¹³C NMR (101 MHz, CDCl₃, 298 K) δ 198.4, 177.0, 174.2, 165.8 (d, *J* = 254.5 Hz), 152.9, 142.9, 137.2, 133.6, 132.7, 130.8 (d, *J* = 9.2 Hz), 129.4, 129.3, 119.1, 118.9, 115.8 (d, *J* = 21.8 Hz), 115.5, 80.7, 63.9, 60.4, 57.3, 49.3, 42.3, 36.4, 33.2, 28.9, 28.5, 21.3; HPLC: System A, *t*_R: 2.68 min, 99% (214 nm), 96% (240 nm); MS: calculated exact mass for C₃₆H₄₄FN₄O₄: 615.3 [M+H]⁺, found by HPLC-MS (ESI): 615.3.

8-[4-(4-fluorophenyl)-4-oxobutyl]-1-phenyl-3-(4-aminophenethyl)-1,3,8-triazaspiro[4.5]decan-4-one (6). Compound **5** (887 mg, 1.44 mmol, 1.0 eq) was dissolved in dioxane (5 mL) and a 4 M solution of HCl in dioxane was added (5 mL, 20 mmol, 14 eq). The resulting mixture was stirred at room temperature for 3 h. The reaction mixture was evaporated to dryness. The crude was partitioned between CH₂Cl₂ and H₂O (30 mL 1:1 v/v) and NaHCO₃ was carefully added until the pH of the aqueous phase was basic

(ca. 8-9). The layers were separated, and then the aqueous phase was extracted with CH₂Cl₂ (3×20 mL). The combined organic extract was washed with brine (1×75 mL), dried with MgSO₄ and evaporated. The resulting crude was purified by flash chromatography on silica using CH₂Cl₂ and MeOH as solvents (0 to 6% MeOH in CH₂Cl₂), affording compound **6** (488 mg, 0.95 mmol, 66%). ¹H NMR (400 MHz, CDCl₃, 298 K) δ 8.07 – 7.98 (m, 2H), 7.25 – 7.19 (m, 2H), 7.16 – 7.09 (m, 2H), 7.04 – 6.98 (m, 2H), 6.87 – 6.78 (m, 3H), 6.65 – 6.59 (m, 2H), 4.51 (s, 2H), 3.61 (t, *J* = 7.1 Hz, 2H), 3.01 (t, *J* = 7.2 Hz, 2H), 2.87 – 2.72 (m, 6H), 2.64 – 2.42 (m, 4H), 2.03 – 1.90 (m, 2H), 1.59 – 1.50 (m, 2H); ¹³C NMR (101 MHz, CDCl₃, 298 K) δ 198.7, 174.4, 165.8 (d, *J* = 253.6 Hz), 145.2, 143.2, 133.8, 130.8 (d, *J* = 9.2 Hz), 129.6, 129.3, 128.0, 119.0, 115.8 (d, *J* = 21.8 Hz), 115.6, 115.5, 64.0, 60.7, 57.7, 49.7, 42.5, 36.6, 33.0, 29.4, 22.0; HPLC: System A, *t*_R: 1.70 min, 98% (214 nm), 98% (240 nm); MS: calculated exact mass for C₃₁H₃₆FN₄O₂: 515.3 [M+H]⁺, found by HPLC-MS (ESI): 515.2.

4-((4-(2-(8-(4-(4-fluorophenyl)-4-oxobutyl)-4-oxo-1-phenyl-1,3,8-triazaspiro[4.5]decan-3-yl)ethyl)phenyl)amino)-4-oxobutanoic acid (7). To a solution of **6** (86.5 mg, 168 μmol, 1.0 eq) in CH₃CN (5 mL) was added succinic anhydride (20.2 mg, 202 μmol, 1.2 eq) and the mixture was stirred at room temperature overnight (16 h). After completion of the reaction the mixture was evaporated to dryness. The resulting crude was dissolved in CH₂Cl₂ (20 mL) and immediately washed with brine (2×20 mL). The resulting organic phase was dried over MgSO₄ and evaporated to afford compound **7** as a white solid (93.3 mg, 152 μmol, 90%). ¹H NMR (400 MHz, DMSO-*d*₆, 298 K) δ 9.94 (s, NH), 8.12 – 8.02 (m, 2H), 7.54 – 7.45 (m, 2H), 7.42 – 7.32 (m, 2H), 7.26 – 7.13 (m, 4H), 7.06 – 6.97 (m, 2H), 6.84 – 6.75 (m, 1H), 4.64 (s, 2H), 3.59 (t, *J* = 7.2 Hz, 2H), 3.45 – 3.24 (m, 4H), 3.18 (t, *J* = 7.0 Hz, 2H), 2.99 (t, *J* = 7.9 Hz, 2H), 2.93 – 2.76 (m, 4H), 2.59 – 2.45 (m, 4H), 2.10 – 1.94 (m, 2H), 1.61 (d, *J* = 14.1 Hz, 2H); ¹³C NMR (101 MHz, DMSO-*d*₆, 298 K) δ 197.5, 173.8, 173.6, 172.1, 169.9, 165.0 (d, *J* = 251.5 Hz), 142.5, 137.6, 133.3, 133.3, 132.8, 130.9 (d, *J* = 9.4 Hz), 129.1, 128.9, 119.0, 118.2, 115.7 (d, *J* = 21.9 Hz), 114.5, 62.9, 58.2, 55.7, 48.3, 41.4, 39.5, 35.3, 32.0, 31.0, 28.9, 28.8, 26.4, 18.6; HPLC: System A, *t*_R: 2.02 min, 99% (214 nm), 99% (240 nm); MS: calculated exact mass for C₃₅H₄₀FN₄O₅: 615.3 [M+H]⁺, found by HPLC-MS (ESI): 615.2.

2-oxo-7,10,13-trioxa-3-azahexadecan-16-aminium chloride (8). To a solution of 1-(*tert*-butoxycarbonyl-amino)-4,7,10-trioxa-13-tridecanamine (401 mg, 1.25 mmol, 1.0 eq) in CH₂Cl₂ (4 mL) was added acetic anhydride (130 μL, 1.38 mmol, 1.1 eq) and DIEA (470 μL, 2.76 mmol, 2.2 eq). The resulting mixture was stirred at room temperature for 3 h. After this time, the crude was washed with saturated NaHCO₃ (2×5 mL) and brine (1×5 mL). The organic phase was dried over MgSO₄ and evaporated. Subsequent treatment of the crude with a 2 M solution of HCl in dioxane (10 mL, 20 mmol, 16 eq) at room temperature for 1 h, followed by the evaporation of dioxane and HCl to dryness, afforded compound **8** as a pale yellow oil (352 mg, 1.10 mmol, 88%). ¹H NMR (400 MHz, D₂O, 298 K) δ 3.73 – 3.64 (m, 10H), 3.58 (t, *J* = 6.4 Hz, 2H), 3.25 (t, *J* = 6.8 Hz, 2H), 3.12 (t, *J* = 7.2 Hz, 2H), 2.01 – 1.92 (m, 5H), 1.83 – 1.75 (m, 2H); ¹³C NMR (101 MHz, D₂O, 298 K) δ 173.9, 69.5, 69.4, 69.3, 69.2, 68.3, 68.2, 37.6, 36.4, 28.1, 26.4, 21.8; MS:

calculated exact mass for C₁₂H₂₇ClN₂O₄ (hydrochloride): 298.2, calculated exact mass for C₁₂H₂₇N₂O₄ (amine): 263.2 [M+H]⁺, found by HPLC-MS (ESI): 263.0.

2-(2-(2-acetamidoethoxy)ethoxy)ethan-1-aminium chloride (9). To a solution of 1-(*tert*-butoxycarbonyl-amino)-3,6-dioxa-8-octanamine (120 mg, 0.48 mmol, 1.0 eq) in CH₂Cl₂ (4 mL) was added acetic anhydride (50 μL, 0.53 mmol, 1.1 eq) and DIEA (181 μL, 1.06 mmol, 2.2 eq). The resulting mixture was stirred at room temperature for 3 h. After this time, the crude was washed with saturated NaHCO₃ (2×5 mL) and brine (1×5 mL). The organic phase was dried over MgSO₄ and evaporated. Subsequent treatment of the crude with a 2 M solution of HCl in dioxane (10 mL, 20 mmol, 16 eq) at room temperature for 1 h, followed by the evaporation of dioxane and HCl to dryness, afforded compound **9** as a pale yellow oil (95.3 mg, 0.42 mmol, 87%). ¹H NMR (400 MHz, D₂O, 298 K) δ 3.76 (t, *J* = 5.0 Hz, 2H), 3.70 (s, 4H), 3.63 (t, *J* = 5.4 Hz, 2H), 3.38 (t, *J* = 5.4 Hz, 2H), 3.21 (br t, *J* = 5.1 Hz, 2H), 1.99 (s, 3H); ¹³C NMR (101 MHz, D₂O, 298 K) δ 174.3, 69.5, 69.4, 68.7, 66.3, 39.0, 38.9, 21.8; MS: calculated exact mass for C₈H₁₉ClN₂O₃: 226.1 (hydrochloride), calculated exact mass for C₈H₁₉N₂O₃ (amine): 191.1 [M+H]⁺, found by HPLC-MS (ESI): 190.9.

18-((4-(2-(8-(4-(4-fluorophenyl)-4-oxobutyl)-4-oxo-1-phenyl-1,3,8-triazaspiro[4.5]decan-3-yl)ethyl)phenyl)amino)-15,18-dioxo-4,7,10-trioxa-14-azaoctadecan-1-aminium chloride (10). To a mixture of **7** (50.7 mg, 82.5 μmol, 1.0 eq), EDC·HCl (23.8 mg, 0.12 mmol, 1.5 eq) and HOBt·H₂O (19.0 mg, 0.12 mmol, 1.5 eq) was added a solution of 1-(*tert*-butoxycarbonyl-amino)-4,7,10-trioxa-13-tridecanamine (39.7 mg, 0.12 mmol, 1.5 eq) in DMF (5 mL). The resulting mixture was stirred at room temperature overnight (18 h). After this time the solvent was evaporated to dryness. The crude was dissolved in AcOEt (15 mL) and washed with saturated NaHCO₃ (3×15 mL), 0.5% w/v citric acid (3×15 mL) and brine (1×15 mL). The organic phase was dried over MgSO₄ and evaporated to obtain the Boc-protected compound (44.3 mg, 48.3 μmol). This compound was dissolved in dioxane (1 mL) and a 4 M solution of HCl in dioxane (0.5 mL, 2.0 mmol, 41 eq) was added. The mixture was stirred at room temperature for 1 h. Then, the dioxane and HCl were evaporated to dryness. Finally, the crude was dissolved in H₂O (1 mL) and lyophilized to afford compound **10** (40.1 mg, 47.0 μmol, 57%). ¹H NMR (400 MHz, D₂O, 298 K) δ 8.05 – 7.97 (m, 2H), 7.43 – 7.32 (m, 4H), 7.32 – 7.19 (m, 4H), 7.10 – 7.02 (m, 1H), 7.02 – 6.93 (m, 2H), 5.45 (s, NH), 4.64 (s, 2H), 3.76 – 3.67 (m, 2H), 3.68 – 3.57 (m, 8H), 3.57 – 3.50 (m, 2H), 3.52 – 3.34 (m, 6H), 3.28 – 3.02 (m, 8H), 2.93 (br t, *J* = 6.5 Hz, 2H), 2.70 – 2.55 (m, 2H), 2.57 – 2.38 (m, 4H), 2.13 – 1.96 (m, 2H), 1.96 – 1.89 (m, 2H), 1.83 – 1.60 (m, 4H); ¹³C NMR (101 MHz, D₂O, 298 K) δ 200.7, 174.3, 173.2, 172.7, 165.9 (d, *J* = 253.6 Hz), 141.7, 135.8, 134.9, 132.4, 131.0 (d, *J* = 9.6 Hz), 129.6, 129.6, 121.9, 121.2, 118.4, 115.8 (d, *J* = 22.0 Hz), 69.4, 69.3, 69.2, 68.2, 63.5, 59.1, 56.0, 48.8, 41.5, 37.6, 36.2, 34.9, 32.0, 31.8, 31.0, 28.2, 27.0, 26.4, 18.0; HPLC: System B, tr: 1.67 min, 98% (214 nm), 97% (240 nm); MS: calculated exact mass for C₄₅H₆₂ClFN₆O₇: 852.4 (hydrochloride), calculated exact mass for C₄₅H₆₂FN₆O₇ (amine): 817.5 [M+H]⁺, found by HPLC-MS (ESI): 817.3.

2-(2-(2-(4-((4-(2-(8-(4-(4-fluorophenyl)-4-oxobutyl)-4-oxo-1-phenyl-1,3,8-triazaspiro[4.5]decan-3-yl)ethyl)phenyl)amino)-4-oxobutanamido)ethoxy)ethoxy)ethan-1-aminium chloride (**11**). To a mixture of **7** (50.6 mg, 82.3 μmol , 1.0 eq), EDC·HCl (23.6 mg, 0.12 mmol, 1.5 eq) and HOBt·H₂O (18.8 mg, 0.12 mmol, 1.5 eq) was added a solution of 1-(*tert*-butoxycarbonyl-amino)-3,6-dioxa-8-octanamine (30.5 mg, 0.12 mmol, 1.5 eq) in DMF (5 mL). The resulting mixture was stirred at room temperature overnight (18 h). After this time the solvent was evaporated to dryness. The crude was dissolved in AcOEt (15 mL) and washed with saturated NaHCO₃ (3×15 mL), 0.5% w/v citric acid (3×15 mL) and brine (1×15 mL). The organic phase was dried over MgSO₄ and evaporated to obtain the Boc-protected compound (50.9 mg, 60.2 μmol). This compound was dissolved in dioxane (1 mL) and a 4 M solution of HCl in dioxane (0.5 mL, 2.0 mmol, 39 eq) was added. The mixture was stirred at room temperature for 1 h. Then, the dioxane and HCl were evaporated to dryness. Finally, the crude was dissolved in H₂O (1 mL) and lyophilized to afford compound **11** (36.0 mg, 46.1 μmol , 56%). ¹H NMR (400 MHz, D₂O, 298 K) δ 8.04 – 7.94 (m, 2H), 7.42 – 7.29 (m, 4H), 7.31 – 7.17 (m, 4H), 7.09 – 7.02 (m, 1H), 7.00 – 6.92 (m, 2H), 4.63 (s, 2H), 3.77 – 3.65 (m, 4H), 3.66 – 3.58 (m, 4H), 3.54 (t, J = 5.5 Hz, 2H), 3.47 – 3.33 (m, 4H), 3.32 (t, J = 5.5 Hz, 2H), 3.25 – 3.04 (m, 6H), 2.92 (br t, J = 6.6 Hz, 2H), 2.69 – 2.57 (m, 2H), 2.57 – 2.50 (m, 2H), 2.52 – 2.38 (m, 2H), 2.11 – 1.93 (m, 2H), 1.65 (d, J = 14.5 Hz, 2H); ¹³C NMR (101 MHz, D₂O, 298 K) δ 200.7, 174.6, 173.2, 172.8, 165.9 (d, J = 253.8 Hz), 141.6, 135.7, 134.9, 132.4, 131.0 (d, J = 9.9 Hz), 129.6, 129.6, 121.8, 121.2, 118.4, 115.8 (d, J = 22.2 Hz), 69.5, 69.4, 68.8, 66.3, 63.4, 59.1, 56.0, 48.7, 41.5, 39.0, 38.8, 34.9, 32.0, 31.6, 30.7, 27.0, 18.0; HPLC: System B, t_{R} : 1.60 min, 99% (214 nm), 97% (240 nm); MS: calculated exact mass for C₄₁H₅₄ClFN₆O₆: 780.4 (hydrochloride), calculated exact mass for C₄₁H₅₄FN₆O₆ (amine): 745.4 [M+H]⁺, found by HPLC-MS (ESI): 745.2.

Methyl 24-((4-(2-(8-(4-(4-fluorophenyl)-4-oxobutyl)-4-oxo-1-phenyl-1,3,8-triazaspiro[4.5]decan-3-yl)ethyl)phenyl)amino)-3-(21-((4-(2-(8-(4-(4-fluorophenyl)-4-oxobutyl)-4-oxo-1-phenyl-1,3,8-triazaspiro[4.5]decan-3-yl)ethyl)phenyl)amino)-2,18,21-trioxo-7,10,13-trioxa-3,17-diazahenicosyl)-5,21,24-trioxo-10,13,16-trioxa-3,6,20-triazatetracosanoate (**12**). Compound **2** (2.6 mg, 12.7 μmol , 1.0 eq), compound **10** (21.6 mg, 25.4 μmol , 2.0 eq), EDC·HCl (7.3 mg, 38.0 μmol , 3.0 eq) and HOBt·H₂O (5.8 mg, 38.0 μmol , 3.0 eq) were dissolved in DMF (2 mL) and DIEA (7.0 μL , 41.1 μmol , 3.2 eq) was added. The resulting mixture was stirred at room temperature overnight (16 h). After this time the solvent was evaporated to dryness, and the crude was purified by semi-preparative reversed-phase HPLC (45 to 72% acetonitrile in aqueous 10 mM NH₄HCO₃ in 8 min, XBridge C₁₈ 19×150 mm 5 μm) affording compound **12** (11.3 mg, 6.27 μmol , 49%). ¹H NMR (400 MHz, CDCl₃, 298 K) δ 9.21 (s, 2 NH), 8.05 – 7.94 (m, 4H), 7.76 – 7.65 (m, 2 NH), 7.52 – 7.42 (m, 4H), 7.33 – 7.21 (m, 4H), 7.20 – 7.08 (m, 8H), 7.05 – 6.97 (m, 2 NH), 6.91 – 6.78 (m, 6H), 4.58 (s, 4H), 3.77 – 3.65 (m, 7H), 3.65 – 3.42 (m, 30H), 3.42 – 3.23 (m, 16H), 3.12 (t, J = 6.7 Hz, 4H), 3.09 – 2.95 (m, 8H), 2.91 (t, J = 7.1 Hz, 4H), 2.71 – 2.50 (m, 8H), 2.17 (br s, 4H), 1.82 – 1.66 (m, 8H), 1.54 (d, J = 14.4 Hz, 4H); ¹³C NMR (101 MHz, CDCl₃, 298 K) δ 172.6, 172.2, 171.1, 170.8, 166.0 (d, J = 255.4 Hz), 142.2, 137.5, 133.0, 132.9, 130.8 (d, J = 9.1 Hz), 129.7, 129.3, 120.2,

119.7, 115.9 (d, $J = 21.9$ Hz), 114.9, 77.2, 70.6, 70.2, 70.1, 69.9, 69.8, 69.4, 63.6, 58.7, 56.6, 56.0, 52.0, 48.8, 41.8, 38.0, 37.2, 35.6, 33.1, 31.7, 29.4, 29.0, 27.4; HPLC: System A, tr: 2.18 min, >99% (214 nm), >99% (240 nm); MS: calculated exact mass for $C_{97}H_{130}F_2N_{13}O_{18}$: 1803.0 $[M+H]^+$, found by HPLC-MS (ESI): 1803.0, 902.3 $[M+2H]^{2+}$, 601.9 $[M+3H]^{3+}$. HRMS (ESI): calculated exact mass for $C_{97}H_{130}F_2N_{13}O_{18}$ $[M+H]^+$: 1802.9619, found 1802.9618.

Methyl 19-((4-(2-(8-(4-(4-fluorophenyl)-4-oxobutyl)-4-oxo-1-phenyl)-1,3,8-triazaspiro[4.5]decan-3-yl)ethyl)phenyl)amino)-3-(16-((4-(2-(8-(4-(4-fluorophenyl)-4-oxobutyl)-4-oxo-1-phenyl)-1,3,8-triazaspiro[4.5]decan-3-yl)ethyl)phenyl)amino)-2,13,16-trioxo-6,9-dioxa-3,12-diazahexadecyl)-5,16,19-trioxo-9,12-dioxa-3,6,15-triazanonadecanoate (**13**). Compound **2** (2.7 mg, 13.1 μ mol, 1.0 eq), compound **11** (20.5 mg, 26.2 μ mol, 2.0 eq), EDC·HCl (7.5 mg, 39.3 μ mol, 3.0 eq) and HOBT·H₂O (6.0 mg, 39.3 μ mol, 3.0 eq) were dissolved in DMF (2 mL) and DIEA (7.0 μ L, 41.1 μ mol, 3.1 eq) was added. The resulting mixture was stirred at room temperature overnight (16 h). After this time the solvent was evaporated to dryness, and the crude was purified by semi-preparative reversed-phase HPLC (45 to 67% acetonitrile in aqueous 10 mM NH_4HCO_3 in 8 min, XBridge C₁₈ 19×150 mm 5 μ m) affording compound **13** (14.0 mg, 8.44 μ mol, 64 %).

¹H NMR (400 MHz, CDCl₃, 298 K) δ 9.11 (s, 2 NH), 8.04 – 7.93 (m, 4H), 7.81 (br t, $J = 5.7$ Hz, 2 NH), 7.51 – 7.41 (m, 4H), 7.30 – 7.23 (m, 4H), 7.22 – 7.16 (m, 2 NH), 7.16 – 7.09 (m, 8H), 6.93 – 6.87 (m, 4H), 6.87 – 6.81 (m, 2H), 4.57 (s, 4H), 3.74 – 3.63 (m, 7H), 3.58 – 3.31 (m, 38H), 3.12 (t, $J = 6.7$ Hz, 4H), 3.05 – 2.94 (m, 8H), 2.91 (t, $J = 6.9$ Hz, 4H), 2.70 – 2.54 (m, 8H), 2.24 – 2.11 (m, 4H), 1.50 (d, $J = 14.2$ Hz, 4H); ¹³C NMR (101 MHz, CDCl₃, 298 K) δ 197.1, 173.2, 172.9, 172.1, 171.1, 171.0, 166.0 (d, $J = 255.0$ Hz), 142.3, 137.4, 133.1, 133.0, 130.8 (d, $J = 9.3$ Hz), 129.7, 129.3, 120.3, 119.6, 115.9 (d, $J = 21.9$ Hz), 115.1, 70.4, 69.8, 63.6, 59.0, 58.5, 56.3, 55.9, 52.0, 48.4, 41.7, 39.5, 39.2, 35.7, 33.0, 31.6, 27.2, 18.8; HPLC: System A, tr: 2.08 min, 98% (214 nm), >99% (240 nm); MS: calculated exact mass for $C_{89}H_{114}F_2N_{13}O_{16}$: 1658.8 $[M+H]^+$, found by HPLC-MS (ESI): 1658.9, 830.3 $[M+2H]^{2+}$, 553.9 $[M+3H]^{3+}$. HRMS (ESI): calculated exact mass for $C_{89}H_{114}F_2N_{13}O_{16}$ $[M+H]^+$: 1658.8469, found: 1658.8454.

Methyl 3-(2,18-dioxo-7,10,13-trioxa-3,17-diazanonadecyl)-24-((4-(2-(8-(4-(4-fluorophenyl)-4-oxobutyl)-4-oxo-1-phenyl)-1,3,8-triazaspiro[4.5]decan-3-yl)ethyl)phenyl)amino)-5,21,24-trioxo-10,13,16-trioxa-3,6,20-triazatetracosanoate (**14**). Compound **2** (45.0 mg, 219 μ mol, 1.0 eq) and EDC·HCl (42.0 mg, 219 μ mol, 1.0 eq) were dissolved in dry DMF (1 mL) and the mixture was stirred at room temperature for 2 h under Ar atmosphere. Then, a solution of compound **8** (65.5 mg, 219 μ mol, 1.0 eq) and DIEA (75 μ L, 441 μ mol, 2.0 eq) in dry DMF (1 mL) was added and the resulting mixture was stirred at room temperature for 90 min. After this time the solvent was evaporated to dryness, and the crude was purified by Waters Porapak™ Rxn RP column (aqueous 10 mM NH_4HCO_3) to afford the intermediate 3-(2-methoxy-2-oxoethyl)-5,21-dioxo-10,13,16-trioxa-3,6,20-triazadocosanoic acid (78.4 mg, 174 μ mol, 79%). ¹H NMR (400 MHz, D₂O, 298 K) δ 3.70 (s, 3H), 3.68 – 3.59 (m, 8H), 3.59 – 3.50 (m, 6H), 3.37 (s,

2H), 3.34 – 3.24 (m, 4H), 3.21 (t, $J = 6.8$ Hz, 2H), 1.95 (s, 3H), 1.85 – 1.70 (m, 4H); ^{13}C NMR (101 MHz, D_2O , 298 K) δ 178.7, 174.0, 173.9, 173.8, 69.5, 69.3, 69.2, 68.3, 68.2, 58.2, 58.2, 55.4, 52.0, 36.4, 35.9, 28.2, 28.1, 21.8; MS: calculated exact mass for $\text{C}_{19}\text{H}_{36}\text{N}_3\text{O}_9$: 450.2 $[\text{M}+\text{H}]^+$, found by HPLC-MS (ESI): 450.2. This intermediate (8.0 mg, 17.8 μmol , 1.0 eq), compound **10** (16.7 mg, 19.6 μmol , 1.1 eq), EDC·HCl (5.1 mg, 26.7 μmol , 1.5 eq) and HOBt·H₂O (4.1 mg, 26.7 μmol , 1.5 eq) were dissolved in DMF (1.5 mL) and DIEA (7.0 μL , 41.1 μmol , 2.2 eq) was added. The resulting mixture was stirred at room temperature overnight (15 h). After this time the solvent was evaporated to dryness, and the crude was purified by semi-preparative reversed-phase HPLC (37 to 45% acetonitrile in aqueous 10 mM NH_4HCO_3 in 8 min, XBridge C₁₈ 19×150 mm 5 μm) affording compound **14** (5.5 mg, 4.40 μmol , 25%). ^1H NMR (400 MHz, CDCl_3 , 298 K) δ 9.19 (br s, NH), 8.03 – 7.94 (m, 2H), 7.68 (br s, 2 NH), 7.51 – 7.43 (m, 2H), 7.31 – 7.22 (m, 2H), 7.20 – 7.09 (m, 4H), 7.00 (br s, NH), 6.90 – 6.78 (m, 3H), 6.56 (br s, NH), 4.58 (s, 2H), 3.76 – 3.66 (m, 5H), 3.66 – 3.42 (m, 28H), 3.42 – 3.26 (m, 14H), 3.22 – 2.97 (m, 6H), 2.93 (t, $J = 7.0$ Hz, 2H), 2.70 – 2.54 (m, 4H), 2.27 – 2.11 (m, 2H), 1.95 (s, 3H), 1.82 – 1.67 (m, 8H), 1.52 (d, $J = 14.8$ Hz, 2H); ^{13}C NMR (101 MHz, CDCl_3 , 298 K) δ 172.7, 172.1, 171.1, 170.8, 170.5, 137.5, 132.8, 130.8 (d, $J = 9.4$ Hz), 129.7, 129.3, 120.2, 119.7, 116.0 (d, $J = 21.8$ Hz), 114.8, 70.6, 70.2, 70.1, 70.0, 69.8, 69.6, 69.5, 63.6, 58.8, 58.7, 56.0, 52.0, 48.8, 41.7, 38.1, 38.0, 37.3, 37.3, 35.5, 33.2, 33.1, 32.1, 31.8, 29.9, 29.8, 29.4, 29.1, 29.0, 27.1, 23.4, 22.8; HPLC: System A, t_{R} : 1.98 min, 99% (214 nm), 98% (240 nm); MS: calculated exact mass for $\text{C}_{64}\text{H}_{95}\text{FN}_9\text{O}_{15}$: 1248.7 $[\text{M}+\text{H}]^+$, found by HPLC-MS (ESI): 1248.5, 624.9 $[\text{M}+2\text{H}]^{2+}$. HRMS (ESI): calculated exact mass for $\text{C}_{64}\text{H}_{95}\text{FN}_9\text{O}_{15}$: 1248.6926 $[\text{M}+\text{H}]^+$, found: 1248.6936.

Methyl 3-(2,13-dioxo-6,9-dioxa-3,12-diazatetradecyl)-19-((4-(2-(8-(4-(4-fluorophenyl)-4-oxobutyl)-4-oxo-1-phenyl-1,3,8-triazaspiro[4.5]decan-3-yl)ethyl)phenyl)amino)-5,16,19-trioxo-9,12-dioxa-3,6,15-triazanonadecanoate (15). Compound **2** (42.1 mg, 205 μmol , 1.0 eq) and EDC·HCl (39.3 mg, 205 μmol , 1.0 eq) were dissolved in dry DMF (1 mL) and the mixture was stirred at room temperature for 2 h under Ar atmosphere. Then, a solution of compound **9** (46.5 mg, 205 μmol , 1.0 eq) and DIEA (70 μL , 412 μmol , 2.0 eq) in dry DMF (1 mL) was added and the resulting mixture was stirred at room temperature for 90 min. After this time the solvent was evaporated to dryness, and the crude was purified by Waters Porapak™ Rxn RP column (aqueous 10 mM NH_4HCO_3) to afford the intermediate 3-(2-methoxy-2-oxoethyl)-5,16-dioxo-9,12-dioxa-3,6,15-triazaheptadecanoic acid (62.1 mg, 164 μmol , 80%). ^1H NMR (400 MHz, D_2O , 298 K) δ 3.71 (s, 3H), 3.68 – 3.56 (m, 10H), 3.44 (t, $J = 5.5$ Hz, 2H), 3.41 (s, 2H), 3.36 (t, $J = 5.3$ Hz, 2H), 3.30 (s, 2H), 1.98 (s, 3H); ^{13}C NMR (101 MHz, D_2O , 298 K) δ 178.6, 174.3, 174.1, 174.0, 69.4, 68.7, 68.7, 58.1, 58.1, 55.2, 52.0, 38.9, 38.5, 21.7; MS: calculated exact mass for $\text{C}_{15}\text{H}_{28}\text{N}_3\text{O}_8$: 378.2 $[\text{M}+\text{H}]^+$, found by HPLC-MS (ESI): 378.1. This intermediate (7.25 mg, 19.2 μmol , 1.0 eq), compound **11** (16.5 mg, 21.1 μmol , 1.1 eq), EDC·HCl (5.5 mg, 28.8 μmol , 1.5 eq) and HOBt·H₂O (4.4 mg, 28.8 μmol , 1.5 eq) were dissolved in DMF (1.5 mL) and DIEA (7.5 μL , 44.1 μmol , 2.3 eq) was added. The resulting mixture was stirred at room temperature overnight (15 h). After this time the solvent was evaporated to dryness, and the crude was purified by semi-

preparative reversed-phase HPLC (35 to 43% acetonitrile in aqueous 10 mM NH_4HCO_3 in 8 min, XBridge C_{18} 19×150 mm 5 μm) affording compound **15** (5.0 mg, 4.53 μmol , 24%). ^1H NMR (400 MHz, CDCl_3 , 298 K) δ 8.87 (br s, NH), 8.04 – 7.95 (m, 2H), 7.69 – 7.57 (m, 2 NH), 7.50 – 7.41 (m, 2H), 7.31 – 7.20 (m, 2H), 7.19 – 7.10 (m, 4H), 6.97 (br s, NH), 6.90 – 6.79 (m, 3H), 6.55 (br s, NH), 4.57 (s, 2H), 3.75 – 3.65 (m, 5H), 3.66 – 3.27 (m, 34H), 3.10 (br s, 6H), 2.92 (t, $J = 6.8$ Hz, 2H), 2.70 – 2.57 (m, 4H), 2.14 (br s, 2H), 1.98 (s, 3H), 1.51 (d, $J = 14.3$ Hz, 2H); ^{13}C NMR (101 MHz, CDCl_3 , 298 K) δ 172.8, 172.2, 170.9, 170.9, 170.8, 170.7, 166.0 (d, $J = 254.9$ Hz), 137.3, 130.8 (d, $J = 9.4$ Hz), 129.6, 129.3, 120.2, 119.6, 115.9 (d, $J = 21.9$ Hz), 115.1, 70.4, 70.3, 70.1, 69.9, 69.8, 63.7, 58.7, 56.0, 52.1, 49.0, 39.6, 39.5, 39.2, 39.2, 33.1, 32.1, 31.7, 29.8, 23.3, 22.8; HPLC: System A, tr: 1.90 min, 96% (214 nm), 96% (240 nm); MS: calculated exact mass for $\text{C}_{56}\text{H}_{79}\text{FN}_9\text{O}_{13}$: 1104.6 $[\text{M}+\text{H}]^+$, found by HPLC-MS (ESI): 1104.8, 552.9 $[\text{M}+2\text{H}]^{2+}$. HRMS (ESI): calculated exact mass for $\text{C}_{56}\text{H}_{79}\text{FN}_9\text{O}_{13}$ $[\text{M}+\text{H}]^+$: 1104.5776, found: 1104.5799.

TM with TAT peptides. A peptide derived from the HIV transactivator of transcription, HIV TAT (YGRKKRRQRRR), was fused to peptides with the amino acid sequences of human A_2AR or D_2R TM domain 6, human D_2R TM domain 5 and human D_2R TM domain 7 (Genemed Synthesis), to promote integration of the TM domains in the plasma membrane. Because HIV TAT binds to the phosphatidylinositol-(4, 5)-bisphosphate found on the inner surface of the membrane, HIV TAT peptide was fused to the *N*-terminus of TM6 and to the *C*-terminus of TM5 and TM7 to obtain the right orientation of the inserted peptide. The amino acid sequences were:

TAT-TM6 of D₂R: YGRKKRRQRRR M³⁷⁴LAIVLGVFIICWLPFFITHIL³⁹⁵;

TAT-TM6 of A_{2A}R: YGRKKRRQRRRL²³⁵AIIVGLFALCWLPLHIINCFTFF²⁵⁸;

TM5-TAT of D₂R: F¹⁸⁹VVYSSIVSFYVPFIVTLLVYIKIY²¹³YGRKKRRQRRR;

TM7-TAT of D₂R: A⁴¹⁰FTWLG YVNSAVNPIIYTTFN⁴³¹YGRKKRRQRRR.

Radioligand binding experiments. Brains of male and female sheep of 4-6 months old were freshly obtained from the local slaughterhouse. Striatal brain tissues were disrupted with a Polytron homogenizer (PTA 20 TS rotor, setting 3; Kinematica, Basel, Switzerland) for two 5 s-periods in 10 volumes of 50 mM Tris-HCl buffer at pH 7.4, containing a proteinase inhibitor cocktail (Sigma, St. Louis, MO, USA). Membranes were obtained by centrifugation, twice at 105000 g for 45 min at 4°C. The pellet was stored at -80°C, washed once more as described above and resuspended in 50 mM Tris-HCl buffer for immediate use. Membrane protein was quantified by the bicinchoninic acid method (Pierce Chemical Co., Rockford, IL, USA) using bovine serum albumin dilutions as standard. Binding experiments were performed with membrane suspensions at room temperature in 50 mM Tris-HCl buffer at pH 7.4, containing 10 mM MgCl_2 . For D_2R competition-binding assays, membrane suspensions (0.2 mg of protein/mL) were incubated for 2 h with a constant free concentration of 0.8 nM of the D_2R antagonist [^3H]YM-09151-2 ($K_{\text{DA1}} = 0.15$ nM) and increasing concentrations of each tested ligand. Non-specific binding was determined in the presence of 30 μM of dopamine, because at

this concentration dopamine does not displace the radioligand from sigma receptors. Competition-binding assays using TAT-TM peptides were performed as described previously, but preincubating peptides and membranes for 1 h before the addition of the ligands and the radioligand. In all cases, free and membrane-bound ligands were separated by rapid filtration of 500 μ L aliquots in a cell harvester (Brandel, Gaithersburg, MD, USA) through Whatman GF/C filters embedded in 0.3% polyethylenimine, that were subsequently washed for 5 s with 5 mL of ice-cold 50 mM Tris-HCl buffer. The filters were incubated with 10 mL of Ecoscint H scintillation cocktail (National Diagnostics, Atlanta, GA, USA) overnight at room temperature and radioactivity counts were determined using a Tri-Carb 2800 TR scintillation counter (PerkinElmer) with an efficiency of 62%. Radioligand competition curves were analyzed by nonlinear regression using the commercial Grafit curve-fitting software (Erithacus Software, Surrey, UK) by fitting the binding data to the mechanistic two-state dimer receptor model.²¹ The macroscopic equilibrium dissociation constants from competition experiments were determined applying the following general equation:

$$A_{\text{bound}} = \frac{\left(K_{\text{DA}2} A + 2 A^2 + \frac{K_{\text{DA}2} A B}{K_{\text{DAB}}} \right) R_T}{K_{\text{DA}1} K_{\text{DA}2} + K_{\text{DA}2} A + A^2 + \frac{K_{\text{DA}2} A B}{K_{\text{DAB}}} + \frac{K_{\text{DA}1} K_{\text{DA}2} B}{K_{\text{DB}1}} + \frac{K_{\text{DA}1} K_{\text{DA}2} B^2}{K_{\text{DB}1} K_{\text{DB}2}}}$$

where A represents the radioligand concentration, B the assayed competing compound concentration and K_{DAB} the hybrid allosteric modulation between A and B. For A and B non-cooperative and non-allosteric modulation between A and B, the equation can be simplified due to the fact that $K_{\text{DA}2} = 4K_{\text{DA}1}$, $K_{\text{DB}2} = 4K_{\text{DB}1}$ and $K_{\text{DAB}} = 2K_{\text{DB}1}$:

$$A_{\text{bound}} = \frac{\left(4 K_{\text{DA}1} A + 2 A^2 + \frac{2 K_{\text{DA}1} A B}{K_{\text{DB}1}} \right) R_T}{4 K_{\text{DA}1}^2 + 4 K_{\text{DA}1} A + A^2 + \frac{2 K_{\text{DA}1} A B}{K_{\text{DB}1}} + \frac{4 K_{\text{DA}1}^2 B}{K_{\text{DB}1}} + \frac{K_{\text{DA}1}^2 B^2}{K_{\text{DB}1}^2}}$$

Cell culture. CHO cells stably co-expressing the human cDNAs of $A_{2A}R$ and D_2R were obtained and tested as described in Orru et al. (2011).²⁵ This clone was grown in Minimum Essential Medium (MEM α ; Gibco) supplemented with 2 mM L-glutamine, 100 μ g/mL sodium pyruvate, MEM nonessential amino acid solution (1/100), 100U/mL penicillin/streptomycin, 5% (vol/vol) of heat-inactivated FBS (all supplements from Invitrogen) and with 600 mg/mL Geneticin (G 418 Sulfate, Calbiochem) and 300 mg/mL Hygromycin B (Invitrogen). HEK-293T cells were grown in Dulbecco's modified Eagle's medium supplemented with 2 mM L-glutamine, 100 μ g/mL sodium pyruvate, MEM nonessential amino acid solution (1/100), 100U/mL penicillin/streptomycin, 5% (vol/vol) of heat-inactivated FBS. All cells were cultured at 37°C and 5% CO₂.

Dynamic Mass Redistribution (DMR) Assay. The global cell signaling profile was measured using an EnSpire Multimode Plate Reader (PerkinElmer, Waltham, Massachusetts, US). This label-free approach uses refractive waveguide grating optical biosensors, integrated into 384-well microplates. Changes in local optical density are measured in a detection zone up to 150 nm above the surface of the sensor. Cellular mass movements induced upon receptor activation are detected by illuminating the underside of the biosensor with polychromatic light and measured as changes in the wavelength of

the reflected monochromatic light. These changes are a function of the refraction index. The magnitude of this wavelength shift (in picometers) is directly proportional to the amount of DMR. CHO cells stably co-expressing A_{2A}R and D₂R were used to perform the DMR assays to mimic the pattern receptor expression of brain striatum, where a high portion of D₂R form heteromers with A_{2A}R.¹³ Briefly, 24 h before the assay, cells were seeded at a density of 7,000 cells per well in 384-well sensor microplates with 30 μ L growth medium and cultured for 24 h (37°C, 5% CO₂) to obtain 70%–80% confluent monolayers. Previous to the assay, cells were washed twice with assay buffer (media with 20 mM HEPES, pH 7.15, 0.1% DMSO and 0.1% BSA) and incubated 2 h in 30 μ L per well of non assay buffer in the reader at 24°C. Hereafter, the sensor plate was scanned, and a baseline optical signature was recorded for 10 min before adding 10 μ L of the antagonist compound dissolved in the assay buffer at different concentrations. The DMR response was recorded for 30 min. Finally, 10 μ L of a 100 nM solution of the agonist (sumanriole) dissolved in the assay buffer was added and recorded for at least 90 min. The resulting shifts of reflected light wavelength (pm) were monitored over time. Kinetic results were analyzed using EnSpire Workstation Software v 4.10.

Expression vectors and fusion proteins. For bimolecular fluorescence complementation experiments, in order to obtain receptors fused to the hemitruncated Venus variant of the YFP, sequences encoding the amino acid residues 1-155 (nYFP) and 156-238 (cYFP) of the YFP Venus, were subcloned in pcDNA3.1 vector. Moreover, the human cDNA for D₂R cloned into pcDNA3.1 was subcloned to be in-frame with restriction sites EcoRI and BamHI of the pcDNA3.1-nYFP and the pcDNA3.1-cYFP. Between the receptor and the hemitruncated fluorescence protein there is a linker of 36 nucleotides.

Bimolecular fluorescence complementation (BiFC). HEK-293T cells were transiently co-transfected with lipofectamine with the cDNA encoding D₂R fused to nYFP and/or with the same amount of the receptor fused to cYFP. After 48 h, cells were treated or not with the indicated TM with TAT peptides (4 μ M) for 4 h at 37°C. To quantify protein reconstructed YFP Venus expression, cells (20 μ g protein; 50,000 cells/well) were distributed in 96-well microplates (black plates with a transparent bottom, Porvair, King's Lynn, UK), and emission fluorescence at 530 nm was determined in a FLUOstar Optima Fluorimeter (BMG Labtechnologies, Offenburg, Germany) equipped with a high-energy xenon flash lamp, using a 10-nm bandwidth excitation filter at 400 nm reading. Protein fluorescence expression was determined as the fluorescence of the sample minus the fluorescence of cells not expressing the fusion proteins.

Computational models of the D₂R monomer and homodimer. A homology model of D₂R (Uniprot code P14416) was constructed from the crystal structure of D₃R (PDB id 3PBL)²⁶ using Modeller 9.12.²⁷ Three computational models of the D₂R homodimer were built using alternative transmembrane (TM) helix interfaces: the TM1/2 (involving TMs1 and 2 and helix 8) and TM5/6 (involving TMs 5 and 6) interfaces using the crystal of the μ -opioid receptor (4DKL)²⁸ as a template, and the TM4/5 (involving TMs 4 and 5) interface using the crystal structure of the β_1 -adrenergic receptor (4GPO).²⁹ Nevertheless,

the results with disrupting peptides indicate a direct interaction exclusively between TM 6 of D₂R in the homodimer (Figure 3). Due to the absence of crystal structures of oligomers using exclusively the TM6 interface, the D₂R homodimer was additionally modelled with HADDOCK2.2³⁰ using residues K367^{6,29} – I384^{6,46} as directly involved in the interaction. The stability of this TM6 interface homodimer was evaluated by molecular dynamic (MD) simulations.

Docking of ligands. The pharmacophore-linker derivative **7** was docked into D₂R using MOE (Chemical computing group Inc., Montreal, QC, Canada). Inspired by computational scripts that link fragments in a binding site for fragment-based drug discovery, we developed a MOE-based computational tool to design the optimal spacer size connecting the attachment points of the pharmacophore-linker derivative **7** (see Table S1). This tool was used to model bivalent ligands **12** and **13** into the D₂R homodimer. The selection of the preferred spacer was based upon the interaction energy between ligand and protein, internal energy of the ligand, and visual inspection.

Molecular dynamic simulations. The pharmacophore-linker derivative **7**, in complex with the D₂R monomer, and bivalent ligand **13**, in complex with the D₂R homodimer constructed via the TM6 interface, were embedded in a pre-equilibrated box (9x9x9 nm³ for monomers and 12x12x10 nm³ for homodimers) containing a lipid bilayer (~205 or ~300 molecules of POPC) with explicit solvent (~14000 or ~30.000 water molecules) and 0.15 M concentration of Na⁺ and Cl⁻ ions (~140 or ~330 ions).³¹ Model systems were energy minimized and subjected to a 6 step MD equilibration (10+5+2+2+2+2 ns) in which constraints on hydrogen atoms, protein loops, and protein and ligand atoms were subsequently relaxed. Next, these restraints were released, and unrestrained MD trajectories were produced for 0.5 μs for compound **7** in complex with the D₂R monomer and for 1 μs for compound **13** in complex with the D₂R homodimer. A 2 fs time step and constant temperature of 300K was used. All bonds and angles were kept frozen using the LINCS algorithm. Lennard-Jones interactions were computed using a cutoff of 10 Å, and electrostatic interactions were treated using PME with the same real-space cutoff. The AMBER99SD-ILDN³² force field was used for the protein, the parameters described by Berger and co-workers for lipids,³³ the general Amber force field (GAFF) and HF/6-31G*-derived RESP atomic charges for ligands.³⁴ This combination of protein and lipid parameters has previously been validated.³⁵ All simulations were performed using GROMACS software v5.1.4.³⁶

ASSOCIATED CONTENT

The following files are available free of charge. Synthetic Schemes for compounds **1-11**, supporting figures **S1-S3**, table **S1**, and ¹H- and ¹³C-NMR spectra of compounds **1-15** (PDF). Molecular formula strings for all synthesized compounds (CSV).

AUTHOR INFORMATION

Corresponding Author

* M. R.: e-mail, mroyo@pcb.ub.es

* V. C.: e-mail, vcasado@ub.edu

* L. P.: e-mail, leonardo.pardo@uab.es

Author Contributions

These authors contributed equally.

Notes

The authors declare no competing financial interest.

ACKNOWLEDGMENT

This study was funded by grants from the Spanish Ministerio de Economía, Industria y Competitividad (SAF2014-60138-R to MR, SAF2014-54840-R to VC, SAF2016-77830-R to LP, and SAF2015-74627-JIN to AC; those grants may include FEDER funds), CIBER-BBN (CB06-01-0074), CIBERNED (CB06/05/0064), Generalitat de Catalunya (2014SGR137, 2014SGR1236, 2017SGR1439 and 2017SGR1497), “Fundació La Marató de TV3” Grant 20140610, and the intramural funds of the National Institute on Drug Abuse (SF).

ABBREVIATIONS

A_{2A}R, adenosine A_{2A} receptor; BiFC, bimolecular fluorescence complementation; CHO, Chinese hamster ovary; D₂R, dopamine D₂ receptor; DIEA, diisopropyl ethylamine; DMR, dynamic mass redistribution; ECL, extracellular loop; EDC·HCl, N-(3-Dimethylaminopropyl)-N'-ethylcarbodiimide hydrochloride; HOBt·H₂O, 1-Hydroxybenzotriazole hydrate; MOE, molecular operating environment; NAPS, N-(p-aminophenethyl)piperone; NTA, nitrilotriacetic acid; OEG, oligoethylene glycol; TAT, transactivator of transcription; TM, transmembrane; YFP, yellow fluorescent protein.

REFERENCES

- (1) Whorton, M. R.; Bokoch, M. P.; Rasmussen, S. G. F.; Huang, B.; Zare, R. N.; Kobilka, B.; Sunahara, R. K. A monomeric G protein-coupled receptor isolated in a high-density lipoprotein particle efficiently activates its G protein. *Proc. Natl. Acad. Sci. USA* **2007**, *104*, 7682-7687.
- (2) Ferré, S.; Casadó, V.; Devi, L. A.; Filizola, M.; Jockers, R.; Lohse, M.J.; Milligan, G.; Pin, J.P.; Guitart, X. G protein-coupled receptor oligomerization revisited: functional and pharmacological perspectives. *Pharmacol. Rev.* **2014**, *66*, 413-434.
- (3) Farran, B. An update on the physiological and therapeutic relevance of GPCR oligomers. *Pharmacol. Res.* **2017**, *117*, 303-327.
- (4) (a) Santos, R.; Ursu, O.; Gaulton, A.; Bento, A.P.; Donadi, R.S.; Bologa, C.G.; Karlsson, A.; Al-Lazikani, B.; Hersey, A.; Oprea, T.I.; Overington, J.P. A comprehensive map of molecular drug targets. *Nat. Rev. Drug Discovery* **2017**, *16*, 19-34. (b) Gaitonde, S. A.; González-Maeso, J. Contribution of heteromerization to G protein-coupled receptor function. *Curr. Opin. Pharmacol.* **2017**, *32*, 23-31.
- (5) Guo, H.; An, S.; Ward, R.; Yang, Y.; Liu, Y.; Guo, X. X.; Hao, Q.; Xu, T. R. Methods used to study the oligomeric structure of G-protein-coupled receptors. *Biosci. Rep.* **2017**, *37*, BSR20160547.
- (6) (a) Hiller, C.; Kühhorn, J.; Gmeiner, P. Class A G-Protein-Coupled Receptor (GPCR) Dimers and Bivalent Ligands. *J. Med. Chem.* **2013**, *56*, 6542-6559. (b) Soriano, A.; Ventura, R.; Molero, A.; Hoen, R.; Casadó, V.; Cortés, A.; Fanelli, F.; Albericio, F.; Lluís, C.; Franco, R.; Royo, M. Adenosine A_{2A} Receptor-Antagonist/Dopamine D₂ Receptor-Agonist Bivalent Ligands as Pharmacological Tools to Detect A_{2A}-D₂ Receptor Heteromers. *J. Med. Chem.* **2009**, *52*, 5590-5602. (c) Daniels, D. J.; Lenard, N. R.; Etienne, C. L.; Law, P. -Y.; Roerig, S. C.; Portoghese, P. S. Opioid-induced tolerance and dependence in mice is modulated by the distance between pharmacophores in a bivalent ligand series. *Proc. Natl. Acad. Sci. U. S. A.* **2005**, *102*, 19208-19213.
- (7) Busnelli, M.; Kleinau, G.; Muttenthaler, M.; Stoev, S.; Manning, M.; Bibic, L.; Howell, L. A.; McCormick, P. J.; Di Lascio, S.; Braida, D.; Sala, M.; Rovati, G. E.; Bellini, T.; Chini, B. Design and Characterization of Superpotent Bivalent Ligands Targeting Oxytocin Receptor Dimers via a Channel-Like Structure. *J. Med. Chem.* **2016**, *59*, 7152-7166.
- (8) Hübner, H.; Schellhorn, T.; Gienger, M.; Schaab, C.; Kaindl, J.; Leeb, L.; Clark, T.; Möller, D.; Gmeiner, P. Structure-guided development of heterodimer-selective GPCR ligands. *Nat. Commun.* **2016**, *7*, 12298.
- (9) Shonberg, J.; Scammells, P. J.; Capuano, B. Design Strategies for Bivalent Ligands Targeting GPCRs. *ChemMedChem* **2011**, *6*, 963-974.
- (10) Jörg, M.; May, L. T.; Mak, F. S.; Lee, K. C. K.; Miller, N. D.; Scammells, P. J.; Capuano, B. Synthesis and Pharmacological Evaluation of Dual Acting Ligands

Targeting the Adenosine A_{2A} and Dopamine D₂ Receptors for the Potential Treatment of Parkinson's Disease. *J. Med. Chem.* **2015**, *58*, 718-738.

(11) (a) Kumar, V.; Moritz, A. E.; Keck, T. M.; Bonifazi, A.; Ellenberger, M. P.; Sibley, C. D.; Free, R. B.; Shi, L.; Lane, J. R.; Sibley, D. R.; Newman, A. H. Synthesis and Pharmacological Characterization of Novel trans-Cyclopropylmethyl-Linked Bivalent Ligands That Exhibit Selectivity and Allosteric Pharmacology at the Dopamine D₃ Receptor (D₃R). *J. Med. Chem.* **2017**, *60*, 1478-1494. (b) Mohr, K.; Schmitz, J.; Schrage, R.; Tränkle, C.; Holzgrabe, U. Molecular Alliance-From Orthosteric and Allosteric Ligands to Dualsteric/Bitopic Agonists at G Protein Coupled Receptors. *Angew. Chem. Int. Ed.* **2013**, *52*, 508-516.

(12) (a) Guo, W.; Shi, L.; Javitch, J. A. The Fourth Transmembrane Segment Forms the Interface of the Dopamine D₂ Receptor Homodimer. *J. Biol. Chem.* **2003**, *278*, 4385-4388. (b) Kern, A.; Albarran-Zeckler, R.; Walsh, H. E.; Smith, R. G. Apo-Ghrelin Receptor Forms Heteromers with DRD2 in Hypothalamic Neurons and Is Essential for Anorexigenic Effects of DRD2 Agonism. *Neuron* **2012**, *73*, 317-332.

(13) Bonaventura, J.; Navarro, G.; Casadó-Anguera, V.; Azdad, K.; Rea, W.; Moreno, E.; Brugarolas, M.; Mallol, J.; Canela, E. I.; Lluís, C.; Cortés, A.; Volkow, N. D.; Schiffmann, S. N.; Ferré, S.; Casadó, V. Allosteric interactions between agonists and antagonists within the adenosine A_{2A} receptor-dopamine D₂ receptor heterotetramer. *Proc. Natl. Acad. Sci. USA* **2015**, *112*, E3609-E3618.

(14) Ferré, S.; Ciruela, F.; Canals, M.; Marcellino, D.; Burgueño, J.; Casadó, V.; Hillion, J.; Torvinen, M.; Fanelli, F.; de Benedetti, P.; Goldberg, S. R.; Bouvier, M.; Fuxe, K.; Agnati, L. F.; Lluís, C.; Franco, R.; Woods, A. Adenosine A_{2A}-dopamine D₂ receptor-receptor heteromers. Targets for neuro-psychiatric disorders. *Parkinsonism Relat. Disord.* **2004**, *10*, 265-271.

(15) (a) Kaczor, A.; Jörg, M.; Capuano, B. The dopamine D₂ receptor dimer and its interaction with homobivalent antagonists: homology modeling, docking and molecular dynamics. *J. Mol. Model.* **2016**, *22*, 203. (b) Carli, M.; Kolachalam, S.; Aringhieri, S.; Rossi, M.; Giovannini, L.; Maggio, R.; Scarselli, M. Dopamine D₂ Receptors Dimers: How can we Pharmacologically Target Them? *Curr. Neuropharmacol.* **2018**, *16*, 222-230.

(16) Pulido, D.; Albericio, F.; Royo, M. Controlling Multivalency and Multimodality: Up to Pentamodal Dendritic Platforms Based on Diethylenetriaminepentaacetic Acid Cores. *Org. Lett.* **2014**, *16*, 1318-1321.

(17) Carriba, P.; Navarro, G.; Ciruela, F.; Ferré, S.; Casadó, V.; Agnati, L.; Cortés, A.; Mallol, J.; Fuxe, K.; Canela, E. I.; Lluís, C.; Franco, R. Detection of heteromerization of more than two proteins by sequential BRET-FRET. *Nat. Methods* **2008**, *5*, 727-733.

(18) (a) Jin, C.; Mayer, L. D.; Lewin, A. H.; Rehder, K. S.; Brine, G. A. Practical Synthesis of p-Aminophenethylpiperone (NAPS), a High-Affinity, Selective D₂-Dopamine Receptor Antagonist. *Synth. Commun.* **2008**, *38*, 816-823. (b) Albizu, L.; Cottet, M.; Kralikova, M.; Stoev, S.; Seyer, R.; Brabet, I.; Roux, T.; Bazin, H.; Bourrier,

- E.; Lamarque, L.; Breton, C.; Rives, M. L.; Newman, A.; Javitch, J.; Trinquet, E.; Manning, M.; Pin, J. P.; Mouillac, B.; Durroux, T. Time-resolved FRET between GPCR ligands reveals oligomers in native tissues. *Nat. Chem. Biol.* **2010**, *6*, 587-594.
- (19) Cordoní, A.; Navarro, G.; Aymerich, M. S.; Franco, R. Structures for G-Protein-Coupled Receptor Tetramers in Complex with G Proteins. *Trends Biochem. Sci.* **2015**, *40*, 548-551.
- (20) Kang, Y. S.; Son, J. H.; Hwang, I. C.; Ahn, K. H. Synthesis of a bis(oxazoline)-*N*-carboxylate ligand and its Zn(II) complex that shows C–H···Cl hydrogen bonding. *Polyhedron* **2006**, *25*, 3025-3031.
- (21) Casadó, V.; Cortés, A.; Ciruela, F.; Mallol, J.; Ferré, S.; Lluís, C.; Canela, E. I.; Franco, R. Old and new ways to calculate the affinity of agonists and antagonists interacting with G-protein-coupled monomeric and dimeric receptors: The receptor–dimer cooperativity index. *Pharmacol. Ther.* **2007**, *116*, 343-354.
- (22) (a) Casadó, V.; Cortés, A.; Mallol, J.; Pérez-Capote, K.; Ferré, S.; Lluís, C.; Franco, R.; Canela, E. I. GPCR homomers and heteromers: A better choice as targets for drug development than GPCR monomers? *Pharmacol. Ther.* **2009**, *124*, 248-257. (b) Casadó, V.; Ferrada, C.; Bonaventura, J.; Gracia, E.; Mallol, J.; Canela, E. I.; Lluís, C.; Cortés, A.; Franco, R. Useful pharmacological parameters for G-protein-coupled receptor homodimers obtained from competition experiments. Agonist–antagonist binding modulation. *Biochem. Pharmacol.* **2009**, *78*, 1456-1463.
- (23) Schröder, R.; Schmidt, J.; Blättermann, S.; Peters, L.; Janssen, N.; Grundmann, M.; Seemann, W.; Kaufel, D.; Merten, N.; Drewke, C.; Gomeza, J.; Milligan, G.; Mohr, K.; Kostenis, E. Applying label-free dynamic mass redistribution technology to frame signaling of G protein–coupled receptors noninvasively in living cells. *Nat. Protoc.* **2011**, *6*, 1748-1760.
- (24) Navarro, G.; Cordoní, A.; Casadó-Anguera, V.; Moreno, E.; Cai, N-S.; Cortés, A.; Canela, E. I.; Dessauer, C. W.; Casadó, V.; Pardo, L.; Lluís, C.; Ferré, S. Evidence for functional pre-coupled complexes of receptor heteromers and adenylyl cyclase. *Nat Commun.* **2018**, *9*, 1242.
- (25) Orru, M.; Bakešová, J.; Brugarolas, M.; Quiroz, C.; Beaumont, V.; Goldberg, S. R.; Lluís, C.; Cortés, A.; Franco, R.; Casadó, V.; Canela, E. I.; Ferré, S. Striatal pre- and postsynaptic profile of adenosine A_{2A} receptor antagonists. *PLoS One* **2011**, *6*, e16088.
- (26) Chien, E. Y.; Liu, W.; Zhao, Q.; Katritch, V.; Han, G. W.; Hanson, M. A.; Shi, L.; Newman, A. H.; Javitch, J. A.; Cherezov, V.; Stevens, R. C. Structure of the human dopamine D₃ receptor in complex with a D₂/D₃ selective antagonist. *Science* **2010**, *330*, 1091-1095.
- (27) Marti-Renom, M. A.; Stuart, A. C.; Fiser, A.; Sanchez, R.; Melo, F.; Sali, A. Comparative protein structure modeling of genes and genomes. *Annu. Rev. Biophys. Biomol. Struct.* **2000**, *29*, 291-325.

- (28) Manglik, A.; Kruse, A. C.; Kobilka, T. S.; Thian, F. S.; Mathiesen, J. M.; Sunahara, R. K.; Pardo, L.; Weis, W. I.; Kobilka, B. Granier, K.; S. Crystal structure of the μ -opioid receptor bound to a morphinan antagonist. *Nature* **2012**, *485*, 321-326.
- (29) Huang, J.; Chen, S.; Zhang, J. J.; Huang, X. Y. Crystal structure of oligomeric β 1-adrenergic G protein-coupled receptors in ligand-free basal state. *Nat. Struct. Mol. Biol.* **2013**, *20*, 419-425.
- (30) de Vries, S. J.; van Dijk, M.; Bonvin, A. M. The HADDOCK web server for data-driven biomolecular docking. *Nat. Protoc.* **2010**, *5*, 883-897.
- (31) Cordomi, A.; Edholm, O.; Perez, J. J. Effect of Force Field Parameters on Sodium and Potassium Ion Binding to Dipalmitoyl Phosphatidylcholine Bilayers. *J. Chem. Theory Comput.* **2009**, *5*, 2125-2134.
- (32) Lindorff-Larsen, K.; Piana, S.; Palmo, K.; Maragakis, P.; Klepeis, J. L.; Dror, R. O.; Shaw, D. E. Improved side-chain torsion potentials for the Amber ff99SB protein force field. *Proteins* **2010**, *78*, 1950-1958.
- (33) Berger, O.; Edholm, O.; Jähnig, F. Molecular dynamics simulations of a fluid bilayer of dipalmitoylphosphatidylcholine at full hydration, constant pressure, and constant temperature. *Biophys. J.* **1997**, *72*, 2002-2013.
- (34) Wang, J.; Wolf, R. M.; Caldwell, J. W.; Kollman, P. A.; Case, D. A. Development and testing of a general amber force field. *J. Comput. Chem.* **2004**, *25*, 1157-1174.
- (35) Cordomi, A.; Caltabiano, G.; Pardo, L. Membrane Protein Simulations Using AMBER Force Field and Berger Lipid Parameters. *J. Chem. Theory Comput.* **2012**, *8*, 948-958.
- (36) Pronk, S.; Pall, S.; Schulz, R.; Larsson, P.; Bjelkmar, P.; Apostolov, R.; Shirts, M. R.; Smith, J. C.; Kasson, P. M.; van der Spoel, D.; Hess, B.; Lindahl, E. GROMACS 4.5: a high-throughput and highly parallel open source molecular simulation toolkit. *Bioinformatics* **2013**, *29*, 845-854.

Supporting Information for

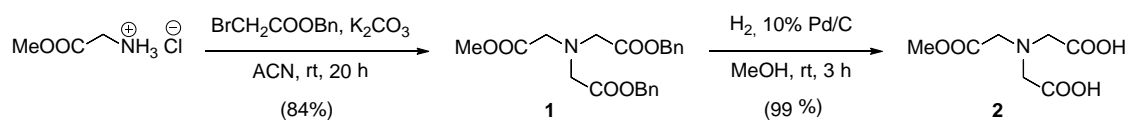
Design of a true bivalent ligand with picomolar binding affinity for a G protein-coupled receptor homodimer

Daniel Pulido,^{†,‡,#} Verònica Casadó-Anguera,^{§,||,⊥,#} Laura Pérez-Benito,^{∇,#} Estefanía Moreno,^{§,||,⊥} Arnau Cordoní,[∇] Laura López,[∇] Antoni Cortés,^{§,||,⊥} Sergi Ferré,[¶] Leonardo Pardo,^{,∇} Vicent Casadó^{*,§,||,⊥} and Miriam Royo^{*,†,‡}*

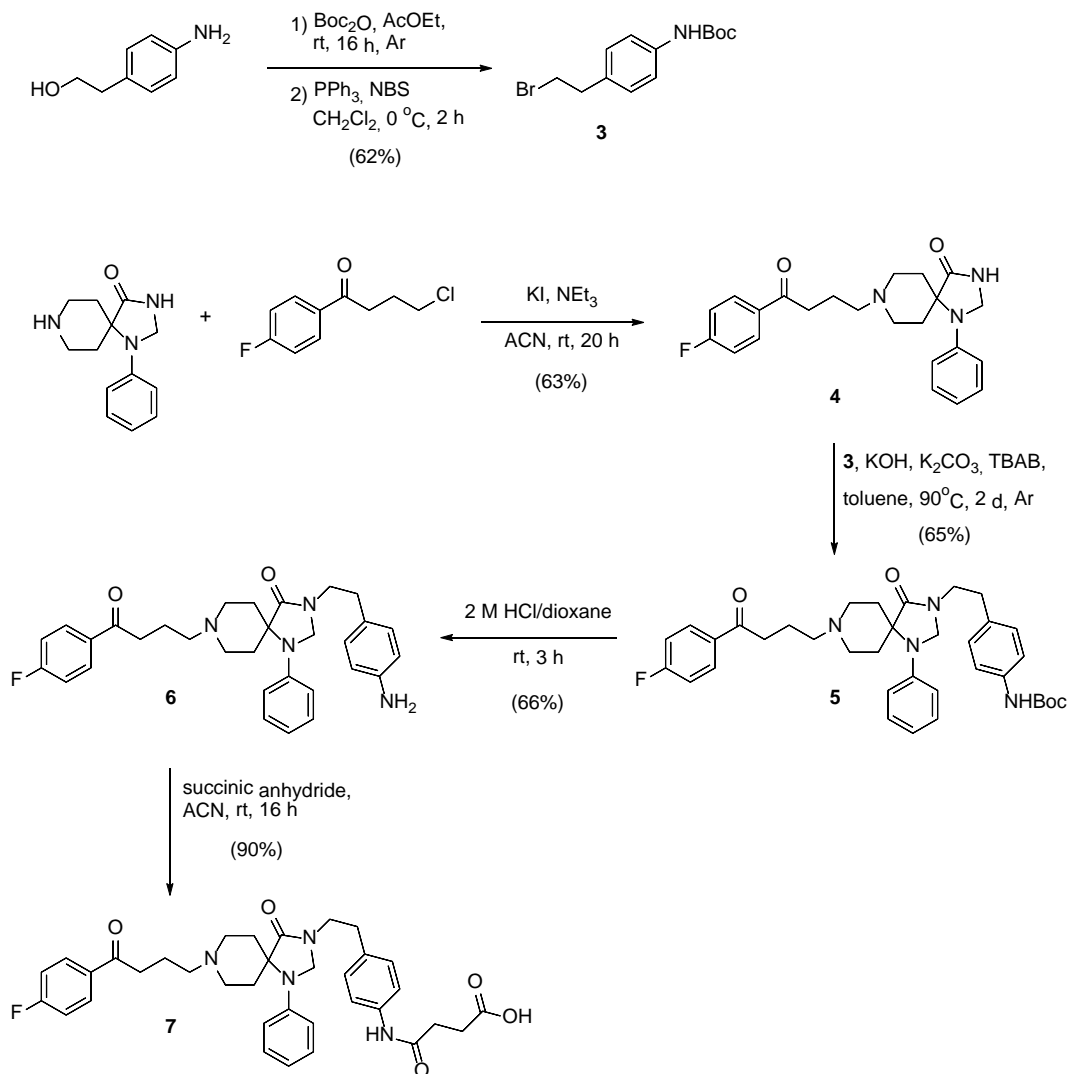
Table of Contents

Scheme S1. Synthesis of the nitrilotriacetic (NTA) derived core 2	S3
Scheme S2. Synthesis of the pharmacophore-linker derivative 7	S3
Scheme S3. Synthesis of the OEG derivatives 8-11	S4
Figure S1	S5
Figure S2	S5
Figure S3	S6
Table S1	S7
NMR Spectra of Compounds 1-15	S8
HPLC traces of compounds 7, 12-15	S23
References	S25

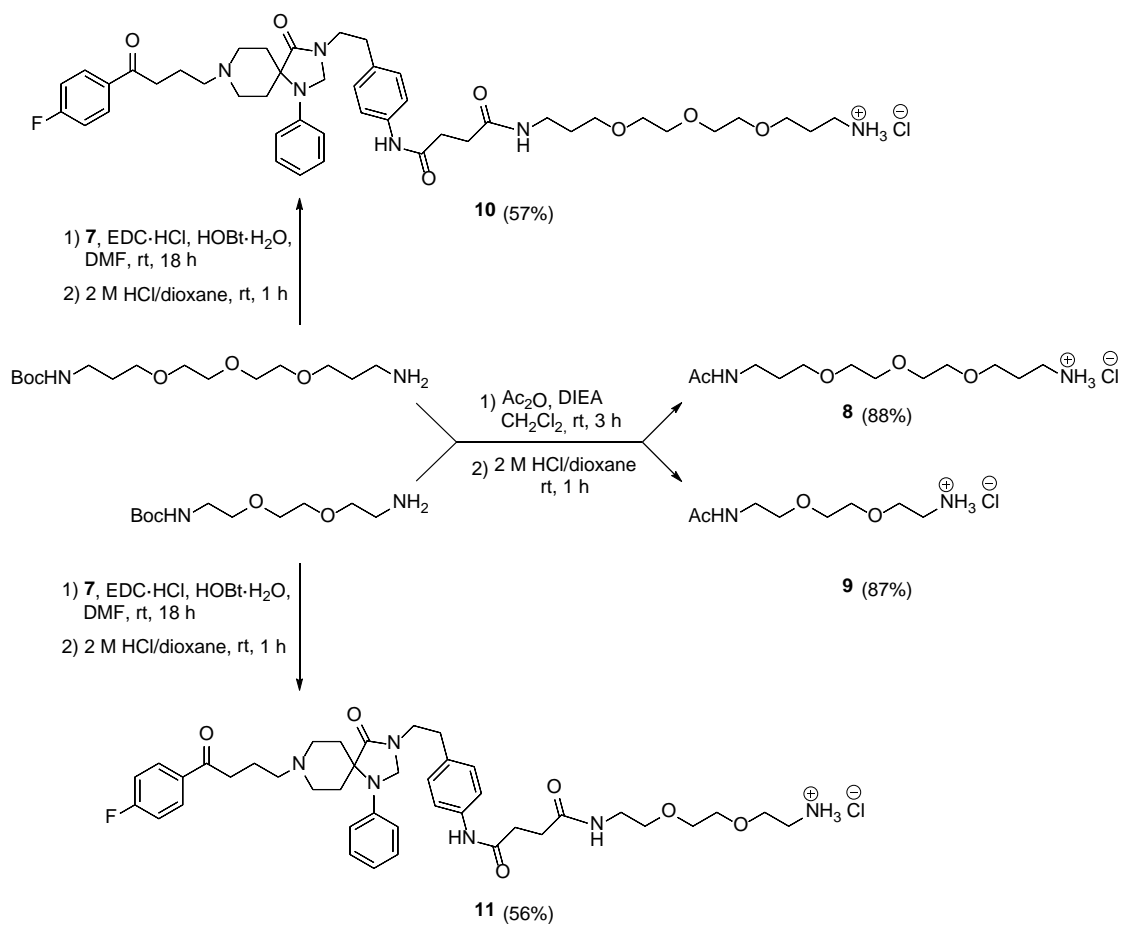
Scheme S1. Synthesis of the nitrilotriacetic (NTA) derived core **2**. (*inspired in*¹)



Scheme S2. Synthesis of the pharmacophore-linker derivative **7**.²



Scheme S3. Synthesis of the OEG derivatives **8-11**.



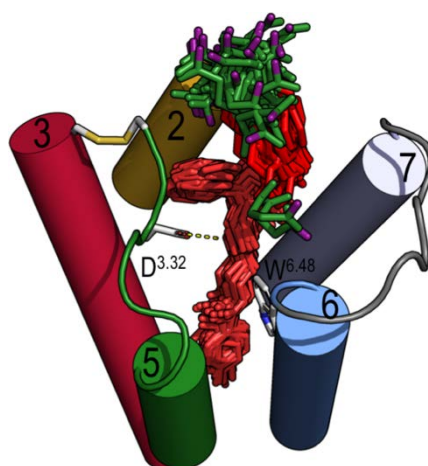


Figure S1. MD simulations of the pharmacophore-linker derivative **7** in complex with the D₂R monomer (extracellular view in which transmembrane helices (TM) are depicted as cylinders and extracellular loops (ECL) as ribbons; TMs 1 and 4, ECL 1, and part of ECL 2 are omitted for clarity). The structures of **7** (the color code of the atoms is as in Figure 1) are extracted from the simulations (50 structures collected every 10 ns), whereas the structure of the D₂R monomer corresponds to the initial model. The stability of the system is analyzed in Figure S3. Clearly, the pharmacophore unit (red) remains highly stable at the binding site during the simulation, whereas the linker moiety (green), at the extracellular aqueous environment, is very flexible and achieves diverse conformations between ECL 2 and 3. The attachment point (purple) is oriented toward different points in space and can be used for linking the spacer group.

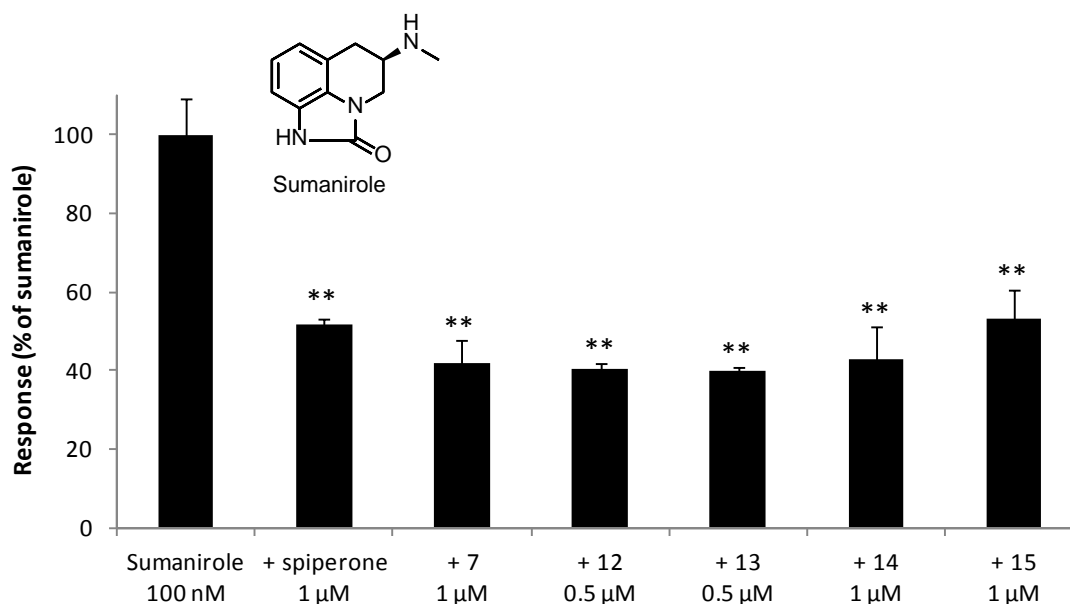


Figure S2. Quantification of the antagonist effect of D₂R ligands on dynamic redistribution mass assays (DMR). Values are mean±SEM from 3 determinations. Statistical significance was calculated by one-way ANOVA followed by Dunnett's post hoc test. **p<0.01 compared to sumanirole alone.

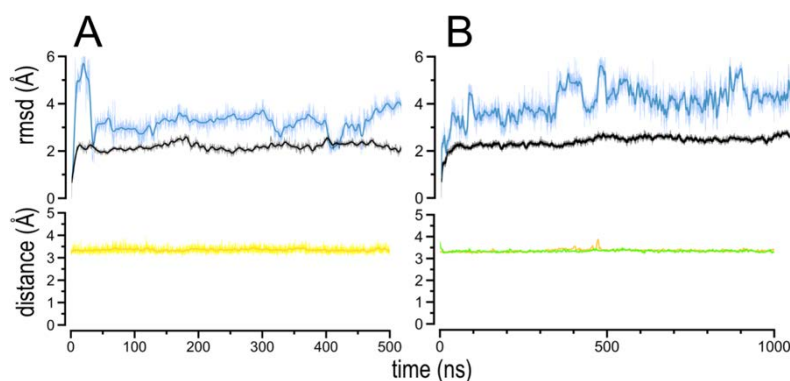
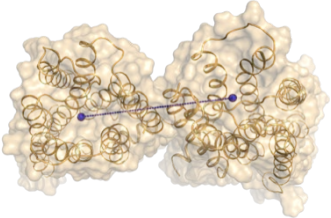
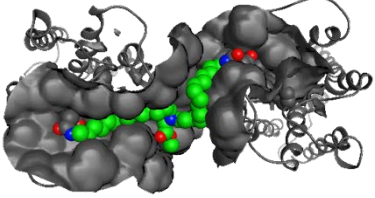
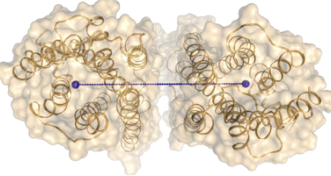
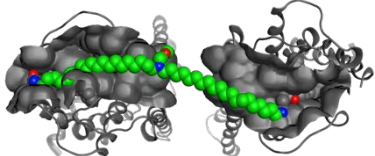
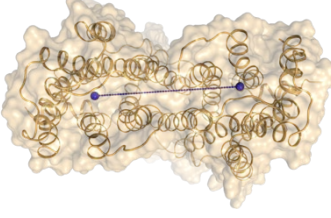
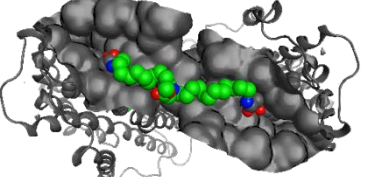
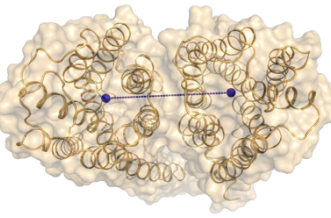
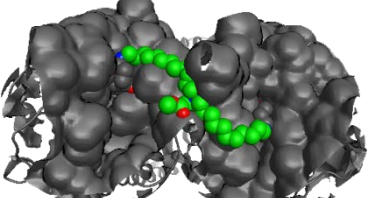
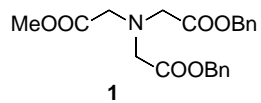


Figure S3. MD simulations of the pharmacophore-linker derivative **7** (A, Figure S1), and bivalent ligand **13** (B, Figure 5) were monitored by the root mean-square deviation (rmsd) of the backbone atoms (black) of the monomer (A) or the homodimer (B) and ligand heavy atoms (blue) along the trajectories. Clearly, rmsd values for the monomer are similar than for the homodimer. Thus, the modeled TM6 interface for the homodimer remains unchanged during the unbiased 1 μ s MD simulation (rmsd \approx 2Å). As expected, rmsd values of bivalent ligand **13** are larger than those of the pharmacophore-linker derivative **7** due to the flexibility of the linker/spacer chain. The binding of the pharmacophore unit to the orthosteric binding site was monitored by the salt bridge distance between the protonated amine of **7** and Asp^{3.32} of the monomer (yellow line in A) or by salt bridge distances between both protonated amines of **13** and Asp^{3.32} of monomers A (yellow line in B) and B (green line in B). These distances (<3.5Å) confirm that the designed bivalent ligand **13** remains stable at the orthosteric binding cavities through the unbiased 1 μ s MD simulation.

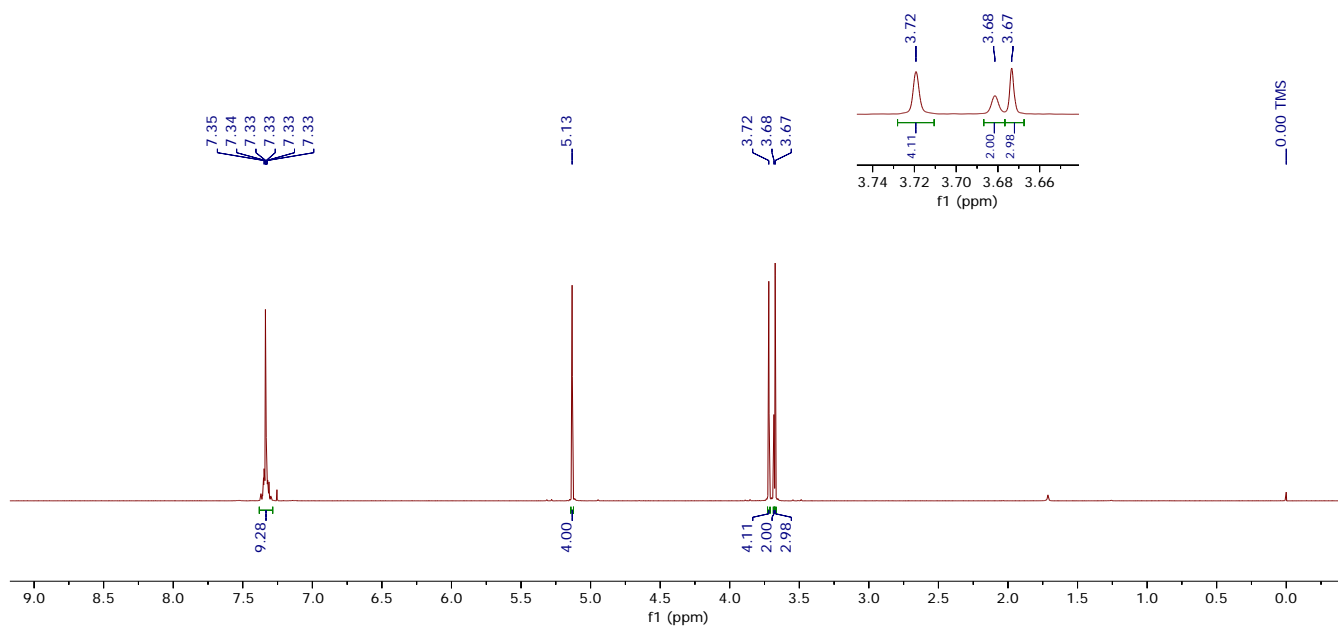
Table S1. Comparison of the distances between the center of mass of the binding site of spiperone (blue sphere) for D₂R homodimers constructed via the TM1/2, TM4/5, TM5/6, and TM6 interfaces. Calculation of the preferred spacer size of bivalent ligands for the D₂R homodimer constructed via these interfaces. We constructed a van der Waals interaction surface on the protein (in gray) that defines 3D positions that could represent a favorable interaction between the dimer and the spacer of the bivalent ligand. The MOE-based tool identifies the shortest path through the surface vertices whilst starting and ending at the attachment points on the pharmacophore-linker derivative **7**. We report the number of heavy atoms between each pharmacophore/linker unit, including the attachment atom.

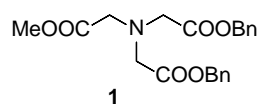
Interface	Distance		Spacer	
TM1/2	36 Å		31	
TM4/5	43 Å		43	
TM5/6	33 Å		25	
TM6	27 Å		25	

NMR Spectra of Compounds 1-15

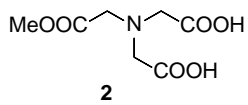
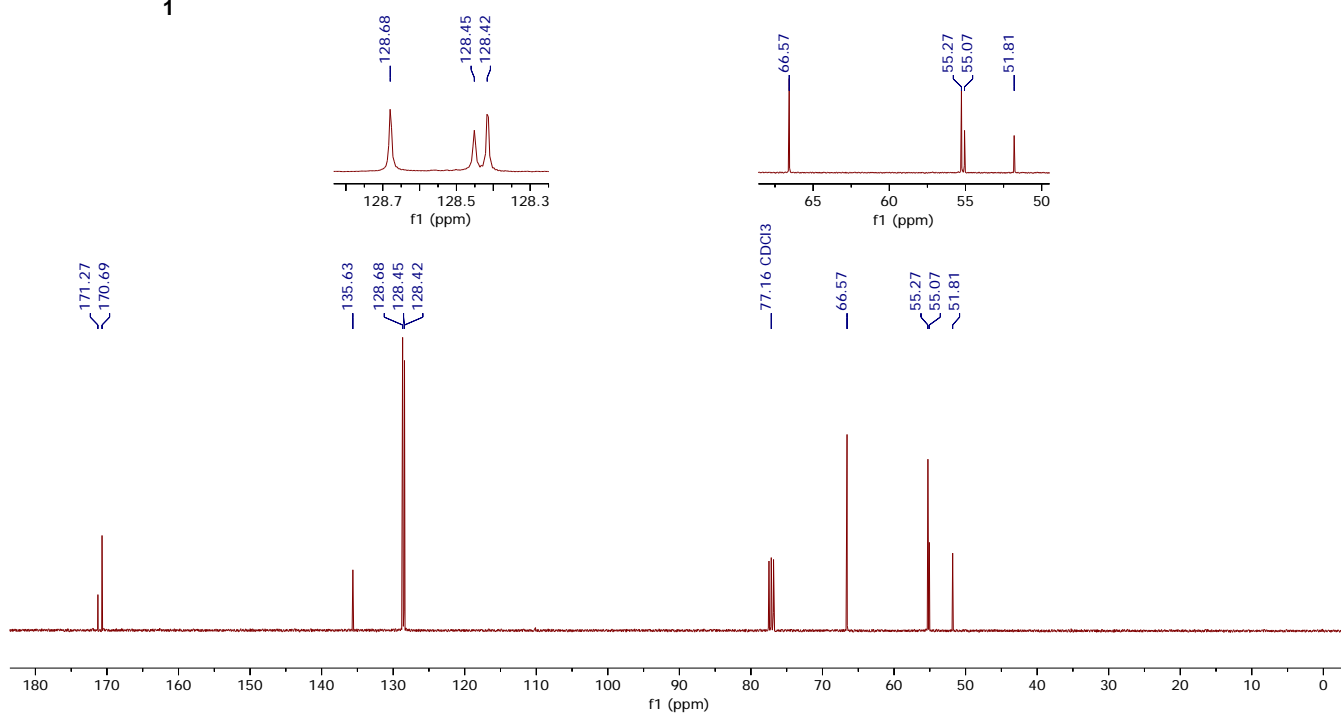


^1H NMR (400 MHz, CDCl_3) δ 7.38 – 7.28 (m, 10H), 5.13 (s, 4H), 3.72 (s, 4H), 3.68 (s, 2H), 3.67 (s, 3H).

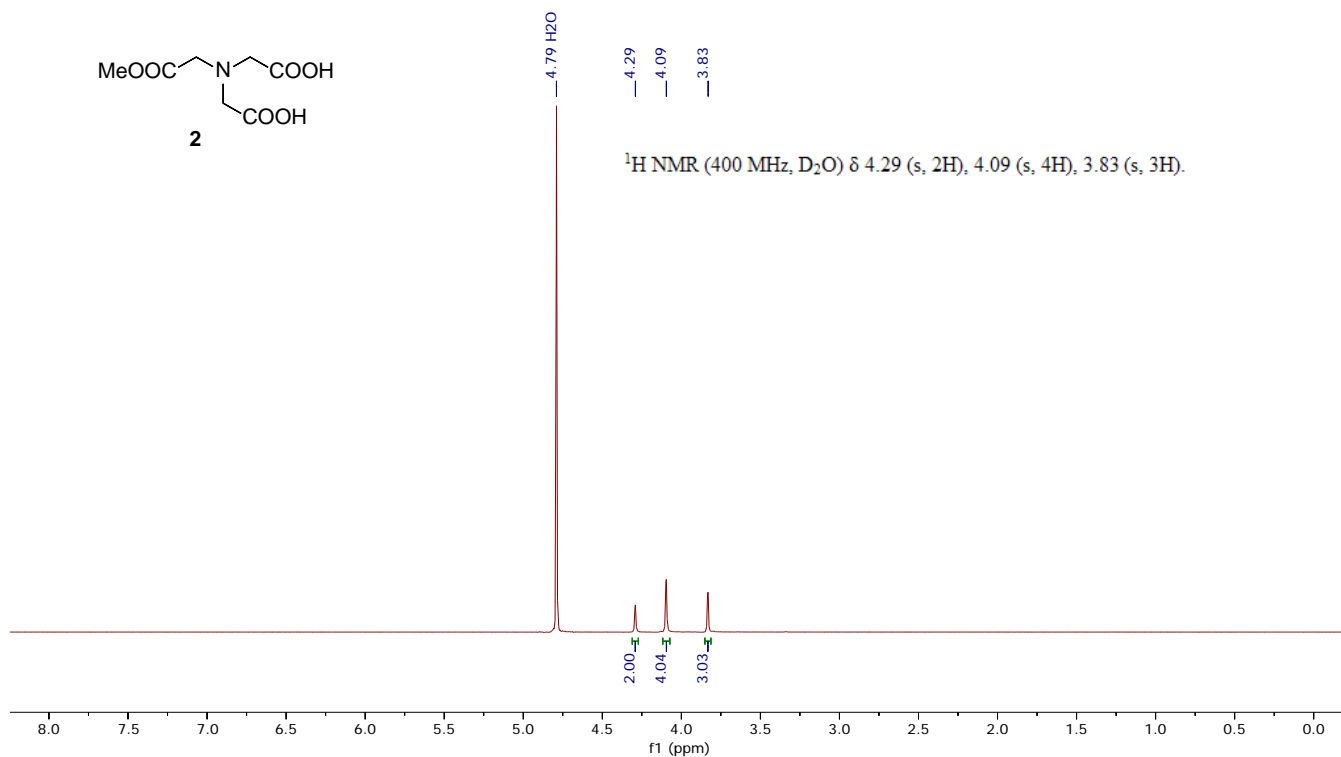


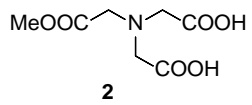


^{13}C NMR (101 MHz, CDCl_3) δ 171.27, 170.69, 135.63, 128.68, 128.45, 128.42, 66.57, 55.27, 55.07, 51.81.

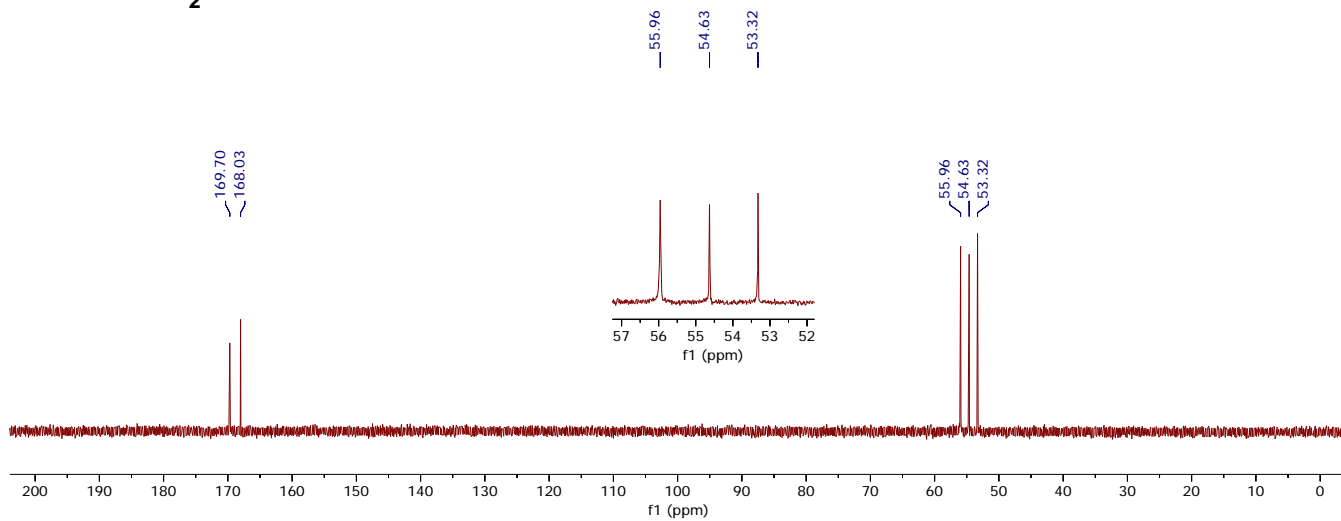


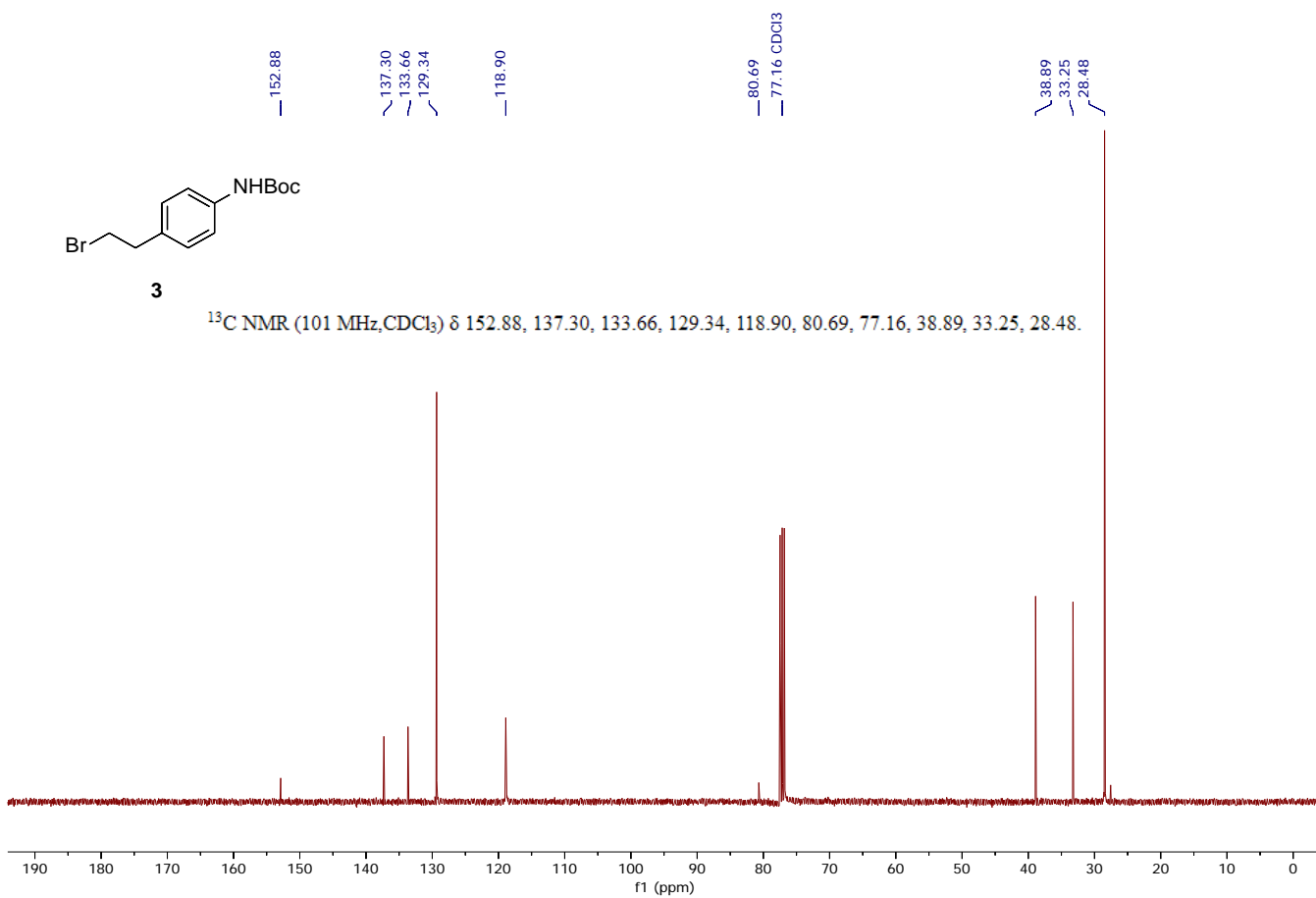
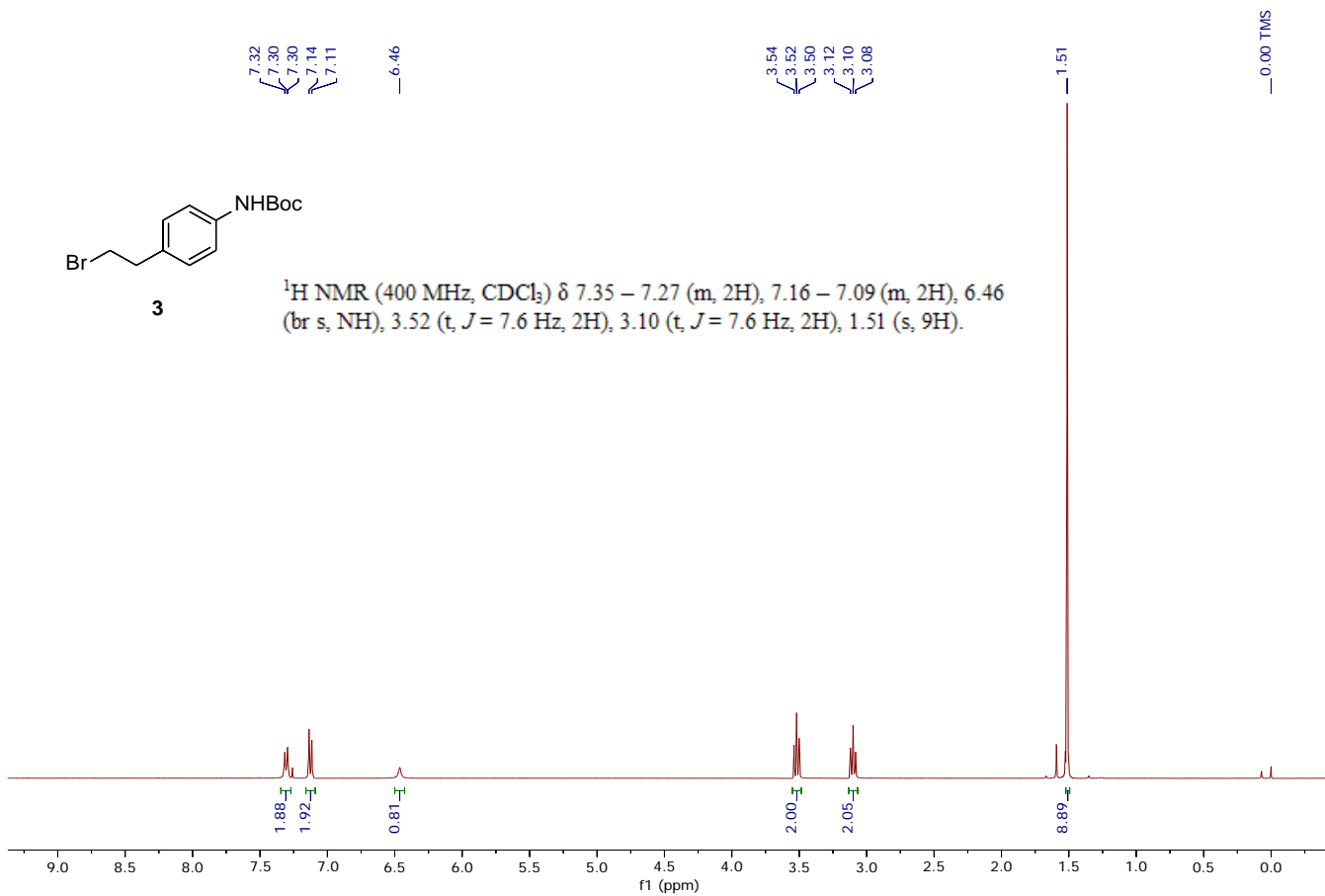
^1H NMR (400 MHz, D_2O) δ 4.29 (s, 2H), 4.09 (s, 4H), 3.83 (s, 3H).

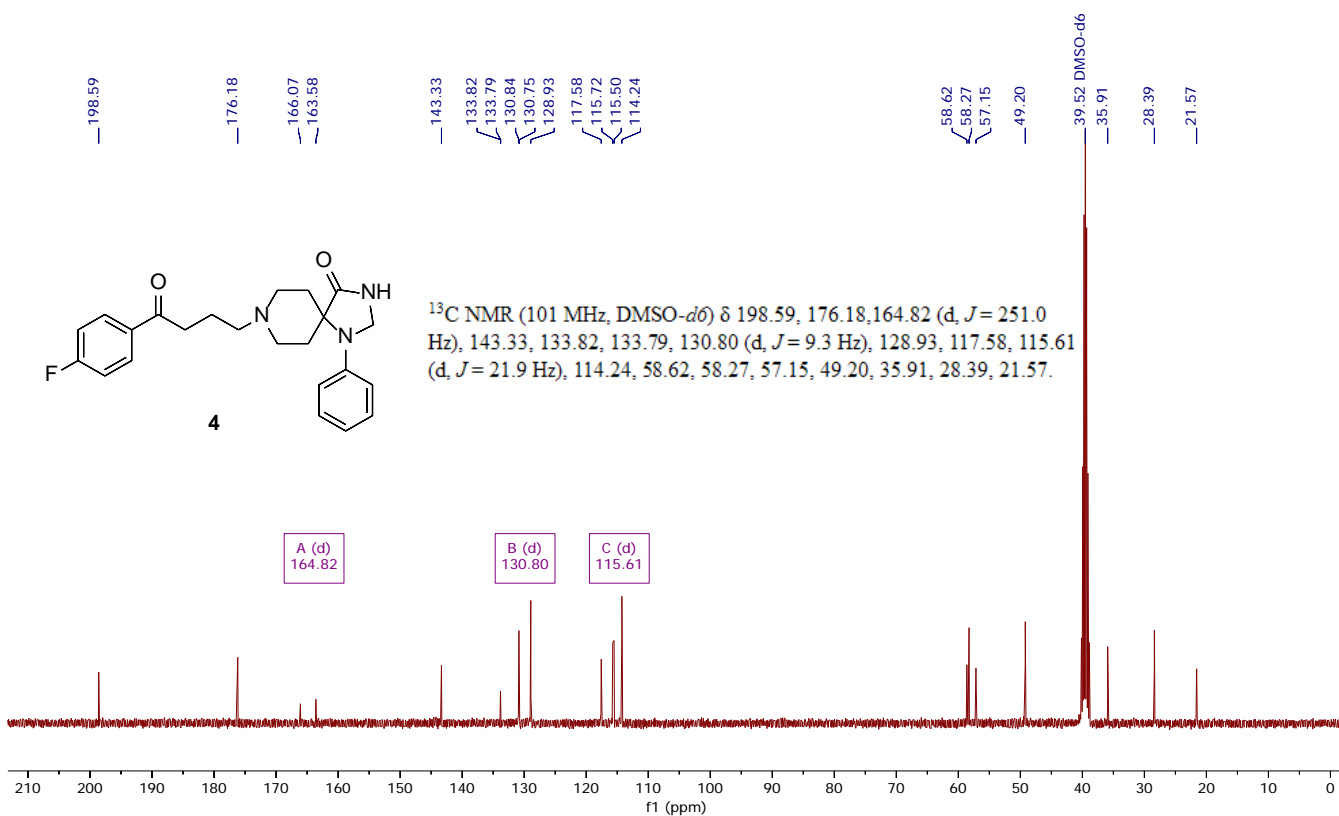
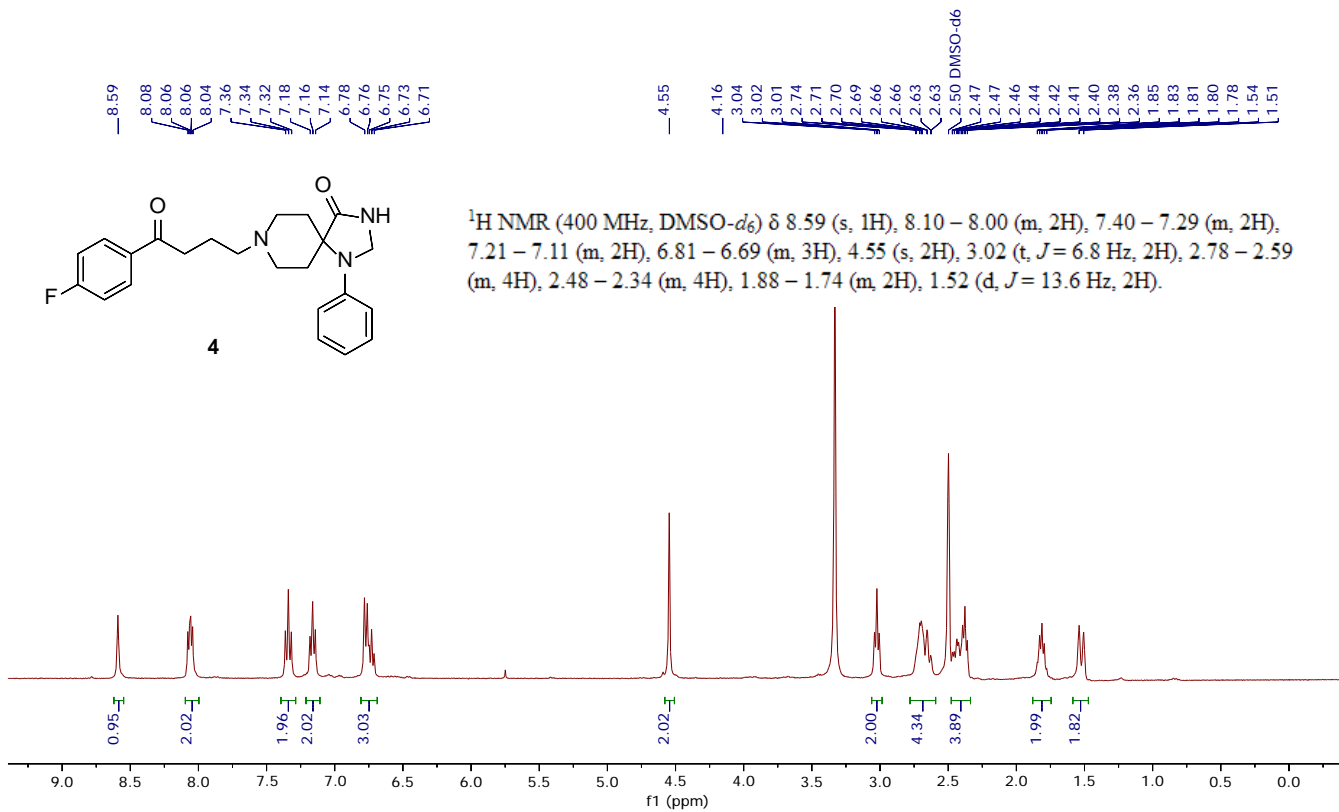


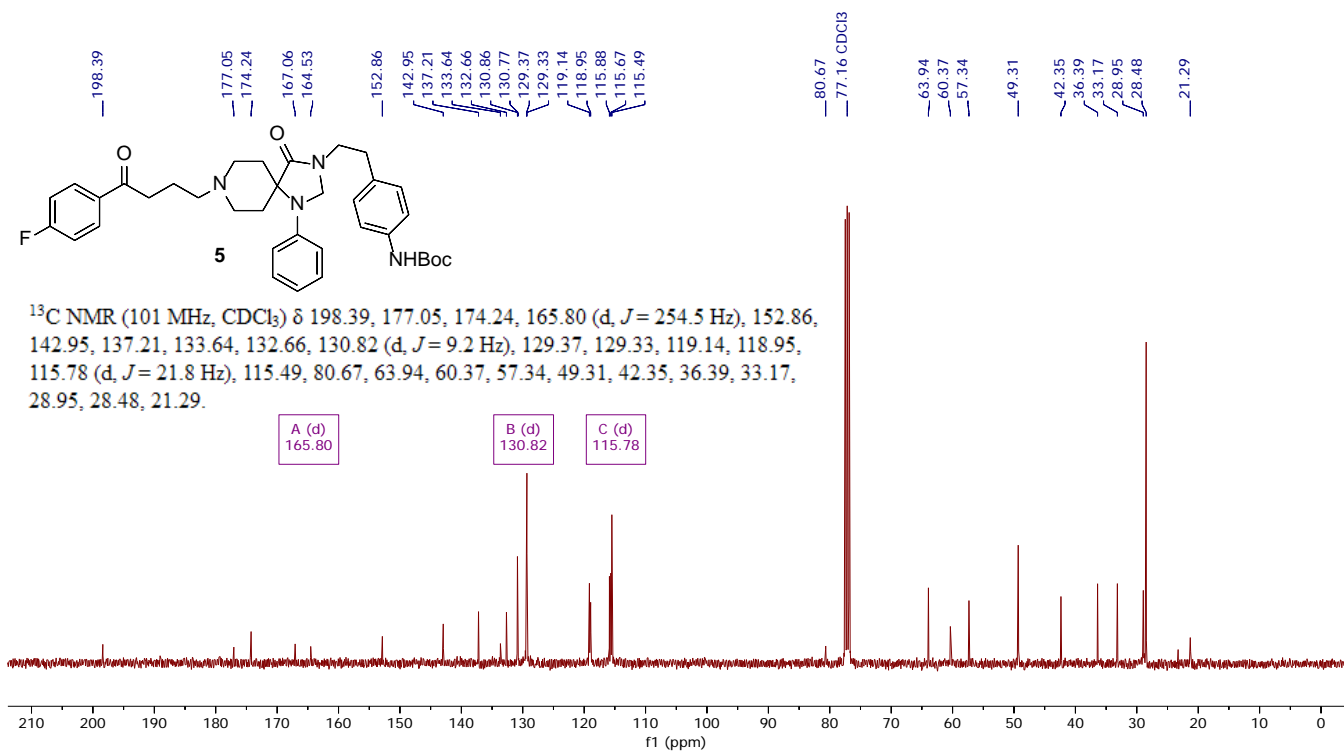
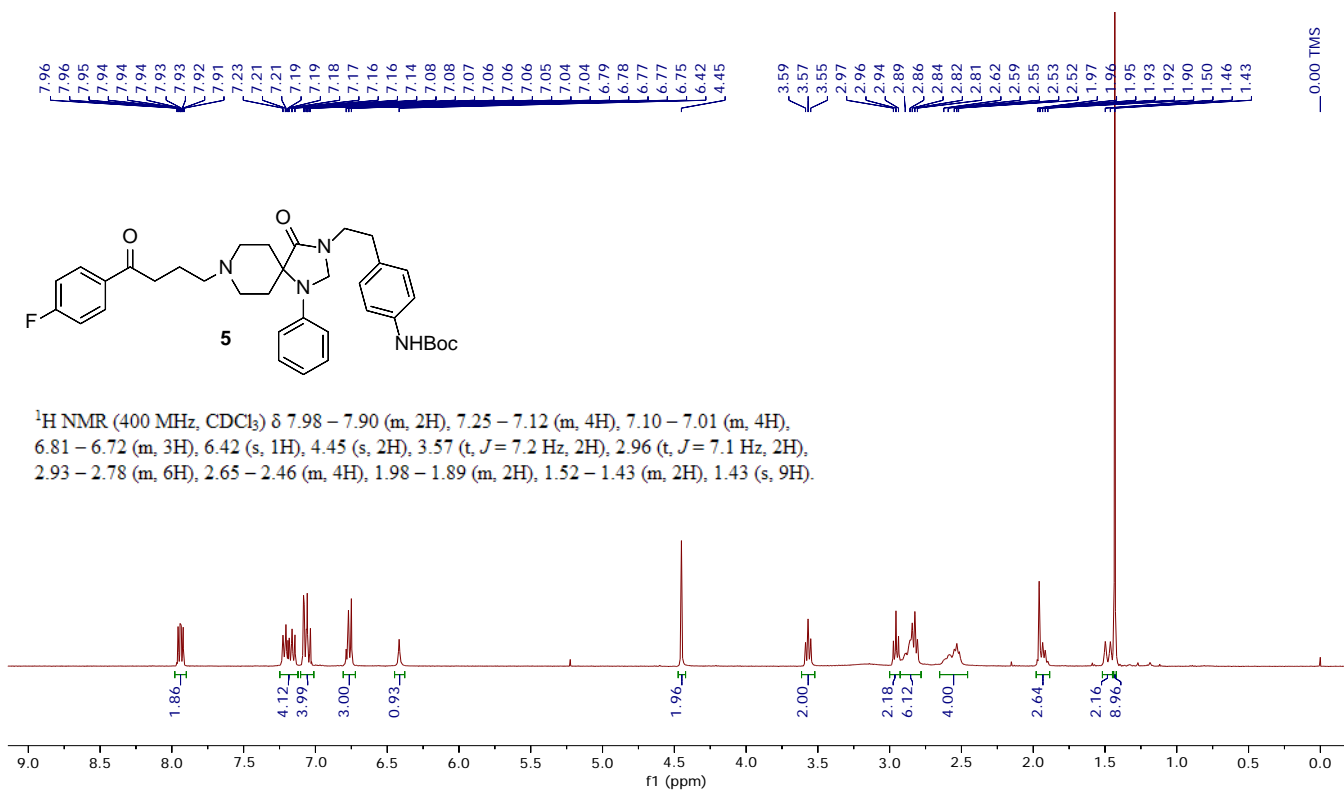


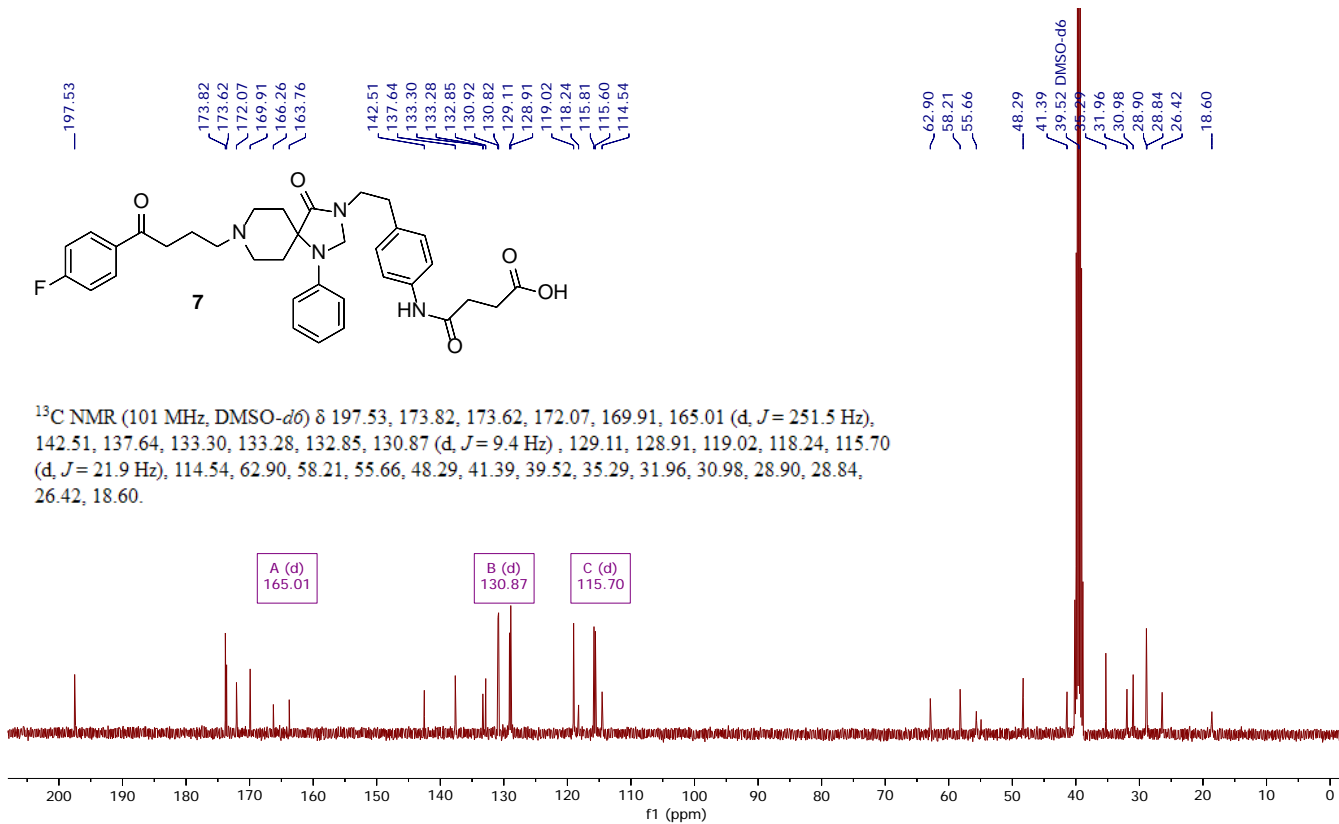
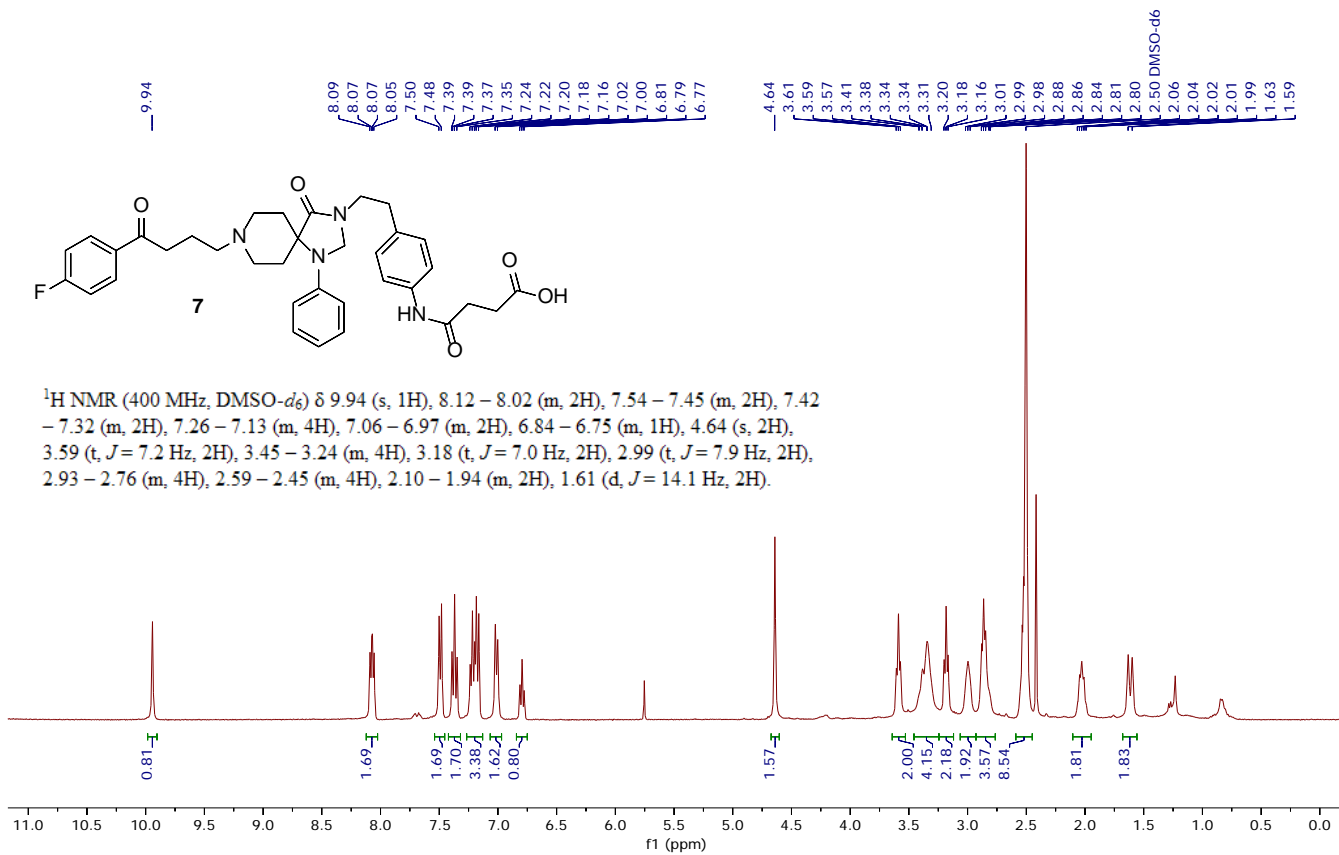
^{13}C NMR (101 MHz, D_2O) δ 169.70, 168.03, 55.96, 54.63, 53.32.

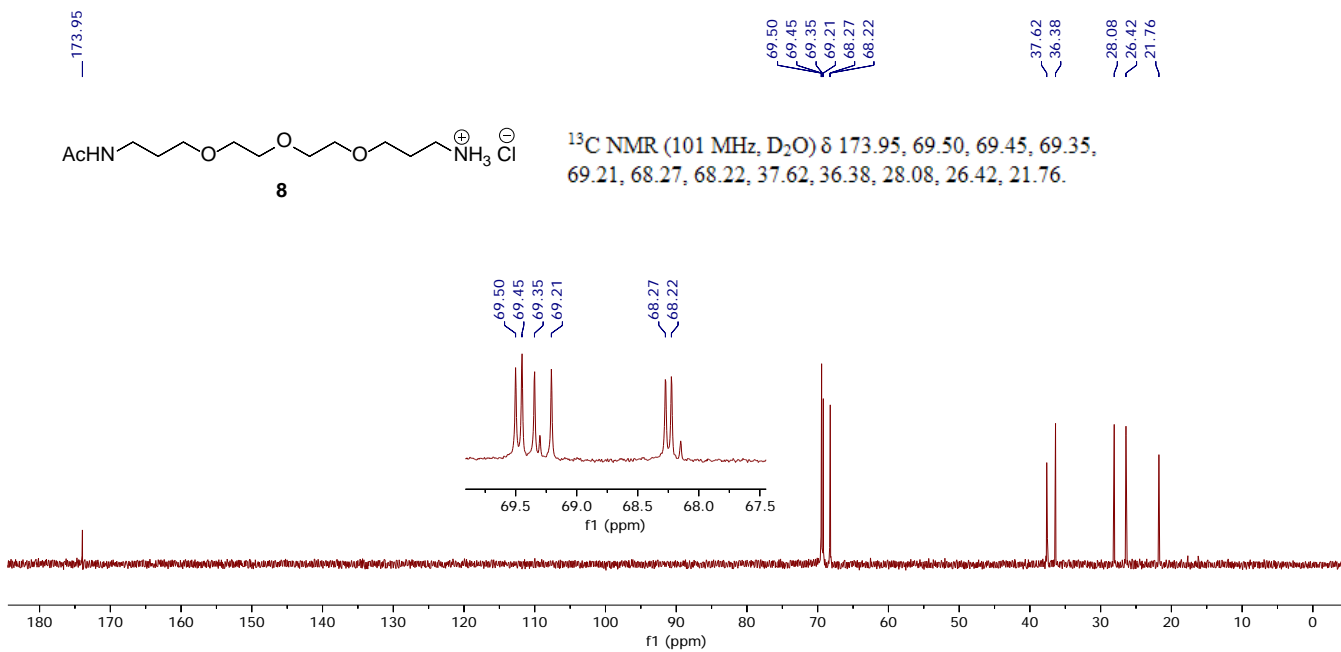
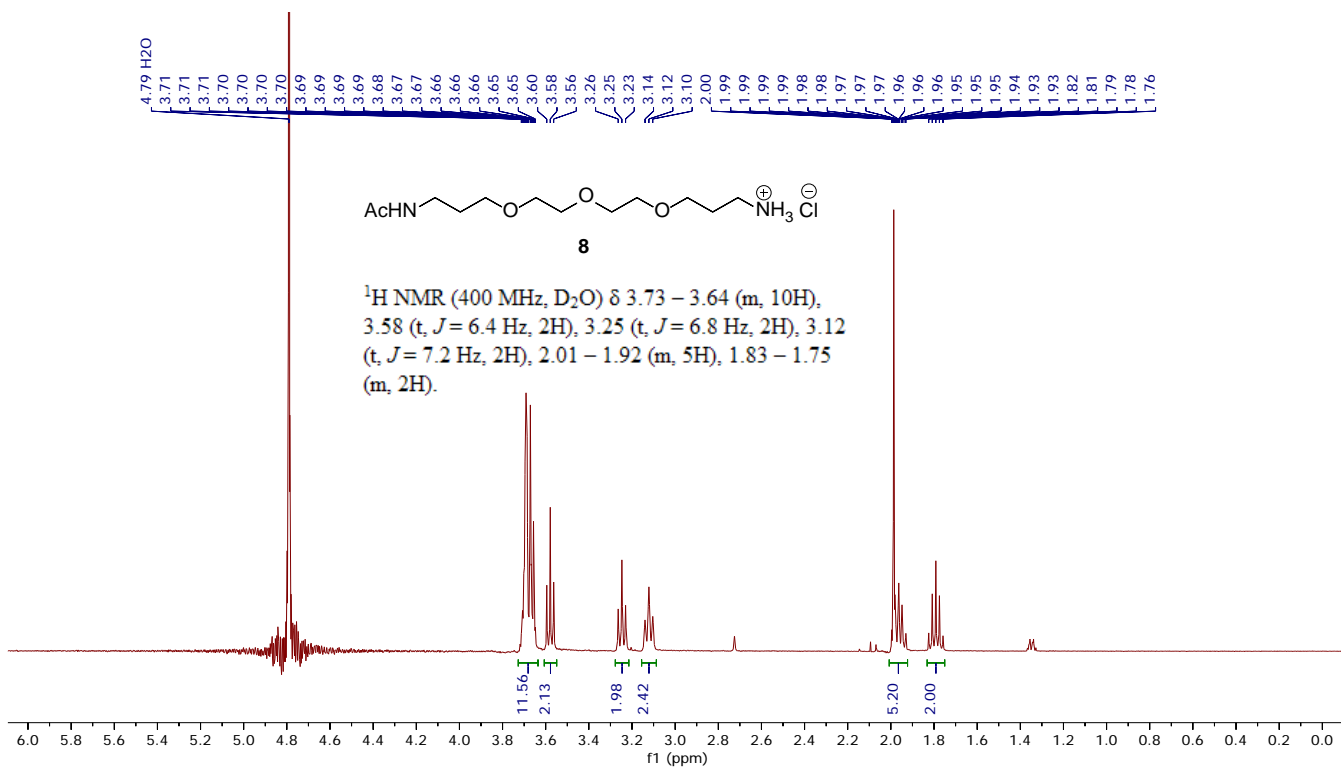


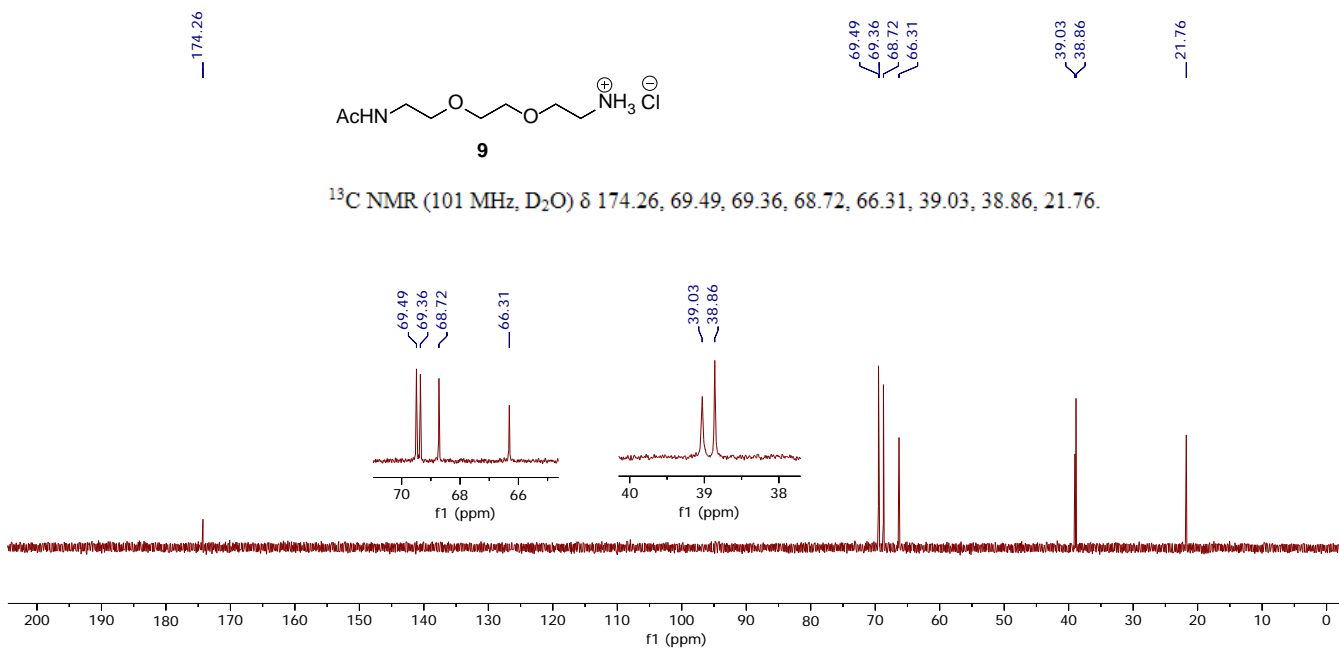
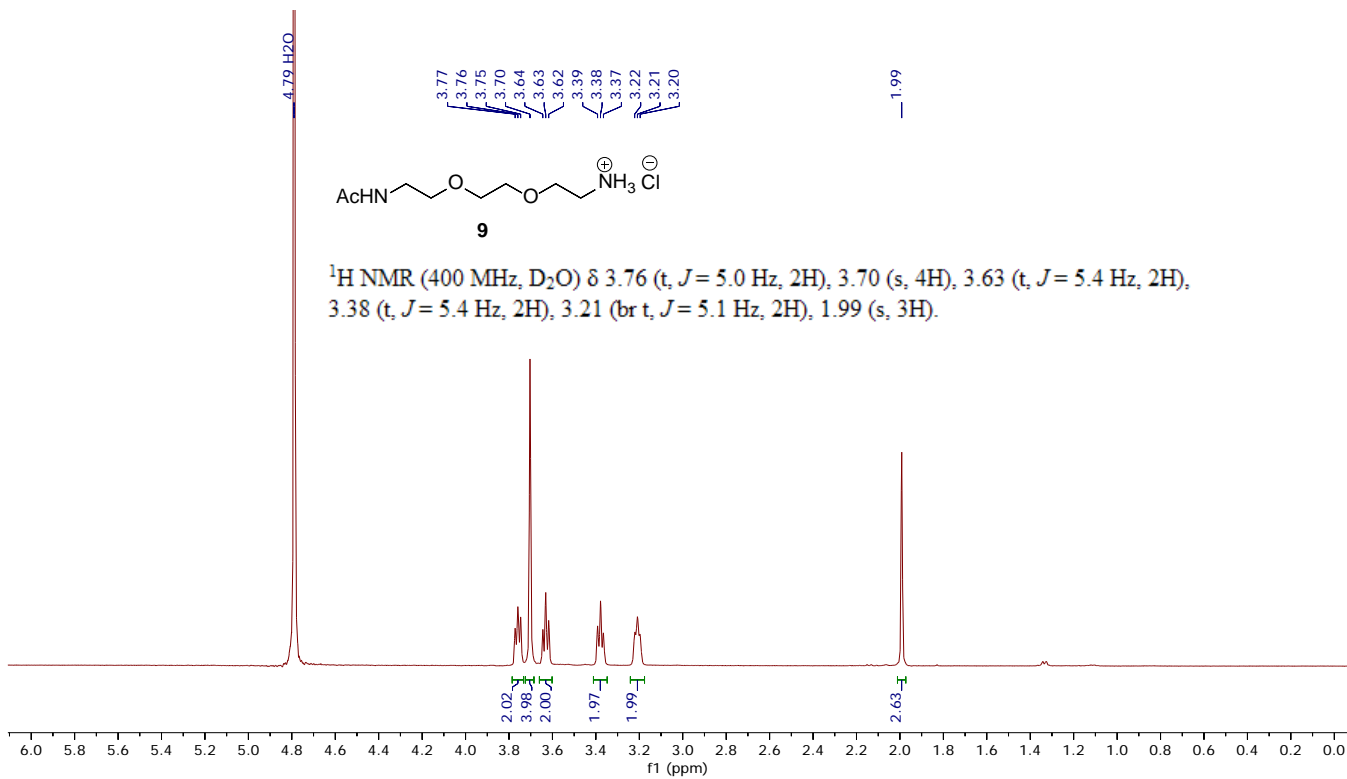


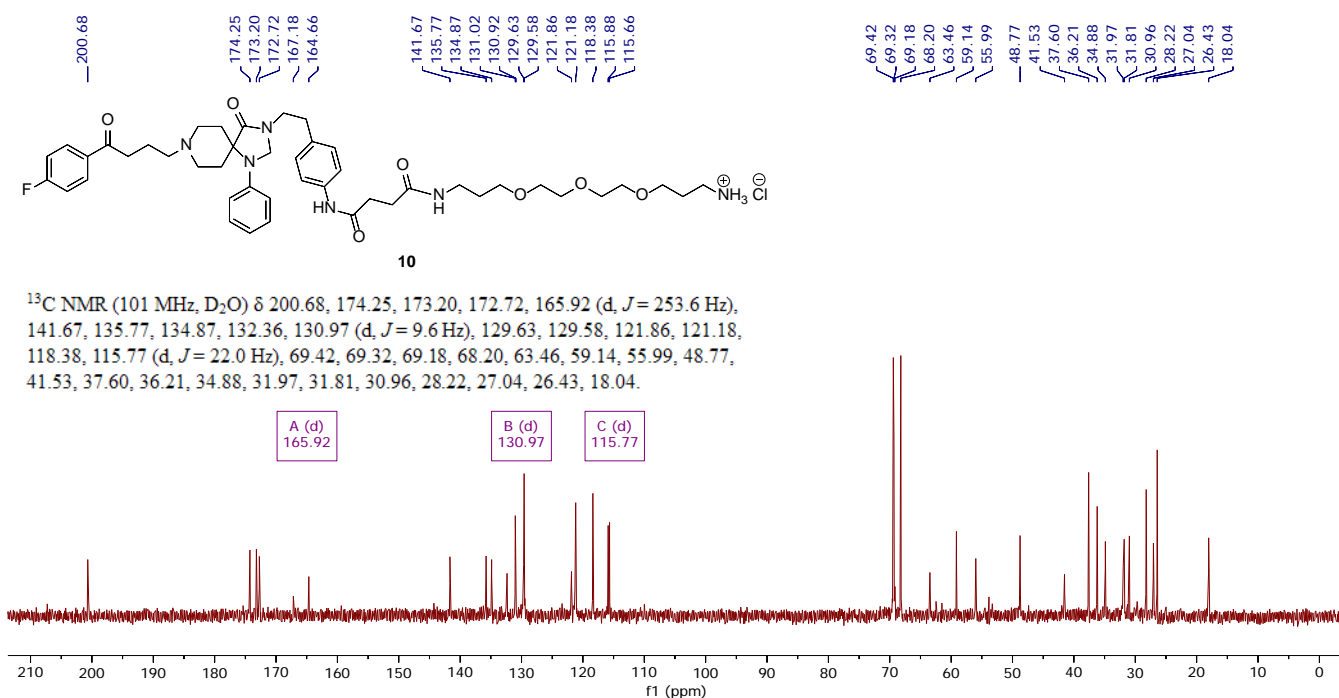
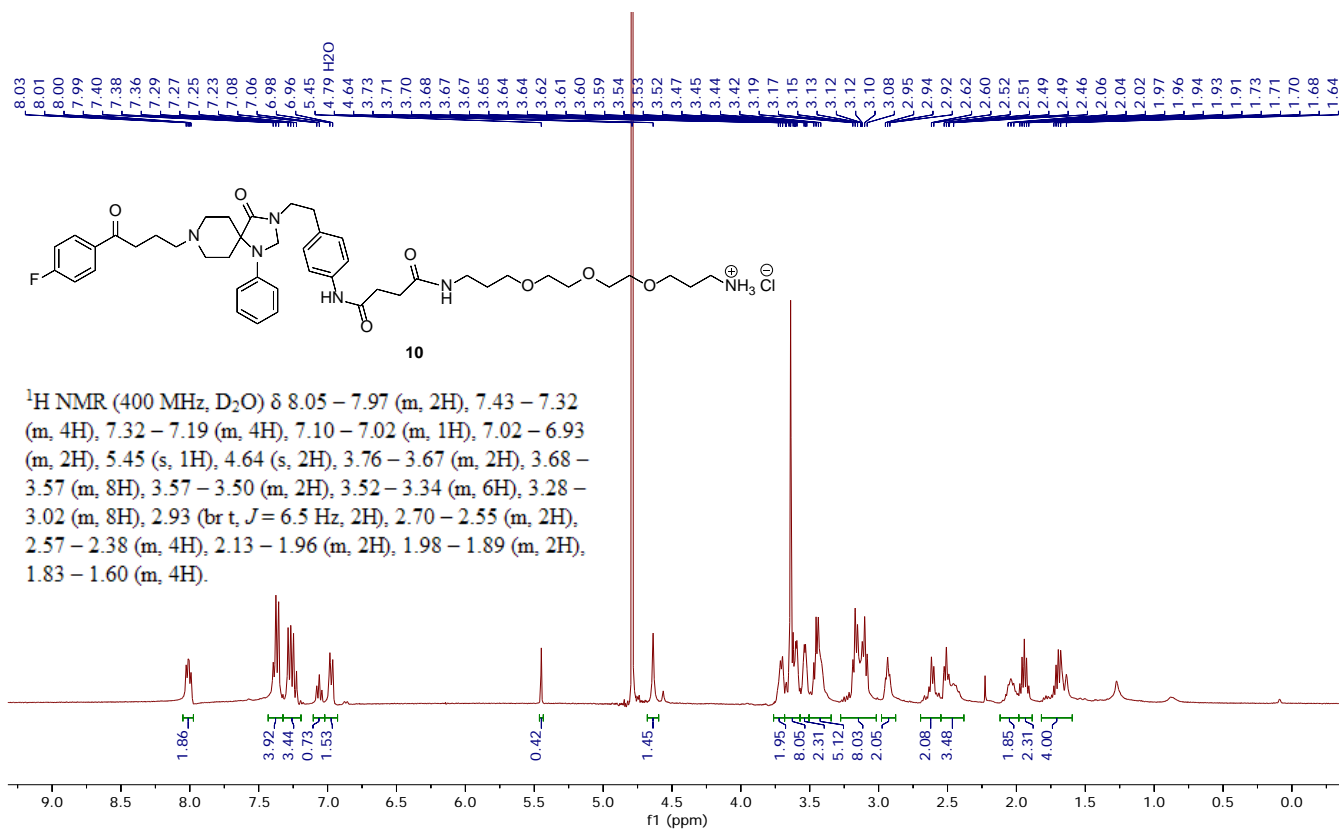


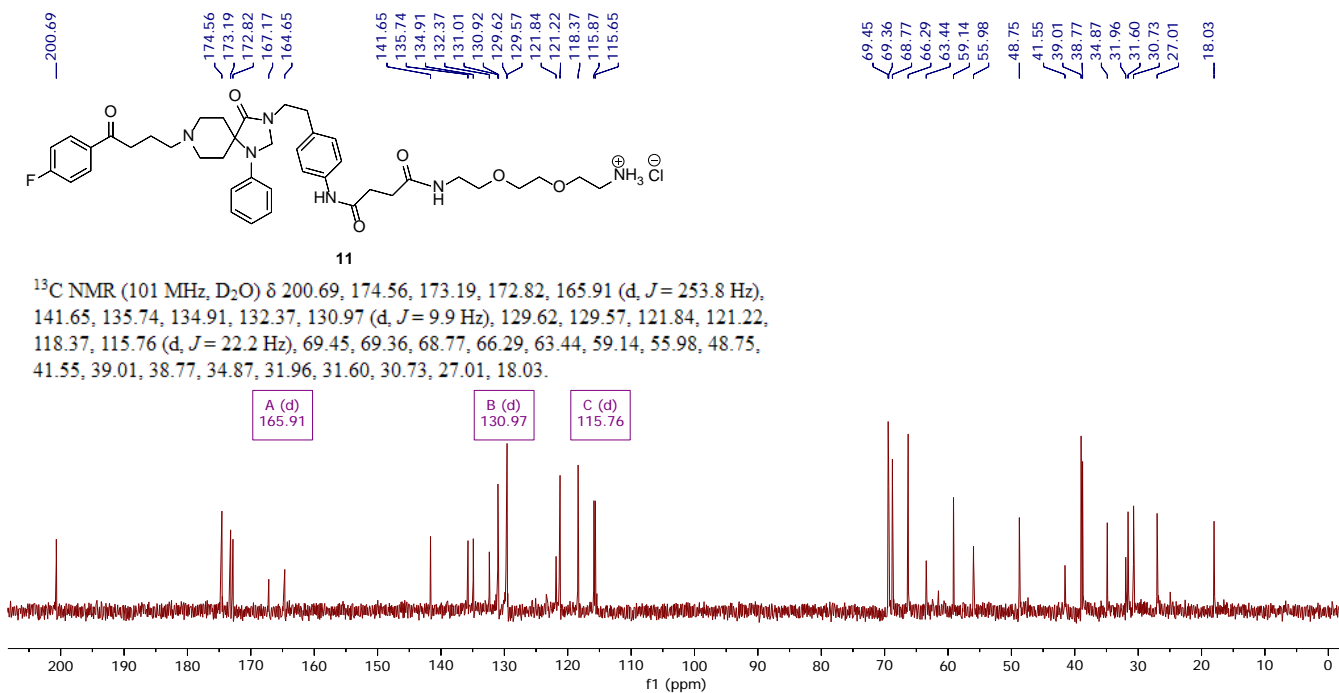
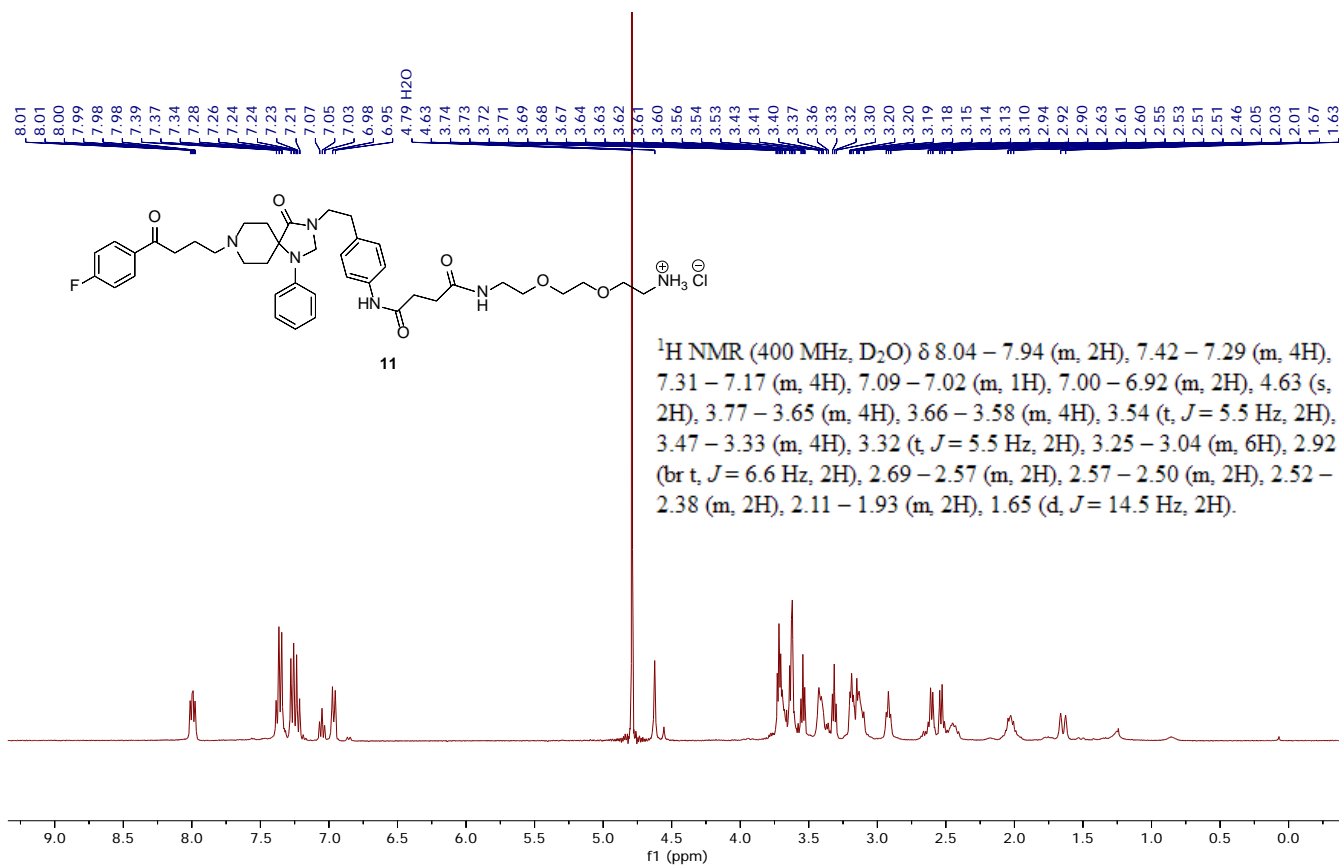


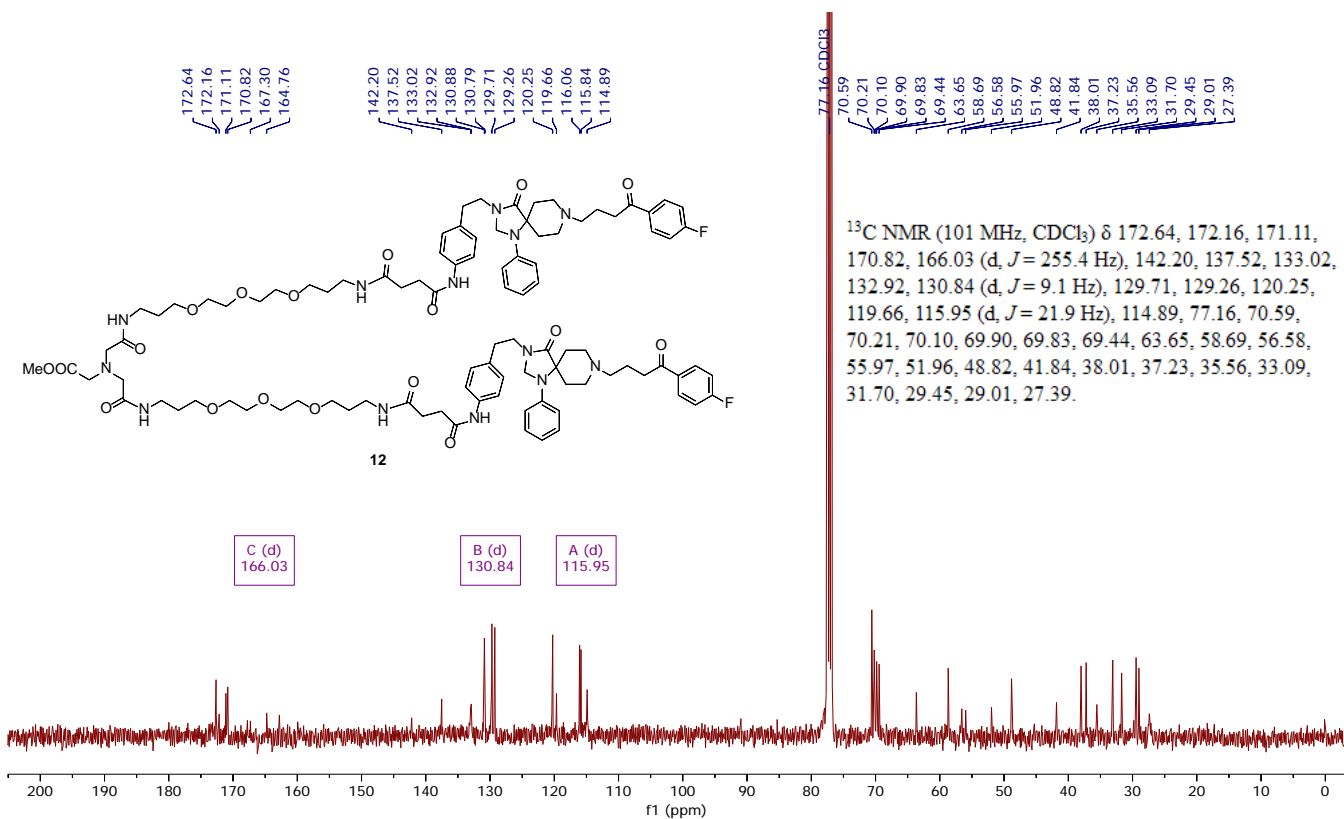
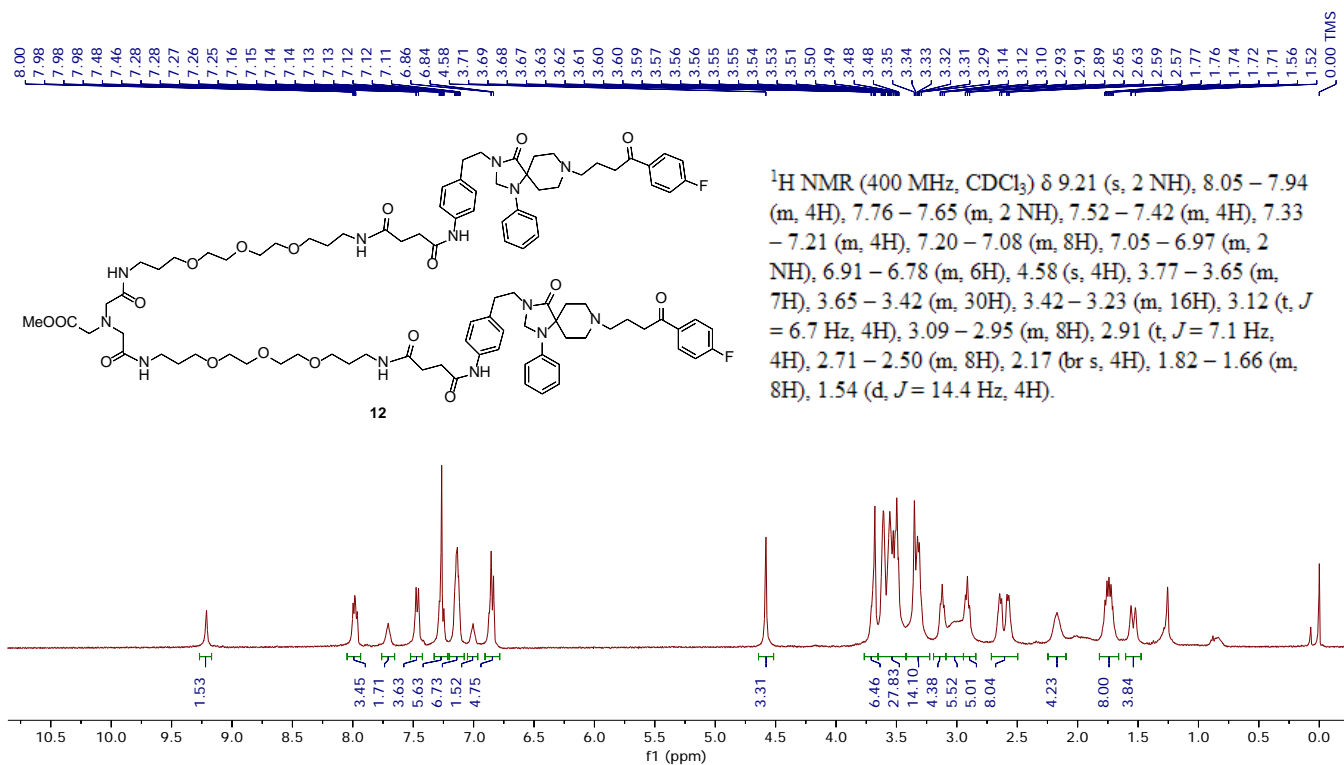


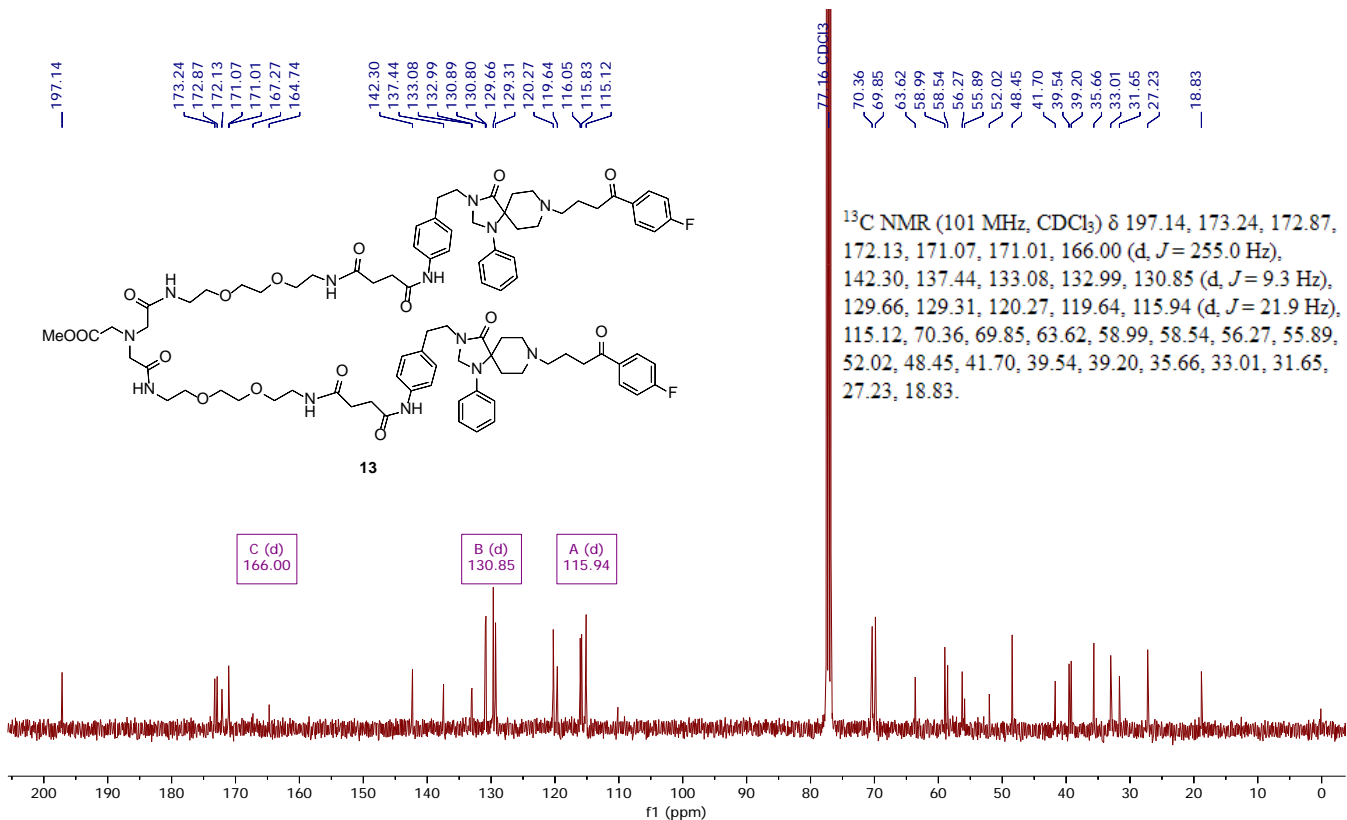
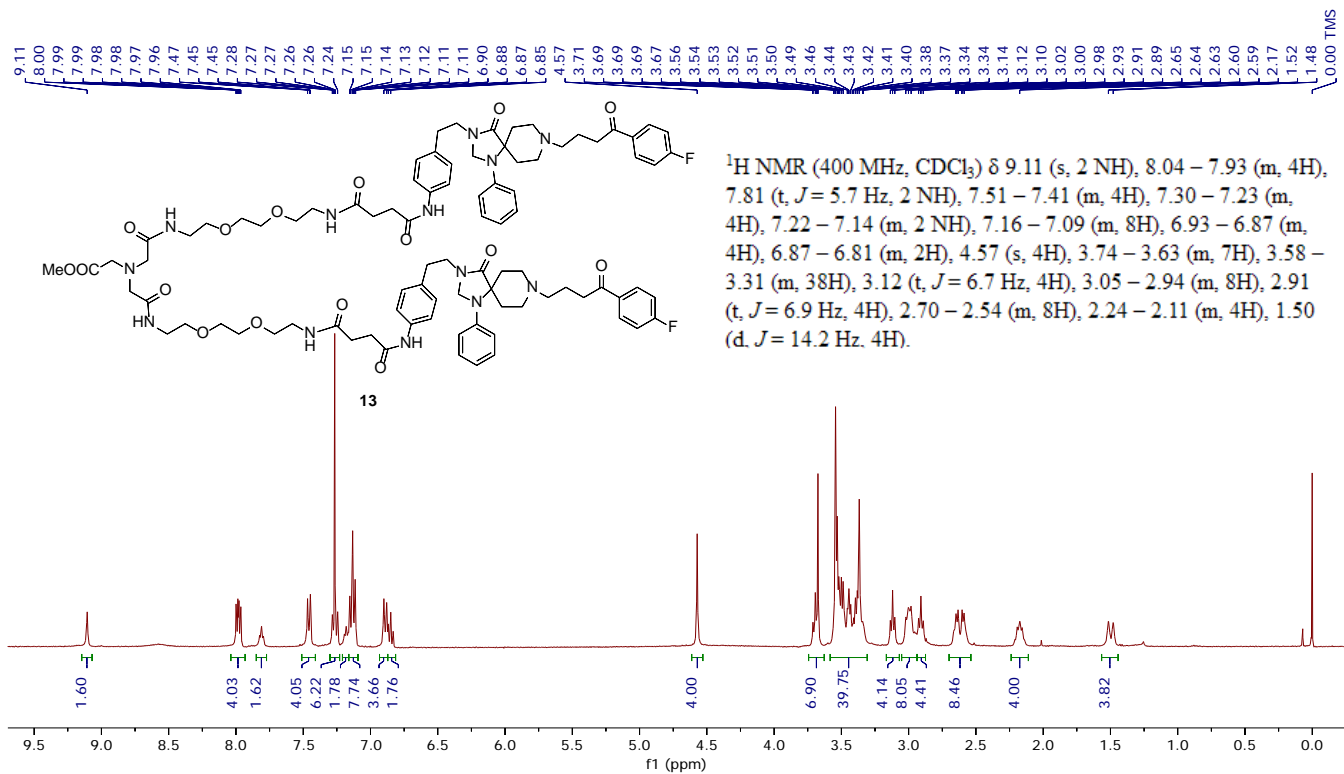


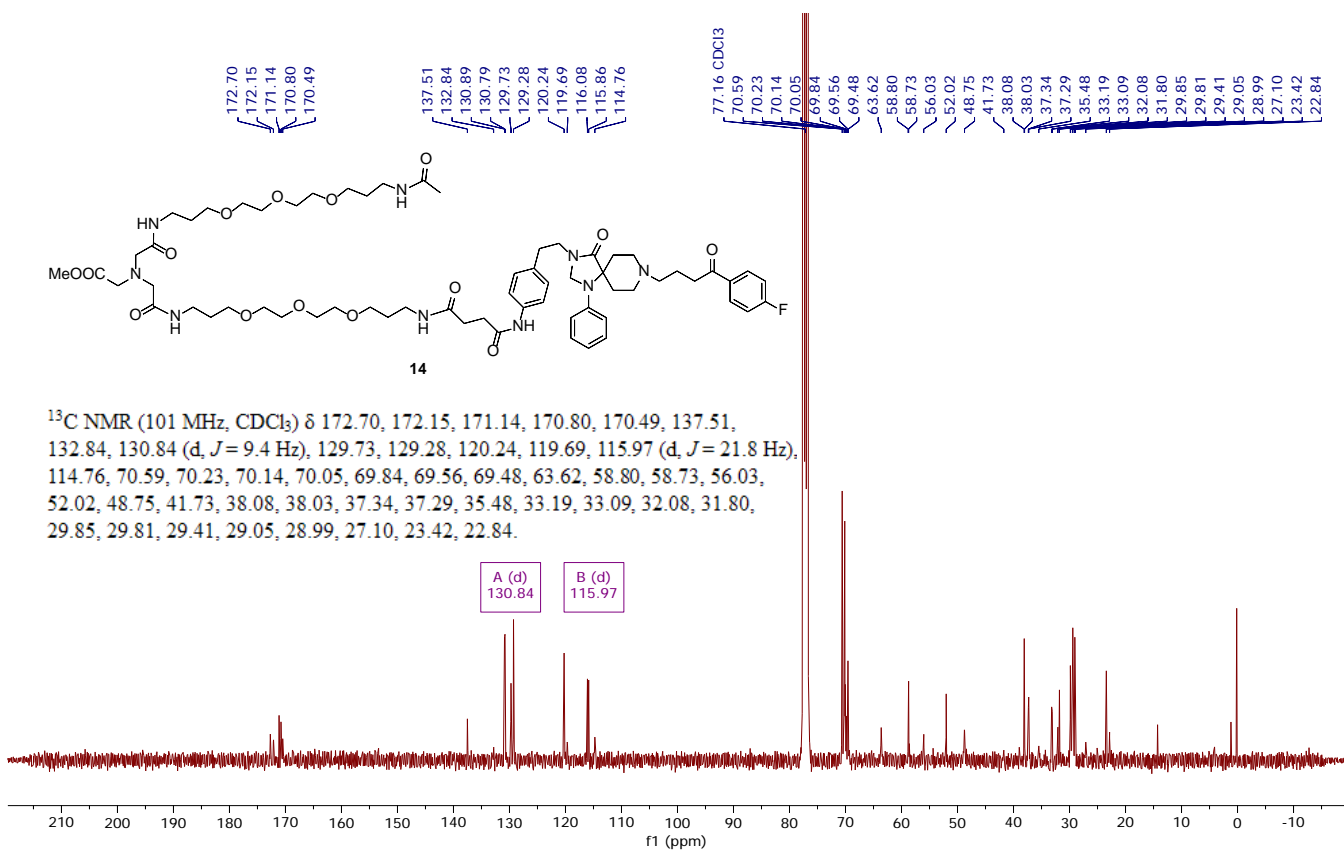
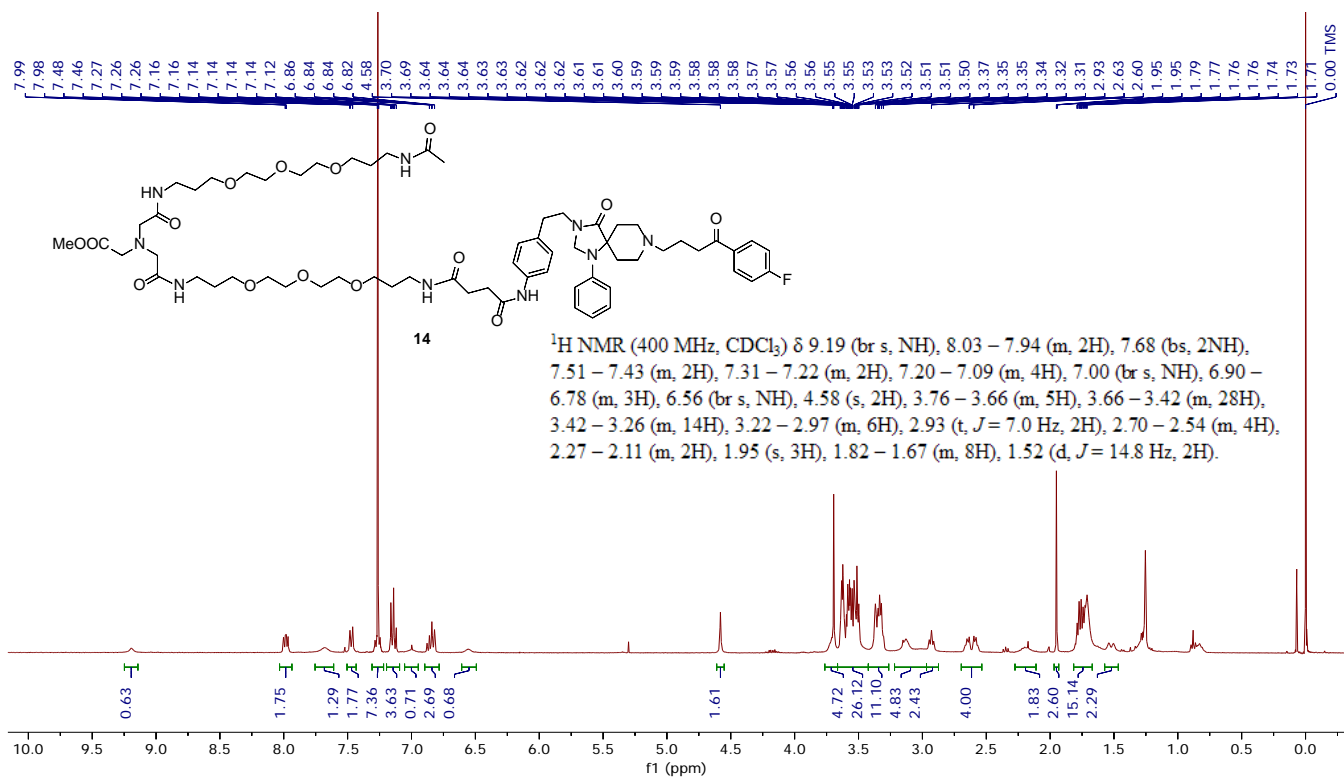


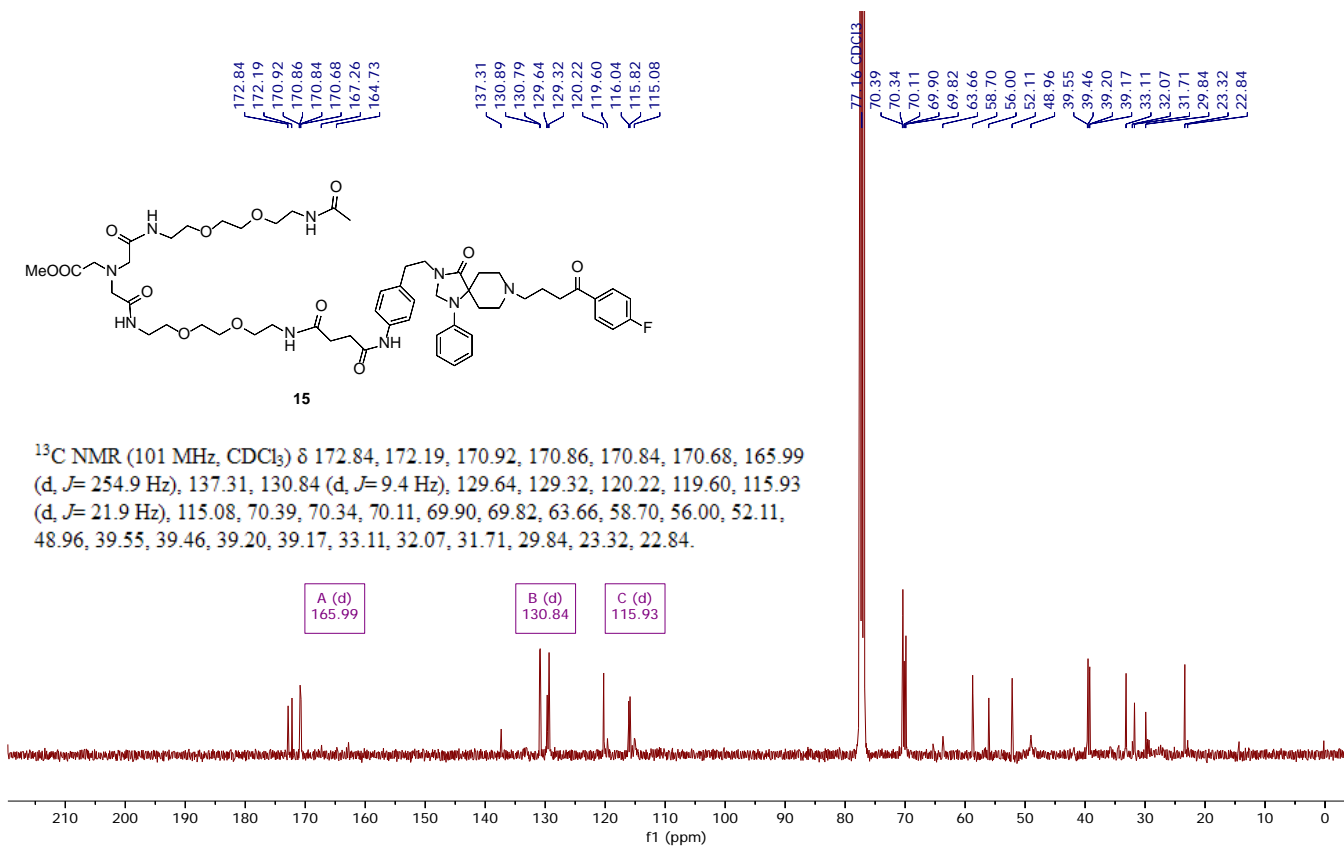
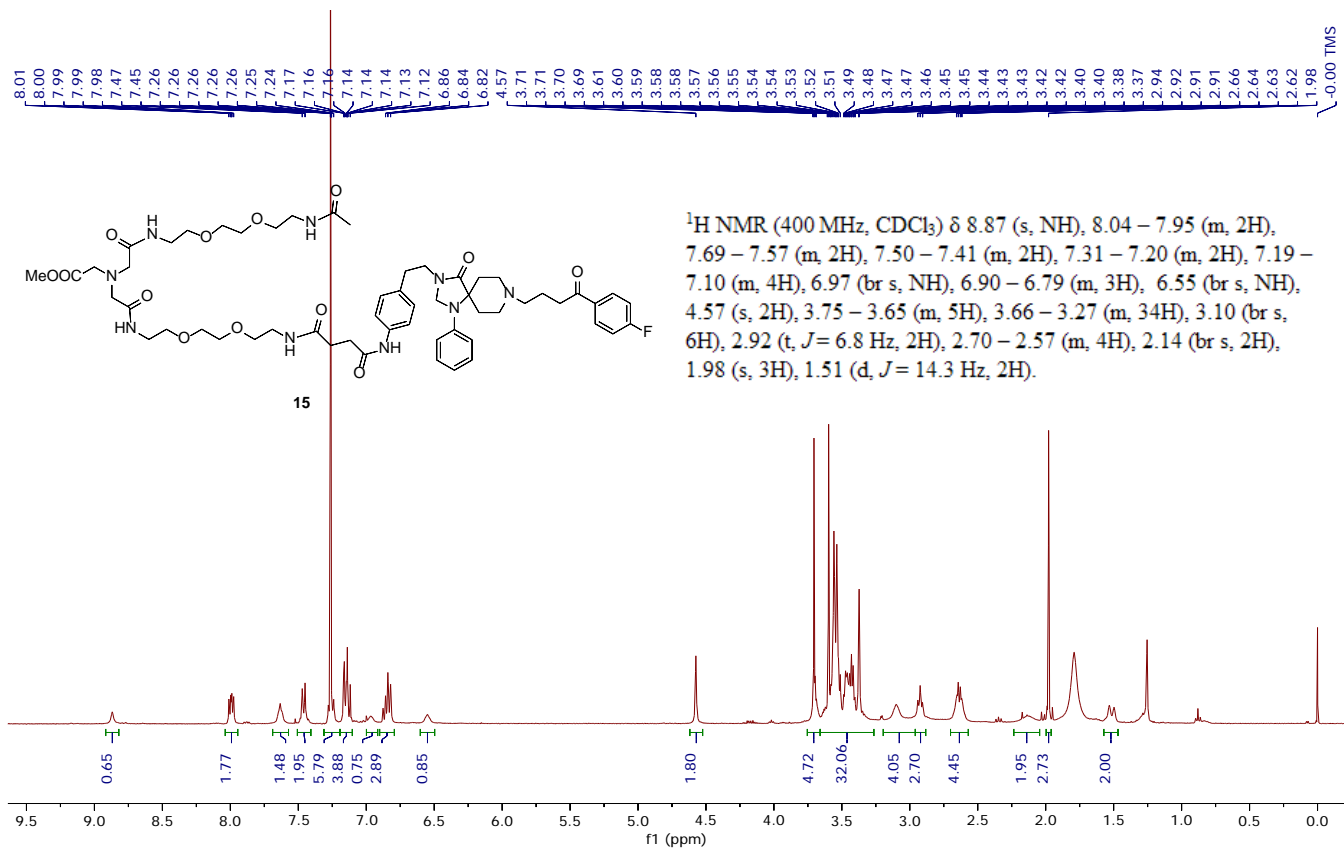




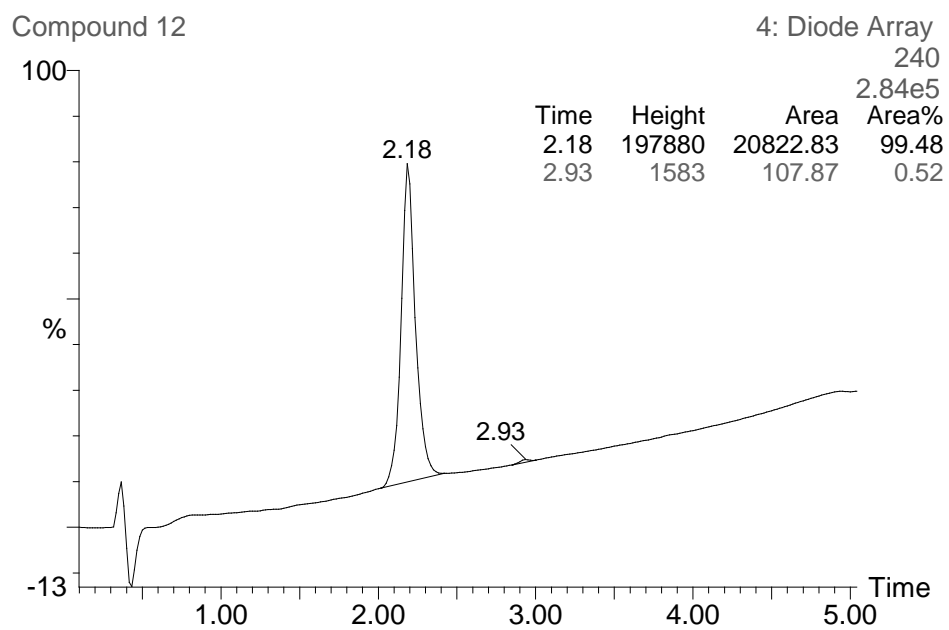
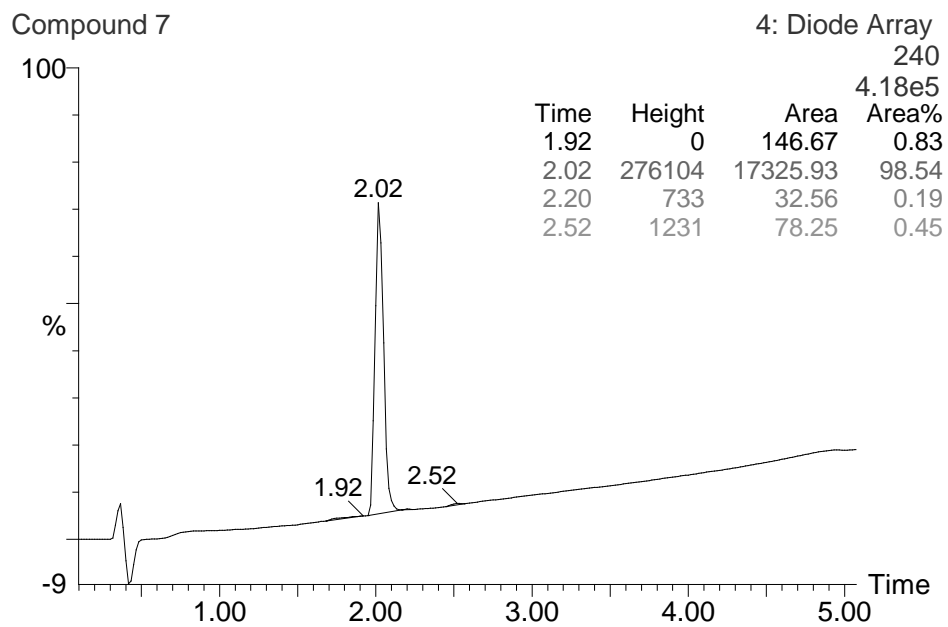






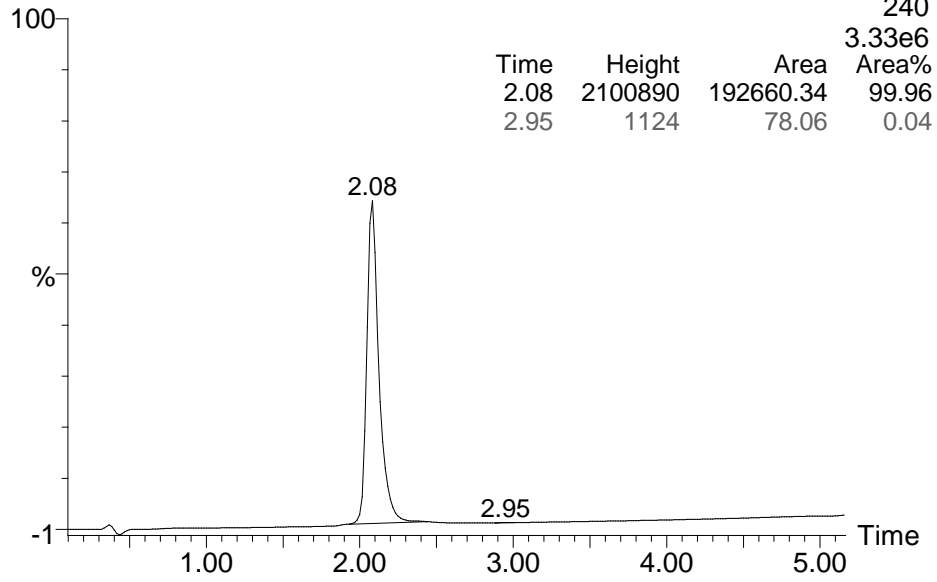


HPLC traces of compounds 7, 12-15



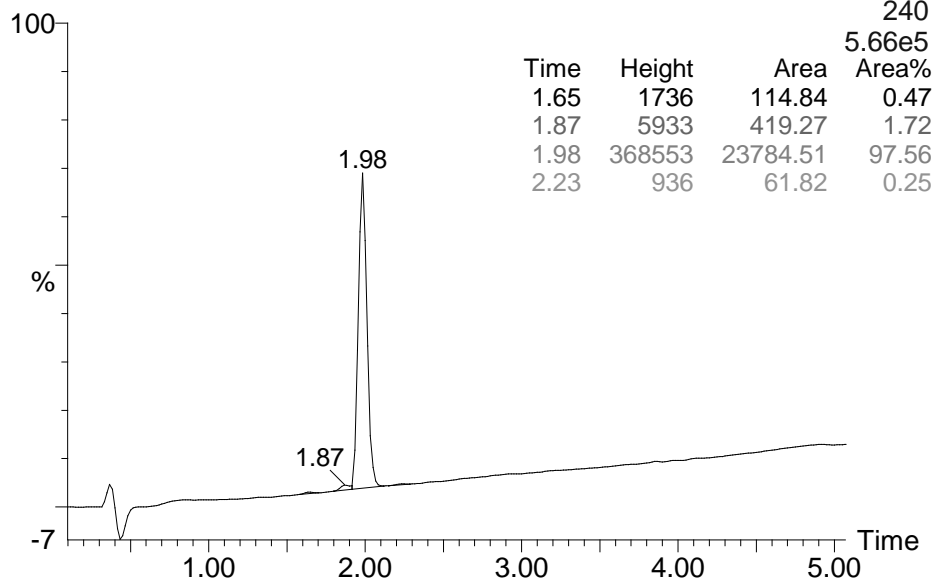
Compound 13

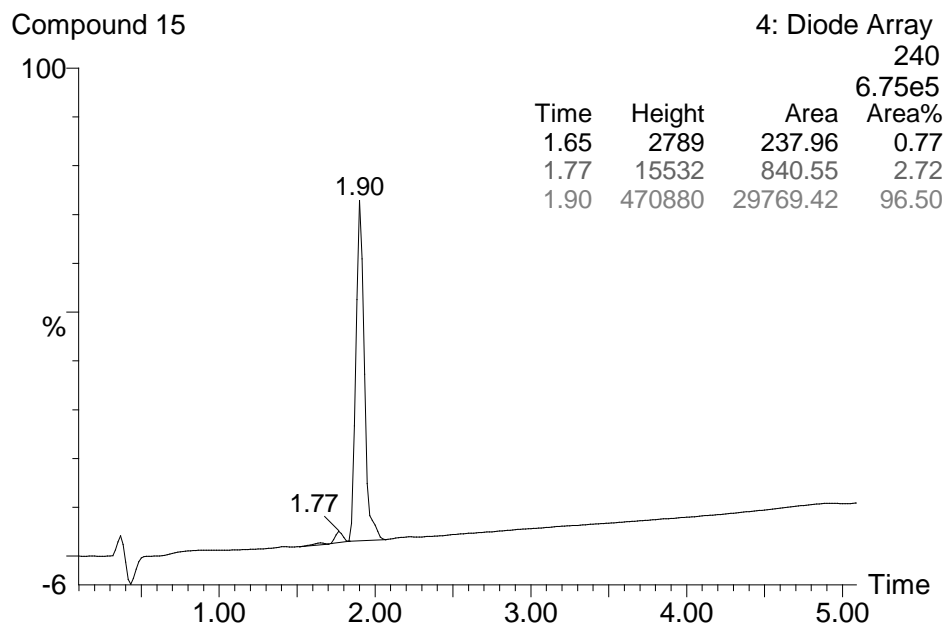
4: Diode Array



Compound 14

4: Diode Array





References

- (1) Kang, Y. S.; Son, J. H.; Hwang, I. C.; Ahn, K. H. Synthesis of a bis(oxazoline)-*N*-carboxylate ligand and its Zn(II) complex that shows C–H···Cl hydrogen bonding. *Polyhedron* **2006**, *25*, 3025-3031.
- (2) Jin, C.; Mayer, L. D.; Lewin, A. H.; Rehder, K. S.; Brine, G. A. Practical Synthesis of *p*-Aminophenethylpiperone (NAPS), a High-Affinity, Selective D₂-Dopamine Receptor Antagonist. *Synth. Commun.* **2008**, *38*, 816-823.


Chapter 4. α_{2A} - and α_{2C} -Adrenoceptors as Targets for Dopamine and Dopamine Receptor Ligands

Sánchez-Soto M*, **Casadó-Anguera V***, Yano H, Bender BJ, Cai NS, Moreno E, Canela EI, Cortés A, Meiler J, Casadó V, Ferré S.

Molecular Neurobiology, 2018, *in press*



α_{2A} - and α_{2C} -Adrenoceptors as Potential Targets for Dopamine and Dopamine Receptor Ligands

Marta Sánchez-Soto^{1,2,3} · Verònica Casadó-Anguera^{2,3} · Hideaki Yano¹ · Brian Joseph Bender^{4,5} · Ning-Sheng Cai¹ · Estefanía Moreno^{2,3} · Enric I. Canela^{2,3} · Antoni Cortés^{2,3} · Jens Meiler^{4,5} · Vicent Casadó^{2,3} · Sergi Ferré¹ 

Received: 14 December 2017 / Accepted: 7 March 2018

© This is a U.S. Government work and not under copyright protection in the US; foreign copyright protection may apply 2018

Abstract

The poor norepinephrine innervation and high density of Gi/o-coupled α_{2A} - and α_{2C} -adrenoceptors in the striatum and the dense striatal dopamine innervation have prompted the possibility that dopamine could be an effective adrenoceptor ligand. Nevertheless, the reported adrenoceptor agonistic properties of dopamine are still inconclusive. In this study, we analyzed the binding of norepinephrine, dopamine, and several compounds reported as selective dopamine D₂-like receptor ligands, such as the D₃ receptor agonist 7-OH-PIPAT and the D₄ receptor agonist RO-105824, to α_2 -adrenoceptors in cortical and striatal tissue, which express α_{2A} -adrenoceptors and both α_{2A} - and α_{2C} -adrenoceptors, respectively. The affinity of dopamine for α_2 -adrenoceptors was found to be similar to that for D₁-like and D₂-like receptors. Moreover, the exogenous dopamine receptor ligands also showed high affinity for α_{2A} - and α_{2C} -adrenoceptors. Their ability to activate Gi/o proteins through α_{2A} - and α_{2C} -adrenoceptors was also analyzed in transfected cells with bioluminescent resonance energy transfer techniques. The relative ligand potencies and efficacies were dependent on the Gi/o protein subtype. Furthermore, dopamine binding to α_2 -adrenoceptors was functional, inducing changes in dynamic mass redistribution, adenylyl cyclase activity, and ERK1/2 phosphorylation. Binding events were further studied with computer modeling of ligand docking. Docking of dopamine at α_{2A} - and α_{2C} -adrenoceptors was nearly identical to its binding to the crystallized D₃ receptor. Therefore, we provide conclusive evidence that α_{2A} - and α_{2C} -adrenoceptors are functional receptors for norepinephrine, dopamine, and other previously assumed selective D₂-like receptor ligands, which calls for revisiting previous studies with those ligands.

Keywords α_2 -Adrenoceptors · BRET · DMR · Adenylyl cyclase · ERK1/2 phosphorylation · Docking

Marta Sánchez-Soto and Verònica Casadó-Anguera contributed equally to this work.

✉ Vicent Casadó
vcasado@ub.edu

✉ Sergi Ferré
sferre@Intra.nida.nih.gov

¹ Integrative Neurobiology Section, National Institute on Drug Abuse, Intramural Research Program, National Institutes of Health, Triad Technology Building, 333 Cassell Drive, Baltimore, MD 21224, USA

² Department of Biochemistry and Molecular Biomedicine, Faculty of Biology, University of Barcelona, Diagonal 643, 08028 Barcelona, Spain

³ Centro de Investigación Biomédica en Red sobre Enfermedades Neurodegenerativas (CIBERNED), Institute of Biomedicine, University of Barcelona, Barcelona, Spain

⁴ Department of Pharmacology, Vanderbilt University, Nashville, TN 37232, USA

⁵ Center for Structural Biology, Vanderbilt University, Nashville, TN 37232, USA

Introduction

The neurotransmitter norepinephrine (NE) binds and activates three subfamilies of adrenoceptors: α_1 -adrenoceptors, subdivided into α_{1A} , α_{1B} , and α_{1D} ; α_2 -adrenoceptors, subdivided into α_{2A} , α_{2B} , and α_{2C} ; and β -adrenoceptors, subdivided into β_1 , β_2 , and β_3 [1]. Classically, α_1 -, α_2 - and β -adrenoceptors couple to Gq/11, Gi/o, and Gs, respectively [1, 2]. In mammalian species, α_{2A} is the main subtype in most brain regions whereas α_{2B} subtype has a limited distribution and is mostly expressed in the thalamus [3, 4]. The α_{2C} subtype is found with particularly high density in the striatum [5, 6] with a moderately lower density than α_{2A} [7, 8]. The high density of dorsal striatal α_{2A} - and α_{2C} -adrenoceptors prompted a fundamental question in view of the well-known paucity of striatal noradrenergic terminals [9–11] and the concomitant low extracellular levels of striatal NE [12]. Yet, a series of studies indicate that both types of receptors are fully

functional in the striatum, where they seem to be localized mostly postsynaptically, preferentially in GABAergic striatal efferent neurons [13, 14]. There is also evidence for α_{2A} -adrenoceptors playing a role as autoreceptors localized in the sparse striatal noradrenergic terminals [15]. It was postulated by Zhang et al. [16] that dopamine (DA) could provide the endogenous neurotransmitter for striatal α_2 -adrenoceptors. In transfected mammalian cells, using radioligand binding experiments, they found only a small preferential affinity of NE versus DA at both α_{2A} - and α_{2C} -adrenoceptors. Similar results were more recently obtained from radioligand binding studies using transfected mammalian and insect cell lines [17] and with radioligand binding and autoradiographic experiments in the bird and rat brain with a non-selective α_2 -adrenoceptor ligand [18]. However, Zhang et al. [16] reported a much lower potency of DA (in the micromolar range) than NE (in the nanomolar range) at the level of α_{2C} -adrenoceptor-mediated signaling (modulation of forskolin-induced adenylyl cyclase activation).

Due to the mismatch between dopaminergic and noradrenergic innervation and the density of their receptors in several brain areas, the controversy about the differential binding affinity of DA versus NE on adrenoceptors, and the potential functional efficacy of this binding, we wanted to study in detail the ability of DA and several synthetic DA receptor ligands to bind to the orthosteric site of α_2 -adrenoceptors in transfected cells and in the sheep brain. Moreover, we further analyzed the ability of these ligands to generate functional responses: activation of G proteins, inhibition of cAMP accumulation, and ERK1/2 phosphorylation. In the present study, we first analyzed the ability of DA and several DA receptor ligands to bind to α_2 -adrenoceptors in cortical tissue, which predominantly expresses α_{2A} -adrenoceptors, and in striatal tissue, which expresses both α_{2A} - and α_{2C} -adrenoceptors. We also studied the potential dopaminergic function of α_{2A} - and α_{2C} -adrenoceptors using the same methodology that recently allowed us to demonstrate the potent activation of all Gi/o-coupled DA D₂-like receptors by NE [19]. This methodology consists on sensitive bioluminescence resonance energy transfer (BRET)-based techniques that allow detection of ligand-dependent interactions between specific receptors and specific G proteins (G protein activation) or receptor-induced activation of effectors (adenylyl cyclase activity) in living cells [19]. Moreover, we compared the ability of NE, DA, and DA receptor ligands to modulate dynamic mass redistribution (DMR) and to activate MAPK signaling. Lastly, we modeled the binding of DA at α_{2A} - and α_{2C} -adrenoceptors, as compared to its binding to the crystallized D₃ receptor. Our results provide conclusive evidence for α_{2A} - and α_{2C} -adrenoceptors being not only NE but also DA receptors and common targets for other D₂-like receptor ligands.

Materials and Methods

DNA Constructs and Transfection

For BRET experiments, human receptor constructs were used for α_{2A} - and α_{2C} -adrenoceptors (cDNA Resource Center). The following human G protein constructs were used: G α 1-, G α 2-, G α 3-, G α o1-, or G α o2-Renilla luciferase 8 (RLuc8) with RLuc8 inserted at position 91, untagged G β 1, and G γ 2 fused to full-length mVenus at its N terminus. The G α -RLuc8 constructs were kindly provided by Céline Galés (INSERM, Toulouse, France). The cAMP sensor using YFP-Epac-Rluc (CAMYEL) biosensor was obtained from the American Type Culture Collection (no. MBA-277; ATCC, Manassas, VA, USA) [20]. All the constructs were confirmed by sequencing analysis. A constant amount of plasmid cDNA (0.5 μ g G α -RLuc8, 4.5 μ g G β 1, 5 μ g G γ 2-mVenus, and 5 μ g receptor) was transfected into HEK-293T cells using polyethylenimine (Sigma-Aldrich) in a 1:2 ratio in 10-cm dishes. Cells were maintained in culture with Dulbecco's modified Eagle's medium supplemented with 10% fetal bovine serum and kept in an incubator at 37 °C and 5% CO₂. The transfected amount and ratio among the receptor and heterotrimeric G proteins were tested for optimized dynamic range in drug-induced BRET. HEK-293T cells were also used in BRET experiments for determination of adenylyl cyclase inhibition (see below). For DMR and ERK1/2 phosphorylation assays, Chinese hamster ovary (CHO) cells were grown in minimum essential medium (MEM α ; Gibco) supplemented with 2 mM L-glutamine, 100 μ g/ml sodium pyruvate, MEM non-essential amino acid solution (1:100), 100 U/ml penicillin/streptomycin, and 5% (v/v) of heat-inactivated fetal bovine serum. These cells were transfected with human α_{2A} -RLuc8 receptor using polyethylenimine in a 1:2 ratio in 25-cm² cell culture flasks. All experiments were performed approximately 48 h after transfection.

BRET

BRET assays were performed to detect receptor ligand-induced events for Gi/o protein activation. Gi/o protein activation assay used RLuc-fused G α i/o protein subunit and mVenus-fused G γ 2 protein for BRET pair. Receptor and untagged G β 1 constructs were co-transfected. As reported previously [19, 20], cells were harvested, washed, and resuspended in phosphate-buffered saline. Approximately 200,000 cells/well were distributed in 96-well plates, and 5 μ M coelenterazine H (substrate for luciferase) was added to each well. One minute after the addition of coelenterazine H, ligands (DA, NE, clonidine, quinpirole, 7-OH-PIPAT, and RO-105824) were added to each well. Antagonists were added 10 min before coelenterazine. The fluorescence of the acceptor was quantified (excitation at 500 nm and emission at

540 nm for 1-s recordings) in Mithras LB940 (Berthold Technologies, Bad Wildbad, Germany) to confirm the constant expression levels across experiments. In parallel, the BRET signal from the same batch of cells was determined as the ratio of the light emitted by mVenus (510–540 nm) over that emitted by RLuc (485 nm). G protein activation was calculated as the BRET change (BRET ratio for the corresponding drug minus the BRET ratio in the absence of the drug) observed 10 min after the addition of the ligands. E_{\max} values were expressed as the percentage of the effect of each ligand over the effect of NE. BRET curves were analyzed by non-linear regression using the commercial Prism 4 (GraphPad Software).

DMR

A global cell signaling profile or DMR was measured using an EnSpire Multimode Plate Reader (PerkinElmer, Waltham, MA, USA). This label-free approach uses refractive waveguide grating optical biosensors, integrated into 384-well microplates. Changes in local optical density are measured in a detection zone up to 150 nm above the surface of the sensor. Cellular mass movements induced upon receptor activation are detected by illuminating the underside of the biosensor with polychromatic light and measured as changes in the wavelength of the reflected monochromatic light. These changes are a function of the refraction index. The magnitude of this wavelength shift (in picometers) is directly proportional to the amount of DMR. Briefly, after 24 h of CHO cell transfection with α_{2A} -RLuc8 receptor, cells were resuspended and seeded at a density of 7000 cells per well in 384-well sensor microplates in 30 μ l growing media and cultured for 24 h at 37 °C and 5% CO₂, to obtain monolayers at 70–80% confluency. Before starting the assay, cells were washed twice with assay buffer (MEM α supplemented with 20 mM HEPES, pH 7.15, 0.1% DMSO, and 0.1% BSA) and incubated 2 h in 40 μ l per well in the reader at 24 °C. Hereafter, the sensor plate was scanned, and a baseline optical signature was recorded for 10 min before adding 10 μ l of the agonist dissolved in assay buffer and recorded for 90 min. Kinetic results were analyzed using EnSpire Workstation Software v 4.10.

Adenylyl Cyclase Activity

BRET assays were performed to detect receptor ligand-induced adenylyl cyclase activity. This assay used the CAMYEL biosensor construct which contains RLuc and YFP. The biosensor detects the conformational changes in Epac that are induced upon its binding to cAMP. The conformational change triggered by an increase in cAMP induced by forskolin results in a decrease in BRET due to the relative orientation change between donor and acceptor. A decrease in forskolin-induced cAMP levels is therefore observed as an

increase in BRET [21]. To study G α i-dependent inhibition activity, cells were treated as described above but pre-stimulated for 10 min with 1 μ M forskolin (Sigma-Aldrich), in the presence of 10 μ M propranolol 10 min before sample reading to control for activation of endogenous β -adrenergic receptors (see “Results”).

ERK1/2 Phosphorylation

CHO cells were transfected with α_{2A} -RLuc8 receptor, obtaining a transfection of about 0.3 pmol/mg protein. The day of the experiment, cells were starved by treating them with serum-free media for 4 h at 37 °C. After that, cells were incubated with the indicated agonist for 5 min at 37 °C. Then, cells were rinsed with ice-cold phosphate-buffered saline and lysed by adding 200 μ l ice-cold lysis buffer (50 mM Tris-HCl (pH 7.4), 50 mM NaF, 150 mM NaCl, 45 mM β -glycerophosphate, 1% Triton X-100, 20 mM phenylarsine oxide, 0.4 mM NaVO₄, and protease inhibitor cocktail). The cellular debris was removed by centrifugation at 13,000g for 5 min at 4 °C, and the protein was quantified. To determine the level of ERK1/2 phosphorylation, equivalent amounts of protein were separated by electrophoresis on a denaturing 10% SDS polyacrylamide gel and transferred onto polyvinylidene fluoride membranes. Odyssey blocking buffer (LI-COR Biosciences, Lincoln, NE, USA) was then added, and the membrane was rocked for 90 min. The membranes were then probed with a mixture of a mouse anti-phospho-ERK1/2 antibody (1:2500; Sigma-Aldrich) and rabbit anti-ERK1/2 antibody that recognizes both phosphorylated and non-phosphorylated ERK1/2 (1:40,000; Sigma-Aldrich) overnight at 4 °C. The 42- and 44-kDa bands corresponding to ERK1 and ERK2 were visualized by the addition of a mixture of IRDye 800 (anti-mouse) antibody (1:10,000; Sigma-Aldrich) and IRDye 680 (anti-rabbit) antibody (1:10,000; Sigma-Aldrich) for 2 h and scanned by the Odyssey infrared scanner (LICOR Biosciences). Band densities were quantified using the scanner software and exported to Excel (Microsoft, Redmond, WA, USA). The level of phosphorylated ERK1/2 isoforms was normalized for differences in loading using the total ERK1/2 protein band intensities.

Radioligand Binding

Brains of male and female sheep of 4–6 months old were freshly obtained from the local slaughterhouse. Brain tissues (cortex and dorsal striatum) and HEK-293T cell suspensions were disrupted with a Polytron homogenizer (PTA 20 TS rotor, setting 3; Kinematica, Basel, Switzerland) for two 5-s periods in 10 volumes of 50 mM Tris-HCl buffer, pH 7.4, containing a proteinase

inhibitor cocktail (Sigma, St. Louis, MO, USA). Membranes were obtained by centrifugation twice at 105,000g for 45 min at 4 °C. The pellet was stored at –80 °C, washed once more as described above, and resuspended in 50 mM Tris-HCl buffer for immediate use. Membrane protein was quantified by the bicinchoninic acid method (Pierce Chemical Co., Rockford, IL, USA) using bovine serum albumin dilutions as standard. Binding experiments were performed with membrane suspensions at room temperature in 50 mM Tris-HCl buffer, pH 7.4, containing 10 mM MgCl₂. For competition-binding assays, membrane suspensions (0.2 mg of protein/ml) were incubated for 2 h with a constant-free concentration of 0.9 nM of the α₂R-antagonist [³H]RX821002 or 1.3 nM of the D₁-like receptor antagonist [³H]SCH 23390 or 0.8 nM of the D₂-like receptor antagonist [³H]YM-09151-2 and increasing concentrations of each tested ligand: NE, DA, clonidine, 7-OH-PIPAT, quinpirole, and RO-105824. For α₂R saturation-binding assays, membrane suspensions (0.2 mg of protein/ml) were incubated for 3 h at room temperature in 50 mM Tris-HCl buffer, pH 7.4, containing 10 mM MgCl₂ with increasing concentrations of the α₂R-antagonist [³H]RX821002. Non-specific binding was determined in the presence of 10 μM of the non-radiolabeled antagonist RX821002 (for α₂R) or 30 μM of DA (for D₁R and D₂R). In all cases, free and membrane-bound ligands were separated by rapid filtration of 500-μl aliquots in a cell harvester (Brandel, Gaithersburg, MD, USA) through Whatman GF/C filters embedded in 0.3% polyethylenimine that were subsequently washed for 5 s with 5 ml of ice-cold 50 mM Tris-HCl buffer. The filters were incubated with 10 ml of Ecoscint H scintillation cocktail (National Diagnostics, Atlanta, GA, USA) overnight at room temperature, and radioactivity counts were determined using a Tri-Carb 2800 TR scintillation counter (PerkinElmer) with an efficiency of 62%.

Binding Data Analysis

Data were analyzed according to the “two-state dimer model” of Casadó et al. [22]. The model assumes GPCR dimers as a main functional unit and provides a more robust analysis of parameters obtained from saturation and competition experiments with orthosteric ligands, as compared with the commonly used “two-independent site model” [22, 23]. In saturation experiments with the radioligand, the model analyzes the total number of radioligand binding sites (B_{\max} ; more specifically, it calculates R_T , the total number of dimers, where $B_{\max} = 2R_T$), the affinity of the radioligand for the first protomer in the unoccupied dimer (K_{DA1}), the affinity of the radioligand for the second protomer when the first protomer is already occupied by the radioligand (K_{DA2}), and an index of

cooperativity of the radioligand (D_{CA}). A positive or negative value of D_{CA} implies either an increase or a decrease in affinity of K_{DA2} versus K_{DA1} , and its absolute value provides a measure of the degree of increase or decrease in affinity. In competition experiments, the model analyzes the interactions of the radioligand with a competing ligand and it provides the affinity of the competing ligand for the first protomer in the unoccupied dimer (K_{DB1}), the affinity of the competing ligand for the second protomer when the first protomer is already occupied by the competing ligand (K_{DB2}) or the radioligand (K_{DAB}), and an index of cooperativity of the competing ligand (D_{CB}). A positive or negative value of D_{CB} implies either an increase or a decrease in affinity of K_{DB2} versus K_{DB1} , and its absolute value provides a measure of the degree of increase or decrease in affinity.

Radioligand competition and saturation curves were analyzed by non-linear regression using the commercial GraFit curve-fitting software (Erithacus Software, Surrey, UK), by fitting the binding data to the mechanistic two-state dimer receptor model, as described in detail elsewhere [24]. The equation describing the saturation experiment with the radioligand A in non-cooperative conditions ($K_{DA2} / K_{DA1} = 4$) is as follows: $A_{\text{bound}} = 2AR_T / (2K_{DA1} + A)$, where A represents the radioligand concentration. To calculate the macroscopic equilibrium dissociation constants from competition experiments, the following general equation must be applied: $A_{\text{bound}} = (K_{DA2}A + 2A^2 + K_{DA2}AB / K_{DAB})R_T / (K_{DA1}K_{DA2} + K_{DA2}A + A^2 + K_{DA2}AB / K_{DAB} + K_{DA1}K_{DA2}B / K_{DB1} + K_{DA1}K_{DA2}B^2 / (K_{DB1}K_{DB2}))$, where B represents the assayed competing compound concentration (F). For A , the non-cooperative and non-allosteric modulation between A and B , the equation is simplified due to the fact that $K_{DA2} = 4K_{DA1}$ and $K_{DAB} = 2K_{DB1}$; $A_{\text{bound}} = (4K_{DA1}A + 2A^2 + 2K_{DA1}AB / K_{DB1})R_T / (4K_{DA1}^2 + 4K_{DA1}A + A^2 + 2K_{DA1}AB / K_{DB1} + 4K_{DA1}^2B / K_{DB1} + 4K_{DA1}^2B^2 / (K_{DB1}K_{DB2}))$. For A and B , the non-cooperative and non-allosteric modulation between A and B , the equation can be simplified due to the fact that $K_{DA2} = 4K_{DA1}$, $K_{DB2} = 4K_{DB1}$, and $K_{DAB} = 2K_{DB1}$; $A_{\text{bound}} = (4K_{DA1}A + 2A^2 + 2K_{DA1}AB / K_{DB1})R_T / (4K_{DA1}^2 + 4K_{DA1}A + A^2 + 2K_{DA1}AB / K_{DB1} + 4K_{DA1}^2B / K_{DB1} + K_{DA1}^2B^2 / K_{DB1}^2)$.

Statistical Analysis

In binding assays, goodness of fit was tested according to reduced chi-square value given by the regression program. The test of significance for two different model population variances was based upon the F -distribution. Using this F -test, a probability greater than 95% ($p < 0.05$) was considered to be the criterion to select a more complex model (cooperativity) over the simplest one (non-cooperativity). In all cases, a probability of less than 70% ($p > 0.30$) resulted when one model was not significantly better than the other. In all cases, results

are given as parameter values \pm SEM and statistical differences were analyzed with Prism 4.

Drugs

Dopamine hydrochloride and L-(−)-norepinephrine (+)-bitartrate salt monohydrate were purchased from Sigma. (−)-Quinpirole hydrochloride, clonidine hydrochloride, 7-OH-PIPAT maleate, RO-105824 dihydrochloride, RX821002, and yohimbine hydrochloride were purchased from Tocris. [³H]RX821002 (63.9 Ci/mmol), [³H]SCH 23390 (81.9 Ci/mmol), and [³H]YM-09151-2 (84.4 Ci/mmol) were from PerkinElmer. Pertussis toxin was purchased from Sigma.

Homology Modeling of α_{2A} - and α_{2C} -Adrenoceptors

Homology models of α_{2A} - and α_{2C} -adrenoceptors were constructed from multiple templates using RosettaCM [25] with a protocol previously described [26]. Sequences of each adrenoceptor were aligned with sequences of the following receptors: D₃ (PDB ID: 3PBL [27]), β_1 (PDB ID: 4BVN [28]), β_2 (PDB ID: 2RH1 [29]), 5HT_{1B} (PDB ID: 4IAR [30]), and 5HT_{2B} (PDB ID: 4IB4 [31]) using BLAST and were modified to ensure alignment of secondary structure elements and conserved residues. The N-terminus was truncated through residues 28 and 46 and the C-terminus was deleted after residues 442 and 456, respectively. Additionally, the long intracellular loop 3 was deleted at residues 229–372 in α_{2A} and 243–381 in α_{2C} and replaced with an eight-residue poly-Gly linker. These sequences were threaded onto each template and hybridized to generate full-length, energy-minimized structures. Models were clustered using automatic radius detection in Rosetta, and the low-energy cluster centers from the top five clusters were selected for additional modeling.

Protein-Ligand Docking

The tridimensional structure of DA was obtained from PubChem (ID 3713609). Conformers of DA were generated using the BCL [32]. To identify the initial starting coordinates for ligand docking, homology models were aligned with the crystal structure of β_2 -adrenoceptor (PDB ID: 4LDO (33)) and DA was aligned with the crystallized ligand. Ligand docking was performed in RosettaLigand using the small perturbation of ligand position protocol and swapping of ligand conformers [33, 34]. One thousand models for each protein-ligand complex were generated. Models were sorted initially by total energy and then culled to the top 5% of models by interface energies for analysis. Per-residue $\Delta\Delta G$ analysis was performed to identify residues involved in ligand binding.

Results

Binding of DA and DA Receptor Ligands to α_2 -Adrenoceptors in Cortical and Striatal Tissue

First, we analyzed the ability of NE, DA, the non-selective α_2 -adrenoceptor agonist clonidine, the non-selective D₂-D₃-D₄ receptor agonist quinpirole, the selective D₃ receptor agonist 7-OH-PIPAT, and the selective D₄ receptor agonist RO-105824 to displace the binding of the non-selective α_2 -adrenoceptor antagonist radioligand [³H]RX821002 in membrane preparations from the sheep cortex and striatum with competitive inhibition experiments. See “Materials and Methods” and refs. [22–24] for description of the variables. Saturation experiments with [³H]RX821002 for cortical and striatal tissue provided B_{\max} values for α_2 -adrenoceptors of 0.33 ± 0.02 and 0.13 ± 0.02 pmol/mg protein and affinity values (K_{DA1}) of 0.06 ± 0.01 and 0.07 ± 0.01 nM ($n = 4-8$), respectively. This implies that the density of α_2 -adrenoceptors in the cortex, which is mostly represented by α_{2A} -adrenoceptors [3, 4], is three times higher than that in the striatum, which expresses similar densities for both α_{2A} - and α_{2C} -adrenoceptors [8]. To test the binding selectivity of [³H]RX821002 for α_2 -adrenoceptors and not for D₂-like receptors, we developed competition experiments of the D₂-like receptor antagonist [³H]YM-09151-2 with increasing concentrations of unlabeled RX821002 in sheep striatal membranes. RX821002 did not displace the radioligand binding at any concentration up to 10 μ M (Fig. 1a). The same experiments were also performed in membranes from HEK-293T cells stably transfected with human D₂, D₃, or D₄ receptors, with identical results (data not shown). These results demonstrate that the radioligand [³H]RX821002 does not bind to D₂-like receptors.

Competition experiments of [³H]RX821002 with NE, DA, clonidine, and the D₂-like receptor ligands in cortical and striatal sheep membranes are shown in Fig. 2a, b, respectively, and the K_{DB1} , K_{DB2} , and D_{CB} values obtained are presented in Table 1. In both tissues, NE, DA, and clonidine showed high affinity for [³H]RX821002 binding sites with an order of potency of clonidine > NE > DA (Fig. 2). The three ligands showed negative cooperativity (negative D_{CB} values). The affinity of NE was higher in the cortex than in the striatum, with higher striatal K_{DB1} , K_{DB2} , and D_{CB} values (stronger negative cooperativity) (Table 1). The affinity of DA was very similar in both tissues, with similar K_{DB1} values and a moderately but significantly higher K_{DB2} value in the striatum, resulting in similar D_{CB} values (Table 1). The affinity of clonidine was also higher in the cortex, with a significantly higher striatal K_{DB1} value and similar D_{CB} values (Table 1). 7-OH-PIPAT and quinpirole also displaced [³H]RX821002 binding with nanomolar and submicromolar affinities, respectively (Table 1, Fig. 2). Interestingly, 7-OH-PIPAT showed negative cooperativity in the cortex, but not in the striatum. The only measurable affinity parameter of 7-OH-PIPAT in the striatum, K_{DB1} , was significantly higher than that in the

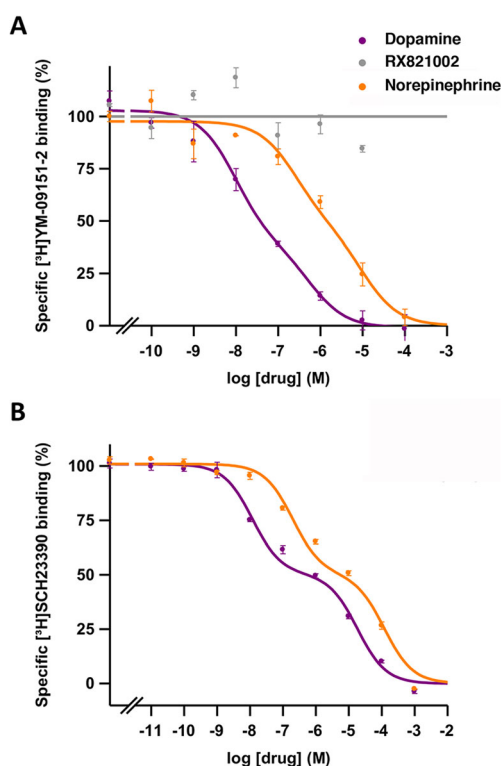


Fig. 1 Radioligand binding to D_2 -like and D_1 -like receptors in the brain striatum. Representative competition curves of D_2 -like receptor antagonist [3 H]-YM-09151-2 vs. increasing concentrations of free competitors NE, DA, and RX821002 (a) and of D_1 -like receptor antagonist [3 H]SCH 23390 vs. increasing concentrations of DA and NE (b) in the sheep brain striatum. Values are expressed as a percentage of the specific binding (100% is 0.13 ± 0.01 pmol/mg protein in a and 0.43 ± 0.04 pmol/mg protein in b). Experimental data were fitted to the two-state dimer receptor model equations, as described in the “Materials and Methods” section. Values are mean \pm SEM from a representative experiment ($n = 3-5$) performed in triplicate

cortex, and it was almost ten times lower than the cortical K_{DB2} value (Table 1). Quinpirole also showed differences in the binding parameters between the cortex and striatum, such as a lower K_{DB1} value but negative cooperativity in the striatum. Finally, RO-105824 also displaced [3 H]RX821002 binding from the cortex and striatum with high affinity (subnanomolar). No cooperativity ($D_{CB} = 0$) was obtained, except for RO-105824 in the cortex ($D_{CB} = -4.3$) (Table 1).

Binding of DA and NE to D_1 -Like and D_2 -Like Receptors in Striatal Tissue

Next, we compared the affinity of endogenous DA and NE binding to DA D_1 -like and D_2 -like receptors with the affinity, determined above, for α_2 -adrenoceptors. In addition to competition experiments with the D_2 -like radioligand antagonist [3 H]YM-09151-2 (Fig. 1a), we performed competition experiments with the D_1 -like radioligand antagonist [3 H]SCH 23390 in sheep striatal

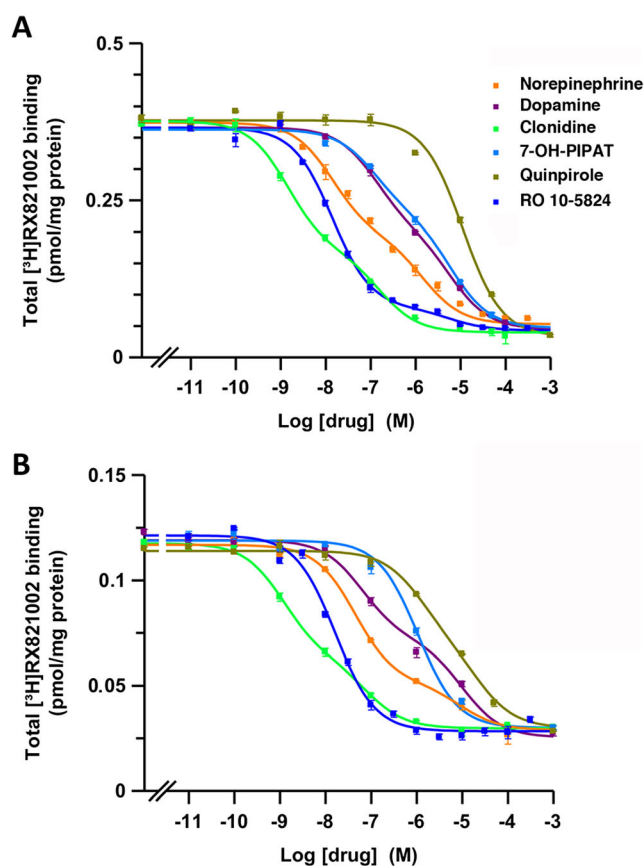


Fig. 2 Radioligand binding of dopaminergic and adrenergic ligands to α_2 -adrenoceptors in brain tissue. Representative competition curves of α_2 -adrenoceptor antagonist [3 H]RX821002 vs. increasing concentrations of free competitors (NE, DA, clonidine, quinpirole, 7-OH-PIPAT, and RO-105824) in sheep brain cortical (a) and striatal (b) membranes. Experimental data were fitted to the two-state dimer receptor model equations, as described in the “Materials and Methods” section. Values are mean \pm SEM from a representative experiment ($n = 3$) performed in triplicate

preparations (Fig. 1b). The equilibrium binding parameters are shown in Table 2. Both NE and DA showed negative cooperativity (Fig. 1) with negative D_c values (Table 2). The affinity of DA for the first protomer of the D_2 -like receptor dimer (K_{DB1}), mostly represented by the D_2R subtype in the dorsal striatum [35], was similar to the affinity for α_2 -adrenoceptors and D_1 -like receptors (Fig. 1, Table 2). The affinity of DA for the second protomer (K_{DB2}) of the D_1 -like receptor was even about ten times lower than that for the α_2 -adrenoceptors and D_2 -like receptors (stronger negative cooperativity; see Table 2). On the other hand, the affinity of NE for α_2 -adrenoceptors in the striatum, represented by α_{2A} - and α_{2C} -adrenoceptors, was significantly higher than that for dopamine receptors (Fig. 1). Specifically, NE had an affinity for DA receptors about 60-fold lower than that for α_2 -adrenoceptors (Table 2, Fig. 1). We can therefore assume that extracellular physiological levels of DA that are

Table 1 Competitive inhibition experiments of [³H]RX821002 versus NE, DA, clonidine, and D₂-like receptor ligands in the sheep brain cortex and striatum

Ligand	Binding parameters	
	Cortex	Striatum
NE	$K_{DB1} = 0.3 \pm 0.2^*$ $K_{DB2} = 250 \pm 100$ $D_{CB} = -2.3$	$K_{DB1} = 0.8 \pm 0.1$ $K_{DB2} = 5000 \pm 3000$ $D_{CB} = -3.2$
DA	$K_{DB1} = 6.9 \pm 0.2$ $K_{DB2} = 350 \pm 10^*$ $D_{CB} = -1.1$	$K_{DB1} = 6 \pm 1$ $K_{DB2} = 1000 \pm 200$ $D_{CB} = -1.6$
Clonidine	$K_{DB1} = 0.014 \pm 0.003^*$ $K_{DB2} = 40 \pm 20$ $D_{CB} = -2.8$	$K_{DB1} = 0.036 \pm 0.005$ $K_{DB2} = 20 \pm 10$ $D_{CB} = -2.1$
7-OH-PIPAT	$K_{DB1} = 9 \pm 2^{**}$ $K_{DB2} = 430 \pm 80$ $D_{CB} = -1.1$	$K_{DB1} = 51 \pm 6$ $D_{CB} = 0$
Quinpirole	$K_{DB1} = 530 \pm 50^{**}$ $D_{CB} = 0$	$K_{DB1} = 110 \pm 10$ $K_{DB2} = 2700 \pm 400$ $D_{CB} = -0.8$
RO-105824	$K_{DB1} = 0.055 \pm 0.003^{***}$ $K_{DB2} = 4000 \pm 2000$ $D_{CB} = -4.3$	$K_{DB1} = 0.42 \pm 0.03$ $D_{CB} = 0$

Binding parameters from competitive inhibition experiments of [³H]RX821002 versus NE, DA, clonidine, and D₂-like receptor ligands in membrane preparations from the sheep brain cortex and striatum (Fig. 2). K_{DB1} , K_{DB2} , and D_{CB} values were obtained according to the two-state dimer model (see “Materials and Methods” and ref. 22). K_{DB1} and K_{DB2} (in nM) are expressed as means \pm SEM of three experiments performed in triplicate. Statistical differences between affinity parameters of cortical versus striatal adrenoceptors were calculated by non-paired, two-tailed Student's *t* test

* $p < 0.05$; ** $p < 0.01$; *** $p < 0.001$

able to activate DA receptors are also able to bind α_2 -adrenoceptors.

α_{2A} - and α_{2C} -Adrenoceptor-Mediated G Protein Activation by DA and Synthetic DA Receptor Ligands

The G protein activation BRET assay (see “Materials and Methods”) was used to determine the potency and efficacy of the above-studied ligands to activate α -adrenoceptors in HEK-293T cells transfected with α_{2A} - or α_{2C} -adrenoceptor and one of the five different RLuc-fused $G\alpha i/o$ subunits ($G\alpha i1$, $G\alpha i2$, $G\alpha i3$, $G\alpha o1$, and $G\alpha o2$) with Venus-fused $G\gamma 2$ protein as BRET acceptor pair. The amount of $G\alpha i/o$ subunits transfected produced values between 0.5 and 1 million luminescence units (arbitrary units). Previously, we found that luminescence values between 200,000 and 1.5 million did not produce a significant alteration of the E_{max} of drug-induced BRET. Moreover, the levels of α_2 -adrenoceptor were around 2 pmol/mg protein. We

Table 2 Competitive inhibition experiments of [³H]SCH 23390, [³H]YM-09151-2, or [³H]RX821002 versus DA and NE in the sheep brain striatum

Receptor	Binding parameters	
	DA	NE
D ₁ -like	$K_{DB1} = 8 \pm 3$ $K_{DB2} = 8000 \pm 1000^{***}$ $D_c = -2.4$	$K_{DB1} = 53 \pm 90^{##}$ $K_{DB2} = 50000 \pm 10,000^{\#}$ $D_c = -2.4$
D ₂ -like	$K_{DB1} = 3.5 \pm 0.6$ $K_{DB2} = 700 \pm 200$ $D_c = -1.7$	$K_{DB1} = 60 \pm 40^{##}$ $K_{DB2} = 3400 \pm 100$ $D_c = -1.2$
α_2	$K_{DB1} = 6 \pm 1$ $K_{DB2} = 1000 \pm 200$ $D_c = -1.6$	$K_{DB1} = 0.8 \pm 0.1$ $K_{DB2} = 5000 \pm 3000$ $D_c = -3.2$

Binding parameters from competitive inhibition experiments of [³H]SCH 23390 (D₁-like receptor antagonist), [³H]YM-09151-2 (D₂-like receptor antagonist), or [³H]RX821002 (α_2 receptor antagonist) versus NE and DA in the sheep brain striatum. K_{DB1} , K_{DB2} , and D_c values were obtained according to the two-state dimer model (see “Materials and Methods” and ref. 22). Values for α_2 -adrenoceptors are from Table 1. K_{DB1} and K_{DB2} (in nM) are expressed as means \pm SEM of three to five experiments performed in triplicate. Statistical differences between affinity parameters obtained were calculated by one-way ANOVA followed by Dunnett's post hoc test

For DA, *** $p < 0.001$ vs. D₂-like receptors; for NE, # $p < 0.05$ and ## $p < 0.01$ vs. α_2 receptors

also previously reported that, using the same cell line and assay conditions, neither DA or NE produces a significant BRET change when transfected with the same fused G protein subunits but without receptor co-transfection [19]. These transfected receptor levels were only slightly higher than those obtained in binding experiments in the sheep brain cortex (see above). A concentration response of the ligand-induced change in BRET values allows to determine the potency as well as the relative efficacy (to NE) at α_{2A} - and α_{2C} -adrenoceptor-mediated G protein activation. Results were largely in agreement with the values obtained with binding experiments, considering that cortical values should represent ligand binding parameters of α_{2A} -adrenoceptors, while striatal values represent combined ligand binding parameters for both α_{2A} - and α_{2C} -adrenoceptors. NE was more potent at α_{2A} - than at α_{2C} -adrenoceptor, except for $G\alpha i2$ and $G\alpha i3$. On the other hand, DA had similar potencies at both adrenoceptors, except for $G\alpha i2$ and $G\alpha o1$. At both α_{2A} - and α_{2C} -adrenoceptors, DA showed high potency and efficacy as compared with NE (Figs. 3 and 4, Tables 3 and 4), although DA was always less potent than NE. The relative DA/NE potency depended on the α -adrenoceptor and on the $G\alpha i/o$ subtype (see Table 3). Therefore, the potencies of DA at activating α_{2A} -adrenoceptor varied from about 15-fold lower, for $G\alpha i1$, to about 30-fold lower, for $G\alpha o1$. On the other hand, the potencies of DA as compared to NE at activating α_{2C} -adrenoceptor were

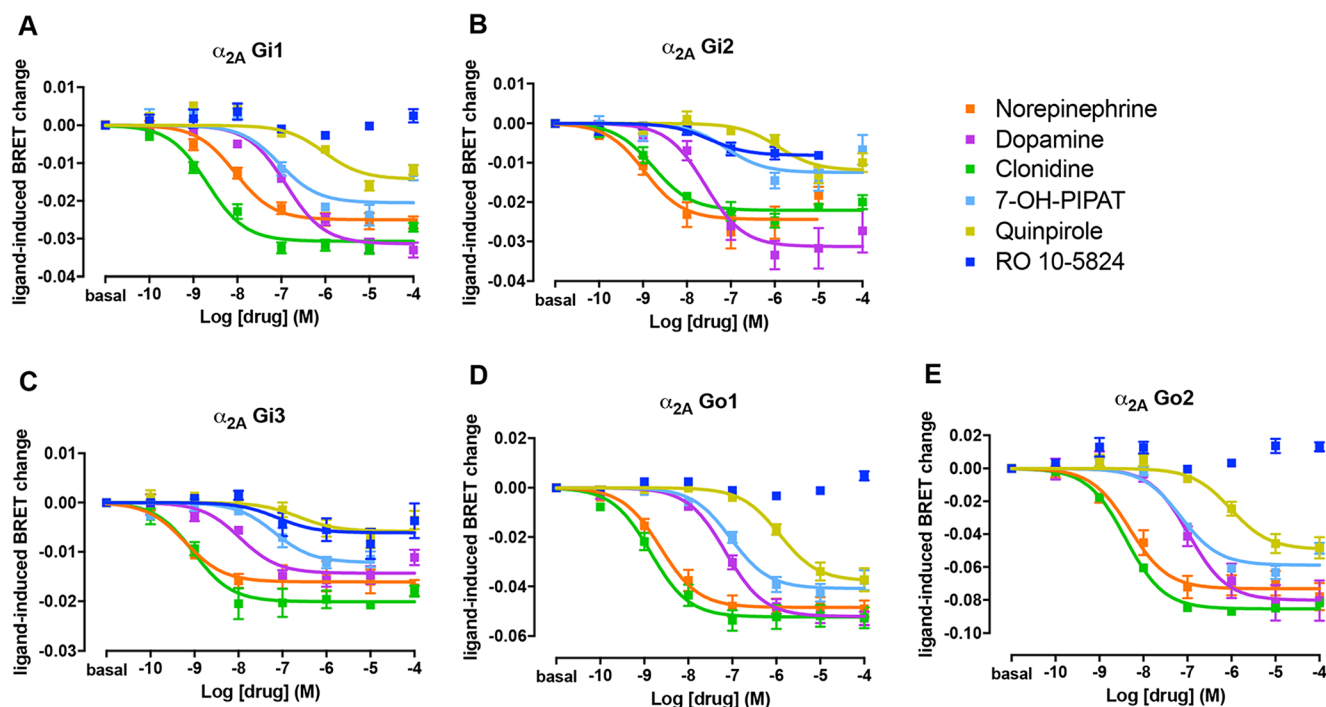


Fig. 3 G protein activation of α_{2A} by dopaminergic and adrenergic ligands. Concentration-response experiments of G protein activation by NE, DA, clonidine, and D_2 -like receptor ligands mediated by α_{2A} in HEK-293T cells transiently transfected with α_{2A} -adrenoceptor; the G protein subunits $G\alpha i1$ -RLuc (a), $G\alpha i2$ -RLuc (b), $G\alpha i3$ -RLuc (c), $G\alpha o1$ -RLuc (d), or $G\alpha o2$ -RLuc (e); $\gamma 2$ -mVenus, and non-fused $\beta 1$. Cells were treated with coelenterazine H followed by increasing concentrations of one of the ligands. Ligand-induced changes in BRET

values were measured as described in the “Materials and Methods” section. BRET values in the absence of ligands were subtracted from the BRET values for each agonist concentration. Data were adjusted to a sigmoidal concentration-response function by non-linear regression analysis and represent means \pm SEM of 3 to 11 experiments performed in triplicate (see Tables 1 and 2 for EC_{50} and E_{max} values and statistical analysis)

very close to those of NE and they varied from less than twofold lower, for $G\alpha i1$, to about 70-fold lower, for $G\alpha i3$ (Table 3).

The prototypical non-selective α -adrenoceptor agonist clonidine only showed a significantly higher potency at α_{2A} - than at α_{2C} -adrenoceptors for $G\alpha o1$ and $G\alpha o2$ (Table 3). An additional difference as compared to NE was that clonidine behaved as a full agonist at α_{2A} - and as a partial agonist at α_{2C} -adrenoceptor, except for $G\alpha i2$ and $G\alpha i3$ (Figs. 3 and 4, Table 4). Intriguingly, the level of efficacy of clonidine for α_{2C} -adrenoceptor varied significantly with the associated $G\alpha i/o$ protein subtypes, from no decrease for $G\alpha i2$ to a very significant loss of efficacy for $G\alpha o1$ (Table 4). Previous studies have already reported a partial agonism of clonidine at α_2 -adrenoceptors, but with disparate results [36, 37], which, at least for α_{2C} , could be related to the $G\alpha i/o$ protein subtypes involved. In summary, the differences in the respective potency values of NE, clonidine, and DA for α_{2A} - and α_{2C} -adrenoceptors in the G protein activation BRET experiments correlate with the higher affinities of NE and clonidine in the cortex and similar affinities of DA in the cortex and striatum.

The non-selective D_2 - D_3 - D_4 receptor agonist quinpirole and the selective D_3 receptor agonist 7-OH-PIPAT also activated α_{2A} - and α_{2C} -adrenoceptors, but with very different profiles (see Figs. 3 and 4, Tables 3 and 4). 7-OH-PIPAT

behaved as a low efficacious agonist at α_{2A} -adrenoceptors for the $G\alpha i2$ subtype. On the other hand, 7-OH-PIPAT behaved as a partial agonist at α_{2C} - $G\alpha i1$ complexes but as a full agonist with the other α_{2C} - $G\alpha i/o$ complexes. This D_3 receptor agonist, at α_{2A} -adrenoceptor, was, in general, as potent as DA and, for both $G\alpha o$ subtypes, was as potent α_{2C} -adrenoceptor agonist as NE. In contrast, quinpirole showed a weak potency (submicromolar range) but also behaved as a partial or full agonist depending on the $G\alpha i/o$ subtype. At α_{2A} , quinpirole behaved as a partial agonist for $Gi1$, $Gi2$, and $Gi3$ and a full agonist for $Go1$ and $Go2$, whereas at α_{2C} , it behaved as a partial agonist for all G protein subtypes except for $Gi3$ (full agonist) and showed no activity when coupled with $G\alpha i1$. As shown in Fig. 5, yohimbine, a non-selective α_2 -adrenoceptor antagonist, completely blocked the effect of 7-OH-PIPAT and quinpirole at both α_{2A} - and α_{2C} -adrenoceptors (for $G\alpha o1$), demonstrating the specificity of the α_2 -adrenoceptor signal produced by both agonists. The potency values of 7-OH-PIPAT and quinpirole in G protein activation BRET experiments correlate with the nanomolar and submicromolar affinities, respectively, as seen in binding assays with brain membranes. Moreover, the higher potencies of 7-OH-PIPAT for α_{2C} - versus α_{2A} -adrenoceptors also correlate with our binding results due to the fact that 7-OH-PIPAT showed negative

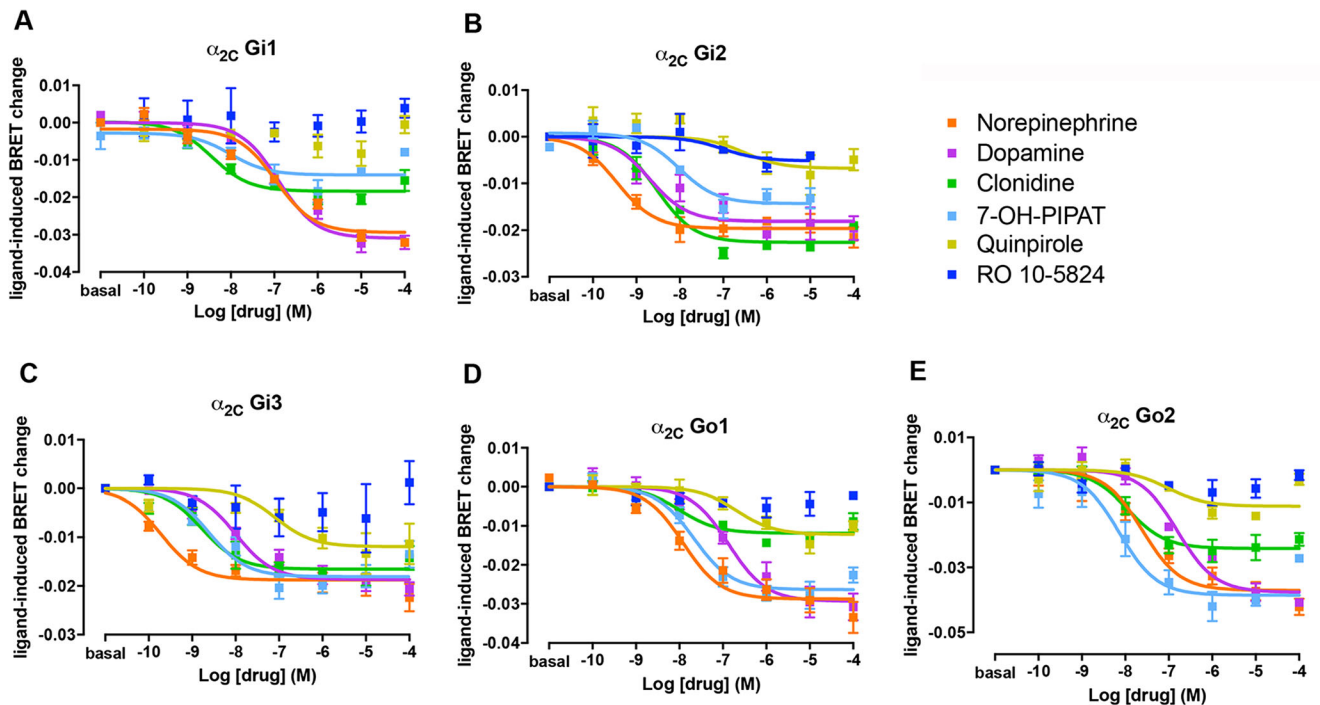


Fig. 4 G protein activation of α_{2C} by dopaminergic and adrenergic ligands. Concentration-response experiments of G protein activation by NE, DA, clonidine, and D₂-like receptor ligands mediated by α_{2C} in HEK-293T cells transiently transfected with α_{2C} receptor; the G protein subunits G α i1-RLuc (a), G α i2-RLuc (b), G α i3-RLuc (c), G α o1-RLuc (d), or G α o2-RLuc (e), γ 2-mVenus; and non-fused β 1. Cells were treated with coelenterazine H followed by increasing concentrations of one of the

ligands. Ligand-induced changes in BRET values were measured as described in the “Materials and Methods” section. BRET values in the absence of ligands were subtracted from the BRET values for each agonist concentration. Data were adjusted to a sigmoidal concentration-response function by non-linear regression analysis and represent means \pm SEM of three to nine experiments performed in triplicate (see Tables 1 and 2 for EC₅₀ and E_{max} values and statistical analysis)

cooperativity in the cortex but not in the striatum. For quinpirole, however, it would be difficult to establish correlations with results from binding assays due to its low efficacy in

BRET assays, which might lead to inaccurate values (Table 3, in parentheses, and Table 4, in italics). Finally, and unexpectedly, the selective D₄ receptor agonist RO-105824 (with

Table 3 Potency of NE, DA, clonidine, 7-OH-PIPAT, and quinpirole obtained from G protein activation experiments mediated by α_{2A} - and α_{2C} -adrenoceptors coupled to the different G α i/o subtypes

G α subunit	Receptor	NE	DA	Clonidine	7-OH-PIPAT	Quinpirole	DA/NE ^a
G α i1	α_{2A}	11 \pm 2**	170 \pm 40	3 \pm 1	80 \pm 20*	700 \pm 250	15
	α_{2C}	90 \pm 30	150 \pm 40	6 \pm 2	(11 \pm 4)	ND	1.7
G α i2	α_{2A}	1.3 \pm 0.3*	30 \pm 3**	2.0 \pm 0.8	120 \pm 6*	(1000 \pm 300)	23
	α_{2C}	0.4 \pm 0.2	5 \pm 3	3 \pm 1	10 \pm 2	(200 \pm 100)	12.5
G α i3	α_{2A}	0.6 \pm 0.2	15 \pm 5	1.0 \pm 0.2	60 \pm 20*	(700 \pm 400)	25
	α_{2C}	0.4 \pm 0.2	30 \pm 20	4 \pm 1	5 \pm 3	400 \pm 100	75
G α o1	α_{2A}	3.0 \pm 0.5*	80 \pm 10**	2.0 \pm 0.4*	100 \pm 20**	1300 \pm 200**	27
	α_{2C}	19 \pm 6	126 \pm 8	(12 \pm 5)	20 \pm 3	(230 \pm 50)	7
G α o2	α_{2A}	6 \pm 1*	100 \pm 20	4.0 \pm 0.2**	66 \pm 7*	820 \pm 80***	17
	α_{2C}	50 \pm 10	140 \pm 20	11 \pm 2	14 \pm 7	(100 \pm 10)	2.8

Potency (EC₅₀ values, in nM) of NE, DA, clonidine, and D₂-like receptor ligands obtained from G protein activation experiments mediated by α_{2A} and α_{2C} coupled to the different G α i/o subtypes (Figs. 3 and 4). EC₅₀ values were obtained from a sigmoidal concentration-response function adjusted by non-linear regression analysis and are expressed as means \pm SEM of 3 to 11 experiments performed in triplicate. In parentheses, values corresponding to experiments show low efficacy, E_{max} lower than 50% (Table 4). Statistical differences between α_{2A} - and α_{2C} -adrenoceptors were calculated by non-paired, two-tailed Student's *t* test

* p < 0.05; ** p < 0.01; *** p < 0.001

^a The ratio of EC₅₀ values of DA and NE for each receptor and G α i/o protein subtype

Table 4 Efficacy of NE, DA, clonidine, 7-OH-PIPAT, and quinpirole obtained from G protein activation experiments mediated by α_{2A} - and α_{2C} -adrenoceptors coupled to the different G α i/o subtypes

G α subunit	Receptor	NE	DA	Clonidine	7-OH-PIPAT	Quinpirole
G α i1	α_{2A}	100 \pm 5	120 \pm 6*	120 \pm 5	94 \pm 6	70 \pm 2*
	α_{2C}	100 \pm 2	105 \pm 5	64 \pm 4***	41 \pm 1**	ND
G α i2	α_{2A}	100 \pm 10	120 \pm 20	89 \pm 6	55 \pm 2*	47 \pm 8*
	α_{2C}	100 \pm 7	80 \pm 10	107 \pm 4	90 \pm 20	46 \pm 9**
G α i3	α_{2A}	100 \pm 10	90 \pm 10	112 \pm 8	71 \pm 6	40 \pm 9**
	α_{2C}	100 \pm 9	95 \pm 6	85 \pm 5	90 \pm 10	80 \pm 15
G α o1	α_{2A}	100 \pm 7	108 \pm 6	110 \pm 10	81 \pm 9	78 \pm 9
	α_{2C}	100 \pm 10	100 \pm 10	41 \pm 3**	98 \pm 7	42 \pm 3**
G α o2	α_{2A}	100 \pm 9	110 \pm 10	120 \pm 2	85 \pm 4	72 \pm 8
	α_{2C}	100 \pm 8	114 \pm 6	70 \pm 8*	106 \pm 3	34 \pm 6**

Efficacy (E_{\max} values, as the percentage of NE values) of NE, DA, clonidine, and D₂-like receptor ligands obtained from G protein activation experiments mediated by α_{2A} and α_{2C} coupled to the different G α i/o subtypes (Figs. 3 and 4). E_{\max} values were obtained from a sigmoidal concentration-response function adjusted by non-linear regression analysis and are expressed as means \pm SEM of 3 to 11 experiments performed in triplicate. In italics, values of E_{\max} are lower than 50%. Statistical differences between NE and the other ligands for each receptor and G α i/o protein subtype were calculated by one-way ANOVA, followed by Dunnett's post hoc test

ND not detectable

* $p < 0.05$; ** $p < 0.01$; *** $p < 0.001$

subnanomolar affinity for α -adrenoceptors) did not produce a significant activation of α_{2A} - or α_{2C} -adrenoceptors coupled to any of the G α i/o subtypes, except for a small efficacy at α_{2A} for G α i2 and G α i3 (Figs. 3 and 4). To confirm the binding of this putative selective D₄ receptor ligand to α_{2A} - and α_{2C} -adrenoceptors, they were tested for their ability to modify the effect of clonidine. RO-105824 did counteract the respective full and partial agonistic effect of clonidine (1 μ M) at the α_{2A} - and α_{2C} -adrenoceptors coupled to G α o1 (Fig. 5c, d). Therefore, the results of BRET and radioligand binding experiments disclosed a previously unknown additional role of the D₄ receptor agonist RO-105824, as a very potent and low-efficacious ligand for α_2 -adrenoceptors at G α i/o activation.

We also determined the effect of DA and synthetic DA receptor ligands on a DMR label-free assay in CHO-transfected cells. This approach detects changes in local optical density due to cellular mass movements induced upon receptor activation (see the “Materials and Methods” section), and DMR responses primarily reflect G protein-dependent signaling in living cells, since it can be abrogated by toxins or inhibitors of the G proteins involved [38]. DA was as capable as NE at activating cellular signaling in CHO cells transfected with α_{2A} -RLuc8 receptor (Fig. 6a). The amount of α_{2A} -RLuc8 receptor expressed was about 0.3 pmol/mg protein. DA and NE activation decreased by adding the α_{2A} -antagonist BRL 44408, indicating the specificity of the cell activation through α_{2A} -receptor. The synthetic DA receptor ligands 7-OH-PIPAT, quinpirole, and RO-105824 at 300 nM were also able to produce a significant response (Fig. 6b), substantially lower for RO-105824, which correlates with the G protein activation BRET assays (Fig. 3). These results indicate that DA and

synthetic DA receptor ligands are also α_2 -adrenoceptor ligands able to activate G α i/o proteins, which correlate with their efficacy with DMR.

α_{2A} - and α_{2C} -Adrenoceptor-Mediated Effects of NE and DA on Adenylyl Cyclase Activity

NE- and DA-induced changes in adenylyl cyclase activity were also analyzed by measuring cAMP levels in intact cells transiently transfected with α_{2A} - or α_{2C} -adrenoceptor, using the CAMYEL BRET biosensor (see the “Materials and Methods” section and ref. 21). HEK-293T cells have been reported to endogenously express β -adrenoceptors [39]. Accordingly, we recently reported that NE, in non-transfected HEK-293T cells, stimulated a Gs-mediated cAMP increase, which could be completely inhibited by the selective β -adrenergic blocker propranolol (10 μ M) (ref. 19; the same website address as above). Therefore, the β -adrenoceptor antagonist propranolol was added throughout the cAMP detection experiments. As shown in Fig. 7, NE and DA produced an increase in BRET, corresponding to a decrease in forskolin-induced cAMP accumulation for both α_{2A} - and α_{2C} -adrenoceptor-transfected cells. The decrease in adenylyl cyclase activity by NE and DA provided apparent half maximal effective concentration (EC_{50}) values that were qualitatively and quantitatively close to those observed with the Gi/o activation BRET assays, as NE was more potent than DA at α_{2A} and α_{2C} (1.4 \pm 0.2 and 7 \pm 4 nM for NE and 140 \pm 40 and 90 \pm 20 nM for DA, respectively). The putative Gi/o-dependent effects mediated by NE and DA were blocked by the non-selective α_2 -adrenoceptor antagonist yohimbine, confirming the receptor specificity of the signal (Fig. 7). In

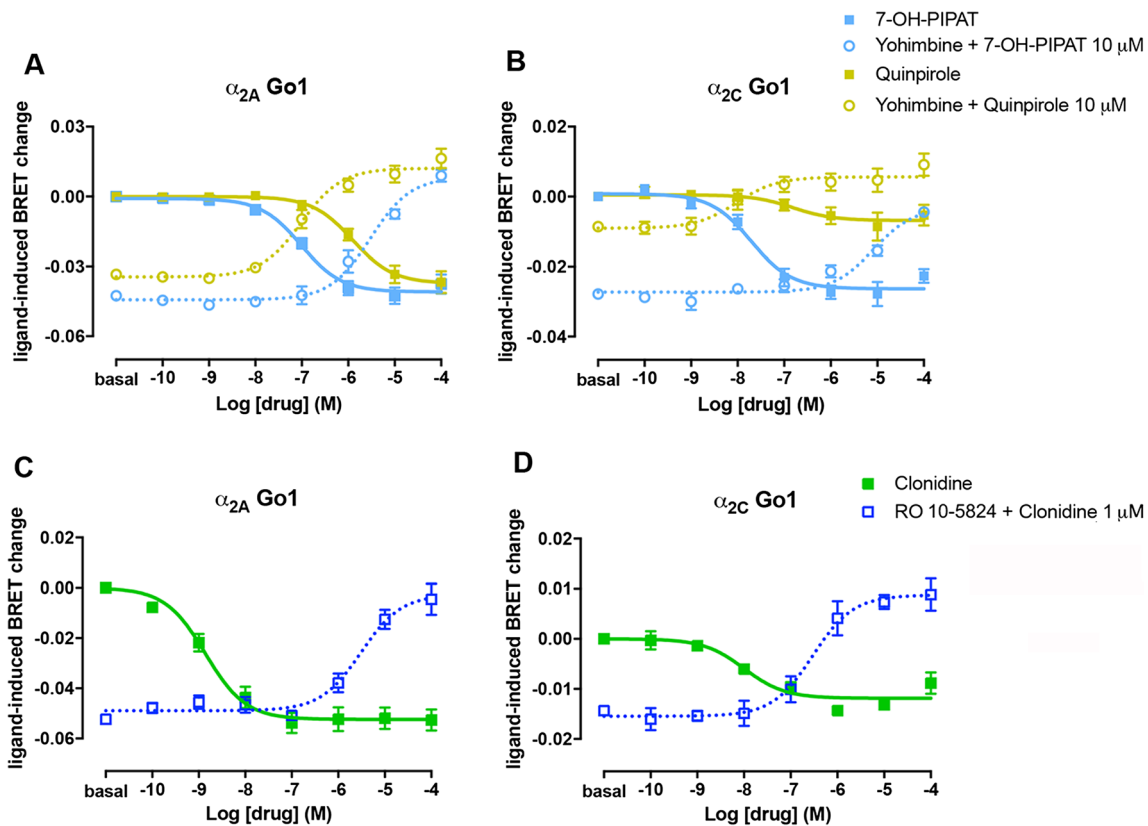


Fig. 5 Specificity of the effect of dopaminergic ligands on α_{2A} - and α_{2C} -adrenoceptors. **a, b** Dose-dependent inhibition by increasing concentrations of the non-selective α_2 receptor antagonist yohimbine of $G\alpha o1$ protein activation induced by 10 μM of the D_2 -like receptor agonists 7-OH-PIPAT (dotted blue) or 10 μM of quinpirole (dotted yellow) in HEK-293T cells transfected with α_{2A} (**a**) or α_{2C} (**b**) adrenoceptors, $G\alpha o1$ -RLuc, γ_2 -mVenus, and non-fused β_1 . As controls, concentration-response curves of $G\alpha o1$ protein activation by 7-OH-PIPAT (full blue) or quinpirole (full yellow) from Figs. 3d and 4d are showed. Cells were treated with coelenterazine H followed by the

addition of 7-OH-PIPAT or quinpirole. Ligand-induced changes in BRET values were measured as described in the “Materials and Methods” section. **c, d** Dose-dependent inhibition of the agonistic effect of clonidine at 1 μM by increasing concentrations of RO-105824 (dark blue) in cells transfected with α_{2A} (**c**) or α_{2C} (**d**) adrenoceptors, $G\alpha o1$ -RLuc, γ_2 -mVenus, and non-fused β_1 . As controls, concentration-response curves of $G\alpha o1$ protein activation by clonidine (full green) from Figs. 3d and 4d are showed. Data were adjusted to a sigmoidal concentration-response function by non-linear regression analysis and represent means \pm SEM of three to six experiments performed in triplicate

addition, cells were treated with pertussis toxin which catalyzes the ADP ribosylation of the α_i subunits of the heterotrimeric G protein, preventing its interaction with the receptor. As expected, pertussis toxin treatment selectively eliminated the initial, therefore Gi-dependent, component of the NE- and DA-mediated effects (Fig. 7). Surprisingly, NE and DA showed inverted U-shaped concentration-response curves with a putative Gs-dependent profile at high ligand concentrations for both α_{2A} - and α_{2C} -adrenoceptor-transfected cells (Fig. 7). These results could be explained by considering previous studies showing that α_2 -adrenoceptors functionally couple not only to Gi/o proteins but also to Gs [40–44]. Typically, the agonist concentrations necessary to elicit detectable stimulation of adenylyl cyclase are significantly higher than those for inhibition. Equivocal results were published by Zhang et al. [16] when comparing the effect of NE and DA on forskolin-induced adenylyl cyclase activation. In their cell systems, NE seemed to predominantly activate Gs with α_{2A} and Gi with α_{2C} , while DA would predominantly activate Gi with both receptors, but at

high micromolar concentrations. In contrast, our experiments show that NE and DA follow the same differential concentration-dependent effects on Gi/o and Gs activation and, at least, at 10 and 100 μM , DA and NE promoted Gs activation mediated by both α_{2A} - and α_{2C} -adrenoceptors (Fig. 7).

α_{2A} - and α_{2C} -Adrenoceptor-Mediated Effects of NE, DA, and Synthetic DA Receptor Ligands on ERK1/2 Phosphorylation

Finally, we studied the ability of DA and synthetic DA receptor ligands to produce MAPK activation. First, we analyzed the increase on ERK1/2 phosphorylation produced by 300 nM of NE in CHO cells transfected with α_{2A} -RLuc8 receptor. This NE concentration increased ERK1/2 phosphorylation levels by threefold over basal, and this effect was similar to that produced by 1 μM of DA (Fig. 8). Next, we demonstrated that the synthetic DA receptor ligands 7-OH-PIPAT, quinpirole, and RO-105824, at 1 μM , were also able to

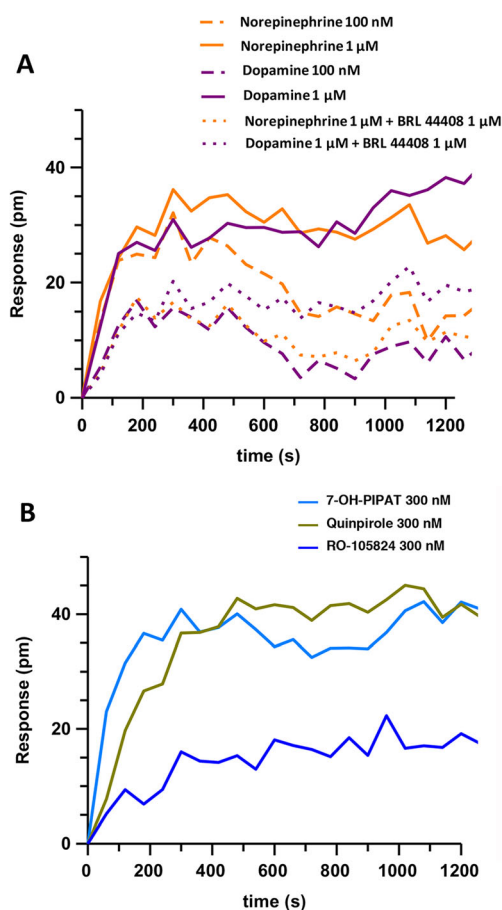


Fig. 6 DMR induced by NE, DA, and synthetic DA receptor ligands using label-free assay. DMR assay was performed in CHO cells transfected with α_{2A} -adrenoceptor. **a** Cells were pretreated (dotted lines) or not (full lines) with the α_{2A} -adrenoceptor antagonist BRL 44408 at 1 μ M for 30 min before adding the endogenous agonists DA or NE at 300 nM or 1 μ M. **b** Cells were treated with 100 nM of several synthetic DA receptor ligands. The resulting shifts of reflected light wavelength (pm) were monitored over time. Each panel is a representative experiment of $n = 3$ different experiments. Each curve is the mean of a representative optical trace experiment carried out in triplicates

produce MAPK activation (Fig. 8). At this concentration, the efficacy of RO-105824 was similar to that of the other ligands. Together with its very low efficacy disclosed on G protein activation and DMR assays, these results indicate that RO-105824 is a biased agonist of α_{2A} -adrenoceptors with functional selectivity for G protein-independent signaling. In summary, adenylyl cyclase activity and ERK1/2 phosphorylation experiments confirm the results from radioligand binding and G protein activation assays, indicating that DA and synthetic DA receptor ligands are efficacious α_2 -adrenoceptor agonists.

Structural Basis for DA at α_{2A} - and α_{2C} -Adrenoceptors

An examination of the binding mode of DA to the adrenoceptors was undertaken to model the activity seen in the biological assays. To generate models of α_{2A} - and α_{2C} -

adrenoceptors, we used the RosettaCM [25] application within the Rosetta suite of macromolecular modeling tools [26, 45]. This method relies on the optimal alignment of a target sequence with multiple template structures obtained from the PDB which are hybridized together to generate novel models. We submitted the sequence of α_{2A} and α_{2C} to BLAST-P and found the top five crystal templates by sequence identity to be the DA D_3 receptor [27], β_1 -adrenoceptor [28], β_2 -adrenoceptor [29], serotonin 5-HT_{1B} receptor [30], and serotonin 5-HT_{2B} receptor [31]. Interestingly, the α_2 -adrenoceptors have more sequence identity in the transmembrane helical bundle with the D_3 receptor than with the related β -adrenoceptors. RosettaCM yielded an ensemble of low-energy models of the receptors, which were clustered by structural similarity. The top five cluster centers were included in the docking studies to account for structural diversity and uncertainty in homology modeling. To understand DA activation, we first examined the binding of DA to the D_3 receptor, the only crystal structure of a DA receptor to date. As there is not a co-crystal structure of DA/ D_3 receptor, we first docked DA to the D_3 receptor using RosettaLigand [33]. The starting coordinates of epinephrine bound to the β_2 -adrenoceptor [46] were used to place DA for docking. Binding pocket analysis identified residue D3.32 interacting with the primary amine in DA and the catechol hydroxyls interacting with S5.42 and S5.46. Important hydrophobic packing against the central portion of DA was achieved by V3.33, H6.55, and F6.51. These are the same interactions that were previously identified in a molecular dynamics simulation of DA binding at D_3 receptor [47]. Comparing the residues at these positions to those in α_{2A} - and α_{2C} -adrenoceptors revealed identity at all residues except position 6.55, in which the His has been replaced with a Tyr in both α_{2A} - and α_{2C} -adrenoceptors. Docking results of DA at either α_{2A} or α_{2C} also identified many of these same residues as critical for binding. Particularly, D3.32, V3.33, S5.42, and F6.51 were present in all receptor models contributing more than -0.4 Rosetta energy units each to the binding of DA (Fig. 9). Residues S5.46 and Y6.55 were also present in all receptor binding modes though contributions varied depending on which receptor type. These results coupled with those from the biological assays provide a strong structural reasoning behind the activity of DA at the α_{2A} - or α_{2C} -adrenoceptors.

Discussion

Previous studies reported DA as a potential α_2 -adrenoceptor ligand on the basis of radioligand binding experiments in transfected mammalian and insect cell lines [16, 17] and in bird and rat brains [18] and also from autoradiographic experiments in tissues [18]. Furthermore, DA has been reported to decrease cAMP intracellular levels in transfected mammalian

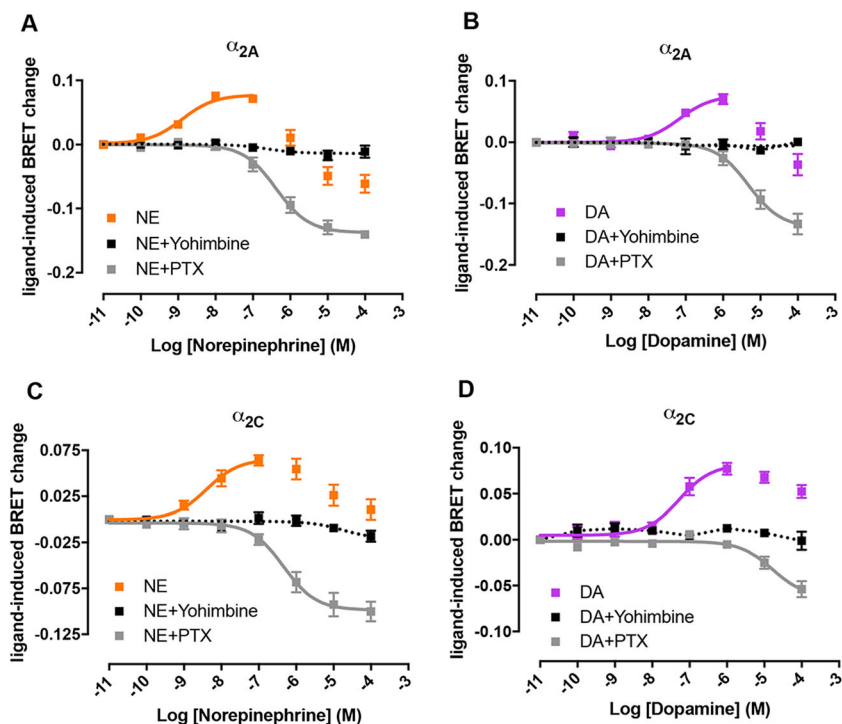


Fig. 7 Effect of NE and DA on the modulation of adenylyl cyclase activity by activation of α_{2A} - and α_{2C} -adrenoceptors. Concentration-response experiments of inhibition of forskolin-induced adenylyl cyclase activity by NE (orange) or DA (purple) mediated by α_{2A} (a, b) or α_{2C} -adrenoceptors (c, d) in HEK-293T cells transiently transfected with the CAMYEL sensor and one of the receptors. Cells were treated with forskolin (1 μ M) for 10 min with or without the selective α_2 antagonist yohimbine (10 μ M) followed by the addition of coelenterazine

H and increasing concentrations of NE or DA. After 10 min, BRET was measured as described in the “Materials and Methods” section. In gray, cells were treated with 100 ng/ml pertussis toxin (PTX) for 16–18 h previous to the experiment. Values obtained with forskolin alone were subtracted from BRET values for each agonist concentration. Data represent the mean \pm SEM of three to seven experiments performed in triplicate

cell lines but only throughout α_{2C} -adrenoceptors, not α_{2A} -adrenoceptors, and at concentrations much higher than NE (EC_{50} in the micromolar range) [18].

In our study, we show that α_{2A} - and α_{2C} -adrenoceptors can bind DA at concentrations in the same order than NE, suggesting that they could be activated by DA at in vivo

concentrations. First, our results demonstrate that endogenous DA, and also common synthetic DA receptor ligands, binds to α_2 -adrenoceptors with moderate to high affinity in the mammalian brain. Second, the affinity of DA for α_2 -adrenoceptors is in the same range as for D₁-like and D₂-like receptors, suggesting that endogenous

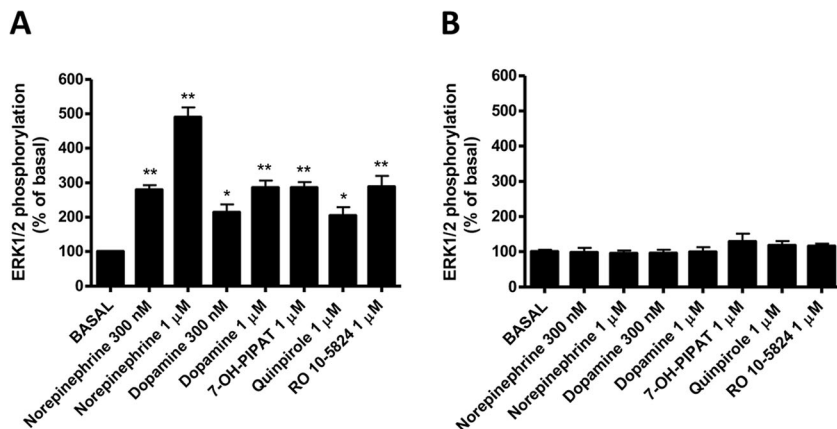


Fig. 8 NE, DA, and synthetic DA receptor ligands signaling via ERK1/2 phosphorylation. ERK1/2 phosphorylation was determined in CHO cells transfected with the α_{2A} -adrenoceptor (a) and non-transfected control cells (b), treated with 300 nM or 1 μ M of the tested ligands for 5 min

at 37 $^{\circ}$ C. Values are expressed as mean \pm SEM ($n = 6$) of percentage of phosphorylation relative to basal levels in non-treated cells. Statistical differences vs. basal conditions were calculated by one-way ANOVA followed by Dunnett’s post hoc test; * $p < 0.05$ and ** $p < 0.01$

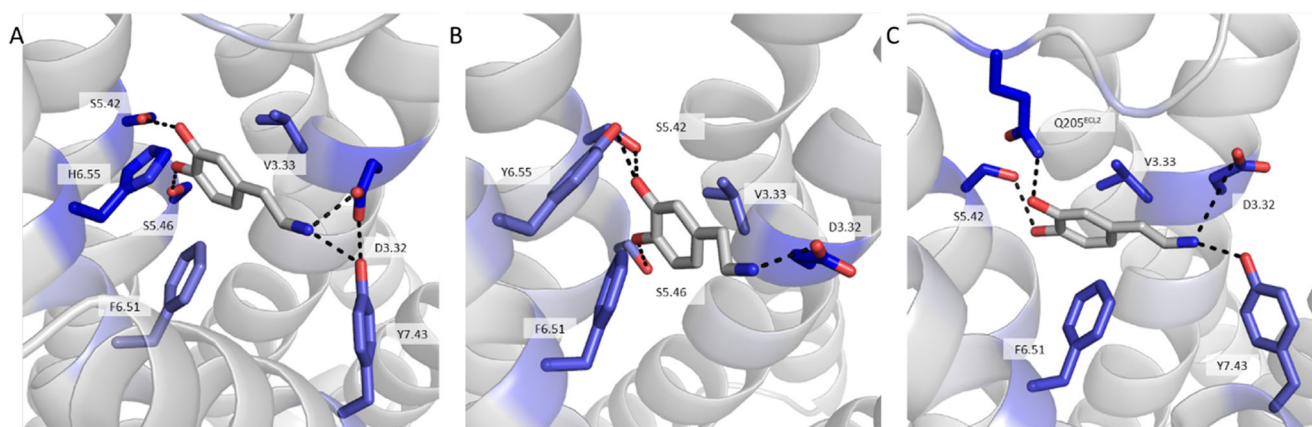


Fig. 9 Binding mode of DA at each receptor type. Shown is the docking orientation of DA at the D_3 receptor (a), α_{2A} -adrenoceptor (b), and α_{2C} -adrenoceptor (c). Residues were scored for binding energy $\Delta\Delta G$, and those most strongly contributing to the binding of DA are shown in stick

representation. The strength of binding interaction is colored by the depth of blue with dark blue being the most strongly contributing. Important hydrogen bonds to the amine group and catechol hydroxyls are formed in all binding poses

levels of DA can activate both α_2 -adrenoceptors and dopamine receptors. Third, DA and synthetic DA receptor ligands can activate G protein and induce cell DMR through α_2 -adrenoceptors. Finally, DA and NE show the same cell signaling pattern, being both capable to modulate adenylyl cyclase activity and ERK1/2 phosphorylation at nanomolar concentrations.

The most conclusive demonstration that DA is an α_2 -adrenoceptor ligand comes from the results obtained with binding and G protein activation BRET assays, where the affinities or potencies of DA for α_2 -adrenoceptors were found to be very similar or even higher than for D_1 -like and some subtypes of D_2 -like receptors [19]. Particularly, the EC_{50} values of DA for α_{2A} - and α_{2C} -adrenoceptors (5–170 nM) were consistently lower across all Gi/o protein subtypes as compared with the EC_{50} values (130–400 nM) for the predominant striatal D_2 -like receptor D_{2L} [19]. Taking into account that the levels of tonic extracellular DA are 20–30 nM (with peaks of 500 nM) [48], DA could reach sufficient extracellular concentration to activate α_{2A} - and α_{2C} -adrenoceptors in the striatum, irrespective of the maximal concentration of extracellular NE. In fact, striatal DA release sites are designed for transmitter spillover [49] and most striatal DA receptors are primarily extrasynaptic [50, 51], as well as striatal adrenoceptors, based on the mismatched low NE innervation [7–11]. Although the specific functional role of the DA-sensitive α_2 -adrenoceptors in neuronal striatal function remains to be established, a previous study suggests that they might mediate an inhibitory modulatory role of the Gs/olf-coupled striatal adenosine A_{2A} and DA D_1 receptors [14].

The possibility of DA-mediated activation of α_{2A} - and α_{2C} -adrenoceptors in extrastriatal areas should not, however, be underestimated. Cortical α_{2A} -adrenoceptors are most probably able to be activated by DA, particularly in the prefrontal cortex, which receives a rather dense DA innervation [52]. In fact,

there is recent evidence for the localization of α_{2A} -adrenoceptors in the cortical terminals from mesencephalic DA neurons [53], which could play a role as “DA autoreceptors.” But, there is also evidence for the localization of both α_{2A} - and α_{2C} -adrenoceptors in the soma and dendrites of the mesencephalic DA cells of both substantia nigra and ventral tegmental areas [53, 54]. Apart from the NE input, these α_{2A} - and α_{2C} -adrenoceptors should be able to act as DA autoreceptors that control the non-synaptic somatodendritic DA release [49]. Adding the present results to our recent study that also indicates a significant role of NE as a Gi/o-coupled D_2 -like receptor agonist [19], we could state that Gi/o-coupled adrenoceptors and DA receptors should probably be considered as members of one “functional” family of catecholamine receptors. A general consideration from the DA and D_2 -like receptor ligand sensitivity of cortical α_{2A} -adrenoceptors is that it should also be involved in the cognitive-enhancing effects associated with their activation, with possible implications for attention deficit hyperactivity disorder [55].

Molecular modeling of DA binding to the various receptors provides a likely binding hypothesis for the results obtained in the biological assays. Of note is the striking similarity between the ligand binding pocket of the D_3 receptor and that of α_{2A} - and α_{2C} -adrenoceptors. Many of the residues that line the binding pocket are identical or chemically well conserved. Given this similarity, it was perhaps unsurprising that the docking of DA at α_{2A} and α_{2C} was nearly identical to DA binding to the D_3 receptor. The lower potency of DA at α_{2A} - and α_{2C} -adrenoceptors compared to NE seems to depend on a lower number of strong interactions as compared to those between DA and D_3 receptors. The pocket may have evolved to bind the slightly bulkier NE and, therefore, is not of an ideal size for DA. However, the differences may also be due to the lower resolution of binding predictions for a comparative model as opposed to a crystal structure. Despite this, the

structural model strongly mimics the results of the binding and activation experiments and therefore provides further evidence of DA acting as a ligand at these receptors.

Another major finding of the present study is that α_{2A} - and α_{2C} -adrenoceptors are also common targets for compounds previously characterized as D_2 -like receptor ligands. Particularly striking was the ability of prototypical D_3 and D_4 receptor agonists 7-OH-PIPAT and RO-105824 to bind with high affinity to α_{2A} - and α_{2C} -adrenoceptors, which might call for revisiting results of previous studies using these compounds. Furthermore, these two compounds and the other DA-synthetic ligands assayed, as well as NE, were able to activate ERK1/2 phosphorylation by binding to α_2 -adrenoceptors. The final pharmacological profile of RO-105824 was that of a potent biased agonist for α_{2A} -adrenoceptor with functional selectivity for a G protein-independent signaling. On the other hand, based on BRET experiments, both potency and efficacy dependence on the receptor and the $G\alpha i/o$ protein subtype were the norm for all ligands, including the endogenous neurotransmitters. We already described that NE and DA show different receptor- and $G\alpha i/o$ subtype-dependent potencies of D_2 -like receptor-mediated G protein activation [19]. The present results extend these findings to other receptors and to non-endogenous ligands, as well as to differences in efficacy. Even though G proteins of the $G\alpha s$ - $G\alpha olf$ family do show contrasting brain expression pattern [56], to our knowledge, no clear region-specific pattern of mRNA expression for $G\alpha i/o$ protein subtypes has been reported. Detailed characterization of the expression patterns for $G\alpha i/o$ protein subtypes would then be central to determine their role in α_{2A} - and α_{2C} -adrenoceptor activation and thus their possible specific targeting with $G\alpha i/o$ subtype functionally selective compounds.

In conclusion, DA is a potent and efficacious ligand at α_2 -adrenoceptors, which modulates forskolin-induced adenylyl cyclase activity and ERK1/2 phosphorylation. The concentration required for these effects is in the range of that for activating D_2 -like and D_1 -like receptors, indicating that these receptors are members of one functional family of catecholamine receptors. Our results provide a clear answer to the mismatch between the low striatal NE innervation and the high density of striatal α_2 -adrenoceptors, which behave as functional DA receptors.

Acknowledgements The authors would like to thank Dr. Céline Galés (INSERM) for generously sharing various Gi-like plasmid constructs for BRET experiments.

Author Contributions M. S.-S., V. C.-A., H. Y., N.-S. C., E. M., A. C., and B. J. B. performed the experiments and analyzed the data. H. Y., B. J. B., J. M., V. C., and S. F. designed the experiments. M. S.-S., V. C.-A., H. Y., B. J. B., J. M., E. I. C., V. C., and S. F. wrote the manuscript.

Funding Information This research was supported by the “Ministerio de Economía y Competitividad” and European Regional Development Funds of the European Union Grant SAF2014-54840-R, the “Centro de Investigación Biomédica en Red sobre Enfermedades Neurodegenerativas” Grant CB06/05/0064, the “Fundació La Marató de TV3” Grant 20140610, the fellowship from the Japan Society for the Promotion of Science, and intramural funds of the National Institute on Drug Abuse. Work in the Meiler Laboratory is supported through the NIH (R01 GM080403, R01 GM099842, R01 DK097376) and NSF (CHE 1305874).

Compliance with Ethical Standards

Conflict of Interest The authors declare that they have no conflicts of interest.

References

- Alexander SP, Mathie A, Peters JA (2011) Guide to Receptors and Channels (GRAC), 5th edition. *Br J Pharmacol* 164(Suppl 1):S1–S324. https://doi.org/10.1111/j.1476-5381.2011.01649_1.x
- MacDonald E, Kobilka BK, Scheinin M (1997) Gene targeting—homing in on alpha 2-adrenoceptor-subtype function. *Trends Pharmacol Sci* 18(6):211–219
- Nicholas AP, Pieribone V, Hokfelt T (1993) Distributions of mRNAs for alpha-2 adrenergic receptor subtypes in rat brain: an in situ hybridization study. *J Comp Neurol* 328(4):575–594. <https://doi.org/10.1002/cne.903280409>
- Scheinin M, Lomasney JW, Hayden-Hixson DM, Schambra UB, Caron MG, Lefkowitz RJ, Fremeau RT Jr (1994) Distribution of alpha 2-adrenergic receptor subtype gene expression in rat brain. *Brain Res Mol Brain Res* 21(1–2):133–149
- Fagerholm V, Rokka J, Nyman L, Sallinen J, Tiihonen J, Tupala E, Haaparanta M, Hietala J (2008) Autoradiographic characterization of alpha(2C)-adrenoceptors in the human striatum. *Synapse* 62(7):508–515. <https://doi.org/10.1002/syn.20520>
- Lehto J, Virta JR, Oikonen V, Roivainen A, Luoto P, Arponen E, Helin S, Hietamaki J et al (2015) Test-retest reliability of (11)C-ORM-13070 in PET imaging of alpha2C-adrenoceptors in vivo in the human brain. *Eur J Nucl Med Mol Imaging* 42(1):120–127. <https://doi.org/10.1007/s00259-014-2899-z>
- Ordway GA, Jaconetta SM, Halaris AE (1993) Characterization of subtypes of alpha-2 adrenoceptors in the human brain. *J Pharmacol Exp Ther* 264(2):967–976
- Uhlen S, Lindblom J, Tiger G, Wikberg JE (1997) Quantification of alpha2A and alpha2C adrenoceptors in the rat striatum and in different regions of the spinal cord. *Acta Physiol Scand* 160(4):407–412. <https://doi.org/10.1046/j.1365-201X.1997.00175.x>
- Lindvall O, Bjorklund A (1974) The organization of the ascending catecholamine neuron systems in the rat brain as revealed by the glyoxylic acid fluorescence method. *Acta Physiol Scand Suppl* 412: 1–48
- Swanson LW, Hartman BK (1975) The central adrenergic system. An immunofluorescence study of the location of cell bodies and their efferent connections in the rat utilizing dopamine-beta-hydroxylase as a marker. *J Comp Neurol* 163(4):467–505. <https://doi.org/10.1002/cne.901630406>
- Aston-Jones G (2004) Locus coeruleus, A5 and A7 noradrenergic cell groups. In: Paxinos G (ed) *The rat nervous system*. Academic, San Diego, pp. 259–294

12. Gobert A, Billiras R, Cistarelli L, Millan MJ (2004) Quantification and pharmacological characterization of dialysate levels of noradrenaline in the striatum of freely-moving rats: release from adrenergic terminals and modulation by alpha2-autoreceptors. *J Neurosci Methods* 140(1–2):141–152. <https://doi.org/10.1016/j.jneumeth.2004.04.040>
13. Holmberg M, Scheinin M, Kurose H, Miettinen R (1999) Adrenergic alpha2C-receptors reside in rat striatal GABAergic projection neurons: comparison of radioligand binding and immunohistochemistry. *Neuroscience* 93(4):1323–1333
14. Hara M, Fukui R, Hieda E, Kuroiwa M, Bateup HS, Kano T, Greengard P, Nishi A (2010) Role of adrenoceptors in the regulation of dopamine/DARPP-32 signaling in neostriatal neurons. *J Neurochem* 113(4):1046–1059. <https://doi.org/10.1111/j.1471-4159.2010.06668.x>
15. Ihalainen JA, Tanila H (2004) In vivo regulation of dopamine and noradrenaline release by alpha2A-adrenoceptors in the mouse nucleus accumbens. *J Neurochem* 91(1):49–56. <https://doi.org/10.1111/j.1471-4159.2004.02691.x>
16. Zhang W, Klimek V, Farley JT, Zhu MY, Ordway GA (1999) alpha2C adrenoceptors inhibit adenylyl cyclase in mouse striatum: potential activation by dopamine. *J Pharmacol Exp Ther* 289(3):1286–1292
17. Alachkar A, Brochie JM, Jones OT (2010) Binding of dopamine and 3-methoxytyramine as l-DOPA metabolites to human alpha(2)-adrenergic and dopaminergic receptors. *Neurosci Res* 67(3):245–249. <https://doi.org/10.1016/j.neures.2010.03.008>
18. Cornil CA, Ball GF (2008) Interplay among catecholamine systems: dopamine binds to alpha2-adrenergic receptors in birds and mammals. *J Comp Neurol* 511(5):610–627. <https://doi.org/10.1002/cne.21861>
19. Sánchez-Soto M, Bonifazi A, Cai NS, Ellenberger MP, Newman AH, Ferré S, Yano H (2016) Evidence for noncanonical neurotransmitter activation: norepinephrine as a dopamine D2-like receptor agonist. *Mol Pharmacol* 89(4):457–466. <https://doi.org/10.1124/mol.115.101808>
20. Urizar E, Yano H, Kolster R, Gales C, Lambert N, Javitch JA (2011) CODA-RET reveals functional selectivity as a result of GPCR heteromerization. *Nat Chem Biol* 7(9):624–630. <https://doi.org/10.1038/nchembio.623>
21. Jiang LI, Collins J, Davis R, Lin KM, DeCamp D, Roach T, Hsueh R, Rebres RA et al (2007) Use of a cAMP BRET sensor to characterize a novel regulation of cAMP by the sphingosine 1-phosphate/G13 pathway. *J Biol Chem* 282(14):10576–10584. <https://doi.org/10.1074/jbc.M609695200>
22. Casadó V, Cortés A, Ciruela F, Mallol J, Ferré S, Lluís C, Canela EI, Franco R (2007) Old and new ways to calculate the affinity of agonists and antagonists interacting with G-protein-coupled monomeric and dimeric receptors: the receptor-dimer cooperativity index. *Pharmacol Ther* 116(3):343–354. <https://doi.org/10.1016/j.pharmthera.2007.05.010>
23. Ferré S, Casadó V, Devi LA, Filizola M, Jockers R, Lohse MJ, Milligan G, Pin JP et al (2014) G protein-coupled receptor oligomerization revisited: functional and pharmacological perspectives. *Pharmacol Rev* 66(2):413–434. <https://doi.org/10.1124/pr.113.008052>
24. Casadó V, Ferrada C, Bonaventura J, Gracia E, Mallol J, Canela EI, Lluís C, Cortés A et al (2009) Useful pharmacological parameters for G-protein-coupled receptor homodimers obtained from competition experiments. Agonist-antagonist binding modulation. *Biochem Pharmacol* 78(12):1456–1463. <https://doi.org/10.1016/j.bcp.2009.07.012>
25. Song Y, DiMaio F, Wang RY, Kim D, Miles C, Brunette T, Thompson J, Baker D (2013) High-resolution comparative modeling with RosettaCM. *Structure* 21(10):1735–1742. <https://doi.org/10.1016/j.str.2013.08.005>
26. Bender BJ, Cisneros A 3rd, Duran AM, Finn JA, Fu D, Lokits AD, Mueller BK, Sangha AK et al (2016) Protocols for molecular modeling with Rosetta3 and RosettaScripts. *Biochemistry* 55(34):4748–4763. <https://doi.org/10.1021/acs.biochem.6b00444>
27. Chien EY, Liu W, Zhao Q, Katritch V, Han GW, Hanson MA, Shi L, Newman AH et al (2010) Structure of the human dopamine D3 receptor in complex with a D2/D3 selective antagonist. *Science* 330(6007):1091–1095. <https://doi.org/10.1126/science.1197410>
28. Miller-Gallacher JL, Nehme R, Warne T, Edwards PC, Schertler GF, Leslie AG, Tate CG (2014) The 2.1 Å resolution structure of cyanopindolol-bound beta1-adrenoceptor identifies an intramembrane Na+ ion that stabilises the ligand-free receptor. *PLoS One* 9(3):e92727. <https://doi.org/10.1371/journal.pone.0092727>
29. Cherezov V, Rosenbaum DM, Hanson MA, Rasmussen SG, Thian FS, Kobilka TS, Choi HJ, Kuhn P et al (2007) High-resolution crystal structure of an engineered human beta2-adrenergic G protein-coupled receptor. *Science* 318(5854):1258–1265. <https://doi.org/10.1126/science.1150577>
30. Wang C, Jiang Y, Ma J, Wu H, Wacker D, Katritch V, Han GW, Liu W et al (2013) Structural basis for molecular recognition at serotonin receptors. *Science* 340(6132):610–614. <https://doi.org/10.1126/science.1232807>
31. Wacker D, Wang C, Katritch V, Han GW, Huang XP, Vardy E, McCorvy JD, Jiang Y et al (2013) Structural features for functional selectivity at serotonin receptors. *Science* 340(6132):615–619. <https://doi.org/10.1126/science.1232808>
32. Kothiwale S, Mendenhall JL, Meiler J (2015) BCL::Conf: small molecule conformational sampling using a knowledge based rotamer library. *J Cheminform* 7:47. <https://doi.org/10.1186/s13321-015-0095-1>
33. Meiler J, Baker D (2006) ROSETTALIGAND: protein-small molecule docking with full side-chain flexibility. *Proteins* 65(3):538–548. <https://doi.org/10.1002/prot.21086>
34. Lemmon G, Meiler J (2012) Rosetta Ligand docking with flexible XML protocols. *Methods Mol Biol* 819:143–155. https://doi.org/10.1007/978-1-61779-465-0_10
35. Meador-Woodruff JH, Damask SP, Wang J, Haroutunian V, Davis KL, Watson SJ (1996) Dopamine receptor mRNA expression in human striatum and neocortex. *Neuropsychopharmacology* 15:17–29
36. Pohjanoksa K, Jansson CC, Luomala K, Marjamaki A, Savola JM, Scheinin M (1997) Alpha2-adrenoceptor regulation of adenylyl cyclase in CHO cells: dependence on receptor density, receptor subtype and current activity of adenylyl cyclase. *Eur J Pharmacol* 335(1):53–63
37. Kukkonen JP, Renvaktar A, Shariatmadari R, Akerman KE (1998) Ligand- and subtype-selective coupling of human alpha-2 adrenoceptors to Ca++ elevation in Chinese hamster ovary cells. *J Pharmacol Exp Ther* 287(2):667–671
38. Schröder R, Schmidt J, Blättermann S, Peters L, Janssen N, Grundmann M, Seemann W, Kaufel D et al (2011) Applying label-free dynamic mass redistribution technology to frame signaling of G protein-coupled receptors noninvasively in living cells. *Nat Protoc* 6(11):1748–1760. <https://doi.org/10.1038/nprot.2011.386>
39. Atwood BK, Lopez J, Wager-Miller J, Mackie K, Straiker A (2011) Expression of G protein-coupled receptors and related proteins in HEK293, AtT20, BV2, and N18 cell lines as revealed by microarray analysis. *BMC Genomics* 12:14. <https://doi.org/10.1186/1471-2164-12-14>
40. Fraser CM, Arakawa S, McCombie WR, Venter JC (1989) Cloning, sequence analysis, and permanent expression of a human alpha 2-adrenergic receptor in Chinese hamster ovary cells. Evidence for independent pathways of receptor coupling to adenylate cyclase attenuation and activation. *J Biol Chem* 264(20):11754–11761

41. Jones SB, Halenda SP, Bylund DB (1991) Alpha 2-adrenergic receptor stimulation of phospholipase A2 and of adenylate cyclase in transfected Chinese hamster ovary cells is mediated by different mechanisms. *Mol Pharmacol* 39(2):239–245
42. Eason MG, Jacinto MT, Liggett SB (1994) Contribution of ligand structure to activation of alpha 2-adrenergic receptor subtype coupling to Gs. *Mol Pharmacol* 45(4):696–702
43. Eason MG, Kurose H, Holt BD, Raymond JR, Liggett SB (1992) Simultaneous coupling of alpha 2-adrenergic receptors to two G-proteins with opposing effects. Subtype-selective coupling of alpha 2C10, alpha 2C4, and alpha 2C2 adrenergic receptors to Gi and Gs. *J Biol Chem* 267(22):11579–11580
44. Eason MG, Liggett SB (1995) Identification of a Gs coupling domain in the amino terminus of the third intracellular loop of the alpha 2A-adrenergic receptor. Evidence for distinct structural determinants that confer Gs versus Gi coupling. *J Biol Chem* 270(42):24753–24760
45. Leaver-Fay A, Tyka M, Lewis SM, Lange OF, Thompson J, Jacak R, Kaufman K, Renfrew PD et al (2011) ROSETTA3: an object-oriented software suite for the simulation and design of macromolecules. *Methods Enzymol* 487:545–574
46. Ring AM, Manglik A, Kruse AC, Enos MD, Weis WI, Garcia KC, Kobilka BK (2013) Adrenaline-activated structure of beta2-adrenoceptor stabilized by an engineered nanobody. *Nature* 502(7472):575–579. <https://doi.org/10.1038/nature12572>
47. Feng Z, Hou T, Li Y (2012) Selectivity and activation of dopamine D3R from molecular dynamics. *J Mol Model* 18(12):5051–5063. <https://doi.org/10.1007/s00894-012-1509-x>
48. Owesson-White CA, Roitman MF, Sombers LA, Belle AM, Keithley RB, Peele JL, Carelli RM, Wightman RM (2012) Sources contributing to the average extracellular concentration of dopamine in the nucleus accumbens. *J Neurochem* 121(2):252–262. <https://doi.org/10.1111/j.1471-4159.2012.07677.x>
49. Rice ME, Patel JC, Cragg SJ (2011) Dopamine release in the basal ganglia. *Neuroscience* 198:112–137. <https://doi.org/10.1016/j.neuroscience.2011.08.066>
50. Hersch SM, Ciliax BJ, Gutekunst CA, Rees HD, Heilman CJ, Yung KK, Bolam JP, Ince E et al (1995) Electron microscopic analysis of D1 and D2 dopamine receptor proteins in the dorsal striatum and their synaptic relationships with motor corticostriatal afferents. *J Neurosci* 15(7 Pt 2):5222–5237. <https://doi.org/10.1016/b978-0-12-381270-4.00019-6>
51. Yung KK, Bolam JP, Smith AD, Hersch SM, Ciliax BJ, Levey AI (1995) Immunocytochemical localization of D1 and D2 dopamine receptors in the basal ganglia of the rat: light and electron microscopy. *Neuroscience* 65(3):709–730
52. Goldman-Rakic PS, Lidow MS, Smiley JF, Williams MS (1992) The anatomy of dopamine in monkey and human prefrontal cortex. *J Neural Transm Suppl* 36:163–177
53. Castelli MP, Spiga S, Perra A, Madeddu C, Mulas G, Ennas MG, Gessa GL (2016) alpha2A adrenergic receptors highly expressed in mesoprefrontal dopamine neurons. *Neuroscience* 332:130–139. <https://doi.org/10.1016/j.neuroscience.2016.06.037>
54. Lee A, Wissekerke AE, Rosin DL, Lynch KR (1998) Localization of alpha2C-adrenergic receptor immunoreactivity in catecholaminergic neurons in the rat central nervous system. *Neuroscience* 84(4):1085–1096
55. Brennan AR, Arnsten AF (2008) Neuronal mechanisms underlying attention deficit hyperactivity disorder: the influence of arousal on prefrontal cortical function. *Ann N Y Acad Sci* 1129:236–245. <https://doi.org/10.1196/annals.1417.007>
56. Herve D (2011) Identification of a specific assembly of the g protein golf as a critical and regulated module of dopamine and adenosine-activated cAMP pathways in the striatum. *Front Neuroanat* 5:48. <https://doi.org/10.3389/fnana.2011.00048>

Chapter 5. Revisiting the functional role of dopamine D4 receptor gene polymorphisms: Heteromerization-dependent gain of function of the D4.7 receptor variant

Sánchez-Soto M, Yano H, Cai NS, **Casadó-Anguera V**, Moreno E, Cortés A, Casadó V, Ferré S.

ACS Chemical Biology, submitted

Revisiting the functional role of dopamine D₄ receptor gene polymorphisms: Heteromerization-dependent gain of function of the D_{4.7} receptor variant

Marta Sánchez-Soto,[†] Hideaki Yano,[†] Ning-Sheng Cai,[†] Verónica Casadó-Anguera,[‡] Estefanía Moreno,[‡] Vicent Casadó[‡] and Sergi Ferré^{*,†}

[†]Integrative Neurobiology Section, National Institute on Drug Abuse, Intramural Research Program, National Institutes of Health, Baltimore, Maryland 21230, United States

[‡]Department of Biochemistry and Molecular Biomedicine, Faculty of Biology, Institute of Biomedicine of the University of Barcelona, University of Barcelona, and Centro de Investigación Biomédica en Red sobre Enfermedades Neurodegenerativas (CIBERNED), Barcelona 08028, Spain

Corresponding author

*E-mail: sferre@intra.nida.nih.gov

ABSTRACT: The two most common polymorphisms of the human *DRD4* gene encode a dopamine D₄ receptor (D4R) with four or seven repeats of a proline-rich sequence of 16 amino acids (D4.4R or D4.7R). Although the seven-repeat polymorphism has been repeatedly associated with attention deficit hyperactivity disorder and substance use disorders, the differential functional properties between D4.4R and D4.7R remained enigmatic until recent electrophysiological and optogenetic-microdialysis experiments indicated a gain of function of D4.7R. Since no clear differences in the biochemical properties of individual D4.4R and D4.7R have been reported, it was previously suggested that those differences emerge upon heteromerization with dopamine D₂ receptor (D2R), which co-localizes with D4R in the brain. However, contrary to a gain of function, experiments in mammalian transfected cells suggested that heteromerization with D2R results in lower MAPK signaling by D4.7R as compared to D4.4R. In the present study, we readdressed the question of functional differences of D4.4R and D4.7R forming homomers or heteromers with the short isoform of D2R (D2SR), using a functional bioluminescence resonance energy transfer (BRET) assay that allows the measurement of ligand-induced changes in the interaction between G protein coupled receptors (GPCRs) forming homomers or heteromers with their cognate G protein. Significant functional and pharmacological differences between D4.4R and D4.7R were only evident upon heteromerization with the short isoform of D2R (D2SR). The most dramatic finding was a significant increase and decrease in the constitutive activity of D2SR upon heteromerization with D4.7R and D4.4R, respectively, providing the first clear mechanism for a functional difference between both products of polymorphic variants and for a gain of function of the D4.7R.

The human *DRD4* gene displays a high number of polymorphisms in its coding sequence. The most extensive polymorphism is found in exon 3, a region that encodes the third intracellular loop of the receptor.¹⁻³ This polymorphism consists of a variable number of tandem repeats (VNTR) in which a 48-base pair sequence exists as 2- to 11-fold repeats. The two most common polymorphisms contain four and seven TRs (with allelic frequencies of about 60% and 20%, respectively)² and encode a dopamine D₄ receptor (D4R) with four and seven repeats of a proline-rich sequence of 16 amino acids (D4.4R and D4.7R).¹⁻³ *DRD4* polymorphisms have been suggested to associate with numerous behavioral individual differences and neuropsychiatric disorders. The most consistent associations are the link between the gene encoding D4.7R and attention deficit hyperactivity disorder (ADHD)^{1,4-6} or substance use disorders (SUDs).⁷

The functional significance of the products of *DRD4* polymorphisms remained enigmatic until recent results from electrophysiological experiments in mouse cortical slices with viral infection of human D4.4R and D4.7R⁸ and immuno-histochemical and optogenetic-microdialysis experiments in a D4.7 knock-in mouse, expressing a humanized D4R with the long intracellular domain of the human D4.7R.⁹ D4.7 or the humanized D4R demonstrated a pronounced *gain of function* when respectively compared with D4.4 or the wild-type (WT) mouse D4R,^{8,9} which expresses a D4R with a shorter third intracellular loop comparable to the human D4.2 receptor.¹⁰ In the brain, D4R is expressed in the prefrontal cortex, particularly in the pyramidal glutamatergic neuron, where D4R exerts a significant inhibitory control at the somatodendritic as well as at its striatal projections.⁸⁻¹⁰ Electrophysiological recording in cortical slices from *DRD4* knockout mice, showed an increased ability of a D4R agonist to suppress glutamatergic excitatory network bursts upon viral infection with human D4.7 as compared with D4.4 receptor cDNA.⁸ D4.7 knock-in mouse showed a blunting of methamphetamine-induced cortical activation and optogenetically- and methamphetamine-induced corticostriatal glutamate release.⁹

The question now remains about the biochemical mechanism responsible for the gain of function of D4.7R. In fact, initial and still canonically cited studies seemed to indicate that the D4.7R signals with less efficiency than D4.4R.¹¹ Nevertheless, in a recent study using functional bioluminescence resonance energy transfer (BRET) experiments with biosensors fused to the different G α i/o subtypes and to the G γ subunit, we could not find significant differences in the ability of D4.4R or D4.7R to promote dopamine-induced G protein activation.¹² It has also been suggested that the potential functional and pharmacological differences between D4.4R and D4.7R signaling become evident upon heteromerization with the dopamine D₂ receptor (D2R). In fact, D4R and the short isoform of the D2R (D2SR) are co-localized in striatal glutamatergic terminals and found to contribute to the inhibitory control of glutamate release exerted by dopamine and dopamine receptor agonists.^{10,13} Two separate studies, based on BRET and co-immunoprecipitation techniques in transfected mammalian cells suggested that D4.7R establishes weaker intermolecular and functional interactions with D2R (both isoforms, D2LR and D2SR) than D4.4R.^{10,14} At the functional level, a significantly stronger MAPK activation could only be observed upon simultaneous activation of D2R and D4.4R,^{10,14} which seems opposite to what it would be expected from a gain of function of D4.7R over D4.4R. In the present study, we readdressed the question of functional differences of D4.4R and D4.7R forming homomers or heteromers with D2SR, using a functional BRET assay¹⁵ that allows the measurement of ligand-

induced changes in the interaction between G protein coupled receptors (GPCRs) forming homomers or heteromers with their cognate G protein.

RESULTS AND DISCUSSION

Ligand-induced changes in the interaction between Gi protein and D4.4R, D4.7R or D2SR homomers. In complemented donor acceptor resonance energy transfer (CODA-RET) assay, two complementary halves of RLuc (nRLuc and cRLuc) are separately fused to two different receptor molecules putatively able to oligomerize and a YFP is fused to a G protein subunit, in this case G α i1.¹⁵ Ligand-induced changes in CODA-RET measurements imply, first, a successful complementation of RLuc and, therefore, oligomerization of the corresponding GPCR units. Second, although CODA-RET does not provide an estimate of the degree of oligomerization (affinity, stoichiometry), it represents the reading of a specific signaling through the GPCR homo- or heterodimer.^{15,16} Concentration-response curves of ligand-induced changes in BRET were then determined with CODA-RET experiments. The ligands used were dopamine and the clinically used D₂-like receptor agonists pramipexole and ropinirole. For each group of experiments with the same transfected cDNA constructs, EC₅₀ and E_{max} values were calculated from concentration-response curves of BRET values expressed as the percentage of the maximal effect of dopamine, considering dopamine as full agonist. Functional D4.4R-D4.4R and D4.7R-D4.7R homodimers could be demonstrated with CODA-RET, and the pattern of response to the different ligands was very similar, with similar EC₅₀ values and E_{max} values (Figure 1 and Table 1). Pramipexole and ropinirole were partial agonists as compared to dopamine and the efficacy of pramipexole was mostly undetectable for the D4.4R-D4.4R homomer (Figure 1 and Table 1). On the other hand, pramipexole behaved as a full agonist on the D2R-D2R homodimer, while ropinirole was a partial agonist with very low efficacy. With dopamine, the qualitative results were the same as those obtained in a previous study.¹² In both assays, dopamine showed a very similar potency for D4.4R and D4.7R and a significantly lower potency for D2SR, which would agree with the general hypothesis that homodimers represent a main functional population of GPCR.¹⁷

Ligand-induced changes in the interaction between Gi protein and D4.4R-D2S or D4.7R-D2SR heteromers. Next, we addressed the question about D4R-D2S heteromerization. CODA-RET experiments demonstrated that both D4.4R-nRLuc and D4.7R-nRLuc can form functional heteromers with D2SR-cRLuc and, importantly, with significantly different pharmacological properties (Figures 2A and 2B and Table 2). First, compared with D2SR-D2SR homomers, dopamine showed a small but significant increase in potency for D4.7R-D2SR, but not for D4.4R-D2SR heteromers (Figures 2A and 2B and Table 2). Second, pramipexole showed full efficacy for D4.7R-D2SR heteromers and significantly higher efficacy than dopamine for the D4.4R-D2SR heteromers. On the other hand, ropinirole was a partial agonist at D4.7R-D2SR heteromers and it lost its efficacy at D4.4R-D2SR heteromers (Figures 2A and 2B). To our knowledge, these results provide the first clear demonstration of pharmacodynamic differences of ligands that depend on the products of the most common *DRD4* polymorphic variants, which are disclosed by heteromerization with D2SR.

In addition, a very differential response of D4.4R-D2SR and D4.7R-D2SR heteromers to raclopride (D₂-like receptor antagonist with very low affinity for D4R) and the selective D4R

antagonist L745-870 was observed. Raclopride, at a concentration (100 nM) that completely antagonized dopamine-mediated G protein activation by D2SR-D2SR homomers and was completely inefficient at D4.7R-D4.7R homomers (Figures 3A and 3B), completely antagonized the effect of dopamine at D4.4R-D2SR and D4.7R-D2SR heteromers (Figures 3C and 3D). On the other hand, L745-870, at a concentration (1 μ M) that completely antagonized dopamine-mediated G protein activation by D4.7R-D4.7R homomers and was mostly inefficient at D2SR-D2SR homomers (Figures 3A and 3B), produced a significant but partial counteraction of the effect of dopamine at D4.4R-D2SR, but a small but consistent increase at D4.7R-D2SR (Figures 3C and 3D). This increase could nevertheless be artefactual, since basal levels before normalization were slightly lower for D4.7R-D2SR heteromers in the presence of L745-870. We therefore investigated the possibility that L745-870 could selectively act as an inverse agonist on the D4.7R-D2SR heteromer, indicating the existence of a specific constitutive activity of the D4.7R-D2SR heteromer. In fact, L745-870 induced a significant concentration-dependent decrease in BRET values in CODA-RET experiments in cells transfected with D4.7R-nRLuc and D2SR-cRLuc, but not in cells transfected with D4.4R-nRLuc and D2SR-cRLuc, D4.4R-nRLuc and D4.4R-cRLuc or D4.7R-nRLuc and D4.7R-cRLuc (Figures 4A and 4B). However, concentrations of L745-870 higher than 1 μ M were necessary to clearly disclose the constitutive activity of the D4.7R-D2SR heteromer (Figure 4A). Since at these concentrations L745-870 also binds to D2R,¹⁸ the results suggests that D2SR provides the constitutive activity in the D4.7R-D2S heteromer. In fact, the effect of L745-870 was counteracted by raclopride, which by itself did not show any inverse agonistic activity (Figure 5A), as previously described in mammalian cell lines selectively expressing D2SR. Finally, and also at micromolar concentrations, L745-870 behaved as an inverse agonist in the D2SR-D2SR homomer, although with less efficacy than in the D4.7R-D2SR heteromer (Figure 5B). As shown in Figure 6, the maximal efficacy of L745-870 to produce inverse agonism in D2SR-D2SR homomers was significantly increased in the D4.7R-D2SR heteromers and significantly decreased in the D4.4R-D2SR (Figure 6).

In summary, the experiments with antagonists provide an additional demonstration that both D4.4R and D4.7R form functional heteromers with D2SR with significantly different functional properties. D2SR determines dopamine-mediated Gi-dependent signaling in both heteromers. Within the D4.4R-D2SR heteromer, D4.4R participates in the dopamine-mediated Gi-dependent activation of D4.4R-D2SR and decreases the constitutive activity of D2SR. Within the D4.7R-D2SR heteromer, D4.7R confers an increase in the potency of dopamine and a significant increase in the constitutive activity of the D2SR.

CONCLUSIONS

In the present study, using functional BRET assays in mammalian transfected cells, we could demonstrate significant functional and pharmacological differences between D4.4R and D4.7R only evident upon heteromerization with D2SR, providing a plausible mechanism for the gain of function of D4.7R versus D4.4R recently demonstrated *in vitro*, in mouse cortical slices with viral infection of human D4.4R and D4.7R⁸, and *in vivo*, in optogenetic-microdialysis experiments in the D4.7R knock-in mouse⁹. The most dramatic finding was the significant increase in the constitutive activity that D4.7R confers to the D2SR upon heteromerization. To our knowledge, this is the first reported example of changes in the constitutive activity of a GPCR upon

heteromerization, which adds to the list of new properties associated with GPCR oligomerization.¹⁷ More significant is the fact that this new property was specifically associated to the product of a *DRD4* polymorphism, conferring a gain of function to the D4.7R *versus* the D4.4R variant. Previous studies already suggested that functional and pharmacological differences between D4.4R and D4.7R could depend on heteromerization with D2R.^{10,14} However, those studies found a stronger agonist-mediated MAPK signaling in cells co-transfected with D4.4R and D2R versus D4.7R and D2R, suggesting the opposite, a loss of function of D4.7R upon heteromerization with D2R and a reduced ability of D4.7R to heteromerize with D2R.^{10,14} Nevertheless, the results of those studies were just correlative and did not unequivocally establish that the interactions at the MAPK signaling depended on receptor heteromerization. On the other hand, in the present study, with the use of the CODA-RET technique, we could demonstrate the existence of functional D4.7R-D2SR heteromers in transfected cells and also dissect the pharmacological profile of D4.4R and D4.7R homodimers and heteromers. The fact that a gain of function of D4.7R *versus* D4.4R could only be demonstrated upon heteromerization with D2SR, strongly suggests that D4R-D2R heteromers represent a significant receptor population that modulates the function of cortico-striatal glutamatergic neurons.

Another significant finding, with possible translational implications, was the differential profile of the clinically used dopamine agonists pramipexole and ropinirole, with their more pronounced relative effect in the D4.4R-D2SR and D4.7R-D2SR, respectively. We have in fact recently suggested that the therapeutic effect of both compounds in Restless Legs Syndrome is most probably related to their ability to activate D4R and D2SR localized in cortico-striatal glutamatergic terminals.¹³ That being the case, we should expect different clinical efficacies of pramipexole and ropinirole depending on the predominant expression of the products of *DRD4* polymorphisms.

METHODS

DNA constructs and transfection. Sequences encoding amino acid residues 1-229 and 230-311 of RLuc protein were subcloned in the pcDNA3.1 vector to obtain complementary hemitruncated RLuc proteins (nRLuc and cRLuc, respectively). D4.4R and D4.7R human cDNAs cloned into pcDNA3.1 were amplified without their stop codons using sense and antisense primers harboring unique *NheI* and *XhoI* restriction sites. The amplified fragment corresponding to D4.4R or D4.7R was subcloned to be in-frame with restriction sites of pcDNA3.1-nRLuc and pcDNA3.1-cRLuc to yield plasmids that express D4.4R or D4.7R fused to the corresponding hemitruncated RLuc on the C-terminal end of the receptor (D4.4R-nRLuc, D4.4R-cRLuc, D4.7R-nRLuc and D4.7R-cRLuc). The following human G protein constructs were used: G α 1-YFP (with the YFP derivative mVenus inserted at position 91), untagged G β 1, and untagged G γ 2. All the constructs were confirmed by sequencing analysis. Plasmid cDNAs were transfected into human embryonic kidney (HEK-293T) cells using polyethylenimine (PEI, Sigma-Aldrich, St. Louis, MO) with a 1 to 2 ratio in 10-cm dishes. Cells were maintained in culture with Dulbecco's modified Eagle's medium supplemented with 10% fetal bovine serum. The amount and proportion of transfected receptor-nRLuc, receptor-cRLuc, G α 1-YFP, G β 1 and G γ 2 were optimized by testing various proportions of plasmids encoding the different sensors. Experiments were performed

~48 hours post-transfection. D2SR-nRLuc, D2SR-cRLuc and Gai1-YFP were kindly provided by J. A. Javitch (Columbia University, New York).

Functional Bioluminescence Resonance Energy Transfer (BRET) assays. Cells were harvested, washed and resuspended in phosphate-buffered saline (PBS). Approximately 200,000 cells/well were distributed in 96-well plates, and 5 μ M coelenterazine H (substrate for BRET1) was added to each well. One minute after addition of coelenterazine, different concentrations of dopamine, pramipexole or ropinirole (or L745-870, when analyzing its possible inverse agonism) were added to each well. In the experiments testing for the effect of antagonists of dopamine, L745-870 or raclopride were added 12 min before the addition of dopamine. Fluorescence of the acceptor was quantified (excitation at 500 nm and emission at 540 nm for 1 s recording) in Mithras LB940 (Berthold technologies, Bad Wildbad Germany) to confirm the constant expression level across experiments. In parallel, BRET signal from the same batch of cells was determined as the ratio of the light emitted by YFP (mVenus variant; 510-540 nm) over RLuc (485 nm). Results were calculated for the BRET change (BRET ratio for the corresponding drug minus BRET ratio in the absence of the drug) 10 minutes after addition of the agonists (or L745-870, when indicated). Data manipulations and statistical analyses (described in the Table legends) were performed with Prism 4 (GraphPad Software).

ACKNOWLEDGEMENTS

Work supported by the intramural funds of the National Institute on Drug Abuse and a grant from the Spanish “Ministerio de Economía y Competitividad” and the European Regional Development Funds of the European Union (SAF2014-54840-R).

REFERENCES

1. LaHoste, G. J., Swanson, J. M., Wigal, S. B., Glabe, C., Wigal, T., King, N., and Kennedy, J. L. (1996) Dopamine D4 receptor gene polymorphism is associated with attention deficit hyperactivity disorder. *Mol. Psychiatry* **1**, 121-124.
2. Chang, F. M., Kidd, J. R., Livak, K. J., Pakstis, A. J., and Kidd, K. K. (1996) The world-wide distribution of allele frequencies at the human dopamine D4 receptor locus. *Hum. Genet.* **98**, 91-101.
3. Wang, E., Ding, Y. C., Flodman, P., Kidd, J. R., Kidd, K. K., Grady, D. L., Ryder, O. A., and Spence, M.A. (2004) The genetic architecture of selection at the human dopamine receptor D4 (DRD4) gene locus. *Am. J. Hum. Genet.* **74**, 931-944.
4. Faraone, S. V., Perlis, R. H., Doyle, A. E., Smoller, J. W., Goralnick, J. J., Holmgren, M. A., and Sklar, P. (2005) Molecular genetics of attention-deficit/hyperactivity disorder. *Biol. Psychiatry* **57**, 1313-1323.
5. Li, D., Sham, P. C., Owen, M. J., and He, L. (2006) Meta-analysis shows significant association between dopamine system genes and attention deficit hyperactivity disorder (ADHD). *Hum. Mol. Genet.* **15**, 2276-2284.
6. Gizer, I.R., Ficks, C., and Waldman, I. D. (2009) Candidate gene studies of ADHD: a meta-analytic review. *Hum. Genet.* **126**, 51-90.
7. Belcher, A. M., Volkow, N. D., Moeller, F. G., and Ferré, S. (2014) Personality traits and vulnerability or resilience to substance use disorders. *Trends Cogn. Sci.* **18**, 211-217.

8. Zhong, P., Liu, W., and Yan, Z. (2016) Aberrant regulation of synchronous network activity by the attention-deficit/hyperactivity disorder-associated human dopamine D4 receptor variant D4.7 in the prefrontal cortex. *J. Physiol.* 594, 135-147.
9. Bonaventura, J., Quiroz, C., Cai, N. S., Rubinstein, M., Tanda, G., and Ferré, S. (2017) Key role of the dopamine D(4) receptor in the modulation of corticostriatal glutamatergic neurotransmission. *Sci. Adv.* 3, e1601631.
10. González, S., Rangel-Barajas, C., Peper, M., Lorenzo, R., Moreno, E., Ciruela, F., Borycz, J., Ortiz, J., Lluís, C., Franco, R., McCormick, P. J., Volkow, N. D., Rubinstein, M., Floran, B., and Ferré, S. (2012) Dopamine D4 receptor, but not the ADHD-associated D4.7 variant, forms functional heteromers with the dopamine D2S receptor in the brain. *Mol. Psychiatry* 17, 650-662.
11. Asghari, V., Sanyal, S., Buchwaldt, S., Paterson, A., Jovanovic, V., and Van Tol H. H. (1995) Modulation of intracellular cyclic AMP levels by different human dopamine D4 receptor variants. *J. Neurochem.* 65, 1157-1165.
12. Sánchez-Soto, M., Bonifazi, A., Cai, N.-S., Ellenberger, M. P., Newman, A. H., Ferré, S., and Yano, H. (2016) Evidence for Noncanonical Neurotransmitter Activation: Norepinephrine as a dopamine D2-like receptor agonist. *Mol. Pharmacol.* 89, 457-466.
13. Yepes, G., Guitart, X., Rea, W., Richard, P. A., Earley, C. J., Quiroz, C., and Ferré, S. (2017) Targeting hypersensitive corticostriatal terminals in Restless Legs Syndrome. *Ann. Neurol.* 82, 951-960.
14. Borroto-Escuela, D. O., Van Craenenbroeck, K., Romero-Fernandez, W., Guidolin, D., Woods, A. S., Rivera, A., Haegeman, G., Agnati, L. F., Tarakanov, A. O., and Fuxe, K. (2011) Dopamine D2 and D4 receptor heteromerization and its allosteric receptor-receptor interactions. *Biochem. Biophys. Res. Commun.* 404, 928-934.
15. Urizar, E., Yano, H., Kolster, R., Galés, C., Lambert, N., and Javitch, J. A. (2011) CODA-RET reveals functional selectivity as a result of GPCR heteromerization. *Nat. Chem. Biol.* 7, 624-630.
16. Guitart, X., Navarro, G., Moreno, E., Yano, H., Cai, N. S., Sánchez-Soto, M., Kumar-Barodia, S., Naidu, Y. T., Mallo, J., Cortés, A., Lluís, C., Canela, E. I., Casadó, V., McCormick, P. J., and Ferré, S. (2014) Functional selectivity of allosteric interactions within G protein-coupled receptor oligomers: the dopamine D1-D3 receptor heterotetramer. *Mol. Pharmacol.* 86, 417-429.
17. Ferré, S., Casadó, V., Devi, L. A., Filizola, M., Jockers, R., Lohse, M. J., Milligan, G., Pin, J.-P., and Guitart, X. (2014) G protein-coupled receptor oligomerization revisited: functional and pharmacological perspectives. *Pharmacol. Rev.* 66, 413-434.
18. Patel, S., Freedman, S., Chapman, K. L., Emms, F., Fletcher, A. E., Knowles, M., Marwood, R., Mcallister, G., Myers, J., Curtis, N., Kulagowski, J. J., Leeson, P. D., Ridgill, M., Graham, M., Matheson, S., Rathbone, D., Watt, A. P., Bristow, L. J., Rupniak, N. M., Baskin, E., Lynch, J. J., and Ragan, C. I. (1997) Biological profile of L-745,870, a selective antagonist with high affinity for the dopamine D4 receptor. *J. Pharmacol. Exp. Ther.* 283, 636-647.
19. Nilsson, C. L., Ekman, A., Hellstrand, M., and Eriksson, E. (1996) Inverse agonism at dopamine D2 receptors. Haloperidol-induced prolactin release from GH4C1 cells transfected with the human D2 receptor is antagonized by R(-)-n-propylnorapomorphine, raclopride, and phenoxybenzamine. *Neuropsychopharmacology* 15, 53-61.

FIGURES

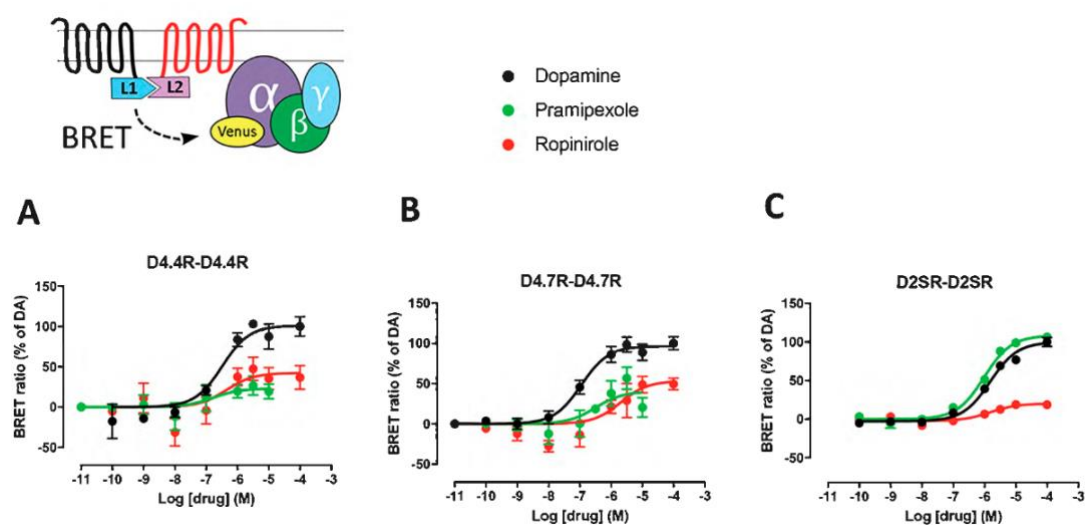


Figure 1. Ligand-induced changes in the interaction between Gi protein and D4.4R-D4.4R, D4.7R-D4.7R or D2SR-D2SR homomers. On top, scheme of the constructs used for the CODA-RET experiments, where two complementary halves of RLuc (nRLuc and cRLuc, L1 and L2, respectively) are fused to the corresponding receptors and YFP (mVenus variant) is fused to the Gαi1 subunit. (A-C) Concentration-response experiments of changes in BRET ratio induced by dopamine, pramipexole or ropinirole, determined by changes in the interaction of D4.4R-D4.4R homomers (A), D4.7R-D4.7R homomers (B) or D2SR-D2SR homomers (C) with Gαi1 protein. HEK-293T cells were transiently transfected with D4.4R-nRLuc and D4.4R-cRLuc (A), D4.7R-nRLuc and D4.7R-cRLuc (B) or D2SR-nRLuc and D2SR-cRLuc (C), the G protein subunits Gαi1-YFP and unfused β1 and γ2. Cells were treated with coelenterazine H followed by increasing concentrations of the ligand. After 10 minutes, BRET between the corresponding complemented RLuc receptor and Gαi1-YFP was measured as described in the Methods. BRET values in the absence of ligands were subtracted from the BRET values for each ligand concentration. BRET values expressed as the percentage of the maximal effect of dopamine (%of DA), considering dopamine as full agonist. Data were fit by nonlinear regression to a sigmoidal concentration-response curve against the agonist concentration and are shown as a percentage of the maximal dopamine effect. Data represent the mean ± S.E.M. of 6-9 experiments performed in triplicate (see Table 1 for EC₅₀ and E_{max} values and statistical comparisons).

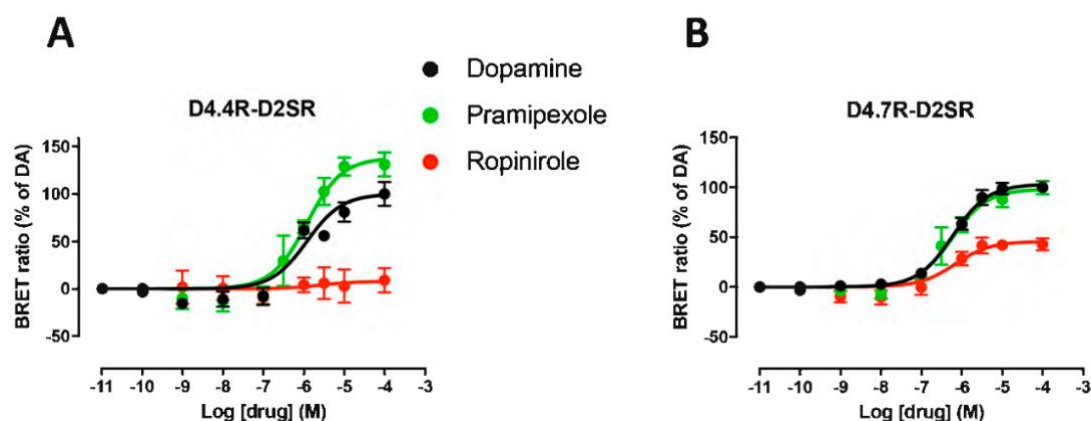


Figure 2. Ligand-induced changes in the interaction between Gi protein and D4.4R-D2SR or D4.7R-D2SR heteromers. (A-B) Concentration-response experiments of changes in BRET ratio induced by dopamine, pramipexole or ropinirole determined by changes in the interaction of D4.4R-D2SR or D4.7R-D2SR heteromers with G α i1 protein. HEK-293T cells were transiently transfected with D4.4R-nRLuc and D2SR-cRLuc (A) or D4.7R-nRLuc and D2SR-cRLuc (B), the G protein subunits G α i1-YFP and unfused β 1 and γ 2. Cells were treated with coelenterazine H followed by increasing concentrations of the ligand. After 10 minutes, BRET between the corresponding complemented RLuc receptor and G α i1-YFP was measured as described in the Methods. BRET values in the absence of ligands were subtracted from the BRET values for each ligand concentration. BRET values expressed as the percentage of the maximal effect of dopamine (%of DA), considering dopamine as full agonist. Data were fit by nonlinear regression to a sigmoidal concentration-response curve against the agonist concentration and are shown as a percentage of the maximal dopamine effect. Data represent the mean \pm S.E.M. of 5-10 experiments performed in triplicate (see Table 2 for EC₅₀ and E_{max} values and statistical comparisons).

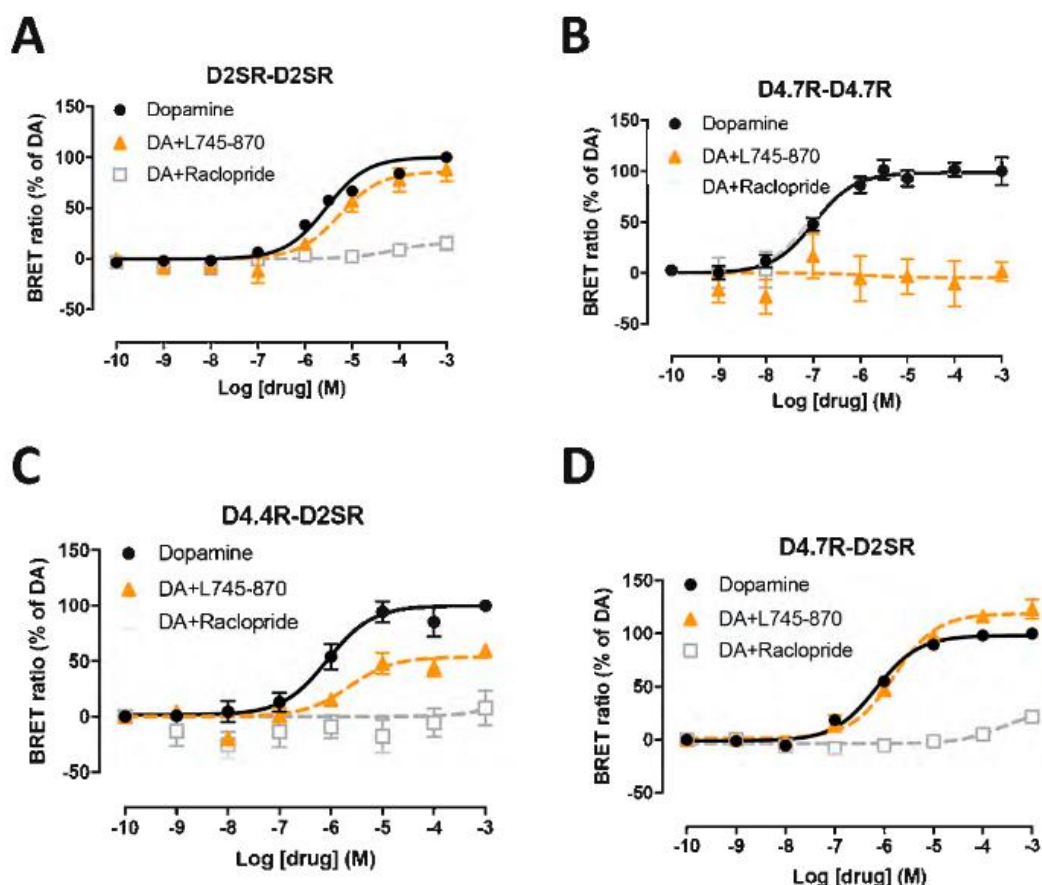


Figure 3. Effect of L745-870 and raclopride on dopamine-induced changes in the interaction between Gi protein and D2SR-D2SR or D4.7R-D4.7R homomers and between Gi protein and D4.4R-D2SR or D4.7R-D2SR heteromers. (A-D) Concentration-response experiments of dopamine-induced changes in BRET ratio that measure changes in the interaction of D2SR-D2SR homomers (A), D4.7R-D4.7R homomers (B), D4.4R-D2SR heteromers (C) or D4.7R-D2SR heteromers (D) with G α i1 protein. HEK-293T cells were transiently transfected with D2SR-nRLuc and D2SR-cRLuc (A), D4.7R-nRLuc and D4.7R-cRLuc (B), D4.4R-nRLuc and D2SR-cRLuc (C) or D4.7R-nRLuc and D2SR-cRLuc (D), the G protein subunits G α i1-YFP and unfused β 1 and γ 2. Cells were treated with coelenterazine H followed by increasing concentrations of dopamine alone or with the presence of the selective D4R antagonist L745-870 or raclopride, a D₂-like receptor antagonist with very low affinity for D4R. After 10 minutes, BRET between the corresponding complemented RLuc receptor and G α i1-YFP was measured as described in the Methods. BRET values in the absence of ligands were subtracted from the BRET values for each ligand concentration. BRET values expressed as the percentage of the maximal effect of dopamine (% of DA), considering dopamine as full agonist. Data were fit by nonlinear regression to a sigmoidal concentration-response curve against the agonist concentration and are shown as a percentage of the maximal dopamine effect. Data represent the mean \pm S.E.M. of 5-13 experiments performed in triplicate.

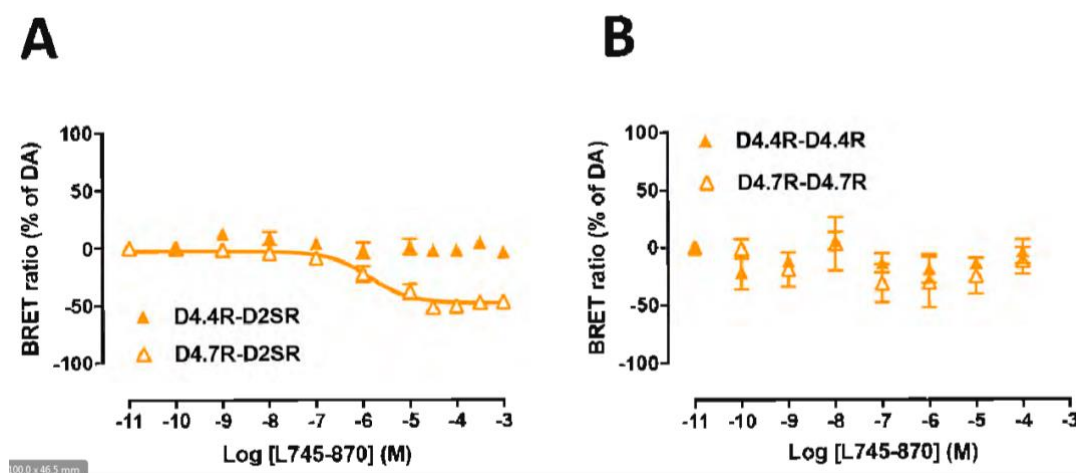


Figure 4. Inverse agonism of L745-870 on D4.7R-D2SR heteromers. (A-B) Concentration-response experiments of the selective D4R antagonist L745-870-induced changes in BRET ratio that measure changes in the interactions of D4.4R-D2SR or D4.7R-D2SR heteromers (A) and D2SR-D2SR or D4.7R-D4.7R homomers (B) with the G α i1 protein. HEK-293T cells were transiently transfected with D4.4R-RLuc or D4.7R-RLuc (A), D4.4R-nRLuc and D4.4R-cRLuc or D4.7R-nRLuc and D4.7R-cRLuc (B), the G protein subunits G α i1-YFP and unfused β 1 and γ 2. Cells were treated with coelenterazine H followed by increasing concentrations of L745-870. After 10 minutes, BRET between the corresponding RLuc- or complemented RLuc receptor and G α i1-YFP was measured as described in the Methods. BRET values in the absence of ligands were subtracted from the BRET values for each ligand concentration. BRET values expressed as the percentage of the maximal effect of dopamine (%of DA), considering dopamine as full agonist. Data were fit by nonlinear regression to a sigmoidal concentration-response curve against the agonist concentration and are shown as a percentage of the maximal dopamine effect. Data represent the mean \pm S.E.M. of 4-8 experiments performed in triplicate.

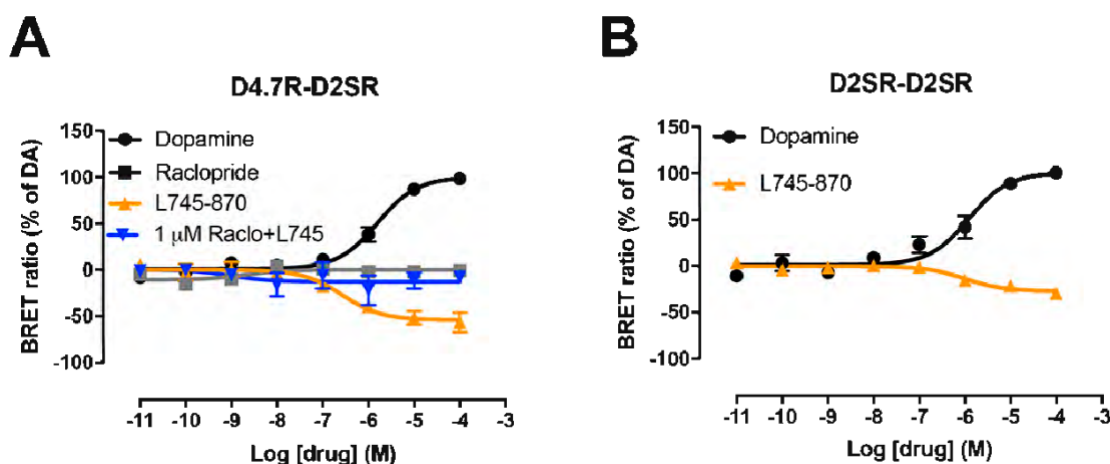


Figure 5. Constitutive activity of D2SR-D2SR homomers and D4.7R-D2SR heteromers. (A-B) Concentration-response experiments of changes in BRET ratio induced by dopamine, the selective D4R antagonist L745-870 or raclopride which measure changes in the interactions of D4.7R-D2SR heteromers (A) or D2SR-D2SR homomers (B) with the $G\alpha i1$ protein. HEK-293T cells were transiently transfected with or D4.7R-nRLuc and D2SR-cRLuc (A) or D2SR-nRLuc and D2SR-cRLuc (B), the G protein subunits $G\alpha i1$ -YFP and unfused $\beta 1$ and $\gamma 2$. Cells were treated with coelenterazine H followed by increasing concentrations of L745-870. After 10 minutes, BRET between the corresponding RLuc- or complemented RLuc receptor and $G\alpha i1$ -YFP was measured as described in the Methods. BRET values in the absence of ligands were subtracted from the BRET values for each ligand concentration. BRET values expressed as the percentage of the maximal effect of dopamine (%of DA), considering dopamine as full agonist. Data were fit by nonlinear regression to a sigmoidal concentration-response curve against the agonist concentration and are shown as a percentage of the maximal dopamine effect. Data represent the mean \pm S.E.M. of 4-8 experiments performed in triplicate.

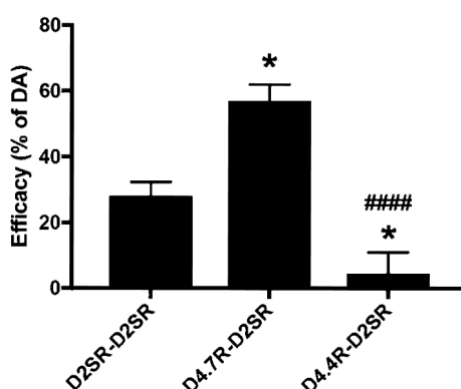


Figure 6. Differences between the constitutive activity of D2SR-D2SR homomers, D4.7R-D2SR heteromers and D4.4R-D2SR heteromers. Statistical comparisons of the maximal efficacy of the inverse agonistic effect of L745-870 obtained in cells expressing D2SR-D2SR homomers (results from Figure 5B), D4.7R-D2SR heteromers (results from Figure 5A) and D4.4R-D2SR heteromers (results from Figure 4A). One way ANOVA followed by Tukey's multiple comparison test: * and **: $p < 0.05$ and $p < 0.01$ as compared to D2SR-D2SR; ####: $p < 0.0001$ as compared to D4.7R-D2SR.

TABLES

Table 1. Ligand-induced changes in the interaction between Gi protein and D4.4R-D4.4R, D4.7R-D4.7R or D2SR-D2SR homomers

		EC ₅₀ (nM)	E _{max} (%)
D4.4R-D4.4R	Dopamine	240 ± 60 **	100 ± 10
	Pramipexole	NA	NA
	Ropinirole	400 ± 200 **	53 ± 4 #
D4.7R-D4.7R	Dopamine	130 ± 30 **	100 ± 5
	Pramipexole	500 ± 350	65 ± 5 ##
	Ropinirole	1300 ± 300	73 ± 8
D2SR-D2SR	Dopamine	1600 ± 200	100 ± 4
	Pramipexole	1200 ± 300	109 ± 2
	Ropinirole	2200 ± 500	28 ± 3 ###

EC₅₀ and E_{max} (% of dopamine) values (mean ± SEM) from concentration-response experiments of changes in BRET ratio induced by dopamine, pramipexole or ropinirole mediated by D4.4R-D4.4R, D4.7R-D4.7R or D2SR-D2SR homomers in HEK-293T cells transiently expressing D4.4R-nRLuc and D4.4R-cRLuc, D4.7R-nRLuc and D4.7R-cRLuc or D2SR-nRLuc and D2SR-cRLuc, the G protein subunits Gαi1-YFP and unfused β1 and γ2. Statistical differences between the EC₅₀ value of each ligand for D4.4R-D4.4R or D4.7R-D4.7R homomers as compared to the EC₅₀ value of the same ligand for D2SR-D2SR were calculated by one-way ANOVA followed by Dunnett post-hoc test; **: p<0.01, respectively. Statistical differences between the E_{max} value of each ligand for each receptor homomer as compared to the E_{max} values of dopamine for the same receptor homomer were calculated by one-way ANOVA followed by Dunnett post-hoc test; #, ## and ###: p<0.05, p<0.01 and p<0.001 respectively.

Table 2: Ligand-induced changes in the interaction between Gi protein and D4.4R-D2SR or D4.7R-D2SR heteromers

		EC ₅₀ (nM)	E _{max} (%)
D4.4R-D2SR	Dopamine	1000 ± 200	100 ± 6
	Pramipexole	1100 ± 200	125 ± 5 #
	Ropinirole	NA	NA
D4.7R-D2SR	Dopamine	700 ± 100 *	100 ± 4
	Pramipexole	625 ± 196	94 ± 5
	Ropinirole	600 ± 150 **	49 ± 5 ##

EC₅₀ and E_{max} (% of dopamine) values (mean ± SEM) from concentration-response experiments of changes in BRET ratio induced by dopamine, pramipexole or ropinirole mediated by D4.4R-D2SR or D4.7R-D2SR heteromers in HEK-293T cells transiently expressing D4.4R-nRLuc and D2SR-cRLuc or D4.7R-nRLuc and D2SR-cRLuc, the G protein subunits Gαi1-YFP and unfused β1 and γ2. Statistical differences between the EC₅₀ value of each ligand for D4.4R-D2SR or D4.7R-D2SR heteromers as compared to the EC₅₀ value of the same ligand for the D2SR-D2SR homomer (Table 1) were calculated by one-way ANOVA followed by Dunnett post-hoc test; * and **: p<0.05 and p<0.01, respectively. Statistical differences between the E_{max} value of each ligand for each receptor heteromer as compared to the E_{max} values of dopamine for the same receptor heteromer were calculated by one-way ANOVA followed by Dunnett post-hoc test; # and ##: p<0.05 and p<0.01, respectively.

Chapter 6. Functional differences between dopamine D4.4 and D4.7 receptor variants within the dopamine D4-adrenergic α 2A receptor heteromer in the brain

Verònica Casadó-Anguera, Estefanía Moreno, Patricia Homar, Marta Sánchez-Soto, Jordi Bonaventura, Josefa Mallol, Sergi Ferré, Antoni Cortés, Enric I. Canela and Vicent Casadó

Neuropsychopharmacology, manuscript in preparation

Functional differences between dopamine D_{4.4} and D_{4.7} receptor variants within the dopamine D₄-adrenergic α_{2A} receptor heteromer in the brain

Verònica Casadó-Anguera^{1,2}, Estefanía Moreno^{1,2}, Patricia Homar^{1,2}, Marta Sánchez-Soto³, Ning Sheng Cai³, Jordi Bonaventura⁴, Josefa Mallol^{1,2}, Sergi Ferré³, Antoni Cortés^{1,2}, Enric I. Canela^{1,2} and Vicent Casadó^{1,2*}

¹ Centro de Investigación Biomédica en Red sobre Enfermedades Neurodegenerativas (CIBERNED), Spain

² Institute of Biomedicine of the University of Barcelona (IBUB), and Department of Biochemistry and Molecular Biomedicine, Faculty of Biology, University of Barcelona, Av. Diagonal 643, 08028 Barcelona

³ Integrative Neurobiology Section, National Institute on Drug Abuse, Intramural Research Program, National Institutes of Health, Baltimore, MD 21224, USA.

⁴ Biobehavioral Imaging and Molecular Neuropsychopharmacology Unit, National Institute on Drug Abuse, Intramural Research Program, Baltimore, MD 21224, USA.

* **Corresponding author:** Vicent Casadó. *E-mail: vcasado@ub.edu

Author's e-mail addresses: vcasadoanguera@gmail.com (V. Casadó-Anguera), marta.sanchezsoto@nih.gov (M. Sánchez-Soto), fifa877@hotmail.com (E. Moreno), patriciahomar25@gmail.com (P. Homar), NCai@intra.nida.nih.gov (NS. Cai), jordi.bonaventura@nih.gov (J. Bonaventura), jmallol@ub.edu (J. Mallol), sferre@intra.nida.nih.gov (S. Ferré), antonicortes@ub.edu (A. Cortés), ecanela@ub.edu (E.I. Canela), vcasado@ub.edu (V. Casadó)

Abstract:

Most medications used to treat attention deficit hyperactivity disorder (ADHD) are directed to modulate NE and DA neurotransmission in the brain. Genetic studies have indicated linkage of vulnerability for developing ADHD and substance use disorders (SUD) and polymorphisms of α_{2A} R-adrenoceptors (α_{2A} R) and dopamine D₄ receptors (D₄R). There are evidences demonstrating that α_{2A} Rs are involved the correct function of working memory and behavioral inhibition and in the protection against distractibility at the level of prefrontal cortex (PFC). α_{2A} Rs are also involved in the basal ganglia motor control inhibiting DA release from the substantia nigra. D₄Rs have also been related to the control of glutamate release both in the PFC and in the basal ganglia, thus in the control of PFC excitability and in the “Go” and “NoGo” GABAergic striatal efferent pathways. However, very little is known and there is controversy about the molecular mechanisms and functional significance of the polymorphisms of the human DRD4 gene. Here, using a combination of approaches including biophysical, pharmacological, functional and immunochemical assays in transfected cells and in cortex and striatum brain slices, we investigated the possibility that D₄R might modify adrenergic receptor function through direct receptor-receptor interaction. We report, to our knowledge, the first heteromer between D₄R and α_{2A} R, which also shows functional differences between both products of D₄R polymorphic variants that are only evident upon heteromerization with α_{2A} R, as reported for D₄R-D₂R heteromers. Concretely, there is a negative cross-talk and a cross-antagonism within the α_{2A} R-D₄R heteromer only evident with D_{4.4}R but not with D_{4.7}R variant. These differences may be responsible for the pathophysiology of ADHD disorder and can give new clues for the rational design of α_{2A} R- D₄R targeted drugs for the treatment of ADHD and SUD.

Introduction

The biogenic amines dopamine (DA) and norepinephrine (NE) constitute a class of conventional neurotransmitters and hormones that occupy key positions in the regulation of physiological processes and in the development of neurological, psychiatric, endocrine and cardiovascular diseases (Eisenhofer et al. 2004; Kreusser et al., 2017). The prefrontal cortex (PFC) is the most recently evolved region of the brain, subserving our highest order cognitive abilities, controlling working memory, attention, and behavioral inhibition and planning (Arnsten et al., 1988; Jäkälä et al., 1999). There is also an old but consistent literature demonstrating that PFC lesions cause locomotor hyperactivity in monkeys (Kennard et al., 1941; French, 1959; Gross, 1963; Gross and Weiskrantz, 1964).

The PFC network activity is fragile, and extremely sensitive to the neurochemical environment, in particular to the catecholamine levels (Arnsten, 2007). Thus, small changes in the arousal systems can markedly alter its connectivity (Arnsten et al., 2010). There are evidences of reduced DA and NE inputs to the PFC in adults with attention deficit hyperactivity disorder (ADHD) (Ernst et al., 1998). ADHD is a disorder characterized by pervasive symptoms of inattention, impulsivity and/or hyperactivity and is a significant risk factor for developing major mental disorders such as substance abuse disorders (SUD) and depression (Philipsen et al., 2008). These results, taken with several genetic studies that have indicated linkage of vulnerability for developing ADHD and a variety of genes related to DA (DA transporter, DA degrading enzyme COMT, D₁ and D₄ receptors) and NE (α_{2A} -adrenoceptors and dopamine beta hydroxylase) (Cook et al., 1995; Gill et al., 1997; Roman et al., 2003; Park et al., 2005; Arnsten and Li, 2005; Belcher et al., 2014), explain why most medications used to treat ADHD modulate DA and NE transmission.

Among the α_2 -adrenoceptors (α_2 Rs), which are coupled to Gai/o proteins, the α_{2A} R subtype is the most prevalent in the PFC and is found presynaptically on noradrenergic terminals acting as autoreceptors inhibiting NE release. α_{2A} Rs are also found postsynaptically on PFC pyramidal cells (Aoki et al., 1998; Wang et al., 2007) playing a critical role in the regulation of the PFC-dependent cognition (MacDonald et al., 1997; Wang et al., 2007) and exerting an opposite effect than α_1 -adrenoceptors (α_1 Rs). Yet, a series of studies indicate that α_{2A} Rs are also fully functional in the striatum, where they seem to be localized mostly postsynaptically, preferentially in GABAergic striatal efferent neurons (Holmberg et al., 1999; Hara et al., 2010).

Cortical function is also regulated by the catecholamine DA acting at D₄Rs in pyramidal neurons or in GABA interneurons that innervate pyramidal neurons (Mrzljak et al., 1996; Goldman-Rakic, 1998) or interneurons (Mrzljak et al., 1996; Wang et al., 2002). D₄Rs are also involved in the modulation of corticostriatal glutamatergic transmission in the striatum, both at the dendritic level (PFC) and at the terminal level (NAc shell) (Maura et al., 1988, Gonzalez et al., 2012a; Bonaventura et al., 2017). The D₄R is strongly linked to neuropsychiatric disorders, such as ADHD and schizophrenia. Concretely, its polymorphic variant D_{4.7}R, with a global frequency of 21% (Chang et al., 1996), has been suggested to be associated with numerous behavioral individual differences and neuropsychiatric disorders such as ADHD (La Hoste et al., 1996; Li et al., 2006; Gizer et al., 2009; Albrecht et al., 2014), and substance use disorders (McGeary, 2009; Belcher et al., 2014; Mallard et al., 2016; Bonaventura et al., 2017). So far, very little is known

and there is controversy about the molecular mechanisms and functional significance of the remarkable polymorphism of the human DRD4 gene (Jovanovic et al., 1999). There are results showing no differences in the ability of DA to activate the three different D₄R variants reconstituted with purified G proteins containing G_{αi1}, G_{αi2}, or G_{αi3} subunits (Kazmi et al., 2000; Sánchez-Soto et al., 2016), which questions the studies that have suggested D₄R variant-dependent differences in the potency of DA or NE to activate G protein [³⁵S]GTPγS binding assays (Czermak et al., 2006) or to inhibit adenylyl cyclase (Asghari et al., 1995). Emerging evidence by electrophysiological studies in cortical slices suggests that ADHD-linked variant D_{4.7}R induces more suppression of glutamatergic excitatory network bursts and less suppression of GABAergic inhibitory network bursts in the PFC circuitry, compared with hD_{4.4}R variant (Zhong et al., 2016). This may explain the significant frontal hypoactivity detected in ADHD patients (Dickstein et al., 2006; Fernández et al., 2009; Brown et al., 2012). In addition, Bonaventura et al. (2017) demonstrated that D₄Rs mediate a significant role in the dopaminergic inhibitory control of corticostriatal neurotransmission, which was higher in D_{4.7}R knock-in mice. A blunted corticostriatal transmission should affect the activity of both the “Go” and “NoGo” GABAergic striatal efferent pathways, decreasing their respective ability to increase the reactivity to reward-related stimuli and to suppress the reactivity to nonrewarded- or aversive-related stimuli (Bromberg-Martin et al., 2010). The outcome should be an increased “interest” for irrelevant stimuli and a reduced inhibition of irrelevant responses, which could be important in explaining the attention deficit and impulsivity of ADHD.

Catecholamine receptors, being GPCRs, form oligomers (homodimers and heterodimers) that are often essential for modulation of GPCR function (Ferré et al., 2007, 2014; Gomes et al., 2016). D₄Rs are able to form homodimers in HEK-293T transfected cells (Borroto-Escuela et al., 2011; Van Craenenbroeck et al., 2011). D_{4.4}Rs but not D_{4.7}Rs form heteromers with D_{2S}Rs in HEK-293T transfected cells and in striatal mice and rat slices (González et al., 2012a). Moreover, both variants heteromerize with D_{2L}Rs in HEK-293T transfected cells but with less potency in the case of D_{4.7}R-D_{2L}R (Borroto-Escuela 2011). In addition, it has been reported that D₄Rs also form heteromers with the adrenergic receptors α_{1B} and β₁ in rat pineal gland and in CHO transfected cells (González et al., 2012b) and that α_{2A}R can form homodimers (Small et al., 2006) and heteromers with α_{2C}R (Small et al., 2006) and β₁R (Xu et al., 2003).

We hypothesize that one important role of D₄Rs in both cortex and striatum can be the modulation of α_{2A}R receptor function. One possibility for such a modulation could be through receptor heteromer formation. Here, using a combination of approaches including biophysical, pharmacological, functional and immunochemical assays in transfected cells and in cortex and striatum brain slices, we explored the possibility that D₄R might modify adrenergic receptor function through direct receptor-receptor interaction. We report, to our knowledge, the first heteromer between D₄R and α_{2A}R, which also shows differences between the D₄R variants. These differences can account for the pathogenesis of ADHD and can give new clues for novel heteromer-based therapeutic strategies for the treatment of ADHD.

Materials and Methods

DNA constructs

For bimolecular fluorescence complementation experiments, human D_{4.4}R, D_{4.7}R, α_{2A} R, α_{1A} R, and A₁R were cloned into pcDNA3.1 expressing the amino acid residues 1-155 (nYFP) and 156-238 (cYFP) of the YFP Venus. For bimolecular luminescence complementation experiments, human D_{4.4}R, D_{4.7}R, α_{2A} R, α_{1A} R, and A₁R were cloned into pcDNA3.1 expressing the amino acid residues 1-229 (nRLuc) and 230-311 (cRLuc) of the RLuc8 protein. For BRET assays, D_{4.4}R-YFP, D_{4.7}R-YFP, α_{1A} R-YFP, α_{2A} R-RLuc8 and A₁R-RLuc constructs were used. For CODA-RET assays, human Gai1-mVenus, untagged G β 1, and G γ 2, α_{2A} R-nRLuc, α_{2A} R-cRLuc, D_{4.4}R-nRLuc, D_{4.4}R-cRLuc, D_{4.7}R-nRLuc and D_{4.7}R-cRLuc were used. For binding and functional assays, α_{2A} R-RLuc8 was used.

TAT-TM peptides

A peptide derived from the HIV transactivator of transcription, HIV TAT (YGRKKRRQRRR), was fused to peptides with the amino acid sequences of human D₄R transmembrane (TM) domains 4-7 (Peptide Synthesis Facility, University Pompeu Fabra, Barcelona), to promote integration of the TM domains in the plasma membrane. Because HIV TAT binds to the phosphatidylinositol-(4, 5)-bisphosphate found on the inner surface of the membrane (He et al., 2011), HIV TAT peptide was fused to the N-terminus of TM4 and TM6 and to the C-terminus of TM5 and TM7 to obtain the right orientation of the inserted peptide. The amino acid sequences were:

TAT-TM4 of D₄R: RRRQRRKKRGYGSRRQLLIGATWLLSAVAAPVLCGL

TM5-TAT of D₄R: YVVYSSVCSFFLPCPLMLLLYWATFYGRKKRRQRRR

TM7-TAT of D₄R: LVSAVTWLGIVNSALNPVIYTVFNAYGRKKRRQRRR

Cell culture

HEK-293T cells were maintained in culture with Dulbecco's modified Eagle's medium supplemented with 5% fetal bovine serum and kept in an incubator at 37°C and 5% CO₂. HEK-293T cells inducible expressing D₄R variants under the control of tetracycline, were obtained with the Flp-In T-Rex system. These cell lines were maintained with hygromycin 50 μ g/ml and blasticidin 15 μ g/ml and the D₄R variant expression was induced for 18-24h with tetracycline 250 ng/ml.

BRET and bimolecular fluorescence/luminescence complementation assays

Cells were transiently co-transfected with polyethylenimine with a constant amount of expression vector encoding for receptor fused to RLuc and with increasing amounts of the expression vector corresponding to receptor fused to YFP (0.55 μ g of α_{2A} R-RLuc and 0.2-3 μ g of D_{4.4}R-YFP or 0.2-3.5 μ g of D_{4.7}R-YFP or 0.2-2 μ g of α_{1A} R-YFP; 0.08 μ g of A₁R-RLuc and 0.2-3 μ g of D_{4.4}R-YFP or 0.1 μ g of A₁R-RLuc and 0.5-3 μ g of D_{4.7}R-YFP). Cells were harvested, washed, and resuspended in PBS. For determining Venus expression, 20 μ g of protein were distributed in 96-well plates (black plates with a transparent bottom) and the emission at 530 nm after the excitation at 500 nm with a Mithras LB940 (Berthold Technologies, Bad Wildbad, Germany) was quantified. Protein fluorescence expression was determined as the fluorescence of the sample minus the fluorescence of cells expressing the receptor fused to RLuc alone. In parallel, luminescence and BRET signal was determined as the ratio of the light emitted by Venus (530

nm) over that emitted by coelenterazine H (485 nm) 1 min after the addition of 5 μ M coelenterazine H (Invitrogen) using a Mithras LB940. To quantify receptor-RLuc expression, luminescence readings were also performed after 10 min of adding coelenterazine H. The net BRET was defined as [(long-wavelength emission)/(short-wavelength emission)]-cf., where cf. corresponds to [(longwavelength emission)/(short-wavelength emission)] for the receptor-RLuc expressed alone in the same experiment. BRET is expressed as milliBRET units (mBU; net BRET 1000). Data were fitted to a nonlinear regression equation, assuming a single-phase saturation curve with GraphPad Prism software.

For fluorescent and luminescent complementation assays, cells were co-transfected with the cDNA encoding for the receptors of interest fused to the Venus or RLuc hemiproteins. The quantification of the receptor-reconstituted Venus expression was performed as described above for BRET assays. The quantification of the receptor-reconstituted RLuc expression was measured at 485 nm after 10 min of adding coelenterazine H. Cells expressing the receptor fused to one hemiprotein showed similar fluorescence or luminescence levels to non-transfected cells.

Radioligand binding experiments

Radioligand binding experiments were performed in HEK-293T cells co-expressing the α_{2A} -RLuc8, about 0.3-0.4 pmols/mg protein, and the D₄R (about 1 pmol/mg protein) and in brains of male and female sheep of 4-6 months old freshly obtained from the local slaughterhouse. Brain tissues and cell suspensions, were disrupted with a Polytron homogenizer (PTA 7 TS rotor, setting 3; Kinematica, Basel, Switzerland) for two 5 s-periods in 10 volumes of 50 mM Tris-HCl buffer, pH 7.4, containing a proteinase inhibitor cocktail (Sigma, St. Louis, MO, USA). Membranes were obtained by centrifugation twice at 105.000 g for 45 min at 4°C. The pellet was stored at -80°C, washed once more as described above and resuspended in 50 mM Tris-HCl buffer for immediate use. Membrane protein was quantified by the bicinchoninic acid method (Pierce Chemical Co., Rockford, IL, USA) using bovine serum albumin dilutions as standard.

Binding experiments were performed with membrane suspensions (0.2 mg of protein/mL) at room temperature in 50 mM Tris-HCl buffer, pH 7.4, containing 10 mM MgCl₂. For competition-binding assays, membrane suspensions were incubated for 2 h with a constant free concentration of 0.9 nM of the α_2 R antagonist [³H]RX821002, or 0.7 nM of the D₂-like receptor antagonist [³H]YM-09151-2 and increasing concentrations of each tested ligand. For α_2 R saturation-binding assays, membrane suspensions were incubated for 3 h at room temperature in 50 mM Tris-HCl buffer, pH 7.4, containing 10 mM MgCl₂ with increasing concentrations of the α_2 R antagonist [³H]RX821002. Non-specific binding was determined in the presence of 10 μ M of the non-radiolabeled antagonist RX821002.

In dissociation kinetic assays, membranes were pre-incubated at 12 °C in Tris-HCl buffer (50 mM, pH 7.4) containing 10 mM MgCl₂ in the absence or presence of A-412997 (30 nM) or YM-09151-2 (30 nM). After 30 min, 0.9 nM of the α_2 R antagonist [³H]RX821002 was added for an additional 1-h period of radioligand association. Dissociation was initiated by the addition of 10 μ M of RX821002. At the indicated time intervals, total binding was measured as described below.

In all cases, free and membrane-bound ligands were separated by rapid filtration of 500 μL aliquots in a cell harvester (Brandel, Gaithersburg, MD, USA) through Whatman GF/C filters embedded in 0.3% polyethylenimine that were subsequently washed for 5 s with 5 mL of ice-cold 50 mM Tris-HCl buffer. The filters were incubated with 10 mL of Ultima Gold MV scintillation cocktail (PerkinElmer, Boston, MA, USA) overnight at room temperature and radioactivity counts were determined using a Tri-Carb 2800 scintillation counter (PerkinElmer, Boston, MA, USA) with an efficiency of 62% (Sarrió et al., 2000).

Binding data analysis

Data were analyzed according to the ‘two-state dimer model’ of Casadó et al. (2007). The model assumes GPCR dimers as a main functional unit and provides a more robust analysis of parameters obtained from saturation and competition experiments with orthosteric ligands, as compared with the commonly used ‘two-independent-site model’ (Casadó et al., 2007; Ferré et al., 2014). In competition experiments the model analyzes the interactions of the radioligand with a competing ligand and it provides the affinity of the competing ligand for the first protomer in the unoccupied dimer (K_{DB1}), the affinity of the competing ligand for the second protomer when the first protomer is already occupied by the competing ligand (K_{DB2}) or the radioligand (K_{DAB}) and an index of cooperativity of the competing ligand (D_{CB}). A positive or negative value of D_{CB} implies either an increase or a decrease in affinity of K_{DB2} versus K_{DB1} and its absolute value provides a measure of the degree of increase or decrease in affinity.

Radioligand competition curves were analyzed by nonlinear regression using the commercial Grafit curve-fitting software (Erithacus Software, Surrey, UK), by fitting the binding data to the mechanistic two-state dimer receptor model, as described in detail elsewhere (Casadó et al., 2009). To calculate the macroscopic equilibrium dissociation constants from competition experiments, the following general equation must be applied:

$$A_{\text{bound}} = \frac{\left(K_{DA2} A + 2 A^2 + \frac{K_{DA2} A B}{K_{DAB}} \right) R_T}{K_{DA1} K_{DA2} + K_{DA2} A + A^2 + \frac{K_{DA2} A B}{K_{DAB}} + \frac{K_{DA1} K_{DA2} B}{K_{DB1}} + \frac{K_{DA1} K_{DA2} B^2}{K_{DB1} K_{DB2}}}$$

where B represents the assayed competing compound concentration.

For an absence of cooperativity and allosteric modulation between A and B, the equation can be simplified due to the fact that: $K_{DA2} = 4K_{DA1}$, $K_{DB2} = 4K_{DB1}$ and $K_{DAB} = 2K_{DB1}$;

$$A_{\text{bound}} = \frac{(4 K_{DA1} A + 2 A^2 + A B) R_T}{4 K_{DA1}^2 + 4 K_{DA1} A + A^2 + A B + 4 K_{DA1} B + B^2}$$

Dissociation kinetic data were fitted to the following empirical equation:

$$A_{\text{total bound}} = \sum_{i=1}^n A_{ei} e^{-t k_i} + A_{\text{nonspecific bound}}$$

where A_{ei} represents the initial radioligand (the $\alpha_2\text{R}$ antagonist $[^3\text{H}]\text{RX821002}$) bound at equilibrium for each molecular specie i , t is time, and k_i is the dissociation rate constants for the n different molecular species. For biphasic curves (or complex dissociation kinetics), $n = 2$.

CODA-RET assays

HEK-293T cells were co-transfected with human $G\alpha i1$ -mVenus, untagged $G_{\beta 1}$, and $G_{\gamma 2}$, and the pair of receptors of interest fused to the corresponding RLuc8 hemiprotein using polyethylenimine in a 1:2 ratio in 100-cm² cell culture plates. All experiments were performed approximately 48-hours after transfection. Cells were harvested, washed and resuspended in phosphate-buffered saline. Approximately 200,000 cells/well were distributed in 96-well plates, and 5 μ M Coelenterazine H was added to each well. One minute after addition of coelenterazine H, agonists were added to each well. Antagonists were added 10 minutes before coelenterazine. The fluorescence of the acceptor was quantified (excitation at 500 nm and emission at 540 nm for 1-second recordings) in Mithras LB940 (Berthold Technologies, Bad Wildbad, Germany) to confirm the constant expression levels across experiments. In parallel, the BRET signal from the same batch of cells was determined as the ratio of the light emitted by mVenus (530 nm) over that emitted by RLuc (485 nm). G protein-activation was calculated as the BRET change (BRET ratio for the corresponding drug minus BRET ratio in the absence of the drug) observed 10 minutes after the addition of the ligands. E_{max} values were expressed as the percentage of the effect of each ligand over the effect of NE or DA depending on the experiment. Data were fitted to a nonlinear regression equation, assuming a single-phase dose-response curve with GraphPad Prism software. The transfected amount and ratio among the receptor and heterotrimeric G proteins were tested for optimized dynamic range in drug-induced BRET.

cAMP production

For cAMP production, homogeneous time-resolved fluorescence energy transfer (HTRF) assays were performed using the Lance Ultra cAMP kit (PerkinElmer, Waltham, Massachusetts, US), based on competitive displacement of a europium chelate-labelled cAMP tracer bound to a specific antibody conjugated to acceptor beads. HEK-293T cells stably expressing $D_{4.4}R$ or $D_{4.7}R$ were transfected with α_{2A} -RLuc8 receptor. First of all we established the optimal cell density and forskolin concentration for an appropriate fluorescent signal that covered most of the dynamic range of cAMP standard curve. Cells (1,200 cells/well) growing in medium containing 50 μ M zardaverine were pretreated with the antagonists or the corresponding vehicle in white ProxiPlate 384-well microplates (PerkinElmer) at 25°C for 15 min and stimulated with agonists for 15 min before adding 0.2 μ M forskolin or vehicle and incubating for an additional 15-min period. Fluorescence at 665 nm was analyzed on a PHERAstar Flagship microplate reader equipped with an HTRF optical module (BMG Lab technologies, Offenburg, Germany).

Dynamic mass redistribution assay

A global cell signaling profile or DMR was measured using an EnSpire Multimode Plate Reader (PerkinElmer, Waltham, Massachusetts, USA). This label-free approach uses refractive waveguide grating optical biosensors, integrated into 384-well microplates. Changes in local optical density are measured in a detection zone up to 150 nm above the surface of the sensor. Cellular mass movements induced upon receptor activation are detected by illuminating the underside of the biosensor with polychromatic light and measured as changes in the wavelength of the reflected monochromatic light. These changes are a function of the refraction index. The magnitude of this wavelength shift (in picometers) is directly proportional to the amount of DMR. Briefly, after 24h of the HEK-D₄R cells transfection with α_{2A} -RLuc8 receptor, cells were resuspended and seeded at a density of 10,000 cells per well in 384-well sensor microplates in 30 μ l growing media plus hygromycin, blasticidin and tetracycline and cultured for 24 h at 37°C and 5% CO₂, to obtain monolayers at 70%–80% confluency. Before starting the assay, cells were washed twice with assay buffer (DMEM supplemented with 20 mM HEPES, pH 7.15, 0.1% DMSO and 0.1% BSA) and incubated 2 h in 40 μ l per well in the reader at 24°C. Hereafter, the sensor plate was scanned, and a baseline optical signature was recorded for 10 min before adding 10 μ l of the antagonist dissolved in assay buffer and recorded for 30 min. After that, 10 μ l of the agonist was added and recorded for 60 min. Kinetic results were analyzed using EnSpire Workstation Software v 4.10.

ERK1/2 phosphorylation assay

HEK-293T cells stably expressing D_{4.4}R or D_{4.7}R were transfected with α_{2A} -RLuc8 receptor. The day of the experiment, cells were starved by treating them with serum free media for 4h at 37°C. After that, cells were incubated with the indicated agonist for 5 minutes at 37°C. Then, cells were rinsed with ice-cold phosphate-buffered saline and lysed by adding 200 μ l ice-cold lysis buffer (50 mM Tris-HCl [pH 7.4], 50 mM NaF, 150 mM NaCl, 45 mM β -glycerophosphate, 1% Triton X-100, 20 mM phenylarsine oxide, 0.4 mM NaVO₄, and protease inhibitor cocktail). The cellular debris was removed by centrifugation at 13,000 x g for 5 minutes at 4°C, and the protein was quantified. To determine the level of ERK1/2 phosphorylation, equivalent amounts of protein were separated by electrophoresis on a denaturing 10% SDS polyacrylamide gel and transferred onto polyvinylidene fluoride membranes. Odyssey blocking buffer (LI-COR Biosciences, Lincoln, NE) was then added, and the membrane was rocked for 90 minutes. The membranes were then probed with a mixture of a mouse anti-phospho-ERK1/2 antibody (1:2500; Sigma-Aldrich) and rabbit anti-ERK1/2 antibody that recognizes both phosphorylated and nonphosphorylated ERK1/2 (1:40,000; Sigma-Aldrich) overnight at 4°C. The 42- and 44-kDa bands corresponding to ERK1 and ERK2 were visualized by the addition of a mixture of IRDye 800 (anti-mouse) antibody (1:10,000; Sigma-Aldrich) and IRDye 680 (anti-rabbit) antibody (1:10,000; Sigma-Aldrich) for 2 hours and scanned by the Odyssey infrared scanner (LICOR Biosciences). Band densities were quantified using the scanner software and exported to Excel (Microsoft, Redmond, WA). The level of phosphorylated ERK1/2 isoforms was normalized for differences in loading using the total ERK1/2 protein band intensities.

Brain slices preparation

Transgenic D_{4.7}R mice, with a humanized mouse DRD4 gene containing seven TRs of the human DRD4 in the homologous region of the mouse gene, which codes for the 3IL (González et al., 2012a), were used. Homozygous (D_{4.7}R) and WT littermates were obtained from a breeding colony of D_{4.7}R heterozygous mice (in a C57Bl/6J background) kept in the National Institute on Drug Abuse, Intramural Research Program (NIDA IRP) breeding facility. Animals were housed (four per cage) and kept on a 12-hour light/12-hour dark cycle with food and water available *ad libitum*. All animals used in the study were maintained in accordance with the guidelines of the National Institutes of Health (NIH) Animal Care, and the animal research conducted to perform this study was approved by the NIDA IRP Animal Care and Use Committee (protocols #12-BNRB-73, #15-BNRB-73, and #12-MTMD-2). Animals were killed by cervical dislocation. Mice brains were rapidly removed and placed in ice-cold oxygenated (95% O₂/5% CO₂) Krebs-HCO₃⁻ buffer (containing [in mM]: 124 NaCl, 4 KCl, 1.25 KH₂PO₄, 1.5 MgCl₂, 1.5 CaCl₂, 10 glucose, and 26 NaHCO₃, pH 7.4). The brains were sliced coronally at 4°C. Slices containing cortex or striatum (500 µm thick) were kept at 4°C in this Krebs-HCO₃-buffer during the dissection and were transferred into an incubation tube containing 1 ml of ice-cold Krebs-HCO₃-buffer. The temperature was raised to 23°C, and after 30 min the medium was replaced by 2 ml of fresh Krebs-HCO₃-buffer (23°C). The slices were incubated under constant oxygenation (O₂/CO₂: 95%/5%) at 30°C for 4–5 h in absence or presence of the TM peptides at 4 µM in an Eppendorf Thermomixer (5 Prime, Boulder, Colorado, USA).

For phospho-ERK 1/2 determination, the media was replaced by 200 µL of fresh Krebs-HCO₃-buffer and incubated for 30 min before the addition of any agent. Slices were treated or not with the indicated ligand for the indicated time (5 min). After the indicated incubation period, the solution was discarded, and slices were frozen on dry ice, lysed by the addition of 500 µL of ice-cold lysis buffer and treated as described for cells.

In situ PLAs in brain tissue

For proximity ligation assays, mouse brain slices were fixed by immersion with 4% paraformaldehyde solution for 1 h at 4°C. Samples were then washed in 50 mM Tris-HCl, 0.9% NaCl pH 7.8 buffer (TBS), cryopreserved in a 30% sucrose solution for 48 h at 4°C, and stored at -20°C until sectioning. 20 µm-thick slices were cut coronally on a freezing cryostat (Leica Jung CM-3000), mounted on slide glass and frozen at -20°C until use. To perform the PLA, slices were thawed at 4°C, washed in TBS, permeabilized with TBS containing 0.01% Triton X-100 for 10 min, and successively washed with TBS. Heteromers were detected using the Duolink II in situ PLA detection Kit (OLink; Bioscience, Uppsala, Sweden) and following the instructions of the supplier. To detect α_{2A}R-D₄R heteromers, a mixture of equal amounts of rabbit anti-α_{2A}R antibody (ab92650) (Thermo Scientific, Fremont, California) and goat anti-D₄R (sc-1439) (Santa Cruz Biotechnology, Santa Cruz, California) antibody were used. Samples were further incubated with anti-rabbit plus and anti-goat minus PLA probes. Slices were mounted using the mounting medium with DAPI and observed in a Leica SP2 confocal microscope (Leica Microsystems, Mannheim, Germany) equipped with an apochromatic 63X oil-immersion objective (N.A. 1.4), and a 405 nm and a 561 nm laser line. For each field of view, a stack of two channels (one per staining) and 9 to 15 Z stacks with a step size of 1 µm were acquired. Images were opened and

processed with Image J confocal. After image processing, the red channel was depicted in green color to facilitate detection on the blue-stained nucleus and to maintain the color intensity constant for all images. In tissue, a quantification of cells containing one or more red spots versus total cells (blue nucleus) was determined considering a total of 1,500–3,000 cells from 4–12 different fields within each region from three different animals. The ImageJ confocal program using the Fiji package (<https://fiji.sc/>) was used. Nuclei and red spots were counted on the maximum projections of each image stack. After getting the projection, each channel was processed individually. The nuclei were segmented by filtering with a median filter, subtracting the background, enhancing the contrast with the contrast limited adaptive histogram equalization (CLAHE) plug-in, and finally applying a threshold to obtain the binary image and the regions of interest (ROIs) around each nucleus. Red spot images were also filtered and thresholded to obtain the binary images. Red spots were counted in each of the ROIs obtained in the nuclei images.

Statistical analysis

In binding assays, goodness of fit was tested according to reduced chi-squared value given by the regression program. The test of significance for two different model population variances was based upon the F-distribution. Using this F-test, a probability greater than 95% ($p < 0.05$) was considered the criterion to select a more complex model (cooperativity) over the simplest one (non-cooperativity). In all cases, a probability of less than 70% ($p > 0.30$) resulted when one model was not significantly better than the other. In all cases, results are given as parameter values \pm SEM and statistical differences were analyzed with GraphPad Prism 4.

Results

D_{4.4}R and D_{4.7}R form heteromers with α_{2A} R in transfected mammalian cells

First, we analyzed the ability of D_{4.4}R and D_{4.7}R to form heteromers with α_{2A} R *in vitro* by bioluminescence resonance energy transfer (BRET). These experiments were performed in HEK-293T cells co-transfected with the cDNA corresponding to α_{2A} R-RLuc and increasing amounts of D_{4.4}R-YFP or D_{4.7}R-YFP cDNA. The BRET saturation curve obtained was hyperbolic, reaching an asymptote at the highest concentrations of the YFP fusion construct used, thus indicating a specific interaction between both fusion proteins (Fig. 1A and 1B). The BRET_{max} for the pair α_{2A} R-D_{4.4}R was 95 ± 8 . A substantially lower BRET_{max} signal (33 ± 2 mBU) was obtained with α_{2A} R-D_{4.7}R. The BRET₅₀ values were 8 ± 2 for α_{2A} R-D_{4.4}R and 56 ± 13 for α_{2A} R-D_{4.7}R. The specificity of the D₄Rs and α_{2A} R to form heteromers was confirmed by the nonspecific (non-saturable) BRET signal obtained when cells were cotransfected with the cDNA corresponding to α_{2A} R-RLuc and increasing amounts of the cDNA corresponding to the α_{1A} R-YFP (Fig. 1C) or with the cDNA corresponding to A₁-RLuc and increasing amounts of the cDNA corresponding to the D₄-YFP receptors (Fig. 1D), as negative controls.

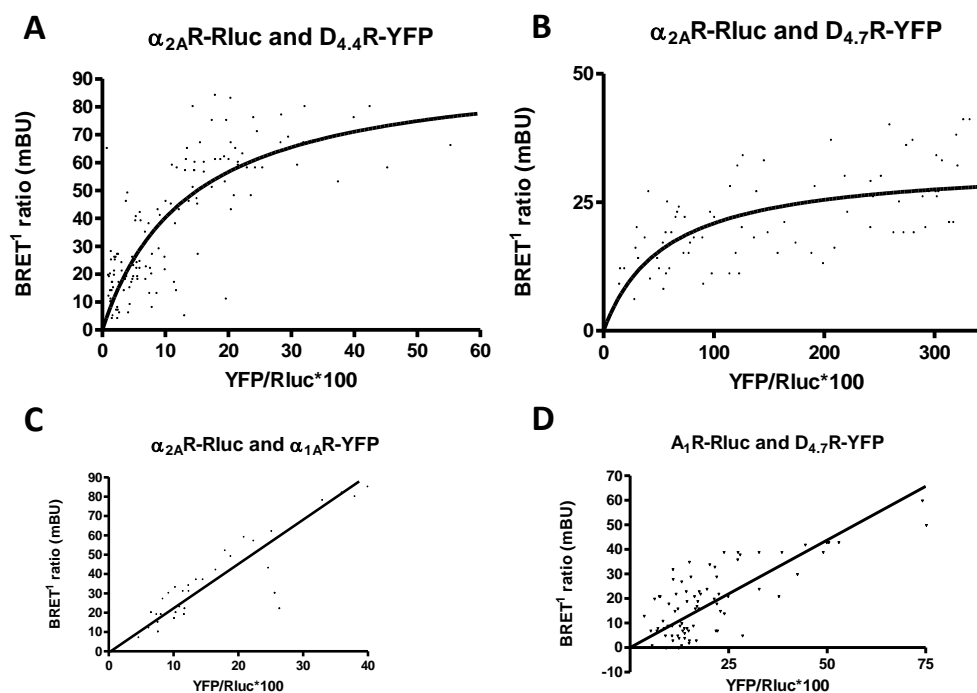


Figure 1. BRET saturation experiments were performed using HEK-293T cells 48 h post-transfection with 0.55 μ g of cDNA corresponding to α_{2A} -RLuc and increasing concentrations of the cDNA encoding for (A) D_{4.4}-YFP (0.2-3 μ g), (B) D_{4.7}-YFP (0.2-3.5 μ g) (C) α_{1A} -YFP (0.2-2 μ g) (D) 0.1 μ g of A₁-RLuc and increasing concentrations of the cDNA of D_{4.7}-YFP (0.5-3 μ g). Both fluorescence and luminescence of each sample were measured before every experiment to confirm similar donor expression (approximately 150,000-200,000 bioluminescence units) while monitoring the increase in acceptor expression (5,000-70,000 fluorescence units). The relative amount of BRET is given as a function of 100 the ratio between the fluorescence of the acceptor (YFP) and the luciferase activity of the donor (Rluc). BRET is expressed as mili BRET units (mBU = net BRETx 1000) and is means \pm SEM. of three to eight different experiments.

Further support for heteromer and also for homodimer formation was obtained from bimolecular luminescence complementation (BiLC) assays in transfected HEK-293 cells showed in Fig. 2A, where luminescence only appears after the correct folding of the two RLuc8 hemiproteins. This occurs when two receptors fused to hemi-RLuc8 proteins (cRLuc or nRLuc) come within proximity. Luminescence was detected in HEK-293T cells transfected with different amounts of cDNA corresponding to D₄R-nRLuc and D₄R-cRLuc or α_{2A} R-nRLuc and α_{2A} R-cRLuc for the homodimer detection and α_{2A} R-nRLuc and D₄R-cRLuc or α_{2A} R-cRLuc and D₄R-nRLuc for the heteromer detection. All three receptors formed homodimers and α_{2A} R heteromerized with both D₄R variants causing the RLuc8 protein reconstitution. This was not the case for α_{2A} R-nRLuc and α_{1A} R-cRLuc, α_{2A} R-cRLuc and α_{1A} R-nRLuc and adenosine A₁R-nRLuc and D₄R-cRLuc, which supports the specificity of those interactions. In addition, we also performed bimolecular fluorescence complementation (BiFC) assays showed in Fig. 2B, where fluorescence only appears after the correct folding of two mVenus hemiproteins. As in BiLC assays, we obtained an mVenus reconstitution for α_{2A} R and D₄R homodimers and heteromers but not for α_{1A} R- α_{2A} R nor for D₄R-A₁R. These results are according with those obtained in BRET assays.

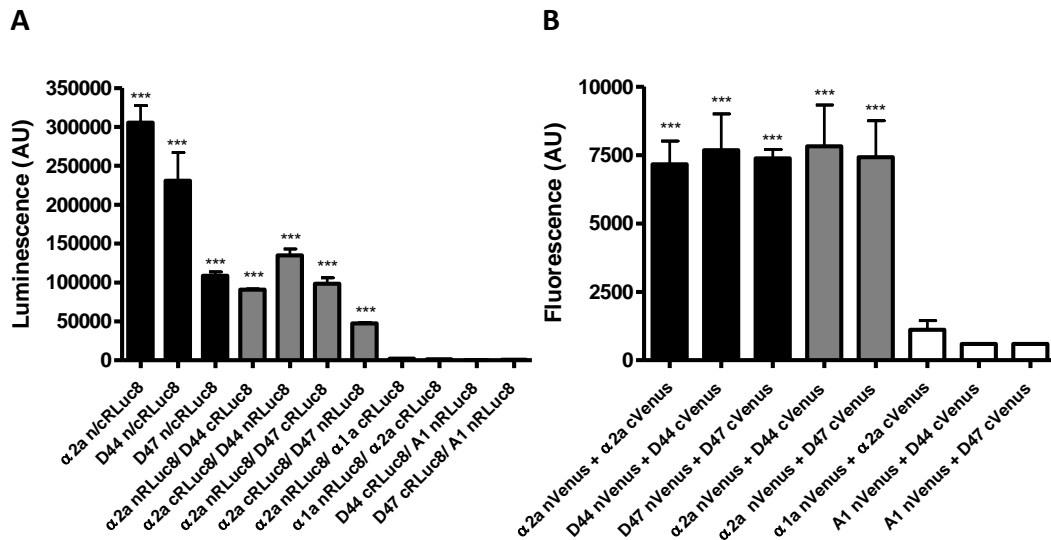


Figure 2. $\alpha_{2A}R$ and D_4R homodimers and heteromers. Luminescence (A) and fluorescence (B) due to complementation [in arbitrary units (AU)] of RLuc and YFP mVenus was determined in HEK-293 cells coexpressing $\alpha_{2A}R$ -nRLuc and $\alpha_{2A}R$ -cRLuc, $D_{4.4}R$ -nRLuc and $D_{4.4}R$ -cRLuc, $D_{4.7}R$ -nRLuc and $D_{4.7}R$ -cRLuc, $\alpha_{2A}R$ -nRLuc and $D_{4.4}R$ -cRLuc, $\alpha_{2A}R$ -nRLuc and $D_{4.7}R$ -cRLuc, $\alpha_{2A}R$ -cRLuc and $D_{4.4}R$ -nRLuc, $\alpha_{2A}R$ -cRLuc and $D_{4.7}R$ -nRLuc, $\alpha_{2A}R$ -nVenus and $\alpha_{2A}R$ -cVenus, $D_{4.4}R$ -nVenus and $D_{4.4}R$ -cVenus, $D_{4.7}R$ -nVenus and $D_{4.7}R$ -cVenus, $\alpha_{2A}R$ -nVenus and $D_{4.4}R$ -cVenus or $\alpha_{2A}R$ -nVenus and $D_{4.7}R$ -cVenus. Negative controls were obtained with the pairs: $\alpha_{2A}R$ -nRLuc and $\alpha_{1A}R$ -cRLuc, $\alpha_{2A}R$ -nRLuc and $\alpha_{1A}R$ -cRLuc, A_1R -nRLuc and $D_{4.4}R$ -cRLuc, A_1R -nRLuc and $D_{4.7}R$ -cRLuc, $\alpha_{2A}R$ -nVenus and $\alpha_{1A}R$ -cVenus, A_1R -nVenus and $D_{4.4}R$ -cVenus or A_1R -nVenus and $D_{4.7}R$ -cVenus. Values represent means \pm SEM from 3 different experiments performed in triplicate. Statistical significance was calculated by one-way ANOVA followed by Dunnett's post hoc test. **P < 0.01, compared with the negative controls.

$\alpha_{2A}R$ – D_4R heteromers assemble into tetrameric complexes

A bimolecular luminescence and fluorescence complementation approach was used to demonstrate the ability of $\alpha_{2A}R$ and D_4R to form heterotetramers. In HEK-293 cells, we reconstituted the RLuc8 after transfection of $D_{4.4}R$ -nRLuc and $D_{4.4}R$ -cRLuc or $D_{4.7}R$ -nRLuc and $D_{4.7}R$ -cRLuc and the mVenus after transfection of $\alpha_{2A}R$ -nVenus and $\alpha_{2A}R$ -cVenus. Complemented RLuc and complemented mVenus were used as donor and acceptor molecules in bioluminescence resonance energy transfer (BRET) experiments (Fig. 3). Significant BRET values were obtained confirming the presence of the heterotetramer $\alpha_{2A}R$ - $D_{4.4}R$ and $\alpha_{2A}R$ - $D_{4.7}R$ formed by a heteromer of homodimers. D_4R - D_4R and $\alpha_{2A}R$ - $\alpha_{1A}R$ pairs (fused to corresponding hemiproteins) again served as negative controls (Fig. 3).

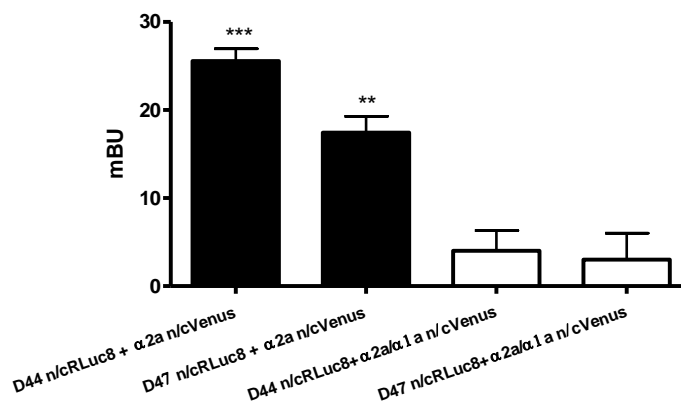


Figure 3. Heterotetrameric structure of the $\alpha_{2A}R$ - D_4R heteromer. BRET was determined in transfected HEK-293T cells expressing $\alpha_{2A}R$ -nVenus, $\alpha_{2A}R$ -cVenus, D_4R -nRLuc and D_4R -cRLuc. As negative controls D_4R - D_4R and $\alpha_{2A}R$ - $\alpha_{1A}R$ pairs were used. Values are mean \pm SEM of three different experiments performed in triplicate. Statistical significance was calculated by one-way ANOVA followed by Dunnett's post hoc test. **P < 0.01, ***P < 0.001 compared with the negative controls.

Functional properties of $\alpha_{2A}R$ - D_4R heteromers in transfected mammalian cells

Then we wanted to functionally characterize this interaction by analyzing if downstream signaling is altered upon dual stimulating of the two receptors in the heteromer. Concretely, we studied the mediated effects on adenylyl cyclase activity both at the level of G protein activation and at the cAMP accumulation, the global cell signaling profile by the dynamic mass redistribution (DMR) technique and, finally, at the level of MAPK phosphorylation.

Due to the fact that we have just published that some synthetic dopamine receptor agonists are actually able to bind with high affinity to α_2R s and generate signaling (i. e. the considered D_4R selective agonist RO 10-5824) (Cornil and Ball, 2008; Sánchez-Soto et al., 2018), we first tested the specificity of the ligands used in these assays. With competitive inhibition experiments using the non-selective α_2R antagonist radioligand [3H]RX821002 in membrane preparations from sheep cortex, we saw that the synthetic D_4R agonists PD168077 and A-412997 had an α_2R affinity of $K_{DB1}=80\pm 10$ and $1,400\pm 200$ nM, respectively. In addition, with competitive inhibition experiments using [3H]YM-09151-2 in membrane preparations from HEK-293T cells expressing $D_{4.4}R$ or $D_{4.7}R$, we saw that the synthetic α_2R agonist dexmedetomidine had a K_{DB1} for D_4R of about 2,000-6,000 nM. For this reason we decided to use A-412997, with a K_{DB1} of 1.1 ± 0.1 nM for transfected D_4R , and dexmedetomidine, with a K_{DB1} of 5.6 ± 0.8 nM for transfected α_2R , as agonists of D_4R s and α_2R s, respectively, for analyzing the signaling fingerprint of the α_2R - D_4R heteromer.

G protein activation by CODA-RET assay

In this assay, two complementary halves of RLuc (nRLuc and cRLuc) are separately fused to two receptor molecules putatively able to oligomerize and an mVenus is fused to the $G_{\alpha i1}$ subunit. Ligand-induced changes in CODA-RET measurements imply, first, a successful complementation of RLuc confirming the oligomerization of the corresponding GPCR units *in vitro* and, second, represents the reading of a specific signaling through the GPCR homo- or heterodimer and not of other species (Urizar et al., 2011; Guitart et al., 2014). Moreover, given that it has been seen that E_{max} is directly related with efficacy (Galés et al., 2005), we can conclude if a given agonist is full or partial at G protein activation. With CODA-RET we determined the potency and efficacy of several adrenergic and dopaminergic ligands: the endogenous DA and NE, the synthetic D_3R selective agonists pramipexole, ropinirole and rotigotine and the α_2R agonists dexmedetomidine, clonidine and guanfacine at mobilizing $G_{\alpha i1}$ through their binding to $\alpha_{2A}R$ - $\alpha_{2A}R$, $\alpha_{2A}R$ - $D_{4.4}R$ and $\alpha_{2A}R$ - $D_{4.7}R$ dimer complexes.

We co-transfected HEK-293T cells with $\alpha_{2A}R$ fused to the C-terminal of RLuc and $\alpha_{2A}R$, $D_{4.4}R$ or $D_{4.7}R$ fused to the N-terminal of the fluorescent protein, the $G_{\alpha i1}$ subunit fused to mVenus and untagged $G_{\beta 1}$, and $G_{\gamma 2}$ subunits. The amount of $G_{\alpha i/o}$ subunits transfected produced values between 10,000 and 20,000 fluorescence units and the amount of RLuc receptor complementation produced a values between 1 and 3 million (arbitrary units). A concentration-response of the ligand-induced change in BRET values allows the determination of the potency as well as the relative efficacy (to NE) in mediating G protein activation of the receptor pair. Data of CODA-RET assays appear in Fig. 4 fitted to a sigmoid dose-response curve and the parameter values deduced are in Table 1. The results show a non-canonical activation of $\alpha_{2A}R$ - $\alpha_{2A}R$ by DA, which is almost as potent as NE for this receptor but less efficient (about 65%). In $\alpha_{2A}R$ - $\alpha_{2A}R$

homodimer, pramipexole also activated $G_{\alpha i1}$ with high EC_{50} value and an E_{max} of about 45% vs. NE when bound to $\alpha_{2A}R$ - $\alpha_{2A}R$; E_{max} was similar than for $\alpha_{2A}R$ - $D_{4.7}R$, where had a lower EC_{50} value. Moreover, for both $\alpha_{2A}R$ - $\alpha_{2A}R$ and $\alpha_{2A}R$ - $D_{4.7}R$ dimers, ropinirole and rotigotine did not produce a significant response. In contrast, ropinirole and rotigotine showed high potency (nM range) for the $\alpha_{2A}R$ - $D_{4.4}R$ heteromer, but with low efficacy (about 15%). The non-canonical effect of DA and DA receptor ligands observed is according to the recently published Sánchez-Soto et al. (2018). In addition, synthetic α_2R agonists dexmedetomidine, clonidine and guanfacine have high potency (in the nanomolar range) but low efficacy at α_2Rs . Concretely, dexmedetomidine and clonidine have an efficacy about 20% and guanfacine about 10% vs. NE for $\alpha_{2A}R$ - $\alpha_{2A}R$. The potency and efficacy of these three ligands for $\alpha_{2A}R$ - $\alpha_{2A}R$ are similar than for $\alpha_{2A}R$ - $D_{4.7}R$ heteromer and, in contrast, they did not produce a significant activation at $\alpha_{2A}R$ - $D_{4.4}R$. In conclusion, the overall qualitative pharmacological profile of the studied ligands is similar between $\alpha_{2A}R$ - $\alpha_{2A}R$ and $\alpha_{2A}R$ - $D_{4.7}R$ dimers but is clearly different than for the $\alpha_{2A}R$ - $D_{4.4}R$ dimer. These results demonstrate different properties of the $D_{4.4}R$ and $D_{4.7}R$ variants upon heteromerization with $\alpha_{2A}R$.

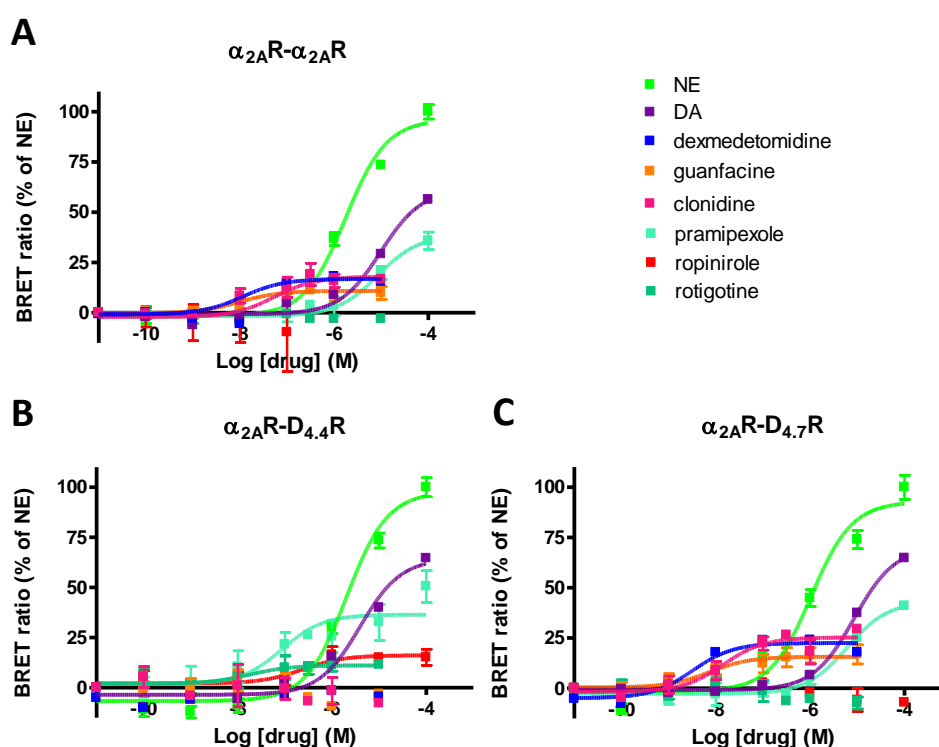


Figure 4. Ligand-induced changes in the interaction between $G_{\alpha i1}$ protein and $\alpha_{2A}R$ - $\alpha_{2A}R$, $\alpha_{2A}R$ - $D_{4.4}R$ or $\alpha_{2A}R$ - $D_{4.7}R$ dimers. Concentration-response experiments of changes in BRET ratio induced by norepinephrine, dopamine, pramipexole, ropinirole, rotigotine, guanfacine, dexmedetomidine and clonidine determined by changes in the interaction of $\alpha_{2A}R$ - $\alpha_{2A}R$ (A), $\alpha_{2A}R$ - $D_{4.4}R$ (B) or $\alpha_{2A}R$ - $D_{4.7}R$ (C) dimers with $G_{\alpha i1}$ protein. HEK-293T cells were co-transfected with $\alpha_{2A}R$ fused to the C-terminal of RLuc, $\alpha_{2A}R$, $D_{4.4}R$ or $D_{4.7}R$ fused to the N-terminal of the fluorescent protein, the $G_{\alpha i1}$ subunit fused to mVenus and untagged $G_{\beta 1}$, and $G_{\gamma 2}$ subunits. Cells were treated with coelenterazine H followed by increasing concentrations of the ligand. After 10 minutes, BRET between the corresponding complemented RLuc receptor and $G_{\alpha i1}$ -YFP was measured as described in Methods section. BRET values in the absence of ligands were subtracted from the BRET values for each ligand concentration. BRET values expressed as the percentage of the maximal effect of NE (% NE), considering NE as full agonist. Data were fit by nonlinear regression to a sigmoidal concentration-response curve against the agonist concentration. Data represent the mean \pm SEM of 3-11 experiments performed in triplicate (see Table 1 for EC_{50} and E_{max} values and statistical comparisons).

Table 1. Ligand-induced changes in the interaction between Gai1 protein and $\alpha_{2A}R$ - $\alpha_{2A}R$, $\alpha_{2A}R$ - $D_{4.4}R$ and $\alpha_{2A}R$ - $D_{4.7}R$ dimers. Experiments were performed in HEK-293T cells transiently expressing $\alpha_{2A}R$ -cRLuc and $\alpha_{2A}R$ -nRLuc, $\alpha_{2A}R$ -cRLuc and $D_{4.4}R$ -nRLuc or $\alpha_{2A}R$ -cRLuc and $D_{4.7}R$ -nRLuc, the G protein subunits $G_{\alpha 11}$ -YFP and unfused β_1 and γ_2 .

	$\alpha_{2A}R$ - $\alpha_{2A}R$		$\alpha_{2A}R$ - $D_{4.4}R$		$\alpha_{2A}R$ - $D_{4.7}R$	
	EC ₅₀ (μ M)	E _{max} vs NE	EC ₅₀ (μ M)	E _{max} vs NE	EC ₅₀ (μ M)	E _{max} vs NE
NE	6 \pm 1	100 \pm 3	10 \pm 3	100 \pm 6	3 \pm 1	100 \pm 4
DA	12 \pm 1	65 \pm 2	7 \pm 2	68 \pm 5	11 \pm 2	71 \pm 2
Pramipexole	20 \pm 10	44 \pm 2	0.13 \pm 0.07	26 \pm 2	5.6 \pm 0.6**	45 \pm 5
Ropinirole	-	0	0.4 \pm 0.2	15 \pm 2	-	0
Rotigotine	-	0	0.007 \pm 0.005	14 \pm 2	-	0
Guanfacine	0.011 \pm 0.005	11 \pm 2	-	0	0.0045 \pm 0.0002	17 \pm 3
Dexmedetomidine	0.024 \pm 0.005	20.5 \pm 0.4	-	0	0.0033 \pm 0.0009	28 \pm 1
Clonidine	0.013 \pm 0.009	19 \pm 4	-	0	0.0033 \pm 0.0009	28 \pm 4

EC₅₀ is expressed as mean \pm SEM and E_{max} as mean \pm SEM in % of NE. ** p<0.01 vs. $\alpha_{2A}R$ - $D_{4.4}R$ (one-way ANOVA followed by Dunnett's post hoc test).

To further study the contribution of each receptor in the G-protein signaling activation by DA and NE within each dimer, we pretreated the cells with the D₄R antagonist L745,870 or the $\alpha_{2A}R$ antagonist BRL44408. The curves obtained are showed in Fig. 5 and the parameter values deduced appear in Table 2. The potency of NE and DA was highly reduced by BRL44408 in the three dimer combinations; similar results were obtained using yohimbine as $\alpha_{2A}R$ antagonist (data not shown). In contrast, L745,870 significantly decreased only the effects of DA and NE in the $\alpha_{2A}R$ - $D_{4.4}R$ heteromer. Concretely, in this heteromer the potency of DA did not vary but the efficacy reduced by half, the opposite than NE, that maintained the efficacy but decreased ten times its potency upon treatment with L745,870. Because the addition of the D₄R antagonist L745,870 does not affect NE nor DA signaling in the $\alpha_{2A}R$ - $D_{4.7}R$ heteromer, we can conclude that $D_{4.7}R$ does not signal upon heteromerization with $\alpha_{2A}R$. To discard any possible artifact with the D₄R cDNAs fused to the hemiproteins, we wanted to confirm that both D₄Rs were able to produce G protein activation after dimerization. By using the same assay and complementing $D_{4.4}R$ - $D_{4.4}R$ and $D_{4.7}R$ - $D_{4.7}R$, we established both potency and efficacy of DA and NE at these homodimers (data not shown). DA and NE had a potency of 0.24 \pm 0.6 μ M and > 100 μ M for $D_{4.4}R$ - $D_{4.4}R$ homodimers and a potency of 0.13 \pm 0.06 μ M and 40 \pm 15 μ M for $D_{4.7}R$ - $D_{4.7}R$ homodimers, respectively. DA and NE acted as full agonists at both homodimers.

On the other hand, in the $\alpha_{2A}R$ - $D_{4.4}R$ heteromer NE signaling is probably only mediated by $\alpha_{2A}R$, because the potency of NE for the heteromer is the same as for the $\alpha_{2A}R$ - $\alpha_{2A}R$ homodimer (Table 2) and significantly different than for the $D_{4.4}R$ - $D_{4.4}R$ homodimer. Thus, we can assume that the decrease in the potency after the addition of L745,870 is due to the receptor-receptor allosteric interaction called cross-antagonism, where an antagonist binding to a protomer can modulate the binding of an agonist to the other protomer within the heteromer (Viñals et al., 2015). This allosteric modulation is not observed in the $\alpha_{2A}R$ - $D_{4.7}R$ heteromer, which is a new difference between D₄R variants, only evident upon heteromerization with $\alpha_{2A}R$. In the $\alpha_{2A}R$ - $D_{4.4}R$ heteromer, DA signaling is most likely mediated by both $\alpha_{2A}R$ and $D_{4.4}R$, since the affinity of DA for the heteromer is 7 \pm 2 μ M, which is an average between the affinity for the $\alpha_{2A}R$ - $\alpha_{2A}R$ homodimer (Table 2) and for the $D_{4.4}R$ - $D_{4.4}R$ homodimer. Thus, in the

$\alpha_2\text{AR-D}_{4.4}\text{R}$ heteromer, we can assume that the decrease in DA efficacy after the addition of L745,870 or BRL44408 is basically due to their antagonism on $\text{D}_{4.4}\text{R}$ and $\alpha_2\text{AR}$, respectively.

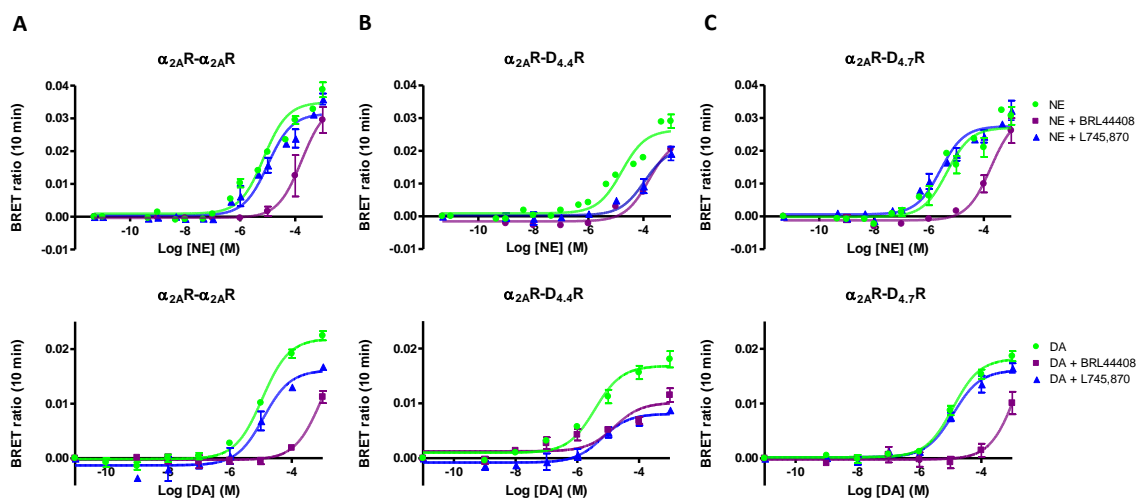


Figure 5. Affinity effects on NE and DA-induced changes in the interaction between $\text{G}_{\alpha i1}$ protein and $\alpha_2\text{AR-}\alpha_2\text{AR}$, $\alpha_2\text{AR-D}_{4.4}\text{R}$ or $\alpha_2\text{AR-D}_{4.7}\text{R}$ dimers. Dose-response experiments of changes in BRET ratio induced by NE, DA, in the presence or absence of the antagonists L745,870 or BRL44408 at 1 μM determined by changes in the interaction of $\alpha_2\text{AR-}\alpha_2\text{AR}$ (A), $\alpha_2\text{AR-D}_{4.4}\text{R}$ (B) or $\alpha_2\text{AR-D}_{4.7}\text{R}$ (C) dimers with $\text{G}_{\alpha i1}$ protein. HEK-293T cells were co-transfected with $\alpha_2\text{AR}$ fused to the C-terminal of RLuc, $\alpha_2\text{AR}$, $\text{D}_{4.4}\text{R}$ or $\text{D}_{4.7}\text{R}$ fused to the N-terminal of the fluorescent protein, the $\text{G}_{\alpha i1}$ subunit fused to mVenus and untagged $\text{G}_{\beta 1}$, and $\text{G}_{\gamma 2}$ subunits. Cells were treated with coelenterazine H followed by increasing concentrations of the ligand. After 10 minutes, BRET between the corresponding complemented RLuc receptor and $\text{G}_{\alpha i1}$ -YFP was measured as described in the Methods. BRET values in the absence of ligands were subtracted from the BRET values for each ligand concentration. BRET values expressed as the percentage of the maximal effect of DA or NE. Data were fit by nonlinear regression to a sigmoidal dose-response curve against the agonist concentration. Data represent the mean \pm SEM of 3-11 experiments performed in triplicate (see Table 2 for EC_{50} and E_{max} values and statistical comparisons).

Table 2. NE and DA-induced changes in the interaction between $\text{G}_{\alpha i1}$ protein and $\alpha_2\text{AR-}\alpha_2\text{AR}$, $\alpha_2\text{AR-D}_{4.4}\text{R}$ and $\alpha_2\text{AR-D}_{4.7}\text{R}$ dimers in the presence or absence of the antagonists L745,870 or BRL44408. Experiments were performed in HEK-293T cells transiently expressing $\alpha_2\text{AR-cRLuc}$ and $\alpha_2\text{AR-nRLuc}$, $\alpha_2\text{AR-cRLuc}$ and $\text{D}_{4.4}\text{R-nRLuc}$ or $\alpha_2\text{AR-cRLuc}$ and $\text{D}_{4.7}\text{R-nRLuc}$, the G protein subunits $\text{G}_{\alpha i1}$ -YFP and unfused β_1 and γ_2 .

	$\alpha_2\text{AR-}\alpha_2\text{AR}$		$\alpha_2\text{AR-D}_{4.4}\text{R}$		$\alpha_2\text{AR-D}_{4.7}\text{R}$	
	EC_{50} (μM)	E_{max} (%)	EC_{50} (μM)	E_{max} (%)	EC_{50} (μM)	E_{max} (%)
NE	6 \pm 1	100 \pm 3	10 \pm 3	100 \pm 5	3 \pm 1	100 \pm 4
NE + L745,870	11 \pm 4	90 \pm 4	130 \pm 40**	89 \pm 7	2.6 \pm 0.5	104 \pm 5
NE + BRL44408	500 \pm 200**	107 \pm 9	160 \pm 20**	109 \pm 10	190 \pm 30**	125 \pm 13
DA	12 \pm 1	100 \pm 3	7 \pm 2	100 \pm 7	11 \pm 2	100 \pm 3
DA + L745,870	13 \pm 4	78 \pm 7*	8 \pm 3	58 \pm 5**	13 \pm 1	87 \pm 5
DA + BRL44408	> 1000**	94 \pm 5	40 \pm 20*	63 \pm 8**	> 1000**	116 \pm 9

EC_{50} is expressed as mean \pm SEM and E_{max} as mean \pm SEM in % of NE or DA. * $p < 0.05$, ** $p < 0.01$ vs. the corresponding cells not treated with antagonists (one-way ANOVA followed by Dunnett's post hoc test).

Inhibition at the level of adenylyl cyclase

Conformational changes caused by GPCR heteromerization can modify signaling properties of a receptor such as leading to signaling empowerment or attenuation (positive or negative cross-talk if both ligands are agonists and cross-antagonism). These changes generate a specific fingerprint of the oligomer. In order to establish the cross-talk within the $\alpha_2\text{AR-D}_{4.4}\text{R}$ heteromer we analyzed the heteromer fingerprint at the level of inhibition of adenylyl cyclase activation

induced by forskolin. In the $\alpha_{2A}R$ - $D_{4.4}R$ cells, we detected a negative cross-talk because the decrease of the cAMP accumulation induced by forskolin due to the co-activation with dexmedetomidine and A-412997 did not produce any additive effect; in contrast, it was not significantly different than the treatment with dexmedetomidine and was even less potent than the treatment with A-412997 alone (Fig. 6). In contrast, we could not detect negative cross-talk between $D_{4.7}R$ and $\alpha_{2A}R$ because the co-activation with these ligands produced an additive effect.

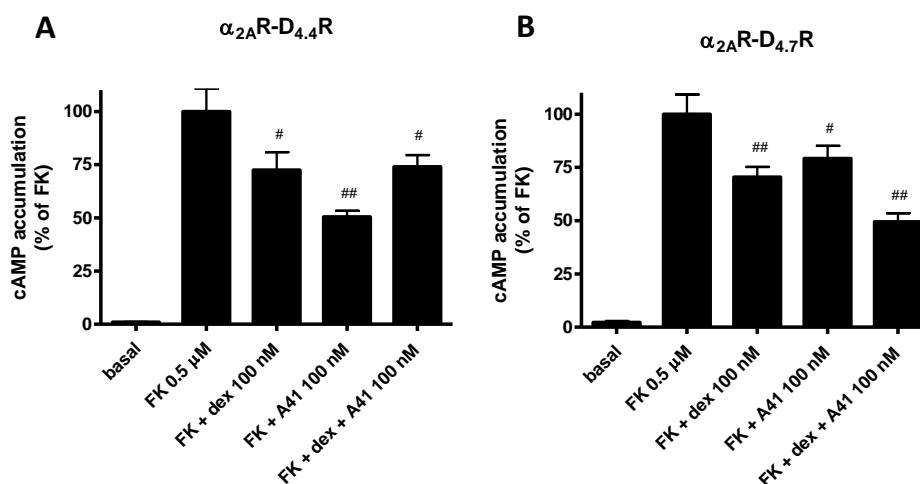


Figure 6. Negative cross-talk within the $\alpha_{2A}R$ - $D_{4.4}R$ heteromer. Agonist induced adenylyl cyclase inhibition assay was performed in tetracycline-inducible HEK-293T cells expressing $D_{4.4}R$ (A) or $D_{4.7}R$ (B) and transiently transfected with $\alpha_{2A}R$. Cells were stimulated with 100 nM of dexmedetomidine (α_{2R} agonist) or with 300 nM of A-412997 (D_{4R} agonist) or costimulated with both agonists in the presence of 0.5 μ M forskolin. Values are expressed as mean \pm SEM in % vs. FK treatment of 3-4 independent experiments performed in triplicates and of percentage of cAMP concentration relative to the forskolin treated cells of each cellular type. One-way ANOVA followed by Dunnett's post hoc test showed statistical differences: # $p < 0.05$, ## $p < 0.01$, vs. FK treatment.

Global cellular response by DMR assays

Furthermore, we measured the global cellular response using DMR label-free assays, which detect changes in the wavelength of the reflected monochromatic light after the illumination of the underside of a biosensor with a polychromatic light. The magnitude of this wavelength shift (in picometers) is directly proportional to the amount of cellular mass redistribution upon receptor activation. DMR experiments showed a similar pattern than that obtained in cAMP assays. We detected a negative cross-talk between $D_{4.4}R$ and $\alpha_{2A}R$ because the DMR signal induced by the α_{2R} agonist dexmedetomidine alone or the D_{4R} agonist A-412997 alone was attenuated when both agonists were added together (Fig. 7, top). In contrast, this negative cross-talk between $D_{4.7}R$ and $\alpha_{2A}R$ was much lower or inexistent because the co-activation with these ligands produced almost an additive effect (Fig. 7, bottom). In addition, we wanted to further confirm the cross-antagonism within the $\alpha_{2A}R$ - $D_{4.4}R$ heteromer suggested by CODA-RET experiments. The DMR signal induced by the $\alpha_{2A}R$ agonist was prevented not only by the $\alpha_{2A}R$ antagonist RX821002 but also partially by the D_{4R} antagonist YM-09151-2 in the case of the $\alpha_{2A}R$ - $D_{4.4}R$ heteromer. In contrast, in the case of the $\alpha_{2A}R$ - $D_{4.7}R$ heteromer, the DMR signal induced by the $\alpha_{2A}R$ agonist was prevented by its antagonist but not by the D_{4R} antagonist YM-09151-2. These results are according to those observed in CODA-RET assays. Surprisingly, the $\alpha_{2A}R$ antagonist RX821002 did not prevent the signal of D_{4R} in any case.

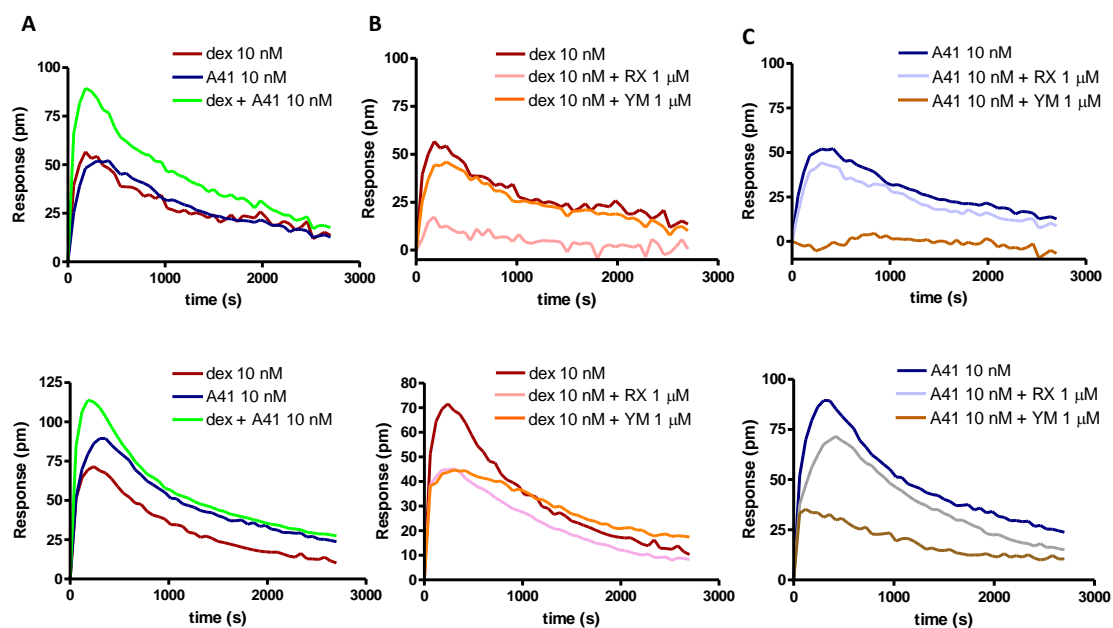


Figure 7. Global cellular response measured by DMR induced by dexmedetomidine and A-412997 in HEK-293T cells expressing $D_{4.4}R$ or $D_{4.7}R$ and $\alpha_{2A}R$. The assay was performed in HEK-293T tetracycline-inducible expressing $D_{4.7}R$ (top) or $D_{4.4}R$ (bottom) and transiently transfected with $\alpha_{2A}R$. These cells were non-treated (A) or treated (B and C) with the D_2 -like receptor antagonist YM-09151-2 or the $\alpha_{2A}R$ antagonist RX821002 at 1 μM for 30 min before the addition of the α_{2R} agonist dexmedetomidine or the D_4R agonist A-412997 or both. In (B), antagonists plus dexmedetomidine and in (C) antagonists plus A-412997. The resulting shifts of reflected light wavelength (pm) were monitored over time. Each panel is a representative experiment of $n=4$ different experiments. Each curve is the mean of a representative optical trace experiment carried out in triplicates.

MAPK activation

Finally, we also studied the allosteric interactions of D_4R and $\alpha_{2A}R$ at the level of MAPK activation (Fig. 8). This signaling pathway also showed a similar pattern than cAMP signaling and the DMR assay. Concretely, we detected a negative cross-talk between $D_{4.4}R$ and $\alpha_{2A}R$ because the ERK1/2 phosphorylation increase due to the co-activation with dexmedetomidine and A-412997 is not significantly different than the activation with A-412997 alone. In contrast, we could not detect negative cross-talk between $D_{4.7}R$ and $\alpha_{2A}R$ because the co-activation with these ligands is additive (Fig. 8). Surprisingly, in DMR assays and in cAMP accumulation and MAPK activation experiments, both D_4R variants are able to activate signaling, in contrast with CODA-RET experiments, where $D_{4.7}R$ did not signal upon heteromerization with $\alpha_{2A}R$. It is because with CODA-RET assays, we can only detect the specific signaling through the GPCR oligomer, and not through other species. In contrast, with the other techniques, combinations of homodimers, heteromers and higher order oligomers may contribute to the final signaling, because these cells commonly express more D_4R than $\alpha_{2A}R$ and not all D_4R s are forming heteromers with $\alpha_{2A}R$ s.

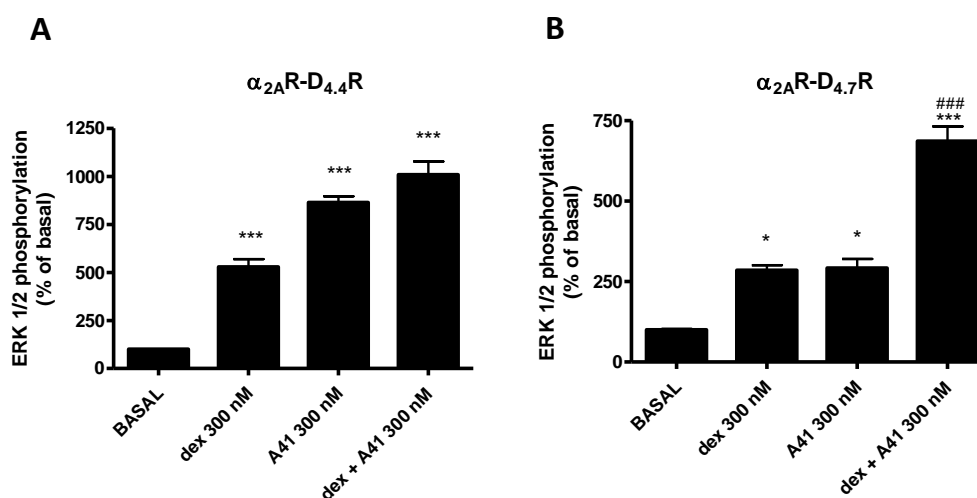


Figure 8. $\alpha_{2A}R-D_{4.4}R$ and $\alpha_{2A}R-D_{4.7}R$ heteromer signaling via ERK 1/2 phosphorylation. ERK phosphorylation was determined in HEK-293T tetracycline-inducible expressing $D_{4.4}R$ (A) or $D_{4.7}R$ (B) and transiently transfected with $\alpha_{2A}R$. Cells were activated with 300 nM of dexmedetomidine (α_2R agonist) or with 300 nM of A-412997 (D_4R agonist) or coactivated with both agonists for 5 min at 37 °C. Values are expressed as mean \pm SEM of 4 independent experiments performed in triplicates of percentage of phosphorylation relative to basal levels in not treated cells. Statistical differences vs. basal conditions were calculated by one-way ANOVA followed by Dunnett's post hoc test; * p <0.05 and ** p <0.01. Differences vs. A-412997 treatment were also calculated ### p <0.001.

Radioligand binding assays

To confirm the allosteric interaction between $\alpha_{2A}R$ and $D_{4.4}R$ s, we performed dissociation experiments with [3H]RX821002 in membranes of HEK-293T, that expressed $\alpha_{2A}R$ and $D_{4.4}R$. Dissociation curves were biphasic (Fig. 9). Both the D_4R agonist A-412997 and the antagonist YM-09151-2 were able to significantly modify the slow dissociation rate constant of the labeled antagonist in membranes with $\alpha_{2A}R$ and $D_{4.4}R$ s, specially the slow kinetic component (Table 3). This would suggest that $D_{4.4}R$ ligands can exert an allosteric modulation of the radiolabeled $\alpha_{2A}R$ antagonist when heteromerizing. It is due to the fact that if two ligands compete for the same orthosteric binding site, one cannot influence in the dissociation kinetics of the other. In contrast, if there is an allosteric modulation within a heteromer, the binding of one ligand to the orthosteric site of one receptor, allosterically alters the kinetic properties of the other ligand bound to the receptor partner, as we have recently determined for the $A_{2A}R-D_2R$ heteromer (Bonaventura et al., 2015; Casadó-Anguera et al., 2016).

Table 3. Effect of D_4R ligands on dissociation kinetic parameters of the $\alpha_{2A}R$ radiolabeled antagonist.

	k_{off1} (min $^{-1}$)	k_{off2} (min $^{-1}$)
control	0,15 \pm 0,05	0,025 \pm 0,007
+ A-412997	0,3 \pm 0,3	0,044 \pm 0,009*
+ YM-09151-2	0,1 \pm 0,2	0,05 \pm 0,01*

Dissociation kinetic assays were performed at 12°C on membranes from HEK-293T cells expressing $D_{4.4}R$ and $\alpha_{2A}R$ receptors. Membranes were incubated with the corresponding radioligand in the absence or presence of 30 nM A-412997 or 30 nM YM-09151-2. k_{off} values are means \pm SEM from three experiments performed in triplicate fitted with the dissociation equation that appears in Methods section. * p <0.05 vs. the control curve (one-way ANOVA followed by Dunnett's post hoc test).

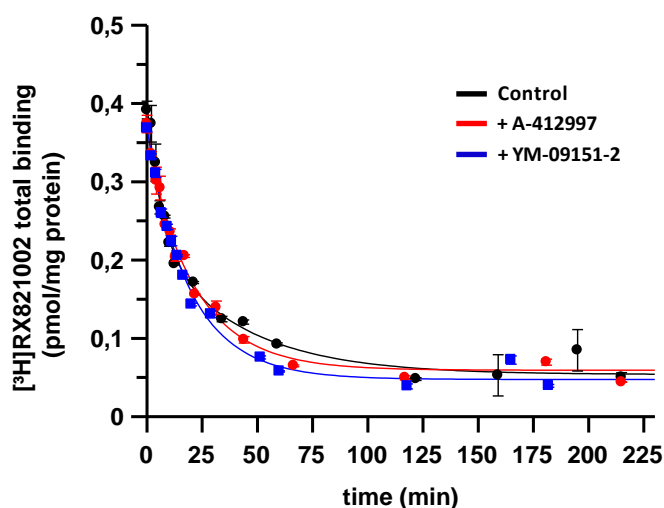


Figure 9. Dissociation kinetics of $[^3\text{H}]\text{RX821002}$ in the presence of A-412997 or YM-09151-2. Dissociation curves of the $[^3\text{H}]\text{RX821002}$ in the absence (black curve) or presence of either the D_4R agonist A-412997 (red curve) or the D_4R antagonist YM-09151-2 (blue curve) were performed at 12°C on membranes from HEK-293T cells expressing $\text{D}_{4,4}\text{R}$ and $\alpha_{2\text{A}}\text{R}$ receptors. Data were fit by the dissociation equation that appears in Methods section. Representative experiment of 3 experiments performed in triplicate (see Table 3 for $k_{\text{off}1}$ and $k_{\text{off}2}$ values and statistical comparisons).

$\text{D}_{4,4}\text{R}$ and $\text{D}_{4,7}\text{R}$ form heteromers with $\alpha_{2\text{A}}\text{R}$ in brain tissues

Biophysical techniques such as BRET assays cannot be easily applied in native tissue, but other direct and indirect methods can be used. Thus, by the proximity ligation assay (PLA) using an anti- D_4R and an anti- $\alpha_{2\text{A}}\text{R}$ antibodies, we looked for evidence of expression of $\alpha_{2\text{A}}\text{R}$ - D_4R heteromers in striatum and cortex of knock-in $\text{hD}_{4,7}$ mice as compared with WT littermates, which express a mouse D_4R with a shorter third intracellular loop comparable to the human $\text{D}_{4,2}\text{R}$ (González et al., 2012a). The PLA technology requires that the two interacting receptors be close enough to allow the antibody-probes to be able to ligate. If the receptors are at <17 nm, a punctuate fluorescent signal can be detected by confocal microscopy (Söderberg et al., 2008). The specificity of the anti- $\alpha_{2\text{A}}\text{R}$ and anti- D_4R antibodies used was tested by immunohistochemistry comparing the labeling in transfected and un-transfected cells (data not shown). $\alpha_{2\text{A}}\text{R}$ - D_4R staining was significantly observed in cortex and in striatum of both animals as compared to the staining in the corpus callosum, showing that the signal is specific (Fig. 10). The same results as with WT mice were obtained with rat cortex and striatum (Fig 10). We found significant more heteromers in cortex than in striatum in WT mice and in rats (Fig 10B). These results are according to the higher expression of $\alpha_{2\text{A}}\text{R}$ found in cortex (0.34 ± 0.01 pmol/mg protein) compared to in striatum (0.11 ± 0.01 pmol/mg protein) in sheep reported by Sánchez-Soto et al. (2018) and also the higher expression of D_4R in cortex than in striatum in several animal species and in humans (Khan et al., 1998; Tarazi et al., 1998; Svingos et al., 2000; Lauzon and Laviolette, 2010).

PLA assay was also used to evaluate the ability of peptides with the amino acid sequence of transmembrane domains (TMs) of D_4R to destabilize $\alpha_{2\text{A}}\text{R}$ - D_4R heteromers, as recently described for other receptors such as adenosine $\text{A}_{2\text{A}}\text{R}$ -dopamine D_2R heteromer (Bonaventura et al., 2015) and for dopamine D_1R - D_3R heteromers (Guitart et al., 2014). These experiments with disrupting peptides suggested the involvement of TM4 from D_4R in the $\alpha_{2\text{A}}\text{R}$ - D_4R heteromer interface in cortex slices from WT mice. TM5 and TM7 did not alter the PLA quantification (Fig. 10C).

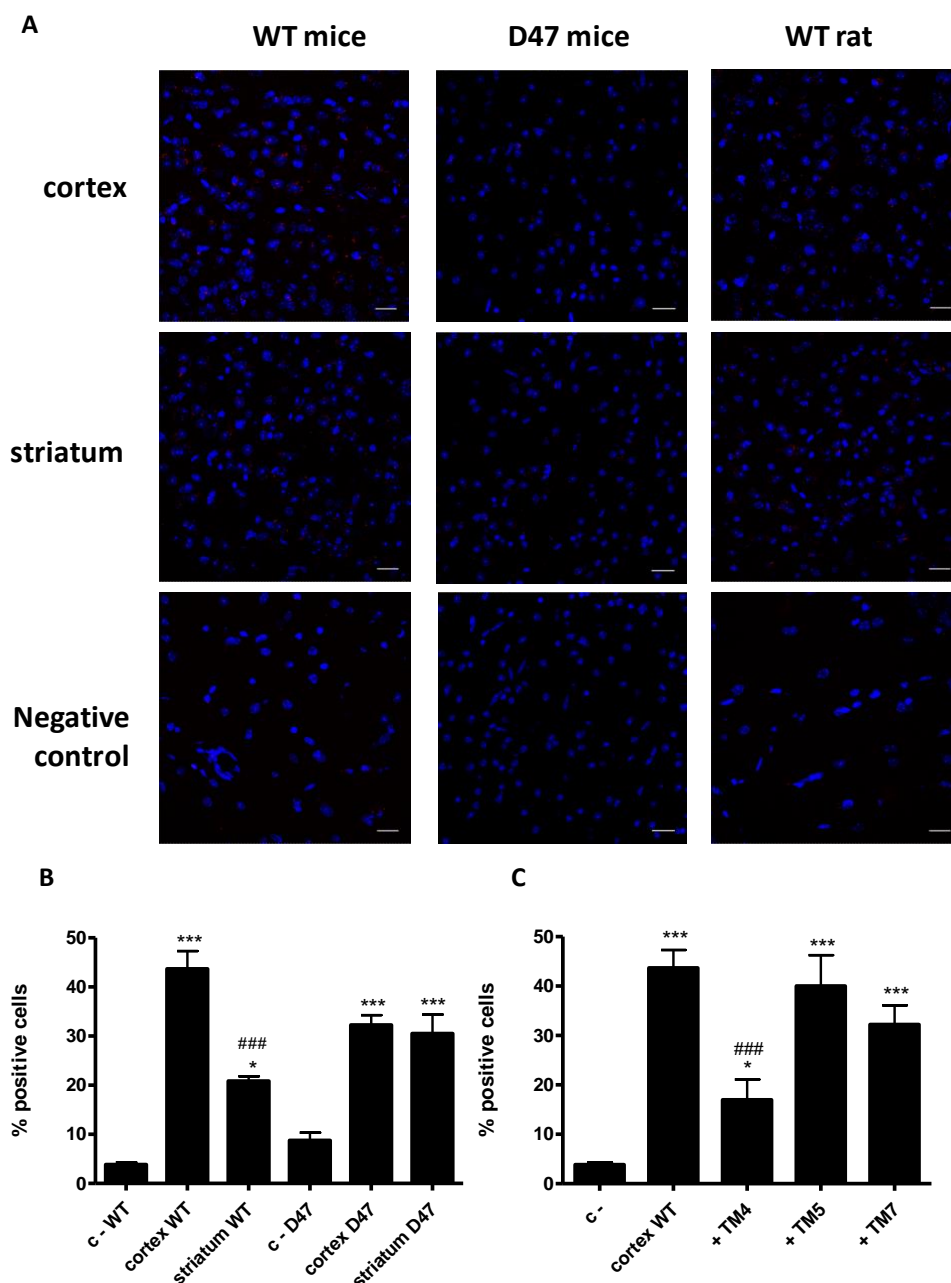


Figure 10. Detection of $\alpha_{2A}R$ -D₄R heteromers by PLA in cortex and striatum slices from rats and knock-in hD_{4,7}R and WT mice and disturbing effect of D₄R TMs peptides. (A) Quantification of PLA assays in cortex and striatum slices from WT rats and WT and knock-in hD_{4,7}R mice (B) Quantification of PLA assays in cortex of WT mice in the absence or presence of peptides with the sequence of several transmembrane domains (TM4, TM5 and TM7) of D₄R. Cortical slices were treated for 4 h with vehicle or with 4 μ M of each interference peptides before performing proximity ligation assays. The number of cells containing one or more red spots ($\alpha_{2A}R$ -D₄R heteromers) is expressed as the percentage of the total number of cells in striatum and cortex. Data (percentage of positive cells) are the mean \pm SEM of counts in 8–12 different fields of 3 different experiments. * $p < 0.05$ ***, $p < 0.001$ vs. the respective negative control; ### $p < 0.01$, ### $p < 0.001$ vs. cortex WT (one-way ANOVA followed by Dunnett's post hoc test). (C) Confocal microscopy images of cortex and striatum slices from WT and knock-in hD_{4,7}R mice (superimposed sections) are shown where heteromers appear as red spots. In all cases, cell nuclei were stained with DAPI (blue). Scale bars = 20 μ m.

After confirming the expression of this heteromers *ex vivo*, we wanted to further characterize the α_{2R} -D₄R heteromer fingerprint in WT mice cortical slices (cross-talk), at the level of MAPK activation (Fig. 11). This signaling pathway also showed a similar pattern than in

transfected cells. As expected, the α_2 R agonist dexmedetomidine and the D₄R agonist A-412997 increased ERK phosphorylation (activation), whereas co-incubation with both agonists abrogated ERK 1/2 phosphorylation confirming the negative cross-talk observed in cells expressing D_{4.4}R and α_{2A} R (Fig 11A). The treatment with TM4 again seemed to disturb the receptor-receptor modulation, reducing the negative cross-talk within the heteromer (Fig. 11B). TM5 seems to not alter the negative cross-talk (Fig 11C).

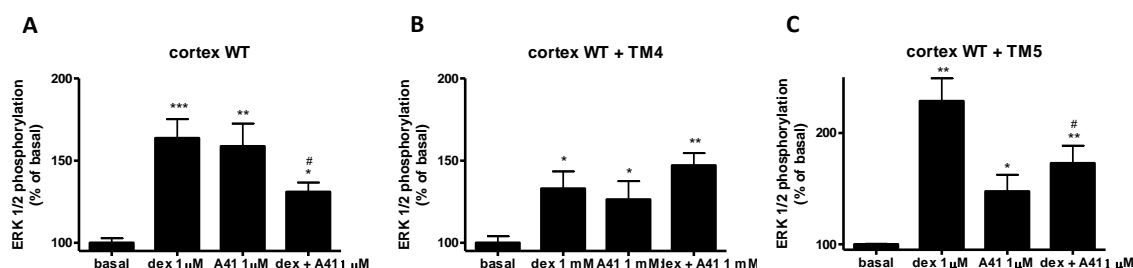


Figure 11. α_2 R-D₄R interaction at the level of ERK 1/2 phosphorylation in cortical brain slices from WT mice. Quantification of phosphorylated ERK 1/2 of cortical brain slices from WT mice was determined by western blot. Cortical slices were treated for 4 h with vehicle or with 4 μ M of each interference peptides before the activation with 1 μ M dexmedetomidine (α_2 R agonist) or with 1 μ M A-412997 (D₄R agonist) or coactivated with both agonists for 5 min at 23°C. Values are expressed as mean \pm SEM of 3-4 independent experiments performed in quadruplicate of percentage of phosphorylation relative to basal levels in not treated cells. * p <0.05, ** p <0.01 and *** p <0.001 vs. the respective basal; # p <0.05 vs. 1 μ M dexmedetomidine (one-way ANOVA followed by Dunnett's post hoc test).

Discussion

DRD4 polymorphic variants have been suggested to be associated with numerous behavioral individual differences and neuropsychiatric disorders. The most reported association is the link between the variant with seven repeats and ADHD (Faraone et al., 2005; Li et al., 2006; Gizer et al., 2009; Kim et al., 2012; Cummins et al., 2014) and SUDs (McGeary, 2009; Belcher et al., 2014). Yet, very little is known about the role of the D₄R in the brain and even less about the functional differences between the products of the different polymorphic variants, which should explain their noticeable influence at the behavioral level.

In the present study, using biophysical, pharmacological, functional and immunochemical independent approaches in transfected cells and in brain slices, we have obtained several findings that lead to four major conclusions. First, we provide strong support for the formation of α_{2A} R-D₄R heteromers that are expressed and functionally active in transfected cells; to our knowledge, it is the first heteromer described between α_2 R and D₄R (both D_{4.4}R and D_{4.7}R variants). Second, the α_{2A} R-D₄R heteromer shows new allosteric properties such as a negative cross-talk upon co-stimulation of both receptors by their agonists, and cross-antagonism, since antagonist binding to D₄R breaks agonist function on α_{2A} R. Third, these allosteric interactions are D₄R variant-dependent, because they are only evident with D_{4.4}R but not with D_{4.7}R variant. Finally, we have demonstrated that the α_{2A} R-D₄R heteromer is also present and functional in rodent brain tissues, even in knock-in hD_{4.7} mice.

Our *in vitro* results of BRET, BiFC and BiLC show, for the first time, that α_{2A} R specifically heteromerizes with D₄R variants. The D_{4.7}R variant, associated with ADHD, showed a decreased affinity (increased BRET₅₀) and lower BRET_{max} when compared to the common variant D_{4.4}R. It therefore may suggest that D_{4.4}R more easily form heteromers with α_{2A} R. This was also the case for the D_{2L}R–D₄R heteromer reported by Borroto-Escuela et al. (2011). In that work, the BRET₅₀

of the D_{2L}R–D_{4.4}R heteromer showed a significantly higher affinity compared with the D_{2L}R–D_{4.7}R. On the other hand, Gonzalez et al. (2012a) indicated a small BRET signal between the D_{4.7}R and the short variant of D₂R (D_{2S}R), but Sánchez-Soto et al. (in preparation) suggest a significant and functional heteromerization between D_{2S}R–D_{4.7}R.

We also propose a heterotetrameric structure of this complex based in BRET with BiLC and BiFC formed by a heteromer of α_{2A} R and D₄R homodimers. A similar structure has been suggested for the dopamine D₁-D₃ receptor (Guitart et al., 2014), the adenosine A_{2A}-dopamine D₂ receptor (Bonaventura et al., 2015; Navarro et al., 2018) and the adenosine A₁-A_{2A} receptor (Navarro et al., 2016) complexes. This structural model could predict complex allosteric modulations after the binding of agonists and/or antagonists within the oligomer, which may have important pharmacological implications, as reported for the A_{2A}R-D₂R heterotetramer (Bonaventura et al., 2015). Despite we have demonstrated the existence of higher order oligomers, the further characterization was performed with heterodimers, which is enough to justify the allosteric interactions analyzed.

By using CODA-RET, we have demonstrated the existence of functional Gi-mediated signaling complexes between α_{2A} R and D₄R *in vitro*. Both D₄R variants have the same potency and efficacy for the endogenous neurotransmitters NE and DA and is the heteromerization with α_{2R} who exposes the functional and pharmacological differences between the variants. α_{2A} R determines NE-mediated Gi-dependent signaling in both heteromers. In contrast, both α_{2A} R and D_{4.4}R, but not D_{4.7}R, determine DA-mediated Gi-dependent signaling. In addition, it is important to notice the differential profile of the D₂-like receptor agonists currently used for the treatment of Restless Leg syndrome and Parkinson's disease, pramipexole, ropinirole and rotigotine, which are more potent at the α_{2A} R-D_{4.4}R than at the α_{2A} R-D_{4.7}R. Moreover, NE agonists clinically used for the treatment of ADHD, clonidine and guanfacine, also have a different profile depending on the heteromer, being more potent and having higher efficacies for the α_{2A} R-D_{4.7}R. So, these drugs may have different clinical efficacies depending on the DRD4 polymorphism expressed. This would suggest the need for genotyping in order to provide the most appropriate therapeutic agent for these diseases and also highlights new differences between the D₄R variants only evident upon heteromerization with α_{2A} R.

We have also observed a negative cross-talk between both receptors within the α_{2R} -D_{4.4}R heteromer by analyzing global cell signaling, cAMP levels and ERK phosphorylation. In addition, a cross-antagonism of D_{4.4}R on α_{2A} R was detected. These allosteric interactions are not evident within the α_{2A} R-D_{4.7}R heteromer upon agonist or antagonist binding. Similar results with ERK phosphorylation were detected within the D₂R-D₄R heteromer, with both D_{2S}R and D_{2L}R variants. In these heteromers, a positive cross-talk was detected with the D_{4.4}R but not with the D_{4.7}R variant (Borroto-Escuela et al., 2011; González et al., 2012a). The 7 tandem repeats of the proline rich sequence of 16 amino acids in the intracellular loop 3 of the D_{4.7}R may cause this protein to have a very high disorder index (Woods, 2010), which may alter the development of cross-talk and cross-antagonism. Our results are of interest because variant differences can have important implications for understanding the pathogenesis of ADHD and can give new clues for the rational design of α_{2A} R-D₄R targeted drugs for its treatment.

By radioligand dissociation experiments in transfected HEK-293T cells we also detected the $\alpha_{2A}R$ -D₄R heteromerization. In these experiments, D₄R ligands were able to modify the slow dissociation rate constant of the $\alpha_{2A}R$ radioligand. The dissociation rate of a pre-bound GPCR orthosteric ligand complex can only be modified by the concomitant binding of a modulator to a topographically distinct site, which can be on the same protomer (allosteric site) or on another protomer in a homodimer (orthosteric or allosteric site) (May et al., 2007).

Apart from giving evidence of dimer-specific properties, like specific signaling or binding properties or the existence of dimer-selective ligands in heterologous system, in order to define the physiological relevance of GPCR heteromers, their physical interaction has to be verified in native tissues (Pin et al., 2007; Gomes et al., 2016). In order to assess this objective, we used the PLA technology, which allow the determination of two interacting receptors in tissue slices if are at <17 nm. We performed PLAs in cortex and striatum of knock-in hD4.7 mice and of WT littermates, confirmed the presence of heteromers between $\alpha_{2A}R$ and the two variants of D₄R *ex vivo*. Previous studies have shown PLA to be semiquantitative and particularly useful at lower expression levels (Mocanu et al., 2011). Viñals et al. (2015) observed an increase in PLA signal with increasing cDNA. Thus, we can conclude that in WT mice there are more heteromers in cortex than in striatum and similar levels can be detected in tissues from knock-in hD4.7 mice.

In this study we have also confirmed the signaling fingerprint of $\alpha_{2A}R$ with the D₄R WT variant at MAPK level detected in transfected cells, confirming their expression in native tissues. In addition, an even more conclusive demonstration can be accomplished by directly probing the biochemical property of the heteromer with the *ex vivo* application of a specific disruptive peptide (Bonaventura et al., 2015; Viñals et al., 2015; Moreno et al., 2017, 2018). In this context, TM4 of the D₄R was able to destabilize $\alpha_{2A}R$ -D₄R heteromers, decreasing the heteromer detection in PLA assays and also disturbing the receptor-receptor modulation, reducing the negative cross-talk within the heteromer, at the level of MAPK activation. TM5 did not alter the PLA nor the negative cross-talk. Determining the transmembrane domains involved in the heteromer interface can facilitate the generation of a model of the heteromeric complex that can give new clues for the rational design of true bivalent compounds heteromer-specific. These compounds may be more selective and potent for the treatment of ADHD and SUD.

The physiological relevance of the present study is that we have identified $\alpha_{2A}R$ -D₄R heteromers in cortex and striatal tissues where both receptors negatively modulate glutamatergic cell activity. Due to the negative cross-talk between $\alpha_{2A}R$ and D₄R within the heteromer, the co-activation of both receptors would produce an attenuation of the inhibition of glutamate in the corticostriatal glutamatergic neurons postsynaptically at the dendritic level in the PFC and presynaptically in the striatum. There are no previous evidences saying that there are presynaptic $\alpha_{2A}R$ s in the striatum but, since D₄R are only presynaptic and we have detected PLA signal in this brain area, we have to assume that these heteromers are located presynaptically. This coactivation could be mediated by NE and/or DA because $\alpha_{2A}R$ and D₄R receptors are able to bind both chatecolamine neurotransmitters and generate a signal (Zhang et al., 1999; Cornil et al., 2008; Alachkar et al., 2010; Sánchez-Soto et al., 2016, 2018). This provides a new mechanism by which NE and DA may regulate glutamatergic neurotransmission. The fact that the heteromer with the D_{4.7}R variant does not show this negative cross-talk may generate presynaptically in the striatum an increase of the glutamate inhibition. This should affect the activity of both the “Go” and “NoGo” GABAergic striatal efferent pathways, decreasing

their respective ability to increase the reactivity to reward-related stimuli and to suppress the reactivity to non-rewarded- or aversive-related stimuli (Bromberg-Martin et al., 2010). This may result in an increased “interest” for irrelevant stimuli and a reduced inhibition of irrelevant responses, which could be important in explaining the attention deficit and impulsivity of ADHD (Bonaventura et al., 2017). In addition, the apparent contradictory clinical results obtained upon treatment with the α_{2A} R agonists clonidine and guanfacine, can be explained by their binding to presynaptic autoreceptors in the PFC decreasing NE release and, thus, reducing stress related to high NE levels that bound to α_1 R and β R and that decreased the ratio signal/noise (Shinba et al., 2001; Broese et al., 2012). Moreover, these agonists, may also bind to post-synaptic α_{2A} R, reducing the activation generated by endogenous catecholamines because they act as partial agonists, as we could detect in CODA-RET assays.

In summary, the present results demonstrate the presence of α_{2A} R-D₄R heteromers in PFC and in striatum, where they exert a fine-tune modulation of glutamate release. Therefore, this heteromer could constitute an important target for drug development for the treatment of ADHD and SUD.

Funding and disclosure

This research was supported by “Ministerio de Economía y Competitividad” and European Regional Development Funds of the European Union (Grant SAF2014-54840-R and SAF2017-87629-R), “Centro de Investigación Biomédica en Red sobre Enfermedades Neurodegenerativas” (Grant CB06/05/0064), the “Fundació La Marató de TV3” (Grant 20140610), and intramural funds of the National Institute on Drug Abuse. The authors declare no biomedical financial interests or potential conflicts of interest.

References

- Alachkar A, Brotchie JM, Jones OT (2010) Binding of dopamine and 3-methoxytyramine as L-DOPA metabolites to human alpha(2)-adrenergic and dopaminergic receptors. *Neurosci Res* **67**:245-249. doi:10.1016/j.neures.2010.03.008.
- Albrecht B, Brandeis D, Uebel-von Sandersleben H, Valko L, Heinrich H, Xu X, Drechsler R, Heise A, Kuntsi J, Müller UC, Asherson P, Steinhausen HC, Rothenberger A, Banaschewski T (2014). Genetics of preparation and response control in ADHD: the role of DRD4 and DAT1. *J Child Psychol Psychiatry* **55**:914-923. doi: 10.1111/jcpp.12212.
- Aoki C, Venkatesan C, Go CG, Forman R, Kurose H (1998) Cellular and subcellular sites for noradrenergic action in the monkey dorsolateral prefrontal cortex as revealed by the immunocytochemical localization of noradrenergic receptors and axons. *Cereb Cortex* **8**:269-277.
- Arnsten AF (2007) Catecholamine and second messenger influences on prefrontal cortical networks of "representational knowledge": a rational bridge between genetics and the symptoms of mental illness. *Cereb Cortex* **1**:6-15.
- Arnsten AF, Li BM (2005) Neurobiology of executive functions: catecholamine influences on prefrontal cortical functions. *Biol Psychiatry* **57**:1377-1384.

Arnsten AF, Cai JX, Goldman-Rakic PS (1988) The alpha-2 adrenergic agonist guanfacine improves memory in aged monkeys without sedative or hypotensive side effects: evidence for alpha-2 receptor subtypes. *J Neurosci* **8**:4287-4298.

Arnsten AF, Paspalas CD, Gamo NJ, Yang Y, Wang M (2010) Dynamic Network Connectivity: A new form of neuroplasticity. *Trends Cogn Sci* **14**:365-375. doi: 10.1016/j.tics.2010.05.003.

Asghari V, Sanyal S, Buchwaldt S, Paterson A, Jovanovic V, Van Tol HH (1995) Modulation of intracellular cyclic AMP levels by different human dopamine D4 receptor variants. *J Neurochem* **65**: 1157-1165.

Belcher AM, Volkow ND, Moeller FG, Ferré S (2014) Personality traits and vulnerability or resilience to substance use disorders. *Trends Cogn Sci* **18**:211-217.

Bonaventura J, Navarro G, Casadó-Anguera V, Azdad K, Rea W, Moreno E, Brugarolas M, Mallol J, Canela EI, Lluís C, Cortés A, Volkow ND, Schiffmann SN, Ferré S, Casadó V (2015) Allosteric interactions between agonists and antagonists within the mechanism adenosine A2A-dopamine D2 receptor heterotetramer. *Proc Natl Acad Sci USA* **11**:E3609–3618.

Bonaventura J, Quiroz C, Cai NS, Rubinstein M, Tanda G, Ferré S (2017) Key role of the dopamine D4 receptor in the modulation of corticostriatal glutamatergic neurotransmission. *Sci Adv* **3**:e1601631. doi: 10.1126/sciadv.1601631.

Borrito-Escuela DO, Van Craenenbroeck K, Romero-Fernandez W, Guidolin D, Woods AS, Rivera A, Haegeman G, Agnati LF, Tarakanov AO, Fuxe K (2011). Dopamine D2 and D4 receptor heteromerization and its allosteric receptor–receptor interactions. *Biochem Biophys Res Commun* **404**:928–934.

Broese M, Riemann D, Hein L, Nissen C (2012) α -Adrenergic receptor function, arousal and sleep: mechanisms and therapeutic implications. *Pharmacopsychiatry* **45**:209-16. doi: 10.1055/s-0031-1299728.

Bromberg-Martin ES, Matsumoto M, Hikosaka O (2010) Dopamine in motivational control: Rewarding, aversive, and alerting. *Neuron* **68**:815-834.

Brown MR, Sidhu GS, Greiner R, Asgarian N, Bastani M, Silverstone PH, Greenshaw AJ, Dursun SM (2012) ADHD-200 Global Competition: diagnosing ADHD using personal characteristic data can outperform resting state fMRI measurements. *Front Syst Neurosci* **6**:69. doi: 10.3389/fnsys.2012.00069.

Casadó V, Cortés A, Ciruela F, Mallol J, Ferré S, Lluís C, Canela EI, Franco R (2007) Old and new ways to calculate the affinity of agonists and antagonists interacting with G-protein-coupled monomeric and dimeric receptors: the receptor-dimer cooperativity index. *Pharmacol Ther* **116**:343-354. doi:10.1016/j.pharmthera.2007.05.010.

Casadó V, Ferrada C, Bonaventura J, Gracia E, Mallol J, Canela EI, Lluís C, Cortés A, Franco R (2009) Useful pharmacological parameters for G-protein-coupled receptor homodimers obtained from competition experiments. Agonist-antagonist binding modulation. *Biochem Pharmacol* **78**:1456-1463. doi:10.1016/j.bcp.2009.07.012.

- Casadó-Anguera V, Bonaventura J, Moreno E, Navarro G, Cortés A, Ferré S, Casadó V (2016) Evidence for the heterotetrameric structure of the adenosine A2A-dopamine D2 receptor complex. *Biochem Soc Trans* **44**:595-600.
- Chang FM, Kidd JR, Livak KJ, Pakstis AJ, Kidd KK (1996) The world-wide distribution of allele frequencies at the human dopamine D4 receptor locus. *Hum Genet* **98**:91–101.
- Cook Jr EH, Stein MA, Krasowski MD, Cox NJ, Olkon DM, Kieffer JE, Leventhal BL (1995) Association of attention-deficit disorder and the dopamine transporter gene. *Am J Hum Genet* **56**:993–998.
- Cornil CA, Ball GF (2008) Interplay among catecholamine systems: dopamine binds to alpha2-adrenergic receptors in birds and mammals. *J Comp Neurol* **511**:610-627. doi:10.1002/cne.21861
- Cummins TD, Jacoby O, Hawi Z, Nandam LS, Byrne MA, Kim BN, Wagner J, Chambers CD, Bellgrove MA (2014) Alpha-2A adrenergic receptor gene variants are associated with increased intra-individual variability in response time. *Mol Psychiatry* **19**:1031–1036.
- Czermak C, Lehofer M, Liebmann PM, Traynor J (2006) [35S]GTPgammaS binding at the human dopamine D4 receptor variants hD4.2, hD4.4 and hD4.7 following stimulation by dopamine, epinephrine and norepinephrine. *Eur J Pharmacol* **531**:20-24.
- Dickstein SG, Bannon K, Castellanos FX, Milham MP (2006) The neural correlates of attention deficit hyperactivity disorder: an ALE meta-analysis. *J Child Psychol Psychiatry* **47**:1051-1062.
- Eisenhofer G, Kopin IJ, Goldstein D (2004) Catecholamine metabolism: a contemporary view with implications for physiology and medicine. *Pharmacol Rev* **56**:331-349.
- Ernst M, Zametkin AJ, Matochik JA, Jons PH, Cohen RM (1998) DOPA decarboxylase activity in attention deficit hyperactivity disorder adults. [fluorine-18]fluorodopa positron emission tomographic study. *J Neurosci* **18**:5901-5907.
- Faraone SV, Perlis RH, Doyle AE, Smoller JW, Goralnick JJ, Holmgren MA, Sklar P (2005) Molecular genetics of attention-deficit/hyperactivity disorder. *Biol Psychiatry* **57**:1313–1323.
- Fernández A, Quintero J, Hornero R, Zuluaga P, Navas M, Gómez C, Escudero J, García-Campos N, Biederman J, Ortiz T (2009) Complexity analysis of spontaneous brain activity in attention-deficit/hyperactivity disorder: diagnostic implications. *Biol Psychiatry* **65**:571-577. doi: 10.1016/j.biopsych.2008.10.046.
- Ferré S, Agnati LF, Ciruela F, Lluís C, Woods AS, Fuxe K, Franco R (2007) Neurotransmitter receptor heteromers and their integrative role in “local modules”: the striatal spine module. *Brain Res Rev* **55**:55-67.
- Ferré S, Casadó V, Devi LA, Filizola M, Jockers R, Lohse MJ, Milligan G, Pin JP, Guitart X (2014) G protein-coupled receptor oligomerization revisited: functional and pharmacological perspectives. *Pharmacol Rev* **66**:413-434.
- French GM (1959) Locomotor effects of regional ablations of frontal cortex in rhesus monkeys. *J Comp Physiol Psychol* **52**:18-24.
- Galés C, Rebois RV, Hogue M, Trieu P, Breit A, Hébert TE, Bouvier M (2005) Real-time monitoring of receptor and G-protein interactions in living cells. *Nat Methods* **2**:177–184.

- Gill M, Daly G, Heron S, Hawi Z, Fitzgerald M (1997) Confirmation of association between attention deficit hyperactivity disorder and a dopamine transporter polymorphism. *Mol Psychiatry* **2**:311–313.
- Gizer IR, Ficks C, Waldman ID (2009) Candidate gene studies of ADHD: A meta-analytic review. *Hum Genet* **126**:51–90.
- Goldman-Rakic PS (1998) The cortical dopamine system: role in memory and cognition. *Adv Pharmacol* **42**:707–711.
- Gomes I, Ayoub MA, Fujita W, Jaeger WC, Pflieger KD, Devi LA (2016) G Protein-coupled receptor heteromers. *Annu Rev Pharmacol Toxicol* **56**:403–425. doi: 10.1146/annurev-pharmtox-011613-135952.
- González S, Rangel-Barajas C, Peper M, Lorenzo R, Moreno E, Ciruela F, Boryc J, Ortiz J, Lluís C, Franco R, McCormick PJ, Volkow ND, Rubinstein M, Floran B, Ferré S. (2012a) Dopamine D4 receptor, but not the ADHD-associated D4.7 variant, forms functional heteromers with the dopamine D2S receptor in the brain. *Mol Psychiatry* **17**:650–662.
- González S, Moreno-Delgado D, Moreno E, Pérez-Capote K, Franco R, Mallol J, Cortés A, Casadó V, Lluís C, Ortiz J, Ferré S, Canela E, McCormick PJ (2012b) Circadian-related heteromerization of adrenergic and dopamine D₄ receptors modulates melatonin synthesis and release in the pineal gland. *PLoS Biol* **10**:e1001347. doi: 10.1371/journal.pbio.1001347.
- Gross CG (1963) Locomotor activity following lateral frontal lesions in rhesus monkeys. *J Comp Physiol Psychol* **56**:232–236.
- Gross CG, Weiskratz L (1964) Some changes in behavior produced by lateral frontal lesions in macaque. In: JM Warren, K Akert (eds.) *The frontal Granular Cortex and Behavior* (pp. 74–101). New York: McGraw-Hill Book Co.
- Guitart X, Navarro G, Moreno E, Yano H, Cai NS, Sánchez-Soto M, Kumar-Barodia S, Naidu YT, Mallol J, Cortés A, Lluís C, Canela EI, Casadó V, McCormick PJ, Ferré S (2014) Functional selectivity of allosteric interactions within G protein coupled receptor oligomers: The dopamine D1-D3 receptor heterotetramer. *Mol Pharmacol* **86**:417–429.
- Guo, W., Urizar, E., Kralikova, M., Mobarec, J. C., Shi, L., Filizola, M., and Javitch, J. A. (2008) Dopamine D2 receptors form higher order oligomers at physiological expression levels. *EMBO J* **27**:2293–2304.
- Hara M, Fukui R, Hieda E, Kuroiwa M, Bateup HS, Kano T, Greengard P, Nishi A (2010) Role of adrenoceptors in the regulation of dopamine/DARPP-32 signaling in neostriatal neurons. *J Neurochem* **113**:1046–1059. doi:10.1111/j.1471-4159.2010.06668.x.
- Holmberg M, Scheinin M, Kurose H, Miettinen R (1999) Adrenergic alpha_{2C}-receptors reside in rat striatal GABAergic projection neurons: comparison of radioligand binding and immunohistochemistry. *Neuroscience* **93**:1323–1333
- Jovanovic V, Guan HC, Van Tol HH (1999) Comparative pharmacological and functional analysis of the human dopamine D4.2 and D4.10 receptor variants. *Pharmacogenetic* **9**:561–568.
- Kazmi MA, Snyder LA, Cypess AM, Graber SG, Sakmar TP (2000) Selective reconstitution of human D4 dopamine receptor variants with Gi alpha subtypes. *Biochemistry* **39**:3734–3744.

- Kennard M A, Spencer S, Fountain G (1941) Hyperactivity in monkeys following lesions of the frontal lobes. *J Neurophysiol* **4**:512-524.
- Khan ZU, Gutiérrez A, Martín R, Peñafiel A, Rivera A, De La Calle A (1998) Differential regional and cellular distribution of dopamine D2-like receptors: an immunocytochemical study of subtype-specific antibodies in rat and human brain. *J Comp Neurol* **402**:353-371.
- Kim S, Bobeica I, Gamo NJ, Arnsten, AF, Lee D (2012) Effects of α -2A adrenergic receptor agonist on time and risk preference in primates. *Psychopharmacology* **219**:363–375.
- Kreusser MM, Lehmann LH, Haass M, Buss SJ, Katus HA, Lossnitzer D (2017) Depletion of cardiac catecholamine stores impairs cardiac norepinephrine re-uptake by downregulation of the norepinephrine transporter. *PLoS One* **12**:e0172070. doi: 10.1371/journal.pone.0172070.
- La Hoste GJ, Swanson JM, Wigal SB, Glabe C, Wigal T, King N, Kennedy JL (1996) Dopamine D4 receptor gene polymorphism is associated with attention deficit hyperactivity disorder. *Mol Psychiatry* **1**:121–124.
- Lauzon NM, Laviolette SR (2010) Dopamine D4-receptor modulation of cortical neuronal network activity and emotional processing: Implications for neuropsychiatric disorders. *Behav Brain Res* **208**:12-22. doi: 10.1016/j.bbr.2009.11.037.
- Li D, Sham PC, Owen MJ, He L (2006) Meta-analysis shows significant association between dopamine system genes and attention deficit hyperactivity disorder (ADHD). *Hum Mol Genet* **15**:2276–2284.
- MacDonald E, Kobilka BK, Scheinin M (1997) Gene targeting homing in on alpha 2-adrenoceptor subtype function. *Trends Pharmacol Sci* **18**:211-219.
- Mallard TT, Doorley J, Esposito-Smythers CL, McGeary JE (2016) Dopamine D4 receptor VNTR polymorphism associated with greater risk for substance abuse among adolescents with disruptive behavior disorders: Preliminary results. *Am J Addict* **25**:56-61. doi: 10.1111/ajad.12320.
- Maura G, Giardi A, Raiteri M (1988) Release-regulating D-2 dopamine receptors are located on striatal glu- tamatergic nerve terminals. *J Pharmacol Exp Ther* **247**:680–684.
- May LT, Leach K, Sexton PM, Christopoulos A (2007) Allosteric modulation of G protein-coupled receptors. *Annu Rev Pharmacol Toxicol* **47**:1-51.
- McGeary J (2009) The DRD4 exon 3 VNTR polymorphism and addiction-related phenotypes: A review. *Pharmacol Biochem Behav* **93**:222–229.
- Mocanu MM, Váradi T, Szöllősi J, Nagy P (2011) Comparative analysis of fluorescence resonance energy transfer (FRET) and proximity ligation assay (PLA). *Proteomics* **11**:2063–2070. doi: 10.1002/pmic.201100028
- Moreno E, Quiroz C, Rea W, Cai NS, Mallol J, Cortés A, Lluís C, Canela EI, Casadó V, Ferré S (2017) Functional μ -opioid-galanin receptor heteromers in the ventral tegmental area. *J Neurosci* **37**:1176-1186. doi: 10.1523/JNEUROSCI.2442-16.2016.
- Moreno E, Chiarlone A, Medrano M, Puigdemívol M, Bibic L, Howell LA, Resel E, Puente N, Casarejos MJ, Perucho J, Botta J, Suelves N, Ciruela F, Ginés S, Galve-Roperh I, Casadó V, Grandes P, Lutz B, Monory K, Canela EI, Lluís C, McCormick PJ, Guzmán M (2018) Singular location and

signaling profile of adenosine A2A-cannabinoid CB1 receptor heteromers in the dorsal striatum. *Neuropsychopharmacology* **43**:964-977. doi: 10.1038/npp.2017.12.

Mrzljak L, Bergson C, Pappy M, Huff R, Levenson R, Goldman-Rakic PS (1996) Localization of dopamine D4 receptors in GABAergic neurons of the primate brain. *Nature* **381**:245-248.

Navarro G, Cordoní A, Zelman-Femiak M, Brugarolas M, Moreno E, Aguinaga D, Perez-Benito L, Cortés A, Casadó V, Mallol J, Canela EI, Lluís C, Pardo L, García-Sáez AJ, McCormick PJ, Franco R (2016) Quaternary structure of a G-protein-coupled receptor heterotetramer in complex with Gi and Gs. *BMC Biol* **14**:26. doi: 10.1186/s12915-016-0247-4.

Navarro G, Cordoní A, Casadó-Anguera V, Moreno E, Cai NS, Cortés A, Canela EI, Dessauer CW, Casadó V, Pardo L, Lluís C, Ferré S (2018) Evidence for functional pre-coupled complexes of receptor heteromers and adenylyl cyclase. *Nat Commun* **9**:1242. doi: 10.1038/s41467-018-03522-3.

Park L, Nigg JT, Waldman ID, Nummy KA, Huang-Pollock C, Rappley M, Friderici KH (2005) Association and linkage of alpha-2A adrenergic receptor gene polymorphisms with childhood ADHD. *Mol Psychiatry* **10**:572–580.

Philipsen A, Hesslinger B, Tebartz van Elst L (2008) Attention deficit hyperactivity disorder in adulthood: diagnosis, etiology and therapy. *Dtsch Arztebl Int* **105**:311-317. doi: 10.3238/arztebl.2008.0311.

Pin JP, Neubig R, Bouvier M, Devi L, Filizola M, Javitch JA, Lohse MJ, Milligan G, Palczewski K, Parmentier M, Spedding M (2007) International union of basic and clinical pharmacology. LXVII. Recommendations for the recognition and nomenclature of G protein-coupled receptor heteromultimers. *Pharmacol Rev* **59**:5–13.

Roman T, Schmitz M, Polanczyk GV, Eizirik M, Rohde LA, Hutz MH (2003) Is the alpha-2A adrenergic receptor gene (ADRA2A) associated with attention-deficit/hyperactivity disorder?. *Am J Med Genetics Part B: Neuropsychiatric Genetics* **120B**:116–120.

Sánchez-Soto M, Bonifazi A, Cai NS, Ellenberger MP, Newman AH, Ferré S, Yano H (2016) Evidence for noncanonical neurotransmitter activation: norepinephrine as a dopamine D2-like receptor agonist. *Mol Pharmacol* **89**:457-466. doi: 10.1124/mol.115.101808.

Sánchez-Soto M, Casadó-Anguera V, Yano H, Bender BJ, Cai NS, Moreno E, Canela EI, Cortés A, Meiler J, Casadó V, Ferré S (2018) α 2A- and α 2C-Adrenoceptors as potential targets for dopamine and dopamine receptor ligands. *Mol Neurobiol* (in press) doi: 10.1007/s12035-018-1004-1.

Shinba T, Shinozaki T, Mugishima G (2001) Clonidine immediately after immobilization stress prevents long-lasting locomotion reduction in the rat. *Prog Neuropsychopharmacol Biol Psychiatry* **25**:1629-1640.

Small KM, Schwarb MR, Glinka C, Theiss CT, Brown KM, Seman CA, Liggett SB (2006) Alpha2A- and alpha2C-adrenergic receptors form homo- and heterodimers: the heterodimeric state impairs agonist-promoted GRK phosphorylation and beta-arrestin recruitment. *Biochemistry* **45**:4760-4767.

- Söderberg O, Leuchowius KJ, Gullberg M, Jarvius M, Weibrecht I, Larsson LG, Landegren U (2008) Characterizing proteins and their interactions in cells and tissues using the in situ proximity ligation assay. *Methods* **45**:227–232.
- Svingos AL, Periasamy S, Pickel VM (2000) Presynaptic dopamine D(4) receptor localization in the rat nucleus accumbens shell. *Synapse* **36**:222–232.
- Tarazi FI, Campbell A, Yeghiayan SK, Baldessarini RJ (1998) Localization of dopamine receptor subtypes in corpus striatum and nucleus accumbens septi of rat brain: comparison of D1-, D2-, and D4-like receptors. *Neuroscience* **83**:169–176.
- Urizar E, Yano H, Kolster R, Galés C, Lambert N, Javitch JA (2011) CODA-RET reveals functional selectivity as a result of GPCR heteromerization. *Nat Chem Biol* **7**:624–630.
- Van Craenenbroeck K, Borroto-Escuela DO, Romero-Fernandez W, Skieterska K, Rondou P, Lintermans B, Vanhoenacker P, Fuxe K, Ciruela F, Haegeman G (2011) Dopamine D4 receptor oligomerization-contribution to receptor biogenesis. *FEBS J* **278**:1333–1344. doi: 10.1111/j.1742-4658.2011.08052.x.
- Viñals X, Moreno E, Lanfumey L, Cordoní A, Pastor A, de La Torre R, Gasperini P, Navarro G, Howell LA, Pardo L, Lluís C, Canela EI, McCormick PJ, Maldonado R, Robledo P (2015) Cognitive impairment induced by delta9-tetrahydrocannabinol occurs through heteromers between cannabinoid CB1 and serotonin 5-HT2A receptors. *PLoS Biol* **13**:e1002194. doi: 10.1371/journal.pbio.1002194.
- Wang X, Zhong P, Yan Z (2002) Dopamine D4 receptors modulate GABAergic signaling in pyramidal neurons of prefrontal cortex. *J Neurosci* **22**:9185–9193.
- Wang M, Ramos BP, Paspalas CD, Shu Y, Simen A, Duque A, Vijayraghavan S, Brennan A, Dudley A, Nou E, Mazer JA, McCormick DA, Arnsten AF (2007) Alpha2A-adrenoceptors strengthen working memory networks by inhibiting cAMP-HCN channel signaling in prefrontal cortex. *Cell* **129**:397–410.
- Woods AS (2010) The dopamine D(4) receptor, the ultimate disordered protein. *J Recept Signal Transduct Res* **30**:331–336. doi: 10.3109/10799893.2010.513842.
- Xu J, He J, Castleberry AM, Balasubramanian S, Lau AG, Hall RA (2003) Heterodimerization of alpha 2A- and beta 1-adrenergic receptors. *J Biol Chem* **278**:10770–10777.
- Zhang W, Klimek V, Farley JT, Zhu MY, Ordway GA (1999) Alpha2C adrenoceptors inhibit adenylyl cyclase in mouse striatum: potential activation by dopamine. *J Pharmacol Exp Ther* **289**:1286–1292.
- Zhong P, Liu W, Yan Z (2016) Aberrant regulation of synchronous network activity by the attention-deficit/hyperactivity disorder-associated human dopamine D4 receptor variant D4.7 in the prefrontal cortex. *J Physiol* **594**:135–147.

IV- GENERAL DISCUSSION

IV. GENERAL DISCUSSION

Catecholamines including dopamine (DA) and norepinephrine (NE) are widely distributed in the body and constitute a class of conventional neurotransmitters and hormones that occupy key positions in the regulation of physiological processes and in the development of neurological, psychiatric, endocrine and cardiovascular diseases (Eisenhofer et al. 2004; Kreusser et al., 2017). DA has been shown to have a key role in regulating affect, attention, behavior and cognition, motivation and reward, sleep and voluntary movement (Jauhar et al., 2017). NE is involved in alertness, mood, arousal, learning and memory, motor control, blood flow, and metabolism (Costa et al., 2012; Schwarz and Luo, 2015; Díaz-Mataix et al., 2017). DA system has been a main focus of interest during the last decades mainly due to its role in pathologies such as Parkinson's disease, attention deficit hyperactivity disorder (ADHD), schizophrenia, Tourette syndrome, Huntington disease, Restless Leg syndrome and substance abuse disorder (SUD), among others. NE system has also been related with several diseases within the CNS such as psychiatric disorders including major depression and ADHD, among others. In addition, adenosine, acting on adenosine receptors (AR) is a modulator of other receptors such as D₁-like and D₂-like DA receptors (Cobbin et al., 1974). DA and adenosine receptor complexes are involved in the control of the direct and indirect pathway of motor control in basal ganglia, in which adrenergic receptors are also involved (Li and Mei, 1994; Ma et al., 2003, 2005).

NE, DA and adenosine receptors belong to the GPCR family, also known as seven transmembrane domain receptors. GPCRs have an enormous biomedical importance. It is estimated that about 35% of approved drugs target GPCRs (Sriram and Insel, 2018). Thus, it is not surprising that lots of models have been developed in order to explain the pharmacological behavior of these receptors. Most of the developed models consider GPCRs as monomeric entities. The majority of these models generate an overparameterization except the "two-independent-site model" that is the approach most simple and most often used to deal with radioligand binding data. The two-independent-site model is based on two assumptions: one is that receptors are monomeric and another is that there are two populations of receptors, one is coupled to a G-protein and displays high-affinity (K_{DH}), whereas another is uncoupled from any G-protein and displays low-affinity (K_{DL}) binding for agonists.

However, during the last two decades a large number of GPCRs have been described to form homodimers, heterodimers and higher order oligomers that are often essential for the fine modulation of GPCR function (Ciruela, 2008; Casadó et al., 2007; Ferré et al., 2009a, 2010a,b, 2014; Milligan, 2009; Rivero Muller et al., 2010; Albizu et al., 2010; Gonzalez-Maeso, 2011; Ciruela et al., 2012; Lane and Canals, 2012; Miller et al., 2012; Steel et al., 2014).

Despite the clear evidence of GPCR dimerization, the fact that biphasic competition curves can be also fitted with the two-independent-site model has caused that, for simplicity, most laboratories still use monomeric classical equations instead of using dimer receptor models. Nevertheless, as oligomers have biochemical properties that are demonstrably different from those of their individual components (Ferré et al., 2009b), it is not surprising that, when working with receptor dimers but using monomeric models, some parameters obtained may be erroneous and some points could be underestimated in the fit. Some examples are: dissociation constants estimated in saturation and in competition experiments are dissimilar (Strange, 2005;

Maggio et al., 2013); the estimated values for the equilibrium dissociation constants and for the number of receptors vary significantly depending on the concentration of the radioligand employed (Casadó et al., 1991; Franco et al., 1996); in competition experiments, the positive cooperativity cannot be explained (Albizu et al., 2006), the same as mismatches in constant values obtained when dissociation is performed by dilution vs. by an excess of unlabeled ligand (De Meyts et al., 1973; Urizar et al., 2005; Kara et al., 2010; Gracia et al., 2013b). Moreover, depending on the radioligand employed the affinity values obtained for the competitor may vary significantly. For this reason, we went deeper into the study of the dimer receptor model (Casadó et al., 2009a) in order to find out the effect of radioligand-competitor allosteric interactions that could explain and overcome anomalous results obtained when fitting competition binding data with classical monomeric models.

In the work, **Reinterpreting anomalous competitive binding experiments assuming radioligand-competitor allosteric interactions within G protein-coupled receptor homodimers**, we have demonstrated that the radioligand-competitor interaction constant (K_{DAB}) explains the fitting of bell-shaped curves and, more importantly, can overcome scenarios where different affinity values for a competitive drug are obtained depending on the radioligand.

Effectively, all of the previous examples indicate a lack of robustness of the two-independent-site model that can be solved by using a dimer receptor model. Concretely, our group demonstrated that the dimer receptor model (Casadó et al., 2009a; Ferré et al., 2014) can explain several unexpected experimental results such as obtaining biphasic, monophasic or bell-shaped curves, and even different affinity values for the competitor (K_{DB}), depending on the radioligand concentration. Moreover, our model can also explain results previously considered erroneous due to their impossibility to be fitted such as the mentioned bell-shaped curves, where increasing concentrations of a competitor produce an increase of the radioligand binding before causing the expected displacement of such binding (Berde et al., 1964; Albizu et al., 2006). Concretely, we have shown that the existence of a radioligand-competitor allosteric interaction, deduced from the dimer receptor model (Casadó et al., 2009b), is the responsible for the correct fitting of bell-shaped curves. It is important to notice that, when bell-shaped curves are experimentally obtained, the estimated affinity values of the competitor using the equations corresponding to the dimer receptor model, which includes the K_{DAB} parameter, are closer to the actual values obtained with saturation experiments. On the contrary, the K_{DB} values obtained from classical monomeric models are commonly much higher. Moreover, applying our dimer receptor model, the affinity values obtained for a competitive drug do not change depending on the radioligand employed (Maggio et al., 2013). This is because our model takes into account that each pair of radioligand-competitor has a particular K_{DAB} value according to the magnitude of its allosteric interaction.

We have also deduced the radioligand concentration responsible for the conversion from biphasic to monophasic or to bell-shaped curves in competitive radioligand binding assays. This concentration depends on the relation among the three dissociation constants: K_{DA1} , K_{DAB} and K_{DB1} . With this information, if $K_{DAB} < K_{DB1}$, decreasing the radioligand concentration under $2K_{DA1} (K_{DB1} - K_{DAB}) / K_{DB1}$, we could deduce if a biphasic competition curve obtained with high A concentration is due to an agonist-antagonist interaction (if the bell-shaped curve appears) or due to a negative cooperativity of the displacer ligand B. This is important because a positive radioligand-competitor interaction also generates biphasic competition curves when the

concentration of A is higher than $2K_{DA1}$, even without a cooperative binding of B. This knowledge will allow the correct fitting of the data in further analysis.

In summary, we have demonstrated that bell-shaped curves are only interpretable assuming the formation of receptor homodimers and, therefore, obtaining bell-shaped curves in competition experiments is a clear evidence of receptor dimerization *in vitro* (working with membrane preparations from transfected cells) and *ex-vivo* (working with membrane preparations from tissues). However, more complex oligomers cannot be discarded.

Dimerization and the biochemical, pharmacological and biological characterization of receptor oligomers is essential for understanding the normal function of the body. Oligomerization alterations have implications in pathologies and have important repercussions in the field of GPCR pharmacology. Catecholamine receptors, especially DA receptors, are modulated by other receptors. In this context, adenosine extracellular levels, which vary according to the energetic state of the organism, control motor activation induced by DA receptors. The most representative example of these interactions, is the adenosine A_{2A} -dopamine D_2 receptor heteromer.

In the articles **“Allosteric interactions between agonists and antagonists within the adenosine A_{2A} receptor-dopamine D_2 receptor heterotetramer”**, **“Evidence for the heterotetrameric structure of the adenosine A_{2A} -dopamine D_2 receptor complex”** and **“Functional pre-coupled complexes of receptor heteromers and adenylyl cyclase”**, we have investigated the allosteric and canonical interactions within the $A_{2A}R$ - D_2R heteromer.

In this way, our study of the $A_{2A}R$ - D_2R heteromer, calls for an awareness of homodimers as predominant GPCR species, providing a significant role of allosteric interactions between orthosteric ligands within GPCR heteromers, which should have important implications in the field of GPCR pharmacology (reviewed in Ferré et al., 2014).

By radioligand dissociation experiments using the $A_{2A}R$ antagonist [3H]ZM 241385 or the D_2R antagonist [3H]YM-09151-2 in the absence or presence of $A_{2A}R$ agonist CGS 21680 or quinpirole, respectively, we demonstrated the presence of both $A_{2A}R$ - $A_{2A}R$ and D_2R - D_2R homodimers in the striatum. In addition, we have also detected $A_{2A}R$ - D_2R heteromers in brain striatum by PLA and functional assays. The effects of TM peptides of $A_{2A}R$ or D_2R on radioligand binding assays and on double complementation of BRET donor and acceptor units indicate that TM6 is involved in the $A_{2A}R$ and D_2R homodimer interfaces and TM4 and TM5 in the heterodimer interface. With this information and with the use of TM of the adenylyl cyclase 5 in double complementation of BRET donor and acceptor units assays, we determined that the $A_{2A}R$ - D_2R heteromer has a tetrameric structure, with two homodimers of $A_{2A}R$ and D_2R bound to the adenylyl cyclase subtype 5 (AC5).

Additionally, we suggest a quaternary structure of zig-zagged arranged $A_{2A}R$ - D_2R -AC5, including G_{α_s} and G_{α_i} . To our knowledge, these are the first data suggesting higher-order linear arrangements of GPCR heteromers and effectors. With all this information, we designed a computational model, where only the two internal protomers participate in the heteromeric interface and the two external protomers participate in the homomeric interface of the $A_{2A}R$ - D_2R heterotetramer. This arrangement can explain not only multiple allosteric interactions produced by different orthosteric ligands, agonists and antagonists, but also the antagonistic canonical interaction at the adenylyl cyclase (AC) level between the $G_{\alpha_{olf}}$ - $A_{2A}R$ and the G_{α_i} - D_2R .

Our structural model assumes that occupancy of the A_{2A}R homodimer with either an agonist or an antagonist produces a conformational change that conduces the same allosteric modulation to the D₂R, a decrease of its function, while simultaneous occupancy of the A_{2A}R homodimer by an agonist and an antagonist would not allow this conformational change (as we have seen by dissociation experiments of radiolabelled A_{2A}R antagonist and confirmed by MAPK signaling assays). Moreover, the zig-zagged model, where AC is between an A_{2A}R of one heterotetramer and a D₂R of a second heterotetramer, also sustains the canonical G_{αs}-G_{αi} interaction at the AC level, in which G_{αi} protein coupled to D₂R, counteract AC activation induced by the G_{αs} protein coupled to A_{2A}R. In this situation, both G_{αs} and G_{αi} must be interacting with the same AC, according to our model. It is worth mentioning that we have confirmed that these interactions constitute biochemical properties of the A_{2A}R-D₂R heteromer since they depend on the integrity of the right quaternary structure of the heteromer, as demonstrated with the application of disturbing TMs that alter the oligomeric conformation, causing an alteration of its fingerprint.

We observed that, in the striatum, under specific experimental conditions, orthosteric A_{2A}R antagonists behave as A_{2A}R agonists and decrease D₂R function, effects that are counteracted upon co-administration of both A_{2A}R agonists and antagonists (electrophysiological and locomotor activity experiments). Since under physiological conditions there are basal levels of adenosine, this could be the main mechanism by which caffeine and A_{2A}R antagonists produce locomotor activation, by counteracting the functional effects that depend on D₂R signaling within the A_{2A}R-D₂R heteromer. Nevertheless, motor depression induced by caffeine or A_{2A}R antagonists imply a significant displacement of endogenous adenosine and occupancy of the A_{2A}R homodimer in the A_{2A}R-D₂R heteromer, which can only be attained by large concentrations of caffeine that are not reached with habitual consumption of coffee. However, it is important to notice that therapeutic doses of more potent and selective A_{2A}R antagonists may have differential effects depending on the levels of endogenous adenosine. Not only that, but when adding larger concentrations of potent and selective A_{2A}R antagonists, they might generate the same effects as agonists, causing problems in the treatment of PD. Therefore, our tetrameric model for the A_{2A}R-D₂R heteromer still provides support for the use of A_{2A}R antagonists in PD, providing new clues as to how to adjust the dosage according to the expected levels of endogenous adenosine. Additionally, the complementing results obtained from functional experiments in mammalian cell culture, in striatal slices and in rats, demonstrate the previously claimed significant dependence of D₂R signaling and A_{2A}R-D₂R heteromerization on the pharmacological effects of caffeine and other A_{2A}R ligands (Azdad et al., 2009; Ferré et al., 2004; Ferré; 2008).

Our results also indicate that a large proportion of D₂R form heteromers with A_{2A}R in transfected cells and striatal tissue. Thus, a very similar degree of allosteric modulation of D₂R by A_{2A}R ligands was observed in both artificial and native systems. Particularly notorious was the ability of caffeine to allosterically (non-competitively) decrease D₂R antagonist binding by about 60% and 40% in membrane preparations of transfected cells and striatal tissue, respectively. Furthermore, the experiments with MAPK signaling in transfected cells and the electrophysiological experiments in striatal neurons demonstrate that there is an additional strong allosteric negative modulation of A_{2A}R ligands on the intrinsic efficacy of D₂R ligands, which can explain, for instance, the complete counteraction by A_{2A}R antagonists on MAPK

activation and on the decrease in neuronal excitability of individual neurons from the rat ventral striatum induced by high concentrations of D₂R agonists, which should surmount the reduction in affinity. This allosteric modulation is called cross antagonism, which is the ability of an antagonist of one receptor to antagonize the signaling of the partner receptor. This is possible because agonists stabilize conformations of TM5 and TM6 that facilitate the opening of the intracellular cavity for the G-protein binding, whereas antagonists stabilize other conformations of these helices that close the cavity. In this scenario, TM5 and TM6 of protomer A, in the closed conformation, can interact with TM5 and 6 of protomer B (via a four-helix bundle) also stabilizing its closed conformation not allowing the G-protein binding to the partner receptor (Viñals et al., 2015). The fact that rearrangement of TM6 constitutes main ligand-induced conformational changes that determine G protein activation and modulation of ligand affinity (Rasmussen et al., 2011), provides a frame for the understanding of allosteric communications through the protomers in GPCR oligomers (Han et al., 2009; Pellissier et al., 2011; Ferré et al., 2014).

The present study represents a proof of concept of the significant functional role of GPCR heteromers within a signalosome, since it demonstrates that GPCR heteromers provide the frame for biochemical interactions previously thought to be independent of intermolecular receptor-receptor interactions, on classical receptor cross-talk at the second-messenger level (Agnati et al., 2005). Therefore, we postulate that pre-coupling should not only apply to other G_{αs}-G_{αi}-AC-coupled heteromers, but also to heteromers coupled to other G proteins and effectors, such as the well-established G_{αi}-G_{αq}-coupled metabotropic glutamate receptor mGlu₂ receptor-serotonin 5-HT_{2A} receptor heteromer (Fribourg et al., 2011), which could be pre-coupled to potassium channels (Baki et al., 2016). At a more general level, the present results represent a very significant support to the still controversial concepts of GPCR pre-coupling and oligomerization. In this context, we also determined that the non-activated or agonist-activated A_{2A}R-D₂R heterotetramer is able to establish different molecular interactions with AC5. These interactions imply a major rearrangement of the TMs of the activated pre-coupled complex facilitating the interaction of AC5 catalytic domains with the corresponding G_α subunit (Sadana et al., 2009). This is allowed by the agonist-induced movement of the G_{βγ} subunits away from the helical-domain of the G_α subunit (Cabrera-Vera et al., 2003; Galés et al., 2006). This key role of the G protein in determining changes in the quaternary structure of the A_{2A}R-D₂R heterotetramer-AC5 complex upon receptor activation would agree with the recently described stable pre-coupling of striatal G_{αolf} and AC5 (Xie et al., 2015) and the here described less stable interactions between TMs of AC5 and A_{2A}R and D₂R.

Previous studies indicate that the same situation occurs *in vivo* in the striatum, where the pharmacological or genetic blockade of D₂R disinhibits adenosine-mediated activation of AC in the striato-pallidal neuron (Taura et al., 2018). In fact, A_{2A}R blockade counteracts most biochemical and behavioral effects induced by interruption of D₂R signaling (Taura et al., 2018). Also in complete agreement are the results obtained by Lee et al. (2002) with AC5 knockout mice, which show that AC5 is the principal AC integrating signals from A_{2A}R and D₂R in the striatum and that the signaling cascade involving AC5 is essential for the behavioral effects of D₂R antagonists, and therefore antipsychotic drugs. The significant control of A_{2A}R signaling by D₂R implied that most A_{2A}R that signal through AC5 are forming heteromers with D₂R in striatal neurons in culture.

The knowledge of the correct rearrangement of this protein complex and of its interprotomer modulations will allow to understand most pharmacological effects of $A_{2A}R$ and D_2R ligands in the striatum, with implications for several neuropsychiatric disorders.

With the knowledge about the structure and function acquired with the $A_{2A}R$ - D_2R heteromer we have developed a precise strategy to create bivalent ligands of GPCR homo- and hetero-dimers based on a versatile multivalent chemical platform that has been summarized in the manuscript **“Design of a true bivalent ligand with picomolar binding affinity for a G protein-coupled receptor homodimer”**.

Using computational tools that considered the TM interfaces, distances between orthosteric binding sites and the mode of interaction of the pharmacophore units, we have obtained a reduction in the number of synthesized bivalent ligands, and a higher success in affinity results. Here we describe the design of a true bivalent ligand with high affinity for the dopamine D_2 receptor (D_2R) homodimer. The selected pharmacophore unit was the D_2R antagonist spiperone which was docked into the D_2R homology model to determine the orientation of the linker and the attachment point at the extracellular domain. The spacer was formed by different length oligoethylene glycol moieties. Specifically, we used two spacer lengths: 25-atoms spacer, representing the shortest possible true bivalent interaction, and a longer alternative formed by 35-atoms. We analyzed the binding affinity of the synthesized ligands and we confirmed their antagonistic nature on D_2R signaling by DMR technique. The selected bivalent ligand 13, showed picomolar binding affinity. The affinity highly decreased in the presence of the TM6 peptide of D_2R . This was evidence of a clear simultaneous interaction with both orthosteric sites of the D_2R homodimer, constituted through TM6. Moreover, it was also a chemical tool to confirm interprotomer interaction in native tissue.

Since bivalent ligands are the best example of oligomer selective-ligands that can interact simultaneously with a homo or hetero- GPCR dimer with high affinity and subtype selectivity, improving safety and efficacy for their therapeutic targets, our protocol is the basis for the synthesis of other bivalent ligands for D_2R heterodimers with other catecholamine or adenosine receptors with therapeutic interest for the treatment of motor dysfunctions.

It is important to notice that, to obtain oligomer-selective bivalent ligands, the selected pharmacophores must be highly specific. However, it is not always easy. As an example, there is compelling evidence indicating that DA and NE promiscuously interact with each other's receptors, especially in some situations where catecholamine innervations do not coincide with the distribution of its receptors. One important example is the D_4R which is known to be both a dopaminergic and noradrenergic receptor and to act as an adrenergic receptor in certain parts of the brain (Lanau et al., 1997; Newman-Tancredi et al., 1997; Czermak et al., 2006; Cummings et al., 2010; Root et al., 2015, Sánchez-Soto et al., 2016). Recently, G_{α_i} activation, adenylyl cyclase inhibition, and β -arrestin recruitment experiments showed a relatively small separation between the potencies of NE for $\alpha_{2A}R$ and D_2 -like receptors (20-fold), verifying D_2 -like receptors as potential signal transducers for NE (Sánchez-Soto et al., 2016).

In general, It has been previously postulated that DA may be a potential α_2R ligand on the basis of radioligand binding experiments in transfected mammalian and insect cell lines (Zhang et al., 1999; Alachkar et al., 2010) and in bird and rat brains and also from autoradiographic experiments in tissues (Cornil et al., 2008). Furthermore, DA has been reported

to decrease cAMP intracellular levels in transfected mammalian cell lines but only throughout $\alpha_{2C}R$, not $\alpha_{2A}R$, and at concentrations much higher than NE (EC_{50} in the micromolar range) (Cornil et al., 2008). However, there was the controversy about the differential binding affinity of DA versus NE on α_2Rs and the potential functional efficacy of this binding.

In our study “ **α_{2A} - and α_{2C} -Adrenoceptors as Targets for Dopamine and Dopamine Receptor Ligands**”, we showed that α_{2A} and α_{2C} adrenoceptors can bind DA at concentrations in the same order than NE suggesting that they could be activated by DA at *in vivo* concentrations. First, our results demonstrated that endogenous DA, and also common synthetic DA-receptor ligands, bind to α_2R with moderate to high affinity in the mammalian brain. Second, the affinity of DA for α_2R is in the same range as for D_1 -like and D_2 -like receptors, suggesting that endogenous levels of DA can activate both α_2R and dopamine receptors. Third, DA and synthetic DA receptor ligands can activate G protein and induce cell DMR through α_2Rs . Finally, DA and NE show the same cell signaling pattern, being both capable to modulate adenylyl cyclase activity and ERK1/2 phosphorylation at nanomolar concentrations.

The most conclusive demonstration that DA is an α_2R ligand comes from the results obtained with binding and G protein activation BRET assays, where the affinities or potencies of DA for α_2Rs were found to be very similar or even higher than for D_1 -like and some subtypes of D_2 -like receptors (Sánchez-Soto et al., 2016). Particularly the EC_{50} values of DA for α_{2A} and α_{2C} adrenoceptors (5-170 nM) were consistently lower across all $G_{i/o}$ protein subtypes as compared with the EC_{50} values (130-400 nM) for the predominant striatal D_2 -like receptor D_{2L} (Sánchez-Soto et al., 2016). Taking into account that the levels of tonic extracellular DA are 20-30 nM (with peaks of 500 nM) (Owesson-White et al., 2012), DA could reach sufficient extracellular concentration to activate $\alpha_{2A}R$ and $\alpha_{2C}R$ in the striatum, irrespective of the maximal concentration of extracellular NE. In fact, striatal DA release sites are designed for transmitter spillover (Rice et al., 2011) and most striatal DA receptors are primarily extrasynaptic (Hersch et al., 1995; Yung et al., 1995), as well as striatal adrenoceptors, based on the mismatched low NE innervation (Ordway et al., 1993; Uhlen et al., 1997; Lindvall and Bjorklund, 1974; Swanson and Hartman, 1975; Aston-Jones, 2004). Although the specific functional role of the DA-sensitive α_2 adrenoceptors in neuronal striatal function remains to be established, a previous study suggests that they might mediate an inhibitory modulatory role of the $G_{s/olf}$ -coupled striatal adenosine A_{2A} and DA D_1 receptors (Hara et al., 2010).

The possibility of DA-mediated activation of α_{2A} and α_{2C} adrenoceptors in extrastriatal areas should not however, be underestimated. Cortical α_{2A} adrenoceptors are most probably able to be activated by DA, particularly in the prefrontal cortex, which receives a rather dense DA innervation (Goldman-Rakic et al., 1992). In fact, there is recent evidence for the localization of α_{2A} adrenoceptors in the cortical terminals from mesencephalic DA neurons (Castelli et al., 2016), which could play a role as “DA autoreceptors”. But there is also evidence for the localization of both α_{2A} and α_{2C} adrenoceptors in the soma and dendrites of the mesencephalic DA cells of both substantia nigra and ventral tegmental area (Castelli et al., 2016; Lee et al., 1998). Apart from the NE input, these α_{2A} and α_{2C} adrenoceptors should be able to act as “DA autoreceptors” that control the non-synaptic somatodendritic DA release (Rice et al., 2011). Adding the present results to our recent study that also indicates a significant role of NE as a $G_{\alpha i/o}$ -coupled D_2 -like receptor agonist (Sánchez-Soto et al., 2016), we could state that $G_{\alpha i/o}$ -

coupled adrenoceptors and DA receptors should probably be considered as members of one 'functional' family of catecholamine receptors. A general consideration from the DA and D₂-like receptor ligand sensitivity of cortical α_{2A} adrenoceptors is that it should also be involved in the cognitive-enhancing effects associated with their activation, with possible implications for attention deficit hyperactivity disorder (Brennan and Arnsten, 2008).

Molecular modeling of DA binding to the various receptors provides a likely binding hypothesis for the results obtained in the biological assays. Of note is the striking similarity between the ligand binding pocket of the D₃ receptor and that of α_{2A} and α_{2C} adrenoceptors. Many of the residues that line the binding pocket are identical or chemically well conserved. Given this similarity it was perhaps unsurprising that the docking of DA at α_{2A} and α_{2C} was nearly identical to DA binding to the D₃ receptor. The lower potency of DA at α_{2A} and α_{2C} adrenoceptors compared to NE seems to depend on a lower number of strong interactions as compared to those between DA and D₃ receptors. The pocket may have evolved to bind the slightly bulkier NE and therefore is not of an ideal size for DA. However, the differences may also be due to the lower resolution of binding predictions for a comparative model as opposed to a crystal structure. Despite this, the structural model strongly mimics the results of the binding and activation experiments and therefore provides further evidence of DA acting as a ligand at these receptors.

Another major finding of the present study is that α_{2A} and α_{2C} adrenoceptors are also common targets for compounds previously characterized as D₂-like receptor ligands. Particularly striking was the ability of prototypical D₃ and D₄ receptor agonists 7-OH-PIPAT and RO-105824 to bind with high affinity to α_{2A} and α_{2C} adrenoceptors, which might call for revisiting results of previous studies using these compounds. Furthermore, these two compounds and the other DA-synthetic ligands assayed, as well as NE, were able to activate ERK1/2 phosphorylation by binding to α_2 adrenoceptors. The final pharmacological profile of RO-105824 was that of a potent biased agonist for α_{2A} adrenoceptor agonist with functional selectivity for a G protein-independent signaling. On the other hand, based on BRET experiments, both potency and efficacy dependence on the receptor and the G_{ai/o} protein subtype was the norm for all ligands, including the endogenous neurotransmitters. We already described that NE and DA show different receptor- and G_{ai/o} subtype-dependent potencies of D₂-like receptor-mediated G protein activation (Sánchez-Soto et al., 20016). The present results extend these findings to other receptors and to non-endogenous ligands, as well as to differences in efficacy. Even though G proteins of the G_{as}-G_{oif} family do show contrasting brain expression pattern (Herve, 2011), to our knowledge no clear region-specific pattern of mRNA expression for G_{ai/o} protein subtypes has been reported. Detailed characterization of the expression patterns for G_{ai/o} protein subtypes would then be central to determine their role in α_{2A} R and α_{2C} R-activation and thus their possible specific targeting with G_{ai/o} subtype functionally selective compounds.

In conclusion, DA is a potent and efficacious ligand at α_2 R, which modulates forskolin-induced adenylyl cyclase activity and ERK1/2 phosphorylation. The concentration required for these effects is in the range of that for activating D₂-like and D₁-like receptors, indicating that these receptors are members of one "functional" family of catecholamine receptors. Our results provide a clear answer to the mismatch between the low striatal NE innervation and the high density of striatal α_2 R, which behave as functional DA receptors.

Both catecholamine D₂ and D₄ receptors co-localize in the corticostriatal pyramidal neurons of the layer V both pre- and post-synaptically, controlling glutamate release in the striatum (Almeida y Mengod, 2010; Bonaventura et al., 2017) and, consequently, the activation of the indirect pathway of the movement. In addition to D₂-like, the catecholamine α_{2A} R has also been associated with ADHD and action impulsivity (Ma et al., 2003, 2005; Arnsten and Li, 2005; Cummins et al. 2014) and is, as well, present both in the PFC and basal ganglia (Fagerholm et al., 2008; Santana N et al., 2013; Zhang et al., 2013; Lehto et al., 2015). Thus, in view of the common epidemiological and pharmacological involvement of D₂R, D₄R and α_{2A} R in impulse control and the observed promiscuity of DA and NE in their ability to activate both G _{α i/o}-coupled receptors, in the manuscripts **“Revisiting the functional role of dopamine D₄ receptor gene polymorphisms: Heteromerization-dependent gain of function of the D_{4.7} receptor variant”** and **“Functional differences between dopamine D_{4.4} and D_{4.7} receptor variants within the dopamine D₄-adrenergic α_{2A} receptor heteromer in the brain”**, we have investigated and demonstrated the existence of the D₄R-D_{2S}R and D₄R- α_{2A} R heteromers, with possible important functions in motor control and action impulsivity, and we have characterized their different pharmacological properties depending on the D₄R variant involved.

The two most common polymorphisms of the human *DRD4* gene encode a D₄R with four or seven repeats of a proline-rich sequence of 16 amino acids (D_{4.4}R or D_{4.7}R). Although D_{4.7}R has been associated with ADHD (Swanson et al., 2007; Froehlich et al., 2011), the differential functional properties between both variants remained enigmatic until recent electrophysiological and optogenetic-microdialysis experiments that indicated a gain of function of D_{4.7}R (Bonaventura et al., 2017). Since no clear differences in the biochemical properties of individual D_{4.4}R and D_{4.7}R (e.g. in their ability to activate G _{α i} protein subtypes, inhibit adenylyl cyclase or recruit β -arrestin) (Sánchez-Soto et al., 2016) have been reported, it became therefore plausible that differential functional interactions with other receptors could provide an explanation for the differential attributes of D₄R variants described at the level of brain function and dysfunction (Borroto-Escuela et al., 2011; González et al., 2012b).

Thus, in the present study, with the use of the CODA-RET technique, we could demonstrate the existence of functional D₄R-D_{2S}R *in vitro*. Moreover, with the use of CODA-RET, radioligand binding and functional assays in transfected cells and in brain slices, we could demonstrate the existence of functional D₄R- α_{2A} R *in vitro* and in rodent brains. PLA assays were also performed in cortex and striatum of knock-in hD_{4.7} mice, confirming indeed the presence of heteromers between α_{2A} R and the D_{4.7}R *ex vivo*. Previous studies have shown PLA to be semiquantitative and particularly useful at lower expression levels (Mocanu et al., 2011). Viñals et al. (2015) observed an increase in PLA signal with increasing cDNA. Thus, we can conclude that in WT mice there are more heteromers in cortex than in striatum and similar levels can be detected in tissues from knock-in hD_{4.7} mice. The description of both heteromers is very important because both α_{2A} R and the D₂-like receptors are involved in the pathophysiology and treatment of disorders related with a lack of impulse control.

BRET experiments showed a decreased affinity (increased BRET₅₀) of the α_{2A} R-D_{4.7}R heteromer, when compared to the common variant D_{4.4}R. It therefore may suggest that D_{4.4}R more easily form heteromers with α_{2A} R. This was also the case as for the D₂LR-D₄R heteromer reported by Borroto-Escuela et al. (2011). In this work, the BRET₅₀ of the D₂LR-D_{4.4}R heteromer showed a significantly higher affinity compared with the D₂LR-D_{4.7}R. Additionally, the PLAs

performed in cortex and striatum of knock-in hD_{4.7} mice and of WT littermates, which express a mouse D₄R with a shorter third intracellular loop comparable to the human D_{4.2}R (González et al., 2012), confirmed the presence of the α_{2A} R-D_{4.7}R heteromer *ex vivo*. To our knowledge, it is the first heteromer described of α_2 R and D₄R, both with D_{4.4}R and D_{4.7}R variants.

In addition, we could also show significant functional and pharmacological differences between D_{4.4}R and D_{4.7}R only evident upon heteromerization with D₂₅R or α_{2A} R, which generates the specific fingerprint of the oligomer. By CODA-RET assays we confirmed that both D₄R variants have the same potency and efficacy for the endogenous neurotransmitters DA and NE and is the heteromerization with α_{2A} R or D₂₅R who exposes the functional and pharmacological differences between the variants. Concerning the D₄R-D₂₅R heteromer, in the D_{4.7}R-D₂₅R but not in D_{4.4}R-D₂₅R heteromer, DA showed a small but significant increase in potency as compared with the D₂₅R-D₂₅R homodimer. Moreover, within the D_{4.7}R-D₂₅R, DA only signals through D₂₅R. In contrast, DA can activate both D₂₅R and D_{4.4}R. Within the D₄R- α_{2A} R heteromer, α_{2A} R determines NE-mediated G_{αi}-dependent signaling in both heteromers; in contrast, both D_{4.4}R and α_{2A} R determine DA-mediated G_{αi}-dependent signaling. D_{4.7}R variant does not signal in any case.

Another significant finding obtained from CODA-RET assays, with possible translational implications, was the differential profile of the clinically used D₂-like agonists for the treatment of Restless Leg syndrome and Parkinson's disease: pramipexole, ropinirole and rotigotine. These agonists are more potent at the α_{2A} R-D_{4.4}R than at the α_{2A} R-D_{4.7}R. In contrast, pramipexole and ropinirole were more potent at D_{4.7}R- D₂R than at D_{4.4}R- D₂R. Moreover, NE agonists clinically used for the treatment of ADHD: clonidine and guanfacine also have a different profile depending on the heteromer, being more potent and having higher efficacies for the α_{2A} R-D_{4.7}R. So, these drugs may have different clinical efficacies depending on the DRD4 polymorphism expressed. These are the first differences in the potency or efficacy of exogenous ligands between the D₄R variants that appear upon heteromerization and would suggest the need for genotyping in order to provide the most appropriate therapeutic agent for each disease.

Finally, the most dramatic finding about the D₄R-D₂₅R heteromer derived from CODA-RET assays was the significant increase in the constitutive activity that D_{4.7}R confers to the D₂₅R upon heteromerization. To our knowledge, this is the first reported example of changes in the constitutive activity of a GPCR upon heteromerization, which adds to the list of new properties associated with GPCR oligomerization (Ferré et al., 2014). More significant is the fact that this new property was specifically associated to the product of a *DRD4* polymorphism, conferring a gain of function to the D_{4.7}R *versus* the D_{4.4}R variant that provide a plausible mechanism for the gain of function of D_{4.7}R *versus* D_{4.4}R recently demonstrated *in vitro*, in mouse cortical slices with viral infection of human D_{4.4}R and D_{4.7}R (Zhong et al., 2016), and *in vivo*, in optogenetic-microdialysis experiments in the D_{4.7}R knock-in mouse (Bonaventura et al., 2017). The fact that a gain of function of D_{4.7}R *versus* D_{4.4}R could only be demonstrated upon heteromerization with D₂₅R, strongly suggests that D_{4.4}R-D₂R heteromers represent a significant receptor population that modulates the function of cortico-striatal glutamatergic neurons.

Apart from demonstrating the formation of α_{2A} R-D₄R heteromers *in vitro* by BRET, BiFC and BiLC complementation, we demonstrated the formation of α_{2A} R homodimers and D₄R homodimers by BiFC and BiLC. Also, a heterotetramer can be detected by double complementation of BRET donor and acceptor units, formed by a heteromer of homodimers.

Moreover, we have observed a negative cross-talk upon co-stimulation of both receptors by their agonists within the α_2R - $D_{4.4}R$ heteromer by analyzing global cell signaling, cAMP levels and ERK phosphorylation. In addition, a cross-antagonism of $D_{4.4}R$ on $\alpha_{2A}R$ was detected, since antagonist binding to D_4R decreases agonist function on $\alpha_{2A}R$. Surprisingly, these allosteric interactions are also D_4R variant-dependent, because they are only evident with $D_{4.4}R$ but not with $D_{4.7}R$ variant. Similar results with ERK phosphorylation were detected within the D_2R - D_4R heteromer, with both $D_{25}R$ and $D_{2L}R$ variants. In these heteromers, a positive cross-talk was detected with the $D_{4.4}R$ but not with the $D_{4.7}R$ variant (Borroto-Escuela et al., 2011; González et al., 2012a). The 7 tandem repeats of the proline rich sequence of 16 amino acids in the intracellular loop 3 of the $D_{4.7}R$ may cause this protein to have a very high disorder index (Woods, 2010), which may alter the development of cross-talk and cross-antagonism. Our results are of interest because variant differences can have important implications for understanding the pathogenesis of ADHD and can give new clues for the rational design of $\alpha_{2A}R$ - D_4R targeted drugs for its treatment.

In this study, we have also confirmed the signaling fingerprint of $\alpha_{2A}R$ with the D_4R detected in transfected cells in brain slices of WT mice at MAPK level, corroborating their expression in native tissues. In addition, an even more conclusive demonstration can be accomplished by directly probing the biochemical property of the heteromer with the *ex vivo* application of a specific disruptive peptide (Bonaventura et al., 2015; Viñals et al., 2015; Moreno et al., 2017, 2018). In this context, TM4 of the D_4R was able to destabilize $\alpha_{2A}R$ - D_4R heteromers, decreasing the heteromer detection in PLA assays and also disturbing the receptor-receptor modulation, reducing the negative cross-talk within the heteromer, at the level of MAPK activation. TM5 did not alter the PLA nor the negative cross-talk. Determining the transmembrane domains involved in the heteromer interface can facilitate the generation of a model of the heteromeric complex that can give new clues for the rational design of true bivalent compounds heteromer-specific. These compounds may be more selective and potent for the treatment of ADHD and SUD.

The physiological relevance of the present study is that we have identified $\alpha_{2A}R$ - D_4R heteromers in cortex and striatal tissues where both receptors negatively modulate glutamatergic cell activity. Due to the negative cross-talk between $\alpha_{2A}R$ and D_4R within the heteromer, the co-activation of both receptors would produce an attenuation of the inhibition of glutamate in the corticostriatal glutamatergic neurons post-synaptically at the dendritic level in the PFC and presynaptically in the striatum. There are no previous evidences saying that there are presynaptic $\alpha_{2A}R$ s in the striatum but, since D_4R are only presynaptic and we have detected PLA signal in this brain area, we have to assume that these heteromers are located presynaptically. This coactivation could be mediated by NE and/or DA because $\alpha_{2A}R$ and D_4R receptors are able to bind both catecholamine neurotransmitters and generate a signal (Zhang et al., 1999; Cornil et al., 2008; Alachkar et al., 2010; Sánchez-Soto et al., 2016, 2018). This provides a new mechanism by which NE and DA may regulate glutamatergic neurotransmission. The fact that the heteromer with the $D_{4.7}R$ variant does not show this negative cross-talk may generate presynaptically in the striatum an increase of the glutamate inhibition. This should affect the activity of both the “Go” and “NoGo” GABAergic striatal efferent pathways, decreasing their respective ability to increase the reactivity to reward-related stimuli and to suppress the reactivity to non-rewarded- or aversive-related stimuli (Bromberg-Martin et al., 2010). This may

result in an increased “interest” for irrelevant stimuli and a reduced inhibition of irrelevant responses, which could be important in explaining the attention deficit and impulsivity of ADHD (Bonaventura et al., 2017). In addition, the apparent contradictory clinical results obtained upon treatment with the α_{2A} R agonists clonidine and guanfacine, can be explained by their binding to presynaptic autoreceptors in the PFC decreasing NE release and, thus, reducing stress related to high NE levels that bound to α_1 R and β R and that decreased the ratio signal/noise (Shinba et al., 2001; Broese et al., 2012). Moreover, these agonists, may also bind to post-synaptic α_{2A} R, reducing the activation generated by endogenous catecholamines because they act as partial agonists, as we could detect in CODA-RET assays.

V- CONCLUSIONS

V. CONCLUSIONS

The conclusions corresponding to the **Objective 1** of this Thesis are:

- The mathematical formulation of the dimer receptor model for competitive ligand binding explains three different patterns: biphasic, monophasic and bell-shaped curves.
- According to this model, when there is a radioligand-competitor positive modulation ($K_{DAB} < 2K_{DB1}$) in a receptor homodimer we can obtain competitive displacement curves with these three different patterns (biphasic, monophasic and bell-shaped). Otherwise, bell-shaped curves do not appear.
- The radioligand concentration responsible for the conversion from biphasic or monophasic to bell-shaped curves in competitive radioligand binding assays is under $2K_{DA1} (K_{DB1} - K_{DAB}) / K_{DB1}$, if $K_{DAB} < K_{DB1}$.
- Bell-shaped curves are only interpretable assuming the formation of receptor homodimers and, therefore, obtaining bell-shaped curves in competition experiments is a clear evidence for receptor dimerization.
- In summary, the existence of a radioligand-competitor interaction, deduced from our dimer receptor model, allows the fitting of bell-shaped curves, typically considered as anomalous or erroneous results. The inclusion of the radioligand-competitor K_{DAB} parameter in the equation allows the obtention of values for the competitor closer to the actual values, irrespective of the radioligand employed in the assay. On the contrary, the K_{DB} values obtained from classical monomeric models are frequently much higher.

The conclusions corresponding to the **Objective 2** of this Thesis are:

- Any orthosteric $A_{2A}R$ ligand, agonist or antagonist, can decrease the affinity and intrinsic efficacy of any orthosteric D_2R ligand, agonist or antagonist. Moreover, there is a canonical G_{α_s} - G_{α_i} interaction at the AC level, i.e. the ability of a G_{α_i} -coupled GPCR to counteract AC activation induced by a G_{α_s} -coupled GPCR. These interactions constitute the biochemical fingerprint of the $A_{2A}R$ - D_2R heteromer and depend on the integrity of its right quaternary structure as demonstrated in transfected mammalian cells and striatal tissue.
- $A_{2A}R$ - D_2R heteromer is constituted by $A_{2A}R$ and D_2R homodimers and the AC5 complex, being TM6 involved in $A_{2A}R$ and D_2R homodimer interfaces and TM4 and TM5 in the heterodimer interface. Moreover, a quaternary structure of zig-zagged arranged $A_{2A}R$ - D_2R -AC5, including G_{α_s} and G_{α_i} , is suggested. This pre-coupled arrangement explains the canonical G_{α_s} - G_{α_i} interaction at the AC level.
- Occupancy of the $A_{2A}R$ homodimer with either an agonist or an antagonist produces a conformational change that leads to the same negative allosteric modulation on the D_2R , while simultaneous occupancy of the $A_{2A}R$ homodimer by an agonist and an antagonist would not allow this conformational change.
- In addition to the well reported negative modulation of $A_{2A}R$ agonists on D_2R signaling, the experiments in transfected cells and in striatal neurons demonstrate that there is also an additional strong allosteric modulation (cross-antagonism) of $A_{2A}R$ antagonists on the intrinsic efficacy of D_2R ligands.
- The main mechanism by which caffeine and $A_{2A}R$ antagonists produce locomotor activation could be due to the co-occupation of the homodimer by the antagonist and the endogenous adenosine. In this case, both ligands counteract each other's effect, allowing D_2R signaling within the $A_{2A}R$ - D_2R heteromer. Thus, therapeutic doses of potent and selective $A_{2A}R$ antagonists may have differential effects, inhibiting or allowing D_2R signaling, depending on the levels of endogenous adenosine.
- The non-activated or agonist-activated $A_{2A}R$ - D_2R heterotetramer is able to establish different molecular interactions with AC5. These interactions imply a major rearrangement of the TMs of the activated pre-coupled complex facilitating the interaction of AC5 catalytic domains with the corresponding G_{α} subunit. This is allowed by the agonist-induced movement of the $G_{\beta\gamma}$ subunits away from the helical-domain of the G_{α} subunit.
- A very similar degree of allosteric modulation of D_2R by $A_{2A}R$ ligands was observed in both artificial and native systems. This confirms that a large proportion of D_2R form heteromers with $A_{2A}R$ in transfected cells and striatal tissue.
- The results obtained represent a very significant support to the still controversial concepts of GPCR pre-coupling to G proteins and other effectors.

The conclusions corresponding to the **Objective 3** of this Thesis are:

- We have developed a precise strategy to create bivalent ligands of GPCR homo- and heterodimers based on a versatile multivalent chemical platform.
- The use of computational tools that consider the TM interfaces, distances between orthosteric binding sites and mode of interaction of the pharmacophore units, allows a reduction in the number of synthesized bivalent ligands, in addition to a high success in affinity results.
- Our bivalent ligand **13** showed picomolar binding affinity, which highly decreased in the presence of the TM6 peptide of D₂R, involved in the homodimer interface of the D₂R-D₂R. This is evidence of a clear simultaneous interaction with both orthosteric sites of the D₂R homodimer and is a chemical tool to confirm inter-protomer interaction in native tissue.
- In summary, our protocol is the basis for the synthesis of other bivalent ligands for D₂R heterodimers with therapeutic interest.

The conclusions corresponding to the **Objective 4** of this Thesis are:

- A promiscuous action mechanism of catecholamines is detected because α_{2A} and α_{2C} adrenoceptors can bind DA at concentrations in the same order than NE suggesting that they could be activated by DA at *in vivo* concentrations.
- Endogenous DA, and also common synthetic DA-receptor ligands, bind to α_2 adrenoceptors with moderate to high affinity in the mammalian brain. Moreover, the affinity of DA for α_2 adrenoceptors is in the same range as for D₁-like and D₂-like receptors, suggesting that endogenous levels of DA may activate both α_2 adrenoceptors and dopamine receptors. This provide a clear answer to the mismatch between the low striatal NE innervation and the high density of striatal α_2 adrenoceptors, which behave as functional DA receptors.
- DA and synthetic DA receptor ligands can activate G protein and induce cellular DMR through α_2 adrenoceptors. Based on BRET experiments, both potency and efficacy dependence on the receptor and the G_{ai/o} protein subtype was the norm for all ligands, including the endogenous neurotransmitters. Detailed characterization of the expression patterns for G_{ai/o} protein subtypes would then be crucial to determine their role in α_{2A} and α_{2C} adrenoceptor-activation and thus their possible specific targeting with G_{ai/o} subtype functionally selective compounds.
- DA and NE show the same cell signaling pattern, both being able to modulate adenylyl cyclase activity and ERK1/2 phosphorylation at nanomolar concentrations. This means that DA is not only able to bind to α_2 adrenoceptors but also to activate the same signaling pathways as NE.
- α_2 adrenoceptors could act as “DA autoreceptors” that control the non-synaptic somatodendritic DA release. We could state that G_{i/o}-coupled adrenoceptors and DA receptors should probably be considered as members of one ‘functional’ family of catecholamine receptors.

The conclusions corresponding to the **Objective 5** of this Thesis are:

- With the use of the CODA-RET technique, we could demonstrate the existence of functional D_{4.7}R-D₂₅R heteromers in transfected cells and also dissect the pharmacological profile of D_{4.4}R and D_{4.7}R homodimers and heteromers.
- There are no differences in the potency or efficacy of the endogenous neurotransmitters DA and NE for D_{4.4}R and D_{4.7}R homodimers, but the association with D₂Rs promoted additional differential modulations by D₄R variants of ligand-induced D₄R-D₂R heteromer-mediated signaling.
- Rotigotine is a very potent agonist for D_{4.7}R-D₂R compared to D_{4.4}R-D₂R or D₂R-D₂R. This could have implications for the treatment of RLS and Parkinson's disease.
- There is a significant increase in the constitutive activity that the D_{4.7}R confers to the D₂₅R upon heteromerization. To our knowledge, this is the first reported example of changes in the constitutive activity of a GPCR upon heteromerization. Moreover, this new property is specifically associated to D_{4.7}R, conferring a gain of function of the D_{4.7}R *versus* the D_{4.4}R variant.

The conclusions corresponding to the **Objective 6** of this Thesis are:

- Using biophysical, pharmacological, functional and immunochemical independent approaches in transfected cells, we provide strong support for the formation of α_{2A} R-D₄R heteromers that are expressed and functionally active in transfected cells; to our knowledge, it is the first heteromer described between α_2 R and D₄R, concretely with both D_{4.4}R and D_{4.7}R variants. Moreover, we have demonstrated that the α_{2A} R-D₄R heteromer is also present and functional in slices of rodent cortex and striatal brain tissues, even in knock-in hD_{4.7} mice.
- α_{2A} R-D₄R heteromer shows new allosteric properties such as a negative cross-talk upon co-stimulation of both receptors by their agonists, and cross-antagonism, since antagonist binding to D₄R decreases agonist function on α_{2A} R.
- These allosteric interactions within the α_{2A} R-D₄R heteromer are D₄R variant-dependent, because they are only evident with D_{4.4}R but not with D_{4.7}R. This means that individuals with the D_{4.7}R variant show a heteromerization-dependent gain of function, i. e. an increase of the inhibition of glutamate release. This should affect the activity of both the "Go" and "NoGo" GABAergic striatal efferent pathways, generating an increased "interest" for irrelevant stimuli and a reduced inhibition of irrelevant responses, which could be important for explaining the attention deficit and impulsivity of ADHD.
- Clinically used D₂-like agonists (pramipexole, ropinirole and rotigotine) are more potent at the α_{2A} R-D_{4.4}R than at the α_{2A} R-D_{4.7}R. NE agonists clinically used (clonidine, guanfacine and dexmedetomidine) are more potent and have higher efficacies for the α_{2A} R-D_{4.7}R. Thus, these drugs may have different clinical efficacies depending on the DRD4 polymorphism expressed and suggests the need for genotyping in order to provide the most appropriate therapeutic agent for each disease.
- Given that D_{4.4}R and D_{4.7}R variants are involved in the pathophysiology of ADHD and SUD, we suggest that α_{2A} R-D₄R heteromers could be target for the therapeutic treatment of such neurological disorders.

In summary, the **general conclusions** of this Thesis are:

- Homodimers are predominant GPCR species, providing a significant role of allosteric interactions between orthosteric ligands of the different protomers within GPCR heteromers, which should have important implications in the field of GPCR pharmacology. A paradigmatic example of complex allosteric interactions is the $A_{2A}R$ - $A_{2A}R$ - D_2R - D_2R - $G_{\alpha S}$ - $G_{\alpha I}$ -AC5 heteromer.
- Since bivalent ligands are the best example of oligomer selective-ligands that can interact simultaneously with a homo or hetero- GPCR dimer with high affinity and subtype selectivity, improving safety and efficacy for their therapeutic targets, our protocol is the basis for the synthesis of other bivalent ligands for D_2R heteromers with other catecholamine or adenosine receptors with therapeutic interest for the treatment of motor dysfunctions.
- Catecholamine receptors constitute a “functional” family of GPCR. We have demonstrated the existence of functional D_4R - $D_{2S}R$ *in vitro* and functional D_4R - $\alpha_{2A}R$ *in vitro* and in rodent brain tissues not only with the $D_{4.4}R$ but also with the $D_{4.7}R$ variant, prevalent in ADHD. Significant different properties of these heteromers were D_4R variant-dependent. Given that D_2R , D_4R and $\alpha_{2A}R$, are involved in the pathophysiology of ADHD and SUD, we suggest that D_4R - D_2R and $\alpha_{2A}R$ - D_4R heteromers could be target for the therapeutic treatment of such neurological disorders.

VI- BIBLIOGRAPHY

VI. BIBLIOGRAPHY

- Abbracchio MP, Burnstock G, Verkhratsky A, Zimmermann H (2009) Purinergic signalling in the nervous System: an overview. *Trends Neurosci.* 32:19-29.
- Acton D, Miles GB (2015) Stimulation of Glia Reveals Modulation of Mammalian Spinal Motor Networks by Adenosine. *PLoS One.* 10:e0134488. doi: 10.1371/journal.pone.0134488.
- Agnati, L. F., Tarakanov, A. O., Ferré, S., Fuxe, K. & Guidolin, D. Receptor-receptor interactions, receptor mosaics, and basic principles of molecular network organization: possible implications for drug development. *J. Mol. Neurosci.* **26**, 193-208 (2005).
- Ahles A, Engelhardt S (2014) Polymorphic variants of adrenoceptors: pharmacology, physiology, and role in disease. *Pharmacol Rev.* 66:598-637. doi: 10.1124/pr.113.008219.
- Ahmad S, Fatteh N, El-Sherbiny NM, Naime M, Ibrahim AS, El-Sherbini AM, El-Shafey SA, Khan S, Fulzele S, Gonzales J, Liou GI (2013) Potential role of A2A adenosine receptor in traumatic optic neuropathy. *J Neuroimmunol.* 264:54-64.
- Alachkar A, Brotchie JM, Jones OT (2010) Binding of dopamine and 3-methoxytyramine as L-DOPA metabolites to human alpha(2)-adrenergic and dopaminergic receptors. *Neurosci Res.* 67:245-9. doi:10.1016/j.neures.2010.03.008
- Albin RL, Young AB, Penney JB (1989) The functional anatomy of basal ganglia disorders. *Trends Neurosci.* 12:366-75.
- Albizu L, Balestre MN, Breton C, Pin JP, Manning M, Mouillac B, Barberis C, Durroux T (2006) Probing the existence of G protein-coupled receptor dimers by positive and negative ligand-dependent cooperative binding. *Mol Pharmacol.* 70:1783-91.
- Albizu L, Cottet M, Kralikova M, Stoev S, Seyer R, Brabet I, Roux T, Bazin H, Bourrier E, Lamarque L, Breton C, Rives ML, Newman A, Javitch J, Trinquet E, Manning M, Pin JP, Mouillac B, Durroux T (2010) Time-resolved FRET between GPCR ligands reveals oligomers in native tissues. *Nat Chem Biol.* 6:587-94. doi: 10.1038/nchembio.396.
- Alexander GE, Crutcher MD (1990) Functional architecture of basal ganglia circuits: neural substrates of parallel processing. *Trends Neurosci.* 13:266-71.
- Almeida J, Mengod G (2010) D2 and D4 dopamine receptor mRNA distribution in pyramidal neurons and GABAergic subpopulations in monkey prefrontal cortex: implications for schizophrenia treatment. *Neuroscience.* 170:1133-9. doi: 10.1016/j.neuroscience.2010.08.025.
- Al-Tikriti MS, Roth RH, Kessler RM, Innis RB (1992) Autoradiographic localization of dopamine D1 and D2 receptors in rat cerebral cortex following unilateral neurotoxic lesions. *Brain Res.* 575:39-46.
- Altman JD, Trendelenburg AU, MacMillan L, Bernstein D, Limbird L, Starke K, Kobilka BK, Hein L (1999) Abnormal regulation of the sympathetic nervous system in alpha2A-adrenergic receptor knockout mice. *Mol Pharmacol.* 56:154-61.
- Amara SG, Kuhar MJ (1993) Neurotransmitter transporters: recent progress. *Annu Rev Neurosci.* 16:73-93.

- Angers S, Salahpour A, Joly E, Hilairet S, Chelsky D, Dennis M, Bouvier M (2000) Detection of beta 2-adrenergic receptor dimerization in living cells using bioluminescence resonance energy transfer (BRET). *Proc Natl Acad Sci USA*. 97:3684-9.
- Antle MC, Steen NM, Mistlberger RE (2001) Adenosine and caffeine modulate circadian rhythms in the Syrian hamster. *Neuroreport*. 12:2901-5.
- Antonioli L, Blandizzi C, Pacher P, Hasko G (2013) Immunity, inflammation and cancer: a leading role for adenosine. *Nat Rev Cancer*. 13:842-57.
- Antonioli L, Hasko G, Fornai M, Colucci R, Blandizzi C (2014) Adenosine pathway and cancer: where do we go from here? *Expert Opin Ther Targets*. 18:973-7.
- Aoki C, Venkatesan C, Go CG, Forman R, Kurose H (1998) Cellular and subcellular sites for noradrenergic action in the monkey dorsolateral prefrontal cortex as revealed by the immunocytochemical localization of noradrenergic receptors and axons. *Cereb Cortex*. 8:269-77.
- Aperia AC (2000) Intrarenal dopamine: a key signal in the interactive regulation of sodium metabolism. *Annu Rev Physiol*. 62:621-47.
- Arch JR, Newsholme EA (1978) Activities and some properties of 5'-nucleotidase, adenosine kinase and adenosine deaminase in tissues from vertebrates and invertebrates in relation to the control of the concentration and the physiological role of adenosine. *Biochem J*. 174:965-77.
- Ariano MA, Wang J, Noblett KL, Larson ER, Sibley DR (1997a) Cellular distribution of the rat D4 dopamine receptor protein in the CNS using anti-receptor antisera. *Brain Res*. 752:26-34.
- Ariano MA, Wang J, Noblett KL, Larson ER, Sibley DR (1997b) Cellular distribution of the rat D1B receptor in central nervous system using anti-receptor antisera. *Brain Res*. 746:141-50.
- Arnatt CK, Zhang Y (2014) Bivalent ligands targeting chemokine receptor dimerization: molecular design and functional studies. *Curr Top Med Chem*. 14:1606-18.
- Arnatt CK, Falls BA, Yuan Y, Raborg TJ, Masvekar RR, El-Hage N, Selley DE, Nicola AV, Knapp PE, Hauser KF, Zhang Y (2016) Exploration of bivalent ligands targeting putative mu opioid receptor and chemokine receptor CCR5 dimerization. *Bioorg Med Chem*. 24:5969-5987.
- Arnsten AF (2007) Catecholamine and second messenger influences on prefrontal cortical networks of "representational knowledge": a rational bridge between genetics and the symptoms of mental illness. *Cereb Cortex*. 17:16-15.
- Arnsten AF, Li BM (2005) Neurobiology of executive functions: catecholamine influences on prefrontal cortical functions. *Biol Psychiatry*. 57:1377-84.
- Arnsten AF, Goldman-Rakic PS (1984) Selective prefrontal cortical projections to the region of the locus coeruleus and raphe nuclei in the rhesus monkey. *Brain Res*. 306:9-18.
- Arnsten AF, Cai JX, Goldman-Rakic PS (1988) The alpha-2 adrenergic agonist guanfacine improves memory in aged monkeys without sedative or hypotensive side effects: evidence for alpha-2 receptor subtypes. *J Neurosci*. 8:4287-98.

- Arnsten AF, Murphy B, Merchant K (2000) The selective dopamine D4 receptor antagonist, PNU-101387G, prevents stress-induced cognitive deficits in monkeys. *Neuropsychopharmacology*. 23:405-10.
- Arnsten AF, Paspalas CD, Gamo NJ, Yang Y, Wang M (2010) Dynamic Network Connectivity: A new form of neuroplasticity. *Trends Cogn Sci*. 14:365-75. doi: 10.1016/j.tics.2010.05.003.
- Aron AR, Robbins TW, Poldrack RA (2004) Inhibition and the right inferior frontal cortex. *Trends Cogn Sci*. 8:170-7.
- Arosio B, Casati M, Gussago C, Ferri E, Abbate C, Scortichini V, Colombo E, Rossi PD, Mari D (2016) Adenosine Type A2A Receptor in Peripheral Cell from Patients with Alzheimer's Disease, Vascular Dementia, and Idiopathic Normal Pressure Hydrocephalus: A New/Old Potential Target. *J Alzheimers Dis*. 54:417-25. doi: 10.3233/JAD-160324.
- Ascherio A, Zhang SM, Hernán MA, Kawachi I, Colditz GA, Speizer FE, Willett WC (2001) Prospective study of caffeine consumption and risk of Parkinson's disease in men and women. *Ann Neurol*. 50:56-63.
- Asghari V, Sanyal S, Buchwaldt S, Paterson A, Jovanovic V, Van Tol HH (1995) Modulation of intracellular cyclic AMP levels by different human dopamine D4 receptor variants. *J Neurochem*. 65:1157-65.
- Aston-Jones, G. (2004) Locus coeruleus, A5 and A7 noradrenergic cell groups, in *The Rat Nervous System* (Paxinos, G., ed.). Academic Press, San Diego, pp 259-294.
- Aston-Jones G, Cohen JD (2005) An integrative theory of locus coeruleus-norepinephrine function: adaptive gain and optimal performance. *Annu Rev Neurosci*. 28:403-50.
- Ayoub MA, Couturier C, Lucas-Meunier E, Angers S, Fossier P, Bouvier M, Jockers R (2002) Monitoring of ligand-independent dimerization and ligand-induced conformational changes of melatonin receptors in living cells by bioluminescence resonance energy transfer. *J Biol Chem*. 277:21522-8
- Ayoub MA, Levoye A, Delagrangé P, Jockers R (2004) Preferential formation of MT1/MT2 melatonin receptor heterodimers with distinct ligand interaction properties compared with MT2 homodimers. *Mol Pharmacol*. 66:312-21.
- Azdad K, Gall D, Woods AS, Ledent C, Ferré S, Schiffmann SN (2009) Dopamine D2 and adenosine A2A receptors regulate NMDA-mediated excitation in accumbens neurons through A2A-D2 receptor heteromerization. *Neuropsychopharmacology*. 34:972-86.
- Babcock GJ, Farzan M, Sodroski J (2003) Ligand-independent dimerization of CXCR4, a principal HIV-1 coreceptor. *J Biol Chem*. 278:3378-85.
- Bagher AM, Laprairie RB, Toguri JT, Kelly MEM, Denovan-Wright EM (2017) Bidirectional allosteric interactions between cannabinoid receptor 1 (CB1) and dopamine receptor 2 long (D2L) heterotetramers. *Eur J Pharmacol*. 813:66-83. doi: 10.1016/j.ejphar.2017.07.034.
- Bahamonde MI, Taura J, Paoletta S, Gakh AA, Chakraborty S, Hernando J, Fernández-Dueñas V, Jacobson KA, Gorostiza P, Ciruela F (2014) Photomodulation of G protein-coupled adenosine receptors by a novel light-switchable ligand. *Bioconjug Chem*. 25:1847-54. doi: 10.1021/bc5003373.

- Baki L, Fribourg M, Younkin J, Eltit JM, Moreno JL, Park G, Vysotskaya Z, Narahari A, Sealfon SC, Gonzalez-Maeso J, Logothetis DE (2016) Cross-signaling in metabotropic glutamate 2 and serotonin 2A receptor heteromers in mammalian cells. *Pflugers Arch.* 468:775-93.
- Baldwin JM (1994) Structure and function of receptors coupled to G proteins. *Curr Opin Cell Biol.* 6:180-190.
- Banères JL and Parello J (2003) Structure-based analysis of GPCR function: evidence for a novel pentameric assembly between the dimeric leukotriene B4 receptor BLT1 and the G-protein. *J Mol Biol.* 329:815–29.
- Barbas H, Medalla M, Alade O, Suski J, Zikopoulos B, Lera P (2005) Relationship of prefrontal connections to inhibitory systems in superior temporal areas in the rhesus monkey. *Cereb Cortex.* 15:1356-70.
- Barki-Harrington L, Luttrell LM, Rockman HA (2003) Dual inhibition of beta-adrenergic and angiotensin II receptors by a single antagonist: a functional role for receptor-receptor interaction in vivo. *Circulation.* 108:1611-8.
- Baron MS, Wichmann T, Ma D, DeLong MR (2002) Effects of transient focal inactivation of the basal ganglia in parkinsonian primates. *J Neurosci.* 22:592-9.
- Beaulieu JM, Gainetdinov RR (2011) The physiology, signaling, and pharmacology of dopamine receptors. *Pharmacol Rev.* 63:182-217. doi: 10.1124/pr.110.002642.
- Belcher AM, Volkow ND, Moeller FG, Ferré S (2014) Personality traits and vulnerability or resilience to substance use disorders. *Trends Cogn Sci.* 18:211-7
- Berde B, Boissonnas RA, Huguenin RL, Sturmer E (1964) Vasopressin analogues with selective pressor activity. *Experientia.* 20:42–3.
- Berque-Bestel I, Lezoualc'h F, Jockers R (2008) Bivalent ligands as specific pharmacological tools for G protein-coupled receptor dimers. *Curr Drug Discov Technol.* 5:312-8.
- Berlanga ML, Simpson TK, Alcantara AA (2005) Dopamine D5 receptor localization on cholinergic neurons of the rat forebrain and diencephalon: a potential neuroanatomical substrate involved in mediating dopaminergic influences on acetylcholine release. *J Comp Neurol.* 492:34-49.
- Berridge CW, Waterhouse BD (2003) The locus coeruleus-noradrenergic system: modulation of behavioral state and state-dependent cognitive processes. *Brain Res Brain Res Rev.* 42:33-84.
- Bertheleme N, Strega A, Bunting SE, Dowell SJ, Byrne B (2014) Arginine 199 and leucine 208 have key roles in the control of adenosine A2A receptor signalling function *PLOS One.* 9, e89613.
- Bertoldi M (2014) Mammalian Dopa decarboxylase: structure, catalytic activity and inhibition. *Arch Biochem Biophys.* 546:1-7. doi: 10.1016/j.abb.2013.12.020.
- Best M, Williams JM, Coccaro EF (2002) Evidence for a dysfunctional prefrontal circuit in patients with an impulsive aggressive disorder. *Proc Natl Acad Sci USA.* 2002 99:8448-53.
- Birnbaum SG, Yuan PX, Wang M, Vijayraghavan S, Bloom AK, Davis DJ, Gobeske KT, Sweatt JD, Manji HK, Arnsten AF (2004) Protein kinase C overactivity impairs prefrontal cortical regulation of working memory. *Science.* 306:882-4.

- Black JW, Leff P (1983) Operational models of pharmacological agonism. *Proc R Soc Lond B Biol Sci.* 220:141-62.
- Bonaventura J, Quiroz C, Cai NS, Rubinstein M, Tanda G, Ferré S (2017) Key role of the dopamine D4 receptor in the modulation of corticostriatal glutamatergic neurotransmission. *Sci Adv.* 3:e1601631. doi: 10.1126/sciadv.1601631.
- Bondar A, Lazar J (2006) The G protein Gi1 exhibits basal coupling but not preassembly with G protein-coupled receptors. *J Biol Chem.* 292:9690-8. doi: 10.1074/jbc.M116.768127.
- Bonifazi A, Yano H, Ellenberger MP, Muller L, Kumar V, Zou MF, Cai NS, Guerrero AM, Woods AS, Shi L, Newman AH (2017) Novel bivalent ligands based on the sumanirole pharmacophore reveal dopamine D₂ receptor (D₂R) biased agonism. *J Med Chem.* 60:2890-907. doi: 10.1021/acs.jmedchem.6b01875.
- Borea PA, Varani K, Vincenzi F, Baraldi PG, Tabrizi MA, Merighi S, Gessi S (2015) The A3 adenosine receptor: history and perspectives. *Pharmacol Rev.* 67:74-102. doi: 10.1124/pr.113.008540.
- Borea PA, Gessi S, Merighi S, Varani K (2016) Adenosine as a multi-signalling guardian angel in human diseases: when, where and how does it exert its protective effects? *Trends Pharmacol Sci.* 37:419-34.
- Borota D, Murray E, Keceli G, Chang A, Watabe JM, Ly M, Yassa M A (2014) Post-study caffeine administration enhances memory consolidation in humans. *Nature Neuroscience.* 17:201–204.
- Borroto-Escuela DO, Van Craenenbroeck K, Romero-Fernandez W, Guidolin D, Woods AS, Rivera A, Haegeman G, Agnati LF, Tarakanov AO, Fuxe K (2011). Dopamine D2 and D4 receptor heteromerization and its allosteric receptor–receptor interactions. *Biochem Biophys Res Commun.* 404:928–34.
- Bouret S, Sara SJ (2005) Network reset: a simplified overarching theory of locus coeruleus noradrenaline function. *Trends Neurosci.* 28:574-82.
- Bourne HR (1997) How receptors talk to trimeric G proteins. *Curr Opin Cell Biol.* 9:134–142.
- Bouvier M, Chidiac P, Hebert TE, Loisel TP, Moffett S, Mouillac B (1995) Dynamic palmitoylation of G-protein-coupled receptors in eukaryotic cells. *Methods Enzymol.* 250:300-14.
- Brady T (1942) Adenosine deaminase. *Biochem J.* 36:478-84.
- Breit A, Lagacé M, Bouvier M (2004). Hetero-oligomerization between beta2-and beta3-adrenergic receptors generates a beta-adrenergic signaling unit with distinct functional properties. *J Biol Chem.* 279:28756-65.
- Brennan AR, Arnsten AF (2008) Neuronal mechanisms underlying attention deficit hyperactivity disorder: the influence of arousal on prefrontal cortical function. *Ann N Y Acad Sci.* 1129:236-45. doi:10.1196/annals.1417.007
- Brette F, Rodriguez P, Komukai K, Colyer J, Orchard CH (2004). beta-adrenergic stimulation restores the Ca transient of ventricular myocytes lacking t-tubules. *J Mol Cell Cardiol.* 36:265-75.
- Broese M, Riemann D, Hein L, Nissen C (2012) α -Adrenergic receptor function, arousal and sleep: mechanisms and therapeutic implications. *Pharmacopsychiatry.* 45:209-16. doi: 10.1055/s-0031-1299728.

- Bromberg-Martin ES, Matsumoto M, Hikosaka O (2010) Dopamine in motivational control: Rewarding, aversive, and alerting. *Neuron*. 68:815-34.
- Brown RM, Short JL (2008) Adenosine A(2A) receptors and their role in drug addiction. *J Pharm Pharmacol*. 60:1409-30. doi: 10.1211/jpp/60.11.0001.
- Brunton LL, Chabner BA, and Knollmann BC (2011) Goodman & Gilman's The pharmacological basis of therapeutics, 12th ed, New York: McGraw-Hill Companies Inc.
- Bücheler MM, Hadamek K, Hein L (2002) Two alpha(2)-adrenergic receptor subtypes, alpha(2A) and alpha(2C), inhibit transmitter release in the brain of gene-targeted mice. *Neuroscience*. 109:819-26.
- Bulenger S, Marullo S, Bouvier M (2005). Emerging role of homoand heterodimerization in G-protein-coupled receptor biosynthesis and maturation. *Trends Pharmacol Sci*. 26:131-7.
- Bunemann M, Frank M, Lohse MJ (2003) Gi protein activation in intact cells involves subunit rearrangement rather than dissociation. *Proc Natl Acad Sci USA*. 100:16077-82.
- Bura SA, Nadal X, Ledent, C Maldonado R., Valverde, O (2008) A2A adenosine receptor regulates glia proliferation and pain after peripheral nerve injury. *Pain*. 140:95-103.
- Burgueño J, Enrich C, Canela EI, Mallol J, Lluís C, Franco R, Ciruela F (2003) Metabotropic glutamate type 1alpha receptor localizes in low-density caveolin rich plasma membrane fractions. *J Neurochem*. 86:785-91.
- Buschman TJ, Miller EK (2007) Top-down versus bottom-up control of attention in the prefrontal and posterior parietal cortices. *Science*. 315:1860-2.
- Busnelli M, Kleinau G, Muttenthaler M, Stoev S, Manning M, Bibic L, Howell LA, McCormick PJ, Di Lascio S, Braida D, Sala M, Rovati GE, Bellini T, Chini B (2016) Design and characterization of superpotent bivalent ligands targeting oxytocin receptor dimers via a channel-like structure. *J. Med Chem* 59:7152-66.
- Bylund DB, Eikenberg DC, Hieble JP, Langer SZ, Lefkowitz RJ, Minneman KP, Molinoff PB, Ruffolo RR Jr, Trendelenburg U (1994) International Union of Pharmacology nomenclature of adrenoceptors. *Pharmacol Rev*. 46:121-36.
- Cabrera-Vera TM, Vanhauwe J, Thomas TO, Medkova M, Preininger A, Mazzoni MR, Hamm HE (2003) Insights into G protein structure, function, and regulation. *Endocr Rev*. 24:765-81.
- Cahill L, McGaugh JL (1996) The neurobiology of memory for emotional events: adrenergic activation and the amygdala. *Proc West Pharmacol Soc*. 39:81-4.
- Calebiro D, Nikolaev VO, Gagliani MC, de Filippis T, Dees C, Tacchetti C, Persani L, Lohse MJ (2009) Persistent cAMP-signals triggered by internalized G-protein-coupled receptors. *PLoS Biol*. 7:e1000172.
- Camici M, Micheli V, Ipata PL, Tozzi MG (2010) Pediatric neurological syndromes and inborn errors of purine metabolism. *Neurochem Int*. 56:367-78. doi: 10.1016/j.neuint.2009.12.003.
- Canals M, Marcellino D, Fanelli F, Ciruela F, de Benedetti P, Goldberg SR, Neve K, Fuxe K, Agnati LF, Woods AS, Ferré S, Lluís C, Bouvier M, Franco R (2003) Adenosine A2A-dopamine D2

receptor-receptor heteromerization: qualitative and quantitative assessment by fluorescence and bioluminescence energy transfer. *J Biol Chem.* 278:46741-9.

Canals M, Angulo E, Casadó V, Canela EI, Mallol J, Viñals F, Staines W, Tinner B, Hillion J, Agnati L, Fuxe K, Ferré S, Lluís C, Franco R (2005) Molecular mechanisms involved in the adenosine A and A receptor-induced neuronal differentiation in neuroblastoma cells and striatal primary cultures. *J Neurochem.* 92:337-48.

Canals M, Sexton PM, Christopoulos A (2011) Allosterism in GPCRs: "MWC" revisited *Trends Biochem Sci.* 36:663-72.

Capra JA, Laskowski RA, Thornton JM, Singh M, Funkhouser TA (2009) Predicting protein ligand binding sites by combining evolutionary sequence conservation and 3D structure. *PLoS Comput Biol.* 5:e1000585. doi: 10.1371/journal.pcbi.1000585.

Carlsson A (2001) A paradigm shift in brain research. *Science.* 294:1021-4.

Carlsson A, Lindqvist M, Magnusson T (1957) 3,4-Dihydroxyphenylalanine and 5-hydroxytryptophan as reserpine antagonists. *Nature.* 180:1200.

Carpenter B, Nehmé R, Warne T, Leslie AG, Tate CG (2016) Structure of the adenosine A_{2A} receptor bound to an engineered G protein. *Nature.* 536:104-7.

Carriba P, Navarro G, Ciruela F, Ferré S, Casadó V, Agnati L, Cortés A, Mallol J, Fuxe K, Canela EI, Lluís C, Franco R (2008) Detection of heteromerization of more than two proteins by sequential BRET-FRET. *Nat Methods.* 5:727-33. doi: 10.1038/nmeth.1229. Epub 2008 Jun 29.

Carús-Cadavieco M, de Andrés I (2012) Adenosine and homeostatic control of sleep. Actions in target structures of the sleep-wake circuits. *Rev Neurol.* 55:413-20.

Casadó V, Cantí C, Mallol J, Canela EI, Lluís C, Franco R (1990) Solubilization of A₁ adenosine receptor from pig brain: characterization and evidence of the role of the cell membrane on the coexistence of high and low-affinity states. *J Neurosci Res.* 26:461-73.

Casadó V, Mallol J, Canela EI, Lluís C, Franco R (1991) The binding of [³H]R-PIA to A₁ adenosine receptors produces a conversion of the high to the low-affinity state. *FEBS Lett.* 286:221-4.

Casadó V, Cortés A, Ciruela F, Mallol J, Ferré S, Lluís C, Canela EI, Franco R (2007) Old and new ways to calculate the affinity of agonists and antagonists interacting with G-protein-coupled monomeric and dimeric receptors: the receptor-dimer cooperativity index. *Pharmacol Ther.* 116:343-54.

Casadó V, Cortés A, Mallol J, Perez-Capote K, Ferré S, Lluís C, Franco R, Canela EI (2009a) GPCR homomers and heteromers: a better choice as targets for drug development than GPCR monomers? *Pharmacol Ther.* 124:248-57.

Casadó V, Ferrada C, Bonaventura J, Gracia E, Mallol J, Canela EI, Lluís C, Cortés A, Franco R (2009b) Useful pharmacological parameters for G-protein-coupled receptor homodimers obtained from competition experiments. Agonist-antagonist binding modulation. *Biochem Pharmacol.* 78:1456-63. doi: 10.1016/j.bcp.2009.07.012.

Casadó V, Barrondo S, Spasic M, Callado LF, Mallol J, Canela EI, Lluís C, Meana J, Cortés A, Sallés J, Franco R (2010) G_i protein coupling to adenosine A₁-A_{2A} receptor heteromers in human brain caudate nucleus. *J Neurochem.* 114:972-80. doi: 10.1111/j.1471-4159.2010.06810.x.

- Casey BJ, Epstein JN, Buhle J, Liston C, Davidson MC, Tonev ST, Spicer J, Niogi S, Millner AJ, Reiss A, Garrett A, Hinshaw SP, Greenhill LL, Shafritz KM, Vitolo A, Kotler LA, Jarrett MA, Glover G (2007) Frontostriatal connectivity and its role in cognitive control in parent-child dyads with ADHD. *Am J Psychiatry*. 164:1729-36.
- Castellanos FX, Lee PP, Sharp W, Jeffries NO, Greenstein DK, Clasen LS, Blumenthal JD, James RS, Ebens CL, Walter JM, Zijdenbos A, Evans AC, Giedd JN, Rapoport JL (2002) Developmental trajectories of brain volume abnormalities in children and adolescents with attention-deficit/hyperactivity disorder. *JAMA*. 288:1740-8.
- Castellanos FX, Margulies DS, Kelly C, Uddin LQ, Ghaffari M, Kirsch A, Shaw D, Shehzad Z, Di Martino A, Biswal B, Sonuga-Barke EJ, Rotrosen J, Adler LA, Milham MP (2008) Cingulate-precuneus interactions: a new locus of dysfunction in adult attention-deficit/hyperactivity disorder. *Biol Psychiatry*. 63:332-7. doi: 10.1016/j.biopsych.2007.06.025.
- Castelli MP, Spiga S, Perra A, Madeddu C, Mulas G, Ennas MG, Gessa GL (2016) alpha2A adrenergic receptors highly expressed in mesoprefrontal dopamine neurons. *Neuroscience* 332:130-139. doi:10.1016/j.neuroscience.2016.06.037.
- Cerione RA, Codina J, Benovic JL, Lefkowitz RJ, Birnbaumer L, Caron MG (1984) The mammalian beta 2-adrenergic receptor: reconstitution of functional interactions between pure receptor and pure stimulatory nucleotide binding protein of the adenylate cyclase system. *Biochemistry*. 23:4519-25.
- Chabre M, Deterre P, Antony B (2009) The apparent cooperativity of some GPCRs does not necessarily imply dimerization. *Trends Pharmacol Sci*. 30:182-7.
- Chan ES, Liu H, Fernandez P, Luna A, Perez-Aso M, Bujor AM, Trojanowska M, Cronstein BN, (2013) Adenosine A2A receptors promote collagen production by a Fli-1 and CTGF-mediated mechanism. *Arthritis Res Ther*. 15:R58.
- Chandler DJ (2016) Evidence for a specialized role of the locus coeruleus noradrenergic system in cortical circuitries and behavioral operations. *Brain Res*. 1641:197-206. doi: 10.1016/j.brainres.2015.11.022.
- Changeux JP (2012) Allosterism and the Monod-Wyman-Changeux model after 50 years. *Annu Rev Biophys*. 41:103-33.
- Changeux JP, Christopoulos A (2016) Allosteric modulation as a unifying mechanism for receptor function and regulation. *Cell*. 166:1084-102.
- Chang FM, Kidd JR, Livak KJ, Pakstis AJ, Kidd KK (1996) The world-wide distribution of allele frequencies at the human dopamine D4 receptor locus. *Hum Genet*. 98:91-101.
- Chen CA, Manning DR (2001) Regulation of G proteins by covalent modification. *Oncogene*. 20:1643-52.
- Chen JF, Sonsalla PK, Pedata F, Melani A, Domenici M R, Popoli P, Geiger J, Lopes LV, de Mendonça A (2007) Adenosine A2A receptors and brain injury: broad spectrum of neuroprotection, multifaceted actions and "fine tuning" modulation. *Progress in Neurobiology*. 83:310-31.

- Chen JF, Eltzhig HK, Fredholm BB (2013) Adenosine receptors as drug targets--what are the challenges? *Nat Rev Drug Discov.* 12:265-86. doi: 10.1038/nrd3955.
- Cheng Y, Prusoff WH (1973) Relationship between the inhibition constant (K₁) and the concentration of inhibitor which causes 50 per cent inhibition (I₅₀) of an enzymatic reaction. *Biochem Pharmacol.* 22:3099-108.
- Chidiac P, Green MA, Pawagi AB, Wells JW (1997) Cardiac muscarinic receptors. Cooperativity as the basis for multiple states of affinity. *Biochemistry.* 36:7361-7379.
- Chiu FL, Lin JT, Chuang CY, Chien T, Chen CM, Chen KH, Hsiao HY, Lin YS, Chern Y, Kuo HC (2015) Elucidating the role of the A_{2A} adenosine receptor in neurodegeneration using neurons derived from Huntington's disease iPSCs. *Hum Mol Genet.* 24:6066-79. doi: 10.1093/hmg/ddv318.
- Cho DI, Beom S, Van Tol HH, Caron MG, Kim KM (2006) Characterization of the desensitization properties of five dopamine receptor subtypes and alternatively spliced variants of dopamine D₂ and D₄ receptors. *Biochem Biophys Res Commun.* 350:634-40.
- Choe HW, Kim YJ, Park JH, Morizumi T, Pai EF, Krauss N, Hofmann KP, Scheerer P, Ernst OP (2011) Crystal structure of metarhodopsin II. *Nature.* 471:651-5.
- Choi WS, Machida CA, Ronnekleiv OK (1995) Distribution of dopamine D₁, D₂, and D₅ receptor mRNAs in the monkey brain: ribonuclease protection assay analysis. *Brain Res Mol Brain Res.* 31:86-94.
- Chondrogiorgi M, Tatsioni A, Reichmann H, Konitsiotis S (2014) Dopamine agonist monotherapy in Parkinson's disease and potential risk factors for dyskinesia: a meta-analysis of levodopa-controlled trials. *Eur J Neurol.* 21:433-40. doi: 10.1111/ene.12318.
- Christopoulos A (2014) Advances in G protein-coupled receptor allostery: from function to structure. *Mol Pharmacol.* 86:463-78.
- Christopoulos A, Kenakin T (2002) G protein-coupled receptor allostery and complexing. *Pharmacol Rev.* 54:323-74.
- Christopoulos, A, Changeux, JP, Catterall, WA, Fabbro, D, Burris, TP, Cidlowski, JA, Olsen, RW, Peters, JA, Neubig, RR, Pin, JP, Sexton, PM, Kenakin, TP, Ehlert, FJ, Spedding, M, Langmead, CJ, (2014) International Union of Basic and Clinical Pharmacology. XC. Multisite pharmacology: recommendations for the nomenclature of receptor allostery and allosteric ligands. *Pharmacol Rev.* 66:918-47.
- Chun M, Liyanage UK, Lisanti MP, Lodish HF (1994) Signal transduction of a G protein-coupled receptor in caveolae: colocalization of endothelin and its receptor with caveolin. *Proc Natl Acad Sci USA.* 91: 11728-32.
- Ciruela F (2008). Fluorescence based methods in the study of protein-protein interactions in living cells. *Curr Opin Biotechnol.* 19:338-43.
- Ciruela F, Saura C, Canela EI, Mallol J, Lluís C, Franco R (1996) Adenosine deaminase affects ligand-induced signalling by interacting with cell surface adenosine receptors. *FEBS Lett.* 380:219-23.

- Ciruela F, Escriche M, Burgueno J, Angulo E, Casado V, Soloviev MM, Canela EI, Mallol J, Chan WY, Lluís C, McIlhinney RA, Franco R (2001) Metabotropic glutamate 1 α and adenosine A₁ receptors assemble into functionally interacting complexes. *J Biol Chem.* 276:18345-51.
- Ciruela F, Burgueño J, Casadó V, Canals M, Marcellino D, Goldberg S.R, Bader M, Fuxe K, Agnati L, Lluís C, Franco R, Ferré S, Woods A.S (2004). Combining mass spectrometry and pull-down techniques for the study of receptor heteromerization. Direct epitope-epitope electrostatic interactions between adenosine A_{2A} and dopamine D₂ receptors. *Anal Chem.* 76:5354-63.
- Ciruela F, Casadó V, Rodrigues R.J, Lujan J, Burgueño J, Canals M, Borycz J, Rebola N, Goldberg S.R, Mallol J, Cortés A, Canela E.I, Lopez-Gimenez J.F, Milligan G, Luis C, Cunha R.A, Ferré S, Franco R (2006) Presynaptic control of striatal glutamatergic neurotransmission by adenosine A₁-A_{2A} heteromers. *J Neurosci.* 26:2080-7.
- Ciruela F, Gomez-Soler M, Guidolin D, Borroto-Escuela D.O, Agnati L.F, Fuxe K, Fernandez-Dueñas V (2011) Adenosine receptor containing oligomers: their role in the control of dopamine and glutamate neurotransmission in the brain. *Biochim Biophys Acta.* 1808:1245-55.
- Ciruela F, Fernandez-Dueñas V, Llorente J, Borroto-Escuela D, Cuffi ML, Carbonell L, Sanchez S, Agnati LF, Fuxe K, Tasca CI (2012) G protein-coupled receptor oligomerization and brain integration: Focus on adenosinergic transmission. *Brain Res.* 1476:86-95.
- Civelli O, Bunzow JR, Grandy DK (1993) Molecular diversity of the dopamine receptors. *Annu Rev Pharmacol Toxicol.* 33:281–307.
- Claing A, Perry SJ, Achiriloaie M, Walker JK, Albanesi JP, Lefkowitz RJ, Premont RT (2000) Multiple endocytic pathways of G protein-coupled receptors delineated by GIT1 sensitivity. *Proc Natl Acad Sci USA.* 97: 1119–24.
- Clapham DE, Neer EJ (1997) G protein beta gamma subunits. *Annu Rev Pharmacol Toxicol.* 37:167–203.
- Cobbin LB, Einstein R, Maguire MH (1974) Studies on the coronary dilator actions of some adenosine analogues. *Br J Pharmacol.* 50:25–33.
- Cohen MX, Frank MJ (2009) Neurocomputational models of basal ganglia function in learning, memory and choice. *Behav Brain Res.* 199:141-56. doi: 10.1016/j.bbr.2008.09.029.
- Cohen LS, Fracchiolla KE, Becker J, Naider F (2014) Invited review: GPCR structural characterization: using fragments as building blocks to determine a complete structure. *Biopolymers.* 102:223-43. doi: 10.1002/bip.22490.
- Colquhoun D (1973) The relationship between classical and cooperative models for drug action. In: A symposium on drug receptors (Rang HP, ed.), Baltimore: University Park Press. p. 149–82.
- Conn PJ, Pin JP (1997). Pharmacology and functions of metabotropic glutamate receptors. *Annu Rev Pharmacol Toxicol.* 37:205-37.
- Conn PJ, Christopoulos A, Lindsley CW (2009) Allosteric modulators of GPCRs: a novel approach for the treatment of CNS disorders. *Nat Rev Drug Discov.* 8:41-54. doi: 10.1038/nrd2760.
- Conway EJ, Cooke R (1939) The deaminases of adenosine and adenylic acid in blood and tissues. *Biochem J.* 33:479-92.

- Cook Jr EH, Stein MA, Krasowski MD, Cox NJ, Olkon DM, Kieffer JE, Leventhal BL (1995) Association of attention-deficit disorder and the dopamine transporter gene. *Am J Hum Genet.* 56:993–8.
- Cornil CA, Ball GF (2008) Interplay among catecholamine systems: dopamine binds to alpha2-adrenergic receptors in birds and mammals. *J Comp Neurol.* 511:610–27. doi:10.1002/cne.21861
- Cortés A, Gracia E, Moreno E, Mallol J, Lluís C, Canela EI, Casadó V (2015) Moonlighting adenosine deaminase: a target protein for drug development. *Med Res Rev.* 35:85–125. doi: 10.1002/med.21324.
- Cortés A, Moreno E, Rodríguez-Ruiz M, Canela EI, Casadó V (2016) Targeting the dopamine D3 receptor: an overview of drug design strategies. *Expert Opin Drug Discov.* 11:641–64. doi: 10.1080/17460441.2016.1185413.
- Costa R, Tamascia ML, Nogueira MD, Casarini DE, Marcondes FK (2012) Handling of adolescent rats improves learning and memory and decreases anxiety. *J Am Assoc Lab Anim Sci.* 51:548–53.
- Costantino L, Barlocco D (2006) Privileged structures as leads in medicinal chemistry. *Curr Med Chem.* 13:65–85.
- Cowan RL, Wilson CJ, Emson PC, Heizmann CW (1990) Parvalbumin-containing GABAergic interneurons in the rat neostriatum. *J Comp Neurol.* 302:197–205.
- Cristóvão-Ferreira S, Navarro G, Brugarolas M, Pérez-Capote K, Vaz S.H, Fattorini G, Conti F, Lluís C, Ribeiro J.A, McCormick PJ, Casadó V, Franco R, Sebastião AM (2013) A1R-A2AR heteromers coupled to Gs and G i/o proteins modulate GABA transport into astrocytes. *Purinergic Signal.* 9:433–49.
- Cui Q, Karplus M (2008) Allosterity and cooperativity revisited. *Protein Science.* 17:1295–307.
- Cummings DF, Ericksen SS, Goetz A, Schetz JA (2010) Transmembrane segment five serines of the D4 dopamine receptor uniquely influence the interactions of dopamine, norepinephrine, and Ro10-4548. *J Pharmacol Exp Ther.* 333:682–95. doi: 10.1124/jpet.109.164962.
- Cummins TD, Jacoby O, Hawi Z, Nandam LS, Byrne MA, Kim BN, Wagner J, Chambers CD, Bellgrove MA (2014) Alpha-2A adrenergic receptor gene variants are associated with increased intra-individual variability in response time. *Mol Psychiatry.* 19: 1031–6.
- Cunha RA (2005) Neuroprotection by adenosine in the brain: From A(1) receptor activation to A (2A) receptor blockade. *Purinergic Signal.* 1:111–34.
- Cunha RA (2008) Caffeine, adenosine receptors, memory and Alzheimer disease. *Med Clin.* 131:790–5.
- Cunha RA (2016) How does adenosine control neuronal dysfunction and neurodegeneration? *J Neurochem.* 139:1019–55. doi: 10.1111/jnc.13724.
- Cunha RA, Ribeiro JA (2000) Purinergic modulation of [(3)H]GABA release from rat hippocampal nerve terminals. *Neuropharmacology.* 39:1156–67.
- Cunha RA, Ferré S, Vaugeois JM, Chen JF (2008) Potential therapeutic interest of adenosine A2A receptors in psychiatric disorders. *Curr Pharm Des.* 14:1512–24.

- Cussac D, Schaak S, Denis C, Flordellis C, Calise D, Paris H (2001) High level of alpha2-adrenoceptor in rat foetal liver and placenta is due to alpha2B-subtype expression in haematopoietic cells of the erythrocyte lineage. *Br J Pharmacol.* 133:1387-95.
- Cutler DL, Tendolkar A, Grachev ID (2012) Safety, tolerability and pharmacokinetics after single and multiple doses of preladenant (SCH-420814) administered in healthy subjects. *J Clin Pharm Ther.* 37:578-87.
- Cvejic S, Devi LA (1997) Dimerization of the delta opioid receptor: implication for a role in receptor internalization. *J Biol Chem.* 272:26959-64.
- Czermak C, Lehofer M, Liebmann PM, Traynor J (2006) [³⁵S]GTPgammaS binding at the human dopamine D4 receptor variants hD4.2, hD4.4 and hD4.7 following stimulation by dopamine, epinephrine and norepinephrine. *Eur J Pharmacol.* 531:20-4.
- Daaka Y, Luttrell LM, Ahn S, Della Rocca GJ, Ferguson SS, Caron MG, Lefkowitz RJ (1998) Essential role for G protein-coupled receptor endocytosis in the activation of mitogen-activated protein kinase. *J Biol Chem.* 273:685-8.
- Dager SR, Friedman SD (2000) Brain imaging and the effects of caffeine and nicotine. *Ann Med.* 32:592-9.
- Dahlström A, Fuxe K (1964) Localization of monoamines in the lower brain stem. *Experientia.* 20:398-9.
- Darracq L, Blanc G, Glowinski J, Tassin JP (1998) Importance of the noradrenaline-dopamine coupling in the locomotor activating effects of D-amphetamine. *J Neurosci.* 18:2729-39
- Daunt DA, Hurt C, Hein L, Kallio J, Feng F, Kobilka BK (1997) Subtype-specific intracellular trafficking of alpha2-adrenergic receptors. *Mol Pharmacol.* 51:711-20.
- Dawaliby R, Trubbia C, Delporte C, Masureel M, Van Antwerpen P, Kobilka BK, Govaerts C. (2016) Allosteric regulation of G protein-coupled receptor activity by phospholipids. *Nat Chem Biol.* 12:35-9. doi: 10.1038/nchembio.1960.
- De Amici M, Dallanoce C, Holzgrabe U, Tränkle C, Mohr K (2010) Allosteric ligands for G protein-coupled receptors: a novel strategy with attractive therapeutic opportunities. *Med Res Rev.* 30:463-549. doi: 10.1002/med.20166.
- Deary A, Gingrich JA, Falardeau P, Fremeau RT, Bates MD, Caron MG (1990) Molecular cloning and expression of the gene for a human D1 dopamine receptor. *Nature.* 347:72-6.
- Defagot MC, Malchiodi EL, Villar MJ, Antonelli MC (1997) Distribution of D4 dopamine receptor in rat brain with sequence-specific antibodies. *Brain Res Mol Brain Res.* 45:1-12.
- Del Castillo J, Katz B (1957) Interaction at end-plate receptors between different choline derivatives. *Proc R Soc Ser B* 146:369-81.
- De Lean A, Stadel JM, Lefkowitz RJ (1980) A ternary complex model explains the agonist-specific binding properties of the adenylate cyclase-coupled b-adrenergic receptor. *J Biol Chem.* 255:7108-17.
- DeLong MR (1990) Primate models of movement disorders of basal ganglia origin. *Trends Neurosci.* 13:281-5.

- De Mei C, Ramos M, Iitaka C, Borrelli E. (2009) Getting specialized: presynaptic and postsynaptic dopamine D2 receptors. *Curr Opin Pharmacol.* 9:53–8.
- De Meyts P, Roth J, Neville DM Jr, Gavin JR 3rd, Lesniak MA (1973) Insulin interactions with its receptors: experimental evidence for negative cooperativity. *Biochem Biophys Res Commun.* 55:154-61.
- Deupi X, Kobilka BK (2010) Energy landscapes as a tool to integrate GPCR structure, dynamics, and function. *Physiology (Bethesda).* 25:293–303.
- Deutch AY (2013) Parkinson's disease redefined. *Lancet Neurol.* 12:422-3. doi: 10.1016/S1474-4422(13)70052-8.
- Díaz-Cabiale Z, Vivó M, Del Arco A, O'Connor WT, Harte MK, Müller CE, Martínez E, Popoli P, Fuxe K, Ferré S (2002) Metabotropic glutamate mGlu5 receptor-mediated modulation of the ventral striopallidal GABA pathway in rats. Interactions with adenosine A(2A) and dopamine D(2) receptors. *Neurosci Lett.* 324:154-8.
- Díaz-Mataix L, Piper WT, Schiff HC, Roberts CH, Campese VD, Sears RM, LeDoux JE (2017) Characterization of the amplificatory effect of norepinephrine in the acquisition of Pavlovian threat associations. *Learn Mem.* 24:432-9. doi: 10.1101/lm.044412.116.
- Di Chiara G, Bassareo V (2007) Reward system and addiction: what dopamine does and doesn't do. *Curr Opin Pharmacol.* 7:69-76.
- Ding YC, Chi HC, Grady DL, Morishima A, Kidd JR, Kidd KK, Flodman P, Spence MA, Schuck S, Swanson JM, Zhang YP, Moyzis RK (2002) Evidence of positive selection acting at the human dopamine receptor D4 gene locus. *Proc Natl Acad Sci USA.* 99:309-14.
- Dixon AK, Gubitza AK, Sirinathsinghji DJ, Richardson PJ, Freeman TC (1996) Tissue distribution of adenosine receptor mRNAs in the rat. *Br J Pharmacol.* 118:1461–8.
- Dohlman HG, Caron MG, DeBlasi A, Frielle T, Lefkowitz RJ (1990) Role of extracellular disulfide-bonded cysteines in the ligand binding function of the beta 2-adrenergic receptor. *Biochemistry.* 29:2335-42.
- Doré AS, Robertson N, Errey JC, Ng I, Hollenstein K, Tehan B, Hurrell E, Bennett K, Congreve M, Magnani F, Tate CG, Weir M, Marshall FH (2011) Structure of the adenosine A(2A) receptor in complex with ZM241385 and the xanthines XAC and caffeine. *Structure.* 19:1283-93. doi: 10.1016/j.str.2011.06.014.
- Dostrovsky JO, Levy R, Wu JP, Hutchison WD, Tasker RR, Lozano AM (2000) Microstimulation-induced inhibition of neuronal firing in human globus pallidus. *J Neurophysiol.* 84:570-4.
- Downes GB, Gautam N (1999) The G protein subunit gene families. *Genomics.* 62:544–52.
- Dror RO, Green HF, Valant C, Borhani DW, Valcourt JR, Pan AC, Arlow DH, Canals M, Lane JR, Rahmani R, Baell JB, Sexton PM, Christopoulos A, Shaw DE (2013) Structural basis for modulation of a G-protein-coupled receptor by allosteric drugs. *Nature.* 503:295-9.
- Drouin C, Darracq L, Trovero F, Blanc G, Glowinski J, Cotecchia S, Tassin JP (2002) Alpha1b-adrenergic receptors control locomotor and rewarding effects of psychostimulants and opiates. *J Neurosci.* 22:2873-84.

- Dubach M, Schmidt R, Kunkel D, Bowden DM, Martin R, German DC (1987) Primate neostriatal neurons containing tyrosine hydroxylase: immunohistochemical evidence. *Neurosci Lett.* 75:205-10.
- Dunwiddie T V, Masino S A (2001) The role and regulation of adenosine in the central nervous system. *Annual Review Neuroscience.* 24:31–55.
- Dungo R, Deeks ED (2013). Istradefylline: first global approval. *Drugs.* 73:875-82.
- Durieux PF, Bearzatto B, Guiducci S, Buch T, Waisman A, Zoli M, Schiffmann SN, de Kerchove d'Exaerde A (2009) D2R striatopallidal neurons inhibit both locomotor and drug reward processes. *Nat Neurosci.* 12:393-5. doi: 10.1038/nn.2286.
- Durroux T (2005) Principles: a model for the allosteric interactions between ligand binding sites within a dimeric GPCR. *Trends Pharmacol Sci.* 26:376–84.
- Eason MG, Kurose H, Holt BD, Raymond JR, Liggett SB (1992) Simultaneous coupling of alpha 2-adrenergic receptors to two G-proteins with opposing effects. Subtype-selective coupling of alpha 2C10, alpha 2C4, and alpha 2C2 adrenergic receptors to Gi and Gs. *J Biol Chem.* 267:15795-801.
- Eason MG, Liggett SB (1995) Identification of a Gs coupling domain in the amino terminus of the third intracellular loop of the alpha 2A-adrenergic receptor. Evidence for distinct structural determinants that confer Gs versus Gi coupling. *J Biol Chem.* 270:24753-60.
- Ehringer H, Hornykiewicz O (1960) Verteilung von noradrenalin and dopamin im gehirn des menschen und ihr verhalten bei erkrankungen des extrapyramidalen systems. *Klin Wschr.* 38:1126–239.
- Eiden LE, Schäfer MK, Weihe E, Schütz B (2004) The vesicular amine transporter family (SLC18): amine/proton antiporters required for vesicular accumulation and regulated exocytotic secretion of monoamines and acetylcholine. *Pflugers Arch.* 447:636-40.
- Eisenhofer G, Kopin IJ, Goldstein D (2004) Catecholamine metabolism: a contemporary view with implications for physiology and medicine. *Pharmacol Rev.* 56:331-49.
- Elmenhorst D, Meyer PT, Winz OH, Matusch A, Ermert J, Coenen HH, Basheer R, Haas HL, Zilles K, Bauer A (2007) Sleep deprivation increases A1 adenosine receptor binding in the human brain: a positron emission tomography study. *J Neurosci.* 27:2410-5.
- Emorine LJ, Marullo S, Briend-Sutren MM, Patey G, Tate K, Delavier-Klutchko C, Strosberg AD (1989) Molecular characterization of the human beta 3-adrenergic receptor. *Science.* 245:1118-21.
- Erickson JD, Schafer MK, Bonner TI, Eiden LE, Weihe E (1996) Distinct pharmacological properties and distribution in neurons and endocrine cells of two isoforms of the human vesicular monoamine transporter. *Proc Natl Acad Sci USA.* 93:5166-71.
- Ernst M, Zametkin AJ, Matochik JA, Jons PH, Cohen RM (1998) DOPA decarboxylase activity in attention deficit hyperactivity disorder adults. A [fluorine-18] fluorodopa positron emission tomographic study. *J Neurosci.* 18:5901-7.

- Evans BE, Rittle KE, Bock MG, DiPardo RM, Freidinger RM, Whitter WL, Lundell GF, Veber DF, Anderson PS, Chang RS, et al (1988) Methods for drug discovery: development of potent, selective, orally effective cholecystokinin antagonists. *J Med Chem.* 31:2235-46.
- Everitt BJ, Robbins TW (2016) Drug Addiction: Updating Actions to Habits to Compulsions Ten Years On. *Annu Rev Psychol.* 67:23-50. doi: 10.1146/annurev-psych-122414-033457.
- Evron T, Daigle TL, Caron MG (2012) GRK2: multiple roles beyond G protein-coupled receptor desensitization. *Trends Pharmacol Sci.* 33:154-64.
- Factor SA, Wolski K, Togasaki DM, Huyck S, Cantillon M, Ho TW, Hauser RA, Pourcher E (2013) Long-term safety and efficacy of preladenant in subjects with fluctuating Parkinson's disease. *Mov Disord.* 28:817-20.
- Fagerholm V, Rokka J, Nyman L, Sallinen J, Tiihonen J, Tupala E, Haaparanta M, Hietala J. (2008) Autoradiographic characterization of alpha(2C)-adrenoceptors in the human striatum. *Synapse.* 62:508-15.
- Fallon JH, Koziell DA, Moore RY (1978) Catecholamine innervation of the basal forebrain. II. Amygdala, suprarhinal cortex and entorhinal cortex. *J Comp Neurol.* 180:509-32.
- Fan QR, Guo WY, Geng Y, Evelyn MG (2017) Class C GPCR: Obligatory Heterodimerization of GABAB Receptor (chapter 12). In: *G-ProteinCoupled Receptor Dimers, The Receptors*, vol 33 (Herrick-Davis K, Milligan G, Di Giovanni G, eds.). Springer, 307-25.
- Faraone SV, Perlis RH, Doyle AE, Smoller JW, Goralnick JJ, Holmgren MA, Sklar P (2005) Molecular genetics of attention-deficit/hyperactivity disorder. *Biol Psychiatry.* 57:1313–23.
- Farré D, Muñoz A, Moreno E, Reyes-Resina I, Canet-Pons J, Dopeso-Reyes IG, Rico AJ, Lluís C, Mallol J, Navarro G, Canela EI, Cortés A, Labandeira-García JL, Casadó V, Lanciego JL, Franco R (2015) Stronger Dopamine D1 Receptor-Mediated Neurotransmission in Dyskinesia. *Mol Neurobiol.* 52:1408-20. doi: 10.1007/s12035-014-8936-x.
- Farrens DL, Altenbach C, Yang K, Hubbell WL, Khorana HG (1996) Requirement of rigid-body motion of transmembrane helices for light activation of rhodopsin. *Science.* 274:768–70.
- Feng Z, Hu G, Ma S, Xie XQ (2015) Computational advances for the development of allosteric modulators and bitopic ligands in G protein-coupled receptors. *AAPS J.* 17:1080-95.
- Ferguson SS (2001) Evolving concepts in G protein-coupled receptor endocytosis: the role in receptor desensitization and signaling. *Pharmacol Rev.* 53:1-24.
- Fernández-Dueñas V, Gómez-Soler M, Morató X, Núñez F, Das A, Kumar TS, Jaumà S, Jacobson KA, Ciruela F (2013) Dopamine D(2) receptor-mediated modulation of adenosine A(2A) receptor agonist binding within the A(2A)R/D(2)R oligomer framework. *Neurochem Int.* 63:42-6. doi: 10.1016/j.neuint.2013.04.006.
- Fernández-Dueñas V, Taura JJ, Cottet M, Gómez-Soler M, López-Cano M, Ledent C, Watanabe M, Trinquet E, Pin JP, Lujan R, Durroux T, Ciruela F (2015) Untangling dopamine-adenosine receptor-receptor assembly in experimental parkinsonism in rats. *Dis. Model. Mech.* 8:57-63.
- Ferrada C, Moreno E, Casadó V, Bongers G, Cortés A, Mallol J, Canela EI, Leurs R, Ferré S, Lluís C, Franco R (2009) Marked changes in signal transduction upon heteromerization of dopamine D1 and histamine H3 receptors. *Br J Pharmacol.* 157:64-75. doi: 10.1111/j.1476-5381.2009.00152.x.

- Ferrandon S, Feinstein TN, Castro M, Wang B, Bouley R, Potts JT, Gardella TJ, Vilardaga JP (2009) Sustained cyclic AMP production by parathyroid hormone receptor endocytosis. *Nat Chem Biol.* 5:734–42 doi: 10.1038/nchembio.206.
- Ferré S (2008) An update on the mechanisms of the psychostimulant effects of caffeine. *J Neurochem.* 105:1067-79.
- Ferré S (2010) Role of the central ascending neurotransmitter systems in the psychostimulant effects of caffeine. *J Alzheimers Dis.* 1:S35-49. doi: 10.3233/JAD-2010-1400.
- Ferré S (2015) The GPCR heterotetramer: challenging classical pharmacology. *Trends Pharmacol Sci.* 36:145-52. doi: 10.1016/j.tips.2015.01.002.
- Ferre S, von Euler G, Johansson B, Fredholm BB, Fuxe K (1991) Stimulation of high-affinity adenosine A2 receptors decreases the affinity of dopamine D2 receptors in rat striatal membranes. *Proc Natl Acad Sci USA.* 88:7238-41.
- Ferré S, O'Connor WT, Svenningsson P, Bjorklund L, Lindberg J, Tinner B, Stromberg I, Goldstein M, Ögren SO, Ungerstedt U, Fredholm BB, Fuxe K (1996) Dopamine D1 receptor-mediated facilitation of GABAergic neurotransmission in the rat strioentopenduncular pathway and its modulation by adenosine A1 receptor-mediated mechanisms. *Eur J Neurosci.* 8:1545-53.
- Ferré S, Fredholm BB, Morelli M, Popoli P, Fuxe K (1997) Adenosine-dopamine receptor-receptor interactions as an integrative mechanism in the basal ganglia. *Trends Neurosci.* 20:482-7.
- Ferré S, Torvinen M, Antoniou K, Irenius E, Civelli O, Arenas E, Fredholm BB, Fuxe K (1998) Adenosine A1 receptor-mediated modulation of dopamine D1 receptors in stably cotransfected fibroblast cells. *J Biol Chem.* 273:4718-24.
- Ferré S, Popoli P, Giménez-Llort L, Rimondini R, Müller CE, Strömberg I, Ögren SO, Fuxe K (2001) Adenosine/dopamine interaction: implications for the treatment of Parkinson's disease. *Parkinsonism Relat Disord.* 7:235-241.
- Ferré S, Karcz-Kubicha M, Hope BT, Popoli P, Burgueño J, Gutierrez MA, Casadó V, Fuxe K, Goldberg SR, Lluís C, Franco R, Ciruela F (2002) Synergistic interaction between adenosine A2A and glutamate mGlu5 receptors: Implications for striatal neuronal function. *Proc Natl Acad Sci.* 99:11940-5.
- Ferré S, Ciruela F, Canals M, Marcellino D, Burgueno J, et al (2004) Adenosine A2A-dopamine D2 receptor-receptor heteromers. Targets for neuro-psychiatric disorders. *Parkinsonism Relat Disord.* 10:265-71.
- Ferré S, Agnati LF, Ciruela F, Lluís C, Woods AS, Fuxe K, Franco R (2007) Neurotransmitter receptor heteromers and their integrative role in “local modules”: the striatal spine module. *Brain Res Rev.* 55:55-67.
- Ferré S, Goldberg SR, Lluís C, Franco R (2009a) Looking for the role of cannabinoid receptor heteromers in striatal function. *Neuropharmacology.* 56:226-34.
- Ferré S, Baler R, Bouvier M, Caron MG, Devi LA, Durroux T, Fuxe K, George SR, Javitch JA, Lohse MJ, Mackie K, Milligan G, Pflieger KD, Pin JP, Volkow ND, Waldhoer M, Woods AS, Franco R (2009b) Building a new conceptual framework for receptor heteromers. *Nat Chem Biol.* 5:131-4. doi: 10.1038/nchembio0309-131.

- Ferré S, Navarro G, Casadó V, Cortés A, Mallol J, Canela EI, Lluís C, Franco R (2010a) G-protein coupled receptor heteromers as new targets for drug development. *Prog. Mol. Biol. Transl. Sci.* 91, 41-52.
- Ferré S, Lluís C, Lanciego JL, Franco R (2010b) Prime time for G-protein-coupled receptor heteromers as therapeutic targets for CNS disorders: the dopamine D₁-D₃ receptor heteromer. *CNS Neurol Disord Drug Targets.* 9:596-600.
- Ferré S, Casadó V, Devi LA, Filizola M, Jockers R, Lohse MJ, Milligan G, Pin JP, Guitart X (2014) G protein-coupled receptor oligomerization revisited: functional and pharmacological perspectives. *Pharmacol Rev.* 66:413-34.
- Ferré S, Bonaventura J, Tomasi D, Navarro G, Moreno E, Cortés A, Lluís C, Casadó V, Volkow ND (2016) Allosteric mechanisms within the adenosine A_{2A}-dopamine D₂ receptor heterotetramer. *Neuropharmacology.* 104:154-60. doi: 10.1016/j.neuropharm.2015.05.028.
- Ferré S (2017) Adenosine control of striatal function-implications for the treatment of apathy in basal ganglia disorders (Chapter 12). In: *Adenosine receptors in Neurodegenerative Diseases.* David Blum, Luisa V. Lopes (eds). Elsevier Inc. 232-54. doi: 10.1016/B978-0-12-803724-9.00012-0
- Filion M, Tremblay L, Bédard PJ (1991) Effects of dopamine agonists on the spontaneous activity of globus pallidus neurons in monkeys with MPTP-induced parkinsonism. *Brain Res.* 547:152-61.
- Fillenz M, Lowry JP (1998) Studies of the source of glucose in the extracellular compartment of the rat brain. *Dev Neurosci.* 20:365-8.
- Fillenz M, Lowry JP, Boutelle MG, Fray AE (1999) The role of astrocytes and noradrenaline in neuronal glucose metabolism. *Acta Physiol Scand.* 167:275-84.
- Filip M, Zaniewska M, Frankowska M, Wydra K, Fuxe K (2012) The importance of the adenosine A_{2A} receptor-dopamine D₂ receptor interaction in drug addiction. *Curr Med Chem.* 19:317-355.
- Fisone G, Borgkvist A, Usiello A (2004) Caffeine as a psychomotor stimulant: mechanism of action. *Cellular and Molecular Life Sciences.* 61:857-872.
- Font J, López-Cano M, Notartomaso S, Scarselli P, Di Pietro P, Bresolí-Obach R, Battaglia G, Malhaire F, Rovira X, Catena J, Giraldo J, Pin JP, Fernández-Dueñas V, Goudet C, Nonell S, Nicoletti F, Llebaria A, Ciruela F (2017) Optical control of pain in vivo with a photoactive mGlu₅ receptor negative allosteric modulator. *Elife.* 11:6. pii: e23545. doi: 10.7554/eLife.23545.
- Franco R, Casadó V, Ciruela F, Mallol J, Lluís C, Canela EI (1996) The cluster-arranged cooperative model: a model that accounts for the kinetics of binding to A₁ adenosine receptors. *Biochemistry* 35:3007-15.
- Franco R, Casadó V, Mallol J, Ferré S, Fuxe K, Cortés A, Ciruela F, Lluís C, Canela EI (2005) Dimer-based model for heptaspanning membrane receptors. *Trends Biochem Sci.* 30:360-66.
- Franco R, Casadó V, Mallol J, Ferrada C, Ferré S, Fuxe K, Cortés A, Ciruela F, Lluís C, Canela EI (2006) The two-state dimer receptor model: a general model for receptor dimers. *Mol Pharmacol* 69:1905-12.

- Frank M, Thumer L, Lohse MJ, Bunemann MG (2005) protein activation without subunit dissociation depends on a Gai-specific region. *J Biol Chem.* 280:24584–90.
- Franowicz JS, Kessler LE, Borja CM, Kobilka BK, Limbird LE, Arnsten AF (2002) Mutation of the alpha2A-adrenoceptor impairs working memory performance and annuls cognitive enhancement by guanfacine. *J Neurosci.* 22:8771-7.
- Frederick AL, Yano H, Trifilieff P, Vishwasrao HD, Biezonski D, Mészáros J, Urizar E, Sibley DR, Kellendonk C, Sonntag KC, Graham DL, Colbran RJ, Stanwood GD, Javitch JA (2015) Evidence against dopamine D1/D2 receptor heteromers. *Mol Psychiatry.* 20:1373-85. doi: 10.1038/mp.2014.166.
- Fredholm BB (2014) Adenosine-a physiological or pathophysiological agent?. *J Mol Med (Berl).* 92:201-6.
- Fredholm BB, Bättig K, Holmén J, Nehlig A, Zvartau EE (1999) Actions of caffeine in the brain with special reference to factors that contribute to its widespread use. *Pharmacol Rev.* 51:83-133.
- Fredholm BB, Chen JF, Cunha RA, Svenningsson P, Vaugeois JM (2005) Adenosine and brain function. *Int Rev Neurobiol.* 63:191-270.
- Fremeau RT, Duncan GE, Fornaretto MG, Dearry A, Gingrich JA, Breese GR, Caron MG (1991) Localization of D1 dopamine receptor mRNA in brain supports a role in cognitive, affective, and neuroendocrine aspects of dopaminergic neurotransmission. *Proc Natl Acad Sci USA.* 88:3772-6.
- French GM (1959) A deficit associated with hypermotility in monkeys with lesions of the dorsolateral frontal granular cortex. *J Comp Physiol Psychol.* 52:25-8.
- Fribourg M, Moreno JL, Holloway T, Provasi D, Baki L, Mahajan R, Park G, Adney SK, Hatcher C, Eltit JM, Ruta JD, Albizu L, Li Z, Umali A, Shim J, Fabiato A, MacKerell AD Jr, Brezina V, Sealton SC, Filizola M, González-Maeso J, Logothetis DE (2011) Decoding the signaling of a GPCR heteromeric complex reveals a unifying mechanism of action of antipsychotic drugs. *Cell.* 147:1011-23.
- Frielle T, Collins S, Daniel KW, Caron MG, Lefkowitz RJ, Kobilka BK (1987) Cloning of the cDNA for the human beta 1-adrenergic receptor. *Proc Natl Acad Sci. USA.* 84:7920-4.
- Froehlich TE, Epstein JN, Nick TG, Melguizo Castro MS, Stein MA, Brinkman WB, Graham AJ, Langberg JM, Kahn RS (2011) Pharmacogenetic predictors of methylphenidate dose-response in attention-deficit/hyperactivity disorder. *J Am Acad Child Adolesc Psychiatry.* 50:1129-39.e2. doi: 10.1016/j.jaac.2011.08.002.
- Fronik P, Gaiser BI, Sejer Pedersen D (2017) Bitopic ligands and metastable binding sites: opportunities for G protein-coupled receptor (GPCR) medicinal chemistry. *J Med Chem.* 60:4126-34. doi: 10.1021/acs.jmedchem.6b01601.
- Fukumitsu N, Ishii K, Kimura Y, Oda K, Sasaki T, Mori Y, Ishiwata K (2005) Adenosine A1 receptor mapping of the human brain by PET with 8-dicyclopropylmethyl-1-11C-methyl-3-propylxanthine. *J Nucl Med.* 46:32-7.
- Galés C, Rebois RV, Hogue M, Trieu P, Breit A, Hébert TE, Bouvier M (2005) Real-time monitoring of receptor and G-protein interactions in living cells. *Nat. Methods* 2, 177–84.

- Galés C, Van Durm JJ, Schaak S, Pontier S, Percherancier Y, Audet M, Paris H, Bouvier M (2006) Probing the activation-promoted structural rearrangements in preassembled receptor-G protein complexes. *Nat Struct Mol Biol.* 13:778-86.
- Gao ZG, Jacobson KA (2006) Keynote review: allosterism in membrane receptors. *Drug Discov Today* 11:191-202.
- Gao ZG, Jacobson KA (2007). Emerging adenosine receptor agonists. *Expert Opin Emerg Drugs.* 12:479-492.
- Gao ZG, Jacobson KA (2013) Allosteric modulation and functional selectivity of G protein-coupled receptors. *Drug Discov Today Technol.* 10:e237-43.
- Gaspar P, Bloch B, Le Moine C (1995) D1 and D2 receptor gene expression in the rat frontal cortex: cellular localization in different classes of efferent neurons. *Eur J Neurosci.* 7:1050-63.
- Gentry PR, Sexton PM, Christopoulos (2015) A Novel Allosteric Modulators of G Protein-coupled Receptors. *J Biol Chem.* 290:19478-88. doi: 10.1074/jbc.R115.662759.
- Gerfen CR (2000a) Dopamine-mediated gene regulation in models of Parkinson's disease. *Ann Neurol.* 47:S42-50.
- Gerfen CR (2000b) Molecular effects of dopamine on striatal-projection pathways. *Trends Neurosci.* 23:S64-70.
- Gerfen CR, Engber TM, Mahan LC, Susel Z, Chase TN, Monsma Jr FJ, Sibley DR (1990) D1 and D2 dopamine receptor-regulated gene expression of striatonigral and striatopallidal neurons. *Science.* 250:1429-32.
- Gessi S, Merighi S, Sacchetto V, Simioni C, Borea PA (2011) Adenosine receptors and cancer. *Biochim Biophys Acta.* 1808:1400-12.
- Gharibi B, Abraham AA, Ham J, Evans BA (2012) Contrasting effects of A1 and A2b adenosine receptors on adipogenesis. *Int J Obes (Lond).* 36:397-406. doi: 10.1038/ijo.2011.129.
- Gherbi K, May LT, Baker JG, Briddon SJ, Hill SJ (2015) Negative cooperativity across β 1-adrenoceptor homodimers provides insights into the nature of the secondary low-affinity CGP 12177 β 1-adrenoceptor binding conformation. *FASEB J.* 29:2859-71. doi: 10.1096/fj.14-265199.
- Gilchrist RL, Ryu KS, Ji I, Ji TH (1996) The luteinizing hormone/chorionic gonadotropin receptor has distinct transmembrane conductors for cAMP and inositol phosphate signals. *J Biol Chem.* 271:19283-7.
- Gill M, Daly G, Heron S, Hawi Z, Fitzgerald M (1997) Confirmation of association between attention deficit hyperactivity disorder and a dopamine transporter polymorphism. *Mol Psychiat.* 2:311-3.
- Gilman AG (1987) G proteins: transducers of receptor-generated signals. *Annu Rev Biochem.* 56:615-49.
- Ginés S, Hillion J, Torvinen M, Le Crom S, Casadó V, Canela EI, Rondin S, Lew JY, Watson S, Zoli M, Agnati LF, Verniera P, Lluís C, Ferré S, Fuxe K, Franco R (2000) Dopamine D1 and adenosine A1 receptors form functionally interacting heteromeric complexes. *Proc Natl Acad Sci USA.* 97:8606-11.

- Gingrich JA, Caron MG (1993) Recent advances in the molecular biology of dopamine receptors. *Annu Rev Neurosci.* 16:299-321.
- Girault JA, Greengard P (2004) The neurobiology of dopamine signaling. *Arch Neurol.* 61:641-4.
- Giros B, Sokoloff P, Martres MP, Riou JF, Emorine LJ, Schwartz JC (1989) Alternative splicing directs the expression of two D2 dopamine receptor isoforms. *Nature.* 342:923-926.
- Giros B, Martres MP, Pilon C, Sokoloff P, Schwartz JC (1991) Shorter variants of the D3 dopamine receptor produced through various patterns of alternative splicing. *Biochem Biophys Res Commun.* 176:1584-92.
- Gizer IR, Ficks C, Waldman ID (2009) Candidate gene studies of ADHD: A meta-analytic review. *Hum Genet.* 126:51-90.
- Glass MJ, Pickel VM (2002) Alpha(2A)-adrenergic receptors are present in mu-opioid receptor containing neurons in rat medial nucleus tractus solitarius. *Synapse.* 43:208-18.
- Glass M, Dragunow M, Faull RL (2000) The pattern of neurodegeneration in Huntington's disease: a comparative study of cannabinoid, dopamine, adenosine and GABA(A) receptor alterations in the human basal ganglia in Huntington's disease. *Neuroscience.* 97:505-19.
- Glass M, Govindpani K, Furkert DP, Hurst DP, Reggio PH, Flanagan JU (2016) One for the Price of Two. Are Bivalent Ligands Targeting Cannabinoid Receptor Dimers Capable of Simultaneously Binding to both Receptors? *Trends Pharmacol Sci.* 37:353-363. doi: 10.1016/j.tips.2016.01.010.
- Gloriam DE, Schioth HB, Fredriksson R (2005). Nine new human Rhodopsin family G-protein coupled receptors: identification, sequence characterisation and evolutionary relationship. *Biochem Biophys Acta.* 1722:235-46.
- Glukhova A, Thal DM, Nguyen AT, Vecchio EA, Jörg M, Scammells PJ, May LT, Sexton PM, Christopoulos A (2017) Structure of the adenosine A1 receptor reveals the basis for subtype selectivity. *Cell.* 168:867-77.e13.
- Göblyös A, Ijzerman AP (2011) Allosteric modulation of adenosine receptors. *Biochim Biophys Acta.* 1808:1309-18.
- Godefroy O, Rousseaux M (1996) Binary choice in patients with prefrontal or posterior brain damage. A relative judgement theory analysis. *Neuropsychologia.* 34:1029-38.
- Godin AG, Rappaz B, Potvin-Trottier L, Kennedy TE, De Koninck Y, Wiseman PW (2015) Spatial intensity distribution analysis reveals abnormal oligomerization of proteins in single cells. *Biophys J.* 109:710-21. doi: 10.1016/j.bpj.2015.06.068.
- Goin JC, Nathanson NM (2006) Quantitative analysis of muscarinic acetylcholine receptor homoand heterodimerization in live cells: regulation of receptor down-regulation by heterodimerization. *J Biol Chem.* 281:5416-25.
- Gold PW (2015) The organization of the stress system and its dysregulation in depressive illness. *Mol Psychiatry.* 20:32-47. doi: 10.1038/mp.2014.163.
- Goldman-Rakic PS (1998) The cortical dopamine system: role in memory and cognition. *Adv Pharmacol.* 42:707-11.

- Goldman-Rakic PS, Lidow MS, Gallager DW (1990) Overlap of dopaminergic, adrenergic, and serotonergic receptors and complementarity of their subtypes in primate prefrontal cortex. *J Neurosci.* 10:2125-38.
- Goldman-Rakic PS, Lidow MS, Smiley JF, Williams MS (1992) The anatomy of dopamine in monkey and human prefrontal cortex. *J Neural Transm Suppl* 36:163-177
- Goldman-Rakic PS, Castner SA, Svensson TH, Siever LJ, Williams GV (2004) Targeting the dopamine D1 receptor in schizophrenia: insights for cognitive dysfunction. *Psychopharmacology.* 174:3–16.
- Gomes CV, Kaster MP, Tome AR, Agostinho PM, Cunha RA (2011) Adenosine receptors and brain diseases: neuroprotection and neurodegeneration. *Biochim Biophys Acta.* 1808:1380–99.
- Gomes I, Ayoub MA, Fujita W, Jaeger WC, Pfleger KD, Devi LA (2016) G Protein-coupled receptor heteromers. *Annu Rev Pharmacol Toxicol.* 56:403-25. doi: 10.1146/annurev-pharmtox-011613-135952.
- González A, Cordero A, Matsoukas M, Zachmann J, Pardo L (2014) Modeling of G protein-coupled receptors using crystal structures: from monomers to signaling complexes. *Adv Exp Med Biol.* 796:15-33. doi: 10.1007/978-94-007-7423-0_2.
- González S, Rangel-Barajas C, Peper M, Lorenzo R, Moreno E, Ciruela F, Boryc J, Ortiz J, Lluís C, Franco R, McCormick PJ, Volkow ND, Rubinstein M, Floran B, Ferré S. (2012a) Dopamine D4 receptor, but not the ADHD-associated D4.7 variant, forms functional heteromers with the dopamine D2S receptor in the brain. *Mol Psychiatry.* 17:650–62.
- González S, Moreno-Delgado D, Moreno E, Pérez-Capote K, Franco R, Mallol J, Cortés A, Casadó V, Lluís C, Ortiz J, Ferré S, Canela EI, McCormick PJ (2012b) Circadian-related heteromerization of adrenergic and dopamine D₄ receptors modulates melatonin synthesis and release in the pineal gland. *PLoS Biol.* 10:e1001347. doi: 10.1371/journal.pbio.1001347.
- González de Mejia E, Ramirez-Mares MV (2014) Impact of caffeine and coffee on our health. *Trends in Endocrinology and Metabolism.* 25:489–92.
- Gonzalez-Islas C, Hablitz JJ (2003) Dopamine enhances EPSCs in layer II-III pyramidal neurons in rat prefrontal cortex. *J Neurosci.* 23:867-75.
- Gonzalez-Maeso J (2011) GPCR oligomers in pharmacology and signaling. *Mol Brain.* 4:20. doi: 10.1186/1756-6606-4-20.
- Goodman OB Jr, Krupnick JG, Santini F, Gurevich VV, Penn RB, Gagnon AW, Keen JH, Benovic JL (1996) β -Arrestin acts as a clathrin adaptor in endocytosis of the β 2-adrenergic receptor. *Nature.* 383:447–50. doi: 10.1038/383447a0.
- Gracia E, Cortés A, Meana JJ, García-Sevilla J, Hershfield M S, Canela EI, Mallol J, Lluís C, Franco R, Casadó V (2008) Human adenosine deaminase as an allosteric modulator of human A1 adenosine receptor: abolishment of negative cooperativity for [3H](R)-PIA binding to the caudate nucleus. *Journal of Neurochemistry.* 107:161–170.
- Gracia E, Pérez-Capote K, Moreno E, Barkešová J, Mallol J, Lluís C, Franco R, Cortés A, Casadó V, Canela EI (2011) A2A adenosine receptor ligand binding and signalling is allosterically modulated by adenosine deaminase. *Biochem J.* 435:701-9. doi: 10.1042/BJ20101749.

- Gracia E, Farré D, Cortés A, Ferrer-Costa C, Orozco M, Mallol J, Lluís C, Canela EI, McCormick PJ, Franco R, Fanelli F, Casadó V (2013a) The catalytic site structural gate of adenosine deaminase allosterically modulates ligand binding to adenosine receptors. *FASEB J.* 27:1048-61. doi: 10.1096/fj.12-212621.
- Gracia E, Moreno E, Cortés A, Lluís C, Mallol J, McCormick PJ, Canela EI, Casadó V (2013b) Homodimerization of adenosine A₁ receptors in brain cortex explains the biphasic effects of caffeine. *Neuropharmacology.* 71:56-69. doi: 10.1016/j.neuropharm.2013.03.005.
- Graf R, Mattera R, Codina J, Evans T, Ho YK, Estes MK, Birnbaumer L (1992) Studies on the interaction of alpha subunits of GTP-binding proteins with beta gamma dimers. *Eur J Biochem.* 210:609-19.
- Graveland GA, DiFiglia M (1985) The frequency and distribution of medium-sized neurons with indented nuclei in the primate and rodent neostriatum. *Brain Res.* 327:307-11.
- Gray JH, Owen RP, Giacomini KM (2004) The concentrative nucleoside transporter family, SLC28. *Pflugers Arch.* 447:728-34.
- Graybiel AM, Kimura M (1995) Adaptive neural networks in the basal ganglia. In: *Models of information processing in the basal ganglia* (Houk JC, Davis JL, Beiser DG, eds.). Cambridge: MIT Press. p. 103-16.
- Graybiel AM, Canales JJ, Capper-Loup C (2000) Levodopa-induced dyskinesias and dopamine-dependent stereotypies: a new hypothesis. *Trends Neurosci.* 23:S71-7.
- Grenhoff J, Nisell M, Ferre S, Aston-Jones G, Svensson TH (1993) Noradrenergic modulation of midbrain dopamine cell firing elicited by stimulation of the locus coeruleus in the rat. *J Neural Transm.* 93:11-25.
- Gross CG (1963) Locomotor activity following lateral frontal lesions in rhesus monkeys. *J Comp Physiol Psychol.* 56:232-6.
- Grundmann M, Tikhonova IG, Hudson BD, Smith NJ, Mohr K, Ulven T, Milligan G, Kenakin T, Kostenis E (2016) A molecular mechanism for sequential activation of a G protein-coupled receptor. *Cell Chem Biol.* 23:392-403. doi: 10.1016/j.chembiol.2016.02.014.
- Grunebaum E, Cohen A, Roifman CM (2013) Recent advances in understanding and managing adenosine deaminase and purine nucleoside phosphorylase deficiencies. *Curr Opin Allergy Clin Immunol.* 13:630-8. doi: 10.1097/ACI.0000000000000006.
- Guillot TS, Miller GW (2009) Protective actions of the vesicular monoamine transporter 2 (VMAT2) in monoaminergic neurons. *Mol Neurobiol.* 39:149-70. doi: 10.1007/s12035-009-8059-y.
- Guitart X, Navarro G, Moreno E, Yano H, Cai NS, Sánchez-Soto M, Kumar-Barodia S, Naidu YT, Mallol J, Cortés A, Lluís C, Canela EI, Casadó V, McCormick PJ, Ferré S (2014) Functional selectivity of allosteric interactions within G protein coupled receptor oligomers: The dopamine D1-D3 receptor heterotetramer. *Mol Pharmacol.* 86:417-29.
- Guixà-González R, Albasanz JL, Rodríguez-Espigares I, Pastor M, Sanz F, Martí-Solano M, Manna M, Martínez-Seara H, Hildebrand PW, Martín M, Selent J (2017) Membrane cholesterol access into a G-protein-coupled receptor. *Nat Commun.* 8:14505. doi: 10.1038/ncomms14505.

- Gundlfinger A, Bischofberger J, Johenning FW, Torvinen M, Schmitz D, Breustedt J (2007) Adenosine modulates transmission at the hippocampal mossy fibre synapse via direct inhibition of presynaptic calcium channels. *J Physiol.* 582:263–77.
- Guo W, Shi L, Javitch JA (2003) The fourth transmembrane segment forms the interface of the dopamine D2 receptor homodimer. *J Biol Chem.* 278:4385-8.
- Guo T, Hobbs DW (2003) Privileged structure-based combinatorial libraries targeting G protein-coupled receptors. *Assay Drug DeV. Technol.* 1:579-92.
- Guo H, An S, Ward R, Yang Y, Liu Y, Guo X, Hao Q, Xu T (2017) Methods used to study the oligomeric structure of G-protein-coupled receptors. *Biosci Rep.* 37:BSR20160547 doi: 10.1042/BSR20160547.
- Gutiérrez-de-Terán H, Massink A, Rodríguez D, Liu W, Han GW, Joseph JS, Katritch I, Heitman LH, Xia L, Ijzerman AP, Cherezov V, Katritch V, Stevens RC (2013) The role of a sodium ion binding site in the allosteric modulation of the A(2A) adenosine G protein-coupled receptor. *Structure.* 21:2175-85. doi: 10.1016/j.str.2013.09.020.
- Haber SN (2014) The place of dopamine in the cortico-basal ganglia circuit. *Neuroscience.* 282:248-57. doi: 10.1016/j.neuroscience.2014.10.008.
- Haber SN, Behrens TE (2014) The neural network underlying incentive-based learning: implications for interpreting circuit disruptions in psychiatric disorders. *Neuron.* 83:1019-39. doi: 10.1016/j.neuron.2014.08.031.
- Haeusler D, Grassinger L, Fuchshuber F, Hörleinsberger WJ, Höftberger R, Leisser I, Girschele F, Shanab K, Spreitzer H, Gerdenitsch W, Hacker M, Wadsak W, Mitterhauser M (2015) Hide and seek: a comparative autoradiographic in vitro investigation of the adenosine A3 receptor. *Eur. J. Nucl Med Mol Imaging.* 42:928-39.
- Hall DA (2000) Modeling the functional effects of allosteric modulators at pharmacological receptors: an extension of the two-state model of receptor activation. *Mol Pharmacol.* 58:1412–23.
- Hamill RW, Shapiro RE, Vizzard MA (2012) Peripheral autonomic nervous system. In: *Primer on the autonomic nervous system* (Robertson D, Biaggioni I, Burnstock G, Low PA, Paton JFR, eds.). London: Academic Press. p. 17–26.
- Hamm HE (1998). The many faces of G protein signaling. *J Biol Chem.* 273:669-72.
- Han Y, Moreira IS, Urizar E, Weinstein H, and Javitch JA (2009) Allosteric communication between protomers of dopamine class A GPCR dimers modulates activation. *Nat Chem Biol.* 5:688–95.
- Hansson E, Ronnback L (1991) Receptor regulation of the glutamate, GABA and taurine high-affinity uptake into astrocytes in primary culture. *Brain Res.* 548:215-21.
- Hanyaloglu AC, von Zastrow M (2008) Regulation of GPCRs by endocytic membrane trafficking and its potential implications. *Annu Rev Pharmacol Toxicol.* 48:537–68.
- Hara M, Fukui R, Hieda E, Kuroiwa M, Bateup HS, Kano T, Greengard P, Nishi A (2010) Role of adrenoceptors in the regulation of dopamine/DARPP-32 signaling in neostriatal neurons. *J Neurochem.* 113:1046-59. doi:10.1111/j.1471-4159.2010.06668.x.

- Harley CW (1987) A role for norepinephrine in arousal, emotion and learning?: limbic modulation by norepinephrine and the Kety hypothesis. *Prog Neuropsychopharmacol Biol Psychiatry*. 11:419-58.
- Harley CW (2007) Norepinephrine and the dentate gyrus. *Prog Brain Res*. 163:299-318.
- Harpsøe K, Isberg V, Tehan BG, Weiss D, Arsova A, Marshall FH, Bräuner-Osborne H, Gloriam DE (2015) Selective negative allosteric modulation of metabotropic glutamate receptors – a structural perspective of ligands and mutants. *Sci Rep*. 5:13869. doi: 10.1038/srep13869.
- Hasko G, Pacher P (2008) A2A receptors in inflammation and injury: lessons learned from transgenic animals. *J Leukoc Biol*. 83:447-55.
- Hasko G, Linden J, Cronstein B, Pacher P (2008) Adenosine receptors: therapeutic aspects for inflammatory and immune diseases. *Nature Rev Drug Discov*. 7:759-70.
- Hatfield SM, Sitkovsky M (2016) A2A adenosine receptor antagonists to weaken the hypoxia-HIF-1 α driven immunosuppression and improve immunotherapies of cancer. *Curr Opin Pharmacol*. 29:90-6. doi: 10.1016/j.coph.2016.06.009.
- Hausdorff WP, Bouvier M, O'Dowd BF, Irons GP, Caron, MG, Lefkowitz RJ (1989) Phosphorylation sites on two domains of the beta 2-adrenergic receptor are involved in distinct pathways of receptor desensitization. *J Biol Chem*. 264:12657-65.
- Hauser SR, Hedlund PB, Roberts AJ, Sari Y, Bell RL, Engleman EA (2015) The 5-HT7 receptor as a potential target for treating drug and alcohol abuse. *Front Neurosci*. 8:448. doi: 10.3389/fnins.2014.00448.
- Hawryluk JM, Ferrari LL, Keating SA, Arrigoni E (2012) Adenosine inhibits glutamatergic input to basal forebrain cholinergic neurons. *J Neurophysiol*. 107:2769-81. doi: 10.1152/jn.00528.2011.
- He L, Fong J, von Zastrow M, Whistler JL (2002). Regulation of opioid receptor trafficking and morphine tolerance by receptor oligomerization. *Cell*. 108:271-82.
- He SQ, Zhang ZN, Guan JS, Liu HR, Zhao B, Wang HB, Li Q, Yang H, Luo J, Li ZY, Wang Q, Lu YJ, Bao L, Zhang X (2011) Facilitation of m-opioid receptor activity by preventing d-opioid receptor-mediated codegradation. *Neuron*. 69:120–31.
- Hebert TE, Moffett S, Morello JP, Loisel TP, Bichet DG, Barret C, Bouvier M (1996) A peptide derived from a beta2-adrenergic receptor transmembrane domain inhibits both receptor dimerization and activation. *J Biol Chem*. 271:16384-92.
- Hein L, Altman JD, Kobilka BK (1999) Two functionally distinct alpha2-adrenergic receptors regulate sympathetic neurotransmission. *Nature*. 402:181-4
- Hermans E, Vanisberg MA, Geurts M, Maloteaux JM (1997). Down-regulation of neurotensin receptors after ligand-induced internalization in rat primary cultured neurons. *Neurochem Int*. 31:291-9.
- Hernan MA, Takkouche B, Caamano-Isorna F, Gestal-Otero JJ (2002) A meta-analysis of coffee drinking, cigarette smoking, and the risk of Parkinson's disease. *Ann Neurol*. 52:276–84. doi: 10.1002/ana.10277.

- Herrera C, Casadó V, Ciruela F, Schofield P, Mallol J, Lluís C, Franco R (2001) Adenosine A2B receptors behave as an alternative anchoring protein for cell surface adenosine deaminase in lymphocytes and cultured cells. *Mol Pharmacol.* 59:127-34.
- Herrick-Davis K, Grinde E, Mazurkiewicz JE (2004) Biochemical and biophysical characterization of serotonin 5-HT_{2C} receptor homodimers on the plasma membrane of living cells. *Biochemistry.* 43:13963-71.
- Herrick-Davis K, Grinde E, Lindsley T, Cowan A, Mazurkiewicz JE (2012) Oligomer size of the serotonin 5-hydroxytryptamine 2C (5-HT_{2C}) receptor revealed by fluorescence correlation spectroscopy with photon counting histogram analysis: evidence for homodimers without monomers or tetramers. *J Biol Chem.* 287:23604-14. doi: 10.1074/jbc.M112.350249.
- Herrick-Davis K, Grinde E, Cowan A, Mazurkiewicz JE (2013) Fluorescence correlation spectroscopy analysis of serotonin, adrenergic, muscarinic, and dopamine receptor dimerization: the oligomer number puzzle. *Mol Pharmacol.* 84:630-42. doi: 10.1124/mol.113.087072.
- Hersch SM, Ciliax BJ, Gutekunst CA, Rees HD, Heilman CJ, Yung KK, Bolam JP, Ince E, Yi H, Levey AI (1995) Electron microscopic analysis of D1 and D2 dopamine receptor proteins in the dorsal striatum and their synaptic relationships with motor corticostriatal afferents. *J Neurosci.* 15:5222-37.
- Hervé D (2011) Identification of a specific assembly of the G protein G_o as a critical and regulated module of dopamine and adenosine-activated cAMP pathways in the striatum. *Front Neuroanat.* 5:48. doi:10.3389/fnana.2011.00048.
- Hettinger BD, Lee A, Linden J, Rosin DL (2001) Ultrastructural localization of adenosine A_{2A} receptors suggests multiple cellular sites for modulation of GABAergic neurons in rat striatum. *J Comp Neurol.* 431:331-46.
- Hillion J, Canals M, Torvinen M, Casado V, Scott R, Terasmaa A, Hansson A, Watson S, Olah M. E, Mallol J, Canela EI, Zoli M, Agnati LF, Ibanez CF, Lluís C, Franco R, Ferre S, Fuxe K (2002) Coaggregation, cointernalization, and codesensitization of adenosine A_{2A} receptors and dopamine D₂ receptors. *J Biol Chem.* 277:18091-7.
- Hoffman BB, Lefkowitz RJ (1996) Catecholamines, sympathomimetic drugs, and adrenergic receptor antagonists. In: Goodman & Gilman's *The Pharmacological Basis of Therapeutics*. Hardman JG, Limbird LE, Molinoff PB, Ruddon RW, Goodman Gilman A (eds) New York, NY, U.S.A.: McGraw-Hill; 199-248.
- Holmberg M, Scheinin M, Kurose H, Miettinen R (1999) Adrenergic alpha_{2C}-receptors reside in rat striatal GABAergic projection neurons: comparison of radioligand binding and immunohistochemistry. *Neuroscience.* 93:1323-33.
- Holmberg M, Fagerholm V, Scheinin M (2003) Regional distribution of alpha_{2C}-adrenoceptors in brain and spinal cord of control mice and transgenic mice overexpressing the alpha_{2C}-subtype: an autoradiographic study with [³H]RX821002 and [³H]rauwolscine. *Neuroscience.* 117:875-98.
- Horn F, Bettler E, Oliveira L, Campagne F, Cohen FE, Vriend G (2003). GPCRDB information system for G protein-coupled receptors. *Nucleic Acids Research.* 31:294-97.

- Horvat RD, Roess DA, Nelson SE, Barisas BG, Clay CM (2001) Binding of agonist but not antagonist leads to fluorescence resonance energy transfer between intrinsically fluorescent gonadotropin-releasing hormone receptors. *Mol Endocrinol.* 15:695–703.
- Hounsou C, Margathe JF, Oueslati N, Belhocine A, Dupuis E, Thomas C, Mann A, Ilien B, Rognan D, Trinquet E, Hibert M, Pin JP, Bonnet D, Durroux T (2015) Time-resolved FRET binding assay to investigate hetero-oligomer binding properties: proof of concept with dopamine D1/D3 heterodimer. *ACS Chem Biol.* 10:466-74. doi: 10.1021/cb5007568.
- Huang Y, Thathiah A (2015) Regulation of neuronal communication by G protein-coupled receptors. *FEBS Lett.* 589:1607-19. doi: 10.1016/j.febslet.2015.05.007.
- Huang C, Hepler JR, Chen LT, Gilman AG, Anderson RG, Mumby SM (1997) Organization of G proteins and adenylyl cyclase at the plasma membrane. *Mol Biol Cell.* 8:2365–78.
- Huang W, Osman R, Gershengorn MC (2005) Agonist induced conformational changes in thyrotropin-releasing hormone receptor type I: disulfide crosslinking and molecular modeling approaches. *Biochemistry.* 44:2419–31.
- Huang NK, Lin JH, Lin JT, Lin CI, Liu EM, Lin CJ, Chen WP, Shen YC, Chen HM, Chen JB, Lai HL, Yang CW, Chiang MC, Wu YS, Chang C, Chen JF, Fang JM, Lin YL, Chern Y (2011) A new drug design targeting the adenosinergic system for Huntington's disease. *PLoS One.* 6:e20934. doi: 10.1371/journal.pone.0020934.
- Huang J, Chen S, Zhang JJ, Huang XY (2013) Crystal structure of oligomeric beta1-adrenergic G protein-coupled receptors in ligand-free basal state. *Nat Struct Mol Biol.* 20:419–25.
- Huang ZL, Zhang Z, Qu W M (2014) Roles of adenosine and its receptors in sleep-wake regulation. *International Review of Neurobiology.* 119:349–371.
- Huang W, Zeng X, Shi Y, Liu M (2017) Functional characterization of human equilibrative nucleoside transporter 1. *Protein Cell.* 8:284-295. doi: 10.1007/s13238-016-0350-x.
- Hübner H, Schellhorn T, Gienger M, Schaab C, Kaindl J, Leeb L, Clark T, Möller D, Gmeiner P (2016) Structure-guided development of heterodimer-selective GPCR ligands. *Nat Commun.* 7:12298. doi: 10.1038/ncomms12298.
- Hurt CM, Feng FY, Kobilka B (2000). Cell-type specific targeting of the alpha 2c-adrenoceptor. Evidence for the organization of receptor microdomains during neuronal differentiation of PC12 cells. *J Biol Chem.* 275:35424-31.
- Hyman SE, Malenka RC, Nestler EJ (2006) Neural mechanisms of addiction: the role of reward-related learning and memory. *Annu Rev Neurosci.* 29:565-98.
- Ihalainen JA, Tanila H (2004) In vivo regulation of dopamine and noradrenaline release by alpha2A-adrenoceptors in the mouse nucleus accumbens. *J Neurochem.* 91:49-56.
- Ikemoto K, Satoh K, Kitahama K, Maeda (1996) T Demonstration of a new dopamine-containing cell group in the primate rostral telencephalon. *Neurosci Lett.* 220:69-71.
- Impellizzeri D, Di Paola R, Esposito E, Mazzon E, Paterniti I, Melani A, Bramanti P, Pedata F, Cuzzocrea S (2011) CGS21680, an agonist of the adenosine (A2A) receptor, decreases acute lung inflammation. *Eur J Pharmacol.* 668:305-16.

- Irannejad R, Tomshine JC, Tomshine JR, Chevalier M, Mahoney JP, Steyaert J, Rasmussen SG, Sunahara RK, El-Samad H, Huang B, von Zastrow M (2013). Conformational biosensors reveal GPCR signalling from endosomes. *Nature*. 495:534–8.
- Issafras H, Angers S, Bulenger S, Blanpain C, Parmentier M, Labbé-Jullié C, Bouvier M, Marullo S (2002) Constitutive agonist-independent CCR5 oligomerization and antibody-mediated clustering occurring at physiological levels of receptors. *J Biol Chem*. 277:34666–73.
- Iversen SD, Iversen LL (2007) Dopamine: 50 years in perspective. *Trends Neurosci*. 30:188-93.
- Izquierdo JM, Majós N, Bonnal S, Martínez C, Castelo R, Guigó R, Bilbao D, Valcárcel J (2005) Regulation of Fas alternative splicing by antagonistic effects of TIA-1 and PTB on exon definition. *Mol Cell*. 19:475-84.
- Jaakola VP, Griffith, MT, Hanson MA, Cherezov V, Chien EYT, Lane JR, Ijzerman AP, Stevens RC (2008) The 2.6 angstrom crystal structure of a human A2A adenosine receptor bound to an antagonist. *Science*. 322:1211-7.
- Jacobson KA, Gao ZG (2006) Adenosine receptors as therapeutic targets. *Nat Rev Drug Discov*. 5:247-64.
- Jacoby E, Bouhelal R, Gerspacher M, Seuwen K (2006). The 7 TM G-protein-coupled receptor target family. *Chem Med Chem*. 1:761-82.
- Jäkälä P, Riekkinen M, Sirviö J, Koivisto E, Kejonen K, Vanhanen M, Riekkinen P Jr (1999a) Guanfacine, but not clonidine, improves planning and working memory performance in humans. *Neuropsychopharmacology*. 20:460-70.
- Jäkälä P, Sirviö J, Riekkinen M, Koivisto E, Kejonen K, Vanhanen M, Riekkinen P Jr (1999b) Guanfacine and clonidine, alpha 2-agonists, improve paired associates learning, but not delayed matching to sample, in humans. *Neuropsychopharmacology*. 20:119-30.
- Janes K, Symons-Liguori AM, Jacobson KA, Salvemini D (2016) Identification of A3 adenosine receptor agonists as novel non-narcotic analgesics. *Br J Pharmacol*. 173:1253-67.
- Jauhar S, Veronese M, Rogdaki M, Bloomfield M, Natesan S, Turkheimer F, Kapur S, Howes OD (2017) Regulation of dopaminergic function: an [18F]-DOPA PET apomorphine challenge study in humans. *Transl Psychiatry*. 7:e1027. doi: 10.1038/tp.2016.270.
- Jenner P (2003) A2A antagonists as novel non-dopaminergic therapy for motor dysfunction in PD. *Neurology*. 61:S32-8.
- Jenner P (2014) An overview of adenosine A2A receptor antagonists in Parkinson's disease. *Int Rev Neurobiol*. 119:71–86. doi:10.1016/B978-0-12-801022-8.00003-9.
- Jenner P, Mori A, Hauser R, Morelli M, Fredholm BB, Chen JF (2009) Adenosine, adenosine A2A antagonists, and Parkinson's disease. *Parkinsonism Relat Disord*. 15:406–13. doi:10.1016/j.parkreldis.2008.12.006.
- Jensen AD, Guarnieri F, Rasmussen SG, Asmar F, Ballesteros JA, Gether U (2001) Agonist-induced conformational changes at the cytoplasmic side of transmembrane segment 6 in the $\alpha 2$ adrenergic receptor mapped by site-selective fluorescent labeling. *J Biol Chem*. 276:9279–90.

- Jensen AA, Hansen JL, Sheikh SP, Bräuner-Osborne H (2002) Probing intermolecular protein-protein interactions in the calcium-sensing receptor homodimer using bioluminescence resonance energy transfer (BRET). *Eur J Biochem.* 269:5076–87
- Jiang LI, Collins J, Davis R, Lin KM, DeCamp D, Roach T, Hsueh R, Rebres RA, Ross EM, Taussig R, Fraser I, Sternweis PC (2007) Use of a cAMP BRET sensor to characterize a novel regulation of cAMP by the sphingosine 1-phosphate/G13 pathway. *J Biol Chem.* 282:10576-84.
- Jin LQ, Wang HY, and Friedman E (2001) Stimulated D(1) dopamine receptors couple to multiple Galpha proteins in different brain regions. *J Neurochem.* 78:981–90.
- Jockers R, Angers S, Da Silva A, Benaroch P, Strosberg AD, Bouvier M, Marullo S (1999) Beta(2)-adrenergic receptor down-regulation. Evidence for a pathway that does not require endocytosis. *J Biol Chem.* 274:28900-8.
- Johansson B, Halldner L, Dunwiddie TV, Masino SA, Poelchen W, Giménez-Llort L, Escorihuela RM, Fernández-Teruel A, Wiesenfeld-Hallin Z, Xu XJ, Hårdemark A, Betsholtz C, Herlenius E, Fredholm BB (2001) Hyperalgesia, anxiety, and decreased hypoxic neuroprotection in mice lacking the adenosine A1 receptor. *Proc Natl Acad Sci U S A.* 98:9407-12.
- Johnston JM, Aburi M, Provasi D, Bortolato A, Urizar E, Lambert NA, Javitch JA, Filizola M (2011) Making structural sense of dimerization interfaces of delta opioid receptor homodimers. *Biochemistry.* 50:1682-90. doi: 10.1021/bi101474v.
- Jordan BA, Devi LA (1999) G-protein-coupled receptor heterodimerization modulates receptor function. *Nature.* 399:697-700.
- Jordan BA, Trapaidze N, Gomes I, Nivarthi R, Devi LA (2001) Oligomerization of opioid receptors with beta 2-adrenergic receptors: a role in trafficking and mitogen-activated protein kinase activation. *Proc Natl Acad Sci USA.* 98:343–8.
- Joseph JD, Wang YM, Miles PR, Budygin EA, Picetti R, Gainetdinov RR, Caron MG, Wightman RM (2002) Dopamine autoreceptor regulation of release and uptake in mouse brain slices in the absence of D(3) receptors. *Neuroscience.* 112:39-49.
- Jovanovic V, Guan HC, Van Tol HH (1999) Comparative pharmacological and functional analysis of the human dopamine D4.2 and D4.10 receptor variants. *Pharmacogenetic.* 9:561-8.
- Kachroo A, Schwarzschild MA (2012) Adenosine A2A receptor gene disruption protects in an alpha-synuclein model of Parkinson's disease. *Ann Neurol.* 71:278–82. doi: 10.1002/ana.22630
- Kaczor AA, Makarska-Bialokoz M, Selent J, de la Fuente RA, Martí-Solano M, Castro M (2014) Application of BRET for studying G protein-coupled receptors. *Mini Rev Med Chem.* 14:411-25.
- Kamiya T, Saitoh O, Yoshioka K, Nakata H (2003) Oligomerization of adenosine A2A and dopamine D2 receptors in living cells. *Biochem Biophys Res Commun.* 306:544-9.
- Kanda T, Uchida S (2014) Clinical/pharmacological aspect of adenosine A2A receptor antagonist for dyskinesia. *Int Rev Neurobiol.* 119:127-50. doi: 10.1016/B978-0-12-801022-8.00006-4.
- Kanda T, Jackson MJ, Smith LA, Pearce RK, Nakamura J, Kase H, Kuwana Y, Jenner P (1998) Adenosine A2A antagonist: a novel antiparkinsonian agent that does not provoke dyskinesia in parkinsonian monkeys. *Ann Neurol.* 43:507-13.

- Kanda T, Jackson MJ, Smith LA, Pearce RK, Nakamura J, Kase H, Kuwana Y, Jenner P (2000) Combined use of the adenosine A_{2A} antagonist KW-6002 with L-DOPA or with selective D₁ or D₂ dopamine agonists increases antiparkinsonian activity but not dyskinesia in MPTP-treated monkeys. *Exp Neurol*. 162:321–7.
- Kang DS, Tian X, Benovic JL (2013) β -Arrestins and G protein-coupled receptor trafficking. *Meth. Enzymol*. 521:91–108.
- Kara E, Lin H, Strange PG (2010) Co-operativity in agonist binding at the D₂ dopamine receptor: evidence from agonist dissociation kinetics. *J Neurochem*. 112:1442-53. doi: 10.1111/j.1471-4159.2009.06554.x.
- Karcz-Kubicha M, Antoniou K, Terasmaa A, Quarta D, Solinas M, Justinova Z, Pezzola A, Reggio R, Müller CE, Fuxe K, Goldberg SR, Popoli P, Ferré S (2003) Involvement of adenosine A₁ and A_{2A} receptors in the motor effects of caffeine after its acute and chronic administration. *Neuropsychopharmacology*. 28:1281-91.
- Kase H (2001) New aspects of physiological and pathophysiological functions of adenosine A_{2A} receptor in basal ganglia. *Biosci Biotechnol Biochem*. 65:1447-57.
- Kase H, Aoyama S, Ichimura M, Ikeda K, Ishii A, Kanda T, Koga K, Koike N, Kurokawa M, Kuwana Y, Mori A, Nakamura J, Nonaka H, Ochi M, Saki M, Shimada J, Shindou T, Shiozaki S, Suzuki F, Takeda M, Yanagawa K, Richardson PJ, Jenner P, Bedard P, Borrelli E, Hauser RA, Chase TN (2003) Progress in pursuit of therapeutic A_{2A} antagonists: the adenosine A_{2A} receptor selective antagonist KW6002: research and development toward a novel nondopaminergic therapy for Parkinson's disease. *Neurology*. 61:S97-100.
- Kawaguchi Y (1993) Physiological, morphological, and histochemical characterization of three classes of interneurons in rat neostriatum. *J Neurosci*. 13:4908-23.
- Kawaguchi Y, Wilson CJ, Augood SJ, Emson PC (1995) Striatal interneurons: chemical, physiological and morphological characterization. *Trends Neurosci*. 18:527-35.
- Kebabian JW, Calne DB (1979) Multiple receptors for dopamine. *Nature*. 277:93–6.
- Kemp JM, Powell TP (1971) The structure of the caudate nucleus of the cat: light and electron microscopy. *Philos Trans R Soc Lond B Biol Sci*. 262:383-401.
- Kenakin T (1995) Agonist-receptor efficacy. II. Agonist trafficking of receptor signals. *Trends Pharmacol Sci*. 16:232–8.
- Kenakin TP (2003) The secret lives of GPCRs. *Drug Discov Today*. 8:674.
- Kenakin T (2005) New concepts in drug discovery: collateral efficacy and permissive antagonism. *Nat Rev Drug Discov*. 4:919-27.
- Kenakin T (2011) Functional selectivity and biased receptor signaling. *J Pharmacol Exp Ther*. 336:296-302. doi: 10.1124/jpet.110.173948.
- Kenakin T (2012) Biased signaling and allosteric machines: new vistas and challenges for drug discovery. *British J Pharmacol*. 165:1659-69.
- Kenakin T, Christopoulos, A (2013). Signalling bias in new drug discovery: detection, quantification and therapeutic impact. *Nat Rev Drug Discov*. 12:205-16.

- Kenakin T, Miller LJ (2010) Seven transmembrane receptors as shapeshifting proteins: the impact of allosteric modulation and functional selectivity on new drug discovery. *Pharmacol Rev.* 62:265–304.
- Kendall RT, Luttrell LM (2009) Diversity in arrestin function. *Cell Mol Life Sci.* 66:2953–73.
- Kennard MA (1941) Abnormal Findings in 246 Consecutive Autopsies on Monkeys. *Yale J Biol Med.* 13:701-12.
- Kennedy ME, Limbird LE (1993) Mutations of the alpha 2A-adrenergic receptor that eliminate detectable palmitoylation do not perturb receptor-G-protein coupling. *J Biol Chem.* 268:8003-11.
- Kerppola TK (2008) Bimolecular Fluorescence Complementation (BiFC) Analysis as a probe of protein interactions in living cells. *Annu. Rev. Biophys.* 37:465-87.
- Khan ZU, Gutiérrez A, Martín R, Peñafiel A, Rivera A, De La Calle A (1998) Differential regional and cellular distribution of dopamine D2-like receptors: an immunocytochemical study of subtype-specific antibodies in rat and human brain. *J Comp Neurol.* 402:353-71.
- Khan ZU, Gutiérrez A, Martín R, Peñafiel A, Rivera A, de la Calle A (2000) Dopamine D5 receptors of rat and human brain. *Neuroscience.* 100:689-99.
- Kienzler MA, Isacoff EY (2017) Precise modulation of neuronal activity with synthetic photoswitchable ligands. *Curr Opin Neurobiol.* 45:202-9. doi: 10.1016/j.conb.2017.05.021.
- Klein S, Reuveni H, Levitzki A (2000) Signal transduction by a nondissociable heterotrimeric yeast G protein. *Proc Natl Acad Sci USA.* 97:3219–23.
- Klotz KN, Lohse MJ (1986) The glycoprotein nature of A1 adenosine receptors. *Biochem Biophys Res Commun.* 140:406-13.
- Knight RT, Scabini D, Woods DL (1989) Prefrontal cortex gating of auditory transmission in humans. *Brain Res.* 504:338-42.
- Ko CH, Koon CM, Yu SL, Lee KY, Lau CB, Chan EH, Wing YK, Fung KP, Leung PC (2016) Hypnotic effects of a novel anti-insomnia formula on *Drosophila* insomnia model. *Chin J Integr Med.* 22:335-43. doi: 10.1007/s11655-014-1625-1.
- Kochman K (2014) Superfamily of G-protein coupled receptors (GPCRs)-extraordinary and outstanding success of evolution. *Postepy Hig Med Dosw.* 68:1225-37. doi: 10.5604/17322693.1127326.
- Kolahdouzan M, Hamadeh MJ (2017) The neuroprotective effects of caffeine in neurodegenerative diseases. *CNS Neurosci Ther.* 23:272-90. doi: 10.1111/cns.12684.
- Kondo T, Mizuno Y, Japanese Istradefylline Study Group (2015) A long-term study of istradefylline safety and efficacy in patients with Parkinson disease. *Clin Neuropharmacol.* 38:41–6. doi:10.1097/WNF.0000000000000073.
- Koob GF (1992) Neural mechanisms of drug reinforcement. *Ann N Y Acad Sci.* 654:171-91.
- Koob GF, Volkow ND (2010) Neurocircuitry of addiction. *Neuropsychopharmacology.* 35:217-38. doi: 10.1038/npp.2009.110.

- Kraft LJ, Kenworthy AK (2012) Imaging protein complex formation in the autophagy pathway: analysis of the interaction of LC3 and Atg4B (C74A) in live cells using Förster resonance energy transfer and fluorescence recovery after photobleaching. *J Biomed Opt.* 17:011008. doi:10.1117/1.JBO.17.1.011008.
- Kravitz AV, Freeze BS, Parker PR, Kay K, Thwin MT, Deisseroth K, Kreitzer AC (2010) Regulation of parkinsonian motor behaviours by optogenetic control of basal ganglia circuitry. *Nature.* 466:622-6. doi: 10.1038/nature09159.
- Kreitzer AC, Malenka RC (2008) Striatal plasticity and basal ganglia circuit function. *Neuron.* 60:543-54. doi:10.1016/j.neuron.2008.11.005.
- Kreusser MM, Lehmann LH, Haass M, Buss SJ, Katus HA, Lossnitzer D (2017) Depletion of cardiac catecholamine stores impairs cardiac norepinephrine re-uptake by downregulation of the norepinephrine transporter. *PLoS One.* 12:e0172070. doi: 10.1371/journal.pone.0172070.
- Kroeger KM, Pflieger KD, Eidne KA (2003) G-protein coupled receptor oligomerization in neuroendocrine pathways. *Front Neuroendocrinol.* 24:254–78.
- Krügel U (2016) Purinergic receptors in psychiatric disorders. *Neuropharmacology.* 104:212-25. doi: 10.1016/j.neuropharm.2015.10.032.
- Krupnick JG, Benovic JL (1998) The role of receptor kinases and arrestins in G protein-coupled receptor regulation. *Annu Rev Pharmacol Toxicol.* 38:289-319.
- Kuhhorn J, Gotz, A, Hubner H, Thompson D, Whistler J, Gmeiner P (2011) Development of a bivalent dopamine D2 receptor agonist. *J Med Chem.* 54:7911-9.
- Kuszak AJ, Pitchiaya S, Anand JP, Mosberg HI, Walter NG, Sunahara RK (2009) Purification and functional reconstitution of monomeric mu-opioid receptors: allosteric modulation of agonist binding by Gi2. *J Biol Chem.* 284:26732-41. doi: 10.1074/jbc.M109.026922.
- Kvetnansky R, Sabban EL, Palkovits M (2009) Catecholaminergic systems in stress: structural and molecular genetic approaches. *Physiol Rev.* 89:535-606. doi: 10.1152/physrev.00042.2006.
- La Hoste GJ, Swanson JM, Wigal SB, Glabe C, Wigal T, King N, Kennedy JL (1996) Dopamine D4 receptor gene polymorphism is associated with attention deficit hyperactivity disorder. *Mol Psychiatry.* 1:121–4.
- Lanau F, Zenner MT, Civelli O, Hartman DS (1997) Epinephrine and norepinephrine act as potent agonists at the recombinant human dopamine D4 receptor. *J Neurochem.* 68:804-12.
- Lane JR, Canals M (2012) Sequential conformational rearrangements dictate the dynamics of class C GPCR activation. *Sci Signal.* 5:pe51. doi: 10.1126/scisignal.2003503.
- Lane JR, Sexton PM, Christopoulos A (2013) Bridging the gap: bitopic ligands of G-protein-coupled receptors. *Trends Pharmacol Sci.* 34:59-66.
- Lane JR, Donthamsetti P, Shonberg J, Draper-Joyce CJ, Dentry S, Michino M, Shi L, López L, Scammells PJ, Capuano B, Sexton PM, Javitch JA, Christopoulos A (2014) A new mechanism of allostery in a G protein-coupled receptor dimer. *Nat Chem Biol.* 10:745–52.
- Langer SZ (1997) 25 years since the discovery of presynaptic receptors: present knowledge and future perspectives. *Trends Pharmacol Sci.* 18:95-9.

- Langer SZ (2015) α 2-Adrenoceptors in the treatment of major neuropsychiatric disorders. *Trends Pharmacol Sci.* 36:196-202. doi: 10.1016/j.tips.2015.02.006.
- Langmead CJ, Christopoulos A (2014) Functional and structural perspectives on allosteric modulation of GPCRs. *Curr Opin Cell Biol.* 27:94-101. doi: 10.1016/j.ceb.2013.11.007.
- Lappas CM, Sullivan GW, Linden J (2005) Adenosine A2A agonists in development for the treatment of inflammation. *Expert Opin Investig Drugs.* 14:797-806.
- Laporte SA, Oakley RH, Holt JA, Barak LS, Caron MG (2000) The interaction of β -arrestin with the AP-2 adaptor is required for the clustering of β 2-adrenergic receptor into clathrin-coated pits. *J Biol Chem.* 275:23120-6.
- Laugwitz KL, Allgeier A, Offermanns S, Spicher K, Van Sande J, Dumont JE, Schultz G (1996) The human thyrotropin receptor: a heptahelical receptor capable of stimulating members of all four G protein families. *Proc Natl Acad Sci USA.* 93:116-20.
- Lauzon NM, Laviolette SR (2010) Dopamine D4-receptor modulation of cortical neuronal network activity and emotional processing: Implications for neuropsychiatric disorders. *Behav Brain Res.* 208:12-22. doi: 10.1016/j.bbr.2009.11.037.
- Lavoie C, Mercier JF, Salahpour A, Umapathy D, Breit A, Villeneuve LR, Zhu WZ, Xiao RP, Lakatta EG, Bouvier M, Hébert TE (2002) Beta 1/beta 2-adrenergic receptor heterodimerization regulates beta 2-adrenergic receptor internalization and ERK signaling efficacy. *J Biol Chem.* 277:35402-10.
- Law PY, Erickson-Herbrandson LJ, Zha QQ, Solberg J, Chu J, Sarre A, Loh HH (2005). Heterodimerization of mu and delta-opioid receptors occurs at the cell surface only and requires receptor-G protein interactions. *J Biol Chem.* 280:11152-64.
- Lee A, Wissekerke AE, Rosin DL, Lynch KR (1998) Localization of alpha2C-adrenergic receptor immunoreactivity in catecholaminergic neurons in the rat central nervous system. *Neuroscience.* 84:1085-96
- Lee KW, Hong JH, Choi IY, Che Y, Lee JK, Yang SD, Song CW, Kang HS, Lee JH, Noh JS, Shin HS, Han PL (2002) Impaired D2 dopamine receptor function in mice lacking type 5 adenylyl cyclase. *J. Neurosci.* 22:7931-40.
- Leff P (1995) The two-state model of receptor activation. *Trends Pharmacol Sci.* 16:89-97.
- Lefkowitz RJ (1998) G protein-coupled receptors. III. New roles for receptor kinases and beta-arrestins in receptor signaling and desensitization. *J Biol Chem.* 273:18677-80.
- Lehto J, Virta JR, Oikonen V, Roivainen A, Luoto P, Arponen E, Helin S, Hietamäki J, Holopainen A, Kailajärvi M, Peltonen JM, Rouru J, Sallinen J, Virtanen K, Volanen I, Scheinin M, Rinne JO (2015) Test-retest reliability of (11)C-ORM-13070 in PET imaging of α 2C-adrenoceptors in vivo in the human brain. *Eur J Nucl Med Mol Imaging.* 42:120-7. doi: 10.1007/s00259-014-2899-z.
- Le Moine C, Bloch B (1995) D1 and D2 dopamine receptor gene expression in the rat striatum: sensitive cRNA probes demonstrate prominent segregation of D1 and D2 mRNAs in distinct neuronal populations of the dorsal and ventral striatum. *J Comp Neurol.* 355:418-26.

- Lensing CJ, Freeman KT, Schnell SM, Adank DN, Speth RC, Haskell-Luevano C (2016). An in vitro and in vivo investigation of bivalent ligands that display preferential binding and functional activity for different melanocortin receptor homodimers. *J Med Chem.* 59:3112-28.
- Levitz J, Habrian C, Bharill S, Fu Z, Vafabakhsh R, Isacoff EY (2016) Mechanism of assembly and cooperativity of homomeric and heteromeric metabotropic glutamate receptors. *Neuron.* 92:143-59. doi: 10.1016/j.neuron.2016.08.036.
- Levitz J, Broichhagen J, Leippe P, Konrad D, Trauner D, Isacoff EY (2017) Dual optical control and mechanistic insights into photoswitchable group II and III metabotropic glutamate receptors. *Proc Natl Acad Sci USA.* 25:114:E3546-E3554. doi: 10.1073/pnas.1619652114.
- Levy R, Dostrovsky JO, Lang AE, Sime E, Hutchison WD, Lozano AM (2001) Effects of apomorphine on subthalamic nucleus and globus pallidus internus neurons in patients with Parkinson's disease. *J Neurophysiol.* 86:249-60.
- Li BM, Mei ZT (1994) Delayed-response deficit induced by local injection of the alpha 2-adrenergic antagonist yohimbine into the dorsolateral prefrontal cortex in young adult monkeys. *Behav Neural Biol.* 62:134-9.
- Li D, Sham PC, Owen MJ, He L (2006) Meta-analysis shows significant association between dopamine system genes and attention deficit hyperactivity disorder (ADHD). *Hum Mol Genet.* 15:2276-84.
- Li N, Csepe TA, Hansen BJ, Sul LV, Kalyanasundaram A, Zakharkin SO, Zhao J, Guha A, Van Wagoner DR, Kilic A, Mohler PJ, Janssen PM, Biesiadecki BJ, Hummel JD, Weiss R, Fedorov VV (2016) Adenosine-Induced Atrial Fibrillation: Localized Reentrant Drivers in Lateral Right Atria due to Heterogeneous Expression of Adenosine A1 Receptors and GIRK4 Subunits in the Human Heart. *Circulation.* 134:486-98. doi: 10.1161/CIRCULATIONAHA.115.021165.
- Lidow MS, Goldman-Rakic PS, Gallager DW, Rakic P (1991) Distribution of dopaminergic receptors in the primate cerebral cortex: quantitative autoradiographic analysis using [3H]raclopride, [3H]spiperone and [3H]SCH23390. *Neuroscience.* 40:657-71.
- Lin R, Karpa K, Kabbani N, Goldman-Rakic P, Levenson R (2001) Dopamine D2 and D3 receptors are linked to the actin cytoskeleton via interaction with filamin A. *Proc Natl Acad Sci USA.* 98:5258-63.
- Lindvall O, Bjorklund A (1974) The organization of the ascending catecholamine neuron systems in the rat brain as revealed by the glyoxylic acid fluorescence method. *Acta Physiol Scand Suppl* 412:1-48
- Liprando LA, Miner LH, Blakely RD, Lewis DA, Sesack SR (2004) Ultrastructural interactions between terminals expressing the norepinephrine transporter and dopamine neurons in the rat and monkey ventral tegmental area. *Synapse.* 52:233-44. 10.1002/syn.20023.
- Llorca-Torrallba M, Borges G, Neto F, Mico JA, Berrocoso E (2016) Noradrenergic Locus Coeruleus pathways in pain modulation. *Neuroscience.* 338:93-113. doi:10.1016/j.neuroscience.2016.05.057.
- Loening AM, Fenn TD, Wu AM, Gambhir SS (2006). Consensus guided mutagenesis of Renilla luciferase yields enhanced stability and light output. *Protein Eng Des Sel.* 19:391-400.

- Lohse MJ, Benovic JL, Codina J, Caron MG, Lefkowitz RJ (1990) β -Arrestin: a protein that regulates β -adrenergic receptor function. *Science*. 248:1547–50.
- Lopez-Garcia E, Guallar-Castillon P, Leon Muñoz L, Graciani A, Rodriguez-Artalejo F (2014) Coffee consumption and health-related quality of life. *Clinical Nutrition*. 33:143–9.
- Lopez-Gimenez, J.F, Canals, M, Pediani, J.D, Milligan, G (2007) The alpha 1b-adrenoreceptor exists as a higher-order oligomer: effective oligomerization is required for receptor maturation, surface delivery and function. *Mol. Pharmacol*. 71:1015-29.
- Łukasiewicz S, Błasiak E, Faron-Górecka A, Polit A, Tworzydło M, Górecki A, Wasylewski Z, Dziedzicka-Wasylewska M (2007) Fluorescence studies of homooligomerization of adenosine A2A and serotonin 5-HT1A receptors reveal the specificity of receptor interactions in the plasma membrane. *Pharmacol Rep*. 59:379-92.
- Luttrell LM, Lefkowitz RJ (2002) The role of beta-arrestins in the termination and transduction of G-protein-coupled receptor signals. *J Cell Sci*. 115:455-65.
- Luttrell LM, Gesty-Palmer D (2010) Beyond desensitization: physiological relevance of arrestin-dependent signaling. *Pharmacol Rev*. 62:305–30.
- Luttrell LM, Maudsley S, Bohn LM (2015) Fulfilling the promise of "biased" G protein-coupled receptor agonism. *Mol Pharmacol*. 88:579–88. doi: 10.1124/mol.115.099630.
- Ma CL, Qi XL, Peng JY, Li BM (2003) Selective deficit in no-go performance induced by blockade of prefrontal cortical alpha 2-adrenoceptors in monkeys. *Neuroreport*. 14:1013-6.
- Ma CL, Arnsten AF, Li BM (2005) Locomotor hyperactivity induced by blockade of prefrontal cortical alpha2-adrenoceptors in monkeys. *Biol Psychiatry*. 57:192-5.
- MacDonald E, Scheinin M (1995) Distribution and pharmacology of alpha 2-adrenoceptors in the central nervous system. *J Physiol Pharmacol*. 46:241-58.
- MacDonald A, Daly CJ, Bulloch JM, McGrath JC (1992) Contributions of alpha 1-adrenoceptors, alpha 2-adrenoceptors and P2x-purinoceptors to neurotransmission in several rabbit isolated blood vessels: role of neuronal uptake and autofeedback. *Br J Pharmacol*. 105:347-54.
- MacDonald E, Kobilka BK, Scheinin M (1997). Gene targeting homing in on alpha 2-adrenoceptor subtype function. *Trends Pharmacol Sci*. 18:211-9.
- MacMillan LB, Hein L, Smith MS, Piascik MT, Limbird LE (1996) Central hypotensive effects of the alpha2a-adrenergic receptor subtype. *Science*. 273:801-3.
- Maguire JJ, Kuc RE, Davenport AP (2012) Radioligand binding assays and their analysis. *Methods Mol Biol*. 897:31-77. doi: 10.1007/978-1-61779-909-9_3.
- Maggio R, Rocchi C, Scarselli M (2013) Experimental strategies for studying G protein-coupled receptor homoand heteromerization with radioligand binding and signal transduction methods. *Methods Enzymol*. 521:295-310. doi: 10.1016/B978-0-12-391862-8.00016-8.
- Mahon MJ, Donowitz M, Yun CC, Segre GV (2002) Na(1)/H(1) exchanger regulatory factor 2 directs parathyroid hormone 1 receptor signalling. *Nature*. 417:858-61.
- Maia L, de Mendonça A (2002) Does caffeine intake protect from Alzheimer's disease? *Eur J Neurol*. 9:377-82.

- Makris N, Buka SL, Biederman J, Papadimitriou GM, Hodge SM, Valera EM, Brown AB, Bush G, Monuteaux MC, Caviness VS, Kennedy DN, Seidman LJ (2008) Attention and executive systems abnormalities in adults with childhood ADHD: A DT-MRI study of connections. *Cereb Cortex*. 18:1210-20
- Manna M, Niemelä M, Tynkkynen J, Javanainen M, Kulig W, Müller DJ, Rog T, Vattulainen I (2016) Mechanism of allosteric regulation of β 2-adrenergic receptor by cholesterol. *Elife*. 5. pii: e18432. doi: 10.7554/eLife.18432.
- Mancia F, Assur Z, Herman AG, Siegel R, Hendrickson WA (2008) Ligand sensitivity in dimeric associations of the serotonin 5HT_{2c} receptor. *EMBO Rep*. 9:363-9. doi: 10.1038/embor.2008.27.
- Mandrika I, Petrovska R, Klovins J (2010) Evidence for constitutive dimerization of niacin receptor subtype. *Biochem Biophys Res Commun*. 395:281-7. doi: 10.1016/j.bbrc.2010.04.011.
- Manglik A, Kruse AC, Kobilka TS, Thian FS, Mathiesen JM, Sunahara RK, Pardo L, Weis WI, Kobilka BK, Granier S (2012) Crystal structure of the micro-opioid receptor bound to a morphinan antagonist. *Nature*. 485:321–6.
- Maramai S, Gemma S, Brogi S, Campiani G, Butini S, Stark H, Brindisi M (2016) Dopamine D3 receptor antagonists as potential therapeutics for the treatment of neurological diseases. *Front Neurosci*. 10:451.
- Marcellino D, Ferré S, Casadó V, Cortés A, Le Foll B, Mazzola C, Drago F, Saur O, Stark H, Soriano A, Barnes C, Goldberg SR, Lluís C, Fuxe K, Franco R (2008) Identification of dopamine D1-D3 receptor heteromers. Indications for a role of synergistic D1-D3 receptor interactions in the striatum. *J Biol Chem*. 283:26016-25. doi: 10.1074/jbc.M710349200.
- Marinissen MJ, Gutkind JS (2001) G-protein-coupled receptors and signaling networks: emerging paradigms. *Trends Pharmacol Sci*. 22:368-76.
- Martinelli A, Ortore G (2013) Molecular modeling of adenosine receptors. *Methods Enzymol*. 522:37-59. doi: 10.1016/B978-0-12-407865-9.00003-0.
- Matsubara E, Shoji M, Abe K (2002) The treatment of Parkinson's disease-adenosine A_{2A} receptor antagonists. *Nihon Rinsho*. 60:112-6.
- Mauger C, Sivan B, Brockhaus M, Fuchs S, Civelli O, Monsma F Jr (1998) Development and characterization of antibodies directed against the mouse D₄ dopamine receptor. *Eur J Neurosci*. 10:529-37.
- Maura G, Giardi A, Raiteri M (1988) Release-regulating D-2 dopamine receptors are located on striatal glutamatergic nerve terminals. *J Pharmacol Exp Ther*. 247:680–4.
- May LT, Leach K, Sexton PM, Christopoulos A (2007) Allosteric modulation of G protein-coupled receptors. *Annu Rev Pharmacol Toxicol*. 47:1-51.
- May LT, Bridge LJ, Stoddart LA, Briddon SJ, Hill SJ (2011) Allosteric interactions across native adenosine-A₃ receptor homodimers: quantification using single-cell ligand-binding kinetics. *FASEB J*. 25:3465-76. doi: 10.1096/fj.11-186296.
- McGeary J (2009) The DRD4 exon 3 VNTR polymorphism and addiction-related phenotypes: A review. *Pharmacol Biochem Behav*. 93:222–9.

- McMillin SM, Heusel M, Liu T, Costanzi S, Wess J (2011) Structural basis of M3 muscarinic receptor dimer/oligomer formation. *J Biol Chem.* 286:28584-98. doi: 10.1074/jbc.M111.259788.
- McVey M, Ramsay D, Kellett E, Rees S, Wilson S, Pope AJ, Milligan G (2001) Monitoring receptor oligomerization using time-resolved fluorescence resonance energy transfer and bioluminescence resonance energy transfer. The human delta -opioid receptor displays constitutive oligomerization at the cell surface, which is not regulated by receptor occupancy. *J Biol Chem.* 276:14092-9.
- Melancon BJ, Hopkins CR, Wood MR, Emmitte KA, Niswender CM, Christopoulos A, Conn PJ, Lindsley CW (2012) Allosteric modulation of seven transmembrane spanning receptors: theory, practice, and opportunities for central nervous system drug discovery. *J Med Chem.* 55:1445-64. doi: 10.1021/jm201139r.
- Mercier JF, Salahpour A, Angers S, Breit A, Bouvier M (2002) Quantitative assessment of beta 1 and beta 2-adrenergic receptor homo and heterodimerization by bioluminescence resonance energy transfer. *J Biol Chem.* 277:44925-31.
- Messer WS (2004) Bivalent ligands for G-protein coupled receptors. *Curr Pharm.* 10:2015-20.
- Miller EK, Li L, Desimone R (1993) Activity of neurons in anterior inferior temporal cortex during a short-term memory task. *J Neurosci.* 13:1460-78.
- Miller LJ, Dong M, Harikumar KG (2012) Ligand binding and activation of the secretin receptor, a prototypic family B G protein-coupled receptor. *Br J Pharmacol.* 166:18-26.
- Miller EM, Pomerleau F, Huettl P, Gerhardt GA, Glaser PE (2014) Aberrant glutamate signaling in the prefrontal cortex and striatum of the spontaneously hypertensive rat model of attention-deficit/hyperactivity disorder. *Psychopharmacology* 231:3019-29.
- Milligan G (2008) A day in the life of a G protein-coupled receptor: the contribution to function of G protein-coupled receptor dimerization. *Br J Pharmacol.* 153:S216-29.
- Milligan G (2009) G protein-coupled receptor hetero-dimerization: contribution to pharmacology and function. *Br J Pharmacol.* 158:5-14.
- Milligan G (2013) The prevalence, maintenance and relevance of G protein-coupled receptor oligomerization. *Mol Pharmacol.* 84:158-69.
- Milligan G, Kostenis E (2006) Heterotrimeric G-proteins: a short history. *Br J Pharmacol.* 147:S46-55.
- Milligan G, White JH (2001) Protein-protein interactions at G-protein-coupled receptors. *Trends Pharmacol Sci.* 22:513-8.
- Milligan G, Canals M, Pediani JD, Ellis J, Lopez-Gimenez JF (2006) The role of GPCR dimerisation/oligomerisation in receptor signaling. *Ernst Schering Found Symp Proc.* 2:145-61.
- Mink JW (2003) The Basal Ganglia and involuntary movements: impaired inhibition of competing motor patterns. *Arch Neurol.* 60:1365-8.
- Mink JW (2006). Neurobiology of basal ganglia and Tourette syndrome: basal ganglia circuits and thalamocortical outputs. *Adv Neurol.* 99:89-98.

- Missale C, Nash SR, Robinson SW, Jaber M, Caron MG (1998) Dopamine receptors: from structure to function. *Physiol Rev.* 78:189–225.
- Mocanu MM, Váradi T, Szöllosi J, Nagy P (2011) Comparative analysis of fluorescence resonance energy transfer (FRET) and proximity ligation assay (PLA). *Proteomics.* 11:2063-70. doi: 10.1002/pmic.201100028.
- Mohr K, Schmitz J, Schrage R, Trankle C, Holzgrabe U (2013) Molecular alliance-From orthosteric and allosteric ligands to dualsteric/bitopic agonists at G protein coupled receptors. *Angew Chem Int Ed.* 52:508-16.
- Molina-Arcas M, Casado FJ, Pastor-Anglada M (2009) Nucleoside transporter proteins. *Curr Vasc Pharmacol.* 7:426-34.
- Mondal S, Khelashvili G, Johner N, Weinstein H (2014) How the dynamic properties and functional mechanisms of GPCRs are modulated by their coupling to the membrane environment. *Adv Exp Med Biol.* 796:55-74.
- Monsma FJ Jr, McVittie LD, Gerfen CR, Mahan LC, Sibley DR. (1989) Multiple D2 dopamine receptors produced by alternative RNA splicing. *Nature.* 342:926–9.
- Moore TJ, Glenmullen J, Mattison DR (2014) Reports of pathological gambling, hypersexuality, and compulsive shopping associated with dopamine receptor agonist drugs. *JAMA Internal Medicine.* 174:1930–3.
- Morello S, Sorrentino R, Pinto A (2009) Adenosine A2A receptor agonists as regulators of inflammation: pharmacology and therapeutic opportunities. *J. Receptor Ligand and Channel Res.* 2, 11-17.
- Moreno E, Vaz SH, Cai NS, Ferrada C, Quiroz C, Barodia SK, Kabbani N, Canela EI, McCormick PJ, Lluís C, Franco R, Ribeiro JA, Sebastião AM, Ferré S. (2011) Dopamine-galanin receptor heteromers modulate cholinergic neurotransmission in the rat ventral hippocampus. *J Neurosci.* 31:7412-23. doi: 10.1523/JNEUROSCI.0191-11.2011.
- Moreno E, Quiroz C, Rea W, Cai NS, Mallol J, Cortés A, Lluís C, Canela EI, Casadó V, Ferré S (2017) Functional μ -Opioid-Galanin Receptor Heteromers in the Ventral Tegmental Area. *J Neurosci.* 37:1176-86. doi: 10.1523/JNEUROSCI.2442-16.2016.
- Moreno E, Chiarlone A, Medrano M, Puigdemívol M, Bibic L, Howell LA, Resel E, Puente N, Casarejos MJ, Perucho J, Botta J, Suelves N, Ciruela F, Ginés S, Galve-Roperh I, Casadó V, Grandes P, Lutz B, Monory K, Canela EI, Lluís C, McCormick PJ, Guzmán M (2018) Singular Location and Signaling Profile of Adenosine A2A-Cannabinoid CB1 Receptor Heteromers in the Dorsal Striatum. *Neuropsychopharmacology.* 43:964-77. doi: 10.1038/npp.2017.12.
- Moro S, Deflorian F, Bacilieri M, Spalluto G (2006) Ligand-based homology modeling as attractive tool to inspect GPCR structural plasticity. *Curr Pharm Des.* 12:2175-85.
- Morphy R, Kay C, Rankovic Z (2004) From magic bullets to designed multiple ligands. *Drug Discov Today.* 9:641-51.
- Mostofsky SH, Cooper KL, Kates WR, Denckla MB, Kaufmann WE (2002) Smaller prefrontal and premotor volumes in boys with attention-deficit/hyperactivity disorder. *Biol Psychiatry.* 52:785-94.

- Mrzljak L, Bergson C, Pappy M, Huff R, Levenson R, Goldman-Rakic PS (1996) Localization of dopamine D4 receptors in GABAergic neurons of the primate brain. *Nature*. 381:245-8.
- Mueller A, Shepard SB, Moore T (2018) Differential expression of dopamine D5 receptors across neuronal subtypes in macaque frontal eye field. *Front Neural Circuits*. 12:12. doi: 10.3389/fncir.2018.00012.
- Mundell S, Kelly E (2011) Adenosine receptor desensitization and trafficking. *Biochim Biophys Acta*. 1808:1319-28. doi: 10.1016/j.bbamem.2010.06.007.
- Murchison CF, Zhang XY, Zhang WP, Ouyang M, Lee A, Thomas SA (2004) A distinct role for norepinephrine in memory retrieval. *Cell*. 117:131-43.
- Nagai T, Ibata K, Park ES, Kubota M, Mikoshiba K, Miyawaki A (2002) A variant of yellow fluorescent protein with fast and efficient maturation for cell-biological applications. *Nat Biotechnol*. 20:87-90.
- Naganuma M, Wiznerowicz EB, Lappas CM, Linden J, Worthington MT, Ernst PB (2006) Cutting edge: Critical role for A2A adenosine receptors in the T cell-mediated regulation of colitis. *J Immunol*. 177:2765-9.
- Nahorski SR, Howlett DR, Redgrave P (1979) Loss of beta-adrenoceptor binding sites in rat striatum following kainic acid lesions. *Eur J Pharmacol*. 60:249-52.
- Nair-Roberts RG, Chatelain-Badie SD, Benson E, White-Cooper H, Bolam JP, Ungless MA (2008) Stereological estimates of dopaminergic, GABAergic and glutamatergic neurons in the ventral tegmental area, substantia nigra and retrorubral field in the rat. *Neuroscience*. 152:1024-31. doi: 10.1016/j.neuroscience.2008.01.046.
- Nambu A (2008) Seven problems on the basal ganglia. *Curr Opin Neurobiol*. 18:595-604. doi: 10.1016/j.conb.2008.11.001.
- Navarro G, Quiroz C, Moreno-Delgado D, Sierakowiak A, McDowell K, Moreno E, Rea W, Cai NS, Aguinaga D, Howell LA, Hausch F, Cortés A, Mallol J, Casadó V, Lluís C, Canela EI, Ferré S, McCormick PJ (2015) Orexin-corticotropin-releasing factor receptor heteromers in the ventral tegmental area as targets for cocaine. *J Neurosci*. 35:6639-53.
- Navarro G, Cordoní A, Zelman-Femiak M, Brugarolas M, Moreno E, Aguinaga D, Perez-Benito L, Cortés A, Casadó V, Mallol J, Canela EI, Lluís C, Pardo L, García-Sáez AJ, McCormick PJ, Franco R (2016) Quaternary structure of a G-protein-coupled receptor heterotetramer in complex with Gi and Gs. *BMC Biol*. 14:26. doi: 10.1186/s12915-016-0247-4.
- Navarro G, Cordoní A, Brugarolas M, Moreno E, Aguinaga D, Pérez-Benito L, Ferré S, Cortés A, Casadó V, Mallol J, Canela EI, Lluís C, Pardo L, McCormick PJ, Franco R (2018) Cross-communication between Gi and Gs in a G-protein-coupled receptor heterotetramer guided by a receptor C-terminal domain. *BMC Biol*. 16:24. doi: 10.1186/s12915-018-0491-x.
- Neubig RR (1994) Membrane organization in G-protein mechanisms. *FASEB J*. 8:939-46.
- Newman-Tancredi A, Audinot-Bouchez V, Gobert A, Millan MJ (1997) Noradrenaline and adrenaline are high affinity agonists at dopamine D4 receptors. *Eur J Pharmacol*. 319:379-83.
- Nicholas AP, Pieribone V, Hokfelt T (1993) Distributions of mRNAs for alpha-2 adrenergic receptor subtypes in rat brain: an in situ hybridization study. *J Comp Neurol*. 328:575-94.

- Nicholas AP, Hokfelt T, Pieribone VA (1996) The distribution and significance of CNS adrenoceptors examined with in situ hybridization. *Trends Pharmacol Sci.* 17:245-55.
- Nickols HH, Conn PJ (2014) Development of allosteric modulators of GPCRs for treatment of CNS disorders. *Neurobiol Dis.* 61:55-71.
- Nicola SM, Surmeier J, Malenka RC (2000) Dopaminergic modulation of neuronal excitability in the striatum and nucleus accumbens. *Annu Rev Neurosci.* 23:185-215.
- Nimczick M, Decker M (2015) New approaches in the design and development of cannabinoid receptor ligands: multifunctional and bivalent compounds. *ChemMedChem.* 10:773-86.
- Nussinov R, Tsai CJ (2015) Tandem domains with tuned interactions are a powerful biological design principle. *PLoS Biol.* 13:e1002306. doi: 10.1371/journal.pbio.1002306.
- Oakley RH, Laporte SA, Holt JA, Barak LS, Caron MG (1999) Association of β -arrestin with G protein-coupled receptors during clathrin-mediated endocytosis dictates the profile of receptor resensitization. *J Biol Chem.* 274:32248-57.
- Obeso JA, Marin C, Rodriguez-Oroz C, Blesa J, Benitez-Temiño B, Mena-Segovia J, Rodríguez M, Olanow CW (2008) The basal ganglia in Parkinson's disease: current concepts and unexplained observations. *Ann Neurol.* 64 (Suppl 2):S30-46. doi: 10.1002/ana.2148.1.
- Offermanns S, Heiler E, Spicher K, Schultz G (1994) Gq and G11 are concurrently activated by bombesin and vasopressin in Swiss 3T3 cells. *FEBS Lett.* 349:201-4.
- Oldham WM, Hamm HE (2008) Heterotrimeric G protein activation by G-protein-coupled receptors. *Nat Rev Mol Cell Biol.* 9:60-71.
- Oldham WM, Van Eps N, Preininger AM, Hubbell WL, Hamm HE (2006) Mechanism of the receptor-catalyzed activation of heterotrimeric G proteins. *Nat Struct Mol Biol.* 13:772-7.
- Ordway GA, Jaconetta SM, Halaris AE (1993) Characterization of subtypes of alpha-2 adrenoceptors in the human brain. *J Pharmacol Exp Ther.* 264:967-76.
- Orrú M, Bakešová J, Brugarolas M, Quiroz C, Beaumont V, Goldberg SR, Lluís C, Cortés A, Franco R, Casadó V, Canela EI, Ferré S (2011) Striatal preand postsynaptic profile of adenosine A(2A) receptor antagonists. *PLoS One.* 6:e16088. doi: 10.1371/journal.pone.0016088.
- Ouyang X, Ghani A, Malik A, Wilder T, Colegio OR, Flavell RA, Cronstein BN, Mehal WZ (2013) Adenosine is required for sustained inflammasome activation via the A2A receptor and HIF-1 α pathway. *Nat Commun.* 4:2909.
- Owesson-White CA, Roitman MF, Sombers LA, Belle AM, Keithley RB, Peele JL, Carelli RM, Wightman RM (2012) Sources contributing to the average extracellular concentration of dopamine in the nucleus accumbens. *J Neurochem.* 121:252-62. doi:10.1111/j.1471-4159.2012.07677.x
- Pak Y, O'Dowd BF, Wang JB, George SR (1999) Agonist-induced, G protein-dependent and -independent down-regulation of the mu opioid receptor. The receptor is a direct substrate for protein-tyrosine kinase. *J Biol Chem.* 274:27610-16.

- Palczewski K, Kumasaka T, Hori T, Behnke CA, Motoshima H, Fox BA, Le Trong I, Teller DC, Okada T, Stenkamp RE, Yamamoto M, Miyano M (2000) Crystal structure of rhodopsin: a G protein-coupled receptor. *Science*. 289:739–45.
- Palmer TM, Stiles GL (1995) Adenosine receptors. *Neuropharmacology*. 34:683-94.
- Palmer TM, Trevethick MA (2008) Suppression of inflammatory and immune responses by the A2a adenosine receptor: an introduction. *Br J Pharmacol*. 153 (Suppl 1): S27-S34.
- Palmer TM, Gettys TW, Jacobson KA, Stiles GL (1994) Desensitization of the canine A2a adenosine receptor: delineation of multiple processes. *Mol Pharmacol*. 45:1082-94.
- Papac DI, Thornburg KR, Büllsbach EE, Crouch RK, Knapp DR (1992) Palmitoylation of a G-protein coupled receptor. Direct analysis by tandem mass spectrometry. *J Biol Chem*. 267:16889-94.
- Papay R, Gaivin R, Jha A, McCune DF, McGrath JC, Rodrigo MC, Simpson PC, Doze VA, Perez, DM (2006) Localization of the mouse alpha1A-adrenergic receptor (AR) in the brain: alpha1AAR is expressed in neurons, GABAergic interneurons, and NG2 oligodendrocyte progenitors. *J Comp Neurol*. 497:209-22.
- Park PS, Wells JW (2003) Monomers and oligomers of the M2 muscarinic cholinergic receptor purified from Sf9 cells. *Biochemistry*. 42:12960-71.
- Park L, Nigg JT, Waldman ID, Nummy KA, Huang-Pollock C, Rappley M, Friderici KH (2005) Association and linkage of alpha-2A adrenergic receptor gene polymorphisms with childhood ADHD. *Molecular Psychiatry*. 10: 572–80.
- Parkinson FE, Damaraju VL, Graham K, Yao SY, Baldwin SA, Cass CE, Young JD (2011) Molecular biology of nucleoside transporters and their distributions and functions in the brain. *Curr Top Med Chem*. 11:948-72.
- Parmar VK, Grinde E, Mazurkiewicz JE, Herrick-Davis K (2017) Beta2-adrenergic receptor homodimers: Role of transmembrane domain 1 and helix 8 in dimerization and cell surface expression. *Biochim Biophys Acta*. 1859(9 Pt A):1445-55. doi: 10.1016/j.bbamem.2016.12.007.
- Parton RG, Simons K (2007) The multiple faces of caveolae. *Nat Rev Mol Cell Biol*. 8:185-94.
- Paul S, Elsinga PH, Ishiwata K, Dierckx RA, Van Waarde A (2011) Adenosine A1 receptors in the central nervous system: their function in health and disease, and possible elucidation by PET imaging. *Curr Med Chem* 18:4820-4835.
- Pedata F, Gianfriddo M, Turchi D, Melani A (2005) The protective effect of adenosine A2A receptor antagonism in cerebral ischemia. *Neurol Res*. 27:169-74.
- Pedata F, Dettori I, Coppi E, Melani A, Fusco I, Corradetti R, Pugliese AM (2016) Purinergic signalling in brain ischemia. *Neuropharmacology*. 104:105-30.
- Pelligrino DA, Xu HL, Vetri F (2010) Caffeine and the control of cerebral hemodynamics. *J Alzheimers Dis*. 20:S51-62. doi: 10.3233/JAD-2010-091261.
- Pellissier LP, Barthet G, Gaven F, Cassier E, Trinquet E, Pin JP, Marin P, Dumuis A, Bockaert J, and Banères JL Claeysen S (2011) G protein activation by serotonin type 4 receptor dimers: evidence that turning on two protomers is more efficient. *J Biol Chem*. 286:9985-97.

- Peng H, Kumaravel G, Yao G, Sha L, Wang J, Van Vlijmen H, Bohnert T, Huang C, Vu CB, Ensinger CL, Chang H, Engber TM, Whalley ET, Petter RC (2004) Novel bicyclic piperazine derivatives of triazolotriazine and triazolopyrimidines as highly potent and selective adenosine A2A receptor antagonists. *J Med Chem.* 47:6218-29.
- Penney JB Jr, Young AB (1986) Striatal inhomogeneities and basal ganglia function. *Mov Disord.* 1:3-15.
- Perez DM, Karnik SS (2005) Multiple signaling states of G-protein-coupled receptors. *Pharmacol Rev.* 57:147-61.
- Perez DM, Hwa J, Gaivin R, Mathur M, Brown F, Graham RM (1996) Constitutive activation of a single effector pathway: evidence for multiple activation states of a G protein-coupled receptor. *Mol Pharmacol.* 49:112–22.
- Pfleger KD, Eidne KA (2005) Monitoring the formation of dynamic G-protein-coupled receptor-protein complexes in living cells. *Biochem J.* 385:625-37.
- Phelps PE, Houser CR, Vaughn JE (1985) Immunocytochemical localization of choline acetyltransferase within the rat neostriatum: a correlated light and electron microscopic study of cholinergic neurons and synapses. *J Comp Neurol.* 238:286-307.
- Philipp M, Hein L (2004) Adrenergic receptor knockout mice: distinct functions of 9 receptor subtypes. *Pharmacol Ther.* 101:65-74.
- Philipp M, Brede ME, Hadamek K, Gessler M, Lohse MJ, Hein L (2002) Placental alpha(2)-adrenoceptors control vascular development at the interface between mother and embryo. *Nat Genet.* 31:311-5.
- Phillis JW, Edstrom JP, Kostopoulos GK, Kirkpatrick JR (1979) Effects of adenosine and adenine nucleotides on synaptic transmission in the cerebral cortex. *Can J Physiol Pharmacol.* 57:1289-312.
- Pieper U, Schlessinger A, Kloppmann E, Chang GA, Chou JJ, Dumont ME, Fox BG, Fromme P, Hendrickson WA, Malkowski MG, Rees DC, Stokes DL, Stowell MH, Wiener MC, Rost B, Stroud RM, Stevens RC, Sali A (2013) Coordinating the impact of structural genomics on the human alpha-helical transmembrane proteome. *Nat Struct Mol Biol.* 20:135–8.
- Pin JP, Neubig R, Bouvier M, Devi L, Filizola M, Javitch JA, Lohse MJ, Milligan G, Palczewski K, Parmentier M, Spedding M (2007) International union of basic and clinical pharmacology. LXVII. Recommendations for the recognition and nomenclature of G protein-coupled receptor heteromultimers. *Pharmacol Rev.* 59:5–13.
- Pinna A (2014) Adenosine A2A receptor antagonists in Parkinson's disease: progress in clinical trials from the newly approved istradefylline to drugs in early development and those already discontinued. *CNS Drugs.* 28:455-74.
- Piirainen H, Taura J, Kursula P, Ciruela F, Jaakola VP (2017) Calcium modulates calmodulin/ α -actinin 1 interaction with and agonist-dependent internalization of the adenosine A2A receptor. *Biochim Biophys Acta.*1864:674-86. doi: 10.1016/j.bbamcr.2017.01.013.

- Popoli P, Betto P, Rimondini R, Reggio R, Pézzola A, Ricciarello G, Fuxe K, Ferré S (1998) Age-related alteration of the adenosine/dopamine balance in the rat striatum. *Brain Res.* 795:297-300.
- Popoli P, Blum D, Domenici MR, Burnouf S, Chern Y (2008) A critical evaluation of adenosine A2A receptors as potentially "druggable" targets in Huntington's disease. *Curr Pharm Des.* 14:1500-11.
- Porkka-Heiskanen T, Zitting KM, Wigren HK (2013) Sleep, its regulation and possible mechanisms of sleep disturbances. *Acta Physiol (Oxf).* 208:311-28. doi: 10.1111/apha.12134.
- Portoghese PS (2001) From models to molecules: opioid receptor dimers, bivalent ligands, and selective opioid receptor probes. *J Med Chem.* 44:2259-69.
- Pou C, Mannoury la Cour C, Stoddart LA, Millan MJ, Milligan G (2012) Functional homomers and heteromers of dopamine D2L and D3 receptors co-exist at the cell surface. *J Biol Chem.* 287:8864-78. doi: 10.1074/jbc.M111.326678.
- Preti D, Baraldi PG, Moorman AR, Borea PA, Varani K (2015) History and perspectives of A2A adenosine receptor antagonists as potential therapeutic agents. *Med Res Rev.* 35:790-848. doi: 10.1002/med.21344.
- Price JL, Carmichael ST, Drevets WC (1996) Networks related to the orbital and medial prefrontal cortex; a substrate for emotional behavior? *Prog Brain Res.* 107:523-36.
- Primus RJ, Thurkauf A, Xu J, Yevich E, McInerney S, Shaw K, Tallman JF, Gallagher DW (1997) II. Localization and characterization of dopamine D4 binding sites in rat and human brain by use of the novel, D4 receptor-selective ligand [3H]NGD 94-1. *J Pharmacol Exp Ther.* 282:1020-7.
- Prinster SC, Hague C, Hall RA (2005) Heterodimerization of G protein-coupled receptors: specificity and functional significance. *Pharmacol Rev.* 57:289-98.
- Prinster SC, Holmqvist TG, Hall RA (2006) Alpha2C-adrenergic receptors exhibit enhanced surface expression and signaling upon association with beta2-adrenergic receptors. *J Pharmacol Exp Ther.* 318:974-81.
- Probst WC, Snyder LA, Schuster DI, Brosius J, Sealfon SC (1992). Sequence alignment of the G-protein coupled receptor superfamily. *DNA Cell Biol.* 11:1-20.
- Pull I, McIlwain H (1972) Adenine derivatives as neurohumoral agents in the brain. The quantities liberated on excitation of superfused cerebral tissues. *Biochem J.* 130:975-81.
- Quiroz C, Luján R, Uchigashima M, Simoes AP, Lerner TN, Borycz J, Kachroo A, Canas PM, Orru M, Schwarzschild MA, Rosin DL, Kreitzer AC, Cunha RA, Watanabe M, Ferré S (2009) Key modulatory role of presynaptic adenosine A2A receptors in cortical neurotransmission to the striatal direct pathway. *ScientificWorldJournal.* 9:1321-44. doi: 10.1100/tsw.2009.143.
- Raicu V, Singh DR (2013) FRET spectrometry: a new tool for the determination of protein quaternary structure in living cells. *Biophys J.* 105:1937-45.
- Rainbow TC, Parsons B, Wolfe BB (1984) Quantitative autoradiography of beta 1 and beta 2-adrenergic receptors in rat brain. *Proc Natl Acad Sci USA.* 81:1585-9.

- Rajagopal S, Rajagopal K, Lefkowitz RJ (2010) Teaching old receptors new tricks: biasing seven-transmembrane receptors. *Nat Rev Drug Discov.* 9:373-86.
- Rämä P, Linnankoski I, Tanila H, Pertovaara A, Carlson S (1996) Medetomidine, atipamezole, and guanfacine in delayed response performance of aged monkeys. *Pharmacol Biochem Behav.* 55:415-22.
- Ramsay D, Kellett E, McVey M, Rees S, Milligan G (2002) Homoand hetero-oligomeric interactions between G-protein-coupled receptors in living cells monitored by two variants of bioluminescence resonance energy transfer (BRET): heterooligomers between receptor subtypes form more efficiently than between less closely related sequences. *Biochem J.* 365:429–40.
- Ramos BP, Colgan L, Nou E, Ovadia S, Wilson SR, Arnsten AF (2005) The beta-1 adrenergic antagonist, betaxolol, improves working memory performance in rats and monkeys. *Biol Psychiatry.* 58:894-900.
- Rangel-Barajas C, Coronel I, Florán B (2015). Dopamine receptors and neurodegeneration. *Aging Dis.* 6:349-68. doi:10.14336/AD.2015.0330.
- Rankovic Z, Brust TF, Bohn LM (2016) Biased agonism: An emerging paradigm in GPCR drug discovery. *Bioorg Med Chem Lett.* 26:241-50. doi: 10.1016/j.bmcl.2015.12.024.
- Rasmussen SG, DeVree BT, Zou Y, Kruse AC, Chung KY, Kobilka TS, Thian FS, Chae PS, Pardon E, Calinski D, Mathiesen JM, Shah ST, Lyons JA, Caffrey M, Gellman SH, Steyaert J, Skiniotis G, Weiss WI, Sunahara RK, Kobilka BK (2011) Crystal structure of the β_2 adrenergic receptor-Gs protein complex. *Nature.* 477:549-55. doi: 10.1038/nature10361.
- Rebois RV, Hebert TE (2003) Protein complexes involved in heptahelical receptor mediated signal transduction. *Receptors Channels.* 9:169–94.
- Rebois RV, Warner DR, Basi NS (1997) Does subunit dissociation necessarily accompany the activation of all heterotrimeric G proteins? *Cell Signal.* 9:141–51.
- Rebola N, Porciúncula LO, Lopes LV, Oliveira CR, Soares-da-Silva P, Cunha RA (2005a) Long-term effect of convulsive behavior on the density of adenosine A1 and A2A receptors in the rat cerebral cortex. *Epilepsia.* 46 Suppl 5:159-65.
- Rebola N, Rodrigues RJ, Lopes LV, Richardson PJ, Oliveira CR, Cunha RA (2005b) Adenosine A1 and A2A receptors are co-expressed in pyramidal neurons and co-localized in glutamatergic nerve terminals of the rat hippocampus. *Neuroscience.* 133:79-83.
- Reggio R, Pèzzola A, Popoli P (1999) The intrastriatal injection of an adenosine A(2) receptor antagonist prevents frontal cortex EEG abnormalities in a rat model of Huntington's disease. *Brain Res.* 831:315-8.
- Rekas A, Alattia JR, Nagai T, Miyawaki A, Ikura M (2002) Crystal structure of venus, a yellow fluorescent protein with improved maturation and reduced environmental sensitivity. *J Biol Chem.* 277:50573-8.
- Ribeiro J A, Sebastião AM (2010) Caffeine and adenosine. *Journal of Alzheimer's Disease,* 20(Suppl. 1):S3–S15.

- Rice ME, Patel JC, Cragg SJ (2011) Dopamine release in the basal ganglia. *Neuroscience*. 198:112-37. doi:10.1016/j.neuroscience.2011.08.066.
- Rimondini R, Ferré S, Giménez-Llort L, Ogren SO, Fuxe K (1998) Differential effects of selective adenosine A1 and A2A receptor agonists on dopamine receptor agonist-induced behavioural responses in rats. *Eur J Pharmacol*. 347:153-8.
- Rissanen E, Virta J, Paavilainen T, Tuisku J, Helin S, Luoto P, Parkkola R, Rinne JO, Airas L (2013) Adenosine A2A receptors in secondary progressive multiple sclerosis: a [(11)C]TMSX brain PET study. *J Cereb Blood Flow Metab*. 33:1394-401.
- Rivera A, Peñafiel A, Megías M, Agnati LF, López-Téllez JF, Gago B, Gutiérrez A, de la Calle A, Fuxe K (2008) Cellular localization and distribution of dopamine D(4) receptors in the rat cerebral cortex and their relationship with the cortical dopaminergic and noradrenergic nerve terminal networks. *Neuroscience*. 155:997-1010. doi: 10.1016/j.neuroscience.2008.05.060.
- Rivero-Muller A, Chou Y.Y, Ji I, Lajic S, Hanyaloglu AC, Jonas K, Rahman N, Ji TH, Huhtaniemi I (2010) Rescue of defective G protein-coupled receptor function in vivo by intermolecular cooperation. *Proc Natl Aca Sci USA*. 107:2319-24.
- Rivero-Muller A, Jonas KC, Hanyaloglu AC, Huhtaniemi I (2013) Di/oligomerization of GPCRs-mechanisms and functional significance. *Prog Mol Biol Transl Sci*. 117:163-85.
- Rivkees SA (1995) The ontogeny of cardiac and neural A1 adenosine receptor expression in rats. *Brain Res Dev Brain Res*. 89:202-13.
- Rivkees SA, Thevananther S, Hao H (2000) Are A3 adenosine receptors expressed in the brain? *Neuroreport*. 11:1025-30.
- Robbins TW, Roberts AC (2007) Differential regulation of fronto-executive function by the monoamines and acetylcholine. *Cereb Cortex*. 17:i151-60.
- Rodríguez-Frade JM, Vila-Coro AJ, de Ana AM, Albar JP, Martínez-A C, Mellado M. (1999) The chemokine monocyte chemoattractant protein-1 induces functional responses through dimerization of its receptor CCR2. *Proc Natl Acad Sci USA*. 96:3628-33.
- Rohrer DK (1998) Physiological consequences of beta-adrenergic receptor disruption. *J Mol Med*. 76:764-72.
- Rohrer DK, Kobilka BK (1998) Insights from in vivo modification of adrenergic receptor gene expression. *Annu Rev Pharmacol Toxicol*. 38:351-73.
- Roman T, Schmitz M, Polanczyk GV, Eizirik M, Rohde LA, Hutz MH (2003) Is the alpha-2A adrenergic receptor gene (ADRA2A) associated with attention-deficit/hyperactivity disorder?. *American Journal of Medical Genetics Part B: Neuropsychiatric Genetics*. 120B: 116-20.
- Rommelfanger KS, Mitrano DA, Smith Y, Weinschenker D (2009) Light and electron microscopic localization of alpha-1 adrenergic receptor immunoreactivity in the rat striatum and ventral midbrain. *Neuroscience*. 158:1530-40.
- Rondou P, Haegeman G, Van Craenenbroeck K (2010) The dopamine D4 receptor: biochemical and signalling properties. *Cell Mol Life Sci*. 67:1971-86.

- Root DH, Hoffman AF, Good CH, Zhang S, Gigante E, Lupica CR, Morales M (2015) Norepinephrine activates dopamine D4 receptors in the rat lateral habenula. *J Neurosci.* 35:3460-9. doi: 10.1523/JNEUROSCI.4525-13.2015.
- Ross GW, Abbott RD, Petrovitch H, Morens DM, Grandinetti A, Tung KH, Tanner CM, Masaki KH, Blanchette PL, Curb JD, Popper JS, White LR (2000) Association of coffee and caffeine intake with the risk of Parkinson disease. *JAMA.* 283:2674-9.
- Rossi M, Fasciani I, Marampon F, Maggio R, Scarselli M. (2017) The first negative allosteric modulator for dopamine D2 and D3 receptors, SB269652 may lead to a new generation of antipsychotic drugs. *Mol Pharmacol.* 91:586-94. doi: 10.1124/mol.116.107607.
- Roth NS, Lefkowitz RJ, Caron MG (1991) Structure and function of the adrenergic receptor family. *Adv Exp Med Biol.* 308:223-38.
- Roth BL, Sheffler DJ, Kroeze WK (2004) Magic shotguns versus magic bullets: selectively non-selective drugs for mood disorders and schizophrenia. *Nat Rev Drug Discov.* 3:353-9.
- Roth S, Kholodenko BN, Smit MJ, Bruggeman FJ (2015) G protein-coupled receptor signaling networks from a systems perspective. *Mol Pharmacol.* 88:604-16. doi: 10.1124/mol.115.100057.
- Rovira X, Roche D, Serra J, Kniazeff J, Pin JP, Giraldo J (2008) Modeling the binding and function of metabotropic glutamate receptors. *J Pharmacol Exp Ther.* 325:443-56. doi: 10.1124/jpet.107.133967
- Rovira X, Vivó M, Serra J, Roche D, Strange PG, Giraldo J (2009) Modelling the interdependence between the stoichiometry of receptor oligomerization and ligand binding for a coexisting dimer/tetramer receptor system. *Br J Pharmacol.* 156:28-35. doi: 10.1111/j.1476-5381.2008.00031.x.
- Rubia K, Overmeyer S, Taylor E, Brammer M, Williams SC, Simmons A, Bullmore ET (1999) Hypofrontality in attention deficit hyperactivity disorder during higher-order motor control: a study with functional MRI. *Am J Psychiatry.* 156:891-6.
- Rubia K, Smith AB, Brammer MJ, Toone B, Taylor E (2005) Abnormal brain activation during inhibition and error detection in medication-naive adolescents with ADHD. *Am J Psychiatry.* 162:1067-75.
- Rubinstein M, Cepeda C, Hurst RS, Flores-Hernandez J, Ariano MA, Falzone TL, Kozell LB, Meshul CK, Bunzow JR, Low MJ, Levine MS, Grandy DK (2001) Dopamine D4 receptor-deficient mice display cortical hyperexcitability. *J Neurosci.* 21:3756-63.
- Ruiz MA, Escriche M, Lluís C, Franco R, Martín M, Andrés A, Ros M. (2000) Adenosine A(1) receptor in cultured neurons from rat cerebral cortex: colocalization with adenosine deaminase. *J Neurochem.* 75:656-64.
- Sadana R, Dascal N, Dessauer CW (2009) N terminus of type 5 adenylyl cyclase scaffolds Gs heterotrimer. *Mol. Pharmacol.* 76:1256-64.
- Sakata M, Ishibashi K, Imai M, Wagatsuma K, Ishii K, Zhou X, de Vries EFJ, Elsinga PH, Ishiwata K, Toyohara J (2017) Initial evaluation of an adenosine A2A receptor ligand, 11C-preladenant, in healthy human subjects. *J Nucl Med.* 58:1464-70. doi: 10.2967/jnumed.116.188474.

- Sakmar TP (1998) Rhodopsin: a prototypical G protein-coupled receptor. *Prog Nucleic Acid Res Mol Biol.* 59:1-34.
- Samama P, Cotecchia S, Costa T, Lefkowitz RJ (1993) A mutation-induced activated state of the beta 2-adrenergic receptor. Extending the ternary complex model. *J Biol Chem.* 268:4625-36.
- Sánchez-Soto M, Bonifazi A, Cai NS, Ellenberger MP, Newman AH, Ferré S, Yano H (2016) Evidence for noncanonical neurotransmitter activation: norepinephrine as a dopamine D2-like receptor agonist. *Mol Pharmacol.* 89:457-66. doi: 10.1124/mol.115.101808.
- Sano H, Yasoshima Y, Matsushita N, Kaneko T, Kohno K, Pastan I, Kobayashi K (2003) Conditional ablation of striatal neuronal types containing dopamine D2 receptor disturbs coordination of basal ganglia function. *J Neurosci.* 23:9078-88.
- Santana N, Mengod G, Artigas F (2013) Expression of $\alpha(1)$ -adrenergic receptors in rat prefrontal cortex: cellular co-localization with 5-HT(2A) receptors. *Int J Neuropsychopharmacol.* 16:1139-51. doi: 10.1017/S1461145712001083.
- Santiago AR, Baptista FI, Santos PF, Cristóvão G, Ambrósio AF, Cunha RA, Gomes CA (2014) Role of microglia adenosine A(2A) receptors in retinal and brain neurodegenerative diseases. *Mediators Inflamm.* 2014:465694. doi: 10.1155/2014/465694.
- Sara SJ, Bouret S (2012) Orienting and reorienting: the locus coeruleus mediates cognition through arousal. *Neuron.* 76:130-41. doi: 10.1016/j.neuron.2012.09.011.
- Sarrió S, Casadó V, Escriche M, Ciruela F, Mallol J, Canela EI, Lluís C, Franco R (2000) The heat shock cognate protein hsc73 assembles with A(1) adenosine receptors to form functional modules in the cell membrane. *Mol Cell Biol.* 20:5164-74.
- Saunders C, Limbird LE (1999) Localization and trafficking of alpha2-adrenergic receptor subtypes in cells and tissues. *Pharmacol Ther.* 84:193-205.
- Saura C, Ciruela F, Casadó V, Canela EI, Mallol J, Lluís C, Franco R (1996) Adenosine deaminase interacts with A1 adenosine receptors in pig brain cortical membranes. *J Neurochem.* 66:1675-82.
- Saura CA, Mallol J, Canela EI, Lluís C, Franco R (1998) Adenosine deaminase and A1 adenosine receptors internalize together following agonist-induced receptor desensitization. *J Biol Chem.* 273:17610-7.
- Savasta M, Dubois A, Scatton B (1986) Autoradiographic localization of D1 dopamine receptors in the rat brain with [3H]SCH 23390. *Brain Res.* 375:291-301.
- Sawynok J, Liu XJ (2003) Adenosine in the spinal cord and periphery: release and regulation of pain. *Prog Neurobiol.* 69:313-40.
- Scheibner J, Trendelenburg AU, Hein L, Starke K (2001) Alpha2-adrenoceptors modulating neuronal serotonin release: a study in alpha2-adrenoceptor subtype-deficient mice. *Br J Pharmacol.* 132:925-33.
- Scheinin M, Lomasney JW, Hayden-Hixson DM, Schambra UB, Caron MG, Lefkowitz RJ, Freneau RT (1994). Distribution of alpha 2-adrenergic receptor subtype gene expression in rat brain. *Brain Res Mol Brain Res.* 21:133-49.

- Schiffmann SN, Fisone G, Moresco R, Cunha RA, Ferré S (2007) Adenosine A_{2A} receptors and basal ganglia physiology. *Prog Neurobiol.* 83:277-92.
- Schmidt CJ, Thomas TC, Levine MA, Neer EJ. (1992) Specificity of G protein β and γ subunit interactions. *J Biol Chem.* 267:13807–10.
- Schmitz J, Van der May D, Bermudez M, Klockner J, Schrage R, Kostenis E, Trankle C, Wolber G, Mohr K, Holzgrabe U (2014) Dualsteric muscarinic antagonists-Orthosteric binding pose controls allosteric subtype selectivity. *J Med Chem* 57:6739-50.
- Schöneberg T, Schulz A, Biebermann H, Hermsdorf T, Römpler H, Sangkuhl K (2004) Mutant G-protein-coupled receptors as a cause of human diseases. *Pharmacol Ther.* 104:173-206.
- Schwarz LA, Luo L (2015) Organization of the locus coeruleus-norepinephrine system. *Curr Biol.* 25:R1051-R1056. doi: 10.1016/j.cub.2015.09.039.
- Schwarzschild MA, Chen JF, Ascherio A (2002) Caffeinated clues and the promise of adenosine A(2A) antagonists in PD. *Neurology.* 58:1154-60.
- Sebastiao AM, Ribeiro JA (2000) Fine-tuning neuromodulation by adenosine. *Trends Pharmacol Sci.* 21:341-6.
- Sebastiao AM, Ribeiro JA (2009) Tuning and fine-tuning of synapses with adenosine. *Curr Neuropharmacol.* 7:180-94.
- Sebastião AM, Ribeiro JA (2015) Neuromodulation and metamodulation by adenosine: Impact and subtleties upon synaptic plasticity regulation. *Brain Res.* 1621:102-13.
- Seeman P, Wilson A, Gmeiner P, Kapur S (2006) Dopamine D₂ and D₃ receptors in human putamen, caudate nucleus, and globus pallidus. *Synapse.* 60:205-11.
- Seidman LJ, Valera EM, Makris N (2005) Structural brain imaging of attention-deficit/hyperactivity disorder. *Biol Psychiatry.* 57:1263-72.
- Seifert S M, Schaechter J L, Hershorin E R, Lipshultz S E (2011) Health effects of energy drinks on children, adolescents and young adults. *Pediatrics.* 127:511–28.
- Serchov T, Clement HW, Schwarz MK, Iasevoli F, Tosh DK, Idzko M, Jacobson KA, de Bartolomeis A, Normann C, Biber K, van Calker D (2015) Increased Signaling via Adenosine A₁ Receptors, Sleep Deprivation, Imipramine, and Ketamine Inhibit Depressive-like Behavior via Induction of Homer1a. *Neuron.* 87:549-62.
- Sesack SR, Pickel VM (1992) Prefrontal cortical efferents in the rat synapse on unlabeled neuronal targets of catecholamine terminals in the nucleus accumbens septi and on dopamine neurons in the ventral tegmental area. *J Comp Neurol.* 320:145–60. doi: 10.1002/cne.903200202.
- Shaw P, Eckstrand K, Sharp W, Blumenthal J, Lerch JP, Greenstein D, Clasen L, Evans A, Giedd J, Rapoport JL (2007) Attention-deficit/hyperactivity disorder is characterized by a delay in cortical maturation. *Proc Natl Acad Sci USA.* 104:19649-54.
- Sheikh SP, Zvyaga TA, Lichtarge O, Sakmar TP, Bourne HR (1996) Rhodopsin activation blocked by metal-ion-binding sites linking transmembrane hélices C and F. *Nature.* 383:347–50.

- Shen HY, Singer P, Lytle N, Wei CJ, Lan JQ, Williams-Karnesky RL, Chen JF, Yee BK, Boison D (2012) Adenosine augmentation ameliorates psychotic and cognitive endophenotypes of schizophrenia. *J Clin Invest.* 122:2567-77. doi: 10.1172/JCI62378.
- Shen HY, Canas PM, Garcia-Sanz P, Lan JQ, Boison D, Moratalla R, Cunha RA, Chen JF (2013) Adenosine A_{2A} receptors in striatal glutamatergic terminals and GABAergic neurons oppositely modulate psychostimulant action and DARPP-32 phosphorylation. *PLoS One.* 8:e80902. doi: 10.1371/journal.pone.0080902. eCollection 2013.
- Sheng M, Kim E (2000) The Shank family of scaffold proteins. *J Cell Sci.* 113:1851-6.
- Shenoy SK, Lefkowitz RJ (2011) β -Arrestin-mediated receptor trafficking and signal transduction. *Trends Pharmacol Sci.* 32:521-33. doi: 10.1016/j.tips.2011.05.002.
- Shenton FC, Hann V, Chazot PL (2005) Evidence for native and cloned H3 histamine receptor higher oligomers. *Inflamm Res.* 54:48-9.
- Shepherd GM (2003) Corticostriatal connectivity and its role in disease. *Nat Rev Neurosci.* 14:278-91. doi: 10.1038/nrn3469.
- Shi WX, Pun CL, Zhang XX, Jones MD, Bunney BS (2000) Dual effects of D-amphetamine on dopamine neurons mediated by dopamine and nondopamine receptors. *J Neurosci.* 20:3504-11.
- Shinba T, Shinozaki T, Mugishima G (2001) Clonidine immediately after immobilization stress prevents long-lasting locomotion reduction in the rat. *Prog Neuropsychopharmacol Biol Psychiatry.* 25:1629-40.
- Shivnaraine RV, Kelly B, Sankar KS, Redka DS, Han YR, Huang F, Elmslie G, Pinto D, Li Y, Rocheleau JV, Gradinaru CC, Ellis J, Wells JW (2016) Allosteric modulation in monomers and oligomers of a G protein-coupled receptor. *Elife.* 5:e11685. doi: 10.7554/eLife.11685.
- Shonberg J, Scammells PJ, Capuano B (2011) Design strategies for bivalent ligands targeting GPCRs. *ChemMedChem.* 6:963-74.
- Shonberg J, Kling RC, Gmeiner P, Löber S (2015) GPCR crystal structures: medicinal chemistry in the pocket. *Bioorg Med Chem.* 23:3880-906.
- Sibley DR (1999) New insights into dopaminergic receptor function using antisense and genetically altered animals. *Annu Rev Pharmacol Toxicol.* 39:313-41.
- Silvano E, Millan MJ, Mannoury la Cour C, Han Y, Duan L, Griffin SA, Luedtke RR, Aloisi G, Rossi M, Zazzaroni F, Javitch JA, Maggio R (2010) The tetrahydroisoquinoline derivative SB269,652 is an allosteric antagonist at dopamine D3 and D2 receptors. *Mol Pharmacol.* 78:925-34. doi: 10.1124/mol.110.065755.
- Simon MI, Strathmann MP, Gautam N (1991). Diversity of G proteins in signal transduction. *Science.* 252:802-8.
- Simões AP, Machado NJ, Gonçalves N, Kaster MP, Simões AT, Nunes A, Pereira de Almeida L, Goosens KA, Rial D, Cunha RA (2016) Adenosine A_{2A} Receptors in the Amygdala Control Synaptic Plasticity and Contextual Fear Memory. *Neuropsychopharmacology.* 41:2862-71.

- Simonneaux V, Ribelayga C (2003) Generation of the melatonin endocrine message in mammals: a review of the complex regulation of melatonin synthesis by norepinephrine, peptides, and other pineal transmitters. *Pharmacol Rev.* 55:325-95.
- Sitkovsky MV, Lukashev D, Apasov S, Kojima H, Koshiba M, Caldwell C, Ohta A, Thiel M (2004) Physiological control of immune response and inflammatory tissue damage by hypoxia inducible factors and adenosine A2A receptors. *Annu Rev Immunol.* 22:657-82.
- Skieterska K, Rondou P, Van Craenenbroeck K (2016) Dopamine D4 receptor ubiquitination. *Biochem Soc Trans.* 44:601-5. doi: 10.1042/BST20150281.
- Small KM, Schwarb MR, Glinka C, Theiss CT, Brown KM, Seman CA, Liggett SB (2006) Alpha2A and alpha2C-adrenergic receptors form homo and heterodimers: the heterodimeric state impairs agonist-promoted GRK phosphorylation and beta-arrestin recruitment. *Biochemistry.* 45:4760-7.
- Smith Y, Villalba R (2008) Striatal and extrastriatal dopamine in the basal ganglia: an overview of its anatomical organization in normal and Parkinsonian brains. *Mov Disord.* 23:S534-47. doi: 10.1002/mds.22027.
- Smith NJ, Milligan G (2010) Allosterism at G protein-coupled receptor homo and heteromers: uncharted pharmacological landscapes. *Pharmacol Rev.* 62:701-25. doi: 10.1124/pr.110.002667.
- Smith JS, Lefkowitz RJ, Rajagopal S. (2018) Biased signalling: from simple switches to allosteric microprocessors. *Nat Rev Drug Discov.* 17:243-60. doi: 10.1038/nrd.2017.229.
- Smotrys JE, Linder ME (2004) Palmitoylation of intracellular signaling proteins: regulation and function. *Annu Rev Biochem.* 73:559-87.
- Snyder SH, Taylor KM, Coyle JT, Meyerhoff JL (1970) The role of brain dopamine in behavioral regulation and the actions of psychotropic drugs. *Am J Psychiatry.* 127:199-207.
- Söderberg O, Leuchowius K-J, Gullberg M, Jarvius M, Weibrecht I, Larsson LG, Landegren U (2008) Characterizing proteins and their interactions in cells and tissues using the in situ proximity ligation assay. *Methods.* 45:227-32. doi: 10.1016/j.ymeth.2008.06.014.
- Sokoloff P, Giros B, Martres MP, Andrieux M, Besancon R, Pilon C, Bouthenet ML, Souil E, Schwartz JC (1992) Localization and function of the D3 dopamine receptor. *Arzneimittelforschung.* 42:224-30.
- Sokoloff P, Diaz J, Le Foll B, Guillin O, Leriche L, Bezard E, Gross C. (2006) The dopamine D3 receptor: a therapeutic target for the treatment of neuropsychiatric disorders. *CNS Neurol Disord Drug Targets.* 5:25-43.
- Sondek J, Bohm A, Lambright DG, Hamm HE, Sigler PB (1996) Crystal structure of a G-protein beta gamma dimer at 2.1 Å resolution. *Nature.* 379:369-374.
- Soriano A, Ventura R, Molero A, Hoen R, Casadó V, Cortés A, Fanelli F, Albericio F, Lluís C, Franco R, Royo, M (2009) Adenosine A2A receptor-antagonist/dopamine D2 receptor-agonist bivalent ligands as pharmacological tools to detect A2A-D2 receptor heteromers. *J Med Chem.* 52:5590-602.

- Spreng M, Cotecchia S, Schenk F (2001) A behavioral study of alpha-1b adrenergic receptor knockout mice: increased reaction to novelty and selectively reduced learning capacities. *Neurobiol Learn Mem.* 75:214-29.
- Springael JY, Le Minh PN, Urizar E, Costagliola S, Vassart G, Parmentier M (2006) Allosteric modulation of binding properties between units of chemokine receptor homoand hetero-oligomers. *Mol Pharmacol.* 69:1652–61.
- Sriram K, Insel PA (2018) G Protein-coupled receptors as targets for approved drugs: how many targets and how many drugs? *Mol Pharmacol.* 93:251-8. doi: 10.1124/mol.117.111062.
- Stanasila L, Perez JB, Vogel H, Cotecchia S (2003) Oligomerization of the alpha 1a and alpha 1b-adrenergic receptor subtypes. Potential implications in receptor internalization. *J Biol Chem.* 278:40239-51.
- Starke K (2001) Presynaptic autoreceptors in the third decade: focus on alpha2-adrenoceptors. *J Neurochem.* 78:685-93.
- Steel E, Murray VL, Liu AP (2014) Multiplex detection by homo- and heterodimerization of G protein-coupled receptors by proximity biotinylation. *PLoS One.* 9:e93646. doi:10.1371/journal.pone.0093646.
- Stocchi F, Rascol O, Kiebertz K, Poewe W, Jankovic J, Tolosa E, Barone P, Lang AE, Olanow CW (2010) Initiating levodopa/carbidopa therapy with and without entacapone in early Parkinson disease: the STRIDE-PD study. *Ann Neurology.* 68:18–27. doi: 10.1002/ana.22060.
- Stockwell J, Jakova E, Cayabyab FS (2017) Adenosine A1 and A2A Receptors in the Brain: Current Research and Their Role in Neurodegeneration. *Molecules.* 22. pii: E676. doi: 10.3390/molecules22040676.
- Stoof JC, Kebabian JW (1981) Opposing roles for D-1 and D-2 dopamine receptors in efflux of cyclic AMP from rat neostriatum. *Nature.* 294:366-8.
- Strange PG (2005) Oligomers of D2 dopamine receptors: evidence from ligand binding. *J Mol Neurosci.* 26:155-60.
- Stratton CF, Poulin MB, Du Q, Schramm VL (2017) Kinetic Isotope Effects and Transition State Structure for Human Phenylethanolamine N-Methyltransferase. *ACS Chem Biol.* 12:342-6. doi: 10.1021/acscchembio.6b00922.
- Strömberg I, Popoli P, Müller CE, Ferré S, Fuxe K (2000) Electrophysiological and behavioural evidence for an antagonistic modulatory role of adenosine A2A receptors in dopamine D2 receptor regulation in the rat dopamine-denervated striatum. *Eur J Neurosci.* 12:4033-7.
- Summers RJ, Papaioannou M, Harris S, Evans BA (1995) Expression of beta 3-adrenoceptor mRNA in rat brain. *Br J Pharmacol.* 116:2547-8.
- Sun WC, Cao Y, Jin L, Wang LZ, Meng F, Zhu XZ (2005) Modulating effect of adenosine deaminase on function of adenosine A1 receptors. *Acta Pharmacol Sin.* 26:160-5.
- Surmeier DJ, Plotkin J, Shen W (2009) Dopamine and synaptic plasticity in dorsal striatal circuits controlling action selection. *Curr Opin Neurobiol.* 19:621-8. doi: 10.1016/j.conb.2009.10.003.

- Svingos AL, Periasamy S, Pickel VM (2000) Presynaptic dopamine D(4) receptor localization in the rat nucleus accumbens shell. *Synapse*. 36:222-32.
- Swanson LW, Hartman BK (1975) The central adrenergic system. An immunofluorescence study of the location of cell bodies and their efferent connections in the rat utilizing dopamine-beta-hydroxylase as a marker. *J Comp Neurol*. 163:467-505. doi:10.1002/cne.901630406.
- Swanson JM, Kinsbourne M, Nigg J, Lanphear B, Stefanatos GA, Volkow N, Taylor E, Casey BJ, Castellanos FX, Wadhwa PD (2007) Etiologic subtypes of attention-deficit/hyperactivity disorder: brain imaging, molecular genetic and environmental factors and the dopamine hypothesis. *Neuropsychol Rev*. 17:39-59.
- Syrovatkina V, Alegre KO, Dey R, Huang, XY (2016). Regulation, Signaling, and Physiological Functions of G-Proteins. *J Mol Biol*. 428:3850-68.
- Szalai B, Barkai L, Turu G, Szidonya L, Várnai P, Hunyady L (2012) Allosteric interactions within the AT₁ angiotensin receptor homodimer: role of the conserved DRY motif. *Biochem Pharmacol*. 84:477-85. doi: 10.1016/j.bcp.2012.04.014.
- Tanila H, Rämä P, Carlson S (1996) The effects of prefrontal intracortical microinjections of an alpha-2 agonist, alpha-2 antagonist and lidocaine on the delayed alternation performance of aged rats. *Brain Res Bull*. 40:117-9.
- Tarazi FI, Yeghiayan SK, Baldessarini RJ, Kula NS, Neumeyer JL (1997) Long-term effects of S(+)-N-n-propylnorapomorphine compared with typical and atypical antipsychotics: differential increases of cerebrocortical D2-like and striatolimbic D4-like dopamine receptors. *Neuropsychopharmacology*. 17:186-96.
- Tarazi FI, Campbell A, Yeghiayan SK, Baldessarini RJ (1998) Localization of dopamine receptor subtypes in corpus striatum and nucleus accumbens septi of rat brain: comparison of D1-, D2-, and D4-like receptors. *Neuroscience*. 83:169–76.
- Taura J, Fernández-Dueñas V, Ciruela F (2015) Visualizing G Protein-Coupled Receptor-Receptor Interactions in Brain Using Proximity Ligation In Situ Assay. *Curr Protoc Cell Biol*. 67:17.17.1-16. doi: 10.1002/0471143030.cb1717s67.
- Taura J, Valle-León M, Sahlholm K, Watanabe M, Van Craenenbroeck K, Fernández-Dueñas V, Ferré S, Ciruela F (2018) Behavioral control by striatal adenosine A2A -dopamine D2 receptor heteromers. *Genes Brain Behav*. 17:e12432. doi: 10.1111/gbb.12432.
- Teitler M, Toohey N, Knight JA, Klein MT, Smith C (2010) Clozapine and other competitive antagonists reactivate risperidone-inactivated h5-HT7 receptors: radioligand binding and functional evidence for GPCR homodimer protomer interactions. *Psychopharmacology (Berl)*. 212:687-97. doi: 10.1007/s00213-010-2001-x.
- Tepper JM, Tecuapetla F, Koós T, Ibáñez-Sandoval O (2010) Heterogeneity and diversity of striatal GABAergic interneurons. *Front Neuroanat*. 4:150. doi: 10.3389/fnana.2010.00150. eCollection 2010.
- Terrillon S, Bouvier M (2004) Roles of G-protein-coupled receptor dimerization. *EMBO Rep*. 5:30–4.

- Terrillon S, Durroux T, Mouillac B, Breit A, Ayoub MA, Taulan M, Jockers R, Barberis C, Bouvier M (2003) Oxytocin and vasopressin V1a and V2 receptors form constitutive homo- and heterodimers during biosynthesis. *Mol Endocrinol.* 17:677–91.
- Thomas TC, Grandy DK, Gerhardt GA, Glaser PEA (2009) Decreased dopamine D4 receptor expression increases extracellular glutamate and alters its regulation in mouse striatum. *Neuropsychopharmacology.* 34:436–45.
- Thompson-Schill SL, Jonides J, Marshuetz C, Smith EE, D'Esposito M, Kan IP, Knight RT, Swick D (2002) Effects of frontal lobe damage on interference effects in working memory. *Cogn Affect Behav Neurosci.* 2:109-20.
- Thron CD (1973) On the analysis of pharmacological experiments in terms of an allosteric receptor model. *Mol Pharmacol.* 9:1–9.
- Trejo J, Hammes SR, Coughlin SR (1998). Termination of signaling by protease-activated receptor-1 is linked to lysosomal sorting. *Proc Natl Acad Sci USA.* 95:13698-702.
- Trendelenburg AU, Starke K, Limberger N (1994) Presynaptic alpha 2A-adrenoceptors inhibit the release of endogenous dopamine in rabbit caudate nucleus slices. *Naunyn Schmiedeberg's Arch Pharmacol.* 350:473-81.
- Trendelenburg AU, Cox SL, Schelb V, Klebroff W, Khairallah L, Starke K (2000) Modulation of (3)H-noradrenaline release by presynaptic opioid, cannabinoid and bradykinin receptors and beta-adrenoceptors in mouse tissues. *Br J Pharmacol.* 130:321-30.
- Trendelenburg AU, Philipp M, Meyer A, Klebroff W, Hein L, Starke K (2003) All three alpha2-adrenoceptor types serve as autoreceptors in postganglionic sympathetic neurons. *Naunyn Schmiedeberg's Arch Pharmacol.* 368:504-12.
- Trincavelli ML, Daniele S, Orlandini E, Navarro G, Casadó V, Giacomelli C, Nencetti S, Nuti E, Macchia M, Huebner H, Gmeiner P, Rossello A, Lluís C, Martini C (2012) A new D₂ dopamine receptor agonist allosterically modulates A(2A) adenosine receptor signalling by interacting with the A(2A)/D₂ receptor heteromer. *Cell Signal.* 24:951-60. doi: 10.1016/j.cellsig.2011.12.018.
- Trincavelli ML, Giacomelli C, Daniele S, Taliani S, Cosimelli B, Laneri S, Severi E, Barresi E, Pugliese I, Greco G, Novellino E, Da Settimo F, Martini C (2014) Allosteric modulators of human A2B adenosine receptor. *Biochim Biophys Acta.* 1840:1194-203. doi: 10.1016/j.bbagen.2013.12.021.
- Tuček S, Proška J (1995) Allosteric modulation of muscarinic acetylcholine receptors. *Trends Pharmacol Sci.* 16:205–11.
- Uberti MA, Hall RA, Minneman KP (2003) Subtype-specific dimerization of alpha 1-adrenoceptors: effects on receptor expression and pharmacological properties. *Mol Pharmacol.* 64:1379-90.
- Uchida S, Soshiroda K, Okita E, Kawai-Uchida M, Mori A, Jenner P, Kanda T (2015) The adenosine A2A receptor antagonist, istradefylline enhances the anti-parkinsonian activity of low doses of dopamine agonists in MPTP-treated common marmosets. *Eur J Pharmacol.* 747:160–5.
- Uhlen S, Lindblom J, Tiger G, Wikberg JE (1997) Quantification of alpha2A and alpha2C adrenoceptors in the rat striatum and in different regions of the spinal cord. *Acta Physiol Scand.* 160:407-12.

- Ulloa-Aguirre A, Zariñan T, Dias JA, Conn PM (2014) Mutations in G protein-coupled receptors that impact receptor trafficking and reproductive function. *Mol Cell Endocrinol.* 382:411-23.
- Ulrich CD, Holtmann M, Miller LJ (1998). Secretin and vasoactive intestinal peptide receptors: members of a unique family of G protein-coupled receptors. *Gastroenterology* 114:382-97.
- Urizar E, Montanelli L, Loy T, Bonomi M, Swillens S, Gales C, Bouvier M, Smits G, Vassart G, Costagliola S (2005) Glycoprotein hormone receptors: link between receptor homodimerization and negative cooperativity. *EMBO J.* 24:1954–64.
- Urizar E, Yano H, Kolster R, Galés C, Lambert N, Javitch JA (2011) CODA-RET reveals functional selectivity as a result of GPCR heteromerization. *Nat Chem Biol.* 7:624-30. doi: 10.1038/nchembio.623.
- Usiello A, Baik JH, Rougé-Pont F, Picetti R, Dierich A, LeMeur M, Piazza PV, Borrelli E. (2000) Distinct functions of the two isoforms of dopamine D2 receptors. *Nature.* 408:199–203.
- Valentino RJ, Van Bockstaele E (2008) Convergent regulation of locus coeruleus activity as an adaptive response to stress. *Eur J Pharmacol.* 583:194-203. doi: 10.1016/j.ejphar.2007.11.062.
- Vallon V, Osswald H (2009) Adenosine receptors and the kidney. *Handb Exp Pharmacol.* 193:443-70. doi: 10.1007/978-3-540-89615-9_15.
- Vallone D, Picetti R, Borrelli E (2000) Structure and function of dopamine receptors. *Neurosci Biobehav Rev.* 24:125-32.
- Van Craenenbroeck K, Borroto-Escuela DO, Romero-Fernandez W, Skieterska K, Rondou P, Lintermans B, Vanhoenacker P, Fuxe K, Ciruela F, Haegeman G (2011) Dopamine D4 receptor oligomerization-contribution to receptor biogenesis. *FEBS J.* 278:1333-44. doi: 10.1111/j.1742-4658.2011.08052.x.
- Van der Westhuizen ET, Valant C, Sexton PM, Christopoulos A (2015) Endogenous allosteric modulators of G protein-coupled receptors. *J Pharmacol Exp Ther.* 353:246-60.
- Vassilatis DK, Hohmann JG, Zeng H, Li F, Ranchalis JE, Mortrud MT, Brown A, Rodriguez SS, Weller JR, Wright AC, Bergmann JE, Gaitanaris GA (2003) The G protein-coupled receptor repertoires of human and mouse. *Proc Natl Acad Sci USA.* 100:4903-8.
- Vecchio EA, Chuo CH, Baltos JA, Ford L, Scammells PJ, Wang BH, Christopoulos A, White PJ, May LT (2016) The hybrid molecule, VCP746, is a potent adenosine A2B receptor agonist that stimulates anti-fibrotic signalling. *Biochem Pharmacol.* 117:46-56. doi: 10.1016/j.bcp.2016.08.007.
- Vendrell M, Angulo E, Casadó V, Lluís C, Franco R, Albericio F, Royo M (2007) Novel ergopeptides as dual ligands for adenosine and dopamine receptors. *J Med Chem.* 50:3062-9.
- Venkatakrishnan AJ, Deupi, X, Lebon G, Tate CG, Schertler GF, and Babu MM (2013). Molecular signatures of G-protein-coupled receptors. *Nature.* 494:185-94. doi: 10.1038/nature11896.
- Vidi PA, Watts VJ (2009) Fluorescent and bioluminescent protein-fragment complementation assays in the study of G protein-coupled receptor oligomerization and signaling. *Mol Pharmacol.* 75:733-9. doi: 10.1124/mol.108.053819.

- Vidi PA, Ejendal KF, Przybyla JA, Watts VJ (2011) Fluorescent protein complementation assays: new tools to study G protein-coupled receptor oligomerization and GPCR-mediated signaling. *Mol Cell Endocrinol.* 331:185-93. doi: 10.1016/j.mce.2010.07.011
- Vijayraghavan S, Wang M, Birnbaum SG, Williams GV, Arnsten AF (2007) Inverted-U dopamine D1 receptor actions on prefrontal neurons engaged in working memory. *Nat Neurosci.* 10:376-84. Epub 2007 Feb 4.
- Villardaga JP, Bünemann M, Krasel C, Castro M, Lohse MJ (2003) Measurement of the millisecond activation switch of G protein-coupled receptors in living cells. *Nat Biotechnol.* 21:807-12
- Villar VA, Jones JE, Armando I, Palmes-Saloma C, Yu P, Pascua AM, Kever L, Arnaldo FB, Wang Z, Luo Y, Felder RA, Jose PA (2009) G protein-coupled receptor kinase 4 (GRK4) regulates the phosphorylation and function of the dopamine D3 receptor. *J Biol Chem.* 284:21425-34.
- Vincent SL, Khan Y, Benes FM (1993) Cellular distribution of dopamine D1 and D2 receptors in rat medial prefrontal cortex. *J Neurosci.* 13:2551-64.
- Viñals, X, Moreno, E, Lanfumey, L, Cordomi, A, Pastor, A, de La Torre, R, Gasperini, P, Navarro, G, Howell, LA, Pardo, Lluís C, Canela EI, McCormick PJ, Maldonado R, Robledo PL (2015) Cognitive impairment induced by delta9-tetrahydrocannabinol occurs through heteromers between cannabinoid CB1 and serotonin 5-HT2A receptors. *PLoS Biol.* 13:e1002194. doi:10.1371/journal.pbio.1002194.
- Volkow ND, Wang GJ, Newcorn J, Telang F, Solanto MV, Fowler JS, Logan J, Ma Y, Schulz K, Pradhan K, Wong C, Swanson JM (2007) Depressed dopamine activity in caudate and preliminary evidence of limbic involvement in adults with attention-deficit/hyperactivity disorder. *Arch Gen Psychiatry.* 64:932-40.
- Von Zastrow M, Link R, Daunt D, Barsh G, Kobilka B (1993) Subtype-specific differences in the intracellular sorting of G protein-coupled receptors. *J Biol Chem.* 268:763-6.
- Waeber C, Rigo M, Chinaglia G, Probst A, Palacios JM (1991) Beta-adrenergic receptor subtypes in the basal ganglia of patients with Huntington's chorea and Parkinson's disease. *Synapse.* 8:270-80.
- Waldhoer M, Fong J, Jones RM, Lunzer MM, Sharma SK, Kostenis E, Portoghese PS, Whistler JL (2005) A heterodimer-selective agonist shows in vivo relevance of G protein-coupled receptor dimers. *Proc Natl Acad Sci U S A.* 102:9050-5.
- Wall MA, Coleman DE, Lee E, Iniguez-Lluhi JA, Posner BA, Gilman AG, Sprang SR (1995) The structure of the G protein heterotrimer Gi alpha 1 beta 1 gamma 2. *Cell.* 83:1047-58.
- Wang CI, Lewis RJ (2013) Emerging opportunities for allosteric modulation of G-protein coupled receptors. *Biochem Pharmacol.* 85:153-62.
- Wang S, Eisenback M, Datskovskaia A, Boyce M, Bickford ME (2002) GABAergic pretectal terminals contact GABAergic interneurons in the cat dorsal lateral geniculate nucleus. *Neurosci Lett.* 323:141-5.
- Wang E, Ding YC, Flodman P, Kidd JR, Kidd KK, Grady DL, Ryder OA, Spence MA, Swanson JM, Moyzis RK (2004) The genetic architecture of selection at the human dopamine receptor D4 (DRD4) gene locus. *Am J Hum Genet.* 74:931-44.

- Wang Y, Ding B, Cheng P, Liao DZ, Yan SP (2007) Tuned triazolatesilver(I) luminescent complexes from zero to three-dimensionality based on bidentate tetrapodal bridged ligands. *Inorg Chem.* 46:2002-10.
- Wang Z, Xuan F, Lin WH, Troyer MD, Tendolkar A, Cutler DL (2013) Preladenant, a selective adenosine A_{2A} receptor antagonist, is not associated with QT/QTc prolongation. *Eur J Clin Pharmacol.* 69:1761-7. doi: 10.1007/s00228-013-1541-5.
- Wang S, Che T, Levit A, Shoichet BK, Wacker D, Roth BL (2018) Structure of the D2 dopamine receptor bound to the atypical antipsychotic drug risperidone. *Nature.* 555:269-73. doi: 10.1038/nature25758.
- Ward SD, Hamdan FF, Bloodworth LM, Siddiqui NA, Li JH, Wess J (2006) Use of an in situ disulfide crosslinking strategy to study the dynamic properties of the cytoplasmic end of transmembrane domain VI of the M3 muscarinic acetylcholine receptor. *Biochemistry.* 45:676–85.
- Wedemeyer C, Goutman JD, Avale ME, Franchini LF, Rubinstein M, Calvo DJ (2007) Functional activation by central monoamines of human dopamine D(4) receptor polymorphic variants coupled to GIRK channels in *Xenopus* oocytes. *Eur J Pharmacol.* 562:165-73.
- Wedzony K, Chocyk A, Maćkowiak M, Fijał K, Czyrak A (2000) Cortical localization of dopamine D4 receptors in the rat brain-immunocytochemical study. *J Physiol Pharmacol.* 51:205-21.
- Wei CJ, Li W, Chen JF (2011) Normal and abnormal functions of adenosine receptors in the central nervous system revealed by genetic knockout studies. *Biochim Biophys Acta.* 1808:1358-79.
- Wei W, Du C, Lv J, Zhao G, Li Z, Wu Z, Hasko G, Xie X (2013). Blocking A_{2B} adenosine receptor alleviates pathogenesis of experimental autoimmune encephalomyelitis via inhibition of IL-6 production and Th17 differentiation. *J Immunol.* 190:138-46.
- Weiner DM, Levey AI, Sunahara RK, Niznik HB, O'Dowd BF, Seeman P, Brann MR (1991) D1 and D2 dopamine receptor mRNA in rat brain. *Proc Natl Acad Sci USA.* 88:1859-63.
- Weiss JM, Morgan PH, Lutz MW, Kenakin TP (1996a) The cubic ternary complex Receptoroccupancy model I. Model description. *J Theor Biol.* 178:151–67.
- Weiss JM, Morgan PH, Lutz MW, Kenakin TP (1996b) The cubic ternary complex Receptoroccupancy model II. Understanding apparent affinity. *J Theor Biol.* 178:169–82.
- Weiss JM, Morgan PH, Lutz MW, Kenakin TP (1996c). The cubic ternary complex receptor-occupancy model III. Resurrecting efficacy. *J Theor Biol.* 181:381–97.
- Weiss SM, Benwell K, Cliffe IA, Gillespie RJ, Knight AR, Lerpiniere J, Misra A, Pratt RM, Revell D, Upton R, Dourish CT (2003) Discovery of nonxanthine adenosine A_{2A} receptor antagonists for the treatment of Parkinson's disease. *Neurology.* 61:S101-6.
- Wells GJ (2014) Allosteric modulators of G protein-coupled receptors. *Curr Top Med Chem.* 14:1735-7.
- White FJ, Bednars LM, Wachtel SR, Hjorth S, Brooderson RJ (1988) Is stimulation of both D1 and D2 receptors necessary for the expression of dopamine-mediated behaviors? *Pharmacol Biochem Behav.* 30:189–93.

- White JF, Grodnitzky J, Louis JM, Trinh LB, Shiloach J, Gutierrez J, Northup JK, Grisshammer R (2007) Dimerization of the class A G protein-coupled neurotensin receptor NTS1 alters G protein interaction. *Proc Natl Acad Sci USA*. 104:12199-204.
- Whorton MR, Bokoch MP, Rasmussen SG, Huang B, Zare RN, Kobilka B, Sunahara RK (2007) A monomeric G protein-coupled receptor isolated in a high-density lipoprotein particle efficiently activates its G protein. *Proc Natl Acad Sci USA*. 104:7682-7.
- Whorton MR, Jastrzebska B, Park PS, Fotiadis D, Engel A, Palczewski K, Sunahara RK (2008) Efficient coupling of transducin to monomeric rhodopsin in a phospholipid bilayer. *J Biol Chem*. 283:4387-94.
- Wilkins AJ, Shallice T, McCarthy R (1987) Frontal lesions and sustained attention. *Neuropsychologia*. 25:359-65.
- Wills AM, Eberly S, Tennis M, Lang AE, Messing S, Togasaki D, Tanner CM, Kamp C, Chen JF, Oakes D, McDermott MP, Schwarzschild MA; Parkinson Study Group (2013) Caffeine consumption and risk of dyskinesia in CALM-PD. *Mov Disord*. 28:380-3. doi: 10.1002/mds.25319.
- Wimalasena K (2011) Vesicular monoamine transporters: structure-function, pharmacology, and medicinal chemistry. *Med Res Rev*. 31:483-519. doi: 10.1002/med.20187.
- Winder DG, Martin KC, Muzzio IA, Rohrer D, Chruscinski A, Kobilka B, Kandel ER (1999) ERK plays a regulatory role in induction of LTP by theta frequency stimulation and its modulation by beta-adrenergic receptors. *Neuron*. 24:715-26.
- Wise RA (2004) Dopamine, learning and motivation. *Nat Rev Neurosci*. 5:483-94.
- Wise RA (2009) Roles for nigrostriatal-not just mesocorticolimbic-dopamine in reward and addiction. *Trends Neurosci*. 32:517-24.
- Witkovsky P (2004) Dopamine and retinal function. *Doc Ophthalmol*. 108:17-40.
- Woehler A, Ponimaskin EG (2009) G protein-mediated signaling: same receptor, multiple effectors. *Curr Mol Pharmacol*. 2:237-48.
- Wolf ME, Roth RH (1990) Autoreceptor regulation of dopamine synthesis. *Ann NY Acad Sci*. 604:323-43.
- Woods AS (2010) The dopamine D(4) receptor, the ultimate disordered protein. *J Recept Signal Transduct Res*. 30:331-6. doi: 10.3109/10799893.2010.513842.
- Woods DL, Knight RT (1986) Electrophysiologic evidence of increased distractibility after dorsolateral prefrontal lesions. *Neurology*. 36:212-6.
- Wooten D, Christopoulos A, Sexton PM (2013) Emerging paradigms in GPCR allostery: implications for drug discovery. *Nat Rev Drug Discov*. 12:630-44.
- Wreggett KA, Wells JW (1995) Cooperativity manifest in the binding properties of purified cardiac muscarinic receptors. *J Biol Chem*. 270:22488-99.
- Wu J, Hablitz JJ (2005) Cooperative activation of D1 and D2 dopamine receptors enhances a hyperpolarization-activated inward current in layer I interneurons. *J Neurosci*. 25:6322-8.

- Wu M, Shanabrough M, Leranath C, Alreja M (2000) Cholinergic excitation of septohippocampal GABA but not cholinergic neurons: implications for learning and memory. *J Neurosci.* 20:3900-8.
- Wu B, Chien EY, Mol CD, Fenalti G, Liu W, Katritch V, Abagyan R, Brooun A, Wells P, Bi FC, Hamel DJ, Kuhn P, Handel TM, Cherezov V, Stevens RC (2010) Structures of the CXCR4 chemokine GPCR with small-molecule and cyclic peptide antagonists. *Science.* 330:1066–71.
- Wu H, Wacker D, Katritch V, Mileni M, Han G.W, Vardy E, Liu W, Thompson AA, Huang XP, Carroll FI, Mascarella SW, Westkaemper RB, Mosier PD, Roth BL, Cherezov V, Stevens RC (2012) Structure of the human κ -opioid receptor in complex with JDTic. *Nature.* 485:327–32.
- Wu H, Wang CH, Gregory KJ, Han GW, Cho HP, Xia Y, Niswender CM, Katritch V, Meiler J, Cherezov V, Conn PJ, Stevens RC (2014) Structure of a class C GPCR metabotropic glutamate receptor 1 bound to an allosteric modulator. *Science.* 344:58-64.
- Xie K, Masuho I, Shih CC, Cao Y, Sasaki K, Lai CW, Han PL, Ueda H, Dessauer CW, Ehrlich ME, Xu B, Willardson BM, Martemyanov KA (2015) Stable G protein-effector complexes in striatal neurons: mechanism of assembly and role in neurotransmitter signaling. *Elife.* 4:e10451.
- Xu J, He J, Castleberry AM, Balasubramanian S, Lau AG, Hall RA (2003) Heterodimerization of alpha 2A and beta 1-adrenergic receptors. *J Biol Chem.* 278:10770-7.
- Xu K, Bastia E, Schwarzschild M (2005) Therapeutic potential of adenosine A2A receptor antagonists in Parkinson's disease. *Pharmacol Ther.* 105:267–310.
- Yamada K, Kobayashi M, Shiozaki S, Ohta T, Mori A, Jenner P, Kanda T (2014) Antidepressant activity of the adenosine A2A receptor antagonist, istradefylline (KW-6002) on learned helplessness in rats. *Psychopharmacology.* 231:2839-49.
- Yamaguchi S, Knight RT (1990) Gating of somatosensory input by human prefrontal cortex. *Brain Res.* 521:281-8.
- Yan H, Zhang E, Feng C, Zhao X (2016) Role of A3 adenosine receptor in diabetic neuropathy. *J Neurosci Res.* 94:936-46.
- Yesilaltay A, Jenness DD (2000) Homo-oligomeric complexes of the yeast alpha-factor pheromone receptor are functional units of endocytosis. *Mol Biol Cell.* 11:2873–84.
- Yoon YR, Baik JH (2015) Melanocortin 4 receptor and dopamine D2 receptor expression in brain areas involved in food intake. *Endocrinol Metab (Seoul).* 30:576-83. doi: 10.3803/EnM.2015.30.4.576.
- Young CE, Yang CR (2005) Dopamine D1-like receptor modulates layer and frequency-specific short-term synaptic plasticity in rat prefrontal cortical neurons. *Eur J Neurosci.* 21:3310-20.
- Yu AJ, Dayan P (2005) Uncertainty, neuromodulation, and attention. *Neuron.* 46:681-92.
- Yung KK, Bolam JP, Smith AD, Hersch SM, Ciliax BJ, Levey AI (1995) Immunocytochemical localization of D1 and D2 dopamine receptors in the basal ganglia of the rat: light and electron microscopy. *Neuroscience.* 65:709-30

- Zang JB, Nosyreva ED, Spencer CM, Volk LJ, Musunuru K, Zhong R, Stone EF, Yuva-Paylor LA, Huber KM, Paylor R, Darnell JC, Darnell RB (2009) A mouse model of the human Fragile X syndrome I304N mutation. *PLoS Genet.* 5:e1000758. doi: 10.1371/journal.pgen.1000758.
- Zhang W, Klimek V, Farley JT, Zhu MY, Ordway GA (1999) α 2C adrenoceptors inhibit adenylyl cyclase in mouse striatum: potential activation by dopamine. *J Pharmacol Exp Ther.* 289:1286-92.
- Zhang Z, Cordeiro Matos S, Jago S, Adamantidis A, Séguéla P (2013) Norepinephrine drives persistent activity in prefrontal cortex via synergistic α 1 and α 2 adrenoceptors. *PLoS One.* 8:e66122. doi: 10.1371/journal.pone.0066122.
- Zhang D, Zhao Q, Wu B (2015) Structural studies of G protein-coupled receptors. *Mol Cells.* 38:836-42. doi: 10.14348/molcells.2015.0263.
- Zhong P, Liu W, Yan Z (2016) Aberrant regulation of synchronous network activity by the attention-deficit/hyperactivity disorder-associated human dopamine D4 receptor variant D4.7 in the prefrontal cortex. *J Physiol.* 594:135–47.
- Zhou F, Filipeanu CM, Duvernay MT, Wu G (2006) Cell-surface targeting of α 2-adrenergic receptors inhibition by a transport deficient mutant through dimerization. *Cell Signal.* 18:318-27.

VII- ANNEXES

VII. ANNEXES

- Franco R, Casadó-Anguera V, Muñoz A, Petrovic M, Navarro G, Moreno E, Lanciego JL, Labandeira-García JL, Cortés A, Casadó V. (2015) Hints on the Lateralization of Dopamine Binding to D1 Receptors in Rat Striatum. *Molecular Neurobiology*; 53:5436-45.

- Book chapter: Cortés A, Casadó-Anguera V, Moreno E, Casadó V (2016) Caffeine, adenosine A1 receptors and the brain cortex. *Molecular aspects. Neuropathology of addiction. vol. 3.* Victor Preedy (ed.). Elsevier, UK. 741-752.

- Ferré S, Quiroz C, Guitart X, Rea W, Seyedian A, Moreno E, Casadó-Anguera V, Díaz-Ríos M, Casadó V, Clemens S, Allen RP, Earley CJ, García-Borreguero D. (2018) Pivotal Role of Adenosine Neurotransmission in Restless Legs Syndrome. *Frontiers in Neuroscience* doi: 10.3389/fnins.2017.00722

- Ferré S, Bonaventura J, Zhu W, Hatcher-Solis C, Taura J, Quiroz C, Moreno E, Casadó-Anguera V, Kravitz AV, Thompson K, Tomasi D, Volkow ND, Casadó V, Ciruela F, Logothetis DE, Zwillling D. (2018) Essential control of the function of the dorsal and the ventral striatopallidal neuron by adenosine A2A-dopamine D2 receptor heteromers. *Frontiers in Pharmacology* 9:243. doi: 10.3389/fphar.2018.00243

Hints on the Lateralization of Dopamine Binding to D₁ Receptors in Rat Striatum

Rafael Franco^{1,2} · Verónica Casadó-Anguera^{1,2} · Ana Muñoz^{1,3} · Milos Petrovic^{4,5} · Gemma Navarro^{1,2} · Estefanía Moreno^{1,2} · José Luis Lanciego^{1,6} · José Luis Labandeira-García^{1,3} · Antoni Cortés^{1,2} · Vicent Casadó^{1,2}

Received: 3 July 2015 / Accepted: 29 September 2015 / Published online: 9 October 2015
© Springer Science+Business Media New York 2015

Abstract Dopamine receptors in striatum are important for healthy brain functioning and are the target of levodopa-based therapy in Parkinson's disease. Lateralization of dopaminergic neurotransmission in striata from different hemispheres occurs in patients, but also in healthy individuals. Our data show that the affinity of dopamine binding to dopamine D₁ receptors is significantly higher in left than in right striatum. Analysis of data from radioligand binding to striatal samples from naïve, 6-hydroxydopamine lesioned, levodopa-treated and levodopa-induced dyskinetic rats shows differential receptor structure and gives hints on the causes of right/left lateralization of dopamine binding to striatal D₁ receptors.

Moreover, binding data showed loss of lateralization in levodopa (L-DOPA)-induced dyskinetic rats.

Keywords Lateralization · Basal ganglia · G-protein-coupled receptor dimer · Dyskinesia · 6-hydroxydopamine · Cooperativity index

Introduction

Motoric lateralization is due to musculoskeletal and brain asymmetries and does occur in both vertebrates and invertebrates (see [1] for review). In mammalian brain, asymmetries have been mainly studied from an anatomic point of view. Thus, early but accurate studies in human entorhinal area showed right-left asymmetry in the number of neurons [2]. Assessment of lateralization at the molecular level was approached by radioligand-binding studies mainly assuming similar receptor species in both hemispheres and reporting differences in receptor expression. For instance, dopamine D₁ receptor lateralization and correlation of dopamine D₁/D₂ receptor expression ratio with apomorphine-induced rotation were assessed by differences in B_{max}, i.e., in differences in the amount of receptors ([3] and references therein). Despite enormous conceptual interests, the lack of suitable tools is delaying the increase in knowledge of the molecular causes of brain asymmetry. Recent discoveries indicate that dopamine receptors, as members of the G-protein-coupled receptor (GPCR) superfamily, interact with a variety of proteins [4] and that the quaternary structure affects GPCR binding characteristics and signaling [5]. Differences in the affinity of neurotransmitters/neuromodulators binding to specific receptors have served to detect molecular differences in pre-synaptic versus post-synaptic GPCRs [6]. These findings open a way to hypothesize that lateralization in mammalian brain

✉ Rafael Franco
rfranco123@gmail.com

- ¹ Centro de Investigación Biomédica en Red sobre Enfermedades Neurodegenerativas (CIBERNED), Instituto de Salud Carlos III, Valderrebollo 5, 28031 Madrid, Spain
- ² Molecular Neurobiology Laboratory, Department of Biochemistry and Molecular Biology, Faculty of Biology, University of Barcelona, 08028 Barcelona, Spain
- ³ Laboratory of Neuroanatomy and Experimental Neurology, Center for Research in Molecular Medicine and Chronic Diseases (CIMUS), University of Santiago de Compostela, 15782 Santiago de Compostela, Spain
- ⁴ School of Pharmacy and Biomedical Sciences, University of Central Lancashire, PR1 2HE, Preston, UK
- ⁵ Institute of Physiology, Academy of Sciences, Videnska 1083, 14220 Prague, Czech Republic
- ⁶ Laboratory of Neuroanatomy of Basal Ganglia, Neurosciences Division, Center for Applied Medical Research (CIMA), University of Navarra, 31008 Pamplona, Spain

may be addressed by careful study of the affinity of agonist binding to receptors in the two hemispheres.

Dopaminergic neurotransmission in the striatum has a key role in motor control. Thus, the lack of nigrostriatal dopaminergic innervation in Parkinson's disease results in motor alterations. Previously published data have clearly established that left and right striata are not the same: apparent asymmetry between neurochemical properties of striata from opposing hemispheres exists [7] and, unsurprisingly, the same applies to dopaminergic neurotransmission [8]. This lateralization in the striatum at the circuit and the cellular levels has both behavioral consequences [9] and therapeutic implications in Parkinson's disease (PD) therapy [10]. For example, lateralization in $D_{2/3}$ receptor binding was (i) found in response to unpredictable reward and could be accounted for by sex differences [11]; (ii) associated with motor activity [12]; (iii) correlated to the body mass index (BMI) of non-obese males [13]; (iv) found to predict individual differences in learning from reward versus punishment, thus underlying human personality and cognition [14]; and (v) found to correlate with incentive motivation, with greater positive incentive motivation being associated with higher receptor availability in the left hemisphere [15]. However, the molecular dissection of such asymmetry is still lacking [16]. Recently, we have reported left versus right asymmetries of dopamine binding to rat striatal dopamine D_1 receptors (D_1 Rs), indicating that the dopamine-mediated signaling has a stronger tone in the left hemisphere [17]. This lateralization, consistently found in samples from healthy rats, is not due to right-left limb preferences and, therefore, it may likely be a property crucial for proper motor control in mammals. The aim of this paper was to look for hints to understand the molecular basis of lateralization of dopamine binding in right and left striata.

Methods

Eight-week-old male Wistar rats were used in the experiments. All experiments were carried out in accordance with the "Principles of laboratory animal care" and approved by the corresponding committee at the University of Santiago de Compostela, Spain. After anesthesia with ketamine/xylazine (1 % ketamine, 75 mg/kg; 2 % xylazine, 10 mg/kg), and placement in a David Kopf stereotaxic apparatus, animals received a unilateral injection in the right medial forebrain bundle of 12 μ g of 6-hydroxydopamine (6-OHDA) HBr Sigma, prepared in 4 μ L of sterile saline containing 0.2 % ascorbic acid. The stereotaxic coordinates were 3.7 mm posterior to bregma, -1.6 mm lateral to midline, and 8.8 mm ventral to the skull at the midline, in the flat

skull position. The solution was injected with a 5- μ L Hamilton syringe coupled with a motorized injector (Stoelting, Wood Dale, IL, USA) at 1 μ L/min, and the cannula was left in situ for 2 min after injection. Three weeks later, the efficacy of the lesion was evaluated by the amphetamine rotation and the cylinder test. The correct nigrostriatal lesion was confirmed by the loss of tyrosine hydroxylase (TH) immunohistochemistry staining.

Animals were divided into four groups as follows: (1) non-lesioned rats (naïve); (2) animals lesioned by 6-OHDA but receiving only vehicle afterward (lesioned); (3) animals lesioned by 6-OHDA receiving a chronic treatment with levodopa (L-DOPA), 6 mg/kg plus 10 mg/kg of benserazide daily for 3 weeks without exhibiting adverse motoric reactions (L-DOPA-treated non-dyskinetic); and (4) same as (3) but showing adverse motoric reactions (L-DOPA-treated dyskinetic). Benserazide is a peripheral decarboxylase inhibitor that increases brain availability of L-DOPA. The development of dyskinesia was tested using the rodent Abnormal Involuntary Movement Scale (AIMS) [18]. For binding studies, animals were sacrificed by decapitation (6 h after the last injection of vehicle or L-DOPA) and the brains were removed rapidly. Brain areas containing the striatum (both from the lesioned and intact hemispheres) were dissected out and immediately frozen on dry ice until use. A more detailed description of procedures may be found in Farré et al. [17], which also describes the radioligand-binding protocols. In brief, membrane suspensions were pre-incubated in 50-mM Tris-HCl buffer, pH 7.4, containing 10 mM $MgCl_2$ with 1 nM of radiolabelled D_1 R antagonist [3H]R-(+)-7-chloro-8-hydroxy-3-methyl-1-phenyl-2,3,4,5-tetra-hydro-1H-3-benzazepine ([3H]SCH 23390), and increasing concentrations of (\pm)-1-phenyl-2,3,4,5-tetrahydro-(1H)-3-benzazepine-7,8-diol hydrobromide (SKF 38393, D_1 R agonist, triplicates of 15 different competitor concentrations from 0.01 nM to 50 μ M), in the absence or the presence of 100 nM of the D_3 receptor agonist trans-7-hydroxy-2-[N-propyl-N-(3'-iodo-2'-propenyl)amino]tetralin (7-OH-PIPAT). Non-specific binding was determined in the presence of 50 μ M SCH 23390.

Radioligand competition curves were analyzed by non-linear regression using the commercial GraFit curve-fitting software (Erithacus Software, Surrey, UK). Two different models were used for data analysis, one assuming receptor monomers and another assuming receptor dimers. First of all, the equations of the classical two-independent-site model were used; the model assumes receptors in two affinity states: low affinity/not coupled to G proteins and high-affinity/G-protein-coupled. Second, equations of the two-state dimer receptor model were used [19, 20]. In the latter, a homodimer is considered the minimal structural unit of a receptor forming

homomers or forming heteromers with another receptor. To calculate the macroscopic equilibrium dissociation constants

[21], data from competition binding experiments were fitted using the following equation:

$$A_{\text{total bound}} = (K_{DA2}A + 2A^2 + K_{DA2}AB / K_{DAB}) R_T / \left(K_{DA1}K_{DA2} + K_{DA2}A + A^2 + K_{DA2}AB / K_{DAB} + K_{DA1}K_{DA2}B / K_{DB1} + K_{DA1}K_{DA2}B^2 / (K_{DB1}K_{DB2}) \right) + A_{\text{non-specific bound}} \quad (1)$$

where A represents free radioligand (the D₁ partial agonist [³H]SCH 23390) concentration, R_T is the total amount of receptor dimers, and K_{DA1} and K_{DA2} are the macroscopic equilibrium dissociation constants describing the binding of the first and the second radioligand molecules (A) to the dimeric receptor; B represents the assayed competing compound (SKF 38393) concentration, and K_{DB1} and K_{DB2} are, respectively, the macroscopic equilibrium dissociation constants for the binding of the first competitor molecule (B) to an unoccupied

dimer and for the binding of the second competitor molecule (B) to the semi-occupied dimer; K_{DAB} is the hybrid equilibrium radioligand/competitor dissociation constant, which is the dissociation constant of B binding to a receptor dimer semi-occupied by A.

As the radioligand A ([³H] SCH 23390) shows non-cooperative behavior, determining K_{DA1} is sufficient to characterize the binding of the radioligand, A, and Eq. (1) leads to Eq. (2) by establishing K_{DA2}=4K_{DA1} [19, 20]:

$$A_{\text{total bound}} = (4K_{DA1}A + 2A^2 + 4K_{DA1}AB / K_{DAB}) R_T / \left(4K_{DA1}^2 + 4K_{DA1}A + A^2 + 4K_{DA1}AB / K_{DAB} + 4K_{DA1}^2B / K_{DB1} + 4K_{DA1}^2B^2 / (K_{DB1}K_{DB2}) \right) + A_{\text{non-specific bound}} \quad (2)$$

The concentration of competitor B that leads to a 50 % of binding sites occupied by the competitor B molecule is the B₅₀ value. Assuming two independent sites, we have devised

Eq. (3) to obtain B₅₀ from calculated parameters, using the equation corresponding to the two-independent-site model (full deduction of Eq. (3) is available upon request).

$$B_{50} = \left[(B_{\text{maxH}} - B_{\text{maxL}})(K_{DH} - K_{DBL}) + (B_{\text{maxH}} - B_{\text{maxL}})^2(K_{DH} - K_{DBL})^2 + 4B_{\text{max}}^2K_{DH}K_{DBL} \right]^{1/2} / 2B_{\text{max}} \quad (3)$$

where B_{max} represents the maximum binding to high- plus low-affinity sites: B_{max}=B_{maxH}+B_{maxL}.

In the case of receptor dimers, the B₅₀ value is readily calculated [20] by the following formula:

$$B_{50} = (K_{DB1}K_{DB2})^{1/2} \quad (4)$$

Goodness of fit was tested according to reduced chi-squared values given by the GraFit program. The test of significance for two different model population variances was based upon the F distribution (see [19, 22] for details). Using this F test, a probability greater than 95 % (p<0.05) was considered the criterion to select a more complex model (i.e., Eq. (1) or two sites in the two-independent-site model) over the more simple one (i.e., Eq. (2) or one site in the two-independent-site model). Competition curves for each animal were performed in triplicates to obtain accurate parameter values (see [17]). Differences were analyzed for significance by two-way ANOVA followed by Bonferroni's post hoc multiple comparison tests.

Results

Binding to dopamine D₁Rs in right and left rat striatal membranes was performed using [³H]SCH 23390, a D₁R antagonist, and SKF38393, a D₁R agonist, as competitor, in the presence or absence of a dopamine D₃ receptor agonist (7-OH-PIPAT) (see [17]). The data from the competition curves were fitted using equations devised from two models: the two-independent-site model and the two-state dimer model.

Fitting Data Using the Two-Independent-Site Paradigm

The two-independent-site model assumes that high- and low-affinity binding is due to, respectively, GPCRs coupled and uncoupled to a given heterotrimeric G protein. Data from competition assays analyzed using this model provide equilibrium constants for high- (K_{DH}) and for low-affinity (K_{DL}) binding, as well as for the amount of high- and low-affinity sites (Table 1). According to the *two-independent-site* model,

Table 1 Parameter values for the agonist SKF 38393 obtained using [³H]SCH 23390 as radioligand and data fitting to equations devised from the two-independent-site model

Sample	Side	7-OH-PIPAT (100 nM)	B _{maxH}	K _{DH}	B _{maxL}	K _{DL}	B ₅₀
Naïve	Right	–	1.1±0.2	28±2	0.85±0.05	410±30	85±20
		+	1.0±0.4	16±3	1.1±0.2	280±50	75±30
	Left	–	0.3±0.1 ^{###}	2±1 ^{###}	1.4±0.4	140±20 ^{###}	90±40
		+	0.34±0.07	5±1 [#]	1.3±0.4	170±40	105±30
Lesioned	Right	–	0.39±0.08 ^{&}	7±3 ^{&&&}	1.16±0.08	220±40 ^{&&}	120±40
		+	0.38±0.05 ^{&}	5±1	1.12±0.05	220±10	115±15
	Left	–	0.41±0.05	2±1	1.52±0.05	190±20	115±10
		+	0.58±0.05 ^{&}	7±2	1.30±0.08	240±20	105±30
L-DOPA-treated (non-dyskinetic)	Right	–	0.47±0.07 ^{&}	7±2 ^{&&&}	1.26±0.07	170±20 ^{&&&}	90±20
		+	0.8±0.2	26±6*	1.0±0.2	200±50	80±35
	Left	–	0.24±0.05	0.7±0.3	1.73±0.02	120±10	90±10
		+	0.37±0.07	5±2 ^{###}	1.65±0.07	150±10	100±15
Dyskinetic	Right	–	1.2±0.1	24±4	0.9±0.1	420±60	75±20
		+	0.8±0.1	5±2*	1.6±0.1 ^{&*}	220±20*	85±20
	Left	–	0.66±0.05 ^{&&###}	4±1 ^{###}	1.3±0.1	190±20 ^{###}	70±20
		+	0.61±0.03 ^{&}	3±1	1.24±0.05	190±20	70±10

Data are mean±SEM values from three experiments (see [17]). B_{max} is the maximum specific binding, and K_D is the equilibrium dissociation constant of the competing ligand B (SKF 38393). B_{maxH} and B_{maxL} are the maximum specific binding corresponding to, respectively, high- and low-affinity sites, and K_{DH} and K_{DL} are the equilibrium dissociation constants for, respectively, high- and low-affinity sites. B₅₀ is the concentration providing half saturation of the receptor for B and is obtained according to Eq. (3)

**p*<0.01 comparing with and without treatment with the D₃ receptor agonist, 7-OH-PIPAT; # *p*<0.05, ## *p*<0.01, and ### *p*<0.001 with respect to the right side; & *p*<0.05, && *p*<0.01, and &&& *p*<0.001 with respect to the naïve after Bonferroni's post hoc test

two D₁R binding species are distinguishable in striatal samples from either hemisphere of naïve rats. Lateralization is observed by the statistically significant lower K_{DH} and K_{DL} values in the left hemisphere compared with values in the right one: K_{DH} is 14-fold lower and K_{DL} is circa 3-fold lower in the left striatum. In addition, the proportion of high-affinity sites is 3-fold lower in the left hemisphere.

Low-affinity species were predominant in hemilesioned animals in which, interestingly, the affinity parameters (K_{DH} or K_{DL}) for the binding of the agonist to D₁R were similar in the striata from two sides (Table 1). Taking into account all four groups of animals, the overall comparison showed that the proportion of high-affinity (B_{maxH}) versus total number of sites was significantly different (inter-group differences detected by two-way ANOVA) in samples from both right ($F_{(3,16)}=7.79$, *p*=0.002) and left ($F_{(3,16)}=12.80$, *p*=0.0002) hemispheres. Right-left lateralization was also found in terms of differential values (inter-hemisphere differences detected by two-way ANOVA) B_{maxH} ($F_{(1,16)}=30.5$, *p*<0.0001), K_{DH} ($F_{(1,16)}=91.0$, *p*<0.0001), and K_{DL} ($F_{(1,16)}=43.1$, *p*<0.0001) (see Table 1). Interpretation of results in terms of D₁R coupled and uncoupled to G proteins is complex. In principle, the preponderance of low-affinity sites (Table 1) indicates that G-protein-coupled D₁R would be the minority species in all samples except in the right striatum of naïve and dyskinetic animals.

In contrast to the results for B_{maxH}, the values for B₅₀ (i.e., the concentration of SKF38393 that leads to a 50 % of binding sites occupied by this agonist), calculated using the two-site model-derived Eq. (3), were similar in the two hemispheres and were also similar in samples from the different groups. However, there are inter-group differences if B₅₀ values are calculated under the dimer paradigm (see later).

Fitting Data Using the Two-State Dimer Receptor Paradigm

The binding to dimers is determined by the total number of dimers (maximum number of binding sites B_{max} would be twice the number of dimers R_T) and two equilibrium constants defining the binding of the competing agonist (B) to the two protomers of the dimer (K_{DB1} and K_{DB2}). If agonist binding to the first protomer in an unoccupied dimer modifies the characteristics of the binding to the second protomer, cooperativity occurs and a homotropic cooperativity index (D_{CB}) may be readily calculated. Apart from higher affinity in the left hemisphere in samples from all animal groups, the cooperativity index is more negative in the left hemisphere (Table 2). Thus, data fitting using equations devised from the dimer receptor model shows right/left lateralization.

Interestingly, the data fit under the dimer paradigm allow calculation of a hybrid constant that quantifies the

Table 2 Parameter values for the agonist SKF 38393 obtained using [³H]SCH 23390 as radioligand and data fitting to equations devised from the dimer receptor model

Sample	Side	7-OH-PIPAT (100 nM)	R _T	K _{DB1}	K _{DB2}	D _{CB}	K _{DAB}	D _{AB}	B ₅₀
Naïve	Right	–	1.0±0.1	22±2	370±40	–0.62	44±4	0	90±9
		+	1.0±0.1	21±6	330±50	–0.59	40±10	0	85±20
	Left	–	1.1±0.1	3±1 ^{###}	80±10 ^{###}	–0.82	2±1 ^{###}	0.5	15±4 ^{###}
		+	1.1±0.1	6±2 [#]	120±30 [#]	–0.70	6±2 ^{###}	0.3	27±8 [#]
Lesioned	Right	–	0.80±0.03	28±3	450±20	–0.60	56±6	0	112±9
		+	0.75±0.05	22±3	470±40	–0.73	44±6	0	100±10
	Left	–	1.0±0.1	3±1 ^{###}	120±20 ^{###}	–1.0	3±1 ^{###}	0.3	19±5 ^{###}
		+	1.0±0.1	7±3 [#]	210±40 ^{###}	–0.77	10±4 ^{###}	0.25	40±15 ^{###}
L-DOPA-treated (non-dyskinetic)	Right	–	0.9±0.1	20±2	330±30	–0.62	40±4	0	81±8
		+	0.9±0.1	28±2	270±30	–0.38	56±4	0	87±8
	Left	–	1.0±0.1	2±1 ^{###}	60±20 ^{###}	–0.88	0.8±0.4 ^{###}	0.7	11±4 ^{###}
		+	1.1±0.1	8±3 ^{###}	90±20 [#]	–0.45	7±3 ^{###}	0.35	27±8 [#]
Dyskinetic	Right	–	1.2±0.1	20±2	340±30	–0.63	40±4	0	82±8
		+	1.2±0.1	5±1 ^{&*}	160±30 ^{&***}	–0.90	6±2 ^{&&***}	0.2	28±6 ^{&}
	Left	–	1.0±0.1	4±1 ^{###}	160±30 ^{###}	–1.0	5±1 ^{###}	0.2	25±5 ^{###}
		+	1.0±0.1	4±1	160±20	–1.0	4±2	0.3	25±5

Data are mean±SEM values from three experiments (see [17]). R_T is the total amount of receptor dimers, and K_{DB1} and K_{DB2} are, respectively, the equilibrium dissociation constants of the first and second binding of B to the dimer. K_{DAB} is the hybrid equilibrium dissociation constant of B binding to a receptor dimer semi-occupied by the A ([³H]SCH 23390). D_{CB} is the dimer cooperativity index for the binding of ligand B, and D_{AB} is the dimer radioligand/competitor modulation index. B₅₀ is the concentration providing half saturation for B. Parameters are obtained according to [19, 20]

p*<0.05 and *p*<0.01 comparing with and without treatment with the D₃ receptor agonist, 7-OH-PIPAT; # *p*<0.05, ### *p*<0.01, and #### *p*<0.001 with respect to the right side; & *p*<0.01 and && *p*<0.001 with respect to the naïve after Bonferroni's post hoc test

modulation due to the binding of another ligand to the partner receptor in a dimer. The hybrid parameter (D_{AB}) denotes whether the binding of the competitor (B) to unoccupied receptors and to receptors hemiooccupied by the radioligand (A) is similar or not. Deviations from zero values for D_{AB} indicate that binding of the radioligand molecule to one protomer affects the binding of the competitor to the second protomer in the dimer. Importantly, D_{AB} was always zero in samples from right striatum, but not in those from left striatum (Table 2); i.e., two-way ANOVA analysis showed significant inter-hemispheric differences in K_{DAB} ($F_{(1,16)}=324.6$, *p*<0.0001). Although differences in values were detected in the left striatum of every experimental group, the D_{AB} was always positive, thus indicating that the binding of the competitor to the left striatal D₁Rs is favored if one molecule of the radioligand is already bound to the receptor dimer. Non-zero D_{AB} values were confirmed by comparing the goodness of the fit with and without considering interactions due to A affecting the binding of B to the dimer. In fact, the fitting was significantly better when D_{AB} was parameterized than when D_{AB} was forced to be zero. Furthermore, the robustness of the overall results from all conditions and from the two hemispheres was higher when the parameter was taken into account. These results indicate the convenience of considering the D_{AB} hybrid parameter under the receptor dimer concept.

The B₅₀ values obtained under the dimer receptor paradigm (see Eq. (4)) confirm lateralization, with lower values in the left hemisphere (significant inter-hemispheric differences in B₅₀ by two-way ANOVA analysis ($F_{(1,16)}=233.9$, *p*<0.0001) and with no major alterations in samples from lesioned animals (with respect to the samples from naïve rats; see Table 2). Therefore, B₅₀ may better reflect agonist-binding characteristics if calculated under the receptor dimer assumption, i.e., using Eq. (4).

Hints on Lateralization of Binding to D₁Rs in Naïve Animals

Lateralization of dopamine binding to D₁Rs in striatum reflects changes in the molecular structure of the binding site that may be due to several circumstances. The different possibilities may be summarized as different degree of coupling of D₁R to other molecules of D₁R itself or to other proteins (see “Discussion” section for D₁R-interacting proteins). It should be noted that the use of isolated membranes simplifies the interpretation of the results; the two more likely types of interactions in membranes are the homomeric/heteromeric, with GPCRs in complex with G proteins. The data from samples of naïve animals using the two-independent-site model may be interpreted as more D₁Rs coupled to G proteins in the right side. The proportion of high- (18 %) and low-affinity

(82 %) sites in the left side (Fig. 1) points to a marked imbalance in the left hemisphere where receptors seem to be less coupled to heterotrimeric G proteins. The K_{DH} and K_{DL} values, both of which were significantly lower in the left hemisphere (Table 1), indicate that, irrespective of G protein coupling, the D_1R in the left hemisphere is structurally different from the D_1R in the right hemisphere. This is either due to the coupling to a different G protein or it reflects allosteric effects due to membrane components other than G proteins. Although D_1Rs may couple to Gq and lead to calcium mobilization via D_1 - D_2 receptor heteromer formation [23, 24] and other less well defined mechanisms [25], the main signaling pathway engaged via striatal D_1Rs seems to be Gs-dependent [26, 27].

The existence of allosteric effectors differentially affecting the binding to D_1R in the two striatal hemispheres is confirmed by results obtained using the two-state dimer receptor model. First of all, negative cooperativity is more marked in the left side (Table 2). From the analysis using the dimer receptor model, a relevant result comes out: there is a lack of

heterotropic agonist/antagonist effect in the binding to D_1Rs on the right side, whereas the heterotropic agonist/antagonist effect in the binding exists on the left side. In fact, D_{AB} is zero in data from the right side and >0 in data from the left side. Main structural differences in the D_1R from right and left sides occur as only the binding of the radiolabelled antagonist to the left D_1R affects the binding of competing agonist. Hence, the D_1R in the left striatum changes its conformation when occupied with the radioligand in such a way that the access of the competitor to a hemioccupied receptor is better than to the empty dimer (Table 2). The underlying mechanisms are difficult to apprehend, but this piece of evidence is in itself very relevant because it allows distinguishing between two qualitatively different D_1R subpopulations. As the binding to the right hemisphere does not display the heterotropic agonist/antagonist effect, the observed lateralization is due to structurally different D_1Rs . Furthermore, the positive effect contrasts with the negative cooperativity found often in agonist binding to GPCRs [19, 28]. In terms of dimers, the results indicate that the access of the second radiolabelled molecule to D_1R dimers is thermodynamically less favored, whereas the opposite occurs when the competitor binds to the dimer already occupied by one radiolabelled molecule. In summary, according to the two-independent-site model, in the left hemisphere, the fraction of D_1Rs coupled to G proteins is lower than the fraction of uncoupled ones. Under the receptor dimer assumption, an allosteric effect may explain why D_1Rs in the left side display higher affinity. Also, the dimer model-devised parameter D_{AB} seems to be a convenient way to describe intradimer interactions.

Hints on Lateralization of Binding to D_1R in Lesioned and Dyskinetic Animals

According to the two-independent-site model, the balance of high- (B_{maxH}) and low-affinity (B_{maxL}) sites does not significantly change in the left hemisphere of lesioned animals or of lesioned animals treated with L-DOPA, but the B_{maxH}/B_{maxL} ratio is markedly reduced in the right striatum. Remarkably, the K_{DH} and K_{DL} values are markedly reduced in the right side, thus indicating a higher affinity of the agonist binding to D_1R in lesioned animals (with or without L-DOPA treatment) than in naïve animals (Table 1).

Comparing the data from lesioned and naïve animals, the use of the dimer receptor model provided K_D (K_{DB1} or K_{DB2}) values that were similar in the right and in the left hemispheres. Similarly, there were no statistical differences in the values of the D_{CB} and of the D_{AB} and K_{DAB} parameters between animal groups or between left and right sides. In contrast to the two-independent-site model, K_{DB1} and K_{DB2} values showed similar lateralization in lesioned and naïve animals (Table 2); two-way ANOVA analysis showed significant inter-hemisphere differences in K_{DB1} ($F_{(1,16)}=237.2$,

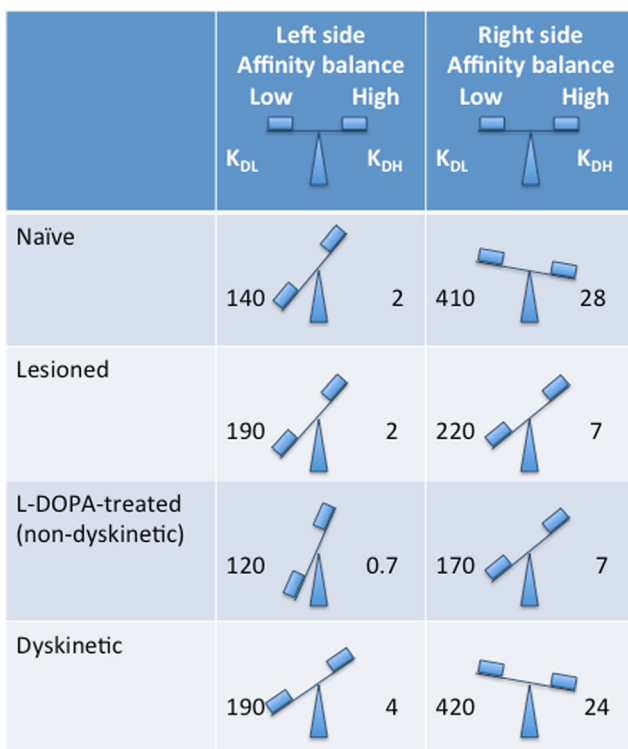


Fig. 1 Balance of high- and low-affinity states in right and left striata from different animals groups. The figure has been constructed using data in Table 1. In each image, the left weighing plate would correspond to the amount of, respectively, low- and high-affinity sites. When the amount of low-affinity site is higher than that of high-affinity site, the left weighing plate is down and the right is up; the opposite (left plate up and the right down) occurs when high-affinity sites are more abundant than low-affinity sites. The degree of dysbalance corresponds to the actual differences in the number of high- and low-affinity states. The numbers correspond to the affinity values (for each condition) of low-affinity (left) and high-affinity (right) species

$p < 0.0001$) and K_{DB2} ($F_{(1,16)} = 204.4$, $p < 0.0001$). The dimer receptor model confirms the similar binding to D_1 Rs in the right side in naïve and dyskinetic animals. In summary, in animals from all treated groups, the dimer assumption model robustly keeps the binding characteristics (lateralization included) found in naïve animals.

According to the two-independent-site model, dyskinesia totally eliminates the high/low-affinity imbalance in the right striatum of lesioned (plus/minus L-DOPA) animals; in fact, the percentage of high-affinity sites in the right side of dyskinetic animals is 57 % (58 % in naïve animals) and the K_{DH} is 24 nM (28 nM in naïve animals). The dopamine binding to D_1 Rs in the left side of dyskinetic animals is more similar to that in naïve animals, but the proportion of high-affinity sites is higher than in any other group (33 vs 12–22 %).

Impact of Agonist Binding to D_3 Receptors on Lateralization of Binding to D_1 R

In samples from all groups except the dyskinetic one, the effect of the D_3 receptor agonist, 7-OH-PIPAT, was monotonous; i.e., it did not affect in a qualitative manner the lateralization in terms of K_D values of agonist binding to striatal D_1 R. In dyskinetic animals, the treatment with the D_3 receptor agonist led to the disappearance of such lateralization. In fact, using the two-independent-site model, K_{DH} values became similar in both hemispheres in dyskinetic animals (also in lesioned animals) (Table 1). Using the receptor dimer paradigm, K_{DB1} , K_{DB2} , or D_{CB} values were similar in the right and left striata of dyskinetic animals (Table 2). Quite noteworthy was that the activation of the D_3 R led to the appearance of the heterotropic D_1 R agonist/antagonist effect in the right side of dyskinetic but not of naïve or lesioned (plus/minus L-DOPA) rats. Furthermore, the B_{50} , calculated according to the dimer receptor model, is reduced in the right striatum to become similar to that in the left striatum. In contrast, B_{50} values calculated according to the two-independent-site model are monotonously high irrespective of the animal group, of the hemisphere, and of treatment (or not) with the D_3 receptor agonist. Comparison of the data in the absence and the presence of the D_3 R agonist confirms lateralization and suggests that parameters obtained using the dimer model are more robust (than using the two-independent-site model) to explain and interpret radioligand-binding results.

Discussion

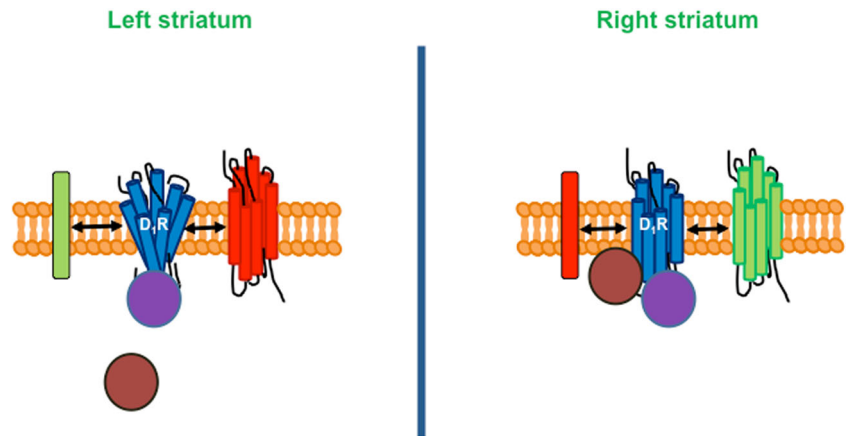
More than three decades ago, Yamamoto et al. [29] reported striatal lateralization of dopamine release in animals under a motor task related to sucrose/water reward. Lateralization of dopamine release mechanisms may run in parallel with lateralization of the dopamine receptor signaling system. In fact,

PET assays using a D_1 R ligand [^{11}C]NNC-112 show asymmetry across hemispheres in healthy humans [30], thus pointing towards differential dopamine-mediated signaling mechanisms in right and left striata. This lateralization occurring at the very molecular level adds further complexity to the neural circuits operating in the most important region for motor control. Elucidation of the causes and consequences of lateralization in dopamine-binding and dopamine-receptor-mediated signaling is key to understand the role of striatal asymmetry in motor control and to design better interventions to prevent and/or manage PD.

Back in the third quarter of the twentieth century, radioligand-binding techniques were instrumental to identify receptors for neurotransmitters. Autoradiography was also instrumental to make the first maps of receptor expression in the CNS. Last but not least, fitting of radioligand-binding data was key to determine the affinity of the transmitter-receptor interaction. More recently, the technique has been mainly used to determine differences of receptor expression in neuropathologies. In Parkinson's disease, alterations in the level of striatal dopamine receptors have been reported [31–34]. Often, the results of the comparison assays are attributed to differences in the level of expression and not to qualitative changes in the characteristics of the binding. Experiments using a single concentration of the radioligand (even in competition assays) cannot provide unequivocal data on the actual levels of receptors. An alteration in specific binding using a single concentration of the radioligand may be due to actual differences in receptor levels or to differential binding characteristics in receptors from the two samples being compared. A proper assessment of receptor levels and ligand-receptor affinity needs optimal experimental design and careful analysis of the data. Indeed, radioligand binding appears as instrumental to detect differential trends in the molecular characteristics of receptors in natural sources.

The information provided by fitting the data to two-independent-site and to two-state dimer receptor models is summarized in Tables 1 and 2 and in Fig. 1. D_1 Rs in the left striatum have higher affinity for agonists than in the right striatum, and this seems to be due to a higher percentage of receptors coupled to G proteins. The potential heteromerization with D_3 Rs does not play any role in lateralization found in naïve and lesioned rats (see below for discussion of data from dyskinetic animals). The homotropic effect, i.e., that exerted by one compound upon the previous binding of the same compound, may be either due to cooperativity in the binding to a receptor dimer or to the occurrence of G-protein-coupled high- and G-protein-uncoupled low-affinity monomers. The binding properties within the left striatum also showed a heterotropic effect, i.e., an effect of the binding of the radiolabelled antagonist on the binding of the competing agonist. Occurrence of receptor dimers in which the binding of the radioligand to a protomer in the dimer affects the

Fig. 2 Scheme of different protein-protein interactions that may impact on the structure of D₁R and give rise to lateralization of dopamine-binding and receptor-mediated signaling. Other G-protein-coupled receptors, other membrane proteins, various G proteins, and scaffolding proteins may likely interact with dopamine receptors



binding of the competitor to the second protomer in the dimer is a reasonable hypothesis to explain the heterotropic agonist/antagonist effect. In summary, our conclusion is that the left striatum displays a D₁R with a tertiary and/or quaternary structure different from that in the right side. Different quaternary structure may be due to a different stoichiometry of the receptor (monomer vs dimer) and/or may be the consequence of allosteric modulation due to differential coupling to G or other proteins, including other GPCRs. Actually, the couple formed by D₁ and adenosine A₁ receptors is recognized as the first identified GPCR heteromer formed by two different receptor types [35, 36]. Heteromerization and allosteric modulation affect the quaternary structure of GPCRs, and therefore, they often affect the affinity of the radioligand/GPCR interaction [5, 37–40]. D₁R may form heteromers with other GPCRs (see www.iiia.csic.es/~ismel/GPCR-Nets/; [41]), and it may also interact with proteins such as NMDA glutamate ionotropic receptors [42–45], N-type calcium channels [46], and calcyon [47].

Coexpression of D₁Rs and calcyon in heterologous systems decreases the proportion of high/low-affinity D₁R sites [48]. As calcyon is elevated in patients with schizophrenia [47], it is likely that the reported decrease in the proportion of D₁R in the disease detected by autoradiography [49] comes from a decrease of high-affinity sites rather than by a decrease in the total amount of receptors. In the 6-hydroxydopamine-hemilesioned rat model of Parkinson's disease, the total amount of D₁Rs does not significantly change ([17]; Tables 1 and 2). In contrast, the characteristics of the binding (high/low-affinity ratio using the two-independent-site model or cooperativity using the dimer receptor model) in samples from lesioned animals were different (Tables 1 and 2 and Fig. 1). Interestingly, the affinity constants and total receptor amounts were similar in right and left striata from naïve and dyskinetic animals. However, in samples from dyskinetic animals, there was a differential trend, namely, the appearance of the heterotropic D₁R agonist/antagonist effect in the right striatum, but only when the D₃R agonist, 7-OH-PIPAT, was

present in the assays. The increase in D₃R expression in dyskinesia leads to a marked D₁-D₃ heteromerization in striatum [17]. The appearance of the peculiar and not previously detected heterotropic agonist/antagonist effect may be due to alterations in the quaternary structure of the D₁R due to activation of D₃R interacting with D₁Rs. L-DOPA therapy results in markedly high concentrations of dopamine in the CNS; consequently, D₃Rs are likely activated under a L-DOPA administration regime such as that used in Parkinson's disease patients. Taken together, the results indicate that a high dopaminergic tone in dyskinetic animals makes D₁Rs similar in right and left striata. Moreover, the lateralization in dopamine binding to striatal D₁Rs, shown in naïve, lesioned, and non-dyskinetic animals, was virtually absent in the dyskinetic state. Abnormal movements in dyskinetic animals may be due to the loss of this D₁R lateralization.

Further experimental effort would be necessary to establish the reasons why dopamine binding to striatal D₁R is lateralized. Differential D₁R structure in right versus left sides may come as a result of interactions with other membrane proteins or with interactions with different scaffolding or G proteins (Fig. 2).

Acknowledgments This work was supported by grants from Spanish *Ministerio de Ciencia y Tecnología* (SAF2009-07276, SAF2011-23813, and SAF2012-39875-C02-01) and from Spanish *Ministerio de Salud* (PI09/01756). MMP is supported by Marie Curie CIG PCIG11-GA-2012-322013.

Conflict of Interest The authors declare no conflict of interest.

References

1. Frasnelli E (2013) Brain and behavioural lateralization in invertebrates. *Front Psychol* 4:939
2. Heinsen H, Henn R, Eisenmenger W, Gotz M, Bohl J, Bethke B, Lockemann U, Puschel K (1994) Quantitative investigations on the human entorhinal area: left-right asymmetry and age-related changes. *Anat Embryol (Berl)* 190(2):181–194

3. Glick SD, Lyon RA, Hinds PA, Soweck C, Titeler M (1988) Correlated asymmetries in striatal D1 and D2 binding: relationship to apomorphine-induced rotation. *Brain Res* 455(1):43–48
4. Pandey P, Mersha MD, Dhillon HS (2013) A synergistic approach towards understanding the functional significance of dopamine receptor interactions. *J Mol Signal* 8(1):13
5. Navarro G, Ferré S, Cordomi A, Moreno E, Mallol J, Casadó V, Cortés A, Hoffmann H et al (2010) Interactions between intracellular domains as key determinants of the Quaternary structure and function of receptor heteromers. *J Biol Chem* 285(35):27346–27359
6. Orru M, Bakešová J, Brugarolas M, Quiroz C, Beaumont V, Goldberg SR, Lluís C, Cortés A et al (2011) Striatal pre- and post-synaptic profile of adenosine A(2A) receptor antagonists. *PLoS One* 6(1):e16088
7. Glick SD, Ross DA, Hough LB (1982) Lateral asymmetry of neurotransmitters in human brain. *Brain Res* 234(1):53–63
8. Thiel CM, Schwarting RKW (2001) Dopaminergic lateralisation in the forebrain: relations to behavioural asymmetries and anxiety in male Wistar rats. *Neuropsychobiology* 43(3):192–199
9. Schwarting RKW, Borta A (2005) Analysis of behavioral asymmetries in the elevated plus-maze and in the T-maze. *J Neurosci Methods* 141(2):251–260
10. Nikkhah G, Falkenstein G, Rosenthal C (2001) Restorative plasticity of dopamine neuronal transplants depends on the degree of hemispheric dominance. *J Neurosci* 21(16):6252–6263
11. Martin-Soelch C, Szczepanik J, Nugent A, Barhaghi K, Rallis D, Herscovitch P, Carson RE, Drevets WC (2011) Lateralization and gender differences in the dopaminergic response to unpredictable reward in the human ventral striatum. *Eur J Neurosci* 33(9):1706–1715
12. Larisch R, Meyer W, Klimke A, Kehren F, Vosberg H, Muller-Gartner HW (1998) Left-right asymmetry of striatal dopamine D2 receptors. *Nucl Med Commun* 19(8):781–787
13. Cho SS, Yoon EJ, Kim SE (2015) Asymmetry of dopamine D2/3 receptor availability in dorsal putamen and body mass index in non-obese healthy males. *Exp Neurobiol* 24(1):90–94
14. Tomer R, Slagter HA, Christian BT, Fox AS, King CR, Murali D, Gluck MA, Davidson RJ (2013) Love to win or hate to lose? Asymmetry of dopamine D2 receptor binding predicts sensitivity to reward versus punishment. *J Cogn Neurosci* 26(5):1039–1048
15. Tomer R, Goldstein RZ, Wang G-J, Wong C, Volkow ND (2008) Incentive motivation is associated with striatal dopamine asymmetry. *Biol Psychol* 77(1):98–101
16. Marin C, Bonastre M, Mengod G, Cortés R, Rodríguez-Oroz MC (2015) From unilateral to bilateral parkinsonism: Effects of lateralization on dyskinesias and associated molecular mechanisms. *Neuropharmacology* 97:365–375
17. Farré D, Muñoz A, Moreno E, Reyes-Resina I, Canet-Pons J, Dopeso-Reyes IG, Rico AJ, Lluís C et al (2015) Stronger dopamine D1 receptor-mediated neurotransmission in dyskinesia. *Mol Neurobiol* 52:1408–1420. doi:10.1007/s12035-014-8936-x
18. Cenci MA, Lee CS, Björklund A (1998) L-DOPA-induced dyskinesia in the rat is associated with striatal overexpression of prodynorphin- and glutamic acid decarboxylase mRNA. *Eur J Neurosci* 10(8):2694–2706
19. Casadó V, Ferrada C, Bonaventura J, Gracia E, Mallol J, Canela EI, Lluís C, Cortés A et al (2009) Useful pharmacological parameters for G-protein-coupled receptor homodimers obtained from competition experiments. Agonist–antagonist binding modulation. *Biochem Pharmacol* 78(12):1456–1463
20. Casadó V, Cortés A, Ciruela F, Mallol J, Ferré S, Lluís C, Canela EI, Franco R (2007) Old and new ways to calculate the affinity of agonists and antagonists interacting with G-protein-coupled monomeric and dimeric receptors: the receptor–dimer cooperativity index. *Pharmacol Ther* 116(3):343–354
21. Franco R, Casadó V, Mallol J, Ferrada C, Ferré S, Fuxe K, Cortés A, Ciruela F et al (2006) The two-state dimer receptor model: a general model for receptor dimers. *Mol Pharmacol* 69(6):1905–1912
22. Casadó V, Canti C, Mallol J, Canela EI, Lluís C, Franco R (1990) Solubilization of A1 adenosine receptor from pig brain: characterization and evidence of the role of the cell membrane on the coexistence of high- and low-affinity states. *J Neurosci Res* 26(4):461–473
23. Lee SP, So CH, Rashid AJ, Varghese G, Cheng R, Lança AJ, O'Dowd BF, George SR (2004) Dopamine D1 and D2 receptor co-activation generates a novel phospholipase C-mediated calcium signal. *J Biol Chem* 279(34):35671–35678
24. Rashid AJ, So CH, Kong MMC, Furtak T, El-Ghundi M, Cheng R, O'Dowd BF, George SR (2007) D1–D2 dopamine receptor heterooligomers with unique pharmacology are coupled to rapid activation of Gq/11 in the striatum. *Proc Natl Acad Sci* 104(2):654–659
25. Chun LS, Free RB, Doyle TB, Huang X-P, Rankin ML, Sibley DR (2013) D1-D2 dopamine receptor synergy promotes calcium signaling via multiple mechanisms. *Mol Pharmacol* 84(2):190–200
26. Jin L-Q, Wang H-Y, Friedman E (2001) Stimulated D1 dopamine receptors couple to multiple G α proteins in different brain regions. *J Neurochem* 78(5):981–990
27. Mannoury-la-Cour C, Vidal S, Pasteau V, Cussac D, Millan MJ (2007) Dopamine D1 receptor coupling to Gs/olf and Gq in rat striatum and cortex: a scintillation proximity assay (SPA)/antibody-capture characterization of benzazepine agonists. *Neuropharmacology* 52(3):1003–1014
28. May LT, Bridge LJ, Stoddart LA, Bridson SJ, Hill SJ (2011) Allosteric interactions across native adenosine-A3 receptor homodimers: quantification using single-cell ligand-binding kinetics. *FASEB J* 25(10):3465–3476
29. Yamamoto BK, Lane RF, Freed CR (1982) Normal rats trained to circle show asymmetric caudate dopamine release. *Life Sci* 30(25):2155–2162
30. Cannon DM, Klaver JM, Peck SA, Rallis-Voak D, Erickson K, Drevets WC (2008) Dopamine type-1 receptor binding in major depressive disorder assessed using positron emission tomography and [^{11}C]NNC-112. *Neuropsychopharmacology* 34(5):1277–1287
31. Ryoo HL, Pierrotti D, Joyce JN (1998) Dopamine D3 receptor is decreased and D2 receptor is elevated in the striatum of Parkinson's disease. *Mov Disord* 13(5):788–797
32. Hurley MJ, Mash DC, Jenner P (2001) Dopamine D1 receptor expression in human basal ganglia and changes in Parkinson's disease. *Mol Brain Res* 87(2):271–279
33. Boileau I, Guttman M, Rusjan P, Adams JR, Houle S, Tong J, Hornykiewicz O, Furukawa Y et al (2009) Decreased binding of the D3 dopamine receptor-preferring ligand [^{11}C](+)-PHNO in drug-naïve Parkinson's disease. *Brain* 132:1366–1375
34. Morin N, Jourdain VA, Morissette M, Grégoire L, Di Paolo T (2014) Long-term treatment with L-DOPA and an mGlu5 receptor antagonist prevents changes in brain basal ganglia dopamine receptors, their associated signaling proteins and neuropeptides in parkinsonian monkeys. *Neuropharmacology* 79:688–706
35. Ginés S, Hillion J, Torvinen M, Le Crom S, Casadó V, Canela EI, Rondin S, Lew JY et al (2000) Dopamine D1 and adenosine A1 receptors form functionally interacting heteromeric complexes. *Proc Natl Acad Sci* 97(15):8606–8611
36. Ferre S, Baler R, Bouvier M, Caron MG, Devi LA, Durrux T, Fuxe K, George SR et al (2009) Building a new conceptual framework for receptor heteromers. *Nat Chem Biol* 5(3):131–134
37. El-Asmar L, Springael J-Y, Ballet S, Andrieu EU, Vassart G, Parmentier M (2005) Evidence for negative binding cooperativity within CCR5-CCR2b heterodimers. *Mol Pharmacol* 67(2):460–469

38. Sohy D, Parmentier M, Springael J-Y (2007) Allosteric transinhibition by specific antagonists in CCR2/CXCR4 heterodimers. *J Biol Chem* 282(41):30062–30069
39. Ferré S, Navarro G, Casadó V, Cortés A, Mallol J, Canela EI, Lluís C, Franco R (2010) Chapter 2—G protein-coupled receptor heteromers as new targets for drug development. *Prog Mol Biol Transl Sci* 91:41–52. doi:10.1016/S1877-1173(10)91002-8
40. Maggio R, Scarselli M, Capannolo M, Millan MJ (2015) Novel dimensions of D3 receptor function: focus on heterodimerisation, transactivation and allosteric modulation. *Eur Neuropsychopharmacol* 25:1470
41. Borroto-Escuela D, Brito I, Romero-Fernandez W, Di Palma M, Oflijan J, Skieterska K, Duchou J, Van Craenenbroeck K et al (2014) The G protein-coupled receptor heterodimer network (GPCR-HetNet) and its hub components. *Int J Mol Sci* 15(5):8570
42. Lee FJS, Xue S, Pei L, Vukusic B, Chéry N, Wang Y, Wang YT, Niznik HB et al (2002) Dual regulation of NMDA receptor functions by direct protein-protein interactions with the dopamine D1 receptor. *Cell* 111(2):219–230
43. Fiorentini C, Gardoni F, Spano P, Di Luca M, Missale C (2003) Regulation of dopamine D1 receptor trafficking and desensitization by oligomerization with glutamate N-methyl-D-aspartate receptors. *J Biol Chem* 278(22):20196–20202
44. Ladepeche L, Yang L, Bouchet D, Groc L (2013) Regulation of dopamine D1 receptor dynamics within the postsynaptic density of hippocampal glutamate synapses. *PLoS One* 8(9):e74512
45. Zheng Q, Liu Z, Wei C, Han J, Liu Y, Zhang X, Ren W (2014) Activation of the D1 receptors inhibits the long-term potentiation in vivo induced by acute morphine administration through a D1-GluN2A interaction in the nucleus accumbens. *Neuroreport* 25(15):1191–1197
46. Kisilevsky AE, Mulligan SJ, Altier C, Iftinca MC, Varela D, Tai C, Chen L, Hameed S et al (2008) D1 receptors physically interact with N-type calcium channels to regulate channel distribution and dendritic calcium entry. *Neuron* 58(4):557–570
47. Koh P, Bergson C, Undie AS, Goldman-Rakic PS, Lidow MS (2003) Up-regulation of the d1 dopamine receptor-interacting protein, calcyon, in patients with schizophrenia. *Arch Gen Psychiatry* 60(3):311–319
48. Lidow MS, Roberts A, Zhang L, Koh P-O, Lezcano N, Bergson C (2001) Receptor crosstalk protein, calcyon, regulates affinity state of dopamine D1 receptors. *Eur J Pharmacol* 427(3):187–193
49. Joyce JN, Lexow N, Bird E, Winokur A (1988) Organization of dopamine D1 and D2 receptors in human striatum: receptor autoradiographic studies in Huntington's disease and schizophrenia. *Synapse* 2(5):546–557

Caffeine, Adenosine A₁ Receptors, and Brain Cortex. Molecular Aspects

Antoni Cortés, Verónica Casadó-Anguera, Estefanía Moreno, Vicent Casadó

Centro de Investigación Biomédica en Red sobre Enfermedades Neurodegenerativas (CIBERNED), Institute of Biomedicine of the University of Barcelona (IBUB), and Department of Biochemistry and Molecular Biology, Faculty of Biology, University of Barcelona, Barcelona, Spain

Abbreviations

- A₁R** Adenosine A₁ receptor
A_{2A}R Adenosine A_{2A} receptor
A_{2B}R Adenosine A_{2B} receptor
A₃R Adenosine A₃ receptor
ADA Adenosine deaminase
BRET Bioluminescence resonance energy transfer
DPCPX Dipropyl-8-cyclopentyl-1-,3-dipropylxanthine
EEG Electroencephalographic
GPCRs G-protein coupled receptors
PDE Cyclic nucleotide phosphodiesterase
PET Positron emission tomography
PLA Proximity ligation assay
R-PIA R-phenyl-isopropyl-adenosine

BRAIN AND PSYCHOSTIMULANTS: CAFFEINE

The efficiency of higher cortical functions, such as memory and speed of complex information processing, tends to decrease with advancing age in normal healthy individuals. Normal aging is typically accompanied by progressive and gradual decline in memory and executive control functions together with morphological changes in the brain. The prominent aging effects are observed mainly in the frontal cortex and some parts of the temporal lobe (Peelle, Cusack, & Henson, 2012). Also, dietary factors may affect cognitive health (Lourida et al., 2013) and dietary control, and prevention of age-related cognitive decline can help maintain quality of life (Lourida et al., 2013). Another factor affecting cognitive functions is psychostimulant usage. Psychostimulants are a broad class of sympathomimetic drugs that, at low doses, can increase arousal, vigilance, vigor and attention, and cognitive enhancement; however, their ability to induce cognitive deficits as well as addiction, especially at high doses, has been described (Wood, Sage, Shuman, & Anagnostaras, 2014). The psychostimulant caffeine (1,3,7-trimethylxanthine) is one of the most important naturally occurring methylated xanthine alkaloids and is the most widely used psychoactive drug in the world (Fisone, Borgkvist, & Usiello, 2004; Fredholm, Battig, Holmen, Nehlig, & Zvartau, 1999).

Once consumed, it is rapidly distributed throughout the body and readily crosses the blood–brain barrier (Dager & Friedman, 2000); once in the brain, it produces a variety of behavioral effects including an increase in performance, subjective alertness and attention (an important prerequisite for many cognitive processes, such as memory and reasoning), and it also reduces fatigue and enhances motor activity (Fisone et al., 2004).

Caffeine does not accumulate in the body but it is extensively metabolized in the liver, primarily by cytochrome P450 1A2 *N*-demethylation, to form three primary metabolites: paraxanthine (1,7-dimethylxanthine), theobromine (3,7-dimethylxanthine), and theophylline (1,3-dimethylxanthine) (Jodynis-Liebert, Flieger, Matuszewska, & Juszczak, 2004). In humans, the formation of paraxanthine accounts for 83.9% of caffeine metabolism, theobromine 12.2%, and theophylline 3.7%, respectively (McLean & Graham, 2002). These metabolites are further metabolized to xanthenes, uric acid, and uracils, which are excreted in the urine, and only a small fraction of caffeine (less than 5% of the ingested dose) is excreted unaffected in the urine. Caffeine is readily available through dietary products, such as coffee, tea, cocoa, different soft and energy drinks, chocolate, caffeine tablets, and certain medications (Heckman, Weil, & Gonzalez de Mejia, 2010). Coffee is among the most widely consumed beverages worldwide, which includes a complex mixture of compounds where caffeine has been the most widely known. Other coffee bioactive substances are diterpenes, chlorogenic acids, niacin, and melanoidins, which can have potential implications on human health (Godos et al., 2014). Caffeine content in coffee beverages has been reported to reach a variability ranging from 130 to 282 mg/cup and up to 322 mg/cup in different commercial espresso coffees (Crozier, Stalmach, Lean, & Crozier, 2012). Although coffee consumption has been historically linked to adverse health effects, new research indicates that coffee consumption may be useful to restore memory dysfunction associated with aging and neurodegenerative diseases (González de Mejia & Ramirez-Mares, 2014). In fact, healthy people can tolerate low and moderate (<400 mg/day for a 70-kg person) ingestions of caffeine, but heavy caffeine consumption has been associated with serious adverse health effects, including tachycardia, hypertension, anxiety, restlessness, and tremors (Seifert, Schaechter, Hershorin, & Lipschultz, 2011).

MOLECULAR TARGETS OF CAFFEINE IN THE BRAIN

The biological effects of caffeine in the brain are developed throughout a wide range of molecular targets (see Figure 1). The most important of them are adenosine receptors in the cytoplasmic membrane, where xanthinic compounds act as antagonists with a low micromolar range of affinities; xanthines like caffeine act as competitive inhibitors of intracellular cyclic nucleotide phosphodiesterase (PDE) isozymes, with low affinity in the high micromolar to millimolar range. Millimolar concentrations of caffeine are also necessary to mobilize calcium from intracellular stores of the endoplasmic reticulum, an effect mediated via activation of ryanodine-sensitive channels. Caffeine also inhibits ligand binding to the benzodiazepine-positive modulatory site of GABA_A receptors but millimolar concentrations are needed. Other proteins such as IP₃ (inositol triphosphate) receptors of the endoplasmic reticulum, voltage-sensitive ion channels of the cytoplasmic membrane, intracellular proteins such as monoamine oxidase, phosphatidylinositol kinase, etc. are further biological targets on which caffeine and other xanthines can act, but at millimolar or high millimolar

concentrations (see Table 1). Caffeine has been historically important as a tool in the study of PDEs, ion channels, ryanodine receptors, and GABA receptors, but its physiological effects cannot be accounted for by its ability to regulate these targets (Daly, 2000). After ingestion of three to five cups of coffee (about 500 mg of caffeine), the peak concentration of free caffeine circulating in 60 μM of plasma and a blood concentration of 0.5–2 mM caffeine produces lethal intoxication (Bruce, Scott, Lader, & Marks, 1986). From all these values, it is clear that caffeine mainly exerts its psychostimulant effects by counteracting the tonic effects of endogenous adenosine on adenosine receptors. This happens because of the ability of adenosine to modulate the function of two principal neurotransmitter systems: one that is involved in motor activation and reward (dopaminergic systems) and another that is involved in arousal processes (cholinergic, noradrenergic, histaminergic, and orexinergic systems) (Ferré, 2010).

ADENOSINE RECEPTORS AND CAFFEINE

Adenosine is a naturally occurring nucleoside that is distributed ubiquitously throughout the body as a metabolic intermediary.

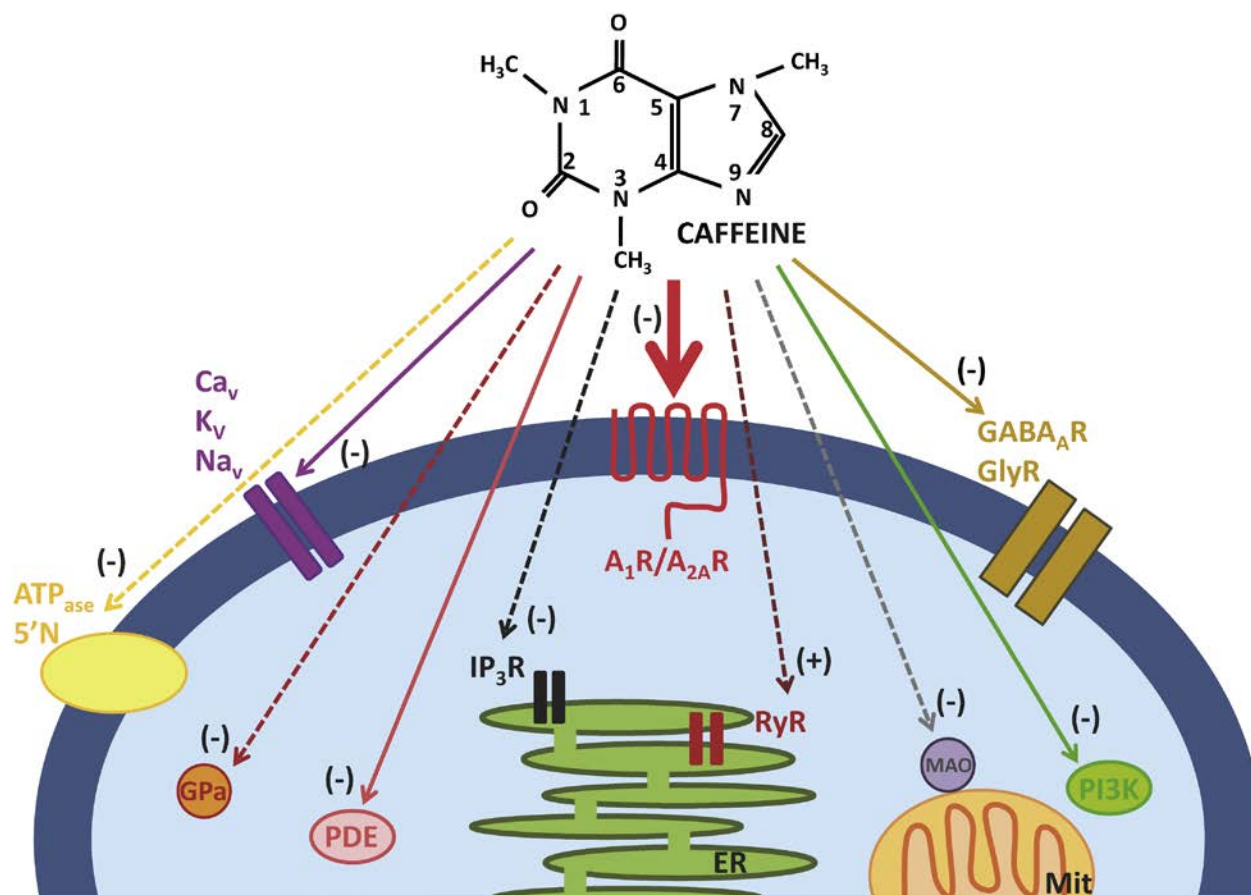


FIGURE 1 Major protein targets of caffeine in neurons. The different arrows show the potency of the interaction of caffeine: thick arrow (low micromolar range); thin arrow (high micromolar range); dashed arrow (millimolar range); (-) inhibition or antagonism; (+) activation or agonism. Mit, Mitochondria; ER, endoplasmic reticulum; A₁R, adenosine A₁ receptor; A_{2A}R, adenosine A_{2A} receptor; ATPase, Na⁺-K⁺-ATPase; Ca_v, voltage-gated calcium channels; GABA_AR, gamma-aminobutyric acid A receptor; GPa, glycogen phosphorylase a; GlyR, glycine receptor; IP₃R, inositol triphosphate receptor; K_v, voltage-gated potassium channels; MAO, monoamine oxidase; Na_v, voltage-gated sodium channels; PDE, phosphodiesterase; PI3K, phosphatidylinositol-3-kinase; RyR, ryanodine-sensitive calcium-release channel; 5'N, 5'-nucleotidase.

TABLE 1 Affinity Parameters of Caffeine Interactions With Different Cellular Proteins

Protein	Parameter (μM)	Source	Research Group
A_1R^a	45, 12	Human brain	C.E. Müller (2004) and B.B. Fredholm (1999)
	44, 20	Rat brain	J.W. Daly (1991) and B.B. Fredholm (1999)
	41, 26, 29	Rat brain cortex	C.E. Müller (1994, 1997) and K.A. Jacobson (1993)
	13, 19	Rat striatum; caf. pretreated	V. Casadó (2006)
	11	Bovine brain	J.W. Daly (1983)
	28	Bovine brain cortex	V. Casadó (2013)
	47	Guinea pig	J.W. Daly (1986)
	44	Bovine and rat brain cortex	J.W. Daly (1986)
	90, 10.7	Transfected HEK cells	V. Casadó (2006) and K.A. Jacobson (1999)
$A_{2A}R^a$	23.4, 2.4	Human brain	C.E. Müller (2004) and B.B. Fredholm (1999)
	45, 8.1	Rat brain	J.W. Daly (1991) and B.B. Fredholm (1999)
	43, 32.5, 48	Rat striatum	C.E. Müller (1994, 2000) and K.A. Jacobson (1999)
	80, 290	Rat striatum; caf. pretreated	V. Casadó (2006)
	7, 9.6	HEK expressing hA _{2A} R	V. Casadó (2006) and K.A. Jacobson (1999)
$A_{2B}R^a$	13	Human brain	B.B. Fredholm (1999)
	17	Rat brain	B.B. Fredholm (1999)
	20.5, 10.4	HEK expressing hA _{2B} R	C.E. Müller (2006) and K.A. Jacobson (2002)
	33.8	CHO expressing hA _{2B} R	C.E. Müller (2009)
	30	Fibroblasts expressing hA _{2B} R	J.W. Daly (1994)
	13	Fibroblasts expressing rat A _{2B} R	J.W. Daly (1994)
A_3^a	190	Human brain	B.B. Fredholm (1999)
	80	Rat brain	B.B. Fredholm (1999)
	>100	CHO expressing rat A ₃ R	K.A. Jacobson (1994)
PDE ^b	>500	–	J.W. Daly (2000)
PDE Ib ^b	480	Rat cardiac ventricle	D. Ukena (1993)
PDE II ^b	708	Rat cardiac ventricle	D. Ukena (1993)
PDE IV ^b	>100	Rat cardiac ventricle	D. Ukena (1993)
PDE V ^b	690	Rat cardiac ventricle	D. Ukena (1993)
PDE IV ^b	747	Cells expressing hPDE IV	V.S. Rao (1999)
RyR ^b	9000	Rabbit myocytes	M. Fill (2011)
	990, 3000	HEK expressing RyR2	D.H. MacLennan (1998) and M.H. Gollob (2010)
	2770	HEK expressing RyR1	D.H. MacLennan (1998)
IP ₃ R	20,000 ^b	Rat cerebellum	F. Michelangeli (1992)
	5000 ^b	Mouse pancreatic cells	O.V. Gerasimenko (2006)
	2000 ^b	Mouse glioblastoma cells+IP ₃ R3	C.J. Lee (2010)
	10,000–70,000 ^c	DT40 expressing rat IP ₃ R1	C.W. Taylor (2014)
	>10,000 ^c	DT40 expressing rat IP ₃ R1	C.W. Taylor (2014)

Continued

TABLE 1 Affinity Parameters of Caffeine Interactions With Different Cellular Proteins—cont'd

Protein	Parameter (μM)	Source	Research Group
GABA _A R	>300 ^a	Rat brain	P.J. Marangos (1979)
	350–500 ^b	Rat brain	G.A. Johnston (1984)
GlyR ^b	500	–	J.W. Daly (2000)
	248–837	HEK expressing GlyR	L. Duan (2009)
Ca _v ^c	>1000	–	J.W. Daly (2000)
K _v ^b	230	Chick ciliary ganglion neuron	S.E. Dryer (1996)
Na _v ^c	>1000	Guinea pig cardiac ventricle	Y. Habuchi (1991) and J.W. Daly (2000)
MAO ^a	700 (MAO-A); 3830 (MAO-B)	Recombinant human enzymes	A. Petzer (2013)
5'N ^b	680	Rat brain	B.B. Fredholm (1983)
ATPase ^c	>1000	–	M.P. Gupta (1990) and J.W. Daly (2000)
GC ^c	>1000	–	R.H. Stellwagen (1984) and J.W. Daly (2000)
GPa ^b	1300	In vitro rabbit muscle GPa	Z. Gregus (2007)
PI3K ^b	110–1000	In vitro kinase assays	P.R. Shepherd (2002)

h, human; caf., caffeine. Abbreviations of protein names are the same as in Figure 1.

^a K_D value.

^b IC_{50} or EC_{50} .

^cUsed range of concentrations.

In the brain, adenosine acts as an important upstream neuromodulator of a broad spectrum of neurotransmitters, receptors, and signaling pathways that converge to contribute to the expression of an array of important brain functions (Gomes, Kaster, Tome, Agostinho, & Cunha, 2011). Adenosine is the main molecule involved in the coordination of brain activity (Sebastião & Ribeiro, 2009) and it has a key endogenous neuroprotective role in this tissue predominantly mediated by the adenosine A₁ receptor (A₁R). This nucleoside maintains brain homeostasis and regulates complex behavior via activation of inhibitory and excitatory adenosine receptors in a brain region-specific manner. Four subtypes of these receptors, A₁R, A_{2A}R, A_{2B}R, and A₃R, have been cloned and pharmacologically characterized. All these receptors are members of the family A of G-protein coupled receptors (GPCRs), a superfamily of integral membrane proteins with a central common core made of seven transmembrane α -helices of approximately 25 residues in length that are connected by intra- and extracellular loops (Fredholm, Ijzerman, Jacobson, Klotz, & Linden, 2001). GPCRs comprise the largest protein superfamily in mammalian genomes and they are the most important class of membrane proteins in clinical medicine, accounting for ~40% of all current therapeutics (Wang & Lewis, 2013). More than 90% of known GPCRs are expressed in the brain and are involved in virtually all functions controlled by the nervous system (Vassilatis et al., 2003).

Among the four cloned adenosine receptors, A₁Rs and A_{2A}Rs are the ones predominantly expressed in the brain; A₃Rs are also expressed in the brain but in lower levels. Caffeine has similar in vitro affinities for A₁R, A_{2A}R, and A_{2B}R and much lower affinity for A₃R (see Table 1). For these reasons, A₁R and A_{2A}R are the preferential

targets for caffeine in the brain, since physiological extracellular levels of adenosine are sufficient to occupy and stimulate these receptors (Solinas et al., 2005). On the other hand, A_{2B}Rs have a lower affinity for adenosine and are only activated by high pathological extracellular levels of adenosine (Fredholm et al., 2001). A₁Rs and A_{2A}Rs show a complementary expression pattern in the brain: A₁Rs are widely expressed in the brain, with particularly high levels in the cerebral cortex, hippocampus, and cerebellum and in numerous hypothalamic nuclei and moderate levels in striatum. A_{2A}Rs are highly concentrated in the striatum, and minimally expressed in the hippocampus and cortex (Dunwiddie & Masino, 2001; Fredholm et al., 2001; Schiffmann, Fisone, Moresco, Cunha, & Ferré, 2007). In the brain, A₁Rs are found at both presynaptic and postsynaptic sites (Rebola, Pinheiro, Oliveira, Malva, & Cunha, 2003); A_{2A}Rs are found predominantly at postsynaptic neurons in the striatum, but they are also detected at significantly lower levels at presynaptic sites in the hippocampus (Rebola, Canas, Oliveira, & Cunha, 2005) and in corticostriatal terminals, controlling glutamate release (Schiffmann et al., 2007) or GABA release (Cunha & Ribeiro, 2000). Karcz-Kubicha et al. (2003) suggests that development of tolerance to the effects of A₁R blockade might be mostly responsible for tolerance to the motor-activating effects of caffeine and that the residual motor-activating effects of caffeine in tolerant individuals might be mostly because of A_{2A}R blockade. Both striatal A₁Rs and A_{2A}Rs are involved in the motor-activating and probably reinforcing effects of caffeine, although they play a different role under conditions of acute or chronic caffeine administration (Ferré, 2008).

The concentration needed to explain the effect of caffeine at the receptor level generally corresponds to following the

consumption of average amounts of caffeine from dietary sources (Porkka-Heiskanen, 2013). Elmenhorst, Meyer, Matusch, Winz, and Bauer (2012) carried out the first in vivo study on cerebral A₁R occupation by caffeine in humans. These authors used ¹⁸F-CPFPX, a positron emission tomography (PET) tracer, to visualize and quantify the occupancy of the most abundant caffeine target in the human brain. Given a biologic half-life of about 5 h, caffeine might therefore occupy up to 50% of the cerebral A₁R when caffeinated beverages are repeatedly consumed during a day. Half-maximal displacement was achieved at a plasma caffeine concentration of 67 μM, which corresponds to 450 mg in a 70-kg subject (Elmenhorst et al., 2012). Caffeine affects the brain by a localized combination of neuronal and vascular responses because increased neuronal activity is thought to be exerted mainly through action on A₁Rs (Dunwiddie & Masino, 2001), whereas vasoconstriction is mediated mainly through action on A_{2A}Rs and also by A_{2B}Rs (low-affinity adenosine receptors that are present in astrocytes and cerebral vascular cells; see Pelligrino, Xu, & Vetri, 2010). Both caffeine-mediated blockade of adenosine receptors and vasoconstriction have direct repercussions on brain connectivity at resting states and during cognitive activation. Whereas the effects of acute caffeine consumption seem mostly to be due to the antagonism of A₁Rs, the effects resulting from the chronic consumption of caffeine seem to be mainly due to the antagonism of A_{2A}Rs (Chen et al., 2007; Ferré, 2008).

MOLECULAR EFFECTS OF CAFFEINE ON COGNITIVE FUNCTIONS

Caffeine acutely increases the functional efficiency of neuronal networks in the human cerebral cortex and, after consumption of moderate amounts of caffeine, cognitive functions are increased (Park et al., 2014). Because A₁Rs are quantitatively the most important neocortical binding sites of caffeine in the human brain, it is likely that the cognition-enhancing effects of caffeine are exerted by this adenosine receptor subtype (Elmenhorst et al., 2012). It has been indicated that the effects of caffeine on cognition are mediated primarily by blockade of the A₁Rs in hippocampal CA1 and CA2 neurons (Dunwiddie & Masino, 2001; Simons, Caruana, Zhao, & Dudek, 2012). Functional magnetic resonance imaging evidence shows that cerebral blood flow is directly proportional to recent caffeine intake (Addicott et al., 2009). A high habitual intake of caffeine was also associated with better verbal memory performance and psychomotor speed in several cross-sectional population studies (Van Boxtel et al., 2003). In animals, caffeine has been found to counteract certain kinds of memory impairments, such as those associated with sleep deprivation or attention deficit disorder. It has been indicated that caffeine administration enhances consolidation of long-term memories in humans (Borota et al., 2014). It has been reported that the regular human consumption of caffeine is associated with the reduced cognitive decline in aging and may have beneficial effects in Alzheimer's disease patients and on Parkinson's disease therapy (Ribeiro & Sebastião, 2010). It has been suggested that chronic (but not acute) caffeine treatment attenuates brain injury by adenosine receptor-mediated suppression of glutamate release, mediated by A₁Rs in ischemic and immunological brain injury models (Xu, Aibiki, & Nagoya, 2002) and by A_{2A}R in Parkinson's and Alzheimer's diseases (Popoli et al., 2002).

MOLECULAR EFFECTS OF CAFFEINE ON SLEEP AND WAKEFULNESS

Arousal is a state of behavioral readiness in response to sensory stimulation, which is associated with cortical electroencephalographic (EEG) activation, and this depends on the activation of ascending arousal systems localized in the pontomesencephalic tegmentum, basal forebrain, and hypothalamus (Ferré, 2010). A₁Rs localized in the basal forebrain and A_{2A}Rs localized in the hypothalamus are believed to be mostly responsible for the arousing properties of caffeine. These properties depend on the blockade of multiple inhibitory mechanisms that adenosine, as an endogenous sleep-promoting substance, exerts on the multiply interconnected ascending arousal systems (Ferré, 2008, 2010). These mechanisms include a direct A₁R-mediated modulation of the corticopetal basal forebrain system and an indirect A_{2A}R-mediated modulation of the hypothalamic, histaminergic, and orexinergic systems (Ferré, 2010).

The blockage of these receptors by caffeine leads to an increase in adenosine within the noradrenergic, cholinergic, dopaminergic, and serotonergic systems, which are regulated by adenosine (Lopez-Garcia, Guallar-Castillon, Leon Muñoz, Graciani, & Rodriguez-Artalejo, 2014). The stimulation of these neurotransmitter systems increases alertness, attention, arousal, and motor activation (Ferré, 2010; Lopez-Garcia et al., 2014). The extracellular level of adenosine increases in the cortex and basal forebrain during prolonged wakefulness and decreases during the sleep-recovery period. Sleep results from the inhibition of wake-promoting systems by homeostatic sleep factors such as adenosine, nitric oxide, and GABAergic neurons in the preoptic area of the hypothalamus, resulting in large amplitude, slow EEG oscillations (Brown, Basheer, McKenna, Strecker, & McCarley, 2012). However, the relative contribution of A₁R and A_{2A}R to sleep induction remains controversial (Huang, Zhang, & Qu, 2014; Porkka-Heiskanen, 2013). Activation of A_{2A}Rs by its agonist infused into the brain potentially increases sleep, and the arousal effect of caffeine was shown to be dependent on the A_{2A}R. On the other hand, inhibition of wake-promoting neurons via the A₁R also mediates the sleep-inducing effects of adenosine, whereas activation of A₁R in the lateral preoptic area of the hypothalamus induces wakefulness. These findings indicate that A_{2A}R plays a predominant role in sleep induction, whereas A₁R regulates the sleep-wake cycle in a site-dependent manner (Huang et al., 2014).

ALLOSTERIC INTERACTIONS BETWEEN CAFFEINE AND ADENOSINE RECEPTORS

It is increasingly recognized that one important mechanism for the regulation of the biological functions of most GPCRs is through allosteric modulation (Christopoulos & Kenakin, 2002; Wootten, Christopoulos, & Sexton, 2013). Allosteric modulators of GPCRs target a site separated from the orthosteric site and modulate receptor functioning. They may have several potential advantages over traditional orthosteric ligands due to their selectivity and pharmacokinetic properties (Kenakin & Miller, 2010; Gao & Jacobson, 2013). Allosteric modulators can either potentiate or inhibit the receptor response by inducing conformational changes in the GPCRs that are transmitted from the allosteric binding site

to the orthosteric site and/or directly to effector protein coupling sites (Kenakin & Miller, 2010). The allosteric binding sites are less structurally conserved than their corresponding orthosteric sites and thus provide new opportunities for the development of more selective drugs (Gao & Jacobson, 2013; Wang & Lewis, 2013). Small molecules and ions have been described as allosteric modulators of A₁Rs (Bruns & Fergus, 1990; Göblyös & Ijzerman, 2011; Jacobson, Gao, Göblyös, & Ijzerman, 2011) as well as proteins such as the adenosine degrading enzyme and adenosine deaminase (ADA), which binds to human striatal A₁R behaving as an allosteric effector that markedly enhances agonist affinity and receptor functionality (Gracia et al., 2008). Furthermore, as previously commented, there is another way of allosteric interaction in GPCRs: the interaction with other receptors. This interaction could be between identical (homomerization) and different (heteromerization) receptors, or with other non-GPCRs and assumes an interaction among protomers in a receptor oligomer (Casadó et al., 2007, 2009a; Ferré et al., 2014). The long perceived notion that GPCRs only function in monomeric form has been changed by the description of a number of GPCRs of classes A, B, and C that are found as homodimers, heterodimers, or as higher-order oligomers (Ciruela et al., 2012; Ferré et al., 2014; Milligan, 2009).

The ability of A₁Rs to form homomers was previously suggested by Western-blot assays (Ciruela et al., 1995) but there was no direct evidence for A₁R homomerization in brain tissues, and thus no indication of physiological relevance. In 2013, using bioluminescence resonance energy transfer (BRET) experiments, Gracia and collaborators showed that A₁Rs can form homomers in transfected cells expressing similar levels of A₁Rs to those found in native tissues. BRET experiments were performed in HEK-293T cells cotransfected with a constant amount of cDNA corresponding to A₁R-Rluc and increasing amounts of cDNA corresponding to A₁R-YFP. The BRET saturation curve was hyperbolic, indicating a specific interaction between both fusion proteins. When BRET saturation curves were determined in the presence of ADA a significant increase of the BRET_{max} without significant modifications of BRET₅₀ was observed (Gracia et al., 2013). These results suggested that ADA binding to the receptor leads to conformational changes in the A₁R quaternary structure that reduces the distance between Rluc and YFP, which were fused to the C-terminal domain of the two A₁R fusion proteins in the receptor homomer. Biophysical techniques to detect homomers cannot be easily applied in native tissue, but other direct and indirect methods can be used. Using the proximity ligation assay (PLA) technique, Gracia et al. (2013) also demonstrated, for the first time, the existence of A₁R homomers in bovine brain cortex *ex vivo*. These homomers were constituted, at least, by two protomers that formed a dimer.

In addition, Gracia et al. (2013) studied the pharmacological and functional role of A₁R homomers in the brain cortex by ligand binding and signaling experiments. Mathematical models that consider dimers as the minimal structure of a GPCR were developed to fit binding data (Casadó et al., 2007; Durroux, 2005; Franco et al., 2005, 2006). Among these models, it is important to note that the two-state dimer receptor model provides the most practical method to analyze ligand-GPCR interactions when considering receptor homomers (Ferré et al., 2014). Moreover, this model allows quantification of cooperativity by defining a new parameter: “the dimer cooperativity index” (Dc) (Casadó et al., 2007). According to the definition of this constant, a zero value indicates lack of cooperativity, whereas a positive or negative value

indicates positive or negative cooperativity. The results obtained with bovine brain cortex A₁Rs demonstrated that these receptors show negative cooperativity in agonist R-phenyl-isopropyladenosine (R-PIA) binding (Dc = -0.65); that is, the agonist binding to one protomer in the empty receptor dimer decreases the agonist affinity for the second protomer in the semioccupied receptor dimer due to a protomer-protomer molecular interaction. In the presence of ADA, the Dc value changed from negative to 0, indicating that ADA abolishes the negative cooperativity in ligand binding. This result suggests that ADA is an example of an enzyme that acts as an allosteric modulator of a GPCR because its binding to A₁R homomers blocks the protomer-protomer interactions in the receptor dimers, stabilizing the high-affinity receptor conformation (Gracia et al., 2013).

Gracia et al. (2013) also investigated if through protomer-protomer interactions in the A₁R homodimer there is a molecular cross-talk when two different compounds, i.e., a radiolabeled agonist ([³H]R-PIA) and a competing antagonist (caffeine), bind to this receptor in a competitive experiment. This cross-talk can be detected and quantified from two new constants that can be obtained using the two-state dimer receptor model (Casadó et al., 2009b), and it constitutes another example of allosteric interaction between protomers in a receptor oligomer (Ferré et al., 2014). These pharmacological parameters are the “hybrid” equilibrium dissociation constant (K_{DAB}) and the dimer radioligand/competitor modulation index (“cross-talk index”, D_{AB}) (see Mini-Dictionary of Terms). It is expected that the caffeine binding to A₁R is not cooperative, and, as a classical antagonist, it should form a monophasic binding competition curve (Gracia et al., 2008). Surprisingly, the competition curve of [³H]R-PIA versus caffeine obtained by Gracia et al. (2013) was biphasic, i.e., a typical cooperative shape (see Figure 2). Although A₁Rs and A_{2A}Rs are the preferential targets for caffeine in the brain (Ferré, 2008; Solinas et al., 2005), the amount of A_{2A}R detected in bovine brain cortex is negligible in comparison with the levels of A₁R (Gracia et al., 2013) and the biphasic behavior for caffeine binding only can be justified by the existence of an agonist-antagonist cross-talk (K_{DAB} = 26 μM; D_{AB} = +0.33) (Table 2). According with the two-state dimer receptor model this cross-talk must be bidirectional (Casadó et al., 2009b), which implies that at low caffeine concentrations (when caffeine only binds to a protomer of the empty homodimer), caffeine binding increases the [³H]R-PIA affinity for the other protomer in the A₁R homomer (K_{DBA} = 0.17 nM; D_{BA} = +0.33) (Table 2). This fact has high physiological relevance because low caffeine doses could increase endogenous adenosine binding to A₁R. Obviously, at high caffeine concentrations (when caffeine highly saturates both protomers of the homodimer) this drug acts as an A₁R antagonist diminishing the agonist binding to the receptor. Interestingly, in the presence of ADA the cross-talk between [³H]R-PIA and caffeine is abolished (D_{AB} = D_{BA} = 0) (see Figure 2 and Table 2). That is in good agreement with the strong modification that this enzyme induces in the quaternary structure of the A₁Rs demonstrated by BRET techniques and by changes in the cooperativity and in the affinity of these receptors for its agonist R-PIA (Gracia et al., 2013). Qualitatively similar results were obtained using dipropyl-8-cyclopentyl-1-,3-dipropylxanthine (DPCPX), a selective nonphysiological A₁R antagonist (K_{DBA} = 0.06 nM and D_{BA} = +0.79).

If it is assumed that the caffeine binding to only one protomer in the homodimer increases the agonist’s affinity for the other protomer

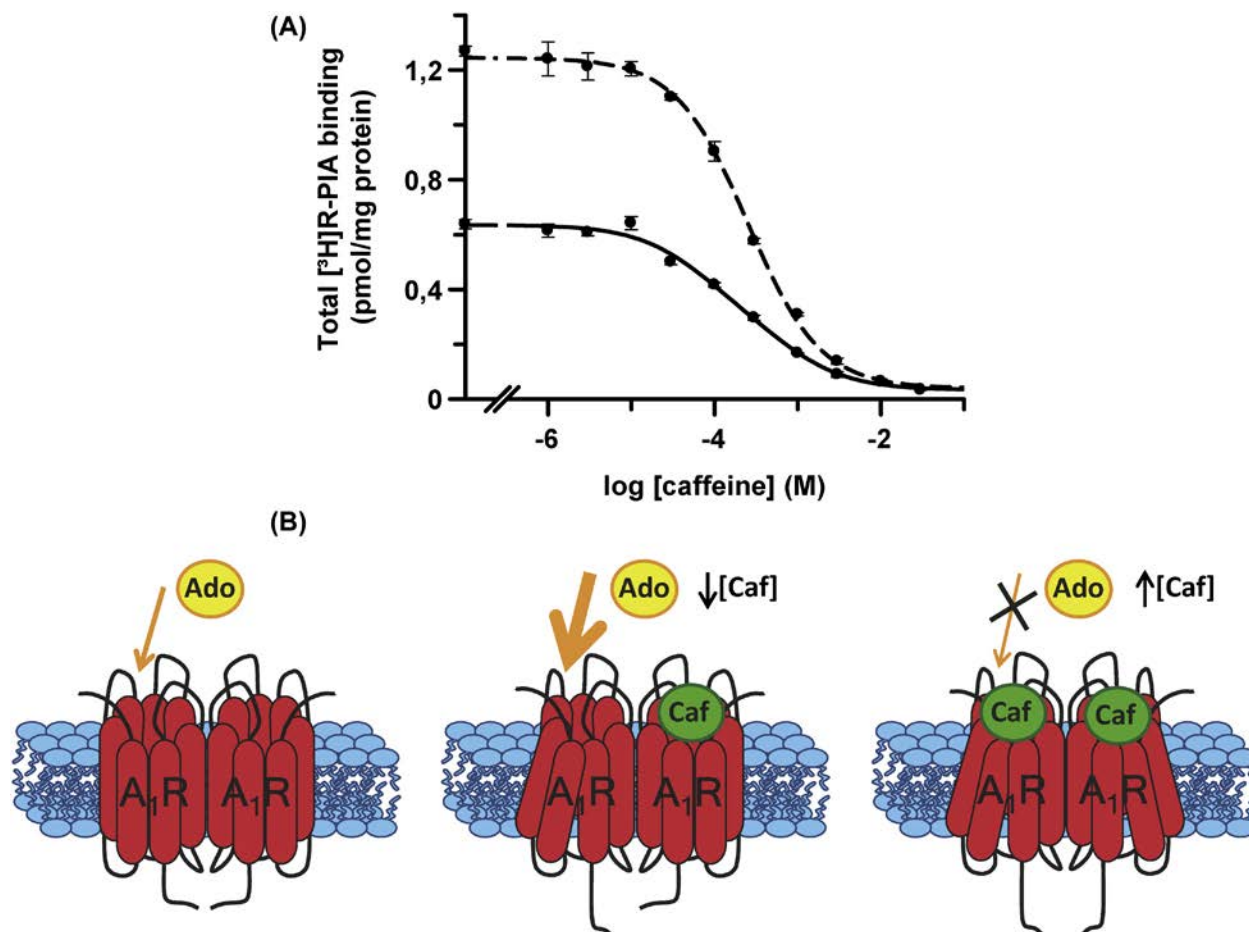


FIGURE 2 Biphasic effects of caffeine binding to A_1R homodimers. In (A), competition curves of the A_1R agonist [3H]R-PIA (0.3 nM) binding versus increasing concentrations of the free antagonist caffeine obtained using bovine brain cortical membranes in the absence (solid line) or presence of 0.2 I.U./ml of ADA (dashed line). Similar results were obtained using Hg^{2+} -inactivated ADA. Experimental data were fitted to the two-state dimer receptor model equations. Parameters' values are in Table 2. See Gracia et al. (2013) for details. In (B), schematic representation showing that at low caffeine (Caf) concentrations it induces an increase of agonist (Ado, adenosine) affinity by A_1R ; conversely, at high caffeine concentrations it behaves as a classical A_1R antagonist and blocks agonist binding. ADA, Adenosine deaminase.

TABLE 2 Binding Parameters of Caffeine to A_1R Obtained With the Dimer Receptor Model

Parameter		Value	
		Caffeine	Caffeine + ADA
K_{DA1}		0.18 nM	0.038 nM
K_{DB1}		28 μ M	18 μ M
K_{DB2}		112 μ M	72 μ M
D_{CB}	Actual	0	0
	Expected without cooperativity	0	0
K_{DAB}	Actual	26 μ M	36 μ M
	Expected without cross-talk	56 μ M	36 μ M
K_{DBA}	Actual	0.17 nM	0.076 nM
	Expected without cross-talk	0.36 nM	0.076 nM
$D_{AB} = D_{BA}$	Actual	+0.33	0
	Expected without cross-talk	0	0

The different parameters were obtained from competition curves of 0.3 nM [3H]R-PIA (ligand A) versus caffeine (ligand B) in the absence or presence of 0.2 I.U./ml of the A_1R allosteric modulator ADA. See Gracia et al. (2013) for details. ADA, Adenosine deaminase.

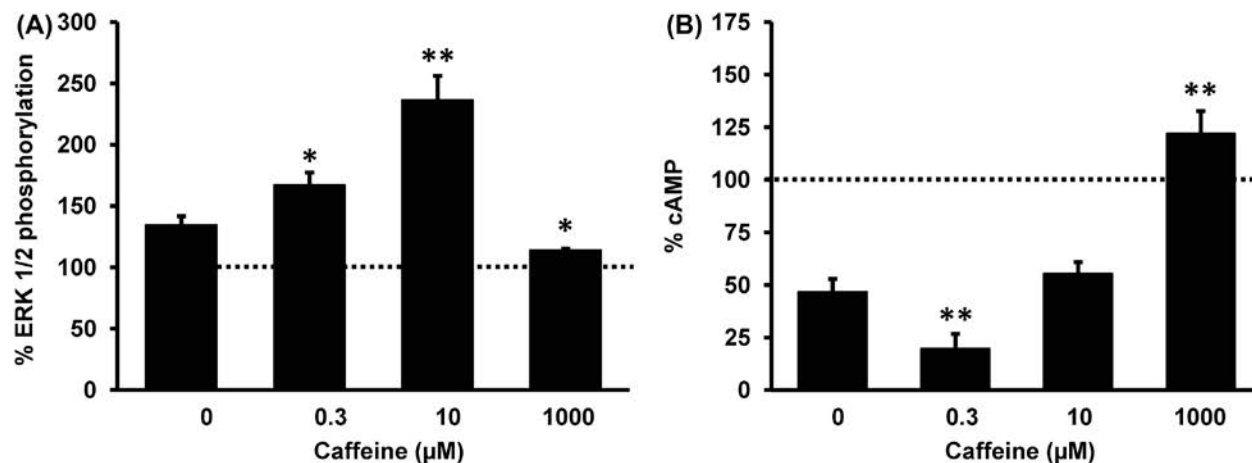


FIGURE 3 Biphasic effects of caffeine on A₁R agonist-induced ERK 1/2 phosphorylation and adenylyl cyclase inhibition. In (A), human A₁R transfected HEK cells were stimulated with 0.5 nM R-PIA in the absence or presence of increasing caffeine concentrations. Values represent the mean \pm SEM of the percentage of phosphorylation relative to basal levels found in untreated cells (100%, dotted line). Statistical significance was calculated by one-way ANOVA followed by a Dunnett's multiple comparison post hoc test; * p < 0.05 and ** p < 0.01 compared with the corresponding cells only treated with R-PIA. In (B), cAMP production was stimulated with 0.5 μ M forskolin. Values represent the mean \pm SEM of the percentage of cAMP concentration relative to the forskolin-treated cells (100%, dotted line, 25 pmols cAMP/10⁶ cells). Statistical significance was calculated by one-way ANOVA followed by a Dunnett's multiple comparison post hoc test; ** p < 0.01 compared with the corresponding cells treated with R-PIA in the absence of caffeine (see details in Gracia et al., 2013).

in the A₁R homodimer, it can be expected that low concentrations of caffeine increase, instead of decrease, the agonist-induced signaling. In fact, Gracia et al. (2013) found that caffeine exerts a biphasic modulation of A₁R agonist-induced cAMP decrease and ERK 1/2 phosphorylation (see Figure 3). For a given agonist concentration, low caffeine concentrations increased agonist-induced signaling; as expected, high caffeine concentrations inhibited agonist-induced signaling (Gracia et al., 2013). The same behavior was also seen for the antagonist DPCPX. It has been reported that caffeine, when administered alone, elicits biphasic effects, showing locomotor depression at lower doses and stimulation at higher doses in mice (Katims, Annau, & Snyder, 1983; Snyder, Katims, Annau, Bruns, & Daly, 1981). Results from Gracia et al. (2013) can account for this behavior since low doses of caffeine can increase the endogenous adenosine binding to brain cortex bovine A₁Rs increasing signaling and locomotor depression while high doses of caffeine obviously act as an A₁R antagonist blocking the effect of endogenous adenosine and inducing locomotor activation (see cartoon in Figure 4). This agonist–antagonist interaction in A₁R homomers could also have biphasic physiological consequences in caffeine regulation of sleep–wakefulness processes.

In summary, using BRET and PLA experiments, Gracia et al. (2013) obtained direct evidence that A₁R form homomers not only in cell cultures but also in the brain cortex, accounting for the first demonstration that A₁R are expressed as homomers in a native tissue. By radioligand binding experiments in the absence or in the presence of the A₁R's allosteric modulator, adenosine deaminase, and by using the two-state dimer receptor model to fit binding data, Gracia et al. (2013) demonstrated that the protomer–protomer interactions in the A₁R homomers account for some of the pharmacological characteristics of agonist and antagonist binding to A₁R. These pharmacological properties include the appearance of cooperativity in agonist binding and the molecular cross-talk detected when two different specific molecules (agonist and antagonist)

bind to the receptor homodimer. In this last case, caffeine binding to one protomer increases the agonist affinity for the other protomer in the A₁R homomer, a pharmacological characteristic that correlates with the low caffeine concentration-induced activation of agonist-promoted A₁R signaling. This pharmacological property, also observed for a synthetic A₁R antagonist as DPCPX, can explain the biphasic effects obtained at low and high concentrations of caffeine on locomotor activity. The usage of antagonist for blocking the effect of agonist drugs has to be taken with caution if an interligand allosteric interaction is detected on the corresponding GPCR target. These results open new perspectives on the actions of antagonists that must be taken into account in drug handling.

APPLICATIONS TO OTHER ADDICTIONS AND SUBSTANCE MISUSE

The paradigm shown in this chapter could have an important role in the research field of most types of drugs of abuse that act across GPCRs. In fact, GPCRs comprise the largest protein superfamily in mammalian genomes and they are the most important class of membrane proteins in clinical medicine, accounting for near 40% of all current therapeutics. Moreover, more than 90% of known GPCRs are expressed in the brain and are involved in virtually all functions controlled by the nervous system. Many GPCRs of classes A, B, and C are found as homodimers, heterodimers, or as higher-order oligomers. These oligomeric structures of GPCRs are essential for receptor activation, maturation, regulation, and signal transduction once they are brought to the cell surface. The two-state dimer receptor model provides the most practical method to analyze ligand–GPCR interactions when considering receptor homomers. As predicted by this model, drug antagonists can show a biphasic effect in their competitive interaction with GPCR endogenous agonists due to a molecular cross-talk between the agonist and the antagonist binding to each protomer in the receptor homodimer.

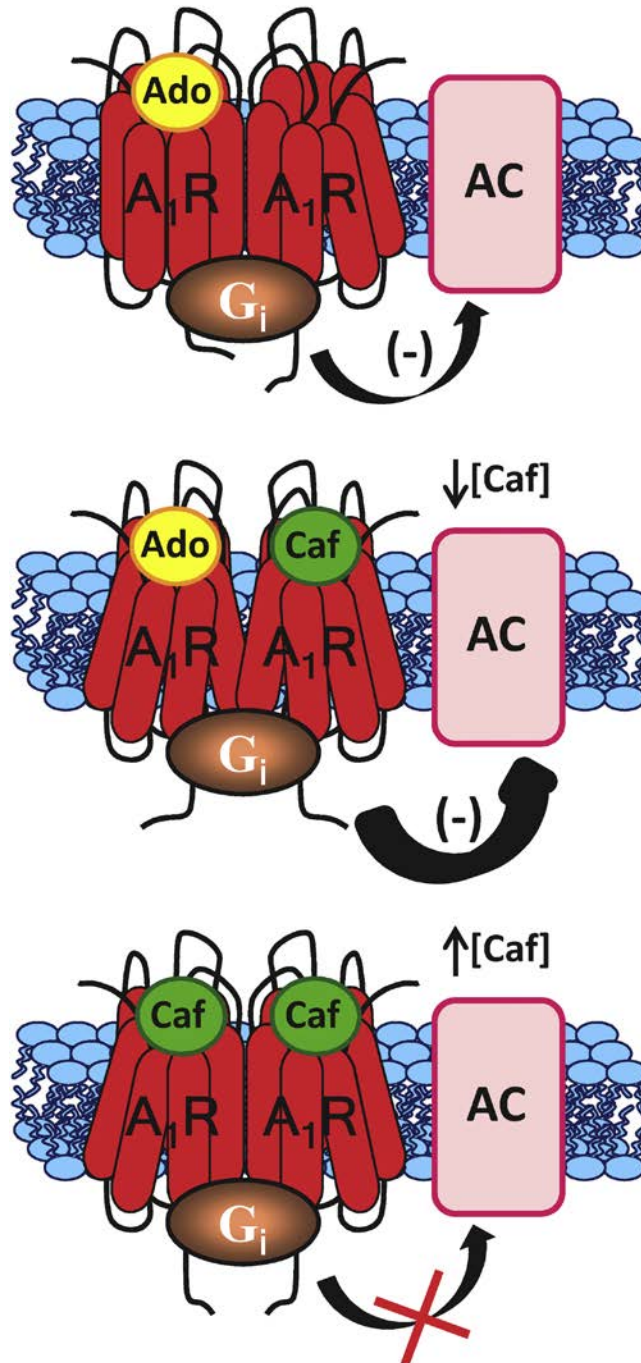


FIGURE 4 Schematic representation of the biphasic effect of caffeine on A_1R agonist-induced adenylyl cyclase (AC) signaling. The molecular cross-talk detected between adenosine (Ado) and caffeine (Caf) is a biochemical fingerprint of the A_1R homodimerization in brain tissue. Cartoon shows how different caffeine concentrations exert different AC effects.

This heterotropic allosteric interaction can be responsible for the fact that low antagonist drug doses increase endogenous agonist effects by an interligand allosteric interaction, but moderate and high drug doses block agonist effects as a classical antagonist. In the same way, the use of antagonists for blocking the effect of agonist drugs (cannabinoids, opioids, amphetamines, hallucinogens, and so on) has to be taken with caution if an interligand allosteric interaction is detected on the corresponding GPCR target.

DEFINITION OF TERMS

Agonist A ligand that combines with a receptor on the orthosteric site and triggers a physiological action.

Allosteric modulator A ligand that binds to an allosteric site on the receptor and modulates binding and/or signaling of an orthosteric ligand. This allosteric site is topographically distinct from, but conformationally linked to, the orthosteric site.

Antagonist A type of receptor ligand that blocks or dampens agonist-mediated responses by binding to the orthosteric site, without triggering a physiological action.

Cooperativity index (D_{CA} , D_{CB}) A constant that estimates the degree of cooperativity in the binding of a radio ligand A (or a competitor ligand B) to a dimeric receptor. Its value is zero for noncooperative binding, whereas positive or negative values indicate the existence of positive or negative cooperativity in the binding of the second molecule of ligand A (or B) to the receptor dimer semioccupied by ligand A (or B).

Cross-talk index (D_{AB} , D_{BA}) A parameter also denominated dimer radioligand/competitor modulation index. Its value is 0 for nonmolecular cross-talk. Positive or negative values of D_{AB} indicate that the presence of a radioligand A bound to one protomer of the receptor increases or decreases, respectively, the affinity of the competitor ligand B for the empty protomer in the receptor dimer semioccupied by ligand A. The analogous definition is valid for D_{BA} .

Dimer receptor model A general mechanistic model that is good for fitting binding data to the dimeric receptors.

GPCR The largest family of cell surface receptors that have in common a characteristic architecture that consists of an extracellular N-terminal domain, an intracellular C-terminal domain, and seven transmembrane spanning domains connected by three extracellular and three intracellular loops.

K_{DA1} Macroscopic equilibrium dissociation constant of the first molecule of ligand A to the receptor dimer.

K_{DAB} Hybrid macroscopic equilibrium dissociation constant of ligand B binding to a receptor dimer semioccupied by ligand A. The analogous definition is valid for K_{DBA} .

K_{DB1} Macroscopic equilibrium dissociation constant of the first molecule of the competitor B to the receptor dimer.

K_{DB2} Macroscopic equilibrium dissociation constant of the second molecule of ligand B to the receptor dimer.

Molecular cross-talk Heterotropic interaction on the receptor oligomer between different structural ligands (i.e., agonist/antagonist).

Orthosteric site The primary binding site of a receptor that binds the endogenous agonist to regulate the activity of the receptor.

Receptor heteromer A macromolecular complex composed of at least two (functional) receptor units with biochemical properties that are demonstrably different from those of its individual components.

Receptor homomer Similar to a receptor heteromer but combining two or more identical (functional) receptor units.

KEY FACTS ON ADENOSINE RECEPTORS

- Adenosine is a naturally occurring nucleoside that is distributed ubiquitously throughout the body as a metabolic intermediary.
- Adenosine is the main molecule involved in the coordination of brain activity and it has a key endogenous neuroprotective role in this tissue predominantly mediated by A_1 Rs.
- Adenosine receptors are members of the family A of GPCRs, a superfamily of integral membrane proteins with a central common core made of seven transmembrane α -helices.
- GPCRs comprise the largest protein superfamily in mammalian genomes and they are the most important class of membrane proteins in clinical medicine, accounting for near 40% of all current therapeutics.
- More than 90% of known GPCRs are expressed in the brain and are involved in virtually all functions controlled by the nervous system.
- Many GPCRs of classes A, B, and C are found as homodimers, heterodimers, or as higher-order oligomers.
- Oligomeric structures of GPCRs are essential for receptor activation, maturation, regulation, and for signal transduction once they are brought to the cell surface.
- Mathematical models that consider dimers as the minimal structure of a GPCR have been developed to fit binding data.
- The two-state dimer receptor model provides the most practical method to analyze ligand–GPCR interactions when considering receptor homomers.

SUMMARY POINTS

- This chapter focuses on the biological effects of caffeine on the brain cortex throughout A_1 Rs.
- Sensory information in the mammalian brain is encoded in the cortex, the brain structure considered to store long-term memories.
- Caffeine is the most widely used psychoactive drug in the world.
- Cortical effects of caffeine are mainly developed throughout binding to adenosine receptors.
- Caffeine acts as an antagonist of A_1 Rs with a low micromolar range of affinity.
- A_1 Rs form homomers in the brain cortex.
- Caffeine shows a biphasic effect in its competitive interaction with A_1 R agonists in binding, cAMP production, and ERK 1/2 phosphorylation assays.
- Low caffeine doses increase adenosine effects by an interligand allosteric interaction.
- Moderate and high caffeine doses block adenosine effects as an antagonist.

ACKNOWLEDGMENT

This study was supported by grants from Spanish Ministerio de Ciencia y Tecnología [grant numbers SAF2008-00146, SAF2011-23813], Government of Catalonia [2009-SGR-12] and Centro de Investigación Biomédica en Red sobre Enfermedades Neurodegenerativas (CIBERNED) [CB06/05/0064].

REFERENCES

- Addicott, M. A., Yang, L. L., Peiffer, A. M., Burnett, L. R., Burdette, J. H., Chen, M. Y., ... Laurienti, P. J. (2009). The effect of daily caffeine use on cerebral blood flow: how much caffeine can we tolerate? *Human Brain Mapping, 30*, 3102–3114.
- Borota, D., Murray, E., Keceli, G., Chang, A., Watabe, J. M., Ly, M., ... Yassa, M. A. (2014). Post-study caffeine administration enhances memory consolidation in humans. *Nature Neuroscience, 17*, 201–204.
- Brown, R. E., Basheer, R., McKenna, J. T., Strecker, R. E., & McCarley, R. W. (2012). Control of sleep and wakefulness. *Physiological Review, 92*, 1087–1187.

- Bruce, M., Scott, N., Lader, M., & Marks, V. (1986). The psychopharmacological and electrophysiological effects of single doses of caffeine in healthy human subjects. *British Journal of Clinical Pharmacology*, *22*, 81–87.
- Bruns, R. F., & Fergus, J. H. (1990). Allosteric enhancement of adenosine A₁ receptor binding and function by 2-amino-3-benzoylthiophenes. *Molecular Pharmacology*, *38*, 939–949.
- Casadó, V., Cortés, A., Ciruela, F., Mallol, J., Ferré, S., Lluís, C., ... Franco, R. (2007). Old and new ways to calculate the affinity of agonists and antagonists interacting with G-protein coupled monomeric and dimeric receptors: the receptor-dimer cooperativity index. *Pharmacology & Therapeutics*, *116*, 343–354.
- Casadó, V., Cortés, A., Mallol, J., Pérez-Capote, K., Ferré, S., Lluís, C., ... Canela, E. I. (2009a). GPCR homomers and heteromers: a better choice as targets for drug development than GPCR monomers? *Pharmacology & Therapeutics*, *124*, 248–257.
- Casadó, V., Ferrada, C., Bonaventura, J., Gracia, E., Mallol, J., Canela, E. I., ... Franco, R. (2009b). Useful pharmacological parameters for G-protein-coupled receptor homodimers obtained from competition experiments. Agonist-antagonist binding modulation. *Biochemical Pharmacology*, *78*, 1456–1463.
- Chen, J. F., Sonsalla, P. K., Pedata, F., Melani, A., Domenici, M. R., Popoli, P., ... de Mendonça, A. (2007). Adenosine A_{2A} receptors and brain injury: broad spectrum of neuroprotection, multifaceted actions and “fine tuning” modulation. *Progress in Neurobiology*, *83*, 310–331.
- Christopoulos, A., & Kenakin, T. (2002). G protein-coupled receptor allosterism and complexing. *Pharmacological Review*, *54*, 323–374.
- Ciruela, F., Casadó, V., Mallol, J., Canela, E. I., Lluís, C., & Franco, R. (1995). Immunological identification of A₁ adenosine receptors in brain cortex. *Journal of Neuroscience Research*, *42*, 818–828.
- Ciruela, F., Fernandez-Dueñas, V., Llorente, J., Borroto-Escuela, D., Cuffi, M. L., Carbonell, L., ... Tasca, C. I. (2012). G protein-coupled receptor oligomerization and brain integration: focus on adenosinergic transmission. *Brain Research*, *1476*, 86–95.
- Crozier, T. W., Stalmach, A., Lean, M. E., & Crozier, A. (2012). Espresso coffees, caffeine and chlorogenic acid intake: potential health implications. *Food & Function*, *3*, 30–33.
- Cunha, R. A., & Ribeiro, J. A. (2000). Purinergic modulation of [³H] GABA release from rat hippocampal nerve terminals. *Neuropharmacology*, *39*, 1156–1167.
- Dager, S. R., & Friedman, S. D. (2000). Brain imaging and the effects of caffeine and nicotine. *Annals of Medicine*, *32*, 292–297.
- Daly, J. W. (2000). Alkylxanthines as research tools. *Journal of the Autonomic Nervous System*, *81*, 44–52.
- Dunwiddie, T. V., & Masino, S. A. (2001). The role and regulation of adenosine in the central nervous system. *Annual Review Neuroscience*, *24*, 31–55.
- Durroux, T. (2005). Principles: a model for the allosteric interactions between ligand binding sites within a dimeric GPCR. *Trends in Pharmacological Science*, *26*, 376–384.
- Elmenhorst, D., Meyer, P. T., Matusch, A., Winz, O. H., & Bauer, A. (2012). Caffeine occupancy of human cerebral A₁ adenosine receptors: in vivo quantification with 18F-CPFPX and PET. *Journal of Nuclear Medicine*, *53*, 1723–1729.
- Ferré, S. (2008). An update of the mechanisms of the psychostimulant effects of caffeine. *Journal of Neurochemistry*, *105*, 1067–1079.
- Ferré, S. (2010). Role of the central ascending neurotransmitter systems in the psychostimulant effects of caffeine. *Journal of Alzheimer's Disease*, *20*(Suppl. 1), S35–S49.
- Ferré, S., Casadó, V., Devi, L. A., Filizola, M., Jockers, R., Lohse, M. J., ... Guitart, X. (2014). G protein-coupled receptor oligomerization revisited: functional and pharmacological perspectives. *Pharmacological Review*, *66*, 413–434.
- Fisone, G., Borgkvist, A., & Usiello, A. (2004). Caffeine as a psychomotor stimulant: mechanism of action. *Cellular and Molecular Life Sciences*, *61*, 857–872.
- Franco, R., Casadó, V., Mallol, J., Ferrada, C., Ferré, S., Fuxe, K., ... Canela, E. I. (2006). The two-state dimer receptor model: a general model for receptor dimers. *Molecular Pharmacology*, *69*, 1905–1912.
- Franco, R., Casadó, V., Mallol, J., Ferré, S., Fuxe, K., Cortés, A., ... Canela, E. I. (2005). Dimer-based model for heptaspanning membrane receptors. *Trends in Biochemical Science*, *30*, 360–366.
- Fredholm, B. B., Battig, K., Holmen, J., Nehlig, A., & Zvartau, E. E. (1999). Actions of caffeine in the brain with special reference to factors that contribute to its widespread use. *Pharmacology Review*, *51*, 83–133.
- Fredholm, B. B., Ijzerman, A. P., Jacobson, K. A., Klotz, K. N., & Linden, J. (2001). International Union of Pharmacology. XXV. Nomenclature and classification of adenosine receptors. *Pharmacology Review*, *53*, 527–552.
- Gao, Z. G., & Jacobson, K. A. (2013). Allosteric modulation and functional selectivity of G protein-coupled receptors. *Drug Discovery Today: Technologies*, *10*, e237–e243.
- Göblyös, A., & Ijzerman, A. P. (2011). Allosteric modulation of adenosine receptors. *Biochimica et Biophysica Acta*, *1808*, 1309–1318.
- Godos, J., Pluchinotta, F. R., Marventano, S., Buscemi, S., li Volti, G., Galvano, F., & Grosso, G. (2014). Coffee components and cardiovascular risk: beneficial and detrimental effects. *International Journal of Food Science and Nutrition*, *65*, 925–936.
- Gomes, C. V., Kaster, M. P., Tome, A. R., Agostinho, P. M., & Cunha, R. A. (2011). Adenosine receptors and brain diseases: neuroprotection and neurodegeneration. *Biochimica et Biophysica Acta*, *1808*, 1380–1399.
- González de Mejia, E., & Ramirez-Mares, M. V. (2014). Impact of caffeine and coffee on our health. *Trends in Endocrinology and Metabolism*, *25*, 489–492.
- Gracia, E., Cortés, A., Meana, J. J., García-Sevilla, J., Hershfield, M. S., Canela, E. I., ... Casadó, V. (2008). Human adenosine deaminase as an allosteric modulator of human A₁ adenosine receptor: abolishment of negative cooperativity for [³H](R)-PIA binding to the caudate nucleus. *Journal of Neurochemistry*, *107*, 161–170.
- Gracia, E., Moreno, E., Cortés, A., Lluís, C., Mallol, J., McCormick, P. J., ... Casadó, V. (2013). Homodimerization of adenosine A₁ receptors in brain cortex explains the biphasic effects of caffeine. *Neuropharmacology*, *71*, 56–69.
- Heckman, M. A., Weil, J., & Gonzalez de Mejia, E. (2010). Caffeine (1,3,7-trimethylxanthine) in foods: a comprehensive review on consumption, functionality, safety, and regulatory matters. *Journal of Food Science*, *75*, R77–R87.
- Huang, Z. L., Zhang, Z., & Qu, W. M. (2014). Roles of adenosine and its receptors in sleep-wake regulation. *International Review of Neurobiology*, *119*, 349–371.
- Jacobson, K. A., Gao, Z. G., Göblyös, A., & Ijzerman, A. P. (2011). Allosteric modulation of purine and pyrimidine receptors. *Advances in Pharmacology*, *61*, 187–220.
- Jodynis-Liebert, J., Flieger, J., Matuszewska, A., & Juszczyk, J. (2004). Serum metabolite/caffeine ratios as a test for liver function. *Journal of Clinical Pharmacology*, *44*, 338–347.

- Karcz-Kubicha, M., Antoniou, K., Terasmaa, A., Quarta, D., Solinas, M., Justinova, Z., ... Ferré, S. (2003). Involvement of adenosine A₁ and A_{2A} receptors in the motor effects of caffeine after its acute and chronic administration. *Neuropsychopharmacology*, *28*, 1281–1291.
- Katims, J. J., Annau, Z., & Snyder, S. H. (1983). Interactions in the behavioral effects of methylxanthines and adenosine derivatives. *Journal of Pharmacology and Experimental Therapeutics*, *227*, 167–173.
- Kenakin, T., & Miller, L. J. (2010). Seven transmembrane receptors as shapeshifting proteins: the impact of allosteric modulation and functional selectivity on new drug discovery. *Pharmacological Review*, *62*, 265–304.
- Lopez-Garcia, E., Guallar-Castillon, P., Leon Muñoz, L., Graciani, A., & Rodriguez-Artalejo, F. (2014). Coffee consumption and health-related quality of life. *Clinical Nutrition*, *33*, 143–149.
- Lourida, I., Soni, M., Thompson-Coon, J., Purandare, N., Lang, I. A., Ukoumunne, O. C., & Llewellyn, D. J. (2013). Mediterranean diet, cognitive function and dementia: a systematic review. *Epidemiology*, *24*, 479–489.
- McLean, C., & Graham, T. E. (2002). Effects of exercise and thermal stress on caffeine pharmacokinetics in men and eumenorrhic women. *Journal of Applied Physiology (1985)*, *93*, 1471–1478.
- Milligan, G. (2009). G protein-coupled receptor hetero-dimerization: contribution to pharmacology and function. *British Journal of Pharmacology*, *158*, 5–14.
- Park, C. A., Kang, C. K., Son, Y. D., Choi, E. J., Kim, S. H., Oh, S. T., ... Cho, Z. H. (2014). The effects of caffeine ingestion on cortical areas: functional imaging study. *Magnetic Resonance Imaging*, *32*, 366–371.
- Peelle, J. E., Cusack, R., & Henson, R. N. (2012). Adjusting for global effects in voxel-based morphometry: gray matter decline in normal aging. *Neuroimage*, *60*, 1503–1516.
- Pelligrino, D. A., Xu, H., & Vetri, F. (2010). Caffeine and the control of cerebral hemodynamics. *Journal of Alzheimer's Disease*, *20*, S51–S62.
- Popoli, P., Pintor, A., Domenici, M. R., Frank, C., Tebano, M. T., Pezzola, A., ... Massotti, M. (2002). Blockade of striatal adenosine A_{2A} receptor reduces, through a presynaptic mechanism, quinolinic acid-induced excitotoxicity: possible relevance to neuroprotective interventions in neurodegenerative diseases of the striatum. *Journal of Neuroscience*, *22*, 1967–1975.
- Porkka-Heiskanen, T. (2013). Sleep homeostasis. *Current Opinion in Neurobiology*, *23*, 799–805.
- Rebola, N., Canas, P. M., Oliveira, C. R., & Cunha, R. A. (2005). Different synaptic and subsynaptic localization of adenosine A_{2A} receptors in the hippocampus and striatum of the rat. *Neuroscience*, *132*, 893–903.
- Rebola, N., Pinheiro, P. C., Oliveira, C. R., Malva, J. O., & Cunha, R. A. (2003). Subcellular localization of adenosine A₁ receptors in nerve terminals and synapses of the rat hippocampus. *Brain Research*, *987*, 49–58.
- Ribeiro, J. A., & Sebastião, A. M. (2010). Caffeine and adenosine. *Journal of Alzheimer's Disease*, *20*(Suppl. 1), S3–S15.
- Schiffmann, S. N., Fisone, G., Moresco, R., Cunha, R. A., & Ferré, S. (2007). Adenosine A_{2A} receptors and basal ganglia physiology. *Progress in Neurobiology*, *83*, 277–292.
- Sebastião, A. M., & Ribeiro, J. A. (2009). Adenosine receptors and the central nervous system. *Handbook of Experimental Pharmacology*, *193*, 471–534.
- Seifert, S. M., Schaechter, J. L., Hershorin, E. R., & Lipshultz, S. E. (2011). Health effects of energy drinks on children, adolescents and young adults. *Pediatrics*, *127*, 511–528.
- Simons, S. B., Caruana, D. A., Zhao, M., & Dudek, S. M. (2012). Caffeine-induced synaptic potentiation in hippocampal CA2 neurons. *Nature Neuroscience*, *15*, 23–25.
- Snyder, S. H., Katims, J. J., Annau, Z., Bruns, R. F., & Daly, J. W. (1981). Adenosine receptors and behavioral actions of methylxanthines. *Proceedings of the National Academy of Sciences of United States of America*, *78*, 3260–3264.
- Solinas, M., Ferré, S., Antoniou, K., Quarta, D., Justinova, Z., Hockemeyer, J., ... Goldberg, S. R. (2005). Involvement of adenosine A₁ receptors in the discriminative-stimulus effects of caffeine in rats. *Psychopharmacology*, *179*, 576–586.
- Van Boxtel, M. P., Schmitt, J. A., Bosma, H., & Jolles, J. (2003). The effects of habitual caffeine use on cognitive change: a longitudinal perspective. *Pharmacology, Biochemistry and Behavior*, *75*, 921–927.
- Vassilatis, D. K., Hohmann, J. G., Zeng, H., Li, F., Ranchalis, J. E., Mortud, M. T., ... Gaitanaris, G. A. (2003). The G protein-coupled receptor repertoire of human and mouse. *Proceedings of the National Academy of Sciences in United States of America*, *102*, 9050–9055.
- Wang, C. I., & Lewis, R. J. (2013). Emerging opportunities for allosteric modulation of G-protein coupled receptors. *Biochemical Pharmacology*, *85*, 153–162.
- Wood, S., Sage, J. R., Shuman, T., & Anagnostaras, S. G. (2014). Psychostimulants and cognition: a continuum of behavioral and cognitive activation. *Pharmacology Review*, *66*, 193–221.
- Wooten, D., Christopoulos, A., & Sexton, P. M. (2013). Emerging paradigms in GPCR allostery: implications for drug discovery. *Nature Review Drug Discovery*, *12*, 630–644.
- Xu, H., Aibiki, M., & Nagoya, J. (2002). Neuroprotective effects of hyperthermic preconditioning on infarcted volume after middle cerebral artery occlusion in rats: role of adenosine receptors. *Critical Care Medicine*, *30*, 1126–1130.

Neuropathology of Drug Addictions and Substance Misuse

Volume 3: General Processes and Mechanisms, Prescription Medications, Caffeine and Areca, Polydrug Misuse, Emerging Addictions and Non-Drug Addictions

Edited by

Victor R. Preedy

King's College London, London, UK



ELSEVIER

AMSTERDAM • BOSTON • HEIDELBERG • LONDON • NEW YORK • OXFORD • PARIS
SAN DIEGO • SAN FRANCISCO • SINGAPORE • SYDNEY • TOKYO

Academic Press is an imprint of Elsevier



Academic Press is an imprint of Elsevier
125 London Wall, London EC2Y 5AS, UK
525 B Street, Suite 1800, San Diego, CA 92101-4495, USA
50 Hampshire Street, 5th Floor, Cambridge, MA 02139, USA
The Boulevard, Langford Lane, Kidlington, Oxford OX5 1GB, UK

Copyright © 2016 Elsevier Inc. All rights reserved.

No part of this publication may be reproduced or transmitted in any form or by any means, electronic or mechanical, including photocopying, recording, or any information storage and retrieval system, without permission in writing from the publisher. Details on how to seek permission, further information about the Publisher's permissions policies and our arrangements with organizations such as the Copyright Clearance Center and the Copyright Licensing Agency, can be found at our website: www.elsevier.com/permissions.

This book and the individual contributions contained in it are protected under copyright by the Publisher (other than as may be noted herein).

Notices

Knowledge and best practice in this field are constantly changing. As new research and experience broaden our understanding, changes in research methods, professional practices, or medical treatment may become necessary.

Practitioners and researchers must always rely on their own experience and knowledge in evaluating and using any information, methods, compounds, or experiments described herein. In using such information or methods they should be mindful of their own safety and the safety of others, including parties for whom they have a professional responsibility.

To the fullest extent of the law, neither the Publisher nor the authors, contributors, or editors, assume any liability for any injury and/or damage to persons or property as a matter of products liability, negligence or otherwise, or from any use or operation of any methods, products, instructions, or ideas contained in the material herein.

British Library Cataloguing-in-Publication Data

A catalogue record for this book is available from the British Library

Library of Congress Cataloging-in-Publication Data

A catalog record for this book is available from the Library of Congress

ISBN: 978-0-12-800634-4

For information on all Academic Press publications
visit our website at <https://www.elsevier.com/>



Publisher: Mara Conner

Acquisition Editor: Mara Conner

Editorial Project Manager: Kathy Padilla

Production Project Manager: Julia Haynes

Designer: Matthew Limbert

Typeset by TNQ Books and Journals

www.tnq.co.in



Pivotal Role of Adenosine Neurotransmission in Restless Legs Syndrome

Sergi Ferré^{1*}, César Quiroz¹, Xavier Guitart¹, William Rea¹, Arta Seyedian¹, Estefanía Moreno², Verónica Casadó-Anguera², Manuel Díaz-Ríos³, Vicent Casadó², Stefan Clemens⁴, Richard P. Allen⁵, Christopher J. Earley⁵ and Diego García-Borreguero⁶

¹ Integrative Neurobiology Section, National Institute on Drug Abuse, Intramural Research Program, National Institutes of Health, Baltimore, MD, United States, ² Center for Biomedical Research in Neurodegenerative Diseases Network and Department of Biochemistry and Molecular Biomedicine, Faculty of Biology, Institute of Biomedicine of the University of Barcelona, University of Barcelona, Barcelona, Spain, ³ Department of Anatomy and Neurobiology and Institute of Neurobiology, University of Puerto Rico, San Juan, PR, United States, ⁴ Department of Physiology, Brody School of Medicine, East Carolina University, Greenville, NC, United States, ⁵ Center for Restless Legs Study, Department of Neurology, Johns Hopkins University, Baltimore, MD, United States, ⁶ Sleep Research Institute, Madrid, Spain

OPEN ACCESS

Edited by:

David Blum,
Institut National de la Santé et de la
Recherche Médicale, France

Reviewed by:

Giuseppe Gangarossa,
Paris Diderot University, France
David Devos,
Centre Hospitalier Régional et
Universitaire de Lille, France

*Correspondence:

Sergi Ferré
sferre@intra.nida.nih.gov

Specialty section:

This article was submitted to
Neurodegeneration,
a section of the journal
Frontiers in Neuroscience

Received: 30 October 2017

Accepted: 11 December 2017

Published: 08 January 2018

Citation:

Ferré S, Quiroz C, Guitart X, Rea W, Seyedian A, Moreno E, Casadó-Anguera V, Díaz-Ríos M, Casadó V, Clemens S, Allen RP, Earley CJ and García-Borreguero D (2018) Pivotal Role of Adenosine Neurotransmission in Restless Legs Syndrome. *Front. Neurosci.* 11:722. doi: 10.3389/fnins.2017.00722

The symptomatology of Restless Legs Syndrome (RLS) includes periodic leg movements during sleep (PLMS), dysesthesias, and hyperarousal. Alterations in the dopaminergic system, a presynaptic hyperdopaminergic state, seem to be involved in PLMS, while alterations in glutamatergic neurotransmission, a presynaptic hyperglutamatergic state, seem to be involved in hyperarousal and also PLMS. Brain iron deficiency (BID) is well-recognized as a main initial pathophysiological mechanism of RLS. BID in rodents have provided a pathogenetic model of RLS that recapitulates the biochemical alterations of the dopaminergic system of RLS, although without PLMS-like motor abnormalities. On the other hand, BID in rodents reproduces the circadian sleep architecture of RLS, indicating the model could provide clues for the hyperglutamatergic state in RLS. We recently showed that BID in rodents is associated with changes in adenosinergic transmission, with downregulation of adenosine A₁ receptors (A1R) as the most sensitive biochemical finding. It was hypothesized that A1R downregulation leads to hypersensitive striatal glutamatergic terminals and facilitation of striatal dopamine release. Hypersensitivity of striatal glutamatergic terminals was demonstrated by an optogenetic-microdialysis approach in the rodent with BID, indicating that it could represent a main pathogenetic factor that leads to PLMS in RLS. In fact, the dopaminergic agonists pramipexole and ropinirole and the $\alpha_2\delta$ ligand gabapentin, used in the initial symptomatic treatment of RLS, completely counteracted optogenetically-induced glutamate release from both normal and BID-induced hypersensitive corticostriatal glutamatergic terminals. It is a main tenet of this essay that, in RLS, a single alteration in the adenosinergic system, downregulation of A1R, disrupts the adenosine-dopamine-glutamate balance uniquely controlled by adenosine and dopamine receptor heteromers in the striatum and also the A1R-mediated inhibitory control of glutamatergic neurotransmission in the cortex and other non-striatal brain areas, which altogether determine both PLMS and hyperarousal. Since A1R agonists would be associated with severe

cardiovascular effects, it was hypothesized that inhibitors of nucleoside equilibrative transporters, such as dipyridamole, by increasing the tonic A1R activation mediated by endogenous adenosine, could represent a new alternative therapeutic strategy for RLS. In fact, preliminary clinical data indicate that dipyridamole can significantly improve the symptomatology of RLS.

Keywords: Restless Legs Syndrome, periodic leg movements during sleep, hyperarousal, dopamine, glutamate, adenosine, ENT1

BID-INDUCED ALTERATIONS IN THE DOPAMINERGIC AND GLUTAMATERGIC SYSTEMS IN RLS

Restless Legs Syndrome (RLS) is a very prevalent neurologic disorder. According to the RLS Epidemiology, Symptoms and Treatment (REST) study, 5% of US and European reported experiencing RLS symptoms at least weekly (Allen et al., 2005). Those symptoms include a periodic, rest-induced, mostly nocturnal, movement-responsive urge to move the legs or periodic leg movements during sleep (PLMS) and hyperarousal (Allen et al., 2010; Ferri et al., 2014; Ferré et al., 2015). Thus, RLS patients do not report sleepiness during daytime, even though the total sleep time averages less than 5.5 h (Allen et al., 2010). The deficits of sensorimotor integration that promote PLMS and hyperarousal are interrelated, but there is no obvious cause-effect relationship between the two phenomena. The interrelation can be demonstrated in polysomnographic studies, which allows measuring the relation between the onset and offset of the arousal events and the concomitant onset and offset of PLMS. These studies have shown that, although it is generally believed that PLMS cause the arousal episodes, these precede the onset of PLMS in more than 40% of cases (Ferré et al., 2015). However, their tight temporal relationship suggests that both events are dependent on a common additional mechanism.

Altered dopaminergic function seems to play an important role in PLMS, which is empirically supported by the significant therapeutic response to L-dopa and dopamine receptor agonists, such as pramipexole and ropinirole (Earley et al., 2014). And it is generally believed that because these drugs have a preferential affinity for dopamine D₃ vs. dopamine D₂ receptors (D3R and D2R, respectively), that D3R constitute a main target responsible for their therapeutic effects (Varga et al., 2009; Manconi et al., 2011). Nevertheless, there is also evidence of biochemical alterations in the dopaminergic system. The dopaminergic profile in RLS includes abnormally high levels of the dopamine metabolite 3-ortho-methyldopa (3-OMD) in the CSF (Allen et al., 2009), a decrease in the density of striatal D2R and a pronounced increase in tyrosine hydroxylase activity in the striatum and substantia nigra (Connor et al., 2009). This would be mostly compatible with a *presynaptic hyperdopaminergic state*, with downregulation of D2R being probably an adaptation secondary to an increased basal dopaminergic tone (Earley et al., 2014). The presence of a hyperdopaminergic state in the basal ganglia obviously posits the question about the mechanism involved in the therapeutic effect of dopamine receptor agonists.

On the other hand, glutamatergic mechanisms probably play an important role in the RLS hyperarousal component. A magnetic resonance spectroscopy imaging study in subjects with RLS showed a significant increase in the thalamic concentration of glutamate (measured by the proxy variable Glx, which represents glutamate plus glutamine), which correlated with the time spent awake during the sleep period (Allen et al., 2013b). These findings therefore suggest a *presynaptic hyperglutamatergic state* in RLS that could underlie the hyperarousal of RLS. In fact, glutamatergic mechanisms play a central role in the therapeutic effects of $\alpha_2\delta$ ligands, such as gabapentin and pregabalin, which are the main therapeutic alternative to dopaminergic ligands for initial treatment of RLS (Garcia-Borreguero et al., 2013). Thus, $\alpha_2\delta$ ligands bind to an auxiliary regulatory protein ($\alpha_2\delta$) of voltage-dependent calcium channels that preferentially modulate neurotransmitter release from glutamatergic terminals (Dooley et al., 2007). The $\alpha_2\delta$ ligands are most effective for the sleep disturbances in RLS, but, although less effective than dopaminergic agonists, they are also effective for PLMS, (Garcia-Borreguero et al., 2014). In summary, RLS pathophysiology seems to depend on alterations in two different, but *somehow interrelated*, neurotransmitter systems, dopamine and glutamate. The dopaminergic system is mostly related to the disturbance in sensorimotor integration with the emergence of PLMS and glutamate seems to be involved with both PLMS and hyperarousal.

Brain iron deficiency (BID) is recognized as a main initial pathophysiological mechanism in the development of RLS (Earley et al., 2014). The association between iron deficiency and RLS was originally described by Nordlander (1953). Further studies showed a high prevalence of RLS symptoms in conditions with compromise of iron availability (Allen and Earley, 2007). The prevalence of RLS in a population of patients with iron-deficient anemia was reported to be as high as 31.5% (Allen et al., 2013a), about six times higher than the prevalence for RLS in the general population (Allen et al., 2005). Nevertheless, most patients with RLS do not have systemic iron deficiency. Although, as already proposed by Nordlander, RLS patients present a specific iron insufficient state in the brain. Thus, all studies of CNS iron have consistently shown BID in RLS (reviewed in Earley et al., 2014). This *brain-specific deficit in iron* seems to be related to a dysregulation of iron transportation by the blood-brain barrier. Thus, postmortem studies suggest alterations in the expression or function of iron management proteins in the choroid plexus and brain microvasculature (Connor et al., 2011). It would therefore be appropriate to address RLS as a brain iron dyshomeostasis, a functional

disorder of iron acquisition by the brain (Connor et al., 2017). Significantly, there is clinical and experimental evidence for a connection between BID and the alterations in the dopaminergic system in RLS. Autopsy analysis have revealed that the immunostaining for iron management proteins is altered in the substantia nigra of RLS brains and the profile of proteins responsible for iron management in the neuromelanin cells of the substantia nigra indicate iron deficiency (Connor et al., 2004). Furthermore, there is significant literature from animal research that indicates a close relationship between brain iron status and the dopaminergic system (for review, see Earley et al., 2014).

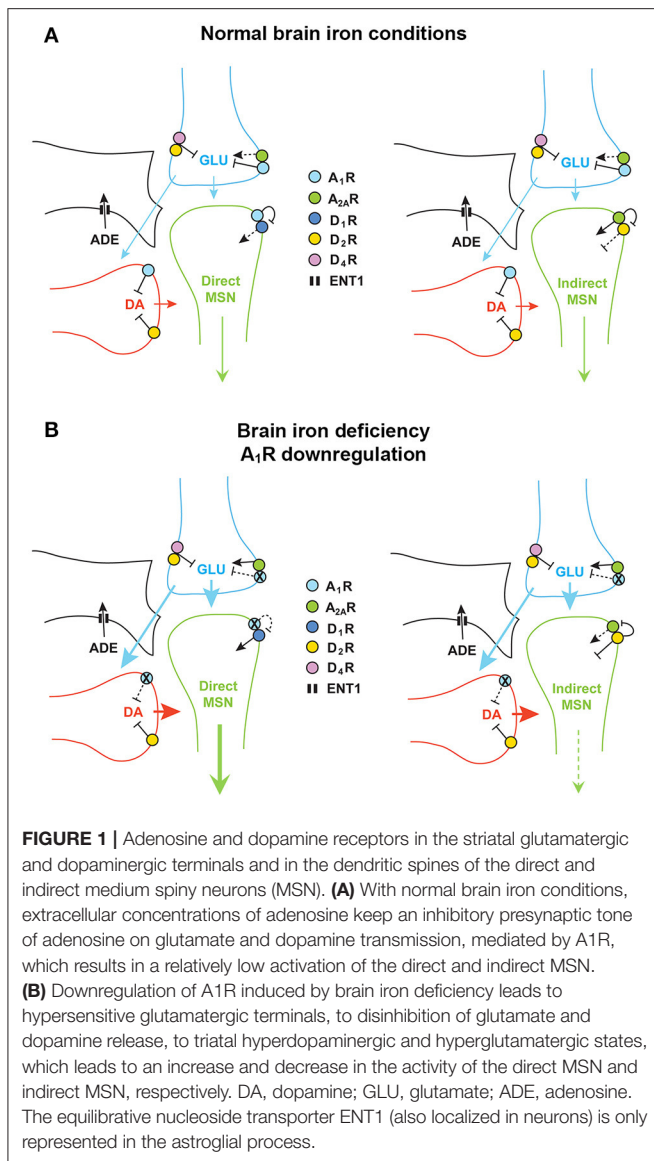
In rodents, BID (including in the ventral midbrain) can be consistently induced by providing a severe iron-deficient diet during the post-weaning period. Even though it does not show motor alterations that would imitate PLMS, the post-weaning, diet-induced BID rodent represents a well-accepted pathophysiological model of RLS (Connor et al., 2009; Earley et al., 2014; Unger et al., 2014). In fact, it provides a biological model for the understanding of the connection of the iron and dopamine alterations in RLS, since it reproduces the main alterations in dopaminergic transmission observed in RLS patients. Those include an increase in striatal extracellular concentrations of dopamine, a reduction in the density of striatal D2R and an increased TH activity in the ventral midbrain (Connor et al., 2009; Unger et al., 2014). Although it does not show motor abnormalities, the BID rodent does reproduce the circadian sleep architecture of RLS, showing an increase in wakefulness at the end of the awake period, which corresponds to the circadian time point where RLS symptoms are associated with maximal disruption of sleep (Dean et al., 2006). This implies that this model could also provide clues for the mechanisms involved in the hyperglutamatergic state of RLS or for alterations in other neurotransmitter systems that could underlie the changes in both the glutamatergic and the dopaminergic systems. A possible candidate is adenosine and its two main receptor subtypes in the brain, A₁ and A_{2A} receptors (A1R and A2AR). Thus, well-known main functions of adenosine are: first, to exert a brake in the function of the ascending dopaminergic system by presynaptic mechanisms and by postsynaptic mechanisms mediated by receptor complexes of specific adenosine and dopamine receptor subtypes, the A1R-dopamine D₁ receptor (D1R) and A2AR-D2R heteromers (Ferré et al., 1997, 2016; Ginés et al., 2000; Hillion et al., 2002; Canals et al., 2003); second, to act as a universal A1R-mediated presynaptic inhibitor of glutamatergic transmission (Wu and Saggau, 1997; Dunwiddie and Masino, 2001; Cunha, 2016); third, to act as a mediator of sleepiness induced by prolonged wakefulness, when adenosine accumulates in the extracellular space and acts mostly on A1R localized in basal forebrain, cortex, and hypothalamus (McCarley, 2007; Ferré, 2010). As here reviewed, adenosine neurotransmission can provide the link between dopamine and glutamate mechanisms in RLS and a hypoadenosinergic state can explain the hyperdopaminergic and hyperglutamatergic state of RLS.

BID-INDUCED ALTERATIONS IN THE ADENOSINERGIC SYSTEM

In view of the established functional and molecular interactions between striatal D2R and A2AR (see below), we first investigated possible alterations in the density or function of striatal A2AR associated with BID in rodents. In fact, in three separate studies we found a consistent upregulation of striatal A2AR in rats and rodents with severe BID, which was behaviorally associated with a higher efficacy of A2AR antagonists to produce locomotor activation (Gulyani et al., 2009; Quiroz et al., 2010, 2016a). The A2AR upregulation could also be reproduced in a mammalian cell line upon exposure to an iron chelator (Gulyani et al., 2009). But, in our most recent study, by analyzing receptor density by Western Blot and by radioligand binding assays, we could also demonstrate a pronounced downregulation of A1R both in the striatum and in the cortex, together with the expected downregulation of striatal D2R (Quiroz et al., 2016a). When administering a less severe iron-deficient diet, still associated with BID (as demonstrated by a significant upregulation of transferrin receptor), the same degree of downregulation of A1R and D2R could be observed, but not the A2AR upregulation (Quiroz et al., 2016a). *These results indicate that downregulation of A1R might constitute a more significant clinical correlate of BID in RLS, while changes on A2AR density would be only observed with severe BID.*

In the brain, the most salient place of interactions of dopamine, glutamate and adenosine is in the striatum, in the striatal GABAergic medium spiny neurons (MSNs), which constitute more than 95% of the striatal neuronal population (Gerfen, 2004). There are two subtypes of MSNs that give rise to the two striatal efferent pathways that connect the striatum with the output structures of the basal ganglia, which are the medial segment of the globus pallidus and the substantia nigra pars reticulata (Gerfen, 2004). The direct MSN constitutes the direct pathway, since directly connects the striatum with the output structures and selectively expresses A1R and D1R, and also D3R in the ventral striatum (Ferré et al., 1996, 1997; Sokoloff and Le Foll, 2017). The indirect MSN connects the striatum with the lateral segment of the globus pallidus and the ventral pallidum, and selectively expresses A2AR and D2R (Ferré et al., 1993, 1997). We have demonstrated that A1R and D1R and A2AR and D2R form specific receptor complexes, the A1R-D1R and A2AR-D2R heteromers (Ferré et al., 1997, 2016; Ginés et al., 2000; Hillion et al., 2002; Canals et al., 2003). The biochemical properties of these heteromers will be analyzed with more detail below, but we can introduce the concept that they act as molecular devices by which endogenous adenosine, by acting on the respective adenosine receptor, tonically inhibits the affinity and signaling of the respective dopamine receptor (see below and **Figure 1A**).

Apart from the postsynaptic striatal A1R-D1R and A2AR-D2R heteromers, adenosine and dopamine receptors are also localized in the terminals of the main striatal afferents, the dopaminergic and the glutamatergic terminals (Bamford et al., 2004; Borycz et al., 2007; González et al., 2012) (**Figure 1A**). In the glutamatergic terminals, A1R form heteromers with A2AR and



D2R form heteromers with D4 receptors (Ciruela et al., 2006; González et al., 2012; Bonaventura et al., 2017) (**Figure 1A**). The A1R-A2AR heteromer acts as a concentration-dependent switch, since adenosine has more affinity for A1R than A2AR receptors, which activation inhibits and stimulates glutamate release, respectively. Under basal conditions, adenosine tonically activates predominantly A1R, which inhibits glutamate release. A2AR is activated with higher concentrations of adenosine, which would normally occur upon strong glutamatergic input (which is associated to neuronal and glial co-release of ATP and its conversion to adenosine by ectonucleotidases; Cunha, 2016). Activation of A2AR negatively modulates A1R signaling in the heteromers and promotes the opposite, glutamate release (Solinas et al., 2002; Borycz et al., 2007). The D2R and D4R localized in the glutamatergic terminals and possibly forming heteromers also play a significant role in the tonic inhibitory modulation of striatal glutamate release by dopamine (González

et al., 2012; Bonaventura et al., 2017) (**Figure 1A**). A1R and D2R are also found in dopaminergic terminals without forming heteromers, where they also exert a tonic inhibitory modulation of dopamine release. Glutamate also modulates local dopamine release, as we have recently demonstrated with optogenetic-microdialysis experiments (Quiroz et al., 2016b), by a mechanism that seems to be mostly indirect, involving activation of cholinergic interneurons and activation of nicotinic receptors localized in the dopaminergic terminals (in preparation). Finally, we should consider another player, the astrocytic process, which is involved in the indirect production of extracellular adenosine, by releasing ATP, and that clears up adenosine from the extracellular space by nucleoside transporters, particularly ENT1 (Pascual et al., 2005; Parkinson et al., 2011; Dulla and Masino, 2013; Cunha, 2016) (**Figure 1A**).

A single alteration in the adenosinergic system, downregulation of A1R, could explain the presynaptic hyperdopaminergic and hyperglutamatergic states in RLS. In particular, downregulation of A1R in the corticostriatal glutamatergic terminals could result in an increased sensitivity of those terminals to release glutamate (**Figure 1B**). These changes recapitulate those observed in A1R knockout mice that show a significant increase in striatal glutamatergic transmission, due to an increased sensitivity of glutamatergic terminals (Salmi et al., 2005). The increased sensitivity of corticostriatal terminals would facilitate stimulated glutamate release and also, secondarily, dopamine release, which could also be potentiated by downregulation of A1R in the dopaminergic terminals (**Figure 1B**). In the direct pathway MSN, this should result in stronger neuronal activation, also dependent on downregulation of A1R and disinhibition of D1R previously forming heteromers with the A1R (**Figure 1B**). We have also previously demonstrated that presynaptic A1R activity facilitates postsynaptic A2AR signaling by keeping a low tone of extracellular dopamine release. Thus, co-administration of A1R and A2AR agonists leads to a significant increase in the activity of the indirect MSN, as measured by *c-fos* and *preproenkephalin* expression (Karcz-Kubicha et al., 2003, 2006). Therefore, in the indirect MSN, presynaptic A1R downregulation should lead to decreased neuronal activity. The increased dopamine release should then lead to a reciprocal interaction in the A2AR-D2R heteromer, by which D2R activation blocks A2AR-mediated signaling through adenylyl cyclase (see below and **Figure 1B**). Since increased activation of the direct and indirect MSN leads to increase and decrease in motor activity, respectively (Gerfen and Surmeier, 2011), the concomitant respective increase and decrease in the activation of the direct and indirect MSN, could explain the akathisia-like symptoms of PLMS. *In conclusion, one single alteration, A1R downregulation-mediated increased sensitivity of corticostriatal terminals, could produce presynaptic striatal hyperglutamatergic and hyperdopaminergic states, which could be a sufficient pathophysiological mechanism to explain PLMS in RLS.* Downregulation of presynaptic D2R localized in glutamatergic and dopaminergic terminals could also be a significant contributing factor.

Consequently, we hypothesized that BID in rodents produces an increased sensitivity of corticostriatal terminals to release

glutamate. In that case, corticostriatal terminals could be a main target for the therapeutic effect of drugs clinically successful in RLS. We tested our hypothesis by using the recently introduced optogenetic-microdialysis method, which involves the use of a modified microdialysis probe with an embedded optogenetic fiber. This method allows the delivery of light surrounding the dialysis membrane, around the same discrete area being sampled for extracellular concentrations of glutamate. In addition, the device allows local perfusion by reverse dialysis of drugs (for details, see Quiroz et al., 2016b). In the first optogenetic-microdialysis study, we injected in the rat prefrontal cortex an adeno-associated virus (AAV) encoding channel-rhodopsin 2 (ChR2) fused to the yellow fluorescent protein (YFP), which allows tracking its localization. After several weeks, ChR2 was expressed by the corticostriatal terminals in the ventral striatum and the implanted optogenetic-microdialysis probe allowed measuring glutamate release by those terminals upon light-induced depolarization. We could then demonstrate that blockade of presynaptic A2AR by perfusion with the A2AR antagonist MSX-3 counteracts optogenetically-induced glutamate release (Quiroz et al., 2016b). For the experiments with BID, we aimed at a more motor-involved striatal area, the dorsal striatal area that receives innervation from the agranular motor cortex. This corticostriatal projection has been anatomically well-defined from different studies analyzing striatal neuronal activation upon cortical-electrical stimulation (Sgambato et al., 1998; Gerfen et al., 2002; Quiroz et al., 2006). A significant glutamate release could be obtained in both iron-deprived animals and controls when using a frequency of stimulation of 100 Hz (Yepes et al., 2017), found to be optimal in previous studies of cortical-electrical and striatal optogenetic stimulation (Gerfen et al., 2002; Quiroz et al., 2006, 2016b). But decreasing the frequency of stimulation to 60 Hz did not produce a significant glutamate release in control animals, although a significant glutamate release could still be observed in the rats with BID (Yepes et al., 2017). These results therefore confirmed the hypothesis of a higher sensitivity of corticostriatal terminals to depolarization-induced glutamate release in the rodent brain with BID. As in our previous study, blockade of A2AR with perfusion with MSX-3 counteracted glutamate release, both in controls at 100 Hz and in iron-deprived animals at 60 Hz (Yepes et al., 2017).

If hypersensitive corticostriatal terminals represent a main pathogenetic mechanism of RLS, they could represent a main target for the therapeutic effect of drugs currently used in RLS. As initial treatment for persistent RLS, the Mayo Clinic Recommendations include either non-ergotic dopamine agonists, such as pramipexole and ropinirole, or $\alpha_2\delta$ ligands, such as gabapentin; for refractory RLS, the recommendations are combination therapy (dopamine agonist + $\alpha_2\delta$ ligands), replenishment of iron stores or considering opioid treatment (empirically found efficient for PLMS) (Garcia-Borreguero et al., 2013; Silber et al., 2013). In fact, perfusion of either the $\alpha_2\delta$ ligand gabapentin or the dopamine agonists pramipexole or ropinirole blocked glutamate release induced by optogenetic stimulation, both in controls (at 100 Hz) and in iron-deprived animals (at 60 Hz) (Yepes et al., 2017). To our knowledge, this represents the

first example of a convergence of the two different mechanisms of action of dopaminergic and glutamatergic compounds in the BID rodent. Subsequently, we questioned the identity of dopamine receptor subtypes involved in the pharmacological effect of pramipexole and ropinirole. We have recently reported results of the optogenetic-microdialysis technique in knock-in mice expressing the long intracellular domain of D4.7, the product of a polymorphic variant of the D4R gene (*DRD4*) associated with attention deficit hyperactivity disorder (ADHD) and substance use disorders (SUD) (Bonaventura et al., 2017). When compared with the wild-type mouse D4R, the expanded intracellular domain of the humanized D4R conferred a gain of function, blunting optogenetically-induced corticostriatal glutamate release (Bonaventura et al., 2017). These results confirmed a key role of striatal D4R localized in glutamatergic terminals in the control of corticostriatal glutamatergic transmission. Since previous studies also indicated that D2SR (the short isoform of D2R) is also localized in striatal glutamatergic terminals, probably forming heteromers with D4R (González et al., 2012), we analyzed the effect of different dopamine receptor antagonists on the effect of pramipexole. Co-perfusion with selective D4R or D2R, but not D3R antagonists, counteracted the effect of pramipexole and the optogenetic stimulation could still increase glutamate release both in controls (at 100 Hz) and in iron-deprived animals (at 60 Hz), therefore indicating that D4R and D2R, but not D3R are the main targets of the inhibitory effects of dopamine receptor agonists on striatal glutamate release (Yepes et al., 2017).

STRIATAL ADENOSINE RECEPTOR HETEROMERS: THE A2AR-D2R HETEROTETRAMER

It is becoming generally accepted that GPCR receptors form pre-coupled functional complexes that include other receptors with the formation of receptor oligomers. The current definition of receptor oligomer is that of “a macromolecular complex composed of at least two (functional) receptor units (protomers) with biochemical properties that are demonstrably different from those of its individual components” (Ferré et al., 2009). To understand these unique biochemical properties, we need to understand the basis of allosterism, which is currently defined as “the process by which the interaction of a chemical or protein at one location on a protein or macromolecular complex (the allosteric site) influences the binding or function of the same or another chemical or protein at a topographically distinct site” (Smith and Milligan, 2010). An orthosteric agonist, which binds to the same receptor site than the endogenous transmitter, has two main and independent properties: affinity (the avidity with which it binds to the receptor) and intrinsic efficacy (the power with which the agonist produces its functional response). In classical GPCR allosterism, the allosteric ligand binds to a non-orthosteric site and modifies either of the properties of the orthosteric agonist. In this frame, the GPCR has been usually considered as a monomeric entity. However, accumulating convincing evidence

indicates that a main GPCR functional unit is constituted by one GPCR homodimer and its cognate G protein (Ferré et al., 2014).

Allosterism in the frame of GPCR homodimers implies the possibility of *allosteric interactions between orthosteric ligands*, either the same or different ligands. The ligand binding to the first protomer modifies either the affinity or intrinsic efficacy of the second protomer. Cooperativity usually refers to the situation where the ligand binding to the first protomer, decreases the affinity of the same ligand binding to the second protomer. But modulator and modulated ligands can also be different orthosteric ligands, agonists or antagonists (Casadó et al., 2009; Ferré et al., 2014). With GPCR heteromers, with two different protomers, we also have two possibilities: first, the same ligand, when the protomers are two different receptor subtypes, such as dopamine D1R and D3R or D2R and D4R, or adenosine A1R and A2AR; second, two obligatory different ligands, when the two protomers bind different endogenous ligands, such as A2AR and D2R or A1R and D1R (Ferré et al., 2014). One of the first clear clues of this type of allosterism in a GPCR heteromer was obtained from radioligand experiments in membrane preparations from rat striatum, where adenosine A2AR ligands were found to modulate the affinity of D2R ligands in rat striatal membrane preparations (Ferré et al., 1991d). In these experiments, the selective A2AR agonist CGS21680 displaced significantly to the right the competitive inhibition curve of dopamine vs. the D2R antagonist tritiated raclopride, indicating a decrease in the affinity of dopamine for the D2R. This experiment also demonstrated, as simultaneously confirmed by Schiffmann et al. (1991) from *in situ* hybridization experiments, that A2AR and D2R are highly co-localized in the same striatal neuron, the indirect MSN.

The possibility of real allosteric interactions between A2AR and D2R ligands strongly suggested direct intermolecular interactions between both receptors. This was later demonstrated first in artificial systems, in mammalian cells transfected with receptors fused to biosensors that only interact when in very close proximity. In Bioluminescence Resonance Energy Transfer (BRET), there is a transfer of energy from a bioluminescent donor, *Renilla* luciferase (Rluc), to a fluorescent acceptor, such as YFP, and this can only occur when both biosensors are closer than 10 nM. In Bimolecular Fluorescence Complementation (BiFC), two complementary halves of the fluorescent sensor separately fused to the putative interacting receptors should complement and reconstitute YFP and, therefore, its ability to produce fluorescence (Canals et al., 2003; Navarro et al., 2010; Bonaventura et al., 2015). These techniques can then be used to determine the biochemical properties of the GPCR heteromer and, indirectly, to allow their identification in the native tissue. *Our rationale is to identify and disrupt the heteromerization interface, the domains of the receptors that establish intermolecular interactions.* We have in fact found evidence for discrete but strong interactions between intracellular domains and extensive but very specific interactions between transmembrane domains (TMs). From *in vitro* experiments of peptide interactions with mass spectrometry we found evidence for a very discrete but powerful electrostatic interaction between an arginine-rich domain of the third intracellular loop of the D2R and a phosphate

group from a specific serine within the tail of the A2AR (Woods and Ferré, 2005). Transfection of receptors with mutations of either of these residues led to a very significant reduction of BRET (Ciruela et al., 2004; Navarro et al., 2010). In addition, the same mutations led to the loss of the ability of the A2AR agonist CGS21680 to decrease the affinity of the D2R agonist quinpirole, which demonstrated that this is, in fact, an allosteric interaction within the A2AR-D2R heteromer (Bonaventura et al., 2015).

Synthetic peptides with the amino acid sequence of the interacting domains are becoming a very successful tool to selectively disrupt the intermolecular interactions in GPCR heteromers, and not only *in vitro*, in transfected mammalian cells, but also *in situ*, in native tissues, and *in vivo*, in the experimental animal. For instance, in patch-clamp experiments with slices of the ventral striatum of mice selectively expressing green fluorescence protein (GFP) in D2R-expressing neurons (which allowed the identification of the indirect MSN), CGS21680 acted as a D2R antagonist and blocked the decrease in the neuronal excitability induced by the D2R agonist norpropylapomorphine (NPA; Azdad et al., 2009). This D2R antagonist-like effect of CGS 21680 was then completely counteracted by the intracellular application of a small peptide with a sequence of the epitope containing the interacting phosphorylated serine of the tail of the A2AR (Azzad et al., 2009). The efficacy of CGS21680 to counteract the effect of a high concentration of NPA indicated that the A2AR agonist modulates not only the affinity, but also the efficacy of the D2R agonist (Azzad et al., 2009). These results demonstrate the very significant role of the allosteric interaction within the A2AR-D2R heteromer in the modulation of the function of the indirect MSN. More recently we used peptides with amino acid sequences of TMs to explore the involvement of the transmembrane intermolecular interactions. First, we studied which TM-peptides can disrupt A2AR-D2R heteromerization *in vitro* by BiFC experiments (which were selected over BRET experiments due to the significant interference of Rluc function by the TM-peptides; Guitart et al., 2014). BiFC was selectively disrupted by peptides with the sequence of TM 5 of A2AR and D2R, but not with the corresponding TM7 peptides (Bonaventura et al., 2015). Then, the same specific disrupting peptides were used in experiments with proximity ligation assay (PLA), an antibody-based technique which allows identification of receptor complexes in native tissues (Trifilieff et al., 2011). Notably, the number of complexes was significantly reduced by the specific disrupting peptides, demonstrating the existence of A2AR-D2R heteromers *in situ*, in the striatum (Bonaventura et al., 2015).

The allosteric interaction in the A2AR-D2R heteromer that determines the ability of A2AR agonists to act D2R antagonists and counteract D2R-mediated decrease in the excitability of the indirect MSN could explain many results of previous behavioral studies, such as the ability of adenosine agonists to reduce the locomotor activity induced by D2R agonists in reserpinized mice or the opposite effect with adenosine receptor antagonists, such as caffeine (Ferré et al., 1991a,b). The effect of adenosine antagonists indicated that endogenous adenosine exerts a tonic influence on D2R signaling through the A2AR-D2R heteromer.

It is now becoming accepted that the psychostimulant effects of caffeine (a non-selective A1R and A2AR antagonist) and selective A2AR antagonists depend on the blockade of the tonic effect of endogenous adenosine mediated by the A2AR-D2R heteromer (Ferré, 2016). Not surprisingly, we also found that A2AR agonists produce catalepsy, which was counteracted by adenosine antagonists, like theophylline (Ferré et al., 1991c). But it was also counteracted by D2R agonists, indicating the existence of a possible *reciprocal interaction*, by which D2R activation decreases the effect of A2AR activation (Ferré et al., 1991c). In fact, A2AR and D2R are respectively coupled to Gs/olf (Gs for short) and Gi/o proteins (Gi for short) and we would expect an antagonistic interaction at adenylyl cyclase level, the canonical interaction by which activation of a Gi-coupled receptor counteracts adenylyl cyclase activation, cAMP accumulation, induced by activation of a Gs-coupled receptor (Gilman, 1987). We explored this possibility in mammalian cells transfected with A2AR and D2R and found that this is the case, that the D2R agonist quinpirole completely antagonizes CGS21680-induced cAMP accumulation and the concomitant downstream signaling, such as an increase in the expression of the immediate-early gene *c-fos* (Kull et al., 1999). This reciprocal D2R-A2AR interaction could also explain the ability of non-selective adenosine receptor antagonists like caffeine and theophylline, as well as selective A2AR antagonists, to counteract the behavioral effects of D2R antagonists, such as catalepsy induced by haloperidol (Casas et al., 1988; Kanda et al., 1994; Shiozaki et al., 1999; Morelli and Wardas, 2001). This would also imply the existence of a *tone of endogenous dopamine mediated by D2R that counteracts the effects of a tone of endogenous adenosine mediated by A2AR*. The blockade of D2R releases A2AR signaling and it is then endogenous adenosine that produces catalepsy upon haloperidol administration. This has been demonstrated in several *ex vivo* studies, where the increase in striatal expression of *c-fos* induced by a D2R antagonist is blocked by non-selective adenosine receptor antagonists and by selective A2AR, but not A1R antagonists (see for instance Pardo et al., 2013).

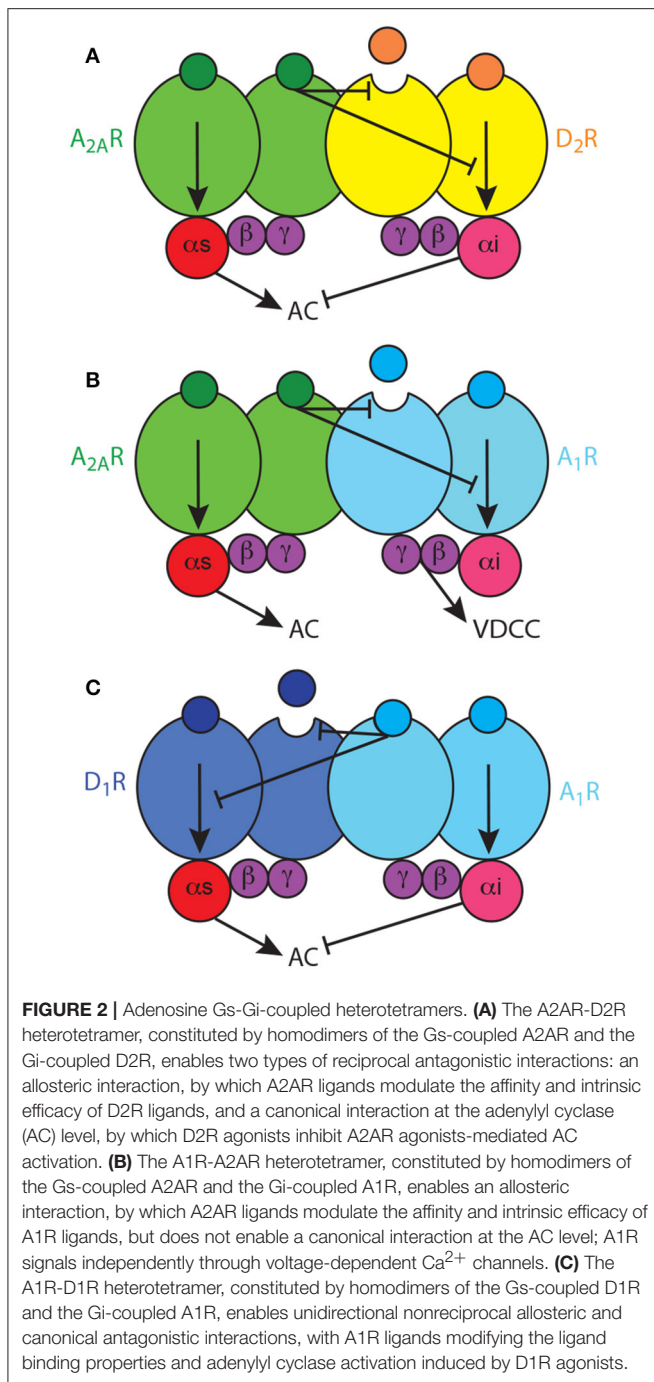
Next obvious question is how two apparently incompatible interactions, the allosteric and the canonical interactions, coexist, and if the canonical interaction also depends on heteromerization. That took us to reconsider the quaternary structure of the A2AR-D2R heteromer, since, just because of steric hindrance, a heterodimer cannot bind simultaneously two G proteins. *We therefore established the following hypotheses: first, that heteromers are often heterotetramers, heteromers of homodimers coupled to their preferred G protein; second, that the heterotetramer enables the canonical antagonistic Gs-Gi interaction; third, that the heterotetramer gives the frame for the pre-coupling of the two receptors involved in the canonical interaction, their respective G proteins and the effector adenylyl cyclase* (Ferré, 2015) (Figure 2A). Using a double complementation assay, with both BiFC and Rluc complementation, fusing the complementary halves of the BRET biosensors to different molecules of A2AR and D2R, we could demonstrate that such a quaternary structure is in fact possible in transfected cells (Bonaventura et al., 2015). Subsequently, we have used all possible 14 TM-peptides corresponding to the

seven TMs of A2AR and the seven TMs of D2R and studied the interface of not only A2AR and D2R, but also the A2AR and D2R homodimers in BiFC experiments. Significantly, only one peptide, TM6 of A2A, disrupted A2AR dimerization, and only one peptide, TM6 of D2R, disrupted D2R dimerization. Furthermore, again TM5, but also TM4, of both A2AR and D2R disrupted A2AR-D2R heteromerization (Navarro et al., submitted). Importantly, taking into account these results, as well as the crystal structure of the A2AR, the D3R (as homologous to the D2R) and the β_2 adrenergic receptor in complex with Gs, computerized modeling allowed only one solution, a linear quaternary structure of the A2AR-D2R heterotetramer, with two internal protomers that provide the heteromeric interface and two external protomers that couple to the alpha subunits of their respective G protein (Navarro et al., submitted).

We have then addressed the possible dependence on heteromerization of the A2AR-D2R canonical interaction in striatal cells in culture, where we previously showed that quinpirole counteracts cAMP accumulation induced by CGS21680 (Navarro et al., 2014). First, we could demonstrate the existence of the A2AR-D2R heteromers in the striatal cultures with PLA. Thus, TM4 and TM5, but not TM6 or TM7, of both A2AR and D2R disrupted the A2AR-D2R complexes (Navarro et al., submitted). Then, only the peptides that disrupted heteromerization disrupted the canonical interaction. Therefore, we could confirm that the canonical interaction is a biochemical property of the A2AR-D2R heterotetramer. *In conclusion, both the allosteric and the canonical interactions are biochemical properties of the A2AR-D2R heterotetramer, which acts as a molecular device that integrates the adenosinergic and dopaminergic signals in the indirect MSN*. The output is mostly determined by the dopaminergic input (high and low for positive and negative reward prediction errors; Ferré, 2017) and amplified by the wining A2AR-D2R interaction, either allosteric or canonical (Ferré, 2016, 2017). In addition, from experiments with BRET and BiFC, fusing the biosensors to the A2AR or D2R and to adenylyl cyclase type 5 (AC5), we obtained evidence for the pre-coupling of the A2AR-D2R heterotetramer, Gs and Gi proteins and the effector adenylyl cyclase subtype 5 (AC5). Taking into account our results with TM peptides corresponding to the putative TMs of adenylyl cyclase, computer modeling (now also including Gs in complex with the catalytic domains of adenylyl cyclase) suggested that one heterotetramer can bind two molecules of AC and that one molecule of AC can bind two heterotetramers, allowing the formation of high-order oligomers with alternative links of heterotetramers and AC (Navarro et al., submitted).

STRIATAL ADENOSINE RECEPTOR HETEROMERS: THE A1R-A2AR AND A1R-D1R HETEROTETRAMERS

The A2AR-D2R heterotetramer is the most studied and best characterized GPCR heteromer. Therefore, it can then be used as a model for establishing similarities and differences in the biochemical properties of other GPCR heteromers. Apart from the



A2AR-D2R heteromer, the same tetrameric quaternary structure has been observed for four additional striatal Gs-Gi-coupled heteromers which could also be involved in the pathophysiology of RLS: the A1R-A2AR heterotetramer (Ciruela et al., 2006; Navarro et al., 2016) and the A2AR-CB1R heterotetramer (in preparation), both localized in the striatal glutamatergic terminals, and the D1R-D3R heterotetramers (Fiorentini et al., 2008; Marcellino et al., 2008; Guitart et al., 2014) and the A1R-D1R heterotetramer (in preparation), both localized in the direct MSN. The D2SR-D4R heteromer, on the other hand, is

only coupled to Gi proteins and, so far, we do not know if its predominant quaternary structure is dimeric or tetrameric. As mentioned above, the A2AR-D2R heteromer is probably indirectly involved in the dysregulation of striatal function that leads to PLMS symptoms, related to a predominant canonical interaction, the D2R-mediated inhibition of A2AR-mediated signaling, associated to the presynaptic hyperdopaminergic state. But, as also mentioned above, BID-induced downregulation of A1R seems could be a main pathogenetic mechanism in RLS, which should imply a more direct involvement of the A1R-A2AR and A1R-D1R heteromers. Interestingly, the analysis of the structure (homo and heteromeric interfaces) and biochemical properties of the different heterotetramers discloses differences that differ from those of the A2AR-D2R heterotetramer. Significantly, those biochemical differences closely relate to their properties as modulators of neuronal function (excitability, neurotransmitter release).

As mentioned above, the A1R-A2AR heterotetramer acts as a concentration-dependent switch, since adenosine has more affinity for the A1R than for the A2AR, allowing low concentrations of adenosine to inhibit and high concentrations to stimulate striatal glutamate release, by activating A1R and A2AR, respectively (Ciruela et al., 2006). Different from postsynaptic receptors (see above), studies with selective antagonists indicate that striatal presynaptic A2AR are not tonically activated by adenosine while presynaptic A1R are tonically activated, particularly in specific striatal compartments. Thus, A1R antagonists increase, while A2AR antagonists do not modify, the striatal extracellular concentration of glutamate (Solinas et al., 2002; Borycz et al., 2007). This might be related to the higher density of postsynaptic receptors and also indicates that *presynaptic A1R are more sensitive than presynaptic A2AR to the variations of endogenous adenosine*. Clearly, the A1R-A2AR heteromer-mediated concentration-dependent switch mechanism cannot be explained in the frame of a canonical interaction at the level of adenylyl cyclase, where the result of the activation of a Gi-coupled receptor depends on its ability to counteract adenylyl cyclase activation by a Gs-coupled receptor. In fact, we have obtained evidence for the lack of existence of canonical interaction in the A1R-A2AR heterotetramer (Navarro et al., submitted) (Figure 2B). Thus, in the glutamatergic terminals, A1R can signal independently of A2AR within the A1R-A2AR heteromer, most probably by a $\beta\gamma$ -dependent-mediated inhibition of presynaptic voltage-dependent Ca²⁺ channels (Wu and Saggau, 1997; Gonçalves and Queiroz, 2008). Yet, when reaching the right concentration to bind A2AR, adenosine inhibits A1R function by a negative allosteric interaction and promotes glutamate release by activating adenylyl cyclase (Ciruela et al., 2006; Gonçalves and Queiroz, 2008) (Figure 2B). The same mechanism has also been described in cortical astrocytes in culture, where A1R-A2AR heteromers modulate GABA uptake (Cristóvão-Ferreira et al., 2013). In addition, evidence for A2AR-D2R heteromers that modulate glutamate release has recently been obtained in striatal astrocytes in culture (Cervetto et al., 2017). The presence and functional significance of these astrocytic adenosine receptor heteromers need still to be determined.

Soon after the discovery of specific pharmacological interactions between A2AR and D2R, similar antagonistic interactions were observed with A1R and D1R ligands, with A1R agonists and antagonists promoting the specific inhibition and facilitation of D1R agonist-mediated locomotor activation, respectively (Ferré et al., 1994, 1996). Similarly, specific biochemical and possibly intermolecular interactions were reported which pointed to the existence of A1R-D1R heteromers (Ferré et al., 1998; Ginés et al., 2000), and which would selectively modulate the function of the direct MSN (Ferré et al., 1994, 1997, 1999). The initial studies in mammalian transfected cells indicated the existence of both allosteric and canonical interactions, but, different to those in the A2AR-D2R heteromer, not reciprocal, with A1R ligands modifying the ligand binding properties and adenylyl cyclase activation induced by D1R agonists (Ferré et al., 1998) (**Figure 2C**). Using TM peptides, BiFC and PLA experiments, we have now obtained experimental evidence for the tetrameric structure of A1R-D1R, for the dependence on heteromerization for the canonical interaction and for the presence of the heteromer in striatal tissue (Moreno et al. in preparation) and the spinal motoneuron (Rivera-Oliver et al., submitted). The spinal A1R-D1R heterotetramer can explain the recently demonstrated spinally-generated caffeine-induced locomotor activation in rats (Acevedo et al., 2016), and we put forward the hypothesis that it can represent a mechanism involved in the spinal component of RLS (Trenkwalder and Paulus, 2010).

TARGETING ADENOSINE NEUROTRANSMISSION IN RLS: THE EQUILBRATIVE TRANSPORTER ENT1

Apart from the striatum, which could represent a main locus for the alteration of sensory-motor integration in RLS, involved in PLMS symptoms, hypoadenosinergic transmission should also occur in other brain areas. In fact, as mentioned above, we could also demonstrate downregulation of A1R in the cortex of mice with severe and less severe BID (Quiroz et al., 2016a). As mentioned above, adenosine is a main mediator of sleepiness following prolonged wakefulness, which determines its extracellular accumulation in the basal forebrain, cortex, and hypothalamus. Upon activation of A1R, this accumulation leads to inhibition of the cells of origin of the corticopetal basal forebrain system (McCarley, 2007; Ferré, 2010) and the prefrontal corticofugal neurons that innervate the cells of origin of the pontine ascending arousal systems (Van Dort et al., 2009). Upon activation of both A1R and A2AR, adenosine also inhibits the hypothalamic histaminergic and orexinergic ascending arousal systems (McCarley, 2007; Ferré, 2010). BID-mediated A1R downregulation in the basal forebrain, cortex, and hypothalamus, could then be the main pathophysiological mechanism responsible for the hyperarousal and sleep disturbances of RLS. In fact, experimental data strongly suggest that A1R is a marker of the homeostatic sleep response, of the need for recovery of lack of sleep. This includes the rebound sleepiness and the cumulative sleepiness after acute and chronic

sleep deprivation, respectively (Bjorness et al., 2009, 2016; Kim et al., 2012). It has in fact been demonstrated that acute and chronic sleep deprivation lead to A1R upregulation in the brain, including both cortex and striatum (Elmenhorst et al., 2007, 2009; Kim et al., 2012, 2015). Finally, as mentioned above, spinal A1R downregulation, and particularly in the motoneuron, could decrease the D1R inhibition, by decreasing the stoichiometry of D1R forming heteromers with D1R.

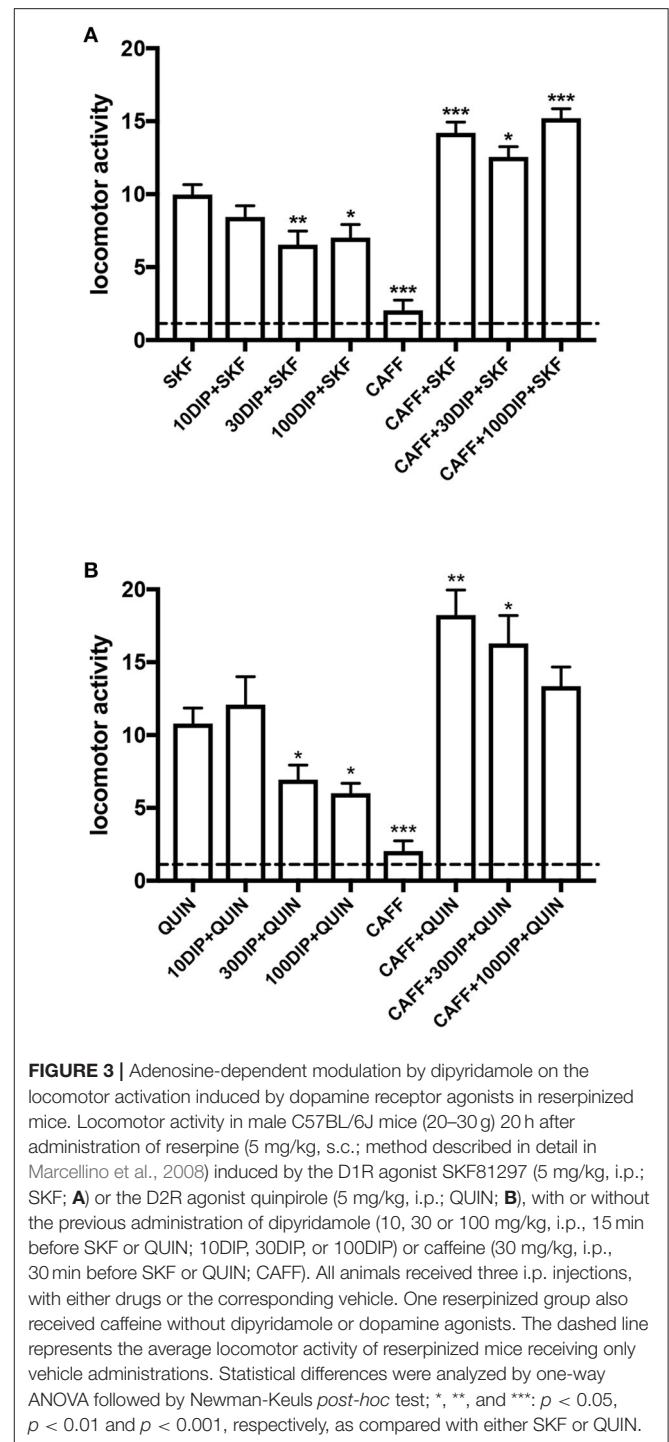
If A1R downregulation-dependent hypoadenosinergic transmission represents a significant pathogenetic factor in RLS and is directly or indirectly involved in the symptoms of both PLMS and hyperarousal, administration of A1R agonist should represent a successful therapeutic strategy. Unfortunately, A1R agonists cannot be used as direct targets, since they produce very significant peripheral effects, namely pronounced bradycardia and hypotension (Schindler et al., 2005). An alternative strategy would be to increase the adenosine tone below the limit of activation of presynaptic A2AR, with inhibitors of adenosine transporters or adenosine metabolism. Our initial choice is focusing on equilibrative nucleoside transporters. Nucleoside transporters are not only important as a mechanism to salvage extracellular nucleosides for intracellular synthesis of nucleotides, but they are also important as regulators of the extracellular levels of adenosine and as providers of an endogenous tone of adenosinergic neurotransmission mediated by adenosine receptors. In mammals, there are two types of nucleoside transporters, equilibrative and concentrative, which mediate a bidirectional equilibrative transport driven by chemical gradient and a unidirectional concentration transport driven by sodium electrochemical gradient, respectively (Parkinson et al., 2011). Adenosine uptake in the brain occurs primarily by facilitated diffusion via equilibrative transporters, which pharmacological blockade is associated with an accumulation of adenosine in the extracellular space (Parkinson et al., 2011; Dulla and Masino, 2013; Cunha, 2016). From the four types of equilibrative transporters so far identified (ENT1, ENT2, ENT3, and ENT4), ENT1 and ENT2 are the most expressed in the brain, both by neurons and astrocytes (Parkinson et al., 2011). Nevertheless, some studies suggest that ENT1 has a more salient role in determining the concentration of extracellular adenosine in the brain and its dependence on glutamate receptor activation (Alanko et al., 2006; Bicket et al., 2016). Furthermore, of importance for the present discussion, ENT1 (but not ENT2) shows a regional co-localization with A1R, which supports an important role of ENT1-mediated transport of adenosine in the control of the neuromodulatory actions mediated by A1R in the human brain (Jennings et al., 2001).

We can therefore deduce that ENT1 inhibitors could be useful therapeutic agents in RLS. Importantly, some non-selective ENT1/ENT2 inhibitors such as dipyridamole are already being medically used for other clinical purposes. Dipyridamole is used as an inhibitor of platelet aggregation to decrease the risk of thromboembolic complications and recurrence of stroke in patients known to have atherosclerotic cerebrovascular disease. Its effect depends on a combination of mechanisms, including cAMP accumulation in platelets induced by phosphodiesterase inhibition and activation of A2AR by an increased extracellular

adenosine secondary to ENT1/2 inhibition in microvascular endothelial cells (Kim and Liao, 2008). However, the possible use of dipyridamole (and other ENT1/ENT2 inhibitors) as a central nervous system agent remains uncertain in view of its reported low ability to cross the blood-brain barrier (Sollevi, 1986; Parkinson et al., 2011) and, to our knowledge, it is not well-established if systemic administration of dipyridamole in the experimental animal leads to behaviorally significant increases in the extracellular levels of adenosine.

Using the classical reserpinized mice model, we evaluated the ability of the systemic administration of dipyridamole to promote an increase in the adenosinergic tone in the brain. In that case, dipyridamole should counteract the locomotor activating effects of D1R and D2R, by acting on striatal A1R-D1R and A2AR-D2R heteromers (Ferré et al., 1991a,b, 1994), and the effect of dipyridamol should then be counteracted by a non-selective A1R/A2AR antagonist, like caffeine. This model, in fact, has been very useful for the discovery of the specific antagonistic interactions between adenosine and dopamine receptor ligands that led to the discovery the A2AR-D2R and A1R-D1R heteromers. As shown in **Figure 3**, dipyridamole, at a minimal dose of 30 mg/kg, significantly decreased the locomotor-activating effect of equipotent doses of the D1R agonist SKF81297 and the D2R agonist quinpirole (5 mg/kg in both cases). As expected, caffeine (30 mg/kg) did not produce a significant effect on its own but significantly potentiated the locomotor activation induced by either agonist. In both cases, the depressant effect of dipyridamole was totally counteracted by caffeine (**Figure 3**). The results, therefore, can entirely be explained by the ability of systemically administered dipyridamole to promote an increase in the basal extracellular levels of striatal adenosine than normally exert a tonic activating effect on postsynaptic A1R-D1R and A2AR-D2R heteromers. Also, such an increase should be expected to increase the activation of presynaptic A1R and hopefully restore the hyperdopaminergic and hyperglutamatergic state in RLS patients. Optogenetic-microdialysis experiments are in progress to demonstrate the ability of dipyridamole to inhibit glutamatergic neurotransmission in hypersensitive corticostriatal terminals in BID rats.

In view of the evidence for the central adenosinergic effect of dipyridamole in reserpinized mice, we explored the possible clinical efficacy of dipyridamole in a prospective 2-month open trial in 13 previously untreated patients diagnosed with idiopathic RLS (García-Borreguero et al., submitted). Therapeutic response was defined as at least a 50% improvement in the “International RLS Scale” and the “Multiple Suggested Immobilization Tests.” Sleep efficiency (SE%), sleep latency and other standard scales were used to evaluate sleep dysfunction and hyperarousal. Dipyridamole was well-tolerated and only two patients had to discontinue at the beginning of the trial due to dizziness. Six and four out of the thirteen patients were full and partial responders, respectively, and only three patients had no significant response. Importantly, not only there was a significant effect of subjective symptoms, but also of PLMS and sleep complaints. These are, of course, preliminary results which could be influenced by a placebo effect and, therefore, await confirmation by a more extensive double-blind clinical trial.



Confirmation of the therapeutic effect of dipyridamole in RLS would bring ENT1 inhibition as a new therapeutic approach for RLS, offering an alternative to dopaminergic drugs and, therefore, to their long-term complications, mainly augmentation. This is an overall increase in symptom severity and intensity and represents a common complication of all dopaminergic drugs, with prevalence rates of nearly 50%, and is a common cause of treatment failure (Earley et al., 2014; Ferré et al., 2017).

Furthermore, our preliminary results suggest that, in contrast to dopaminergic agonists, ENT1 inhibitors should be effective not only for the treatment of dysesthesias and PLMS, but also for sleep complaints and hyperarousal in RLS. In addition to dipyrindamole, there are other marketed compounds with ENT1 inhibitory activity already used at the clinical level for their vascular relaxation and platelet inhibition (ticagrelor, dilazep) or their anti-inflammatory effects (sulindac). The challenge would nevertheless be to obtain new potent and selective ENT1 (or ENT1/ENT2) inhibitors with significant brain penetration.

It conclusion, the main tenet of this essay is that a main mechanism responsible for PLMS and hyperarousal in RLS can be a BID-induced hypoadenosinergic state, with downregulation of A1R. This mechanism may disrupt the adenosine-dopamine-glutamate balance uniquely controlled by adenosine and dopamine receptor heteromers in the striatum and also the A1R-mediated inhibitory control of glutamatergic neurotransmission in the cortex and other non-striatal brain areas and in the spinal cord. We then provide preclinical and clinical evidence for a possible new alternative therapeutic strategy for RLS, increasing the adenosinergic tone in the CNS with ENT1 inhibitors.

REFERENCES

- Acevedo, J., Santana-Almansa, A., Matos-Vergara, N., Marrero-Cordero, L. R., Cabezas-Bou, E., and Díaz-Ríos, M. (2016). Caffeine stimulates locomotor activity in the mammalian spinal cord via adenosine A1 receptor-dopamine D1 receptor interaction and PKA-dependent mechanisms. *Neuropharmacology* 101, 490–505. doi: 10.1016/j.neuropharm.2015.10.020
- Alanko, L., Porkka-Heiskanen, T., and Soynila, S. (2006). Localization of equilibrative nucleoside transporters in the rat brain. *J. Chem. Neuroanat.* 31, 162–168. doi: 10.1016/j.jchemneu.2005.12.001
- Allen, R. P., Auerbach, S., Bahrain, H., Auerbach, M., and Earley, C. J. (2013a). The prevalence and impact of restless legs syndrome on patients with iron deficiency anemia. *Am. J. Hematol.* 88, 261–264. doi: 10.1002/ajh.23397
- Allen, R. P., Barker, P. B., Horská, A., and Earley, C. J. (2013b). Thalamic glutamate/glutamine in restless legs syndrome: increased and related to disturbed sleep. *Neurology* 80, 2028–2034. doi: 10.1212/WNL.0b013e318294b3f6
- Allen, R. P., Connor, J. R., Hyland, K., and Earley, C. J. (2009). Abnormally increased CSF 3-Ortho-methyl-dopa (3-OMD) in untreated restless legs syndrome (RLS) patients indicates more severe disease and possibly abnormally increased dopamine synthesis. *Sleep Med.* 10, 123–128. doi: 10.1016/j.sleep.2007.11.012
- Allen, R. P., and Earley, C. J. (2007). The role of iron in restless legs syndrome. *Mov. Disord.* 18, S440–S448. doi: 10.1002/mds.21607
- Allen, R. P., Stillman, P., and Myers, A. J. (2010). Physician-diagnosed restless legs syndrome in a large sample of primary medical care patients in western Europe: prevalence and characteristics. *Sleep Med.* 11, 31–37. doi: 10.1016/j.sleep.2009.03.007
- Allen, R. P., Walters, A. S., Montplaisir, J., Hening, W., Myers, A., Bell, T. J., et al. (2005). Restless legs syndrome prevalence and impact: REST general population study. *Arch. Intern. Med.* 165, 1286–1292. doi: 10.1001/archinte.165.11.1286
- Azdad, K., Gall, D., Woods, A. S., Ledent, C., Ferré, S., and Schiffmann, S. N. (2009). Dopamine D2 and adenosine A2A receptors regulate NMDA-mediated excitation in accumbens neurons through A2A-D2 receptor heteromerization. *Neuropsychopharmacology* 34, 972–986. doi: 10.1038/npp.2008.144
- Bamford, N. S., Zhang, H., Schmitz, Y., Wu, N. P., Cepeda, C., Levine, M. S., et al. (2004). Heterosynaptic dopamine neurotransmission

ETHICS STATEMENT

All animals used in the study were maintained in accordance with the guidelines of the National Institutes of Health Animal Care and the animal research conducted to perform this study was approved by the NIDA IRP Animal Care and Use Committee (protocol #: 15-BNRB-73).

AUTHOR CONTRIBUTIONS

WR, AS, and DG-B performed the experiments; SF, XG, AS, WR, and DG-B analyzed data; SF, WR, and DG-B designed the experiments; SF, CQ, WR, EM, VC-A, MD-R, VC, SC, RA, CE, and DG-B wrote the manuscript.

ACKNOWLEDGMENTS

Work supported by the intramural funds of the National Institute on Drug Abuse, RLS Foundation, “Ministerio de Economía y Competitividad,” MINECO/FEDER (SAF2014-54840-R), Generalitat de Catalunya (2014-SGR-1236), and Fundació la Marató de TV3 (20140610).

- selects sets of corticostriatal terminals. *Neuron* 42, 653–663. doi: 10.1016/S0896-6273(04)00265-X
- Bicket, A., Mehrabi, P., Naydenova, Z., Wong, V., Donaldson, L., Staglar, I., et al. (2016). Novel regulation of equilibrative nucleoside transporter 1 (ENT1) by receptor-stimulated Ca²⁺-dependent calmodulin binding. *Am. J. Physiol. Cell Physiol.* 310, C808–C820. doi: 10.1152/ajpcell.00243.2015
- Bjorness, T. E., Dale, N., Mettlach, G., Sonneborn, A., Sahin, B., Fienberg, A. A., et al. (2016). An adenosine-mediated glial-neuronal circuit for homeostatic sleep. *J. Neurosci.* 36, 3709–3721. doi: 10.1523/JNEUROSCI.3906-15.2016
- Bjorness, T. E., Kelly, C. L., Gao, T., Poffenberger, V., and Greene, R. W. (2009). Control and function of the homeostatic sleep response by adenosine A1 receptors. *J. Neurosci.* 29, 1267–1276. doi: 10.1523/JNEUROSCI.2942-08.2009
- Bonaventura, J., Navarro, G., Casadó-Anguera, V., Azdad, K., Rea, W., Moreno, E., et al. (2015). Allosteric interactions between agonists and antagonists within the adenosine A2A receptor-dopamine D2 receptor heterotetramer. *Proc. Natl. Acad. Sci. U.S.A.* 112, E3609–E3618. doi: 10.1073/pnas.1507704112
- Bonaventura, J., Quiroz, C., Cai, N. S., Rubinstein, M., Tanda, G., and Ferré, S. (2017). Key role of the dopamine D(4) receptor in the modulation of corticostriatal glutamatergic neurotransmission. *Sci. Adv.* 3:e1601631. doi: 10.1126/sciadv.1601631
- Borycz, J., Pereira, M. F., Melani, A., Rodrigues, R. J., Köfalvi, A., Panlilio, L., et al. (2007). Differential glutamate-dependent and glutamate-independent adenosine A1 receptor-mediated modulation of dopamine release in different striatal compartments. *J. Neurochem.* 101, 355–363. doi: 10.1111/j.1471-4159.2006.04386.x
- Canals, M., Marcellino, D., Fanelli, F., Ciruela, F., de Benedetti, P., Goldberg, S. R., et al. (2003). Adenosine A2A-dopamine D2 receptor-receptor heteromerization: qualitative and quantitative assessment by fluorescence and bioluminescence energy transfer. *J. Biol. Chem.* 278, 46741–46749. doi: 10.1074/jbc.M306451200
- Casadó, V., Ferrada, C., Bonaventura, J., Gracia, E., Mallol, J., Canela, E. I., et al. (2009). Useful pharmacological parameters for G-protein-coupled receptor homodimers obtained from competition experiments. Agonist-antagonist binding modulation. *Biochem. Pharmacol.* 78, 1456–1463. doi: 10.1016/j.bcp.2009.07.012
- Casas, M., Ferré, S., Guix, T., and Jane, F. (1988). Theophylline reverses haloperidol-induced catalepsy in the rat. Possible relevance to the

- pharmacological treatment of psychosis. *Biol. Psychiatry*. 24, 642–648. doi: 10.1016/0006-3223(88)90138-2
- Cervetto, C., Venturini, A., Passalacqua, M., Guidolin, D., Genedani, S., Fuxe, K., et al. (2017). A2A-D2 receptor-receptor interaction modulates gliotransmitter release from striatal astrocyte processes. *J. Neurochem*. 140, 268–279. doi: 10.1111/jnc.13885
- Ciruela, F., Burgueño, J., Casadó, V., Canals, M., Marcellino, D., Goldberg, S. R., et al. (2004). Combining mass spectrometry and pull-down techniques for the study of receptor heteromerization. Direct epitope-epitope electrostatic interactions between adenosine A2A and dopamine D2 receptors. *Anal. Chem*. 76, 5354–5363. doi: 10.1021/ac049295f
- Ciruela, F., Casadó, V., Rodrigues, R. J., Luján, R., Burgueño, J., Canals, M., et al. (2006). Presynaptic control of striatal glutamatergic neurotransmission by adenosine A1-A2A receptor heteromers. *J. Neurosci*. 26, 2080–2087. doi: 10.1523/JNEUROSCI.3574-05.2006
- Connor, J. R., Patton, S. M., Oexle, K., and Allen, R. P. (2017). Iron and restless legs syndrome: treatment, genetics and pathophysiology. *Sleep Med*. 31, 61–70. doi: 10.1016/j.sleep.2016.07.028
- Connor, J. R., Ponnuru, P., Wang, X. S., Patton, S. M., Allen, R. P., and Earley, C. J. (2011). Profile of altered brain iron acquisition in restless legs syndrome. *Brain* 134, 959–968. doi: 10.1093/brain/awr012
- Connor, J. R., Wang, X. S., Allen, R. P., Beard, J. L., Wiesinger, J. A., Felt, B. T., et al. (2009). Altered dopaminergic profile in the putamen and substantia nigra in restless leg syndrome. *Brain* 132, 2403–2412. doi: 10.1093/brain/awp125
- Connor, J. R., Wang, X. S., Patton, S. M., Menzies, S. L., Troncoso, J. C., Earley, C. J., et al. (2004). Decreased transferrin receptor expression by neuromelanin cells in restless legs syndrome. *Neurology* 62, 1563–1567. doi: 10.1212/01.WNL.0000123251.60485.AC
- Cristóvão-Ferreira, S., Navarro, G., Brugarolas, M., Pérez-Capote, K., Vaz, S. H., Fattorini, G., et al. (2013). A1R-A2AR heteromers coupled to Gs and G_{i/o} proteins modulate GABA transport into astrocytes. *Purinergic Signal*. 9, 433–449. doi: 10.1007/s11302-013-9364-5
- Cunha, R. A. (2016). How does adenosine control neuronal dysfunction and neurodegeneration? *J. Neurochem*. 139, 1019–1055. doi: 10.1111/jnc.13724
- Dean, T. Jr., Allen, R. P., O'Donnell, C. P., and Earley, C. J. (2006). The effects of dietary iron deprivation on murine circadian sleep architecture. *Sleep Med*. 7, 634–640. doi: 10.1016/j.sleep.2006.07.002
- Dooley, D. J., Taylor, C. P., Donevan, S., and Feltner, D. (2007). Ca²⁺ channel alpha2delta ligands: novel modulators of neurotransmission. *Trends Pharmacol. Sci*. 28, 75–82. doi: 10.1016/j.tips.2006.12.006
- Dulla, C. G., and Masino, S. A. (2013). “Physiology and metabolic regulation of adenosine: mechanisms,” in *Adenosine. A Key Link Between Metabolism and Brain Activity*, eds S. Masino and D. Boison (New York, NY: Springer), 87–107.
- Dunwiddie, T. V., and Masino, S. A. (2001). The role and regulation of adenosine in the central nervous system. *Annu. Rev. Neurosci*. 24, 31–55. doi: 10.1146/annurev.neuro.24.1.31
- Earley, C. J., Connor, J., García-Borreguero, D., Jenner, P., Winkelman, J., Zee, P. C., et al. (2014). Altered brain iron homeostasis and dopaminergic function in Restless Legs Syndrome (Willis-Ekbom Disease). *Sleep Med*. 15, 1288–1301. doi: 10.1016/j.sleep.2014.05.009
- Elmenhorst, D., Basheer, R., McCarley, R. W., and Bauer, A. (2009). Sleep deprivation increases A(1) adenosine receptor density in the rat brain. *Brain Res*. 1258, 535–538. doi: 10.1016/j.brainres.2008.12.056
- Elmenhorst, D., Meyer, P. T., Winz, O. H., Matusch, A., Erment, J., Coenen, H. H., et al. (2007). Sleep deprivation increases A1 adenosine receptor binding in the human brain: a positron emission tomography study. *J. Neurosci*. 27, 2410–2415. doi: 10.1523/JNEUROSCI.5066-06.2007
- Ferré, S. (2010). Role of the central ascending neurotransmitter systems in the psychostimulant effects of caffeine. *J. Alzheimers Dis*. 20, S35–S49. doi: 10.3233/JAD-2010-1400
- Ferré, S. (2015). The GPCR heterotetramer: challenging classical pharmacology. *Trends Pharmacol. Sci*. 36, 145–152. doi: 10.1016/j.tips.2015.01.002
- Ferré, S. (2016). Mechanisms of the psychostimulant effects of caffeine: implications for substance use disorders. *Psychopharmacology* 233, 1963–1979. doi: 10.1007/s00213-016-4212-2
- Ferré, S. (2017). “Adenosine control of striatal function. Implications for the treatment of apathy in basal ganglia disorders,” in *Adenosine Receptors in Degenerative Diseases*, eds D. Blum and L. V. Lopes (Amsterdam: Elsevier), 231–255.
- Ferré, S., Baler, R., Bouvier, M., Caron, M. G., Devi, L. A., Durrux, T., et al. (2009). Building a new conceptual framework for receptor heteromers. *Nat. Chem. Biol*. 5, 131–134. doi: 10.1038/nchembio0309-131
- Ferré, S., Bonaventura, J., Tomasi, D., Navarro, G., Moreno, E., Cortés, A., et al. (2016). Allosteric mechanisms within the adenosine A2A-dopamine D2 receptor heterotetramer. *Neuropharmacology* 104, 154–160. doi: 10.1016/j.neuropharm.2015.05.028
- Ferré, S., Casadó, V., Devi, L. A., Filizola, M., and Jockers, R., Lohse, M. J., et al. (2014). G protein-coupled receptor oligomerization revisited: functional and pharmacological perspectives. *Pharmacol. Rev*. 66, 413–434. doi: 10.1124/pr.113.008052
- Ferré, S., Earley, C., Gulyani, S., and García-Borreguero, D. (2017). In search of alternatives to dopaminergic ligands for the treatment of restless legs syndrome: iron, glutamate, and adenosine. *Sleep Med*. 31, 86–92. doi: 10.1016/j.sleep.2016.08.019
- Ferré, S., Fredholm, B. B., Morelli, M., Popoli, P., and Fuxe, K. (1997). Adenosine-dopamine receptor-receptor interactions as an integrative mechanism in the basal ganglia. *Trends Neurosci*. 20, 482–487. doi: 10.1016/S0166-2236(97)01096-5
- Ferré, S., Herrera-Marschitz, M., Grabowska-Andén, M., Ungerstedt, U., Casas, M., and Andén, N. E. (1991a). Postsynaptic dopamine/adenosine interaction: I. Adenosine analogues inhibit dopamine D2-mediated behaviour in short-term reserpinized mice. *Eur. J. Pharmacol*. 192, 25–30.
- Ferré, S., Herrera-Marschitz, M., Grabowska-Andén, M., Ungerstedt, U., Casas, M., and Andén, N. E. (1991b). Postsynaptic dopamine/adenosine interaction: II. Postsynaptic dopamine agonism and adenosine antagonism of methylxanthines in short-term reserpinized mice. *Eur. J. Pharmacol*. 192, 31–37.
- Ferré, S., O'Connor, W. T., Fuxe, K., and Ungerstedt, U. (1993). The striopallidal neuron: a main locus for adenosine-dopamine interactions in the brain. *J. Neurosci*. 13, 5402–5406.
- Ferré, S., O'Connor, W. T., Svenningsson, P., Bjorklund, L., Lindberg, J., Tinner, B., et al. (1996). Dopamine D1 receptor-mediated facilitation of GABAergic neurotransmission in the rat strioentopeduncular pathway and its modulation by adenosine A1 receptor-mediated mechanisms. *Eur. J. Neurosci*. 8, 1545–1553. doi: 10.1111/j.1460-9568.1996.tb01617.x
- Ferré, S., Popoli, P., Giménez-Llort, L., Finnman, U. B., Martínez, E., Scotti de Carolis, A., et al. (1994). Postsynaptic antagonistic interaction between adenosine A1 and dopamine D1 receptors. *Neuroreport* 6, 73–76. doi: 10.1097/00001756-199412300-00020
- Ferré, S., Rimondini, R., Popoli, P., Reggio, R., Pèzzola, A., Hansson, A. C., et al. (1999). Stimulation of adenosine A1 receptors attenuates dopamine D1 receptor-mediated increase of NGFI-A, c-fos and jun-B mRNA levels in the dopamine-denervated striatum and dopamine D1 receptor-mediated turning behaviour. *Eur. J. Neurosci*. 11, 3884–3892. doi: 10.1046/j.1460-9568.1999.00810.x
- Ferré, S., Rubio, A., and Fuxe, K. (1991c). Stimulation of adenosine A2 receptors induces catalepsy. *Neurosci. Lett*. 130, 162–164.
- Ferré, S., Torvinen, M., Antoniou, K., Irenius, E., Civelli, O., Arenas, E., et al. (1998). Adenosine A1 receptor-mediated modulation of dopamine D1 receptors in stably cotransfected fibroblast cells. *J. Biol. Chem*. 273, 4718–4724. doi: 10.1074/jbc.273.8.4718
- Ferré, S., von Euler, G., Johansson, B., Fredholm, B. B., and Fuxe, K. (1991d). Stimulation of high-affinity adenosine A2 receptors decreases the affinity of dopamine D2 receptors in rat striatal membranes. *Proc. Natl. Acad. Sci. U.S.A*. 88, 7238–7241.
- Ferri, R., Cosentino, F. I., Manconi, M., Rundo, F., Bruni, O., and Zucconi, M. (2014). Increased electroencephalographic high frequencies during the sleep onset period in patients with restless legs syndrome. *Sleep* 37, 1375–1381. doi: 10.5665/sleep.3934
- Ferré, R., Rundo, F., Zucconi, M., Manconi, M., Bruni, O., Ferini-Strambi, L., et al. (2015). An evidence-based analysis of the association between periodic leg movements during sleep and arousals in Restless Legs Syndrome. *Sleep* 38, 919–924. doi: 10.5665/sleep.4740
- Florentini, C., Busi, C., Gorruso, E., Gotti, C., Spano, P., and Missale, C. (2008). Reciprocal regulation of dopamine D1 and D3 receptor

- function and trafficking by heterodimerization. *Mol. Pharmacol.* 74, 59–69. doi: 10.1124/mol.107.043885
- García-Borreguero, D., Kohnen, R., Silber, M. H., Winkelmann, J. W., Earley, C. J., Högl, B., et al. (2013). The long-term treatment of restless legs syndrome/Willis-Ekbom disease: evidence-based guidelines and clinical consensus best practice guidance: a report from the International Restless Legs Syndrome Study Group. *Sleep Med.* 14, 675–684. doi: 10.1016/j.sleep.2013.05.016
- García-Borreguero, D., Patrick, J., DuBrava, S., Becker, P. M., Lankford, A., Chen, C., et al. (2014). Pregabalin versus pramipexole: effects on sleep disturbance in restless legs syndrome. *Sleep* 37, 635–643. doi: 10.5665/sleep.3558
- Gerfen, C. R. (2004). “Basal ganglia,” in *The Rat Nervous System*, eds G. Paxinos (Amsterdam: Elsevier Academic Press), 445–508.
- Gerfen, C. R., Miyachi, S., Paletzki, R., and Brown, P. (2002). D1 dopamine receptor supersensitivity in the dopamine-depleted striatum results from a switch in the regulation of ERK1/2/MAP kinase. *J. Neurosci.* 22, 5042–5054.
- Gerfen, C. R., and Surmeier, D. J. (2011). Modulation of striatal projection systems by dopamine. *Annu. Rev. Neurosci.* 34, 441–466. doi: 10.1146/annurev-neuro-061010-113641
- Gilman, A. G. (1987). G proteins: transducers of receptor-generated signals. *Annu. Rev. Biochem.* 56, 615–649. doi: 10.1146/annurev.bi.56.070187.003151
- Ginés, S., Hillion, J., Torvinen, M., Le Crom, S., Casadó, V., Canela, E. I., et al. (2000). Dopamine D1 and adenosine A1 receptors form functionally interacting heteromeric complexes. *Proc. Natl. Acad. Sci. U.S.A.* 97, 8606–8611. doi: 10.1073/pnas.150241097
- Gonçalves, J., and Queiroz, G. (2008). Presynaptic adenosine and P2Y receptors. *Handb. Exp. Pharmacol.* 184, 339–732. doi: 10.1007/978-3-540-74805-2_11
- González, S., Rangel-Barajas, C., Peper, M., Lorenzo, R., Moreno, E., Ciruela, F., et al. (2012). Dopamine D4 receptor, but not the ADHD-associated D4.7 variant, forms functional heteromers with the dopamine D2S receptor in the brain. *Mol. Psychiatry* 17, 650–662. doi: 10.1038/mp.2011.93
- Guitart, X., Navarro, G., Moreno, E., Yano, H., Cai, N. S., Sánchez-Soto, M., et al. (2014). Functional selectivity of allosteric interactions within G protein-coupled receptor oligomers: the dopamine D1-D3 receptor heterotetramer. *Mol. Pharmacol.* 86, 417–429. doi: 10.1124/mol.114.093096
- Gulyani, S., Earley, C. J., Camandola, S., Maudsley, S., Ferré, S., Mughal, M. R., et al. (2009). Diminished iron concentrations increase adenosine A(2A) receptor levels in mouse striatum and cultured human neuroblastoma cells. *Exp. Neurol.* 215, 236–242. doi: 10.1016/j.expneurol.2008.10.007
- Hillion, J., Canals, M., Torvinen, M., Casadó, V., Scott, R., Terasmaa, A., et al. (2002). Coaggregation, cointernalization, and codesensitization of adenosine A2A receptors and dopamine D2 receptors. *J. Biol. Chem.* 277, 18091–18097. doi: 10.1074/jbc.M107731200
- Jennings, L. L., Hao, C., Cabrita, M. A., Vickers, M. F., Baldwin, S. A., Young, J. D., et al. (2001). Distinct regional distribution of human equilibrative nucleoside transporter proteins 1 and 2 (hENT1 and hENT2) in the central nervous system. *Neuropharmacology* 40, 722–731. doi: 10.1016/S0028-3908(00)00207-0
- Kanda, T., Shiozaki, S., Shimada, J., Suzuki, F., and Nakamura, J. (1994). KF17837: a novel selective adenosine A2A receptor antagonist with anticonvulsant activity. *Eur. J. Pharmacol.* 256, 263–268. doi: 10.1016/0014-2999(94)90551-7
- Karcz-Kubicha, M., Ferré, S., Díaz-Ruiz, O., Quiroz-Molina, C., Goldberg, S. R., Hope, B. T., et al. (2006). Stimulation of adenosine receptors selectively activates gene expression in striatal enkephalinergic neurons. *Neuropsychopharmacology* 31, 2173–2179. doi: 10.1038/sj.npp.1301035
- Karcz-Kubicha, M., Quarta, D., Hope, B. T., Antoniou, K., Müller, C. E., Morales, M., et al. (2003). Enabling role of adenosine A1 receptors in adenosine A2A receptor-mediated striatal expression of c-fos. *Eur. J. Neurosci.* 18, 296–302. doi: 10.1046/j.1460-9568.2003.02747.x
- Kim, H. H., and Liao, J. K. (2008). Translational therapeutics of dipyridamole. *Arterioscler. Thromb. Vasc. Biol.* 28, s39–s42. doi: 10.1161/ATVBAHA.107.160226
- Kim, Y., Bolortuya, Y., Chen, L., Basheer, R., McCarley, R. W., and Strecker, R. E. (2012). Decoupling of sleepiness from sleep time and intensity during chronic sleep restriction: evidence for a role of the adenosine system. *Sleep* 35, 861–869. doi: 10.5665/sleep.1890
- Kim, Y., Elmenhorst, D., Weissaupt, A., Wedekind, F., Kroll, T., McCarley, R. W., et al. (2015). Chronic sleep restriction induces long-lasting changes in adenosine and noradrenaline receptor density in the rat brain. *J. Sleep Res.* 24, 549–558. doi: 10.1111/jsr.12300
- Kull, B., Ferré, S., Arslan, G., Svenningsson, P., Fuxe, K., Owman, C., et al. (1999). Reciprocal interactions between adenosine A2A and dopamine D2 receptors in Chinese hamster ovary cells co-transfected with the two receptors. *Biochem. Pharmacol.* 58, 1035–1045. doi: 10.1016/S0006-2952(99)00184-7
- Manconi, M., Ferri, R., Zucconi, M., Clemens, S., Giarolli, L., Bottasini, V., et al. (2011). Preferential D2 or preferential D3 dopamine agonists in restless legs syndrome. *Neurology* 77, 110–117. doi: 10.1212/WNL.0b013e3182242d91
- Marcellino, D., Ferré, S., Casadó, V., Cortés, A., Le Foll, B., Mazzola, C., et al. (2008). Identification of dopamine D1-D3 receptor heteromers. Indications for a role of synergistic D1-D3 receptor interactions in the striatum. *J. Biol. Chem.* 283, 26016–26025. doi: 10.1074/jbc.M710349200
- McCarley, R. W. (2007). Neurobiology of REM and NREM sleep. *Sleep Med.* 8, 302–330. doi: 10.1016/j.sleep.2007.03.005
- Morelli, M., and Wardas, J. (2001). Adenosine A(2a) receptor antagonists: potential therapeutic and neuroprotective effects in Parkinson's disease. *Neurotoxicol. Res.* 3, 545–556. doi: 10.1007/BF03033210
- Navarro, G., Aguinaga, D., Moreno, E., Hradsky, J., Reddy, P. P., Cortés, A., et al. (2014). Intracellular calcium levels determine differential modulation of allosteric interactions within G protein-coupled receptor heteromers. *Chem. Biol.* 21, 1546–1556. doi: 10.1016/j.chembiol.2014.10.004
- Navarro, G., Cordero, A., Zelman-Femiak, M., Brugarolas, M., Moreno, E., Aguinaga, D., et al. (2016). Quaternary structure of a G-protein-coupled receptor heterotetramer in complex with Gi and Gs. *BMC. Biol.* 14:26. doi: 10.1186/s12915-016-0247-4
- Navarro, G., Ferré, S., Cordero, A., Moreno, E., Mallol, J., Casadó, V., et al. (2010). Interactions between intracellular domains as key determinants of the quaternary structure and function of receptor heteromers. *J. Biol. Chem.* 285, 27346–27359. doi: 10.1074/jbc.M110.115634
- Nordlander, N. B. (1953). Therapy in restless legs. *Acta Med. Scand.* 145, 453–457. doi: 10.1111/j.0954-6820.1953.tb07042.x
- Pardo, M., López-Cruz, L., Valverde, O., Ledent, C., Baqi, Y., Müller, C. E., et al. (2013). Effect of subtype-selective adenosine receptor antagonists on basal or haloperidol-regulated striatal function: studies of exploratory locomotion and c-Fos immunoreactivity in outbred and A(2A)R KO mice. *Behav. Brain Res.* 247, 217–226. doi: 10.1016/j.bbr.2013.03.035
- Parkinson, F. E., Damaraju, V. L., Graham, K., Yao, S. Y., Baldwin, S. A., Cass, C. E., et al. (2011). Molecular biology of nucleoside transporters and their distributions and functions in the brain. *Curr. Top. Med. Chem.* 11, 948–972. doi: 10.2174/156802611795347582
- Pascual, O., Casper, K. B., Kubera, C., Zhang, J., Revilla-Sanchez, R., Sul, J. Y., et al. (2005). Astrocytic purinergic signaling coordinates synaptic networks. *Science* 310, 113–116. doi: 10.1126/science.1116916
- Quiroz, C., Gomes, C., Pak, A. C., Ribeiro, J. A., Goldberg, S. R., Hope, B. T., et al. (2006). Blockade of adenosine A2A receptors prevents protein phosphorylation in the striatum induced by cortical stimulation. *J. Neurosci.* 26, 10808–10812. doi: 10.1523/JNEUROSCI.1661-06.2006
- Quiroz, C., Gulyani, S., Ruiqian, W., Bonaventura, J., Cutler, R., Pearson, V., et al. (2016a). Adenosine receptors as markers of brain iron deficiency: implications for Restless Legs Syndrome. *Neuropharmacology* 111, 160–168. doi: 10.1016/j.neuropharm.2016.09.002
- Quiroz, C., Orrú, M., Rea, W., Ciudad-Roberts, A., Yepes, G., Britt, J. P., et al. (2016b). Local control of extracellular dopamine levels in the medial nucleus accumbens by a glutamatergic projection from the infralimbic cortex. *J. Neurosci.* 36, 851–859. doi: 10.1523/JNEUROSCI.2850-15.2016
- Quiroz, C., Pearson, V., Gulyani, S., Allen, R., Earley, C., and Ferré, S. (2010). Up-regulation of striatal adenosine A(2A) receptors with iron deficiency in rats: effects on locomotion and cortico-striatal neurotransmission. *Exp. Neurol.* 224, 292–298. doi: 10.1016/j.expneurol.2010.04.004
- Salmi, P., Chergui, K., and Fredholm, B. B. (2005). Adenosine-dopamine interactions revealed in knockout mice. *J. Mol. Neurosci.* 26, 239–244. doi: 10.1385/JMN:26:2-3:239
- Schiffmann, S. N., Jacobs, O., and Vanderhaeghen, J. J. (1991). Striatal restricted adenosine A2 receptor (RDC8) is expressed by enkephalin but not by substance P neurons: an *in situ* hybridization histochemistry study. *J. Neurochem.* 57, 1062–1067. doi: 10.1111/j.1471-4159.1991.tb08257.x
- Schindler, C. W., Karcz-Kubicha, M., Thorndike, E. B., Müller, C. E., Tella, S. R., Ferré, S., et al. (2005). Role of central and peripheral adenosine receptors in the cardiovascular responses to intraperitoneal injections of adenosine

- A1 and A2A subtype receptor agonists. *Br. J. Pharmacol.* 144, 642–650. doi: 10.1038/sj.bjp.0706043
- Sgambato, V., Pagès, C., Rogard, M., Besson, M. J., and Caboche, J. (1998). Extracellular signal-regulated kinase (ERK) controls immediate early gene induction on corticostriatal stimulation. *J. Neurosci.* 18, 8814–8825.
- Shiozaki, S., Ichikawa, S., Nakamura, J., Kitamura, S., Yamada, K., and Kuwana, Y. (1999). Actions of adenosine A2A receptor antagonist KW-6002 on drug-induced catalepsy and hypokinesia caused by reserpine or MPTP. *Psychopharmacology* 147, 90–95. doi: 10.1007/s002130051146
- Silber, M. H., Becker, P. M., Earley, C., Garcia-Borreguero, D., and Ondo, W. G. (2013). Willis-Ekbom Disease Foundation revised consensus statement on the management of restless legs syndrome. *Mayo Clin. Proc.* 88, 977–986. doi: 10.1016/j.mayocp.2013.06.016
- Smith, N. J., and Milligan, G. (2010). Allosteric at G protein-coupled receptor homo- and heteromers: uncharted pharmacological landscapes. *Pharmacol. Rev.* 62, 701–725. doi: 10.1124/pr.110.002667
- Sokoloff, and Le Foll, B. (2017). The dopamine D3 receptor, a quarter century later. *Eur. J. Neurosci.* 45, 2–19. doi: 10.1111/ejn.13390
- Solinas, M., Ferré, S., You, Z. B., Karcz-Kubicha, M., Popoli, P., and Goldberg, S. R. (2002). Caffeine induces dopamine and glutamate release in the shell of the nucleus accumbens. *J. Neurosci.* 22, 6321–6324.
- Sollevi, A. (1986). Cardiovascular effects of adenosine in man; possible clinical implications. *Prog. Neurobiol.* 27, 319–349. doi: 10.1016/0301-0082(86)90005-5
- Trenkwalder, C., and Paulus, W. (2010). Restless legs syndrome: pathophysiology, clinical presentation and management. *Nat. Rev. Neurol.* 6, 337–346. doi: 10.1038/nrneurol.2010.55
- Trifilieff, P., Rives, M. L., Urizar, E., Piskorski, R. A., Vishwasrao, H. D., Castrillon, J., et al. (2011). Detection of antigen interactions *ex vivo* by proximity ligation assay: endogenous dopamine D2-adenosine A2A receptor complexes in the striatum. *Biotechniques* 51, 111–118. doi: 10.2144/000113719
- Unger, E. L., Bianco, L. E., Jones, B. C., Allen, R. P., and Earley, C. J. (2014). Low brain iron effects and reversibility on striatal dopamine dynamics. *Exp. Neurol.* 261, 462–468. doi: 10.1016/j.expneurol.2014.06.023
- Van Dort, C. J., Baghdoyan, H. A., and Lydic, R. (2009). Adenosine A(1) and A(2A) receptors in mouse prefrontal cortex modulate acetylcholine release and behavioral arousal. *J. Neurosci.* 29, 871–881. doi: 10.1523/JNEUROSCI.4111-08.2009
- Varga, L. I., Ako-Agugua, N., Colasante, J., Hertweck, L., Houser, T., Smith, J., et al. (2009). Critical review of ropinirole and pramipexole – putative dopamine D(3)-receptor selective agonists - for the treatment of RLS. *J. Clin. Pharm. Ther.* 34, 493–505. doi: 10.1111/j.1365-2710.2009.01025.x
- Woods, A. S., and Ferré, S. (2005). Amazing stability of the arginine-phosphate electrostatic interaction. *J. Proteome Res.* 4, 1397–1402. doi: 10.1021/pr050077s
- Wu, L. G., and Saggau, P. (1997). Presynaptic inhibition of elicited neurotransmitter release. *Trends Neurosci.* 20, 204–212. doi: 10.1016/S0166-2236(96)01015-6
- Yepes, G., Guitart, X., Rea, W., Newman, A. H., Allen, R. P., Earley, C. J., et al. (2017). Targeting corticostriatal terminals in Restless Legs Syndrome. *Ann. Neurol.* 82, 951–960. doi: 10.1002/ana.25104

Conflict of Interest Statement: The authors declare that the research was conducted in the absence of any commercial or financial relationships that could be construed as a potential conflict of interest.

Copyright © 2018 Ferré, Quiroz, Guitart, Rea, Seyedian, Moreno, Casadó-Anguera, Díaz-Ríos, Casadó, Clemens, Allen, Earley and García-Borreguero. This is an open-access article distributed under the terms of the Creative Commons Attribution License (CC BY). The use, distribution or reproduction in other forums is permitted, provided the original author(s) or licensor are credited and that the original publication in this journal is cited, in accordance with accepted academic practice. No use, distribution or reproduction is permitted which does not comply with these terms.



Essential Control of the Function of the Striatopallidal Neuron by Pre-coupled Complexes of Adenosine A_{2A}-Dopamine D₂ Receptor Heterotetramers and Adenylyl Cyclase

Sergi Ferré^{1*}, Jordi Bonaventura¹, Wendy Zhu², Candice Hatcher-Solis¹, Jaume Taura^{3,4}, César Quiroz¹, Ning-Sheng Cai¹, Estefanía Moreno⁵, Verónica Casadó-Anguera⁵, Alexxai V. Kravitz⁶, Kimberly R. Thompson², Dardo G. Tomasi⁷, Gemma Navarro⁸, Arnau Cordero⁹, Leonardo Pardo⁹, Carme Lluís⁵, Carmen Dessauer¹⁰, Nora D. Volkow⁷, Vicent Casadó⁵, Francisco Ciruela^{3,4}, Diomedes E. Logothetis¹¹ and Daniel Zwillig²

OPEN ACCESS

Edited by:

Vsevolod V. Gurevich,
Vanderbilt University, United States

Reviewed by:

Kevin D. G. Pflieger,
Harry Perkins Institute of Medical
Research, Australia
Dominique Massotte,
UPR3212 Institut des Neurosciences
Cellulaires et Intégratives (INCI),
France

*Correspondence:

Sergi Ferré
sferre@intra.nida.nih.gov

Specialty section:

This article was submitted to
Experimental Pharmacology and Drug
Discovery,
a section of the journal
Frontiers in Pharmacology

Received: 05 October 2017

Accepted: 05 March 2018

Published: xx March 2018

Citation:

Ferré S, Bonaventura J, Zhu W,
Hatcher-Solis C, Taura J, Quiroz C,
Cai N-S, Moreno E,
Casadó-Anguera V, Kravitz AV,
Thompson KR, Tomasi DG,
Navarro G, Cordero A, Pardo L,
Lluís C, Dessauer C, Volkow ND,
Casadó V, Ciruela F, Logothetis DE
and Zwillig D (2018) Essential
Control of the Function of the
Striatopallidal Neuron by Pre-coupled
Complexes of Adenosine
A_{2A}-Dopamine D₂ Receptor
Heterotetramers and Adenylyl
Cyclase. *Front. Pharmacol.* 9:243.
doi: 10.3389/fphar.2018.00243

¹ Integrative Neurobiology Section, National Institute on Drug Abuse, Intramural Research Program, National Institutes of Health, Baltimore, MD, United States, ² Circuit Therapeutics, Inc., Menlo Park, CA, United States, ³ Unitat de Farmacologia, Departament de Patologia i Terapèutica Experimental, Facultat de Medicina i Ciències de la Salut, IDIBELL, Universitat de Barcelona, Barcelona, Spain, ⁴ Institut de Neurociències, Universitat de Barcelona, Barcelona, Spain, ⁵ Center for Biomedical Research in Neurodegenerative Diseases Network, Department of Biochemistry and Molecular Biomedicine, Faculty of Biology, Institute of Biomedicine of the University of Barcelona, University of Barcelona, Barcelona, Spain, ⁶ Eating and Addiction Section, Diabetes, Endocrinology and Obesity Branch, National Institute of Diabetes and Digestive and Kidney Diseases, Intramural Research Program, National Institutes of Health, Bethesda, MD, United States, ⁷ Laboratory of Neuroimaging, National Institute on Alcohol Abuse and Alcoholism, Intramural Research Program, National Institutes of Health, Rockville, MD, United States, ⁸ Department of Biochemistry and Physiology, Faculty of Pharmacy, University of Barcelona, Barcelona, Spain, ⁹ Laboratory of Computational Medicine, School of Medicine, Autonomous University of Barcelona, Bellaterra, Spain, ¹⁰ Department of Integrative Biology and Pharmacology, McGovern Medical School, University of Texas Health Science Center at Houston, Houston, TX, United States, ¹¹ Department of Pharmaceutical Sciences, Bouvé College of Health Sciences, Northeastern University, Boston, MA, United States

The central adenosine system and adenosine receptors play a fundamental role in the modulation of dopaminergic neurotransmission. This is mostly achieved by the strategic co-localization of different adenosine and dopamine receptor subtypes in the two populations of striatal efferent neurons, striatonigral and striatopallidal, that give rise to the direct and indirect striatal efferent pathways, respectively. With optogenetic techniques it has been possible to dissect a differential role of the direct and indirect pathways in mediating “Go” responses upon exposure to reward-related stimuli and “NoGo” responses upon exposure to non-rewarded or aversive-related stimuli, respectively, which depends on their different connecting output structures and their differential expression of dopamine and adenosine receptor subtypes. The striatopallidal neuron selectively expresses dopamine D₂ receptors (D2R) and adenosine A_{2A} receptors (A2AR), and numerous experiments using multiple genetic and pharmacological *in vitro*, *in situ* and *in vivo* approaches, demonstrate they can form A2AR-D2R heteromers. It was initially assumed that different pharmacological interactions between dopamine and adenosine receptor ligands indicated the existence of different subpopulations of A2AR and D2R in the striatopallidal neuron. However, as elaborated in the present essay, most evidence now indicates that all interactions can

be explained with a predominant population of striatal A2AR-D2R heteromers forming complexes with adenylyl cyclase subtype 5 (AC5). The A2AR-D2R heteromer has a tetrameric structure, with two homodimers, which allows not only multiple allosteric interactions between different orthosteric ligands, agonists, and antagonists, but also the canonical Gs-Gi antagonistic interaction at the level of AC5. We present a model of the function of the A2AR-D2R heterotetramer-AC5 complex, which acts as an integrative device of adenosine and dopamine signals that determine the excitability and gene expression of the striatopallidal neurons. The model can explain most behavioral effects of A2AR and D2R ligands, including the psychostimulant effects of caffeine. The model is also discussed in the context of different functional striatal compartments, mainly the dorsal and the ventral striatum. The current accumulated knowledge of the biochemical properties of the A2AR-D2R heterotetramer-AC5 complex offers new therapeutic possibilities for Parkinson's disease, schizophrenia, SUD and other neuropsychiatric disorders with dysfunction of dorsal or ventral striatopallidal neurons.

Keywords: striatopallidal neuron, adenosine A_{2A} receptor, dopamine D₂ receptor, GPCR heteromers, adenylyl cyclase, caffeine, akinesia, apathy

INTRODUCTION

One of the most noticeable functions of adenosine in the brain is the ability to impose a brake on the central dopaminergic system. This inhibitory role of adenosine is largely mediated by the activation of one subtype of adenosine receptor, the A_{2A} receptor (A2AR), particularly expressed by one type of neuron localized in the striatum, the striatopallidal neuron. The striatum is the brain area with the highest innervation of dopamine and the highest expression of dopamine receptors in the brain (Gerfen, 2004), and the striatopallidal neuron expresses the highest density of A2AR and dopamine receptors of the D₂ subtype (D2R) than any other neuron in the central nervous system (Gerfen, 2004; Schiffmann et al., 2007). It is now well accepted that adenosine controls the function of the striatopallidal neuron through intermolecular interactions between A2AR and D2R, with the formation of receptor heteromers.

Since its initial discovery, now more than 25 years ago (Ferré et al., 1991b), A2AR-D2R interactions have become a model for the study of allosteric interactions within G protein-coupled receptor (GPCR) heteromers, with the emergence of a new concept: allosteric interactions between orthosteric ligands (reviewed in Ferré et al., 2014). But recent findings indicate that the A2AR-D2R heteromer will also become a model for receptor-receptor interactions previously thought to take place downstream, on converging signaling molecules, which were often labeled as “interactions at the second messenger level.” The antagonistic canonical interaction at the level of adenylyl cyclase (AC), between a Gs/olf-coupled receptor, such as the A2AR, and a Gi/o-coupled receptor, such as the D2R, represents a classical example. Thus, a recent study demonstrates that this canonical interaction is dependent on the oligomerization of A2AR and D2R and the AC subtype AC5 (Navarro et al., 2018). This discovery implies that the striatal A2AR-D2R heteromer could explain most pharmacological effects of A2AR and D2R ligands, with implications for various neuropsychiatric disorders.

The understanding of the role of striatal adenosine and A2AR-D2R heteromers in striatal function and dysfunction will be here revisited within the framework of, not only the new developments on A2AR-D2R heteromers, but also most recent developments on the function of different striatal compartments and striatal dopamine, particularly on the function of the striatopallidal neuron. First, we summarize the current knowledge of the role of dopamine in the different striatal compartments. Next, we analyze the role of adenosine-dopamine interactions in the modulation of the function of the striatopallidal neuron. We then propose a functional model for the A2AR-D2R heterotetramer-AC5 complex in the striatopallidal neuron, a complex formed by one A2AR homodimer coupled to a Golf protein, a D2R homodimer coupled to a Gi protein and its signaling molecule AC5. The model is then used to reevaluate the pharmacological effects of adenosine receptor ligands, including caffeine. Finally, it is proposed that A2AR-D2R heterotetramer-AC5 complexes localized in striatopallidal neurons can be used as targets for the treatment of neuropsychiatric symptoms, such as akinesia and apathy. We also present new results of the effect of the A2AR antagonist SCH 442416 in radioligand binding, locomotor activation and optogenetic experiments in mice, which reconcile previous studies with the same compound that were apparently incompatible with our hypothesis of a predominant population of striatal A2AR-D2R heteromers that modulate striatopallidal neuronal function.

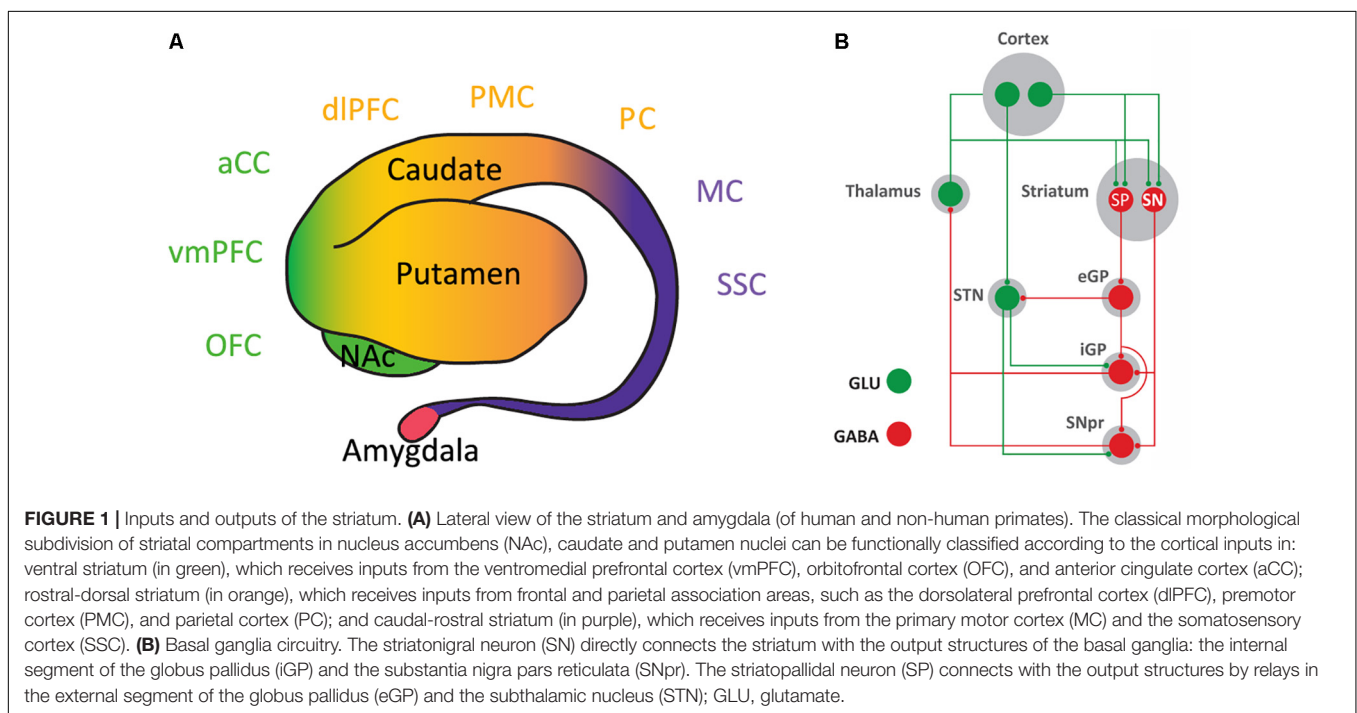
FUNCTIONAL DISTINCTION OF STRIATAL COMPARTMENTS

The striatum is the main input structure of the basal ganglia. Although in humans and non-human primates it has been classically subdivided into nucleus accumbens (NAc), caudate and putamen, it can be functionally subdivided in three different compartments: ventral, rostral-dorsal and caudal-dorsal striata (Figure 1A). The ventral striatum concept has expanded from

its initial inclusion of areas innervated by the dopaminergic cells of the ventral tegmental area (VTA), mostly the NAc with its two compartments core and shell and the olfactory tubercle, to the striatal areas receiving glutamatergic inputs from the ventromedial prefrontal cortex, orbitofrontal cortex and anterior cingulate cortex (Haber and Behrens, 2014) (Figure 1A). In fact, the orbitofrontal cortex and the anterior cingulate cortex, respectively, receive partial and predominant dopaminergic innervation from the substantia nigra pars compacta (SNpc; Haber and Behrens, 2014). Furthermore, the ventral striatum receives afferent glutamatergic projections from the insular cortex, amygdala and hippocampus (Haber and Behrens, 2014). The rostral-dorsal striatum receives glutamatergic input from frontal and parietal association areas and the caudal-dorsal striatum from the primary motor and somatosensory cortices (Figure 1A). Both rostral-dorsal and caudal-dorsal striata receive their dopaminergic input from the SNpc (Haber, 2014; Haber and Behrens, 2014).

The ventral striatum forms part of decision-making brain circuits involved in reward valuation tasks, which determine and store reward values (often named as “subjective values of rewards”) and constantly choose the reward to be obtained by a process of maximizing utilities associated with different options, the highest benefit/cost ratio (Kable and Glimcher, 2009). ‘Delay discounting’ (DD), ‘effort discounting’ (ED), and ‘low-probability discounting’ (LPD) refer to the empirical finding that both humans and animals value immediate, low-effort and high probability rewards more than delayed, high-effort and low probability rewards. A large number of behavioral and clinical studies indicate that DD, ED, and LPD are independent variables possibly involving corticostriatal circuits with different ventral striatal compartments differentially connected to different

prefrontal cortical areas (Prévost et al., 2010; Stopper and Floresco, 2011). A main role of the ventral striatum, classically labeled as an interface between motivation and action (Mogenson et al., 1980), can be synthesized as determining “whether to respond” while that of the dorsal striatum is “how to respond” to reward-associated stimuli (Ferré, 2017). All reward-related, dopamine-dependent functions, including the facilitation of reward-oriented behavior and learning of stimulus-reward and reward-response associations (positive reinforcement; Wise, 2004), are simultaneously processed by the rostral-dorsal and caudal-dorsal striata. In relation to positive reinforcement, the rostral-dorsal striatum is predominantly involved in an initial, more controlled (contingent on the outcome) and less permanent learning, while the caudal-dorsal striatum is involved in a slower, less controlled (non-contingent on the outcome) but long-lasting learning (Kim and Hikosaka, 2015). The same functional dichotomy, “volitional” and “automatic” learning, but with a medial-lateral distribution, can also be demonstrated in the rodent striatum (Voorn et al., 2004; Yin and Knowlton, 2006; Balleine and O’Doherty, 2010). However, it is becoming increasingly evident that dopaminergic mesencephalic cells also process aversive-related and non-rewarded stimuli and are involved in negative reinforcement. Most dopamine cells respond by decreasing their activity upon exposure to aversive stimuli and to omission of expected rewards. Dopaminergic cells, therefore, code for positive and negative reward prediction errors, increasing their firing upon presentation of reward-related stimuli or better than expected rewards or with the termination of aversive-related stimuli and decreasing their firing upon omission of reward-related stimuli or presentation of a worse than expected reward (Steinberg et al., 2013; Chang et al., 2016).



THE A2AR-D2R-EXPRESSING STRIATOPALLIDAL NEURON

In the striatum, glutamatergic and dopaminergic inputs converge in the dendritic spines of the GABAergic medium-sized spiny neurons, which constitute more than 95% of the striatal neuronal population (Gerfen, 2004). There are two types of medium-sized spiny neurons, which define the two striatal efferent pathways that connect the striatum with the output structures of the basal ganglia, substantia nigra pars reticulata (SNpr) and internal segment of the globus pallidus (Figure 1B). The striatonigral neuron constitutes the *direct efferent pathway* since it connects directly with the output structures (Gerfen, 2004). The striatopallidal neuron gives rise to the *indirect efferent pathway* and connects with the pallidal complex (the external segment of the globus pallidus and the ventral pallidum), which connects with the output structures directly and through a relay in the subthalamic nucleus (Gerfen, 2004) (Figure 1B). While there are no apparent qualitative or quantitative differences between the glutamatergic inputs impinging on the striatonigral and striatopallidal neurons, there is a clear distinction with the receptors that process the dopaminergic signals. Thus, the striatonigral neuron expresses dopamine D₁ receptors (D1R), a prototypical G_s/olf-coupled stimulatory receptor (more specifically Golf), while the striatopallidal neuron expresses D2R, a prototypical G_{i/o}-coupled inhibitory receptor (Gerfen, 2004; Bertran-Gonzalez et al., 2008). This established scheme breaks down in the most ventral striatal compartment, the shell of the NAc. The most ventral striatopallidal neurons project to the ventromedial and ventrolateral parts of the ventral pallidum, which does not connect with the output structures or relay in the subthalamic nucleus (Root et al., 2015). Instead, these regions of the ventral pallidum represent output structures of the basal ganglia themselves, since they project to the medio-dorsal thalamus, lateral hypothalamus and lateral habenula (Root et al., 2015). Furthermore, some ventral striatopallidal neurons also express D1R, with some degree of co-localization but still largely segregated from D2R (Bertran-Gonzalez et al., 2008; Frederick et al., 2015).

A mechanism by which dopamine is directly involved with positive and negative reinforcement is emerging from the study of the functional role of the direct and indirect striatal efferent pathways. Using recently developed optogenetic techniques, it has been possible to dissect a differential role of the direct and indirect pathways in mediating “Go” responses upon exposure to reward-related stimuli and “NoGo” responses upon exposure to non-rewarded or aversive-related stimuli, respectively, which depends on their different connecting output structures and their differential expression of dopamine receptor subtypes (Hikida et al., 2010, 2013; Kravitz et al., 2010, 2012; Freeze et al., 2013; Danjo et al., 2014). The differential connectivity entails that activation of striatonigral and striatopallidal neurons lead to qualitatively different behavioral responses, with the most obvious being the respective facilitation and inhibition of psychomotor activity. At this point, following Wise and Bozarth (1987), we should make the distinction between “psychomotor” and simply “motor” responses. Psychomotor responses, which

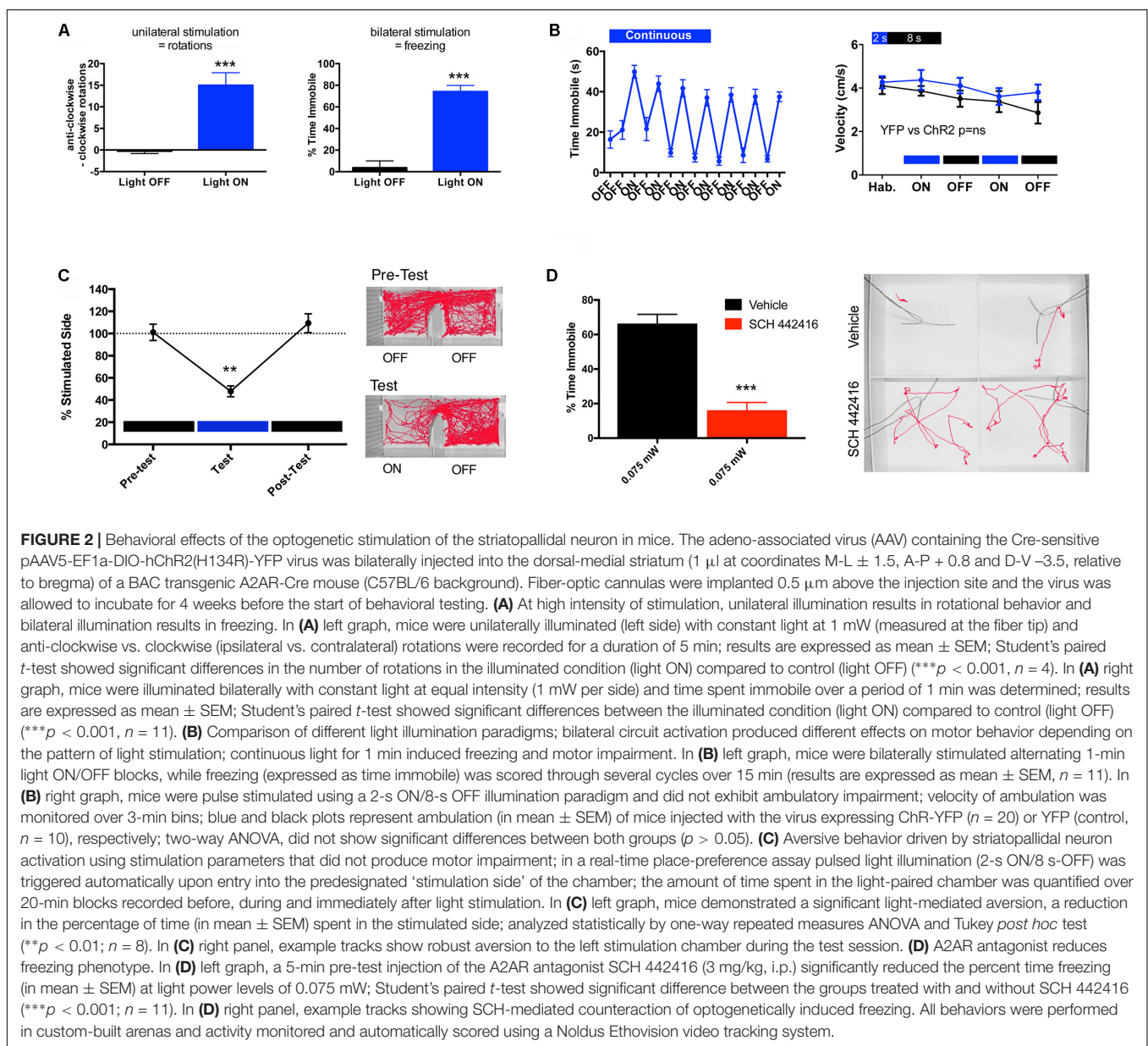
include forward locomotion or withdraw, have a characteristic dependence on external stimuli; increases or decreases of dopamine enhance or diminish the responsiveness to those stimuli, respectively. The differential affinities of D1R and D2R for endogenous dopamine and their respective predominant expression in striatonigral and striatopallidal neurons provide a fine-tuning device by which bursts and pauses of dopamine neurons can differentially influence their activity (Roitman et al., 2008; Bromberg-Martin et al., 2010; Macpherson et al., 2014). Dopamine has significantly higher affinity for D2R than for D1R. Therefore, D2R are more activated than D1R by basal dopamine levels and are more sensitive to the effects of dopamine pauses, while D1R are more sensitive to dopamine bursts, to conditions of larger dopamine release. Bursts of dopamine neurons result in large dopamine release, which predominantly increases the activation of stimulatory D1R and causes the direct pathway to promote high-value reward-associated movements, whereas the lower basal dopamine levels predominantly activate D2R, which are inhibitory and remove activation of the indirect pathway, thus suppressing low-value reward-associated or high-value punishment-associated movements (Frank, 2005; Hikosaka, 2007; Dreyer et al., 2010; Hikida et al., 2010, 2013; Kravitz et al., 2012; Danjo et al., 2014). Nevertheless, we should not ignore the fact that D2R are not completely occupied by endogenous dopamine and that bursts of dopamine are also able to enhance D2R signaling, therefore participating to the psychomotor activation guided by the stimuli associated with the concomitant increase in dopaminergic cell firing. However, strong dopamine receptor activation basically promotes potentiation of corticostriatal synapses onto the direct pathway and learning from positive outcomes (positive reinforcement), while weak dopamine receptor activation promotes potentiation of corticostriatal synapses onto the indirect pathway and learning from negative outcomes (negative reinforcement) (Frank et al., 2004; Shen et al., 2008; Voon et al., 2010).

Another important phenotypical difference between the striatopallidal and striatonigral neurons is their differential expression of adenosine receptor subtypes. The striatopallidal neurons selectively express A2AR, in fact, the highest density in the brain (Schiffmann et al., 2007). On the other hand, A2AR are absent from the striatonigral neurons, which express adenosine A₁ receptors (A1R) (Ferré et al., 1997). A2AR can then be used as a marker of the striatopallidal neuron. For instance, to identify the function of the striatopallidal neuron, studies using Bacterial Artificial Chromosome (BAC) transgenic mice have targeted the regulatory elements of either the D2R or the A2AR (Durieux et al., 2009; Valjent et al., 2009; Freeze et al., 2013). We used BAC transgenic mouse lines that express Cre recombinase under the control of regulatory elements of the D2R (D2R-Cre mice) or the A2AR (A2AR-Cre mice), allowing the selective expression of channelrhodopsin 2 (ChR2) by striatopallidal neurons (Kravitz et al., 2010; Freeze et al., 2013; Zwilling et al., 2014). This was achieved by bilateral injection of an adeno-associated virus (AAV) containing a Cre-sensitive vector with a double-floxed inverted open reading frame encoding a fusion of ChR2 and enhanced yellow fluorescence

457 protein into the dorsomedial striatum. Then, fiber-optic cannulas
 458 implanted immediately above the injection site allowed the local
 459 delivery of light with the concomitant selective optogenetic
 460 activation of a large fraction of dorsal striatopallidal neurons.
 461 Unilateral optogenetic stimulation led to significant ipsilateral
 462 rotational behavior, while bilateral optogenetic stimulation led to
 463 a significant decrease in locomotor activity (Kravitz et al., 2010;
 464 Freeze et al., 2013; Zwilling et al., 2014) (Figure 2A). These results
 465 were opposite to those obtained by the selective ablation of a
 466 large proportion of dorsal and ventral striatopallidal neurons in
 467 BAC transgenic A2AR-Cre mice by Cre-mediated expression of
 468 a diphtheria toxin receptor and diphtheria toxin injection, which
 469 led to hyperlocomotion (Durieux et al., 2009).

470 Altogether, these optogenetic and genetic targeting
 471 experiments agree with the increase and decrease of “NoGo”
 472

responses upon the respective activation or inactivation of
 514 striatopallidal neurons. Hypo- or hyperlocomotion represents an
 515 outcome of the respective sustained activation or deactivation of
 516 a large number of striatopallidal neurons, which more discretely
 517 should represent the respective facilitation and inhibition of
 518 withdrawal behavior from low-value reward-associated or high-
 519 value punishment-associated movements. We addressed more
 520 directly this assumption in optogenetic experiments with A2AR-
 521 Cre mice, by selectively inducing the expression of ChR2 in dorsal
 522 striatopallidal neurons and by using more discrete parameters
 523 of stimulation (Zwilling et al., 2014). Figure 2B shows the
 524 comparison of two different parameters of bilateral optogenetic
 525 stimulation in the dorso-medial striatum on locomotor activity.
 526 Continuous light for 1 min induced freezing and therefore an
 527 impairment of motor activity that would interfere with the
 528



571 analysis of behavior in a real-time place-preference study. On the
572 other hand, mice that were pulse-stimulated using a 2-s ON/8-s
573 OFF illumination paradigm did not demonstrate ambulatory
574 impairment (**Figure 2B**). When this pulse-stimulation was
575 triggered when the mouse entered one of the chambers of a
576 place-preference box, the animal showed a very significant
577 aversion-like behavior to that side (**Figure 2C**) (Zwilling et al.,
578 2014). These results also complement those obtained by Hikida
579 et al. (2010, 2013) in experiments with selective bilateral
580 inactivation of the dorsal or ventral striatopallidal neuron by
581 means of doxycycline-dependent, pathway-specific expression
582 of tetanus toxin (driven by the promoter of the gene coding the
583 neuropeptide enkephalin, selectively expressed by striatopallidal
584 neurons). A counteraction of the expression in addition to the
585 acquisition of aversion-like behavior was also demonstrated by
586 using an asymmetric design, with targeted unilateral inactivation
587 of the ventral striatopallidal neurons with tetanus toxin and the
588 contralateral infusion of a D2R agonist (but not a D2R antagonist
589 or D1R agonists or antagonists) or an A2AR antagonist (Hikida
590 et al., 2013). Similarly, we could demonstrate that the systemic
591 administration of the A2AR antagonist SCH 442416 (3 mg/kg
592 i.p.) significantly decreases the locomotor depression induced
593 by low-intensity optogenetic stimulation of the dorsal-medial
594 striatopallidal neurons (**Figure 2D**). These results would imply
595 a significant role of an endogenous adenosinergic tone in the
596 facilitation of the striatopallidal neuronal function mediated
597 by A2AR. In fact, numerous neurochemical studies imply that
598 A2AR signaling is especially involved in driving the activation of
599 the striatopallidal neuron upon D2R disinhibition (see below),
600 therefore in driving the suppression of the behavior associated
601 with non-rewarded and punishment-associated stimuli.

602 603 604 **THE A2AR-D2R RECEPTOR** 605 **HETEROTETRAMER-AC5 COMPLEX** 606

607 There is a large amount of experimental evidence indicating
608 the existence of a predominant striatal population of A2AR
609 and D2R that control striatopallidal neuronal function (Ferré
610 et al., 1993; Azdad et al., 2009; Bonaventura et al., 2015;
611 Ferré et al., 2016). Recent studies suggested that A2AR-
612 D2R heteromers assemble into a heterotetrameric structure,
613 with A2AR and D2R homodimers coupled to their respective
614 cognate Gs (more precisely the Golf isoform) and Gi proteins
615 (Bonaventura et al., 2015). The heterotetrameric structure
616 would provide the frame for multiple adenosine-dopamine
617 interactions and for interactions between exogenous A2AR
618 and D2R ligands (Navarro et al., 2014; Ferré et al., 2016).
619 One of the most prominent interactions is the allosteric
620 negative effect of A2AR ligands on the affinity and efficacy
621 of D2R ligands (*allosteric interaction*) (Ferré et al., 1991b;
622 Azdad et al., 2009; Bonaventura et al., 2015), which has been
623 demonstrated to depend on A2AR-D2R heteromerization by
624 the use of synthetic peptides that selectively interfere with
625 the heteromeric interface, both in mammalian transfected cells
626 and in striatal tissue (Azdad et al., 2009; Bonaventura et al.,
627 2015).

628 In addition to the allosteric interaction, a strong reciprocal
629 antagonistic interaction, with the ability of D2R agonists to
630 inhibit A2AR agonist-mediated activation of AC, was first
631 identified in mammalian transfected cells (Kull et al., 1999;
632 Hillion et al., 2002) and more recently characterized in
633 striatal cells in culture (Navarro et al., 2014). This represents
634 an antagonistic Gs-Gi *canonical interaction*, the ability of
635 an activated Gi-coupled receptor to inhibit a Gs-coupled
636 receptor-mediated activation of AC. The A2AR-D2R canonical
637 interaction was first observed *in situ*, in the striatum. The
638 evidence came initially from experiments that demonstrated
639 that the increase in the expression of the immediate-early gene
640 *c-fos* in the striatopallidal neurons upon treatment with D2R
641 antagonists or acute dopamine depletion could be counteracted
642 by blocking A2AR signaling (Boegman and Vincent, 1996;
643 Svenningsson et al., 1999). This A2AR signaling is initiated
644 by the second messenger cyclic-AMP (cAMP), the product of
645 AC activation. The cascade includes protein kinase A (PKA)
646 activation, with phosphorylation of the cAMP-response element
647 binding protein (CREB), a mechanism which is amplified
648 by the PKA-dependent phosphorylation of 'dopamine- and
649 cAMP-regulated phosphoprotein of molecular weight 32,000'
650 (DARPP-32) (Svenningsson et al., 1998; Kull et al., 1999)
651 (**Figure 3A**). A2AR-mediated activation of PKA also promotes
652 phosphorylation of voltage dependent Ca^{2+} channels (VDCC),
653 NMDA, and AMPA receptors (Håkansson et al., 2006; Azdad
654 et al., 2009; Higley and Sabatini, 2010), which determines their
655 degree of activation and, therefore, the degree of excitability
656 of the striatopallidal neurons, which determines the degree of
657 psychomotor depression (**Figure 3A**).

658 Activation of the D2R, when uninterrupted by co-activation
659 of the A2AR (allosteric interaction), can also signal through
660 phospholipase C (PLC) by a $G\beta\gamma$ subunit-dependent mechanism,
661 which induces the release of inositol (1,4,5)-triphosphate (IP₃),
662 a second messenger that causes the release of intracellular
663 Ca^{2+} . This, in turn results in the subsequent activation of the
664 Ca^{2+} /calmodulin-dependent protein phosphatase calcineurin
665 (also called protein phosphatase 2B or PP2B) (Hernandez-Lopez
666 et al., 2000; Azdad et al., 2009) (**Figure 3A**). Phosphorylated
667 forms of VDCC, NMDA, and AMPA receptors and DARPP-32
668 are main targets of PP2B. Therefore, activation of PP2B leads to
669 a decreased neuronal excitability and represents a downstream
670 additional mechanism of D2R-mediated inhibition of A2AR
671 signaling (Lindskog et al., 1999) (**Figure 3A**). In addition,
672 A2AR and D2R activation can modify gene expression through
673 respective G protein-dependent and independent mechanisms
674 of MAPK activation, which plays a predominant role in the
675 mailing of signals from the synapse to the nucleus by directly
676 activating the constitutive transcription factor Elk-1 (Besnard
677 et al., 2011) (**Figure 3A**). Our previous work indicates that
678 the outcome of co-activation of striatal A2AR and D2R on
679 MAPK activation depends on the intracellular levels of Ca^{2+} ,
680 which determines the binding of two different neuronal Ca^{2+} -
681 binding proteins, NCS-1 and calneuron-1 (Navarro et al., 2014).
682 NCS-1 and calneuron bind to the A2AR-D2R heteromer upon
683 low and high concentrations of Ca^{2+} , respectively. Binding
684 of calneuron specifically alters the ability of A2AR ligands

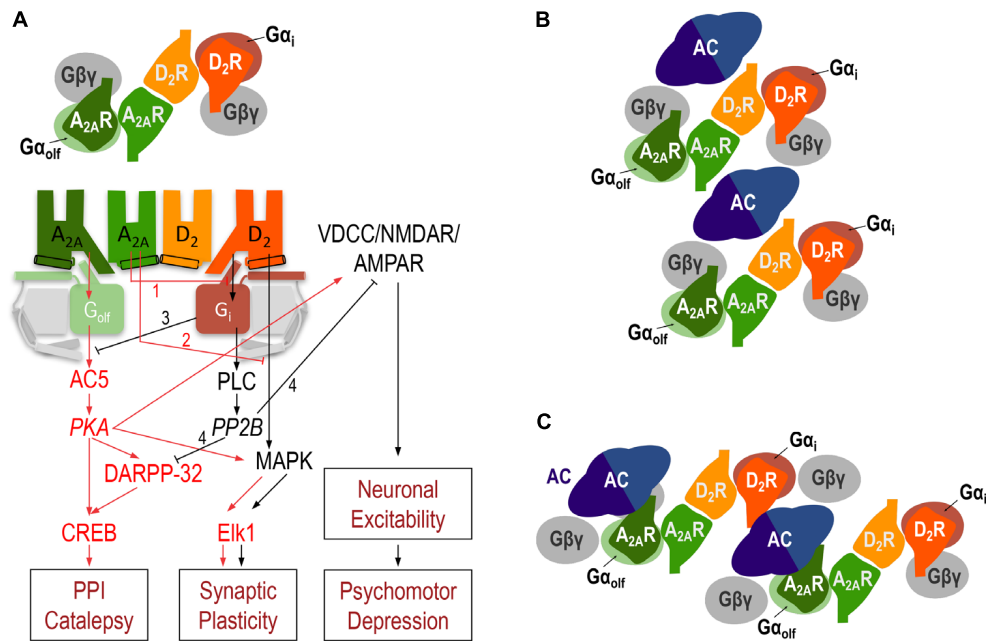


FIGURE 3 | The A2AR-D2R heterotetramer. **(A)** Model representing the striatal A2AR-D2R heteromer-dependent mechanisms that modulate different biochemical and behavioral outputs. The heterotetrameric structure of the A2AR-D2R heteromer allows multiple simultaneous and reciprocal interactions between adenosine and dopamine and exogenous A2AR and D2R ligands. Mainly, the ability of adenosine or exogenous A2AR ligands to decrease G protein-dependent (1) or G protein-independent (2) signaling by dopamine or exogenous D2R ligands (allosteric interactions) and a reciprocal antagonistic interaction, the ability of D2R agonists to inhibit the A2AR agonist-mediated activation of AC5, by means of the antagonistic Gs-Gi canonical interaction at the AC5 level (3). When uninterrupted by the canonical interaction, A2AR signals through activation of AC5 and protein kinase A (PKA) with phosphorylation of ‘dopamine- and cAMP-regulated phosphoprotein of molecular weight 32,000’ (DARPP-32), which facilitates PPI and catalepsy, and voltage-dependent Ca²⁺ channels (VDCC), NMDA and AMPA receptors, resulting in an increase in the excitability of the striatopallidal neuron. When uninterrupted by the allosteric interaction, D2R signals through PLC, which leads to activation of calcineurin (PP2B). PP2B dephosphorylates PKA substrates, DARPP-32, VDCC, NMDA and AMPA receptors, providing a downstream additional mechanism of D2R-mediated inhibition of A2AR signaling (4) and leading to a decrease in the excitability of the striatopallidal neuron, which facilitates psychomotor activation. A2AR and D2R activation can also modify gene expression through different mechanisms, including G protein-dependent and independent MAPK activation and activation of the transcription factor Elk-1 (see text). In **(B,C)**, schematic slice-representation viewed from the extracellular side of the minimal functional unit of the A2AR-D2R heterotetramer in complex with AC5 (see text), in the absence **(B)** and presence **(C)** of agonists, which induce a rearrangement of the heterotetramer-AC5 interfaces (modified from Navarro et al., 2018).

to allosterically modulate the GTP-independent D2R ligand-mediated MAPK activation, while binding of NCS-1 also counteracts the A2AR-mediated allosteric modulation of D2R-ligand-mediated G protein signaling (and therefore the canonical interaction). This provides a mechanism by which co-activation of A2AR and D2R in the heteromer promotes and counteracts MAPK activation upon low and high concentrations of Ca²⁺, respectively (Navarro et al., 2014).

The question is how two apparently simultaneous reciprocal interactions between A2AR- and D2R signaling (allosteric and canonical interactions) can take place in the same cell. Based on some studies obtained with the A2AR antagonist SCH 442416, we initially hypothesized the existence of two populations of A2AR in striatopallidal neurons (Orrú et al., 2011b). One population would be forming heteromers with D2R and would mediate the allosteric interaction, while another population would not be forming heteromers with D2R and would allow the antagonistic interaction at the second messenger level, cAMP (Ferré et al., 2011; Orrú et al., 2011b). However, we recently hypothesized that the putative heterotetrameric structure of the A2AR-D2R heteromer could sustain both the allosteric and the

canonical interactions (Navarro et al., 2014). In addition, based on the emergent view that considers GPCR homodimers as main functional units (Ferré et al., 2014), we postulated that heteromers are constituted by different interacting homodimers (Ferré et al., 2014; Ferré, 2015). This could be of special functional importance with heteromers formed by one homodimer coupled to a Gs/olf protein and another different homodimer coupled to a Gi/o protein. Our hypothesis was that such a GPCR *heterotetramer* would be part of a pre-coupled macromolecular complex that also includes AC5, the predominant AC subtype in the striatum (Lee et al., 2002), a necessary frame for the canonical antagonistic interaction at the AC level (Ferré, 2015). In fact, in mammalian transfected cells, using synthetic peptides with amino acid sequences of all transmembrane domains (TM) of A2AR and D2R and the putative TMs of AC5, we recently provided clear evidence for the existence of functional pre-coupled complexes of A2AR and D2R homodimers, their cognate Golf and Gi proteins and AC5 (Navarro et al., 2018). We first identified a symmetrical TM 6 interface for the A2AR and D2R homodimers and a symmetrical TM 4/TM 5 A2AR-D2R heteromeric interface. Computational analysis provided

799 one minimal solution, a linear arrangement with two internal
800 interacting A2AR and D2R protomers and two external non-
801 interacting A2AR and D2R protomers in which the α -subunits
802 of Gi and Gs bind to the corresponding external protomers
803 of the D2R or A2AR homodimers (**Figure 3**). Second, we
804 found asymmetrical interfaces formed by TMs of the receptors
805 and putative TMs of AC5 which rearrange upon agonist
806 exposure. Computational analysis indicated the existence of
807 a minimal functional complex formed by two A2AR-D2R
808 heterotetramers and two AC5 molecules (**Figures 3B,C**). In
809 fact, this quaternary structure suggests the possible formation of
810 zig-zagged arranged high-order oligomeric structures, a higher-
811 order linear arrangement of GPCR heteromers and effectors
812 (Navarro et al., 2018). Finally, we could demonstrate that this
813 macromolecular complex provides the sufficient but necessary
814 condition for the canonical Gs-Gi interactions at the AC level
815 (Navarro et al., 2018). The most demonstrative experiment was
816 that destabilization of the quaternary structure of the A2AR-
817 D2R heterotetramer, with interfering synthetic peptides with
818 the amino acid sequence of the TMs involved in heteromeric
819 interface, blocked the ability of a D2R agonist to counteract AC5
820 activation by an A2AR agonist in striatal neurons in culture
821 (Navarro et al., 2018).

822 The A2AR-D2R heterotetramer therefore acts as an integrative
823 molecular device, which allows reciprocal antagonistic
824 interactions between adenosine and dopamine to facilitate
825 a switch in the activation-inhibition of the striatopallidal neuron:
826 A preferential A2AR vs. D2R activation leads to an increase in
827 neuronal activity determined by the A2AR-mediated activation
828 of the AC5/PKA pathway, which is potentiated by the allosteric
829 counteraction of D2R signaling (“1” and “2” in **Figure 3A**);
830 a preferential D2R vs. A2AR activation leads to a decrease in
831 neuronal activity by activation of the PLC/PP2B pathway and
832 switching off the A2A-mediated activation of AC5 through the
833 canonical interaction (“3” in **Figure 3A**), which we have shown
834 depends on the integrity of the A2AR-D2R heterotetramer-AC5
835 complex (Navarro et al., 2008, 2014; Azdad et al., 2009; Higley
836 and Sabatini, 2010; Bonaventura et al., 2015; Ferré, 2016; Ferré
837 et al., 2016).

838 The heterotetrameric structure of the A2AR-D2R heteromer
839 provides the framework for allosteric mechanisms of A2AR
840 ligands that could explain recent experimental findings
841 apparently incompatible with classical pharmacology, such as
842 the agonist-like behavior of A2AR antagonists, which includes
843 caffeine, a non-selective adenosine receptor antagonist. The
844 initial unexpected finding came from a human PET study. In
845 this study, the acute administration of caffeine produced an
846 increase in the binding of [¹¹C]raclopride, a D2R antagonist, in
847 the putamen and ventral striatum (Volkow et al., 2015). As a
848 significant additional finding, the caffeine-dependent increase
849 in D2R antagonist binding in the ventral striatum correlated
850 with an increase in alertness (Volkow et al., 2015). Considering
851 that previous studies demonstrated antagonistic allosteric
852 interactions between A2AR and D2R agonists, caffeine should
853 have induced the opposite effect, a decrease in [¹¹C]raclopride
854 binding, due to an increase in the affinity of endogenous
855 dopamine. We therefore studied the possibility of a direct

856 allosteric modulation of caffeine on D2R agonist binding. Both
857 the A2AR agonist CGS 21680 and caffeine significantly decreased
858 the binding of the D2R agonist [³H]quinpirole in membrane
859 preparations from sheep striatum and mammalian cells
860 transfected with A2AR and D2R. We could also demonstrate
861 that both agonist-agonist and antagonist-agonist allosteric
862 modulations were dependent on heteromerization, since they
863 were not observed when transfecting a mutated A2AR with
864 impaired ability to heteromerize with D2R (Bonaventura et al.,
865 2015). Therefore, we initially assumed that the caffeine-induced
866 increase in [¹¹C]raclopride binding demonstrated in PET
867 experiments could be explained by a caffeine-induced decrease in
868 the affinity of endogenous dopamine. However, the observation
869 that both A2AR agonists and A2AR antagonists can produce
870 the same allosteric interaction in the A2AR-D2R heteromer, a
871 reduction in the affinity of agonists for the D2R, contradicts
872 the hypothesis of a key role of allosteric interactions within the
873 A2AR-D2R heteromer as a main mechanism involved in the
874 opposite behavioral effects of A2AR agonists and antagonists
875 (Ferré, 2008, 2016). Nevertheless, a biphasic effect was observed
876 when analyzing the effect of increasing concentrations of caffeine
877 or the selective A2AR antagonists SCH 58261 and KW 6002 on
878 the ability of a single concentration of CGS 21680 to decrease
879 [³H]quinpirole binding. Low concentrations of caffeine and
880 the A2AR antagonists significantly counteracted the effect
881 of CGS 21680, while high concentrations further decreased
882 [³H]quinpirole binding (Bonaventura et al., 2015). Therefore, the
883 results implied that orthosteric A2AR agonists and antagonists
884 produce the same allosteric modulation of D2R agonist binding
885 within the A2AR-D2R heteromer when applied individually, but,
886 when co-applied, they cancel out each other's effect. This could be
887 explained by the existence of two A2AR protomers in the A2AR-
888 D2R heteromer and allosteric interactions between orthosteric
889 agonists and antagonists, by which simultaneous occupation of
890 the A2AR homodimer by an agonist and an antagonist would
891 “freeze” the ability of either ligand to allosterically modulate
892 D2R agonist binding. The existence of allosteric interactions
893 between orthosteric A2AR agonists and antagonists could be
894 confirmed through binding kinetics experiments with the A2AR
895 antagonist [³H]ZM 241385. Thus, when analyzing the effect of
896 CGS 21680, caffeine and SCH 58261, only CGS 21680 modified
897 the dissociation rate of [³H]ZM 241385 (Bonaventura et al.,
898 2015). Considering that CGS 21680 and [³H]ZM 241385 bind to
899 the same orthosteric site (Lebon et al., 2011), the effect of CGS
900 21680 could be explained by co-occupation of both ligands of the
901 two orthosteric sites in an A2AR homodimer.

902 The same allosteric effects on D2R agonist binding
903 demonstrated by A2AR agonists and antagonists were also
904 shown for the efficacy of D2R agonists. By measuring ERK1/2
905 phosphorylation in transfected cells, we could demonstrate that
906 CGS 21680 counteracts quinpirole-induced MAPK activation,
907 that this effect of CGS 21680 can be counteracted by low
908 concentrations of caffeine or the A2AR antagonist SCH 58261
909 and that high concentration of the antagonists induce the
910 opposite effect (Bonaventura et al., 2015). We should therefore
911 expect that in the experimental animal A2AR antagonists
912 behave as A2AR agonists under specific conditions. In fact, in

patch-clamp experiments, we could demonstrate that the A2AR antagonist SCH 58261 counteracts the D2R antagonist-like properties of CGS 21680, but it reproduces the effect of the A2AR agonist when administered alone (Bonaventura et al., 2015). These results challenge the traditional view of competitive antagonism as the mechanism of the psychostimulant effects of caffeine (and selective A2AR antagonists). According to our model, the psychostimulant effect of caffeine can be explained by the counteraction of the allosteric interaction by co-occupation of the A2AR homodimer with caffeine and endogenous adenosine in the A2AR-D2R heterotetramer.

However, these allosteric interactions between A2AR agonists and antagonists and D2R agonists do not yet explain the increase in striatal [¹¹C]raclopride binding in human PET experiments induced by caffeine. Again, counteraction by caffeine of the inhibitory effect of endogenous adenosine on the binding of endogenous dopamine should lead to a decrease of [¹¹C]raclopride binding. It was then demonstrated that CGS 21680 and caffeine also inhibit the binding of [³H]raclopride binding in membrane preparations from striatum or transfected cells (Bonaventura et al., 2015). That these results imply allosteric interactions within the A2AR-D2R heteromer was demonstrated by their disappearance upon transfection of a mutated A2AR with impaired ability to heteromerize with D2R and by using a synthetic peptide that disrupts A2AR-D2R heteromerization (Bonaventura et al., 2015). Therefore, within the A2AR-D2R heteromer, any orthosteric A2AR ligand, agonist or antagonist, exerts a negative allosteric modulation on the affinity of any orthosteric D2R ligand, agonist or antagonist. Finally, the same as with [³H]quinpirole binding, we could also demonstrate a biphasic effect of caffeine on CGS 21680-mediated decrease of [³H]raclopride binding (Bonaventura et al., 2015). These results would at last provide a plausible mechanism for the effect of caffeine on [¹¹C]raclopride binding in humans, by its ability to antagonize the effect of endogenous adenosine on the binding of the exogenous D2R antagonist. An alternative explanation could still be that caffeine blocks an adenosine-mediated internalization of A2AR-D2R heteromers (Hillion et al., 2002; Huang et al., 2013), thus leading to higher D2R availability along with higher [¹¹C]raclopride binding. The positive association between caffeine-induced increases in D2R availability and caffeine-induced increases in alertness (Volkow et al., 2015) would support this interpretation, since increased D2R signaling contributes to alertness (Isaac and Berridge, 2003). Irrespective of the mechanism involved, the effect of caffeine on [¹¹C]raclopride binding in human PET experiments implies its dependence on the A2AR-D2R heteromer and, therefore, that a significant proportion of striatal [¹¹C]raclopride binding visualized with PET labels A2AR-D2R heteromers. Furthermore, these results call for the need to control caffeine intake when evaluating the effect of D2R ligands in humans, not only when using them as probes for imaging studies, but also when using them as therapeutic agents in neuropsychiatric disorders.

Very different qualitative differences between several A2AR antagonists emerged when evaluating their potencies and efficacies on different *in vitro* and *in vivo* techniques. Particularly significant was the demonstration of different binding properties

of the A2AR antagonist SCH 442416 depending on the presence and absence of D2R, when forming or not forming heteromers with D2R (Orrú et al., 2011a). In cells expressing A2AR and D2R, competitive-inhibition curves of the A2AR antagonist [³H]ZM 241388 binding vs. increasing concentrations of SCH 442416 were clearly biphasic. On the other hand, in cells expressing only A2AR, or A1R and A2AR, the curves were monophasic. When analyzing the radioligand binding experiments with the two-state dimer model (Casadó et al., 2007; Ferré et al., 2014), the data indicated a negative cooperativity of SCH 442416 binding to the A2AR (Orrú et al., 2011b; Ferré et al., 2014), an additional demonstration of A2AR homomerization. This, in fact, was the first indication that the A2AR-D2R comprises at least two A2AR protomers, in agreement with a tetrameric structure of the A2AR-D2R heteromer. We have now been able to reproduce these findings in striatal tissue, comparing the results of competitive-inhibition experiments of [³H]ZM 241388 binding vs. increasing concentrations of SCH 442416 in striatal membrane preparations of wild-type (WT) and striatal D2R knockout mice with a CRE-mediated deletion of D2R expression in A2AR-expressing neurons. The same as with mammalian transfected cells, the curves were biphasic or monophasic in the presence or absence of the D2R, respectively (Figure 4). The demonstration of the same binding properties of SCH 442416 in striatal tissue than in A2AR-D2R transfected cells implies that the A2AR-D2R heterotetramer represents the predominant population of A2AR and D2R in the striatum. Nevertheless, as mentioned below, striatal A2AR are also localized presynaptically, in glutamatergic terminals, where most probably do not form heteromers with D2R. These receptors, although playing a significant role in the modulation of striatal glutamate release, represent a very small fraction of the total of striatal A2AR, as compared to the postsynaptic A2AR.

REVISITING THE BEHAVIORAL EFFECTS OF ADENOSINE RECEPTOR LIGANDS IN THE FRAME OF ONE MAIN POPULATION OF STRIATAL A2AR AND D2R FORMING HETEROMERS

Considering that increases or decreases in the activity of the GABAergic striatopallidal neuron lead to the respective opposite effect on psychomotor activity and using a model that considers the A2AR-D2R heteromer as a key modulator of striatopallidal neuronal function, we could recently explain most psychomotor effects of caffeine (Ferré, 2016). This included the enigmatic caffeine-induced rotational behavior in rats with unilateral striatal dopamine denervation (Fuxe and Ungerstedt, 1974; Herrera-Marschitz et al., 1988; Casas et al., 1989; Garrett and Holtzman, 1995) and the ability of caffeine to significantly counteract the adipic-aphagic syndrome in rodents with 6-hydroxy-dopamine-induced or genetic-induced dopamine deficiency (Casas et al., 2000; Kim and Palmiter, 2003, 2008). According to the model, under resting conditions there is a tonic activation of A2AR and D2R by the endogenous neurotransmitters which results in a predominant A2AR vs. D2R

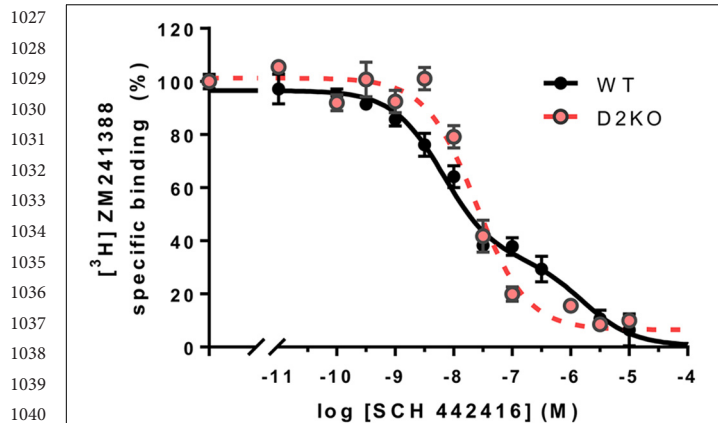


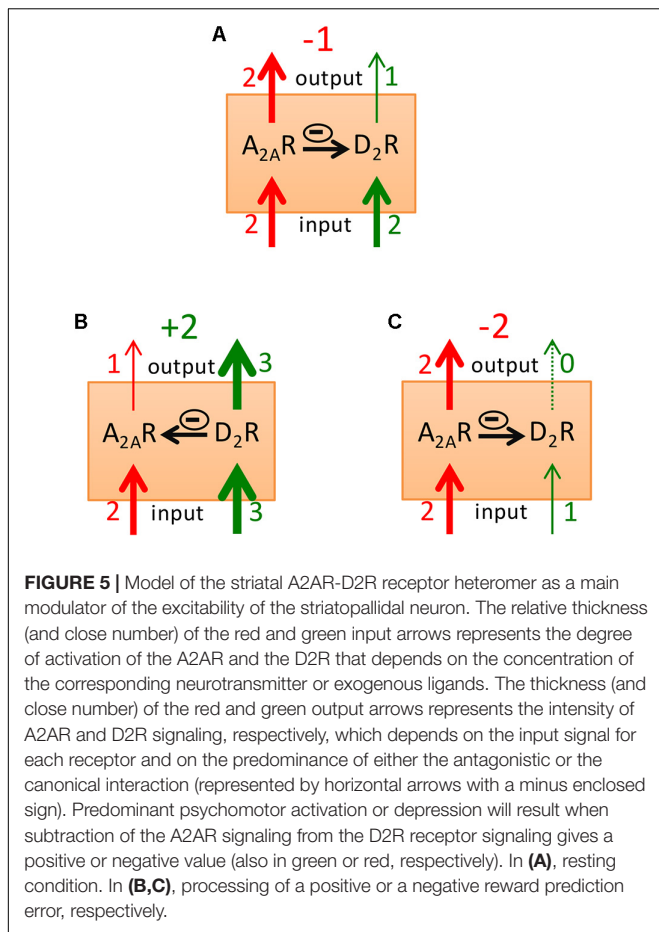
FIGURE 4 | Specific A2AR-D2R heteromer-dependent properties of SCH 442416 in mouse striatum. Transgenic conditional knockout striatopallidal neuron-Drd2-KO mice were generated by crossing mice expressing Cre driven by regulatory elements of the A2AR gene (*Adora2a*) [B6.FVB(Cg)-Tg(*Adora2a-Cre*)KG139Gsat/Mmucd; GENSAT; 036158-UCD] with mice carrying conditional D2R gene (*Drd2*) null alleles B6.129S4(FVB)-*Drd2*^{tm1.1Mrub/J}, JAX020631 (Bello et al., 2017). Membrane preparations from the striatum of striatopallidal-Drd2-KO (red) and their CRE negative littermates (WT, black) were incubated with [³H]ZM 241388 (2 nM) and increasing concentrations of SCH 442416 as described elsewhere (Bonaventura et al., 2015). Data points were fit to the two-state dimer receptor model (Casadó et al., 2007; Ferré et al., 2014), showing a biphasic curve due to negative cooperativity of SCH 442416 in WT mice (DCB = -1.8), but a monophasic curve in the conditional D2R null mice, thus reproducing the same behavior of SCH 442416 previously demonstrated in mammalian cells co-expressing A2AR and D2R and only A2AR, respectively (Orrú et al., 2011a).

signaling and a predominant allosteric interaction (Figure 5A), which results in low psychomotor activity. Reward-related stimuli and, particularly a “better than expected” rewarding stimulus (positive reward prediction error), leads to striatal dopamine release with a predominant D2R vs. A2AR signaling, potentiated by the canonical interaction (Figure 5B), leading to psychomotor activation. Aversive-related stimuli or a “worse than expected” rewarding stimuli (negative reward prediction error) leads to inhibition of dopamine release, to the weakest D2R and strongest A2AR signaling, which is potentiated by the canonical interaction (Figure 5C), leading to psychomotor arrest.

A pathogenic hallmark of akinesia in Parkinson’s disease is a pronounced hyperactivity of the striatopallidal neuron associated with the dopamine deficiency and pronounced decrease in the tonic D2R signaling. The discoveries on A2AR localization and function in striatopallidal neurons gave the rationale for the recently implemented A2AR antagonists in this disease (Müller and Ferré, 2007; Morelli et al., 2009; Armentero et al., 2011). It was initially suggested that the value of A2AR antagonists as antiparkinsonian agents would depend mostly on the allosteric interaction, on the ability of A2AR antagonists to potentiate D2R signaling by concomitant administration of L-dopa or a selective D2R agonist (Ferré et al., 1991b, 1992). This was followed by behavioral studies with genetic inactivation of A2AR and D2R, which stressed the value of the canonical interaction, which

was assumed to be independent of intermolecular interactions between A2AR and D2R (Chen et al., 2001). As mentioned above, the existence of the two apparently incompatible simultaneous allosteric and canonical interactions led to the hypothesis of the existence of two populations of A2AR in the striatopallidal neuron, one population forming heteromers with D2R and sustaining the allosteric interaction and another population not forming heteromers with D2R and sustaining the canonical interaction (Ferré et al., 2011; Orrú et al., 2011b). The unique pharmacological properties of SCH 442416, with its specific reduced affinity for the A2AR-D2R heteromer, due to negative cooperativity, were then exploited to attempt a pharmacological dissection of the two populations of postsynaptic A2AR. In fact, we previously used this strategy to dissect postsynaptic from presynaptic A2AR, which forms heteromers with A1R in the striatal glutamatergic terminals, where they play an important role in the modulation of glutamate release (Ciruela et al., 2006; Quiroz et al., 2009). A correlation had been shown with the higher potency of SCH 442416 to block presynaptic A1R-A2AR heteromers vs. postsynaptic A2AR-D2R heteromers and its higher potency to inhibit corticostriatal glutamate release than to produce locomotor activation (Orrú et al., 2011a). The preferential presynaptic profile of SCH 442416 was confirmed by other studies including other research groups (Hobson et al., 2013; O’Neill et al., 2014) and was suggested to provide a therapeutic approach for conditions with increased corticostriatal transmission, such as cannabinoid use disorder (Justinová et al., 2014). An apparently stronger potency of SCH 442416 to counteract locomotor depression induced by the D2R antagonist raclopride, as compared to that produced by the A2AR agonist CGS 2160, was then interpreted as the ability of SCH 442416 to also dissect the two putative postsynaptic populations of A2AR. The more sensitive population to SCH 442416 would be A2AR that do not form heteromers with D2R and that would sustain the canonical interaction (Orrú et al., 2011b). However, as mentioned before, we now know that the canonical interaction requires receptor heteromerization (Navarro et al., 2018). Therefore, we recently performed new studies on the behavioral effects of SCH 442416 upon genetic blockade of A2AR or D2R and upon administration of the A2AR agonist CGS 21680 and the D2R antagonist haloperidol, to reevaluate if they could all be explained within the framework of a predominant population of striatal postsynaptic A2AR-D2R heteromers (Taura et al., 2017).

To control strain-dependent behavioral differences and differences in drug responses, using CRISPR-Cas9 technology, we generated a D2R deficient mouse with the same genetic background as the CD-1 A2AR^{-/-} mouse (Ledent et al., 1997). CD-1 D2R^{-/-} mice showed a significant but relatively small reduction in spontaneous locomotor activity (Taura et al., 2017), as previously reported in D2R^{-/-} C57BL/6 mice (Baik et al., 1995). This is in contrast with the pronounced akinesia and catalepsy that characterize pharmacological D2R blockade (Ferré et al., 1990; Kanda et al., 1994; Shiozaki et al., 1999). Therefore, genetic D2R blockade is associated with neuroadaptations that counteract the loss of a D2R-mediated tonic stimulatory effect of endogenous dopamine on psychomotor activity. Indeed, a recent study in inducible D2R knockout adult mice that obviated



developmental compensations reported that the loss of D2R was associated with severe hypolocomotion and catalepsy (Bello et al., 2017). Likewise, the spontaneous locomotor activity of A2AR^{-/-} mice was also significantly reduced, as previously reported in the A2AR C57BL/6 mouse (Yang et al., 2009). Since pharmacological blockade leads to significant locomotor activation (see below and Karcz-Kubicha et al., 2003; Orrú et al., 2011a), the reduced activity of A2AR^{-/-} mice indicates the development of neuroadaptations that counteract the loss of an A2AR-mediated tonic inhibitory effect of endogenous adenosine on psychomotor activity. We also assessed sensorimotor processing of A2AR^{-/-} and D2R^{-/-} CD-1 mice by monitoring pre-pulse inhibitory responses (PPI) (Taura et al., 2017). As compared with WT mice, D2R^{-/-} mice did not show significant differences, while A2AR^{-/-} mice showed a significantly reduced PPI as previously reported (Wang et al., 2003; Moscoso-Castro et al., 2016), demonstrating a significant dependence on A2AR, but not D2R, signaling for a normal PPI. We also evaluated drug-induced catalepsy in A2AR^{-/-} and D2R^{-/-} mice. Our results showed that haloperidol-induced catalepsy was abolished and partially but significantly reduced in D2R^{-/-} and A2AR^{-/-} mice, respectively, as compared with WT mice (Taura et al., 2017), which is in agreement with previous work (Usiello et al., 2000; Chen et al., 2001; El Yacoubi et al., 2001). The results

support the dependence on A2AR signaling in the catalepsy induced by pharmacological blockade of D2R, which would agree with the existence of the tonic inhibition of A2AR signaling by endogenous dopamine driven by the canonical interaction in the A2AR-D2R heteromer. Neuroadaptations occurring in the A2AR^{-/-} mouse should explain the partial effect of genetic blockade of A2AR on D2R antagonist-induced catalepsy, which contrasts with the very effective blockade with A2AR antagonists (see below and Kanda et al., 1994; Shiozaki et al., 1999; Morelli and Wardas, 2001). We also assessed catalepsy induced by the A2AR agonist CGS 21680 (Ferré et al., 1991a; Kanda et al., 1994; Hauber and Münkler, 1997) in A2AR^{-/-} and D2R^{-/-} mice. As expected, CGS 21680 failed to induce catalepsy in A2AR^{-/-} mice, but its effect was partially but significantly reduced in D2R^{-/-} mice (Taura et al., 2017). Again, these results might reflect a functional antagonism related to neuroadaptations associated with genetic D2R blockade, which would tend to counteract the loss of the D2R-mediated tonic stimulatory effect of endogenous dopamine on psychomotor activity.

We then reevaluated the effect of SCH 442416 on locomotion, PPI and drug-induced catalepsy in WT, but also in A2AR^{-/-} and D2R^{-/-} mice. In WT CD-1 mice, SCH 442416 produced a significant and effective locomotor activation at 1 mg/kg (i.p.) (Taura et al., 2017), a dose three times lower than the minimal effective dose in Sprague-Dawley rats (Orrú et al., 2011a). As expected, SCH 44241 was unable to alter the locomotor activity in A2AR^{-/-} mice and it only moderately, but significantly, increased the activity in D2R^{-/-} mice (Taura et al., 2017). The decrease in the effect of the A2AR antagonist in D2R^{-/-} mice would agree with a dependence on D2R signaling in the locomotor activation induced by pharmacological blockade of A2AR, due to the tonic inhibition of D2R signaling by endogenous adenosine driven by the allosteric interaction in the A2AR-D2R heteromer. In agreement with the dependence on A2AR for PPI, SCH 442416 (at the minimal dose of 3 mg/kg, i.p.) induced a blockade of PPI in WT mice (Taura et al., 2017). This is also in agreement with a previous study in rats with intracranial infusion of another A2AR antagonist (MSX-3) in the NAc (Nagel et al., 2003). SCH 442416 was obviously ineffective on the already disrupted PPI in A2AR^{-/-} mice, but its disruptive effect was reduced in D2R^{-/-} mice (Taura et al., 2017). This could be related to the competing effect of endogenous adenosine by the released tonic inhibition of A2AR signaling by endogenous dopamine driven by the canonical interaction in the A2AR-D2R heteromer. Finally, SCH 442416 significantly reduced haloperidol-induced catalepsy, as previously reported for other A2AR antagonists (Kanda et al., 1994; Shiozaki et al., 1999; Morelli and Wardas, 2001), but with a higher minimal dose than the one needed to produce locomotor activation (3 vs. 1 mg/kg, i.p., respectively; Taura et al., 2017). To confirm the preferential pre- vs. postsynaptic profile of SCH 442416 in mice, we also performed dose-response experiments in C57BL/6 mice on locomotor activity and counteraction of corticostriatal glutamate release using a recently introduced optogenetic-microdialysis technique (Quiroz et al., 2016; Bonaventura et al., 2017). Different to previous experiments in rats, SCH 442416 showed the same potency

and efficiency as the selective A2AR antagonist KW 6002 at eliciting locomotor activation. Both drugs produced significant activation at 1 mg/kg (i.p.) but were inefficient at 0.1 mg/kg (Figure 6A). At this moment, we do not have an explanation for the lower potency and efficacy of SCH 442416 in rats as compared to mice. On the other hand, SCH 442416 was able to block optogenetically induced striatal glutamate release at 0.1 mg/kg, while KW 6002 was ineffective at 1 mg/kg (Figure 6B). This confirmed the experimental findings in rats, demonstrating a predominant striatal presynaptic and postsynaptic A2AR blocking properties of SCH 442416 and KW 6002, respectively (Orrú et al., 2011a).

Altogether, the results with genetic and pharmacological blockade of A2AR and D2R agree with a main role of A2AR-D2R heteromers in the striatopallidal neuron in conveying locomotor activation and PPI disruption induced by A2AR antagonists and D2R agonists and catalepsy mediated by A2AR agonists and D2R antagonists. More specifically, they also agree with A2AR-D2R heteromers in striatopallidal neurons mediating all postsynaptic pharmacological effects of SCH 442416, locomotor activation, blockade of PPI and counteraction of D2R antagonist-induced catalepsy. As shown in the scheme of Figure 3A, the A2AR-D2R heteromer explains the qualitatively different behavioral outputs depending on direct A2AR-Golf-AC-PKA-mediated increase in excitability or indirect D2R-Gi-PLC-PP2B-mediated disinhibition of the excitability of the striatopallidal neuron, leading to catalepsy and PPI (more related to the direct activation of the PKA-DARPP-32-CREB signaling; Bateup et al., 2010;

Berger et al., 2011) or just psychomotor depression, respectively. In fact, it is well known that catalepsy, with its rigidity component, is not qualitatively equivalent to a high degree of locomotor depression. Finally, and as mentioned before, depending on the intracellular concentrations of Ca^{2+} , A2AR, and D2R activation and co-activation lead to differential MAPK and Elk-1 activation, with implications for gene expression and synaptic plasticity (Figure 3A).

A2AR-D2R HETEROMER-MEDIATED CONTROL OF THE VENTRAL VS. DORSAL STRIATOPALLIDAL FUNCTION AND IMPLICATIONS FOR NEUROPSYCHIATRIC DISORDERS. 'APATHY' VS. 'AKINESIA'

Dysfunction of the central dopamine system is involved in a variety of disorders, including Parkinson's disease, schizophrenia, and substance use disorders (SUD). The functional separation of striatal compartments in ventral, rostral-dorsal and caudal-dorsal striata allows a more syndromic sub-classification of those disorders with potentially significant new therapeutic approaches. Parkinson's disease and non-human primate models of Parkinson's disease provide the clearest illustration. The cardinal motor symptoms of Parkinson's disease, bradykinesia, rigidity and tremor (Jankovic, 2008), have been classically

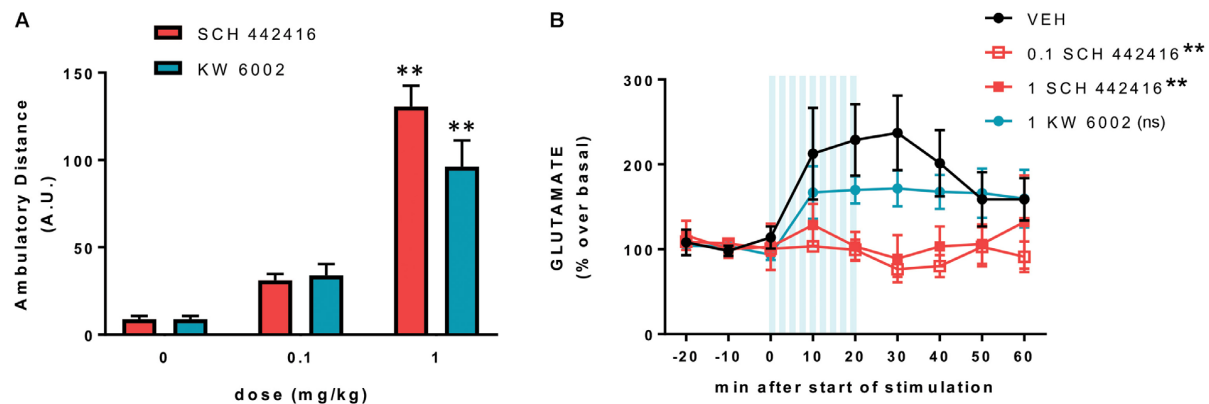


FIGURE 6 | Preferential presynaptic profile of SCH 442416 in C57BL/6 mice. **(A)** SCH 442416 shows similar potency and efficacy to KW 6002 at producing locomotor activation. Locomotor activity was measured in an open field arena as described elsewhere (Bonaventura et al., 2015); animals were injected intraperitoneally (i.p.) with vehicle (saline with 10% DMSO and 10% Tween-80) and the indicated concentrations of SCH 442416 or KW 6002 and the locomotor activity was measured for 2 h in activity chambers with 42.0 cm × 42.0 cm open fields (Coulbourn Instruments); values are mean ± SEM of the traveled distance (arbitrary units, A.U.); two-way ANOVA with Newman-Keuls *post hoc* test did not demonstrate significant differences between the two A2AR antagonists and, for both drugs, it only showed significant differences with the dose of 1 mg/kg as compared to the corresponding vehicle-treated groups (***p* < 0.01 compared to vehicle; *n* = 8–11). **(B)** Optogenetic-microdialysis experiments were performed as described elsewhere (Bonaventura et al., 2017); briefly, C57BL/6 mice received a unilateral injection of an AAV encoding Chr2 (Chr2/H134R) fused to EYFP under control of the CaMKIIα neuronal promoter [AAV-CaMKIIα-hChr2(H134R)-EYFP] in the motor cortex. One month later, an optogenetic-microdialysis probe (Quiroz et al., 2016; Bonaventura et al., 2017) was implanted in the dorsal striatum, and glutamate in the dialysate was measured at 10-min intervals before, during, and after optogenetic stimulation of the corticostriatal terminals. Vehicle (black plot, see above) or the indicated doses of SCH 442416 (red plot) or KW 6002 (blue plot) were administered (i.p.) 10 min before the start of the stimulation. Values (in % over basal) represent mean ± SEM, normalized to the mean of the concentration of GLU present in the three samples preceding stimulation; one-way ANOVA with Newman-Keuls *post hoc* test showed a significant decrease of the transformed values (area under the curve, data from min 0 to min 60) from both groups treated with SCH 442416 (1 and 0.1 mg/kg), but not from the group treated with KW 6002, compared to the vehicle group (***p* < 0.01 compared to vehicle; ns, non-significant; *n* = 7–8).

1369 attributed to dysfunction of the skeletomotor system, the brain
1370 circuits involved in the execution and coordination of body
1371 movements. Contemporary theories embracing parallel cortical-
1372 striatal-thalamic-cortical circuits in the pathogenesis of this
1373 disorder emphasize the particular involvement of the “motor
1374 circuit,” which includes motor cortical areas (DeLong and
1375 Wichmann, 2015). In fact, in Parkinson’s disease, dopamine
1376 cell degeneration tends to occur initially and predominantly
1377 in the lateral part of the SNpc, which projects mainly to the
1378 caudal-dorsal striatum. Thus, there is a predominant deficit of
1379 the more “automatic” vs. “volitional” action skills and most
1380 sequential psychomotor responses need to be performed with
1381 full attention (Kim and Hikosaka, 2015). Nevertheless, with
1382 more advanced stages of Parkinson’s disease the function of the
1383 more rostral striatum becomes also compromised, with deficits
1384 in “volitional” actions skills (Kim and Hikosaka, 2015). With
1385 further (or preferential) ventral degeneration of the dopamine
1386 mesencephalic nuclei (VTA) we move to the pathology of the
1387 ventral striatum, to apathy (Tremblay et al., 2015), as it has also
1388 been demonstrated experimentally in the non-human primate
1389 (Brown et al., 2012; Tian et al., 2015).

1390 Initial studies on the psychomotor-activating effects of
1391 caffeine or selective A2AR antagonists dealt with general
1392 locomotor activity and were translationally applied to the
1393 treatment of akinesia in Parkinson’s disease (see above and
1394 Müller and Ferré, 2007; Morelli et al., 2009; Armentero
1395 et al., 2011). Those initial studies implicitly considered A2AR-
1396 D2R heteromers in the dorsal striatum, but a large number
1397 of studies indicated that not only dorsal but also ventral
1398 striatopallidal neurons express A2R and A2AR-D2R heteromers
1399 (Ferré et al., 1994; Ferré, 1997; Hauber and Münkler, 1997;
1400 Pinna et al., 1997; Svenningsson et al., 1997; Ishiwari et al.,
1401 2007). More recent studies have also analyzed the effect of
1402 caffeine and A2AR antagonists on more specific reward-oriented
1403 behaviors, showing that they can increase the responsiveness
1404 to food-related stimuli, sucrose solutions, stimuli that elicit
1405 maternal behavior and self-administration (Pereira et al., 2011;
1406 Randall et al., 2011; Sheppard et al., 2012; Nunes et al.,
1407 2013; Lazenka et al., 2015). The work by Salamone’s group
1408 has specifically addressed the role of adenosine and A2AR in
1409 effort-related choice behavior. Direct administration of A2AR
1410 agonists in the NAc altered effort-related choice behavior in
1411 a manner closely resembling the effects of interference with
1412 ventral striatal dopamine neurotransmission, decreasing the
1413 degree of responsiveness (“effort”) to reward-associated stimuli.
1414 Furthermore, A2AR antagonists reversed the effort discounting
1415 effects of D2R antagonists (Salamone et al., 2012; Nunes et al.,
1416 2013).

1417 Clinically, apathy has been defined as “a syndrome consisting
1418 of loss of motivation not attributable to disturbances in
1419 emotion, intellect or consciousness” (Marin, 1991). However,
1420 it is becoming obvious that apathy is a multifaceted concept
1421 that includes dissociable constructs that should correspond to
1422 dissociable neurobiological correlates (Sinha et al., 2013). We
1423 hypothesize that some if not all those dissociable correlates
1424 correspond to corticostriatal circuits involving the different
1425 functional striatal compartments and their “Go” and “NoGo”

1426 pathways. In fact, attuned with the role of dopamine in reward-
1427 associated behavior in all striatal compartments, recent studies
1428 even allow conceptualizing Parkinson’s disease bradykinesia in
1429 a motivational framework (Mazzoni et al., 2007; Chong et al.,
1430 2015). Nevertheless, as defined clinically, apathy is a common
1431 non-motor symptom of Parkinson’s disease (den Brok et al.,
1432 2015) that correlates negatively with dopamine innervation
1433 in the ventral striatum (Remy et al., 2005; Chaudhuri et al.,
1434 2006; Brown et al., 2012). In fact, a deficit in the dopamine
1435 modulation of the ventral striatum should translate, first, in
1436 a deficit in responsiveness, with a global inability to respond
1437 to reward- and punishment-associated stimuli (attuned with
1438 the “whether to respond” vs. “how to respond” functions of
1439 ventral vs. dorsal striatum). Second, it should lead to dysfunction
1440 of reward valuation, in alterations (increase) in DD, ED and
1441 LPD (attuned with the ventral striatum as forming part of
1442 corticostriatal circuits involved in reward valuation tasks).
1443 Indeed, non-medicated patients with Parkinson’s disease have
1444 shown increases in DD and ED (Al-Khaled et al., 2015; Chong
1445 et al., 2015).

1446 Interestingly, apathy is also a major negative symptom of
1447 schizophrenia, classically considered as a disorder associated
1448 with central hyperdopaminergic tone. Several studies have found
1449 evidence for selective dysfunction of the ventral striatum in
1450 schizophrenia, specifically hypoactivation with reward-associated
1451 stimuli (Simon et al., 2010, 2015; Strauss et al., 2015; Kirschner
1452 et al., 2016). Ventral striatal activation during reward anticipation
1453 was in fact found to be selectively and inversely correlated with
1454 apathy but not with other negative symptoms (Simon et al.,
1455 2010; Kirschner et al., 2016). Two additional findings give a
1456 clue for the mechanisms of apathy in schizophrenia, which
1457 seem to be dopamine-independent or at least not related to
1458 a decrease in the dopamine tone. First, there is a reduced
1459 functional connectivity between the orbito-frontal cortex (OFC)
1460 and the ventral striatum (Simon et al., 2015); second, there
1461 is consistent evidence that schizophrenic patients suffer from
1462 selective deficits in learning from positive outcomes, with intact
1463 learning from negative outcomes (Strauss et al., 2015). Therefore,
1464 the apathetic schizophrenic patient seems to have a selective
1465 decreased activation of the “Go” pathway, a reduction in the
1466 ratio of activation of “Go” vs. “NoGo” pathways secondary
1467 to impaired cortical-ventral striatal connectivity (Strauss et al.,
1468 2015). A similar situation would also be present in the patient
1469 with SUD, a decreased “Go”/“NoGo” pathway activation, also
1470 with reduced ventral striatal activation to reward stimuli
1471 (which can basically only be activated by the addictive drugs)
1472 (Volkow et al., 2011). Apathy is a well-known symptom in
1473 SUD, although it has been scarcely addressed experimentally
1474 (Verdejo-García et al., 2006; Verdejo-García and Pérez-García,
1475 2008; Gjini et al., 2014). The SUD patient is motivated to
1476 procure the drug but tends to be withdrawn and apathetic
1477 when exposed to non-drug-related activities (Verdejo-García
1478 et al., 2006). In this case, however, the pathogenesis seems to
1479 follow from an initial reduction in D2R density (maybe with
1480 a concomitant relative increase of A2AR which would not be
1481 opposed by D2R forming heteromers), leading to an increased
1482 activity of the ventral striatopallidal neuronal function, of the

1483 “NoGo” pathway. The tonic decrease in feedback activation of the
 1484 ventromedial prefrontal cortex, orbitofrontal cortex and anterior
 1485 cingulate cortex leads to additional dysfunction of the decision-
 1486 making cortical-ventral striatal circuits (Volkow et al., 2011;
 1487 Belcher et al., 2014). These changes lead to a similar situation than
 1488 the non-motor symptoms in patients with Parkinson’s disease,
 1489 to apathy and choice impulsivity, as demonstrated by several
 1490 studies indicating increase DD in patients with SUD (Belcher
 1491 et al., 2014; Hamilton et al., 2015). In summary, for all types
 1492 of apathy, the relative increase in the ventral striopallidal vs.
 1493 striatonigral neuronal function should benefit from the treatment
 1494 with A2AR antagonists, targeting A2AR-D2R heterotetramer-
 1495 AC5 complexes.

1496
 1497
 1498 **CONCLUSION**

1499
 1500 A significant amount of experimental and clinical evidence
 1501 demonstrates that A2AR and D2R localized in the ventral and
 1502 dorsal striatopallidal neurons cannot be considered anymore
 1503 as single functional units, but as forming part of complexes
 1504 of the A2AR-D2R heterotetramer-AC5 complexes, which
 1505 exert a fine-tuned integration of adenosine and dopamine
 1506 neurotransmission. The current accumulated knowledge of
 1507 the biochemical properties of the A2AR-D2R heteromer
 1508 offer new therapeutic possibilities for Parkinson’s disease,
 1509 schizophrenia, SUD and other neuropsychiatric disorders with
 1510 dysfunction of dorsal or ventral striatopallidal neurons. More
 1511 generally, this knowledge implies we should modify classical
 1512 views of GPCR physiology and pharmacology and include
 1513 GPCR heteromers as main targets for drug development.
 1514 The understanding of the biochemical properties of GPCR
 1515 heteromers specifically localized in neuronal elements that
 1516 form part of neuronal circuits involved in the pathophysiology
 1517 of specific neuropsychiatric disorders should provide new
 1518
 1519

1520 **REFERENCES**

1521 Al-Khaled, M., Heldmann, M., Bolstorff, I., Hagenah, J., and Münte, T. F.
 1522 (2015). Intertemporal choice in Parkinson’s disease and restless legs syndrome.
 1523 *Parkinsonism Relat. Disord.* 21, 1330–1335. doi: 10.1016/j.parkreldis.2015.09.
 1524 026
 1525 Armentero, M. T., Pinna, A., Ferré, S., Lanciego, J. L., Müller, C. E., and Franco, R.
 1526 (2011). Past, present and future of A(2A) adenosine receptor antagonists in the
 1527 therapy of Parkinson’s disease. *Pharmacol. Ther.* 132, 280–299. doi: 10.1016/j.
 1528 pharmthera.2011.07.004
 1529 Azdad, K., Gall, D., Woods, A. S., Ledent, C., Ferré, S., and Schiffmann, S. N.
 1530 (2009). Dopamine D2 and denosine A2A receptors regulate NMDA-mediated
 1531 excitation in accumbens neurons through A2A-D2 receptor heteromerization.
 1532 *Neuropsychopharmacology* 34, 972–986. doi: 10.1038/npp.2008.144
 1533 Baik, J. H., Picetti, R., Saiardi, A., Thiriet, G., Dierich, A., Depaulis, A., et al.
 1534 (1995). Parkinsonian-like locomotor impairment in mice lacking dopamine D2
 1535 receptors. *Nature* 377, 424–428. doi: 10.1038/377424a0
 1536 Balleine, B. W., and O’Doherty, J. P. (2010). Human and rodent homologies
 1537 in action control: corticostriatal determinants of goal-directed and
 1538 habitual action. *Neuropsychopharmacology* 35, 48–69. doi: 10.1038/npp.20
 1539 09.131
 1540 Bateup, H. S., Santini, E., Shen, W., Birnbaum, S., Valjent, E., Surmeier, D. J.,
 1541 et al. (2010). Distinct subclasses of medium spiny neurons differentially regulate

selective pharmacological approaches with less secondary 1540
 effects. 1541

1542
 1543 **ETHICS STATEMENT**

1544
 1545 All animals used in the study were maintained in accordance with
 1546 the guidelines of the National Institutes of Health (NIH) Animal
 1547 Care, and the animal research conducted to perform this study
 1548 was approved by the NIDA IRP Animal Care and Use Committee
 1549 (protocols #12-BNRB-73, #15-BNRB-73, and #12-MTMD-2). 1550
 1551

1552
 1553 **AUTHOR CONTRIBUTIONS**

1554
 1555 JB, WZ, CH-S, and KT performed the experiments and analyzed
 1556 the data. SF, JB, AK, VC, DL, and DZ designed the experiments.
 1557 SF, JB, JT, CQ, N-SC, EM, VC-A, AK, DT, GN, AC, LP, CL, CD,
 1558 NV, VC, FC, DL, and DZ wrote the manuscript. 1559
 1560

1561
 1562 **FUNDING**

1563
 1564 This work was supported by the intramural funds of the
 1565 National Institute on Drug Abuse, “Ministerio de Economía
 1566 y Competitividad”, MINECO/FEDER (SAF2014-55700-P,
 1567 SAF2014-54840-R, and PIE14/00034), Generalitat de Catalunya
 1568 (2014 SGR 1054 and 2014-SGR-1236), and Fundació la Marató
 1569 de TV3 (20140610 and 20152031). 1570
 1571

1572
 1573 **ACKNOWLEDGMENTS**

1574
 1575 The authors apologize if they unwittingly omitted other relevant
 1576 studies about the interactions between A2AR and D2R in the
 1577 functional control of striatopallidal neurons. 1578
 1579

1580 striatal motor behaviors. *Proc. Natl. Acad. Sci. U.S.A.* 107, 14845–14850.
 1581 doi: 10.1073/pnas.1009874107
 1582 Belcher, A. M., Volkow, N. D., Moeller, F. G., and Ferré, S. (2014). Personality traits
 1583 and vulnerability or resilience to substance use disorders. *Trends Cogn. Sci.* 18,
 1584 211–217. doi: 10.1016/j.tics.2014.01.010
 1585 Bello, E. P., Casas-Cordero, R., Galiñanes, G. L., Casey, E., Belluscio, M. A.,
 1586 Rodríguez, V., et al. (2017). Inducible ablation of dopamine D2 receptors
 1587 in adult mice impairs locomotion, motor skill learning and leads to severe
 1588 parkinsonism. *Mol. Psychiatry* 22, 595–604. doi: 10.1038/mp.2016.105
 1589 Berger, A. K., Green, T., Siegel, S. J., Nestler, E. J., and Hammer, R. P. Jr.
 1590 (2011). cAMP response element binding protein phosphorylation in nucleus
 1591 accumbens underlies sustained recovery of sensorimotor gating following
 1592 repeated D₂-like receptor agonist treatment in rats. *Biol. Psychiatry* 69, 288–294.
 1593 doi: 10.1016/j.biopsych.2010.08.032
 1594 Bertran-Gonzalez, J., Bosch, C., Maroteaux, M., Matamales, M., Hervé, D.,
 1595 Valjent, E., et al. (2008). Opposing patterns of signaling activation in dopamine
 1596 D1 and D2 receptor-expressing striatal neurons in response to cocaine and
 1597 haloperidol. *J. Neurosci.* 28, 5671–5685. doi: 10.1523/jneurosci.1039-08.2008
 1598 Besnard, A., Galan-Rodriguez, B., Vanhoutte, P., and Caboche, J. (2011). Elk-1
 1599 a transcription factor with multiple facets in the brain. *Front. Neurosci.* 5:35.
 1600 doi: 10.3389/fnins.2011.00035
 1601 Boegman, R. J., and Vincent, S. R. (1996). Involvement of adenosine and glutamate
 1602 receptors in the induction of c-fos in the striatum by haloperidol. *Synapse*
 1603 1594
 1604 1595
 1605 1596

- 1597 22, 70–77. doi: 10.1002/(SICI)1098-2396(199601)22:1<70::AID-SYN8>3.0.
1598 CO;2-F
- 1599 Bonaventura, J., Navarro, G., Casadó-Anguera, V., Azdad, K., Rea, W., Moreno, E.,
1600 et al. (2015). Allosteric interactions between agonists and antagonists within
1601 the adenosine A2A receptor-dopamine D2 receptor heterotetramer. *Proc. Natl.
1602 Acad. Sci. U.S.A.* 112, E3609–E3618. doi: 10.1073/pnas.1507704112
- 1602 Bonaventura, J., Quiroz, C., Cai, N. S., Rubinstein, M., Tanda, G., and Ferré,
1603 S. (2017). Key role of the dopamine D(4) receptor in the modulation
1604 of corticostriatal glutamatergic neurotransmission. *Sci. Adv.* 3:e1601631.
1605 doi: 10.1126/sciadv.1601631
- 1605 Bromberg-Martin, E. S., Matsumoto, M., and Hikosaka, O. (2010). Dopamine in
1606 motivational control: rewarding, aversive, and alerting. *Neuron* 68, 815–834.
1607 doi: 10.1016/j.neuron.2010.11.022
- 1608 Brown, C. A., Campbell, M. C., Karimi, M., Tabbal, S. D., Loftin, S. K., Tian,
1609 L. L., et al. (2012). Dopamine pathway loss in nucleus accumbens and ventral
1610 tegmental area predicts apathetic behavior in MPTP-lesioned monkeys. *Exp.
1611 Neurol.* 236, 190–197. doi: 10.1016/j.expneurol.2012.04.025
- 1611 Casadó, V., Cortés, A., Ciruela, F., Mallol, J., Ferré, S., Lluís, C., et al. (2007). Old
1612 and new ways to calculate the affinity of agonists and antagonists interacting
1613 with G-protein-coupled monomeric and dimeric receptors: the receptor-dimer
1614 cooperativity index. *Pharmacol. Ther.* 116, 343–354. doi: 10.1016/j.pharmthera.
1615 2007.05.010
- 1615 Casas, M., Ferré, S., Cobos, A., Grau, J. M., and Jané, F. (1989). Relationship
1616 between rotational behaviour induced by apomorphine and caffeine in rats with
1617 unilateral lesion of the nigrostriatal pathway. *Neuropharmacology* 28, 407–409.
1618 doi: 10.1016/0028-3908(89)90037-3
- 1618 Casas, M., Prat, G., Robledo, P., Barbanj, M., Kulisevsky, J., and Jané, F. (2000).
1619 Methylxanthines reverse the adipsic and aphagic syndrome induced by bilateral
1620 6-hydroxydopamine lesions of the nigrostriatal pathway in rats. *Pharmacol.
1621 Biochem. Behav.* 66, 257–263. doi: 10.1016/S0091-3057(00)00189-1
- 1622 Chang, C. Y., Esber, G. R., Marrero-Garcia, Y., Yau, H. J., Bonci, A., and
1623 Schoenbaum, G. (2016). Brief optogenetic inhibition of dopamine neurons
1624 mimics endogenous negative reward prediction errors. *Nat. Neurosci.* 19, 111–
1625 116. doi: 10.1038/nn.4191
- 1625 Chaudhuri, K. R., Martinez-Martin, P., Schapira, A. H., Stocchi, F., Sethi, K.,
1626 Odin, P., et al. (2006). International multicenter pilot study of the
1627 first comprehensive self-completed nonmotor symptoms questionnaire for
1628 Parkinson's disease: the NMSQuest study. *Mov. Disord.* 21, 916–923.
1629 doi: 10.1002/mds.20844
- 1629 Chen, J. F., Moratalla, R., Impagnatiello, F., Grandy, D. K., Cuellar, B.,
1630 Rubinstein, M., et al. (2001). The role of the D(2) dopamine receptor (D(2)R)
1631 in A(2A) adenosine receptor (A(2A)R)-mediated behavioral and cellular
1632 responses as revealed by A(2A) and D(2) receptor knockout mice. *Proc. Natl.
1633 Acad. Sci. U.S.A.* 98, 1970–1975. doi: 10.1073/pnas.98.4.1970
- 1633 Chong, T. T., Bonnelle, V., Manohar, S., Veromann, K. R., Muhammed, K., Tofaris,
1634 G. K., et al. (2015). Dopamine enhances willingness to exert effort for reward in
1635 Parkinson's disease. *Cortex* 69, 40–46. doi: 10.1016/j.cortex.2015.04.003
- 1635 Ciruela, F., Casadó, V., Rodrigues, R. J., Luján, R., Burgueño, J., Canals, M.,
1636 et al. (2006). Presynaptic control of striatal glutamatergic neurotransmission
1637 by adenosine A1-A2A receptor heteromers. *J. Neurosci.* 26, 2080–2087.
1638 doi: 10.1523/JNEUROSCI.3574-05.2006
- 1639 Danjo, T., Yoshimi, K., Funabiki, K., Yawata, S., and Nakanishi, S. (2014).
1640 Aversive behavior induced by optogenetic inactivation of ventral tegmental
1641 area dopamine neurons is mediated by dopamine D2 receptors in the nucleus
1642 accumbens. *Proc. Natl. Acad. Sci. U.S.A.* 111, 6455–6460. doi: 10.1073/pnas.
1643 1404323111
- 1643 DeLong, M. R., and Wichmann, T. (2015). Basal ganglia circuits as targets
1644 for neuromodulation in Parkinson disease. *JAMA Neurol.* 72, 1354–1360.
1645 doi: 10.1001/jamaneurol.2015.2397
- 1645 den Brok, M. G., van Dalen, J. W., van Gool, W. A., Moll van Charante, E. P., de
1646 Bie, R. M., and Richard, E. (2015). Apathy in Parkinson's disease: a systematic
1647 review and meta-analysis. *Mov. Disord.* 30, 759–769. doi: 10.1002/mds.26208
- 1648 Dreyer, J. K., Herrik, K. F., Berg, R. W., and Hounsgaard, J. D. (2010). Influence
1649 of phasic and tonic dopamine release on receptor activation. *J. Neurosci.* 30,
1650 14273–14283. doi: 10.1523/jneurosci.1894-10.2010
- 1650 Durieux, P. F., Bearzatto, B., Guiducci, S., Buch, T., Waisman, A., Zoli, M., et al.
1651 (2009). D2R striatopallidal neurons inhibit both locomotor and drug reward
1652 processes. *Nat. Neurosci.* 12, 393–395. doi: 10.1038/nn.2286
- 1653 El Yacoubi, M., Ledent, C., Parmentier, M., Costentin, J., and Vaugeois, J. M. 1654
1655 (2001). Adenosine A2A receptor knockout mice are partially protected against
1656 drug-induced catalepsy. *Neuroreport* 12, 983–986. doi: 10.1097/00001756-
1657 200104170-00024
- 1657 Ferré, S. (1997). Adenosine-dopamine interactions in the ventral striatum.
1658 Implications for the treatment of schizophrenia. *Psychopharmacology* 133,
1659 107–120. doi: 10.1007/s002130050380
- 1660 Ferré, S. (2008). An update on the mechanisms of the psychostimulant effects of
1661 caffeine. *J. Neurochem.* 105, 1067–1079. doi: 10.1111/j.1471-4159.2007.05196.x
- 1661 Ferré, S. (2015). The GPCR heterotetramer: challenging classical pharmacology.
1662 *Trends Pharmacol. Sci.* 36, 145–152. doi: 10.1016/j.tips.2015.01.002
- 1662 Ferré, S. (2016). Mechanisms of the psychostimulant effects of caffeine:
1663 implications for substance use disorders. *Psychopharmacology* 233, 1963–1979.
1664 doi: 10.1007/s00213-016-4212-2
- 1664 Ferré, S. (2017). “Adenosine control of striatal function. Implications for the
1665 treatment of apathy in basal ganglia disorders,” in *Adenosine Receptors in
1666 Degenerative Diseases*, eds D. Blum and L. V. Lopes (Amsterdam: Elsevier),
1667 231–255. doi: 10.1016/B978-0-12-803724-9.00012-0
- 1668 Ferré, S., Bonaventura, J., Tomasi, D., Navarro, G., Moreno, E., Cortés, A.,
1669 et al. (2016). Allosteric mechanisms within the adenosine A2A-dopamine
1670 D2 receptor heterotetramer. *Neuropharmacology* 104, 154–160. doi: 10.1016/
1671 j.neuropharm.2015.05.028
- 1671 Ferré, S., Casadó, V., Devi, L. A., Filizola, M., Jockers, R., Lohse, M. J., et al. 1672
1673 (2014). G protein-coupled receptor oligomerization revisited: functional and
1674 pharmacological perspectives. *Pharmacol. Rev.* 66, 413–434. doi: 10.1124/pr.
1675 113.008052
- 1675 Ferré, S., Fredholm, B. B., Morelli, M., Popoli, P., and Fuxe, K. (1997). Adenosine-
1676 dopamine receptor-receptor interactions as an integrative mechanism in the
1677 basal ganglia. *Trends Neurosci.* 20, 482–487. doi: 10.1016/S0166-2236(97)
1678 01096-5
- 1678 Ferré, S., Fuxe, K., von Euler, G., Johansson, B., and Fredholm, B. B. (1992).
1679 Adenosine-dopamine interactions in the brain. *Neuroscience* 51, 501–512.
1680 doi: 10.1016/0306-4522(92)90291-9
- 1680 Ferré, S., Guix, T., Prat, G., Jane, F., and Casas, M. (1990). Is experimental
1681 catalepsy properly measured? *Pharmacol. Biochem. Behav.* 35, 753–757. doi: 10.1016/
1682 0091-3057(90)90354-K
- 1682 Ferré, S., O'Connor, W. T., Fuxe, K., and Ungerstedt, U. (1993). The striopallidal
1683 neuron: a main locus for adenosine-dopamine interactions in the brain.
1684 *J. Neurosci.* 13, 5402–5406.
- 1684 Ferré, S., O'Connor, W. T., Snaprud, P., Ungerstedt, U., and Fuxe, K. (1994).
1685 Antagonistic interaction between adenosine A2A receptors and dopamine D2
1686 receptors in the ventral striopallidal system. *Implications for the treatment
1687 of schizophrenia. Neuroscience* 63, 765–773. doi: 10.1016/0306-4522(94)90
1688 521-5
- 1688 Ferré, S., Quiroz, C., Orru, M., Guitart, X., Navarro, G., Cortés, A., et al. 1690
1691 (2011). Adenosine A(2A) receptors and A(2A) receptor heteromers as key
1692 players in striatal function. *Front. Neuroanat.* 5:36. doi: 10.3389/fnana.2011.0
1693 0036
- 1693 Ferré, S., Rubio, A., and Fuxe, K. (1991a). Stimulation of adenosine A2 receptors
1694 induces catalepsy. *Neurosci. Lett.* 130, 162–164.
- 1694 Ferré, S., von Euler, G., Johansson, B., Fredholm, B. B., and Fuxe, K. (1991b).
1695 Stimulation of high-affinity adenosine A2 receptors decreases the affinity of
1696 dopamine D2 receptors in rat striatal membranes. *Proc. Natl. Acad. Sci. U.S.A.*
1697 88, 7238–7241.
- 1697 Frank, M. J. (2005). Dynamic dopamine modulation in the basal ganglia:
1698 a neurocomputational account of cognitive deficits in medicated and
1699 nonmedicated Parkinsonism. *J. Cogn. Neurosci.* 17, 51–72. doi: 10.1162/
1700 0898929052880093
- 1700 Frank, M. J., Seeberger, L. C., and O'Reilly, R. C. (2004). By carrot or by stick:
1701 cognitive reinforcement learning in parkinsonism. *Science* 306, 1940–1943.
1702 Frederick, A. L., Yano, H., Trifilieff, P., Vishwasrao, H. D., Biezonski, D.,
1703 Mészáros, J., et al. (2015). Evidence against dopamine D1/D2 receptor
1704 heteromers. *Mol. Psychiatry* 20, 1373–1385. doi: 10.1038/mp.2014.166
- 1705 Freeze, B. S., Kravitz, A. V., Hammack, N., Berke, J. D., and Kreitzer, A. C. (2013).
1706 Control of basal ganglia output by direct and indirect pathway projection
1707 neurons. *J. Neurosci.* 33, 18531–18539. doi: 10.1523/JNEUROSCI.1278-13.2013
- 1707 Fuxe, K., and Ungerstedt, U. (1974). Action of caffeine and theophyllamine
1708 on supersensitive dopamine receptors: considerable enhancement of receptor
1709
- 1710

- 1711 response to treatment with DOPA and dopamine receptor agonists. *Med. Biol.* 52, 48–54.
- 1712 Garrett, B. E., and Holtzman, S. G. (1995). Does adenosine receptor blockade
- 1713 mediate caffeine-induced rotational behavior? *J. Pharmacol. Exp. Ther.* 274,
- 1714 207–214.
- 1715 Gerfen, C. R. (2004). “Basal ganglia,” in *The Rat Nervous System*, ed. G. Paxinos
- 1716 (Amsterdam: Elsevier), 445–508.
- 1717 Gjini, K., Qazi A., Greenwald, M. K., Sandhu, R., Gooding, D. C., and Boutros,
- 1718 N. N. (2014). Relationships of behavioral measures of frontal lobe dysfunction
- 1719 with underlying electrophysiology in cocaine-dependent patients. *Am. J.*
- 1720 *Addict.* 23, 265–271. doi: 10.1111/j.1521-0391.2014.12095.x
- 1721 Haber, S. N. (2014). The place of dopamine in the cortico-basal ganglia circuit. *Neuroscience* 282, 248–257. doi: 10.1016/j.neuroscience.2014.10.008
- 1722 Haber, S. N., and Behrens, T. E. (2014). The neural network underlying incentive-
- 1723 based learning: implications for interpreting circuit disruptions in psychiatric
- 1724 disorders. *Neuron* 83, 1019–1039. doi: 10.1016/j.neuron.2014.08.031
- 1725 Håkansson, K., Galdi, S., Hendrick, J., Snyder, G., Greengard, P., and Fisone, G.
- 1726 (2006). Regulation of phosphorylation of the GluR1 AMPA receptor by
- 1727 dopamine D2 receptors. *J. Neurochem.* 96, 482–488. doi: 10.1111/j.1471-4159.
- 1728 2005.03558.x
- 1729 Hamilton, K. R., Mitchell, M. R., Wing, V. C., Balodis, I. M., Bickel, W. K.,
- 1730 Fillmore, M., et al. (2015). Choice impulsivity: definitions, measurement issues,
- 1731 and clinical implications. *Personal. Disord.* 6, 182–198. doi: 10.1037/per0000099
- 1732 Hauber, W., and Münkler, M. (1997). Motor depressant effects mediated by
- 1733 dopamine D2 and adenosine A2A receptors in the nucleus accumbens and
- 1734 the caudate-putamen. *Eur. J. Pharmacol.* 323, 127–131. doi: 10.1016/S0014-
- 1735 2999(97)00040-X
- 1736 Hernandez-Lopez, S., Tkatch, T., Perez-Garci, E., Galarraga, E., Bargas, J.,
- 1737 Hamm, H., et al. (2000). D2 dopamine receptors in striatal medium spiny
- 1738 neurons reduce L-type Ca²⁺ currents and excitability via a novel PLC[β]1-
- 1739 IP3-calcineurin-signaling cascade. *J. Neurosci.* 20, 8987–8995.
- 1740 Herrera-Marschitz, M., Casas, M., and Ungerstedt, U. (1988). Caffeine produces
- 1741 contralateral rotation in rats with unilateral dopamine denervation:
- 1742 comparisons with apomorphine-induced responses. *Psychopharmacology*
- 1743 94, 38–45. doi: 10.1007/BF00735878
- 1744 Higley, M. J., and Sabatini, B. L. (2010). Competitive regulation of synaptic
- 1745 Ca²⁺ influx by D2 dopamine and A2A adenosine receptors. *Nat. Neurosci.* 13,
- 1746 958–966. doi: 10.1038/nn.2592
- 1747 Hikida, T., Kimura, K., Wada, N., Funabiki, K., and Nakanishi, S. (2010). Distinct
- 1748 roles of synaptic transmission in direct and indirect striatal pathways to reward
- 1749 and aversive behavior. *Neuron* 66, 896–907. doi: 10.1016/j.neuron.2010.05.011
- 1750 Hikida, T., Yawata, S., Yamaguchi, T., Danjo, T., Sasaoka, T., Wang, Y., et al. (2013).
- 1751 Pathway-specific modulation of nucleus accumbens in reward and aversive
- 1752 behavior via selective transmitter receptors. *Proc. Natl. Acad. Sci. U.S.A.* 110,
- 1753 342–347. doi: 10.1073/pnas.1220358110
- 1754 Hikosaka, O. (2007). Basal ganglia mechanisms of reward-oriented eye movement. *Ann. N. Y. Acad. Sci.* 1104, 229–249. doi: 10.1196/annals.1390.012
- 1755 Hillion, J., Canals, M., Torvinen, M., Casado, V., Scott, R., Terasmaa, A., et al.
- 1756 (2002). Coaggregation, cointernalization, and codesensitization of adenosine
- 1757 A2A receptors and dopamine D2 receptors. *J. Biol. Chem.* 277, 18091–18097.
- 1758 doi: 10.1074/jbc.M107731200
- 1759 Hobson, B. D., O'Neill, C. E., Levis, S. C., Monteggia, L. M., Neve, R. L.,
- 1760 Self, D. W., et al. (2013). Adenosine A1 and dopamine d1 receptor
- 1761 regulation of AMPA receptor phosphorylation and cocaine-seeking behavior. *Neuropsychopharmacology* 38, 1974–1983. doi: 10.1038/npp.2013.96
- 1762 Huang, L., Wu, D. D., Zhang, L., and Feng, L. Y. (2013). Modulation of A2a
- 1763 receptor antagonist on D2 receptor internalization and ERK phosphorylation. *Acta Pharmacol. Sin.* 34, 1292–1300. doi: 10.1038/aps.2013.87
- 1764 Isaac, S. O., and Berridge, C. W. (2003). Wake-promoting actions of dopamine
- 1765 D1 and D2 receptor stimulation. *J. Pharmacol. Exp. Ther.* 307, 386–394.
- 1766 doi: 10.1124/jpet.103.053918
- 1767 Ishiwari, K., Madson, L. J., Farrar, A. M., Mingote, S. M., Valenta, J. P.,
- 1768 DiGianvittorio, M. D., et al. (2007). Injections of the selective adenosine A2A
- 1769 antagonist MSX-3 into the nucleus accumbens core attenuate the locomotor
- 1770 suppression induced by haloperidol in rats. *Behav. Brain Res.* 178, 190–199.
- 1771 doi: 10.1016/j.bbr.2006.12.020
- 1772 Jankovic, J. (2008). Parkinson's disease: clinical features and diagnosis. *J. Neurol.*
- 1773 *Neurosurg. Psychiatry* 79, 368–376. doi: 10.1136/jnnp.2007.131045
- 1774 Justinová, Z., Redhi, G. H., Goldberg, S. R., and Ferré, S. (2014). Differential
- 1775 effects of presynaptic versus postsynaptic adenosine A2A receptor blockade
- 1776 on Δ9-tetrahydrocannabinol (THC) self-administration in squirrel monkeys. *J. Neurosci.* 34, 6480–6484. doi: 10.1523/jneurosci.5073-13.2014
- 1777 Kable, J. W., and Glimcher, P. W. (2009). The neurobiology of decision: consensus
- 1778 and controversy. *Neuron* 63, 733–745. doi: 10.1016/j.neuron.2009.09.003
- 1779 Kanda, T., Shiozaki, S., Shimada, J., Suzuki, F., and Nakamura, J. (1994). KF17837:
- 1780 a novel selective adenosine A2A receptor antagonist with anticataleptic activity. *Eur. J. Pharmacol.* 256, 263–268. doi: 10.1016/0014-2999(94)90551-7
- 1781 Karcz-Kubicha, M., Antoniou, K., Terasmaa, A., Quarta, D., Solinas, M.,
- 1782 Justinova, Z., et al. (2003). Involvement of adenosine A1 and A2A receptors
- 1783 in the motor effects of caffeine after its acute and chronic administration. *Neuropsychopharmacology* 28, 1281–1291. doi: 10.1038/sj.npp.1300167
- 1784 Kim, D. S., and Palmiter, R. D. (2003). Adenosine receptor blockade reverses
- 1785 hypophagia and enhances locomotor activity of dopamine-deficient mice. *Proc. Natl. Acad. Sci. U.S.A.* 100, 1346–1351. doi: 10.1073/pnas.252753799
- 1786 Kim, D. S., and Palmiter, R. D. (2008). Interaction of dopamine and adenosine
- 1787 receptor function in behavior: studies with dopamine-deficient mice. *Front. Biosci.* 13, 2311–2318.
- 1788 Kim, H. F., and Hikosaka, O. (2015). Parallel basal ganglia circuits for voluntary
- 1789 and automatic behaviour to reach rewards. *Brain* 138, 1776–1800. doi: 10.1093/brain/awv134
- 1790 Kirschner, M., Hager, O. M., Bischof, M., Hartmann, M. N., Kluge, A., Seifritz, E.,
- 1791 et al. (2016). Ventral striatal hypoactivation is associated with apathy but not
- 1792 diminished expression in patients with schizophrenia. *J. Psychiatry Neurosci.*
- 1793 41, 152–161. doi: 10.1503/jpn.140383
- 1794 Kravitz, A. V., Freeze, B. S., Parker, P. R., Kay, K., Thwin, M. T., Deisseroth, K., et al.
- 1795 (2010). Regulation of parkinsonian motor behaviours by optogenetic control of
- 1796 basal ganglia circuitry. *Nature* 466, 622–626. doi: 10.1038/nature09159
- 1797 Kravitz, A. V., Tye, L. D., and Kreitzer, A. C. (2012). Distinct roles for direct and
- 1798 indirect pathway striatal neurons in reinforcement. *Nat. Neurosci.* 15, 816–818.
- 1799 doi: 10.1038/nn.3100
- 1800 Kull, B., Ferré, S., Arslan, G., Svenningsson, P., Fuxe, K., Owman, C., et al. (1999).
- 1801 Reciprocal interactions between adenosine A2A and dopamine D2 receptors
- 1802 in Chinese hamster ovary cells co-transfected with the two receptors. *Biochem. Pharmacol.* 58, 1035–1045. doi: 10.1016/S0006-2952(99)00184-7
- 1803 Lazenka, M. F., Moeller, F. G., and Negus, S. S. (2015). Effects of caffeine and its
- 1804 metabolite paraxanthine on intracranial self-stimulation in male rats. *Exp. Clin. Psychopharmacol.* 23, 71–80. doi: 10.1037/pha0000012
- 1805 Lebon, G., Warne, T., Edwards, P. C., Bennett, K., Langmead, C. J., Leslie, A. G.,
- 1806 et al. (2011). Agonist-bound adenosine A2A receptor structures reveal common
- 1807 features of GPCR activation. *Nature* 474, 521–525. doi: 10.1038/nature10136
- 1808 Ledent, C., Vaugeois, J. M., Schiffmann, S. N., Pedrazzini, T., El Yacoubi, M.,
- 1809 Vanderhaeghen, J. J., et al. (1997). Aggressiveness, hypoalgesia and high blood
- 1810 pressure in mice lacking the adenosine A2a receptor. *Nature* 388, 674–678.
- 1811 doi: 10.1038/41771
- 1812 Lee, K. W., Hong, J. H., Choi, I. Y., Che, Y., Lee, J. K., Yang, S. D., et al. (2002).
- 1813 Impaired D2 dopamine receptor function in mice lacking type 5 adenylyl
- 1814 cyclase. *J. Neurosci.* 22, 7931–7940.
- 1815 Lindskog, M., Svenningsson, P., Fredholm, B. B., Greengard, P., and
- 1816 Fisone, G. (1999). Activation of dopamine D2 receptors decreases
- 1817 DARPP-32 phosphorylation in striatonigral and striatopallidal projection
- 1818 neurons via different mechanisms. *Neuroscience* 88, 1005–1008.
- 1819 doi: 10.1016/S0306-4522(98)00411-4
- 1820 Macpherson, T., Morita, M., and Hikida, T. (2014). Striatal direct and
- 1821 indirect pathways control decision-making behavior. *Front. Psychol.* 5:1301.
- 1822 doi: 10.3389/fpsyg.2014.01301
- 1823 Marin, R. S. (1991). Apathy: a neuropsychiatric syndrome. *J. Neuropsychiatry Clin. Neurosci.* 3, 243–254. doi: 10.1176/jnp.3.3.243
- 1824 Mazzoni, P., Hristova, A., and Krakauer, J. W. (2007). Why don't we move faster?
- 1825 Parkinson's disease, movement vigor, and implicit motivation. *J. Neurosci.* 27,
- 1826 7105–7116. doi: 10.1523/JNEUROSCI.0264-07.2007
- 1827 Mogenson, G. J., Jones, D. L., and Yim, C. Y. (1980). From motivation to action:
- 1828 functional interface between the limbic system and the motor system. *Prog. Neurobiol.* 14, 69–97. doi: 10.1016/0301-0082(80)90018-0
- 1829 Morelli, M., Carta, A. R., and Jenner, P. (2009). Adenosine A2A receptors and
- 1830 Parkinson's disease. *Handb. Exp. Pharmacol.* 193, 589–615. doi: 10.1007/978-
- 1831 3-540-89615-9_18
- 1832
- 1833
- 1834

- 1825 Morelli, M., and Wardas, J. (2001). Adenosine A(2a) receptor antagonists: potential
1826 therapeutic and neuroprotective effects in Parkinson's disease. *Neurotox. Res.* 3,
1827 545–556. doi: 10.1007/BF03033210
- 1828 Moscoso-Castro, M., Gracia-Rubio, I., Ciruela, F., and Valverde, O. (2016).
1829 Genetic blockade of adenosine A2A receptors induces cognitive impairments
1830 and anatomical changes related to psychotic symptoms in mice. *Eur.*
1831 *Neuropsychopharmacol.* 26, 1227–1240. doi: 10.1016/j.euroneuro.2016.04.003
- 1832 Müller, C. E., and Ferré, S. (2007). Blocking striatal adenosine A2A receptors:
1833 a new strategy for basal ganglia disorders. *Recent Pat. CNS Drug Discov.* 2, 1–21.
1834 doi: 10.2174/157488907779561772
- 1835 Nagel, J., Schladebach, H., Koch, M., Schwienbacher, I., Müller, C. E., and
1836 Hauber, W. (2003). Effects of an adenosine A2A receptor blockade in the
1837 nucleus accumbens on locomotion, feeding, and prepulse inhibition in rats.
1838 *Synapse* 49, 279–286. doi: 10.1002/syn.10240
- 1839 Nakamura, K., and Hikosaka, O. (2006). Role of dopamine in the primate
1840 caudate nucleus in reward modulation of saccades. *J. Neurosci.* 26, 5360–5369.
1841 doi: 10.1523/JNEUROSCI.4853-05.2006
- 1842 Navarro, G., Aguinaga, D., Moreno, E., Hradsky, J., Reddy, P. P., Cortés, A.,
1843 et al. (2014). Intracellular calcium levels determine differential modulation of
1844 allosteric interactions within G protein-coupled receptor heteromers. *Chem.*
1845 *Biol.* 21, 1546–1556. doi: 10.1016/j.chembiol.2014.10.004
- 1846 Navarro, G., Cordero, A., Casadó-Anguera, V., Moreno, E., Cai, N.-S., Cortés, A.,
1847 et al. (2018). Evidence for functional pre-coupled complexes of receptor
1848 heteromers and adenylyl cyclase. *Nat. Commun.* (in press). doi: 10.1038/s41467-
1849 018-03522-3
- 1850 Nunes, E. J., Randall, P. A., Podurgiel, S., Correa, M., and Salamone, J. D. (2013).
1851 Nucleus accumbens neurotransmission and effort-related choice behavior
1852 in food motivation: effects of drugs acting on dopamine, adenosine, and
1853 muscarinic acetylcholine receptors. *Neurosci. Biobehav. Rev.* 37, 2015–2025.
1854 doi: 10.1016/j.neubiorev.2013.04.002
- 1855 O'Neill, C. E., Hobson, B. D., Levis, S. C., and Bachtell, R. K. (2014). Persistent
1856 reduction of cocaine seeking by pharmacological manipulation of adenosine A1
1857 and A2A receptors during extinction training in rats. *Psychopharmacology* 231,
1858 3179–3188. doi: 10.1007/s00213-014-3489-2
- 1859 Orrú, M., Bakešová, J., Brugarolas, M., Quiroz, C., Beaumont, V., Goldberg, S. R.,
1860 et al. (2011a). Striatal pre- and postsynaptic profile of adenosine A(2A) receptor
1861 antagonists. *PLoS One* 6:e16088. doi: 10.1371/journal.pone.0016088
- 1862 Orrú, M., Quiroz, C., Guitart, X., and Ferré, S. (2011b). Pharmacological evidence
1863 for different populations of postsynaptic adenosine A2A receptors in the rat
1864 striatum. *Neuropharmacology* 61, 967–974. doi: 10.1016/j.neuropharm.2011.06.
1865 025
- 1866 Pereira, M., Farrar, A. M., Hockemeyer, J., Müller, C. E., Salamone, J. D., and
1867 Morrell, J. I. (2011). Effect of the adenosine A2A receptor antagonist MSX-
1868 3 on motivational disruptions of maternal behavior induced by dopamine
1869 antagonism in the early postpartum rat. *Psychopharmacology* 213, 69–79.
1870 doi: 10.1007/s00213-010-2015-4
- 1871 Pinna, A., Wardas, J., Cristalli, G., and Morelli, M. (1997). Adenosine A2A receptor
1872 agonists increase Fos-like immunoreactivity in mesolimbic areas. *Brain Res.*
1873 759, 41–49. doi: 10.1016/S0006-8993(97)00214-X
- 1874 Prévost, C., Pessiglione, M., Météreau, E., Cléry-Melin, M. L., and Dreher, J. C.
1875 (2010). Separate valuation subsystems for delay and effort decision costs.
1876 *J. Neurosci.* 30, 14080–14090. doi: 10.1523/jneurosci.2752-10.2010
- 1877 Quiroz, C., Luján, R., Uchigashima, M., Simoes, A. P., Lerner, T. N., Borycz, J.,
1878 et al. (2009). Key modulatory role of presynaptic adenosine A2A receptors in
1879 cortical neurotransmission to the striatal direct pathway. *ScientificWorldJournal*
1880 9, 1321–1344. doi: 10.1100/tsw.2009.143
- 1881 Quiroz, C., Orrú, M., Rea, W., Ciudad-Roberts, A., Yepes, G., Britt, J. P.,
1882 et al. (2016). Local control of extracellular dopamine levels in the medial
1883 nucleus accumbens by a glutamatergic projection from the infralimbic cortex.
1884 *J. Neurosci.* 36, 851–859. doi: 10.1523/jneurosci.2850-15.2016
- 1885 Randall, P. A., Nunes, E. J., Janniere, S. L., Stopper, C. M., Farrar, A. M., Sager, T. N.,
1886 et al. (2011). Stimulant effects of adenosine antagonists on operant behavior:
1887 differential actions of selective A2A and A1 antagonists. *Psychopharmacology*
1888 216, 173–186. doi: 10.1007/s00213-011-2198-3
- 1889 Remy, P., Doder, M., Lees, A., Turjanski, N., and Brooks, D. (2005). Depression
1890 in Parkinson's disease: loss of dopamine and noradrenergic innervation in the
1891 limbic system. *Brain* 128, 1314–1322. doi: 10.1093/brain/awh445
- 1892 Roitman, M. F., Wheeler, R. A., Wightman, R. M., and Carelli, R. M. (2008). Real-time chemical responses in the nucleus accumbens differentiate
1893 rewarding and aversive stimuli. *Nat. Neurosci.* 11, 1376–1377. doi: 10.1038/nn.
1894 2219
- 1895 Root, D. H., Melendez, R. I., Zaborszky, L., and Napier, T. C. (2015). The
1896 ventral pallidum: subregion-specific functional anatomy and roles in motivated
1897 behaviors. *Prog. Neurobiol.* 130, 29–70. doi: 10.1016/j.pneurobio.2015.03.005
- 1898 Salamone, J. D., Correa, M., Nunes, E. J., Randall, P. A., and Pardo, M. (2012).
1899 The behavioral pharmacology of effort-related choice behavior: dopamine,
1900 adenosine and beyond. *J. Exp. Anal. Behav.* 97, 125–146. doi: 10.1901/jeab.2012.
1901 97-125
- 1902 Schiffmann, S. N., Fisone, G., Moresco, R., Cunha, R. A., and Ferré, S. (2007).
1903 Adenosine A2A receptors and basal ganglia physiology. *Prog. Neurobiol.* 83,
1904 277–292. doi: 10.1016/j.pneurobio.2007.05.001
- 1905 Shen, W., Flajolet, M., Greengard, P., and Surmeier, D. J. (2008). Dichotomous
1906 dopaminergic control of striatal synaptic plasticity. *Science* 321, 848–851.
1907 doi: 10.1126/science.1160575
- 1908 Sheppard, A. B., Gross, S. C., Pavelka, S. A., Hall, M. J., and Palmatier, M. I. (2012).
1909 Caffeine increases the motivation to obtain non-drug reinforcers in rats. *Drug*
1910 *Alcohol Depend.* 124, 216–222. doi: 10.1016/j.drugalcdep.2012.01.008
- 1911 Shiozaki, S., Ichikawa, S., Nakamura, J., Kitamura, S., Yamada, K., and
1912 Kuwana, Y. (1999). Actions of adenosine A2A receptor antagonist KW-6002
1913 on drug-induced catalepsy and hypokinesia caused by reserpine or MPTP.
1914 *Psychopharmacology* 147, 90–95. doi: 10.1007/s002130051146
- 1915 Simon, J. J., Biller, A., Walther, S., Roesch-Ely, D., Stippich, C., Weisbrod, M., et al.
1916 (2010). Neural correlates of reward processing in schizophrenia—relationship to
1917 apathy and depression. *Schizophr. Res.* 118, 154–161. doi: 10.1016/j.schres.2009.
1918 11.007
- 1919 Simon, J. J., Cordeiro, S. A., Weber, M. A., Friederich, H. C., Wolf, R. C.,
1920 Weisbrod, M., et al. (2015). Reward system dysfunction as a neural substrate
1921 of symptom expression across the general population and patients with
1922 schizophrenia. *Schizophr. Bull.* 41, 1370–1378. doi: 10.1093/schbul/sbv067
- 1923 Sinha, N., Manohar, S., and Husain, M. (2013). Impulsivity and apathy in
1924 Parkinson's disease. *J. Neuropsychol.* 7, 255–283. doi: 10.1111/jnp.12013
- 1925 Steinberg, E. E., Keiflin, R., Boivin, J. R., Witten, I. B., Deisseroth, K., and Janak,
1926 P. H. (2013). A causal link between prediction errors, dopamine neurons and
1927 learning. *Nat. Neurosci.* 16, 966–973. doi: 10.1038/nn.3413
- 1928 Stopper, C. M., and Floresco, S. B. (2011). Contributions of the nucleus accumbens
1929 and its subregions to different aspects of risk-based decision making. *Cogn.*
1930 *Affect. Behav. Neurosci.* 11, 97–112. doi: 10.3758/s13415-010-0015-9
- 1931 Strauss, G. P., Morra, L. F., Sullivan, S. K., and Gold, J. M. (2015). The role of low
1932 cognitive effort and negative symptoms in neuropsychological impairment in
1933 schizophrenia. *Neuropsychology* 29, 282–291. doi: 10.1037/neu0000113
- 1934 Svenningsson, P., Fourreau, L., Bloch, B., Fredholm, B. B., Gonon, F., and Le
1935 Moine, C. (1999). Opposite tonic modulation of dopamine and adenosine on
1936 c-fos gene expression in striatopallidal neurons. *Neuroscience* 89, 827–837.
1937 doi: 10.1016/S0306-4522(98)00403-5
- 1938 Svenningsson, P., Le Moine, C., Kull, B., Sunahara, R., Bloc, H. B., and Fredholm,
1939 B. B. (1997). Cellular expression of adenosine A2A receptor messenger
1940 RNA in the rat central nervous system with special reference to dopamine
1941 innervated areas. *Neuroscience* 80, 1171–1185. doi: 10.1016/S0306-4522(97)00
1942 180-2
- 1943 Svenningsson, P., Lindskog, M., Rognoni, F., Fredholm, B. B., Greengard, P.,
1944 and Fisone, G. (1998). Activation of adenosine A2A and dopamine D1
1945 receptors stimulates cyclic AMP-dependent phosphorylation of DARPP-32 in
1946 distinct populations of striatal projection neurons. *Neuroscience* 84, 223–228.
1947 doi: 10.1016/S0306-4522(97)00510-1
- 1948 Taura, J., Valle-León, M., Sahlhom, K., Watanabe, M., Van Craenebroeck, K.,
1949 Fernández-Dueñas, V., et al. (2017). Behavioral control by adenosine A2A-
1950 dopamine D2 receptor heteromers. *Genes Brain Behav.* doi: 10.1111/gbb.12432
1951 [Epub ahead of print].
- 1952 Tian, L., Xia, Y., Flores, H. P., Campbell, M. C., Moerlein, S. M., and Perlmutter, J. S.
1953 (2015). Neuroimaging analysis of the dopamine basis for apathetic behaviors in
1954 an MPTP-lesioned primate model. *PLoS One* 10:e0132064. doi: 10.1371/journal.
1955 pone.0132064
- 1956 Tremblay, L., Worbe, Y., Thobois, S., Sgambato-Faure, V., and Féger, J.
1957 (2015). Selective dysfunction of basal ganglia subterritories: from movement
1958 1937
1959 1938

1939 to behavioral disorders. *Mov. Disord.* 30, 1155–1170. doi: 10.1002/mds.2
 1940 6199

1941 Usiello, A., Baik, J. H., Rougé-Pont, F., Picetti, R., Dierich, A., LeMeur, M., et al.
 1942 (2000). Distinct functions of the two isoforms of dopamine D2 receptors.
 1943 *Nature* 408, 199–203. doi: 10.1038/35041572

1944 Valjent, E., Bertran-Gonzalez, J., Hervé, D., Fisone, G., and Girault, J. A. (2009).
 1945 Looking BAC at striatal signaling: cell-specific analysis in new transgenic mice.
 1946 *Trends Neurosci.* 32, 538–547. doi: 10.1016/j.tins.2009.06.005

1947 Verdejo-García, A., Bechara, A., Recknor, E. C., and Pérez-García, M. (2006).
 1948 Executive dysfunction in substance dependent individuals during drug use
 1949 and abstinence: an examination of the behavioral, cognitive and emotional
 1950 correlates of addiction. *J. Int. Neuropsychol. Soc.* 12, 405–415. doi: 10.1017/
 1951 S1355617706060486

1952 Verdejo-García, A., and Pérez-García, M. (2008). Substance abusers' self-awareness
 1953 of the neurobehavioral consequences of addiction. *Psychiatry Res.* 158, 172–180.
 1954 doi: 10.1016/j.psychres.2006.08.001

1955 Volkow, N. D., Wang, G. J., Fowler, J. S., Tomasi, D., and Telang, F. (2011).
 1956 Addiction: beyond dopamine reward circuitry. *Proc. Natl. Acad. Sci. U.S.A.* 108,
 1957 15037–15042. doi: 10.1073/pnas.1010654108

1958 Volkow, N. D., Wang, G. J., Logan, J., Alexoff, D., Fowler, J. S., Thanos, P. K., et al.
 1959 (2015). Caffeine increases striatal dopamine D₂/D₃ receptor availability in the
 1960 human brain. *Transl. Psychiatry* 5:e549. doi: 10.1038/tp.2015.46

1961 Voon, V., Pessiglione, M., Brezing, C., Gallea, C., Fernandez, H. H., Dolan,
 1962 R. J., et al. (2010). Mechanisms underlying dopamine-mediated reward bias in
 1963 compulsive behaviors. *Neuron* 65, 135–142. doi: 10.1016/j.neuron.2009.12.027

1964 Voorn, P., Vanderschuren, L. J., Groenewegen, H. J., Robbins, T. W., and Pennartz,
 1965 C. M. (2004). Putting a spin on the dorsal-ventral divide of the striatum. *Trends*
 1966 *Neurosci.* 27, 468–474. doi: 10.1016/j.tins.2004.06.006

1967 Wang, J. H., Short, J., Ledent, C., Lawrence, A. J., and van den Buuse, M.
 1968 (2003). Reduced startle habituation and prepulse inhibition in mice lacking the
 1969 adenosine A2A receptor. *Behav. Brain Res.* 143, 201–207. doi: 10.1016/S0166-
 1970 4328(03)00036-6

1971 Wise, R. A. (2004). Dopamine, learning and motivation. *Nat. Rev. Neurosci.* 5,
 1972 483–494. doi: 10.1038/nrn1406

1973 Wise, R. A., and Bozarth, M. A. (1987). A psychomotor stimulant theory of
 1974 addiction. *Psychol. Rev.* 94, 469–492. doi: 10.1037/0033-295X.94.4.469

1975 Yang, J. N., Chen, J. F., and Fredholm, B. B. (2009). Physiological roles of A1
 1976 and A2A adenosine receptors in regulating heart rate, body temperature, and
 1977 locomotion as revealed using knockout mice and caffeine. *Am. J. Physiol. Heart*
 1978 *Circ. Physiol.* 296, H1141–H1149. doi: 10.1152/ajpheart.00754.2008

1979 Yin, H. H., and Knowlton, B. J. (2006). The role of the basal ganglia in habit
 1980 formation. *Nat. Rev. Neurosci.* 7, 464–476. doi: 10.1038/nrn1919

1981 Zwilling, D., Zhu, W., Lee, H., Gallager, I., Braithwaite, S. P., and Thompson,
 1982 K. R. (2014). *An optogenetic Model to Study Motor and Psychiatric Symptoms*
 1983 *of Parkinson's Disease. 2014 Neuroscience Meeting Planner.* Washington, DC:
 1984 Society for Neuroscience.

1985
 1986
 1987
 1988
 1989
 1990
 1991
 1992
 1993
 1994
 1995

Conflict of Interest Statement: The authors declare that the research was
 conducted in the absence of any commercial or financial relationships that could
 be construed as a potential conflict of interest.

Copyright © 2018 Ferré, Bonaventura, Zhu, Hatcher-Solis, Taura, Quiroz, Cai,
 Moreno, Casadó-Anguera, Kravitz, Thompson, Tomasi, Navarro, Cordero, Pardo,
 Lluís, Dessauer, Volkow, Casadó, Ciruela, Logothetis and Zwilling. This is an open-
 access article distributed under the terms of the Creative Commons Attribution
 License (CC BY). The use, distribution or reproduction in other forums is permitted,
 provided the original author(s) and the copyright owner are credited and that the
 original publication in this journal is cited, in accordance with accepted academic
 practice. No use, distribution or reproduction is permitted which does not comply
 with these terms.

